第18卷 第5期 医学研究生学报 Vol. 18 No. 5
2005年5月 Journal of Medical Postgraduates May. 2005

· 综 述 ·

钬激光生物学效应的研究进展

丁新民综述，保庭毅审校
（第四军医大学唐都医院泌尿外科，陕西西安 710038）

摘要：钬激光以其优良的特性，在医学上的应用不断扩展。不同输出功率的钬激光对生物组织产生不同的效应。Cecchetti W 针对高功率钬激光产生的良好消融、汽化、切割及碎石效应，提出了等离子体理论，较好地解释了钬激光作用过程中出现的各种物理现象，进一步指导临床应用；逐渐降低钬激光的输出功率，可分别引起组织凝固、生物良性刺激，促进组织、细胞代谢及修复等效应。

关键词：钬激光；生物学效应；等离子
中图分类号：R362 文献标识码：A 文章编号：1008-8199(2005)05-0465-02*

Progress of study of holmium : YAG laser in biological effect

DING Xin-min *reviewing*, BAO Ting-yi *checking*
(*Department of Urology, Tangdu Hospital, the Fourth Military Medical University, Xi' an* 710038, *Shaanxi, China*)

Abstract: With its excellent character , Holmium: Yag laser had been used in more and more areas of medicine. It's growing success is a result of its excellent performance as both a lithotriptor and a surgical laser on soft tissues. The low level laser power is a good stimulator to the growth of biological tissue and the metabolism of cells.

Key words: YAG laser; Biological effect; Plasma formation

0 引 言

激光技术自20世纪60年代诞生以来，在医学上的应用不断地扩展，解决了医学中的许多难题。钬激光（Ho:YAG lasers）以其对软组织精确的消融、汽化、切割、凝固、止血作用，以及良好的碎石功能等多种用途，在临床各科得到了广泛的应用，尤其是在泌尿外科的经腔道治疗中具有不可替代的优势。为进一步推广应用，现对其近年来在基础研究方面的进展作一综述。

1 钬激光的光学特性

钬激光是由掺钬的钇铝石榴石激光器（Ho:YAG）产生的中红外激光，波长为2 120 nm，非常接近水的1 950 nm吸收峰，其吸收系数为24 cm^{-1}，能很好地被生物组织吸收，热弛豫时间（thermalrelaxation time）为310 ms。目前世界上Ho:YAG的技术数据为：脉冲能量0.2～4 J，持续时间250～350 μs，频率为5～50 Hz，平均能量输出为3.0～100 W。可非常容易地由低水含量的石英光纤传输。

2 钬激光对生物组织的作用及其机制

钬激光随着输出功率的不同，可对生物组织产生不同的效应，其作用机制也不同。

2.1 钬激光对生物组织的消融、切割及碎石效应 动物实验及临床实践[1-5]均证实，高功率钬激光（> 30 W）对各种生物组织有良好的消融、切割效应，其特点是：①钬激光器可根据不同的使用目的，调整不同的能量和脉冲设置，所产生的热穿透不深，弥散很少，可以起到精细雕刻的作用；②对被切割组织周围

* 收稿日期：2004-10-25；修订日期：2004-11-28
作者简介：丁新民（1969-），男，河南千城人，主治医师，医学硕士研究生，从事泌尿外科专业。
万方数据

的热凝固损伤较小，但同时可产生有效止血效果，使操作几乎在无血的视野下进行；③既可作用于软组织，又可碎石；④既可在流体介质中以接触方式进行，也可以非接触方式进行。传递钬激光能量的光纤特别适用于软质和硬质输尿管镜、膀胱镜和切除镜，光纤有侧方开口和末端开口两种，直径为 200～1 000 μm。

钬激光对生物组织的上述作用机制有不同的诠释，传统的观点强调热效应[6]，即受激光辐射的组织直接吸收光能，瞬间产生高热，使受照射软组织被汽化、消融，结石被熔化。在此基础上还针对非接触的组织切割提出了" 摩西效应"（Mose effect）[7] 以及汽化小球的爆破碎石理论等。但是，根据热效应理论仍有不能解释的现象，如钬激光穿透组织的深度只有 0.4 mm，不足以产生良好的凝血作用，而事实则相反；再者，如果结石是在高温作用下破碎，其排出的残渣应该呈熔化后的晶体状，而事实上排出的却是性状未变的碎石沫或小石块。此外，激光治疗过程中伴随的爆裂声也无法解释等。因此，Cecchetti 等[8] 提出了钬激光的 等离子体" 理论，即钬激光先导致组织内产生等离子体，等离子体再进一步作用于生物组织，从而对钬激光的各种生物效应作出了合理的解释，并通过实验，验证了等离子泡的存在，且测量了其大小。这种解释也符合公认的两级激光生物作用理论，即第一步生物组织吸收激光能量，将光能转换成热能、化学能、机械能等，产生理化改变；第二步，这些理化因子进一步导致靶组织发生形态或功能等生物学改变。不同波长的短脉冲激光照射生物组织均可产生等离子体，但形成的机制不同。波长为 504 nm 的染料激光通过强电场（脉冲能量峰值可达 10^5 W）照射固体靶，使生物分子外层电子逸出成为自由电子，导致生物组织电离，产生致密的已电离的气体云，即等离子体或等离子泡；钬激光是通过其光纤头端的水分迅速吸收激光能量，产生热电离而形成等离子体。形成的等离子体可吸收各种波长的激光，其对激光的吸收比产生等离子体的生物组织大得多。一旦形成等离子体，其强烈吸收入射激光，等离子体本身以超音速膨胀，产生压强很高的冲击波，伴随爆裂声发出[9]，生物组织可因冲击波或等离子体形成的空腔崩溃产生的压强，引起局部破坏。Cecchetti 等在实验中测得直径 550 μm 的光纤，当脉冲能量达 1.4 J、频率达 10 Hz 时，在光纤头端开始形成等离子体，在 1.5 J×20 Hz 时测得的等离子体大小，光纤前端为 2 mm，侧面为 1.5 mm。随着脉冲能量和频率的加大，等离子泡可以略有增大，等离子体内部产生可导致金属热电欧熔化的高温，估计在 1 500℃ 以上，在等离子体外 1 mm内温度可达数十度至数百度，系热传导所致。等离子体本身导致组织汽化、消融或碎石，传导的热量使周围组织凝固、止血。根据理论推算的钬激光作用范围与在体内试验中产生的实际效果基本一致。该试验中所测定的等离子泡，其大小与以前通过缩影照片[10] 所取得的钬激光头端产生的泡大小基本一致，说明过去所描述的蒸汽泡本质上就是等离子泡。

上述机制的阐明对钬激光的实际应用具有重要意义。在应用钬激光时，可根据需要选择适当的参数，根据等离子泡大小，正确放置光纤，通过其正面或侧面进行治疗。此外，在钬激光治疗的过程中一定要保持清晰、准确的视野，以保持光纤与正常组织间适当的距离，以避免损伤；同时光纤与导丝及取石篮等也要有适当的距离，以避免对其破坏；在应用钬激光时，一定要把光纤头浸入水中，以保证产生有效的切割、凝固或碎石作用。

2.2 钬激光对生物组织的热凝固效应 当钬激光输出功率不足以产生等离子体时，可通过组织直接吸收光能产生热凝固效应。这是钬激光的初级生物作用。属于中红外的钬激光光子能量较小，生物组织吸收后，只能引起其振动和转动，并转化为平动能，即增加生物分子的热运动[11]，在宏观上表现为该处生物组织的温度升高，不能引起光化学反应，因此，不会引起组织细胞的癌变。当受照射组织温度达到 60～100℃，持续 10 s，便可导致凝固性损伤。由于钬激光主要是被组织中的水分吸收，扩散系数很小，激光脉冲小于热弛豫时间（相对于一个光学吸收长度）时，热凝固的范围较小。

2.3 钬激光的生物刺激作用 当钬激光的输出功率控制在较弱水平，使组织温度控制在 38～40℃ 时，可产生良好的生物刺激作用[4]，使生物组织代谢率增高，毛细血管扩张，血流加速，改善局部血液循环，改善组织营养，促进代谢和修复等，还可改善神经系统功能。在基因转染试验中证明，应用钬激光辐射供能可以显著提高裸 DNA 向移行细胞癌[11] 及前列腺癌[12] 细胞内的转染率，提示钬激光在肿瘤的基因治疗中有应用价值。Beckham 等[13] 通过测定细胞内荧光标记的热休克蛋白 70（HSP 70）的改变，表明了钬激光辐射对细胞代谢的影响，标志着人们对钬激光生物效应的研究已从组织学水平进入分子水平。

（下转第 468 页）

践发现，对远段肺动脉小分支栓塞的诊断价值不大，而且并发症发生率为 6%，病死率为 0.5%。急性 PE 患者病情危重，此项检查几乎不能进行。

近年来，随着 CT、螺旋 CT、核磁共振和 EBCT 等影像学技术的发展，EBCT 诊断 PE 的临床价值得到体现。CT 诊断 PE 的敏感性和特异性分别为 87% 和 95%[3]，但对肺段以下分支血管敏感性低，同时因扫描时间长，心搏、呼吸运动伪影显著，而在临床应用中受限。MRI 诊断 PE 具有快速、无创性的特点，敏感性和特异性分别为 72% 和 59%，但对肺段以下血管敏感性低，伪影多，而且有检查禁忌证（如心脏瓣膜置换术后、永久起搏器安装术后等）。EBCT 可行电影扫描，提供心功能指标。

EBCT 扫描速度达 50 m/s，能完全消除呼吸及心搏产生的运动伪影，可在几秒内获得清晰的肺动脉图像，可显示肺段及亚段等小分支。Boonbarichaiyapruok 等[5]对 20 例临床怀疑 PE 的患者分别进行 V/Q、肺动脉造影、EBCT 检查，以肺血管造影为金标准，对上述三种方法的敏感性和特异性作比较，EBCT 分别为 95% 和 100%。三种方法的正相关和负相关系数为 60%，结果表明，EBCT 是快速诊断 PE 的替代手段。Goldin JG 等[6]在猪模型中用 EBCT 对肺段/亚段 PE 的准确度进行研究，用增强 EBCT 对 18/21 的段/亚段 PE 作出正确诊断，敏感性为 86%。证明增强 EBCT 对段/亚段 PE 是一种敏感的方法，同时 EBCT 具有较高的时间、密度分辨率和无创性，实现了电影 CT 及 SSD 和 MPR 等三维重建技术[7]。EBCT 可清晰显示 PE 的部位和范围，能显示肺动脉四级分支内病灶，而且可同时显示肺动脉血栓和管壁，对 PE 作出直接评价和分型。由于扫描快速，患者无需屏气也可得到清晰的图像，尤其对急性 PE 患者，需要立即溶栓或手术治疗的急危重患者更能体现其临床价值。

参考文献：

[1] 罗慰慈. 肺栓塞的诊治进展[J]. 中华老年医学杂志, 2001, 20(3): 165-167.

[2] 戴汝平. 重视肺动脉栓塞的影像学诊断[J]. 中华放射学杂志, 1999, 33(5): 293-294.

[3] 张少雄, 戴汝平, 程显声 等. EBCT 在诊断肺栓塞治疗中的应用评价(CT)[J]. 中华放射学杂志, 1999, 33(5): 306-308.

[4] 于 淼, 张金山, 王艳萍 等. 肺栓塞的影像学诊断[J]. 中华放射学杂志, 1999, 33(5): 303-305.

[5] Boonbaichaiyapruok S, panpunnang S, Siripornpilaks *et al*. Utilization of electron beam CT scan in diagnosis of pulmonary embolism [J]. Med Assoc Thai, 1997, 80(8): 527-531.

[6] Goldin JG, Yoon HC, Greaser LE *et al*. Detection of pulmonary emboli at the segmental and subsegmental level with electron-beam CT validation in a porcine model[J]. Acad Radiol, 1998, 5(7): 503-508.

[7] 陈君坤, 张宗军. 电子束 CT 三维重建的应用和评价[J]. 医学研究生学报, 2000, 13(6): 371-374.

（责任编辑：张 锐）

（上接第 466 页）

参考文献：

[1] de la Rosette JJMCH, Granas S, Muschter R *et al*. Present Practice and Development of Minimally Invasive Techniques, Imaging andTraining in European Urology: Results of a Survey of the European Society of Uro-Technology (ESUT)[J]. Euro Urol, 2003, 44(5): 346-351.

[2] Tooher R, Sutherland P, Costello A *et al*. A systematic review of holmium laser prostatectomy for benign prostatic hyperplasia[J]. J Urol, 2004, 171(5): 1773-1781.

[3] Monga M, Beerman WW. Advanced intramenal ureteroscopic procedures[J]. Urol Clin North Am, 2004, 31(1): 129-135.

[4] Hayashi K, Hecht P, Thalut G 3rd *et al*. The biologic response to laser thermal modification in an in vivo sheep model[J]. Clin Orthop, 2000, 373(4): 265-276.

[5] 马建军, 保庭毅. 钬激光在泌尿外科应用的新进展[J]. 医学研究生学报, 2003, 16(2): 132-134.

[6] Jansen ED, Asshauer T, Frenz M *et al*. Effect of pulse duration on bubble formation and laser induced pressure waves during holmium laser ablation[J]. Laser Surg Med, 1996, 18(3): 287-293.

[7] Van Leeuwen TG, Vander Veen MJ, Verdaasdonk RM *et al*. Non-contact tissue ablation by Holmium: YSSG laser pulses in blood [J]. Lasers Surg Med, 1991, 11(1): 26-34.

[8] Cecchetti W, Zattoni F, Nigro F *et al*. Plasma bubble formation induced by holmium laser: an in vitro study[J]. Urology, 2004, 63(3): 586-590.

[9] Conesa S, Palanco S, Laserna JJ. Acoustic and optical emission during laser-induced plasma formation[J]. Spectrochimica Acta Part B, 2004, 59(6): 1395-1401.

[10] Dushinski JW, Lingeman JE. High speed photographic evaluation of holmium laser[J]. J Endourol, 1998, 12(2): 177-181.

[11] Knoll T, Trojan L, Langhein S *et al*. Impact of holmium: YAG and neodymium: YAG lasers on the efficacy of DNA delivery in transitional cell carcinoma[J]. Lasers Med Sci, 2004, 19(1): 33-36.

[12] Sagi S, Knoll T, Trojan L *et al*. Gene delivery into prostate cancer cells by holmium laser application[J]. Prostate Cancer Prostatic Dis, 2003, 6(2): 127-130.

[13] Berkham JT, Mackanos MA, Crooke C *et al*. Assessment of cellular response to thermal laser injury through bioluminescence imaging of heat shock protein 70[J]. Photochem Photobiol, 2004, 79(1): 76-85.

（责任编辑：鲁 立； 英文编辑：李幼生）

万方数据

· 综述 ·

钬激光碎石机制研究进展

崔杰 肖波

结石症是一种常见的多发性疾病，其治疗方法除了传统手术外，还有：液电碎石术(electrohydraulic lithotripsy，EHL)、体外冲击波碎石术(extracorporeal shockwave lithotripsy，ESWL)、激光碎石术(laser lithotripsy，LL)、超声碎石术(ultrasound lithotripsy，USL)、气压弹道碎石术(pneumatic lithotripsy，PL)。其中，EHL只适合软脆的结石而且容易造成穿孔[1]；ESWL是非侵入性的，但是容易形成石街[2]，而且其一次碎石成功率低；USL的碎石效率高，但是不能击碎高硬度的结石，而且该方法不适用于输尿管结石；PL能够击碎高硬度结石，但是其效率不高，且容易引起并发症[3,4]；LL由于传输光纤的柔韧性，可以配合较为柔软的内窥镜(如输尿管软镜)使用，这是USL和PL无法做到的。研究人员研究了不同波长的激光的应用及碎石效果：染料激光(Dye Laser，λ=504 nm)，调Q钕激光(Q-switch Nd:YAG laser，λ=1064 nm)，双频双脉冲激FREDDY(Frequency-doubled double-pluse Nd:YAG laser，λ_1=532 nm，λ_2=1064 nm)不能击碎一水草酸钙(COM)等高硬度结石[5]；染料激光需要定期更换染料[6]；调Q钕激光因为水对1064 nm的激光吸收系数很小(0.1 cm)，所以穿透深度深，容易对周围组织造成热损伤；钬激光(Ho:YAG laser，λ=2100 nm)能够击碎所有成分的结石[7]，并且该波长接近水吸收谱的峰值(吸收系数30cm^{-1})[7]，对周围组织热损伤小，而且容易用低OH浓度的光纤传输；铒激光(Er:YAG laser，λ=2940 nm)虽然也具有与钬激光相似的特点，甚至碎石效率比钬激光高[8]，但是目前没有一种光纤能够有效地传输饵激光[7,9]。所以，目前激光碎石术中较多采用的是钬激光。

目前，国内医院使用比较多的体内碎石术是超声碎石术、气压弹道碎石术和钬激光碎石术，实际应用中超声碎石术经常与气压弹道碎石术或者钬激光碎石术结合使用。由于钬激光碎石术具有损伤小、可配合软镜使用等其他技术不具备的优势，因此就目前来说，它是不可替代的。

了解钬激光的碎石机制，掌握不同的参数对碎石效果的影响对于钬激光治疗机的研制方向及临床应用都至关重要。二十世纪九十年代以来，研究人员对此进行了大量的研究，其碎石机制的主要观点集中在光机/光声机制和光热机制。

为了下文的叙述方便，涉及到的参数用以下符号表示：单脉冲能量—E_0，脉冲宽度—τ_p，脉冲重复频率—f，纤芯直径—d_f，能流密度(单脉冲能量/纤芯面积)—H。

碎石机制研究

一、光机/光声机制

光机/光声机制简单地说是指结石周围的水吸收激光能量，产生等离子泡(或蒸气泡)，利用其在膨胀或破碎过程中产生的冲击波击碎结石[5,10,11]。

瑞士、英国的学者[12-14]认为钬激光的碎石机制与短脉冲激光一样[15-17]，也是光机/光声机制，与短脉冲激光产生等离子泡不同，结石周围的水吸收钬激光能量，温度升高形成蒸气泡，蒸气泡破碎产生冲击波，击碎结石。

瑞士的Rink K[12]等人利用快速照相机和PVDF针尖水听器展开实验。E_0=244 mJ，τ_p=230 us，d_f=600 um时，光纤端头产生的气泡近似球形，激光脉冲开始350 us后，气泡体积达到最大，600 us时气泡破碎，破碎前最小直径约150 um。此时，在距光纤端头4 mm处测得的声压为180 bar，如果按照声压以球形波1/r衰减规律进行修正[11,18,19]，气泡破碎点的声压高达3600 bar，与短脉冲dye激光产生的声压相当，足以击碎结石。

英国Malcolm Sperrin等[13,14]用双薄膜水听器和

作者单位：100190 北京市，中国科学院声学研究所医用声学实验室

万方数据

针尖水听器测量了距离激光传输光纤端头不同距离的声压，E_0=2J，τ_p=300 μs，d_f=600 μm时，在距离光纤端头4 mm处测得的声压经过方位修正后高达510 MPa，该冲击波强度足以击碎结石。另外，他们还根据测得的声压用有限元方法计算了结石内部的应力分布，进一步证明光机/光声机制。

二、光热机制

光热机制是结石或者周围的水吸收激光能量，激发电子和分子到较高的能级，并通过分子间的碰撞把能量传递到周围的部分，引起微动能增加，表现为温度升高，由此造成结石的熔化或者化学分解[5,11]。

较早提出这一观点的是Oklahoma州立大学的Schafer SA等人[12]，他们认为结石表面吸收激光能量并熔化，而结石周围的水吸收激光能量形成气泡，气泡破碎有助于冲散碎片。E_0=220 mJ，τ_p=300 μs，d_f=320 μm，H=311 J/cm^{2}时，用PVDF水听器距离光纤端头5 mm测得的峰值声压大约为15 kPa，考虑水听器的积分效应，实际声压大约为15 bar，研究人员认为这个量级不足以击碎结石。用频闪观测仪观察，光纤垂直结石表面时，只有光纤离结石表面足够近，破碎才发生；光纤平行结石表面时，即使气泡完全接触结石表面，也只有非常小的消融现象，直到激光辐射面接触结石表面，消融才发生。用光学多通道分析仪进行光谱分析，得到350 nm～900 nm的连续宽带谱，他们认为这是一个5000 K的黑体温度。另外，用显微镜观察到，钬激光碎石产生的碎片为丝状，不同于机械方法碎石的粒状。以上实验现象都为钬激光的光热机制提供了证据。

美国Texas大学的K. F. Chan等[13,14]除了采用传统的高速摄像机记录气泡动态和水听器测量声压的手段外，还进行了质量损耗比较和化学分析。经过测量碎石后结石的质量损耗发现：空气中结石脱水＞空气中结石含水＞结石浸在水中；-80度的结石＜常温结石。这都说明了光热机制的主导作用，因为前一个实验中，水吸收了一部分激光能量，后一个实验中，一部分激光能量被用来升温。用红外谱分析仪分析激光作用前后结石的成分：COM(一水草酸钙)，CHPD(二水磷酸氢钙)和MAPH(六水磷酸铵镁)结石的碎片中都发现新成分；cystine(胱氨酸)结石所处的水中发现硫磺和少量cysteine(半胱氨酸)；uric acid(尿酸)结石处的水中发现cyanide(氰化物)[15]。以上结果都表明光热效应引起了化学分解。

另外，Dushinski JW[16]和Zhong. P[17]等也用高速照相设备进行实验，并得到相似的结果。Zhong. P认为钬激光在光纤端头形成的被拉长的梨形的气泡形成了一个通道，引导激光能量传输到结石表面，即"Moses effect"，最终利用光热效应"消融"结石。

与以上的实验方法不同，意大利的科学[18]家利用220 μm直径的热电偶测量光纤端头附近的温度，试图解释钬激光的碎石机制。他们认为由于水对钬激光的吸收系数很大，相当于充当了光敏物质的作用，所以与短脉冲激光相比，其形成等离子泡的阈值大大降低，正是由于等离子泡破碎产生的热效应消除了结石。他们在不同的钬激光参数下，测量了不同距离处的温度，并根据测量的温度和破裂声的发生估计了等离子泡的尺寸以及不同光纤直径对应的等离子泡的产生阈值。当E_0=1.5J；f=20 Hz；d_f=550 μm时，在距离光纤2 mm处测得的温度为750℃，重复频率上升到30 Hz时热电偶被损坏，根据制造热电偶的材料铁康铜的熔点(1400℃)估计，此时测量点的温度远高于1400℃，研究者认为只有等离子泡能产生如此高温。该研究团队认为之前研究所描述的蒸汽泡实际应为等离子泡。

三、相关参数对钬激光碎石效果的影响

影响钬激光碎石效果的因素包括激光单脉冲能量、激光脉冲宽度、激光脉冲重复频率、激光平均功率、激光能流密度、传输光纤纤芯直径、结石成分等。明确这些参数对碎石效果的影响对钬激光碎石技术安全，有效地用于临床治疗有重要的指导作用，因此研究人员在研究钬激光碎石机制的同时，也非常重视以上参数对碎石效果的影响，并且得到一些有用的结果，其中美国Taxes大学的研究最为集中。

研究与应用中发现，钬激光碎石的过程中会发生结石"后退"(retropulsion)现象，造成损伤周围组织，需重新定位光纤端头，延长手术时间等不利影响。其原因有多种可能，例如激光引起的冲击波，气泡的膨胀和破碎或者碎片溅射时的反作用力[19,20]。在其他参数相同的情况下，激光脉冲宽度越小，结石后退越厉害[19-21]；脉冲重复频率越高，后退距离越大[21]。Lee H等[22,23]计算了后退动量，并把测量结果用"steady-state vaporization"模型解释，得到以下结论：光纤直径相同的情况下，后退动量与能流密度成正比；能流密度相同的情况下，光纤直

万方数据

径越大后退动量越大，但其比例系数与结石产生的"坑洼"(crater)轮廓有关。

钬激光的碎石效率可以用结石的质量损耗或者激光在结石表面产生的"坑洼"情况来衡量，与单脉冲能量、脉冲宽度、光纤直径、重复频率等参数都有关系。研究发现一定条件下，E_p增大或f升高都导致质量损耗增大，但其增大并不是单调的，例如小直径光纤(200 μm、365 μm)对应的质量损耗在f=10 Hz出现拐点：f>10 Hz，质量损耗没有明显增加[9]。这是因为小直径光纤比较容易受到损耗[10,11]，使其实际输出能量小于额定脉冲能量。在光纤没有受到损耗的情况下，较大的单脉冲能量和光纤直径能产生较大体积的"坑洼"[12]，也有人总结为能流密度的增大会提高碎石效率[13]。另外，如果不考虑脉冲宽度对结石"后退"的影响，脉冲宽度较小的情况碎石效率较高[14]。所以，激光参数的选择是一个复杂的，需要综合考虑的问题。除了以上与钬激光治疗机有关的参数外，不同成分的结石对应的碎石效率也有很大的差异，光纤直径和单脉冲能量相同时，MAPH结石产生最大最深的"坑洼"，CHPD、cystine、uric acid产生中等大小和深度的"坑洼"，COM产生最小的"坑洼"[15]。作者分析不同成分结石的易碎程度与其热效应阈值有关，但是结石的硬度、不同成分对钬激光的吸收系数等因素对碎石效率的影响还有待确定。

讨 论

到目前为止，国外研究人员主要利用实验手段探究钬激光的碎石机制，大部分研究者认为钬激光的光热效应对碎石起主要作用，但是其中仍然存在一些问题没有解决，还有一些现象没有得到合理的解释。

首先，由于钬激光的脉冲宽度较宽，其形成的空腔泡比短脉冲激光形成的等离子泡形状要复杂地多，只有在某些参数条件下是球形或者近球形，大部分情况下都是梨形，甚至产生柱状通道，其破碎情况也比较复杂，产生多个破碎中心[7,16,17]，影响声压幅值。美国Texas大学的Jansen ED[18,19]等研究了没有结石参与的情况下，纯水或PAA(Polyacrylamide)凝胶中激光脉冲宽度和能流密度对气泡形成、气泡尺寸及声压的影响：其他参数相同情况下，脉冲宽度越小对应的最大气泡尺寸越大，声压值越高；能流密度增大，气泡持续时间增长，产生的声压值增大，但是能流密度大到一定程度，其声压反而会随之减小[19]。表1列出了一部分研究人员的声压测量结果，可以发现每次实验测得的声压值差别很大，这可能有水听器的原因，也可能是因为每次测

表1 已报道不同参数设置下测量的声压值

相关参数				距离 (mm)	声压 (bar)	归一化声压 (bar)
E_p(mJ)	τ_t(us)	d_f(μm)	H(J/cm²)			
244[13]	230	600	86	4	180	720
360[13]	230	200	1146	3	25	75
2000[14]	300	600	707.7	4	5100	20400
220[20]	300	320	311	5	15	45
400[21]	350	550	168.4	1	20	20
200[16]	100	400	159.2	1	66	66
480[16]	180	600	170	3	120	360

注：以上数值都是在水中没有结石(或固体界面)参与的情况下得到的；归一化声压为按回球形波1/r衰减规律修正到距离光纤端头1 mm处的声压。

万方数据

量所用的参数不同，所以针对钬激光引起的声压的测量，各种参数对声压的影响以及声压幅度对碎石的作用还需要进行较系统、全面的研究。这对于进一步研究钬激光的碎石机制，探讨治疗过程中对周围组织的损伤程度及对光纤的损耗有重要意义。

其次，钬激光碎石机制的研究工作中所用的钬激光的参数与目前市场上的钬激光治疗机的参数有很大的差距，例如，前文提到的文献中钬激光E_p<1.5J，但是目前E_p最大可以达到4J；另外，除了文献[20]之外，其他研究人员都是在单激光脉冲的情况下进行气泡观察或者声场测量，而临床应用中脉冲重复频率可以高达50 Hz。如此高的单脉冲能量的碎石机制是否与低能量的情况有所不同，较高的脉冲频率对声场及碎石效果的影响，以及临床应用中是否需要如此高的设置，都有待于进一步研究。而且各参数对碎石效率、结石"后退"、光纤损耗的影响是非常复杂的，能否找出一个定性的模型，以指导碎石时的参数设置，提高治疗效率，都是具有挑战性的问题。

最后，多篇文章中报道了钬激光碎石时伴随的模糊的"白光"现象，文献[21]认为这是5000K黑体温度的能量辐射，与文献[20]中根据热电偶估计的结果(>1400℃)具有一定的可比性，但是与根据胆固醇的对钬激光的吸收系数及胆固醇的比热计算的温度不符；文献[21]认为白光是钬激光器的泵浦光泄露引起，但是本文作者实验中发现只有激光的E_p>1J时才有"白光"发生。另外对于碎石时产生的"爆裂"声[20,22]，只有文献[20]解释为等离子泡破碎引起的，但是本文作者的实验中发现在任何一种参数设置下，都有这种声音产生，而不是文献中提到的在一定的阈值下才产生这种现象。如果能把这两种伴随现象解释清楚，将有助于钬激光碎石机制的明了。

总 结

明确钬激光的碎石机制，及激光参数设置对碎石效率、周围组织的影响具有重要的现实意义：为钬激光碎石的临床应用提供参考，可以在尽可能的减小患者痛苦的前提下安全有效地完成碎石；为钬激光治疗机的研制提供依据与指导；为碎石效率更高的钬激光碎石机制的研究准备理论与实验经验。

参考文献

1 周水根，孙西钊，叶章群. 体内碎石术的原理与临床应用. 临床泌尿外科杂志，2000，15(7)：332-334.

2 袁同强，魏佳莉，李志坚，等. 钬激光、ESWL、气压弹道碎石术治疗输尿管结石的疗效比较. 临床泌尿外科杂志，2001，16(11)：456-457.

3 徐留玉，李杰，魏学斌，等. 钬激光碎石术与气压弹道碎石术治疗输尿管结石的疗效比较. 中国激光医学杂志，2007，15(4)：228-230.

4 孙宁，高新，陈育彬，等. 双频双脉冲激光碎石术与电子弹道碎石术治疗肾输尿管结石的比较. 中国内镜杂志，2004，10(5)：33-36.

5 Welch AJ, Kang HW, Lee H, et al. Calculus fragmentation in laser lithotripsy. MINERVA UROL NEFROL. 2004, 56(1): 49-63.

6 Spindel ML, Moslem A, Bhatia KS, et al. Comparison of Holmium and Flashlamp Pumped Dye Lasers for Use in Lithotripsy of Biliary Calculi. Lasers Surg Med. 1992, 12(5): 482-489.

7 Curcio JA, Petty CC. The Near-Infrared absorption spectrum of liquid water. J. Opt. Soc. Am. 1951, 41(3): 302-304.

8 Sayer J, Johnson DE, Price RE, et al. Endoscopic laser fragmentation of ureteral calculi using the Holmium:YAG. Proc SPIE. 1993, 1879(1): 143-148.

9 Lee H, Kang HW, Teichman JM, et al. Urinary calculus fragmentation during Ho:YAG and Er:YAG lithotripsy. Lasers Surg Med. 2006, 38(1): 39-51.

10 Chan KF, Lee H, Teichman JM, et al. Erbium: YAG laser lithotripsy mechanism. J Urol. 2002, 168(2): 436-441.

11 Jacques SL. Laser-tissue Interactions: Photochemical, photothermal, and photomechanical. Surg Clin North Am. 1992, 72(3): 531-558.

12 Jiang ZX, Whitehurst C, King TA. Fragmentation methods in laser lithotripsy. Proc SPIE, 1991, 1421: 88-99.

13 Asshauer T, Rink K, Delacretaz G. Acoustic transient generation by holmium-laser-induced cavitation bubble. Journal of Applied Physics, 1994, 76(9): 5007-5013.

14 Sperrin M, Rogers K. Determination of the shock wave intensity from a laser lithotriptor using a bi-laminar hydrophone. IEE Colloquium on Innovative Pressure, Force and Flow Measurements, 1999(2): 311-315.

15 Rink K, Delacretaz G, and Salathe RP. Fragmentation process of current laser lithoriptors. Laser Surg Med. 1995, 16(2): 134-146.

16 Rink K, Delacretaz G, and Salathe RP. Fragmentation process induced by nanosecond laser pulses. Applied Physics Letters, 1992, 61 (22): 2644-2646.

17 Zorcher T, Hochberger J, Schrott K, et al. In vitro study concerning the efficiency of the frequency-doubled double-pulse Neodymium:YAG laser (FREDDY) for lithotripsy of calculi in the urinary tract. Lasers Surg. Med. 1999, 25(1): 38-42.

18 Jansen ED, Asshauer T, Frenz M, et al. Effect of pulse duration on bubble formation and laser-induced pressure waves during holmium laser ablation. Lasers Surg Med. 1996, 18(3): 278-293.

19 Asshauer T, Delacretaz G, Jansen ED, et al. Pulsed holmium laser ablation of tissue phantoms (correlation between bubble formation and acoustic transients. Applied Physics B (Lasers and Optics). 1997, 65 (4-5): 647-657.

20 Schafer SA, Durville FM, Jassemnejad B, et al. Mechanisms of biliary stone fragmentation using the Ho:YAG laser. IEEE Transactions on Biomedical Engineering. 1994, 41(3): 276-283.

万方数据

21 Chan KF, Vassar GJ, Pfefer TJ, et al. Holmium: YAG laser lithotripsy: a dominant photothermal ablative mechanism with chemical decomposition of urinary calculi. Lasers Surg Med, 1999, 25(4): 22-37.
22 Vassar GJ, Chan KF, Teichman JM, et al. Holmium: YAG lithotripsy: photothermal mechanism. J Endourol. 1999, 13(3): 181-90.
23 Teichman JM, Vassar GJ, Glickman RD, et al. Holmium: YAG lithotripsy: photothermal mechanism converts uric acid calculi to cyanide. J Urol, 1998, 160(2): 320-324.
24 Dushinski JW and Lingeman JE, High-speed photographic evaluation of holmium laser. J Endourology. 1998, 12(2): 177-181.
25 Zhong P, Tong HL, Malenhamm J, et al. Transient cavitation and acoustic emission produced by different laser lithotripters. J Endourology, 1998, 12(4): 371-378.
26 Cecchetti W, Zattoni F, Nigro F, et al. Plasma bubble formation induced by holmium laser an in vitro study. UROLOGY, 2004, 63(3): 586-590.
27 Lee H, Ryan RT, Kim J, et al. Dependence of Calculus Retropulsion Dynamics on Fiber Size and Radiant Exposure During Ho:YAG Lithotripsy. J. Biomech. Eng. 2004, 126(4): 506-515.
28 Lee H, Ryan RT, Teichman JM, et al. Stone retropulsion during Holmium:YAG lithotripsy. J Urol. 2003, 169(3): 881-885.
29 Finley DS, Petersen J, Abdelshehid C, et al. Effect of holmium: YAG laser pulse width on lithotripsy retropulsion in vitro. Journal of Endourology, 2005, 19(8): 1041-1044.
30 Kalra P, Le NB, Bagley D. Effect of pulse width on object movement in vitro using Holmium:YAG laser. J Endourol, 2007, 21(2): 228-231.
31 Kang HW, Lee H, Teichman JM, et al. Dependence of calculus retropulsion on pulse duration during Ho: YAG laser lithotripsy. Lasers Surg Med. 2006, 38(8): 762-772.
32 Margret CG, Sung JC, Springhart WP, et al. In vitro comparison of stone retropulsion and fragmentation of the frequency doubled, double pulse Nd:yag laser and the holmium: yag laser. J Urol., 2005, 173(5): 1797-1800.
33 Kuo RL, Aslan P, Zhong P, et al. Impact of holmium laser settings and fiber diameter on stone fragmentation and endoscope deflection. J Endourol. 1998, 12(6): 523-527.
34 Lee H, Robert TR, Joel MH, et al. Effect of Lithotripsy on Holmium: YAG Optical Beam Profile. J Endourol. 2003, 17(2): 63-67.
35 Vassar GJ, Teichman JM, Glickman RD. Holmium:YAG lithotripsy efficiency varies with energy density. J Urol. 1998, 160(2): 471-476.
36 Yoshida T, Fujimura K, Yamazaki T, et al. Experimental and clinical study of a holmium:YAG laser with adjustable pulse duration. Aktuelle Urol 2003, 34(4): 276-278.
37 Teichman JM, Vassar GJ, Glickman RD. Holmium:yttrium-aluminum-garnet lithotripsy efficiency varies with stone composition. Urology, 1998, 52(3): 392-397.

(收稿日期:2008-09-02)
(本文编辑:肖恒军)

崔杰, 肖灵. 钬激光碎石机制研究进展[J/CD]. 中华腔镜泌尿外科杂志: 电子版, 2008, 2(4): 358-362.

·读者·作者·编者·

本刊投稿注意事项

作者来稿必须附第一作者的单位介绍信,文稿宋体,五号字,1.5倍行距打印一式两份寄至编辑部,文稿的电子版(包括图片)存入光盘或发E-mail:chinaendourology@126.com,图片不需排版至word中,标示图的序号及名称,如(图1 右输尿管壁内段降起),同时在文章中对应位置注明图的序号。另外,请附上100字左右的第一作者简介,并注明联系方式,包括手机号码,办公室电话,E-mail,以便及时联系。

论文所涉及的课题如取得国家或部、省级以上基金或属攻关基金项目,应脚注于文题左下方,如"基金项目:xx基金资助(基金编号xxxx)",并附证书复印件。

请勿一稿多投!

本刊编辑部

万方数据

输尿管镜下钬激光碎石术后并发输尿管狭窄回顾性分析

刘为池[1]　刘刚[1]　唐锦护[1]　曾志玮[1]　廖松柏[1]　于洋[1]　武英杰[1]　于永刚[1]

[摘要] 目的：探讨输尿管镜下钬激光碎石术后输尿管狭窄的原因及其预防和处理。方法：回顾性分析我院 2009 年 1 月～2012 年 12 月期间对 635 例输尿管结石患者行输尿管镜钬激光碎石术的临床资料，总结输尿管镜碎石术后发生输尿管狭窄的特点及处理方法。结果：术后出现输尿管狭窄 26 例(4.09%)；其中输尿管完全闭锁 11 例(1.73%)。结论：钬激光碎石对输尿管有损伤作用，可导致输尿管狭窄，尤其对嵌顿性结石要注意操作技巧和术后正确的预防及随访。

[关键词] 输尿管镜；钬激光；输尿管狭窄；并发症；输尿管结石
doi：10.13201/j.issn.1001-1420.2014.07.004
[中图分类号] R693.4　[文献标识码] A

Retrospective analysis of ureteral stricture after ureteroscopic holmium: YAG laser lithotripsy

LIU Weichi　LIU Gang　TANG Jinhu　ZENG Zhiwei　LIAO Songbai
YU Yang　WU Yingjie　YU Yonggang
(Department of Urology, 181st Hospital of Chinese People's Liberation Army, Guilin, Guangxi, 541002, China)
Corresponding author: LIU Gang, E-mail: lgsuperapple@126.com

Abstract **Objective**: To study the causes and prevention of the ureteral stricture after ureteroscopic holmium: YAG laser lithotripsy. **Method**: From January 2009 to December 2012, 635 patients of ureteral stones underwent ureteroscopic lithotripsy using holmium: YAG laser in our hospital. The clinical data were retrospectively analysed. **Result**: There were 26 cases (4.09%) who suffered from ureteral stricture after holmium: YAG laser lithotripsy, including 11 cases (1.73%) of ureteral atresia. **Conclusion**: Holmium: YAG laser lithotripsy can do damage to ureter and induce ureteral stricture, especially in those patients with impacted stone. Thus, surgical techniques, postoperative prevention and follow-up plan should be paid attention to.

Key words ureteroscopy; holmium laser; ureteral stricture; complication; ureteral stone

输尿管狭窄常见于输尿管的炎症、结石、外伤以及医源性操作后，输尿管结石术后输尿管狭窄是常见的远期并发症[1]。无论是开放取石，还是经腔镜取石、内镜碎石术，发病率均报道不一，发生率为 3%～11%[2-4]，而且缺乏独立的大样本报告，大多作为术后并发症之一予以讨论，并且把输尿管穿孔、撕裂等损伤归为狭窄的主要原因。杨后猛等[5]也注意到钬激光对输尿管黏膜的损伤是引起输尿管狭窄的高危因素，事实上输尿管穿孔，撕裂等损伤发生率很低，经留置双 J 管或手术处理后极少有狭窄发生。我院于 2009 年 1 月～2012 年 12 月对 635 例输尿管结石患者行输尿管镜下钬激光碎石术，术后出现输尿管狭窄再次手术者 26 例，现将这些患者的临床特点及处理进行回顾性分析，现报告如下。

1　资料与方法

[1] 解放军第 181 医院泌尿外科(广西桂林，541002)
通信作者：刘刚，E-mail：lgsuperapple@126.com

1.1　临床资料

本组 635 例，男 368 例，女 267 例，年龄 16～72 岁，平均 40.2 岁。其中输尿管上段结石 226 例，中段 135 例，下段 274 例。全部患者均行 B 超、CT 确诊，结石大小 5～35 mm，平均 13.2 mm，均有不同程度积水；集合系统分离 10～80 mm，平均 25.3 mm。排除标准：既往曾行体外冲击波碎石术或输尿管手术者不纳入本组研究对象，术中无输尿管穿孔及撕裂者。

1.2　方法

应用钬激光碎石设备 HLM-1-30(合肥科瑞达公司)；Wolf $F_{8.5}$ 半硬性输尿管镜。连续硬膜外麻醉，膀胱截石位，直视下通过尿道置入输尿管镜，以斑马导丝或输尿管导管引导，液压灌注泵扩张输尿管管口(入镜后关水或严格控制进水量及速度，避免结石上移入肾盂)，缓慢向上进镜至结石下缘，部分输尿管上段结石较大、积水明显者行经皮输尿管镜微造瘘钬激光碎石术，插入钬激光光纤，功率设

中国知网 https://www.cnki.net

置为 1.0～1.5 J/15～20 Hz；用钬激光光纤抵住结石，结石粉碎至 3 mm 以下，合并息肉者行钬激光切除术，碎石后检查输尿管有无病变，常规留置 F_5 或 F_6 双 J 管，术后 2～4 周拔除。

2 结果

635 例患者术后发生输尿管狭窄而再次住院者 26 例(4.09%)，其中大部分于拔除双 J 管后 1～30 天出现患侧腰部胀痛，其他患者无临床症状，复查 B 超或 CT 检查未见结石梗阻，但积水恢复到术前大小，甚至加重，经逆行插管造影明确输尿管狭窄存在，其中输尿管闭锁者 11 例(1.73%)。狭窄部位上段 10 例(4.42%，10/226)，中段 3 例(2.22%，3/135)，下段 13 例(4.74%，13/274)，发生输尿管闭锁的患者结石平均大小 15.5 mm，梗阻侧肾积水平均 38.6 mm，呈嵌顿结石状，与梗阻部位无关。26 例患者中行输尿管钬激光肉切开 15 例，术后留置双 J 管 3～6 个月；11 例输尿管闭锁者行输尿管狭窄段切除端端吻合术 7 例，4 例输尿管下段闭锁行输尿管膀胱再植术；15 例钬激光肉切开患者，2 例因再次输尿管狭窄改开放手术，其中 1 例因肾功能严重受损行肾切除术。

3 讨论

自从我院应用钬激光碎石后，发现输尿管结石术后输尿管狭窄患者明显增多，尤其是输尿管完全闭锁的患者。除了新技术应用及相应的输尿管镜下碎石患者增多的样本因素外，我们认为钬激光碎石对输尿管有损伤作用。在结石长期存在，引起输尿管黏膜破坏的基础上，钬激光碎石加重输尿管损伤，此二者为输尿管结石激光碎石术后输尿管狭窄的主要原因。理论上，输尿管的损伤是输尿管狭窄的必要条件，损伤的程度与狭窄正相关，尤其是环状的输尿管黏膜的损伤，轻微的损伤对输尿管修复无明显影响，因此输尿管狭窄极少见于 1 mm 以下的结石患者。虽然理论上钬激光组织穿透深度不足 0.5 mm，一般不会导致穿孔，术后输尿管黏膜损伤轻微，很少会造成瘢痕致输尿管狭窄，但反复多次的重叠效果就难以估计。实际上，早期我们应用钬激光处理结石合并息肉的时候，就发现钬激光切除息肉导致输尿管黏膜明显苍白和输尿管的挛缩，在结石明显与输尿管粘连时，边缘结石碎石后输尿管黏膜广泛被破坏。后来，我们处理这种结石时，尽量从结石中间开始，边缘结石用输尿管钳夹离输尿管后再碎，输尿管息肉只在其根部烧灼一下，破坏其血供即可，避免反复凝切导致输尿管损伤。在改变处理方式后，术后输尿管狭窄比早期减少。腔内气压弹道碎石对输尿管没有热损伤，但存在着机械的物理损伤，理论上可减少术后输尿管狭窄，国内报告输尿管镜气压弹道碎石术后输尿管狭窄的发生率一般在 1%以下[3,4]。我们在排除输尿管穿孔、反复体外冲击波碎石等可能引起输尿管结石术后狭窄的可能因素的基础上，统计输尿管钬激光碎石术后狭窄发生率为 4.09%，尤其是术后输尿管闭锁的发生率明显多见(1.73%)，在拔除输尿管双 J 管后很快需再次处理，这在过去的气压弹道碎石术后极少见，也充分说明钬激光碎石对输尿管存在这不同程度的损伤，尤其在嵌顿结石的情况下。但是比较钬激光和气压弹道碎石术后狭窄的发生率还需要进一步的配对资料研究。

术后输尿管双 J 管的留置是预防输尿管术后狭窄的措施之一，常规我们留置 $F_{4.7}$ 双 J 管 2～4 周，在发现多例输尿管术后狭窄后，对术中存在输尿管损伤明显的患者延长至 8～12 周，对防止术后输尿管狭窄有一定作用。最长者在术后拔除双 J 管后出现输尿管狭窄的患者留置进口双 J 管半年，随访大部分未再狭窄，但也有 2 例仍再度狭窄而行开放狭窄段切除端端吻合术，提示输尿管黏膜损伤严重，甚至有肌层损伤可能，导致瘢痕的形成，输尿管黏膜无法再生。因此，对术中有明显输尿管黏膜损伤者，可适当延长双 J 管留置时间，由此带来的是给患者长期带管的不适，包括尿频、尿急、尿痛及肉眼血尿，以及可能潜在的感染，拔管后及时复查 B 超或静脉肾盂造影，如再度狭窄及时行狭窄段切除，并行相应吻合手术。

腔内微创碎石已成为输尿管结石的主要处理方式，开放手术理论上可以避免输尿管的环状损伤，其术后狭窄的主要原因与吻合技术相关，且多见相对狭窄。随着腹腔镜技术的发展，腹腔镜下输尿管切开取石术也在进行，但相对于腔内碎石而言，对大多数的输尿管结石，腹腔镜在医疗费用、手术时间及损伤程度，术后恢复、并发症及普及方面没有优势，但在较大的输尿管结石，存在着明显肾积水以及粘连的嵌顿结石，腹腔镜下取石或开放取石或许给我们更多合适的选择[5,6]。

综上所述，我们认为钬激光碎石可以导致输尿管的损伤，导致术后输尿管的狭窄，对结石较大、结石嵌顿时间较长、合并明显肾积水的患者在行钬激光碎石时或处理合并的息肉时，应尽量减少对输尿管的损伤，适当延长术后双 J 管留置时间，或者选择其他合适的取石方式。输尿管结石术后拔除双 J 管 1 个月内及时复查，早期发现输尿管狭窄并及时治疗。

[参考文献]

1 何云锋，吴小候，唐伟，等. 输尿管镜下钬激光治疗输尿管狭窄 73 例分析[J]. 重庆医学，2012，41(2)：133－134.

2 孟晓，屈国欣，王梅叶，等. 输尿管镜下钬激光治疗输尿管息肉(附 32 例报告)[J]. 中国内镜杂志，2007，13(3)：309－310.

(下转第 580 页)

中国知网 https://www.cnki.net

(上接第 574 页)

3 舒向晖，黄百生，邹建华，等. 输尿管镜下气压弹道碎石术并发症分析[J]. 现代泌尿外科杂志，2009，14(1)：47—49.

4 杨后猛，曾国华，邵法明，等. 输尿管镜碎石术常见并发症的处理和预防[J]. 临床泌尿外科杂志，2011，26(10)：747—749.

5 王大伟，鲁军，夏术阶，等. 输尿管镜钬激光碎石治疗肉芽包裹输尿管(附 358 例报告)[J]. 临床泌尿外科杂志，2008，23(2)：91—93.

6 王永传，夏术阶，孙晓文，等. 逆行输尿管镜手术常见并发症及防治策略[J]. 现代泌尿外科杂志，2011，16(1)：18—20.

7 毛峥，商庆兵，王婵，等. 三种腔镜技术治疗复杂性输尿管上段结石的疗效比较[J]. 临床泌尿外科杂志，2010，25(8)：595—598.

8 赵国防，杨春亭，杜冬岭，等. 三种不同微创手术方法治疗嵌顿性输尿管上段结石的疗效探讨[J]. 中华腔镜泌尿外科杂志(电子版)，2010，4(5)：44—47.

(收稿日期：2014-01-03)

中国知网 https://www.cnki.net

·论　著·

国产钬激光手术对兔肾热损伤的初步研究



龚春雨[1]，李黎[1]，屈锐[1]，杨罗[1]，冯洋阳[1]，邓旭卓[1]，罗小蓉[1]，杨静[2]

1. 四川大学华西第四医院外科（成都 610041）
2. 四川大学华西医院麻醉手术中心（成都 610041）

【摘要】 **目的**　探索用新西兰大白兔的新鲜离体肾脏和输尿管进行初步实验，观察国产钬激光热损伤的效果。**方法**　在手术室内（恒定温度 22℃，湿度 60%），选用国产钬 60 W 激光设备，将新西兰大白兔的新鲜离体肾脏放入已注入 50 mL 生理盐水的 50 mL 一次性使用无菌注射器内，同时将 550 μm 的钬激光光导纤维放入其中，用水银温度计测定生理盐水的温度；钬激光参数设定为频率 20 Hz，能量 2 J，激发 15 s，间歇 5 s，反复进行，分别在 2、5、7 min 测定生理盐水的温度，解剖并拍摄兔肾，进行病理学检查。**结果**　钬激光激发 2 min 时，注射器内生理盐水温度从 22℃ 升高到 38℃，兔肾皮质和髓质基本红润，病理检查提示肾皮质、髓质及输尿管均接近正常；5 min 时，注射器内生理盐水温度升至 57℃，兔肾皮质呈白色，皮质、髓质分界欠清，肾髓质色泽红润，病理检查提示皮质肾单位大部分坏死，髓质变性不明显，输尿管明显变性；7 min 时，注射器内生理盐水温度高达 78℃，肾皮质、髓质分界不清，均呈白色，皮质、髓质凝固，病理检查提示肾小球、肾小管均基本变性、坏死。**结论**　国产钬激光常用的碎石功率会产生渐增的热损伤，水温超过 50℃ 以后，将有可能对人体组织产生损伤。

【关键词】 钬激光；肾脏；输尿管；热损伤；兔

A primary research of the thermal damage of rabbit kidney by domestic holmium laser in surgery

GONG Chunyu[1], LI Li[1], QU Rui[1], YANG Luo[1], FENG Yangyang[1], DENG Huizhuo[1], LUO Xiaorong[1], YANG Jing[2]

1. Department of Surgery, No. 4 West China Teaching Hospital, Sichuan University, Chengdu, Sichuan 610041, P. R. China
2. Department of Anesthesiology, West China Hospital, Sichuan University, Chengdu, Sichuan 610041, P. R. China
Corresponding author: YANG Jing, Email: macrobun@163.com

【**Abstract**】 **Objective**　To observe the effect of thermal damage in the fresh isolated kidneys of New Zealand white rabbits caused by domestic holmium laser. **Methods**　In the operation room (constant temperature 22℃, humidity 60%), Guangdong electric (POTENT) domestic holmium laser equipment was chosen. The fresh isolated kidney of New Zealand white rabbit was put into a disposable sterilized syringe with 50 mL normal saline, then the holmium laser optical fiber (550 μm) was put into it, and the temperature of normal saline was measured by a mercury thermometer. The parameters of holmium laser were setted as frequency 20 Hz, energy 2 J, stimulating time 15 seconds, intermittent time 5 seconds, which was repeated. The temperature was measured 2, 5 and 7 minutes after stimulation. Then the kidney was dissected, phtographed, haematoxylin-eosin stained, and pathologically examined. **Results**　At the 2nd minute of stimulation, the temperature of normal saline in the syringe increased from 22℃ to 38℃; the cortex and medulla of rabbit kidney were ruddy, and the cortex, medulla and ureter were almost normal in pathological section. At the 5-minute point, the temperature increased to 57℃, and the cortex turned to be white, while the medulla remained ruddy, but the demarcation between the cortex and medulla was not very clear. At the 7th minute, the temperature was 78℃, and the cortex and medulla were both white and solidification with no clear demarcation. Pathological examination showed severe degeneration and necrosis of glomerulus and renal tubule. **Conclusion**　Common power of domestic holmium laser would produce increasing thermal damage, which may cause tissue damage in the human body when the temperature increases above 50℃.

【**Key words**】 Holmium laser; Kidney; Ureter; Thermal damage; Rabbit

DOI：10.7507/1002-0179.201601009
通信作者：杨静，Email：macrobun@163.com

(C)1994-2023 China Academic Journal Electronic Publishing House. All rights reserved.　http://www.cnki.net

钬激光是一种当代泌尿外科常用的激光，为脉冲式激光，工作介质为固定在钇铝石榴石晶体中的钬，波长为 2 100 nm，通过软/硬光导纤维（光纤）传送，在泌尿外科领域广泛应用，适合泌尿外科的结石、肿瘤等体腔内手术。钬激光具有以下特性：① 组织穿透度<0.5 mm，可用于精确的外科切割和止血；② 高能脉冲，常用于处理泌尿系统结石、前列腺切除、尿道或输尿管狭窄切开和膀胱肿瘤切除等。钬激光使用时约 95% 能量被周围 5 mm 的水介质吸收，方向性好，碎石效率高，是泌尿系统腔内手术理想的碎石工具，能够高效处理泌尿系统结石等[1-3]。但是随着钬激光在国内的普及，泌尿外科医生发现有些泌尿系统结石术后随诊患者出现了输尿管狭窄、粘连甚至管腔闭锁甚至肾功能受损[4]，需要后续治疗。其原因除与结石损伤、感染、手术操作等有关外，是否与术中钬激光的热效应有关？目前其相关研究较少，特别是缺乏国产钬激光设备的文献。为此，我们采用国产钬激光设备对成年新西兰大白兔的新鲜离体肾脏和输尿管进行了尝试性实验，探究钬激光手术时热效应导致的热损伤产生的不良反应。现报告如下。

1 材料与方法

1.1 材料

本研究在手术室内进行，室内恒定温度为 22℃，湿度为 60%，标准电源 220 V，频率 50 Hz。实验动物为 5 只健康新西兰大白兔，雌雄不限，年龄 6 个月，体质量 4 – 5 kg，由四川大学华西医学中心动物实验中心提供。采用广东普电自动化科技股份有限公司生产的钬激光治疗机（型号：POTENT-H2），最大输出功率 60 W，波长 2 100 nm，标准配置 550 μm 传导光纤。一次性使用无菌 BD 注射器，注射用生理盐水，实验室常用水银温度计。

1.2 方法

钬激光治疗机连接标准配置的 550 μm 钬激光光纤，钬激光功率参数设定为频率 20 Hz，能量 2 J 状态，保持待机。尖段光纤放入 50 mL 的一次性无菌 BD 注射器，固定在金属架上，注射器中为 50 mL 室温生理盐水；采用过量空气耳缘静脉注射处死新西兰大白兔后，立即采集肾脏并放入注射器中，保持密闭，钬激光激发 15 s，间歇 5 s，重复进行，分别在进行到 2、5、7 min 时用实验室常用的标准水银温度计在此 3 个时间点分别测定注射器内生理盐水的温度，每个时间点均取出大白兔肾脏，每个时间点重复 3 只兔，取 3 次温度的平均值。仔细观察并用普通数码相机拍摄完整兔肾脏和剖开后的肾皮质、髓质及输尿管，随后处理标本，用苏木精-伊红（hematoxylin and eosin，HE）染色，奥林巴斯显微镜不同放大倍数观察其病理切片，并拍摄分析。

2 结果

2.1 2 min 时钬激光热效应

钬激光激发 2 min 时，注射器内生理盐水温度从 22℃ 升高到 38℃。解剖兔肾脏，其皮质和髓质基本红润；病理检查提示肾脏皮质、髓质及输尿管均接近正常。见图 1。

2.2 5 min 时钬激光热效应

钬激光激发 5 min 时，注射器内生理盐水温度升至 57℃。解剖兔肾脏，其皮质部分有比较明显的变化，色泽泛白色，皮质、髓质分界欠清，肾脏的内层包括肾髓质色泽红润；病理检查提示皮质肾单位大部分坏死，髓质变性不明显，输尿管明显变性。见图 2。

2.3 7 min 钬激光热效应

钬激光激发 7 min 时，注射器内生理盐水温度高达 78℃。解剖兔肾，其内外层皮质、髓质分界不清，色泽几乎全部为白色，皮质、髓质凝固；病理检查提示肾小球、肾小管均基本变性、坏死。见图 3。

3 讨论

3.1 钬激光热效应的手术价值

钬激光属于多用途的一种临床治疗激光技术，在泌尿外科领域中应用广泛[5-6]，其优点主要包括凝固特性好、切割精确、能量易于被水介质吸收、穿透性弱、方向性好[7-8]。泌尿系统属于管道系统，针对碎石、切除、切开等操作可达到满意的效果，因此钬激光在内镜的配合下治疗泌尿外科疾病具有重要的临床价值[9]。

因为钬激光使用时约 95% 的能量被周围 5 mm 的水介质吸收，根据能量守恒原则，钬激光的能量假设完全转化成水的热能。根据比热容公式：$Q=cm\Delta t$，即 $Q=cm(t-t_1)$，其中 Q 为能量，c 为比热，m 为质量，t 为末温，t_1 为初温。而 Q=钬激光功率（W）×激发时间（s），由此可得：激发时间=$cm\Delta t$/钬激光功率。考虑到 95% 的能量被吸收的情况，水的比热在液态情况下是 4.2×10^3 J/（kg·℃），如钬激光功率为 40 W，可以算出理论上加热 10 mL 水每升高 1℃ 需要的时间为 $4.2\times10^3\times0.01/(40\times95\%)=1.11$ s，加热 50 mL 水每升高 1℃ 需要 $4.2\times10^3\times0.05/(40\times95\%)=5.53$ s[10]。考虑到实际手术

(C)1994-2023 China Academic Journal Electronic Publishing House. All rights reserved. http://www.cnki.net



图 1　钬激光激发 2 min 时兔肾脏彩色像　a. 肾脏完整，外观基本正常；b. 剖开观察肾脏皮质、髓质基本红润；c. 病理检查示肾皮质、肾小球基本正常（HE ×200）

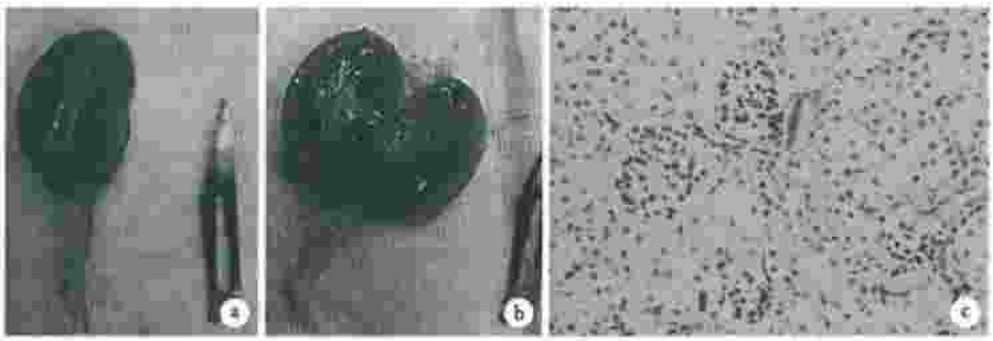


图 2　钬激光激发 5 min 时兔肾脏彩色像　a. 肾脏完整，颜色泛白；b. 剖开观察肾脏皮质、髓质分界欠清，髓质红润；c. 病理检查示皮质肾单位大部分坏死，髓质变性不明显，输尿管明显变性（HE ×400）

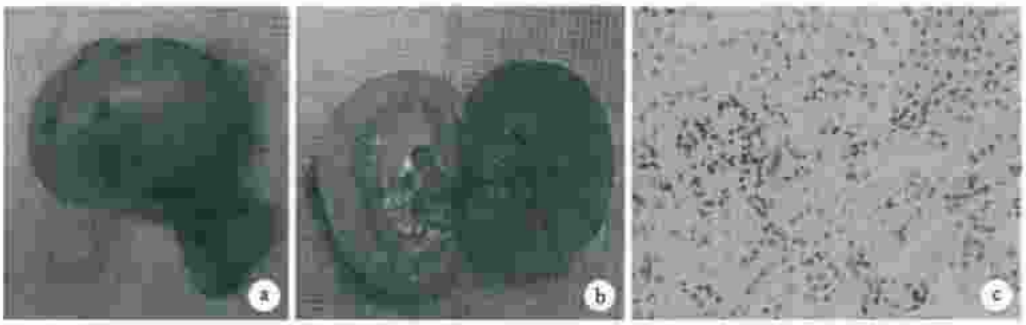


图 3　钬激光激发 7 min 时兔肾脏彩色像　a. 肾脏完整，颜色全部呈白色；b. 剖开观察肾脏皮质、髓质凝固；c. 病理检查示肾小球、肾小管均基本变性、坏死（HE ×400）

中钬激光激发环境是生理盐水混合尿液，其比热略大于水和操作过程中热量散失的具体情况后，其实和我们的实验数据结果是比较一致的[13-14]。

3.2　手术中钬激光的热损伤

泌尿系统如输尿管和肾盂内部体积一般不大，液体量有限（取决于积水程度），手术数量较多时，外科医生为快速碎石特别是上尿路结石、处理狭窄等，钬激光的功率常倾向调大[13-14]。我们前期的实验研究发现，因钬激光工作原理，常用的功率会产生明显的热效应，介质温度增高，手术室内，钬激光功率 40 W（频率 20 Hz，能量 2 J），激发 15 s，间歇 5 s，10 mL 生理盐水不到 1 min 水温将超过 50℃，可能对人体组织产生损伤作用；115 s 时水温会超过 70℃，产生的热效应会导致包括血管收缩在内的明显损伤组织[15]。钬激光常用的功率会产生热效应，随时间延长而明显增加，水温超过 50℃ 以后，可能对机体组织产生危害即损伤作用，对 50 mL 生理盐水中的兔肾、输尿管有明确损伤作用，特别是在 5、7 min 时水温分别增高至 57、78℃。况且，人体基础体温是 37℃，热量散失小于室温 22℃，提示钬激光用于肾盂和输尿管碎石术时，使用数分钟后，即可能产生积累的热损伤。而钬激光术后一些患者出现肾功能下降、泌尿管道狭窄，如输尿管狭窄、粘连甚至管腔闭锁，除结石引起的炎症和感染因素外，钬激光的热效应导致介质水温增加引起的人体组织损伤亦不可忽视[16]。

(C)1994-2017 China Academic Journal Electronic Publishing House. All rights reserved. http://www.cnki.net

必须承认，体外实验的钬激光介质水是静止的，实际手术时医生会持续灌注生理盐水，循环的介质可明显带走部分热量，以减少温度损伤；且根据术中情况，功率亦可调整，激发和间歇的时间也会不同。所以，体外钬激光对新鲜离体兔肾的热损伤实验并不能完全等同于人体内手术的实际情况，这有待临床医生实施钬激光碎石等手术时进一步明确。

因为工作原理，钬激光常用的碎石功率会产生渐增的热损伤，当肾盂和输尿管结石体积较大、质地较硬，预计碎石时间偏长时，应当引起临床医生注意；增加水循环，适当降低功率等是可以选择的方法。

参考文献

1 孙颖浩. 钬激光在泌尿外科中的应用. 中国现代手术学杂志, 2003, 7(5): 331-334.
2 罗建仕. 钬激光技术在泌尿系结石中的应用. 微创医学, 2006, 1(2): 115-117.
3 刘庆. 多用途钬激光: 泌尿外科的新技术. 医疗设备信息, 2005, 20(1): 27-28.
4 王坤杰, 李虹. 输尿管软镜联合钬激光在特殊上尿路结石治疗中的运用. 现代泌尿外科杂志, 2015, 20(11): 761-763.
5 顾锦江. 输尿管镜下钬激光治疗输尿管结石伴息肉疗效分析. 浙江临床医学, 2017, 19(2): 296-297.
6 俞宇宙, 胡明进, 朱琪翔, 等. 微创经皮肾镜钬激光碎石取石术在肾结石中的应用效果分析. 临床医药文献杂志, 2016, 3(43): 8565.
7 袁磊, 马永, 娄腾飞, 等. 改良方法在输尿管镜钬激光治疗输尿管结石中的应用. 淮海医药, 2016, 34(5): 545-546.
8 瞿甜全, 荀兴连, 杜龙. 输尿管钬激光碎石术和微创经皮肾镜碎石术治疗输尿管上段结石疗效观察. 陕西医学杂志, 2014, 43(4): 443-444.
9 张俊岩, 王德刚, 王文刚. 斜卧位经皮肾输尿管镜下钬激光碎石术治疗复杂性肾结石. 中国医药指南, 2017, 15(2): 153-154.
10 李良菊, 宋泉玉, 胡海燕. 经输尿管镜钬激光碎石日间手术的安全及质量评价. 海南医学, 2017, 28(1): 141-143.
11 崔增林, 张峰, 卞建强. 输尿管镜联合钬激光碎石治疗嵌顿性输尿管上段结石体会. 河南外科学杂志, 2016, 22(2): 112-113.
12 吕国强, 宋东奎, 郝凯. 输尿管镜钬激光碎石术治疗老年输尿管结石疗效及对肾功能的影响观察. 基层医学论坛, 2016, 20(35): 4950-4951.
13 罗魁德, 殷凡荣. 经输尿管钬激光碎石术治疗输尿管结石 100 例临床疗效. 世界最新医学文摘, 2106, 16(12): 199-120.
14 Grasso M, Fraiman M, Levine M. Ureteropyeloscopic diagnosis and treatment of upper urinary tract urothelial malignancies. Urology, 1999, 54(2): 240-246.
15 Ng EY, Tan HM, Ooi EH. Boundary element method with bioheat equation for skin burn injury. Burns, 2009, 35(7): 987-997.
16 龚云辉. 输尿管镜弹道与钬激光碎石治疗输尿管结石致肾功能衰竭的临床分析. 中国医药指南, 2016, 4(26): 194-195.

收稿日期：2016-11-30 修回日期：2017-04-19
本文编辑：张元芬

(C)1994-2023 China Academic Journal Electronic Publishing House. All rights reserved. http://www.cnki.net

· 临床研究 ·

输尿管结石行输尿管镜下碎石术后并发输尿管狭窄的危险因素分析

叶照华　米其武　罗杰鑫　李德君　陈祐君

【摘要】 目的　探讨输尿管镜下治疗输尿管结石术后并发输尿管狭窄的危险因素。方法　以 2014 年 1 月至 2015 年 12 月间来我院就诊的 708 例行输尿管镜下碎石的输尿管结石患者的临床资料为基础，分析造成术后输尿管狭窄的危险因素。结果　术后共发现输尿管狭窄患者 36 例 (5.1%)。导致输尿管狭窄发生的危险因素依次为：嵌顿结石 (OR=3.61, 95%CI=2.12~6.08, *P*<0.001)，多发结石 (OR=3.22, 95%CI=1.01~5.77, *P*<0.001)，大结石 (OR=2.41, 95%CI=1.14~4.18, *P*<0.001)、钬激光手术 (OR=1.36, 95%CI=1.02~3.93, *P*=0.031)，长病程 (OR=1.12, 95%CI=1.02~3.42, *P*=0.038)。结论　对于嵌钝性结石、多发结石、结石较大及行钬激光碎石者，应注意手术操作对输尿管的损伤，积极防治输尿管狭窄的发生。

【关键词】 输尿管镜；　输尿管结石；　输尿管狭窄；　危险因素；　多因素

Analysis of the risk factors of ureterostenosis after ureteroscopic lithotripsy in patients with ureteral calculi

Ye Zhaohua, Mi Qiwu, Luo Jiexin, Li Dejun, Chen Youjun. Department of Urology, Dongguan People's Hospital, Guangdong 523000, China

Corresponding author: Ye Zhaohua, Email: 66567664@qq.com

【Abstract】 Objective　To investigate the risk factors of ureteral stricture after ureteroscopic lithotripsy in patients with ureteral calculi. Methods　The risk factors of ureteral stricture after ureteroscopic lithotripsy based on the clinical data of 708 patients from January 2014 to December 2015 in our hospital were analyzed retrospectively. Results　A total of 36 patients (5.1%) with ureteral stricture were found. The risk factors for the ureteral stricture were: impacted calculi (OR=3.61, 95%CI=2.12~6.08, *P*<0.001), multiple calculi(OR=3.22, 95%CI=1.01~5.77, *P*<0.001), big stone(OR=2.41, 95%CI=1.14~4.18, *P*<0.001), holmium laser lithotripsy (OR=1.36, 95% CI=1.02~3.93, *P*=0.031), long course of disease (OR=1.12,95% CI=1.02~3.42, *P*=0.038). Conclusion　For patients with impacted calculi, multiple stones, large stones and patients who were treated with holmium laser lithotripsy, we should be careful not to injury the ureter, and actively prevent and control the occurrence of ureteral stenosis

【Key words】 Ureteroscope;　Ureteral calculi;　Ureteral stricture;　Risk factors;　Multiple factors

输尿管结石是常见的泌尿系统结石，以往传统的外科手术取石，患者创伤大、并发症发生率高。近年来随着输尿管镜技术的发展，使得输尿管结石、肿瘤等疾病的诊断和治疗都产生了质的飞跃[1]。然而由于输尿管镜的侵入操作所造成的输尿管的损伤的比例也在增大，文献报道其发生率为 2%左右[2]。输尿管的损伤可直接引起损伤性的输尿管狭窄[3]，后者进一步发展可引发肾积水及肾功能减退甚至肾脏萎缩。本研究以 708 例接受输尿管镜下碎石治疗的输尿管结石患者为研究对象，分析了造成患者术后发生输尿管狭窄的危险因素，现报道如下。

DOI: 10.3877/cma.j.issn.1674-3253.2017.01.011

作者单位：523000 广东，东莞市人民医院泌尿外科

通讯作者：叶照华，Email：66567664@qq.com

(C)1994-2023 China Academic Journal Electronic Publishing House. All rights reserved.　http://www.cnki.net

资料和方法

一、临床资料

708例输尿管结石均经超声，平片、静脉尿路造影等检查确诊。其中男405例，女303例，年龄18~70岁，平均年龄(43±13)岁，上段结石98例，中段结石283例，下段结石327例，结石大小0.4 cm×0.5 cm~1.5 cm×2.4 cm，患者病程3 d~7年，平均病程(7±3)个月。584例接受钬激光碎石治疗，124例接受气压弹道碎石。

二、治疗方法

患者均采用硬膜外麻醉，在输尿管镜的引导下完成碎石、取石操作。钬激光组使用光纤传导激光能量，从结石中央向周边以"虫噬"法将结石粉碎至2 mm以下。如结石下方合并有息肉或者狭窄等，则先切除息肉或狭窄环。对于嵌顿性结石，则先切开包裹组织，再进行碎石。气压弹道组则用冲击针在连续脉冲或者单个脉冲下，将结石粉碎至2 mm以下，结石可随尿液自行排除，较大结石用结石钳取出。结石周边息肉也可同时钳取。患者术后置留双J管2~4周，如果术中存在输尿管损伤，则延长至8~12周。

三、纳入和排除标准

纳入标准：患者均为首次接受输尿管镜下碎石治疗，具有完整的临床随访资料，年龄在18~70岁；排除标准：患者有输尿管手术史或者碎石前已经合并有输尿管狭窄者，合并严重的内外科疾病或者肿瘤者。

四、统计学处理

用SPSS16.0进行统计分析，先采用卡方检验或秩和检验行单因素分析，再用Logistic回归进行多因素分析，P<0.05表示差异有统计学意义。

结　果

一、输尿管狭窄情况：术后共发现输尿管狭窄患者36例，发生率为5.1%，患者表现为拔除双J管1个月内出现病变部位的腰部胀痛，相关影像学检查未发现明确的结石梗阻，但可见明显加重的肾积水，经逆行插管造影可见存在输尿管狭窄。其中输尿管上段狭窄17例，中段狭窄11例，下段狭窄8例。

二、单因素分析结果：单因素统计分析发现病程超过3个月、大结石、多发结石、嵌顿结石、使用钬激光碎石可增加输尿管结石术后输尿管狭窄的发生率(表1)。

三、多因素统计分析：通过多因素统计分析发现导致输尿管狭窄发生的危险因素依次为：嵌顿结石(OR=3.61，95% CI=2.12~6.08，P<0.001)、多发结石(OR=3.22，95% CI=1.01~5.77，P<0.001)、大结石(OR=2.41，95%CI=1.14~4.18，P<0.001)、钬激光手术(OR=1.36，95%CI=1.02~3.93，P=0.031)、长病程(OR=1.12，95% CI=1.02~3.42，P=0.038)(表2)。

表1　708例患者不同影响因素的输尿管狭窄发生情况分析(例)

因素	例数	性别		年龄		病程		结石长径			结石部位		
		男	女	<50岁	≥50岁	<3月	≥3月	<1 cm	1~2 cm	>2 cm	上部	中部	下部
狭窄	36	21	15	20	16	12	24	12	8	16	5	16	15
无狭窄	672	384	288	357	315	426	246	462	153	57	82	297	293
χ^2值		0.020		0.081		13.087		−5.328			0.109		
P值		0.888		0.776		<0.001		<0.001			0.947		

因素	多发结石		合并息肉		嵌顿结石		治疗方式		置留双J管时间	
	是	否	是	否	是	否	钬激光	气压弹道	≤4周	>4周
狭窄	13	23	10	26	28	8	30	6	16	20
无狭窄	115	557	147	525	228	444	395	277	366	306
χ^2值	8.327		0.690		24.655		8.585		1.381	
P值	0.004		0.406		<0.001		0.003		0.240	

表2　输尿管狭窄多因素分析结果

因素	嵌顿结石	多发结石	大结石	钬激光手术	长病程
β值	1.30	1.169	0.880	0.307	0.113
OR	3.61	3.22	2.41	1.36	1.12
95%CI	2.12~6.08	1.01~5.77	1.14~4.18	1.02~3.93	1.02~3.42
Wald χ^2值	11.43	8.24	9.34	5.15	5.02
P值	<0.001	<0.001	<0.001	0.031	0.038

(C)1994-2023 China Academic Journal Electronic Publishing House. All rights reserved. http://www.cnki.net

讨　论

输尿管结石碎石术是常见的引起输尿管狭窄的原因之一，无论是内镜取石、开放取石、腹腔镜取石均有一定的概率发生术后输尿管狭窄，不同文献报道的发生率略有差异，在3%~10%之间[1-7]。本研究中输尿管狭窄发生率为5.1%，与相关文献的报道类似。

嵌顿结石具有病理类型及局部解剖的特殊性，由于嵌顿所致的输尿管水肿，使得安全导丝极易穿破输尿管黏膜进而引起黏膜的损伤，导致出血、感染及瘢痕的产生，因而嵌顿结石患者更容易发生输尿管狭窄[8]。温海东等[9]研究发现，输尿管镜碎石术中，输尿管黏膜损伤、输尿管穿孔为造成术后狭窄的主要危险因素。因而对于嵌顿结石，应自结石的中间开始碎石，周边与输尿管黏膜相接触的部分应夹离输尿管后，再行碎石。同时，在实际工作中我们发现，如果结石过大、过多、结石滞留时间过长，可刺激输尿管黏膜发生明显的炎性反应，进而出现黏膜增生、水肿和息肉的形成，甚至可以发生黏膜下结石；或者由于同时伴有纤维组织的增生修复，使得患有结石的同时伴有输尿管狭窄。为了消除混杂因素的影响，本研究剔除了这部分术前就伴有纤维组织增生而致输尿管狭窄的病例。通过多因素分析发现，除了嵌顿结石外，多发结石、结石较大及长病程均为造成患者术后发生输尿管狭窄的危险因素。可能原因除了结石刺激导致的炎性增生外，结石多、大、病程长往往存在不同程度的输尿管梗阻及肾积水或者肾积脓；这也一定程度增加了碎石术的复杂性，增加了输尿管损伤的发生概率。

输尿管镜下气压弹道碎石与钬激光碎石是两种原理不同的碎石方式，前者通过机械力将结石击碎而后者是通过激光的热能使得水分汽化膨胀冲击结石而碎石。由于钬激光的局部高热，可造成输尿管黏膜的局部热损伤，使用钬激光处理黏膜息肉时，如果处理不当，可造成明显的输尿管黏膜苍白或者输尿管挛缩；击碎结石边缘后，可见被广泛破坏的输尿管黏膜[4]。使用钬激光碎石造成输尿管损伤的原因除了与初学者经验、技术不丰富有关外，未充分暴露视野，强行进、退镜也是其中的原因[10,11]。

碎石术后双J管的置入，可提高患者结石的排净率及肾绞痛的发生率[9]。对于术中发现输尿管损伤的患者，延长双J管的置留时间可以降低术后输尿管狭窄的发生[4]。本研究未发现延长双J管置留时间为输尿管狭窄的保护因素，相反，置留时间超过4周者，输尿管狭窄的发生率略高。这可能与延长双J管置留时间者多存在输尿管损伤有关。另外相关的研究发现，延长双J管的置留时间能显著增加患者的并发症的发生率[12]。

参 考 文 献

[1] Baldie K, Angell J, Ogan K, et al. Robotic management of benign mid and distal ureteral strictures and comparison with laparoscopic approaches at a single institution [J]. Urology, 2012, 80(3): 596-601.

[2] Han PK, Rohan M, Mohd Adam B. The short-term outcome of laser endoureterotomy for ureteric stricture [J]. Med J Malaysia, 2013, 68(3): 222-226.

[3] Harraz AM, Shoma AM, Shokeir AA. Ureteroscopy for Ureteral Strictures[M]. Springer London, 2013: 235-244.

[4] 刘为池, 刘刚, 唐锦护, 等. 输尿管镜下钬激光碎石术后并发输尿管狭窄回顾性分析 [J]. 临床泌尿外科杂志, 2014, 29(7): 573-575.

[5] Gu SP, Zeng GH, You ZY, et al. Types of renal calculi and management regimen for Chinese minimally invasive percutaneous nephrolithotomy [J]. Indian J Surg, 2015, 77(Suppl 3): 872-876.

[6] 刘亚东, 田河, 安瑞华. 经尿道输尿管镜气压弹道碎石治疗单发输尿管结石后发生输尿管狭窄的危险因素分析[J]. 现代泌尿外科杂志, 2016, 21(4): 252-255.

[7] 高永涛, 王岩. 输尿管结石行体外冲击波碎石治疗后发生输尿管狭窄的危险因素分析 [J]. 现代泌尿外科杂志, 2014, 19(6): 384-386.

[8] 杨亮. 钬激光碎石术治疗输尿管结石后发生输尿管狭窄的危险因素分析[J]. 临床和实验医学杂志, 2015, 14(14): 1210-1212.

[9] 温海东, 陈结能, 廖昊, 等. 输尿管镜下钬激光治疗输尿管嵌顿性结石引起输尿管狭窄的相关因素分析 [J]. 临床泌尿外科杂志, 2016, 31(2): 127-130.

[10] Razzaghi MR, Razi A, Mazloomfard MM, et al. Safety and efficacy of pneumatic lithotripters versus Holmium laser in management of ureteral calculi: a randomized clinical trial[J]. Urol J, 2013, 10(1): 762-766.

[11] 覃斌, 黄向华, 李长赞, 等. 输尿管镜下钬激光碎石与气压弹道碎石术治疗输尿管结石的疗效比较 [J]. 中华腔镜泌尿外科杂志(电子版), 2012, 6(1): 38-41.

[12] 夏朝晖. 输尿管镜钬激光碎石术后留置双J管并发症危险因素分析[J]. 医学综述, 2014, 20(24): 4566-4567.

(收稿日期: 2016-05-23)
(本文编辑: 阮星星 李文标)

叶照华, 米其武, 罗杰鑫, 等. 输尿管结石行输尿管镜下碎石术后并发输尿管狭窄的危险因素分析[J/CD]. 中华腔镜泌尿外科杂志: 电子版, 2017, 11(1): 46-48.

(C)1994-2023 China Academic Journal Electronic Publishing House. All rights reserved. http://www.cnki.net

·综述·

泌尿系结石钬激光碎石热效应研究进展

刘凡[1] 原小斌[2] 张敏[2] 王东文[1,2] 曹晓明[2] 综述 张旭辉 审校

[1]山西医科大学第一临床医学院，太原 030001；[2]山西医科大学第一医院泌尿外科，太原 030001

通信作者：张旭辉，Email：zhangxuhui7576@sina.com

【摘要】 钬激光碎石术以其碎石效果可靠、对组织损伤较小的优势而被广泛应用于泌尿系结石的微创治疗。但输尿管结石钬激光碎石术后常合并输尿管狭窄、粘连等并发症，其原因除输尿管黏膜局部病变、合并感染之外，一定程度上与钬激光的热效应有关。钬激光热效应的常见影响因素包括：钬激光脉冲能量和频率、脉宽模式、光纤直径、灌注速度、灌注液的温度、碎石模式等，现就钬激光碎石术热效应的研究进展作一综述。

【关键词】 尿路结石；碎石术，激光；激光，固体；钬

DOI：10.3760/cma.j.issn.1673-4416.2019.02.049

泌尿系结石是我国常见的泌尿外科疾病[1]。泌尿系结石的治疗除传统的切开取石外，还有体外冲击波碎石术（extracorporeal shock wave lithotripsy，ESWL）、钬激光碎石术（holmium laser lithotripsy，HLL）、超声碎石术（ultrasound lithotripsy，USL）、气压弹道碎石术（pneumatic lithotripsy，PL）等。钬激光碎石术因其可观的临床碎石效率以及可与经皮肾镜、输尿管硬镜、输尿管软镜等设备配合使用等突出优势，在泌尿系结石腔内治疗中得以广泛应用[2]。

1 钬激光的特点

钬激光具有以下特点：① 高能脉冲式激光，可以击碎各种成分的泌尿系结石；② 对结石冲击力小，可以有效减少碎石过程中的结石后移效应；③ 组织穿透深度较浅，不易引起输尿管或膀胱穿孔[3]。钬激光吸收峰与水接近，其释放的能量95%可被周围水介质吸收[4]，进而转化为水分子的热能，使周围环境中的水温升高，对周围组织产生明显的热效应。

2 钬激光的碎石机制及热效应原理

目前认为钬激光碎石机制主要有光热机制（photothermal decomposition）和光机械机制（photomechanical mechanisms）[4-5]；Sperrin 等[6]研究测量了光纤尖端不同距离处的冲击波压力，当脉冲能量为 2 J 时，在光纤尖端 4 mm 处的压力为 510 MPa，该压力水平足以击碎结石。光热机制是指钬激光光纤尖端的水介质吸收能量后温度升高发生汽化形成微气泡，大量微气泡形成传递激光能量的汽化通道，结石吸收激光能量后温度急速升高，高温使结石发生热分解，最终消融结石[5]。这种由微气泡形成的汽化通道被称之为"摩西效应"[7]。Chan 等[8]利用高速摄像设备拍摄钬激光碎石的过程发现在激光作用于结石约 50 us 时，结石表面便出现碎裂迹象，而此时微气泡尚未形成，因此并没有冲击波产生。同时他们研究发现当光纤与结石表面平行时，结石表面受到的冲击波压力最强，但此时却没有结石碎裂。Cecchetti 等[9]研究发现在能量设置为 1.5 J 时，光纤尖端 2 mm 处的温度为 750℃，当频率升高为 30 Hz 时，温度达到 1400℃以上，它们认为这些微气泡其实便是等离子气泡，只有等离子气泡破碎产生的热效应才能达到如此高温。这些均是光热机制的有力证据。Finley 等[10]认为钬激光的碎石机制与钬激光的能量和脉宽呈正相关，脉宽越长，光热机制作用就越明显，钬激光脉宽相对较长，因此，光热机制在钬激光碎石过程中发挥主要作用，而光机械机制则起到冲散结石碎片的作用。

3 钬激光热效应对细胞的影响

Bettaieb 等[11]研究显示 43℃可引起细胞钙稳态的破坏，细胞导致蛋白质变性，在此环境中 120 min 会导致细胞死亡。Molina 等[12]研究证明时间和温度对细胞损伤具有共同作用，温度每升高 1℃，造成相同细胞损伤所需的时间便减少一半，当温度达到 56℃时，细胞在 1 s 内即可死亡。钬激光碎石时能量密度相对较高，灌注液和周围组织的温度迅速升高[13]，Wollin 等[14]在体外使用 200 μm 的光纤，分别测量 0.2 J×50 Hz、0.6 J×6 Hz、0.8 J×8 Hz、1.0 J×10 Hz、1.0 J×20 Hz 等五组能量设置组合在无灌注条件下 60 s 内的温度变化，发现五组的最高温度均超过 43℃，0.8 J×8 Hz、1.0 J×10 Hz 组的最高温度超过 60℃，1.0 J×20 Hz 组的最高温度甚至超过 100℃，由此可见钬激光热效应所致的高温远超细胞所能承受的极限温度，无疑会对细胞造成严重影响。

4 钬激光热效应与输尿管狭窄

临床研究发现钬激光碎石术后常出现输尿管狭窄、闭锁等并发症[15]，输尿管狭窄的主要原因有：①合并感染；②结石长期炎症刺激引起的输尿管局部黏膜病变；③碎石过程中因操作视野不清导致的管壁组织直接损伤；④由于结石完全梗阻，镜端水流不畅，长时间钬激光碎石，局部易致高温，对

输尿管黏膜、肌层甚至浆膜层造成热灼伤，损伤局部呈凝固样坏死，组织修复后形成病理性瘢痕组织，最终导致输尿管狭窄甚至闭锁[35-37]。由此可见，钬激光的热效应是引起输尿管狭窄的重要因素，然而，钬激光热效应的高低尚与诸多因素相关。

5 钬激光热效应的影响因素

钬激光热效应的影响因素包括：脉冲能量和频率、脉宽模式、光纤直径、灌注速度、灌注液温度以及碎石模式等。

5.1 脉冲能量和频率对钬激光热效应的影响

Aldoukhi 等[18]用热电偶测量了0.5 J×10 Hz、1.0 J×10 Hz、1.0 J×20 Hz、1.0 J×40 Hz 等4组能量设置组合在无灌注时钬激光连续激发60 s内的温度变化。结果显示4组的最高温度分别为45.2℃、50.1℃、55.6℃、70.3℃，0.5 J×10 Hz与1.0 J×10 Hz组数据表明脉冲频率不变时，钬激光的热效应随着脉冲能量增加呈现增强趋势；1.0 J×10 Hz、1.0 J×20 Hz、1.0 J×40 Hz 等三组数据表明脉冲能量不变时，钬激光热效应随脉冲频率增加呈现增强趋势。Wollin 等[14]监测了0.2 J×50 Hz组与1.0 J×10 Hz组在无灌注时钬激光连续激发60 s内的温度变化，发现1.0 J×10 Hz组的灌注液温度明显高于0.2 J×50 Hz组。可见，脉冲能量对钬激光的热效应影响更明显。Kallidonis 等[19]通过体外实验测量了在灌注开放时钬激光功率为5 W、10 W、20 W 时灌注液的温度，发现随着功率增大，灌注液的温度也随着升高。

5.2 脉宽模式对钬激光热效应的影响

随着碎石设备的发展，最新的钬激光能量平台可以选择不同的脉宽进行碎石。Yoshida 等[20]研究了不同脉宽对钬激光热效应的影响，与初始温度相比，150 us、300 us、450 us、600 us、800 us 组灌注液温度分别升高了1.2℃、1.3℃、1.4℃、1.9℃、2.4℃，这说明在钬激光脉冲能量、频率等一致的情况下，增加脉宽会使钬激光热效应增加。钬激光释放热量所需要的时间约为100 us，而钬激光的脉冲宽度为150－1000 us，脉宽越长，脉冲持续时间内释放的热量就越多，钬激光的热效应就越显著[10,21]。

5.3 光纤直径与灌注速度对钬激光热效应的影响

Buttice 等[22]研究表明在无灌注时，272 μm 光纤比200 μm 光纤热效应更明显，能量组合为0.5 J×20 Hz时，两组的最高温度均超过45℃，但272 μm 光纤比200 μm 光纤温度升高更快。而当灌注开放时，两种直径的光纤对灌注液温度影响无明显差异。可见在无灌注时，减小光纤直径可以降低钬激光的热效应。Wollin 等[14]测量了0.2 J×50 Hz、0.6 J×6 Hz、0.8 J×8 Hz、1.0 J×10 Hz、1.0 J×20 Hz 组在灌注速度为0、50、100 mL/min时钬激光连续激发60 s内的温度变化，发现灌注速度为0 mL/min时，五组最高温度均超过43℃，灌注速度为50 mL/min时，仅有1 J×20 Hz组的最高温度超过43℃，当灌注速度为100 mL/min时，五组的最高温度均未超过43℃。可见，增加灌注速度，可以降低钬激光的热效应。随着钬激光使用功率不断增大，充足顺畅的腔内灌注是降低钬激光热效应的有效措施，灌注不足时，即便功率很低也会对周围组织产生明显热效应。输尿管软镜碎石时，灌注液和钬激光光纤使用共同的通道，根据泊肃叶定律，灌注流量与灌注通道半径的四次方成正比，因此，光纤直径的轻微改变即可引起灌注流量的巨大变化。有研究表明使用大直径的钬激光光纤，会降低软镜的灌注流量，使灌注液的温度升高，对周围组织产生明显热效应，同时会降低软镜的弯曲度及手术视野的清晰度，增加手术时间[23-24]。

5.4 灌注液温度对钬激光热效应影响

由于常温生理盐水可能会引起术后低体温、寒战、低氧血症等不良反应，因此在腔镜手术中常使用36.5℃生理盐水作为灌注液[25]。而在钬激光碎石术中，为了降低钬激光的热效应，常选择常温生理盐水作为灌注液。Buttice 等[22]对比研究20℃和36.5℃生理盐水作为灌注液的安全性，结果显示在无灌注时，二者最高温度均超到45℃，36.5℃的灌注液组用时更短，温度升高更快；而在灌注开放时，二者温度均未超过45℃。研究表明在无灌注时，钬激光在不同温度的灌注液中均会产生明显的热效应，灌注液的温度越高则钬激光热效应越明显；而在灌注开放时，使用20℃和36.5℃的生理盐水作为灌注液均是安全的，同时36.5℃灌注液可以减少术后低体温等不良反应。

5.5 碎石模式对钬激光热效应的影响

目前，钬激光热效应研究多为体外试验，这些试验均是在钬激光空激发的条件下测量温度，并未对比研究结石在腔内碎石模式下对于钬激光热效应的影响。钬激光碎石时，钬激光的能量转化为灌注液的热能和碎石的动能。因此，在碎石条件下，结石吸收了部分钬激光的能量，这有助于降低钬激光热效应[21]。此外，持续碎石模式模式和间断碎石模式也会影响钬激光的热效应。Aldoukhi 等[18]测量了在灌注速度为14－15 mL/min时，0.5 J×10 Hz、1.0 J×10 Hz、0.5 J×20 Hz、1.0 J×20 Hz、0.5 J×40 Hz、1.0 J×40 Hz、0.5 J×80 Hz 等能量设置组合在钬激光持续激发60 s及停止之后20 s内灌注液的温度变化，发现灌注液温度在钬激光激发前20 s内快速升高，之后达到平台期，在钬激光停止工作后5 s内灌注液温度快速下降，10 s时温度基本恢复至正常温度，因此钬激光持续激发时间少于20 s、间歇时间长于5 s，有助于降低钬激光的热效应。钬激光碎石中不可避免的一个问题是结石的后移效应，结石后移时，寻找结石、光纤尖端与结石的重新接触等均会使钬激光短暂停止工作，这些也有助于降低钬激光的热效应。输尿管本身的弹性扩张、血管分布、血液流动、尿液的连续产生等均可能对钬激光热效应产生影响[23]。此外，光纤尖端的保护涂层、光纤的修剪方式、弯曲程度等也可能会影响钬激光的热效应。

6 小结

综上所述，钬激光热效应受钬激光脉冲能量和频率、脉宽模式、灌注速率、灌注液温度、光纤直径以及碎石模式等诸多因素的影响：增加脉冲能量和频率可以使钬激光的热效应

明显增强，增加灌注速度可以降低钬激光热效应，但应避免肾内压过高；减少脉宽可以降低钬激光热效应；在无灌注时，小直径光纤可以降低钬激光的热效应，但可能会增加光纤的损耗；在灌注开放的条件下，36.5℃的灌注液可能是安全的，同时可以减少术后低体温等并发症；间断的碎石模式及结石对能量的吸收也有助于降低钬激光的热效应。目前，钬激光热效应研究尚缺乏多因素的系统体外试验以及在体动物实验，尚需要进一步研究。

利益冲突 所有作者均声明不存在利益冲突

参 考 文 献

[1] 那彦群，叶章群，孙光. 中国泌尿外科疾病诊疗指南：2014 版[M]. 北京：人民卫生出版社，2013.

[2] 孙颖浩，高小峰. 钬激光在泌尿外科中的应用[J]. 医学研究杂志，2010，39(8)：2－5. DOI：10.3969/j.issn.1673－548X.2010.08.002.

[3] Patel AP, Knudsen BE. Optimizing use of the holmium:YAG laser for surgical management of urinary lithiasis[J]. Curr Urol Rep, 2014, 15(4): 397. DOI: 10.1007/s11934－014－0397－2.

[4] 崔杰，肖灵. 钬激光碎石机制研究进展[J]. 中华腔镜泌尿外科杂志(电子版)，2008，2(4)：59－63. DOI：10.3969/j.issn.1674－3253.2008.04.019.

[5] Welch AJ, Kang HW, Lee H, et al. Calculus fragmentation in laser lithotripsy[J]. Minerva Urol Nefrol, 2004, 56(1): 49－63.

[6] Sperrin M, Rogers K. Determination of the shock wave intensity from a laser lithotriptor using a bi－laminar hydrophone[J]. IEE Colloquium Innovative Pressure, Force and Flow Measurement, 1999. DOI: 10.1049/ic:19990493.

[7] Jacques SL. Laser－tissue interactions. Photochemical, photothermal, and photomechanical[J]. Surg Clin North Am, 1992, 72(3): 531－558.

[8] Chan KF, Vassar GJ, Pfefer TJ, et al. Holmium:YAG laser lithotripsy: A dominant photothermal ablative mechanism with chemical decomposition of urinary calculi[J]. Lasers Surg Med, 1999, 25(1): 22－37.

[9] Grocchetti W, Zattoni F, Nigro F, et al. Plasma bubble formation induced by holmium laser: an in vitro study[J]. Urology, 2004, 63(3): 586－590. DOI: 10.1016/j.urology.2003.09.010.

[10] Finley DS, Petersen J, Abdelshehid C, et al. Effect of holmium: YAG laser pulse width on lithotripsy retropulsion in vitro[J]. J Endourol, 2005, 19(8): 1041－1044. DOI: 10.1089/end.2005.19.1041.

[11] Benaich A, Averill－Bates DA. Thermotolerance induced at a mild temperature of 40°C alleviates heat shock－induced ER stress and apoptosis in HeLa cells[J]. Biochim Biophys Acta, 2015, 1853(1): 52－62. DOI: 10.1016/j.bbamcr.2014.09.016.

[12] Molina WR, Silva IN, Donalisio dSR, et al. Influence of saline on temperature profile of laser lithotripsy activation[J]. J Endourol, 2015, 29(2): 235－239. DOI: 10.1089/end.2014.0305.

[13] Hermann TR, Liatsikos EN, Nagele U, et al. EAU guidelines on laser technologies[J]. Eur Urol, 2012, 61(4): 783－795. DOI: 10.1016/j.eururo.2012.01.010.

[14] Wollin DA, Carlos EC, Tom WR, et al. Effect of Laser Settings and Irrigation Rates on Ureteral Temperature During Holmium Laser Lithotripsy, an In Vitro Model[J]. J Endourol, 2018, 32(1): 59－63. DOI: 10.1089/end.2017.0658.

[15] 刘为池，刘翔，唐锦护，等. 输尿管镜下钬激光碎石术后并发输尿管狭窄回顾性分析[J]. 临床泌尿外科杂志，2014，7)：573－574. DOI：10.13201/j.issn.1001－1420.2014.07.004.

[16] Wang CJ, Kang DB, Shen BH, et al. Ureteral obstruction and urinary fistula due to fibrin glue after partial nephrectomy: A case report and review of the literature[J]. Oncol Lett, 2013, 5(3): 825－828. DOI: 10.3892/ol.2013.1114.

[17] 张波，王朝晖，陈志，等. 双镜种联合治疗输尿管镜钬激光碎石术引起的输尿管狭窄的疗效分析[J]. 中华泌尿外科杂志，2017，38(10)：778－781. DOI：10.3760/cma.j.issn.1000－6702.2017.10.014.

[18] Aldoukhi AH, Ghani KR, Hall TL, et al. Thermal Response to High－Power Holmium Laser Lithotripsy[J]. J Endourol, 2017, 31(12): 1308－1312. DOI: 10.1089/end.2017.0679.

[19] Kallidonis P, Annatides L, Panagopoulos V, et al. Does the Heat Generation by the Thulium:Yttrium Aluminum Garnet Laser in the Irrigation Fluid Allow Its Use on the Upper Urinary Tract An Experimental Study[J]. J Endourol, 2016, 30(4): 422－427. DOI: 10.1089/end.2015.0252.

[20] Yoshida T, Fujimura K, Yamazaki T, et al. Experimental and clinical study of a holmium: YAG laser with adjustable pulse duration[J]. Aktuelle Urol, 2003, 34(4): 276－278. DOI: 10.1055/s－2003－41617.

[21] Teichmann HO, Herrmann TR, Bach T. Technical aspects of lasers in urology[J]. World J Urol, 2007, 25(3): 221－225. DOI: 10.1007/s00345－007－0184－5.

[22] Buttice S, Sener TE, Proietti S, et al. Temperature Changes Inside the Kidney: What Happens During Holmium: Yttrium－Aluminium－Garnet Laser Usage?[J]. J Endourol, 2016, 30(5): 574－579. DOI: 10.1089/end.2015.0747.

[23] Bach T, Geavlete B, Herrmann TR, et al. Working tools in flexible ureterorenoscopy－－influence on flow and deflection: what does matter?[J]. J Endourol, 2008, 22(8): 1639－1643. DOI: 10.1089/end.2008.0184.

[24] Baghdadi M, Emilhani E, Talso M, et al. Comparison of laser fiber passage in ureteroscopic maximum deflection and their influence on deflection and irrigation: Do we really need the ball tip concept[J]. World J Urol, 2017, 35(2): 313－318. DOI: 10.1007/s00345－016－1873－8.

[25] Singh R, Asthana V, Sharma JP, et al. Effect of irrigation fluid temperature on core temperature and hemodynamic changes in transurethral resection of prostate under spinal anesthesia[J]. Anesth Essays Res, 2014, 8(2): 209－215. DOI: 10.4103/0259－1162.134508.

（本文编辑：刘珩）

（收稿日期：2018-02-05）

输尿管结石行输尿管镜下碎石术后并发输尿管狭窄的危险因素分析

耿超 游刚* 徐连荣 韦伟
（重庆宏仁一医院，重庆 408400）

[摘要] 目的 探究输尿管结石行输尿管镜下碎石术后并发输尿管狭窄的危险因素。方法 本次研究对象选择2017年5月～2019年5月期间于本院接受输尿管镜下碎石术的360例输尿管结石患者。结果 手术完成后18例患者出现输尿管狭窄，其中9例患者为输尿管上段狭窄，6例患者为输尿管中段狭窄，3例患者为输尿管下段狭窄。输尿管狭窄发生率为5.00%；通过单因素分析发现，患者病程、结石长径、是否为多发结石、是否为嵌顿结石、治疗方式等均为输尿管狭窄发生的影响因素；多因素分析发现输尿管狭窄危险因素依次为：嵌顿结石、多发结石、大结石、钬激光手术、长病程。结论 输尿管狭窄危险因素有嵌顿结石、多发结石、大结石、钬激光手术和长病程等。

[关键词] 输尿管结石；输尿管镜；碎石术；输尿管狭窄
[中图分类号] R693+.4 [文献标识码] A
DOI:10.19738/j.cnki.psy.2019.23.172

输尿管结石在泌尿系统结石中较为常见，传统的手术取石，会对患者造成较大的创伤，且术后并发症较为高发。输尿管镜技术在近年来得到快速的发展，在输尿管结石的诊断和治疗中得到了广泛的使用。但是输尿管镜的侵入，会对输尿管造成较大的损伤，而且输尿管的损伤有可能会导致输尿管狭窄的发生。

1 资料与方法

1.1 一般资料

本次研究对象选择2017年5月～2019年5月期间于本院接受输尿管镜下碎石术的360例输尿管结石患者。所有接受本次研究的患者中，有206例男性患者和154例女性患者；最小年龄患者18岁，最大年龄患者70岁，平均（43.2±13.7）岁；50例患者为上段结石，144例患者为中段结石，166例患者为下段结石；最小结石0.4 cm×0.5 cm，最大结石为1.5 cm×2.4 cm；最短病程3天，最长病程7年，平均（7.8±3.2）月。钬激光碎石治疗的患者297例，气压弹道碎石治疗的患者63例。

1.2 研究方法

所有接受本次研究的患者均接受硬膜外麻醉，碎石与取石的操作均在输尿管镜的引导下进行。接受钬激光碎石治疗的患者，通过光纤进行激光能量的传导，利用“雕”法将结石从中央向周边进行粉碎，粉碎到2 mm以下。如果结石的下方有息肉，则应该先将息肉切除后在进行结石的粉碎。若为嵌顿性结石，需要先将包裹组织切开，然后实施碎石操作。接受气压弹道碎石治疗的患者，使用冲击针在脉冲作用下进行结石的粉碎操作，同样粉碎到2 mm以下，结石可随着尿液被清除，对于比较大的结石，则使用结石钳将其取出。手术完成后，将双J管置留2～4周，若术中有输尿管损伤情况，则需要置留8～12周。

1.3 统计学方法

本院在进行数据分析时，所应用分析的软件是SPSS22.0。用（$\bar{x}\pm s$）表示计量资料，通过t检验对研究中的数据进行检验，χ^2检验计数资料，以$P<0.05$为有统计学意义。

2 结果

手术完成后18例患者出现输尿管狭窄，其中9例患者为输尿管上段狭窄，6例患者为输尿管中段狭窄，3例患者为输尿管下段狭窄。输尿管狭窄发生率为5.00%。

由表1，通过单因素分析发现，患者病程、结石长径、是否为多发结石、是否为嵌顿结石、治疗方式等均为输尿管狭窄发生的影响因素。

表1 不同影响因素的输尿管狭窄发生情况分析

因素		狭窄（n=18）	无狭窄（n=342）	χ^2	P
性别	男	11	195	0.020	>0.05
	女	7	147		
年龄	<50岁	10	182	0.082	>0.05
	≥50岁	8	160		
病程	<3月	6	217	13.85	<0.001
	≥3月	12	125		
结石长径	<1 cm	6	235	-5.326	<0.001
	1~2 cm	4	78		
	>2 cm	8	29		
结石部位	上部	3	42	0.108	>0.05
	中部	8	273		
	下部	7	27		
多发结石	是	6	59	8.325	<0.05
	否	12	283		
合并息肉	是	5	135	0.692	>0.05
	否	13	207		
嵌顿结石	是	14	210	24.653	<0.001
	否	4	132		
治疗方式	钬激光	15	201	8.583	<0.05
	气压弹道	3	141		
置留双J管时间	≤4周	8	186	1.383	>0.05
	>4周	10	156		

由表2，多因素分析发现输尿管狭窄危险因素依次为：嵌顿结石、多发结石、大结石、钬激光手术、长病程。

表2 输尿管狭窄多因素分析结果

因素	B值	OR	95%CI	χ^2	P
嵌顿结石	1.31	3.62	2.11～6.09	11.42	<0.001
多发结石	1.168	3.23	1.02～5.78	8.25	<0.001
大结石	0.882	2.42	1.15～4.19	9.35	<0.001
钬激光手术	0.305	1.35	1.01～3.94	5.12	0.032
长病程	0.114	1.13	1.01～3.43	5.01	0.038

3 讨论

导致输尿管狭窄发生的常见因素为输尿管结石碎石术。嵌顿结石会由于嵌顿引起的输尿管水肿，导致输尿管黏膜被安全导丝穿破，使黏膜被损伤，产生感染、出血，因此嵌顿结石患者出现输尿管狭窄的概率较高[1]。另外，在本次研究中发现多发结石、大结石、钬激光手术、长病程同样是导致输尿管狭窄发生的影响因素。

参考文献

[1] 温海东,陈新胜,廖灵,等.输尿管镜下钬激光治疗输尿管嵌顿性结石引起输尿管狭窄的相关因素分析[J].临床泌尿外科杂志,2016,31(2):127-130.

通讯作者：游刚 [China Academic Journal Electronic Publishing House. All rights reserved. http://www.cnki.net

输尿管镜钬激光碎石术后继发输尿管狭窄的危险因素分析

刘跃闻[1,2] 李建中[1] 周亚军[1,2] 李昕[1]

[摘要] 目的：探讨经尿道输尿管镜钬激光碎石术(URL)后继发输尿管狭窄的危险因素。方法：回顾性分析我院 2016 年 3 月～2017 年 5 月收治的 312 例接受经尿道 URL 患者的临床资料，对可能引起输尿管狭窄的病因先行单因素分析，再对有统计学意义的指标行多因素 Logistic 分析。结果：本研究共收集 312 例患者的临床资料，其中发生输尿管狭窄 15 例，发生率为 4.79%。单因素分析显示，肾积水程度、息肉包裹、手术时间、接受 ESWL、结石长径与术后狭窄有关；多因素 Logistic 分析显示，肾积水程度、息肉包裹、手术时间、接受 ESWL、结石长径是导致术后输尿管狭窄的独立危险因素。结论：对于肾积水程度较大、息肉包裹、接受 ESWL、结石较大、手术时间较长的患者行经尿道 URL 时，需要注意手术操作，预防输尿管狭窄的发生。

[关键词] 输尿管镜；输尿管结石；钬激光；输尿管狭窄；危险因素
doi:10.13201/j.issn.1001-1420.2019.08.008
[中图分类号] R693 [文献标志码] A

Analysis of risk factors of ureterostenosis after ureteroscopic holmium laser lithotripsy for ureteral stones

LIU Yuewen[1,2] *LI Jianzhong*[1] *ZHOU Yajun*[1,2] *LI Xin*[1]

([1]Department of Urology, Northern Theater General Hospital, Shenyang, 110016, China; [2]Jinzhou Medical University)

Corresponding author: LI Jianzhong, E-mail: 174030098@qq.com

Abstract **Objective**: To investigate the risk factors of ureteral stricture after transurethral ureteroscopic lithotripsy (URL) with holmium laser. **Method**: A retrospective analysis of the clinical data of 312 patients undergoing transurethral URL with holmium laser admitted to our hospital from March 2016 to May 2017 was done. A single factor analysis of the causes of ureteral stricture was done, Logistic analysis was performed on statistically significant indicators, and renal function changes were followed up to observe the influence of ureteral stricture on renal function. **Result**: A total of 312 clinical patients were included in the study, including 15 cases of ureteral stricture, with an incidence of approximately 4.79%. Univariate analysis showed that hydronephrosis, polyp encapsulation, operative time, ESWL history, long stone diameter were associated with postoperative stenosis. Multivariate logistic analysis showed hydronephrosis, polyp encapsulation, operative time, ESWL history, long stone diameter were independent risk factors for postoperative ureteral stricture. **Conclusion**: For transurethral URL with holmium laser in patients with severe hydronephrosis, polyp encapsulation, ESWL history, large stones and long operation time, it is necessary to pay attention to the operation and prevent the occurrence of ureteral stricture.

Key words ureteroscopy; ureteral calculi; holmium laser; ureteral stricture; risk factors

输尿管结石是泌尿系最常见的结石种类之一，随着医疗水平及设备的不断发展进步，输尿管结石的治疗方法也多种多样，如体外冲击波碎石术(ESWL)、输尿管镜钬激光碎石术(URL)、经皮肾镜取石术(PCNL)、腹腔镜输尿管切开取石术等。根据最近的一份报告，URL 已取代 ESWL 成为美国上尿路结石的主要治疗方式[1]。结合欧洲泌尿外科学会推荐的输尿管结石的治疗选择，钬激光是最有效的碎石系统，已成为输尿管镜碎石和输尿管软镜碎石的"金标准"[2-3]。但随着此项技术在临床的大面积广泛应用，其固有的手术缺陷也开始逐渐显现，如可能引起的输尿管狭窄、穿孔等[4]。输尿管狭窄可导致输尿管梗阻和肾功能进行性恶化。对于无症状输尿管梗阻的患者，如果不进行常规术后随访，可能会发生不可逆的肾功能衰竭。本文旨在研究可能导致经尿道 URL 术后输尿管狭窄的危险因素，为临床预防输尿管狭窄的发生提供依据。现报告如下。

1 资料与方法

1.1 临床资料

回顾性分析我院 2016 年 3 月～2017 年 5 月收

[1]北部战区总医院泌尿外科(沈阳，110016)
[2]锦州医科大学
通信作者：李建中，E-mail：174030098@qq.com

(C)1994-2020 China Academic Journal Electronic Publishing House. All rights reserved. http://www.cnki.net

治的 312 例接受经尿道 URL 患者的临床资料，术后发生狭窄 15 例，发生率为 4.79%，大多发生于术后 1 个月拔出输尿管支架后的第 2～12 个月。患者复查时泌尿系彩超提示不同程度肾盂、输尿管扩张积水，行泌尿系 CTU 或肾盂造影后诊断为输尿管狭窄。其中男 216 例，女 96 例；结石位于左侧 172 例，右侧 140 例；青年(18～39 岁)87 例，中年(40～55 岁)131 例，老年(≥56 岁)94 例。

1.2 手术方法

所有患者均于全麻或腰麻下取截石位行 URL，使用钬激光碎石机，9.8F 输尿管镜，550 μm 光纤，所有手术均由我科同一位高年资医师完成。

1.3 入组和排除标准

入组标准：①所有患者均为首次接受 URL；②临床资料完整。排除标准：①双侧输尿管单发结石；②一侧输尿管多发结石或合并肾结石；③既往有输尿管相关手术史或曾留置双 J 管；④既往输尿管狭窄病史或合并输尿管息肉；⑤术中输尿管撕裂或损伤或先天性输尿管开口狭窄；⑥合并心、肺、脑等器官重度衰竭或恶性肿瘤患者。

1.4 研究方法

回顾性分析 312 例患者资料，根据患者术后随访结果将其分为狭窄组和非狭窄组，其中狭窄组 15 例，非狭窄组 297 例。诊断输尿管狭窄根据泌尿系 CTU 或静脉肾盂造影提示输尿管狭窄伴积水，泌尿系彩超常提示某一输尿管节段未见结石但伴有肾盂及输尿管扩张积水。比较两组患者性别、年龄、BMI、患侧、结石位置、积水程度、息肉包裹、手术时间、是否接受 ESWL、结石长径、是否术前合并感染的相关情况。①肾积水程度主要根据患者 B 超检查结果判断。轻度肾积水：肾盂肾盏轻微扩张或无扩张(肾盂肾盏形态关系仍在)，无实质萎缩，肾集合系统分离 1～2 cm；中度肾积水：肾盂肾盏中度扩张，杯口变钝和乳头变平，皮质轻微变薄，肾集合系统分离 2.1～3.5 cm；重度肾积水：肾盂肾盏气球样膨胀、扩张明显，或肾盂肾盏界限消失皮质变薄肾萎缩，肾盂集合系统分离>3.5 cm。②BMI：18.5～23.9 正常、24.0～27.9 过重、28.0～32.0 肥胖、>32.0 非常肥胖。③合并感染：按照《内科学》第 8 版标准，新鲜尿离心沉渣检查每高倍镜视野白细胞超过 5 个或镜下白细胞超过一个“+”号；清洁外阴后无菌技术下采集的中段尿标本，涂片每高倍镜视野均见细菌，或尿液中亚硝酸盐阳性。④结石位置：依据影像学分段标准：将位于肾盂输尿管连接处到骶髂关节上缘之间的结石定义为输尿管上段结石；将位于骶髂关节上缘到骶髂关节下缘之间的结石定义为输尿管中段结石；将位于骶髂关节下缘到输尿管膀胱连接处的结石定义为输尿管下段结石。

1.5 统计学方法

采用 SPSS 24.0 统计学软件进行数据分析，首先采用 χ^2 检验对两组患者的 11 个危险因素进行单因素分析，然后对单因素分析具有统计学意义的因素进行 Logistic 多因素回归分析。以 $P<0.05$ 为差异有统计学意义。

2 结果

2.1 单因素分析结果

单因素分析发现，结石长径、肾积水程度、息肉包裹、手术时间及接受 ESWL 与 URL 术后输尿管狭窄有关($P<0.05$)。见表 1。

表 1 URL 术后输尿管狭窄单因素分析 例(%)

变量	总例数	狭窄	χ^2	P 值
性别			0.123	0.810
男	216	11(5.09)		
女	96	4(4.17)		
年龄/岁			0.604	0.422
18～39	87	6(6.89)		
40～55	131	7(5.34)		
≥56	94	2(2.12)		
BMI			1.717	0.931
正常	87	6(6.89)		
过重	92	3(3.26)		
肥胖	62	3(4.38)		
非常肥胖	71	3(4.22)		
患侧			0.151	0.592
左侧	172	9(5.23)		
右侧	140	6(4.28)		
结石位置			0.244	0.816
上段	176	8(4.55)		
中段	59	4(6.78)		
下段	77	3(3.90)		
息肉包裹			38.186	0.000
有	51	12(23.53)		
无	261	3(1.15)		
手术时间/min			6.712	0.032
<30	21	1(4.76)		
30～60	144	3(2.08)		
>60	147	11(7.48)		
肾积水程度			24.707	0.000
轻度	107	1(0.93)		
中度	153	4(2.61)		
重度	52	10(19.23)		
ESWL			11.632	0.000
是	64	9(6.38)		
否	248	6(2.42)		
结石长径/cm			6.141	0.047
<1	152	5(3.29)		
1～2	146	8(5.48)		
>2	24	2(8.33)		
术前感染			0.228	0.644
有	189	10(5.29)		
无	123	5(4.06)		

(C)1994-2020 China Academic Journal Electronic Publishing House. All rights reserved. http://www.cnki.net

2.2　多因素分析结果

将上述单因素分析有统计学意义的危险因素进行多因素 Logistic 回归分析，结果显示：结石长径、积水深度、息肉包裹、手术时间及接受 ESWL 均是 URL 术后输尿管狭窄的独立危险因素（$P<0.05$）。见表 2。

表 2　URL 术后输尿管狭窄多因素分析

危险因素	回归系数	标准误	χ^2	P 值	OR	95%CI	
						下限	上限
结石长径	−1.840	1.711	1.155	0.032	0.159	0.006	4.549
积水深度	2.999	1.489	4.509	0.044	0.050	1.829	23.977
息肉包裹	4.550	1.314	11.898	0.001	94.661	7.204	243.963
手术时间	0.338	1.529	0.269	0.025	0.713	0.036	14.291
接受 ESWL	2.191	0.886	6.117	0.013	8.941	1.576	50.798

3　讨论

激光技术是用于治疗泌尿系结石的标准方式[11]。引入钬激光技术治疗输尿管结石拓宽了输尿管镜手术(URS)的适应证，包括处理较大尺寸的上尿路结石[12]。钬激光具有精确而强大的热分解机制以及优异的安全性，能够通过小而柔韧的光纤传递激光能量，为上尿路碎石术后的结石碎片开辟了排出通路[13]。钬激光对各种成分的泌尿系结石均能够高效粉碎，其具有以下 2 种特性：①组织穿透深度浅：组织穿透深度<0.5 mm，可用于精确的外科切割和止血；②高能脉冲式：瞬间电压达 10 kW，碎石效率高且不受结石大小和成分的影响[14]。而输尿管狭窄则是 URL 术后最常见的一种远期并发症，发生率为 4.1%～7.8%[15]；除了形成狭窄的危险因素外，输尿管狭窄的发生率也受术后影像学随访策略的影响。在一些研究中，由于随访不足，可能会低估输尿管狭窄的发生率[3]。若能有效地评估患者 URL 术后继发输尿管狭窄的可能性，并降低相关的风险因素，则可以进一步提高手术治疗效果，同时还可以减轻患者的医疗负担。

本研究 312 例患者中，发生输尿管狭窄患者 15 例，狭窄率约为 4.79%。本文共研究了性别、年龄、BMI、患侧、结石位置、肾积水程度、息肉包裹、手术时间、术前感染、术前是否接受 ESWL 及结石长径 11 个因素，单因素分析发现，手术时间、肾积水程度、接受 ESWL、结石长径、息肉包裹这 5 个因素与术后输尿管狭窄有关。结石伴息肉包裹即临床常见的嵌顿性结石，是指结石长期滞留于输尿管刺激黏膜炎性增生，导致输尿管黏膜损伤。由黏膜产生的纤维蛋白渗出物沉积在受损区域，刺激黏附，最后形成狭窄[16]。嵌顿性结石周围息肉增生较为严重且输尿管黏膜水肿，导丝通过时极易穿破输尿管黏膜形成假道或穿孔；输尿管水肿导致的有限操作空间增加了在结石碎裂时损坏黏膜的机会[11]。钬激光虽然组织切割程度浅碎石效率高，但不可避免的会引起周围组织的热损伤；根据之前的文献，钬激光治疗上尿路肿瘤继发输尿管狭窄的发生率为 8.57%～13.67%[17]，输尿管狭窄高发病率证实了狭窄与钬激光热效应之间的关系。我们还经常可以见到在处理完嵌顿性结石过后，结石床表面凹凸不平，黏膜苍白缺血，甚至出现黏膜下结石；据 Dretler 等[4]报道，嵌入输尿管壁的草酸钙颗粒可能导致随后的肉芽肿反应和狭窄疾病；此外，在提取术后出现输尿管狭窄患者的狭窄部位组织内发现了大量对草酸钙晶体产生反应的巨噬细胞及异物巨细胞，故嵌入输尿管黏膜的结石碎片可引发炎症，导致狭窄形成。所以，在临床上处理息肉包裹性结石时，应从结石的中心开始碎石，待结石碎成几个大块后再继续处理；若部分结石仍附着于结石床上，应使用异物钳将其夹下来或使用输尿管镜、导丝撬动结石，待结石脱落后再继续碎石。同时，嵌顿性结石多伴有不同程度的肾盂输尿管扩张积水，结石长径越大，引起的梗阻程度也就越大，肾盂积水可能就越重，碎石时间也就越长。输尿管结石的直径与输尿管镜碎石后狭窄发生关系密切。直径越大的结石，手术时间越长；术中灌洗时间越长，术后发生感染概率越大[18]。由于术中输尿管黏膜对水压或结石成分的免疫反应所引起的缺血会导致输尿管黏膜水肿或纤维化，包括：Ⅰ型病变即输尿管黏膜细胞的水肿或半球形病变；Ⅱ型病变外观呈绒毛状改变，并在显微镜下显示为由柱状间充质细胞构成。Yamaguchi 等[19]发现这 2 种微观变化可能与结石有关，他们推断结石大小和手术时间是导致输尿管病变发展的可能因素。

ESWL 自 20 世纪 80 年代推广以来，已经大大改变了尿石症的治疗方法，目前被认为是大多数(90%)肾和输尿管结石患者首选和侵入性最小的一线治疗方案[16]。ESWL 产生的冲击波穿过身体软组织而不会损失强度，并通过直接剪切力侵蚀或空化结石，将其击碎成较小的碎片[17,20]。而且形状大小不一的结石在缓慢排出过程中容易对输尿管

(C)1994-2020 China Academic Journal Electronic Publishing House. All rights reserved.　http://www.cnki.net

黏膜造成损伤，出血，形成瘢痕，进而可能导致狭窄的发生。国内外尚无明确的临床资料证明 ESWL 术后继发输尿管狭窄的发生概率或风险因素，结合陈静[18]报道及我院临床经验，ESWL 次数越多，越容易继发术后的输尿管狭窄。故建议行 ESWL 超过 2 次而无临床效果的患者，应立即接受手术治疗，不应再继续体外碎石。

叶照华等[20]研究显示，结石嵌顿时间越长，输尿管镜碎石术后继发输尿管狭窄的可能越大，这与 El-abd 等[21]研究相符合。但本文中绝大多数患者均为常规体检或突发不适行影像学检查时发现输尿管结石，且均为首次入院，故无法依据患者提供的结石嵌顿时间作为临床依据。同时，本文还探讨了 BMI、术前感染、结石位置等因素对继发输尿管狭窄的影响，但研究结果显示以上因素均与继发输尿管狭窄无关。此外术后留置输尿管支架时间的长短或许与输尿管狭窄有关，叶照华等[20]还认为，术后置留时间超过 4 周者，输尿管狭窄的发生率略高。而我院行 URL 后常规留置输尿管支架 1 个月，现并无临床证据显示输尿管支架与术后狭窄有关，这可能与输尿管支架留置时间过长导致的输尿管损伤有关。故需要对此问题进行大量前瞻性的研究来阐明其效用。

综上所述，结石息肉包裹、手术时间、接受 ESWL、结石长径、积水深度是 URL 后输尿管狭窄的危险因素。临床医师要根据患者不同情况建立个体化诊疗方案，综合评估患者病情及相关风险因素，根据术中结石是否嵌顿选择不同的碎石工具，合理控制手术时间，并告知患者定期随访，做到早发现早治疗。

[参考文献]

1 Oberlin D T，Flum A S，Bachrach L，et al.Contemporary surgical trends in the management of upper tract calculi[J].J Urol，2015，193(3)：880－884.

2 Turk C，Petrik A，Sarica K，et al.EAU guidelines on diagnosis and conservative management of urolithiasis[J].Eur Urol，2015，69(3)：468－474.

3 Ibrahim H M，Mohyelden K，Abdel-Bary A，et al.Single versus double ureteral stent placement after laser endoureterotomy for the management of benign ureteral strictures：A randomized clinical trial[J].J Endourol，2015，29(10)：1204－1209.

4 Breda A，Ogunyemi O，Leppert J T，et al.Flexible ureteroscopy and laser lithotripsy for multiple unilateral intrarenal stones[J].Eur Urol，2009，55(5)：1190－1197.

5 Tepeler A，Resorlu B，Sahin T，et al.Categorization of intraoperative ureteroscopy complications using modified Satava classification system[J].World J Urol，2014，32(1)：131－136.

6 Kijvikai K，Hafeblian G E，Preminger G M，et al.Shock wave lithotripsy or ureteroscopy for the management of proximal ureteral calculi：an old discussion revisited[J].J Urol，2007，178(4 Pt 1)：1157－1163.

7 Hibi H，Ohori T，Taki T，et al.Long－term results of endoureterotomy using a holmium laser[J].Int J Urol，2007，14(9)：872－874.

8 袁耀基，苏郑明，梁健，等.泌尿外科中输尿管狭窄的医源性危险因素及预防[J/CD].中华腔镜泌尿外科杂志(电子版)，2017，11(6)：423－425.

9 Chen S，Zhou L，Wei T，et al.Comparison of holmium：YAG laser and pneumatic lithotripsy in the treatment of ureteral stones：an update meta-analysis[J].Urol Int，2017，98(2)：125－133.

10 Roberts W W，Cadeddu J A，Micali S，et al.Ureteral stricture formation after removal of impacted calculi[J].J Urol，1998，159(3)：723－726.

11 Fam X I，Singam P，Ho C C，et al.Ureteral stricture formation after ureteroscope treatment of impacted calculi：A prospective study[J].Korean J Urol，2015，56(1)：63－67.

12 Johnson G B，Fraiman M，Grasso M.Broadening experience with the retrograde endoscopic management of upper urinary tract urothelial malignancies[J].BJU Int，2005，95(Suppl 2)：110－113.

13 Dretler S P，Young R H.Stone granuloma：a cause of ureteral stricture[J].J Urol，2003，150(6)：1800－1802.

14 Devarajan R，Ashraf M，Beck R O，et al.Holmium：YAG-Glasertripsy for ureteric calculi：an experience of 300 procedures[J].Br J Urol，1998，82(3)：342－347.

15 Yamaguchi K，Minei S，Yamazaki T，et al.Characterization of ureteral lesions associated with impacted stones[J].Int J Urol，2009，6(6)：281－285.

16 Dong H，Peng Y，Li L，et al.Prevention strategies for ureteral stricture following ureteroscopic lithotripsy[J].Asian J Urol，2018，5(2)：94－100.

17 Ceban E.The treatment of the reno－ureteral calculi by extracorporeal shockwave lithotripsy(ESWL)[J].J Med Life，2012，5(2)：135－138.

18 Tonolini M，Villa F，Ippolito S，et al.Cross－sectional imaging of iatrogenic complications after extracorporeal and endourological treatment of urolithiasis[J].Insights Imaging，2014，5(6)：677－689.

19 陈静.体外冲击波碎石治疗输尿管结石后发生输尿管狭窄的危险因素探究[J].中华继续医学教育杂志，2017，9(8)：107－109.

20 叶照华，米其武，罗杰鑫，等.输尿管结石行输尿管镜下碎石术后并发输尿管狭窄的危险因素分析[J/CD].中华腔镜泌尿外科杂志(电子版)，2017，11(1)：46－48.

21 El-abd A S，Sulaiman M G，Abo Farha M O，et al.The development of ureteric strictures after ureteroscopic treatment for ureteric calculi：A long-term study at two academic centres[J].Arab J Urol，2014，12(2)：168－172.

(收稿日期：2018-10-05)

(C)1994-2020 China Academic Journal Electronic Publishing House. All rights reserved. http://www.cnki.net

·论著·

单发输尿管结石患者行输尿管镜下钬激光碎石术后狭窄的危险因素分析

周乐 胡焕春 汪波
武汉京都结石泌尿外科医院泌尿外科，武汉 430061
通信作者：汪波，Email：1084829466@qq.com

【摘要】 目的 探讨单发输尿管结石患者行输尿管镜下钬激光碎石（URSL）后发生狭窄的危险因素，为患者的治疗提供参考。**方法** 回顾性分析2017年11月至2018年11月在本院行URSL术的单发输尿管结石患者230例，按照术后随访结果将其中输尿管狭窄患者26例作为观察组，输尿管非狭窄患者204例作为对照组，分析患者术后发生狭窄的危险因素。**结果** 结石直径≥2 cm，严重肾积水、结石嵌顿、病程较长均是患者术后发生狭窄的危险因素，两组比较差异有统计学意义（$P<0.05$）；输尿管狭窄多因素logistic回归分析显示，大结石、严重肾积水、嵌顿结石以及长病程均是影响患者URSL术后输尿管狭窄的独立危险因素，差异有统计学意义（$P<0.05$）。**结论** 严重肾积水、结石较大、结石嵌顿以及较长病程均是患者术后发生输尿管狭窄的高危因素，因此在对患者进行治疗的过程中应远离引起患者输尿管狭窄的高风险因素、提高患者治疗效果。

【关键词】 输尿管结石；碎石术，激光；尿道狭窄
DOI：10.3760/cma.j.issn.1673-4416.2020.02.012

Analysis of risk factors for postoperative stenosis with single ureteral calculi treated with ureteroscopic holmium laser listhotripsy

Zhou Le, Hu Huanchun, Wang Bo
Department of Urology, Wuhan Institute of Urology, Wuhan 430061, China
Corresponding author: Wang Bo, Email: 1084829466@qq.com

Abstract **Objective** To explore the risk factors of stricture after ureteroscopic holmium laser lithotripsy (URSL) in patients with single ureteral calculi, and to provide reference for the treatment of patients. **Methods** Retrospective analysis of 230 patients with single ureteral calculi who underwent URSL between November 2017 and November 2018 was performed. According to the postoperative follow-up results, 26 patients with ureteral stricture were treated as observation group, and ureteral non-stenosis patients were 204 patients as a control group. The risk factors for stenosis after surgery were analyzed. **Results** The risk factors of postoperative stenosis showed that the diameter of calculus ≥2 cm, severe hydronephrosis, stone incarceration, and long course of disease were the risk factors for postoperative stenosis. The difference between the two groups was statistically significant ($P<0.05$). Multivariate logistic regression analysis of ureteral stricture showed that large stones, severe hydronephrosis, incarcerated stones and long-term disease were independent risk factors for ureteral stricture after URSL, and the difference was statistically significant ($P<0.05$). **Conclusions** Severe hydronephrosis, large stones, stone incarceration and long course of disease are high risk factors for postoperative ureteral stricture. Therefore, patients should be kept away from the high risk factors causing ureteral stricture in patients during treatment for better therapeutic efficiency.

Key words Ureteral Calculi; Lithotripsy, Laser; Urethral Stricture

DOI: 10.3760/cma.j.issn.1673-4416.2020.02.012

输尿管结石作为最常见的上尿路结石。在泌尿系结石中，约20%的结石位于输尿管，其中70%位于输尿管下段。输尿管结石多来源于肾脏，且为单侧结石，其症状也与肾结石症状基本相同[1-2]。患者疼痛多呈绞痛，可放射到同侧下腹部、睾丸或阴唇，大多数患者仅有镜下血尿[3-4]。随着近年来微创技术的发展，创伤小、效果明确、并发症少使微创手术成为直径较大结石的主要治疗手段，但输尿管镜的侵入操作也会引起患者输尿管损伤，增加患者输尿管狭窄的发生率。因此，为探讨单发输尿管结石患者行URSL术后发生狭窄的危险因素，为患者的治疗提供参考。

1 资料与方法

1.1 临床资料

回顾性分析2017年11月至2018年11月间在本院行URSL术的单发输尿管结石患者230例，按照术后随访结果将其中输尿管狭窄患者26例作为观察组，输尿管非狭窄患者204例作为对照组。纳入标准：①患者术前均确诊为输尿管结石；②患者均首次接受输尿管镜下碎石治疗；③患者知情并签署同意书。排除标准：①合并严重肝肾功能不全患者；②术前合并输尿管狭窄患者；③治疗依从性较差患者。观察组中男20例，女6例，年龄22～73（49.5±13.2）岁，对照组中男152例，女52例，年龄20～76（50.3±12.7）岁，两组患者在性别、年龄等临床资料方面比较差异无统计学意义（$P>0.05$）。

1.2 方法

患者取截石位，采用硬膜外麻醉，选择德国Wolf 8～9.5F输尿管镜及瑞科恩钬激光碎石机，经尿道直视下进入患者膀胱；确认患者患侧输尿管口后，向输尿管内放入斑马导丝，顺斑马导丝旋转进镜，推入输尿管镜到达结石处；设置钬激光碎石机功率为50 W，于直视下将结石粉碎成2～3 mm大小的碎片，然后采用套石网篮将结石碎片取出置于膀胱；完成碎石、取石后，留置F5～F7双J管于输尿管内引流1周，同时于膀胱内留置气囊导尿管，所有操作均由同一医生完成。采用肾盂输尿管膀胱三维CT、泌尿系彩超以及静脉泌尿系造影等方式检查患者是否出现输尿管狭窄以及上段积水。记录患者输尿管狭窄相关危险因素及多因素logistic回归分析。

1.3 统计学分析

采用SPSS 18.0进行统计学分析，以率（%）表示计数资料，使用χ^2检验，然后对两组患者各项资料进行单因素分析，对于单因素分析具有统计学意义的各因素采取logistic多因素回归分析，$P<0.05$表示差异有统计学意义。

2 结果

2.1 患者术后狭窄危险因素分析

患者术后狭窄危险因素结果显示，观察组患者结石直径≥2 cm、严重肾积水、存在结石嵌顿、病程较长患者占比明显高于对照组，两组比较差异有统计学意义（$P<0.05$，表1）。

表 1 单发输尿管结石患者术后狭窄危险因素分析[例(%)]

组别	例数	性别		年龄		结石直径		肾积水程度			结石嵌顿		合并尿路感染		患侧		病程	
		男	女	≤60 岁	>60 岁	≤2 cm	>2 cm	轻度	中度	重度	是	否	有	无	左	右	≤3 个月	>3 个月
观察组	26	20(76.9)	6(23.1)	16(61.5)	10(38.5)	16(61.5)	10(38.5)	4(15.4)	8(30.8)	14(53.8)	8(30.8)	20(76.9)	20(76.9)	6(23.1)	14(53.8)	12(46.2)	10(38.5)	16(61.5)
对照组	204	152(74.5)	52(25.5)	108(52.9)	96(47.1)	182(89.2)	22(10.8)	51(25.0)	101(49.5)	52(25.5)	110(53.9)	94(46.1)	122(59.8)	82(40.2)	102(50.0)	102(50.0)	58(28.4)	146(71.6)
χ^2 值	-	0.8532		0.2238		25.9531		19.0054			31.5008		0.6390		0.8123		15.8947	
P 值	-	>0.001		>0.001		<0.001		<0.001			<0.001		>0.001		>0.001		<0.001	

2.2 输尿管狭窄多因素 logistic 回归分析

输尿管狭窄多因素 logistic 回归分析显示，大结石、严重肾积水、嵌顿结石以及长病程均是影响患者 URSL 术后输尿管狭窄的独立危险因素，差异有统计学意义($P<0.05$，表 2)。

表 2 输尿管狭窄多因素 logistic 回归分析

危险因素	β 值	OR 值	95%CI	χ^2 值	P 值
大结石	1.15	2.83	1.1~4.2	8.25	<0.001
严重肾积水	1.35	3.12	1.2~2.4	11.18	<0.001
嵌顿结石	1.42	3.65	2.2~6.1	10.28	<0.001
长病程	0.79	1.75	1.1~3.4	7.24	0.039

3 讨论

输尿管结石作为一种多来源于肾脏的结石，它包括了肾结石以及体外震波后碎块降落的结石。由于尿盐晶体较容易随尿液排入膀胱，因此原发性输尿管结石极为少见。临床研究发现，输尿管结石多为单个，左右两侧发病大致相似，且结石位于输尿管下段最为多见[6-8]。

目前微创手术作为输尿管结石主要治疗手段之一。因此，在术前或术中对术后输尿管狭窄发生的风险进行预测以及预防能够有效地改善患者预后，提高患者治疗效果。输尿管镜下钬激光碎石作为输尿管结石的一种微创治疗手段，通过"钻孔效应"将结石碎成细小的颗粒，能够高效粉碎各种泌尿系结石。结石大小作为影响患者治疗效果的一项重要因素，在对较大的结石进行碎石、取石的过程中，手术时间增加导致灌洗时间的延长，增加了患者术后感染的风险[9-11]。

输尿管产生炎症刺激后会导致局部出现炎性肉芽组织，形成输尿管息肉，息肉包绕结石后会导致结石体积增大，阻梗加重，导致输尿管狭窄的发生[12-13]。嵌顿结石作为一种较为特殊的病理类型，嵌顿结石长时间压迫输尿管导管后会导致管壁间质逐渐变得纤维化，促进上皮增生以及水肿的发生，从而改变了嵌顿部位的输尿管壁性质，限制了结石的移动，导致成膜的损伤、出血、感染以及瘢痕的形成，诱发输尿管狭窄的发生，增加了手术难度以及对输尿管壁损伤的风险。肾积水、病程作为输尿管狭窄的又一影响因素，这是因为患者通常存在不同程度的输尿管梗阻或肾积脓，增加了碎石的复杂性以及输尿管损伤的发生率[14-16]。

上述因素的影响也提示了患者在治疗的过程中，应从结石中间开始碎石，周边与输尿管黏膜相接触的部分应夹离输尿管后再进行碎石。同时在面对结石较大、质地较硬、持续灌注时间较长的患者，因碎石较为困难，因此可选择分为二次手术，减少患者术后狭窄的发生。本研究显示，患者术后狭窄危险因素结果显示，结石直径≥2 cm、严重肾积水、嵌顿结石、较长病程均是患者术后发生输尿管狭窄的危险因素，并且输尿管狭窄多因素 logistic 回归分析显示、大结石、严重肾积水、嵌顿结石以及长病程均是影响患者 URSL 术后输尿管狭窄的独立危险因素。因此在对患者进行治疗的过程中应远离引起患者输尿管狭窄的高风险因素，提高患者治疗效果。

利益冲突 所有作者均声明不存在利益冲突

参 考 文 献

[1] 黄永红，朱丹，宋昭祥. 综合护理干预对输尿管结石 URSL 术后治疗效果的影响[J]. 护士进修杂志，2014，(4)：346－347.

[2] 戚俊，邹小鹏，王鹏. 输尿管镜钬激光碎石术治疗老年输尿管结石的疗效及对肾功能的影响[J]. 中国老年学杂志，2016，36(3)：683－685. DOI：10.3969/j. issn. 1005－9202. 2016. 03. 076.

[3] Lebentrau S, Müller PF, Miernik A, et al. Risk Factors for Ureteral Damage in Ureteroscopic stone Treatment: Results of the German Prospective Multicentre Benchmarks of Ureterorenoscopic Stone Treatment－Results in Terms of Complications, Quality of Life, and Stone－Free Rates Project[J]. Urol Int, 2019, 102(2)：187－193. DOI：10.1159/000495072.

[4] 林峰，陈军，王鸿果. 不同手术方式治疗输尿管结石的效果分析[J]. 中国全科医学，2014，(17)：2036－2039. DOI：10.3969/j. issn. 1007－9572. 2014. 17. 029.

[5] 陈波特，杨煜，张小明，等. 输尿管镜下气压弹道碎石术和体外冲击波碎石术治疗输尿管结石的疗效比较[J]. 现代预防医学，2014，41(22)：4186－4188.

[6] 陈勇杰，张贵生. 输尿管镜下钬激光碎石术与气压弹道碎石术治疗输尿管结石效果比较[J]. 山东医药，2016，56(37)：87－89. DOI：10.3969/j. issn. 1002－266X. 2016. 37. 030.

[7] 张国辉，程艳，许陈祥，等. 输尿管结石伴急性肾周积液的超声观察与分析[J]. 中国超声医学杂志，2013，29(11)：1038－

1041.

[8] Rohloff M, Shakuri-Rad J, McElrath C, et al. Which Objective Parameters Are Associated with a Positive Urine Culture in the Setting of Ureteral Calculi: The Ureteral Calculi Urinary Culture Calculator[J]. J Endourol, 2018, 32(12): 1168-1172. DOI: 10.1089/end.2018.0668.

[9] 高永锋, 王岩. 输尿管结石行体外冲击波碎石治疗后发生输尿管狭窄的危险因素分析[J]. 现代泌尿外科杂志, 2014, 19(6): 384-386. DOI: 10.3969/j.issn.1009-8291.2014-06-010.

[10] 刘亚东, 田河, 安瑞华. 经尿道输尿管镜气压弹道碎石治疗单发输尿管结石后发生输尿管狭窄的危险因素分析[J]. 现代泌尿外科杂志, 2016, 21(4): 252-255. DOI: 10.3969/j.issn.1009-8291.2016.04.005.

[11] 吴佳成, 陆雅君, 姜力. 经尿道输尿管镜气压弹道治疗输尿管结石后发生输尿管狭窄的危险因素[J]. 中国临床研究, 2018, 31(9): 1267-1270. DOI: 10.13429/j.cnki.cjcr.2018.09.030.

[12] 叶照华, 米其武, 罗杰鑫, 等. 输尿管结石行输尿管镜下碎石术后并发输尿管狭窄的危险因素分析[J]. 中华腔镜泌尿外科杂志(电子版), 2017, 11(1): 40-42. DOI: 10.3877/cma.j.issn.1674-3253.2017.01.011.

[13] Zhou R, Han C, Hao L, et al. Ureteroscopic lithotripsy in the Trendelenburg position for extracting obstructive upper ureteral obstruction stones: a prospective, randomized, comparative trial[J]. Scand J Urol, 2018, 52(4): 291-295. DOI: 10.1080/21681805.2018.1492966.

[14] 史博文, 徐科, 黄云腾. 经皮肾镜取石术在儿童肾结石中的应用及进展[J]. 临床小儿外科杂志, 2017, 16(6): 617-621. DOI: 10.3969/j.issn.1671-6353.2017.06.021.

[15] 杨亮. 钬激光碎石术治疗输尿管结石后发生输尿管狭窄的危险因素分析[J]. 临床和实验医学杂志, 2015, (14): 1210-1212. DOI: 10.3969/j.issn.1671-4695.2015.014.026.

[16] 商向涛, 作亚迪. 尿石症并发尿路感染的危险因素和病原学分析[J]. 中国医学前沿杂志(电子版), 2017, 9(9): 87-91. DOI: 10.12037/YXQY.2017.09-21.

(本文编辑: 骆凤)

(收稿日期: 2019-02-28)

输尿管镜下钬激光碎石术后输尿管狭窄的危险因素分析

张志成　廖祖强

输尿管结石是最常见的上尿路结石，中年人群为高发人群，男性高于女性。输尿管结石主要临床表现为肾绞痛和血尿。若不及时治疗，极易造成上尿路感染及输尿管梗阻，严重影响患者生活质量[1]。传统治疗方法以外科切开取石术和体外冲击波碎石为主，但切开取石术对患者创伤大、并发症发生率高、术后恢复慢；体外冲击波碎石具有碎石率低、排石困难等缺点[2]。而目前临床上迅速发展的输尿管镜钬激光碎石具有碎石效果确切、创伤小、恢复快等优点，已成为泌尿外科处理输尿管结石的重要方法[3]。但由于输尿管镜为侵入性操作，难免会对输尿管产生一定损伤，进而发生输尿管狭窄，术后残留结石等相关并发症。本研究通过对输尿管镜下钬激光碎石术治疗患者的临床资料进行调查，探讨输尿管镜下钬激光碎石术后发生输尿管狭窄的相关危险因素，为输尿管结石患者术后进一步治疗及相关并发症的预防提供参考依据。

1　对象与方法

1.1　调查对象：本研究选取 2016 年 1 月至 2019 年 6 月在我院泌尿外科接受治疗的输尿管结石患者作为研究对象。纳入标准：①均经 CT 或 B 超等检查确诊为输尿管结石，且首次采用输尿管镜钬激光碎石术进行治疗；②均为单侧结石；③无精神或语言功能障碍；④愿意参加本次调查，并填写知情同意书，同时具有完整随访资料的患者。排除标准：①有既往输尿管手术史的患者；②在本次住院前已合并输尿管狭窄的患者；③合并有严重的内、外科疾病或肿瘤的患者。

1.2　调查内容：本次调查采用的调查表是参考以往文献，结合自身临床经验并反复咨询泌尿外科专家设计而成。参与本次调查的人员均为经过统一培训的泌尿外科医师。调查表内容包括：①输尿管结石患者基本情况：性别、年龄、身高、体质量、既往病史等；②输尿管结石患者疾病情况：输尿管结石病程、结石位置、结石个数、结石大小、是否伴有炎性包裹或息肉、是否合并上尿路感染、是否造成肾功能损伤等；③输尿管结石治疗情况：激光碎石时间、钬激光是否损伤黏膜等；④术后随访情况：随访并记录患者术后 3 个月内输尿管狭窄发生情况。

1.3　统计学分析：采用 SPSS 17.0 软件进行统计分析，单因素分析采用 χ^2 检验；并将单因素分析中有统计学意义的因素引入多因素 Logistic 回归模型中进行分析（变量筛选采用 Backward method，入选标准取 $\alpha_{入}$=0.05，剔出标准取 $\alpha_{出}$=0.10），并计算 *OR* 值和 95%*CI* 置信区间；P<0.05 为差异有统计学意义。

2　结　　果

2.1　输尿管术后狭窄率调查：参与本次调查并有完整随访资料的输尿管结石患者共 485 例，术后 3 个月内共发现输尿管狭窄患者 38 例，其发生率 7.84%。其中输尿管上段狭窄 11 例（占 10.58%），中段狭窄 15 例（占 8.06%），下段狭窄 12 例（占 6.15%）。

2.2　影响输尿管狭窄率的单因素分析：输尿管结石病程（输尿管结石病程越长，输尿管狭窄率越高）、多发结石（结石个数越多，输尿管狭窄率越高）、结石最大径（结石体积越大，输尿管狭窄率越高）、嵌顿结石伴有息肉（嵌顿结石伴有息肉的患者，其术后发生输尿管狭窄的风险较高）、炎性黏膜包裹结石（有炎性黏膜包裹结石的患者，其术后发生输尿管狭窄的风险较高）、激光碎石时间（术中激光碎石所需时间越长，术后发生输尿管狭窄率就越高）及钬激光损伤黏膜（术中被钬激光损伤黏膜的患者，其术后发生输尿管狭窄的风险较高）是影响输尿管镜下钬激光碎石术后发生输尿管狭窄的危险因素，见表 1。

2.3　影响输尿管狭窄率的多因素 Logistic 回归分析：见表 2、3。输尿管结石病程、结石最大径、嵌顿结石伴有息肉及钬激

DOI:10.11655/zgywylc2020.08.010

作者单位：037003 大同煤矿集团总医院泌尿外科

(C)1994-2023 China Academic Journal Electronic Publishing House. All rights reserved.　http://www.cnki.net

表 1 影响输尿管镜下钬激光碎石术后发生输尿管狭窄的单因素分析

影响因素		例数	输尿管未狭窄		输尿管狭窄		χ^2值	P值
			例数	%	例数	%		
性别	男性	282	259	91.84	23	8.16	0.096	0.757
	女性	203	188	92.61	15	7.39		
年龄	<65 岁	178	168	94.38	10	5.62	1.914	0.167
	≥65 岁	307	279	90.88	28	9.12		
	<25 岁	204	192	94.12	12	5.88		
体质量指数	25~30 kg/m^2	172	157	91.28	15	8.72	2.033	0.362
	≥30 kg/m^2	109	98	89.91	11	10.09		
患侧肾功能	正常	365	338	92.60	27	7.40	0.392	0.531
	受损	120	109	90.83	11	9.17		
合并上尿路感染	无	403	375	93.05	28	6.95	2.598	0.107
	有	82	72	87.80	10	12.20		
结石病程	<3 个月	183	178	97.27	5	2.73	14.181	<0.001
	3~6 个月	211	192	91.00	19	9.00		
	≥6 个月	91	77	84.62	14	15.38		
结石位置	上段	104	93	89.42	11	10.58	1.860	0.395
	中段	186	171	91.94	15	8.06		
	下段	195	183	93.85	12	6.15		
多发结石(≥2 个)	否	136	131	96.32	5	3.68	4.526	0.033
	是	349	316	90.54	33	9.46		
结石最大径	<0.7 cm	234	225	96.15	9	3.85	12.053	0.002
	0.7~1.0 cm	139	126	90.65	13	9.35		
	≥1.0 cm	112	96	85.71	16	14.29		
嵌顿结石伴有息肉	无	323	306	94.74	17	5.26	10.272	<0.001
	有	152	131	86.18	21	13.82		
炎性黏膜包裹结石	无	287	271	94.43	16	5.57	4.973	0.026
	有	198	176	88.89	22	11.11		
激光碎石时间	<30 min	297	281	94.61	16	5.39		
	30~60 min	151	135	89.40	16	10.60	7.602	0.022
	≥60 min	37	31	83.78	6	16.22		
钬激光损伤黏膜	否	368	346	94.02	22	5.98	7.283	0.007
	是	117	101	86.32	16	13.68		

表 2 影响因素及赋值说明

因素	赋值说明
结石病程(X1)	1:≤3 个月,2:3~6 个月,3:>6 个月
多发结石(X2)	0=否,1=是
结石最大径(X3)	1:<0.7 cm,2:0.7~1.0 cm,3:>1.0 cm
嵌顿结石伴有息肉(X4)	0=无,1=有
炎性黏膜包裹结石(X5)	0=无,1=有
激光碎石时间(X6)	1:<30 min,2:30~60 min,3:>60 min
钬激光损伤黏膜(X7)	0:否,1:是
输尿管狭窄情况(Y)	0:未狭窄,1:狭窄

光损伤黏膜是影响输尿管镜下钬激光碎石术后发生输尿管狭窄的独立危险因素，即在其他因素相同的情况下，输尿管结石病程每升高一个等级，术后输尿管狭窄的发生率增加 1.213 倍；结石最大径每增大一个等级，术后输尿管狭窄的发生率增加 0.896 倍；嵌顿结石伴有息肉的患者术后发生输尿管狭窄的风险是无息肉患者的 2.421 倍；术中被钬激光损伤黏膜的患者术后发生输尿管狭窄的风险是黏膜未损伤患者的 2.877 倍。

3 讨 论

输尿管镜碎石术是引起输尿管狭窄的较为常见的因素之一，无论是何种方式的取石，术后都有发生输尿管狭窄的风险。Kallidonis 等[4]研究显示输尿管镜下钬激光碎石术后输尿管狭窄率约为 3.5%~11.2%，王俊等[5]临床研究发现钬激光

(C)1994-2023 China Academic Journal Electronic Publishing House. All rights reserved. http://www.cnki.net

表 3　多因素 Logistic 回归分析

影响因素	B值	S.E值	Wald χ^2值	P值	OR值	95%CI
结石病程(X1)	0.879	0.238	10.027	0.007	2.213	1.516,2.914
结石最大径(X3)	0.712	0.219	8.944	0.027	1.896	1.136,2.650
嵌顿结石伴有息肉(X4)	1.340	0.341	14.650	<0.001	2.421	1.850,3.194
钬激光损伤黏膜(X7)	1.428	0.332	17.336	<0.001	2.877	2.055,3.391
常数项	0.855	0.234	0.234	1.762	0.324	1.531

碎石术后输尿管狭窄率为 5.95%。本研究中患者术后输尿管狭窄率约为 7.84%，与相关文献所报道结果基本相近。

本研究显示：输尿管结石病程、结石最大径、嵌顿结石伴有息肉及钬激光损伤黏膜是影响输尿管镜下钬激光碎石术后发生输尿管狭窄的独立危险因素。分析其原因：首先，若患者的结石较大且在输尿管内嵌顿时间较长，则结石周围可形成大量息肉而造成输尿管炎性水肿的发生。引导导丝通过该段输尿管时，极易造成黏膜损伤、导致出血、感染、瘢痕等不良事件发生，故嵌顿结石更易导致输尿管狭窄[4]。因而在处理嵌顿结石，尤其是较大较硬的结石时，不应沿结石与黏膜间用较大功率的钬激光碎石，而应该采用中央穿孔法由内向外逐步碎石。其次，由于钬激光能量较高，长时间使用可造成输尿管黏膜局部热损伤，尤其在击碎结石边缘后，可见广泛破坏的输尿管黏膜[5]。本次研究也发现多数患者均为由于输尿管黏膜损伤所致的瘢痕性狭窄。可见，钬激光在粉碎结石碎块时，极易损伤输尿管黏膜。所以，我们建议选择点踩、点碎或取石钳取出小结石。此外，输尿管镜操作技巧有关，输尿管镜属于泌尿外科较易上手的微创技术，难免对输尿管黏膜有机械性损伤。例如，在没有充分暴露视野时，盲目进镜、退镜均会造成输尿管黏膜损伤；在使用取石钳取出结石时，如果取石钳未暴露在镜子视野中央，则极易造成输尿管黏膜的划伤，最终导致输尿管狭窄的发生。

综上所述，输尿管结石病程越长、结石直径越大且有息肉形成，或者在术中有钬激光损伤黏膜的患者，在术后发生输尿管狭窄的可能性较高。因此，泌尿外科医生在术前应进行有效评估，选择合适的方案进行治疗。

参考文献

[1] 李晓明，阮殿喜.钬激光碎石术治疗输尿管结石后并发输尿管狭窄的相关因素研究[J].中国社区医师，2019，35(1)：31-32.

[2] 叶旭华，米其武，罗杰鑫，等.输尿管结石行输尿管镜下碎石术后并发输尿管狭窄的危险因素分析[J/CD].中华腔镜泌尿外科杂志(电子版)，2017，11(1)：40-42.

[3] 邓定凯.输尿管镜钬激光碎石术与体外冲击波碎石术治疗输尿管结石的临床比较[J].健康必读，2019，27(14)：73.

[4] Kallidonis P, Ntasiotis P, Knoll T. Minimally invasive surgical ureterolithotomy versus ureteroscopic lithotripsy for large ureteric stones: a systematic review and meta-analysis of the literature[J]. Eur Urol Focus, 2017, 3(6): 554-566.

[5] 王俊，郭志新，吴洪磊，等.输尿管软镜钬激光碎石术治疗输尿管上段结石并发输尿管狭窄的危险因素分析[J].临床泌尿外科杂志，2018，33(7)：532-536.

[6] 钟华，廖开森，王斌，等.输尿管镜下钬激光碎石术治疗输尿管结石后出现输尿管狭窄原因分析[J].浙江临床医学，2018，20(5)：868-869.

[7] 杜江.输尿管镜钬激光碎石术治疗输尿管结石的可行性及优势分析[J/CD].临床医药文献电子杂志，2019，6(19)：86-87.

(收稿日期：2019-11-04)

(C)1994-2023 China Academic Journal Electronic Publishing House. All rights reserved.　http://www.cnki.net

输尿管结石行输尿管镜下碎石术后并发输尿管狭窄的危险因素分析

古源

摘　要：目的：探究并分析输尿管结石行输尿管镜下碎石术后并发输尿管狭窄的危险因素。方法：选取2017年6月-2018年12月我院收治的输尿管结石行输尿管镜下碎石术后并发输尿管狭窄的患者142例为该研究对象，按照术后随访结果的不同，将其分为两组，各71例，非狭窄组，即对照组，狭窄组，即研究组，详细分析两组患者的危险因素。结果：单因素结果表明：结石直径、病程以及输尿管损伤等因素和输尿管软镜碎石术后输尿管狭窄的产生息息相关，差异具有统计学意义（$P<0.05$）；采用多因素Logistic分析可得：结石直径、病程、输尿管损伤等因素是导致该疾病发生的关键危险因素，差异具有统计学意义（$P<0.05$）。结论：由于输尿管结石行输尿管镜下碎石术后的病程长、输尿管受损与结石直径大等因素会大大提高患者输尿管发狭窄的几率，故术前对患者的病情进行详细的评估显得格外重要，同时术中操作须谨慎，术后及时预防。

关键词：输尿管结石；输尿管镜下碎石术；并发输尿管狭窄；危险因素

输尿管狭窄在输尿管结石碎石术中属于一种最为普遍的疾病。不管是开放取石、内镜取石，还是腹腔镜取石皆会引起术后输尿管狭窄的现象。根据不同的文献显示，术式不同可能发生率存在一定的差异性，其处于3%~10%之间[1]。所以本研究为了分析输尿管结石行输尿管镜下碎石术后并发输尿管狭窄的危险因素，选取了142例实施了该手术患者的临床资料为此研究对象，现报道如下：

1 资料与方法

1.1 一般资料

选取2017年6月-2018年12月我院收治的输尿管结石行输尿管镜下碎石术后并发输尿管狭窄的患者142例为该研究对象，按照术后随访结果的不同，将其分为两组，各71例，其中年龄26~78岁，平均（56.7±2.9）岁。所有入选患者的临床资料具有可比性（$P>0.05$），且均知情同意本研究，同时经过医院伦理委员会批准。

纳入标准：（1）全部患者在术前皆通过腹部平片、全泌尿系CT、泌尿系彩超以及静脉尿路造影等被确诊成为输尿管上段结石；（2）首次进行输尿管软镜钬激光碎石者；（3）病例资料齐全者。排除标准：（1）伴有合并肾结石或者输尿管多发结石患者；（2）原有输尿管手术病史者；（3）伴有合并凝血功能异常、心肺功能障碍者。

1.2 方法

所有受试对象皆使用硬膜外麻醉，在输尿管镜的指导下完成碎石、取石等操作。对照组采用光纤传导激光能量，从结石核心部位向周围粉碎到2mm下即可。若结石下面狭窄或息肉等，就先去除息肉及狭窄环。针对嵌顿性结石，就先把包裹组织切开，再碎石。研究组就用冲击针把结石粉碎到2mm之下，使结石随尿液排出，直径相对较大的结石，则使用结石钳取出。两组患者在术后将双J管留置2-3周，若术中出现输尿管受训的现象，则延长到8-10周[2]。

1.3 观察指标

观察并分析两组患者的危险因素，其主要包括结石直径、病程、结石嵌顿、手术时间和输尿管损伤等。

1.4 统计学方法

数据统计使用SPSS22.0，计数使用X^2（%），计量资料使用t检测（$\bar{x}\pm s$），以$P<0.05$为有统计学意义。

2 结果

单因素结果表明：结石直径、病程以及输尿管损伤等因素和输尿管软镜碎石术后输尿管狭窄的产生息息相关，差异具有统计学意义（$P<0.05$），具体见表1。

表1 输尿管结石行输尿管镜下碎石术后发生输尿管狭窄文献因素上分析（例）

影响因素	对照组（n=71）	研究组（n=71）	X^2	P
性别				
男	38	40	0.056	>0.05
女	33	31		
年龄/岁				
≥60	35	37	0.853	>0.05
<60	36	34		
糖尿病				
是	33	39	1.689	>0.05
否	38	32		
病程/月			9.885	<0.05
≥3	45	22		
<3	26	49		
结石直径/cm				
<1	50	20	5.695	<0.05
≥1	21	51		
输尿管受损				
有	53	48	10.136	<0.05
无	18	23		

采用多因素Logistic分析可得：结石直径、病程、输尿管损伤等因素是导致该疾病发生的关键危险因素，差异具有统计学意义（$P<0.05$），具体见表2。

表2 术后输尿管狭窄的多因素Logistic分析

因素	β	OR值	95%CI	标准误	P
病程	1.479	4.372	1.098-17.568	4.326	<0.05
结石直径	-1.389	0.265	0.086-0.745	0.469	<0.05
输尿管损伤	-1.967	0.287	0.032-0.557	0.726	<0.05

3 讨论

近几年，伴随着输尿管医疗科技的改进，使得肿瘤、输尿管结石等疾病的诊治取得了很大的进步，但是因为输尿管镜的入侵操作，对输尿管也造成了严重的损伤。

采用钬激光碎石导致输尿管手术的原因不仅和初学者的经验、操作是否娴熟密切相关，还与强制性进、退镜等操作有关。但在本研究中并未发现双J管置留时间的延长是保护输尿管狭窄重要因素，反之，置留时间过长者，输尿管狭窄的产生率偏高，此外，还会大大提高患者并发症的产生率[3]。本研究结果显示，结石直径、病程、输尿管损伤等因素是导致该疾病发生的关键危险因素，差异具有统计学意义（$P<0.05$）。

参考文献

[1]吕佳,章超龙,纪阿林,etal.输尿管软镜碎石术后肾包膜下血肿的危险因素分析[J].重庆医科大学学报,2018,v.43(04):62-64.

[2]王强,边家盛.输尿管镜下气压弹道碎石治疗输尿管下段结石的临床疗效[J].山东医药,2017,57(1):94-96.

[3]王强,边家盛.输尿管镜下气压弹道碎石治疗输尿管下段结石的临床疗效[J].山东医药,2017,18(01):100-102.

（作者单位：安徽省第二人民医院）

(C)1994-2023 China Academic Journal Electronic Publishing House. All rights reserved. http://www.cnki.net

激光腔内碎石术后并发输尿管狭窄的预防研究进展

秦鹏飞[1] 黄挺[2] 方立[2] 程跃[2△]

［摘要］ 激光技术的广泛应用极大提高了泌尿外科腔内碎石的手术效率，而其术后出现的输尿管狭窄是一种非常危险的并发症，一旦发生便难以处理。目前认为术中机械损伤和热损伤是其主要成因，尤其是激光热损伤，近年来引起了学者们的重点关注。本文就激光腔内碎石术后并发输尿管狭窄的发生机制、危险因素及预防策略的研究进展作一综述。

［关键词］ 激光；碎石术；输尿管狭窄；热损伤；预防
DOI：10.13201/j.issn.1001-1420.2021.08.015
［中图分类号］ R693.5 ［文献标志码］ A

Research progress on the prevention of ureteral stricture after laser lithotripsy

QIN Pengfei[1] *HUANG Ting*[2] *FANG Li*[2] *CHENG Yue*[2]
([1]School of Medicine, Ningbo University, Ningbo, Zhejiang, 315211, China; [2]Center of Urology and Nephrology, Ningbo First Hospital)
Corresponding author: CHENG Yue, E-mail: dongbaba2@hotmail.com

Abstract The wide application of laser technology has greatly improved the efficiency of lithotripsy in urology. However, postoperative ureteral stricture is a very dangerous complication which is difficult to deal with once it occurs. Currently, it is believed that mechanical damage and thermal damage are the main causes, especially laser thermal damage, which has attracted the attention of scholars in recent years. In this paper, the pathogenesis, risk factors and prevention strategies of ureteral stricture after laser lithotripsy are reviewed.

Key words laser; lithotripsy; ureteral stricture; thermal damage; prevention

激光技术目前已广泛应用于泌尿外科各类腔内碎石术式中[1]，其中钬激光（Holmium：YAG laser）是临床较为主流的选择。伴随着较高的碎石效率与清石率[2]，激光腔内碎石术后并发输尿管狭窄的发生率也在逐渐增长，有国外文献报道其发生率可达 2.95%[3]，国内研究也出现过 4.09%的术后高狭窄率[4]，这引起了学者们的广泛关注。输尿管狭窄会导致不同程度肾积水，且被发现时往往已伴有肾功能的损害，属于较严重的并发症。因此，术后高狭窄率背后的原因以及如何减少此类并发症的发生是学者们研究聚焦的方向。本文就激光腔内碎石术后并发输尿管狭窄的可能发生机制、相关危险因素及相应预防策略作一综述，为临床医师们解决这类问题提供一些思路。

1 术后输尿管狭窄的可能发生机制

1.1 机械性损伤-炎症纤维化

传统研究中，更多关注点往往在机械性因素于术后输尿管狭窄中的作用。包括术前结石长期嵌顿产生的黏膜慢性损伤[5]，术中腔镜、激光光纤、导引鞘等对输尿管黏膜的机械性牵拉和刮擦，激光对黏膜的直接击打作用以及术后残留结石碎块的损伤等[6]。机械性损伤会破坏输尿管组织造成局部缺血和炎症反应，黏膜上皮细胞出现肥大、增生和水肿并进一步导致纤维化-管腔狭小的发生[7]。然而，Fam 等[8]通过一项前瞻性研究得出输尿管黏膜的机械性损伤及炎症反应其实是可逆的，尚不能认为其是导致输尿管狭窄的危险因素。

1.2 激光热效应损伤

近些年越来越多的学者开始关注到激光的热效应在术后输尿管狭窄形成中的作用。钬激光的工作原理是利用光-热效应（photothermal）和光-机械效应（photomechanical）进行熔石、碎石[9]。虽然钬激光的碎石范围只有 0.5～1.0 mm，但由于其波长（2120 nm）与水的最大吸收峰（1940 nm）非常接近[10]，大部分能量会被激光纤维头周围的液体吸收从而产生热效应[11]。已有研究表明，人体组织的热损伤阈值大约为 43℃，在该温度下输尿管组织已开始发生蛋白质凝固变性，异常的转录、翻译及 DNA 复制，引起细胞凋亡，进而产生病理性瘢痕组织并引起输尿管狭窄[12-14]。若在 43℃下暴露 120 min，则直接可致细胞组织发生不可逆性的坏死。且每超过阈值温度 1℃，对相同数量的细胞造成损伤所需的时间将减少一半[15]。在 Winship 等[16]的体外模型实验中，常规灌注流量及钬激光

[1] 宁波大学医学院（浙江宁波，315211）
[2] 宁波市第一医院泌尿肾病中心
△ 审校者
通信作者：程跃，E-mail：dongbaba2@hotmail.com

(C)1994-2022 China Academic Journal Electronic Publishing House. All rights reserved. http://www.cnki.net

设置下(尤其在输尿管软镜下且钬激光功率≥10 W时),钬激光头端附近液体的温度可在 1 s 内达到热损伤阈值。这提示热效应也是激光腔内碎石术后输尿管狭窄形成的重要机制。

2 输尿管狭窄形成的主要危险因素

2.1 嵌顿性结石

长时间嵌顿的结石,其周围输尿管黏膜往往水肿严重且常伴息肉形成,这使管腔操作空间变小从而间接增大术中激光对黏膜直接损伤的机会[9]。且这类患者输尿管黏膜受到慢性炎症刺激更持久,组织增生和纤维化严重。Darwish 等[10]认为,嵌顿的结石因堵塞管腔而使术中灌注液的循环减弱,可导致结石周围的压力和温度升高,这加重了对输尿管的损害。

2.2 大负荷结石

结石负荷大的患者常伴有输尿管梗阻与肾积水,尤其高位结石,这类病例碎石难度大[11],手术时间久。Sorokin 等[12]通过对 10 年来病例的回顾性研究得出:结石体积对手术时间的影响最大,并且结石体积每增加 100 mm^3,手术碎石时间约增加 2 min。这就意味着,术中激光热效应对输尿管黏膜的损伤也随之增加。

2.3 灌注不足

灌注液的循环引流可有效带走激光产生的多余热量,在灌注量相对不足的情况下,术中输尿管腔内、肾盂内很快出现高温[13],输尿管壁受到热损伤,引起其术后纤维化狭窄的出现。Wollin 等[14]测量了 0.2 J×50 Hz、0.6 J×6 Hz、0.8 J×8 Hz、1.0 J×10 Hz、1.0 J×20 Hz 5 组分别在灌注量为 0、50、100 mL/min 时钬激光持续激活 60 s 内的水温变化,结果显示灌注量为 0 时,5 组最高温度均超过热损伤阈值(43℃),灌注量为 50 mL/min 时,仅有 1.0 J×20 Hz 组的最高温度到阈值,当灌注量达 100 mL/min 时,5 组的最高温度均未超过阈值。这表明,要想在术中防止热损伤的发生,对灌注量的要求可能会非常高。

2.4 术中危险操作

缺乏经验的术者往往操作不熟练,除了会发生牵拉刮擦输尿管、反复进退镜等机械性伤害外[15],还会出现因激光纤维定位不精准而对黏膜造成直接破坏、单次长时间持续激活激光碎石产生高温热损伤等现象,这些不当操作也是导致术后并发症不可忽视的因素[16]。

3 术后输尿管狭窄的预防策略

近年来国内外学者进行了大量的随机对照试验、回顾性分析以及体外/体内模型研究,旨在寻找出有效的手段以解决激光腔内碎石术后输尿管狭窄的问题。相比于以往着眼于输尿管狭窄形成后的治疗方式,今天的学者们则把更多的目光聚焦在并发症出现之前的预防策略上,力求降低该并发症的发生率。

3.1 术式的选择

以往指南建议,对于直径≥2 cm 的结石更推荐行 PCNL 治疗[17]。然而,设备仪器的改进包括镜径的缩小、镜体偏转力的加强、光学成像的优化以及一次性器材的应用,尤其是输尿管镜通道鞘(ureteral access sheath,UAS)的应用与改良十分有效地保护了输尿管黏膜免受重复的机械性损伤并且改善了灌注液的引流[18-20],这些都导致越来越多的术者在处理 2 cm 以上大结石时尝试选择 URL/FURL[21]。已有系统综述报道,对于≥2 cm 的结石,目前 RIRS 的清石率可达到达 91%[22]。但陈珂宇等[23]研究发现,输尿管镜/软镜在治疗大结石(直径≥2 cm)时,激光持续激活时间可从几秒延长达几十秒,热效应显著。同时,在实际操作中灌流率其实并不恒定且往往低于设定值,击打高位结石时为防止结石被冲回肾盂,如果调低灌注量甚至会有零灌注的情况出现,这更使局部温度短时间内骤增至安全临界点[24-25]。而在 PCNL 术中,由于鞘的直径较大,使灌注液回水通畅,且体积稍大的结石也能被直接取出,避免了长时间的钬激光激活,碎石过程中局部热效应控制较好。因此,对于直径≥2 cm 的结石,尤其是高位结石,PCNL 在术中温度控制及对术后输尿管狭窄的预防中,较 URL/FURL 仍具有一定理论优势[26]。

另外,对于术前评估结石情况复杂合并危险因素的病例(如长期嵌顿结石、大负荷结石、合并感染)[27],为减少因手法不娴熟导致的不当操作如在术野不清的情况下盲目碎石、单次长时间激活激光等,缩短输尿管在危险因素下的暴露时间,降低术后输尿管狭窄发生率,更推荐由高年资的医生施行手术。

3.2 激光参数的设置

合理的激光参数即能量和频率设置是非常重要的,Liang 等[27]建立了体外模型来模拟输尿管镜碎石的过程,他们认为碎石应首先从低功率设置开始,对大多数设备来说功率设置不应超过 20 W,因为此功率已能处理绝大部分的结石。他们的实验中,在 1.0 J×20 Hz 的功率设置配合 10 mL/min 的灌流量下,连续激活钬激光仅 3 s,即可使周围水温达到 56.3℃之高,这已经远高于热损伤阈值[13-14]。另外,在同样的功率设置下,比如 1.0 J×20 Hz 与 2.0 J×10 Hz 均为 20 W,但前者测得的水温在任何时间点都明显高于后者,这表明高频低能模式可能比高能低频模式的热效应更显著。而在清石率上,Li 等[28]的研究认为低能高频设置与高能低频设置的表现相似。因此,尽量避免在输尿管中使用相对高频模式碎石可能更有助于预防术

(C)1994-2022 China Academic Journal Electronic Publishing House. All rights reserved. http://www.cnki.net

后管腔狭窄的发生。

3.3　灌注液的引流

在腔内手术中，灌注液除了能清晰视野、冲回碎石外，还能吸收大部分激光热量，所以灌注量对术后并发症的预防也至关重要。前文提到 Wollin 等[18]的对照试验表明，要想在术中做到杜绝热损伤的发生，适当增加灌注即能有效缓冲激光的热效应。然而，盲目要求高灌注量可能会导致肾盂内压过高而增加术后感染的风险。所以，在灌注量问题上如何平衡热损伤的风险与肾盂高压的风险值得学者们进一步的探究。目前，负压吸引工作鞘(negative pressure ureteral access sheath)的应用已为解决此问题提供了一个可行的角度。例如，邓小林等[19]研发了一种可监测肾盂内压的输尿管软镜负压吸引鞘，吸引口与负压泵相连，持续抽吸灌注液，实现腔内“降压”的同时还能“降温”。因传统 URL/FURL 术中液体流出通道较小较长，灌注液循环受阻，致输尿管腔内散热效果不佳；又无高效的排石方法，主要通过高压灌注回流和手动钳取，花费了大量取石时间[20]。而使用负压吸引鞘后，灌注量就可适当增大，在高循环流速下，击碎的结石连同多余的热量被快速排出体外[21]，既阻止了热量的累积又节省了部分取石时间以缩短输尿管壁在危险因素下的暴露时间，这对管壁损伤乃至术后狭窄的预防有积极作用。相似的，Fang 等[22]也着眼于灌注液的引流问题，他们在体外猪肾模型中模拟钬激光碎石术以对比不同“镜鞘比”下的肾盂内压及灌注液流速。镜鞘比越小，即镜的外径与鞘内通道直径之比越小，镜与鞘之间的出水通道越大，会加速灌注液的引流，所以适当减小镜鞘比理论上可保护肾脏及输尿管免受高压、高温的损害。最终得出镜鞘比≤0.75 是较为安全的。目前，他们仅对镜鞘比与肾盂内压的关系研究作了报道，而镜鞘比对钬激光热效应的影响仍有待更进一步的探究。

3.4　灌注液的选择

有学者提出应用低温灌注液的想法，试图用低于生理温度(36.5℃)的灌注液来吸收更多热量以保护肾脏及输尿管[23]。然而，Buttice 等[24]的研究表明常温盐水(24.5℃)与 36.5℃盐水在相同钬激光设置及灌注量下的散热能力差异无统计学意义，但常温盐水会降低人体核心温度反而会引起低体温、寒战、低氧血症等并发症。所以，实际操作中仍然更推荐使用接近生理温度的盐水。

3.5　激光碎石方法

对于较大结石，尤其是嵌顿性结石，碎石方法尤为重要。刘为池等[7]报道了击碎结石边缘发现输尿管黏膜损伤的经验。叶照华等[4]认为长期嵌顿的大结石周围输尿管黏膜往往水肿严重，管壁黏膜与结石贴合紧密，甚至存在黏膜下结石，故此时采用“钻孔法”从结石中部开始击打比“周边蚕食法”会更安全稳妥[25]。结石周边与管壁黏膜相接触的部分应夹离管壁后，再行碎石[26]。也有学者[27]建议先将嵌顿结石朝输尿管近端移动后再行碎石以获得更大的操作空间，但仍需进一步实验验证。Dretler 等[28]有报道，激光碎石术后遗留的残余草酸钙结石容易定植于输尿管壁上引发异物巨细胞反应生成异物肉芽肿最终堵塞管腔使之狭窄。对此，我国学者提出的“粉末化碎石”[4]概念有一定的理论指导意义，即在术中将结石粉碎至＜2 mm的碎片，此等大小的结石能在术后顺利排出体外而不会残留形成石街。术者可以 200 μm 钬激光光纤为参照，将结石粉碎至其直径的 10 倍以下(即 2 mm)，减少残余结石的沉积定植。

另外，手术中术者为了提高碎石效率，激光处于持续激活状态的情况时常发生，Aldoukhi 等[29]进行了体内猪肾模型实验，结果表明相邻两次钬激光激活所需要的间隔时间实际应大于有效碎石时间，即采取“间歇性激活”能有效减少热效应的产生。可以预见，“操作者占空比(operator duty cycle)”将会是未来研究的一个重要方向。

3.6　双 J 管的留置

钬激光碎石术后常规留置双 J 管引流，但术后双 J 管的留置一直是较富争论的话题，Ozyer 等[30]通过回顾性分析发现在同侧输尿管内留置两根双 J 管的引流效果更佳。这与刘杰等[31]的报道相符，他们认为单根双 J 管在一些狭小输尿管中会像“塞子”一样堵塞管腔，尿液只能从引流管管腔流出，一旦管腔堵塞则形成无效引流。而两根双 J 管之间可相互支撑，使尿液从双管的间隙中也可流出，减少尿外渗，降低输尿管瘢痕发生率，且两根双 J 管间的相对运动可减少粘连的形成[32]。因此，对于存在较严重输尿管损伤(包括机械性损伤和热损伤)可能性的患者，术后留置两根双 J 管是一种可尝试的选择。关于双 J 管的留置时间问题，刘为池等[7]的经验是对术中存在明显黏膜损伤的患者，应适当延长留置时间至 8～12 周。然而，叶照华等[33]的研究并未发现延长双 J 管留置时间为输尿管狭窄的保护因素，相反，他们认为留置超过 4 周者输尿管狭窄率会更高。另外，Assimos 等[34]通过一项多中心前瞻性研究发现，术前留置双 J 管可明显提高肾结石手术清石率并减少并发症的发生，这可能与通道鞘置入成功率的提高使输尿管损伤减少有关[35]。

3.7　药物预防

有学者研究发现，血管紧张素转换酶抑制剂(ACE-I)如卡托普利可通过降低表皮生长因子(EGF)、纤维蛋白原、Ⅰ型胶原蛋白 a2(Col Ⅰa2)

(C)1994-2022 China Academic Journal Electronic Publishing House. All rights reserved.　http://www.cnki.net

等的表达以抑制纤维化瘢痕的形成，也可应用于预防激光腔内碎石术后并发输尿管狭窄[60]，但目前该理论仍需进一步研究验证。

4 总结与展望

激光腔内碎石术因其微创、安全、清石效率高等众多优点，已成为泌尿系结石的主流治疗手段。但由于其存在对输尿管壁的机械性损伤和热损伤，术后并发输尿管狭窄的问题正逐渐得到关注。目前，对其预防的重点主要在激光设置、灌注问题以及碎石方法上。部分危险因素如嵌顿、大负荷结石仍无法从根源上去除，并且对于术中持续存在的激光热损伤，依然缺乏切实可靠的术中监测手段及保护措施。这是一项复杂但具有意义的任务，有待之后的学者继续探索，以期进一步提高激光腔内碎石术的安全性及减少术后输尿管狭窄并发症的发生率。

参考文献

[1] 那彦群，叶章群.中国泌尿外科疾病诊断治疗指南手册 2014 版[M].北京：人民卫生出版社，2014：141.

[2] Ercil H，Alma E，Bas O，et al.Safety and Efficacy of Pneumatic Lithotripters Versus Holmium Laser on Multiple Ureteral Calculi[J].Arch Iran Med，2016，19(11)：786-790.

[3] Li L，Pan Y，Weng Z，et al.A Prospective Randomized Trial Comparing Pneumatic Lithotripsy and Holmium Laser for Management of Middle and Distal Ureteral Calculi[J].J Endourol，2015，29(8)：883-887.

[4] 刘为池，刘刚，唐锦护，等.输尿管镜下钬激光碎石术后并发输尿管狭窄回顾性分析[J].临床泌尿外科杂志，2014，29(7)：573-574，580.

[5] Roberts WW，Cadeddu JA，Micali S，et al.Ureteral stricture formation after removal of impacted calculi[J].J Urol，1998，159(3)：723-726.

[6] Dretler SP，Young RH.Stone granuloma：a cause of ureteral stricture[J].J Urol，1993，150(6)：1800-1802.

[7] Morgentaler A，Bridge SS，Dretler SP.Management of the impacted ureteral calculus[J].J Urol，1990，143(2)：263-266.

[8] Fam XI，Singam P，Ho CC，et al.Ureteral stricture formation after ureteroscope treatment of impacted calculi：a prospective study[J].Korean J Urol，2015，56(1)：63-67.

[9] Jacques SL.Laser-tissue interactions.Photochemical，photothermal，and photomechanical[J].Surg Clin North Am，1992，72(3)：531-558.

[10] Molina WR，Silva IN，Donalisio da Silva R，et al.Influence of saline on temperature profile of laser lithotripsy activation[J].J Endourol，2015，29(2)：235-239.

[11] Wang XK，Jiang ZQ，Tan J，et al.Thermal effect of holmium laser lithotripsy under ureteroscopy[J].Chin Med J(Engl)，2019，132(16)：2004-2007.

[12] Winship B，Wollin D，Carlos E，et al.The Rise and Fall of High Temperatures During Ureteroscopic Holmium Laser Lithotripsy[J].J Endourol，2019，33(10)：794-799.

[13] van Rhoon GC，Samaras T，Yarmolenko PS，et al.CEM43℃ thermal dose thresholds：a potential guide for magnetic resonance radiofrequency exposure levels?[J].Eur Radiol，2013，23(8)：2215-2227.

[14] Kampinga HH.Thermotolerance in mammalian cells.Protein denaturation and aggregation，and stress proteins[J].J Cell Sci，1993，104(Pt 1)：11-17.

[15] Sapareto SA，Dewey WC.Thermal dose determination in cancer therapy[J].Int J Radiat Oncol Biol Phys，1984，10(6)：787-800.

[16] Darwish AE，Gadelmoula MM，Abdelkawi IF，et al.Ureteral stricture after ureteroscopy for stones：A prospective study for the incidence and risk factors[J].Urol Ann，2019，11(3)：276-281.

[17] Sorokin I，Cardona-Grau DK，Rehfuss A，et al.Stone volume is best predictor of operative time required in retrograde intrarenal surgery for renal calculi：implications for surgical planning and quality improvement[J].Urolithiasis，2016，44(6)：545-550.

[18] Wollin DA，Carlos EC，Tom WR，et al.Effect of Laser Settings and Irrigation Rates on Ureteral Temperature During Holmium Laser Lithotripsy：an In Vitro Model[J].J Endourol，2018，32(1)：59-63.

[19] Leijte JA，Oddens JR，Lock TM.Holmium laser lithotripsy for ureteral calculi：predictive factors for complications and success[J].J Endourol，2008，22(2)：257-260.

[20] Kaplan AG，Lipkin ME，Scales CD Jr，et al.Use of ureteral access sheaths in ureteroscopy[J].Nat Rev Urol，2016，13(3)：135-140.

[21] Turk C，Neisius A，Petrik A，et al.EAU guidelines on urolithiasis[S].2020.

[22] Geraghty R，Abourmarzouk O，Rai B，et al.Evidence for Ureterorenoscopy and Laser Fragmentation (URSL) for Large Renal Stones in the Modern Era[J].Curr Urol Rep，2015，16(8)：54.

[23] 陈柯宇，王亮.钬激光碎石术后输尿管狭窄的相关因素分析[J].四川医学，2018，39(12)：1345-1349.

[24] Buttice S，Sener TE，Proietti S，et al.Temperature Changes Inside the Kidney：What Happens During Holmium：Yttrium-Aluminium-Garnet Laser Usage?[J].J Endourol，2016，30(5)：574-579.

[25] Aldoukhi AH，Hall TL，Ghani KR，et al.Caliceal Fluid Temperature During High-Power Holmium Laser Lithotripsy in an In Vivo Porcine Model[J].J Endourol，2018，32(8)：724-729.

[26] 周乐，胡换春，汪波.单发输尿管结石患者行输尿管镜下钬激光碎石术后狭窄的危险因素分析[J].国际泌尿系统杂志，2020，40(2)：231-234.

[27] Liang H，Liang L，Yu Y，et al.Thermal effect of holmium laser during ureteroscopic lithotripsy[J].BMC

(C)1994-2022 China Academic Journal Electronic Publishing House. All rights reserved. http://www.cnki.net

Urol，2020，20(4)：69.

[28] Li R，Ruckle D，Kehoila M，et al. High-Frequency Dusting Versus Conventional Holmium Laser Lithotripsy for Intrarenal and Ureteral Calculi[J]. J Endourol，2017，31(3)：272-277.

[29] 邓小林，宋乐明，钟久庆，等. 可智能监控肾盂内压的输尿管软镜吸引取石术的临床应用[J]. 中华泌尿外科杂志，2016，37(5)：385-388.

[30] Yang Z，Song L，Xie D，et al. The New Generation Mini-PCNL System-Monitoring and Controlling of Renal Pelvic Pressure by Suctioning Device for Efficient and Safe PCNL in Managing Renal Staghorn Calculi[J]. Urol Int，2016，97(1)：61-66.

[31] 李天，盛明，李逊，等. 输尿管负压吸引鞘在输尿管软镜碎石术中的价值探讨[J]. 中国内镜杂志，2018，24(2)：33-37.

[32] Fang L，Xie G，Zheng Z，et al. The Effect of Ratio of Endoscope-Sheath Diameter on Intrapelvic Pressure During Flexible Ureteroscopic Lasertripsy[J]. J Endourol，2019，33(2)：132-139.

[33] 叶照华，米其武，罗杰鑫，等. 输尿管结石行输尿管镜下碎石术后并发输尿管狭窄的危险因素分析[J/OL]. 中华腔镜泌尿外科杂志(电子版)，2017，11(1)：40-42.

[34] 程跃，严泽军，谢国海，等. "粉末化碎石"在输尿管软镜治疗肾结石中的应用[J]. 微创泌尿外科杂志，2013，2(3)：210-212.

[35] Ozyer U，Dirim A. Tandem ureteral stents in the management of double-J stent dysfunction in gynecological malignancies[J]. Diagn Interv Imaging，2017，98(9)：601-608.

[36] 刘杰，薛江辉，冉光勇，等. 同侧两根双 J 管引流在结石伴息肉导致输尿管狭窄患者中的应用[J/OL]. 中华腔镜泌尿外科杂志(电子版)，2019，13(4)：251-254.

[37] 何永忠，李逊，杨炜青，等. 电刀内切开联合球囊扩张治疗输尿管狭窄[J/OL]. 中华腔镜泌尿外科杂志(电子版)，2017，11(2)：37-40.

[38] Assimos D，Crisci A，Culkin D，et al. Preoperative JJ stent placement in ureteric and renal stone treatment：results from the Clinical Research Office of Endourological Society (CROES) ureteroscopy (URS) Global Study[J]. BJU Int，2016，117(4)：648-654.

[39] 杨炜青，李逊，何永忠，等. 输尿管软镜碎石术前留置双 J 管的随机对照研究[J/OL]. 中华腔镜泌尿外科杂志(电子版)，2016，10(2)：26-29.

[40] Pan J，Xue W，Chen Q，et al. Antifibrotic role of captopril after ureteral injury[J]. Urol Int，2012，89(4)：418-424.

(收稿日期：2020-12-12)

(上接第 662 页)

[49] Anan G，Yoneyama T，Noro D，et al. The Impact of Glycosylation of Osteopontin on Urinary Stone Formation[J]. Int J Mol Sci，2019，21(1)：93.

[50] Li X，Liu K，Pan Y，et al. Roles of osteopontin gene polymorphism (rs1126616)，osteopontin levels in urine and serum，and the risk of urolithiasis：a meta-analysis [J]. Biomed Res Int，2015，2015：315043.

[51] Safarinejad MR，Shafiei N，Safarinejad S. Association between polymorphisms in osteopontin gene (SPP1) and first episode calcium oxalate urolithiasis[J]. Urolithiasis，2013，41(4)：303-313.

[52] Qin J，Cai Z，Xing J，et al. Association between calcitonin receptor gene polymorphisms and calcium stone urolithiasis：A meta-analysis [J]. Int Braz J Urol，2019，45(5)：901-909.

[53] Chou YH，Juo SH，Chiu YC，et al. A polymorphism of the ORAI1 gene is associated with the risk and recurrence of calcium nephrolithiasis[J]. J Urol，2011，185(5)：1742-1746.

[54] Stechman MJ，Loh NY，Thakker RV. Genetics of hypercalciuric nephrolithiasis：renal stone disease [J]. Ann N Y Acad Sci，2007，1116：461-484.

(收稿日期：2020-04-30)

(C)1994-2022 China Academic Journal Electronic Publishing House. All rights reserved.　http://www.cnki.net

·论著·

输尿管软镜钬激光碎石术后继发输尿管狭窄的相关性因素分析

王淇超[1] 曹敬毅[1] 孙卫兵[2] 王乾[1] 宋墨[1] 吴刚[1] 葛艳[1]
[1]江苏大学附属徐州医院,徐州市肿瘤医院泌尿外科,徐州 221005;[2]大连医科大学附属第二医院泌尿外一科,大连 116027
通信作者:曹敬毅,Email:cjy_197510@163.com

【摘要】 **目的** 探讨影响输尿管软镜钬激光碎石术治疗输尿管上段结石继发输尿管狭窄的相关因素。**方法** 回顾性分析2011年1月至2020年6月于徐州市肿瘤医院行输尿管软镜下钬激光碎石术治疗的258例输尿管上段结石患者的临床资料,依据术后是否出现输尿管狭窄分为狭窄组(15例)及非狭窄组(243例)。分析两组患者的年龄、结石直径、是否合并糖尿病等临床资料的差异,运用logistic回归分析术后引发输尿管狭窄的相关因素。**结果** 单因素分析显示:病程、结石直径、结石嵌顿、息肉包裹、输尿管损伤、手术时间与术后输尿管狭窄的发生均具有相关性(均$P<0.05$)。多因素logistic回归分析显示:病程、结石直径、结石嵌顿及输尿管损伤为术后发生输尿管狭窄的独立危险因素(均$P<0.05$)。**结论** 病程长、结石较大、存在结石嵌顿及术中输尿管损伤的患者行输尿管软镜钬激光碎石术治疗时,术后易出现输尿管狭窄,因此术中应注意精细操作,术后注意严密随访。

【关键词】 输尿管结石;输尿管镜检查;碎石术;尿道狭窄
基金项目:徐州市科委资助课题(KC16SH038)
DOI:10.3760/cma.j.cn431460-20200930-00118

Correlation analysis of secondary ureteral stricture after flexible ureteroscopic holmium laser lithotripsy

Wang Qichao[1], Cao Jingyi[1], Sun Weibing[2], Wang Qian[1], Song Mo[1], Wu Gang[1], Ge Yan[1]

[1]Department of Urology, Xuzhou Hospital Affiliated to Jiangsu University, Tumor Hospital of Xuzhou City, Xuzhou 221005, China; [2]Department of Urology, the Second Hospital Affiliated to Dalian Medical University, Dalian 116027, China

Corresponding author: Cao Jingyi, Email: cjy_197510@163.com

Abstract **Objective** To investigate the influence of soft ureteroscopic holmium laser lithotripsy in the treatment of ureteral stricture secondary to upper ureteral calculi. **Methods** The clinical data of 258 patients with upper ureteral calculi treated by holmium laser lithotripsy under soft ureteroscope in tumor hospital of Xuzhou city from January 2011 to June 2020 were retrospectively analyzed, and they were divided into stricture group (15 cases) and non-stricture group (243 cases) according to the occurrence of postoperative ureteral stricture. The differences in age, stone diameter, diabetes mellitus, stone incarceration and hydronephrosis between the two groups were analyzed, and the related factors of postoperative ureteral stricture were analyzed by logistic regression. **Results** Univariate analysis showed that the course of disease, stone diameter, stone incarceration, polyp encapsulation, ureteral injury, operation time were correlated with the occurrence of postoperative ureteral stricture ($P<0.05$). Multivariate logistic regression analysis showed that the course of disease, stone diameter, stone incarceration and ureteral injury were independent risk factors for postoperative ureteral stricture ($P<0.05$). **Conclusions** The patients with long duration of disease, larger diameter stone, stone incarceration and ureter injury were more likely to develop ureteral stricture after flexible ureteroscopic holmium laser lithotripsy, so full preoperative evaluations, improvement of surgical skill sand prevention as early as possible after operation should be considered.

Key words Ureteral Calculi; Ureteroscopy; Lithotripsy; Urethral Stricture

Fund program: Project Supported by Xuzhou Science and Technology Commission (KC16SH038)

DOI: 10.3760/cma.j.cn431460-20200930-00118

泌尿系结石为泌尿外科常见疾病，目前发病率为15%左右[1]。上尿路结石多数为肾结石下行所致，少数可因输尿管狭窄引起。目前处理上尿路结石的方式有体外冲击波碎石治疗、输尿管硬镜、输尿管软镜及经皮肾镜治疗等，但对于肾盂内或者肾盏内结石，输尿管硬镜常无法触及且经皮肾镜创伤相对较大，而输尿管软镜可有效处理部分输尿管结石及肾盏内结石，同时具有创伤小、出血少及术后恢复快等优点。输尿管软镜常见的并发症有尿源性感染、输尿管狭窄及输尿管黏膜撕脱等，其中输尿管狭窄又可导致输尿管梗阻，从而影响手术的本身意义，因此如何预防手术所带来的不良反应极为重要[2-3]。本研究分析了影响输尿管软镜钬激光碎石术后继发输尿管狭窄的相关因素，现报道如下。

1 资料与方法

1.1 一般资料

回顾性分析2011年1月至2020年6月于徐州市肿瘤医院行输尿管软镜治疗的258例输尿管上段结石患者的临床资料，其中男性144例，女性114例，合并糖尿病患者105例，患者年龄为(52.1±8.3)岁。排除标准为既往存在输尿管手术史、输尿管多发结石、合并肾结石及术前发现存在输尿管狭窄的患者。

入组患者均经过泌尿系CT、腹部平片(KUB)及CT尿路系统成像(CTU)检查诊断为输尿管结石，同时行泌尿系超声评估肾积水程度。轻度：集合系统扩张1~2 cm；中度：集合系统扩张2.1~3.5 cm；重度：集合系统扩张>3.5 cm。其中输尿管狭窄及肾积水定义为：术后复查CTU提示输尿管存在输尿管上段及肾盂扩张，且集合系统扩张>1 cm。依据术后是否存在输尿管狭窄分为狭窄组(15例)及非狭窄组(243例)，两组患者的基本资料比较，差异无统计学意义($P>0.05$，表1)。本研究经徐州市肿瘤医院伦理委员会批准，且所有患者或家属均签署知情

同意书。

表1 两组输尿管上段结石患者的一般资料比较

组别	例数	年龄（岁，$\bar{x}\pm s$）	性别（例）		结石直径（cm，$\bar{x}\pm s$）	手术时间（min，$\bar{x}\pm s$）
			男	女		
狭窄组	15	53.7±6.8	9	6	1.5±2.1	57.4±10.2
非狭窄组	243	51.9±9.1	135	108	1.6±1.9	56.8±7.8
t/χ^2值	-	0.015	0.126		0.007	0.026
P值	-	0.794	0.061		0.916	0.653

1.2 方法

所有患者均行输尿管软镜钬激光碎石术治疗，手术方法：麻醉成功后，患者取截石位，常规术区消毒、铺巾。使用F8/9.8 Wolf输尿管硬镜由尿道外口顺利进入膀胱，见患侧尿管开口处D-J管一根，尾端弯曲好，置入异物钳，夹住D-J管尾端，将其完整取出。输尿管硬镜再次进入膀胱，将斑马导丝置入患侧输尿管，输尿管硬镜沿导丝进入输尿管，将导丝置入肾盂内，退出输尿管硬镜，在导丝引导下将F14输尿管软镜鞘置入输尿管，输尿管软镜沿镜鞘置入至结石位置，置入220 μm钬激光光纤，调整功率为20 W，将结石击碎成粉末状，依次检查上、中、下各盏，见无较大结石残留，退镜，引导留置F6 D-J管，保留导尿管。术后均通过门诊复查泌尿系超声以了解病情变化，必要时完善CTU检查。收集两组患者的性别、年龄、是否合并糖尿病、病程、手术时间、结石发生于左侧或右侧、结石直径、肾积水程度、结石嵌顿与否、是否合并输尿管息肉、术中有无输尿管损伤及手术时间等临床资料。

1.3 统计学方法

采用SPSS 19.0统计软件对数据进行处理，计量资料以（$\bar{x}\pm s$）表示，采用t检验；计数资料采用χ^2检验；单因素及多因素分析采用logistic回归分析，术后发生输尿管狭窄的相关因素。以$P<0.05$为差异有统计学意义。

2 结果

2.1 输尿管软镜术后影响输尿管狭窄的单因素logistic回归分析

术后对患者随访3-12个月。单因素分析结果显示：病程、结石直径、结石嵌顿、输尿管息肉、输尿管损伤、手术时间与术后输尿管狭窄的发生均具有相关性，组间比较差异均有统计学意义（均$P<0.05$，表2）。

表2 术后影响输尿管狭窄的单因素logistic回归分析（例）

组别	例数	性别		年龄		糖尿病		病程		结石直径			肾积水程度			结石嵌顿		输尿管息肉	
		男	女	<60岁	≥60岁	有	无	≤3个月	>3个月	<1 cm	1-2 cm	>2 cm	轻度	中度	重度	有	无	有	无
狭窄组	15	9	6	9	6	9	6	3	12	3	3	9	3	9	3	12	3	12	3
非狭窄组	243	135	108	168	75	96	147	159	84	69	129	45	78	99	66	60	183	90	153
χ^2值	-	0.034		0.784		1.687		4.997		9.889			0.427			5.712		2.162	
P值	-	0.849		0.647		0.190		0.028		0.008			0.978			0.016		0.142	

续表2 术后影响输尿管狭窄的单因素logistic回归分析（例）

组别	例数	输尿管损伤		手术时间		结石位置	
		有	无	≤1 h	>1 h	左侧	右侧
狭窄组	15	12	3	3	12	9	6
非狭窄组	243	57	186	114	129	135	108
χ^2值	-	10.241		8.814		0.094	
P值	-	0.001		0.003		0.781	

2.2 输尿管软镜术后影响输尿管狭窄的多因素logistic回归分析

将上述单因素分析提示与输尿管狭窄有相关性的指标行多因素logistic回归分析，结果显示：病程、结石直径、结石嵌顿及输尿管损伤为术后发生输尿管狭窄的独立危险因素（均$P<0.05$，表3）。

表3 术后影响输尿管狭窄的多因素logistic回归分析

因素	SE	OR	95%CI	P值
病程	0.694	4.372	1.084-17.574	0.036
结石直径	0.551	1.254	0.087-0.742	0.011
结石嵌顿	0.824	4.421	1.186-16.487	0.021
输尿管损伤	0.714	5.135	0.032-0.557	0.003

3 讨论

泌尿系结石为泌尿外科常见疾病，具有发病形式多样等特点；其中输尿管上段结石的处理更为多样化，主要治疗方案有体外冲击波碎石、输尿管硬镜、腹腔镜切开取石及输尿管软镜等；其中输尿管软镜术式具有创伤较小且可有效处理上行结石等优点而得到广泛运用[4-6]。输尿管软镜常见的并发症有尿源性感染、输尿管狭窄及输尿管黏膜撕脱等，其中输尿管狭窄仍是其不可忽视的并发症，输尿管狭窄又可导致输尿管梗阻，严重影响了手术疗效并增加了患者的负担[5,7]。因此探讨导致输尿管狭窄的相关因素极为重要，可将输尿管狭窄的发生率降至最低，进而提升手术疗效。

本研究的多因素分析结果提示患者病程、结石直径、结石嵌顿及输尿管损伤与术后输尿管狭窄的发生密切有关。病程长往往导致积水加重，尿液引流不畅又易引发结石逐渐增大；同时病程长易导致

梗阻处输尿管炎性增生、息肉形成，诱发结石嵌顿，嵌顿处输尿管可因局部缺血而导致输尿管纤维化瘢痕形成，瘢痕挛缩导致输尿管狭窄形成，同时梗阻远端输尿管萎缩折曲；这一病理生理变化目前认为是输尿管狭窄形成的主要病理机制。而手术操作又可导致表皮细胞生长因子（EGF）等炎性介质的产生，从而促进输尿管瘢痕形成，进一步加重输尿管狭窄[5-9]。输尿管损伤亦是导致输尿管狭窄的重要因素之一，既包括结石本身对输尿管所产生的损伤，也包括手术本身对输尿管的损伤；输尿管损伤形式主要包含激光直接损伤、黏膜撕脱、输尿管出血穿孔及热损伤等[10]。

因此术中精细操作，可有效减小术后出现输尿管狭窄的概率，鉴于此，笔者总结输尿管上段结石手术治疗的经验如下：①碎石过程中尽量保持光纤在视野范围内，避免激光直接接触输尿管黏膜，相关操作常可导致输尿管直接损伤；②避免长时间碎石，既往研究显示40 W钬激光1 min内间隔激发可使水温升至50 ℃，高温水可导致输尿管黏膜热损伤[9]。因此在保证引流通畅的情况下尽量保证流动水，进而减小激光的热叠加效应；同时输尿管软镜常需要置入F14/16通道鞘，长时间手术可增加输尿管压迫缺血的风险，尽管本调查结果显示手术时间并不是引发术后输尿管狭窄的危险因素，但不排除其与其他因素为同一主因素，同时不容易忽视的是随着手术时间的延长，感染的风险亦随之增加；③通畅鞘的置入常为非可视性，目前认为其是导致输尿管穿孔及黏膜撕脱的主要原因，因此在通畅鞘的置入过程中切勿暴力操作，期间应注意调试导丝活动性以间接观察输尿管鞘是否位于输尿管管腔内，如遇阻力较大，可置入输尿管软镜直视观察输尿管情况；④对于输尿管息肉的处置仅建议处理突入输尿管管腔内的部分，且建议从息肉基底部开始处理，而不宜广泛的烧灼输尿管息肉，此操作常可导致输尿管的直接损伤。

总之，输尿管狭窄为输尿管软镜治疗后较为严重的并发症，相比出现后的治疗，不如防患于未然，严格把握输尿管软镜的手术适应证。对于病程长、结石较大的患者，术中应注意精细操作，避免输尿管损伤，必要时行二期手术，对于术中发现存在结石嵌顿情况，术中可适当增加D-J管留置时间，同时注意术后随访。

利益冲突 所有作者均声明不存在利益冲突

参 考 文 献

[1] Heldt JP, Smith JC, Anderson KM, et al. Ureteral calculi detection using low dose computerized tomography protocols is compromised in overweight and underweight patients[J]. J Urol, 2012, 188(1): 124-129. DOI: 10.1016/j.juro.2012.02.2568.

[2] Basa O, Tuygun C, Dede O, et al. Factors affecting complication rates of retrograde flexible ureterorenoscopy: analysis of 1571 procedures-a single-center experience[J]. World J Urol, 2017, 35(5): 819-826. DOI: 10.1007/s00345-016-1930-3.

[3] Oberlin DT, Flum AS, Bachrach L, et al. Contemporary surgical trends in the management of upper tract calculi[J]. J Urol, 2015, 193(3): 880-884. DOI: 10.1016/j.juro.2014.09.006.

[4] Ibrahim HM, Mohyelden K, Abdel-Bary A, et al. Single versus double ureteral stent placement after laser endoureterotomy for the management of benign ureteral strictures: a randomized clinical trial[J]. J Endourol, 2015, 29(10): 1204-1209. DOI: 10.1089/end.2015.0445.

[5] 叶照华, 米其武, 罗杰鑫, 等. 输尿管结石行输尿管镜下碎石术后并发输尿管狭窄的危险因素分析[J]. 中华腔镜泌尿外科杂志(电子版), 2017, 11(1): 40-42. DOI: 10.3877/cma.j.issn.1674-3253.2017.01.011.

[6] 万克松, 王传圣, 程华根, 等. 输尿管镜碎石术后并发输尿管狭窄风险的列线图模型预测[J]. 国际泌尿系统杂志, 2021, 41(2): 323-327. DOI: 10.3760/cma.j.cn431460-20191016-00033.

[7] 胡卫国, 苏博兴. 影响钬激光碎石效率的细节问题：参数设置及光纤使用[J]. 临床泌尿外科杂志, 2017, 32(4): 267-269. DOI: 10.13201/j.issn.1001-1420.2017.04.006.

[8] 曹文锋, 王亮, 黄晓科, 等. 微创经皮肾镜联合输尿管软镜治疗嵌顿性输尿管上段结石[J]. 中国微创外科杂志, 2012, 12(10): 933-934, 937. DOI: 10.3969/j.issn.1009-6604.2012.10.023.

[9] Sun YT, Lee KS, Hung SH, et al. Sialendoscopy with holmium: YAG laser treatment for multiple large sialolithiases of the Wharton duct: a case report and literature review[J]. J Oral Maxillofac Surg, 2014, 72(12): 2491-2496. DOI: 10.1016/j.joms.2014.06.448.

[10] Fam XI, Singam P, Ho CC, et al. Ureteral stricture formation after ureteroscope treatment of impacted calculi: a prospective study[J]. Korean J Urol, 2015, 56(1): 63-67. DOI: 10.4111/kju.2015.56.1.63.

（本文编辑：刘珩）
（收稿日期：2020-09-30）

·论著·

输尿管镜钬激光碎石术后输尿管狭窄的危险因素分析

潘飞飞 马森 孙雪彪 马佳伟
南京同仁医院泌尿外科，南京 211100
通信作者：马森，Email：710884673@qq.com

【摘要】 目的 探讨输尿管结石患者经输尿管镜钬激光碎石术后输尿管狭窄情况及其对预后的影响。**方法** 回顾性分析 2018 年 1 月—2019 年 8 月于南京同仁医院行输尿管镜钬激光碎石术治疗的 406 例患者的临床资料，根据患者术后输尿管狭窄情况将患者分为狭窄组（$n=28$）和非狭窄组（$n=378$），采用单因素和多因素 Logistic 回归分析评价输尿管结石患者术后输尿管狭窄的独立危险因素，并比较两组患者术后复发率及预后生存情况。根据独立危险因素构建列线图模型，采用受试者操作特征（ROC）曲线、GiViTI 校准曲线带及临床决策曲线验证模型的准确性。计量资料以均数±标准差（$\bar{x}\pm s$）表示，组间比较采用 t 检验；计数资料组间比较采用 χ^2 检验。**结果** 单因素分析结果显示，非狭窄组与狭窄组患者在结石病程、结石最大径、息肉包裹、肾积水程度、嵌顿结石、输尿管损伤及手术时间方面，差异均具有统计学意义（$P<0.05$）；多因素 Logistic 回归分析结果显示，结石病程、结石最大径、息肉包裹、肾积水程度、嵌顿结石及输尿管损伤均为输尿管结石患者术后输尿管狭窄的独立危险因素（$P<0.05$）。采用电话查询、门诊复查、病历查询等方式对输尿管结石患者进行 1 年随访，结果显示，输尿管结石复发 106 例，狭窄组患者术后 1 年（21.43% 比 8.99%）、术后 2 年复发率（35.71% 比 14.81%）均显著高于非狭窄组，差异均有统计学意义（$\chi^2=4.54$、8.36，$P<0.05$）。与非狭窄组比较，狭窄组患者生理功能评分［（79.28±8.17）分比（65.22±10.53）分］、生理职能评分［（78.54±9.33）分比（69.23±7.86）分］及总体健康评分［（81.03±10.54）分比（70.43±7.38）分］均显著降低，差异均具有统计学意义（$t=7.70$、5.29、5.43，$P<0.05$）。构建的列线图模型 ROC 曲线下面积为 0.882（95% CI：0.774～0.928），在 GiViTI 校准曲线带的 80%～90% 置信区间区域均未穿过 45° 角平分线（$P=0.176$），临床决策曲线提示净获益率高。**结论** 输尿管结石病程、结石最大径、息肉包裹、肾积水程度、嵌顿结石及输尿管损伤均为输尿管结石患者术后输尿管狭窄的独立危险因素，临床医师应积极采取干预措施，降低患者术后输尿管狭窄的发生率，改善患者预后，提高患者生活质量。

【关键词】 输尿管结石；碎石术，激光；输尿管狭窄；预后
DOI：10.3760/cma.j.cn115396-20211102-00424

Risk factors of ureteral stricture after ureteroscopic holmium laser lithotripsy

Pan Feifei, Ma Sen, Sun Xuebiao, Ma Jiawei
Department of Urology, Nanjing Tongren Hospital, Nanjing 211100, China
Corresponding author: Ma Sen, Email: 710884673@qq.com

【Abstract】 Objective To investigate the ureteral stricture after ureteroscopic holmium laser lithotripsy in patients with ureteral calculi and its effect on prognosis. **Methods** The clinical data of 406 patients who underwent ureteroscopic holmium laser lithotripsy in Nanjing Tongren Hospital from January 2018 to August 2019 were

analyzed retrospectively, according to postoperative ureteral stricture, the patients were divided into stricture group ($n=28$) and non-stricture group ($n=378$). The independent risk factors of postoperative ureteral stricture in patients with ureteral calculi were evaluated by univariate and multivariate Logistic regression analysis, and the postoperative recurrence rate and prognosis of the two groups were compared. The nomogram model was constructed according to independent risk factors, and the accuracy of the model was verified by receiver operating characteristic (ROC) curve, GiViTI calibration band and clinical decision curve. Measurement data were expressed as mean ± standard deviation ($\bar{x} \pm s$), comparison between groups used t-test, and comparison of count data between groups used Chi-square. **Results** Univariate analysis showed that there were significant differences in course of ureteral calculi, stone diameter, polyp wrapping, degree of hydronephrosis, incarcerated stone, ureteral injury and operation time between non-stricture group and stricture group ($P<0.05$). Multivariate Logistic regression analysis showed that the course of ureteral calculi, stone diameter, polyp wrapping, degree of hydronephrosis, incarcerated stone and ureteral injury were independent risk factors for postoperative ureteral stricture in patients with ureteral calculi ($P<0.05$). The patients with ureteral calculi were followed up for 1 year by telephone, outpatient reexamination and medical record inquiry. During the follow-up period, 106 cases of ureteral calculi recurred. The recurrence rate of 1 year (21.43% *vs* 8.99%) and 2 years (35.71% *vs* 14.81%) in the stricture group was significantly higher than that in the non-stricture group, the differences were statistically significant ($\chi^2=4.54$, 8.36, $P<0.05$). Compared with the non-stricture group, the physiological function score [(79.28 ± 8.17) *vs* (65.22 ± 10.53)], physiological function score [(78.54 ± 9.33) *vs* (69.23 ± 7.86)] and overall health score [(81.03 ± 10.54) *vs* (70.43 ± 7.38)] in the stricture group were significantly lower, the differences were statistically significant ($t=7.70$, 5.29, 5.43, $P<0.05$). The area under curve of the constructed nomogram model ROC curve was 0.882 (95% *CI*: 0.774-0.928). In the 80%-90% confidence interval area of the GiViTI calibration curve belt, it does not pass through the 45° angle bisector ($P=0.176$). The clinical decision curve indicates that the net benefit rate was high. **Conclusions** The course of ureteral calculi, stone diameter, polyp wrapping, degree of hydronephrosis, incarcerated stone and ureteral injury are independent risk factors for postoperative ureteral stricture in patients with ureteral calculi. Clinicians should actively take intervention measures to reduce the incidence of postoperative ureteral stenosis, improve the prognosis and improve the quality of life of patients.

[Key words] Ureteral calculi; Lithotripsy, laser; Ureteral stricture; Prognosis
DOI:10.3760/cma.j.cn115396-20211102-00424

输尿管结石是临床常见的泌尿外科疾病，是由输尿管缩水引起的一种梗阻性病变[1]，可导致上尿路积水扩张、肾绞痛，若不及时治疗将导致不可逆的肾功能衰竭[2]。近年来，随着输尿管镜操作技术的发展，体外冲击波碎石术[3]、输尿管镜钬激光碎石术[4]等被广泛应用于临床输尿管结石治疗中。钬激光具有高效的碎石能力及小组织穿透性，输尿管镜钬激光碎石术可治疗不同成分及不同部位的输尿管结石[5]，已成为临床治疗泌尿系统结石的有效手段。但输尿管镜为侵入性操作，容易导致患者输尿管损伤，从而增加患者术后发生输尿管狭窄的概率[6]。因此本研究旨在探讨输尿管结石患者行输尿管镜钬激光碎石术后发生输尿管狭窄的影响因素，并分析输尿管狭窄对患者预后的影响，以期为临床治疗提供科学依据。

1　资料与方法

1.1　一般资料

回顾性分析2018 年 1 月—2019 年 8 月于南京同仁医院行输尿管镜钬激光碎石术治疗的 406 例输尿管结石患者的临床资料，其中男性 246 例，女性 160 例；年龄 24～76 岁，平均(48.26 ± 12.35)岁；上段输尿管结石 126 例，中段输尿管结石 80 例，下段输尿管结石 200 例。本研究经南京同仁医院伦理委员会审查批准(批号：20170539)，纳入患者均知悉本研究内容并签署知情同意书。

1.2　纳入与排除标准

纳入标准：(1)经静脉尿路造影、B 超、泌尿系平片及 CT 检查明确诊断为输尿管结石；(2)首次行输尿管镜钬激光碎石术；(3)患者年龄≥18 岁。排除标准：(1)多发输尿管结石；(2)合并肾结石、输尿管畸形、恶性肿瘤，以及心、肝、肾、肺及免疫系统功能障碍；(3)既往输尿管结石治疗史；(4)留置输尿管支架；(5)术前影像学提示输尿管狭窄。

1.3　方法

1.3.1　手术方法　患者气管全身麻醉或腰麻后取截石位，经尿道置入输尿管硬镜确定患侧输尿管开口位置，经由输尿管导管和镍钛合金超滑导丝将输尿管镜

输送至输尿管口，持续进镜至结石部位，沿导丝置入 F14/12 波科输尿管软镜通道鞘，退出鞘芯和导丝，沿通道鞘电子输尿管软镜，将 200 μm 钬激光光纤置入输尿管软镜通道，击碎结石并联合套石篮将碎块取出，将导丝上行置入肾盂，退出输尿管镜，沿导丝滞留 F6 双 J 管和 F16 导尿管。导尿管留置 2 d，双 J 管留置 3～4 周，复查无结石残留可将双 J 管拔除。

1.3.2 临床资料收集 通过查阅电子病历收集患者的临床资料，包括性别、年龄、结石病程、结石部位、结石最大径、患侧、息肉包裹情况、术前感染情况、肾积水程度、输尿管损伤情况及手术时间等。采用健康调查简表（SF-36）[7]评价患者术后生活质量，该量表共 36 个条目，8 个维度，分别为总体健康、躯体功能、躯体角色功能、躯体疼痛、精力、社会功能、情绪角色功能和心理健康，每个维度总分为 100 分，采用标准评分法计算生理功能评分和生理职能评分，分数越高提示患者生活质量越好。

1.3.3 随访 采用电话查询、门诊复查、病历查询等方式对输尿管结石患者进行 1 年随访，记录患者输尿管狭窄情况及复发情况；拔除双 J 管后 1 周、2 周、1 个月及半年均需行彩超检查，若积水加重，则进一步行计算机断层扫描术（Computer tomography，CT）、静脉尿路造影（Intravenous urography，IVU）检查，明确为输尿管狭窄所致的肾积水加重，则判定为术后发生输尿管狭窄[8]，根据输尿管狭窄情况将患者分为狭窄组和非狭窄组，并记录患者 1 年随访期间复发情况。

1.4 统计学方法

采用 SPSS 23.0 软件对数据进行统计学分析。计量资料以均数 ± 标准差（$\bar{x} \pm s$）表示，组间比较采用 t 检验；计数资料组间比较采用 χ^2 检验。采用单因素和多因素 Logistic 回归分析筛选出输尿管结石患者行输尿管镜钬激光碎石术后发生输尿管狭窄的影响因素，并构建列线图预测模型。采用受试者操作特征（Receive operating characteristic，ROC）曲线、GiViTI 校准曲线带及临床决策曲线检验评价模型的预测效能。$P<0.05$ 认为差异具有统计学意义。

2 结果

2.1 输尿管狭窄的单因素分析

纳入研究的 406 例输尿管结石患者均行输尿管镜钬激光碎石术，术后随访 8～24 个月，共 28 例患者术后发生输尿管狭窄，其中男性 16 例，女性 12 例。单因素分析结果显示，非狭窄组与狭窄组患者在结石病程、结石最大径、息肉包裹、肾积水程度、嵌顿结石、输尿管损伤及手术时间方面，差异均具有统计学意义（$P<0.05$），在性别、年龄、结石部位、患侧、术前感染及术后双 J 管留置时间方面，差异均无统计学意义（$P>0.05$）。见表 1。

表 1 输尿管结石患者输尿管镜钬激光碎石术后输尿管狭窄的单因素分析[例(%)]

因素	狭窄组（$n=28$）	非狭窄组（$n=378$）	χ^2 值	P 值
性别				
男性	16(57.14)	230(60.85)	0.15	0.699
女性	12(42.86)	148(39.15)		
年龄				
<50 岁	15(53.57)	208(55.03)	0.02	0.881
≥50 岁	13(46.43)	170(44.97)		
结石病程				
<3 个月	7(25.00)	238(62.96)	15.70	<0.001
≥3 个月	21(75.00)	140(37.04)		
结石部位				
上段	3(10.71)	52(13.76)	0.29	0.866
中段	12(42.86)	166(43.92)		
下段	13(46.23)	160(42.32)		
结石最大径				
<2 cm	16(57.14)	339(89.68)	25.13	<0.001
≥2 cm	12(42.86)	39(10.32)		
患侧				
左侧	16(57.14)	219(57.94)	0.01	0.935
右侧	12(42.86)	159(42.06)		
息肉包裹				
是	18(64.29)	156(41.27)	5.64	0.018
否	10(35.71)	222(58.73)		
术前感染				
是	17(60.71)	171(45.24)	2.51	0.113
否	11(39.29)	207(54.76)		
肾积水程度				
轻度	4(14.29)	207(54.76)	17.80	<0.001
中度	9(32.14)	53(14.02)		
重度	15(53.57)	118(31.22)		
嵌顿结石				
是	21(75.00)	129(34.13)	18.70	<0.001
否	7(25.00)	249(65.87)		
输尿管损伤				
是	20(71.43)	90(23.81)	19.93	<0.001
否	8(28.57)	288(76.19)		
手术时间				
<60 min	5(17.86)	177(46.83)	8.85	0.003
≥60 min	23(82.14)	201(53.17)		
术后双 J 管留置时间				
<4 周	13(46.43)	204(53.97)	0.60	0.440
≥4 周	15(53.57)	174(46.03)		

注：狭窄组：CT 和 IVU 提示输尿管狭窄所致肾积水加重；非狭窄组：CT 和 IVU 提示无输尿管狭窄所致肾积水加重。CT：计算机断层扫描术；IVU：静脉尿路造影。

2.2　输尿管狭窄的多因素分析

将单因素分析中差异具有统计学意义的因素进行赋值(表 2),采用似然比前进法对变量进行筛选,以多因素 Logistic 回归分析进行评价。结果显示,结石病程、结石最大径、息肉包裹、肾积水程度、嵌顿结石及输尿管损伤均为输尿管结石患者术后输尿管狭窄的独立危险因素($P<0.05$)。见表 3。

表 2　变量赋值量表

变量	赋值
结石病程	<3 个月 =0,≥3 个月 =1
结石最大径	<2 cm =0,≥2 cm =1
息肉包裹	否 =0,是 =1
肾积水程度	轻度 =0,中度 =1,重度 =2
嵌顿结石	否 =0,是 =1
输尿管损伤	否 =0,是 =1
手术时间	<60 min=0,≥60 min=1

表 3　输尿管结石患者输尿管钬激光碎石术后输尿管狭窄的多因素 Logistic 回归分析

因素	β 值	SE 值	$Wald$ χ^2 值	OR 值	95%CI	P 值
结石病程	0.663	0.398	1.173	1.941	1.532～2.191	0.017
结石最大径	0.788	0.759	1.224	2.198	1.749～2.517	0.013
息肉包裹	0.616	0.574	1.329	1.852	1.215～2.893	0.024
肾积水程度	0.501	0.315	1.919	1.651	1.294～1.827	0.012
嵌顿结石	0.169	0.686	1.168	1.184	1.007～1.327	0.003
输尿管损伤	0.133	0.392	1.449	1.142	1.003～1.845	0.008
手术时间	0.457	0.703	1.108	1.580	0.742～2.355	0.198

2.3　风险预测模型构建

基于多因素 Logistic 回归分析结果,采用 R 语言统计软件构建输尿管结石患者术后输尿管狭窄的风险预测模型,结果显示,重度肾积水积分为 80 分,嵌顿结石积分为 50 分,结石最大径≥2 cm 积分为40 分,息肉包裹积分为 15 分,输尿管损伤积分为35 分,病程≥3 个月积分为 55 分,所得总分为275 分,该分数预测输尿管结石患者输尿管镜钬激光碎石术后输尿管狭窄的概率为95.00%。见插页,图 1。

2.4　预测模型评估

2.4.1　区分度　绘制本研究列线图模型预测患者术后发生输尿管狭窄的 ROC 曲线,计算 ROC 曲线下面积(Area under curve, AUC)为 0.882(95% CI: 0.774～0.928),表明该模型的区分度尚可。见插页,图 2。

2.4.2　校准度　预测模型在 GiViTI 校准曲线带的 80%～90% 置信区间区域均未穿过 45° 角平分线($P=0.176$),模型的预测概率与实际观测概率接近,具有较强的一致性。见插页,图 3。

2.4.3　临床决策曲线　采用临床决策曲线评价列线图模型有效性,决策曲线中,高风险阈值设为 0～1.0,列线图预测模型的阈值概率为 0.01～0.91,净获益率 >0,列线图模型预测的有效性较好。见插页,图 4。

2.5　输尿管狭窄对患者预后的影响

2.5.1　输尿管狭窄对结石复发的影响　406 例患者均获得随访,输尿管结石复发 106 例,狭窄组术后 1、2 年复发率均显著高于非狭窄组,差异均具有统计学意义($P<0.05$)。见表 4。

表 4　狭窄组和非狭窄组输尿管结石患者结石复发率比较[例(%)]

组别	例数	术后 1 年	术后 2 年
狭窄组	28	6(21.43)	10(35.71)
非狭窄组	378	34(8.99)	56(14.81)
χ^2 值		4.54	8.36
P 值		0.030	<0.001

注:狭窄组:CT 和 IVU 提示输尿管狭窄所致肾积水加重;非狭窄组:CT 和 IVU 提示无输尿管狭窄所致肾积水加重。CT:计算机断层扫描术;IVU:静脉尿路造影。

2.5.2　输尿管狭窄对患者生活质量的影响　与非狭窄组比较,狭窄组患者各项生活质量评分均显著降低,差异均具有统计学意义($P<0.05$)。见表 5。

表 5　狭窄组和非狭窄组输尿管结石患者生活质量评分比较(分,$\bar{x}\pm s$)

组别	例数	生理功能	生理职能	总体健康
狭窄组	28	65.22±10.53	69.23±7.86	70.43±7.38
非狭窄组	378	79.28±8.17	78.54±9.33	81.03±10.54
t 值		7.70	5.29	5.43
P 值		<0.001	<0.001	<0.001

注:狭窄组:CT 和 IVU 提示输尿管狭窄所致肾积水加重;非狭窄组:CT 和 IVU 提示无输尿管狭窄所致肾积水加重。CT:计算机断层扫描术;IVU:静脉尿路造影。

3　讨论

输尿管狭窄是输尿管结石钬激光碎石术后常见的远期并发症,输尿管镜下钬激光碎石术作为临床治疗输尿管结石的微创技术,通过钬激光瞬间产生的高能量将结石击碎,在使用时组织穿透度 <0.5 mm,且

95%的能量能被周围 5 mm 的水介质吸收，具有微创、术后并发症少、恢复快等优点[9]。但随着输尿管镜钬激光碎石术的普及和使用功率的不断提高，其间接性热损伤作用逐渐得到临床医师的重视。研究表明，热损伤后部分患者输尿管局部出现凝固样坏死，进而形成病理性瘢痕组织，导致输尿管狭窄[10]。因此，探讨输尿管结石患者输尿管镜钬激光碎石术后继发输尿管狭窄的影响因素，对临床制定干预措施、提高手术疗效具有重要意义。

无论采用何种碎石术，术后均可能继发输尿管狭窄，发生率为 3% ~ 11%[11-12]，本研究中输尿管狭窄发生率为 6.90%，与既往研究一致。目前已有临床研究探讨了输尿管结石患者行碎石术后发生输尿管狭窄的影响因素，但研究结果不一。吴佳成等[13]通过对 1 800 例输尿管结石患者的临床资料进行回顾性分析发现，嵌顿结石、多发结石、大结石、钬激光手术、长病程、肾积水程度及息肉包裹均为输尿管镜钬激光碎石术后患者发生输尿管狭窄的危险因素。而万优等[14]研究表明，结石以上输尿管宽度、结石所在部位输尿管壁厚度、结石周围输尿管伴息肉生长是输尿管上段嵌顿结石患者术后发生输尿管狭窄的独立预测因素。本研究通过单因素和多因素 Logistic 回归分析发现结石病程、结石最大径、息肉包裹、肾积水程度、嵌顿结石及输尿管损伤均为输尿管结石患者术后输尿管狭窄的独立危险因素。输尿管结石最大径与输尿管镜钬激光碎石术后输尿管狭窄密切相关，结石最大径越大，相应的手术时间及术中灌洗时间越长，从而增加术后输尿管感染及狭窄的概率[15-16]。对于病程较长的患者，由于结石长期在输尿管内嵌顿[17]，嵌顿结石长期压迫输尿管导致管壁间质纤维化、尿路上皮增生及输尿管黏膜水肿，导致炎性息肉的形成及纤维组织增生，术中置入导丝时极容易损伤输尿管，增加术后发生输尿管狭窄的风险[18]。肾积水程度也是导致输尿管狭窄的危险因素之一，钬激光激发产生的能量通过光纤进行传导，将气化后的高能量传导至结石部位，从而高效粉碎各种成分的泌尿系统结石，但输尿管管径狭窄，输尿管镜钬激光碎石术中输尿管镜与结石之间的空间狭小，若灌流率较低，钬激光所产生的局部高热，将对输尿管黏膜、肌层及浆膜层造成损伤，输尿管损伤部位形成病理性瘢痕组织，导致输尿管狭窄，甚至引起输尿管堵塞[19-20]。除钬激光对输尿管造成的损伤外，未能充分暴露手术视野以及多次进镜、退镜也可能导致输尿管损伤，增加患者术后狭窄的风险[21]。基于影响输尿管结石患者术后发生输尿管狭窄的独立危险因素，本研究建立了列线图预测模型，对结石病程、结石最大径、息肉包裹、肾积水程度、嵌顿结石及输尿管损伤量化评分并计算总分。AUC 为 0.882(95% *CI*:0.774 ~ 0.928)，提示区分度高，临床决策曲线模型远离极端曲线，净获益率高，安全可靠。但为避免预测模型在建立数据中出现过度拟合，本研究在建立预测模型后前瞻性收集输尿管结石患者的临床资料进行外部验证，GiViTI 校准曲线带是通过拟合多项式 Logistic 回归函数来揭示模型预测概率和实际观测概率之间的关系，并计算校准曲线带中 80% 置信区间(浅灰色区)和 95% 置信区间(暗灰色区)[22]。本研究中模型外部验证人群 GiViTI 校准曲线带的 95% 置信区间区域未穿过 45°角平分线，提示预测模型拟合度良好。

此外，本研究结果显示，输尿管结石患者经输尿管镜钬激光碎石术后 2 年结石复发 106 例，复发率为 26.11%，且狭窄组患者术后 1、2 年复发率均显著高于非狭窄组，生活质量评分显著低于非狭窄组，分析可能与输尿管狭窄患者尿路异常、代谢紊乱加重致使结石黏附有关。

4 总结

结石病程、结石最大径、息肉包裹、肾积水程度、嵌顿结石及输尿管损伤均为输尿管结石患者术后输尿管狭窄的独立危险因素，临床医师应积极采取干预措施，降低患者术后输尿管狭窄的发生率，改善患者预后，提高患者生活质量。

利益冲突 所有作者均声明不存在利益冲突

作者贡献声明 潘飞飞：研究设计、论文构思和写作；马鑫：质量控制及审校；孙雪彪：数据收集和分析；马佳伟：结果分析与解释

参 考 文 献

[1] 毕志雄，王建峰，毕建斌. 输尿管软镜碎石术和输尿管硬镜联合 NTmp 阻石网篮碎石术治疗输尿管上段结石疗效分析[J]. 国际外科学杂志，2020，47(9)：599-604. DOI：10.3760/cma.j.cn115396-20190421-00056.

[2] Faw C, Wan J, Hollingsworth JM, et al. Impact of the timing of ureteral stent placement on outcomes in patients with obstructing ureteral calculi and presumed infection[J]. J Endourol, 2019, 33(9): 736-740. DOI: 10.1089/end.2019.0138.

[3] Wu Q, Liang R, Huang Y, et al. Association between renal urolithiasis after extracorporeal shock wave lithotripsy therapy and new-onset hypertension: an updated meta-analysis[J]. J Int Med Res, 2021, 49(4): 3000605211002003. DOI: 10.1177/03000605211002003.

[4] Chunlin Y, Wanlin D, Jinhua D. Analysis of the efficacy of holmium laser and pneumatic ballistic in the treatment of impacted ureteral calculi[J]. Medicine (Baltimore), 2020, 99(36): e21692. DOI: 10.1097/MD.0000000000021692.

[5] Lu P, Chen K, Wang Z, et al. Clinical efficacy and safety of flexible ureteroscopic lithotripsy using 365 μm holmium laser for nephrolithiasis: a prospective, randomized, controlled trial[J]. World J Urol, 2020, 38(2): 481-487. DOI: 10.1007/s00345-019-02776-w.

[6] Mohyelden K, Hussein HA, El Helaly HA, et al. Long-term outcomes of two ipsilateral vs single double-J stent after laser endoureterotomy for bilharzial ureteral strictures[J]. J Endourol, 2021, 35(6): 775-780. DOI: 10.1089/end.2020.0956.

[7] 胡彩平, 陈毅, 李秋萍. SF-36 量表与 QLQ-C30 量表在老年癌症病人生活质量评估中的应用及其相关性研究[J]. 护理研究, 2015, 29(24): 2968-2972. DOI: 10.3969/j.issn.1009-6493.2015.24.008.

[8] 王俊, 郭志新, 吴洪森, 等. 输尿管软镜钬激光碎石术治疗输尿管上段结石并发输尿管狭窄的危险因素分析[J]. 临床泌尿外科杂志, 2018, 33(7): 532-536.

[9] 杨登科, 王俊, 胡伟, 等. 术前未预置双J管一期输尿管软镜碎石治疗上尿路结石的疗效观察[J]. 中国内镜杂志, 2019, 25(6): 56-61. DOI: 10.3969/j.issn.1007-1989.2019.06.010.

[10] 陈柯宇, 王亮. 钬激光碎石术后输尿管狭窄的相关因素分析[J]. 四川医学, 2018, 39(12): 1345-1349. DOI: 10.16252/j.cnki.issn1004-0501-2018.12.008.

[11] 李文智, 韦自卫, 徐明曦, 等. 双镜联合治疗输尿管结石术后输尿管狭窄的效果[J]. 江苏医药, 2020, 46(2): 210-212. DOI: 10.19460/j.cnki.0253-3685.2020.02.028.

[12] 孟凯, 李东. 钬激光碎石术治疗输尿管结石后发生输尿管狭窄的危险因素分析[J]. 贵州医药, 2020, 44(9): 1440-1441. DOI: 10.3969/j.issn.1000-744X.2020.09.050.

[13] 吴佳成, 陆雅君, 姜力. 经尿道输尿管镜气压弹道治疗输尿管结石后发生输尿管狭窄的危险因素[J]. 中国临床研究, 2018, 31(9): 1267-1270. DOI: 10.13429/j.cnki.cjcr.2018.09.030.

[14] 万优, 许长宝, 赵兴华, 等. 输尿管上段嵌顿性结石术后发生输尿管狭窄的影响因素分析[J]. 微创泌尿外科杂志, 2020, 9(5): 324-329. DOI: 10.19538/j.cnki.10-1020/r.2020.05.008.

[15] Molina WR, Carrera BV, Chew BH, et al. Temperature rise during ureteral laser lithotripsy: comparison of super pulse thulium fiber laser (SPTF) vs high power 120 W holmium-YAG laser (Ho:YAG)[J]. World J Urol, 2021, 39(10): 3951-3956. DOI: 10.1007/s00345-021-03619-3.

[16] Cornelius J, Zumbühl D, Afferi L, et al. Immediate shockwave lithotripsy vs delayed shockwave lithotripsy after urgent ureteral stenting in patients with ureteral or pyeloureteral urolithiasis: a matched-pair analysis[J]. J Endourol, 2021, 35(5): 721-727. DOI: 10.1089/end.2020.0384.

[17] 程传宇, 郝建伟, 武玉东, 等. HIV 感染肾结石患者行输尿管软镜钬激光碎石术后发生尿路感染的危险因素分析[J]. 中华泌尿外科杂志, 2019, 40(9): 690-694. DOI: 10.3760/cma.j.issn.1000-6702.2019.09.010.

[18] 王翼, 豆海锋. 后腹腔镜下输尿管切开取石术治疗输尿管结石患者术后并发输尿管狭窄的危险因素分析[J]. 医学临床研究, 2022, 39(2): 271-273. DOI: 10.3969/j.issn.1671-7171.2022.02.031.

[19] He Z, Yin S, Duan X, et al. Does the presence or degree of hydronephrosis affect the stone disintegration efficacy of extracorporeal shock wave lithotripsy? A systematic review and meta-analysis[J]. Urolithiasis, 2020, 48(6): 517-526. DOI: 10.1007/s00240-019-01165-7.

[20] 陈松, 唐宇哲, 付猛, 等. 输尿管镜碎石术后输尿管狭窄的治疗[J]. 现代泌尿外科杂志, 2022, 27(1): 39-42. DOI: 10.3969/j.issn.1009-8291.2022.01.008.

[21] Hou CP, Lin YH, Juang HH, et al. Effect of ureteral calculus in outpatients receiving semirigid ureteroscope laser lithotripsy[J]. Medicine (Baltimore), 2020, 99(10): e19324. DOI: 10.1097/MD.0000000000019324.

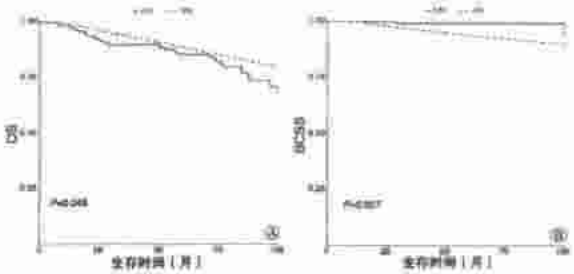
[22] 胡明, 杨云杰, 赵振华, 等. 预测输尿管结石进展为尿脓毒血症的列线图模型的外部验证[J]. 天津医药, 2019, 47(9): 975-978. DOI: 10.11958/20182210.

(收稿日期:2021-11-02)



注：IDC：浸润性导管癌；EPC：包裹性乳头状癌；OS：总生存；BCSS：乳腺癌特异性生存。

图 1　IDC 和 EPC 的 OS 及 BCSS 曲线　Ⓐ：OS 曲线；Ⓑ：BCSS 曲线



注：IDC：浸润性导管癌；EPC：包裹性乳头状癌；OS：总生存；BCSS：乳腺癌特异性生存。

图 2　倾向得分匹配调整后 IDC 和 EPC 的 OS 及 BCSS 曲线　Ⓐ：OS 曲线；Ⓑ：BCSS 曲线

注释：图 1 ~2 见原文：基于 SEER 数据库回顾性分析乳腺包裹性乳头状癌的临床特征及预后（正文见第 381 页）

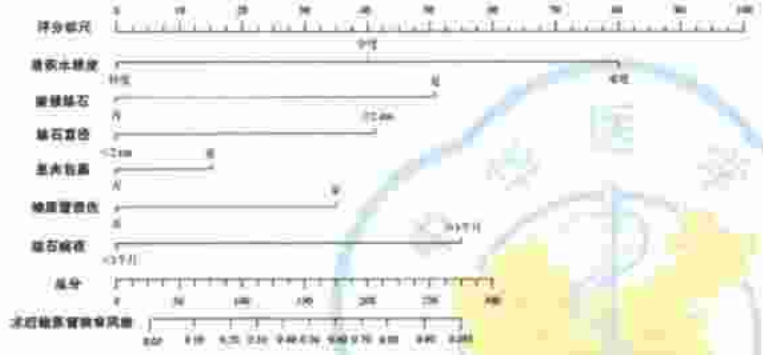
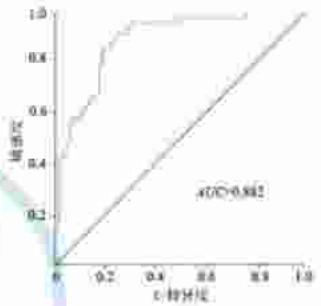


图 1　输尿管结石患者行输尿管镜钬激光碎石术后输尿管狭窄的列线图预测模型



注：ROC：受试者操作特征。

图 2　列线图模型预测输尿管结石患者术后发生输尿管狭窄的 ROC 曲线

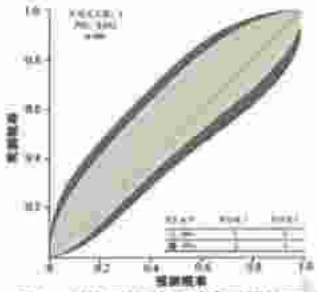


图 3　列线图模型预测输尿管结石患者术后发生输尿管狭窄的外部验证人群 GiViTI 校准曲线带

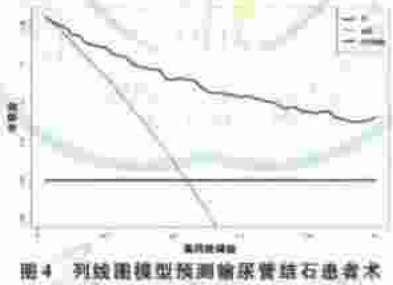
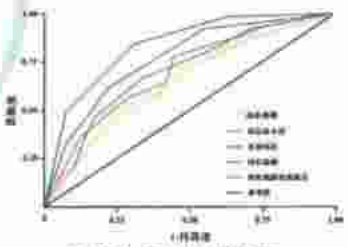


图 4　列线图模型预测输尿管结石患者术后发生输尿管狭窄的临床决策曲线

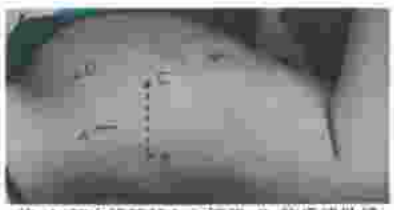


注：ROC：受试者操作特征。

图 1　各影响因素对患者术后发生输尿管狭窄预测价值的 ROC 曲线

注释：图 1 ~4 见原文：输尿管镜钬激光碎石术后输尿管狭窄的危险因素分析（正文见第 387 页）

注释：图 1 见原文：输尿管结石患者气压弹道碎石术后发生输尿管狭窄情况调查及对预后的影响（正文见第 393 页）



注：A：腋中线髂棘上 2 横指；B：腋后线肋缘下 1 横指；C：腋前线与肋缘交点；D：脐旁线髂棘上 1 横指。

图 1　预防性切除原位多囊肾患者体位及 Trocar 安放位置

注释：图 1 见原文：预防性切除原位多囊肾对 ADPKD 患者肾移植围手术期并发症及手术难度的影响（正文见第 399 页）

DOI: 10.3969/j.issn.1000-744X.2019.03.015.

·论著·

钬激光碎石后发生输尿管狭窄的病因及临床意义

岳栋 郑苗 李忠海
济宁医学院附属医院泌尿外科，济宁 272000
通信作者：岳栋，Email：yuedong2021@163.com

【摘要】 **目的** 探讨钬激光碎石后发生输尿管狭窄的病因，为临床治疗及预防提供指导意义。**方法** 回顾性分析2020年5月至2022年5月在本院诊断为输尿管结石的482例患者的临床资料，其中65例行后腹腔镜输尿管切开取石术，417例行输尿管镜钬激光碎石术。对正常输尿管行HE染色，提取输尿管平滑肌细胞并用钬激光处理，采用Transwell实验检测其对巨噬细胞的趋化作用，采用Western blot法检测α-平滑肌肌动蛋白（α-SMA）的表达情况。**结果** 输尿管镜钬激光碎石术后的输尿管狭窄发生率高于后腹腔镜输尿管切开取石（$P=0.008$）。机制上碎石过程中钬激光可造成输尿管平滑肌细胞损伤，促进巨噬细胞迁移并诱导其高表达α-SMA。**结论** 钬激光碎石容易造成输尿管平滑肌细胞损伤，招募巨噬细胞参与纤维化过程，导致输尿管狭窄，术中尽量避免肌层的损伤及减少巨噬细胞的浸润有助于减少输尿管狭窄的发生。

【关键词】 输尿管镜检查；腹腔镜检查；碎石术；输尿管狭窄
DOI：10.3760/cma.j.cn431460-20220531-00278

Basic study and clinical significance of ureteral stricture after holmium laser lithotripsy

Yue Dong, Zheng Miao, Li Zhonghai

Department of urology, Affiliated Hospital of Jining Medical University, Jining 272000, China

Corresponding author: Yue Dong, Email: yuedong2021@163.com

Abstract **Objective** To investigate the etiology of ureteral stricture after holmium laser lithotripsy, and to provide guidance for clinical treatment and prevention. **Methods** The clinical data of 482 patients diagnosed with ureteral calculi in our hospital from May 2020 to May 2022 were retrospectively analyzed. Among them, 65 patients underwent retroperitoneal laparoscopic ureterolithotomy and 417 patients underwent ureteroscopic holmium laser lithotripsy. The normal ureter was stained with HE, and the ureteral smooth muscle cells were extracted and treated with holmium laser. Transwell assay was used to detect the chemotaxis of macrophages, and Western blot was used to detect the expression of α-smooth muscle actin (α-SMA). **Results** The incidence of postoperative ureteral stricture was higher than in retroperitoneal laparoscopic ureterotomy, and the difference was statistically significant ($P=0.008$). Mechanically, holmium laser damage ureteral smooth muscle cells during lithotripsy promotes macrophage migration and induces high expression of α-SMA. **Conclusions** Holmium laser lithotripsy is easy to cause ureteral smooth muscle cell injury and recruit macrophages to participate in the fibrosis process, resulting in ureteral stricture. During operation, muscle layer injury should be avoided as much as possible and macrophages infiltration should be reduced, which is helpful to reduce occurrence of ureteral stricture.

Key words Ureteroscopy; Laparoscopy; Lithotripsy; Stricture of Ureter

DOI:10.3760/cma.j.cn431460-20220531-00278

随着输尿管镜和腹腔镜技术的进步，绝大部分输尿管结石可以通过微创手术进行治疗[1]。相对于后腹腔镜输尿管切开取石，钬激光碎石操作简单，结石不易移位，碎石效率高，在临床应用比较普遍，但其造成输尿管狭窄的问题不容忽视。据统计，输尿管结石钬激光术后狭窄的发生率为 3% ~ 24%[2]。钬激光具有消融和凝固作用，导致结石碎裂的同时造成致输尿管热损伤[3]。钬激光组织穿透能力有限，约为 0.5 mm，在碎石时对周围组织损伤小，安全性高[4]。组织损伤后的修复过程中往往伴有免疫细胞浸润，巨噬细胞参与了电离辐射、肾脏缺血再灌注损伤修复[5-6]。迄今为止，有关钬激光碎石后发生输尿管狭窄的机制尚未达成共识，巨噬细胞在输尿管损伤后的作用尚未明了，对如何预防输尿管结石术后狭窄的经验甚少，本研究利用细胞模型证实了钬激光对输尿管平滑肌的热损伤，损伤后的平滑肌细胞趋化巨噬细胞并诱导纤维化，最终导致输尿管狭窄，这为手术方式的选择及优化提供了理论基础。

1 资料与方法

1.1 一般资料

回顾性收集 2020 年 5 月至 2022 年 5 月在本院诊断为输尿管结石的 482 例患者的临床资料，其中 65 例行后腹腔镜输尿管切开取石，417 例行输尿管镜钬激光碎石术，采用静脉肾盂输尿管造影、输尿管逆行插管造影或输尿管磁共振水成像等检查评估狭窄位置及长度[7]。正常输尿管组织来源于肾输尿管全程切除患者。所有患者均获得术前知情同意。入选标准：①输尿管结石行钬激光碎石或后腹腔镜输尿管切开取石；②结石直径≤ 2 cm。排除标准：①保守治疗、体外碎石或行经皮肾取石患者；②合并高热、脓毒血症，糖尿病血糖控制不佳者；③存在手术禁忌证者，如高龄、心、肺、肾等重要脏器功能不全、严重血液病等。

1.2 实验方法

1.2.1 细胞培养 输尿管平滑肌原代细胞培养：在肾输尿管全程切除术后 24 h 内的输尿管标本中提取原代平滑肌细胞。用手术刀片纵行剖开输尿管，去除黏膜和浆膜层，将平滑肌层剪碎，用胶原酶Ⅱ消化 1 h，通过 100 μm 孔径的筛子过滤。细胞悬液离心后使用 DMEM 完全培养基重悬并在培养瓶中培养。人单核细胞（THP-1）来源于美国菌种保藏中心（ATCC），使用 RPMI 1640 完全培养基，佛波酯（PMA）诱导成巨噬细胞。37 ℃、5% CO_2 培养。

1.2.2 HE 染色 输尿管组织经过固定、脱水、透明后切片，65 ℃烘片 2 h 后放入二甲苯、梯度酒精脱蜡，蒸馏水清洗切片，苏木素染色 3～8 min，自来水冲洗，1% 的盐酸酒精分化数秒，自来水冲洗，0.6% 氨水返蓝，流水冲洗后入伊红染液中染色 1～3 min。脱水封片后制成病理切片使用扫描仪扫片。

1.2.3 鬼笔环肽染色 在 6 孔板中将已爬好细胞的盖玻片用 PBS 浸洗 3 次，每次 3 min；4% 多聚甲醛固定 20 min，0.5% 曲拉通破膜 5 min 后，加入 200 μL 鬼笔环肽溶液（2.5 mg /L）避光孵育 30 min；PBS 冲洗 3 次后，用含 DAPI 的抗荧光猝灭剂封片。然后在荧光显微镜下采集图像。

1.2.4 Transwell 迁移实验 将输尿管平滑肌细胞（5×10^4 细胞）接种于 6 孔板，采用科瑞达（HANS-H75）钬激光处理（能量 1.5 J，频率 20 Hz），处理后的在 -80 ℃培养基中保存。将巨噬细胞接种于 Transwell 上室（8 μm，康宁公司生产），不同培养基处理 24 h 后收集小室，4% 多聚甲醛固定 20 min，用 0.1% 结晶紫染色 20 min 后显微镜观察并计数。

1.2.5 Western blot 检测 巨噬细胞在 RIPA 裂解液中裂解。采用 BCA 法检测蛋白浓度。在 10% 的十二烷基硫酸钠-聚丙烯酰胺凝胶（SDS-PAGE）中电泳，PVDF 膜转膜后脱脂奶粉封闭 1 h，一抗 4 ℃孵育过夜。二抗孵育 1 h 后使用 ECL 发光液进行曝光，曝光仪使用天能 5800。抗体：以 α-平滑肌肌动蛋白（α-SMA）（1∶ 1 000，14395-1-AP）、GAPDH（1∶ 1 000）作为内参。山羊抗小鼠 IgG（1∶ 5 000）；山羊抗兔 IgG（1∶ 5 000）。

1.3 统计学方法

使用 GraphPad Prism、Adobe Illustrator CS6 进行统计分析及做图。计数资料以百分率（%）表示，采用 Fisher 检验，计量资料采用非参数 t 检验，以 $P<0.05$ 为差异有统计学意义。

2 结果

2.1 两组术后输尿管狭窄发生率比较

后腹腔镜输尿管切开取石术后发生输尿管狭窄 1 例，发生率为 1.5%，钬激光碎石术后发生输尿管狭窄 49 例，发生率为 11.8%，两者比较差异有统计学意义（$P=0.008$）。

2.2 输尿管狭窄的临床特点

输尿管狭窄的影像学诊断主要依据强化 CT 和术中情况，患者一为输尿管结石钬激光碎石术后 9 个月、拔除双 J 管 3 个月后复查可见残余结石周围输尿管呈“S”型迂曲（图 1A 箭头所示），狭窄上段肾盂扩张积水（图 1B）。患者二为输尿管末段狭窄，采用德国狼牌（Wolf）电切镜下见狭窄周围瘢痕形成（图 1C 箭头所示），针状电极切开瘢痕组织。为了研究钬激光碎石术后输尿管狭窄，取肾输尿管全程切除后的正常输尿管组织（图 1D），行横断面 HE 染色，发现输尿管静息状态下从黏膜到肌层最厚处约为 0.5 mm，相对薄弱处 <0.5 mm（图 1E）。

2.3 钬激光损伤输尿管的基础研究

为了进一步研究钬激光对输尿管平滑肌的影响，采用胶原酶消化提取输尿管平滑肌原代细胞并培养，见细胞呈长纤维状（图 2A）。鬼笔环肽染色见细胞内微丝，从细胞骨架层面证实了提取的细胞为平滑肌细胞（图 2B、C、D）。为了模拟钬激光损伤输尿管平滑肌，采用钬激光瞬时处理 6 孔板内的平滑肌细胞，选择碎石常用参数为能量 1.5 J，频率 20 Hz（图 2E），钬激光激发后显微镜观察 6 孔板底部，可见钬激光将 6 孔板底部击碎，形成微小裂纹（图 2F），能量激发中心部位细胞悬浮死亡，周围细胞状态不佳（图 2G）。损伤后巨噬细胞常常参与修复，在体外通过佛波酯（PMA）诱导单核细胞 THP1 获得贴壁的巨噬细胞（图 2H），通过 Transwell 实验发现钬激光处理平滑肌细胞后能够明显趋化巨噬细胞（图 2I、J），并能够从蛋白层面诱导巨噬细胞高表达 α-SMA（图 2K）。

2.4 后腹腔镜切开取石的注意事项

后腹腔镜切开取石中的经验是手术过程中尽可能长切开输尿管取出结石（图 3A），清理结石周围炎症组织，暴露新鲜组织切面（图 3B），严格对位缝合切开创面（图 3C）。

3 讨论

输尿管镜碎石术是一种临床广泛应用的碎石方法，尤其是随着数字化可弯曲软镜技术的进步和大功率钬激光的应用[8-9]。目前大部分研究集中在碎石效率及安全性方面[10-11]。由于钬激光的热损伤作用，碎石后输尿管狭窄的发生率高于气压弹道及输尿管切开取石[3,12]。一项 Meta 分析比较了钬激光和气压弹道治疗输尿管结石的有效性和安全性，结果显示虽然钬激光可缩短手术时间，增加早期结石清除率和延迟排石率，但术后输尿管狭窄率高于气压弹道碎石组[3]。有学者发现后腹腔镜下输尿管切开取石较钬激光碎石的结石清除率更高，但术后并发症较多，两者术后输尿管狭窄风险相似[13]。

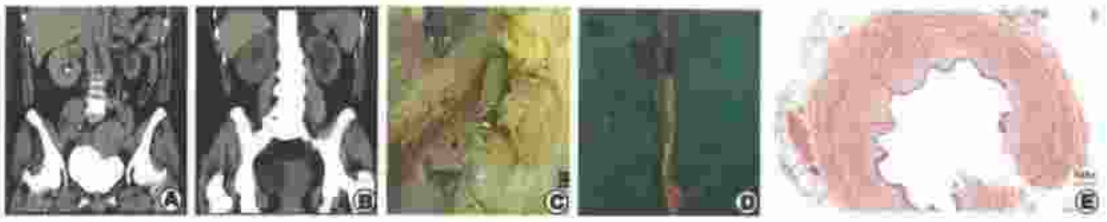


图1　输尿管狭窄的临床特点　A,B:输尿管狭窄的CT图像(A中箭头表示输尿管狭窄处);C:输尿管狭窄段瘢痕形成(箭头表示输尿管狭窄处瘢痕);D:输尿管形态;E:输尿管横断面病理图像(HE染色,×40,红线代表黏膜到肌层距离)

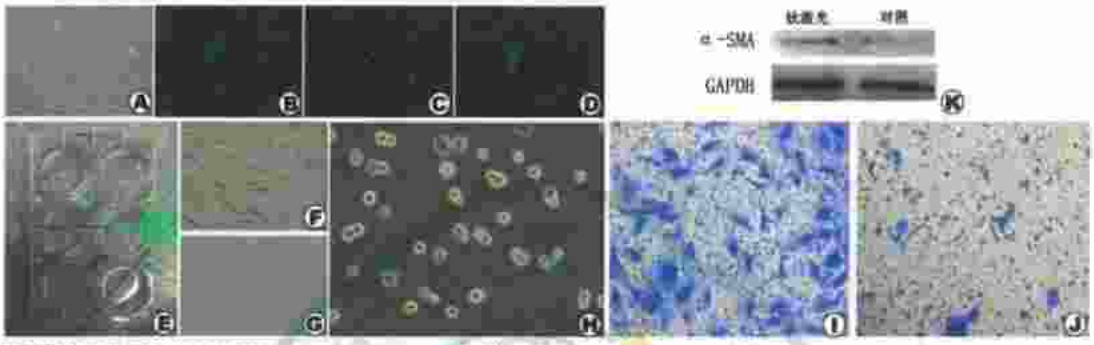


图2　输尿管钬激光损伤后的体外模拟实验(×200)　A:输尿管平滑肌细胞形态;B~D:输尿管平滑肌鬼笔环肽染色;E~G:钬激光处理6孔板内细胞;H:单核细胞在体外诱导成巨噬细胞;I,J:不同处理后的培养基对巨噬细胞的趋化实验(结晶紫染色);K:不同处理后的培养基对巨噬细胞α-SMA蛋白表达的影响



图3　后腹腔镜切开取石手术步骤　A:后腹腔镜切开输尿管取出结石;B:清理结石周围炎性组织及瘢痕;C:缝合输尿管切开面

相对于钬激光碎石,后腹腔镜输尿管切开取石的并发症明显减少,输尿管狭窄率也明显降低[12]。输尿管结石嵌塞处热损伤后输尿管局部狭窄伴有明显的肾盂积水[14]。输尿管内膜切开术是治疗良性输尿管狭窄的首选方法,术后可以同侧置入2个双J管[15]。对于结核性输尿管狭窄,可顺行置入双J管[16]。对于不适合手术重建的患者,也可以通过球囊扩张行输尿管旁路术[17-18]。内镜手术可作为输尿管狭窄治疗的首选方案,如果治疗失败,二期可选择开放或腹腔镜输尿管成形术[19]。为了研究输尿管狭窄的发生原因,本研究进行了临床与基础研究相结合的方法。先取正常输尿管进行免疫组化和HE染色,考虑到碎石过程中水流灌注及镜体扩张,结石周围输尿管处于扩张状态,钬激光的热损伤不可避免会达到肌层,故提取输尿管平滑肌原代细胞作为钬激光损伤的细胞模型。国外有研究比较了15 W和30 W钬激光碎石在输尿管镜碎石术中的有效性和安全性,证实了30 W效果更佳[20]。临床中选择30 W碎石比较温和,但体外实验发现钬激光在此能量下可瞬间将6孔板板底击碎,能量中心位置细胞死亡,这也证实了钬激光的损伤作用远远大于本研究术中所见。本研究发现输尿管狭窄周围伴有瘢痕形成,既往有研究发现创伤愈合相关的巨噬细胞在损伤输尿管中通过旁分泌TGF-β1促使成纤维细胞瘢痕形成,导致狭窄形成[21]。笔者推测钬激光损伤输尿管平滑肌细胞后通过趋化巨噬细胞参与纤维化瘢痕形成,为了进一步证实这一推断,本研究通过钬激光处理平滑肌细胞模拟钬激光对输尿管损伤,划痕处理平滑肌细胞模拟切开取石对输尿管损伤,然后与巨噬细胞共培养,通过比较发现钬激光处理平滑肌细胞后能够明显趋化巨噬细胞。近年来,在肾损伤模型患者中,通过巨噬细胞标记物(CD68

或 F4/80）和肌成纤维细胞标记物 α-SMA 的共表达证实受损肾脏中肌成纤维细胞可能来自单核细胞/巨噬细胞[22]。本研究发现共培养后巨噬细胞的 α-SMA 表达水平升高，表明巨噬细胞向成纤维细胞转化增强。另外，巨噬细胞 M2 型通过表达相关细胞因子参与基质重塑，促进胶原蛋白和纤维组织的形成，导致伤口收缩和闭合，但是这种表型的持续激活可能导致有害的组织修复和病理性纤维化[23]。基于基础研究结果，笔者在手术中总结经验：输尿管镜钬激光碎石尽量不要原位碎石，可将结石推入肾盂，行软镜下碎石；如必须原位碎石，可先留置输尿管导管，使输尿管处于松弛状态，以减少钬激光损伤肌层的概率。对于结石嵌顿时间久、周围炎性肉芽组织包裹的患者，应考虑行后腹腔镜输尿管切开取石，过程中注意保护肌层，避免过多损伤。本文阐明了钬激光碎石后可造成输尿管平滑肌细胞损伤，巨噬细胞被招募并参与纤维化，最终导致瘢痕形成、输尿管狭窄，术中尽量避免肌层的损伤，减少巨噬细胞的浸润，有助于减少输尿管狭窄的发生。

利益冲突 所有作者均声明不存在利益冲突。

参 考 文 献

[1] Assimos D, Krambeck A, Miller NL, et al. Surgical management of stones: American urological association/endourological society guideline, PART I[J]. J Urol, 2016, 196(4): 1153-1160. DOI: 10.1016/j.juro.2016.05.090.

[2] Fam XI, Singam P, Ho CC, et al. Ureteral stricture formation after ureteroscopic treatment of impacted calculi: a prospective study[J]. Korean J Urol, 2015, 56(1): 63-67. DOI: 10.4111/kju.2015.56.1.63.

[3] Chen S, Zhou L, Wei T, et al. Comparison of holmium: YAG laser and pneumatic lithotripsy in the treatment of ureteral stones: an update Meta-analysis[J]. Urol Int, 2017, 98(2): 125-133. DOI: 10.1159/000448692.

[4] Esposito C, Masieri L, Bagnara V, et al. Ureteroscopic lithotripsy for ureteral stones in children using holmium: yag laser energy: results of a multicentric survey[J]. J Pediatr Urol, 2019, 15(4): 391.e1-e7. DOI: 10.1016/j.jpurol.2019.05.004.

[5] Forsberg MH, Kink JA, Thickens AS, et al. Exosomes from primed MSCs can educate monocytes as a cellular therapy for hematopoietic acute radiation syndrome[J]. Stem Cell Res Ther, 2021, 12(1): 459. DOI: 10.1186/s13287-021-02491-7.

[6] Weng X, Zhao H, Guan Q, et al. Clusterin regulates macrophage expansion, polarization and phagocytic activity in response to inflammation in the kidneys[J]. Immunol Cell Biol, 2021, 99(3): 274-287. DOI: 10.1111/imcb.12405.

[7] 谢超群，吴泰山，谢丽红，等. 腹腔镜和输尿管镜联合治疗 15 例医源性输尿管狭窄[J]. 中国内镜杂志, 2021, 27(9): 75-80. DOI: 10.12235/E20210383.

[8] Weiss B, Shah O. Evaluation of ilusting versus basketing-can new technologies improve stone-free rates?[J]. Nat Rev Urol, 2016, 13(12): 726-733. DOI: 10.1038/nrurol.2016.172.

[9] 魏双平，史红雷，焦志敏，等. 输尿管软镜钬激光碎石治疗上尿路感染性结石的临床疗效分析（附 28 例报告）[J]. 国际泌尿系统杂志, 2022, 42(1): 98-101. DOI: 10.3760/cma.j.cn431460-0200515-00024.

[10] Tracy CR, Chareeb GM, Paul CJ, et al. Increasing the size of ureteral access sheath during retrograde intrarenal surgery improves surgical efficiency without increasing complications[J]. World J Urol, 2018, 36(6): 971-978. DOI: 10.1007/s00345-018-2204-z.

[11] 冯战启，景治安，刘彦军. 改良输尿管镜钬激光碎石术治疗输尿管嵌顿性结石的疗效研究[J]. 国际泌尿系统杂志, 2022, 42(3): 430-433. DOI: 10.3760/cma.j.cn431460-20200917-00117.

[12] Li J, Chang X, Wang Y, et al. Laparoscopic ureterolithotomy versus ureteroscopic laser lithotripsy for large proximal ureteral stones: a systematic review and meta-analysis[J]. Minerva Urol Nefrol, 2020, 72(1): 30-37. DOI: 10.23736/S0393-2249.19.03557-4.

[13] Hu H, Xu L, Wang S, et al. Ureteral stricture formation after removal of proximal ureteral stone: retroperitoneal laparoscopic ureterolithotomy versus ureteroscopy with holmium: YAG laser lithotripsy[J]. PeerJ, 2017, 5: e3483. DOI: 10.7717/peerj.3483.

[14] Roberts WW, Cadeddu JA, Micali S, et al. Ureteral stricture formation after removal of impacted calculi[J]. J Urol, 1998, 159(3): 723-726.

[15] Mohyelden K, Hussein HA, El Helaly HA, et al. Long-term outcomes of two ipsilateral vs. single double-J stent after laser endoureterotomy for bilharzial ureteral strictures[J]. J Endourol, 2021, 35(6): 775-780. DOI: 10.1089/end.2020.0956.

[16] 薛小明，吴学荣，更藏尖措，等. 顺行和逆行输尿管双 J 管支架置入术在结核性输尿管狭窄中的疗效对比研究[J]. 临床泌尿外科杂志, 2021, 36(9): 732-734. DOI: 10.13201/j.issn.1001-1420.2021.09.012.

[17] Gao X, Chen J, Wang W, et al. Step-by-step technique for the endoscopic treatment of ureteral stricture[J]. BJU Int, 2021, 28(6): 692-696. DOI: 10.1111/bju.15558.

[18] 招云亮，高媛，王跃强，等. 双镜联合钬激光内切开+球囊扩张治疗术后输尿管肠吻合口狭窄的临床研究[J]. 国际泌尿系统杂志, 2022, 42(2): 340-342. DOI: 10.3760/cma.j.cn431460-20200525-00090.

[19] 熊松，唐宇哲，付猛，等. 良性输尿管狭窄的治疗：90 例单中心回顾分析[J]. 中华腔镜泌尿外科杂志（电子版）, 2021, 15(4): 313-316. DOI: 10.3877/cma.j.issn.1674-3253.2021.04.010.

[20] Kayghi O, Aydin YM, Çiçek MÇ, et al. 15 and 30 W holmium: YAG laser lithotriptor in ureteroscopic lithotripsy: Which one is more effective and safe?[J]. J Laparoendosc Adv Surg Tech A, 2021, 31(7): 839-842. DOI: 10.1089/lap.2021.0090.

[21] Ueshima E, Fujimori M, Kodama H, et al. Macrophage-secreted

TGF-β1 contributes to fibroblast activation and ureteral stricture after ablation injury[J]. Am J Physiol Renal Physiol, 2019, 317(7): F52-F64. DOI: 10.1152/ajprenal.00260.2018.

[22] Xiong Y, Chang Y, Hao J, et al. Eplerenone attenuates fibrosis in the contralateral kidney of UUO rats by preventing macrophage-to-myofibroblast transition[J]. Front Pharmacol, 2021, 12: 620433. DOI: 10.3389/fphar.2021.620433.

[23] 刘俊, 聂宇, 王玉旭, 等. 巨噬细胞代谢与组织修复研究进展[J]. 现代免疫学, 2022, 42(3): 248-253. DOI: 1001 2478(2002)03 0248 06.

(本文编辑:彭文忠)
(收稿日期:2022-05-31)

输尿管镜下钬激光碎石术后并发输尿管狭窄的影响因素分析

杨文军 卢 友 董志灵
江西省上饶东信第五医院生殖男科，江西上饶 334000

[摘要]**目的** 分析输尿管镜下钬激光碎石术后并发输尿管狭窄的影响因素。**方法** 回顾性分析2019年1月至2021年12月上饶东信第五医院收治的100例输尿管镜下行钬激光碎石术输尿管结石患者的临床资料，根据术后是否并发输尿管狭窄分为未发生组（n=87）和发生组（n=13），比较两组可能的影响因素，分析输尿管镜下钬激光碎石术后并发输尿管狭窄的影响因素。**结果** 患者病程（β=0.963，OR=2.620，95%CI=1.945～3.529，P<0.001）、结石直径（β=1.247，OR=3.480，95%CI=2.827～4.283，P<0.001）、息肉包绕结石情况（β=2.248，OR=9.469，95%CI=0.595～150.734，P=0.013）、结石嵌顿情况（β=1.692，OR=5.430，95%CI=0.660～44.657，P=0.015）、输尿管镜类型（β=1.216，OR=3.374，95%CI=1.119～10.170，P<0.001）是输尿管镜下钬激光碎石术后并发输尿管狭窄的影响因素（P<0.05）。**结论** 对于病程较长、结石嵌顿、结石直径较大、息肉包绕结石的患者来说，并发输尿管狭窄的风险较大，此外输尿管镜较粗也是并发输尿管狭窄的危险因素。

[关键词]钬激光碎石术；输尿管结石；输尿管狭窄；影响因素
[中图分类号] R693 [文献标识码] A [文章编号] 1674-4721(2023)3(a)-0109-04

Analysis of influencing factors of ureteral stricture after ureteroscopic holmium laser lithotripsy

YANG Wenjun LU You DONG Zhiling
Department of Reproductive Andrology, Shangrao Dongxin Fifth Hospital, Jiangxi Province, Shangrao 334000, China

[Abstract] Objective To analyze the influencing factors of ureteral stricture after ureteroscopic holmium laser lithotripsy. **Methods** The clinical data of 100 patients with ureteral calculi undergoing ureteroscopic holmium laser lithotripsy admitted to Shangrao Dongxin Fifth Hospital from January 2019 to December 2021 were retrospectively analyzed. According to whether ureteral stenosis was complicated after operation, the patients were divided into the non-occurrence group (n=87) and the occurrence group (n=13). The possible influencing factors of the two groups were compared, and the influencing factors of ureteral stenosis complicated after ureteroscopic holmium laser lithotripsy were analyzed. **Results** The course of disease (β=0.963, OR=2.620, 95%CI=1.945-3.529, P<0.001), stone diameter (β=1.247, OR=3.480, 95%CI=2.827-4.283, P<0.001), polyp surrounding calculus (β=2.248, OR=9.469, 95%CI=0.595-150.734, P=0.013), stone entrapment (β=1.692, OR=5.430, 95%CI=0.660-44.657, P=0.015), type of ureteroscopy (β=1.216, OR=3.374, 95%CI=1.119-10.170, P<0.001) were influential factors for ureteral stricture after ureteroscopic holmium laser lithotripsy (P<0.05). **Conclusion** For patients with long course of disease, stone incarceration, large stone diameter and polyp around the stone, the risk of complicated ureteral stenosis is greater. In addition, thicker ureteroscope is also a risk factor for complicated ureteral stenosis.

[Key words] Holmium laser lithotripsy; Ureteral calculi; Ureteral stricture; Influencing factors

泌尿系统结石发病率较高，其中输尿管结石是常见的类型，目前治疗输尿管结石方法主要分为药物治疗、开放性手术治疗与微创治疗，其中药物治疗在发病短、结石直径大的患者中疗效较好[1]。开放性手术创口较大恢复慢，随着技术发展，微创治疗被逐渐确立为首选[2]。目前微创治疗主要分为体外碎石和体内取石。体外冲击波碎石方便快捷，价格低廉，在直径<1 cm结石中疗效较好，但清除不彻底，适用范围有限制。而输尿管镜下钬激光碎石术创伤小、成功率高，是一种具有前景的治疗方法[3-4]。但在一些情况下，微创手术也会造成输尿管出血、撕脱、狭窄等一系列并发症，输尿管狭窄是较为严重并发症之一，会造成患者预后不良，影响治疗效果。因此明确术后并发输尿管狭窄的

[基金项目]江西省卫生计生委科技计划项目（20167279）。

(C)1994-2023 China Academic Journal Electronic Publishing House. All rights reserved. http://www.cnki.net

可能原因意义重大。为此，本研究分析了输尿管镜下钬激光碎石术后并发输尿管狭窄的影响因素。

1 资料与方法

1.1 一般资料

回顾性分析江西省上饶东信第五医院2019年1月至2021年12月收治的100例输尿管镜下行钬激光碎石术输尿管结石患者临床资料，其中男69例，女31例；年龄17~72岁，平均(55.76±4.88)岁。根据术后是否并发输尿管狭窄分为未发生组(n=87)和发生组(n=13)。本研究在院内医学伦理委员会审核批准下实施(伦理批号：201901DX308)。诊断标准：参照《中国泌尿外科疾病诊断治疗指南》[4]中标准，经B超、X线平片、CT及尿路造影明确诊断为输尿管结石或输尿管狭窄。纳入标准：①符合上述诊断标准；②临床资料完整；③首次进行钬激光碎石术。排除标准：①合并其他重大疾病；②有输尿管手术史或有输尿管结石、狭窄病史；③术前有输尿管狭窄；④输尿管畸形；⑤多发输尿管结石或合并其他部位结石。

1.2 方法

收集并记录患者基本资料和疾病资料，所有患者均行钬激光碎石术，术后以门诊或电话方式随访6~24个月，记录输尿管狭窄发生情况。单因素分析患者各因素与发生输尿管狭窄的关系，并以P<0.05为标准将多变量纳入多元logistic回归分析以筛选输尿管镜下钬激光碎石术后并发输尿管狭窄的影响因素。

1.3 观察指标及评价标准

①一般资料：查阅病案明确患者性别、年龄等信息；②生化指标：使用生化分析仪(西门子，型号：AD-VIA2400)监测患者血钙和血肌酐(serum creatinine，SCr)含量；③疾病情况：通过影像学检查患者结石及肾积水情况。尿路感染标准为有膀胱刺激征、白细胞升高、同时尿培养清洁中段菌落>10^5 cfu/ml[5]。肾积水B超情况判定。轻度：肾脏大小、实质无明显异常，肾集合系统分离<3 cm；中度：肾脏轻微增大，实质变薄，集合系统分离3~4 cm；重度：肾脏变形，实质显著变薄或不可见，放射状肾柱回声，肾集合分离>4 cm[6]。④手术资料：记录患者手术时间及所用输尿管镜尺寸。

1.4 统计学方法

使用SPSS 21.0统计学软件进行数据分析，计量资料用均数±标准差($\bar{x}\pm s$)表示，两组间比较采用t检验；计数资料用率表示，两组间比较采用χ^2检验，等级资料采用秩和检验。多因素分析采用多元logistic回归分析，以P<0.05为差异有统计学意义。

2 结果

2.1 单因素分析

单因素分析结果显示，两组患者的病程、结石直径、息肉包绕结石情况、结石嵌顿情况、肾积水程度、输尿管镜类型、手术时间比较，差异有统计学意义(P<0.05)(表1)。

表1 输尿管镜下钬激光碎石术后并发输尿管狭窄单因素分析(例)

因素	发生组(n=13)	未发生组(n=87)	χ^2/Z值	P值
性别			0.439	0.749
男	10	59		
女	3	28		
年龄(岁，$\bar{x}\pm s$)	55.34±4.42	55.82±4.97	0.900	0.370
体重指数(kg/m^2，$\bar{x}\pm s$)	23.62±2.26	24.35±2.78	0.902	0.369
病程(月，$\bar{x}\pm s$)	5.15±1.34	3.08±1.79	3.998	<0.001
基础疾病				
高血压	2	9	0.293	0.633
糖尿病	1	5	0.076	0.576
高脂血症	2	8	0.481	0.615
术前治疗情况			0.024	1.000
无	11	75		
药物治疗	2	12		
血钙(mmol/L，$\bar{x}\pm s$)	2.59±0.13	2.53±0.15	1.366	0.175
SCr(μmol/L，$\bar{x}\pm s$)	77.34±6.28	78.11±6.74	0.387	0.699
结石直径			3.367	0.001
<1 cm	2	54		
1~2 cm	7	26		
>2 cm	4	7		
患侧			0.186	0.666
左	8	48		
右	5	39		
结石位置			0.022	0.982
上	6	40		
中	3	21		
下	4	26		
息肉包绕结石			13.521	0.001
是	9	18		
否	4	69		
结石嵌顿			5.826	0.016
是	12	50		
否	1	37		
尿路感染			0.202	0.754
是	8	59		
否	5	28		
肾积水程度			3.199	0.001
轻	3	61		
中	7	18		
重	3	8		
输尿管镜类型			8.265	0.009
F8.9/9.8	8	29		
F6/7.5	5	58		
手术时间			2.615	0.009
<1 h	1	37		
1~1.5 h	5	28		
>1.5 h	7	22		

注 SCr：血肌酐

2.2 多因素分析

将单因素分析所示具有统计学意义的因素进行

(C)1994-2023 China Academic Journal Electronic Publishing House. All rights reserved. http://www.cnki.net

多元 logistic 回归分析，以是否发生输尿管狭窄为因变量，赋值未发生=0，发生=1，自变量赋值见表2。多元 logistic 回归分析结果显示，患者病程、结石直径、息肉包绕结石情况、结石嵌顿情况、输尿管镜类型是输尿管镜下钬激光碎石术后患者并发输尿管狭窄的影响因素（$P<0.05$）（表3）。

表2 钬激光碎石术后并发输尿管狭窄 logistic 回归自变量赋值

自变量因素	赋值方式
结石直径	>2 cm=2，1~2 cm=1，<1 cm=0
息肉包绕结石	发生=1，未发生=0
结石嵌顿	发生=1，未发生=0
肾积水程度	重=2，中=1，轻=0
输尿管镜类型	F8.9/9.8=1，F6/7.5=0
手术时间	>1.5 h=2，1~1.5 h=1，<1 h=0

表3 输尿管镜下钬激光碎石术后并发输尿管狭窄多因素分析

相关危险因素	回归系数（β）	标准误	Wald χ^2 值	P 值	OR 值	95%CI 值	
						下限	上限
病程	0.963	0.152	40.139	<0.001	2.620	1.945	3.529
结石直径	1.247	0.106	138.395	<0.001	3.480	2.827	4.283
息肉包绕结石	2.248	1.412	2.535	0.013	9.469	0.595	150.734
结石嵌顿	1.692	1.075	2.477	0.015	5.430	0.660	44.657
肾积水程度	1.833	1.961	0.874	0.384	6.253	0.134	291.943
输尿管镜类型	1.216	0.563	4.665	<0.001	3.374	1.119	10.170
手术时间	0.367	0.735	0.249	0.804	1.443	0.342	6.096

3 讨论

钬激光可有效粉碎结石，且持续时间短术后创口小，在管镜辅助操作下内部视野清晰，便于医师操作。钬激光碎石术后患者可能并发输尿管狭窄，输尿管狭窄致病因素复杂，除先天畸形外，常作为术后并发症出现。输尿管狭窄可导致患者尿液引流受限，肾积水加重，甚至严重损害肾脏功能[9]。虽然目前治疗输尿管狭窄方法众多，但目前并无公认较好的权威治疗方法[9]。因此输尿管狭窄的预防或及早发现显得尤为重要。

本研究经 logistic 回归分析筛选得出，患者病程（β=0.963，OR=2.620，95%CI=1.945~3.529，P<0.001）、结石直径（β=1.247，OR=3.480，95%CI=2.827~4.283，P<0.001）、息肉包绕结石情况（β=2.248，OR=9.469，95%CI=0.595~150.734，P=0.013）、结石嵌顿情况（β=1.692，OR=5.430，95%CI=0.660~44.657，P=0.015）、输尿管镜类型（β=1.216，OR=3.374，95%CI=1.119~10.170，P<0.001）是输尿管镜下钬激光碎石术后并发输尿管狭窄的影响因素（P<0.05）。叶照华等[10]的研究发现，病程长、结石大、结石嵌顿均是并发输尿管狭窄的危险因素，与本研究结论一致。病程长短可影响许多疾病的转归程度，如陈湛等[11]指出，病程长可增大尿路梗阻肾炎患者不良临床结局的风险。本研究患病时间长会导致患者并发输尿管狭窄风险上升，可能由于结石随时间推移产生炎症并加重扩散，因此发现疾病后需要及早治疗，以免延误病情。结石直径过大，可能延长手术时间，进一步提升发生并发症的概率[12]。大直径结石也会加重输尿管梗阻，造成输尿管局部缺血水肿，管壁磨损可能性也越大。目前在面对直径>2 cm的结石时常采用经皮肾镜碎石取石术[13]。输尿管息肉是上皮细胞增殖或化生而来，分为原发性与继发性，继发性占比最多。目前息肉形成原因仍不明确，较为常见的说法认为和感染及慢性刺激有关[14]。输尿管壁因为结石的长时间刺激，可能导致免疫细胞分泌炎症因子，促使纤维组织形成息肉[15]。结石被息肉包绕后，更不易被排出，且息肉增加了结石体积，更易形成梗阻，也提升了手术难度。结石易嵌顿在输尿管较为狭窄部位，常被炎性组织包裹，易造成严重梗阻，患者肾积水程度也会加重[16]。嵌顿结石在碎石过程中，易上移进入肾脏区域，结石残余风险高[17]。结石嵌顿与息肉常常同时出现，可能结石嵌顿会造成输尿管壁的炎症损伤，炎症加剧息肉的形成，造成恶性循环。且嵌顿患者结石易残存，造成输尿管狭窄风险增大。在本研究中，息肉与结石嵌顿是主要的风险因素，提示出现此两类症状的患者需要重点预防可能并发症带来的风险。此外，如果上述因素导致手术时间延长或术中激光对同一部位用时延长，可能会加剧输尿管损伤，因此有研究者提出对于有类似风险的患者，应在术后延长双J管留置时间[18]。随着输尿管镜手术的普及，医源性损伤造成的输尿管狭窄越来越多，术中因素也是不得忽视的重点，有研究表明，手术时间会影响术后感染概率[19]。但患者差异、病情复杂程度、医师熟练度等，都会造成手术时间的变化[20-21]，相对而言输尿管镜型号因素的差异更为客观，输尿管镜的尺寸会影响患者预后，原因可能为尺寸较大管镜易导致输尿管壁损伤。F8.9/9.8为常见型号，但可能无法到达较狭窄部位，相比于小口径更易造成管壁撕扯性损伤。蒋廷森等[22]的研究发现F6/7.5相比于F8.9/9.8在治疗输尿管上段嵌顿性结石中安全性与可行性都更高，这提示应根据具体情况选择合适型号的输尿管镜。

综上所述，对于病程较长、结石直径较大或嵌顿、息肉包绕的患者来说，并发输尿管狭窄的风险较大，此外输尿管镜较粗也是并发输尿管狭窄的危险因素。

[参考文献]

[1]杨福星，叶章群.再谈尿路结石治疗中需重视的几个关键问题[J].中华泌尿外科杂志，2018，39(9)：644-646.

(C)1994-2023 China Academic Journal Electronic Publishing House. All rights reserved. http://www.cnki.net

[2]李勇,陈在贤.输尿管镜下钬激光治疗输尿管结石的临床研究[J].重庆医学,2017,46(26):3666-3667.
[3]颜燕,姜宁,李健,等.体外冲击波碎石和输尿管镜钬激光碎石治疗输尿管上段结石疗效对比[J].实用医学杂志,2018,34(24):4123-4126.
[4]王敏捷,陈颖红,唐丽芳,等.输尿管软镜与体外冲击波碎石治疗经皮肾镜术后残留结石的比较[J].中国微创外科杂志,2019,19(11):1012-1015.
[5]那彦群,叶章群,孙颖浩,等.中国泌尿外科学疾病诊断治疗指南[M].北京:人民卫生出版社,2014:129.
[6]尿路感染诊断与治疗中国专家共识编写组.尿路感染诊断与治疗中国专家共识(2015版)——复杂性尿路感染[J].中华泌尿外科杂志,2015,36(4):241-244.
[7]曹海根,王金锐.实用腹部超声诊断学[M].北京:人民卫生出版社,2005:267.
[8]廖文彪,杨嗣星,宋超,等.输尿管镜钬激光碎石术后输尿管狭窄的处理方法:5年单中心回顾性研究[J].中华泌尿外科杂志,2021,42(12):910-914.
[9]王坤杰,周亮,李虹.输尿管狭窄治疗中几个关键问题的探讨[J].中华泌尿外科杂志,2020,41(12):881-883.
[10]叶照华,米其武,罗杰鑫,等.输尿管结石行输尿管镜下碎石术后并发输尿管狭窄的危险因素分析[J].中华腔镜泌尿外科杂志(电子版),2017,11(1):46-48.
[11]陈湛,陈伟伟.尿路结石梗阻致化脓性肾盂肾炎患者不良临床结局的相关因素分析[J].中国现代医学杂志,2021,31(2):29-32.
[12]李鑫,何云锋,吴小候,等.上尿路结石腔道手术后并发尿脓毒血症的危险因素分析[J].重庆医科大学学报,2018,43(4):590-594.
[13]高让,廖邦华,陈云天,等.输尿管软镜钬激光碎石取石术治疗大于2 cm上尿路结石的疗效及安全性分析[J].重庆医科大学学报,2018,43(4):527-531.
[14]杨金龙,周云,耿红全,等.小儿输尿管管腔内息肉的临床诊断特点及治疗方案[J].实用医学杂志,2018,34(15):2626-2627.
[15]曹阿丹,郭海燕,翟曼丽,等.输尿管息肉双源CT泌尿系造影表现[J].临床放射学杂志,2018,37(8):1338-1341.
[16]杨明,朱文静,阎荣良,等.中药联合输尿管镜钬激光碎石术治疗嵌顿性输尿管上段结石的临床观察[J].辽宁中医杂志,2017,44(12):2561-2564.
[17]周益军,朱喜山,戴晓农,等.螺旋状套石篮辅助输尿管软镜钬激光碎石术治疗单侧直径大于1厘米输尿管上段结石临床研究[J].中国内镜杂志,2017,23(1):61-64.
[18]吴铁球,汪志民.输尿管硬镜联合软镜碎石术与微创经皮肾镜取石术处理输尿管上段嵌顿结石的比较[J].中国微创外科杂志,2017,17(11):970-973.
[19]孟娟,蔡宏瑜,张旭辉,等.输尿管结石患者术后尿源性脓毒症的影响因素及外周血NLR、PLR、PCT的诊断价值[J].中华医院感染学杂志,2021,31(20):3082-3085.
[20]黄雷,王建国.输尿管镜下钬激光碎石术与开放手术治疗老年输尿管结石疗效比较[J].中国医药科学,2021,11(3):218-220.
[21]万滨,张文圣.输尿管镜钬激光碎石术治疗输尿管结石的效果及安全性[J].中国当代医药,2021,28(31):103-106.
[22]蒋廷森,吴锦昌,陈宗证,等.6/7.5F输尿管硬镜钬激光碎石治疗输尿管上段嵌顿性结石[J].中国微创外科杂志,2017,17(7):641-643.

(收稿日期:2022-09-19)

(C)1994-2023 China Academic Journal Electronic Publishing House. All rights reserved. http://www.cnki.net

UROLOGY RESEARCH &PRACTICE

ORIGINAL ARTICLE
Endourology
Urology Research and Practice 2023;49(3):198-204
DOI: 10.5152/tud.2023.22264

Incidence of Ureteric strictures Following Ureteroscopic Laser Lithotripsy: Holmium:YAG Versus Thulium Fiber Laser

ABSTRACT

Objective: We aimed to compare the incidence of ureteric strictures between holmium:yttrium aluminum garnet and thulium fiber laser following ureteroscopic laser lithotripsy. In the present era of miniaturization of endourologic armamentarium and better optics, how safe are lasers to fire inside ureter?

Materials and Methods: It is a prospective comparative study over a period of 2 years that included patients who underwent ureteroscopic laser lithotripsy for ureteric stones. Patients were randomly divided into 2 groups: group A underwent holmium:yttrium aluminum garnet laser lithotripsy and group B underwent thulium fiber laser lithotripsy.

Results: A total of 478 patients were analyzed after excluding patients not willing to participate and patients lost to follow-up. Two hundred forty patients underwent holmium:yttrium aluminum garnet laser lithotripsy (group A) and 238 patients underwent thulium fiber laser lithotripsy (group B). The demographic data of 2 groups were comparable. The mean age of patients in group A and group B was 36.5 ± 12.52 years and 38.62 ± 10.71 years, respectively. The mean operative time in group A and group B was 47 ± 15 and 36 ± 13 minutes, respectively, while the mean laser time in group A and group B was 13.5 ± 45 minutes and 9.25 ± 3.2 minutes, respectively. Four (1.67%) patients in group A and 11 (4.62%) patients in group B developed ureteric strictures during follow-up, and the difference was statistically significant ($P < .001$). The mean length of stricture was 2.67 ± 1.27 cm in group A and 4.42 ± 2.2 cm in group B, and the difference was statistically significant.

Conclusion: Thulium fiber laser, projected as safe laser previously, has a higher incidence of ureteric strictures compared to holmium:yttrium aluminum garnet laser when used for ureteroscopic laser lithotripsy.

Keywords: Holmium, YAG laser, thulium fiber laser, ureteric strictures, ureteroscopy, ureteroureterostomy

Introduction

Ureteric stones presenting as acute flank pain is a common cause of emergency department visits, and a large number of patients require definitive treatment in the form of ureteroscopic lithotripsy. Ureteroscopic lithotripsy by lasers or pneumatic lithotripters allows fragmentation of larger stones and subsequent clearance. Lasers have outclassed pneumatic lithotriptors in the management of ureteric strictures, with less retropulsion and better fragmentation o all types of stones.[1]

Holmium:yttrium aluminum garnet (Ho:YAG) laser, being an efficient lithotripter and compatible with both flexible and rigid uretroscopes, has been considered as the gold standard for ureteroscopic lithotripsy.[2] Because of some inherent flaws in the Ho:YAG laser, thulium

Copyright © Author(s) – Available online at http://urologyresearchandpractice.org/
Content of this journal is licensed under a Creative Commons Attribution 4.0 International License.

Sajad Ahmad Para[1]
Mohammad Saleem Wani[2]
Arif Hamid[1]
Sajad Ahmad Malik[1]
Abdul Rouf Khawaja[1]
Saqib Mehdi[1]

[1]*Department of Urology, Sher-i-Kashmir Institute of Medical Sciences, Srinagar, India*
[2]*Department of Urology and Renal Transplant, Sher-i-Kashmir Institute of Medical Sciences, Srinagar, India*

*The work attributed to Department of Urology Sher-i-kashmir Institute of Medical Sciences, Srinagar, India.

Corresponding author:
Sajad Ahmad Para
sajadpara96@gmail.com

Received: November 23, 2022
Accepted: February 15, 2023
Publication Date: May 17, 2023

Cite this article as: Ahmad Para S, Saleem Wani M, Hamid A, Ahmad Malik S, Rouf Khawaja A, Mehdi S. Incidence of ureteric strictures following ureteroscopic laser lithotripsy: holmium:YAG versus thulium fiber laser. *Urol Res Pract.* 2023;49(3):198-204.

fiber laser (TFL) was introduced into the armamentarium of laser lithotripters to overcome these deficiencies. As a lithotripter, TFL outclasses the Ho:YAG laser in many aspects as follows: it uses fine fibers to deliver energy with core diameter as low as 50 µm; it is possible to operate TFL at modest pulse energy as low as 0.025 J; (3) it has a peak operating frequency up to 2000 Hz; (4) it has a pulsed infrared energy emission at a wavelength of 1940 nm that has a 4-fold absorption coefficient compared to the Ho:YAG laser and therefore has low threshold for lithotripsy and tissue ablation.[3] Comparative studies have suggested faster stone ablation rates (1.5-4 times) in favor of TFL.[4] With the use of Ho:YAG laser lithotripsy through small-size uretroscopes, the incidence of ureteric strictures was reduced compared to the use of rigid lithotripters through larger-sized uretroscopes.

Thermal effect of lasers on ureteric mucosa leads to mucosal ablation and subsequent ureteric stricture formation in many cases. Thulium fiber laser has a low depth of penetration and has been projected as safe laser for intracorporeal lithotripsy. However, studies have shown that rise in ureteric temperature was 9°C-12°C higher for TFL than the Ho:YAG laser when operated at higher frequency and slow irrigation flow, leading to increased thermal stress to the surrounding tissues.[5] In the present study, we compared the incidence of ureteric strictures between TFL and Ho:YAG laser when used for ureteroscopic lithotripsy.

Materials and Methods

This is a 2-year prospective comparative study, carried at our institute from January 2020 to December 2021. This study includes all the cases of ureteric stones that underwent ureteroscopic laser lithotripsy. Patients with ureteric stones were evaluated with computed tomography (CT) urography and subsequently planned for ureteroscopic laser lithotripsy. Patients were randomized to undergo lithotripsy with the Ho:YAG laser (Lumenis pulse 100H Ho laser, group A) or TFL (IPG photonics 50/500-QCW, group B). Written informed consent was taken from the patients, and ethical committee clearance was obtained to carry out this study. The study has been approved by Ethical committee of Sher-i-Kashmir Institute of Medical Sciences Srinagar Jammu and Kashmir India. Approval number is IEC/Skims protocol #231E/2020. Patients with past history of extracorporeal shockwave lithotripsy, ureteroscopy, or open surgery done on the ureter were excluded from study. Also, patients with past history of genitourinary strictures, endometriosis, retroperitoneal fibrosis, or pyonephrosis were also excluded from the study.

Ureteroscopy was done under spinal anesthesia using 6/7.5 Fr semi-rigid ureteroscope with normal saline irrigation by continuous and pulsatile irrigation bulb. The steps of the procedure were same except the type of laser used in 2 groups. In both groups 200 µm fiber was used to deliver laser energy. Lithotripsy was started with 0.4 J and 8 Hz in both the groups and gradually increased if disintegration was ineffective. After lithotripsy, larger stone fragments were removed with a forceps and a double J (DJ) stent was deployed at the end of the procedure. Stone clearance and placement of DJ stent was confirmed with fluoroscopy. A follow-up x-ray kidney ureters and bladder (KUB) was done after 2 weeks to look for any residual fragments. The DJ stent was removed 4 weeks after the procedure. An ultrasound examination of the abdomen was done 6 weeks after stent removal to look for any residual hydronephrosis. Patients with fever, flank pain, increase in hydroureteronephrosis, or obstructive uropathy underwent CT urography to identify any stricture. Patients with pyonephrosis or urosepsis underwent percutaneous nephrostomy tube placement. The length and site of stricture was estimated by CT urography (Figure 1), table retrograde pyelography (Figure 2), and antegrade pyelography (Figure 3). All those patients with ureteric strictures underwent Tc^{99m} diethylenetriamine pentaacetate (DTPA) scan to quantify renal function. Patients with ureteric strictures underwent endoureterotomy, ureteroureterostomy (Figure 4), ureteroneocystostomy, Boari flap reconstruction, or nephrectomy depending on the length of stricture, site of stricture, and salvageability of renal function. Patients treated for ureteric strictures were followed at 3 months post-surgery with Tc^{99m} DTPA

MAIN POINTS

- *Thulium fiber laser has low threshold for lithotripsy and tissue ablation compared to holmium:yttrium aluminum garnet (Ho:YAG) laser.*
- *Although the optical penetration depth of thulium fiber laser (TFL) is less compared to the Ho:YAG laser, the TFL energy is absorbed 16 000 times more than the Ho:YAG laser after passing 1 mm depth of tissue, reflecting into severe tissue ablation associated with TFL.*
- *Thulium fiber laser has a higher incidence of ureteric strictures compared to the Ho:YAG laser when used for ureteroscopic laser lithotripsy.*
- *Thulium fiber laser should be used cautiously inside the ureter with low energy at lower frequency setting with continuous irrigation.*

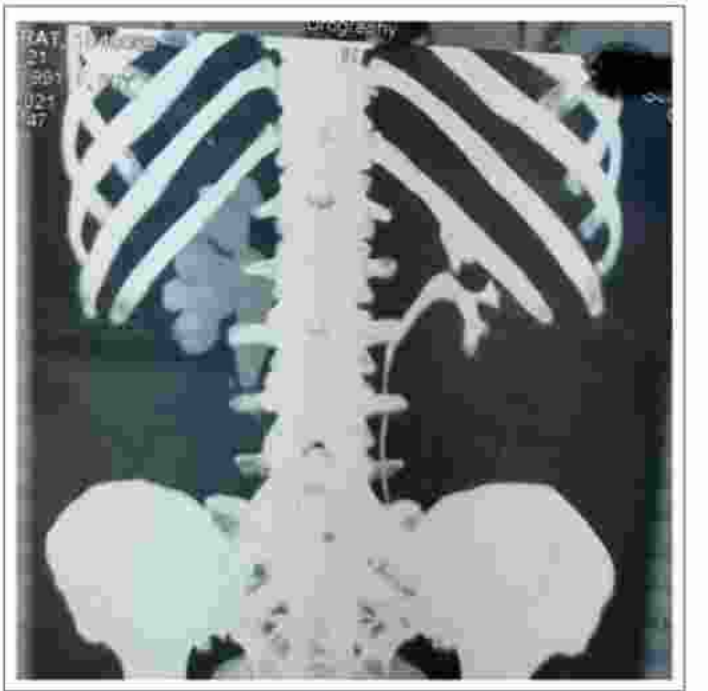


Figure 1. Computed tomography urography: reconstructed image showing right-sided hydroureteronephrosis due to upper ureteric stricture.



Figure 2. Antegrade and retrograde pyelography delineating the length of stricture (red arrow).

scan and CT urography. Statistical analysis was done using Statistical Package for Social Sciences (SPSS) version 22.0. (IBM SPSS Corp.; Armonk, NY, USA). The qualitative data are presented as numbers and percentages, while the quantitative data are presented as mean (SD). The normal distribution of quantitative data was assessed by



Figure 3. Left antegrade pyelography showing complete cutoff in the upper ureter.

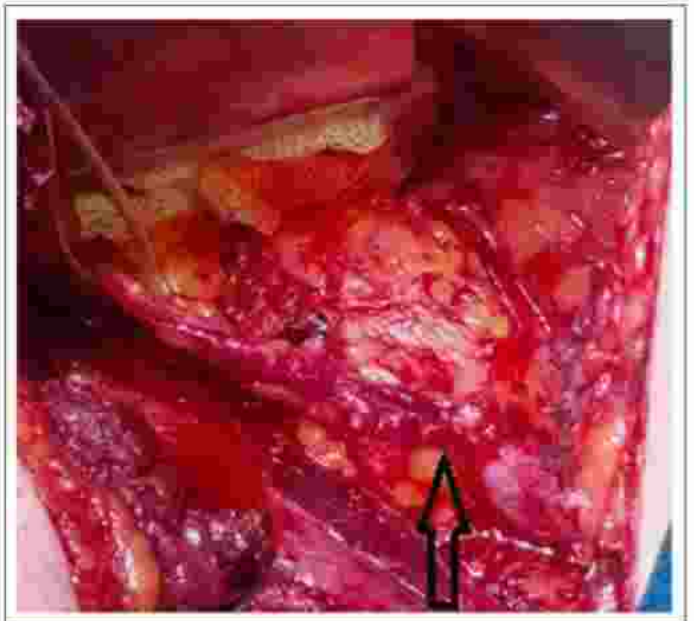


Figure 4. Intraoperative picture of the upper ureteric stricture (black arrow).

an independent sample *t*-test. Comparison of qualitative variables between the groups was done using the chi-square test. Statistical significance of any parameter was defined as *P*-value <.05.

Results

Between January 2020 and December 2021, 540 patients with ureteric calculi were planned for ureteroscopic laser lithotripsy. Out of these 21 declined to participate and a further 30 patients were excluded as they did not qualify to participate in the study. The remaining 489 patients were randomly divided into 2 groups: group A (246 patients) who underwent Ho:YAG laser lithotripsy and group B (243 patients) who underwent TFL lithotripsy. During the study, 6 patients from group A and 5 patients from group B lost to follow-up. Figure 5 shows the stages of our study in a Consolidated Standards of Reporting Trials diagram.

The demographic profile of our study groups is shown in Table 1, and there was no statistically significant difference between the 2 groups. The percentage of females in group A and group B was 36.25% and 35.29%, respectively. The average age of patients in group A and group B was 36.5 ± 12.52 years and 38.62 ± 10.71 years, respectively, and the difference was not statistically significant ($P = .45$). The average waiting period to undergo procedure is 7.5 ± 1.5 days and 8 ± 2.5 days in group A and group B, respectively, and the difference was not statistically significant. The average stone size in group A was 8.9 ± 3.5 mm and that in group B was 9.1 ± 3.2 mm ($P = .25$). Stone density was 922 ± 241 hounsfield unit (HU) and 918 ± 235 HU in group A and group B, respectively ($P = .82$). The stone parameters of 2 groups were comparable. The percentage of stones in the upper ureter (above crossing of iliac vessels) was 40% and 39% in group A and group B, respectively ($P = .21$).

The intraoperative parameters of the 2 groups are shown in Table 2. The mean operative time in group A and group B was 47 ± 15 and 36 ± 13 minutes, respectively, and the difference was

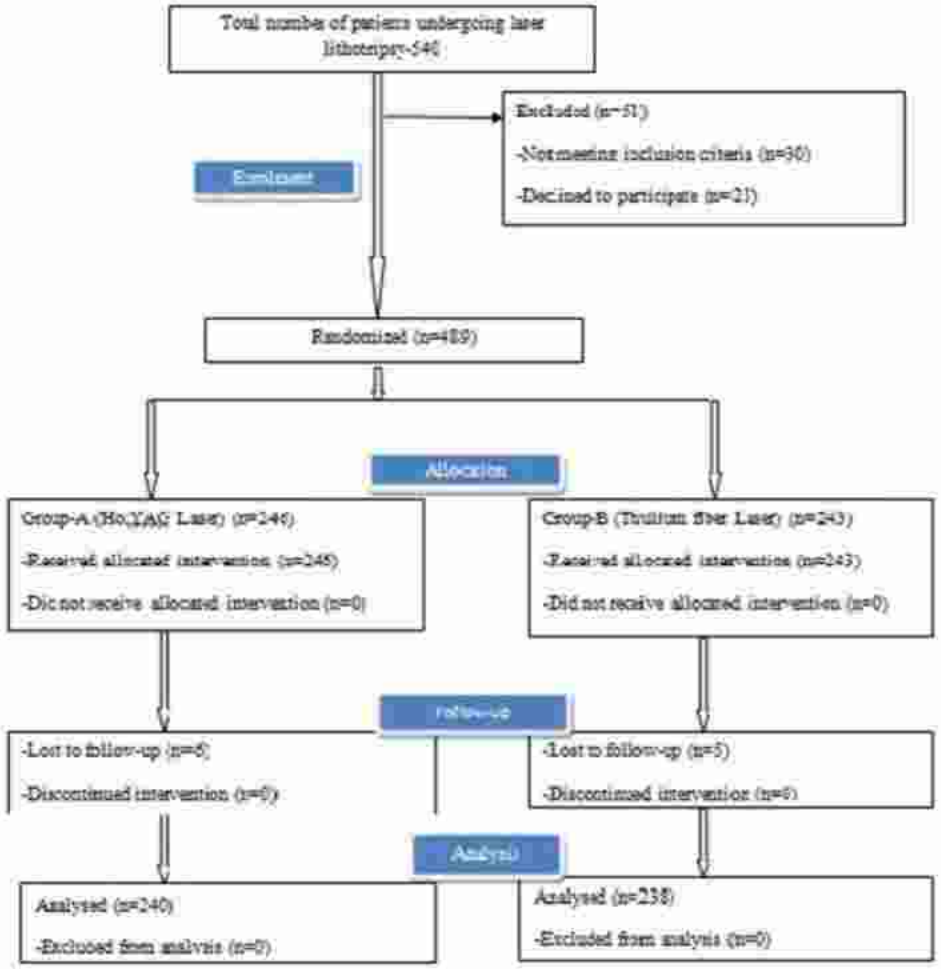


Figure 5. Stages of our study in a Consolidated Standards of Reporting Trials diagram.

statistically significant ($P < .05$). The mean laser time in group A was 13.5 ± 4.5 minutes and that in group B it was 9.25 ± 3.2 minutes. The difference in the laser time was statistically significant ($P < .001$). Forty-eight percent of patients in group A and 37% of cases in group B required augmentation in frequency and energy to achieve the desirable fragmentation after starting with low-energy setting, and the difference was significant ($P < .05$). The average laser energy spent in group A and group B was 4.4 ± 1.2 and 3.12 ± 1.3 kJ/case, respectively, and the difference was not statistically significant ($P < .23$). Fifteen percent of patients in group A and 13.02% of patients in group B had adverse events recorded intraoperatively that included bleeding impairing vision (10% in group A and 8.82% in group B), visible mucosal ablation (8.75% in group A and 7.56% in group B), and ureteric perforation (1.25% in group A and 0.84% in group B). The difference was not statistically significant ($P < .42$).

Table 1. Demographic Profile of Patients

Demographic Profile	Group A (Ho:YAG), n = 240	Group B (TFL), n = 238	*P*
Age in years (mean ± SD)	36.5 ± 12.52	38.62 ± 10.71	.45
Sex (male/female)	153/87	154/84	.28
Stone size in mm (mean ± SD)	8.9 ± 3.5	9.1 ± 3.2	.25
Stone density in HU (mean ± SD)	922 ± 241	918 ± 235	.82
Location of stone in percent (upper ureter/lower ureter)	40/60	39/61	.21

Ho, holmium; TFL, thulium fiber laser; YAG, yttrium aluminum garnet.

The incidence of postoperative ureteric strictures following ureteroscopic laser lithotripsy is shown in Table 3. Four (1.67%) patients in group A and 11 (4.62%) patients in group B developed ureteric strictures during follow-up, and the difference was statistically significant ($P < .001$). Majority of patients with strictures presented with flank pain and fever (75% in group A and 82% in group B). Asymptomatic progressive hydronephrosis was reported in 1 patient of group A and 2 patients of group B. The mean time of presentation following removal of DJ stent was 41 ± 19 days in group A and 39 ± 17 days in group B, and the difference was not significant ($P < .45$). Percutaneous nephrostomy tube placement was required to drain pyonephrosis and control sepsis in 3 patients of group A and 9 patients of group B. Strictures were predominantly located in the upper ureter in both the groups (75% in group A and 78% in group B). The mean length of stricture documented on CT urography/antegrade or retrograde pyelography was 2.67 ± 1.27 cm in group A and 4.42 ± 2.2 cm in group B, and the difference was statistically significant ($P < .001$).

Table 2. Intraoperative Parameters of the 2 Study Groups

Intraoperative Parameters	Group A (Ho:YAG), n = 240	Group B (TFL), n = 238	*P*
Operative time in minutes (mean ± SD)	47 ± 15	36 ± 13	.05
Laser time in minutes (mean ± SD)	13.5 ± 4.5	9.25 ± 3.2	.001
Laser energy spent in kJ/case (mean ± SD)	4.4 ± 1.2	3.12 ± 1.3	.23
Adverse events recorded (%)	15%	13.02%	.42
–Bleeding impairing vision	10%	8.82%	
–Visible mucosal ablation	8.75%	7.56%	
–Ureteric perforation	1.25%	0.84%	

Ho, holmium; TFL, thulium fiber laser; YAG, yttrium aluminum garnet.

Laser endoureterotomy was done to treat small passable strictures. One patient in each group had strictures amenable to laser endoureterotomy. Two patients in group A and 5 patients in group B required ureteroureterostomy to restore continuity of ureter. Short-segment lower ureteric strictures, 1 in group A and 2 in group B, required ureteroneocystostomy. One patient in group B with long-segment lower ureteric stricture required Boari flap reconstruction. Two patients in group B required nephrectomy for non-functional kidney; however, no nephrectomy was reported in group A.

Discussion

Ureteroscopic lithotripsy is considered as the gold standard treatment for ureteric stones. Conventional lithotripsy by pneumatic lithotripters had the problem of poor fragmentation of harder stones and retropulsion. Introduction of laser lithotripters has allowed the use of small-size uretroscopes, better vision because of good flow of irrigation fluid through ureteroscope, efficient fragmentation, and less retropulsion, thus reducing the operative time and the incidence of ureteric strictures.[6] Holmium:YAG laser became the gold standard in laser lithotripsy with its ability to fragment all kinds of stones and a better safety profile. Safety was attributed to its limited tissue penetration and high absorption coefficient in water, thus reducing the collateral damage.[7]

Table 3. Comparison of Ureteric Strictures in 2 Study Groups

Ureteric Strictures Following Procedure	Group A (Ho:YAG), n = 240	Group B (TFL), n = 238	*P*
Incidence of ureteric strictures, n (%)	4 (1.67%)	11 (4.62%)	.001
Presenting symptom, n (%)			.22
–Fever and pain	3 (75%)	9 (82%)	
–Asymptomatic progressive hydronephrosis	1 (25%)	2 (18%)	
Time of presentation following the removal of DJ stent, in days (mean ± SD)	41 ± 19	39 ± 17	.45.
Percutaneous nephrostomy tube placed, n (%)	3 (75%)	9 (81.81%)	.42
Location of stricture, n (%)			.35
–Upper ureter	3 (75%)	8 (72.72%)	
–Lower ureter	1 (25)	3 (27.27%)	
Mean length of stricture in cm (mean ± SD)	2.67 ± 1.27	4.42 ± 2.2	.001
Procedures done for ureteric strictures			
–Laser endoureterotomy	1	1	
–Ureteroureterostomy	2	5	
–Ureteroneocystostomy	1	2	
–Boari flap reconstruction	0	1	
–Nephrectomy	0	2	

DJ, double J; Ho, holmium; TFL, thulium fiber laser; YAG, yttrium aluminum garnet.

There are some flaws associated with the Ho:YAG laser generator. The generator requires an adequate cooling system that contributes to its large size. High-power Ho:YAG generator employs numerous crystal cavities to integrate the overall power output. These architectural anomalies result in an output beam that is multimodal and nonuniform with hotspots. This type of laser beam is difficult to precisely focus onto a small target and therefore demands the use of thicker optical fiber with a core diameter of 200 µm or larger.[8] The architecture of the Ho:YAG generator makes it susceptible to external shocks, leading to the misalignment of reflecting mirrors within the crystal cavity causing enduring damage to the generator and the optical fiber. These limitations paved the way for TFL into intracorporeal lithotripsy. The TFL uses a thin (10-20 µm core diameter) and long silica fiber doped with thulium ions. Multiple diodes are used to excite thulium ions. The final output beam has a wavelength of 1940 nm that can be operated in continuous or pulsed mode. The diode laser used for laser pumping has an emission spectrum that precisely matches the thulium ion absorption line. There is less heat dissipation and a potential to operate at high-power setting (>50 W) and higher frequencies (up to 2000 Hz). It uses small-sized fans for forced air cooling, reducing the size of the machine.[9]

Thulium fiber laser is an efficient lithotripter with 2 times faster fragmentation and 4 times superior dusting compared to the Ho:YAG laser. Schembri et al[10] reported that TFL attains high ablation rates and surpasses Ho:YAG laser over a range of different settings and ablation modes. The ability of TFL to operate at low pulse energy reduces retropulsion and need of ancillary procedures for residual stones. In our study, the mean operative time and mean laser time were less in the TFL group compared to the Ho:YAG laser group, and the difference was statistically significant. Besides efficient lithotripsy, better vision and less retropulsion by TFL may be the reason for less operative time compared to the Ho:YAG laser. The mean laser energy spent in lithotripsy did not differ in the 2 groups. Stone factors like density, composition, and size of the stone determine the mean laser energy spent during the procedure, and these factors were comparable in the 2 groups.

There is a significant variability about the ureteric stricture rate following ureteroscopic lithotripsy reported in the literature, with incidence ranging from 0.30% to 23.81%. Adiyat et al[11] and Li et al reported a stricture rate of 1.4% and 2.95%, respectively, following Ho:YAG laser lithotripsy, and the results are comparable with our study. The incidence of ureteric strictures in our study was reported to be higher in the TFL group as compared to the Ho:YAG laser group, and the difference was statistically significant. The TFL used for the procedure in our study was IPG photonics 50/500-QCW TFL. The TFL beam has a wavelength of 1940 nm, which is equivalent to the near-infrared absorption peak of water at 22 °C. The absorption coefficient of the TFL is 14 mm^{-1}, which corresponds to the optical penetration depth of 0.077 mm in water and is much less than that of the Ho:YAG laser having an optical penetration depth of 0.4 mm.[12] These features

should add to the safety profile of the TFL, but what is the reason for clustering of stricture cases in our study that is predominantly related to TFL use? The answer needs to be dug out.

The intensity of the laser beam diminishes while travelling through a medium because of absorption, and the rate of decay in intensity is determined by the absorption coefficient of the material α. According to Beer–Lambert law, the intensity of laser beam diminishes exponentially with the depth as it travels through the medium.[11]

$$I_z = I_0 e^{-\alpha z}$$

where I_z is the intensity after penetrating the depth z, z is the depth penetrated, e ($e = 2.7182$) is the Euler's number, and α is the absorption coefficient of the material α.

According to this mathematical equation, the energy of a laser beam will decay by a factor of e (2.71828) while traversing each successive optical penetration depth of that medium. The energy of the Ho:YAG laser beam will be reduced to 37% of its energy at origin after travelling through a medium for a distance corresponding to its optical penetration depth. For TFL, energy will reduce to 1.7% of its energy at source after travelling the distance equivalent to the optical penetration depth of that medium. Practically after traversing 1 mm depth of water, the Ho:YAG laser pulse will possess about 4% of its energy at source, while the TFL beam will have a mere intensity of 0.00024% left with it after travelling the same distance. No doubt, the optical penetration depth of TFL is less compared to the Ho:YAG laser. Because of the logarithmical pattern of laser energy absorption in the tissue, the TFL energy is absorbed 16 000 times more than the Ho:YAG laser after travelling 1 mm depth. This high absorption coefficient reflects in low threshold for tissue ablation and more tissue damage in favor of TFL. The TFL has a natural "moses" potential attributed to its uniform pulse energy.[14] The depth traversed is again augmented by the "Moses" effect. The TFL pulse has a low threshold for tissue ablation and vapor channel initiation because of its high water absorption coefficient that translates into worse tissue damage in the ureter during laser lithotripsy.[15]

Another factor suggested for more stricture rate is the high temperature generated during TFL laser lithotripsy. Ureteric temperatures have exceeded physiological limits after TFL use at high-energy setting and low irrigation rate.[16] Lack of ureteric access sheath and poor return of irrigation fluid in rigid ureteroscopy are the obvious reasons for raised intraurethric temperature. The threshold temperature for cellular damage being 43°C is crossed within the first 1 second of laser use in the absence of adequate irrigation. Surgical factors increasing the chance of thermal ureteric injury are low irrigation flow, higher laser energy setting, and instrument use without access sheath.[17] Liang et al[18] reported a marked rise in the ureteric temperature at higher frequency compared to lower frequency setting at equal power. So these might be contributing factors to the high stricture rate in the TFL group. Tokas et al[19] studied the effect of rise in the intraurethric temperature during laser lithotripsy and its effect on the course of healing. At higher energy settings, TFL causes a marked rise in intraurethric temperature and worse tissue damage reflecting into dense scars on subsequent healing. They proposed brief on/off laser activation intervals, cold continuous irrigation, and use of access sheaths for better irrigation to maintain physiological intraurethric temperature.

The average length of stricture in our study was 2.67 ± 1.27 cm in the Ho:YAG group and 4.42 ± 2.2 cm in the TFL group. Larger stricture length in the TFL group can be attributed to low threshold for tissue ablation and more pronounced rise in the intraurethric temperature. Small-length upper ureteric strictures are well managed by ureteroureterostomy with excellent results.[20] Two patients in group A and 5 patients in group B needed ureteroureterostomy to restore the continuity of ureter. Laser endoureterotomy has a success rate of 62% for small-length ureteric strictures.[21] One patient in each group underwent laser endoureterotomy with successful outcome. Small-segment lower ureteric strictures are amenable to ureteroneocystostomy, while long-segment lower ureteric strictures require Boari flap reconstruction.[22] One patient in the Ho:YAG group and 2 in the TFL group required ureteroneocystostomy, while 1 patient in the TFL group required Boari flap reconstruction for long-segment lower ureteric stricture. Non-salvageable renal function with pyonephrosis was managed by nephrectomy in the TFL group.

Conclusion

There is a higher incidence of ureteric strictures following the use of TFL for ureteroscopic lithotripsy. Although projected as a safe laser, TFL should be used cautiously inside the ureter especially at higher power/frequency settings. Low energy at low frequency setting with continuous irrigation can reduce the incidence of ureteric strictures in TFL lithotripsy.

Ethics Committee Approval: *Ethical committee approval was received from the Ethical committee of Sher-i-Kashmir Institute of Medical Sciences Srinagar Jammu and Kashmir India (Approval number: IEC/Skims protocol #231E/2020).*

Informed Consent: *Written informed consent was obtained from patients who participated in this study.*

Peer-review: *Externally peer-reviewed.*

Author Contributions: *Concept – S.A.P.; Design – M.S.W.; Supervision – A.H.; Resources – S.A.M.; Materials – A.R.K.; Data Collection and/or Processing – S.A.P.; Analysis and/or Interpretation – A.H.; Literature Search – S.M.; Writing Manuscript – A.R.K.; Critical Review – M.S.W.*

Declaration of Interests: *The authors declare that they have no competing interest.*

Funding: *The authors declare that this study had received no financial support.*

References

1. Maghsoudi R, Amjadi M, Norizadeh D, Hassanzadeh H. Treatment of ureteral stones: A prospective randomized controlled trial on comparison of Ho:YAG laser and pneumatic lithotripsy. *Indian J Urol.* 2008;24(3):352-354. [CrossRef]
2. Sayer J, Johnson DE, Price RE, Cromeens DM. Ureteral lithotripsy with the holmium:YAG laser. *J Clin Laser Med Surg.* 1993;11(2):61-65. [CrossRef]
3. Fried NM, Irby PB. Advances in laser technology and fiber-optic delivery systems in lithotripsy. *Nat Rev Urol.* 2018;15(9):563-573. [CrossRef]
4. Traxer O, Keller EX. Thulium fiber laser: the new player for kidney stone treatment? A comparison with holmium: YAG laser. *World J Urol.* 2020;38(8):1883-1894. [CrossRef]
5. Hardy LA, Wilson CR, Irby PB, Fried NM. Thulium fiber laser lithotripsy in an *in vitro* ureter model. *J Biomed Opt.* 2014;19(12):128001. [CrossRef]

6. Erhard MJ, Bagley DH. Urologic applications of the holmium laser: preliminary experience. *J Endourol*. 1995;9(5):383-386. [CrossRef]
7. Emiliani E, Talso M, Haddad M, et al. The true ablation effect of Holmium YAG laser on soft tissue. *J Endourol*. 2018;32(3):230-235. [CrossRef]
8. Haddad M, Emiliani E, Rouchausse Y, et al. Impact of the curve diameter and laser settings on laser fiber fracture. *J Endourol*. 2017;31(9):918-921. [CrossRef]
9. Jackson SD, Lauto A. Diode-pumped fiber lasers: a new clinical tool? *Lasers Surg Med*. 2002;30(3):184-190. [CrossRef]
10. Schembri M, Sahu J, Aboumarzouk O, et al. Thulium fiber laser: the new kid on the block. *Turk J Urol*. 2020;46:S1-S10.
11. Adiyat KT, Meuleners R, Monga M. Selective postoperative imaging after ureteroscopy. *Urology*. 2009;73(3):490-493. [CrossRef]
12. Jansen ED, van Leeuwen TG, Motamedi M, Borst C, Welch AJ. Temperature dependence of the absorption coefficient of water for midinfrared laser radiation. *Lasers Surg Med*. 1994;14(3):258-268. [CrossRef]
13. Allmen MV, Blatter A. *Laser-Beam Interactions with Materials: Physical Principles and Applications*. Vol. 1. Springer Series in Materials Science. springer verlag berlin Heidelberg.1995;1:115-165.
14. Chiron PH, Berthe LL, Coninck VD. Comparison of vapor bubbles induced by an holmium:YAG Laser and a SuperPusled Thulium Fiber Laser. *J Endourol*. 2018;32:40-45.
15. Schomacker KT, Domankevitz Y, Flotte TJ, Deutsch TF. Co:MgF2 laser ablation of tissue: effect of wavelength on ablation threshold and thermal damage. *Lasers Surg Med*. 1991;11(2):141-151. [CrossRef]
16. Belle JD, Srikureja N, Chen N, et al. MP65-03 Does the novel thulium laser generate more heat than the conventional holmium laser? *J Urol*. 2021;206(suppl 3):1119-1110. [CrossRef]
17. Aldoukhi AH, Roberts WW, Hall TL, Ghani KR. Watch your distance: the role of laser fiber working distance on fragmentation when altering pulse width or modulation. *J Endourol*. 2019;33(2):120-126. [CrossRef]
18. Liang H, Liang L, Yu Y, et al. Thermal effect of holmium laser during ureteroscopic lithotripsy. *BMC Urol*. 2020;20(1):69. [CrossRef]
19. Tokas T, Rice P, Seitz C, Gauhar V, Somani B. Temperature change during laser upper-tract endourological procedures: current evidence and future perspective. *Curr Opin Urol*. 2023;33(2):108-115. [CrossRef]
20. Knight RB, Hudak SJ, Morey AF. Strategies for open reconstruction of upper ureteral strictures. *Urol Clin North Am*. 2013;40(3):351-361. [CrossRef]
21. Hardy JD, Eraslan S. Autotransplantation of the kidney for high ureteral injury. *J Urol*. 1963;90:563-574. [CrossRef]
22. Meretyk S, Albala DM, Clayman RV, Denstedt JD, Kavoussi LR. Endoureterotomy for the treatment of ureteric strictures. *J Urol*. 1992;147(6):1502-1506. [CrossRef]

泌尿外科
研究与实践

原文尿路外科
泌尿外科研究与实践2023；49(3)：198-204
DOI：10.5152/tud.2023.22264

输尿管镜激光碎石术后输尿管狭窄的发生率：钬YAG激光与铥光纤激光

摘要

目的：本研究旨在比较钬：钇铝石榴石激光与铥光纤激光在输尿管镜激光碎石术后输尿管狭窄的发生率。在当前内镜器械小型化和光学性能提升的时代，输尿管内发射激光的安全性如何？

材料与方法：本研究为前瞻性对比研究，为期2年，纳入接受输尿管镜激光碎石术治疗输尿管结石的患者。患者随机分为两组：A组采用钬：钇铝石榴石激光碎石术，B组采用铥光纤激光碎石术。

结果：经过剔除不参与研究的患者和失访患者后，共纳入478例患者进行分析。其中240例接受钬：钇铝石榴石激光碎石术（A组），238例接受铥光纤激光碎石术（B组）。两组患者人口学资料基本一致。A组和B组患者的平均年龄分别为36.5±12.52岁和38.62±10.71岁。两组平均手术时间分别为47±15分钟和36±13分钟，激光治疗时间分别为13.5±45分钟和9.25±3.2分钟。随访期间，A组有4例（1.67%）患者出现输尿管狭窄，B组有11例（4.62%）患者出现，两组差异具有统计学意义（P <.001）。A组狭窄平均长度为2.67±1.27厘米，B组为4.42±2.2厘米，两组差异同样具有统计学意义。

结论：在输尿管镜激光碎石术中，铥光纤激光器与钬：钇铝石榴石激光器相比，发生输尿管狭窄的几率更高，而此前认为铥光纤激光器是安全的。

关键词：钬、YAG激光、铥光纤激光、输尿管狭窄、输尿管镜、输尿管尿道造口术

萨贾德·艾哈迈德·帕拉[1]
Mohammad Saleem Wani[2]
阿里夫·哈米德[1]
萨贾德·艾哈迈德·马利克[1]
Abdul Rouf Khawaja[1]
萨基卜·迈赫迪[1]

印度斯利那加克什米尔医学科学研究所[1]尿科和肾脏移植科

克什米尔医学科学研究所[2]尿科和肾脏移植科

*本研究由印度斯利那加克什米尔大学医学院泌尿外科系完成

通讯作者：SajadAhmadPara
sajadpara96@gmail.com

收到日期：11月25日 2022
接受日期：2月15日 2023
出版日期：5月17日 2023

本文引用格式：Ahmad Para S., Saleem Wani M., Hamid A., Ahmad Malik S., Rouf Khawaja A., Mohdi S.输尿管镜激光碎石术后输尿管狭窄发生率：钬：YAG与铥光纤激光。*Urol Res Pract.* 2023;49(3):198-204.

介绍

输尿管结石急性发作引发的剧烈腰痛是急诊科常见病例，多数患者需通过输尿管镜碎石术进行根治。该手术采用激光或气压式碎石器，能有效粉碎大块结石并完成碎石排石。在治疗输尿管狭窄方面，激光碎石技术已超越传统气压式碎石器，其回弹力更小，对各类结石的碎石效果更佳。[1]

钬酸钇铝石榴石（Ho：YAG）激光作为高效碎石器，可与软硬式输尿管镜兼容，一直被视为输尿管镜碎石术的金标准。[2]但由于钬酸钇铝石榴石激光器本身存在一些缺陷，铥

版权归作者所有，由AVES出版有限公司在线发布http://urologyresearchandpractice.org/
本期刊内容采用知识共享署名4.0国际许可协议授权。

为弥补传统激光碎石仪的不足，光纤激光（TFL）被引入临床应用。作为新型碎石设备，TFL在多个方面超越了钬：钇铝石榴石（Ho：YAG）激光器：其核心直径低至50μm的细光纤即可实现高效能量传输；可采用低至0.025焦耳的脉冲能量进行操作；(3)工作频率峰值可达2000赫兹；(4)其脉冲红外能量波长为1940纳米，吸收系数是Ho：YAG激光器的四倍，因此在碎石和组织消融方面具有更低的阈值。[5]比较研究表明，TFL的结石消融速度比Ho：YAG激光器快1.5-4倍。[6]通过小型尿道镜进行Ho：YAG激光碎石术时，相较于使用大型尿道镜配合刚性碎石器，输尿管狭窄的发生率显著降低。

激光对输尿管黏膜的热效应常导致黏膜消融及继发性狭窄。钬光纤激光器因其穿透深度较浅，曾被视为内镜碎石术的安全选择。但研究表明，当采用高频操作和低流量冲洗时，钬光纤激光器使输尿管温度升高幅度比钬：钇铝石榴石激光器高出9-12℃，从而对周围组织产生更大的热应力。[7]本研究通过对比输尿管镜碎石术中使用TFL和钬：钇铝石榴石激光器的输尿管狭窄发生率，探讨不同激光器的临床差异。

材料和方法

本研究为一项为期两年的前瞻性对比研究，于2020年1月至2021年12月在本院开展。研究纳入所有接受输尿管镜激光碎石术治疗的输尿管结石病例。患者经计算机断层扫描（CT）尿路造影评估后，计划接受输尿管镜激光碎石术治疗。患者随机分组接受Ho：YAG激光（Lumenis脉冲100H Ho激光，A组）或TFL激光（IPG photonics 50/500-QCW，B组）碎石治疗。所有患者均签署书面知情同意书。本研究已获得印度查谟和克什米尔地区斯利那加舍尔-克什米尔医学科学研究所伦理委员会批准，批准号为IEC/Skims协议#231E/2020。研究对象既往曾接受过体外冲击波碎石术、输尿管镜检查或开放手术治疗的患者

要点

- *与钬铝石榴石（Ho：YAG）激光相比，钬光纤激光在碎石和组织消融方面具有更低的阈值。*
- *虽然钬光纤激光（TFL）的光穿透深度比Ho：YAG激光低，但当穿透1毫米组织深度后，TFL能量被吸收的量是Ho：YAG激光的16 000 倍，这导致TFL出现严重的组织烧蚀。*
- *在输尿管镜激光碎石术中，钬光纤激光器引发输尿管狭窄的风险高于钬：钇铝石榴石激光器。*
- *使用钬光纤激光治疗输尿管时，应采用低能量、低频设置，并配合持续冲洗，操作需格外谨慎。*

本研究排除了输尿管患者，同时排除了有泌尿生殖道狭窄、子宫内膜异位症、腹膜后纤维化或肾盂肾炎病史的患者。

输尿管镜检查在脊髓麻醉下进行，采用6/7.5 Fr半刚性输尿管镜，通过连续灌注和脉冲灌注球进行生理盐水冲洗。两组手术步骤相同，仅激光类型不同。两组均使用200 μ m光纤传输激光能量。碎石术初始能量为0.4焦耳、频率8赫兹，若碎石效果不佳则逐步增加能量。碎石后用镍子取出较大结石碎块，并在手术结束时置入双J型支架。通过X光透视确认结石清除及支架置入情况。术后2周进行肾输尿管膀胱造影（KUB）复查残留碎石。双J支架于术后4周取出，取出支架6周后进行腹部超声检查，观察是否残留肾积水。发热、腰痛、输尿管肾积水加重或梗阻性尿路病变患者需行CT尿路造影检查狭窄情况。出现肾脓肿或尿脓毒症的患者需行经皮肾造瘘管置入术。通过CT尿路造影（图1）、平卧位逆行肾盂造影（图2）和直立位肾盂造影（图3）评估输尿管狭窄的长度和部位。所有输尿管狭窄患者均接受^{99m}乙二胺五乙酸（DTPA）显像扫描以量化肾功能。根据狭窄长度、部位及肾功能可挽救性，患者将接受输尿管内切开术、输尿管吻合术（图4）、输尿管肾造瘘术、博亚里瓣修复术或肾切除术。术后3个月通过^{99m}DTPA对接受治疗的输尿管狭窄患者进行随访。

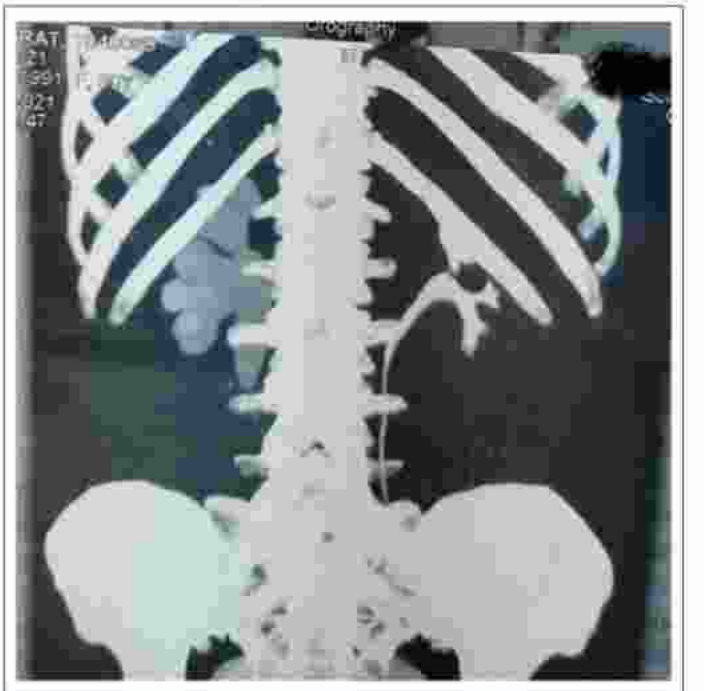


图1.计算机断层扫描尿路造影：重建图像显示因上尿路狭窄导致的右侧输尿管肾积水。



图2.前向与逆行肾盂造影显示狭窄部位长度（红色箭头）。

采用扫描和CT尿路造影进行检查。统计分析使用社会科学统计软件包（SPSS）22.0版（IBM SPSS公司，美国纽约州阿蒙克市）完成。定性数据以数量和百分比呈现，定量数据则以均值（标准差）表示。通过统计学方法评估了定量数据的正态分布情况。



图3.左侧顺行肾盂造影显示上尿路完全闭塞。

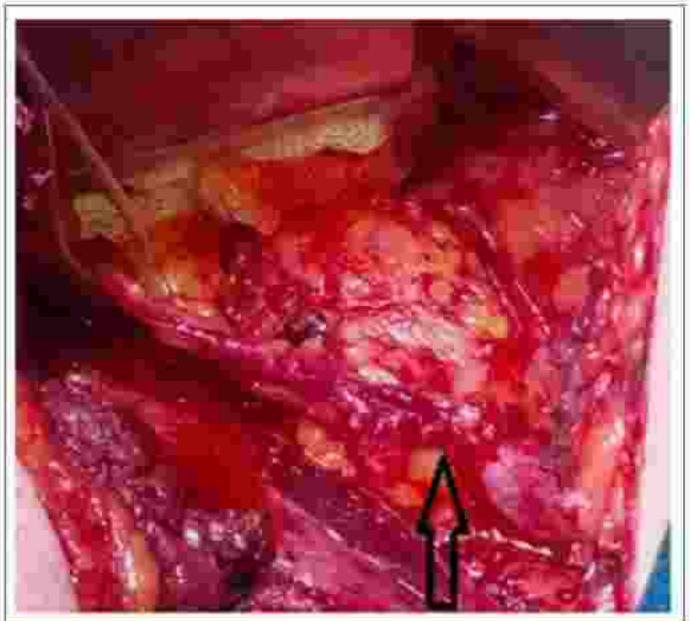


图4.上尿路狭窄术中影像（黑色箭头所示）。

采用独立样本*t*检验。使用卡方检验比较组间定性变量。任何参数的统计学显著性定义为*P*值<.05。

结果

2020年1月至2021年12月期间，共有540名输尿管结石患者计划接受输尿管镜激光碎石术。其中21人拒绝参与研究，另有30名患者因不符合研究条件被排除。剩余489名患者被随机分为两组：A组（246人）接受Ho：YAG激光碎石术，B组（243人）接受TFL碎石术。研究期间，A组6人和B组5人失访。图5以《临床试验报告统一标准》图表形式展示了本研究的实施阶段。

我们研究组的人口学特征详见表1，两组间未发现统计学显著差异。A组和B组女性比例分别为36.25%和35.29%。两组患者的平均年龄分别为36.5±12.52岁和38.62±10.71岁，差异无统计学意义（*P*=0.45）。两组患者接受手术前的平均等待时间分别为7.5±1.5天和8±2.5天，差异同样无统计学意义。A组结石平均大小为8.9±3.5毫米，B组为9.1±3.2毫米（*P*=0.25）。两组结石密度分别为922±241亨氏单位（HU）和918±235 HU（*P*=0.82），结石参数两组基本一致。两组患者输尿管上段（髂血管交叉以上）结石占比分别为40%和39%（*P*=0.21）。

两组术中参数见表2，A组与B组平均手术时间分别为47±15分钟和36±13分钟，差异无统计学意义

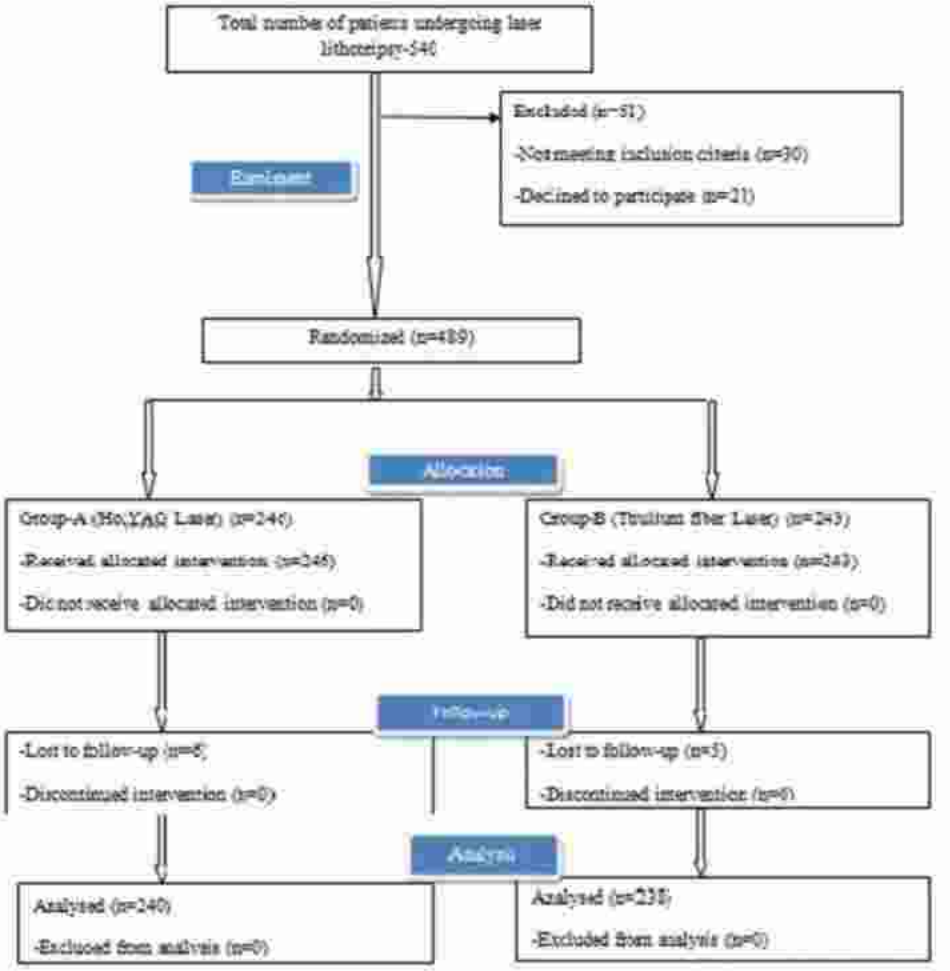


图5.本研究在《临床试验报告统一标准》（CONSORT）框架中的各阶段示意图。

统计学显著性（P<0.05）。A组平均激光治疗时间为13.5±4.5分钟，B组为9.25±3.2分钟，两组差异具有统计学显著性（P<0.001）。A组48%的患者和B组37%的病例在初始低能量设置下仍需通过频率和能量增强才能达到理想的碎石效果，两组差异具有统计学显著性（P<0.05）。A组和B组每例平均激光能量消耗分别为4.4±1.2kJ和3.12±1.3kJ，差异无统计学显著性（P<0.23）。A组15%的患者和B组13.02%的患者出现不良事件记录。

表1.患者人口统计学特征

人口统计学资料	A组（Ho: YAG），n=240	B组（TFL），n=238	P
年龄（岁，平均值±SD）	36.5 ± 12.52	38.62 ± 10.71	.45
性别（男/女）	153/87	154/84	.28
石块尺寸（mm，平均值±标准差）	8.9 ± 3.5	9.1 ± 3.2	.25
HU中的结石密度（平均值±标准差）	922 ± 241	918 ± 235	.82
结石位置百分比（上输尿管/下输尿管）	40/60	39/61	.21

Ho，钬；TFL，铥光纤激光器；YAG，钇铝石榴石。

术中包括影响视力的出血（A组10%，B组8.82%）。可见的粘膜消融（A组8.75%，B组7.56%）和输尿管穿孔（A组1.25%，B组0.84%）。差异无统计学意义（P<.42）。

表3显示了输尿管镜激光碎石术后输尿管狭窄的发生率。A组4例（1.67%）患者和B组11例（4.62%）患者在随访期间出现输尿管狭窄，差异具有统计学意义（P<0.001）。多数狭窄患者表现为腰痛和发热（A组75%，B组82%）。A组1例、B组2例患者报告出现无症状进行性肾积水。A组患者取出DJ支架后平均就诊时间为41±19天，B组为39±17天，差异无统计学意义（P<0.45）。A组3例、B组9例患者需经皮肾造瘘引流脓肾和控制脓毒症。两组狭窄部位主要位于输尿管上段（A组75%，B组78%）。CT尿路造影/顺行或逆行肾盂造影显示的狭窄平均长度分别为A组2.67±1.27厘米、B组4.42±2.00厘米，B组为2 cm，差异具有统计学意义（P<.001）。

表2.2组研究的术中参数

术中参数	A组（Ho：YAG），n=240	B组（TFL），n=238	P
手术时间（分钟，平均值±SD）	47 ± 15	36 ± 13	.05
激光时间（分钟，平均值±SD）	13.5 ± 4.5	9.25 ± 3.2	.001
每例激光能量消耗（kJ，平均值±标准差）	4.4 ± 1.2	3.12 ± 1.3	.23
记录的不良事件（%）	15%	13.02%	.42
-出血影响视力	10%	8.82%	
-可见粘膜消融	8.75%	7.56%	
输尿管穿孔	1.25%	0.84%	

Ho，钬；TFL，铥光纤激光器；YAG，钇铝石榴石。

为治疗可经尿道通过的小型狭窄，我们采用激光输尿管内切术。A组和B组各有一例适合进行激光输尿管内切术的狭窄病例。A组有2例、B组有5例患者需要通过输尿管尿路吻合术来恢复输尿管连续性。A组1例、B组2例短节段下尿路狭窄患者需行输尿管肾囊吻合术。B组1例长节段下尿路狭窄患者需进行博阿里瓣重建术，B组2例因肾功能不全需行肾切除术，而A组未报告此类病例。

讨论

输尿管镜碎石术是治疗输尿管结石的金标准疗法。传统气压碎石器存在碎石效果差、结石易反冲等缺陷。随着激光碎石器的问世，不仅可使用更小型的输尿管镜，还能通过优化的碎石流获得更清晰的视野。

表3.2个研究组输尿管狭窄的比较

术后输尿管狭窄	A组（Ho：YAG），n=240	B组（TFL），n=238	P
输尿管狭窄发生率，n（%）	4 (1.67%)	11 (4.62%)	.001
首发症状，n（%）			.22
发烧和疼痛	3 (75%)	9 (82%)	
-无症状进行性肾积水	1 (25%)	2 (18%)	
取出DJ支架后症状出现的时间（天，平均值±标准差）	41 ± 19	39 ± 17	.45.
置入经皮肾造瘘管，n（%）	3 (75%)	9 (81.81%)	.42
狭窄部位，n（%）			.35
-上输尿管	3 (75%)	8 (72.72%)	
-下输尿管	1 (25)	3 (27.27%)	
狭窄平均长度（cm，平均值±SD）	2.67 ± 1.27	4.42 ± 2.2	.001
为以下对象执行的流程			
输尿管狭窄			
-激光内镜下经皮内膜切除术	1	1	
-Ureteroureterostomy	2	5	
-Ureteroneocystostomy	1	2	
-膜白质重建术	0	1	
-肾切除术	0	2	

DJ，双J；Ho，钬；TFL，铥光纤激光器；YAG，钇铝石榴石。

通过输尿管镜进行碎石时，该技术能有效碎石且反冲力较小，从而缩短手术时间并降低输尿管狭窄的发生率。[8]钇铝石榴石（Holmium：YAG）激光因其能碎裂各类结石且安全性更高，已成为激光碎石术的金标准。其安全性源于组织穿透深度有限且在水中吸收系数高，从而减少附带损伤。[9]

钬：钇铝石榴石（Ho：YAG）激光器存在若干缺陷。该设备需要配备完善的冷却系统，这也导致其体积较大。高功率Ho：YAG激光器采用多个晶体腔来整合整体功率输出，这种结构缺陷会导致输出光束呈现多模态且分布不均，形成热点区域。此类激光束难以精确聚焦于小目标，因此需要使用芯径200μm或更大的粗光纤。[9]该激光器的结构使其容易受到外部冲击影响，可能导致晶体腔内反射镜错位，进而对激光器和光纤造成永久性损伤。这些局限性促使了铥光纤（TFL）在体内碎石术中的应用。TFL采用掺铥离子的纤细（10-20μm芯径）长硅光纤，通过多个二极管激发铥离子。最终输出光束波长为1940 nm，可实现连续或脉冲工作模式。用于激光泵浦的二极管激光器具有与铥离子吸收线精确匹配的发射光谱。它具有较少的热量散发，且具有在高功率设置（>50W）和更高频率（高达2000Hz）下运行的潜力。它使用小型风扇进行强制空气冷却，从而减小了机器的尺寸。[9]

铥光纤激光器是一种高效的碎石设备，其碎石速度比钬：钇铝石榴石（Ho：YAG）激光器快两倍，碎石粉尘量更是高出四倍。Schembri等学者[10]研究表明，TFL在不同参数设置和碎石模式下均能实现高消融效率，性能超越Ho：YAG激光器。TFL采用低脉冲能量工作模式，有效减少了碎石后反冲现象，也无需额外处理残留结石。本研究数据显示，TFL组的平均手术时间和激光治疗时间均显著短于Ho：YAG组，且差异具有统计学意义。除高效碎石外，TFL更佳的视野清晰度和更低反冲率可能是缩短手术时间的关键因素。两组在碎石过程中平均激光能量消耗无显著差异。结石的密度、成分及大小等特性决定了术中平均激光能量消耗，而这些参数在两组间具有可比性。

文献报道的输尿管镜碎石术后输尿管狭窄发生率差异显著，其发生率范围介于0.30%至23.81%之间。Adiyat等[11]和Li等分别报道Ho：YAG激光碎石术后狭窄发生率为1.4%和2.95%，与本研究结果具有可比性。本研究中TFL组的输尿管狭窄发生率较Ho：YAG激光组显著升高，且差异具有统计学意义。本研究采用的TFL设备为IPG光子学50/500-QCW TFL，其波长1940nm与22℃水体近红外吸收峰波长一致。TFL的吸收系数为14mm^{-1}，对应水体中光穿透深度0.077mm，远低于Ho：YAG激光0.4mm的光穿透深度。[9]这些特性表明

应有助于完善TFL的安全性特征，但本研究中狭窄病例的聚集现象主要与TFL使用相关，其成因尚需进一步探究。

激光束在介质中传播时，由于吸收作用，其强度会逐渐衰减，衰减的快慢由材料的吸收系数决定 α。根据比尔-朗伯定律，激光束的强度会随着在介质中传播的深度增加呈指数衰减。[11]

$I_z = I_0 e^{(-\alpha z)}$

其中z是穿透深度后的强度，z是穿透深度，

根据这个数学方程，激光束的能量在穿透介质的每个连续光学穿透深度时会衰减e（2.71828）倍。当Ho：YAG激光束穿过相当于其光学穿透深度的介质后，其能量将降至初始值的37%。而TFL激光在相同穿透深度下，能量仅剩1.7%。实际应用中，Ho：YAG激光脉冲在水下1毫米深度后，能量仅剩约4%；而TFL光束在相同深度后，强度仅剩0.00024%。显然，TFL的光学穿透深度远低于Ho：YAG激光。由于激光能量在组织中的吸收呈现对数衰减特性，TFL在1毫米深度后被吸收的能量是Ho：YAG的16 000倍。这种高吸收系数使得TFL在组织消融方面具有更低的阈值和更强的组织损伤效果。TFL脉冲因其均匀的能量分布而具有天然的"摩西效应"特性。[14]这种效应能显著增强其穿透深度。由于TFL脉冲具有高吸水系数，其组织消融阈值和气道形成阈值较低，这使得在输尿管激光碎石术中对组织的损伤程度更严重。[15]

TFL激光碎石术中产生的高温是导致狭窄率升高的另一个潜在因素。当使用高能量设置和低冲洗速率时，输尿管温度会超过生理极限。[16]无输尿管套管且刚性输尿管镜冲洗液回流不良，是导致输尿管内温度升高的主要原因。若未充分冲洗，在激光使用最初1秒内温度就会突破43℃的细胞损伤临界值。增加热性输尿管损伤风险的手术因素包括：冲洗流量不足、激光能量设置过高以及未使用套管进行器械操作。[17] Liang等[18]研究者发现，在功率相同的情况下，高频设置会导致输尿管温度显著升高。这些因素可能是TFL组狭窄率较高的促成因素。Tokas等[19]研究者则探讨了输尿管内温度升高对激光碎石术愈合进程的影响。当能量设置较高时，TFL会导致尿道内温度显著升高，造成更严重的组织损伤，愈合后会形成致密瘢痕。为此，研究者建议采用短时激光开关模式、持续冷冲洗，并使用导管鞘辅助冲洗，以维持尿道内生理温度。

本研究显示，Ho：YAG组的平均狭窄长度为2.67±1.27厘米，TFL组则为4.42±2.2厘米。TFL组狭窄长度更大的原因在于组织消融阈值较低，且尿道内温度升高更为显著。对于短段上尿路狭窄，输尿管吻合术能取得良好疗效。[20]Ahlawat等[21]研究者采用经腹腔镜输尿管对输尿管吻合术（腹腔镜输尿管吻合术）的成功率为62%。[21]两组各有1例患者接受该术式并获得成功。[22]短段下尿路狭窄可采用输尿管膀胱吻合术，而长段下尿路狭窄需进行博阿里瓣重建。Ho：YAG组有1例、TFL组有2例患者需行输尿管肠膀胱吻合术，TFL组另1例因长段下尿路狭窄需采用博阿里瓣重建。对于伴有肾盂肾炎的不可逆肾功能衰竭，TFL组采取肾切除术进行治疗。

结论

在输尿管镜碎石术中使用TFL激光时，输尿管狭窄的发生率较高。尽管TFL被视作安全激光，但在输尿管内操作时仍需谨慎，尤其在高功率/高频设置下。采用低能量、低频设置并配合持续冲洗，可有效降低经尿道碎石术中输尿管狭窄的发生率。

伦理委员会批准：*已获得印度透凉和迈什米尔斯利塞加尔谢尔-迈什米尔医学科学研究所伦理委员会的批准（批准编号：IEC/Skims方案编号231E/2020）。*

知情同意：*从参与本研究的患者处获得书面知情同意。*

同行评审：*外部同行评审。*

作者贡献：*概念——S.A.P.；设计——M.S.W.；监督——A.H.；资源——S.A.M.；材料——A.R.K.；数据收集和或处理——S.A.P.；分析和或解释——A.H.；文献检索——S.M.；撰写论文——A.R.K.；批判性审查——M.S.W.*

利益声明：*作者声明无利益冲突。*

资金：*作者声明本研究没有获得任何资金支持。*

参考文献

1. 马格莫迪R、阿姆贾迪M、诺里扎德D、哈桑扎德H.肾肌结石的治疗：Ho：YAG激光与气压碎石术的比较研究。*印度泌尿学杂志* 2008；24(3)：352-354. [交叉引用]
2. Sayer J，Johnson DE，Price RE，Cromeens DM.留尔米亚：YAG激光输尿管碎石术.*J Clin Laser Med Surg*.1993；11(2)：61-65. [交叉引用]
3. Fried NM，Irby PB.激光技术与光纤传输系统在碎石术中的应用进展.*Nat Rev Urol*.2018；15(9)：563-573.[交叉引用]
4. Traxer O，Keller EX.钬光纤激光：治疗肾结石的新选择？与铥，YAG激光的对比。*世界泌尿学杂志*.2020；38(8)：1883-1894. [交叉引用]
5. Hardy LA，Wilson CR，Irby PB，Fried NM.体外输尿管模型中的钬光纤激光碎石术.*生物医学光学杂志*.2014；19（12）：128001.[交叉引用]

6. Erhard MJ，Bagley DH.钬激光的泌尿外科应用：初步经验。*J Endourol*.1995；9(5)：383-386。[交叉引用]
7. Emiliani E, Talso M, Haddad M, 等.钬YAG激光对软组织的真正消融效果.*J Endourol*.2018;32(3):230-235.[交叉引用]
8. Haddad M, Emiliani E, Rouchausse Y, 等.曲线直径和激光设置对激光光纤断裂的影响.*J Endourol*.2017;31(9):918-921.[交叉引用]
9. Jackson SD，Lauto A.二极管泵浦光纤激光器：一种新的临床工具？*Lasers Surg Med*.2002；30(3)：184-190.[交叉引用]
10. Schembri M, Sahu J, Aboumarzouk O, 等.钬光纤激光器:行业新宠.*女王伊莉莎白泌尿学杂志*.2020;46:S1-S10.
11. 阿迪亚特KT，梅伦斯R，霍加M.输尿管镜术后选择性影像学检查.*泌尿外科*.2009；73(3)：490-493.[交叉引用]
12. Jansen ED，van Leeuwen TG，Motamedi M，Borst C，Welch AJ.中红外激光组织水吸收系数的温度依赖性。*Lasers Surg Med*.1994；14(3)：258-268。[交叉引用]
13. Allmen MV，Blatter A.*激光束与材料的相互作用：物理原理与应用*.第1卷.斯普林格材料科学丛书.springer verlag berlin Heidelberg.1995：1：115-165.
14. Chiron PH，Berthe LL，ConinckVD.钬：钇铝石榴石激光器与超脉冲钬光纤激光器诱导的气泡比较。*J Endourol*.2018；32：40-45.
15. Schomacker KT，Domankevitz Y，Flotte TJ，Deutsch TF.Co：氟化钡激光组织消融：波长对消融阈值和热损伤的影响.*Lasers Surg Med*.1991；11(2)：141-151.[交叉引用]
16. Belle JD, Srikureja N, Chen N, 等.MP65-03新型钬激光器是否比传统钬激光器产生更多热量?*J Urol*.2021;206(suppl 3):1119-1110.[交叉引用]
17. Aldoukhi AH，Roberts WW，Hall TL，Ghani KR.注意你的距离：改变脉冲宽度或调制对激光光纤工作距离对碎石的作用。*J Endourol*.2019；33(2)：120-126。[交叉引用]
18. Liang H, Liang L, Yu Y, 等.钬激光在输尿管镜碎石术中的热效应.*BMC Urol*.2020;20(1):69.[交叉引用]
19. 托卡斯丁，赖斯P，赛沃C，尚哈尔V，索马尼R.激光上尿路内镜手术过程中的温度变化：现有证据与未来展望.*Curr Opin Urol*.2023；33(2)：108-115.[交叉引用]
20. Knight RB，Hudak SJ，Morey AF.上尿路狭窄开放重建的策略.*Urol Clin North Am*.2013；40(3)：351-361.[交叉引用]
21. Hurdy JD，Eraslan S.肾脏自体移植治疗输尿管高损伤.*J Urol*.1963；90：563-574.[交叉引用]
22. Meretyk S，Albala DM，Clayman RV，Denstedt JD，Kavoussi LR.输尿管狭窄的内输尿管切开术治疗.*J Urol*.1992；147(6)：1502-1506.[交叉引用]

·综述·

热损伤致输尿管狭窄机制的研究进展

吴桐 赵驰宇 综述 姚旭东 张海民 审校
同济大学附属第十人民医院泌尿外科，上海 200072
通信作者：姚旭东，Email：yaoxudong67@sina.com；张海民，Email：zhm1064@163.com

【摘要】 输尿管狭窄是钬激光碎石术的常见并发症之一，其病因可能与热损伤有关。钬激光能量在碎石时可使灌注液和组织温度升高从而导致细胞代谢等发生变化从而诱发局部炎症。随着炎症进展，成纤维细胞可在TGF-β1等因子的作用下分化为肌成纤维细胞并分泌胶原等细胞外基质，发生纤维化。上皮细胞也可发生上皮间质转化，共同促进纤维化的发生，当输尿管发生严重的纤维化时，即表现为输尿管狭窄。通过改变激光功率和灌注液的灌注压等参数可降低组织受到的热损伤，从而降低发生输尿管狭窄的概率。

【关键词】 碎石术；输尿管狭窄；热损伤
基金项目： 上海市崇明区“可持续发展科技创新行动计划”项目（CXY2022-42）
DOI：10.3760/cma.j.cn431460-20220129-00240

近年来，钬激光因其精确切割、方向性好、碎石效率高等优点而广泛应用于泌尿系结石手术治疗中[1]。钬激光在提高碎石效率的同时也增加了输尿管狭窄的发生率[2]。Li等[3]研究报道钬激光碎石术后输尿管狭窄的发生率可高达4.9%。Chen等[2]研究分析囊括了8项相关研究，包括了1 555例患者，其结果表明钬激光碎石术后的输尿管狭窄发生率显著高于气压弹道碎石。输尿管狭窄是钬激光碎石术后严重的晚期并发症，可导致上尿路梗阻并引起肾积水，如不治疗可进一步发展致肾功能丧失[4]。钬激光导致输尿管狭窄的机制，包括机械损伤和热损伤。机械损伤包括结石嵌顿和手术器械或术者操作不当对输尿管壁造成的损伤，而热损伤机制尚未完全明晰，难以完全避免。目前已有研究主要聚焦于探索激光参数设置，如功率、激发时间等，以及灌注液的流速和压力，寻找减少热损伤的临界条件，但在组织层面上对热损伤造成输尿管狭窄的机制研究较少。对热损伤机制的研究有助于早期识别有高危因素的患者，及时进行针对性治疗以改善预后。本文就钬激光碎石术中灌注液的温度变化及热损伤导致输尿管狭窄的可能机制进行阐述。

1 热损伤的模拟实验

1.1 体外实验

有些学者构建了体外模型模拟钬激光碎石术的过程，并在不同条件下探究肾盏及输尿管中灌注液的温度变化。简易的体外模型中，以圆柱形玻璃管模拟输尿管，以玻璃球模拟肾，然后将该模型置于37 ℃恒温水浴箱中模拟体温环境，实验中，研究者插入钬激光导丝模拟手术过程并用热电偶实时测温，实验中改变的条件包括激光功率、激发模式、激发持续时间及灌注液的灌注压、流速等。通过绘制温度-时间曲线发现，灌注液的温度变化首先经历快速上升期，然后缓慢上升，最后达到平台期，不同条件下达到的最高温度不同[5]。Dau等[5]研究发现提高灌注液的流速或使用低温灌注液均可使平台期的灌注液温度降低。Wollin等[6]研究也证实了提高灌注液流速可降低灌注液所能达到的最高温度。有研

究报道了激光功率对灌注液温度的影响并发现在激光频率一定时，功率越高即单次激发能量越高，灌注液升温越快。这些研究的结果均表明钬激光碎石术中激光的光热效应可以直接提高灌注液的温度。体外模型装置简单，便于研究不同条件下灌注液的温度变化曲线并计算热剂量从而根据理论临界值找到最佳设置方案，然而，由于玻璃与组织的物理参数有所不同，且缺乏血流灌注的散热效应，故其不能反映组织受热的真实情况。

1.2 体内实验

体内实验因小鼠或大鼠手术操作难度高，故多在猪身上进行。Aldoukhi等[7]用雌猪进行动物实验模拟输尿管镜钬激光碎石术并记录温度，结果发现激光功率越高，产生热损伤的可能性越大。Noureldin等[8]则探究了不同直径通路鞘和泵灌注或重力灌注对肾内温的影响，发现大直径通路鞘和泵灌注可降低手术期间肾内温的升高程度。这些研究结果表明，应用大直径输尿管鞘、高灌注液流速及高灌注压可以降低灌注液温度升高的程度，但在激光功率过大时仍有可能造成热损伤[7-9]。值得一提的是，为降低热损伤而提高灌注压或灌注液流速可能使肾盂内压升高从而增加肾盂静脉回流和败血症的风险[10-11]。有研究报道为27例输尿管结石患者实施输尿管镜钬激光碎石术的同时记录了术中灌注液的温度变化，术中以室温作为灌注液温度，所有患者术中记录的最高温度均超过了43 ℃，其中17例最高温度超过56 ℃，且在随访过程中，其中3例通过彩色多普勒超声发现肾积水，提示可能存在输尿管狭窄，而这3例患者的术中灌注液温度均超过56 ℃[12]。体内实验能更好地模拟和反应上尿路结石患者接受钬激光碎石术时灌注液的温度变化，从而间接反应周围组织的温度变化。但这些研究只关注了激光或灌注液设置而未对肾或输尿管取组织标本研究。

2 热损伤致输尿管狭窄的机制

2.1 生物组织的热效应

虽然钬激光碎石术中激光产生的能量大部分被光纤和结石之间的水吸收并用于碎石而被消耗，但剩余的能量仍能使灌注液和周围组织温度升高，使肾或输尿管处于热损伤的风险中[13]。升温的灌注液可降低组织酶活性并影响代谢，还可通过热传递直接使周围组织温度升高而产生热损伤。组织温度在42 ℃～50 ℃内，会对化学键造成破坏并可能改变膜结构；当温度超过50 ℃时，组织内酶活性明显减弱，会导致能量生成障碍从而影响细胞代谢；当组织温度超过60 ℃时，蛋白质和胶原蛋白会变性，导致组织坏死[14]。组织环境温度升高除代谢改变外，还可能因为热损伤引起组织应答产生非感染性炎症[15]。若炎症及纤维修复过程失调而表现持续输尿管纤维化，可最终发展为输尿管狭窄[16-17]。有研究为了量化组织的热效应和热损伤，在既往实验结果的基础上提出了热剂量的概念，并总结出当组织在43 ℃环境中处理超过120 min即可造成热损伤，且温度每较43 ℃升高1 ℃，组织接受相同热剂量所需时间减少一半。

2.2 组织病理学改变

热损伤会破坏正常输尿管结构并导致纤维化。正常输尿管由黏膜、肌层和外膜三层结构组成，黏膜由尿路上皮细胞和固有结缔组织组成。尿路上皮的细胞形态和层数可随扩张和空虚状态变化而变化，有利于适应排尿功能。Ho等[18]，黄春雨等[19]，王鑫[20]在研究中均使用新西兰兔进行动物实验，在用激光对其输尿管造成热损伤后取组织标本染色镜检发现，较低剂量的热损伤处理后输尿管内膜完整但肌层显著增厚，较高剂量的热损伤会使黏膜、肌层和外膜均出现不同程度的断裂，而组织一旦发生热损伤，随后均会出现纤维组织明显增生。王鑫[20]还研究了机械损伤后新西兰兔输尿管的变化并与热损伤组比较发现，早期热损伤组的输尿管黏膜下层及肌层增生较机械损伤组明显，且Ⅰ型胶原蛋白、Ⅲ型胶原蛋白及TGF-β表达量明显高于机械损伤组，说明热损伤较机械损伤引起的输尿管纤维化发生时间较早。Barros-Becker等[21]研究发现，热损伤会在损伤组织区域周围招募中性粒细胞和巨噬细胞，从而引起非感染性炎症。在炎症发展过程中，巨噬细胞可由促炎表型转为抗炎表型并分泌TGF-β介导成纤维细胞转化为肌成纤维细胞，而肌成纤维细胞可通过分泌细胞外基质，如胶原发挥促纤维化作用[22]。因此，热损伤可使输尿管上皮的变性坏死并在局部引发非感染性炎症，同时启动纤维修复过程，严重的输尿管纤维化即可导致输尿管狭窄。

2.3 上皮间质和成纤维细胞-肌成纤维细胞转化

热损伤后，输尿管损伤的局部组织产生非感染性炎症并可能伴有上皮间质转化，两者共同促进了纤维化并导致输尿管狭窄。Luo等[23]在研究中建立了大鼠尿路梗阻及输尿管狭窄模型，均证明了输尿管瘢痕中高表达TGF-β1和Smad蛋白。TGF-β1通过TGF-β/Smad通路不仅可以诱导上皮间质转化，还可促进成纤维细胞向肌成纤维细胞转化并分泌细胞外基质和胶原，从而发挥促纤维化作用[24-25]。Ho等[18]研究发现输尿管狭窄处沉积的胶原主要为COL3A1和COL1A2。陈柯宇和王亮[26]研究则在通过电灼烧新西兰兔的输尿管造成热损伤后，取标本检测部分细胞因子，发现随着热损伤严重程度的增加，TGF-β1的表达量也增加，同时伴有IL-1β和TNF-α的表达增加以及高迁移率族蛋白1（HMGB1）的增加。HMGB1作为一种重要的损伤相关分子模式蛋白（damage-associated molecular pattern，DAMP），在细胞核内参与DNA的复制、转录和修复过程。在热作用下，HMGB1可以被释放至细胞外，并通过与TLR4受体结合激活NF-κB通路，从而促进炎症发生发展[27]。HMGB1也可以由巨噬细胞和树突状细胞等炎症细胞迁移至损伤位点主动分泌产生[28]。在对上皮间质转化的标志物研究中发现，热损伤后的输尿管上皮组织中E-钙黏蛋白表达减少而波形蛋白表达增加[18,26]。E-钙黏蛋白是与细胞粘附相关的跨膜糖蛋白，是典型的上皮细胞标志物。而波形蛋白是Ⅲ型中间纤维蛋白之一，主要在内皮细胞等间充质起源的细胞中表达。

E-钙黏蛋白的表达减少和波形蛋白的表达增加意味着输尿管上皮可能发生了上皮间质转化。根据上皮间质转化发生的生物学背景可将其分为三型：Ⅰ型与着床、胚胎形成和器官发育相关；Ⅱ型与伤口愈合、组织再生和器官纤维化相关；Ⅲ型发生在肿瘤细胞中[28]。其中，Ⅱ型上皮间质转化与炎症相关，通常产生成纤维细胞和其他相关细胞来重建创伤或炎症损伤后的组织，并在炎症减弱后停止。尿路上皮细胞在热刺激下可能发生上皮间质转化，但热刺激移除后一段时间，上皮间质转化过程也随之停止。因此，上皮间质转化在参与热损伤导致输尿管狭窄的过程中可能并非主要原因，而由尿路上皮细胞转化而来的间充质细胞在纤维化中到底发挥多少作用尚不清楚。

3 总结与展望

钬激光碎石术中，在激光的光热效应下灌注液温度升高，升温后的灌注液再将热量传递到输尿管，导致尿路上皮细胞热损伤并破坏输尿管组织结构。当热损伤超过临界值，组织细胞可通过招募巨噬细胞等免疫细胞产生非感染性炎症进行应答。随着炎症进展，部分尿路上皮细胞发生上皮间质转化并协同间质中肌成纤维细胞分泌胶原从而促进输尿管的纤维化，最终形成输尿管狭窄。目前对钬激光碎石术中输尿管热损伤的研究多着眼于激光及灌注液参数设置，而热损伤致输尿管狭窄的细胞及分子机制研究较少。热损伤致输尿管狭窄的机制虽未完全阐明，但其核心仍为纤维化，一些抗纤维化药物或治疗手段可能对其有效，具体效果还需实验验证。对热损伤致输尿管狭窄机制的深入研究，有助于早期识别钬激光碎石术后输尿管狭窄高危患者并进行针对性治疗，避免发展至输尿管狭窄后肾积水而影响肾功能。

利益冲突 所有作者均声明不存在利益冲突

参 考 文 献

[1] 孙颖浩，杨波. 钬激光在泌尿外科中的应用[J]. 中华泌尿外科杂志，2005，26(1)：62-64. DOI：10.3760/j:issn:1000-6702.2005.01.020.

[2] Chen S, Zhou L, Wei T, et al. Comparison of holmium: YAG laser and pneumatic lithotripsy in the treatment of ureteral stones: an update Meta-analysis[J]. Urol Int, 2017, 98(2): 125-133. DOI: 10.1159/000448692.

[3] Li L, Pan Y, Weng Z, et al. A prospective randomized trial comparing pneumatic lithotripsy and holmium laser for management of middle and distal ureteral calculi[J]. J Endourol, 2015, 29(8): 883-887. DOI: 10.1089/end.2014.0856.

[4] Jeong IG, Han KS, Joung JY, et al. The outcome with ureteric stents for managing non-urological malignant ureteric obstruction[J]. BJU Int, 2007, 100(6): 1288-1291. DOI: 10.1111/j.1464-410X.2007.07172.x.

[5] Dau JJ, Hall TL, Maxwell AD, et al. Effect of chilled irrigation on caliceal fluid temperature and time to thermal injury threshold during laser lithotripsy: in vitro model[J]. J Endourol, 2021, 35(5): 700-705. DOI: 10.1089/end.2020.0896.

[6] Wollin DA, Carlos EC, Tom WR, et al. Effect of laser settings and irrigation rates on ureteral temperature during holmium Laser lithotripsy, an in vitro model[J]. J Endourol, 2018, 32(1): 59-63. DOI: 10.1089/end.2017.0658.

[7] Aldoukhi AH, Hall TL, Ghani KR, et al. Caliceal fluid temperature during high-power holmium laser lithotripsy in an in vivo porcine model[J]. J Endourol, 2018, 32(8): 724-729. DOI: 10.1089/end.2018.0395.

[8] Noureldin YA, Farsari E, Ntasiotis P, et al. Effects of irrigation parameters and access sheath size on the intra-renal temperature during flexible ureteroscopy with a high-power laser[J]. World J Urol, 2021, 39(4): 1257-1262. DOI: 10.1007/s00345-020-03287-9.

[9] Kallidonis P, Kamal W, Panagopoulos V, et al. Thulium laser in the upper urinary tract: Does the heat generation in the irrigation fluid pose a risk? Evidence from an in vivo experimental study[J]. J Endourol, 2016, 30(5): 555-559. DOI: 10.1089/end.2015.0768.

[10] Noureldin YA, Kallidonis P, Ntasiotis P, et al. The effect of irrigation power and ureteral access sheath diameter on the maximal intra-pelvic pressure during ureteroscopy: in vivo experimental study in a live anesthetized pig[J]. J Endourol, 2019, 33(9): 725-729. DOI: 10.1089/end.2019.0317.

[11] Auge BK, Pietrow PK, Lallas CD, et al. Ureteral access sheath provides protection against elevated renal pressures during routine flexible ureteroscopic stone manipulation[J]. J Endourol, 2004, 18(1): 33-36. DOI: 10.1089/089277904322836631.

[12] Wang XK, Jiang ZQ, Tan J, et al. Thermal effect of holmium laser lithotripsy under ureteroscopy[J]. Chin Med J (Engl), 2019, 132(16): 2004-2007. DOI: 10.1097/CM9.0000000000000300.

[13] Buttice S, Sener TE, Proietti S, et al. Temperature changes inside the kidney: What happens during holmium: Yttrium-aluminium-garnet laser usage? [J]. J Endourol, 2016, 30(5): 574-579. DOI: 10.1089/end.2015.0747.

[14] 江世臣，张学学. 生物组织热损伤及最小热损伤剂量分析[C]. 中国工程热物理学会第十一届年会，2005：817-820.

[15] Cornish PB, Carlson D, Kang R, et al. Damage-associated molecular patterns and the systemic immune consequences of severe thermal injury[J]. J Immunol, 2020, 205(5): 1189-1197. DOI: 10.4049/jimmunol.2000439.

[16] Luo J, Zhao S, Wang J, et al. Bone marrow mesenchymal stem cells reduce ureteral stricture formation in a rat model via the paracrine effect of extracellular vesicles[J]. J Cell Mol Med, 2018, 22(9): 4449-4459. DOI: 10.1111/jcmm.13744.

[17] Ichii O, Otsuka S, Namiki Y, et al. Molecular pathology of murine ureteritis causing obstructive uropathy with hydronephrosis[J]. PLoS One, 2011, 6(11): e27783. DOI: 10.1371/journal.pone.0027783.

[18] Ho DR, Su SH, Chang PJ, et al. Biodegradable stent with mTOR inhibitor-eluting reduces progression of ureteral stricture[J]. Int J Mol Sci, 2021, 22(11): 5664. DOI: 10.3390/ijms22115664.

[19] 龚春雨，李黎，屈锐，等. 国产钬激光手术对兔肾热损伤的初步研究[J]. 华西医学，2017，32(7)：984-987. DOI：10.7507/1002-0179.201601009.

[20] 王鑫. 输尿管损伤后瘢痕狭窄形成机制及干预的实验研究[D]. 苏州大学泌尿外科，2014.

[21] Barros-Becker F, Squirrell JM, Burke R, et al. Distinct tissue damage and microbial cues drive neutrophil and macrophage recruitment to thermal injury[J]. iScience, 2020, 23(11): 101699. DOI: 10.1016/j.isci.2020.101699.

[22] Eming SA, Martin P, Tomic-Canic M. Wound repair and regeneration: mechanisms, signaling, and translation[J]. Sci Transl Med, 2014, 6(265): 265sr6. DOI: 10.1126/scitranslmed.3009337.

[23] Liao J, Zhao S, Wang J, et al. Bone marrow mesenchymal stem cells reduce ureteral stricture formation in a rat model via the paracrine effect of extracellular vesicles[J]. J Cell Mol Med, 2018, 22(9): 4449-4459. DOI: 10.1111/jcmm.13744.

[24] Sun M, Zhou W, Yao F, et al. MicroRNA-302b mitigates renal fibrosis via inhibiting TGF-β/Smad pathway activation[J]. Braz J Med Biol Res, 2021, 54(3): e9206. DOI: 10.1590/1414-431X20209206.

[25] Yu XY, Sun Q, Zhang YM, et al. TGF-β/Smad signaling pathway in tubulointerstitial fibrosis[J]. Front Pharmacol, 2022, 13: 860588. DOI: 10.3389/fphar.2022.860588.

[26] 陈柯宇，王亮. 高迁移率族蛋白1在钬激光致输尿管狭窄患者中的作用及甘草酸苷的体外抑制研究[J]. 中国免疫学杂志，2020，36(13)：1631-1635. DOI：10.3969/j.issn.1000-484X.2020.13.018.

[27] Andersson U, Yang H, Harris H. Extracellular HMGB1 as a therapeutic target in inflammatory diseases[J]. Expert Opin Ther Targets, 2018, 22(3): 263-277. DOI: 10.1080/14728222.2018.1439924.

[28] VanPatten S, Al-Abed Y. High mobility group box-1 (HMGb1): current wisdom and advancement as a potential drug target[J]. J Med Chem, 2018, 61(12): 5093-5107. DOI: 10.1021/acs.jmedchem.7b01136.

[29] Kalluri R, Weinberg RA. The basics of epithelial-mesenchymal transition[J]. J Clin Invest, 2009, 119(6): 1420-1428. DOI: 10.1172/JCI39104.

（本文编辑：骆凤）
（收稿日期：2022-01-29）

文章编号:1009-6612(2023)11-0859-08
DOI:10.13499/j.cnki.fqjwkzz.2023.11.859

·论 著·

输尿管镜钬激光碎石术后输尿管狭窄的危险因素分析及再次手术的术式选择策略

张冠英[1],徐 云[2],余泉峰[1],李泽宇[1],谷欣权[3],余沁楠[1]
(1.新乡医学院第一附属医院泌尿外科,河南 新乡,453100;
2.新乡医学院第一附属医院内分泌科;3.吉林大学中日联谊医院泌尿外科)

【摘要】 **目的**:探讨输尿管镜钬激光碎石术(URHL)后输尿管狭窄(US)的危险因素及患者再次手术的术式选择与效果。**方法**:选择2019年3月至2022年1月接受URHL治疗的502例输尿管结石患者作为研究对象,设为训练集;按照相同标准将2022年2-10月接受URHL治疗的150例输尿管结石患者设为验证集,进行外部验证。根据术后是否发生US,分为狭窄组(n=50)与未狭窄组(n=452);对比分析两组患者的临床资料。根据US患者再次手术的术式选择,分为微创组(n=25)与开放组(n=25),对比分析两组患者临床资料、手术指标、术后并发症及复发情况。通过多因素Logistic回归分析影响术后US发生的危险因素,绘制森林图,构建列线图预测模型,并进行模型评价。**结果**:病程>3个月、结石最大径≥2 cm、重度肾积水、嵌顿结石伴有息肉、钬激光损伤黏膜均为术后US发生的独立危险因素(P<0.05)。列线图预测模型结果显示,各危险因素总计304分。受试者工作特征曲线、校准曲线及临床决策曲线分析法的评价结果显示,该预测模型的区分度、准确度及有效性均较高。与开放组相比,微创组手术时间、术后肾功能恢复时间、住院时间更短(P<0.05),术中出血量更少(P<0.05);两组并发症发生率、复发率差异均无统计学意义(P>0.05)。**结论**:病程、结石最大径、肾积水程度、嵌顿结石伴有息肉、钬激光损伤黏膜均为术后US发生的独立影响因素。微创手术是URHL术后US的优选术式,手术指标优于开放手术,值得临床推广应用。

【关键词】 输尿管结石;输尿管狭窄;碎石术,激光;输尿管镜检查;危险因素;再手术
中图分类号:R693⁺.4 **文献标识码**:A

Risk factors analysis of ureteral stricture after ureteroscopic holmium laser lithotripsy and the selection of reoperation methods

ZHANG Guanying[1], XU Yun[2], YU Quanfeng[1], et al.
1. Department of Urology, the First Affiliated Hospital of Xinxiang Medical College, Xinxiang 453100, China;
2. Department of Endocrinology, the First Affiliated Hospital of Xinxiang Medical College

【**Abstract**】 **Objective**: To explore the risk factors of the ureteral stricture (US) after ureteroscopic holmium laser lithotripsy (URHL), the choice and effect of reoperation. **Methods**: From Mar. 2019 to Jan. 2022, 502 patients with ureteral calculus who received URHL were selected as the study objects and set as the training set; according to the same criteria, 150 patients with ureteral calculus who received URHL treatment from Feb. 2022 to Oct. 2022 were selected as the validation set for external validation. According to whether the US occurred after the operation, patients were divided into the stricture group (n=50) and non stricture group (n=452). The clinical data of the two groups were collected for comparative analysis. The patients with US were divided into the minimally invasive group (n=25) and open group (n=25) according to the choice of reoperation methods, the clinical data, surgical indexes, postoperative complications and recurrence of the two groups were compared and analyzed. The risk factors of postoperative US were analyzed by multifactor logistic regression, a forest map was drawn, a nomogram prediction model was constructed, and the model was evaluated. **Results**: Multivariate logistic regression analysis showed that the course of disease>3 months, the maximum diameter of the calculus≥2 cm, severe hydronephrosis, incarcerated stones with polyps, and mucosa damage by holmium laser were all independent risk factors for postoperative US (P<0.05). The results of the nomogram prediction model showed that the total risk factors were 304 points. The evaluation results of the receiver operating characteristic curve, calibration curve, and clinical decision curve analysis showed that

通讯作者:谷欣权,E-mail:1090649251@qq.com;余沁楠,E-mail:xuyun2016728@163.com
作者简介:张冠英(1988—),男,新乡医学院第一附属医院泌尿外科主治医师,主要从事泌尿外科的研究。

(C)1994-2024 China Academic Journal Electronic Publishing House. All rights reserved. http://www.cnki.net

the prediction model had high discrimination, accuracy, and effectiveness. Compared with the open group, the minimally invasive group had shorter operation time, postoperative renal function recovery time and hospital stay ($P<0.05$), and less intraoperative blood loss ($P<0.05$). There was no statistically significant difference in the incidence of complications and recurrence between the two groups ($P>0.05$). **Conclusions**: The course of the disease, the maximum diameter of the calculi, the degree of hydronephrosis, incarcerated stones accompanied by polyps and mucosal damage caused by holmium laser are all independent influencing factors for the occurrence of postoperative US. Minimally invasive surgery is the preferred method for treating US after URHL, with better surgical indicators than open surgery, and is worthy of clinical promotion.

[Key words] Ureteral calculi; Ureteral stricture; Lithotripsy, laser; Ureteroscopy; Risk factors; Reoperation

输尿管结石(ureteral calculus, UC)是泌尿外科常见疾病,可导致上尿路积水扩张、肾绞痛,严重时甚至发生肾功能衰竭[1-2]。近年,随着医疗技术的发展,体外冲击波碎石术、输尿管镜钬激光碎石术(ureteroscopic holmium laser lithotripsy, URHL)等已被广泛用于UC的治疗[3-4]。钬激光具有较高的碎石能力及小组织穿透性,URHL可用于治疗不同成分、部位的UC,是泌尿系统结石有效的临床治疗手段[5]。但URHL为侵入性操作,难免会损伤输尿管,从而发生术后输尿管狭窄(ureteral stricture, US)。因此,明确URHL术后影响US发生的危险因素对于改善患者预后十分重要。临床上,治疗US的原则是解除梗阻、恢复尿路的连续性与通畅性,并且保护肾功能。通常情况下,单纯输尿管镜下高压气囊扩张术或钬激光内切开梗阻段术无法取得令人满意的远期疗效,复发率较高;完整切除狭窄段、连续性重建输尿管可取得令人满意的疗效[6-7]。目前,尚缺乏对于US后再次手术术式选择方面的研究。因此,深入研究US后再次手术的术式选择,对于指导临床治疗具有重要意义。本研究选择接受URHL治疗的502例UC患者为研究对象,探讨URHL术后影响US发生的危险因素及再次手术的术式选择。现将结果报道如下。

1 资料与方法

1.1 临床资料

本研究为回顾性分析,选择2019年3月至2022年1月在我院接受URHL治疗的502例UC患者为研究对象,设为训练集,其中男282例,女220例;25~75岁,平均(46.28±10.35)岁;UC位置:上段108例,中段193例,下段201例。按照相同标准选取2022年2~10月接受URHL治疗的150例UC患者设为验证集,行外部验证。两集患者年龄、性别、UC位置差异均无统计学意义($P>0.05$),具有可比性。本研究经我院医学伦理委员会审核批准,受试者及家属均签署知情同意书。纳入标准:(1)经静脉尿路造影、B超、泌尿系平片及CT检查明确为UC;(2)首次行URHL;(3)年龄≥18岁。排除标准:(1)合并肾结石、输尿管畸形、恶性肿瘤;(2)心、肝、肾、肺及免疫系统功能障碍;(3)既往UC治疗史;(4)留置输尿管支架;(5)术前影像学检查存在US。

1.2 研究方法

1.2.1 资料的收集

包括年龄、性别、身体质量指数(body mass index, BMI)、糖尿病、病程、结石位置、多发结石(≥2枚)、结石最大径、上尿路感染、肾积水程度、嵌顿结石伴息肉、炎性黏膜包裹结石、钬激光损伤黏膜、激光碎石时间、术后双J管留置时间、狭窄位置、术后发病原因、就诊原因、手术时间、术中出血量、术后肾功能恢复时间、住院时间、并发症、复发等情况。

1.2.2 手术方法

URHL:麻醉,患者取截石位,经尿道置入输尿管硬镜,确定患侧开口位置,将输尿管镜持续进镜至结石部位,置入F14/12通道鞘,沿通道鞘置入200 μm钬激光光纤,击碎结石并取出碎块,退出输尿管镜,留置F6双J管(3~4周)、导尿管(2 d)。复查未发现残留结石后可拔除双J管。再次手术:采用磁共振尿路成像对US部位进行评价,应用输尿管镜检查患侧输尿管。接受开放狭窄段切除术者,游离肾盂及上段输尿管,切除狭窄段,剪裁多余肾盂(严格依据扩张形态与程度),输尿管切开1~1.5 cm。输尿管壁内段狭窄者,采用狭窄段切除+膀胱输尿管再植术,余者采用梗阻段切除+端端无张力吻合术,若吻合张力较大,可将肾脏或膀胱进行游离松解,以减少张力。行输尿管镜下钬激光内切开术进行微创治疗,激光功率1.8~2 J,频率8~10 Hz,全层切开狭窄段。术中留置F6双J管(12周),导尿管(2~3 d),每3个月彩超复查,以了解肾积水情况,每6个月通过MRI及输尿管腔检查,了解US情况。

(C)1994-2024 China Academic Journal Electronic Publishing House. All rights reserved. http://www.cnki.net

1.3 随访

采用电话、门诊、病历等方式随访1年，记录US及复发情况。拔除双J管后1周、2周、1个月及6个月均需行彩超检查，若肾积水加重，则行CT、经静脉尿路造影检查，以明确是否为US所致。根据术后是否发生US，分为狭窄组（$n=50$）与未狭窄组（$n=452$），并记录随访期间患者复发情况。

1.4 统计学处理

采用SPSS 23.0软件进行数据分析，呈正态分布的计量资料以（$\bar{x}\pm s$）表示，采用t检验；率及构成比的比较采用χ^2检验。多因素Logistic回归分析影响术后US发生的危险因素，采用Empower Stats与统计软件包"R"绘制森林图，采用R软件与软件包rms构建列线图预测模型。采用R3.5.3软件包与rms程序包计算一致性指数，并绘制校正曲线及受试者工作特征曲线，评估模型的预测效能。采用临床决策曲线分析法评价模型的精准度。检验水准$\alpha=0.05$。

2 结 果

2.1 未狭窄组与狭窄组患者临床资料的比较

两组患者年龄、性别、BMI、糖尿病、结石位置、合并上尿路感染、术后双J管留置时间差异均无统计学意义（$P>0.05$）。与未狭窄组相比，狭窄组病程>3个月、多发结石、结石最大径≥2 cm、重度肾积水、嵌顿结石伴有息肉、炎性黏膜包裹结石，钬激光损伤黏膜、激光碎石时间≥60 min的患者比例均更高（$P<0.05$），见表1。

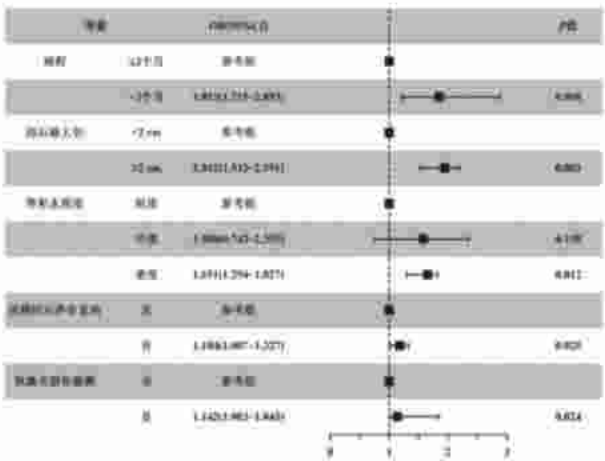


图1 US发生的危险因素森林图

2.2 多因素Logistic回归分析

将表1中两组差异有统计学意义的指标（$P<0.05$）作为自变量，URHL术后发生US为因变量，进行多因素Logistic回归分析，结果显示，病程>3个月、结石最大径≥2 cm、重度肾积水、嵌顿结石伴有息肉、钬激光损伤黏膜，均为术后US发生的独立危险因素（$P<0.05$），见图1。

2.3 建立列线图预测模型

基于危险因素建立列线图预测模型，依据多因素Logistic回归分析中的β值进行赋分：病程>3个月赋予74分、结石最大径≥2 cm赋予80分、中度肾积水赋予20分、重度肾积水赋予60分、嵌顿结石伴有息肉赋予40分、钬激光损伤黏膜赋予30分，总分304分，见图2。

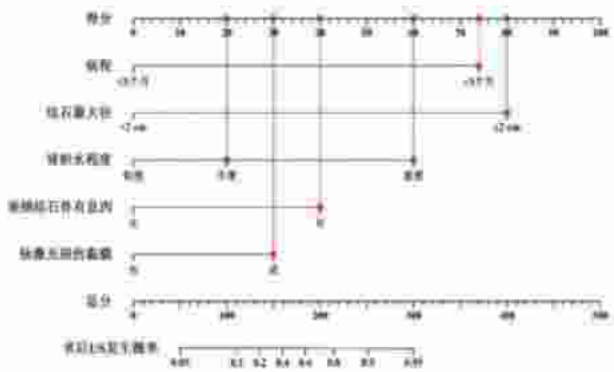


图2 列线图预测模型

2.4 模型验证

采用Bootstrap法（原始数据重复抽样1 000次后）进行内部验证，外部验证通过验证集验证。结果显示：训练集与验证集的一致性指数分别为0.791（95% CI：0.727～0.855）、0.779（95% CI：0.685～0.873）；两集的校正曲线均与理想曲线拟合良好，见图3。训练集与验证集受试者工作特征曲线下面积分别为0.807（95% CI：0.742～0.872）、0.797（95% CI：0.725～0.869），见图4。列线图预测模型的临床决策曲线显示阈值概率在1%～94%时，具有较高的净获益值，见图5。以上均显示本模型具有较好的区分度、准确度及有效性。

2.5 微创组与开放组患者临床资料的比较

根据URHL术后发生US的50例患者再次手术的术式选择分为微创组（$n=25$例）与开放组（$n=25$）。两组患者年龄、性别、BMI、糖尿病、狭窄位置、肾积水程度、术后双J管留置时间、术后发病原因、就诊原因差异均无统计学意义（$P>0.05$），见表2。

(C)1994-2024 China Academic Journal Electronic Publishing House. All rights reserved. http://www.cnki.net

表1 未狭窄组与狭窄组患者临床资料的比较[n(%)]

指标	未狭窄组(n=452)	狭窄组(n=50)	χ^2值	P值
年龄			1.689	0.194
<60岁	312(69.03)	30(60.00)		
≥60岁	140(30.97)	20(40.00)		
性别			0.765	0.382
男	251(55.53)	31(62.00)		
女	201(44.47)	19(38.00)		
BMI			1.522	0.217
≤24 kg/m^2	267(59.07)	25(50.00)		
>24 kg/m^2	185(40.93)	25(50.00)		
糖尿病			0.655	0.418
无	262(57.96)	26(52.00)		
有	190(42.04)	24(48.00)		
病程			39.138	<0.001
≤3个月	296(65.49)	10(20.00)		
>3个月	156(34.51)	40(80.00)		
结石位置			2.017	0.365
上段	94(20.80)	14(28.00)		
中段	173(38.27)	20(40.00)		
下段	185(40.93)	16(32.00)		
多发结石(≥2枚)			3.903	0.048
否	132(29.20)	8(16.00)		
是	320(70.80)	42(84.00)		
结石最大径			42.875	<0.001
<2 cm	405(89.60)	28(56.00)		
≥2 cm	47(10.40)	22(44.00)		
合并上尿路感染			1.972	0.160
否	379(83.85)	38(76.00)		
是	73(16.15)	12(24.00)		
肾积水程度			20.863	<0.001
轻度	235(51.99)	9(18.00)		
中度	77(17.04)	14(28.00)		
重度	140(30.97)	27(54.00)		
嵌顿结石伴息肉			8.567	0.003
无	310(68.58)	24(48.00)		
有	142(31.42)	26(52.00)		
炎性黏膜包裹结石			4.665	0.031
无	262(57.96)	21(42.00)		
有	190(42.04)	29(58.00)		
钬激光损伤黏膜			5.382	0.020
否	340(75.22)	30(60.00)		
有	112(24.78)	20(40.00)		
激光碎石时间			10.542	0.005
<30 min	266(58.85)	20(40.00)		
30~60 min	150(33.19)	20(40.00)		
≥60 min	36(7.96)	10(20.00)		
术后双J管留置时间			1.217	0.270
<4周	245(54.20)	23(46.00)		
≥4周	207(45.80)	27(54.00)		

(C)1994-2024 China Academic Journal Electronic Publishing House. All rights reserved. http://www.cnki.net

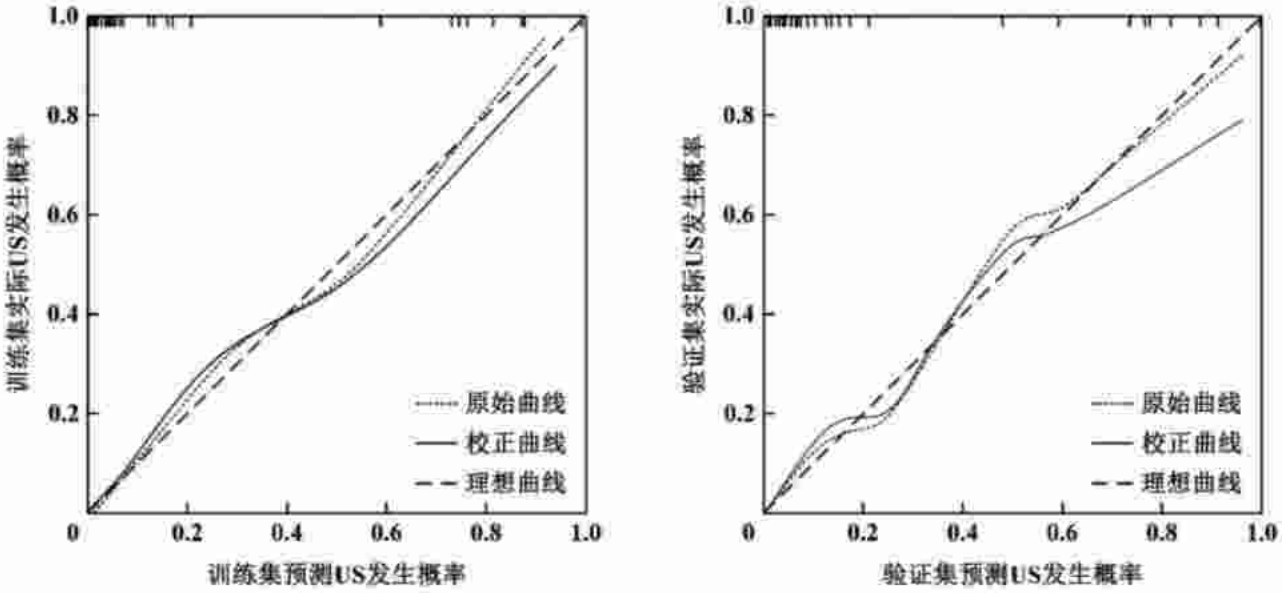


图 3　训练集与验证集的校正曲线

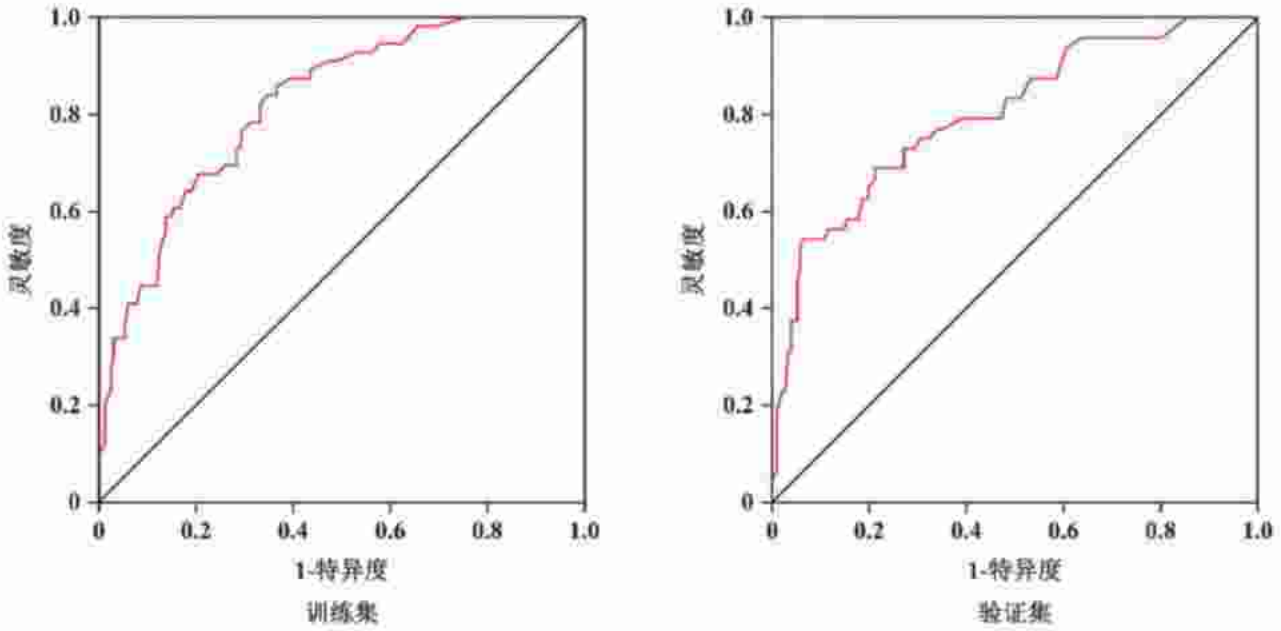


图 4　训练集与验证集的受试者工作特征曲线

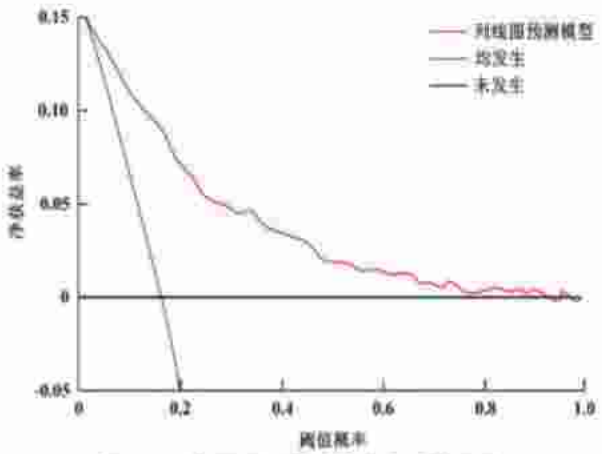


图 5　列线图预测模型的临床决策曲线

2.6　微创组与开放组手术指标的比较

与开放组相比，微创组手术时间、术后肾功能恢复时间、住院时间更短（$P<0.05$），术中出血量更少（$P<0.05$），见表 3。两组并发症发生率、复发率差异均无统计学意义（$P>0.05$），见表 4。

3　讨　论

UC 中约 90% 来自于肾脏，因此该结石成分与肾结石相似，形状主要为枣核与圆形[8]。可导致患者出现发热、恶心、呕吐、血尿等临床症状，严重时会出现梗阻、感染、肾积水等，严重威胁患者的身体健康与生活质量。UC 治疗方法包括保守治疗与手术治疗，均具有一定疗效。开放手术对机体创伤较大，

(C)1994-2024 China Academic Journal Electronic Publishing House. All rights reserved.　http://www.cnki.net

且结石难以彻底清除，随着腔内微创技术的迅速发展，在临床UC治疗中开放手术的应用已越来越少[9-10]。钬激光的碎石能力非常出色，激发产生的能量可通过光纤传导，通过“钻孔效应”将各种成分、密度的泌尿系结石粉碎为细小颗粒排出体外，疗效较好[11-12]。US是URHL术后最严重的并发症，相关研究资料证实[13-14]，开放取石、经腔镜取石或内镜碎石术后均可发生US，发病率有所不同，为3%～11%。因此明确URHL术后影响US发生的危险因素，可有效提高治疗效果。

表2 微创组与开放组患者临床资料的比较[n(%)]

指标	微创组(n=25)	开放组(n=25)	χ^2值	P值
年龄			0.333	0.564
<60岁	14(56.00)	16(64.00)		
≥60岁	11(44.00)	9(36.00)		
性别			0.765	0.382
男	17(68.00)	14(56.00)		
女	8(32.00)	11(44.00)		
BMI			0.080	0.777
≤24 kg/m^2	12(48.00)	13(52.00)		
>24 kg/m^2	13(52.00)	12(48.00)		
糖尿病			2.885	0.089
无	10(40.00)	16(64.00)		
有	15(60.00)	9(36.00)		
狭窄位置			1.486	0.476
上段	6(24.00)	8(32.00)		
中段	9(36.00)	11(44.00)		
下段	10(40.00)	6(24.00)		
肾积水程度			3.958	0.138
轻度	6(24.00)	3(12.00)		
中度	9(36.00)	5(20.00)		
重度	10(40.00)	17(68.00)		
术后双J管留置时间			2.013	0.156
<4周	14(56.00)	9(36.00)		
≥4周	11(44.00)	16(64.00)		
术后发病原因			0.397	0.529
输尿管部分黏膜撕脱或中上段穿孔	19(76.00)	17(68.00)		
输尿管假道形成或下段穿孔	6(24.00)	8(32.00)		
就诊原因			0.407	0.816
腰部胀痛不适	14(56.00)	12(48.00)		
患侧上尿路梗阻伴急性肾盂肾炎	2(8.00)	3(12.00)		
复诊时发现患侧US	9(36.00)	10(40.00)		

表3 两组患者手术指标的比较($\bar{x}\pm s$)

组别	手术时间(min)	术中出血量(mL)	术后肾功能恢复时间(d)	住院时间(d)
微创组	32.12±5.33	16.34±2.10	5.21±1.37	6.43±1.60
开放组	75.12±10.80	150.45±10.36	6.87±1.71	12.32±3.09
t值	17.852	63.435	3.788	8.463
P值	<0.001	<0.001	0.005	<0.001

本研究选择接受URHL治疗的UC患者为研究对象，探讨URHL术后US发生的危险因素，URHL治疗后US发生率为9.96%(50/502)。多因素Logistic回归分析结果显示，病程>3个月、结石最大径≥2 cm、重度肾积水、嵌顿结石伴有息肉、钬激光损伤黏膜均为术后US发生的独立危险因素。孟凯等[15]的研究表明，UC直径与碎石术后US密切相关。结石最大径越大，相应的手术及术中灌洗时间

(C)1994-2024 China Academic Journal Electronic Publishing House. All rights reserved. http://www.cnki.net

越长，从而增加术后输尿管感染及狭窄风险。对于病程较长的患者，由于结石长时间嵌顿于输尿管内，压迫输尿管导致管壁间质纤维化、尿路上皮增生及输尿管黏膜水肿，其周围形成炎性息肉及纤维组织增生，造成炎性水肿[16]。当导丝通过该段输尿管时，容易损伤管内黏膜，引发出血、感染等并发症，因此嵌顿结石更容易造成US。同时，大多数嵌顿结石会伴有一定程度的肾盂积水，结石越大，狭窄程度越大，积水越重，碎石时间越长。钬激光产生的能量通过光纤传导，将高能量传导至结石部位，从而高效粉碎，但由于输尿管管径狭窄，导致输尿管镜与结石之间空隙狭小，若灌流率低，则激光产生的局部高热会热损伤输尿管黏膜、肌层及浆膜层，形成病理性瘢痕组织，导致US，甚至堵塞。结石伴息肉包裹是临床常见的嵌顿性结石，是指结石长期滞留于输尿管并刺激黏膜炎性增生，损伤输尿管黏膜，导致受损区域沉积纤维蛋白渗出物，刺激黏附，最后形成狭窄[17]。嵌顿性结石周围息肉增生严重且输尿管黏膜水肿，通过导丝时极易穿破黏膜形成假道或穿孔。其次，水肿限制了操作空间，有增加碎裂结石损伤黏膜的风险。张志成等[18]的研究表明，嵌顿结石更易致US，因此处理时尤其结石较大且硬，在结石与黏膜间不应使用较大功率的激光，可采用中央穿孔法由内向外逐步碎石。

表4 两组患者术后并发症及复发情况的比较[n(%)]

组别	并发症				复发
	发热	感染	血尿	总计	
微创组	1(4.00)	1(4.00)	0	2(8.00)	1(4.00)
开放组	3(12.00)	2(8.00)	1(4.00)	6(24.00)	3(12.00)
χ^2值				2.381	1.087
P值				0.123	0.297

列线图是临床事件个体化预测分析的统计模型。与其他预测性统计学方法相比，列线图分析可通过直观、可视化的方式提供更好的个体化预测风险评估[19]。本研究评价结果显示，列线图预测模型的精准度较高，且有效性较好，安全可靠，实用性强。在US的作用下，肾盂、集合管等内压均上升，若梗阻时间较长，可对肾功能造成损害，甚至丧失功能。因此，应尽早进行及时、有效的手术治疗，以使患者恢复正常排尿功能，保护肾功能，利于改善预后。本研究中，对于URHL术后发生的US患者采用了两种手术治疗方式，对比分析结果显示，与开放组相比，微创组手术时间、术后肾功能恢复时间、住院时间均更短，术中出血量更少。表明治疗URHL术后US的再次手术，微创手术较开放手术优势显著，更利于患者恢复。这可能因钬激光照射瞬间即可达高温，切割、精确汽化组织极好，同时止血效果好，对瘢痕组织处理良好[20]。本研究仅对比了钬激光输尿管内切开术与开放手术的疗效，微创手术还包括腹腔镜下梗阻段切除+端端吻合术、机器人梗阻段切除+端端吻合术，并未阐述，希望在下一步的学习与研究中进行探讨。

本研究具有一定的局限性：(1)纳入病例数量较少，随着医学技术的发展，笔者相信针对性的前瞻性、大样本量的研究可为URHL术后US治疗提供更高级别的医学证据。(2)随访时间较短，此后的研究中需进一步完善。

综上所述，病程>3个月、结石最大径≥2 cm、重度肾积水、嵌顿结石伴有息肉、钬激光损伤黏膜均为术后US发生的独立危险因素。微创手术是治疗URHL术后US的优选术式，手术指标优于开放手术，值得临床推广使用。

参考文献：

[1] Hou CP, Lin YH, Juang HH, et al. Effect of ureteral calculus in outpatients receiving semirigid ureteroscope laser lithotripsy[J]. Medicine (Baltimore), 2020, 99(10): e19324.
[2] 刘迪，李铁，薛超，等. 不同微创术式治疗输尿管上段结石的疗效比较[J]. 腹腔镜外科杂志，2022，27(11)：858-861.
[3] Mayali JAA, Habeeb ZD, Ghazi MJ, et al. Efficacy and safety of ureteroscopy using holmium-YAG laser lithotripsy in treatment of pediatric ureteral stones[J]. Curr Pediatr Res, 2021, 25(3): 427-432.
[4] Wu ZH, Liu TZ, Wang XH, et al. Negative-Pressure Ureteroscopic Holmium-YAG Laser Lithotripsy for Ureteral Stones[J]. Urol Int, 2020, 104(9-10): 752-757.
[5] Ibrahim A, Elhilali MM, Fahmy N, et al. Double-Blinded Prospective Randomized Clinical Trial Comparing Regular and Moses Modes of Holmium Laser Lithotripsy[J]. J Endourol, 2020, 34(5): 624-628.
[6] 廖文彪，杨嗣星，宋超，等. 输尿管镜钬激光碎石术后输尿管狭窄的处理方法：5年单中心回顾性研究[J]. 中华泌尿外科杂志，2021，42(12)：910-914.
[7] Reus C, Breluner M. Minimally invasive management of ureteral strictures: a 5-year retrospective study[J]. World J Urol, 2019,

(C)1994-2024 China Academic Journal Electronic Publishing House. All rights reserved. http://www.cnki.net

37(8):1733-1738.
[8] Li M, Zhang H, Jiang D, et al. Calculus-related functional protein expression in ureteral calculus-adhered polyp: A preliminary study[J]. Medicine(Baltimore), 2021, 100(25): e26512.
[9] Zhang Z, Wang X, Chen D, et al. Minimally invasive management of acute ureteral obstruction and severe infection caused by upper urinary tract calculi[J]. J Xray Sci Technol, 2020, 28(1): 125-135.
[10] Isogai M, Hamamoto S, Hasebe K, et al. Dual ureteral stent placement after redo laser endoureterotomy to manage persistent ureteral stricture[J]. IJU Case Rep, 2020, 3(3): 93-95.
[11] 吴东东, 张金强, 马富平. 双镜联合经胆囊管钬激光碎石术治疗胆囊结石合并胆总管结石[J]. 腹腔镜外科杂志, 2022, 27(9): 706-710.
[12] Aggarwal D, Parmar K, Mathew J, et al. Sheathless synchronous flexible ureterorenoscopy with holmium laser lithotripsy in complete duplex renal collecting system with stones[J]. Urol Case Rep, 2021, 37: 101707.
[13] 陈华, 刘泰荣, 宋乐明, 等. 腹腔镜手术治疗钬激光碎石术后输尿管狭窄的疗效观察[J]. 中华泌尿外科杂志, 2018, 39(3): 218-221.
[14] 张波, 王朝晖, 陈志, 等. 双镜种联合治疗输尿管镜钬激光碎石术引起的输尿管狭窄的疗效分析[J]. 中华泌尿外科杂志, 2017, 38(10): 778-781.
[15] 孟凯, 李东. 钬激光碎石术治疗输尿管结石后发生输尿管狭窄的危险因素分析[J]. 贵州医药, 2020, 44(9): 1440-1441.
[16] 王翼, 豆海锋. 后腹腔镜下输尿管切开取石术治疗输尿管结石患者术后并发输尿管狭窄的危险因素分析[J]. 医学临床研究, 2022, 39(2): 271-273.
[17] 刘跃闻, 李建中, 周亚军, 等. 输尿管镜钬激光碎石术后继发输尿管狭窄的危险因素分析[J]. 临床泌尿外科杂志, 2019, 34(8): 621-624.
[18] 张志成, 廖继强. 输尿管镜下钬激光碎石术后输尿管狭窄的危险因素分析[J]. 中国药物与临床, 2020, 20(8): 1270-1272.
[19] Jiang S, Fang J, Yu T, et al. Novel Model Predicts Diabetic Nephropathy in Type 2 Diabetes[J]. Am J Nephrol, 2020, 51(2): 130-138.
[20] Li X, Qiao J, Xiong S, et al. The surgical outcomes of reconstruction for the treatment of ureteral stricture after holmium laser lithotripsy: The comprehensive experiences[J]. Asian J Surg, 2022, 45(12): 2713-2718.

(收稿日期: 2023-03-10)
(英文编辑: 梁贻泽)

(C)1994-2024 China Academic Journal Electronic Publishing House. All rights reserved. http://www.cnki.net

World Journal of Urology (2024) 42:157
https://doi.org/10.1007/s00345-024-04821-9

ORIGINAL ARTICLE

WATTS happening? Evaluation of thermal dose during holmium laser lithotripsy in a high-fidelity anatomic model

Christopher Wanderling[1] · Aaron Saxton[1] · Dennis Phan[1] · Karen Doersch[1] · Lauren Shepard[1,2] · Nathan Schuler[1,2] · Thomas Osinski[1] · Scott Quarrier[1] · Ahmed Ghazi[1,2]

Received: 20 August 2023 / Accepted: 16 January 2024 / Published online: 14 March 2024
© The Author(s), under exclusive licence to Springer-Verlag GmbH Germany, part of Springer Nature 2024

Abstract

Purpose To evaluate the thermal profiles of the holmium laser at different laser parameters at different locations in an in vitro anatomic pelvicalyceal collecting system (PCS) model. Laser lithotripsy is the cornerstone of treatment for urolithiasis. With the prevalence of high-powered lasers, stone ablation efficiency has become more pronounced. Patient safety remains paramount during surgery. It is well recognized that the heat generated from laser lithotripsy has the potential to cause thermal tissue damage.

Methods Utilizing high-fidelity, 3D printed hydrogel models of a PCS with a synthetic BegoStone implanted in the renal pelvis, laser lithotripsy was performed with the Moses 2.0 holmium laser. At a standard power (40 W) and irrigation pressure (100 cm H_2O), we evaluated operator duty cycle (ODC) variations with different time-on intervals at four different laser settings. Temperature was measured at two separate locations—at the stone and away from the stone.

Results Temperatures were highest closest to the laser tip with a decrease away from the laser. Fluid temperatures increased with longer laser-on times and higher ODCs. Thermal doses were greater with increased ODCs and the threshold for thermal injury was reached for ODCs of 75% and 100%.

Conclusion Temperature generation and thermal dose delivered are greatest closer to the tip of the laser fiber and are not dependent on power alone. Significant temperature differences were noted between four laser settings at a standardized power (40 W). Temperatures can be influenced by a variety of factors, such as laser-on time, operator duty cycle, and location in the PCS.

Keywords Thermal dose · Temperature · Laser lithotripsy · Holmium · Anatomic model

Abbreviations

RIRS	Retrograde intrarenal surgery
Ho: YAG	Holmium: Yttrium–Aluminum–Garnet
TD_{43}	Thermal dose threshold of injury at 43 °C
CEM	Cumulative equivalent
URS	Ureteroscopy
PCS	Pelvicalyceal collecting system
CFD	Computational fluid dynamics
PVA	Polyvinyl alcohol
ODC	Operator duty cycle
DICOM	Digital imaging and communications in medicine
CAD	Computer-aided design
UPJ	Ureteropelvic junction

Introduction

Retrograde intrarenal surgery (RIRS) is a common treatment for urolithiasis. Advances in laser technology have been integral for success with Holmium: Yttrium–Aluminum–Garnet (Ho:YAG) as a standard lithotripsy laser for its ability to pulverize stones of many compositions [1]. Ho:YAG fragmentation occurs predominantly through photothermal effects with some photoacoustic contribution [2]. The stone absorbs laser energy leading to fragmentation and melting. Energy generation during lasing is the main mechanism of

✉ Christopher Wanderling
Christopher_Wanderling@urmc.rochester.edu

1 Department of Urology, University of Rochester Medical Center, Rochester, NY, USA

2 Department of Urology, Johns Hopkins University, Baltimore, MD, USA

heat production, increasing fluid temperatures potentially causing thermal tissue injury [3–5].

High-powered lasers (≥ 100 W) can deliver energy at greater frequencies (> 120 Hz), improving treatment efficiency. As power increases, so does heat generated. It is crucial to determine the most efficient method of lithotripsy while preserving patient safety. The threshold of thermal injury (TD_{43}) is the thermal dose, in cumulative equivalent minutes (CEM), held at 43 °C. Tissue denaturation occurs when $TD_{43} \geq 120$ min ($TD_{43} = 120$ CEM); this was first evaluated by Sapareto and Dewey with further evaluation during ureteroscopy (URS) in contemporary studies [6–8]. Current in vitro models have produced valuable information but may be challenging to translate clinically. In vivo and ex vivo animal models more closely simulate human RIRS but are expensive, may not replicate human anatomy, and encompass ethical dilemmas.

The goal of this study was to build on prior studies, using a high-fidelity anatomic human kidney model of a pelvicalyceal collecting system (PCS) which has previously been validated with mechanical and computational fluid dynamics (CFD) testing [9]. Thermal properties of polyvinyl (PVA) hydrogel have been validated as an accurate analog of human tissue [10, 11]. The aims of this study are:

1. Evaluate the temperature profile of the Moses 2.0 Ho:YAG laser at and away from the stone for four different 40 W laser settings using four operator duty cycles (ODCs) with three time-on intervals.
2. Evaluate and compare time to TD_{43} for each laser setting.

Materials and methods

Simulation model fabrication

Digital Imaging and Communications in Medicine (DICOM) data from a patient's CT scan were segmented into a 3D computer-aided design (CAD) model using Mimics software (Materialize, Leuven, Belgium). The 3D CAD model (PCS; PCS volume = 25.1 ml) was 3D printed using hydrogel filament (Fusion3 Design, Greensboro, NC) with a synthetic BegoStone (10:1 powder-to-water ratio by weight) positioned in the renal pelvis and coated with a second PVA mixture (Figure S1A & B). This was then implanted into a hydrogel kidney block. The final product underwent extensive mechanical and CFD testing to replicate PCS properties, stone lithotripsy, and fluid flow (Figure S1C & D) [10].

Laser lithotripsy

Lithotripsy was performed at a standardized power (40 W, short pulse width, Moses technology activated) with continuous normal saline irrigation (100 cm $H_2O = 17.9$ ml/min) via retrograde access with a flexible ureteroscope (LithoVue, Boston Scientific) and a 200 µm Ho:YAG laser fiber (Moses 2.0, Boston Scientific; Figure S2). 40 W was selected for the standardized power given the ability to test four laser settings—two fragmentation (1 J × 40 Hz, 2 J × 20 Hz) and two dusting (0.5 J × 80 Hz, 0.4 J × 100 Hz). We evaluated 3 ODCs (50, 75, and 100%) with different laser-on (30, 60, and 120 s) times. Each experiment consisted of 10 ODCs (1 ODC = one laser-on/pedal activated and one laser-off/pedal off sequence. Also defined as laser time-on divided by total lithotripsy time); the 100% ODC consisted of pedal-on time of 12 min straight with no laser-off time. Ten permutations of each laser setting were tested. A total of 80 (40 tests × 2 runs) experiments were performed. Temperature was measured continuously.

Data collection and analysis

Fluid temperature was recorded with K-type needle thermocouple probes and data logger (Omega, Norwalk, CT) at two positions within the PCS—at the stone (renal pelvis) and away from the stone (upper pole calyx). Thermal dose was calculated with the Sapareto and Dewey formula. Thermal dose is an accepted measure of thermal load and has been extensively tested with the known TD_{43} of human tissue being sustained at 43 °C for 120 min when tissue denaturation occurs and is measured in CEM ($TD_{43} = 120$ CEM) [7, 8, 12–15]. Statistical analysis for thermal dose was analyzed via area under the curve (AUC) and Kruskal–Wallis comparison. Temperature data were analyzed via linear regression in a third-order polynomial (Prism 9). $p < 0.05$ was considered statistically significant.

Synthesized (37 °C starting temperature) data were calculated by taking the difference from 37 °C and the baseline experimental data, then adding this difference to experimental starting temperature (room temperature). Synthesized thermal dose data were calculated from the synthesized temperature data in the same manner as the experimental data.

Results

Fluid temperature increased during all tests. For 100% ODC, recorded temperatures continuously increased until a plateau. At 50% and 75% ODCs, a sinusoidal temperature curve resulted in correlation with laser-on period of the ODC. The

highest cumulative thermal doses and maximum temperatures were recorded mostly at the stone and during longer laser-on times. 100% ODCs delivered the greatest cumulative thermal dose (Fig. 1).

Table 1 shows the thermal dose, time to TD_{43}, and statistical comparisons at versus away from the stone. For 100% ODC, the cumulative thermal dose and time to TD_{43} at the stone was highest/fastest for 2 J × 20 Hz (23,812.3CEM/270 s) and lowest/longest for 0.4 J × 100 Hz (1193.9CEM/490 s); 1 J × 40 Hz was 3994.4CEM/360 s and 0.5 J × 80 Hz was 1289.02CEM/300 s. Away from the stone, the highest/fastest was 2 J × 20 Hz (48,273.2CEM/350 s) and lowest/longest was for 1 J × 40 Hz (81.02CEM/threshold not reached); 0.5 J × 80 Hz was 3757.4CEM/400 s and 0.4 J × 100 Hz was 1193.9/490 s. There was a statistically significant difference between the thermal doses at and away from the stone for 1 J × 40 Hz ($p < 0.0001$) and 0.5 J × 80 Hz ($p = 0.008$).

For 75% ODC, TD_{43} was exceeded during 30 s on/10 s off only for 2 J × 20 Hz away from the stone (156.5 CEM). For 60 s on/20 s off, TD_{43} was reached both at and away from the stone for 2 J × 20 Hz (804.2 and 627.9 CEM), it was reached at the stone only for 1 J × 40 Hz (374.2 CEM) and 0.5 J × 80 Hz (1270.6 CEM). TD_{43} was not reached for 0.4 J × 100 Hz. For 120 s on/40 s off, the threshold was reached for each laser setting at and away from the stone except for 0.4 J × 100 Hz where it was only reached at the stone. The TD_{43} was not reached for any laser settings tested at 50% ODC.

Generally, fragmentation settings delivered higher thermal doses at the stone (0.5 J × 80 Hz had the highest cumulative thermal dose for 75% ODC, 60 s on/20 s off and 50% ODC, and 120 s on/120 s off) and away from the stone (Table S1).

As laser-on time increased, so did the thermal dose. For both the 50% and 75% ODCs, a laser-on time of 120 s delivered the greatest cumulative thermal dose for each laser setting. Table S2 depicts the comparison of thermal dose for ODC- time-on of 50% and 75% ODC separately of each laser setting. When comparing data for 50% ODC, at the stone, all laser-on permutations were significantly different except for 30 s on versus 60 s on for 0.4 J × 100 Hz. For 50% ODC away from the stone, a significant difference was achieved for each comparison except for 30 s on versus 60 s on for 0.5 J × 80 Hz and during 60 s on versus 120 s on for 1 J × 40 Hz and 2 J × 20 Hz. Evaluating 75% ODC, there were statistically significant differences for each time-on cycle except for 0.5 J × 80 Hz for 60 s on/20 s off versus 120 s on/40 s off at the stone and 30 s on/10 s off versus 60 s on/20 s off for 2 J × 20 Hz away from the stone.

Considering laser-off times independent of laser-on times, comparing between 50% versus 75% ODC (30 s on/30 s off versus 30 s on/10 s off, 60 s on/60 s off vs 60 s on/20 s off, and 120 s on/120 s off versus 120 s on/40 s off), a significant difference ($p < 0.0001$) for each ODC permutation at all four laser settings was recorded both at and away from the stone.

When adapting our experimental data to synthesize simulated data at a starting temperature of 37 °C, maximal temperatures were higher and every trial exceeded TD_{43} at both locations except 2 J × 20 Hz, 30 s on/30 s off away from the stone. The time to TD_{43} was reached significantly faster when starting at body temperature. Similar statistical results were appreciated for this synthesized data as well.

Complete temperature data, 50% ODC graphs, and synthesized data for the body-temperature analyses are included in the supplemental material.

Discussion

This study demonstrated significant differences in temperature and thermal dose between four laser settings while varying frequency, energy, and ODC with a standardized power (40 W) and irrigation (17.9 ml/min). When evaluating these results and data, it is important to recognize that, while this high-fidelity model can simulate the PCS during URS, it is not able to fully replicate the surgical environment and every confounding variable that is present during RIRS and laser lithotripsy. Additionally, these studies were performed via in vitro anatomic model at room temperature. We do acknowledge that the raw data may not provide a completely accurate clinical correlation; however, correcting for the baseline starting temperature with the synthesized data, this may allow for a stronger consideration with regards to a more accurate clinical correlation.

While significant differences were recognized, there were no overall trends related to fluid temperatures with relation to the frequency or energy tested. Regardless of ODC and laser settings, the total energy delivered was consistent based on laser-on time (30 s-on = 12 ± 0.2 kJ, 60 s-on = 24 ± 0.1 kJ, 120 s-on = 48 ± 0.1 kJ, 100% = 28.3–30.1 kJ). If the dogma and laws of thermodynamics state that power determines temperature independent of frequency and energy held true [8, 16–18], closer results should have been expected between laser settings. A possible explanation, based on expert opinion, is that even though the laser system was set to 40 W, total power may not be delivered consistently during lasing. The FDA requires Ho:YAG lasers produce an output within 15% of the power setting displayed. Based on flashlamp laser technology, some energy pulses may be closer to the selected settings than others. Power output has been found to fluctuate with the temperatures inside of the laser system, which varies with duration of laser activation.

In a survey of 414 urologists, 67% of responses indicated that dusting (high frequency/low energy) was preferred [19]. Urologists must proceed judiciously as high-powered lasers

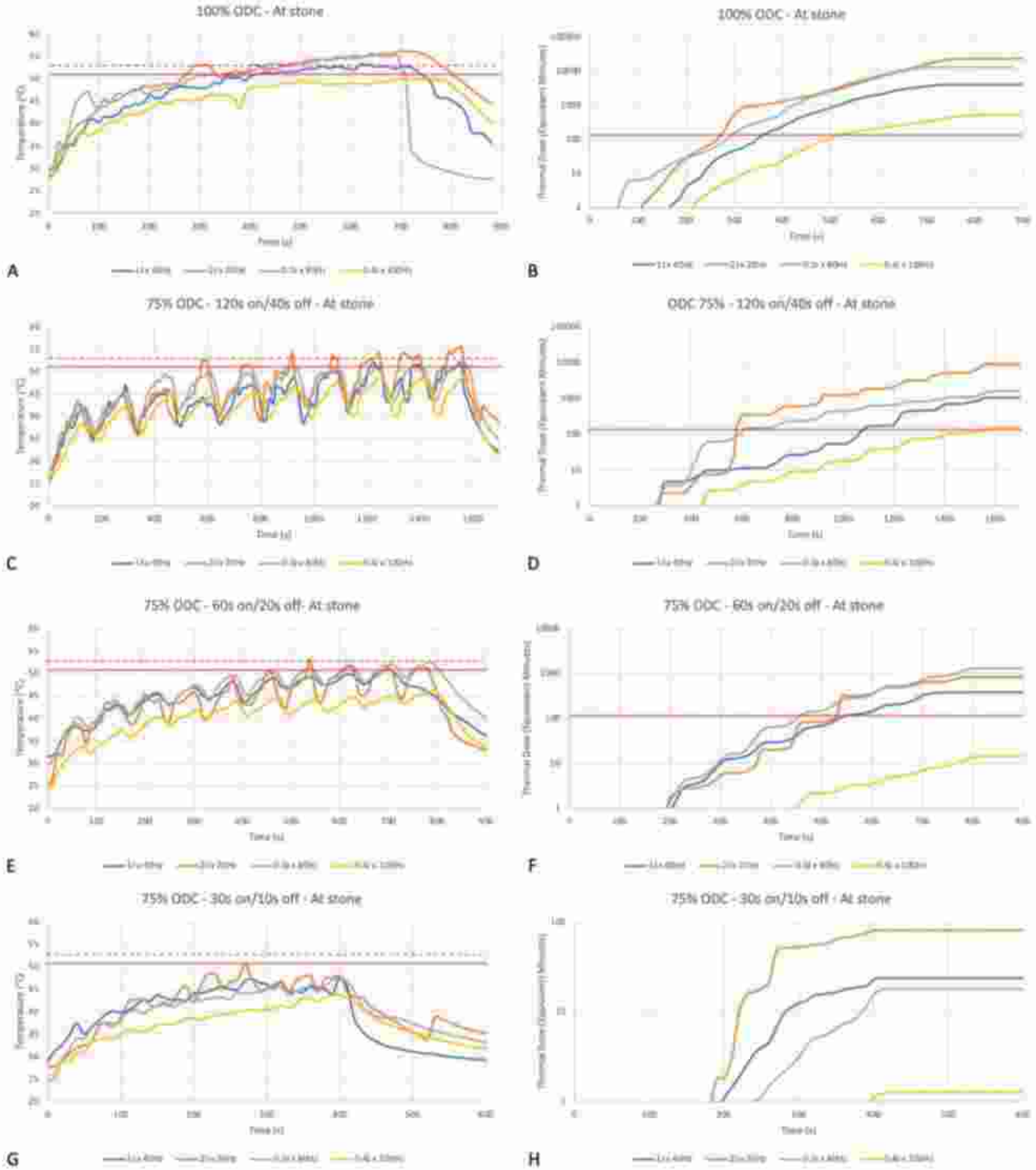


Fig. 1 Temperature and thermal dose graphs of each laser setting at the stone. Critical temperatures of 51 °C (solid red line) and 53 °C (dashed red line) are on temperature graphs. TD_{43} (solid red line) is on the thermal dose graphs. 100% ODC (**A**) temperature and (**B**) thermal dose. 75% ODC: 120 s on/40 s off (**C**) temperature and (**D**) thermal dose; 60 s on/20 s off (**E**) temperature and (**F**) thermal dose; 30 s on/10 s off (**G**) temperature and (**H**) thermal dose

Table 1 Room temperature (experimental) and 37 °C (synthesized) data for cumulative thermal dose (CEM), time to TD_{43}, and statistical comparison at the stone versus away from the stone

Laser setting	ODC	Time on (s)/time off (s)	Cumulative thermal dose (CEM)		Time to thermal injury threshold (s)		P at versus away from Stone
			At stone	Away from stone	At stone	Away from stone	
Experimental starting temperature at room temperature							
1 J×40 Hz	100%		**3994.372408**	81.01790325	360	NR	<0.0001
	75%	30/10	23.74853563	5.44836126	NR	NR	<0.0001
		60/20	**374.2499514**	61.7420721	570	NR	<0.0001
		120/40	**1008.87866**	**370.2939787**	1080	1060	0.0141
	50%	30/30	1.184148196	0.003849885	NR	NR	<0.0001
		60/60	6.533942312	2.584527506	NR	NR	0.0101
		120/120	17.34302074	1.170469434	NR	NR	<0.0001
2 J×20 Hz	100%		**23,812.30995**	**48,273.20725**	270	350	0.4059
	75%	30/10	79.15143878	**156.5133206**	NR	390	0.1908
		60/20	**804.2165105**	**627.9591831**	540	560	0.4538
		120/40	**8944.85014**	**4270.637634**	580	690	0.0307
	50%	30/30	0.016903765	0.000624035	NR	NR	<0.0001
		60/60	2.541680503	5.39947926	NR	NR	0.0321
		120/120	73.32476729	6.34378446	NR	NR	<0.0001
0.5 J×80 Hz	100%		**12,897.02513**	**3757.371719**	300	400	0.008
	75%	30/10	17.77461774	0.625119376	NR	NR	<0.0001
		60/20	**1270.627218**	87.21824929	470	NR	<0.0001
		120/40	**1568.099796**	**566.4515832**	610	940	<0.0001
	50%	30/30	0.019893315	0.003267131	NR	NR	0.0023
		60/60	0.835863942	0.016868467	NR	NR	<0.0001
		120/120	49.59701998	9.762252576	NR	NR	<0.0001
0.4 J×100 Hz	100%		**496.7329568**	**1193.887628**	520	490	0.0951
	75%	30/10	1.272085656	0.022888439	NR	NR	0.003
		60/20	14.40175912	9.806241275	NR	NR	0.4042
		120/40	**160.0905257**	28.62056023	1550	NR	<0.0001
	50%	30/30	0.027268611	0.001571028	NR	NR	<0.0001
		60/60	0.091726583	0.040731872	NR	NR	0.0533
		120/120	7.797394552	1.332162056	NR	NR	<0.0001
Synthesized starting temperature of 37 °C							
1 J×40 Hz	100%		**1,908,310.053**	**3222.019151**	125	395	<0.0001
	75%	30/10	**7322.655539**	**913.1144351**	145	285	<0.0001
		60/20	**16,378.61107**	**8254.505973**	225	295	0.0260
		120/40	**1,739,669.622**	**407,362.0577**	115	235	0.0034
	50%	30/30	**1443.021766**	**146.2747411**	280	580	<0.0001
		60/60	**10,627.60964**	**3768.877438**	275	190	0.0251
		120/120	**81,137.7316**	**8242.847493**	115	320	<0.0001
2 J×20 Hz	100%		**2,843,906.409**	**15,214,508.32**	105	135	0.0932
	75%	30/10	**46,790.00092**	**160,584.8182**	115	110	0.0199
		60/20	**4,502,069.297**	**3,397,500.191**	85	120	0.3611
		120/40	**21,788,051.72**	**7,106,049.871**	95	115	0.0252
	50%	30/30	**141.4346719**	107.4275158	620	NR	>0.9999
		60/60	**5230.702309**	**6402.409149**	385	300	>0.9999
		120/120	**45,458.29682**	**3332.703988**	125	615	<0.0001

Table 1 (continued)

Laser setting	ODC	Time on (s)/time off (s)	Cumulative thermal dose (CEM)		Time to thermal injury threshold (s)		P at versus away from Stone
			At stone	Away from stone	At stone	Away from stone	
0.5 J × 80 Hz	100%		**4,064,796.22**	**634,663.1546**	55	155	0.0003
	75%	30/10	**109,286.5641**	**1746.843721**	115	240	< 0.0001
		60/20	**325,400.0589**	**25,879.8443**	140	270	< 0.0001
		120/40	**831,654.9703**	**172,884.6415**	105	275	< 0.0001
	50%	30/30	**511.5047966**	**155.9222927**	360	530	0.0200
		60/60	**4069.699667**	**202.5558009**	340	1130	< 0.0001
		120/120	**365,374.0152**	**91,416.32437**	55	85	< 0.0001
0.4 J × 100 Hz	100%		**413,479.7619**	**752,733.7017**	145	165	> 0.9999
	75%	30/10	**4010.392836**	**355.5392631**	225	310	0.0603
		60/20	**86,184.97564**	**65,075.70654**	195	215	0.7942
		120/40	**211,310.8757**	**24,788.63573**	255	295	< 0.0001
	50%	30/30	**895.0846398**	**129.6287396**	275	500	0.0045
		60/60	**2527.187859**	**551.2766972**	400	620	0.0003
		120/120	**70,227.88752**	**23,026.15331**	105	150	< 0.0001

Bold indicate test that exceeded threshold of thermal injury. NR indicates that the threshold of thermal injury was not reached. Statistics comparing thermal dose and calculated with Kruskal–Wallis

pose the risk of thermal injury. Human tissue can be rendered nonviable after sustaining a thermal dose equivalent of 43 °C for 120 min, 21.8 s at 51 °C, 15 s at 53 °C, and only 1 s at 56 °C; thus, temperature and thermal dose are not linearly related [6–8]; even TD_{43} of as little as 20 min may result in minor renal thermal injury [20]. We demonstrated that higher cumulative thermal doses were generated with longer laser-on times and higher ODCs for all laser settings.

The Laser Research Lab at the University of Michigan has extensively evaluated laser parameters and thermal dose via in vitro bench models and computational modeling. They have evaluated laser power (2.5–50 W), frequency (5–80 Hz), irrigation rate (0–40 ml/min) and temperature (~0 °C and 19 °C), and ODC (50–100%) [7, 8, 12–15]. They sought to adapt their findings into an in vivo porcine model. Continuous temperature monitoring was performed as irrigation rates were manipulated with a standardized power (40 W) and lasing time (100 s). They found that temperatures capable of tissue damage were easily achieved but can be negated by increasing irrigation flow [21].

Our study demonstrated that greater temperatures and thermal doses were delivered with higher ODCs and longer laser-on times. The TD_{43} was reached for ODCs of 100% and 75%. These findings support previously published studies that the threshold for thermal injury was only exceeded for ODCs ≥ 70% while this threshold was reached quicker at higher ODCs [13]. Aldoukhi, et al. performed a chart review of 63 URS cases and determined that mean ODCs are 32%, while the ODC was 63% during the 60 s of greatest power delivered [15]. These findings along with the results of our study indicate that the ODC, laser-on time, and off-times play a crucial role in regulating the fluid temperatures during laser lithotripsy. Advancements in laser technology provide more opportunity in managing large renal stones via RIRS with prolonged ODCs due to wider range of settings and availability of pulsed lasers that limit retropulsion.

Maxwell, et al. compared a simulation with their in vitro test tube model. They recognized that heat was delivered away from the laser tip toward the distal end of the test tube and bounced back to the opening of the tube, causing a more uniform temperature throughout their system [7]. In our study, maximal temperatures and thermal doses were most often recorded at the probe closest to the tip of the laser fiber. Temperatures and thermal dose variations between probe locations can be attributed to ureteroscope manipulation while lasing along with positioning of the stone and laser tip in the PCS. It is important to recognize that the location of the laser tip and stone are decisive in the thermal loads.

It is important to recognize that the power was standardized in this study due to the ability to manipulate the frequency and energy without changing power and 40 W is a high power which can result in dangerous fluid temperatures during RIRS. There have been recommendations to consider performing lithotripsy in the kidney at a power less than 30 W to minimize the risk of thermal injury [16]. Even when higher power settings are utilized, the risk of thermal injury

can be mitigated by taking breaks from lasing, increasing irrigation rates, or using cooled irrigation.

This study had several strengths. First, this study evaluated four factors: temperature, thermal dose, ODC, and laser-on time in an anatomically correct, high-fidelity model. Second, we were able to evaluate thermal load in multiple locations in the PCS. Finally, we were able to measure the temperatures during active lithotripsy. While prior studies have compared some of these factors affecting fluid temperature, the majority of these studies focus on fewer variables [7, 8, 12, 13, 15]. The majority of studies analyzing thermal dose were performed via in vivo or ex vivo animal models or in vitro glass test tube models.

There are several limitations in this study. We acknowledged that these tests were performed on a model starting at room temperature. Despite the lower starting temperature, we demonstrated that dangerous temperatures can be achieved with aggressive lasering. Our results even more strongly demonstrated that TD_{43} can be reached easily starting at corporal temperature based on our more detailed calculations to simulate starting at body temperature. We also recognize that this model only includes a partial ureter segment and this may lead to difficulty transferring results to clinical situations. While some of the data presented may be challenging to correlate to the surgical environment, it is paramount to recognize that dangerous thermal loads can easily be reached in a clinical setting if one is not diligent during laser lithotripsy. Further studies are indicated to pursue increasingly accurate simulations of RIRS for laser lithotripsy.

Conclusion

This study demonstrated that higher temperatures, greater cumulative thermal dose, and TD_{43} were reached faster closer to the tip of the Ho:YAG laser fiber, with longer laser-on times, coupled with shorter laser-off times, and higher ODCs. Both frequency and energy are crucial in temperature generation and thermal dose delivered, even at a standardized power. Fragmentation settings in general elicited greater thermal doses during Ho:YAG RIRS laser lithotripsy compared with dusting settings. Further studies and model development may allow for a more accurate clinical correlation during in vitro laser studies.

Supplementary Information The online version contains supplementary material available at https://doi.org/10.1007/s00345-024-04821-9.

Acknowledgements The authors would like to graciously thank Dr. William Roberts, MD from the University of Michigan for providing his expertise, input, and guidance in our project. The authors are largely based our project on the excellent work his lab has produced. He reviewed our data and provided insight for data evaluation to provide impactful results.

Author contributions CW: project development, data collection, data analysis, and manuscript writing; AS: data collection and data analysis; DP: data analysis and manuscript writing; KD: data analysis and manuscript writing; LS: project development, data collection, and data analysis; NS: project development, data collection, and data analysis; TO: project development and manuscript writing; SQ: project development and data analysis; AG: project development, data collection, and data analysis. All of the listed authors have contributed substantially to the production of this research and manuscript.

Funding There was no source of funding for this project.

Data Availability The data collection has been included as a supplementary file.

Declarations

Conflict of interest There are no conflicts of interest nor are there any financial or non-financial interests of any author for any author included in the production of this manuscript.

Human or animals rights This research project does not involve any human participants nor animal studies.

Informed consent Informed consent was not required for this study.

References

1. Kronenberg P, Somani B (2018) Advances in lasers for the treatment of stones-a systematic review. Curr Urol Rep 19(6):45
2. Chan KF et al (1999) Holmium:YAG laser lithotripsy: a dominant photothermal ablative mechanism with chemical decomposition of urinary calculi. Lasers Surg Med 25(1):22–37
3. Zarrabi A, Gross AJ (2011) The evolution of lasers in urology. Ther Adv Urol 3(2):81–89
4. Zhang JJ et al (2015) Water content contribution in calculus phantom ablation during Q-switched Tm:YAG laser lithotripsy. J Biomed Opt 20(12):128001
5. Rice P et al (2022) Generated temperatures and thermal laser damage during upper tract endourological procedures using the holmium: yttrium–aluminum–garnet (Ho:YAG) laser: a systematic review of experimental studies. World J Urol 40(8):1981–1992
6. Sapareto SA, Dewey WC (1984) Thermal dose determination in cancer therapy. Int J Radiat Oncol Biol Phys 10(6):787–800
7. Maxwell AD et al (2019) Simulation of laser lithotripsy-induced heating in the urinary tract. J Endourol 33(2):113–119
8. Aldoukhi AH et al (2017) Thermal response to high-power holmium laser lithotripsy. J Endourol 31(12):1308–1312
9. Ghazi A, Melnyk R, Cook A et al (2022) PD37–06 Comparison of computational simulation and hydrogel kidney phantoms for in vivo assessment of intrarenal pressure (IRP) dynamics during ureteroscopy under various experimental conditions. J Urol 207:e641
10. Saba P et al (2020) Development of a high-fidelity robot-assisted kidney transplant simulation platform using three-dimensional printing and hydrogel casting technologies. J Endourol 34(10):1088–1094
11. Braunstein L et al (2022) Characterization of acoustic, cavitation, and thermal properties of poly(vinyl alcohol) hydrogels for use as therapeutic ultrasound tissue mimics. Ultrasound Med Biol 48(6):1095–1109
12. Aldoukhi AH et al (2020) Defining thermally safe laser lithotripsy power and irrigation parameters. J Endourol 34(1):76–81

13. Louters MM et al (2022) Laser operator duty cycle effect on temperature and thermal dose: in-vitro study. World J Urol 40(6):1575–1580
14. Dau JJ et al (2021) Effect of chilled irrigation on caliceal fluid temperature and time to thermal injury threshold during laser lithotripsy. J Endourol 35(5):700–705
15. Aldoukhi AH et al (2021) Patterns of laser activation during ureteroscopic lithotripsy: effects on caliceal fluid temperature and thermal dose. J Endourol 35(8):1217–1222
16. De Coninck V, Defraigne C, Traxer O (2022) Watt determines the temperature during laser lithotripsy. World J Urol 40(5):1257–1258
17. Petzold R, Suarez-Ibarrola R, Miernik A (2021) Temperature assessment of a novel pulsed thulium solid-state laser compared with a holmium:yttrium–aluminum–garnet laser. J Endourol 35(6):853–859
18. Molina WR et al (2021) Temperature rise during ureteral laser lithotripsy: comparison of super pulse thulium fiber laser (SPTF) vs high power 120 W holmium-YAG laser (Ho:YAG). World J Urol 39(10):3951–3956
19. Dauw CA et al (2015) Contemporary practice patterns of flexible ureteroscopy for treating renal stones: results of a worldwide survey. J Endourol 29(11):1221–1230
20. Yarmolenko PS et al (2011) Thresholds for thermal damage to normal tissues: an update. Int J Hyperth 27(4):320–343
21. Aldoukhi AH et al (2018) Caliceal fluid temperature during high-power holmium laser lithotripsy in an in vivo porcine model. J Endourol 32(8):724–729

Publisher's Note Springer Nature remains neutral with regard to jurisdictional claims in published maps and institutional affiliations.

Springer Nature or its licensor (e.g. a society or other partner) holds exclusive rights to this article under a publishing agreement with the author(s) or other rightsholder(s); author self-archiving of the accepted manuscript version of this article is solely governed by the terms of such publishing agreement and applicable law.

《世界泌尿外科杂志》（2024）第42卷第157页
https://doi.org/10.1007/s00345-024-04821-9

原文

发生了什么？高保真解剖模型中钬激光碎石术热剂量的评估

克里斯托弗·沃林德[1] Aaron Saxton [1]·Dennis Phan [1]·Karen Doersch [1]·Lauren Shepard [1,2]·Nathan Schuler [1,2]·Thomas Osinski [1]·Scott Quarrier [1]·Ahmed Ghazi [1,2]

接收日期：2023年8月20日/接受日期：2024年1月16日/网络发表日期：2024年3月14日
©作者（们）于2024年获得德国Springer-Verlag GmbH（Springer Nature旗下）的独家授权

摘要

目的：评估钬激光在不同激光参数下，于人体不同部位的热分布情况。

体外解剖盆腔肾盂集合系统（PCS）模型。激光碎石术是治疗尿路结石的基础疗法。随着高功率激光技术的应用，结石消融效率显著提升。手术中患者安全始终是首要考量。众所周知，激光碎石术产生的高温可能造成组织热损伤。

方法：采用高保真3D打印水凝胶模型的PCS，将合成BegoStone植入肾脏

在进行盆腔激光碎石术时，我们使用Moses 2.0钬激光器。在标准功率（40W）和灌注压力（100cm $_2$H$_2$O）条件下，我们评估了在四种不同激光设置下，操作员工作循环（ODC）随不同工作时间间隔的变化情况。温度分别在结石位置和远离结石的位置进行测量。

结果激光头附近温度最高，远离激光头时温度逐渐降低。流体温度升高

随着激光作用时间延长和ODC值升高，热剂量也随之增加，当ODC值达到75%和100%时，热损伤阈值被触发。

结论激光光纤尖端附近温度生成和热剂量递送最大，且不

仅依赖功率。在40 W标准功率下，四种激光设置显示出显著的温度差异。温度受多种因素影响，包括激光开启时间、操作员工作周期以及在PCS中的位置。

关键词热剂量·温度·激光碎石术·钬·解剖模型

缩写

RIRS逆行肾内手术

Ho：钇铝石榴石（YAG）：Holmium：钇铝石榴石（Yttrium-Aluminum-Garnet）

TD_{43}	43°C时的热剂量损伤阈值
厘米	累计等效
单位	输尿管镜检查
pc	肾盂肾盏集合系统
CFD	计算流体动力学
PVA	聚乙烯醇
鸟氨酸脱羧酶	操作员值班周期
dicom数字图像与通信	医学
CAD	计算机辅助设计
UPJ	输尿管肾盂连接处

介绍

逆行肾内碎石术（RIRS）是治疗尿路结石的常用方法。激光技术的进步对治疗效果至关重要，钬铝石榴石（Ho：YAG）作为标准碎石激光器，因其能粉碎多种成分的结石而被广泛采用[1]。Ho：YAG碎石过程主要通过光热效应实现，同时伴有光声效应的辅助作用[2]。结石吸收激光能量后发生碎裂和熔融，而激光工作时产生的能量生成是其主要作用机制。

✉ 克里斯托弗·沃兰德Christopher_Wanderling@urmc.rochester.edu

1 美国纽约州罗切斯特市罗切斯特大学医学中心泌尿外科

2 美国马里兰州巴尔的摩市约翰霍普金斯大学泌尿外科

热量产生，流体温度升高可能造成热组织损伤[3-5]。

大功率激光（≥100瓦）能在更高频率（>120赫兹）下输出能量，显著提升治疗效率。但功率越高，产生的热量也越大。在确保患者安全的前提下，选择最高效的碎石方法至关重要。热损伤阈值（TD_{43}）是指在43℃环境下能承受的热剂量，单位为累积当量分钟（CEM）。当TD_{43}≥120分钟（即$_{TD\,43}$=120 CEM）时，组织会发生变性。这一标准最初由萨帕雷托和杜威提出，并在后续输尿管镜检查（URS）研究中得到验证[6–8]。虽然现有体外模型提供了宝贵数据，但其临床转化仍面临挑战。相比之下，活体和离体动物模型虽能更贴近人体RIRS（输尿管结石）的生理特征，但存在成本高昂、解剖结构难以复现以及伦理争议等局限性。

本研究旨在基于既往研究成果，采用经机械测试与计算流体动力学（CFD）验证的高精度解剖学人肾模型构建盆腔肾盂集合系统（PCS）[9]。聚乙烯醇（PVA）水凝胶的热学特性已被证实可精准模拟人体组织[10，11]。本研究的主要目标包括：

1. 本研究通过四种不同40瓦激光功率设置，采用四种操作员工作周期（ODCs）及三种开启时间间隔，系统评估了Moses 2.0 Ho：YAG激光器在石料表面及远离石料区域的温度分布特征。
2. 评估并比较每个激光设置的TD时间$_{43}$。

材料和方法

模拟器制造

使用比利时鲁汶Materialize公司开发的Mimics软件，将患者CT扫描的数字医学影像与通信（DICOM）数据分割为三维计算机辅助设计（CAD）模型。该三维CAD模型（PCS，体积25.1毫升）采用北卡罗来纳州格林斯伯勒Fusion3Design公司生产的水凝胶线材进行3D打印，其中合成BegoStone材料（粉末与水重量比10：1）被精准定位在肾盂区域，并覆盖第二层聚乙烯醇（PVA）混合涂层（图S1A和B）。随后将模型植入水凝胶肾脏模型中。最终产品经过全面的力学测试和流体动力学模拟测试，成功复现了PCS的物理特性、结石碎石效果及流体流动状态（图S1C和D）[10]。

激光碎石术

碎石术采用标准化功率（40 W，短脉冲宽度，激活Moses技术）进行，通过逆行通道使用柔性输尿管镜（LithoVue，Boston Scientific）和200μm Ho：YAG激光光纤（Moses 2.0，Boston Scientific；图S2）进行连续生理盐水冲洗（100 cm H_2O=17.9 ml/min）。选择40 W作为标准化功率，因为可以测试四种激光设置——两种碎石模式（1 J×40 Hz，2 J×20 Hz）和两种碎粉模式（0.5 J×80 Hz，0.4 J×100 Hz）。我们评估了三种ODC（50%、75%和100%）在不同激光开启时间（30、60和120秒）下的效果。每个实验包含10个ODC（1 ODC=一个激光开启/踏板激活和一个激光关闭/踏板关闭序列；激光开启时间除以总碎石时间）；100% ODC的踏板开启时间为12分钟，无激光关闭时间。每种激光设置测试了10种排列组合。总共进行了80次实验（40次测试×2次运行），温度持续监测。

数据收集和分析

使用K型针式热电偶探头和数据记录仪（Omega公司，康涅狄格州诺沃克市）在PCS系统内的两个位置——结石部位（肾盂肾盏）和远离结石部位（上极盏）记录液体温度。热剂量采用Sapareto和Dewey公式计算。热剂量是公认的热负荷测量指标，其已通过大量实验验证$_{，}$当人体组织发生变性时，以43℃为基准温度可维持$_{43}$分钟，此时热剂量$TD43_{43}$为120单位[7，8，12–15]。热剂量的统计分析采用曲线下面积（AUC）和Kruskal-Wallis检验。温度数据通过三次多项式线性回归分析（Prism9软件）处理，p<0.05视为具有统计学意义。

合成数据（起始温度37°C）的计算方法是：先将37°C与基线实验数据相减，再将所得差值加到实验起始温度（室温）上。合成热剂量数据的计算方式与实验数据相同，均基于合成温度数据进行。

结果

所有测试中液体温度均持续升高。当使用100%ODC时，记录的温度持续上升直至达到稳定状态。在50%和75%ODC条件下，温度曲线呈现正弦波形，与ODC的激光开启周期存在相关性。

累积热剂量和最高温度记录显示，主要在石质区域且激光照射时间较长时达到峰值。其中，100%ODCs组的累积热剂量最大（图1）。

表1展示了结石位置与远离结石位置时的热剂量、热剂量达到时间43及统计学对比结果。对于100%ODC能量密度，结石位置的累积热剂量和达到热剂量时间$_{43}$分别以2 J×20 Hz（23,812.3CEM/270秒）最快/最高，0.4 J×100 Hz（1193.9 CEM/490秒）最慢/最长；1 J×40 Hz为中等（3994.4CEM/360秒），0.5 J×80 Hz为最低（1289.02CEM/300秒）。远离结石位置时，最快/最高值为2 J×20 Hz（48,273.2CEM/350秒），最低/最长值为1 J×40 Hz（未达到统计学显著性，即未达到显著性水平，记为“未达到”）；0.5 J×80 Hz为中等（3757.4 CEM/400秒），0.4 J×100 Hz为最低（记为“1193.9/490秒”）。1 J×40 Hz（p<0.0001）和0.5 J×80 Hz（p=0.008）在结石位置与远离结石位置时的热剂量存在统计学显著差异。

在75%ODC条件下，仅当使用2 J×20 Hz能量密度且远离结石时（156.5 CEM），TD$_{43}$在30秒开启/10秒关闭模式下被突破。对于60秒开启/20秒关闭模式，TD$_{43}$在2 J×20 Hz能量密度下，无论是否靠近结石均达到阈值（分别为804.2 CEM和627.9 CEM），而1 J×40 Hz仅在结石处达到（374.2 CEM），0.5 J×80 Hz则在结石处达到（1270.6 CEM）。0.4 J×100 Hz未达到TD$_{43}$阈值。120秒开启/40秒关闭模式下，除0.4 J×100 Hz仅在结石处达到阈值外，其他激光设置在结石处和远离结石处均达到阈值。50%ODC测试的所有激光设置均未达到TD$_{43}$阈值。

总体而言，碎裂设置在结石部位（0.5 J×80 Hz在75%ODC、60秒开/20秒关和50%ODC、120秒开/120秒关时累积热剂量最高）和结石部位外（表S1）均能提供更高热剂量。

随着激光开启时间的延长，热剂量也随之增加。对于50%和75%的ODC设置，120秒的激光开启时间在各激光设置中均产生了最大的累积热剂量。表S2展示了50%和75% ODC开启时间下，不同激光设置的热剂量对比数据。在结石位置进行50%ODC时，除0.4焦耳×100赫兹的30秒与60秒开启时间外，其他所有激光开启时间组合均存在显著差异。对于结石位置外的50%ODC，除0.5焦耳×80赫兹的30秒与60秒开启时间外，其他所有对比均呈现显著差异；而在1焦耳×40赫兹和2焦耳×20赫兹条件下，60秒与120秒开启时间的对比也显示出显著差异。评估75%ODC时，除结石位置外的0.5焦耳×80赫兹外，所有开启时间周期均存在统计学显著差异；结石位置的60秒/20秒与120秒/40秒开启时间，以及2焦耳×20赫兹的30秒/10秒与60秒/20秒开启时间均存在显著差异。

考虑到激光关闭时间与开启时间无关，比较50%与75%的ODC（30秒开/30秒关与30秒开/10秒关，60秒开/60秒关与60秒开/20秒关，在结石位置和远离结石位置时，两种激光设置（120秒开/120秒关与120秒开/40秒关）的ODC置换均显示出显著差异（p <0.0001）。

在将实验数据适配以在37°C初始温度下合成模拟数据时，最大温度值更高，且除2 J×20 Hz、30秒开/30秒关的石块远离位置外，所有试验均超过阈值温度$_{43}$。从体温开始时达到阈值温度$_{43}$的时间显著缩短。这种合成数据也显示出相似的统计学结果。

完整的温度数据、50%ODC曲线以及用于体温分析的综合数据均收录于补充材料中。

讨论

本研究在频率、能量和ODC参数变化时，展示了四种激光设置在温度和热剂量上的显著差异，同时保持了标准化功率（40 W）和灌注（17.9 ml/min）。在评估这些结果和数据时，重要的是要认识到，虽然这种高保真模型可以在URS期间模拟PCS，但它无法完全复制手术环境以及RIRS和激光碎石术期间存在的所有干扰变量。此外，这些研究是在室温下的体外解剖模型中进行的。我们承认原始数据可能无法提供完全准确的临床相关性；然而，通过使用合成数据校正基线起始温度，这可能有助于更准确地考虑临床相关性。

虽然研究发现存在显著差异，但就流体温度与测试频率或能量之间的整体趋势而言，并未发现明显关联。无论ODC参数和激光器设置如何调整，基于激光开启时间计算的总能量始终稳定（30秒开启=12±0.2千焦，60秒开启=24±0.1千焦，120秒开启=48±0.1千焦，100%功率=28.3–30.1千焦）。若热力学定律中“功率决定温度而频率和能量无关”的理论成立[8，16–18]，理论上不同激光设置间应呈现更接近的结果。专家推测，尽管激光系统设定为40瓦，但实际输出功率在激光工作时可能存在波动。根据美国食品药品监督管理局（FDA）规定，钬：钇铝石榴石（Ho：YAG）激光器的输出功率需在设定值的15%范围内。基于闪光灯激光技术原理，部分能量脉冲可能比其他脉冲更接近设定值。研究发现，激光系统内部温度随工作时长变化会产生波动，从而导致功率输出不稳定。

在一项针对414名泌尿科医生的调查中，67%的受访者表示更倾向于使用高频低能激光碎石[19]。泌尿科医生必须谨慎使用高功率激光

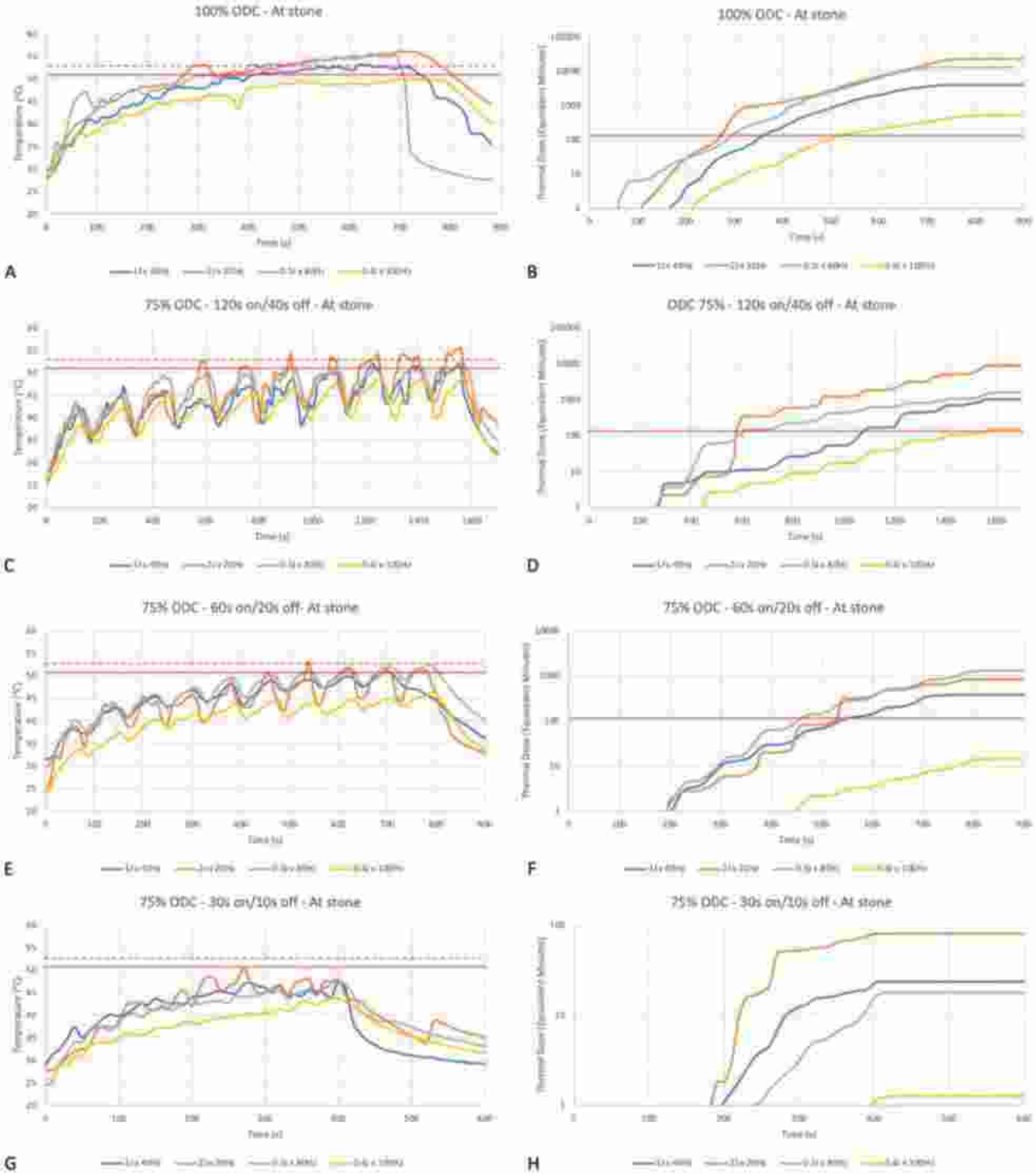


图1每个激光设置在结石处的温度和热剂量曲线。温度曲线上的临界温度为51°C（红色实线）和53°C（红色虚线）。热剂量曲线上的$_{TDM}$（红色实线）为。100%ODC（**A**）温度和（**B**）热剂量。75%ODC：120秒开/40秒关（**C**）温度和（**D**）热剂量；60秒开/20秒关（**E**）温度和（**F**）热剂量；
30秒开/10秒关（**G**）温度和（**H**）热剂量

表1展示了室温（实验）与37°C（合成）条件下累积热剂量（CEM）、至TD时间$_{43}$及石体与非石体对比的统计学比较数据

激光设置	ODC持续时间（秒）/休息时间(s)		累积热剂量（CEM）		达到热损伤阈值的时间(s)		P与对比远离石头
			在石头上	远离石头	在石头上	远离石头	
实验起始温度为室温			编号				
1 J×40 Hz	100%		**3994.372408**	81.01790325	360	编号	<0.0001
	75%	30/10	23.74853563	5.44836126	编号	编号	<0.0001
		60/20	**374.2499514**	61.7420721	570	编号	<0.0001
		120/40	**1008.87866**	**370.2939787**	1080	1060	0.0141
	50%	30/30	1.184148196	0.003849885	编号	编号	<0.0001
		60/60	6.533942312	2.584527506	编号	编号	0.0101
		120/120	17.34302074	1.170469434	编号	编号	<0.0001
2 J×20 Hz	100%		**23,812.30995**	**48,273.20725**	270	350	0.4059
	75%	30/10	79.15143878	**156.5133206**	编号	390	0.1908
		60/20	**804.2165105**	**627.9591831**	540	560	0.4538
		120/40	**8944.85014**	**4270.637634**	580	690	0.0307
	50%	30/30	0.016903765	0.000624035	编号	编号	<0.0001
		60/60	2.541680503	5.39947926	编号	编号	0.0321
		120/120	73.32476729	6.34378446	编号	编号	<0.0001
0.5 J×80 Hz	100%		**12,897.02513**	**3757.371719**	300	400	0.008
	75%	30/10	17.77461774	0.625119376	编号	编号	<0.0001
		60/20	**1270.627218**	87.21824929	470	编号	<0.0001
		120/40	**1568.099796**	**566.4515832**	610	940	<0.0001
	50%	30/30	0.019893315	0.003267131	编号	编号	0.0023
		60/60	0.835863942	0.016868467	编号	编号	<0.0001
		120/120	49.59701998	9.762252576	编号	编号	<0.0001
0.4 J×100 Hz	100%		**496.7329568**	**1193.887628**	520	490	0.0951
	75%	30/10	1.272085656	0.022888439	编号	编号	0.003
		60/20	14.40175912	9.806241275	编号	编号	0.4042
		120/40	**160.0905257**	28.62056023	1550	编号	<0.0001
	50%	30/30	0.027268611	0.001571028	编号	编号	<0.0001
		60/60	0.091726583	0.040731872	编号	编号	0.0533
		120/120	7.797394552	1.332162056	编号	编号	<0.0001
合成起始温度为37°C							
1 J×40 Hz	100%		**1,908,310.053**	**3222.019151**	125	395	<0.0001
	75%	30/10	**7322.655539**	**913.1144351**	145	285	<0.0001
		60/20	**16,378.61107**	**8254.505973**	225	295	0.0260
		120/40	**1,739,669.622**	**407,362.0577**	115	235	0.0034
	50%	30/30	**1443.021766**	**146.2747411**	280	580	<0.0001
		60/60	**10,627.60964**	**3768.877438**	275	190	0.0251
		120/120	**81,137.7316**	**8242.847493**	115	320	<0.0001
2 J×20 Hz	100%		**2,843,906.409**	**15,214,508.32**	105	135	0.0932
	75%	30/10	**46,790.00092**	**160,584.8182**	115	110	0.0199
		60/20	**4,502,069.297**	**3,397,500.191**	85	120	0.3611
		120/40	**21,788,051.72**	**7,106,049.871**	95	115	0.0252
	50%	30/30	**141.4346719**	107.4275158	620	编号	>0.9999
		60/60	**5230.702309**	**6402.409149**	385	300	>0.9999
		120/120	**45,458.29682**	**3332.703988**	125	615	<0.0001

表1（续）

激光设置	******	开启时间（秒）/休息时间(s)	累积热剂量（CEM）		达到热损伤阈值的时间(s)		P与对比
			在石头上	远离石头	在石头上	远离石头	远离石头
0.5 J×80 Hz	100%		**4,064,796.22**	**634,663.1546**	55	155	0.0003
	75%	30/10	**109,286.5641**	**1746.843721**	115	240	<0.0001
		60/20	**325,400.0589**	**25,879.8443**	140	270	<0.0001
		120/40	**831,654.9703**	**172,884.6415**	105	275	<0.0001
	50%	30/30	**511.5047966**	**155.9222927**	360	530	0.0200
		60/60	**4069.699667**	**202.5558009**	340	1130	<0.0001
		120/120	**365,374.0152**	**91,416.32437**	55	85	<0.0001
0.4 J×100 Hz	100%		**413,479.7619**	**752,733.7017**	145	165	>0.9999
	75%	30/10	**4010.392836**	**355.5392631**	225	310	0.0603
		60/20	**86,184.97564**	**65,075.70654**	195	215	0.7942
		120/40	**211,310.8757**	**24,788.63573**	255	295	<0.0001
	50%	30/30	**895.0846398**	**129.6287396**	275	500	0.0045
		60/60	**2527.187859**	**551.2766972**	400	620	0.0003
		120/120	**70,227.88752**	**23,026.15331**	105	150	<0.0001

加粗表示温度超过热损伤阈值的测试结果，NR表示未达到热损伤阈值。统计学比较热剂量与Kruskal-Wallis检验计算结果。

存在热损伤风险。人体组织在承受43°C热剂量当量120分钟、51°C21.8秒、53°C15秒以及56°C仅1秒后，可能变得无法存活；因此，温度与热剂量并非线性相关[6–8]；即使热剂量当量43仅20分钟也可能导致轻微肾热损伤[20]。我们证明，所有激光设置下，激光开启时间越长、光密度值（ODCs）越高，累积产生的热剂量就越大。

密歇根大学激光研究实验室通过体外实验模型和计算建模，对激光参数和热剂量进行了广泛评估。他们评估了激光功率（2.5–50 W）、频率（5–80 Hz）、冲洗速率（0–40 ml/min）和温度（约0°C和19°C），以及ODC值（50–100%）[7，8，12–15]。他们试图将这些发现应用于活体猪模型。在保持标准功率（40 W）和激光时间（100 s）的情况下，通过调节冲洗速率进行连续温度监测。研究发现，虽然很容易达到可造成组织损伤的温度，但通过增加冲洗流量即可消除这种损伤[21]。

我们的研究表明，随着ODC值升高和激光作用时间延长，治疗过程中产生的温度和热剂量也随之增加。当ODC值达到100%和75%时，治疗时长TD_{43}会达到阈值。这些发现支持了既往研究结论：热损伤阈值通常在ODC≥70%时才会被突破，且该阈值在ODC值较高时达到得更快[13]。阿尔杜基（Aldoukhi）团队通过对63例上尿路结石（URS）病例的病历分析发现，平均ODC值为32%，而热损伤阈值（ODC）则达到63%。

在60秒最大功率输出期间[15]，这些发现结合本研究结果表明，激光头（ODC）、激光开启时间与关闭时间对调控激光碎石术中的液体温度具有关键作用。随着激光技术的进步，由于脉冲激光器能有效抑制后向冲击波，加之更广泛的参数设置范围，使得通过超声碎石术（RIRS）处理大型肾结石时延长碎石时间成为可能。

麦克斯韦团队将模拟实验与体外试管模型进行对比研究。他们发现热量从激光头端向外传导至试管远端后反弹回管口，这种能量传递方式使整个系统温度分布更加均匀[7]。在我们的研究中，最高温度和热剂量通常出现在最靠近激光光纤尖端的探头位置。不同探头位置的温度与热剂量差异，主要源于输尿管镜操作时的激光照射位置、结石定位方式以及激光头在碎石系统中的摆放位置。需要特别指出的是，激光头与结石的位置关系对热负荷产生决定性影响。

需要特别说明的是，本研究之所以采用标准化功率设置，是因为在保持功率不变的前提下可以灵活调节频率和能量输出。需要强调的是，40瓦属于高功率参数，可能导致体外冲击波碎石术（RIRS）过程中液体温度升高，存在安全隐患。目前医学界建议，肾脏碎石治疗应选择功率低于30瓦的参数设置，以最大限度降低热损伤风险[16]。即使采用更高功率参数，仍需警惕热损伤风险。

可通过暂停激光作业、提高灌溉频率或采用冷却灌溉来缓解。

本研究具有多项优势。首先，我们通过解剖学精确的高保真模型，系统评估了温度、热剂量、ODC值及激光照射时间四个关键参数。其次，能够在碎石系统（PCS）的多个部位同步监测热负荷。最后，成功实现了碎石术过程中温度的实时测量。尽管既有研究对比过影响液体温度的某些因素，但多数研究仅聚焦少数变量[7，8，12，13，15]。值得注意的是，热剂量相关研究多采用动物活体/离体模型或玻璃试管体外实验进行。

本研究存在若干局限性。我们承认这些实验是在室温条件下启动的模型进行的。尽管初始温度较低，但通过激进的激光治疗仍能达到危险温度。基于更详细的计算模拟（假设从体温开始），我们的结果更有力地证明了在体温条件下启动时，热损伤阈值（TD）$_{43}$可能轻易达到危险水平。同时需要指出，该模型仅包含部分输尿管段，这可能导致临床应用时结果转移存在困难。虽然部分数据可能难以与手术环境对应，但必须认识到：在临床环境中，若操作人员在激光碎石术中不够谨慎，极易产生危险热负荷。未来研究应致力于开发更精确的激光碎石术热损伤阈值（RIRS）模拟模型。

结论

本研究表明，随着激光运行时间延长、关闭时间缩短以及氧损伤系数（ODC）升高，钬：钇铝石榴石（Ho：YAG）激光光纤尖端附近温度更快上升，累积热剂量（TD）和热剂量$_{43}$值也更高。即使在标准化功率下，频率和能量对温度生成及热剂量传递仍起关键作用。相较于碎石模式，碎石碎石术（Ho：YAG RIRS laser lithotripsy）的碎石设置通常会引发更高热剂量。未来研究和模型开发有望在体外激光实验中建立更精准的临床相关性。

补充信息在线版本包含可在https://doi.org/10.1007/s00345-024-04821-9上获得的补充材料。

致谢作者谨向Dr.致以诚挚谢意。
我们衷心感谢密歇根大学的威廉·罗伯茨博士（William Roberts，MD）在本项目中提供的专业指导与宝贵建议。本研究的大部分成果基于其实验室的卓越研究成果。罗伯茨博士审阅了我们的数据，并就数据评估方法提出了深刻见解，从而获得了具有重要影响的研究成果。

作者贡献：CW：项目开发、数据收集、数据分析及论文撰写；AS：数据收集与数据分析；DP：数据分析及论文撰写；KD：数据分析及论文撰写；LS：项目开发、数据收集与数据分析；NS：项目开发、数据收集与数据分析；TO：项目开发及论文撰写；SQ：项目开发与数据分析；AG：项目开发、数据收集与数据分析。所有署名作者均对本研究及论文的完成作出了实质性贡献。

资金本项目无资金来源。

数据可用性数据收集已作为补充文件纳入。

声明

利益冲突：参与本手稿制作的作者均不存在利益冲突，亦无任何财务或非财务利益。

人类或动物权利本研究项目不涉及任何人类受试者或动物研究。

知情同意本研究不需要知情同意。

参考文献

1. 克罗嫩伯格P，索马尼B（2018）《激光治疗结石的最新进展——系统综述》，载于《当代泌尿外科报告》第19卷第6期，第45页。
2. Chan KF等（1999）研究指出，钬：钇铝石榴石激光碎石术是尿路结石化学分解的主要光热消融机制。该成果发表于《激光外科与医学》25(1)：22-37。
3. Zarrabi A，Gross AJ（2011）原位激光技术的发展。《治疗与泌尿学进展》3(2)：81-89
4. 张JJ等（2015）《Q开关Tm：YAG激光碎石术中结石乳膨消融的水分含量贡献》，《生物医学光学杂志》20（12）：128001
5. Rice P等学者（2022年）在《世界泌尿学杂志》第40卷第8期发表系统综述《钬：钇铝石榴石（Ho：YAG）激光在上尿路内镜手术中的温度生成与热损伤研究》，系统评述了相关实验研究。
6. 萨帕雷托·SA，杜威·WC（1984）癌症治疗中的热剂量测定。《国际放射肿瘤学、生物学与物理学杂志》第10卷第6期：787-800
7. 麦克斯韦AD等（2019）《激光碎石术引发的尿路加热模拟研究》，《泌尿外科学杂志》33(2)：113-119
8. 阿尔杜基·A·H等（2017）《高功率快激光碎石术的热响应研究》，载于《泌尿外科学杂志》第31卷第12期，第1308-1312页
9. 加齐·A、梅尔尼克·R、库克·A等（2022）PD37-06计算模拟与水凝胶肾脏模型在不同实验条件下输尿管镜检查中评估肾内压力（IRP）动态变化的对比研究。《泌尿学杂志》207：e641
10. Saba P等（2020）开发基于三维打印与水凝胶铸造技术的高精度机器人辅助肾移植模拟平台。《泌尿外科学杂志》34（10）：1088-1094
11. Braunstein L等（2022）研究了聚乙烯醇水凝胶的声学、空化及热学特性，用于开发治疗性超声组织模拟材料。相关成果发表于《超声医学与生物学》第48卷第6期，页码1095-1109。
12. Aldoukhi AH等（2020）《热安全激光碎石术功率与灌洗参数的界定》，《泌尿外科学杂志》34(1)：76-81

13. Louters MM等（2022）激光操作员工作周期对温度和热剂量的影响：体外研究。《世界泌尿学杂志》40(6)：1575–1580
14. Dau JJ等（2021）研究了冷冻冲洗对激光碎石术中肾盏液温度及热损伤阈值时间的影响。《泌尿外科学杂志》35(5)：700–705
15. Aldoukhi AH等（2021）输尿管镜碎石术中激光激活模式：对盖状体液体温度及热剂量的影响。《泌尿外科学杂志》35(8)：1217–1222
16. 迪康尼克V、德弗兰C、特拉克瑟O（2022）激光碎石术中瓦特值对温度的调控作用。《世界泌尿学杂志》40(5)：1257–1258
17. 佩措尔德R、苏亚雷斯-伊巴罗拉R、米尔尼克A（2021）新型脉冲钬固体激光器与钬钇铝石榴石激光器的温度评估。《泌尿内镜杂志》35(6)：853–859
18. 莫利纳WR等学者（2021）在《世界泌尿外科杂志》第39卷第10期发表《输尿管激光碎石术温度升高的研究：超脉冲钬光纤激光器（SPTF）与120瓦高功率钬掺杂钇铝石榴石激光器（Ho: YAG）的对比》一文，详细比较了两种设备的温度变化特征。
19. Dauw CA等（2015）《肾结石治疗中灵活输尿管镜的当代实践模式：全球调查结果》。《泌尿外科学杂志》29（11）：1221–1230
20. 亚尔莫连科PS等（2011）正常组织热损伤阈值：最新进展。Int J Hyperth 27(4)：320–343
21. Aldoukhi AH等（2018）猪体内高功率钬激光碎石术中膀胱腔内液体温度研究。《泌尿外科学杂志》32(8)：724–729

出版商声明：Springer Nature对已发表地图和机构隶属关系中的司法管辖权主张保持中立。

Springer Nature或其授权方（例如学会或其他合作伙伴）根据与作者或其他权利持有人签订的出版协议，对本文拥有独家权利；作者对本文已接受的稿件版本进行自我存档，完全受该出版协议条款和适用法律的约束。

World Journal of Urology (2024) 42:197
https://doi.org/10.1007/s00345-024-04896-4

ORIGINAL ARTICLE

Assessing renal tissue temperature changes and perfusion effects during laser activation in an in vivo porcine model

Ron Marom[1] · Julie J. Dau[1] · Khurshid R. Ghani[1] · Timothy L. Hall[2] · William W. Roberts[1,2]

Received: 9 September 2023 / Accepted: 21 February 2024 / Published online: 26 March 2024
© The Author(s), under exclusive licence to Springer-Verlag GmbH Germany, part of Springer Nature 2024

Abstract

Introduction High fluid temperatures have been seen in both in vitro and in vivo studies with laser lithotripsy, yet the thermal distribution within the renal parenchyma has not been well characterized. Additionally, the heat-sink effect of vascular perfusion remains uncertain. Our objectives were twofold: first, to measure renal tissue temperatures in response to laser activation in a calyx, and second, to assess the effect of vascular perfusion on renal tissue temperatures.

Methods Ureteroscopy was performed in three porcine subjects with a prototype ureteroscope containing a temperature sensor at its tip. A needle with four thermocouples was introduced percutaneously into a kidney with ultrasound guidance to allow temperature measurement in the renal medulla and cortex. Three trials of laser activation (40W) for 60 s were conducted with an irrigation rate of 8 ml/min at room temperature in each subject. After euthanasia, three trials were repeated without vascular perfusion in each subject.

Results Substantial temperature elevation was observed in the renal medulla with thermal dose in two of nine trials exceeding threshold for tissue injury. The temperature decay time ($t½$) of the non-perfused trials was longer than in the perfused trials. The ratio of $t½$ between them was greater in the cortex than the medulla.

Conclusion High-power laser settings (40W) can induce potentially injurious temperatures in the in vivo porcine kidney, particularly in the medullary region adjacent to the collecting system. Additionally, the influence of vascular perfusion in mitigating thermal risk in this susceptible area appears to be limited.

Keywords In vivo porcine model · Temperature · Thermal injury · Safety · Ureteroscopy

Introduction

Laser lithotripsy with higher-power laser settings not only can yield smaller stone fragments [1] and faster endoscopic treatments [2] but also imposes a thermal risk to the adjacent renal and ureteral tissues. Several computer simulations, in vitro experiments, and in vivo pre-clinical studies have demonstrated high fluid temperature up to 70 degrees Celsius when utilizing 40 Watt laser settings [3–9].

A clinical study evaluating fluid temperature during Ho:YAG laser lithotripsy of ureteral stones [10] also revealed that temperature of the ureteral fluid exceeded 56 degrees Celsius in most patients, including some treated with 10 Watt laser settings. Additionally, following the introduction of the Thulium Fiber Laser (TFL) several years ago, incidents of ureteral thermal injuries were reported, leading to an Urgent Medical Device Correction by the manufacturer not to exceed 20 W settings in the ureter [11].

Despite this collection of data on temperature elevation from laser activation and several reports of thermal tissue injury, exploration of the relationship between calyceal fluid temperatures and renal tissue temperatures has thus far been limited to a single in vivo porcine study by Okhunov et al. that examined temperature in the collecting system, papilla, medulla, and cortex during ureteroscopy [12]. Only minimal tissue temperature elevation was observed in the papilla in several trials; however, the cessation of laser activation when a ureteroscope thermocouple reached 44 °C (occurring in as quickly as 4 s in some cases) precluded a full sampling of the thermal conditions experienced during ureteroscopy

✉ Ron Marom
ronmarom@gmail.com

1 Department of Urology, University of Michigan, 4432 Medical Science I, 1301 Catherine Street, Ann Arbor, MI 48109-5330, USA

2 Department of Biomedical Engineering, University of Michigan, Ann Arbor, MI, USA

[12]. For example, laser lithotripsy in a small calyx with a tight infundibulum (limiting irrigation) with longer periods of laser activation can produce higher and sustained temperatures—between 60 and 80 °C. [4] Thus, it is important to challenge the hypothesis that parenchymal tissue will not experience meaningful temperature elevation with laser activation in a calyx under this more expansive range of conditions as well.

Additionally, the distribution of blood vessels in different regions of the kidney must be considered to more fully understand heat transfer and heat-sink effects within different regions of the kidney. Hence, the objectives of this study were twofold: first, to measure renal tissue temperatures in response to laser activation in a calyx, and second, to assess the effect of vascular perfusion on renal tissue temperatures.

Methods

After obtaining approval from the Institutional Animal Care and Use Committee (IACUC), three female Yorkshire cross pigs (45–55 kg) were anesthetized with telazol and xylazine, intubated, and positioned supine. Animals were ventilated via positive pressure ventilation and maintained under anesthesia with isoflurane and oxygen. Intravenous fluid was provided (0.9% NaCl) and animals were continuously monitored via pulse oximetry and core body temperature.

At the beginning of each procedure, a flexible cystoscope (CYF-3; Olympus) was inserted into the bladder and used to identify the ureteral orifices and advance a 0.035-inch guidewire (Sensor; Boston Scientific) up the ureter. After visualization of the ureter and collecting system with a single-use ureteroscope (LithoVue; Boston Scientific), the initial guidewire was exchanged for a 0.035-inch Amplatz Superstiff guidewire (Boston Scientific).

An Outflow Resistance Altering Tool (ORAT) was passed over the wire into the proximal ureter or renal pelvis. The ORAT is essentially a modified Ureteral Access Sheath (UAS) that allows for adjustment of the outflow resistance to simulate various clinical scenarios, ranging from a narrow ureter to use of an access sheath [13]. In this particular study, the outflow resistance was adjusted to achieve a targeted IRP of 40 cmH_2O while maintaining an irrigation rate of 8 ml/min at room temperature. A prototype flexible ureteroscope with a temperature sensor located at its tip was inserted through the ORAT and fixed in a lower pole calyx for the duration of the trials using an endoscopic fixation device (CystoAssist; Mediflex). A 6 Fr ureteral access catheter (Axxcess; Boston Scientific) was placed into the bladder to maintain drainage.

A multipoint temperature sensing (MTS) needle (MultiPoint 1.5 Thermal Sensor, Boston Scientific) with thermal sensors located 5, 15, 25, and 35 mm from the needle tip was inserted percutaneously with ultrasound guidance through the kidney to the calyx in which the ureteroscope was located. This positioning was intended to locate the four MTS sensors in the collecting system, renal medulla (5 mm from the collecting system), outer region of the renal cortex, and outside the renal capsule, as depicted in Fig. 1. To facilitate data collection, the connectors of the MTS were modified for compatibility with a standard thermocouple data logger (TC-08, Pico Technology).

The ureteroscope position was checked to ensure the laser fiber was not trained directly on the MTS and was not too close to urothelial tissue. A peristaltic pump (Masterflex™ L/S™) delivered 0.9% NaCl irrigation at 8 ml/min at room temperature. A Ho:YAG laser at 40 Watt settings (0.5 J pulse energy, 80 Hz frequency) was activated for 60 s for each trial. Three trials were conducted consecutively in the same calyx in each subject. Adequate time was allotted between trials to ensure temperatures returned to baseline at all thermal sensors before initiating subsequent trials.

Upon completing the experiment, the kidney was carefully harvested with the needle position maintained, and the



Fig. 1 Placement of the MTS within the renal parenchyma. The green marks indicate the locations of the thermal sensors

kidney was sectioned to correlate the temperature sensors' locations with anatomic landmarks (Fig. 1).

A customized MATLAB code was utilized to align the laser and temperature data and perform further calculation. In each trial, thermal dose was computed for each temperature sensor by applying the Dewey and Sapareto methodology to the corresponding temperature curve [14]. Thermal dose is a way to quantify the biological risk of thermal injury, and it depends on the magnitude of temperature elevation and the period of time exposed to elevated temperatures. The threshold for thermal tissue injury and cell death has been established as 120 equivalent minutes [14, 15], which means maintaining a temperature of 43 °C for 120 min. This is equivalent to 44 °C for 60 min, 45 °C for 30 min, and so forth. Even short (1 s) exposures to a temperature of 56 °C will also reach the threshold of thermal injury.

To evaluate the impact of vascular perfusion, temperature decay was examined in the medullary and cortical portions of the kidney. Following euthanasia, additional non-perfusion trials were conducted in the same calyces in each pig. Since core temperature decayed rapidly after euthanasia, a direct comparison of temperatures and thermal dose between perfused and non-perfused trials was not meaningful. Instead, the half-life ($t½$) of temperature decay after laser deactivation was determined from each trial by measuring the time between temperature at the end of laser activation and the midpoint toward baseline temperature. To facilitate comparison, a ratio of $t½$ values for perfused and non-perfused trials was calculated.

Results

Time–temperature curves from each temperature sensor are displayed in Fig. 2. Each curve represents the range of temperatures from three trials. The red line at the bottom designates the 60-s period of laser activation at 40 W settings. Temperature of the collecting system fluid exceeded 60 °C in each trial. Thermal energy propagated into the medulla with peak temperatures ranging from 48 to 52 °C. Cortical temperatures also increased with peak values recorded between 38 and 48 °C. No significant elevation in temperature was observed outside the renal capsule. Following deactivation of the laser, temperature decayed to baseline.

The calculated thermal dose in the medulla of subject #3 ranged from 119 to 380 equivalent minutes. Two of the trials

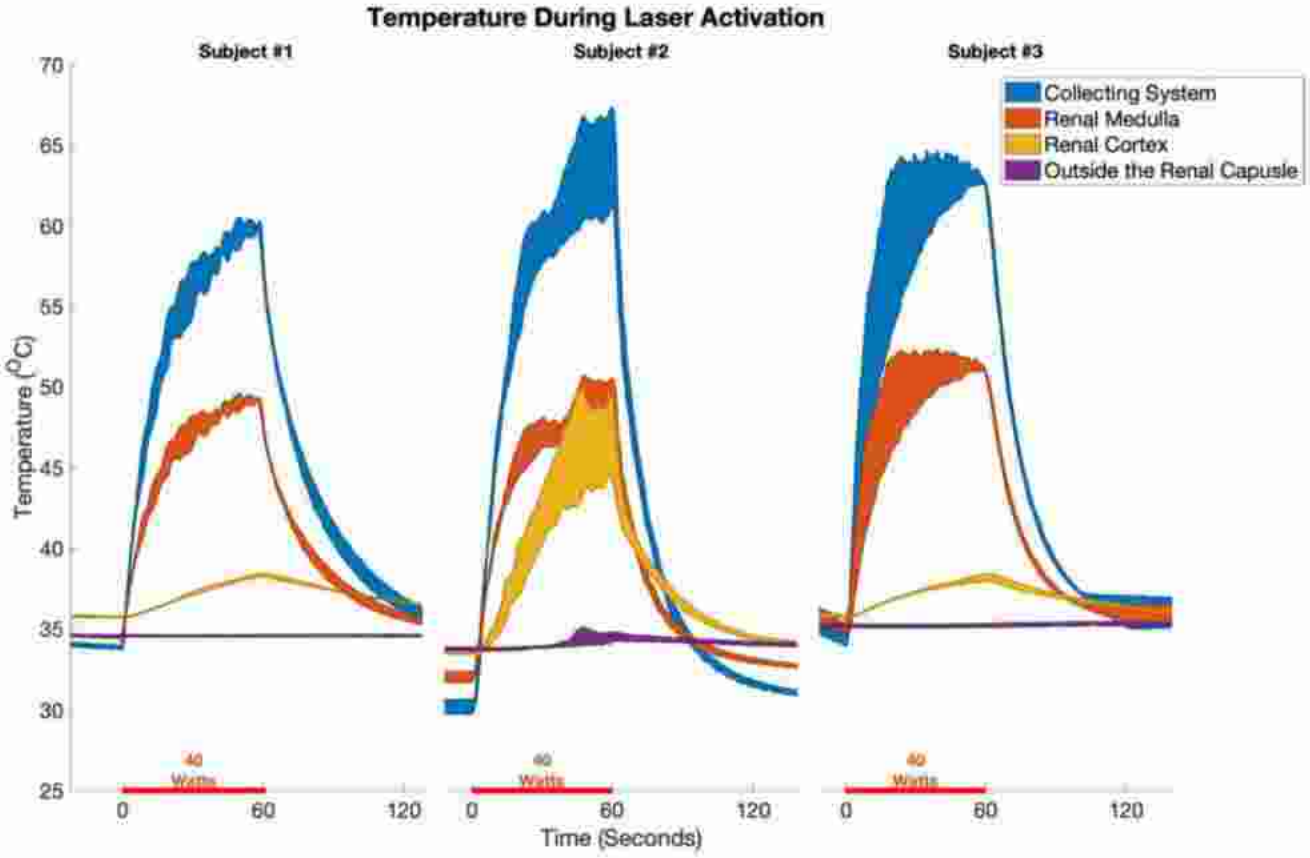


Fig. 2 Time–temperature curves for each subject. Each curve represents the range of temperatures from the three trials conducted. The red line at the bottom designates the 60-s period of laser activation at 40 W settings

exceeded the threshold for thermal injury (120 equivalent minutes), while the third trial was just short. Thermal dose in the medulla of the other subjects ranged from 20 to 55 but did not exceed the thermal threshold for tissue injury (Table 1).

When comparing temperature decay, the ratio of $t½$ for non-perfused trials averaged 1.48 ± 0.14 (range 1.3–1.6) times longer in the medullary tissue and 2.6 ± 1.28 (range 1.7–4.1) times longer in the cortical tissue (Fig. 3).

Discussion

This in vivo study utilized MTS to assess the change in temperature within the collecting system, renal medulla, renal cortex, and outside the renal capsule during laser activation in a renal calyx. In the first part of this study, a consistent gradation in temperature was noted from the collecting system to outside of the renal capsule. Substantial temperature elevation was observed in the renal medulla with thermal dose in two of nine trials exceeding threshold for tissue injury.

Table 1 Mean and maximum calculated t43 values of the different thermal sensors across all subjects and trials

	Mean thermal dose	Max thermal dose
Collecting system	709,300	3,954,200
Renal medulla	90	380
Renal cortex	3	24
Outside renal capsule	0	0

These findings diverge from the study conducted by Okhunov et al. [12] primarily due to variations in the study design. Okhunov's study consisted of two main parts. In the first part, the temperature in the collecting system was limited to a maximum of 44 degrees Celsius. However, this temperature limit makes it highly improbable to surpass the threshold for thermal injury. Thus, it does not fully encompass the range of clinical scenarios, as observed in numerous in vitro, pre-clinical in vivo studies, and clinical studies [3–8].

In the second part of Okhunov's study, restrictions were placed on the highest power output, which was capped at 30 Watts. Additionally, an operator duty cycle known to mitigate temperature elevation was imposed on laser activation [16, 17]. Although Okhunov's study conditions, which incorporate robust temperature mitigation techniques, reflect good clinical practice and provide protection under ideal circumstances, not all ureteroscopic cases can be performed under such ideal circumstances. When assessing the risk of thermal injury, it is essential to explore the limits at which high temperatures may be encountered.

The kidneys receive substantial blood flow, approximately 20% of the overall circulation [18]. It seems reasonable to assume that vascular perfusion alone could mitigate temperature elevation from laser activation. A cooling effect has been observed in radiofrequency ablation, where perfusion-mediated tissue cooling has reduced the extent of coagulation necrosis during tumor ablation [19]. However, the dynamics in the kidney are more intricate than the simplified heat diffusion and conduction equation, primarily due to the non-uniform distribution of blood supply within the organ [20].

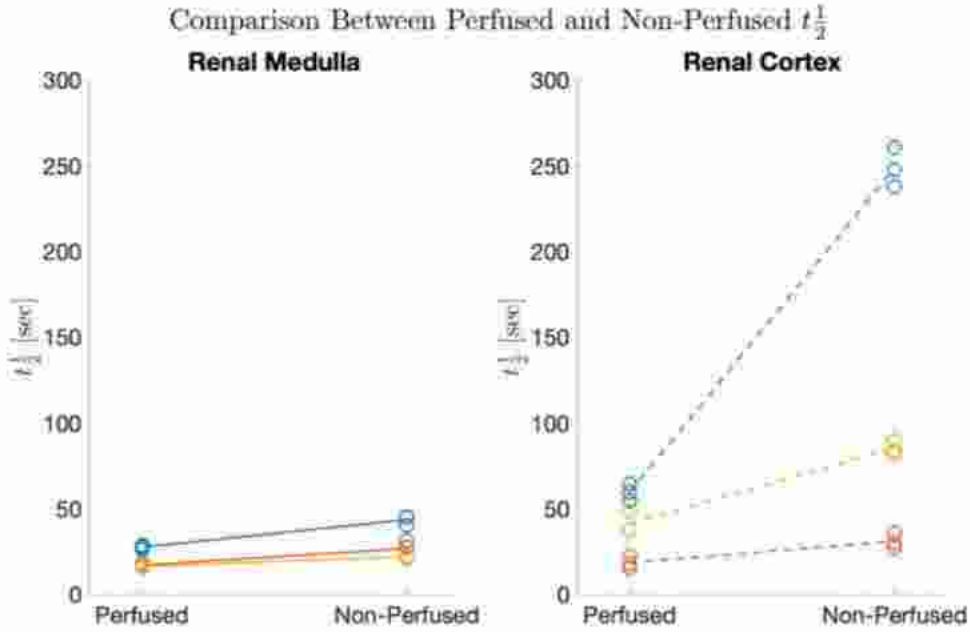


Fig. 3 Comparison of temperature decay ($t½$) between perfused and non-perfused trials, represented by different colors for each subject. The left panel displays the medulla, while the right panel displays the cortex

In the second part of this study, three additional trials were carried out in each porcine subject after euthanasia, without vascular perfusion. Unsurprisingly, the temperature decay time ($t½$) of the non-perfused trials was longer than in the perfused trials. However, the ratio of $t½$ between the non-perused and perfused trials was greater in the cortex than the medulla. This suggests that the vascular heat-sink effect in the cortex is more pronounced than in the medulla. On this basis, the medulla of the kidney appears to be more susceptible to thermal injury than the cortex.

This study has certain limitations. First, the use of the MTS needle with thermal sensors positioned 10 mm apart resulted in only two thermosensors being positioned within the renal parenchyma. Furthermore, our experiment utilized only one needle. Therefore, while this study demonstrates a genuine thermal risk to areas of the kidney adjacent to the calyx in which laser activation occurs, it does not provide a comprehensive thermal assessment of the entire renal parenchyma.

Second, the assessment of the role of perfusion in thermal mitigation, specifically the contribution of convection to thermal spread, was only conducted in a comparative manner and did not quantitatively evaluate perfusion. This is important to note since rapid changes in blood flow during the time of laser activation may be induced due to a combined effect of the intrarenal pressure and potentially temperature changes caused by the laser activation itself. However, our study provides evidence indicating the presence of a thermal injury risk in the renal medulla during ureteroscopy, which exhibits lower perfusion compared to the cortex.

Future studies will focus on thermal mapping of the kidney during laser activation with increased sampling and spatial resolution. This will enable the development of a mathematical model linking thermal dose in the collecting system fluid to thermal injury risk in various kidney regions.

Conclusion

High-power laser settings (40 W) with lower irrigation rates can induce potentially injurious temperatures in the in vivo porcine model, particularly in the medullary region adjacent to the collecting system. Additionally, the influence of vascular perfusion in mitigating the thermal risk in this susceptible area appears to be limited.

Authors contribution R Marom: Project development, Data Collection, Manuscript writing, Data analysis. WW Roberts: Manuscript writing/editing, Data analysis, Critical Revision, Study management. JJ Dau: Manuscript editing. KR Ghani: Manuscript editing. TL Hall: Manuscript editing.

Funding Funding for this study was provided, in part, by a Faculty Catalyst Award, Department of Urology, University of Michigan, and, in part, by a research grant from Boston Scientific.

Data availability The datasets generated during and/or analyzed during the current study are available from the corresponding author on reasonable request.

Declarations

Conflict of interest K.R.G. has consulting relationships with Boston Scientific, Ambu, Olympus, Coloplast, and Karl Storz. W.W.R. has a consulting relationship with Boston Scientific. R.M., J.J.D., and T.L.H. have no disclosures.

Ethical approval All procedures performed in the study involving animal subjects were in accordance with the ethical standards of the institutional research committee and were approved by the University of Michigan's Institutional Animal Care and Use Committee (IACUC).

Disclaimer The prototype ureteroscope used in this study was a concept device/technology, which was not available for sale at the time the study was conducted. Pre-clinical study results may not necessarily be indicative of clinical performance.

References

1. Aldoukhi AH, Roberts WW, Hall TL et al (2017) Holmium laser lithotripsy in the new stone age: dust or bust? Front Surg 4:57
2. Pietropaolo A, Mani M, Hughes T et al (2022) Role of low- versus high-power laser in the treatment of lower pole stones: prospective non-randomized outcomes from a university teaching hospital. Ther Adv Urol 14:17562872221097344
3. Aldoukhi AH, Ghani KR, Hall TL et al (2017) Thermal response to high-power holmium laser lithotripsy. J Endourol 31(12):1308–1312
4. Aldoukhi AH, Hall TL, Ghani KR et al (2018) caliceal fluid temperature during high-power holmium laser lithotripsy in an in vivo porcine model. J Endourol 32(8):724–729
5. Hein S, Petzold R, Schoenthaler M et al (2018) Thermal effects of Ho: YAG laser lithotripsy: real-time evaluation in an in vitro model. World J Urol 36(9):1469–1475
6. Maxwell AD, MacConaghy B, Harper JD et al (2019) Simulation of laser lithotripsy-induced heating in the urinary tract. J Endourol 33(2):113–119
7. Wollin DA, Carlos EC, Tom WR et al (2018) Effect of laser settings and irrigation rates on ureteral temperature during holmium laser lithotripsy, an in vitro model. J Endourol 32(1):59–63
8. Hein S, Petzold R, Suarez-Ibarrola R et al (2020) Thermal effects of Ho:YAG laser lithotripsy during retrograde intrarenal surgery and percutaneous nephrolithotomy in an ex vivo porcine kidney model. World J Urol 38(3):753–760
9. Marom R, Dau JJ, Hall TL et al (2023) Thermal safety boundaries for laser power and irrigation rate during ureteroscopy: in-vivo porcine assessment with a Ho:YAG laser. Urology. https://doi.org/10.1016/j.urology.2023.07.014
10. Wang X-K, Jiang Z-Q, Tan J et al (2019) Thermal effect of holmium laser lithotripsy under ureteroscopy. Chin Med J 132(16):2004–2007
11. U.S. Food & Drug Administration (FDA). Class 2 Device Recall Olympus. 2021. https://www.accessdata.fda.gov/scripts/cdrh/cfdocs/cfres/res.cfm?id=188172. Accessed 3 Jul 2023.

12. Okhunov Z, Jiang P, Afyouni AS et al (2021) Caveat emptor: the heat is "ON"-an in vivo evaluation of the thulium fiber laser and temperature changes in the porcine kidney during dusting and fragmentation modes. J Endourol 35(11):1716–1722
13. Marom R, Dau JJ, Hall TL et al (2023) Effect of outflow resistance on intrarenal pressure at different irrigation rates during ureteroscopy: in vivo evaluation. Urolithiasis 51(1):98
14. Sapareto SA, Dewey WC (1984) Thermal dose determination in cancer therapy. Int J Radiat Oncol Biol Phys 10(6):787–800
15. Yarmolenko PS, Moon EJ, Landon C et al (2011) Thresholds for thermal damage to normal tissues: an update. Int J Hyperthermia 27(4):320–343
16. Aldoukhi AH, Dau JJ, Majdalany SE et al (2021) Patterns of laser activation during ureteroscopic lithotripsy: effects on caliceal fluid temperature and thermal dose. J Endourol 35(8):1217–1222
17. Louters MM, Dau JJ, Hall TL et al (2022) Laser operator duty cycle effect on temperature and thermal dose: in-vitro study. World J Urol 40(6):1575–1580
18. Dalal R, Bruss ZS, Sehdev JS (2022) Physiology, renal blood flow and filteration. StatPearls Publishing, Florida
19. Goldberg SN, Hahn PF, Tanabe KK et al (1998) Percutaneous radiofrequency tissue ablation: does perfusion-mediated tissue cooling limit coagulation necrosis? J Vasc Interv Radiol 9(1 Pt 1):101–111
20. Pallone TL, Edwards A, Mattson DL (2012) Renal medullary circulation. Compr Physiol 2(1):97–140

Publisher's Note Springer Nature remains neutral with regard to jurisdictional claims in published maps and institutional affiliations.

Springer Nature or its licensor (e.g. a society or other partner) holds exclusive rights to this article under a publishing agreement with the author(s) or other rightsholder(s); author self-archiving of the accepted manuscript version of this article is solely governed by the terms of such publishing agreement and applicable law.

《世界泌尿外科杂志》（2024）第42卷第197页
https://doi.org/10.1007/s00345-024-04896-4

原文

活体猪模型中激光激活过程中肾组织温度变化及灌注效应的评估

Ron Marom[1] · Julie J. Dau[1] · Khurshid R. Ghani[1] · Timothy L. Hall[2] · William W. Roberts[1,2]

接收日期：2023年9月9日/接受日期：2024年2月21日/网络发表日期：2024年3月26日
©作者（们）于2024年获得德国Springer-Verlag GmbH（Springer Nature旗下）的独家授权

摘要

引言激光碎石术的体外和体内研究均显示液体温度升高，但肾实质内部的热分布尚未得到充分阐明。此外，血管灌注的散热效应仍存在争议。本研究旨在实现双重目标：首先测量肾盏区域激光激活时的肾组织温度变化，其次评估血管灌注对肾组织温度的影响。

方法使用配备温度监测功能的原型输尿管镜对三头猪实施了输尿管镜检查。传感器位于其尖端。在超声引导下，将带有四个热电偶的针头经皮插入肾脏，以测量肾髓质和皮质的温度。在室温下，以8 ml/min的灌注速率对每位受试者进行了三次激光激活（40W）60秒的试验。实施安乐死后，每位受试者在无血管灌注的情况下重复进行了三次试验。

结果在九项试验中，有两项发现肾髓质温度随热剂量增加而显著升高组织损伤的临界温度。非灌注试验的温度衰减时间（$t_{½}$）比灌注试验长。$t_{½}$的比值在皮质中比在髓中大。

结论高功率激光设置（40W）可在猪肾脏体内诱导具有潜在损伤性的温度，尤其是在邻近集合系统的髓质区域。此外，血管灌注对缓解该易感区域热风险的作用似乎有限。

关键词体内猪模型·温度·热损伤·安全性·输尿管镜检查

介绍

采用高功率激光设置进行碎石术不仅能产生更小的结石碎块[1]和更快的内镜治疗速度[2]，但同时也给邻近的肾组织和输尿管组织带来热损伤风险。多项计算机模拟、体外实验及临床前研究显示，使用40瓦激光设置时，液体温度可高达70摄氏度[3-9]。

一项评估输尿管结石Ho：YAG激光碎石术中液体温度的临床研究[10]研究显示，多数患者输尿管液温超过56摄氏度，其中部分患者使用10瓦激光治疗。此外，自数年前引入钬光纤激光（TFL）以来，输尿管热损伤事件频发，促使制造商紧急发布医疗器械修正案，规定输尿管激光功率不得超过20瓦[11]。

尽管已有大量关于激光激活引发的温度升高的数据记录，以及多篇关于热损伤组织的报道，但关于盏状窝液体温度与肾组织温度关系的研究，目前仅限于奥赫诺夫团队在猪体内进行的一项研究。该研究通过尿路镜检查，检测了收集系统、乳头、髓质和皮质的温度变化[12]。多项试验显示，乳头组织的温度升高幅度微乎其微；然而，当尿路镜热电偶温度达到44°C时（某些情况下仅需4秒即可触发激光关闭），导致无法完整采集尿路镜检查期间的热环境数据。

✉ 罗恩·马罗姆
ronmarom@gmail.com

1 密歇根大学泌尿外科，4432 Medical Science I，1301 Catherine Street，Ann Arbor，MI 48109-5330，美国

2 美国密歇根大学生物医学工程系，密歇根州安娜堡市

[12]例如，对于小叶盏且漏斗部狭窄（限制冲洗）的情况，采用较长的激光激活时间进行碎石术，可使温度持续升高至60-80°C。[4] 因此，有必要对以下假设提出质疑：在更广泛的实验条件下，激光激活下叶状结构的实质组织不会出现显著的温度升高。

此外，要全面理解肾脏各区域的热传递与散热效应，必须考虑其血管分布特征。本研究旨在实现双重目标：首先测量肾盏区域激光激活后的组织温度变化，其次评估血管灌注对肾组织温度的影响。

方法

在获得机构动物护理与使用委员会（IACUC）的批准后，三头雌性约克夏杂交猪（45–55公斤）被用特拉唑和木糖素麻醉，插管后仰卧位。动物通过正压通气进行通气，并在异氟烷和氧气麻醉下维持。静脉输注液体（0.9%氯化钠），并通过脉搏血氧饱和度和核心体温持续监测动物状况。

在每次操作开始时，医生会先将柔性膀胱镜（型号CYF-3；奥林巴斯）插入膀胱，用于定位输尿管开口并推进0.035英寸导丝（Sensor；波士顿科学）。当使用一次性输尿管镜（LithoVue；波士顿科学）观察输尿管及收集系统后，将初始导丝更换为0.035英寸的Amplatz Superstiff导丝（波士顿科学）。

将一种流出阻力调节工具（ORAT）沿导丝送入近端输尿管或肾盂。ORAT本质上是一种改良的输尿管通路鞘（UAS），可调节流出阻力以模拟各种临床场景，范围从狭窄输尿管到使用通路鞘[13]。在本研究中，通过调节流出阻力，在室温下保持8 ml/min的灌洗速率的同时，实现了40 cmH $_2$O的目标尿流率（IRP）。将带有温度传感器的原型柔性输尿管镜通过ORAT插入，并使用内镜固定装置（CystoAssist；Mediflex）在试验期间固定于下极盏部。为维持引流，将6 Fr输尿管通路导管（Axxcess；Boston Scientific）置入膀胱。

多点温度传感（MTS）针（MultiPoint 1.5 Thermal Sensor，Boston Scientific），其热传感器分别位于距针尖5、15、25和35毫米处

在超声引导下，经肾脏皮下穿刺至盏部（输尿管镜所在位置），将MTS传感器组置入该区域。该定位方案旨在将四个传感器分别部署于集合系统、肾髓质（距集合系统5毫米处）、肾皮质外缘及肾包膜外侧，具体位置如图1所示。为便于数据采集，我们对MTS传感器的连接器进行了改造，使其与标准热电偶数据记录仪（型号TC-08，Pico Technology）兼容。

检查输尿管镜位置以确保激光光纤未直接对准MTS且未过于接近尿路上皮组织。蠕动泵（Masterflex™L/S™）在室温下以8 ml/min的流速输送0.9%氯化钠冲洗液。每次试验中，使用40瓦霍氏钇铝石榴石激光器（脉冲能量0.5焦耳，频率80赫兹）持续激活60秒。每位受试者在同一盏盏叶内连续进行三次试验。试验间留有充足时间以确保所有热传感器温度恢复至基线值，随后再开始下一次试验。

实验完成后，肾脏被小心取出，同时保持针头位置不变，随后



图1 MTS在肾实质中的定位。绿色标记表示热传感器的位置

对肾脏进行切片处理，以将温度传感器的位置与解剖标志进行关联（图1）。

本研究采用定制的MATLAB代码对激光与温度数据进行对齐处理并开展后续计算。每次实验中，通过将杜威-萨帕雷托法应用于对应温度曲线[14]，为每个温度传感器计算热剂量。热剂量是量化热损伤生物学风险的指标，其数值取决于温度升幅的大小及暴露于高温环境的时间长短。目前热组织损伤与细胞死亡的临界值被确定为120等效分钟[14，15]，这意味着当温度维持在43°C时

120分钟。这相当于在44°C下持续60分钟，或在45°C下持续30分钟，依此类推。即使短至1秒的56°C高温暴露，也会达到热损伤的临界点。

为评估血管灌注的影响，研究人员对肾脏髓质和皮质区域的体温衰减情况进行了检测。实施安乐死后，研究者在每头猪的同侧肾盏中进行了额外的非灌注实验。由于核心体温在安乐死后迅速下降，因此无法直接比较灌注与非灌注实验中的体温变化及热剂量差异。

有意义。相反，通过测量激光激活结束时的温度与基线温度中点之间的间隔时间，确定了激光失活后温度衰减的半衰期（$t_{1/2}$）。为了便于比较，计算了灌注和非灌注试验的$t_{1/2}$值的比值。

结果

各温度传感器的温度-时间曲线如图2所示。每条曲线代表三次实验的温度范围。底部红线标示了40瓦激光设置下60秒的激活周期。采集系统液体温度在每次实验中均超过60°C。热能向髓质区域传导，峰值温度介于48至52°C之间。皮质温度同样升高，峰值记录在38至48°C区间。在肾包膜外未观察到显著温度升高。激光停用后，温度逐渐回落至基线水平。

受试者3的髓质中计算出的热剂量范围为119至380等效分钟。其中两项试验

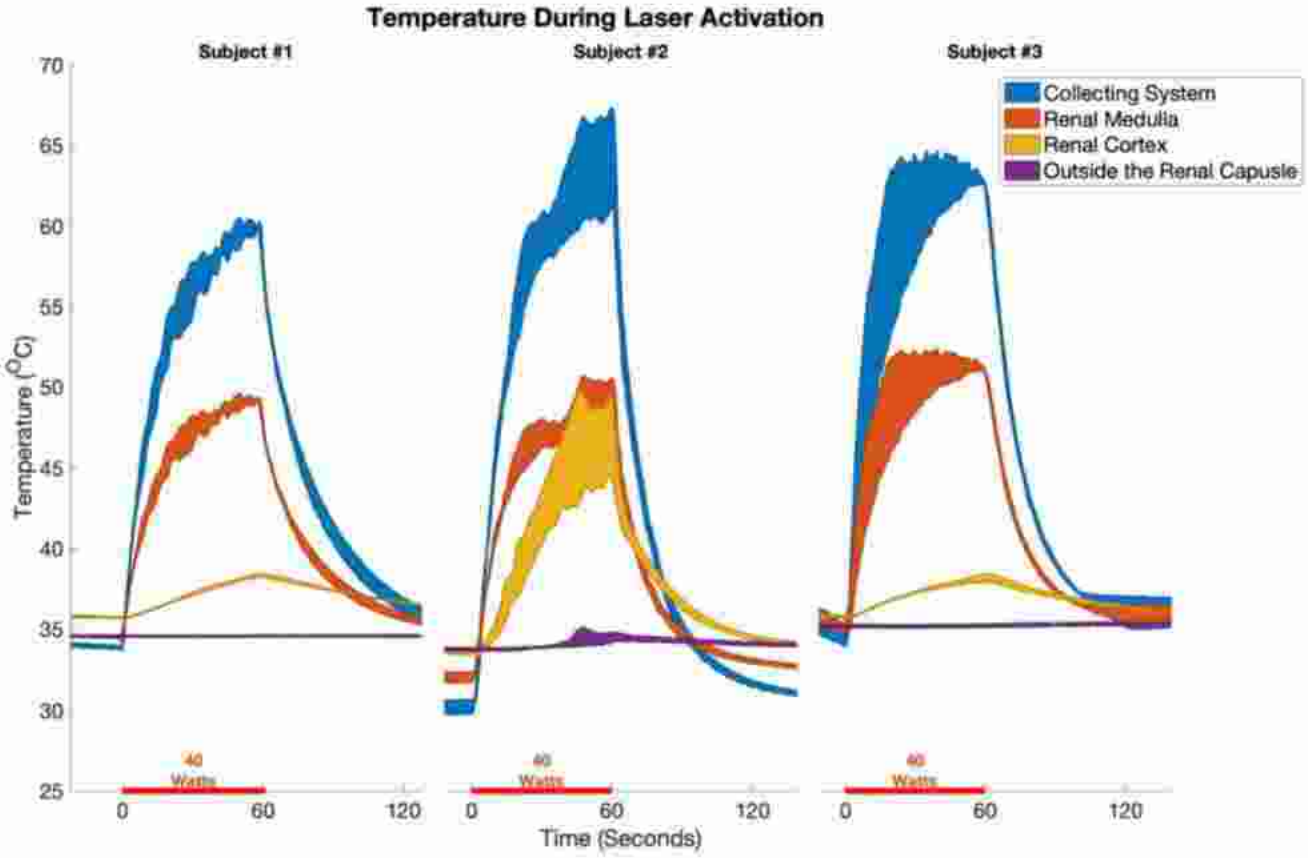


图2为各受试者的时间-温度曲线，每条曲线代表三次试验的温度范围，底部红线表示40W激光激活60秒的周期

超过了热损伤的阈值（120分钟等效时间），而第三次试验刚好未超过。其他受试者脊髓中的热剂量范围为20到55，但没有超过组织损伤的热阈值（表1）。

在比较温度衰减时，非灌注试验的$t_{½}$比值在髓质组织中平均长1.48±0.14倍（范围1.3-1.6倍），在皮质组织中平均长2.6±1.28倍（范围1.7-4.1倍）（图3）。

讨论

本项体内研究采用MTS技术，监测肾盏激光激活过程中收集系统、肾髓质、肾皮质及肾包膜外温度变化。研究初期发现，温度从收集系统向肾包膜外呈梯度递增。在九次实验中，有两次肾髓质温度显著升高，其热剂量已超过组织损伤阈值。

表1所有受试者和试验中不同热传感器的平均和最大计算t43值

	平均热剂量	最大热剂量
收集系统	709,300	3,954,200
肾髓质	90	380
肾皮质	3	24
肾外囊	0	0

这些发现与奥赫诺夫等人[的研究结果存在差异。12]这主要源于研究设计的差异。奥赫诺夫的研究包含两个主要部分。在第一部分中，采集系统的温度被限制在最高44摄氏度。然而，这种温度上限使得超过热损伤阈值的可能性极低。因此，该研究未能完全涵盖临床场景的多样性，正如我们在大量体外实验、临床前体内研究及临床试验中所观察到的[3–8]。

在奥赫诺夫研究的第二阶段，研究人员对最高功率输出进行了限制，将其上限设定为30瓦。此外，还对激光激活施加了已知能降低温度升高的操作员工作周期[16，17]。尽管奥赫诺夫的研究条件采用了完善的温度控制技术，符合良好的临床实践标准，并在理想条件下提供了保护措施，但并非所有输尿管镜手术都能在如此理想的条件下进行。在评估热损伤风险时，必须探索高温可能达到的极限值。

肾脏的血流量占全身循环总量的约20%[18]。可以合理推测，仅通过血管灌注作用就能缓解激光激活引发的温度升高。在射频消融术中已观察到冷却效应，其中灌注介导的组织冷却作用可减少肿瘤消融过程中的凝固性坏死[19]。然而，肾脏的动态变化比简化版的热扩散与传导方程更为复杂，这主要源于器官内部血液供应分布的不均匀性[20]。

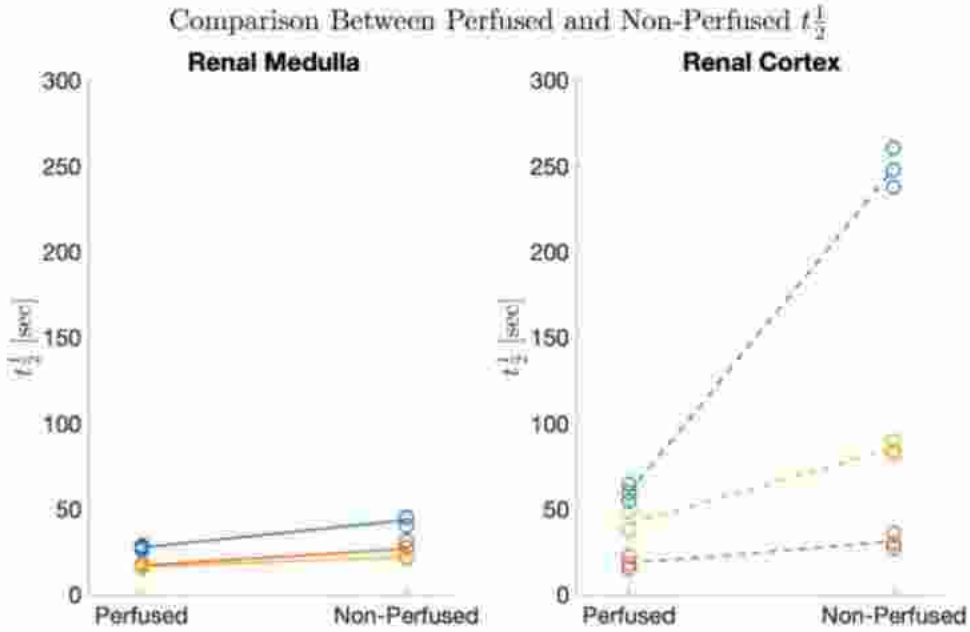


图3血液灌注与非灌注试验的温度衰减（$t_{½}$）对比，不同颜色代表不同受试者。左图显示延髓，右图显示大脑皮层

在本研究的第二阶段，我们对每只接受安乐死处理的猪只进行了三次额外实验，这些实验均未进行血管灌注。不出所料，未灌注组的体温衰减时间（$t_{½}$）明显长于灌注组。但值得注意的是，皮层区域未灌注与灌注组的$t_{½}$比值差异大于脊髓区域。这表明皮层的血管散热效应比脊髓更为显著。由此可以推断，肾脏的脊髓区域比皮层更容易受到热损伤。

本研究存在若干局限性。首先，采用间距10毫米的MTS针头搭配热传感器时，仅有两个传感器能定位在肾实质内。其次，实验仅使用单根针头。因此，尽管本研究证实了激光激活区域邻近肾盏的肾脏组织确实存在热损伤风险，但未能对整个肾实质进行全面的热学评估。

其次，关于灌注在热缓解中的作用评估——特别是对流对热扩散的贡献——仅以比较方式展开，未对灌注进行定量分析。这一点需要特别注意，因为在激光激活期间，肾内压力与激光激活本身可能引发的温度变化共同作用，可能导致血流快速变化。不过，我们的研究提供了证据表明：在输尿管镜检查过程中，肾髓质存在热损伤风险，其灌注水平较肾皮质更低。

未来研究将重点开展肾脏激光激活过程中的热成像分析，通过提升采样频率和空间分辨率，建立数学模型，将采集系统液体中的热剂量与肾脏不同区域的热损伤风险相关联。

结论

高功率激光（40瓦）配合较低的冲洗速率，可能在猪体内模型中引发损伤性温度，尤其在靠近收集系统的髓质区域。此外，血管灌注对缓解该敏感区域热风险的作用似乎有限。

作者贡献R Marom：项目开发、数据收集、论文撰写、数据分析。WW Roberts：论文撰写/编辑、数据分析、批判性修订、研究管理。JJ Dau：论文编辑。KR Ghani：论文编辑。TL Hall：论文编辑。

资金本研究的部分资金由密歇根大学泌尿外科系的Faculty Catalyst Award提供，部分资金由Boston Scientific的研究资助提供。

数据可用性本研究期间生成和/或分析的数据集，可向通讯作者提出合理请求获取。

声明

利益冲突：K.R.G.与Boston Scientific、Ambu、Olympus、Coloplast和Karl Storz有咨询关系。W.W.R.与Boston Scientific有咨询关系。R.M.、J.J.D.和T.L.H.没有披露。

伦理审批本研究中涉及动物受试者的所有程序均符合机构研究委员会的伦理标准，并获得了密歇根大学机构动物护理和使用委员会（IACUC）的批准。

免责声明本研究中使用的输尿管镜原型是概念器械/技术，研究进行时未上市。临床前研究结果不一定能反映临床性能。

参考文献

1. Aldoukhi AH，Roberts WW，Hall TL等人（2017）钬激光碎石术在新石器时代：尘埃还是失败？《外科前沿》4：57
2. Pietropaolo A，Mani M，Hughes T等（2022）低功率与高功率激光治疗下极结石的对比：某大学附属教学医院的前瞻性非随机研究结果。Ther Adv Urol 14：17562872221097344
3. 阿尔杜基AH、加尼KR、霍尔TL等人（2017）高功率钬激光碎石术的热反应。《泌尿外科学杂志》31（12）：1308–1312
4. Aldoukhi AH，Hall TL，Ghani KR等学者（2018）在猪体内模型中研究了高功率钬激光碎石术期间的肾盂肾盏液温。《泌尿外科学杂志》32(8)：724–729
5. 海因S、佩措尔德R、舍恩塔勒M等（2018）《钬：钇铝石榴石激光碎石术的热效应：体外模型实时评估》。《世界泌尿学杂志》36(9)：1469–1475
6. 麦克斯韦AD、麦克康纳吉B、哈珀JD等（2019）《尿路激光碎石术致热效应的模拟研究》。《泌尿外科学杂志》33(2)：113–119
7. Wollin DA，Carlos EC，Tom WR等（2018）激光参数与冲洗速率对钬激光碎石术中输尿管温度的影响（体外模型）。《泌尿内镜杂志》32(1)：59–63
8. 海因S、佩措尔德R、苏亚雷斯-伊巴罗拉R等（2020）在离体猪肾模型中研究了逆行肾内手术与经皮肾镜碎石术期间Ho：YAG激光碎石术的热效应。《世界泌尿学杂志》38(3)：753–760
9. Marom R，Dau JJ，Hall TL等（2023）输尿管镜检查过程中激光功率和冲洗速率的热安全边界：Ho：YAG激光的活体猪评估。《泌尿外科》。https://doi.org/10.1016/j.urology.2023.07.014
10. 王旭科，蒋志清，谭军等（2019）输尿管镜下钬激光碎石术的热效应研究。《中华医学杂志》132（16）：2004–2007
11. 美国食品药品监督管理局（FDA）。奥林巴斯公司2类器械召回，2021。https://www.accessdata.fda.gov/scripts/cdrh/cfdocs/cfres/res.cfm?id=188172。2023年7月3日访问。

12. 奥赫诺夫·Z、姜·P、阿蒂尤尼·AS等（2021）《买者自慎：热能持续激活——猪肾脏在除尘与碎石模式下钬光纤激光器温度变化的体内评估》。《泌尿外科学杂志》35（11）：1716–1722
13. Marom R，Dau JJ，Hall TL等人（2023）在输尿管结石形成过程中不同冲洗速率下流出阻力对肾内压力的影响：体内评估。《泌尿系统结石》5(1)：98
14. 萨姆雷托·SA，杜威·WC（1984）癌症治疗中的热剂量测定。《国际放射肿瘤学、生物学与物理学杂志》第10卷第6期：787–800
15. 亚尔莫连科PS、穆恩EJ、兰登C等（2011）正常组织热损伤阈值：最新进展。《国际热疗杂志》27(4)：320–343
16. 阿尔杜基AH、道JJ、马吉达兰尼SE等（2021）输尿管镜碎石术中激光激活模式：对盲状体液体温度及热剂量的影响。《泌尿外科学杂志》35(8)：1217–1222
17. Louters MM，Dau JJ，Hall TL等（2022）《激光操作员工作周期对温度和热剂量的影响：体外研究》。《世界泌尿学杂志》40(6)：1575–1580
18. Dalal R，Bruss ZS，Sehdev JS（2022）《生理学，肾血流与滤过》.StatPearls出版社，佛罗里达州
19. 戈德堡SN，哈恩PF，田边KK等（1998）经皮射频组织消融术：靶注介导的组织冷却是否限制凝固性坏死？《血管介入放射学杂志》第9卷第1期增刊1):101–111
20. Pallone TL，Edwards A，Mattson DL（2012）肾髓质循环.Compr Physiol 2(1)：97–140

出版商注Springer Nature对已发表地图和机构隶属关系的司法管辖权主张保持中立。

Springer Nature或其授权方（例如学会或其他合作伙伴）根据与作者或其他权利持有人签订的出版协议，对本文拥有独家权利；作者对本文已接受的稿件版本进行自我存档，完全受该出版协议条款和适用法律的约束。

International Urology and Nephrology (2024) 56:2539–2545
https://doi.org/10.1007/s11255-024-03943-8

UROLOGY - ORIGINAL PAPER

Comparison of temperature and renal tissue thermal damage by holmium laser with different energy parameters during lithotripsy: in vitro porcine kidney model

Wei Wei[1] · Ming Chen[2] · Le Xie[3] · Yuan Mai[1] · Huacai Zhu[1] · Zhanping Xu[1]

Received: 8 November 2023 / Accepted: 31 December 2023 / Published online: 14 March 2024
© The Author(s), under exclusive licence to Springer Nature B.V. 2024

Abstract

Objective Holmium laser percutaneous nephrolithotripsy was simulated by porcine kidney calculus model in vitro to investigate thermal damage of renal tissue by different energy parameters of the holmium laser.

Methods We placed human kidney calculus specimen in fresh vitro porcine kidney, then insert thermocouple temperature probes into the submucosa of the renal pelvis and reheated in a 37 °C water bath. A percutaneous nephrological sheath was used to penetrate the renal parenchyma with a moderate irrigation rate of 30 ml/min at 18 ℃. The Holmium laser was used to fragment the stones under a nephroscope, and the temperature was recorded.

Results The four independent models were lithotripsy with 30 W and 60 W laser for 5 and 10 min, respectively; the mean temperature of 30 W vs. 60 W within 5 min was 36.06 °C vs. 39.21 °C ($t=5.36$, $P<0.01$) and the highest temperature was 43.60 °C vs. 46.60 °C; the mean temperature of 30 W vs. 60 W within 10 min was 37.91 °C vs. 40.13 ℃ ($t=5.28$, $P<0.01$), maximum temperature 46.80 ℃ vs. 49.20 ℃. Pathologically, each kidney was observed to have different degrees of thermal damage lesions, and the higher power and longer time the more severe the injury, but the injury was mainly limited to the uroepithelial and subepithelial tissues, with rare damage to renal tubules.

Conclusion The higher laser excitation power and longer duration raised the intrarenal temperature significantly and caused a certain degree of thermal damage to the kidney tissue, but overall it was found to be safe and reliable. Urologists can avoid further side effects through surgical expertise.

Keywords Holmium laser · Lithotripsy · Thermal damage · Intrarenal temperature

Background

The incidence of urinary calculus is gradually increasing worldwide, and in some cases, complex calculus require surgical intervention. With the continuous development of minimally invasive surgery, the treatment of upper urinary tract stones has shifted from open surgery to endoluminal surgery. Percutaneous nephrolithotomy (PCNL) and flexible ureteroscopy (FURS) are widely performed in clinical practice due to their less invasive nature, precise efficacy, and maturity of application [1]. The advancement of lithotripsy energy output modalities has also contributed to the progress of minimally invasive surgery. Since the 1980s, lasers have been officially used in medicine, and the unique physical effect of the holmium laser on human calculus makes it highly efficient for lithotripsy. Although it has been shown that the thulium fiber laser is not inferior for this purpose, the holmium laser remains a state-of-the-art device for endoscopic lithotripsy [2]. The holmium laser is the most commonly used laser in urology surgery due to its outstanding advantages, with approximately 95% of its energy absorbed by the surrounding 5 mm water medium and good directivity [3].

✉ Zhanping Xu
xuzhanping2004@163.com

1 Department of Urology, Foshan Hospital of Traditional Chinese Medicine, Guangzhou University of Chinese Medicine, Foshan, Guangdong, China

2 Department of Urology, The First Affiliated Hospital of Guangzhou University of Chinese Medicine, Guangzhou, Guangdong, China

3 Department of Pathology, Foshan Hospital of Traditional Chinese Medicine, Guangzhou University of Chinese Medicine, Foshan, Guangdong, China

However, despite the increasing popularity of the holmium laser, we have observed that patients undergoing holmium laser lithotripsy exhibit a higher frequency of complications such as ureteral and pelvic stenosis adhesions or even impaired renal function [4]. Most previous thermal studies on the holmium laser did not consider the absorption of laser energy by calculus or discuss tissue pathological changes in depth. Therefore, our study aimed to simulate reality with a more detailed experiment.

Materials and methods

Experimental model

Kidney model

Fresh porcine kidney models were obtained directly from a meat plant and stored in frozen transit at − 4 to 0 °C. The kidneys were used for the study within one hour of isolation. Porcine kidney morphology and size were basically the same, no other lesions, perirenal fat, envelope were trimmed and cleaned before the experiment operating.

Calculus

The human urinary calculus used in this study underwent harmless treatment and compositional analysis. The primary components of these calculus are calcium oxalate dihydrate and calcium oxalate pentahydrate, which are the most prevalent types. The calculus were surgically extracted from the kidney or ureter, and patients provided informed consent for the use of their calculus specimens in this research. The calculus were then reduced and polished to a size of approximately 2–2.5 cm and inserted into the incision made in the porcine renal pelvis. Subsequently, the assembly system was sutured using silk thread (Fig. 1).

Equipment

The equipment included holmium laser lithotripsy system (HZ Series, Potent Optoelectronics, China), endoscopic monitoring system (Richard Wolf, Germany), nephroscope (F9.5, Richard Wolf, Germany), renal puncture sheath (F20, Veili Medical, China), thermostatic water bath system (HH420, YuNuo Instrument, China), thermocouple thermometer and probe (TA612 Series, Suzhou TASI Electronics, China), lavage pump (Fig. 2).

Procedure

1. A fresh vitro porcine kidney combined with a urinary calculus model was prepared. Two thermocouple temperature probes were inserted into the kidney tissue in the proposed lithotripsy area, with a probe phase distance of 1 cm. The probes were positioned as close as possible to the urothelial layer of the collecting system, approximately 5 mm away from the epithelial tissue, ensuring avoidance of penetration into the renal pelvis cavity.
2. The porcine kidneys were rewarmed in a 37 ℃ thermostatic saline bath. The experiment was started by monitoring the kidney temperature until it reached 37 ℃. The renal pelvis was punctured with an F20 nephroscopic sheath, and the nephroscope combined with a holmium laser was used to smash the stones in the kidney. Machine-controlled continuous saline irrigation was used at a uniform moderate rate of 30 ml/min and an irrigation fluid temperature of 18 °C (room temperature). Following urologists' surgical habits, the holmium laser was activated in a trial by the same surgeon for 20–25 s per continuous relay with a 5 s pause. The urologist who conducted the trial was surgically experienced, with more than 10 years of experience in the specialty, and performed approximately 200 laser lithotripsy procedures per year.
3. Experimental groups: The study was divided into four groups with different laser parameters: Group A setting 30 W (2 J, 15 Hz), for 5 min; Group B setting 60 W (3 J, 20 Hz), 5 min; Group C setting 30 W (1 J, 30 Hz), 10 min; Group D setting 60 W (2 J, 30 Hz), 10 min.
4. Once the allotted time for each group was reached, lithotripsy was discontinued, and the kidney was dissected to visually assess histopathological changes within the lithotripsy area. Tissue samples from potential thermal damage sites were collected and preserved in formalin. Microscopic examination of the prepared tissue sections was subsequently conducted to observe any pathological alterations.

Data statistics

Temperature recording software was provided by TASI, Inc, with a recording interval of 5 s. Two probe temperature data within the same kidney model were recorded by taking the average value after data export. All data were imported into Microsoft Excel and SPSS 22.0 to produce graphs. The mean temperature of each group was compared, and the difference was examined by t test, the calibration level $\alpha = 0.05$.

Results

In each group, two kidney models were employed for two independent trials. The maximum temperature for Group A in two trials was 43.60 ℃., the mean temperature was



Fig. 1 Porcine kidney with calculus model

36.01 ℃ and 36.10 ℃. While the maximum temperature of Group B was 46.60 ℃, the mean temperature was 39.39 ℃ and 39.02 ℃. The temperature profiles of Group A and B are shown in Fig 3a, b. After data consolidation, the mean temperature in Group B was higher than in Group A(39.21 °C vs. 36.06 °C, $t = 5.36$, $P = 0.00$), and the heat generated by the 60 W laser during the 5 minute laser lithotripsy had a greater effect on the increased kidney temperature.

A comparison was made between Group C, where Holmium laser excitation was performed for 10 min, and Group D. The maximum temperature of Group C was 46.8 °C with mean temperatures of 37.56 °C and 38.25 °C in both trials. While the maximum temperature of Group D was 49.2 °C with mean temperatures of 40.08 °C and 40.18 °C, respectively (Fig. 3c, d). Group D, with 60 W laser for 10 min, when compared to Group C (30 W), had more significant elevation of renal parenchymal temperature and may have caused thermal damage to the tissue (40.13 °C vs. 37.91 °C, $t = 5.28$, $P = 0.00$).

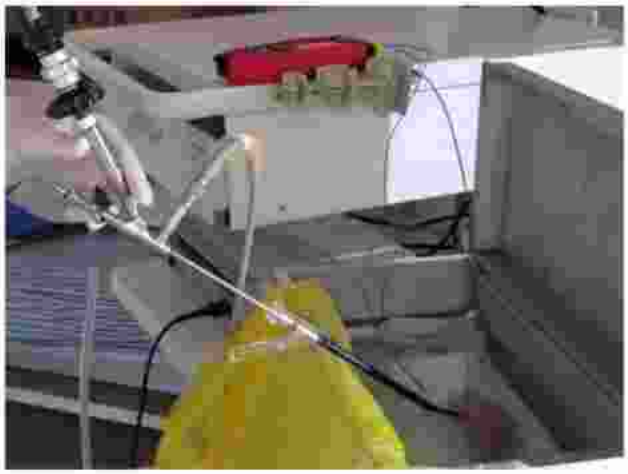


Fig. 2 Equipment and procedure

We dissected each kidney after laser excitation. For each kidney we took 3–5 pieces of tissue for pathological observation, near the thermocouple probe. Mild to moderate thermal damage was more common in Group A and C. Microscopically, the mucosal epithelium of the renal pelvis was detached from the underlying tissue to varying degrees, with some of the superficial umbrella cells only missing and some of the whole layer missing, exposing the bare basement membrane and edema of the mucosal lamina propria (Fig. 4a, b). More severe thermal damage was seen in specimens from groups B and D. The mucosal epithelium was degenerated and detached, with edema of the lamina propria and varying degrees of degeneration and necrosis of the mucosal muscle, myocytes and collagen fibers of the outer membrane (Fig. 4c). We classified the damage in the 53 pathological sections produced, defining 19 sections with severe thermal damage, 2 in Group A, 4 in Group B, 5 in Group C, and 8 in Group D; 24 sections with moderate thermal damage, 8 in Group A, 6 in Group B, 6 in Group C and 4 in Droup D, respectively; and 10 sections with mild damage, 3 in Group A, 3 in Group B, 2 in Group C and 2 in Group D. Ranking the proportion of severe thermal injuries from highest to lowest, we had Group D at 57.1%, Group C at 38.5%, Group B at 30.8%, and Group A at 15.4%.

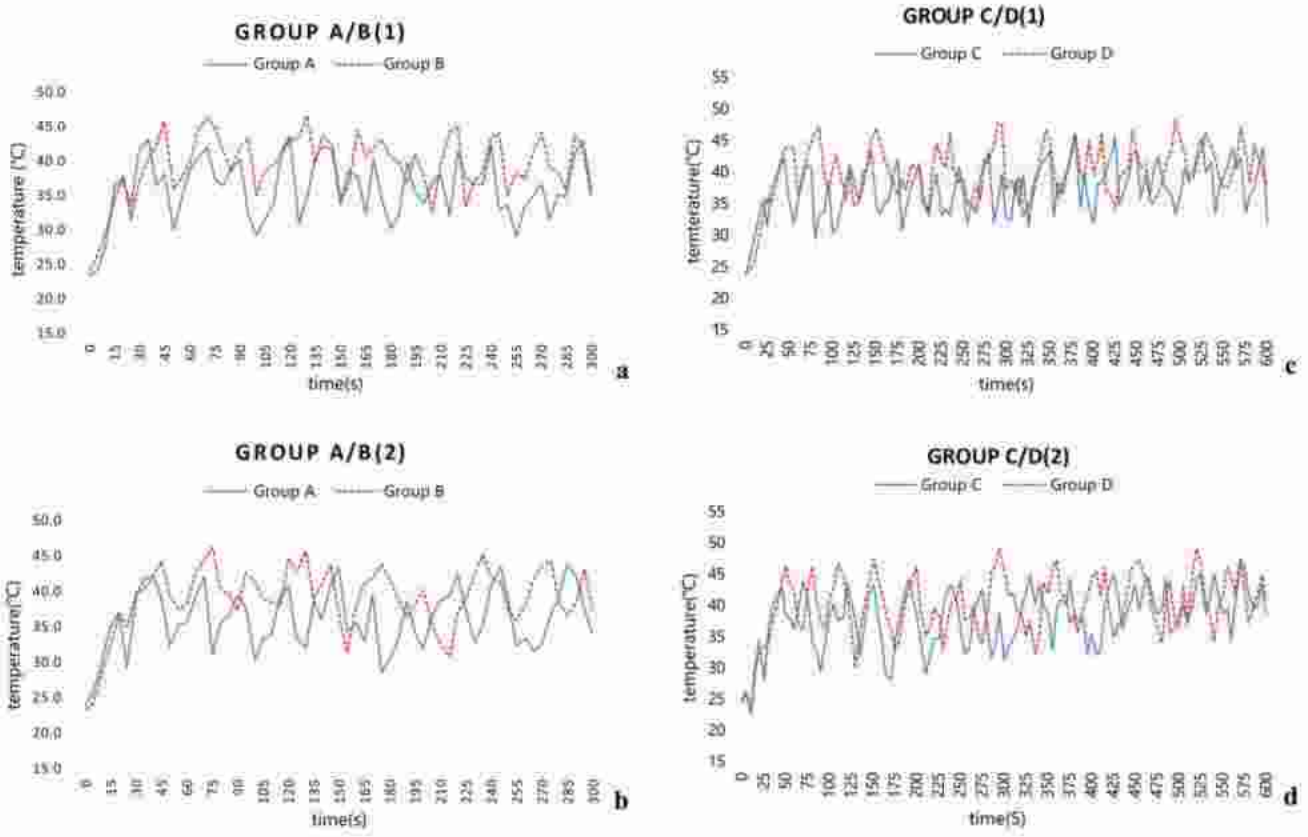


Fig. 3 Temperature profiles of different laser energy parameters. **a** Group A/B 1st trail. **b** Group A/B 2nd trail. **c** Group C/D 1st trail. **d** Group C/D 2nd trail

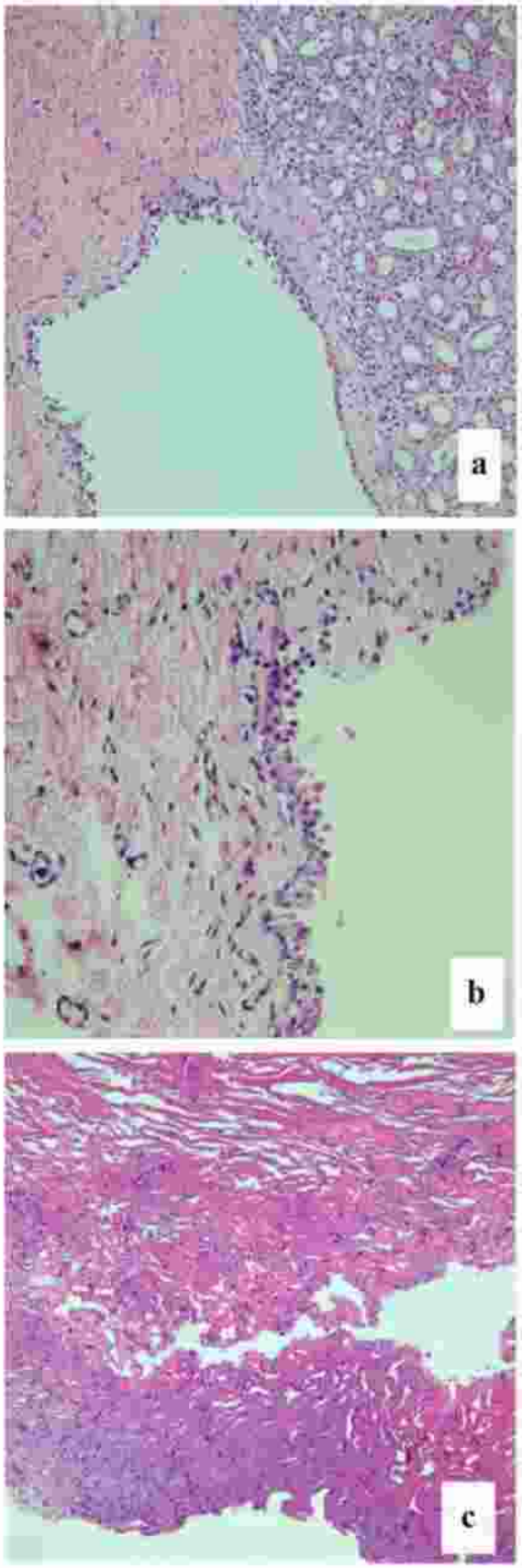


Fig. 4 Pathological pictures of thermal damage renal tissue. **a** Mild. **b** Moderate. **c** Severe

Discussion

Holmium laser lithotripsy has emerged as the preferred treatment modality for urolithiasis. However, most of the previous experiments on isolated animal organs or equipment were only for the purpose of observing temperature changes, and less attention was paid to actual histopathological damage [5]. In vivo animal experiments fully consider the influence of blood flow on temperature changes, and the monitored temperature is closer to reality [6]. However, creating a urinary calculus model in vivo animals is very difficult, and the accuracy of temperature monitoring is not as good as that in vitro. Moreover, model consistency and sample size are both major challenges to controlling bias. Our study innovatively integrates the advantages of in vitro and in vivo experiments, especially in the production of calculus models and pathological observation, which better simulates the actual situation compared with previous studies.

Holmium laser primarily relies on the photothermal mechanism of lithotripsy, where the aqueous medium at the tip of the transmitting fiber absorbs energy and undergoes rapid vaporization to form microbubbles [7]. However, not all of the energy is absorbed by the water and transmitted to the target stone. This laser-emitted energy that does not reach the stone can spill out, elevating intrarenal temperature, damaging the urinary epithelium, and possibly creating complications [8]. Direct impact of laser energy on the flushing fluid is less likely to occur in real procedures. Therefore, we included human calculus samples in our study.

The water flow rate is one of the most important factors affecting the temperature during lithotripsy [8]. A higher water flow rate can significantly lower intrarenal temperature; however, it also leads to increased intrarenal pressure, thereby augmenting the risk of infection. Several studies have pointed out that the water flow rate, the risk is higher, and the temperature after 10 and 60 s of laser activation did not exceed 38.5 °C at a rinse fluid flow rate of 40 mL/min, regardless of the laser configuration [9]. Actual operations encompass intricate factors, including bleeding and infection. To ensure operational safety, urologists often adjust the flow rate to its lowest value, ensuring a clear visual field through the nephroscope's water valve, thus rendering quantification of flow velocity challenging. Hence, we standardized the ideal perfusion flow rate at 30 mL/min. We employ constant pressure pump irrigation without considering factors like lithotripsy discharge and optimal field of view clarity, eliminating the need for manual adjustment of the nephroscope's water valve. Aligned with our surgical practice, the laser was activated for approximately 25 s,

paused for 5 s to enable efficient cooling of the kidney by the irrigation fluid, thus explaining the peaks and valleys observed in our temperature profile.

The proportion of laser energy reaching the stone can be used to estimate the efficiency of laser lithotripsy. An in vitro study reported that 52% of the emitted pulses reached the stone when using a frequency of 20 Hz; when using a frequency of 50 Hz, only 23% reached the target, and at 80 Hz only 4% [10]. It seems that the frequency of laser and lithotripsy efficiency is inversely proportional at a constant power level. Thus, we used different frequency settings in groups A and C with a laser power of 30 W, 15 Hz in Group A vs. 30 Hz in Group C. During the first 5min of intermittent excitation, no significant difference in mean temperature (36.06 ℃ vs. 36.36 ℃, $t=0.52$, $P>0.05$). Similarly, in groups B and D with laser power of 60W set at frequencies of 20 Hz and 30 Hz, the mean temperatures were almost the same (39.21 ℃ vs. 39.27 ℃, $t=0.09$, $P>0.05$). We believe that under sufficient lavage and good laser excitation habit, the residual energy has minimal impact on the renal temperature.

A comparative study of high-power vs. low-power laser lithotripsy showed significantly shorter procedure times but higher joules/mm^3 values for high-power lasers [11]. In another laboratory study simulating the renal calyx, the authors investigated the use of different energies and frequencies to measure the temperature of the medium at various irrigation flows. They found that the higher the delivered energy, the greater the increase in fluid temperature, reaching 50 °C and 70 °C in 10 s and 60 s, respectively, without irrigation [9]. However, most experiments still did not include the calculus factor.

We observed that as the power increased, the energy spillover grew greater, and the intrarenal temperature rose higher and faster, obviously. But the exponential increase in power does not result in a significant increase in temperature. Instead, the higher power may lead to increased lithotripsy efficiency and a decrease in operative time, ultimately translating to a lower risk of bleeding and infection. Although a recent meta-analysis showed no evidence of an advantage of higher power lasers over lower power lasers in terms of shorter operative times when dealing with same volume calculus [12], this is strongly correlated with the fact that calculus composition varies in different populations. Therefore, the surgeon must fully evaluate the mutual advantages and disadvantages of laser thermal damage and procedure time within the context of the actual situation, such as the patient's calculus location, load and infection status.

Thermal damage to tissues depends on the temperature reach and its ability to be sustained over time (thermal dose), which it was showed that tissue and cellular damage occurs at 43 °C and maintain 240 min [13]. A human body temperature exceeding 42 °C can causes substantial cellular damage, when the local temperature is > 45 °C, there will be damage to tissue, and when the local temperature is > 60 °C, the tissue proteins are thermally coagulated and denatured and irreversible damage occurs [14]. In a study, rabbit kidneys were placed in a closed container and subjected to holmium laser excitation, and there was an increase in water temperature and rabbit kidney tissue damage for a certain period of time, but it did not have the conditions of flowing water flushing and energy absorption by stones also [15]. Our results the submucosal mean temperature did not exceed 40 °C during the trail in all groups; the highest temperature was observed in Group D (60 W), at 49.2 °C. In each group, there were periods during which the temperature exceeded 42 °C, but thanks to the intermittent laser excitation and constant-rate irrigation as in human surgery, the high-temperature periods were relatively brief, lasting only about 20 s, and the temperature dropped back quickly after the pause in laser excitation.

After completely recording the temperature data for each individual model, the porcine kidney was promptly handed over to an assistant for dissection. Different degrees of thermal damage lesions were observed visually within each renal parenchyma, as the laser excitation time was longer and the number of lesions was higher in Groups C and D. We mainly excised the tissues near the temperature probe for pathological analysis. It was found in the specimen sections that Group D had the most serious lesions. The number of pathological section with serious urothelium thermal damage accounted for 57.1%, while Group A, the least, was only 15.4%. Thus, we can judge that the higher power and longer Holmium laser excitation caused more thermal damage to the kidney urothelium tissues. At the same time, we also observed very limited degenerative necrosis of the submucosal tissue glomeruli and tubules at the injury site (< 25%, mild) from all sections. Notably, despite Groups B and C having similar maximum temperatures, Group C had a lower mean temperature and a higher percentage of severe thermal injuries.We believe that tissue injury is not only caused by transient high temperatures but is also influenced by the duration of exposure to those temperatures. Evidently, renal tissue in Group C remained within the damaging temperature range for a longer duration.

However, the study has some limitations. Although only two kidney models were used per group, their temperature characteristics were largely consistent within each group. This suggests that the experiments are reproducible and the experimental data is scientifically reliable. Because of the isolated organ experiment, we could not simulate the effect of blood flow on the renal temperature. In vivo conditions, actual renal temperatures may be lower due to blood flow's regulatory effects. The thermal damage observed in our study represents a short-term complication; however, ex vivo organ experiments cannot provide insights into long-term

consequences, which must be observed in real-world clinical settings.

Conclusion

In conclusion, various energy parameter configurations of holmium laser during PCNL result in differing degrees of thermal damage to the kidney. Higher laser power and longer time for a certain irrigation speed lead to higher intrarenal temperature and more tissue damage, but the effect of rapid and high-power excitation on intrarenal temperature is not a concern. Moderate irrigation and intermittent laser excitation habits are very good at avoiding excessive elevation of intrarenal temperature. Little damage to the renal tubules from heat was observed in vitro experiment, with effects mostly limited to the renal mucosa and subepithelium. Overall, under various parameter settings, holmium laser applications for lithotripsy are generally safe and reliable. Urologists can confidently rely on their surgical expertise to minimize any additional side effects.

Author contributions WW: project development, data management, manuscript writing. ZX: project development, manuscript writing. MC: data management, manuscript editing. LX: data collection, pathological observation. YM: data collection. HZ: data collection.

Funding Foshan Health Commission Medical Research Project (Guangdong, China). No. 20220331.

Data availability All relevant data are within the paper. The original data are available from the corresponding author on reasonable request.

Declarations

Conflict of interest The authors declared no potential conflict of interest with respect to the research, author-ship, and publication of this manuscript.

Ethical approval Medical Ethics Committee of Foshan Hospital of Traditional Chinese Medicine. IRB No. 2021138.

Informed consent The experimental calculus was surgically removed from human. Patients signed informed consent for the calculus to be used in this study.

Approval of the research protocol by an institutional reviewer board Foshan Health Commission Medical Research Project (China).

Registry and the registration no. of the study/trial N/A.

Animal studies N/A.

References

1. Tok A, Akbulut F, Buldu I et al (2016) Comparison of microperc and minipercutaneous nephrolithotomy for medium-sized lower calyx stones. Urolithiasis 44(2):155–159
2. Enikeev D, Herrmann TRW et al (2023) Thulium fiber laser in endourology: current clinical evidence. Curr Opin Urol 33(2):95–107. https://doi.org/10.1097/MOU.0000000000001057
3. Skolarikos A, Jung HU, Somani, B et al (2022) Guidelines Urolithiasis. In: EAU Guidelines Office: Arnhem, The Netherlands ISBN 978-94-92671-16-5
4. Dong H, Peng Y, Li L, Gao X et al (2018) Prevention strategies for ureteral stricture following ureteroscopic lithotripsy. Asian J Urol 5(2):94–100
5. Gallegos H, Bravo JC et al (2021) Intrarenal temperature measurement associated with holmium laser intracorporeal lithotripsy in an ex vivo model. Cent Eur J Urol 74(4):588–594. https://doi.org/10.5173/ceju.2021.0092
6. Simon H, Ralf P et al (2020) Thermal effects of Ho:YAG laser lithotripsy during retrograde intrarenal surgery and percutaneous nephrolithotomy in an ex vivo porcine kidney model. World J Urol 38(3):753–760. https://doi.org/10.1007/s00345-019-02808-5. (**Epub 2019 May 16**)
7. Cecchetti W, Zattoni F, Nigro F et al (2004) Plasma bubble formation induced by holmium laser: an in vitro study [J]. Urology 63(3):586–590
8. Felipe P, Eugenio V et al (2022) A practical guide for intra-renal temperature and pressure management during RIRS: what is the evidence telling us. J Clin Med 11(12):3429. https://doi.org/10.3390/jcm11123429
9. Aldoukhi AH, Ghani KR, Hall TL et al (2017) Thermal response to high-power holmium laser lithotripsy. J Endourol 31:1308–1312
10. Aldoukhi A, Hall T, Ghani K et al (2020) Analysis of laser fiber to stone distance during different modes of laser lithotripsy. J Urol 203:e626
11. Mekayten M, Lorber A, Katafigiotis I et al (2019) Will stone density stop being a key factor in endourology? the impact of stone density on laser time using lumenis laser p120 w and standard 20 w laser—a comparative study. J Endourol 33:585–589
12. Ventimiglia E, Panchard F, Quadrini F et al (2021) High- and low-power laser lithotripsy achieve similar results: a systematic review and meta-analysis of available clinical series. J Endourol 35:1146–1152
13. Sapareto SA, Dewey WC (1984) Thermal dose determination in cancer therapy. Int J Radiat Oncol Biol Phys 10:787–800
14. Izzard AS, Rizzoni D et al (2005) Small artery structure and hypertension: adaptive changes and target organ damage. J Hypertens 23(2):247–250
15. Molina WR, Silva IN, Donalisio da Silva R et al (2015) Influence of saline on temperature profile of laser lithotripsy activation. J Endourol 29(2):235–239

Publisher's Note Springer Nature remains neutral with regard to jurisdictional claims in published maps and institutional affiliations.

Springer Nature or its licensor (e.g. a society or other partner) holds exclusive rights to this article under a publishing agreement with the author(s) or other rightsholder(s); author self-archiving of the accepted manuscript version of this article is solely governed by the terms of such publishing agreement and applicable law.

国际泌尿与肾脏病学（2024）56：2539–2545
https://doi.org/10.1007/s11255-024-03943-8

泌尿外科-原始论文

温度与肾组织热损伤的比较在碎石术过程中采用不同能量参数的钬激光：猪肾体外模型

魏巍[1]·明陈[2]·莱谢[3]·元迈[1]·舒华才[1]·徐晨平[1]

接收日期：2023年11月8日/接受日期：2023年12月31日/网络发表日期：2024年3月14日
©作者（们），经Springer Nature B.V.独家授权，2024年

摘要

目的本研究通过猪肾结石模型体外模拟钬激光经皮肾结石碎石术，以进行研究利用钬激光的不同能量参数，有效抑制肾脏组织的热损伤。

方法将人肾结石标本置于新鲜猪肾组织中，随后插入热电偶进行温度监测。将探针插入肾盂黏膜下层，并在37°C的水浴中重新加热。使用经皮肾鞘以中等灌注速率30 ml/min在18**℃**下渗透肾实质。采用钬激光在肾镜下碎石，并记录温度。

结果四个独立模型分别为：使用30瓦和60瓦激光分别进行5分钟和10分钟的碎石术；平均30W与60W组5分钟内的温度分别为36.06**℃**与39.21**℃**（t=5.36，P<0.01），最高温度分别为43.60℃与46.60℃；10分钟内的平均温度分别为37.91℃与40.13℃（t=5.28，P<0.01），最高温度分别为46.80℃与49.20℃。病理观察发现，每只肾脏均存在不同程度的热损伤病变，功率越高、时间越长损伤越严重，但损伤主要局限于尿路上皮和上皮下组织，肾小管损伤罕见。

结论激光能量功率越高、作用时间越长，肾内温度升高越显著、导致虽然对肾脏组织造成一定程度的热损伤，但总体上被证明是安全可靠的。泌尿科医生可通过手术技术避免进一步的副作用。

关键词钬激光·碎石术·热损伤·肾内温度

背景

全球尿路结石发病率持续攀升，部分复杂病例需通过手术治疗。随着微创手术技术的不断进步，上尿路结石的治疗方案碎石技术已从开放手术转向内镜手术。经皮肾镜碎石术（PCNL）和输尿管软镜术（FURS）因其微创特性、精准疗效及成熟应用，在临床实践中得到广泛应用[1]。碎石能量输出模式的进步也推动了微创手术的发展。自20世纪80年代起，激光技术正式应用于医学领域，钬激光对结石的独特物理作用使其在碎石术中表现出色。尽管铥光纤激光在该领域已证明不逊色，但钬激光仍是内镜碎石术的顶尖设备[2]。由于其显著优势——约95%的能量可被周围5毫米水介质吸收且具有良好定向性[3]，钬激光成为泌尿外科手术中最常用的激光设备。

✉ 徐晨平
xuzhanping2004@163.com

1 广州中医药大学佛山中医医院泌尿外科，中国广东省佛山市

2 中国广东省广州市中医药大学第一附属医院泌尿外科

3 广东省佛山市中医院病理学部，广州中医药大学，中国

然而，尽管钬激光的普及率持续攀升，但我们观察到接受钬激光碎石术的患者并发症发生率更高，例如输尿管狭窄、盆腔粘连甚至肾功能受损[4]。以往大多数关于钬激光的热效应研究，既未考虑结石对激光能量的吸收效应，也未深入探讨组织病理学变化。因此，本研究旨在通过更精细的实验设计，还原临床真实场景。

材料和方法

实验模型

肾脏模型

新鲜猪肾样本直接从肉类加工厂获取，经冷冻运输后保存于-4至0℃的低温环境中。样本在分离后一小时内即用于实验。所有猪肾的形态与尺寸基本一致，实验前已去除肾周脂肪及包膜等组织，并进行彻底清洁。

微积分

本研究采用的人体尿路结石样本均经过无害化处理并完成成分分析。这些结石主要由草酸钙二水合物和草酸钙五水合物构成，属于最常见的类型。研究人员通过手术方式从患者肾脏或输尿管中取出结石样本，并获得患者对其样本用于本研究的知情同意。随后将结石研磨抛光至约2-2.5厘米大小，置入猪肾盂切口处。最后使用丝线缝合组装系统（图1）。

设备

设备包括钬激光碎石系统（HZ系列，Potent Optoelectronics，中国）、内窥镜监护系统（Richard Wolf，德国）、肾镜（F9.5，Richard Wolf，德国）、肾穿刺鞘（F 20，Veili Medical，中国）、恒温水浴系统（HH420，YuNuo Instrument，中国）、热电偶温度计和探头（TA 612系列，Suzhou TASI Electronics，中国）、冲洗泵（图2）。

操作步骤

1. 研究人员制备了新鲜的体外培养猪肾，并结合尿路结石模型进行研究。两个热电偶tem-

将温度探头插入肾脏组织的碎石术预定区域，探头与组织表面保持1厘米间距。探头尽可能靠近集合系统的尿路上皮层，与上皮组织保持约5毫米距离，确保探头不会穿透至肾盂腔。

2. 将猪肾脏置于37℃恒温盐水浴中复温。实验开始时监测肾脏温度，直至达到
37 ℃。使用F20肾镜鞘管穿刺肾盂后，通过结合钬激光的肾镜对肾脏结石进行碎石。采用机器控制的连续盐水灌洗，以30毫升/分钟的均匀中等流速进行，灌洗液温度为18℃（室温）。根据泌尿外科医生的手术习惯，同一位外科医生在试验中以20-25秒的连续循环配合5秒暂停的方式激活钬激光。进行试验的泌尿外科医生具有丰富的手术经验，拥有超过10年的专业领域经验，每年完成约200例激光碎石手术。
3. 实验分组：本研究将受试者分为四组，各组采用不同激光参数设置，其中A组为初始参数组。
30 A组：2焦耳（15赫兹）功率，持续5分钟；B组：60焦耳（20赫兹）功率，持续5分钟；C组：30焦耳（30赫兹）功率，持续10分钟；D组：60焦耳（30赫兹）功率，持续10分钟。
4. 当各组完成规定时间后，立即停止碎石术，对肾脏进行解剖以直观观察碎石区域的组织病理学变化。随后采集可能受热损伤部位的组织样本，并用福尔马林保存。最后对制备好的组织切片进行显微镜检查，以观察是否存在病理改变。

数据统计

温度记录软件由TASI公司提供，记录间隔为5秒。通过数据导出后取平均值，记录了同一肾脏模型内的两个探头温度数据。所有数据均导入Microsoft Excel和SPSS 22.0以生成图表。比较了各组的平均温度，并通过*t*检验检验差异，校准水平 α=0.05。

结果

每组采用两种肾脏模型进行两次独立试验。A组在两次试验中的最高温度为43.60℃，平均温度为



图1带结石的猪肾脏模型

36.01 ℃和36.10℃。B组最高温度为46.60℃，平均温度为39.39℃和39.02℃。A组和B组的温度曲线如图3 a、b所示。数据合并后，B组的平均温度高于A组（39.21℃ vs.36.06℃，t=5.36，P=0.00），并且60W激光在5分钟的激光碎石术期间产生的热量对肾脏温度的升高有更大的影响。

研究人员对C组（接受10分钟钬激光激发）与另一组进行了对比。

D组。C组的最高温度为
46.8 在两次试验中，温度均达到37.56℃和38.25℃。而该组的最大温度为
D值为49.2°C，平均温度为40.08°C。
40.18 °C，分别（图3 c、d）。与使用30W激光的C组相比，使用60W激光照射10分钟的D组，肾实质温度升高更显著，可能对组织造成热损伤（40.13°Cvs37.91°C，t=5.28，P=0.00）。

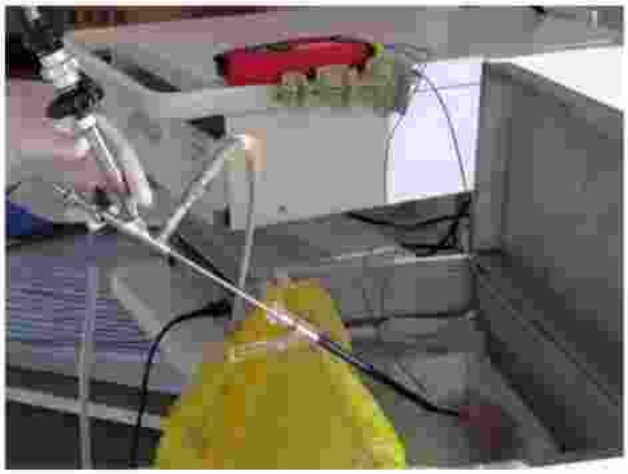


图2设备及流程

我们对每个肾脏进行激光激发后解剖。每个肾脏取3-5块组织用于病理学观察，取自热电偶探头附近区域。轻度至A组和C组的中度热损伤更为常见。显微镜下可见肾盂黏膜上皮与下方组织不同程度脱离，部分浅层伞状细胞仅缺失，部分则缺失整个细胞层，暴露出裸露的基底膜及黏膜固有层水肿（图4 a、b）。B组和D组标本显示更严重的热损伤：黏膜上皮发生变性脱落，固有层水肿伴黏膜肌层、肌细胞及外膜胶原纤维不同程度的变性坏死（图4 c）。通过对53例病理切片的损伤分级，共定义19例重度热损伤：A组2例，B组4例，C组5例，D组8例；24例中度热损伤：A组8例，B组6例，C组6例，D组4例；10例轻度损伤：A组3例，B组3例，C组2例，D组2例。按重度热损伤比例从高到低排序，D组占比最高达57.1%，C组为38%。5%，B组为30.8%，A组为15.4%。

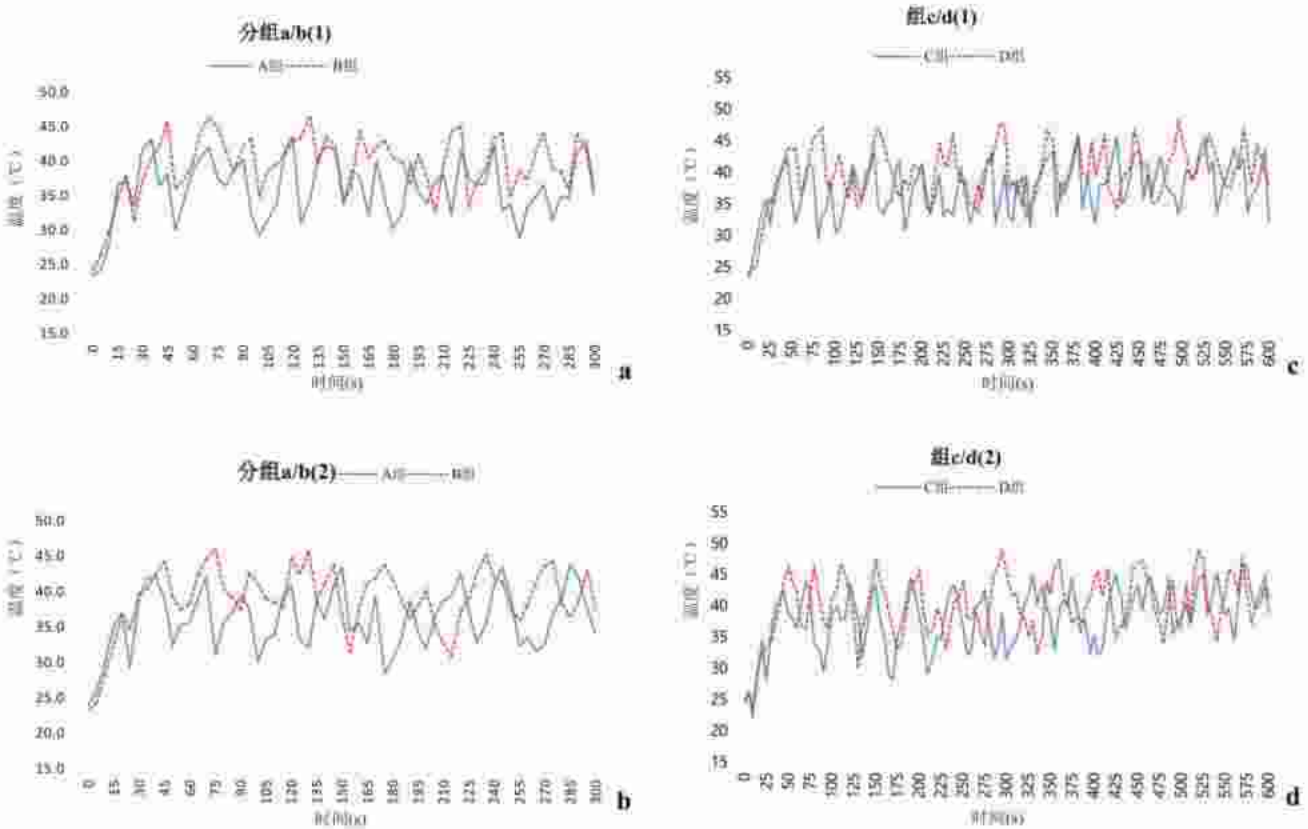


图3不同激光能量参数的温度分布曲线。**a**组A/B第一次试验。**b**组A/B第二次试验。**c**组C/D第一次试验。**d**组C/D第二次试验。

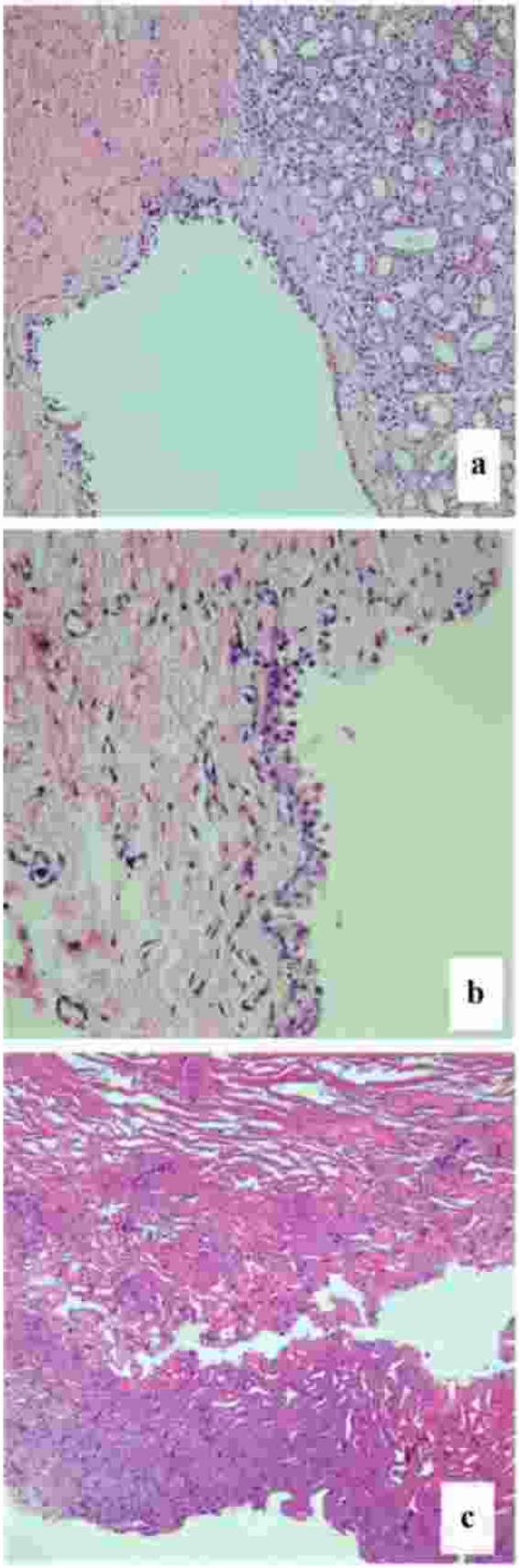


图4热损伤肾组织病理图片。**a**轻度。**b** 中度。**c**重度

讨论

钬激光碎石术已成为治疗尿路结石的首选方案。然而，以往针对孤立动物器官或设备的实验大多仅用于观察温度变化，对实际组织病理损伤的关注较少[5]。活体动物实验充分考虑了血流对温度变化的影响，监测温度更贴近实际情况[6]。但活体动物建立尿结石模型难度较大，且温度监测精度不及体外实验。此外，模型一致性与样本量不足都是控制偏差的主要挑战。本研究创新性地整合了体外与活体实验的优势，特别是在结石模型制备和病理观察方面，相比以往研究更能模拟真实临床场景。

钬激光治疗主要通过碎石的光热机制发挥作用，其工作原理是：传输光纤尖端的水介质吸收能量后迅速汽化形成微气泡[7]。但并非所有能量都能被水介质吸收并传递至结石部位。未抵达结石的激光能量会外泄，导致肾内温度升高，损伤尿路上皮组织，甚至可能引发并发症[8]。在实际临床操作中，激光能量直接作用于冲洗液的情况较为少见。因此，我们在研究中采用了人类结石样本进行验证。

水流速率是影响碎石术期间温度的最重要因素之一[8]。较高的水流速率可显著降低肾内温度，但也会导致肾内压力升高，从而增加感染风险。多项研究表明，水流速率越高，感染风险越大。在冲洗液流速为40 mL/min时，无论激光配置如何，激光激活10秒和60秒后的温度均未超过38.5°C[9]。实际操作涉及出血和感染等复杂因素。为确保手术安全，泌尿科医生通常将流速调整至最低值，以确保通过肾镜水阀获得清晰视野，这使得流速量化变得困难。因此，我们将理想的灌注流速标准化为30 mL/min。我们采用恒压泵冲洗，无需考虑碎石术排出液和最佳视野清晰度等因素，从而消除了手动调节肾镜水阀的需要。根据手术规范，激光器持续工作约25秒。

暂停5秒以促进灌注液对肾脏的高效冷却，这解释了温度曲线中出现的波动现象。

激光能量到达结石的比例可用于评估激光碎石术的效率。一项体外研究表明，当使用20Hz频率时，52%的发射脉冲能到达结石；使用50Hz频率时仅有23%达到目标，而80Hz时仅剩4%[10]。在功率恒定条件下，激光频率与碎石效率呈反比关系。因此，我们在A组和C组分别采用30W功率的激光器，设置15Hz与30Hz两种频率。间歇性激发的前5分钟内，两组平均温度无显著差异（36.06℃ 对比36.36℃，t=0.52，P>0.05）。类似地，在B组和D组中，60W功率的激光器以20Hz和30Hz频率设置时，平均温度几乎相同（39.21℃ 对比39.27℃，t=0.09，P>0.05）。我们认为在充分冲洗和良好激光激发习惯下，残留能量对肾脏温度的影响微乎其微。

一项高功率与低功率激光碎石术的对比研究表明，高功率激光的手术时间显著缩短，但焦耳/毫米^{3}值更高[11]。另一项针对肾盏结构的实验室模拟研究中，研究人员通过调节不同能量和频率参数，测量了不同冲洗流量下介质温度的变化。实验发现，能量输出越高，介质温度升幅越大——在无冲洗条件下，温度分别在10秒和60秒内达到50°C和70°C[9]。不过需要指出的是，多数实验仍未纳入结石因素的考量。

我们观察到，随着功率增加，能量溢出效应显著增强，肾内温度上升幅度和速度也明显加快。但功率的指数级增长并不会导致温度显著升高。相反，更高功率可能提升碎石效率并缩短手术时间，最终降低出血和感染风险。尽管近期荟萃分析显示，在处理相同体积结石时，高功率激光在缩短手术时间方面并未优于低功率激光[12]，但这与结石成分在不同人群中的差异密切相关。因此，外科医生必须根据患者结石位置、结石负荷及感染状况等实际情况，全面权衡激光热损伤与手术时间的利弊得失。

组织的热损伤取决于温度达到的程度及其持续时间（热剂量）。研究表明，组织和细胞损伤发生在43°C并持续240分钟[13]。当人体温度超过42°C时，可造成严重损伤。当局部温度超过45°C时，细胞组织会受到损伤；当温度超过60°C时，组织蛋白会发生热凝固和变性，导致不可逆损伤[14]。有研究将兔肾置于密闭容器中进行钬激光照射，虽然在一定时间内水温升高且兔肾组织受损，但缺乏水流冲洗和结石能量吸收的条件[15]。我们的实验结果显示，所有组别在试验过程中黏膜下平均温度均未超过40°C，其中D组（60瓦）温度最高达到49.2°C。各组均出现温度超过42°C的时段，但由于采用了与人体手术相同的间歇性激光照射和恒定流速冲洗技术，高温持续时间较短，每次仅约20秒，且在激光照射暂停后温度会迅速回落。

在完成各模型温度数据记录后，研究人员立即把猪肾交给助手进行解剖。通过观察发现，随着激光激发时间延长和病灶数量增加，C组和D组肾实质内可见不同程度的热损伤病灶。我们主要切除温度探头附近的组织进行病理分析。切片结果显示，D组损伤最为严重，严重尿路上皮热损伤的病理切片占比达57.1%，而A组仅占15.4%。由此可见，高功率和长脉冲的钬激光对肾尿路上皮组织损伤更严重。同时，所有切片显示损伤部位的肾小球和肾小管间质组织退行性坏死程度极轻微（<25%，轻度）。值得注意的是，尽管B组和C组最高温度相近，但C组平均温度更低，且严重热损伤比例更高。我们认为，组织损伤不仅由短暂的高温引起，还受暴露于这些温度的持续时间影响。显然，C组的肾组织在更长时间内仍处于损伤温度范围内。

不过，本研究存在一些局限性。虽然每组仅使用了两种肾脏模型，但各组温度特征基本一致。这表明实验具有可重复性，实验数据在科学上具有可靠性。由于采用离体器官实验，我们无法模拟血流对肾脏温度的影响。在体内条件下，由于血流的调节作用，实际肾脏温度可能更低。本研究观察到的热损伤属于短期并发症；然而，离体器官实验无法提供关于长期影响的深入见解。

这些后果必须在真实临床环境中加以考量。

结论

综上所述，钬激光在体外冲击波碎石术（PCNL）中采用不同能量参数配置时，会对肾脏造成不同程度的热损伤。当激光功率较高且冲洗速度固定时、持续时间较长会导致肾内温度升高和组织损伤加剧，但快速高功率激发对肾内温度的影响无需过分担忧。采用适度冲洗与间歇性激光激发的常规操作，能有效避免肾内温度过度升高。体外实验显示，热损伤对肾小管的影响微乎其微，主要损伤部位集中在肾黏膜和上皮下层。总体而言，无论参数设置如何，钬激光在碎石术中的应用都具有安全可靠的特点。泌尿科医生完全可以通过娴熟的手术操作，将潜在副作用控制在最低限度。

作者贡献WW：项目开发、数据管理、论文撰写；ZX：项目开发、论文撰写、MC：数据管理、论文编辑、LX：数据收集、病理学观察、YM：数据收集、HZ：数据收集。

资助广东佛山市卫生局医学研究项目（中国广东），编号20220331。

数据可用性所有相关数据均在论文中。原始数据可应合理要求向通讯作者索取。

声明

利益冲突作者声明在研究、作者和出版本手稿方面没有潜在的利益冲突。

伦理审批由佛山市中医院医学伦理委员会审批，IRB编号：2021138。

知情同意本研究通过手术从患者体内取出结石，所有患者均签署了知情同意书，同意将结石用于本研究。

研究方案经机构审查委员会批准福山市卫生局医学研究项目（中国）。

注册号和研究/试验注册号无。

动物研究N/A。

参考文献

1. Tok A，Akbulut F，Buldu I等（2016）微经皮肾镜取石术与经皮肾镜取石术治疗中等大小下盏结石的对比研究。《泌尿系统结石》44(2)：155–159
2. Enikeev D，Herrmann TRW等人（2023）《钬光纤激光在泌尿内镜中的应用：最新临床证据》。Curr Opin Urol 33(2)：95–107. https://doi.org/10.1097/MOU.0000000000001057
3. Scholarikos A，Jung HJ，Somani，B等（2022）尿路结石诊疗指南。见于：EAU Guidelines Office：Arnhem，荷兰ISBN 978-94-92671-16-5
4. 董浩，彭勇，李立，高翔等（2018）输尿管镜碎石术后输尿管狭窄的预防策略。《亚洲泌尿外科杂志》5(2)：94–100
5. Gallegos H，Bravo JC et al（2021）肾内温度测量与钬激光体腔碎石术在离体模型中的相关性。Cent Eur J Urol 74(4)：588–594。https://doi.org/10.5173/ceju.2021.0092
6. Simon H，Ralf P et al（2020）Ho：YAG激光碎石术逆行肾内手术和经皮肾镜碎石术的热效应在离体猪肾模型中。World J Urol 38(3)：753–760。https://doi.org/10.1007/s00345-019-02808-5。（**2019年5月16日电子版**）
7. 切凯蒂W、扎托尼F、尼格罗F等（2004）钬激光诱导的血浆气泡形成：体外研究[J]《泌尿外科》63(3)：586–590
8. Felipe P，Eugenio V等（2022）肾内温度和压力管理在RIRS期间的实用指南：证据告诉我们什么。J Clin Med 11（12）：3429。https://doi.org/10.3390/jcm11123429
9. 阿尔杜基AH，加尼KR，霍尔TL等人（2017）《高功率钬激光碎石术的热反应》。《泌尿外科杂志》31:1308–1312
10. Aldoukhi A，Hall T，Ghani K等（2020）不同激光碎石术模式下激光光纤至结石距离的分析。《泌尿学杂志》203：e626
11. Mekayten M，Lorber A，Kataflgiotis I等人（2019）研究：结石密度是否将成为泌尿内镜手术的关键因素？以Lumenis激光P120 W和标准设备为例，探讨结石密度对激光治疗时间的影响20W激光治疗的比较研究。《泌尿外科学杂志》33：585–589
12. 文垂采利亚E、帕净尔F、蒂德里尼F等学者（2021）发表于《泌尿外科学杂志》的研究表明，高功率与低功率激光碎石术疗效相当：基于现有临床数据的系统综述与荟萃分析。35:1146–1152
13. 萨帕雷托SA、杜威WC（1984）癌症治疗中的热剂量测定。《国际放射肿瘤学、生物学与物理学杂志》10：787–800
14. Izzard AS，Rizzoni D等（2005）小动脉结构与高血压：适应性改变及靶器官损伤。《高血压杂志》23(2)：247–250
15. 莫利纳WR、塔尔瓦IN、多纳利西奥-达席尔瓦R等（2015）盐水对激光碎石术激活温度曲线的影响。《泌尿外科学杂志》29(2)：235–239

出版商声明：Springer Nature对已发表地图和机构隶属关系中的司法管辖权主张保持中立。

Springer Nature或其授权方（例如学会或其他合作伙伴）根据与作者或其他权利持有人签订的出版协议，对本文拥有独家权利；作者对本文已接受的稿件版本进行自我存档，完全受该出版协议条款和适用法律的约束。

INTERNATIONAL JOURNAL OF UROLOGY

International Journal of Urology (2024) 31, 795–801 doi: 10.1111/iju.15466

Original Article
Clinical Investigation

Japanese survey of perioperative complications and ureteral stricture after ureteroscopy with laser lithotripsy for upper urinary tract stones in multicenter collaborative study

Takaaki Inoue,[1,2] Hirokazu Tanaka,[3] Tomoko Masuda,[4] Akinori Iba,[5] Mitsuhiro Tambo,[6] Shinsuke Okada,[7] Terunobu Hou,[8] Ryoji Takazawa,[9] Hirofumi Izaki,[10] Shuzo Hamamoto[11] and Masato Fujisawa[2]

[1]Department of Urology and Stone Center, Hara Genitourinary Hospital, Hyogo, Japan, [2]Division of Urology, Department of Surgery Related, Kobe University Graduate School of Medicine, Hyogo, Japan, [3]Department of Urology, Hyogo Prefectural Kakogawa Medical Center, Kakogawa, Japan, [4]Department of Urology, Tokyo Metropolitan Police Hospital, Nakano-ku, Japan, [5]Department of Urology, Rinku General Medical Center, Izumisano, Japan, [6]Department of Urology, Kyorin University School of Medicine, Tokyo, Japan, [7]Department of Urology, Gyotoku General Hospital, Chiba, Japan, [8]Department of Urology, Teikyo University, Chiba Medical Center, Chiba, Japan, [9]Department of Urology, Tokyo Metropolitan Otsuka Hospital, Toshima-ku, Japan, [10]Department of Urology, Tokushima Prefectural Central Hospital, Toshima-ku, Japan, and [11]Department of Nephro-Urology, Medical School, Nagoya City University Graduate School of Medical Sciences, Nagoya, Aichi, Japan

Abbreviations & Acronyms
BMI = body mass index
CROES = Clinical Research Office of Endourological Society
ESUT = European Society of Uro-technology
EULIS = European Association of Urologists Sections of Urolithiasis
HU = Hounsfield unit
IQR = interquartile range
JSER = Japanese Society of Endourology and Robotics
PULS = proposed postoperative ureteroscopic lesion scale
SWL = shockwave lithotripsy
URS = ureteroscope
URS-L = ureteroscopy with laser lithotripsy

Correspondence
Takaaki Inoue M.D., Department of Urology and Stone Center, Hara Genitourinary Hospital, 5-7-17 Kitanagasadori, Chuo-ku, Kobe City, Hyogo, Japan.
Email: inouetak@harahospital.jp

Received 15 December 2023; accepted 31 March 2024. Online publication 15 April 2024

Objectives: This study aimed to investigate perioperative complications and the details of postoperative ureteral stricture after ureteroscopy with laser lithotripsy (URS-L) for upper urinary tract stones in Japan.

Methods: Patient data on intra- and postoperative complications after ureteroscopy using URS-L were retrospectively collected from multiple centers in Japan between April 2017 and March 2020 with the cooperation of the Japanese Society of Endourology and Robotics. Data included the number of patients undergoing URS-L, number and type of intra- and postoperative complications, and detailed characteristics of postoperative ureteral stricture.

Results: In total, 14 125 patients underwent URS-L over 3 years at 82 institutions. Annual URS-L numbers gradually increased from 4419 in 2017, to 4760 in 2018, and 4946 in 2019. The total complication rate was 10.5%, which was divided into intra-operative complications in 1.40% and postoperative complications in 9.18%. The annual incidences of intra- and postoperative complications were not significantly different from year to year ($p = 0.314$ and $p = 0.112$). Ureteral perforation, ureteral avulsion, and the intra-operative conversion rate were 1.35%, 0.03%, and 0.02%, respectively. Fever >38°C, septic shock, blood transfusion, and postoperative mortality were 7.44%, 0.81%, 0.07%, and 0.04%, respectively. Ureteral stricture occurred in 0.8% of cases. The median length of stricture site was 10.0 mm and the success rate of stricture treatment was 54.6%.

Conclusion: Although URS-L utilization has increased in Japan, the annual complication rate has remained steady. Although URS-L is a useful and less invasive procedure, devastating complications can still occur.

Key words: postoperative complication, ureteral stricture, ureteroscopy with laser lithotripsy.

INTRODUCTION

The prevalence of urolithiasis in the upper urinary tract has been increasing globally due to metabolic syndrome, climate change, and increased utilization of diagnostic modalities such as CT and ultrasonography.[1] Current treatment regimens for upper urinary tract stones have also shifted: while the use of shockwave lithotripsy (SWL) has decreased, use of ureteroscopy (URS) has significantly increased with the development of laser technologies and the

© 2024 The Japanese Urological Association.

evolution of flexible URS.[2] Lithotripter devices to break apart the stones have gradually changed from pneumatic lithotripter systems to holmium YAG lasers and thulium fiber lasers in Japan as a result of development of finer laser fibers, along with increased flexibility, versatility, and usability of these lasers.[3] These laser lithotripsic devices are also quite effective for breaking ureteral stones than kidney stones. In addition, the introduction of flexible URS systems has also increased the range of treatment indications for ureteral stones and kidney stones.

Thus, we refer to this as the "ureteroscopy era with lasers" for stone management. However, as new technology results in novel discoveries and improved clinical efficacy, it is also accompanied by critical risks such as unknown complications and variable clinical outcomes. In this study, we aimed to survey recent intra- and postoperative complications after ureteroscopy with a holmium YAG laser for upper urinary tract stones in Japan. In addition, we also investigated the details of postoperative ureteral stricture.

METHODS

Study design and patients

We retrospectively collected patient data on intra- and postoperative complications after URS-L for upper urinary tract stones. Data were collected from multiple Japanese centers between April 2017 and March 2020 and were acquired with the cooperation of the Japanese Society of Endourology and Robotics (JSER). This study was approved by the institutional review board at Kobe University (No. B190331). We acquired patient consent by an opt-out approach at each institution. We retrospectively extracted only relevant data from each patient's medical record at each participating institution.

Data collection

The following postoperative early complication data were collected from each institution for incidents <1 month after ureteroscopy: annual cases of URS-L, number of ureteral perforations, number of ureteral avulsions, frequency of conversion to open or laparoscopy as an intra-operative complication, number of patients with fever >38°C, frequency of septic shock, blood transfusion, or subcapsular hematoma, and mortality. The number of ureteral strictures, which were diagnosed after 1 month postoperatively, were collected as postoperative late complications. Additionally, we collected the characteristics of patients with postoperative ureteral stricture including age, gender, body mass index (BMI), preoperative hydronephrosis status, preoperative stent placement, stone location, maximum stone size, and stone density by Hounsfield Unit (HU).

Furthermore, we collected data on the diagnostic method, surgical and clinical outcomes: diagnostic imaging studies, time to diagnosis of ureteral stricture after URS-L, length of ureteral stricture, location of ureteral stricture, treatment methods, and success rate of stricture treatment. Additionally, we defined the criteria for specific complications by the following: ureteral perforation was defined as injury involving the full thickness of the ureteral wall, including the adventitia with retroperitoneal fat; fever was indicated by a temperature greater than 38°C related to surgery occurring even once within 1 month after URS-L; septic shock was indicated by unstable mean blood pressure less than 65 mmHg despite fluid infusion and due to infectious status related to surgery; and ureteral stricture was defined as worse hydronephrosis or hydronephrosis equivalent to that before surgery as assessed by postoperative CT or ultrasound sonography. The success of stricture treatment was defined as the amelioration of postoperative hydronephrosis compared with preoperative status.

Statistical analysis

Data were analyzed using IBM SPSS Statistics version 26. Continuous variables and nominal variables from retrospectively collected clinical data were described as medians with interquartile ranges (IQR) and numbers with percentages, respectively. Moreover, Pearson's χ^2-test was used for univariate analysis to compare data for complications between each year. Statistical significance was set at a two-sided p-value of <0.05.

RESULTS

URS-L for upper urinary tract stones was performed on 14 125 patients at 82 institutions between April 2017 and March 2020. Annual URS-L numbers gradually increased from 4419 in 2017 to 4760 in 2018 and 4946 in 2019 (Figure 1). The total complication rate was 10.5%, including intra-operative complications in 1.40% of cases and postoperative complications in 9.18% of cases. Of the intra-operative complications, ureteral perforation, ureteral avulsion, and conversion to open/laparoscopy rates were 1.35%, 0.03%, and 0.02%, respectively. Postoperative early complication rates for events occurring less than 1 month after ureteroscopy were fever >38°C (7.44%), septic shock (0.81%), blood transfusion (0.07%), subcapsular hematoma (0.05%), and mortality (0.04%). The incidence of ureteral stricture as a postoperative late complication was 0.8% (Table 1). Annual incidence rates of intra- and postoperative complications were not significantly different from year to year ($p = 0.314$ and $p = 0.112$; Figure 2). Annual incidence rates of ureteral perforation, fever, septic shock, and ureteral stricture were also not significantly different from year to year ($p = 0.163$, $p = 0.182$, $p = 0.906$, and $p = 0.635$; Figure 3).

From 108 ureteral strictures, which were diagnosed after 1 month postoperatively, 68.4% were diagnosed within 3 months after ureteroscopy by using CT in 42.5% of cases and by ultrasound in 17.5% of cases. The median length of ureteral stricture was 10.0 mm. The most frequently occurring stricture site was in the proximal ureter (38.8%), followed by the distal ureter (24.0%) and the middle ureter (22.2%). The most often selected treatment for ureteral stricture was transurethral balloon dilation. (54.6%) followed by observation (22.2%), ureteroureterostomy (10.1%), and ureteral stent/nephrostomy replacement (10.1%). The total success rate of stricture treatment was 54.6%. Transurethral balloon dilation was the most effective method of all the procedures (Table 2).

© 2024 The Japanese Urological Association.

14425405, 2024, 7, Downloaded from https://onlinelibrary.wiley.com/doi/10.1111/iju.15494 by University Of Bristol, Cochrane Wiley Online Library on [26/10/2024]. See the Terms and Conditions (https://onlinelibrary.wiley.com/terms-and-conditions) on Wiley Online Library for rules of use; OA articles are governed by the applicable Creative Commons License

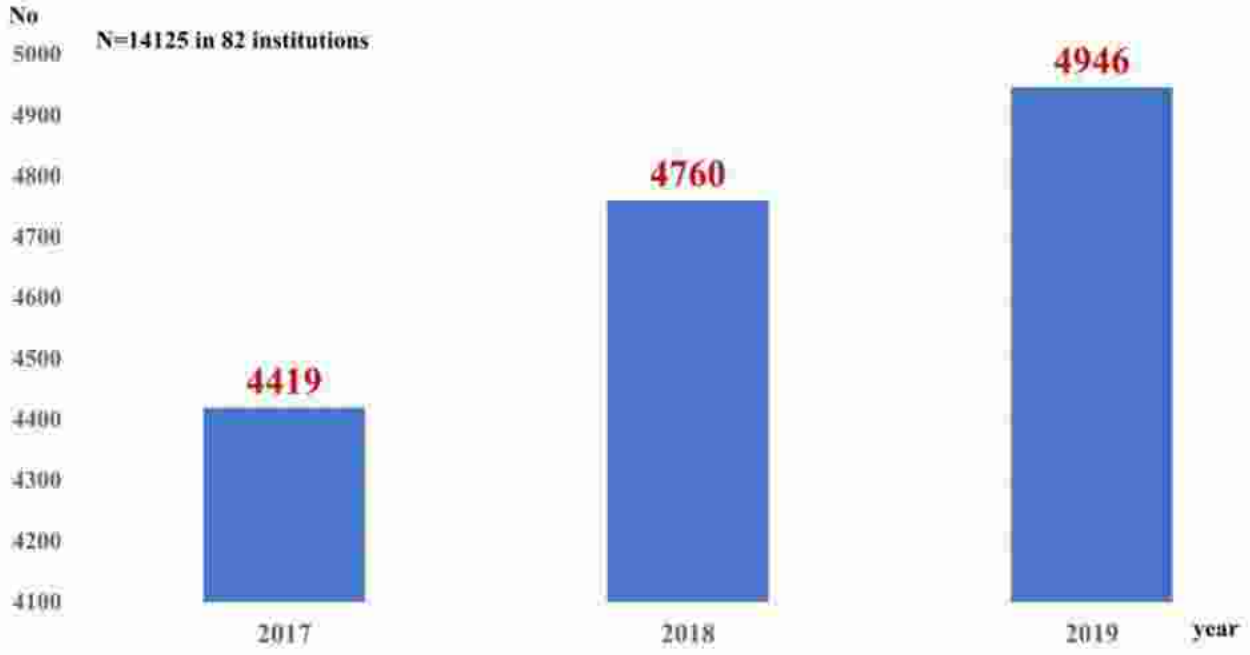


FIGURE 1 Rates of ureteroscopy for upper urinary tract stones by laser lithotripsy in Japan.

TABLE 1 Intra- and postoperative complications after ureteroscopy with laser lithotripsy

Total complication rate (*n*, %)	1496 (10.5)
Intra-operative complication rate (*n*,%)	199 (1.40)
Ureteral perforation	191 (1.35)
Ureteral avulsion	5 (0.03)
Conversion to open/laparoscopy	3 (0.02)
Postoperative early complication rate (<1 month) (*n*, %)	1189 (8.41)
Fever-up (>38°C)	1051 (7.44)
Septic shock	115 (0.81)
Blood transfusion	10 (0.07)
Sup-capsular hematoma	7 (0.05)
Mortality	6 (0.04)
Postoperative late complication (*n*, %)	108 (0.80)
Ureteral stricture	108 (0.80)

Note: *N* = 14 125.

DISCUSSION

In this survey, we found that annual URS-L cases for upper urinary stones in Japan have gradually increased. Although the total complication rate was 10.5%, including intra-operative complications in 1.40% of cases and postoperative complications in 9.18% of cases, the annual incidence rates of intra- and postoperative complications were not significantly different year over year.

The trend of surgical procedures for stone management in the upper urinary tract has changed with the expanded use of laser technology and the innovation of the flexible ureteroscope. In 2014, Ordon et al. found that in an analysis of administrative databases, of 194 781 kidney stone treatments performed between 1991 and 2010, URS utilization significantly increased from 25% in 1991 to 59% in 2010. Conversely, SWL utilization decreased from 69% in 1991 to 34%

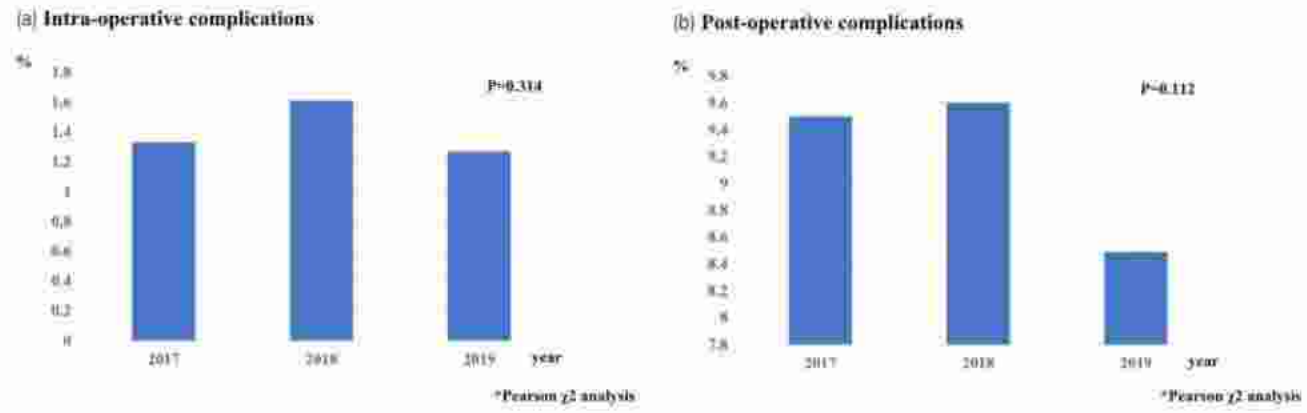


FIGURE 2 Perioperative complication rate for ureteroscopy with laser lithotripsy (a) Intra-operative complications (b) Postoperative complications.

© 2024 The Japanese Urological Association.

14425642, 2024, 7, Downloaded from https://onlinelibrary.wiley.com/doi/10.1111/iju.15409 by University Of British Columbia, Wiley Online Library on [26/10/2025]. See the Terms and Conditions (https://onlinelibrary.wiley.com/terms-and-conditions) on Wiley Online Library for rules of use; OA articles are governed by the applicable Creative Commons License

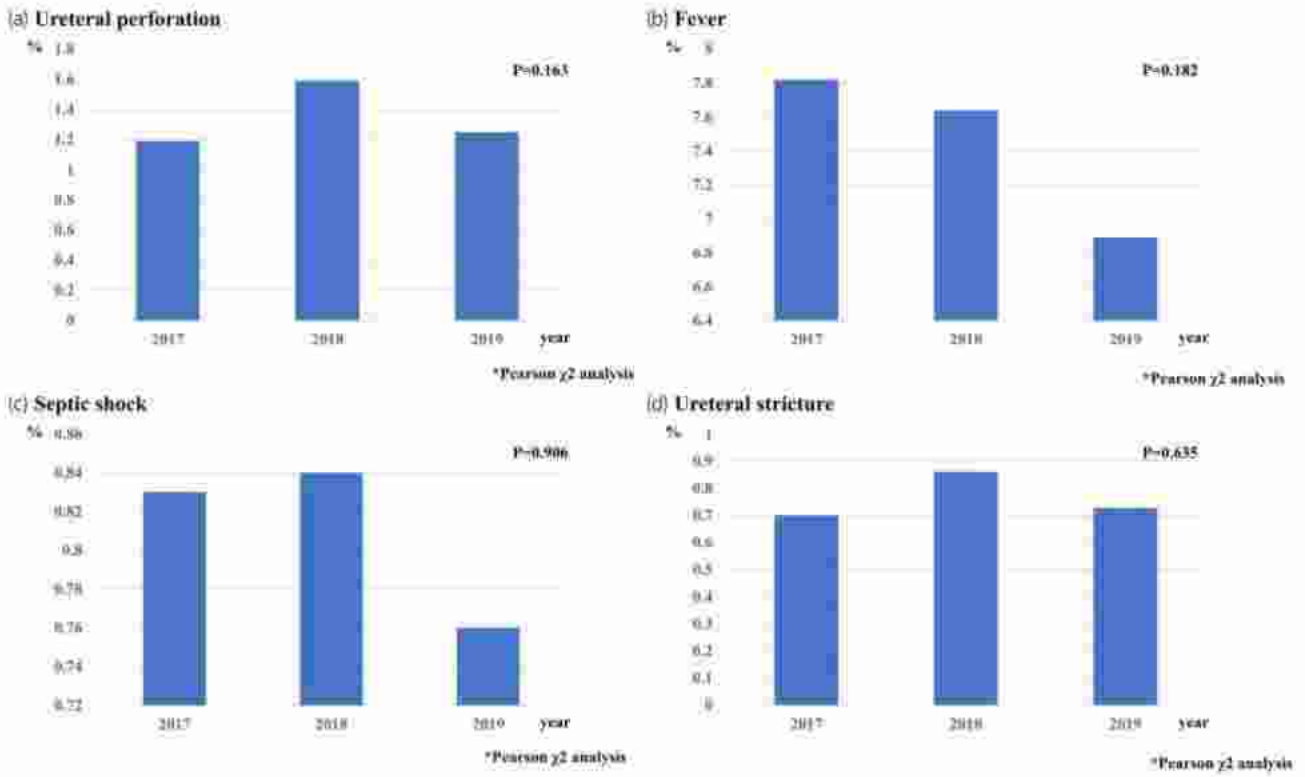


FIGURE 3 Major complication rates for ureteral perforation, fever, septic shock, and ureteral stricture during and after ureteroscopy with laser lithotripsy. (a) Ureteral perforation, (b) Fever, (c) Septic shock, (d) Ureteral Stricture.

in 2010 and was inferior to URS.[4] Additionally, Herout et al. showed that the number of URS significantly increased by 143% between 2006 and 2019.[5] Likewise, Isotani et al reported in 2019 that the annual trend of URS utilization in Japan has been increasing and surpassed the number of SWL performed per year in 2014.[2]

With the current rise in URS utilization, novel technologies might bring additional complications and increase the rate of perioperative complications. The EAU guidelines describe that the overall complication rate after URS is 9%–25%, however, most complications are minor and do not require surgical intervention.[6] According to a global study by the Clinical Research Office of the Endourological Society (CROES), there was a complication rate of 7.4% out of 11 885 patients, including 4.2% intra-operative, 2.6% postoperative, and 0.5% both intra- and postoperative complications, almost all of which were minor complications. However, it should be noted that critical complications still occurred.[7] In the present study, the total complication rate out of 14 125 patients undergoing URS with laser lithotripsy was 10.5%, including intra-operative complications in 1.40% and postoperative complications in 9.18%, which were equivalent to another report. However, severe complications still occurred in our study.

Ureteral perforation, which is a devastating intra-operative complication, occurs in 0.3%–7.4% of cases as a result of ureteroscopic surgery with a ureteral access sheath, laser emission, basketing, and from the ureteroscope itself.[8] Currently, ureteral wall injury as an intra-operative major complication is classified by endoscopic grade. Traxer et al. initially suggested the intra-operative endoscopic classification of ureteral wall injury when using a ureteral access sheath.[9] Subsequently, Schoentaler et al. proposed a postoperative ureteroscopic lesion scale (PULS).[10] In accordance with the Traxer grading system, 13.3% of cases using a 12/14F ureteral access sheath resulted in a damaged ureteral wall involving muscle layers.[9] The ureteral perforation rate in our study was relatively lower, at 1.35%. On the contrary, although ureteral avulsion is a relatively rare intra-operative complication with an incidence of 0.04%–0.9% during ureteroscopy, it is one of the most calamitous complications.[8] Our rate of ureteral avulsion in this study was 0.03%, which was not a lower rate because upper urinary stones are considered a benign disease. Therefore, it is necessary to avoid this serious complication. Once ureteral avulsion has occurred, immediate repair is required, or repair can be performed as a staged procedure. In our study, 0.02% of patients converted from URS to open or laparoscopic procedures due to ureteral avulsion.

Postoperative fever is a well-known early complication following URS, with a reported rate between 0.2% and 15%.[8] In our study, 7.44% of patients experienced fever >38°C postoperatively. Furthermore, urosepsis, which is defined as sepsis resulting in life-threatening organ dysfunction caused by urogenital tract infection is also a serious complication with an incidence between 0.1% and 4.3% post-ureteroscopy.[11] Urosepsis accompanied by septic shock occurs with a frequency of 0.3% to 4.6%, resulting in a mortality rate of 28.3–41.1%.[12,13] The rate of septic shock in our study was 0.81%.

© 2024 The Japanese Urological Association.

TABLE 2 Characteristics and outcomes of postoperative ureteral stricture after ureteroscopy with laser lithotripsy

N = 108 Age (year, median, IQR)	63.0 (54.0–71.0)
Gender (No. %)	*M*: 72 (66.6), F: 36 (33.3)
BMI (kg/m^2, median, IQR)	24.4 (22.1–27.2)
Pre-operative hydronephrosis (No. %)	85 (78.7)
Pre-ureteral stenting (No. %)	31 (28.7)
Stone location (No. %)	
Ureteral orifice	1 (0.9)
Distal ureter	17 (15.7)
Middle ureter	23 (21.2)
Proximal ureter	47 (43.5)
Ureter-pelvic junction	14 (12.9)
Kidney	6 (5.5)
Max stone size (mm, median, IQR)	10.2 (7.4–13.5)
CT-value (HU, median, IQR)	1070.5 (781.5–1320.5)
Diagnosed period of ureteral stricture after ureteroscopy	
POD 1 months	33 (30.5)
POD 1–3 months	41 (37.9)
POD 3–6 months	23 (21.2)
POD 6–12 months	8 (7.4)
POD > 12 months	3 (2.7)
Diagnostic imaging study (No. %)	
CT	46 (42.5)
Ultrasound	19 (17.5)
IVP	1 (0.9)
RP	20 (18.5)
Ureteroscopy	19 (17.5)
Others	3 (2.7)
Length of ureteral stricture (mm median, IQR)	10.0 (5.0–17.0)
Location of ureteral stricture (No. %)	
Ureteral orifice	2 (1.8)
Distal ureter	26 (24.0)
Middle ureter	24 (22.2)
Proximal ureter	42 (38.8)
Ureter-pelvic junction	14 (12.9)
Treatment of ureteral stricture (No. %)	
Transurethral balloon dilation	59 (54.6)
Ureteroureterostomy (Open or laparoscopic)	11 (10.1)
Nephrectomy	2 (1.8)
Ureteral stent or nephrostomy replacement	11 (10.1)
Observation	24 (22.2)
Success rate (No. %)	
Total	59 (54.6)
Transurethral balloon dilation	37 (62.7)
Ureteroureterostomy (Open or laparoscopic)	5 (45.4)
Ureteral stent or nephrostomy replacement	11 (100)
Observation	7 (29.1)

Abbreviations: BMI, body mass index; HU, Hounsfield Unit; IQR, interquartile range; IVP, intravenous pyelogram; POD, postoperative day; RP, retrograde pyelogram.

Blood transfusion following URS for stone treatment is also an early complication, with 1.3%–1.6% incidence.[14,15] Intra-operative bleeding during URS often occurs as a result of ureteral wall injury due to the use of a ureteral access sheath or laser shooting, renal injury due to laser shooting, or renal fornix rupture from high intrarenal pressure. High intrarenal pressure, as well as longer operation time and higher irrigation perfusion pressure intra-operatively are also causes of subcapsular perirenal hematoma, exhibiting 0.4% –2.2% incidence.[16] Patients continuing to take anticoagulation or antiplatelet agents prior to surgery often continue to bleed more intra- and postoperatively.[17,18] In our study, there were 0.07% patients who underwent blood transfusion and 0.05% who experienced subcapsular hematoma, both of which were observed at a relatively lower rate than that previously reported.

Although ureteroscopy for stone management is a safe and minimally invasive procedure, lethal morbidities have occurred. According to a current systematic review from the European Association of Urologists Sections of Urolithiasis (EULIS) and Uro-technology (ESUT), Bhanot et al. demonstrated that there were 72 patient deaths in 15 studies following URS. For the 42 patients in which the etiology could be determined, causes of death included sepsis in 57.1%, multiple organ dysfunction, cardiac-related incidences such as infarction of arrhythmia in 14.2%, hemorrhagic complications in 4.7%, and respiratory-related incidences such as lung thromboemolisms in 7.1%.[19] The mortality rate following URS in the present study was 0.04% which was not a lower incidence than that reported previously.

Ureteral stricture is a major late postoperative complication, with up to 3% incidence.

Ureteral stricture was defined as the focal narrowing of the ureter at the site of previous stone impaction with identifiable hydroureteronephrosis on IVP or retrograde pyelography for generations.[20] However, the usage of contrast agents currently should avoid to be less contrast allergy when anatomical condition before stone surgery is evaluated. In addition, there are not only site of previous stone impaction but also the other site of ureter due to excessive manipulation of ureteroscope and stone basket, miss laser shooting, thermal injury due to leaser setting as well as impacted stone.[21] Therefore, ureteral stricture was defined as worse hydronephrosis or hydronephrosis equivalent to that before surgery in our present study. Especially, the thermal injury might be one of the latest causes to postoperative ureteral stricture when shooting the laser into ureter. Intrarenal temperatures during ureteroscopic laser lithotripsy correlated directly with the laser power setting.[22] In our study, the rate of ureteral stricture was 0.8%. Sunaryo et al. reported that ureteral stricture developed in 2.9% of patients after URS.[23] Some causes of ureteral stricture formation following URS are classified as iatrogenic factors, including ureteral wall injury due to direct and indirect thermal injury, ischemia of the ureteral mucosa due to use of a ureteral access sheath, remaining stone fragments within the mucosa, and intrinsic stone factors such as impacted stone and stone size. Once a ureteral stricture has occurred postoperatively, a complete cure is difficult to achieve. From a population-based assessment, Sunaryo et al. reported that 35% of ureteral strictures required drainage including placement of a ureteral stent or percutaneous nephrostomy, 21% required endoscopic intervention, 4.8% required ureteral reconstruction, and 1.7% underwent simple nephrectomy.[23] In our study, intervention for postoperative ureteral strictures was performed as follows: 54.6% underwent transurethral balloon dilation, 10.1% underwent ureteroureterostomy, 1.8% underwent nephrectomy, 10.1% underwent ureteral stent or nephrostomy replacement, and 22.2% continued observation. The success

© 2024 The Japanese Urological Association.

rate is dependent on the kind of interventional procedure performed. Xiong et al. reported that the overall success rate was 60.9% with endourological intervention for post ureteroscopic ureteral stricture; however, 97.3% underwent reconstructive surgery.[24] In our study, the total success rate for resolution of ureteral stricture was 54.6%, and out of all the interventions, transurethral balloon dilation and ureteroureterostomy successfully managed strictures in 62.7% and in 45.4%, of cases, respectively.

This study has some limitations. First, as a main limitation, the data in this study were collected from experienced institutions actively performing stone surgeries. Therefore, institutions where limited numbers of annual stone surgeries were performed were not included. Second, we collected data on only major complications after URS-L. Therefore, data on minor complications, like breakage of URS, postoperative pain, and ureteral stent-related events, were not collected. Third, we could not analyze the difference between complications related to ureteral versus kidney stones or rigid versus flexible URS because that data was not available from the patient's chart. Fourth, ureteral strictures were diagnosed after 1 month postoperatively using a mix of US and CT. In some cases, postoperative hydronephrosis might mitigate at 2, or 3 months after operation. And then, to compare the degree of hydronephrosis between pre-operation and post-operation, we used the mix evaluation image of US and CT. Nevertheless, to the best of our knowledge, this is the first report to have reported the rates of intra- and postoperative complications after URS-L for upper urinary tract stones in Japan. Additionally, we evaluated the rates of postoperative ureteral stricture. In conclusion, although URS-L utilization has increased in Japan with increasing technological advancements, the annual complication rate has remained steady. Although URS-L is a useful and minimally invasive procedure, devastating complications have still occurred. Careful management for URS-L is needed to prevent additional invasive procedures.

ACKNOWLEDGMENTS

We would like to thank the 82 cooperating institutions in Japan for their dedicated data collection and collaboration.

AUTHOR CONTRIBUTIONS

Takaaki Inoue: Conceptualization; Methodology; Software; Data curation; Formal analysis; Investigation; Project administration; Writing—original draft. **Hirokazu Tanaka:** Data curation. **Tomoko Masuda:** Data curation. **Akinori Iba:** Data curation. **Mitsuhiro Tambo:** Data curation. **Shinsuke Okada:** Data curation; Writing—review & editing. **Terunobu Hou:** Data curation. **Ryoji Takazawa:** Data curation. **Hirofumi Izaki:** Data curation. **Shuzo Hamamoto:** Data curation; Writing—review & editing. **Masato Fujisawa:** Writing—review & editing.

CONFLICT OF INTEREST STATEMENT

None declared.

APPROVAL OF THE RESEARCH PROTOCOL BY AN INSTITUTIONAL REVIEWER BOARD

Yes (No. B190331).

INFORMED CONSENT

Yes due to Opt-out in our hospital.

REGISTRY AND THE REGISTRATION NO. OF THE STUDY/TRIAL

N/A.

ANIMAL STUDIES

N/A.

FUNDING INFORMATION

We have no relevant funding with respect to the present article.

REFERENCES

1. Sakamoto S, Miyazawa K, Yasui T, Iguchi T, Fujita M, Nishimatsu H, et al. Chronological changes in the epidemiological characteristics of upper urinary tract urolithiasis in Japan. *Int J Urol*. 2018;**25**:373–8.
2. Isotani S, Noma Y, Wakumoto Y, Muto S, Horie S. Endourological treatment trend of upper urinary tract urolithiasis in Japan from the Japanese diagnosis procedure combination database. *Int J Urol*. 2019;**26**:1007–8.
3. Rosette JD, Denstedt J, Geavlete P, Keeley F, Matsuda T, Pearle M, et al. The clinical research office of the endourological society ureteroscopy global study: indications, complications, and outcomes in 11,885 patients. *J Endourol*. 2014;**28**:131–9.
4. Ordon M, Urbach D, Mamdani M, Saskin S, D'A Honey RJ, Pace KT. The surgical management of kidney stone disease: a population-based time series analysis. *J Urol*. 2014;**192**:1450–6.
5. Herout R, Baumacke M, Grosben C, Aksoy C, Volkmer B, Schmidt M, et al. Contemporary treatment trends for upper urinary tract stones in a total population analysis in Germany from 2006 to 2019: will shock wave lithotripsy become extinct? *World J Urol*. 2022;**40**:185–91.
6. Skolarikos A, Jung H, Neisius A, Petrik A, Somani B, Tailly T, et al. EAU guidelines on urolithiasis. Complications of ureteroscopy. 2023:21.
7. Somani BK, Giusti G, Sun Y, Osther PJ, Frank M, De Sio M, et al. Complications associated with ureteroscopy (URS) related to treatment of urolithiasis: the clinical research Office of Endourological Society URS global study. *World J Urol*. 2017;**35**:675–81.
8. De Coninck V, Keller EX, Somani B, Giusti G, Proietti S, Rodriguez-Socarras M, et al. Complications of ureteroscopy: a complete overview. *World J Urol*. 2020;**38**:2147–66.
9. Traxer O, Thomas A. Prospective evaluation and classification of ureteral wall injuries resulting from insertion of a ureteral access sheath during retrograde intrarenal surgery. *J Urol*. 2013;**189**:580–4.
10. Schoenthaler M, Buchholz N, Fairus E, Ather H, Bach C, Bach T, et al. The post-ureteroscopic lesion scale (PULS): a multicenter video-based evaluation of inter-rater reliability. *World J Urol*. 2014;**32**:1033–40.
11. Singer M, Deutschman CS, Seymour C, Shankar-Hari M, Annane D, Bauer M, et al. The third international consensus definitions for sepsis and septic shock (Sepsis-3). *JAMA*. 2016;**315**:801–10.
12. Corrales M, Sierra A, Doizi S, Traxer O. Risk of sepsis in retrograde intrarenal surgery. A systematic review of the literature. *Eur Urol Open Sci*. 2022;**30**:84–91.
13. Wagenlehner FME, Lichtenstern C, Rolfes C, Mayer K, Uhle F, Weidner W, et al. Diagnosis and management for urosepsis. *Int J Urol*. 2013;**20**:963–70.

© 2024 The Japanese Urological Association.

14422042, 2024, 7, Downloaded from https://onlinelibrary.wiley.com/doi/10.1111/iju.15469 by University Of Bristol, Cochrane Wiley Online Library on [26/10/2025]. See the Terms and Conditions (https://onlinelibrary.wiley.com/terms-and-conditions) on Wiley Online Library for rules of use; OA articles are governed by the applicable Creative Commons License

14 Castellani D, Traxer O, Ragoori D, Galosi AB, De Stefano V, Gadzhiev N, et al. Improveing outcomes of same-sitting bilateral flexible ureteroscopy for renal stones in real-world practice-lessons learn from global multicenter experience of 1250 patients. *Eur Urol Open Sci*. 2023;**38**:51–9.
15 Fayad MK, Fehmy O, Abulazayem KM, Salama NM. Retrograde intrarenal surgery versus percutaneous nephrolithotomy for treatment of renal pelvic stone more than 2 centimeters: a prospective randomized controlled trial. *Urolithiasis*. 2022;**50**:113–7.
16 Bai J, Li C, Wang S, Liu J, Ye Z, Yu X, et al. Subcapsular renal hematoma after holmium:yttrium-aluminum-garnet laser ureterolithotripsy. *BJU Int*. 2012;**109**:1230–4.
17 Westerman ME, Sharma V, Scales J, Gearman DJ, Ingimarsson JP, Krambeck AE. The effect of antiplatelet agents on bleeding-related complications after ureteroscopy. *J Endourol*. 2016;**30**:1073–8.
18 Westerman ME, Scales J, Sharma V, Gearman DJ, Ingimarsson JP, Krambeck AE. The effect of anticoagulation on bleeding-related complications following ureteroscopy. *Urology*. 2017;**100**:45–52.
19 Bhanot R, Pietropaolo A, Kallidonis TP, Skolarikos A, Keller EX, Cominck VD, et al. Predictors and strategies to avoid mortality following ureteroscopy for stone disease. A systematic revied from European Association of Urologists Sections of urolithiasis (EULIS) and Uro-technology (ESUT). *Eur Urol Focus*. 2022;**8**:598–607.
20 Roberts WW, Cadeddu JA, Micali S, Kavoussi LR, Moore RG. Ureteral stricture formation after removal of impacted calculi. *J Urol*. 1998;**159**:723–6.
21 Ortner G, Somani BK, Guven S, Katzbichler G, Traxer O, Giusti G, et al. Expert's recommendations in laser use for the treatment oof urolithiasis: a comprehensive guide by the European section of Uro-technology (ESUT) and training-research in urological surgery and technology (TRUST)-group. *World J Urol*. 2024;**42**:33.
22 Assoy MS, Jones PJ, Beisland C, Ulvik O. Temperature measurements during flexible ureteroscopic laser lithotripsy—a prospective clinical trial. *J Endourol*. 2024;**38**:308–15.
23 Sunaryo PL, May PC, Holt SK, Sorensen MD, Sweet RM, Harper JD. Ureteral strictures following ureteroscopy for kidney stone disease: a population-based assessment. *J Urol*. 2022;**208**:1268–75.
24 Xiong M, Zhu X, Chen D, Hossain MA, Xie Y, Guo X. Post ureteroscopic stone surgery ureteral strictures management: a retrospective study. *Int Urol Nephrol*. 2020;**52**:841–9.

Editorial Comment

Editorial Comment on Japanese survey of perioperative complications and ureteral stricture after ureteroscopy with laser lithotripsy for upper urinary tract stones in multicenter collaborative study

In this study, Inoue et al. have comprehensively catalogued the key adverse effects associated with ureteroscopy (URS) and laser lithotripsy among a sample exceeding 14 000 patients in Japan.[1] Rates of intra and postoperative complications were reported at 1.4% and 9.2%, respectively. The latter included fever (7.4%) and septic shock (0.8%). The successful execution of orchestrating data collection from 82 contributing centers should be highly lauded. The fruits of this collaborative labor is the development of real-world reference data at a national level. While URS has become the stone intervention of choice among many urologists worldwide, the associated morbidity burden cannot be overlooked. The reported mortality of 0.07% in this study reminds us that deaths related to kidney stones and their surgical removal *can* and *do* occur.[2] Therefore, while URS is commonly purported as a procedure of "no limits," there do exist certain patient groups, for example, extreme elderly where highly selective patient selection is critical. In a recent study of URS in patients ≥85 years, the overall complication rate was 47% while the mortality was 23% at 1 year.[3]

In the operation theater, it is imperative that the surgeon takes ownership of how their incorrect technique and improper use of equipment can potentially lead to complications. This is highly relevant for ureteral strictures, which Inoue et al. reported to have occurred in 0.8% of the study sample. Newer generation laser systems offer the option of high-power settings. While it can be tempting to select these automatically in the pursuit of zero residual fragments, care and caution is required. A recent prospective trial of intrarenal temperature during URS in a clinical setting found that the threshold for cellular thermal injury (43°C) was reached in as quickly as 12 s when 30 W was applied.[4] The argument for employing only lower settings during stone lithotripsy is therefore mounting. Currently, however, practice patterns for laser settings do vary widely and the large variation in company pre-settings likely fuels this further. While there are some recommendations among experts now available, more research is needed in order to determine what is truly considered safe. This needs to be complemented by further research into laser activation times and patterns. Debate and controversy also persist surrounding the relationship between ureteral access sheath use and ureteral stricture formation. The introduction of vacuum-assisted access sheaths will likely see use of sheaths heightened further in clinical practice.[5] Like with high-power settings, while their potential to increase stone free rate attracts most attention when they are discussed, it is important to not overlook their potential link to later stricture formation.

The findings from Inoue et al. therefore prompt us to reflect on how complications like strictures can occur and what steps

This is an open access article under the terms of the Creative Commons Attribution-NonCommercial-NoDerivs License, which permits use and distribution in any medium, provided the original work is properly cited, the use is non-commercial and no modifications or adaptations are made.

14422042, 2024, 7, Downloaded from https://onlinelibrary.wiley.com/doi/10.1111/iju.15469 by University Of British Columbia, Wiley Online Library on [26/10/2025]. See the Terms and Conditions (https://onlinelibrary.wiley.com/terms-and-conditions) on Wiley Online Library for rules of use; OA articles are governed by the applicable Creative Commons License

INTERNATIONAL JOURNAL OF
泌尿外科
国际泌尿外科杂志（2024）第4卷，795-801页 doi: 10.1111/iju.15466

Check for updates

原文
临床研究

一项多中心合作研究对激光碎石术治疗上尿路结石术后围手术期并发症及输尿管狭窄的日本调查

井上隆明，[1,2] 田中博和，[3]武田智子，[4]伊部明纪，[5]田村光弘，[6]冈田信介，[7] Terunobu Hou，[8] Ryoji Takazawa，[9] Hirofumi Izaki、[10] Shuzo Hamamoto [11]和Masato Fujisawa [2]

日本兵库县原泌尿外科及结石中心，[1,2]泌尿外科系、神户大学医学研究生院附属外科相关科、

3456789101111111111

随着更精细激光光纤的开发，日本的[2]灵活输尿管碎石系统逐渐从气动碎石系统升级为钬YAG激光器和铥光纤激光器，这些设备在灵活性、多功能性和易用性方面都有显著提升。[3]这类激光碎石设备对输尿管结石的治疗效果甚至优于肾结石。此外，灵活输尿管碎石系统的引入，也使得输尿管结石和肾结石的治疗适应症范围得到拓展。

因此，我们将这一时期称为“激光输尿管镜时代”，用于结石治疗。然而，随着新技术带来新发现和临床疗效的提升，也伴随着未知并发症和疗效差异等关键风险。本研究旨在调查日本采用钬YAG激光输尿管镜治疗上尿路结石术后近期并发症情况，并详细探讨术后输尿管狭窄的具体表现。

方法

研究设计和患者

本研究通过回顾性分析收集了经尿道碎石术（URS-L）治疗上尿路结石术后患者术中及术后并发症的相关数据。数据采集时间为2017年4月至2020年3月期间，由日本内镜泌尿外科与机器人学会（JSER）协助完成。该研究经神户大学机构审查委员会批准（编号B190331），所有参与机构均采用自愿退出机制获取患者知情同意。我们仅从各参与机构患者病历中提取了相关数据。

数据收集

我们从各医疗机构收集了输尿管镜术后早期并发症数据，涵盖术后1个月内发生的事件：输尿管镜下输尿管结石（URS-L）年发病率、输尿管穿孔数量、输尿管夹层数量、术中转为开放手术或腹腔镜手术的频率、发热（体温＞38℃）患者数量、脓毒性休克发生率、输血次数及肾包膜下血肿情况，以及死亡率。术后1个月确诊的输尿管狭窄病例被列为术后晚期并发症。此外，我们还收集了术后输尿管狭窄患者的特征数据，包括年龄、性别、体重指数（BMI）、术前肾积水状态、术前支架置入情况、结石位置、最大结石尺寸以及按亨氏单位（HU）计算的结石密度。

此外，我们系统收集了诊断方法、手术及临床疗效的相关数据，具体涵盖：诊断影像学检查、经尿道输尿管镜检查（URS-L）后输尿管狭窄的诊断时间、狭窄长度、狭窄部位、治疗方式及狭窄治疗成功率。同时，我们根据以下标准明确了特定并发症的界定：输尿管穿孔定义为累及输尿管壁全层的损伤，包括外膜层。腹膜后脂肪堆积；发热指体温超过38℃且在URS-L术后一个月内至少发生过一次相关手术；脓毒性休克指尽管输液仍存在低于65mmHg的不稳定平均血压，且与手术相关的感染状态有关；输尿管狭窄定义为术后CT或超声检查显示的更严重肾积水或与术前相当的肾积水。狭窄治疗的成功定义为术后肾积水较术前状况有所改善。

统计分析

本研究采用IBM SPSS Statistics 26版软件进行数据分析。回顾性临床数据中的连续变量和名义变量分别以中位数（带四分位距IQR）和频数（百分比）呈现。通过皮尔逊χ^2检验进行单因素分析，比较不同年份的并发症发生率。统计学显著性水平设定为双侧p值<0.05。

结果

2017年4月至2020年3月期间，82家医疗机构共对14 125名患者实施了上尿路结石的逆行性尿路镜碎石术（URS-L）。每年URS-L手术数量逐年递增，从2017年的4419例增至2018年的4760例，2019年达到4946例（图1）。总体并发症发生率为10.5%，其中术中并发症占1.40%，术后并发症占9.18%。术中并发症中输尿管穿孔、输尿管剥离和转为开放/腹腔镜手术的发生率分别为1.35%、0.03%和0.02%。术后早期并发症（输尿管镜术后1个月内发生）包括发热>38℃（7.44%）、脓毒性休克（0.81%）、输血（0.07%）、肾盂下血肿（0.05%）及死亡（0.04%）。术后晚期并发症输尿管狭窄的发生率为0.8%（表1）。术中和术后并发症的年发生率无显著差异（p=0.314和p=0.112；图2）。输尿管穿孔、发热、脓毒性休克和输尿管狭窄的年发病率也与年与年之间无显著差异（p=0.163、p=0.182、p=0.906和p=0.635；图3）。

在术后1个月确诊的108例输尿管狭窄病例中，68.4%的病例通过CT检查在输尿管镜检查后3个月内确诊（占42.5%），超声检查占17.5%。输尿管狭窄的中位长度为10.0毫米。最常见的狭窄部位是近端输尿管（38.8%），其次是远端输尿管（24.0%）和中段输尿管（22.2%）。治疗选择方面，经尿道球囊扩张术占比最高（54.6%），其次是观察治疗（22.2%）、输尿管吻合术（10.1%）和输尿管支架/肾造瘘术（10.1%）。输尿管狭窄治疗的总体成功率为54.6%。经尿道球囊扩张术是所有治疗手段中效果最佳的（见表2）。

©2024日本泌尿外科学会。

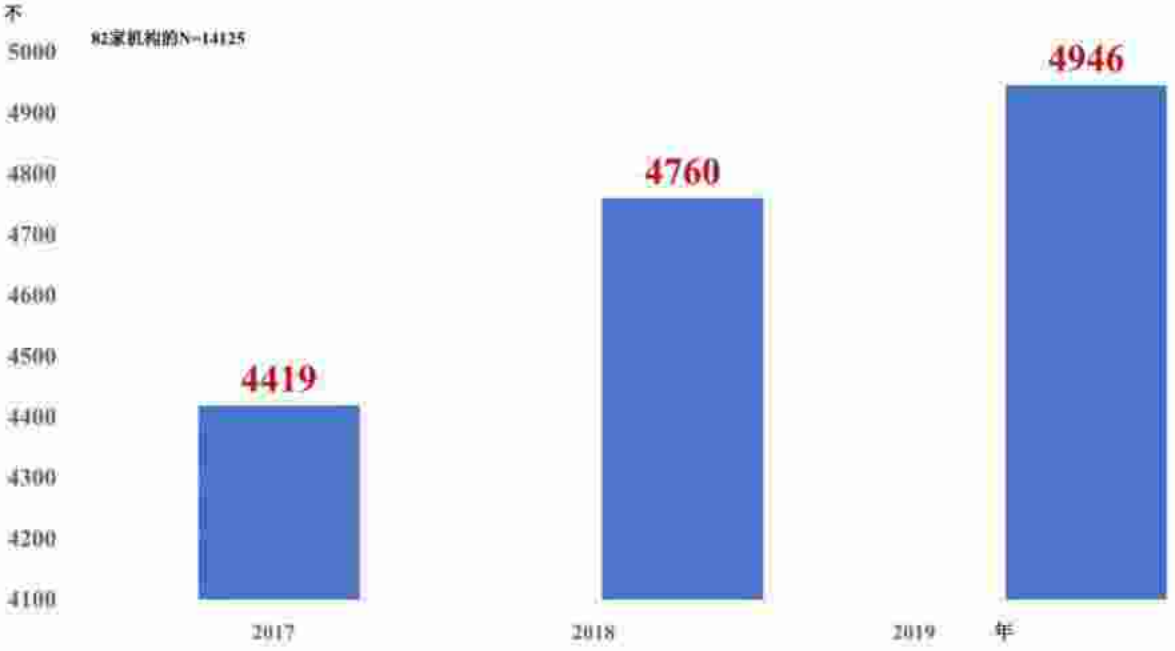


图1日本采用激光碎石术治疗上尿路结石的输尿管镜检查率

表1激光碎石输尿管镜术后并发症分析

总并发症率（n，%）	1496 (10.5)
术中并发症发生率（n，%）	199 (1.40)
输尿管穿孔	191 (1.35)
[illegible]	5 (0.03)
转为开腹/腹腔镜手术	3 (0.02)
术后早期并发症发生率（<1个月）（n，%）	1189 (8.41)
发热（>38℃）	1051 (7.44)
脓毒性休克	115 (0.81)
输血	10 (0.07)
腰肌上血肿	7 (0.05)
死亡率	6 (0.04)
术后晚期并发症（n，%）	108 (0.80)
输尿管狭窄	108 (0.80)

注：N=14125。

讨论

本次调查发现，日本每年上尿路结石（URS-L）病例数呈持续上升趋势。尽管总并发症发生率达10.5%，其中术中并发症占1.40%，术后并发症占9.18%，但术中与术后并发症的年发生率均未达到显著水平。
与往年相比有显著差异。

随着激光技术的广泛应用和柔性输尿管镜的创新，上尿路结石的外科治疗方式发生了显著变化。2014年，Ordon团队通过分析1991至2010年间194,781例肾结石治疗的行政数据库发现，经尿道输尿管镜（URS）的使用率从1991年的25%显著提升至2010年的59%，而经皮肾镜取石术（SWL）的使用率则从1991年的69%下降至2010年的34%。

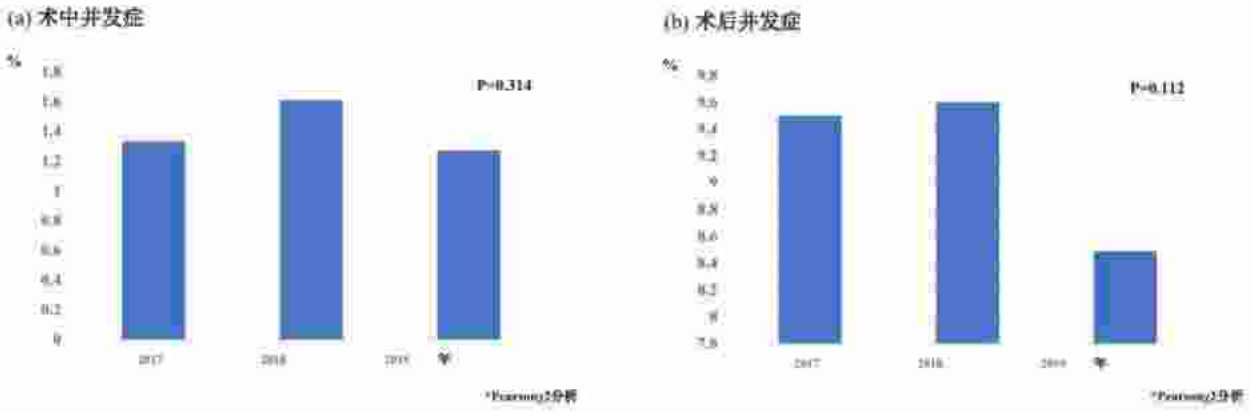


图2激光碎石联合输尿管镜检查的围手术期并发症发生率。(a)术中并发症。(b)术后并发症。

©2024日本泌尿外科学会。

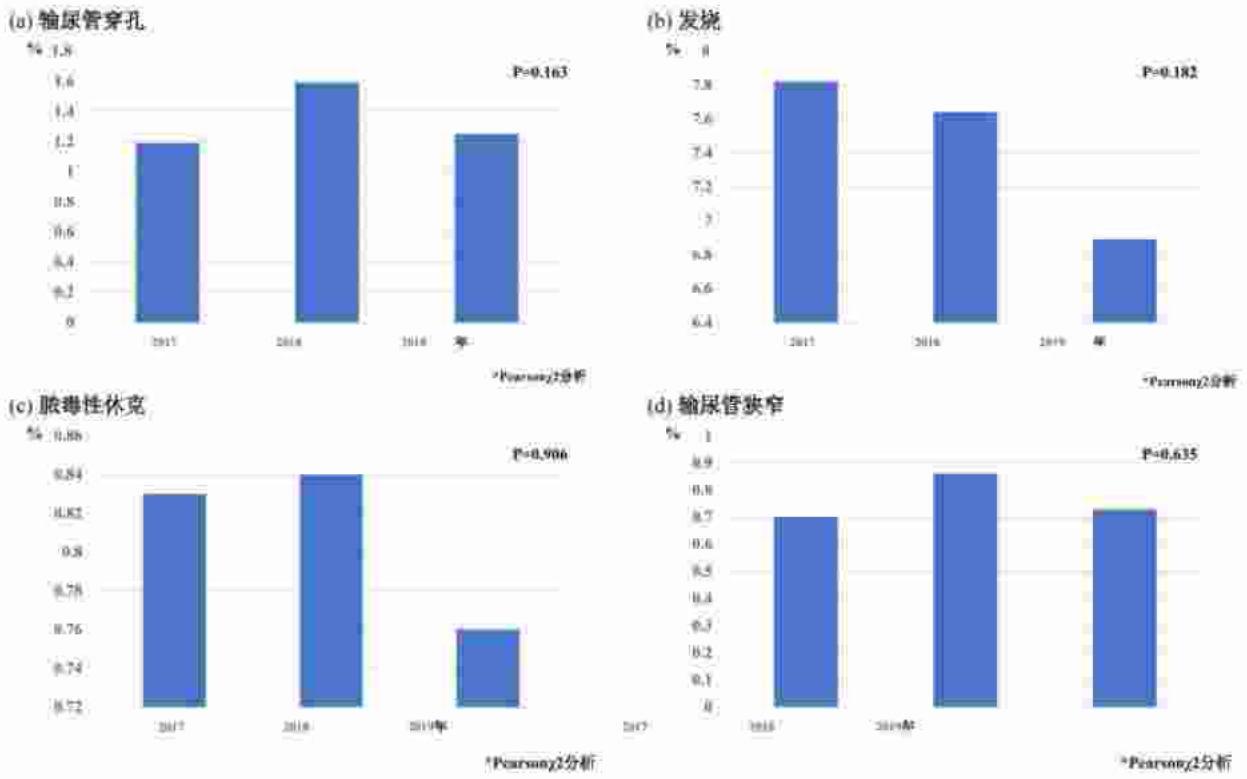


图3激光碎石输尿管镜检查术中及术后输尿管穿孔、发热、脓毒性休克和输尿管狭窄的主要并发症发生率。(a)输尿管穿孔，(b)发热，(c)脓毒性休克，(d)输尿管狭窄。

2010年，其数量低于URS。[4]此外，Herout等人显示，2006年至2019年间URS数量显著增加143%。[5]同样，Isotani等人在2019年报告称，日本URS使用量的年度趋势一直在增加，并且在2014年超过了每年进行的SWL数量。[2]

随着经尿道碎石术（URS）应用的日益普及，新型技术的引入可能引发更多并发症，从而增加围手术期并发症的发生率。欧洲泌尿外科学会（EAU）指南指出，URS术后总体并发症发生率为9%-25%，但多数并发症属于轻微范畴，无需手术干预。[6]根据内镜泌尿外科学会（CROES）临床研究办公室的全球研究数据显示，在11,885例患者中，并发症发生率为7.4%，其中术中并发症占4.2%，术后并发症占2.6%，术中术后并发症合计0.5%，且绝大多数为轻微并发症。但需注意的是，仍存在严重并发症的发生。[7]本研究对14,125例采用激光碎石术联合URS的患者进行分析，结果显示总并发症发生率为10.5%，其中术中并发症占1.40%，术后并发症占9.18%，该数据与另一项研究结果基本一致。但需要强调的是，本研究中仍存在严重并发症的发生。

输尿管穿孔作为极具破坏性的术中并发症，发生率在0.3%-7.4%之间，主要由输尿管镜手术中的尿道套管、激光发射、篮式电切操作及内窥镜本身引发。[8]当前该并发症的严重程度已通过内镜分级系统进行分类。Traxer等学者最初提出研究建议在使用输尿管套管时，术中应通过内镜对输尿管壁损伤进行分类。[9]此后，Schoentaler团队提出了术后输尿管镜损伤评分标准（Puls）。[10]根据Traxer分级系统，使用12/14F输尿管套管的病例中，13.3%出现累及肌层的输尿管壁损伤。[9]本研究中输尿管穿孔发生率相对较低，仅为1.35%。值得注意的是，尽管输尿管剥离术是输尿管镜检查中较为罕见的术中并发症（发生率0.04%-0.9%），但其危害性极高。[8]本研究中输尿管剥离术发生率为0.03%，这一比例并不低，因为上尿路结石本身属于良性病变。因此必须避免这种严重并发症。一旦发生输尿管剥离术，需立即进行修复，或分阶段实施修复。本研究中，仅有0.02%的患者因输尿管剥离术需要从经尿道输尿管镜手术转为开放手术或腹腔镜手术。

输尿管镜手术后发热是该手术常见的早期并发症，文献报道发生率介于0.2%至15%之间。[8]本研究数据显示，术后发热体温超过38℃的患者比例达7.44%。尿脓毒症作为严重并发症，其定义为泌尿生殖道感染引发危及生命的器官功能障碍，发生率在输尿管镜术后0.1%至4.3%之间。伴有脓毒性休克的[11]尿脓毒症发生率0.3%至4.6%，死亡率28.3-41.1%。[12,13]本研究中脓毒性休克的发生率为0.81%。

©2024日本泌尿外科学会.

表2激光碎石输尿管镜术后输尿管狭窄的临床特征与治疗效果

N=108（中位数，年，中位数，IQR）	63.0 (54.0-71.0)
性别（例，%）	M: 72 (66.6), F: 36 (33.3)
BMI（kg/m^2，中位数，IQR）	24.4 (22.1-27.2)
术前肾积水（例，%）术前输尿管	85 (78.7)
支架置入术（例，%）	31 (28.7)
结石位置（无，%）	
输尿管开口近端输尿	1 (0.9) 17
管中段输尿管近端输	(15.7) 23
尿管	(21.2) 47
	(43.5) 14
输尿管-肾盂连接处附	(12.9) 6
近	(5.5)
结石最大径（毫米，中位数，	10.2 (7.4-13.5) 1070.5
IQR），CT值（HU，中位数，IQR）	(781.5-1320.5)
输尿管镜检查后诊断的输尿管狭窄期	
POD 1个月	33 (30.5)
POD 1-3个月	41 (37.9)
POD 3-6个月	23 (21.2)
6-12个月POD	8 (7.4)
POD>12个月	3 (2.7)
诊断性影像学检查（例，%）	
CT	46 (42.5)
超声	19 (17.5)
IVP	1 (0.9)
RP	20 (18.5)
输尿管镜检查	19 (17.5)
其他	3 (2.7)
输尿管狭窄长度（mm，中位数IQR），10.0（5.0-17.0），狭窄部位分布（例数，%）	
输尿管口	2 (1.8)
输尿管壁间	26 (24.0)
中输尿管	24 (22.2)
近端输尿管	42 (38.8)
输尿管-盆腔连接处	14 (12.9)
输尿管狭窄治疗（例，%）	
经尿道球囊扩张术	59 (54.6)
输尿管狭窄切开术（开放或腹腔镜）11例（10.1）肾切除术	2
(1.8)	
输尿管支架或肾造瘘术置换11（10.1）	
观察结果	24 (22.2)
成功率（例，%）	
总计	59 (54.6)
经尿道球囊扩张术	37 (62.7)
输尿管尿路造口术（开放或腹腔镜）5例（45.4）	
输尿管支架或肾造瘘术置换11（100）	
观察结果	7 (29.1)

缩写：BMI，体重指数；HU，亨氏单位；IQR，四分位距；IVP，静脉肾盂造影；POD，术后日；RP，逆行肾盂造影。

经输尿管肾镜取石术后输血是该手术的早期并发症之一，发生率为1.3%-1.6%。[14,15]术中出血常由输尿管穿刺鞘或激光碎石导致的输尿管壁损伤、激光碎石引发的肾脏损伤，或因肾内高压导致的肾囊韧带破裂所致。此外，肾内高压、手术时间延长以及术中灌注压升高也是引发肾周囊下血肿的因素，其发生率为0.4%。
-2.2%的发病率。[16]患者继续服用抗凝剂或者在手术前使用的抗血小板药物通常在术中和术后继续出血。[17,18]在我们的研究中，有0.07%的患者接受了输血，0.05%的患者发生了包膜下血肿，这两者都比之前报道的相对较低。

尽管输尿管镜取石术是一种安全且微创的治疗手段，但仍有致死性并发症发生。根据欧洲泌尿外科学会泌尿系结石分会（EULIS）与泌尿技术分会（ESUT）最新发布的系统综述，Bhanot等学者的研究显示，在15项输尿管镜取石术（URS）相关研究中，共有72例患者死亡。在42例明确病因的病例中，死亡原因包括：脓毒症57.1%、多器官功能障碍14.2%、心脏相关并发症（如心肌梗死和心律失常）4.7%、出血性并发症4.7%，以及呼吸系统相关事件（如肺血栓栓塞）7.1%。[19]本研究显示URS术后死亡率为0.04%，这一数据与既往报道的发病率持平。

输尿管狭窄是术后晚期的主要并发症，发生率高达3%。

输尿管狭窄的定义是：在既往结石嵌顿部位出现输尿管局灶性狭窄，并通过IVP或历代逆行肾盂造影检查可明确显示输尿管肾积水。[20]然而，当前使用造影剂时应避免因术前解剖结构评估导致的造影剂过敏反应。此外，除结石手术前的结石嵌顿部位外，输尿管镜和碎石篮操作过度、激光照射遗漏、激光设置不当引发的热损伤以及结石残留等因素，都可能导致输尿管狭窄的发生。[21]因此，本研究将输尿管狭窄定义为术后出现比术前更严重的肾积水或等同程度的肾积水。特别值得注意的是，当将激光射入输尿管时，热损伤可能是术后输尿管狭窄的最新诱因之一。输尿管镜激光碎石术期间的肾内温度与激光功率设置直接相关。[22]本研究中输尿管狭窄发生率为0.8%。孙亚罗等学者曾报道，经尿道碎石术后2.9%的患者会出现输尿管狭窄。经尿道输尿管结石碎石术（URS）术后输尿管狭窄的成因可分为医源性因素和结石本身因素。医源性因素包括直接或间接热损伤导致的输尿管壁损伤、使用输尿管套管造成的黏膜缺血、黏膜内残留结石碎片，以及结石因素如结石嵌顿和结石大小。术后一旦形成输尿管狭窄，往往难以完全治愈。Sunaryo等学者基于人群研究数据显示：35%的狭窄病例需通过置入输尿管支架或经皮肾造瘘术进行引流，21%需内镜介入治疗，4.8%需输尿管重建，1.7%需单纯肾切除术。[23]本研究中术后狭窄干预方案如下：54.6%采用经尿道球囊扩张术，10.1%实施输尿管吻合术，1.8%进行肾切除术，10.1%更换输尿管支架或肾造瘘装置，22.2%采取观察治疗。手术成功率

©2024日本泌尿外科学会。

成功率取决于所采用的介入手术类型。Xiong等学者报告称，采用经尿道介入治疗输尿管镜术后输尿管狭窄的总体成功率为60.9%，但97.3%的患者需要接受重建手术。[24]在我们的研究中，输尿管狭窄完全缓解的总体成功率为54.6%，在所有介入治疗中，经尿道球囊扩张术和输尿管吻合术分别成功处理了62.7%和45.4%的病例。

本研究存在若干局限性。首先，作为主要局限，本研究数据采集自常年开展结石手术的成熟医疗机构，因此未纳入年手术量较少的机构。其次，我们仅收集了经尿道碎石术后（URS-L）的主要并发症数据，未纳入输尿管结石、术后疼痛及输尿管支架相关事件等次要并发症数据。第三，由于患者病历中未提供相关数据，我们无法分析输尿管结石与肾结石、刚性输尿管碎石术与柔性输尿管碎石术相关并发症的差异。第四，输尿管狭窄诊断采用超声与CT联合影像检查，术后1个月进行评估。部分病例术后2-3月可能出现肾积水缓解现象，为比较术前术后肾积水程度，我们采用超声与CT的联合影像评估。尽管如此，据我们所知，这是
首份报告中已报告术中及术后发生率
经尿道碎石术后出现上尿路结石并发症
在日本。此外，我们还评估了术后并发症的发生率。
我曾患有输尿管狭窄。总之，尽管随着技术进步，日本对URS-L的应用有所增加
尽管取得进展，但年并发症率仍居高不下
尽管URS-L是一种实用且微创的手术，但仍会出现严重并发症。因此，需谨慎管理URS-L，以避免进一步进行侵入性操作。

致谢

我们谨向日本82家合作机构致以诚挚谢意，感谢他们为数据收集与合作付出的辛勤努力。

作者贡献

井上隆明：概念化；方法论；软件；数据管理；正式分析；调查；项目管理；撰写初稿。田中博和：数据管理。正田智子：数据管理。伊部明纪：
数据管理。Mitsuhiro Tambo：数据管理。Shinsuke
冈田：数据管理；撰写—审阅与编辑。Teru
Hou：数据管理。高泽良二：数据管理。
Izaki Hirofumi：数据管理。Hamamoto Shuzo：数据管理；撰写—审阅与编辑。Fujisawa Masato：撰写—审阅与编辑。

利益冲突声明

无声明。

研究批准
机构制定的协议
评审委员会

是（否。B190331）。

知情同意

是，因为在我院实行了选择退出机制。

注册表和注册号
研究/试验的

N/A.

动物研究

N/A.

资金信息

就目前情况而言，我们没有相关的资金
文章

参考文献

1 Sakamoto S, Miyazawa K, Yasui T, Iguchi T, Fujita M, Nishimatsu H, 等.日本上尿路结石流行病学特征的时序变化.国际泌尿学杂志.2018;25:373-8.
2 Isotani S, Noma Y, Wakumoto Y, Muto S, Horie S.日本上尿路结石的内镜治疗趋势——基于日本诊断程序组合数据库的研究。《国际泌尿学杂志》2019;26：1007-8。
3 Rosette JD, Denstedt J, Geavlete P, Keeley F, Matsuda T, Pearle M, 等.内镜外科学会输尿管镜全球研究的临床研究办公室:11,885例患者的适应症、并发症及结局。《内镜外科学杂志》2014;28:131-9.
4 Ordon M, Urbach D, Mamdani M, Saskin S, D 'A Honey RJ, Pace KT.肾结石的外科治疗：基于人群的时间序列分析。J Urol.2014；192：1450-6.
5 Herout R, Baumacke M, Groeben C, Aksoy C, Volkmer B, Schmidt M, et al.2006至2019年德国全人群分析显示：上尿路结石的当代治疗趋势——冲击波碎石术会退出历史舞台吗？《世界泌尿学杂志》2022;40:185-91。
6 Skolarikos A, Jung H, Neisius A, Petrik A, Somani B, Tailly T, 等.EAU关于尿路结石的指南:输尿管镜检查的并发症.2023:21.
7 Somani BK, Giusti G, Sun Y, Osther PJ, Frank M, De Sio M, et al.肾结石治疗中输尿管镜检查（URS）相关并发症：内镜外科学会URS全球研究的临床研究办公室。World J Urol.2017；35：675-81.
8 De Coninck V, Keller EX, Somani B, Giusti G, Proietti S, Rodriguez-Socarras M, et al.输尿管镜检查并发症:全面综述.世界泌尿外科杂志.2020;38:2147-66.
9 Traxer O, Thomas A.逆行性肾内手术中置入输尿管导管所致输尿管壁损伤的前瞻性评估与分类.J Urol.2013；189：580-4.
10 Schoenthaler M, Buchholz N, Farm E, Ather H, Bach C, Bach T, et al.尿道镜术后损伤评分量表（Puls）：基于多中心前瞻性评分者间可靠性评估。《世界泌尿外科杂志》2014；32：1033-40。
11 Singer M, Deutschman CS, Seymour C, Shankar-Hari M, Annane D, Bauer M, et al.第三版国际共识定义脓毒症和脓毒性休克定义（Sepsis-3）.JAMA.2016；315：801-10.
12 Corrales M, Sierra A, Doizi S, Traxer O.肾后入路手术的感染风险：文献综述。Eur Urol Open Sci.2022；30：84-91.
13 Wagenlehner FME, Lichtenstern C, Rolfes C, Mayer K, Uhle F, Weidner W, 等.尿脓毒症的诊断与治疗.国际泌尿学杂志.2013;20:963-70.

©2024日本泌尿外科学会.

14 卡斯特拉尼D，特拉克塞O，拉古雷D，加诺南AB，摩斯特凡诺V，加泰都克N，等.著在真实临床实践中改进间断双侧输尿管镜检查治疗肾结石的疗效——基于1250例患者全球多中心经验的实践启示。《欧洲泌尿外科开放科学》2023；30：51-9。
15 法亚德MK，费赫莱O，阿布勒扎塔斯KM，萨拉马NM.进行肾内手术与经皮肾镜碎石术治疗直径超过2厘米肾盂结石的对比：一项前瞻性随机对照试验。《泌尿系统结石》2022；50：113-7。
16 Bai J, Li C, Wang S, Liu J, Ye Z, Yu X, et al.泌尿系统激光碎石术后肾盂下盏肿.BJU Int.2012;109:1230-4.
17 韦斯特曼ME，莫尔马V，斯凯尔斯J，吉尔曼DJ，莫格马拉JP，克拉姆贡克AE。抗血小板药物对输尿管镜检查后出血相关并发症的影响。《泌尿内镜杂志》2016；30：1073-8。
18 韦斯特曼ME，斯凯尔斯J，莫尔马V，吉尔曼DJ，莫格马拉JP，克拉姆贡克AE。抗凝治疗对输尿管镜检查后出血相关并发症的影响。《泌尿外科》2017；100：45-52。
19 Bhanot R, Pietropaolo A, Kallidonis TP, Skliarikas A, Keller EX, Connick VD等学者。输尿管镜检查后死亡率的预测因素与预防策略关于肾结石的系统性综述，由欧洲泌尿外科学会发布
输尿素结石（EULIS）与泌尿科技（ESUT）研究综述。《欧洲泌尿学焦点》2022年第8卷第598-607页。
20 罗伯茨WW，卡德拉JA，米卡帕S，卡沃西LR，摩尔RG。结石排出后输尿管狭窄形成。《泌尿学杂志》1998；159：723-6。
21 费特纳G，索马尼BK，古艾S，基茨比希斯G，特拉克塞O，塞斯蒂G等。《激光治疗泌尿系结石专家指南：欧洲泌尿技术分会（ESUT）与泌尿外科技术培训研究（TRUST）小组联合编撰》。《世界泌尿学杂志》2024年第42卷第33页。
22 Aesoy MS, Jones PJ, Beisland C, Ulvik O.柔性输尿管镜激光碎石术中的温度监测——一项前瞻性临床试验。《泌尿内镜杂志》2024；38：308-15。
23 Sunaryo PL, May PC, Holt SK, Sorensen MD, Sweet RM, Harper JD.肾结石输尿管镜检查后输尿管狭窄：一项基于人群的研究。《泌尿学杂志》2022，208：1268-73。
24 唐梦、王琨、陈丹、位雅国*马、谢毅。弓旭.输尿管镜下输尿管结石术后狭窄的处理：回顾性研究.国际泌尿与肾脏病学杂志.2020；52：841-9.

编辑评论

多中心协作研究中日本对输尿管镜联合激光碎石术治疗上尿路结石围手术期并发症及输尿管狭窄的调查编辑评论

在本研究中，井上团队对日本超过14,000名患者的输尿管镜检查（URS）和激光碎石术相关主要不良反应进行了全面统计。术中并发症发生率为1.4%，术后并发症发生率为9.2%，后者包括发热（7.4%）和脓毒性休克（0.8%）。82家合作中心协同完成数据收集的高效运作值得高度赞扬。这项协作成果构建了国家级真实世界参考数据。尽管输尿管镜检查已成为全球泌尿科医生首选的结石干预手段，但其伴随的并发症负担不容忽视。本研究报道的0.07%死亡率提醒我们，与肾结石及其手术切除相关的死亡确实可能发生。[2]因此，虽然输尿管镜检查常被誉为“无限制”的手术，但某些特定患者群体（如高龄患者）仍需严格筛选。近期一项针对85岁以上患者的研究显示，输尿管镜检查的总体并发症发生率达47%，1年死亡率达23%。[3]

在手术室中，外科医生必须对自己的错误操作负责。设备使用不当可能引发并发症，这一点在输尿管狭窄治疗中尤为关键。井上团队的研究数据显示，该病症在样本中发生率高达0.8%。新一代激光系统具备高功率调节功能，虽然追求零残留碎石时可能倾向于自动选择高功率，但必须保持谨慎。近期一项临床研究发现，当使用30瓦功率进行输尿管碎石术时，仅需12秒即可达到细胞热损伤阈值（43°C）。[4]因此，主张在碎石术中优先选择低功率的呼声日益高涨。然而当前激光功率的临床实践差异显著，不同厂商预设参数的差异可能加剧这种不一致性。尽管专家已提出部分建议，但要确定真正安全的功率阈值仍需更多研究。同时，关于激光激活时长和模式的研究也应同步推进。关于输尿管套管与输尿管狭窄形成的关系，学界至今仍存在争议。随着真空辅助输尿管套管的引入，这类器械在临床应用中的使用频率预计将进一步提升。[5]与高功率设备类似，虽然这类器械在提高无结石率方面的潜力最受关注，但其可能引发的术后狭窄风险同样不容忽视。

因此，井上等人研究结果促使我们思考狭窄等并发症的形成机制及应对措施。

本文为知识共享署名-非商业性使用-禁止演绎许可协议下的开放获取文章，允许在任何媒介中使用和传播，但需满足以下条件：正确引用原始作品、非商业用途且不作任何修改或改编。

©2024作者版权所有。《国际泌尿学杂志》由约翰·威利父子出版公司旗大利亚有限公司代表日本泌尿外科学会出版。

Asian Journal of Urology 12 (2025) 23–32

Available online at www.sciencedirect.com

ScienceDirect

journal homepage: www.elsevier.com/locate/ajur

Review

Factors affecting the thermal effects of lasers in lithotripsy: A literature review

Kiron Krishnaprasad*, **Ravi Teja Pathi**, **Mustafa Nazar**

Department of Urology, Government TD Medical College, Vandanam, Alappuzha, Kerala, India

Received 26 July 2023; accepted 31 October 2023
Available online 23 April 2024

KEYWORDS
Stone disease;
Laser lithotripsy;
Irrigation;
Thermal effect;
Operator duty cycle

Abstract *Objective:* The use of lasers has been an important part of urology in the treatment of stone and prostate disease. The thermal effects of lasers in lithotripsy have been a subject of debate over the years. The objective of this review was to assess the current state of knowledge available on the thermal effects of lasers in lithotripsy, as well as explore any new areas where studies are needed.

Methods: In August 2022, a keyword search on Google Scholar, PubMed, and Scopus for all papers containing the phrases "thermal effects" AND "laser" AND "lithotripsy" AND "urology" was done followed by citation jumping to other studies pertaining to the topic and 35 relevant papers were included in our study. The data from relevant papers were segregated into five groups according to the factor studied and type of study, and tables were created for a comparison of data.

Results: Temperature above the threshold of 43 °C was reached only when the power was >40 W and when there was adequate irrigation (at least 15–30 mL/min). Shorter lasing time divided by lithotripsy time or operator duty cycles less than 70% also resulted in a smaller temperature rise.

Conclusion: At least eight factors modify the thermal effects of lasers, and most importantly, the use of chilled irrigation at higher perfusion rates, lower power settings of <40 W, and with a shorter operator duty cycle will help to prevent thermal injuries from occurring. Stones impacted in the ureter or pelvi-ureteric junction further increase the probability of thermal injuries during laser firing.

© 2025 Editorial Office of Asian Journal of Urology. Production and hosting by Elsevier B.V. This is an open access article under the CC BY-NC-ND license (http://creativecommons.org/licenses/by-nc-nd/4.0/).

* Corresponding author.
E-mail address: kironkrishnaprasaduro@gmail.com (K. Krishnaprasad).
Peer review under responsibility of Tongji University.

https://doi.org/10.1016/j.ajur.2024.04.002
2214-3882/© 2025 Editorial Office of Asian Journal of Urology. Production and hosting by Elsevier B.V. This is an open access article under the CC BY-NC-ND license (http://creativecommons.org/licenses/by-nc-nd/4.0/).

1. Introduction

Laser is an acronym for "light amplification by stimulated emission of radiation". In 1968, Mulvaney and Beck [1] published a study on the fragmentation of calculi using a ruby crystal laser, which was one of the first studies in laser lithotripsy. The use of lasers has been an important part of urology in the treatment and management of stone diseases and benign prostatic hyperplasia especially after the 1980s. The urological community would benefit from a review article that provides an overview of the current state of knowledge on the thermal effects of lasers, as well as identifies potential new areas of research that require further investigation. Also, the safety of the long-term use of lasers on injury to the pelvicalyceal system and the ureters as well as the factors that may lead to causation of this photothermal injury is not well documented and requires further detailed studies.

During laser lithotripsy, the operator can modify three factors to achieve the necessary effect of stone fragmentation: pulse energy (J), pulse frequency (Hz), and pulse duration (μs). Any changes in energy and frequency can change the power (W), and higher power results in higher temperatures and therefore thermal damage [2]. This thermal damage occurs as a result of the photothermal effect of lasers leading to absorption of the heat energy by the surrounding tissue [3].

Temperature measured using thermocouples placed near the laser probe has been the surrogate used in various experimental studies to extrapolate on safety of *in vivo* laser use. Sapareto and Dewey [4] proposed a "time–temperature relationship" for tissue thermal damage stating that for every 1 °C exceeding the "threshold (43 °C)", the time required to cause damage to the same number of cells will decrease by half. For example, when the tissue is in a 45 °C environment for 15 s, the degree of thermal damage to cells is similar to that at 44 °C for 30 s or 43 °C for 1 min. Most of the articles in this review used this temperature threshold as the standard for assessing the thermal end point.

A long-term sequela of thermal injury of particular concern is that of ureteral strictures. It was found to be approximately three times more common in patients treated by laser lithotripsy over pneumatic lithotripsy in a meta-analysis study [5]. However, a prospective study published in 2019 found that the incidence rate was quite low (1.5%) and seen mostly in the presence of stone impaction [6]. Whether this result was due to an increase in the local temperature or direct injury to the surrounding tissue could not be determined. This is an area of interest which may need further investigation and can be considered for future studies.

The objectives of this review article were to study the following questions in relation to lasers in lithotripsy.

i. What were the factors affecting the thermal effects of lasers on non-target tissue during lithotripsy?
ii. Was the thermal injury to non-target tissue during laser lithotripsy significant?
iii. What were the areas that need further investigation to prevent laser-related injuries?

2. Materials and methods

In August 2022, a keyword search on Google Scholar, PubMed, and Scopus for all papers containing the keywords "thermal effects" AND "laser" AND "lithotripsy" AND "urology" was done in various combinations, followed by citation jumping to other studies pertaining to the topic. All accepted and published English language full articles were studied and filtered wherein articles not pertaining to the aims of our review were excluded by reading the title, abstract, and full article. Thirty-five relevant papers were included in our study and the findings are presented as a narrative literature review.

There were several factors that stood out while the review was conducted and they were segregated into five groups according to the factor studied and type of study, and tables were created for a comparison of data.

3. Results

3.1. Irrigation

The majority of the studies were done on irrigation (its presence or absence, with irrigation pump or only gravity, and chilled or warm). Out of 12 studies, two were *in vivo* in sheep or pig [7,8], two were *ex vivo* [9,10], while the remaining eight [2,11–17] were *in vitro* studies. They all used thermocouples for measuring the temperature but the placement of the probe was inconsistent among the studies. An average distance of 0.5 mm from the laser tip is ideal corresponding to the depth of penetration of holmium:yttrium-aluminium-garnet (Ho:YAG) laser in the water medium [18].

One of the first laser thermography study was conducted in 2015 by Molina et al. [9], where two *ex vivo* models (clinical model and open ureteral model) were studied for temperature rises during Ho:YAG laser with 365 μm firing at 10 W (1 J/10 Hz). They showed an increase in the temperature during laser activation and that ureteral thermal values decreased with saline irrigation. This was further cemented in 2016 by Butticè et al. [11], when they compared 200 μm with 272 μm fibers in a bench model inserted into a saline-filled heating tank at two temperatures (room 24.5 °C and body 36.5 °C). They found that when the irrigation was open, the maximum temperature limit was never reached. Dau et al. [8,16] conducted studies *in vivo* (in 2022) and *in vitro* (in 2021), respectively, most importantly studying the effect of chilled irrigation on caliceal fluid temperatures and the laser heating of fluid with and without stone ablation. They showed that the temperature rise and thermal dose during lithotripsy, especially at higher power were reduced by using chilled irrigation at 1 °C as compared to room temperature irrigation at 19 °C.

More studies since then have come to similar conclusions in various different settings as enumerated in Tables 1 and 2, and the general consensus was that irrigation is essential during laser activation preferably at higher flow rates and higher pressure. Most studies showed a temperature beyond the threshold of 43 °C, only at higher power settings (≥40 W), and the power of the laser must be regulated to stay below the threshold. One article also showed that high

Table 1 Studies pertaining to irrigation with the holmium:yttrium-aluminium-garnet laser.

Study	Study subject	Laser fiber used (μm)	Lasing time	Power setting (W or J/Hz)	Irrigation setting	Temperature recorded (°C)	Mode of temperature measurement
Molina et al., 2015 [9]	Ovis aries	365	NA	1/10	• With • Without	• 37.4±2.5[a] • 49.5±2.3[a]	• Temperature on external surface using infrared Fluke Ti55 Thermal Imager
Butticè et al., 2016 [11]	Bench model with saline heating tank	200 or 272	Stopped when a limit reached	0.5/20, 1/10, 2/5, 3/5, or 4/5	• With or without	• Threshold surpassed when irrigation not used	• Endotracheal thermometer inside the model
Aldoukhi et al., 2017 [12]	Glass test tube	200	1 min	(0.5–1)/(10–80)	• 0, 7–8, 14–15, or 38–40 mL/min	• Max 70.3±2.7° at 40 W, no irrigation	• Thermocouple placed 5 mm from bottom of the test tube
Aldoukhi et al., 2018 [7]	Pig	242	1 min	0.5/80	• 0.1, 15, or 40 mL/min	• 0.1 mL/min: 84.8 • 15 mL/min: 63.9 • 40 mL/min: 43.6	• Thermocouples in calyx, by open exposure, puncture, and retrograde beside the scope
Wollin et al., 2018 [2]	PVC tubing	200	1 min	(0.2–1)/(6–50)	• 0, 50, or 100 mL/min	• 0 mL/min: >100 • 50 mL/min: >43.4 • 100 mL/min: 30.7	• Probe tip thermometer placed 1 mm from tip of fiber
Hein et al., 2018 [13]	20 mL test tube in water bath	272 or 940	2 min	0.5/33, 1/18, 1.5/30, 2/2, or 4.5/(4.12, or 22.3)	• 0–100 mL/min	• Max 68 at 100 W	• Thermocouple in the test tube and water bath
Winship et al., 2019 [17]	Saline bag with reservoir	365	45 s	(0.2–1)/(6–80)	• 0, 100, or 200 mmHg	• Threshold >6 rose at 100 mmHg and below	• Thermocouple placed adjacent to the fiber
Hein et al., 2020 [10]	Porcine kidney in water bath	272, 550, or 940	1min	5–100 W	• 0–100 mL/min	• Critical temperature rose above 30 W	• Three thermocouples in kidney with one flexible thermocouple placed 4 mm proximal to fiber
Ghanim et al., 2020 [14]	Water tank with PVC pipe	365	70 s	(0.375, 0.675, or 1)/20	• 0, 1, 10, or 30 mL/min	• Max 70 at high power and closest to thermometer	• Thermometer in one end of the PVC tube
Liang et al., 2020 [15]	Ligated F20 rubber tube	200	3, 5, or 10 s	(0.5, 1, 1.5, 2, or 3)/(10 or 20)	• 10, 15, 20, or 30 mL/min	• Max 78 at 30 W power at 10 mL/min	• Thermocouple 5 mm from bottom of the tube

(*continued on next page*)

Table 1 (*continued*)

Study	Study subject	Laser fiber used (μm)	Lasing time	Power setting (W or J/Hz)	Irrigation setting	Temperature recorded (°C)	Mode of temperature measurement
Dau et al., 2021 [16]	Glass test tube in water bath	242	1 min	0.5/80	• Chilled irrigation at 1 °C and room temperature at 19 °C at 0, 8, 12, 15, or 40 mL/min	• Threshold temperature delayed in chilled	• Wire thermocouple 3 mm proximal to the ureteroscope tip
Dau et al., 2022 [8]	Female Yorkshire pig	242	1 min	NA	• Chilled irrigation at 1 °C to 4 °C and room temperature at 19 °C at 0–40 mL/min	• Threshold temperature delayed in chilled	• Thermocouple fixed 5 mm from the ureteroscope tip

Max, maximum; NA, not available; PVC, polyvinyl chloride.
* Mean±standard deviation

energy (3.0 J) and low frequency (10 Hz) mode has slightly less thermal damage than its counterpart settings at the same power [15] and needs further evaluation.

The use of ureteric access sheath (UAS) and its effect on the intrarenal temperature were also studied by one group [19]. They found that the UAS decreases intrarenal temperatures at a power setting of 20 W, when compared with not using one. At a power setting greater than 40 W, however, the protective effect was lost and only remedied by increasing irrigation rates [19]. This study also compared the use of the manual pump with the gravity pump for irrigation, and observed that the dangerous threshold temperature was never reached with the manual pump (0.33 pumps/s), but the temperature rise was detrimental at the higher power of >40 W with the gravity pump. Therefore, this indicates that the manual pump could be preferred over the simple gravity irrigation.

3.2. Type of laser

Apart from the Ho:YAG laser, another laser being used frequently recently in lithotripsy is the thulium:YAG (Th:YAG) laser. Since the Th:YAG (2000 nm) laser has a slightly lesser wavelength compared with the Ho:YAG (2140 nm), the depth of penetration is also less. The power efficiency of Th:YAG laser is also said to be five times more than the Ho:YAG laser [18]. But the main advantage during lithotripsy for the Th:YAG is that it is a continuous wave laser, which is better suited for tissue ablation; to overcome this, a thulium fiber laser (TFL; 1940 nm wavelength) was introduced, which was a thulium ion laser with semiconductor diodes instead of a flash pump [20]. This TFL had both the continuous and pulsed wave modes.

The major aspects of studies comparing the Ho:YAG with thulium laser have been summarized in Table 3. In 2016, Kallidonis et al. [21,22] performed two separate studies to evaluate the effect of the Th:YAG laser when compared with Ho:YAG laser. One was *ex vivo* in the porcine upper urinary tract, while the other was an *in vitro* model. They showed comparable results in both studies while studying the temperature rises using both lasers, and concluded that up to 20 W Th:YAG laser was a safe alternative to the Ho:YAG laser, with adequate irrigation. Similar results were obtained by Taratkin et al. [23] and Peng et al. [24] when comparing the Ho:YAG laser with the TFL, finding that irrigation reduced the respective temperatures in the same manner for both lasers.

More recently, Molina et al. [25] compared the temperature rise seen during the super pulse TFL versus the high power Ho:YAG laser during dusting and fragmenting separately in *ex vivo* porcine kidneys. The intra-luminal temperature rise during laser activation was equivalent during dusting and higher in the super pulse TFL during fragmentation, but neither reached the threshold for thermal injury based on the duration of exposure. Therefore, there seems to be a risk of an increased temperature rise with a TFL during fragmentation, but it warrants further investigation.

3.3. Operator duty cycle (ODC) and pedal time

The ODC indicates the ratio of "on/off" of the laser power. The higher the "duty", the higher the ratio of "on"

Table 2 Inferences from the irrigation studies.

Study	Inference
Molina et al., 2015 [9]	• The study was one of the first studies that showed an increase in the temperature during laser activation and that ureteral thermal values decreased with saline irrigation
Butticè et al., 2016 [11]	• Rapid increases of temperature must be avoided when irrigation is closed and water at lower temperatures during irrigation helped delay the rise of temperature
Aldoukhi et al., 2017 [12]	• The highest temperature seen with 1 J/40 Hz power and no irrigation, counter measures for same can be exploited by urologists
Aldoukhi et al., 2018 [7]	• Thermal damage threshold reached in no and medium irrigation but not in high irrigation, so high-power lasers pose a threat for thermal damage at lower irrigation rates
Wollin et al., 2018 [2]	• Despite increasing laser settings, adequate irrigation can maintain relatively stable temperatures within an *in vitro* ureteral system
Hein et al., 2018 [13]	• Laser devices should, therefore, always be applied in conjunction with continuous, closely monitored irrigation whenever performing holmium:yttrium-aluminium-garnet laser lithotripsy
Winship et al., 2019 [17]	• High temperatures were achieved in as little as 1 s at common irrigation pressure and laser settings, particularly with a flexible ureteroscope and power ≥10 W; however, with laser cessation, temperatures quickly returned to a safe level at each irrigation pressure
Hein et al., 2020 [10]	• A formula to calculate the approximate ΔT for irrigation rates ≥30 mL/min was developed: $\Delta T = 15\ K \times$ (power [W]/irrigation [mL/min])
Ghanim et al., 2020 [14]	• All three parameters (pulse energy, irrigation rate, and distance) showed highly significant effect on measured temperatures; the holmium:yttrium-aluminium-garnet laser might be safely provided when there was sufficient irrigation with optimal selected laser power
Liang et al., 2020 [15]	• Safe temperature of laser firing can be ensured at laser power less than 10 W, irrigation greater than 30 mL/min, and high-energy low-frequency firing
Dau et al., 2021 [16] and Dau et al., 2022 [8]	• Chilled irrigation slows temperature rise, decreases plateau temperature, and lowers thermal dose during high-power laser lithotripsy

compared with "off", and therefore, it gives more output energy. The 100% ODC means continuous on, which is the continuous wave cutting [26]. In the setting of lithotripsy, it may be calculated as lasing time divided by lithotripsy time.

In 2021, Aldoukhi et al. [27] performed *in vitro* tests, wherein 1200 J of laser energy was applied in five different patterns at 20 W average power for 60 s. The mean ODC was 32% overall among the five patterns and the mean time of pedal activation was 3.6 s. *In vitro* studies revealed a longer pedal activation time produced a higher peak temperature and thermal dose. Louters et al. [28] in 2022, conducted a similar study to determine the effect of the ODC on the thermal dose delivered. A higher ODC resulted in a greater maximum temperature and thermal dose, with an ODC ≥70% exceeding the threshold of 43 °C. Use of a 50% ODC compared with 60% of the ODC resulted in a ten-fold increase in time required to reach the threshold of thermal injury and an eight-fold increase in maximal allowable energy. These studies fortify the statement that judicious laser ODC control can help to prevent thermal damage from lasers.

3.4. *In vivo* studies

One of the only *in vivo* studies was conducted in patients undergoing ureteroscopy laser lithotripsy for stone disease in China in 2019 by Wang et al. [29]. A total of 30 patients (16 males and 14 females) with a mean age of 47.4 (standard deviation 13.7) years, and a mean calculi diameter of 14.2 (standard deviation 8.1) mm, undergoing ureterorenoscopic lithotripsy were studied. A temperature measurement guidewire was inserted and extended slightly beyond the ureteroscope, while the other end was connected to a thermometer that fed real-time temperature change data to a computer.

The highest temperatures in the 30 sets of data were all higher than 43 °C (100%), with 19 sets (63.3%) having peak temperatures higher than 56 °C. This study showed that with the increase in the power of the holmium laser, or with impacted calculi, the increase in the temperature of the lavage solution around the calculi was even greater, often exceeding the temperature that could be safely tolerated by the tissue; therefore, temperature might be one of the factors that caused ureteral thermal injury and resulted in postoperative strictures [24]. However, the study by Wang et al. [29] was not without limitations as it only studied the thermal effect with respect to the laser power, and also the surgeon was different for each case, which meant the laser settings, time of lasing, and intraoperative conditions were different for each case.

3.5. Other factors like volume and pulse duration

In 2022, Dau et al. [30] performed an *in vitro* study keeping the laser fiber above the stone at 3.5 mm (no ablation) and 0.5 mm (ablation), and the temperature of the fluid was recorded using two thermocouples once per second, to determine the percentage of applied laser energy that is converted to heat and the percentage used for stone ablation. They found that even under conditions of energy-efficient stone ablation, the majority of applied laser energy (91%–96%) was converted to heat [30]. The pelvicalyceal volume in which laser activation occurs was also later found to be an important factor in the thermal effects caused

Table 3 Studies pertaining to the type of lasers.

Study	Study subject	Laser studied	Laser fiber diameter or type	Lasing time	Power settings (W), energy (J)/frequency (Hz)	Irrigation setting	Temperature recorded (°C)
Kallidonis et al., 2016 [21]	Pig	Ho:YAG *vs.* Th:YAG	Continuous wave	NA	• 10 W, 20 W, 30 W, or 40 W	• With	• 33.5
Kallidonis et al., 2016 [22]	Burette with a stopcock and a 40 mL vessel	Ho:YAG *vs.* Th:YAG	Both pulsed and continuous waves	10 min	• 5 W, 10 W, 20 W, 50 W, or 100 W	• Without	• 45.6–68.7
Taratkin et al., 2020 [23]	*In vitro* model	Ho:YAG *vs.* SP TFL	200 μm	1 min	• 40 W, 0.2 J	• 0 or 35 mL/min	• Temperature reduction after irrigation - Ho:YAG: 2.6 - TFL: 1.9
Peng et al., 2020 [24]	Test tube in water tank	TFL	Continuous wave	1 min	• Different settings up to 30 W	• 0, 15, 25, or 50 mL/min	• 0 and 15 mL/min: more than 6.5 °C rise above threshold seen; 25 and 50 mL/min: no rise of temperature over threshold
Molina et al., 2021 [25]	Porcine kidney	Ho:YAG *vs.* SP TFL	200 μm	5 s each for 15 times	• Ho:YAG dusting: 0.3 J/70 Hz; SP TFL dusting: 0.1 J/200 Hz; fragmenting: 0.8 J/8 Hz	• With	• During fragmenting setting - Ho:YAG: 30 - SP TFL: 33.3 • During dusting setting - Ho:YAG: 35.8 - SP TFL: 40.6

Ho:YAG, holmium:yttrium-aluminium-garnet; Th:YAG, thulium:yttrium-aluminium-garnet; TFL, thulium fiber laser; SP, super pulse; NA, not available.

by lasers [31]. The authors found that the volume of fluid in each model was inversely related to the extent of temperature elevation. Therefore, the thermal dose in laser firing reached the threshold for injury faster in smaller volumes. Louters et al. [32] performed a study to determine the volume of fluid mixing during laser activation in a plastic tube with dyed irrigation by evaluating the distance travelled by the dyed fluid during laser activation. The volume of total fluid mixing within the ureter model was found to be small, thus conferring a greater risk of ureteral thermal injury.

The pulse duration of laser activation has also been found to play a role in the thermal effects in a study by Sugiwaka et al. [33] in 2022, where the bubble behavior and temperature distribution around bubbles were studied in an *in vitro* experiment. They found long pulse bubbles had a higher temperature around the bubble and may lead to increased thermal damage to surrounding tissue. The factors mentioned above have not been studied in detail enough to know whether they influence the thermal damage to much extent. However, they should be considered in subsequent analyses, as preliminary studies show that they do play a role.

The main study parameters and settings with respect to these factors are listed in Table 4.

4. Discussion

The use of lasers for lithotripsy is widespread with newer technology and different lasers being developed for this specific purpose. The photothermal effect as mentioned earlier is the main mechanism for the fragmentation of stones, but there are some factors of the laser and fiber used that can modify these effects to a certain extent. At higher power, irrigation is required at higher flow rates to keep temperatures low. However, one must be judicious as overzealous pumping of irrigation can lead to pyelovenous backflow and extravasation due to an increased intrarenal pressure [34].

High-power laser energy can cause a significant increase in fluid temperature in the collecting system and ureter, leading to histologic injury in the surrounding tissue [2,7,12,17]. It is crucial to develop methods to predict and control the thermal dose to ensure patient safety during high-power laser lithotripsy. As mentioned earlier, the time duration of temperature also plays an important role as elucidated in the "time–temperature relationship" by Sapareto and Dewey [4]. This is further encountered as the ODC, or the time duration of "on/off". One study has shown that while the temperature may reach below the threshold between laser firing attempts, the thermal dose is cumulative and can reach very large proportions [27]. Therefore, it is essential that these factors which may lead to an increased thermal dosage are studied in order to prevent thermal damage, especially in the *in vivo* settings. This study attempted to consolidate the various factors that modify the thermal effects of lasers, so that future studies may concentrate their efforts in studying these factors in detail.

From our review, it can be inferred that there are at least eight factors that modify the thermal effects of lasers:

i. Irrigation: the irrigation at higher perfusion flow rates with open systems, at higher pressure, and chilled irrigation over warm irrigation provided better control of the temperature rise during laser lithotripsy. A UAS when feasible may be recommended to reduce temperatures.
ii. The type of laser: the TFL may have slightly higher potential for damage, but further studies are required.
iii. Power settings: in general, higher power means increased risk for damage. Staying below a maximum of 40 W is advisable.
iv. The ODC and pedal time: the higher ODC (on time > off time) and longer pedal times increase risk for injury. Intermittent lasing should be advocated as opposed to continuous.
v. Pulse duration: longer pulse duration increase temperature around bubble and thereby can cause damage.
vi. Volume of fluid: this includes the total pelvicalyceal volume in which laser activation occurs as well as the volume of fluid mixing, with lower fluid volumes resulting in increased thermal doses.
vii. The distance from stone: preliminary studies show that the energy transfer may be equivalent at further distances as well; however, more studies are needed to come to an apt conclusion.
viii. Stone impaction: with impacted stones, the temperature of the lavage solution was significantly higher, often exceeding the temperature that could be safely tolerated by the tissue.

There are plenty of studies to show the importance of the first three factors, and further studies should focus on the remaining lesser researched factors to ensure that thermal injury can be completely avoided during laser activation.

The major deficiency in the studies was that none of them assessed how the temperature changes actually affect the physiology of the pelvi-ureteric system and kidney function due to their *in vitro* nature. There are obvious ethical issues that come up as well that prevent one from experimenting at higher temperature at the cost of safety. However, one is encouraged to pursue more randomized control human studies comparing temperature changes at laser settings below 40 W, at different irrigation rates (preferably chilled), and at lower ODCs (*i.e.*, intermittent activation) in order to find the ideal settings for safety. The use of a UAS and manual pump during irrigation can also be seen to help mitigate the temperature rise seen during laser activation, and more studies are advised comparing the manual pump with gravity irrigation both with and without access sheaths.

Our study had some limitations notably that the reviewed data were mostly from experimental studies conducted on various *in vitro*, *in vivo*, and *ex vivo* subjects, and not clinical data from patients. Also notably, it was a narrative study that reflects the heterogeneity of data, such as the various laser settings, lasers used, and flow rates. As the adage goes, "prevention is better than cure", and additional research is required to prevent laser thermal damage.

Table 4 Other factors affecting thermal damage by lasers.

Study	Factor studied	Study subject	Laser studied	Laser fiber diameter and laser setting	Lasing time	Power settings (J/Hz)	Irrigation setting	Temperature recorded
Dau et al., 2022 [30]	Percentage of laser energy converted to heat	Double walled glass Dewar	Moses 200 D/F/L	200 μm, short pulse and Moses distance modes	30 s	0.5/5	NA	• Rise in control: 1.03±0.01 °C[a] • Rise in experiment: 0.99±0.06 °C[a]
Rezakahn Khajeh et al., 2022 [31]	Pelvicalyceal system volume	Glass tubes of different volumes in the water tank	Ho:YAG laser	230 μm	1 min	0.5/80	0, 8, 15, or 40 mL/min	• Threshold reached faster in smaller volume
Tsaturyan et al., 2022 [36]	Continuous prolonged activation	20 mL syringe with the access sheath	Ho:YAG laser	Continuous wave	10 min	(0.3, 1, or 1.5)/40	10, 20, or 30 mL/min	• Max 83 °C at 10 mL/min
Sugiwaka et al., 2022 [33]	Pulse duration	*in vitro* model	NA	Pulsed wave	NA	NA	NA	• NA
Louters et al., 2022 [32]	Volume of fluid mixing	Plastic tube	Ho:YAG laser	NA	NA	0.5/40	8—40 mL/min	• Threshold crossed at lower irrigation rates with the mixing volume only 1.26±0.10 cm^3[a]

Ho:YAG, holmium:yttrium-aluminium-garnet; Max, maximum; NA, not available.
[a] Mean±standard deviation.

5. Future perspective

It is well known that the theoretical depth of penetration of the Ho:YAG laser into tissue is only 0.4 mm, but there has been speculation that the actual depth of penetration exceeds it [35]. This may account for the thermal damage seen during the use of lasers. However, whether the injury was related to contact damage or due to the thermal effects of the heat generated by laser firing has not been studied in depth. Whether it is due to either cause, the risks that stem from thermal damage cannot be easily ignored and thus the factors which may influence this damage have to be studied thoroughly.

Many studies in the past decade have been dedicated to studying the effects of irrigation on the thermal damage caused; however, the recent studies focused more on other factors such as pulse duration, ODC, type of laser, and *in vivo* studies. These need to be studied further in detail to fill the voids in our knowledge regarding the impact these factors have on laser related injury. In addition, there is a lack of studies which consider patient factors like age, degree of hydronephrosis, and coexisting infections; this may confound the temperature rise seen. However, this is probably due to the fact that the majority of studies are *in vitro* ones, and when *in vivo* studies are done in the future, these factors should be studied prudently.

6. Summary

This review explores the thermal effects of lasers in urology, particularly in lithotripsy for stone and prostate disease. The study was conducted by searching for relevant papers on thermal effects, lasers, lithotripsy, and urology. A total of 35 papers were included in the study, and the results were categorized into five groups for analysis. The findings reveal that temperatures above 43 °C are typically reached with laser power exceeding 40 W and sufficient irrigation (at least 15–30 mL/min). Shorter lasing times and an ODC of less than 70% also lead to smaller temperature increases. The study concludes that several factors influence the thermal effects of lasers including the irrigation, type of laser, power, ODC, pulse duration, volume of fluid, and stone impaction. The key recommendations from the study include the use of chilled irrigation at higher perfusion rates, lower power settings (<40 W), and a shorter ODC to prevent thermal injury, especially in cases involving impacted stones.

7. Conclusion

The thermal effect of lasers with respect to urology is one of the up-and-coming areas of research, even though studies date almost back to 2015. A better understanding of the thermal injury that may result from lasers is essential to prevent the improper technique and consequent sequelae. The use of chilled irrigation at higher perfusion rates, lower power settings of <40 W, and with a shorter ODC will help to prevent thermal injuries from occurring, especially during stone impaction. This review article hopes to highlight the important lessons to be learnt from previous studies and encourage the reader to endeavor into the various gaps in knowledge which are present to further ensure safe and efficient laser usage.

Author contributions

Study concept and design: Kiron Krishnaprasad.
Data acquisition: Kiron Krishnaprasad, Ravi Teja Pathi.
Data analysis: Kiron Krishnaprasad.
Drafting of manuscript: Kiron Krishnaprasad, Ravi Teja Pathi.
Critical revision of the manuscript: Kiron Krishnaprasad, Mustafa Nazar.

Conflicts of interest

The authors declare no conflict of interest.

References

[1] Mulvaney WP, Beck CW. The laser beam in urology. J Urol 1968;99:112–5.
[2] Wollin DA, Carlos EC, Tom WR, Simmons WN, Preminger GM, Lipkin ME. Effect of laser settings and irrigation rates on ureteral temperature during holmium laser lithotripsy, an *in vitro* model. J Endourol 2018;32:59–63.
[3] Rice P, Somani BK, Nagele U, Herrmann TRW, Tokas T. Generated temperatures and thermal laser damage during upper tract endourological procedures using the holmium: yttrium-aluminium-garnet (Ho:YAG) laser: a systematic review of experimental studies. World J Urol 2022;40:1981–92.
[4] Sapareto SA, Dewey WC. Thermal dose determination in cancer therapy. Int J Radiat Oncol Biol Phys 1984;10:787–800.
[5] Chen S, Zhou L, Wei T, Luo D, Jin T, Li H, et al. Comparison of holmium:YAG laser and pneumatic lithotripsy in the treatment of ureteral stones: an update meta-analysis. Urol Int 2017;98:125–33.
[6] Darwish A, Gadelmoula MM, Abdelkawi I, Abdellatif A, Abdel-Moneim A, Hammouda H. Ureteral stricture after ureteroscopy for stones: a prospective study for the incidence and risk factors. Urol Ann 2019;11:276. https://doi.org/10.4103/UA.UA_110_18.
[7] Aldoukhi AH, Hall TL, Ghani KR, Maxwell AD, MacConaghy B, Roberts WW. Caliceal fluid temperature during high-power holmium laser lithotripsy in an *in vivo* porcine model. J Endourol 2018;32:724–9.
[8] Dau JJ, Khajeh NR, Hall TL, Roberts WW. Chilled irrigation for control of temperature elevation during ureteroscopic laser lithotripsy: *in vivo* porcine model. J Endourol 2022;36:403–9.
[9] Molina WR, Silva IN, Donalisio Da Silva R, Gustafson D, Sehrt D, Kim FJ. Influence of saline on temperature profile of laser lithotripsy activation. J Endourol 2015;29:235–9.
[10] Hein S, Petzold R, Suarez-Ibarrola R, Müller PF, Schoenthaler M, Miernik A. Thermal effects of Ho:YAG laser lithotripsy during retrograde intrarenal surgery and percutaneous nephrolithotomy in an *ex vivo* porcine kidney model. World J Urol 2020;38:753–60.
[11] Buttice S, Sener TE, Proietti S, Dragos L, Tefik T, Doizi S, et al. Temperature changes inside the kidney: what happens during holmium:yttrium-aluminium-garnet laser usage? J Endourol 2016;30:574–9.
[12] Aldoukhi AH, Ghani KR, Hall TL, Roberts WW. Thermal response to high-power holmium laser lithotripsy. J Endourol 2017;31:1308–12.

[13] Hein S, Petzold R, Schoenthaler M, Wetterauer U, Miernik A. Thermal effects of Ho:YAG laser lithotripsy: real-time evaluation in an *in vitro* model. World J Urol 2018;36:1469–75.

[14] Ghanim SQ, Hassan JA, Mahmood AS. Temperature changes during irradiation of Ho:YAG laser lithotripsy in an *in vitro* urinary bladder model. AIP Conf Proc 2020;38:2213. https://doi.org/10.1063/5.0000462.

[15] Liang H, Liang L, Yu Y, Huang B, Chen J, Wang C, et al. Thermal effect of holmium laser during ureteroscopic lithotripsy. BMC Urol 2020;20:1–4.

[16] Dau JJ, Hall TL, Maxwell AD, Ghani KR, Roberts WW. Effect of chilled irrigation on caliceal fluid temperature and time to thermal injury threshold during laser lithotripsy: *in vitro* model. J Endourol 2021;35:700–5.

[17] Winship B, Wollin D, Carlos E, Peters C, Li J, Terry R, et al. The rise and fall of high temperatures during ureteroscopic holmium laser lithotripsy. J Endourol 2019;33:794–9.

[18] Sourial MW, De SK, Monga M, Knudsen BE. Chapter 15—basic energy modalities in urology. In: Partin AW, Wein AJ, Kavoussi LR, Peters CA, Dmochowski RR, editors. Campbell walsh wein urology. Elsevier; 2021. p. 240.

[19] Noureldin YA, Farsari E, Ntasiotis P, Adamou C, Vagionis A, Vrettos T, et al. Effects of irrigation parameters and access sheath size on the intra-renal temperature during flexible ureteroscopy with a high-power laser. World J Urol 2021;39:1257–62.

[20] Martov AG, Ergakov DV, Guseynov M, Andronov AS, Plekhanova OA. Clinical comparison of super pulse thulium fiber laser and high-power holmium laser for ureteral stone management. J Endourol 2021;35:795–800.

[21] Kallidonis P, Kamal W, Panagopoulos V, Vasilas M, Amanatides L, Kyriazis I, et al. Thulium laser in the upper urinary tract: does the heat generation in the irrigation fluid pose a risk? Evidence from an *in vivo* experimental study. J Endourol 2016;30:555–9.

[22] Kallidonis P, Amanatides L, Panagopoulos V, Kyriazis I, Vrettos T, Fligou F, et al. Does the heat generation by the thulium:yttrium aluminum garnet laser in the irrigation fluid allow its use on the upper urinary tract? An experimental study. J Endourol 2016;30:422–7.

[23] Taratkin M, Laukhtina E, Singla N, Kozlov V, Abdusalamov A, Ali S, et al. Temperature changes during laser lithotripsy with Ho:YAG laser and novel Tm-fiber laser: a comparative *in-vitro* study. World J Urol 2020;38:3261–6.

[24] Peng Y, Liu M, Ming S, Yu W, Li L, Lu C, et al. Safety of a novel thulium fiber laser for lithotripsy: an *in vitro* study on the thermal effect and its impact factor. J Endourol 2020;34:88–92.

[25] Molina WR, Carrera RV, Chew BH, Knudsen BE. Temperature rise during ureteral laser lithotripsy: comparison of super pulse thulium fiber laser (SPTF) *vs.* high power 120 W holmium-YAG laser (Ho:YAG). World J Urol 2021;39:3951–6.

[26] Al-Sulaiman F, Yilbas BS, Karatas C, Keles O, Uslan I, Usta Y, et al. Laser cutting of Kevlar and mild steel composite structure: end product quality assessment. J Mater Eng Perform 2007;16:22–9.

[27] Aldoukhi AH, Dau JJ, Majdalany SE, Hall TL, Ghani KR, Hollingsworth JM, et al. Patterns of laser activation during ureteroscopic lithotripsy: effects on caliceal fluid temperature and thermal dose. J Endourol 2021;35:1217–22.

[28] Louters MM, Dau JJ, Hall TL, Ghani KR, Roberts WW. Laser operator duty cycle effect on temperature and thermal dose: *in-vitro* study. World J Urol 2022;40:1575–80.

[29] Wang K, Jiang Z, Tan J, Yin G, Huang K, Chen X. Thermal effect of holmium laser lithotripsy under ureteroscopy. Chin Med J (Engl) 2019;132:2004–7.

[30] Dau JJ, Hall TL, Matzger AJ, Louters MM, Khajeh NR, Ghani KR, et al. Laser heating of fluid with and without stone ablation: *in vitro* assessment. J Endourol 2022;36:1607–12.

[31] Rezakahn Khajeh N, Hall TL, Ghani KR, Roberts WW. Pelvicaliceal volume and fluid temperature elevation during laser lithotripsy. J Endourol 2022;36:22–8.

[32] Louters MM, Kim HJ, Dau JJ, Hall TL, Ghani KR, Roberts WW. Characterization of fluid dynamics and temperature profiles during ureteroscopy with laser activation in a model ureter. J Endourol 2022;36:1593–8.

[33] Sugiwaka I, Sugimoto Y, Fukue T. Bubble behavior and temperature distribution around bubble induced by pulsed laser for medical treatment. Int J Multiphas Flow 2022;36:107–14.

[34] Tokas T, Herrmann TRW, Skolarikos A, Nagele U. Pressure matters: intrarenal pressures during normal and pathological conditions, and impact of increased values to renal physiology. World J Urol 2019;37:125–31.

[35] Emiliani E, Talso M, Haddad M, Pouliquen C, Derman J, Côté JF, et al. The true ablation effect of holmium:YAG laser on soft tissue. J Endourol 2018;32:230–5.

[36] Tsaturyan A, Petelnaris A, Pantazis L, Farsari E, Pagonis K, Adamou C, et al. The effect of prolonged laser activation on irrigation fluid temperature: an *in vitro* experimental study. World J Urol 2022;40:1873–8.

可在线获取www.sciencedirect.com
科学直接
期刊主页：www.elsevier.com/locate/ajur

评审

影响激光碎石热效应的因素：文献综述

Kiron Krishnaprasad*，Ravi Teja Pathi，Mustafa Nazar

印度喀拉拉邦阿拉普扎市万丹纳姆政府TD医学院泌尿外科

2023年7月26日收到；2023年10月31日接受
2024年4月23日上线

关键词肾结石；
激光碎石术；冲洗；热效应；
操作员值班周期

摘要目的：激光技术在泌尿外科治疗结石及前列腺疾病中具有重要地位。然而，激光碎石术中的热效应问题多年来始终存在争议。本综述旨在系统梳理当前关于激光碎石术热效应的研究现状，并探索亟待深入研究的新领域。

研究方法：2022年8月，我们通过谷歌学术、PubMed和Scopus数据库进行关键词检索，筛选出包含“热效应”、“激光”、“碎石术”和“泌尿外科”等关键词的论文。通过文献跳跃法获取相关研究后，最终纳入35篇相关论文。根据研究因素和研究类型对数据进行五类分组，并制作表格进行数据对比分析。

结果：只有当功率>40 W且存在充足灌注（至少15-30 mL/min）时，温度才会超过43 ℃的阈值。激光作用时间较短或碎石时间，以及操作员工作周期低于70%，也会导致温度升高幅度减小。

结论：至少有八个因素会影响激光的热效应，其中最关键的是采用低温冲洗配合高灌注速率，功率设置低于40瓦以及缩短操作者工作周期，这些措施能有效预防热损伤的发生。当结石阻塞输尿管或肾盂输尿管连接部时，激光治疗过程中热损伤的风险会显著增加。*2025《亚洲泌尿外科杂志》编辑部。本文由爱思唯尔出版集团负责制作与托管。本刊为CC BY-NC-ND许可协议（知识共享署名-非商业性使用-禁止演绎http://creativecommons.org/licenses/by-nc-nd/4.0/）下的开放获取期刊。

*通讯作者。
电子邮件地址：kironkrishnaprasaduro@gmail.com（K.Krishnaprasad）。
由同济大学负责同行评审。

https://doi.org/10.1016/j.ajur.2024.04.002
2214-3882*2025《亚洲泌尿外科杂志》编辑部。由爱思唯尔出版集团负责制作与托管。本文为CC BY-NC-ND许可协议（http://creativecommons.org/licenses/by-nc-nd/4.0/）下的开放获取文章。

1. 介绍

激光是“通过受激发射放大光”的缩写。1968年，穆尔瓦尼和贝克[1]发表了关于使用红宝石晶体激光器粉碎结石的研究，这是激光碎石术的早期研究之一。自20世纪80年代以来，激光技术在泌尿科领域发挥着重要作用，尤其在治疗结石疾病和良性前列腺增生方面成效显著。泌尿学界亟需一篇综述文章，既能全面梳理当前激光热效应的研究进展，又能明确需要深入探索的潜在研究方向。此外，激光长期使用对盆腔肾盂系统和输尿管造成的损伤风险，以及引发这种光热损伤的具体因素，目前尚未得到充分论证，亟需开展更深入的专项研究。

在进行激光碎石术时，操作者可通过调节三个关键参数来实现结石粉碎效果：脉冲能量(J)、脉冲频率（Hz）和脉冲持续时间（μs）。能量和频率的任何调整都会改变功率(W)，功率越高温度随之升高，从而引发热损伤[2]。这种热损伤源于激光的光热效应，即周围组织吸收热能所导致的[3]。

在多种实验研究中，研究人员常采用激光探头附近的热电偶测温数据作为替代指标，用于评估体内激光治疗的安全性。萨帕雷托和杜威[4]提出了一种组织热损伤的“时间-温度关系”理论，指出当温度超过“阈值（43℃）”1 ℃时，造成相同数量细胞损伤所需时间将缩短一半。例如，当组织在45℃环境中持续15秒时，其热损伤程度相当于44℃环境30秒或43℃环境1分钟的损伤效果。本综述中大多数文献都将这一温度阈值作为评估热损伤终点的标准。

热损伤的长期后遗症中，输尿管狭窄尤为值得关注。一项荟萃分析研究[5]显示，接受激光碎石术治疗的患者发生该并发症的概率是气压碎石术患者的三倍左右。然而2019年发表的前瞻性研究发现，其发生率其实相当低（1.5%），且主要出现在结石嵌顿的情况下[6]，目前尚无法确定这一结果是由于局部温度升高所致，还是周围组织受到直接损伤。这一研究方向值得深入探讨，未来可作为重点研究课题。

本综述旨在探讨激光碎石术的相关问题。

i. 在碎石术过程中，哪些因素会影响激光对非靶组织的热效应？

ii.激光碎石术中非目标组织的热损伤是否显著？

iii.需要进一步调查哪些领域以预防激光相关伤害？

2. 材料和方法

2022年8月，我们在谷歌学术、PubMed和Scopus数据库中对包含“热效应”、“激光”、“碎石术”和“泌尿外科”关键词的论文进行了多组组合检索，并通过引文跳转至相关研究文献。我们系统筛选了所有被接受并发表的英文全文论文，通过阅读标题、摘要和全文内容，排除了与本综述研究目的无关的文献。最终纳入35篇相关论文，以叙述性文献综述的形式呈现研究结果。

在进行审查时，有几个突出的因素，根据研究因素和研究类型，将它们分成了五组，并创建了表格来比较数据。

3. 结果

3.1. 灌溉

大多数研究集中在灌溉系统（包括是否存在灌溉系统、是否配备灌溉泵、是否采用重力灌溉，以及是否使用冷水或温水）方面。在12项研究中，有两项采用活体实验（绵羊或猪）[7，8]，两项为离体实验[9，10]，其余八项[2，11-17]为体外实验。所有研究均采用热电偶进行温度测量，但不同研究中探头的放置位置存在差异。激光头与目标组织的平均距离为0.5毫米，这一距离与钬铝石榴石（Ho：YAG）激光在水介质中的穿透深度最为匹配[18]。

莫利纳等人于2015年率先开展了激光热成像研究。9]本研究采用两种离体模型（临床模型与开放输尿管模型），测试了10瓦功率（1焦耳/10赫兹）365μm脉冲Ho：YAG激光治疗时的温度升高情况。实验数据显示，激光激活期间温度显著上升，而输尿管热值在生理盐水冲洗后有所下降。该结论于2016年被Buttice等人进一步证实。11]在实验台上，研究人员将200μm与272μm纤维置于装有生理盐水的加热槽中，分别在室温（24.5℃）和体温（36.5℃）下进行对比。当冲洗系统处于开启状态时，温度始终未达到极限值。Dau等人[8,16]研究人员分别于2022年开展体内研究，2021年进行体外研究，重点考察了冰水冲洗对结石周围液体温度的影响，以及激光加热液体时是否进行碎石手术的对比效果。研究发现，在碎石过程中（尤其是高功率操作时），采用4℃冰水冲洗可显著降低温度升高幅度和热剂量，相较于19℃室温冲洗效果更佳。

此后多项研究在不同实验条件下得出了相似结论（详见表1和2），学界普遍认为：激光激活过程中必须进行灌溉，且建议采用更高流速和压力。多数研究显示，只有当功率设置达到40瓦及以上时，温度才会突破43摄氏度的临界值，因此需通过调节激光功率确保温度始终低于该阈值。另有研究指出，高

表1　关于钬钇铝石榴石激光灌溉的研究。

研究	研究对象	激光光纤直径值（μm）	激光时间	功率设置（W或J/Hz）	灌注设置	记录温度（℃）	温度测量方式
Molina等人，2015[9]	猪羊	365	否	1/10	• 和 • 无	• 37.4±2.5[a] • 49.5±2.3[a]	• 使用红外线Fluke Ti55热成像仪测量外部表面温度
Buttice等人，2016[11]	带盐水加热槽的试验台模型	200或272	达到上限后停止	0.5/20、1/10、2/5、3/5或4/5	• 有或无	• 未使用灌注时超过阈值	• 模型内的气管内温度计
阿尔杜基等人，2017 [12]	玻璃试管	200	1 min	(0.5–1)/(10–80)	• 0、7-8、14-15 或38-40 mL/min	• 最大70.3±2.7 °，40 W，无灌注	• 热电偶5号mm，自试管底部起
阿尔杜基等人，2018 [7]	猪	242	1 min	0.5/80	• 0.1、15或40 mL/min	• 0.1 mL/min：84.8 • 15 mL/min：63.9 • 40 mL/min：43.6	• 通过开放暴露、穿刺及逆行方式在输下观察杯状结构中的热电偶
Wollin等人，2018[2]	聚氯乙烯管	200	1 min	(0.2–1)/(6–50)	• 0、50或100 mL/min	• 0 mL/min：>100 • 50 mL/min：>43.4 • 100 mL/min：30.7	• 探针温度计放置在距离光纤尖端1 mm处
Hein等人，2018[13]	20 mL试管，置于水浴中	[illegible]		4.5/（4、12 或22.3）	[illegible]		
Winship等人，2019[17]	盐水袋和输液器	365	45 s	(0.2–1)/(6–80)	• 0、100或200 mmHg	• 阈值>6在100 mmHg和以下上升	• 热电偶紧贴光纤放置●肾脏内设有三个热电偶，其中一个柔性热电偶位于光纤近端4毫米处
Hein等人，2020[10]	水浴中的输尿管	272、550或940	1min	5–100 W	• 0–100 mL/min	• 临界温度上升至30 W以上	
Ghanim等人，2020[14]	带聚氯乙烯管的水箱	365	70 s	（0.375,0.675，或1）/20	• 0、1、10或30 mL/min	• 高功率时最大值为70，且最接近温度计读数	• 聚氯乙烯管一端的温度计
梁等，2020 [15]	连接的F20橡胶管	200	3、5或10秒	（0.5、1、1.5、2或3）/（10或20）	• 10、15、20或30 mL/min	• 最大78，功率30瓦，速率10毫升/分钟	• 热电偶，距离管底5 mm

（续下页）

表1（续）。

研究	研究对象	激光光纤用量（μm）	激光时间	功率设置（W或J/Hz）	灌注设置		（°C）	温度记录模式
头晕和肾脓肿，2021年[15]			头晕和肾脓肿，2021年[15]	玻璃试管在水浴中	242	1 min	0.5/80	●供水点●阈值温度●3毫米金属丝热电偶1.5°C和室温，8、12、15或40 mL/min 0时的25°C温度，温度为25°C在0-40 mL/min时	●供水点●阈值温度●3毫米金属丝热电偶1.5°C和室温，LED灯的角均范围提示
头晕和肾病，2022 [8]	女性的约克夏猪	242	1 min	否				●在●阈值温度下进行LED灯测试，热电偶固定于5毫米处1.5°C至4.5°C，室温提高至室内	从输尿管鞘尖端

Max，最大值；NA，不适用；PVA，聚乙烯醇；polyvinyl alcohol。
* Mean±标准差

能量（3.0J）和低频（10Hz）模式在相同功率下的热损伤略小于其对应设置[15]，需要进一步评估。

有研究团队[19]还探讨了输尿管套管（UAS）的使用及其对肾内温度的影响。研究发现，当功率设置为20瓦时，使用UAS可有效降低肾内温度，而未使用时则无此效果。但当功率超过40瓦时，这种保护作用会消失，此时只能通过提高冲洗速率来缓解[19]。该研究还对比了手动泵与重力泵的冲洗效果，发现手动泵（0.33次/秒）从未达到危险温度阈值，但在功率超过40瓦时，重力泵会导致温度升高。因此，这表明在冲洗过程中，手动泵可能比简单的重力冲洗方式更值得推荐。

3.2. 激光类型

除了钬：钇铝石榴石（Ho：YAG）激光器外，铥：钇铝石榴石（Th：YAG）激光器近年来在碎石术中也得到广泛应用。由于Th：YAG（2000纳米）激光波长比Ho：YAG（2140纳米）略短，其穿透深度也相应减少。据称Th：YAG激光器的功率效率是Ho：YAG的五倍[18]。但Th：YAG在碎石术中的主要优势在于其连续波特性，更适合组织消融；为此，研究人员推出了铥光纤激光器（TFL，波长1940纳米），这是一种采用半导体二极管替代闪光泵浦的铥离子激光器[20]。该TFL设备同时具备连续波和脉冲波两种工作模式。

表3概述了Ho：YAG与铥激光治疗的对比研究主要方面。2016年，Kallidonis等学者[21,22]为评估Th：YAG激光与Ho：YAG激光的疗效差异，研究人员开展了两项独立研究。其中一项采用猪上尿路离体模型，另一项则使用体外实验模型。研究发现，两种激光在测量温度升高时效果相当，且在确保充分冲洗的前提下，20瓦Th：YAG激光可作为Ho：YAG激光的安全替代方案。塔拉特金团队[...]的研究也得出了类似结论。23] 以及彭等人[24] 在对比Ho：YAG激光与TFL时，发现两种激光的温度下降幅度完全一致，这表明两种激光的冲洗效果相当。

最近，Molina等人[25] 本研究通过体外猪肾脏实验，分别对比了超脉冲TFL与高功率Ho：YAG激光在碎石和碎石碎石过程中的温度升高情况。结果显示：激光激活时的腔内温度升高幅度在碎石过程中相当，而超脉冲TFL在碎石过程中温度升高更为显著。但两者均未达到基于暴露时间判定的热损伤阈值。因此，超脉冲TFL在碎石过程中可能存在温度升高的风险，但需进一步研究验证。

3.3. 操作员当班周期（ODC）和踩踏时间

ODC表示激光功率的“开/关”比。占空比越高，激光器“开”的时间就越长。

表2灌水研究的推论。

研究	推理
Molina等人，2015[9]	• 该研究是最早发现激光激活时温度升高的研究之一，同时发现输尿管热值随生理盐水冲洗而降低。
Buttice等人，2016[11]	• 在关闭灌溉系统时，必须避免温度快速上升；而灌溉过程中采用低温水则有助于延缓温度上升。
Aldoukhi等人，2017[12]	• 在1 J/40 Hz功率且无灌注的情况下测得的最高温度，泌尿科医生可利用针对该情况的对策
Aldoukhi等人，2018[7]	• 在无灌溉和中等灌溉条件下，热损伤阈值被达到，但在高灌溉条件下未达到，因此高功率激光在低灌溉率下对热损伤构成威胁
Wollin等人，2018[2]	• 尽管激光功率调高，但通过充分冲洗仍能维持体外输尿管系统内的相对稳定温度。
Hein等人，2018[13]	• 因此，进行钬：钇铝石榴石激光碎石术时，应始终将激光设备与持续、密切监测的灌注结合使用。
Winship等人，2019[17]	• 在常规灌注压力和激光参数下，使用柔性输尿管镜且功率≥10瓦时，仅需1秒即可达到高温；然而，当采用激光切割技术时—— 在不同灌溉压力下，温度迅速恢复至安全水平
Hein等人，2020[10]	• 开发了一个计算灌溉速率≥30 mL/min时近似ΔT的公式：ΔT=15 K×（功率[W]/灌溉[ML/min]）
Ghanim等人，2020[14]	• 所有三个参数（脉冲能量、灌注速率和距离）均对测量温度产生高度显著的影响；钬：钇铝石榴石激光器可能安全 当采用最佳激光功率进行充分灌注时可实现
梁等，2020[15]	• 在激光功率小于10 W、灌注量大于30 mL/min以及高能低频点火的情况下，可确保激光点火的安全温度。
Dau等人（2021）[16]和Dau等人，2022[8]	• 冷冻灌洗可减缓温度上升，降低平台温度，并降低高功率激光碎石术中的热剂量

与“关闭”状态相比，因此输出能量更大。100%ODC表示持续开启，即连续波切割[26]。在碎石术中，可计算为激光时间除以碎石时间。

2021年，阿尔杜基等人[27]在体外实验中，研究人员采用20瓦平均功率的激光，以五种不同模式施加1200焦耳能量，持续60秒。结果显示，五种模式的平均ODC值均为32%，踏板激活平均时长为3.6秒。实验数据表明，延长踏板激活时间会显著提升峰值温度和热剂量。Louters等人[28]2022年，研究人员开展了一项类似研究以评估脉冲能量密度（ODC）对热剂量的影响。研究发现，ODC值越高，最大温度和热剂量也越大，当光密度转换效率（ODC）≥70%时，温度会超过43 °C的损伤阈值。与使用60%ODC值相比，采用50%ODC值时达到热损伤阈值所需时间增加十倍，最大允许能量则增加八倍。这些研究有力证明，通过合理调控激光ODC值，可有效预防激光引发的热损伤。

3.4. 体内研究

2019年，王等学者在中国开展了一项罕见的体内研究，对象是接受输尿管镜激光碎石术治疗结石的患者。29]本研究共纳入30例患者（男性16例，女性14例），平均年龄47.4岁（标准差13.7岁），结石平均直径14.2毫米（标准差8.1毫米），均接受输尿管肾镜碎石术。术中置入温度监测导丝并精作延伸。

输尿管镜的另一端连接着温度计，实时监测温度变化数据并传输至计算机。

在30组数据中，所有样本的最高温度均超过43 摄氏度（100%），其中19组（63.3%）的峰值温度甚至突破56 摄氏度。研究表明，随着钬激光功率的提升或结石受压程度加重，结石周围冲洗液的温度升高更为显著，常常超过组织安全耐受温度阈值。因此，温度可能是导致输尿管热损伤并引发术后狭窄的重要因素[24]。不过，王等学者的研究[29]该研究存在局限性，仅考察了激光功率对热效应的影响，且不同病例的主刀医生存在差异，导致各病例的激光参数设置、激光持续时间及术中条件均不一致。

3.5. 其他因素，如音量和脉冲持续时间

2022年，Dau等人[30]研究人员通过体外实验对比了两种激光光纤与结石的距离：3.5毫米（非消融模式）和0.5毫米（消融模式）。实验采用双热电偶实时监测液体温度，每秒记录一次数据，以确定激光能量转化为热能的比例及结石消融所占比例。研究发现，即便在能量高效消融条件下，仍有91%-96%的激光能量转化为热能[30]。后续研究还发现，激光激活发生的Pelvic Lyceal Volume（盆腔腔隙）是影响热效应的重要因素。

表3　　与激光类型有关的研究。

研究	研究对象	激光研究	激光光纤直径或类型	激光时间功率设置(W)、能量(J)/频率薄雾	灌注设置	记录温度（℃）
卡利多尼斯等，2016 [21]	猪	Ho：YAG与Th：YAG连续波数值孔径		• 10 W，20 W，30 W，or 40 W	• 和	• 33.5
卡利多尼斯等，2016年和[22]	带旋塞的布雷特瓶（Ho：YAG与Th：YAG）；一个40 mL容器	脉冲模式及10分钟持续模式，连续不断的波		功率分别为5 W，10 W，20 W，50 W或100 W	• 无	• 45.6–68.7
Taratkin等人，2020 [23]	体外模型	Ho：YAG vs.SP TFL 200 μ m	1 min	• 40 W，0.2 J	• 0 或 35 mL/min	• 冲洗后温度降低 - Ho:YAG: 2.6 - TFL: 1.9
Peng等人，2020年[24]	水箱中的试管TFL	连续波1分钟	•最多可设置为	30 W	• 0，15，25或50 mL/min	• 0和15 mL/min：超过6.5 °C的温度上升超过阈值；25和50 mL/min：温度没有超过阈值
Molina等人，2021年[25]	猪肾脏	Ho：YAG vs.SP TFL 200 μ m	每项耗时5秒；	•Ho：YAG抛光：0.3焦耳/15×70 Hz；SP TFL防尘：0.1 J/200 Hz；碎裂：0.8 J/8 Hz	• 和	• 正在设置片段 - Ho:YAG: 30 - SP TFL: 33.3 • 除尘设置期间 - Ho:YAG: 35.8 - SP TFL: 40.6

Ho：钬铝石榴石），钬：钬　　-铝石榴石；Th：钇铝石榴石（YAG）；TFL：钬　　光纤激光器；SP：超脉冲；NA：不可用。

通过激光照射[31]。研究发现，各模型中的液体体积与温度升幅呈反比关系。因此，当液体体积较小时，激光照射产生的热剂量会更快达到损伤阈值。Louters等人[32]研究人员通过测量激光激活过程中染色液体的移动距离，对塑料管内激光激活时的液体混合体积进行了研究。结果显示，输尿管模型内的液体混合总量较少，这会显著增加输尿管热损伤的风险。

Sugiwaka等人研究发现，激光激活的脉冲持续时间对热效应具有显著影响。33] 2022年的一项体外实验研究了气泡行为及其周围温度分布。研究发现，长脉冲气泡周围温度更高，可能导致周围组织热损伤加剧。目前上述因素尚未得到充分研究，尚无法确定其对热损伤的影响程度。不过，后续分析中应考虑这些因素，因为初步研究表明它们确实会产生影响。

这些因素的主要研究参数和设置列于表4。

4. 讨论

激光碎石技术已得到广泛应用，随着技术进步，针对该用途的新型激光设备和不同波长的激光器正不断研发。如前所述，光热效应是碎石的主要作用机制，但所用激光器和光纤的特性会在一定程度上影响这一效果。当功率较高时，需要加大冲洗流量以维持低温环境。但需谨慎操作，因为过度冲洗可能导致肾盂静脉逆流和肾盂渗漏，这是由于肾内压升高所致[34]。

高功率激光能量会导致收集系统和输尿管内的流体温度显著升高，进而引发周围组织的组织学损伤[2，7，12，17]。在进行高功率激光碎石术时，开发预测和控制热剂量的方法对保障患者安全至关重要。如前所述，温度持续时间同样扮演着关键角色，正如萨帕雷托和杜威提出的“时间-温度关系”理论所阐明的[4]。这种现象在“ODC”（即“开启/关闭”时间周期）中尤为明显。有研究表明，虽然温度可能在两次激光发射尝试之间降至阈值以下，但热剂量会持续累积，最终可能达到极高水平[27]。因此，必须深入研究可能导致热剂量增加的因素，以预防热损伤，特别是在体内实验环境中。本研究试图整合各种影响激光热效应的因素，以便未来的研究可以集中精力详细研究这些因素。

通过我们的综述可以推断，至少有八个因素会影响激光的热效应：

i. 灌注：在开放系统中采用高流量灌注、高压灌注及冷灌注，相较于温灌注更能有效控制激光碎石术中的温度升高。若条件允许，建议使用UAS设备以降低体温。

ii.激光类型：TFL可能具有稍高的损伤风险，但需进一步研究。

iii.功率设置：一般来说，功率越高，损坏风险越大。建议将功率控制在40瓦以内。

四、ODC与踏板时间：ODC值越高（开启时间长于关闭时间）且踏板时间越长，受伤风险越大。应提倡间歇性激光治疗，而非持续性治疗。

v. 脉冲持续时间：脉冲持续时间过长会升高气泡周围的温度，从而可能造成损伤。

六.液体体积：该指标包含激光激活发生的总肾盂肾盏体积及液体混合体积，液体体积越小，热剂量越高。

七.石头的距离：初步研究表明，能量传递在更远的距离上可能同样有效；然而，仍需更多研究才能得出确切结论。

viii.石头撞击：当存在结石阻塞时，冲洗液的温度会显著升高，通常会超过组织安全耐受的温度。

已有大量研究证实前三个因素的重要性，后续研究应重点探索其他较少被关注的因素，从而确保在激光激活过程中完全避免热损伤。

现有研究的主要缺陷在于，由于实验均采用体外环境，未能评估温度变化对盆腔输尿系统及肾脏功能的实际生理影响。此外，实验中涉及的安全风险也引发了伦理争议，限制了在更高温度下开展实验的可能性。但建议开展更多随机对照人体试验，通过对比40瓦以下激光功率、不同冲洗速率（优选冷却状态）以及间歇性激活（ODC）等参数，寻找安全阈值。值得注意的是，使用UAS和手动泵进行冲洗可有效缓解激光激活时的温度升高现象。建议进一步开展对比研究，验证手动泵与重力冲洗在使用导管鞘与不使用导管鞘两种情况下的效果差异。

本研究存在若干局限性：首先，所分析数据主要来自体外、体内及离体实验，而非临床患者数据；其次，研究采用叙述性研究设计，数据呈现异质性特征，包括不同激光参数设置、所用激光器及流速差异。俗话说“预防胜于治疗”；因此需要开展更多研究来预防激光热损伤。

表4　其他影响激光热损伤的因素。

研究	因素研究	研究对象	激光研究	激光光纤直径和激光设置	激光时间	电源设置（J/Hz）	灌注设置	记录的温度
Dau 等人，2022[30]	激光能量转化为热能的百分比	双层玻璃锥瓦瓶	摩西200 D/F/L	200 μm、短脉冲和Moses距离模式	30 s	0.5/5	否	• 对照组血清中Rise的增加：1.03±0.01 °C[a] • 实验温度升高：0.99±0.06 °C[a]
Rezakahn Khajeh 等人，2022[31]	肾盂系统容积	水箱中不同体积的玻璃管	Ho：YAG激光	230 μm	1 min	0.5/80	0、8、15、或40 mL/min	• 小号容量更快达到阈值
Tsaturyan等人，2022[36]；Sugiwaka等人，2022[33]；Louters 等人，2022[32]	持续长时间激活 脉冲持续时间 液体混合体积	20 mL注射器，带穿刺靶体外模型 塑料管	Ho：YAG激光 否 Ho：YAG激光	连续波 脉冲波 否	10 min 否 否	（0.3、1或1.5）/40 否 0.5/40	10、20、或30 mL/min NA 否 8—40 mL/min	• 最高38°C 10 mL/min • 否 • 当灌溉率较低时，仅混合体积达到阈值1.26±0.10厘米[3][a]

Ho：钬钇石榴石；YAG：钇铝石榴石；Max：最大值；NA：不可用。[a]Mean±标准差

5. 未来展望

众所周知，钬掺杂钇铝石榴石（Ho：YAG）激光器的理论穿透深度仅为0.4毫米，但有推测认为实际穿透深度可能超过该数值[35]。这或许可以解释激光使用过程中观察到的热损伤现象。然而，这种损伤究竟是由接触损伤引起，还是源于激光发射产生的热效应，目前尚未得到深入研究。无论具体原因如何，由此引发的热损伤风险不容忽视，因此必须对可能影响该损伤的因素进行系统性研究。

过去十年间，大量研究致力于探究灌溉对热损伤的影响，但近期研究更多聚焦于脉冲持续时间、ODC值、激光类型及体内实验等其他因素。这些因素对激光相关损伤的影响仍需深入研究，以填补现有知识空白。此外，缺乏考虑患者年龄、肾积水程度及合并感染等个体差异的研究，可能导致观察到的温度升高现象被混淆。不过这可能是因为多数研究采用体外实验，未来开展体内实验时，这些因素需要谨慎考量。

6. 摘要

本综述探讨了激光在泌尿外科中的热效应，特别是在碎石术治疗结石和前列腺疾病中的应用。研究通过检索相关论文，涵盖热效应、激光、碎石术及泌尿外科领域，共纳入35篇论文，并将结果分为五类进行分析。研究发现，当激光功率超过40瓦且灌注充足（至少15-30 mL/min）时，温度通常会达到43 ℃以上。较短的激光作用时间和低于70%的ODC也会导致温度升高幅度减小。研究结论表明，影响激光热效应的因素包括灌注方式、激光类型、功率、ODC、脉冲持续时间、液体体积及结石嵌顿情况。研究的关键建议包括：在高灌注速率下使用冷却灌注、降低功率设置（<40瓦）以及缩短ODC以防止热损伤，尤其适用于结石嵌顿病例。

7. 结论

尽管相关研究可追溯至2015年，但激光在泌尿外科领域的热效应研究仍是新兴热点。深入理解激光可能引发的热损伤机制，对于避免操作不当导致的并发症至关重要。采用低温冲洗配合高灌注速率、功率设置低于40瓦且缩短ODC（激光脉冲持续时间）等措施，能有效预防热损伤，尤其在结石阻塞时更为关键。本文旨在梳理前人研究的重要经验，为临床医生提供参考，并鼓励学界深入探索该领域。

various gaps in knowledge which are present to further ensure safe and efficient laser usage.

作者贡献

研究概念和设计：Kiron Krishnaprasad。
数据采集：Kiron Krishnaprasad，Ravi Teja Pathi。
数据分析：Kiron Krishnaprasad。
手稿起草：Kiron Krishnaprasad，Ravi Teja Pathi。
手稿的批判性修订：Kiron Krishnaprasad，Mustafa Nazar。

利益冲突

作者声明不存在利益冲突。

参考文献

[1] Mulvaney WP，Beck CW.激光束在泌尿外科中的应用。J Urol 1968；99：142-5

[2] Wollin DA，Carlos EC，Tam WR，Simmons WN，Preminger GM，Lipkin ME.器具设置和冲洗速率对钬激光碎石术中输尿管温度的影响。体外模型。J Endourol 2018；32：59-63.

[3] Rice P，Somani BK，Nagele U，Herrmann TRW，Tokas T.上尿路内镜镜下术中钬：钇铝石榴石（Ho：YAG）激光产生的温度和热激光输出：重检研究的系统综述（世界泌尿学杂志）2022；40：1981-92

[4] Saporito SA，Dewey WC.温度测量对细胞存活率的影响。辐射研究。生物学与物理学杂志。1984；16：787-800

[5] Chen S，Zhou L，Wei T，Luo D，Jin T，Li H，et al.氪氟准分子激光与气压弹道碎石术治疗输尿管结石的比较：最新荟萃分析12533

[6] Darwish A，Gadelmoula MM，Abdelkawi I，Abdellatif A，Abdel-Moneim A，Hammouda H.肾结石输尿管镜检查后输尿管狭窄：发病率和危险因素的前瞻性研究。Urol Ann 2019；11：276。<sp

[7] Aldoukhi AH，Hall TL，Ghani KR，Maxwell AD，MacConaghy B，Roberts WW.上尿路钬激光碎石术中管体内和肾盂内液体温度。

[8] Dia D，Khajah NR，Hall TL，Roberts WW.冷盐冲洗用于控制输尿管镜激光碎石术期间的温度升高：活体猪模型。J Endourol 2022；36：403-9.

[9] Molina WR，Silva IN，Donalisio Da Silva R，Gustafson D，Sehn D，Kim FJ.基本对激光碎石灌洗温度抑制的影响。J Endourol2015；29：235-9.

[10] Hein S，Petzold R，Suarez-Ibarrola R，Miller PF，Schoenthaler M，Miernik A.Ho：YAG激光碎石术介导行肾内手术和经皮肾镜取石术中的热效应在离体猪肾管腔模型中World J Urol 2020；38：753-60.

[11] Buttice S，Sener TE，Proietti S，Dragos L，Tefik T，Doizi S，et al.肾盂内温度变化：钇铝石榴石钬激光使用时会发生什么？J Endourol 2016；30：574-9

[12] Aldoukhi AH，Ghani KR，Hall TL，Roberts WW.简述半坚激光碎石术的热安全J Endourol 2017；31：1308-12

[13] Herin S，Petzold R，Schoenthaler M，Wetterauer U，Miernik A. Ho：YAG激光碎石术的热效应：体外模型中温度评估。泌尿道结石科杂志；2018；36：1469.

[14] Ghanim SQ，Hassan JA，Mahmood AS.Ho：YAG激光碎石术体外膀胱模型辐照过程中的温度变化。AIP会议论文集2020；38：2213。

[15] Liang H，Liang L，Yu Y，Huang B，Chen J，Wang C，et al.钬激光在输尿管鳞状石术中的热效应[J].BMC Urol 2020；20：1-4.

[16] Dao JJ，Hall TL，Maxwell AD，Ghani KR，Roberts WW.冷盐对激光碎石术中肾盂温度及钬激光脉冲时间的影响。体外检测。J Endourol 2021；35：700-5.

[17] Winship B，Wollin D，Carlos E，Peters C，Li J，Terry R，et al.输尿管镜下钬激光碎石术中温控的升级。J Endourol 2019；33：794-9.

[18] Soucisse ML，De SK，Monga M，Knudsen BE.第15章——输尿道尿外科微创模式.输出：Partin AW，Wein AJ，Kavoussi LR，Peters CA，Dmochowski RR.Campbell walsh wein urology。

[19] Noureldin YA，Farsari E，Nimeiri P，Adamou C，Vagionis A，Vrettos T，et al.潘生丁和维拉帕米对大鼠动脉血流和输尿管蠕动收缩期间管内温度的影响。世界泌尿外科杂志2021；39：1257-62.

[20] Martov AG，Ergakov DV，Guseynov M，Andronov AS，Plekhanova OA.膀胱冲洗光纤激光器与高功率铥激光器治疗输尿管结石的临床比较

[21] Kallidonis P，Kamal W，Panagopoulos V，Vasilas M，Amanuel-idet L，Kyrmizi I，et al.Thulium laser in the upper urinary tract, does the.hem generation in the irrigation fluid pose a risk? Evidence from an in vivo experimental study.J Endourol 2016；30：555-9.

[22] Kallidonis P，Amanuelidet L，Panagopoulos V，Kyrtsaris I，Vrettos T，Fligou F，et al.Thulium: Yttrium Aluminum Garnet Laser Tissue Generation in Irrigation Fluid Allows Its Use on Upper Urinary Tract? An Experimental Study.J Endourol 2016；30：422-7.

[23] Tarakin M，Laukhtina E，Snigur N，Kozlov V，Abdusalamov A，Ali S，et al.Ho：YAG激光治疗Tm光纤激光在激光碎石术中的温度变化体外对比研究.《世界泌尿外科杂志》2020；38：3261-6.

[24] 赵毅，刘明，史哲，赵伟，李立。钬能量和脉冲宽度对光纤激光在膀石术中的安全性：体外研究

热效应及其影响[J].J Endourol 2020；34：88-92.

[25] Molina WR，Carrera RV，Chew BH，Knudsen BE.输尿管激光碎石术中温度升高的比较：超脉冲铥光纤激光器（SPTF）与高功率120W氙氯离子超短脉冲钬：YAG）.的

[26] Al-Sulaiman F，Yilbas BS，Karatas C，Keles O，Usdin L，Unal Y，等.异型轮与低碳钢复合结构的激光切割：成品质量评估.《材料与控制能杂志》2007；16：22-9

[27] Aldoukhi AH，Dau JJ，Majdalany SE，Hall TL，Ghani KR，Hollingsworth JM，et al.输尿管钬纤维石术中激光激活模式：对盐状体温度和热剂量的影响。

[28] Louters MM，Dau JJ，Hall TL，Ghani KR，Roberts WW.激光操作头与结石间距对温度和热剂量的影响：体外研究。World J Urol 2022；40：1575-80.

[29] 王宏，薛志，潘静，叶欣，黄科，高铁锐等.钬激光碎石的热效应.[中华医学前刊]

[30] Dau JJ，Hall TL，Metzger AJ，Louters MM，Khajeh NR，Ghani KR，等.激光应用激活对光纤尖端温度的影响：体外评估.J Endourol 2022；36：1607-12.

[31] Rezakabn Khajeh N，Hall TL，Ghani KR，Roberts WW.激光碎石术中盐溶液温度升高的准体温度补偿

[32] Louters MM，Kim JH，Dau D，Hall TL，Ghani KR，Roberts WW.激光脉冲输尿管内窥镜检查模型输尿管壁的流体动力学和温度响应特征.J

[33] Sugiwaka I，Sugimoto Y，Fukue T.脉冲激光在活动组织中诱导气泡的气泡行为及周围温度分布.Int J Multiphas Flow 2022；36：107-14.

[34] Tokas T，Herrmann TRW，Skolarikos A，Nagele U.压力调整：三维模拟预测术中肾盂内压力，以优化压力指导高对理想生理学的影响。世界泌尿学杂志2019；37：125-31.

[35] Emiliani E，Talso M，Traddad M，Pouliquen C，Dermont J，Corrales M，et al.钬：YAG激光碎石期间肾盂内的最大瞬时温度

[36] Tsaturyan A，Petrichuk A，Panfutik L，Farsari E，Pagonis K，Adamou C，et al.经肝间激光消融对脊髓血流的影响：一项体外实验研究。World J Urol 2022；40：1873-8.

Urolithiasis (2024) 52:86
https://doi.org/10.1007/s00240-024-01592-1

RESEARCH

Monitoring Intrarenal temperature changes during Ho: YAG laser lithotripsy in patients undergoing retrograde intrarenal surgery: a novel pilot study

Ertugrul Kose[1] · Yakup Bostanci[2] · Murat Gulsen[2] · Fevzi Sahin[3] · Onur Kalayci[2] · Ender Ozden[2] · Yarkin Kamil Yakupoglu[2] · Saban Sarikaya[2]

Received: 1 April 2024 / Accepted: 6 June 2024 / Published online: 13 June 2024
© The Author(s), under exclusive licence to Springer-Verlag GmbH Germany, part of Springer Nature 2024

Abstract

Ho: YAG laser lithotripsy is widely used for urinary stone treatment, but concerns persist regarding its thermal effects on renal tissues. This study aimed to monitor intrarenal temperature changes during kidney stone treatment using retrograde intrarenal surgery with Ho: YAG laser. Fifteen patients were enrolled. Various laser power settings (0.8 J/10 Hz, 1.2 J/12 Hz) and irrigation modes (10 cc/min, 15 cc/min, 20 cc/min, gravity irrigation, and manual pump irrigation) were used. A sterile thermal probe was attached to a flexible ureterorenoscope and delivered into the calyceal system via the ureteral access sheath. Temperature changes were recorded with a T-type thermal probe with ±0.1 °C accuracy. Laser power significantly influenced mean temperature, with a 4.981 °C difference between 14 W and 8 W laser power ($p<0.001$). The mean temperature was 2.075 °C higher with gravity irrigation and 2.828 °C lower with manual pump irrigation ($p=0.038$ and $p=0.005$, respectively). Body mass index, laser power, irrigation model, and operator duty cycle explained 49.5% of mean temperature variability (Adj. $R^2=0.495$). Laser power and operator duty cycle positively impacted mean temperature, while body mass index and specific irrigation models affected it negatively. Laser power and irrigation rate are critical for intrarenal temperature during Ho: YAG laser lithotripsy. Optimal settings and irrigation strategies are vital for minimizing thermal injury risk. This study underscores the need for ongoing research to understand and mitigate thermal effects during laser lithotripsy.

Keywords Retrograde intrarenal surgery · Ho:YAG laser · Intrarenal temperature · Laser lithotripsy

Introduction

Retrograde intrarenal surgery (RIRS) is a minimally invasive procedure used to treat urinary stones located within the kidney and upper urinary tract and has become increasingly popular as a first-line treatment for many patients [1]. Its success in achieving high stone clearance rates with minimal morbidity has contributed to its growing popularity and widespread adoption in clinical practice. Since its introduction in the 1990s, the Holmium: Yttrium-Aluminum-Garnet (Ho: YAG) laser has emerged as a standard tool in urological practice for intracorporeal treatment of urinary stone disease, displaying efficacy in fragmenting stones of various compositions [2].

With technological advancements, high-power laser systems have emerged as alternatives to traditional low-power laser systems in endourology. High-power Ho: YAG laser and Thulium Fiber Laser (TFL) systems are particularly noteworthy due to their high-frequency settings, which enable effective stone dusting and result in less retropulsion, making them ideal alternatives [3, 4]. The main concern regarding using these high-power laser systems is the increased risk of thermal tissue damage due to their ability to deliver higher energy transfer than traditional low-power

✉ Ertugrul Kose
ertugrul_kose@hotmail.com

1 Department of Urology, Gazi State Hospital, Ilkadım, Samsun, Turkey

2 Department of Urology, Faculty of Medicine, Ondokuz Mayıs University, Samsun, Turkey

3 Department of Mechanical Engineering, Faculty of Engineering, Ondokuz Mayıs University, Samsun, Turkey

laser settings [5]. TFLs offer advantages over other types of lasers due to their wavelength and mode of operation. However, it's important to note that thermal tissue damage can still occur with TFL procedures if the laser parameters are not properly controlled or if excessive energy is delivered to the tissue. Careful attention to settings and technique is necessary to ensure optimal outcomes and minimize adverse effects.

When laser energy is applied to the stone, it causes rapid vaporization of water molecules within the stone, leading to the generation of a shock wave that fragments the stone into smaller pieces. Additionally, laser energy absorbed by the calyceal fluid increases temperature locally.The main concern regarding the use of the Ho: YAG laser is its potential thermal effects on the surrounding urothelium and kidney tissue [6]. The extent of temperature increase depends on factors like laser power settings, laser application duration, irrigation rate, stone characteristics, and composition and volume of the calyceal fluid.

An increase in the intrarenal temperature (IRT) during laser lithotripsy of urinary system stones has been demonstrated in animal models and 3D modelling studies, with discussions on the effective parameters and outcomes of temperature increase [7–19]. However, the clinical significance of this temperature increase is still a topic of debate. While moderate temperature increases are generally well tolerated by the surrounding tissues, excessive heat could cause thermal injury to the renal parenchyma or surrounding structures. Studies have been designed with 43 °C as the threshold temperature value, based on research showing protein denaturation at 43 °C in the porcine urinary system [20]. Currently, few clinical studies have addressed the monitoring of IRT during laser lithotripsy for kidney stones [21–23].

The primary aim of this study was to monitor IRT changes during Ho: YAG laser treatment of kidney stones, while the secondary aim was to investigate the effects of different variables on the mean temperature.

Patients and methods

Patients undergoing flexible ureteroscopic Ho: YAG laser lithotripsy at our center from March to August 2023 were enrolled after ethics approval (Approval no. 2023/13). The inclusion criteria were as follows: (1) 18 years or older, (2) diagnosed with kidney stones, and (3) whose longest diameter of the stone was less than 2 cm. The exclusion criteria were (1) pediatric patients, (2) patients with congenital kidney/ureter anomalies, (3) patients with ureteral stricture or concurrent ureteral stone, and (4) patients who were pregnant or lactating. Informed consent was obtained from eligible patients before inclusion in the study.

Surgery was performed 7–10 days after inserting a 6/26 DJ stent (Boston Scientific, USA) to improve ureteral access sheath insertion success and reduce ureteral damage risk. All patients had a sterile urine culture five days before surgery. A single experienced surgeon (Y.B.) performed all operations.

We used a thermometer (model 88.598 4ch K SD Logger) capable of recording data at 1-second intervals for the temperature measurement system. The measurement range of the thermometer was −200 °C to +350 °C, with a measurement accuracy of ±0.1 °C. It employs a T-type thermal probe with a diameter of 0.3 mm. To measure the IRT during the operation, the thermal probe was attached to a disposable flexible ureterorenoscope (WiScope®, Germany) with its tip 10 mm from the distal end (Fig. 1) and inserted

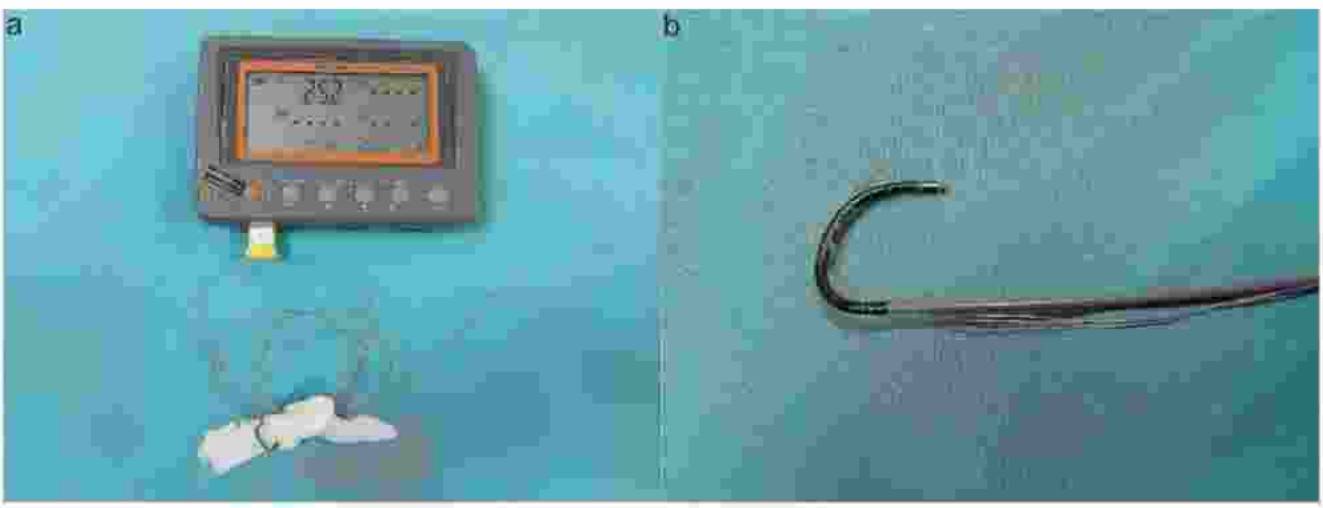


Fig. 1 Temperature measurement system **a** T-type wire temperature sensor and thermometer. **b** The temperature sensor secured to flexible ureterorenoscope

into the collecting system with a flexible ureterorenoscope through a 13/15 single lumen ureteral access sheath (Navigator™ HD, Boston Scientific, USA).

We utilized a holmium laser system (Sphinx Jr., Promed, Germany) equipped with a 272 µm laser fibre (FlexiFib, LISA Laser Products, Germany) to carry out lithotripsy. Each patient underwent lithotripsy using saline solution at room temperature (25.41 ± 2.82 °C). The experimental protocol included mechanical pump irrigation, specifically using a serum infusion pump, at flow rates of 10 ml/min, 15 ml/min, and 20 ml/min. The laser employed for this purpose was 8 W (0.8 J/10 Hz). In addition to the mechanical pump irrigation models, gravity (60 cm above the operating table) and manual pump (pumping as needed to enhance visualization quality) irrigation models were employed for the 14 W (1.2 J/12 Hz) laser setting.

When the flexible ureterorenoscope reached the calyceal system, temperature measurements began. The measurements ended when no clinically significant residual fragments (< 3 mm) were confirmed by endoscopic or fluoroscopic examination. For each study model, many characteristics were recorded, including lasing time (the duration of the active laser pedal on time), lithotripsy time (the time interval from the beginning of laser activation to the conclusion of the final laser activation, considering the durations of pedal on and off), operator duty cycle (ODC) (lasing time/lithotripsy time), total energy, and IRT.

Table 1 Perioperative and clinical characteristics of the patients

Characteristics	Overall ($n = 15$)
Gender, n (%)	
Male	8 (53)
Female	7 (47)
Age (years)	51,27 ± 15,50
Body mass index (kg/m²)	26,43 ± 4,47
Stone side, n (%)	
Right	7 (47)
Left	8 (53)
Stone number, n (%)	
Single	13 (86)
Multiple	2 (14)
Stone location, n (%)	
Renal pelvis	9 (60)
Upper calyx	2 (13)
Middle calyx	2 (13)
Multiple calyx	2 (13)
Stone size (mm²)	139,49 ± 15,07
Stone CT value (HU)	1240 (520–1520)
Opacity, n (%)	
Opaque	12 (80)
Non-opaque	3 (20)
Preoperative creatinine (mg/dL)	0,82 ± 0,13
Fluoroscopy time (sec)	18 (12–48)
Lasing time (min)	15,26 ± 7,04
Lithotripsy time (min)	20,44 ± 8,91
Total energy (J)	17188 ± 11430
Postoperative creatinine (mg/dL)	0,80 ± 0,12
Complication rate (%)	None
Postoperative stay (days)	1

CT computed tomography, *HU* hounsfield unit

Statistical analysis

The data were analysed using the Statistics Package for Social Sciences version 25 (IBM SPSS®, Armonk, NY). The Shapiro–Wilk test was used to verify normal distribution compliance. Normally distributed data are presented as the mean ± standard deviation, while nonnormally distributed data are presented as the median (minimum-maximum). For normally distributed data, repeated measures analysis of variance was used to compare the effects of different irrigation modes across different laser working modes, with multiple comparisons performed using the Bonferroni correction. For nonnormally distributed data, the Friedman test was used to compare the effects of different irrigation modes across different laser working modes, with multiple comparisons conducted using the Dunn test. Generalized linear mixed models were used to assess the effects of the independent variables on the mean temperature, with multiple comparisons performed using the Bonferroni correction. Linear regression analysis was used to identify predictors of mean temperature. $p < 0.05$ was considered to indicate statistical significance.

Results

Overall, 15 patients were included in our study. Table 1 shows the clinical and perioperative characteristics of the patients. The mean age was 51,27 ± 15,50 years, and the mean body mass index (BMI) was 26,43 ± 4,47 kg/m². The mean stone size was 139.49 ± 15.07 mm², and the stone location was the renal pelvis in 60% of patients.

For demonstration, the intrarenal temperature–time graph of "patient 2" is shown in Fig. 2. The IRT sharply decreased with irrigation before laser lithotripsy began, increased with decreasing irrigation rate at 8 W, and decreased with increasing irrigation rate at 14 W. There was a sharp decrease in IRT when transitioning from the gravity irrigation model to the manual pump irrigation model.

We analyzed temperature records from cases with around forty seconds of continuous laser activation, investigating different laser powers and irrigation settings. As the laser power increased and the irrigation rate decreased, the calyceal fluid heated more rapidly and eventually reached a plateau temperature. It was also noted that the time to reach the

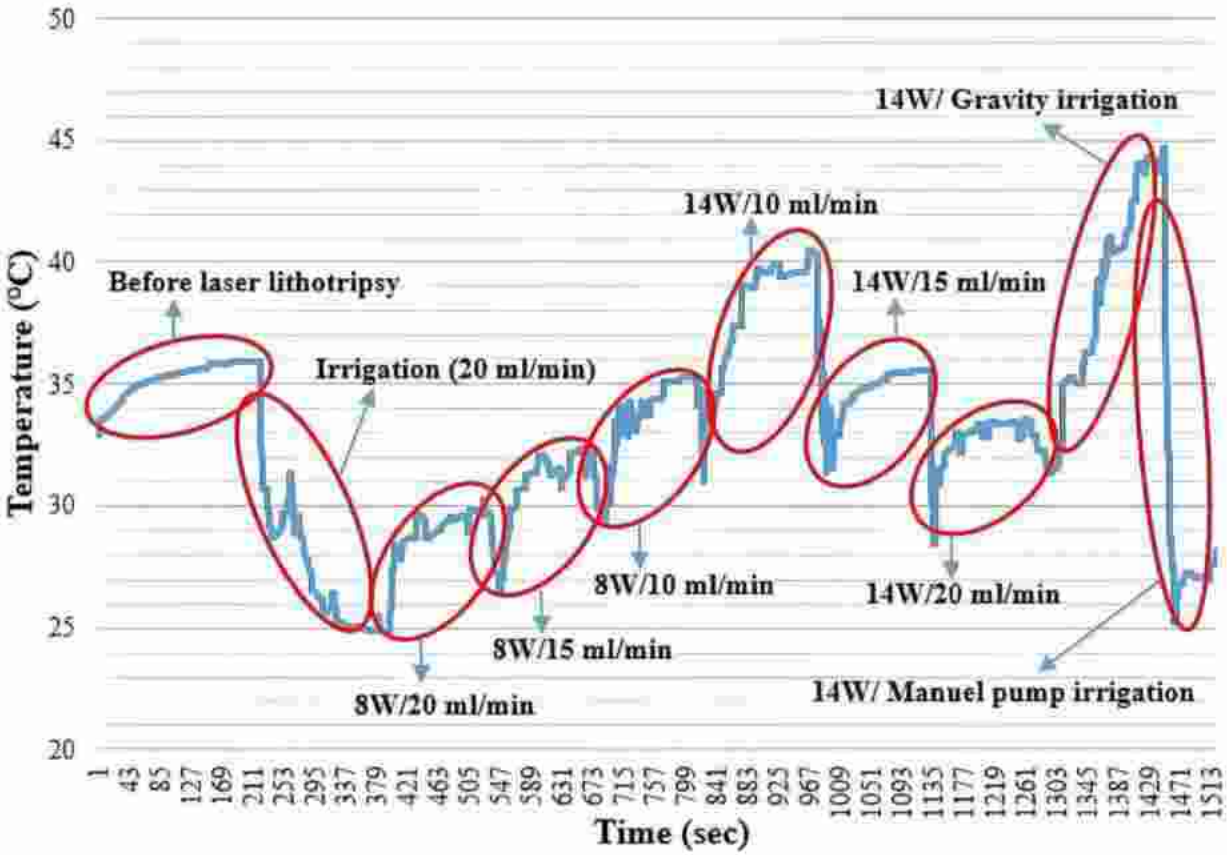


Fig. 2 The temperature-time graph of "patient 2"

plateau temperature was prolonged with a similar relationship between the laser power and irrigation model (Fig. 3).

The overall surgical parameters are summarized in Table 2. In the 8 W working model, the lowest minimum, mean, and maximum IRT were obtained in the 20 ml/min irrigation model (27.5±2.8 °C, 30.2±2.2 °C, and 31.7±2.1 °C; $p=0.017$, $p=0.002$, and $p=0.001$, respectively). In the 14 W working model, while the minimum and mean IRT values were lowest in the manual pump irrigation model (median 26.76 °C and 31.80 °C, respectively; $p<0.001$), the lowest maximum IRT was obtained in the 20 ml/min irrigation model (35.21±2.30 °C; $p=0.005$). The total energy values in the 8 W and 14 W working models were comparable.

The effects of demographic and operative variables on the mean IRT are shown in Table 3. In the univariate analysis examining the purification effects, age, sex, stone size, stone computed tomography (CT) value, laser power, irrigation model, and ODC were the parameters that significantly affected the mean IRT. In the multiple analysis evaluating the interactions of parameters, unlike the results of the univariate analysis, sex was not found to have a significant effect on the mean temperature ($p=0.616$). In contrast, total energy had a significant effect ($p=0.012$). According to the standardized β coefficients, the laser power had the most significant effect on the mean IRT, with the mean IRT being 4.981 °C greater for the 14 W laser power than for the 8 W laser power ($p<0.001$). Compared to the 20 ml/min irrigation model, the mean IRT value was 2.075 °C higher in the gravity irrigation model and 2.828 °C lower in the manual pump irrigation model ($p=0.038$ and $p=0.005$, respectively).

A multiple linear regression model was constructed to predict the mean IRT based on BMI, laser power, the irrigation model, and ODC (Table 4). The calculated regression model was statistically significant ($p<0.001$). While laser power and ODC had positive effects on the mean IRT, increases in BMI and irrigation were expected to decrease the mean IRT. The current variables could explain approximately 49.5% of the mean IRT (Adj. $R^2=0.495$).

In the 8 W laser power treatment group, none of the irrigation treatments reached the threshold of 43 °C. Additionally, in the 14 W laser power group, one patient reached an

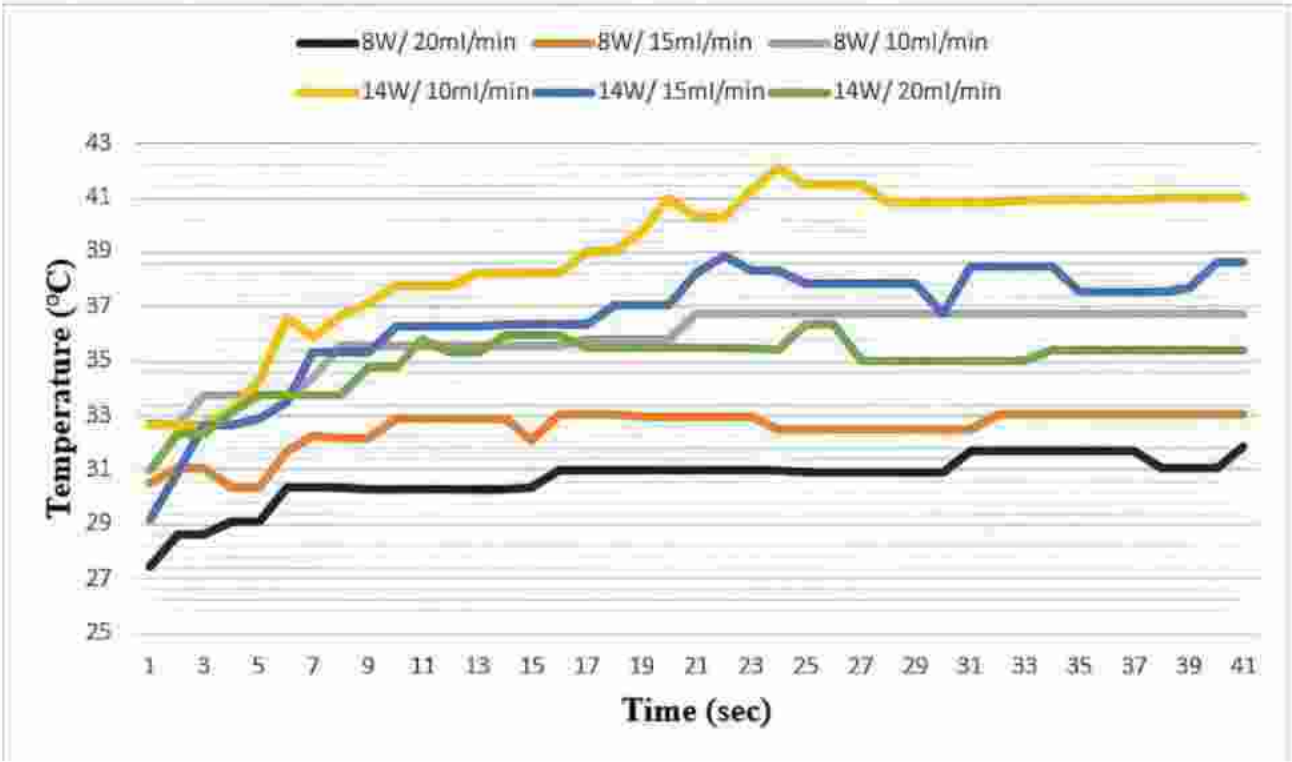


Fig. 3 Temperature-time curve at various power and irrigation settings

Table 2 Baseline characteristics and comparison of surgical parameters

	8 W						
	10 ml/min	15 ml/min	20 ml/min	Manuel pump	Gravity	Test statistic	*p*
Total Energy (J)	1069,7 ± 628,2	999,4 ± 377,1	883,8 ± 325.4	NA	NA	0,833	0,659**
Operator Duty Cycle	$0,90(0,61-0,94)^{ab}$	$0,86(0,47-0,93)^{a}$	$0,91(0,52-1)^{b}$	NA	NA	9,176	**0,01***
Temperature (°C)				NA	NA		
Minimum	$30,7 \pm 2^{a}$	$29 \pm 2,7^{ab}$	$27,5 \pm 2,8^{b}$	NA	NA	8,174	**0,017****
Mean	$33,7 \pm 2,3^{a}$	$31,4 \pm 2,3^{b}$	$30,2 \pm 2,2^{b}$	NA	NA	12,516	**0,002****
Maximum	$35,1 \pm 2,6^{a}$	$32,8 \pm 1,7^{b}$	$31,7 \pm 2,1^{b}$	NA	NA	13,367	**0,001****
	14 W						
	10 ml/min	**15 ml/min**	**20 ml/min**	**Manuel pump**	**Gravity**	**Test statistic**	**p**
Total Energy (J)	2730,67 ± 2590,70	2076,22 ± 1702,33	1737,44 ± 1205,76	3470,33 ± 6801,19	2704,33 ± 4703,37	5,689	0,224**
Operator Duty Cycle	$0,80 \pm 0,14^{a}$	$0,72 \pm 0,21^{ab}$	$0,69 \pm 0,23^{ab}$	$0,60 \pm 0,11^{b}$	$0,58 \pm 0,25^{ab}$	10,96	**0,027****
Temperature (°C)							
Minimum	32,65 $(30,98-35,73)^{c}$	31,38 $(29,21-36,31)^{bc}$	29,92 $(27,04-33,93)^{b}$	26,76 $(25,28-29,21)^{a}$	31,38 $(28,46-33,34)^{bc}$	22,922	**< 0,001***
Mean	37,67 $(32,22-39,90)^{c}$	36,27 $(30,80-40,42)^{c}$	34,06 $(28,66-36,57)^{b}$	31,80 $(28,25-33,24)^{a}$	36,51 $(31,67-38,93)^{bc}$	24,884	**< 0,001***
Maximum	$39,53 \pm 3,68^{b}$	$36,89 \pm 3,02^{ab}$	$35,21 \pm 2,30^{a}$	$38,62 \pm 3,92^{ab}$	$40,01 \pm 5,83^{ab}$	15,039	**0,005****

*Friedman test, **Repeated measures analysis, $^{a-c}$There is no significant difference between irrigation models with the same letter

Table 3 Effects of independent variables on mean temperature

	Univariate					Multivariate				
	β1 (%95 CI)	S.E.M	β2	t	*p**	β1 (%95 CI)	S.E.M	β2	t	*p**
(Constant)						24,644 (20,843 – 28,444)	1,899	0,000	12,975	**< 0,001**
Age	-0,074 (-0,127 - -0,022)	0,026	-0,275	-2,819	**0,006**	-0,105 (-0,137 - -0,072)	0,016	-0,390	-6,475	**< 0,001**
Gender (Ref: male)	-2,087 (-3,345 - -0,829)	0,631	-0,318	-3,308	**0,001**	0,201 (-0,597–1)	0,399	0,031	0,504	0,616
BMI	-0,113 (-0,255–0,029)	0,071	-0,163	-1,593	0,116	0,064 (-0,018 – 0,145)	0,041	0,093	1,569	0,122
Stone size	0,024 (0,008 – 0,04)	0,008	0,292	2,997	**0,004**	0,019 (0,009 – 0,029)	0,005	0,231	3,769	**< 0,001**
Stone CT value	0,003 (0,001 – 0,005)	0,001	0,272	3,095	**0,003**	0,003 (0,001 – 0,005)	0,001	0,272	3,363	**0,001**
Laser power (Ref: 8 W)	3,515 (2,208–4,822)	0,655	0,522	5,364	**< 0,001**	4,981 (4,072 – 5,89)	0,454	0,740	10,965	**< 0,001**
Irrigation model (Ref: 20 ml/min)										
15 ml/min	1,763 (-0,273–3,798)	1,020	0,234	1,728	0,089	1,169 (0,257–2,082)	0,456	0,155	2,565	**0,013**
10 ml/min	2,719 (0,952–4,486)	0,885	0,361	3,071	**0,003**	-1,128 (-2,326–0,07)	0,599	-0,150	-1,885	0,064
Gravity	5,181 (2,894–7,468)	1,146	0,526	4,522	**< 0,001**	2,075 (-0,027 – 4,176)	1,050	0,211	1,976	**0,038**
Manuel pump	0,177 (-1,64 – 1,993)	0,910	0,018	0,194	0,847	-2,828 (-4,745 - -0,911)	0,958	-0,287	-2,952	**0,005**
Total energy	0 (-0,0002 – 0,0003)	0,000	0,030	0,280	0,780	-0,0002 (-0,0004 - -0,0001)	0,000	-0,232	-2,577	**0,012**
Operator Duty Cycle	6,568 (3,045 – 10,092)	1,767	0,390	3,718	**< 0,001**	3,997 (0,545–7,449)	1,725	0,238	2,317	**0,024**

BMI body mass index, *CT* computed tomography, *S.E.M* standart error of mean, *Generalized linear mixed models

Table 4 Analysis results on predictors of mean temperature

	β^1 (%95 CI)	β^2	t	*p**
(Constant)	29,227 (23,977–34,478)		11,111	**< 0,001**
BMI	-0,126 (-0,245 - -0,007)	-0,182	-2,118	**0,038**
Laser power	4,740 (3,462–6,018)	0,704	7,402	**< 0,001**
Irrigation model	-1,173 (-1,627 - -0,719)	-0,474	-5,160	**< 0,001**
Operator duty cycle	4,231 (1,091 – 7,371)	0,251	2,690	**0,009**

BMI *body mass index*, *Linear regression model (Stepwise method)

$p < 0,001$; $R^2 = 0,523$; Adj.$R^2 = 0,495$; Durbin-Watson = 1,611

IRT of 43 °C in the 10 ml/min irrigation model, and one patient reached this IRT in the gravity irrigation model.

Discussion

Our study revealed that in patients who underwent RIRS with a Ho: YAG laser, the laser power, irrigation model and ODC affect and predict the IRT. To our knowledge, this is the first clinical study to investigate the effects of variables other than laser power and irrigation models in RIRS patients treated with the Ho: YAG laser.

According to the essential laws of thermodynamics, in a constant environment, the amount of heat energy per unit time should remain constant, thus resulting in a constant temperature change ($Q = mc\Delta T$). Our study revealed that a continuous active laser could be used for forty seconds without interruption, i.e., when a constant amount of heat energy could be produced in a unit, the IRT increased for a period and then reached a plateau (Fig. 3). In this model, where the environment is not constant, the attainment of a plateau can be explained by the inflow of unheated irrigation fluid into the caliceal system and the outflow of heated irrigation fluid from the caliceal system. This phenomenon is consistent with previous studies reported in the literature [8, 19, 23, 24]. The fact that the IRT reaches a plateau at constant irrigation rates suggests that the mean IRT is a more important parameter than the peak IRT in clinical studies.

The laser settings are personalized. The pulse energy can then be gradually increased until an effective dusting or fragmentation effect is achieved. In our study, the laser power was the most effective parameter for determining the mean IRT. In the regression analysis evaluating predictors, it is predicted that there will be a 4.74 °C increase in the mean IRT with a one-unit increase in laser power (Table 4). In an experimental study by Aldoukhi et al., the highest

temperature (70.3 °C) was reached with 40 W laser power and no irrigation mode among laser powers ranging from 5 W to 40 W [8]. In the pig model study of Peteinaris et al., which considered 54 °C as the thermal threshold, the threshold value was reached with laser powers above 40 W in the gravity irrigation model. In contrast, a safe thermal range was maintained with 20 W and 40 W laser powers [25]. In the pig model study conducted by Noureldin et al., the IRT remained within safe ranges at 20 W laser power when an access sheath was used, and in the gravity irrigation model, threshold temperature values that could cause thermal damage in the urinary system were reached with higher laser powers [17].

The irrigation model has emerged as an influential parameter of IRT. According to a survey study conducted among urologists interested in endourology in 2019, 46% preferred manual pump irrigation, and 27% preferred gravity irrigation as an irrigation method [26]. In this study, the highest mean IRT values were obtained in the gravity irrigation model compared to those in the other irrigation models, while the lowest mean IRT was obtained in the manual irrigation model (Table 3). In the study by Peteinaris et al., the thermal threshold was reached in the gravity irrigation model at 40 W and 60 W laser powers with 30 s of laser activation, while the safe thermal range was maintained in the manual pump irrigation model under similar laser settings [27]. In another in vivo porcine model study, hazardous IRT values were reached in the gravity irrigation model at laser powers exceeding 40 W, regardless of the use of a ureteral access sheath. However, the manual pump irrigation model only reached the thermal threshold with 100 W laser power and without using a ureteral access sheath [25].

In daily practice, suspending irrigation flow can prevent stone retropulsion during lithotripsy. However, careful attention must be paid during this manoeuvre. In one patient in our study, the IRT increased by 9 °C in a very short period of 5 s during lithotripsy when irrigation was inadvertently closed, which is not known. An in vitro study by Buttice et al. demonstrated that irrigation limits temperature increase when any laser setting is used, and rapid increases occur when irrigation is closed [10]. Another experimental ureteroscopy model by Wolin et al. reached the threshold thermal value in all laser power models ranging from 3.6 W to 20 W without continuous irrigation [28]. Hein et al. reported that laser application without irrigation led to a rapid temperature increase of up to Δ28 K, reaching 68 °C at 100 W [24]. Considering all these findings, continuous irrigation flow is essential for maintaining a safe thermal range.

Louters et al.'s in vitro study investigating the effect of ODC on temperature showed that as ODC increased, higher temperatures were reached in shorter periods [29]. In an in vitro study by Aldoukhi et al., the thermal injury threshold was reached in as little as 9 s with 50% ODC at 40 W laser power [7]. An in vitro experiment suggested utilizing ODC as a method to restrict the increase in temperature in small cavities, such as the ureter or minor calyxes [30]. Pauchard et al.'s review on intrarenal temperature and pressure during RIRS suggested halting laser activation to mitigate the risk of high temperatures [31]. In our study, consistent with the literature, when laser activation was stopped during transitions between each working model, we observed a dramatic decrease in the IRT (Fig. 2). Additionally, according to both univariate and multivariate analyses, ODC had a positive effect on the mean IRT (Table 3).

In our study, the thermal threshold was not reached in any irrigation model at 8 W laser power. In contrast, at 14 W laser power, an IRT of 43 °C was reached in the 10 ml/min and gravity irrigation models. An in vitro study by Maxwell et al. modelled the human urinary system using laser powers ranging from 5 to 40 W and irrigation modes, including no irrigation, 15 ml/min, and 40 ml/min. Laser activation was performed for 60 s. Consistent with our study, they found that the thermal threshold was not reached with a laser power of 20 W or less and irrigation rates of 15 ml/min above [14]. Similarly, Teng et al. reported that in their clinical study, the IRT remained within a safe thermal range with low laser power (< 20 W) and an irrigation rate of at least 15 ml/min [23]. In a clinical study by Æsøy et al. utilizing a Thulium fibre laser, similar findings were reported where temperatures of 43 °C were not reached with laser powers of 5 W and 10 W and an irrigation rate of 15 ml/min [22]. Currently, there is no defined optimal laser setting or irrigation model for RIRS. However, low laser power (< 20 W) and moderate irrigation flow (15–30 ml/min) appear to be feasible options for managing the IRT [31].

We are aware that laser frequency is an important parameter affecting IRT. In an in-vitro study by Aldoukhi et al., it was found that at 20 Hz, only 52% of emitted pulses reached the stone, while at 50 Hz and 80 Hz, only 23% and 4% reached the stone, respectively [32]. Thus, with increased frequency, more energy will be absorbed in the liquid medium, leading to higher IRT. In their experimental ureteroscopic lithotripsy model, Liang et al. reported that higher frequencies at the same laser powers resulted in more heat production [33]. In an in-vitro study comparing low-frequency high single-pulse energy with high-frequency, low single-pulse energy models, Hein et al. associated higher frequency settings with 3.5% and 8.8% higher temperatures at low and high laser powers, respectively [24]. In a porcine model study by Gallegos et al., the IRT value was measured at the beginning of the study and one minute after laser use, and the difference between these two measurements was defined as delta temperature (DT). Energy, frequency, use of ureteral access sheath, and liquid height were

found to be parameters significantly affecting DT, with a predicted increase of 2.1 °C in DT at 15 Hz frequency compared to 5 Hz [34]. Maxwell et al. conducted a study with laser powers ranging from 5 to 40 W and different irrigation models, finding that peak temperature values were nearly the same at the same laser powers regardless of frequency and pulse setting [14].

Does IRT truly matter in clinical practice? Aldoukhi et al. performed intrarenal laser activation with a Ho: YAG laser at 40 W power for 60 s, without irrigation, and with low- and high-flow-rate irrigation in four in vivo pig models and achieved maximum IRTs of 84.8 °C, 63.9 °C and 43.6 °C, respectively. On histopathological examination, gross macroscopic changes were observed in the no-irrigation model. At the same time, it was reported that there were minimal changes in low-flow irrigation and no signs of thermal damage in high-flow irrigation [9]. Molina et al. created a ureteral stone model in ex vivo porcine models using manual irrigation, a Ho: YAG laser (6.4 W and 21 W), and a spTFL (6.4 W and 20 W). Both systems remained below the threshold temperature (43 °C). According to histopathological examination, there was no thermal damage to the ureters after lithotripsy [15]. Peteinaris et al. created a kidney stone model in two in vivo porcine models and performed laser lithotripsy using an 8 W Thulium fibre laser for 60 min. The IRT was between 44 °C and 46 °C in both models. The kidneys were histopathologically examined on the 7th and 14th days. On the 7th day, severe histopathological findings such as hemorrhagic areas, separated urothelium, fibrin accumulation, and inflammation in the lamina propria were observed, while on the 14th day, histopathology was reported as "minimal changes" [35]. Therefore, it is not easy to provide a definitive answer when evaluating these findings in light of the study findings. However, given the lack of sufficient evidence regarding the long-term effects of high temperatures, a lower IRT appears safer.

The thermal cytotoxic effect occurring in living tissues can be explained by the temperature and duration of exposure. Sapareto and Dewey developed an equation known as the cumulative equivalent minutes at 43 °C (CEM43) to assess the thermal dose, which is calculated based on an exposure time at a reference temperature of 43 °C [36]. Animal studies have shown that protein denaturation occurs in the urinary system at 43 °C [20], and a CEM43 duration exceeding 70 min leads to significant kidney damage [37]. Since there is no defined safe thermal dose for the human urinary system, we adopted 43 °C as the thermal threshold for our study based on the current literature.

During RIRS, delivering the probe to the calyceal system either retrogradely or percutaneously is necessary to enable IRT monitoring. Despite its fine calibration, which may influence irrigation flow and misrepresent actual IRT readings, the retrograde approach appears less morbid than percutaneous access. The retrograde method, contingent upon using a ureteral access sheath, is reliable. However, there is a need for more clinical studies regarding routine IRT monitoring during RIRS. Currently, flexible ureterorenoscopes capable of intrarenal pressure monitoring are used in clinical practice during RIRS [38], yet an instrument that facilitates IRT monitoring has yet to be developed. Future research in this area will inevitably involve the use of thermal probes.

The present study has several limitations. First, our study has a small sample size, which may introduce bias when estimating population means. Second, since each patient's calyceal anatomy and volume may vary, different IRT results may have been obtained with similar variables. Third, since it is not always possible to keep the laser fibre at the same distance from the stone and from the thermal probe, different IRT results may have been obtained with similar variables. Fourth, a multipoint thermal probe could not be utilized, and the temperature of each major calyx could not be measured; thus, the recorded temperature might not have accurately reflected the mean IRT. Fifth, as the recording device monitor could not provide real-time temperature information, laser activation was continued in cases where critical temperatures were reached. Sixth, due to the lack of chemical stone analysis, the possible effect on the temperature profile could not be investigated.

Conclusion

This preliminary study investigated the impact of Ho: YAG laser lithotripsy on intrarenal calyceal fluid temperature, focusing on the influence of laser power and irrigation rate. The results revealed that the Ho: YAG laser power and irrigation rate had opposite effects on the average temperature, with the laser power being the most influential parameter for temperature elevation. Continuous irrigation at a minimum rate of 15 ml/min helps maintain temperatures within the safe range, particularly at moderate laser powers. Furthermore, this study revealed ODC as a significant parameter affecting IRT, suggesting the importance of the periodic cessation of laser activation. These findings underscore the necessity for further clinical studies with larger populations to elucidate additional factors impacting IRT dynamics during laser lithotripsy.

Author contributions E.K.: Conceptualization, data curation, investigation, methodology, writing-orginal draft. Y.B.: Conceptualization, data curation, methodology, writing-review and editing. M.G.: Data curation, formal analysis. F.S.: Resources, data curation, formal analysis. O.K. and E.O.: Data curation, writing-review and editing. Y.K.Y.: Supervision, writing-review and editing. S.S.: Supervision, writing-review and editing. All the authors have read and approved the final

version of the manuscript.

Funding The authors did not receive support from any organization for the submitted work.

Data availability No datasets were generated or analysed during the current study.

Declarations

Conflict of interest The authors have no relevant financial or non-financial interests to disclose.

References

1. Zeng G, Zhao Z, Mazzon G, Pearle M, Choong S, Skolarikos A et al (2022) European Association of Urology Section of Urolithiasis and International Alliance of Urolithiasis Joint Consensus on Retrograde Intrarenal surgery for the management of Renal stones. Eur Urol Focus 8(5):1461–1468 Epub 2021/11/28. https://doi.org/10.1016/j.euf.2021.10.011
2. Knudsen BE (2019) Laser fibers for Holmium:YAG lithotripsy: what is important and what is New. Urol Clin North Am 46(2):185–191 Epub 2019/04/10. https://doi.org/10.1016/j.ucl.2018.12.004
3. Traxer O, Keller EX (2020) Thulium fiber laser: the new player for kidney stone treatment? A comparison with Holmium:YAG laser. World J Urol 38(8):1883–1894 Epub 2019/02/08. https://doi.org/10.1007/s00345-019-02654-5
4. Traxer O, Rapoport L, Tsarichenko D, Dymov A, Enikeev D, Sorokin N et al (2018) V03-02 first clinical study on superpulse thulium fiber laser for lithotripsy. J Urol 199(4S):e321–e2
5. White C, Aziz M (1985) Energy deposition, heat flow, and rapid solidification during laser and electron beam irradiation of materials. Oak Ridge National Lab
6. Lopes ACN, Dall'Aqua V, Carrera RV, Molina WR, Glina S (2021) Intra-renal pressure and temperature during ureteroscopy: does it matter? Int Braz J Urol 47(2):436–442 Epub 2020/12/08. https://doi.org/10.1590/s1677-5538.ibju.2020.0428
7. Aldoukhi AH, Dau JJ, Majdalany SE, Hall TL, Ghani KR, Hollingsworth JM et al (2021) Patterns of laser activation during ureteroscopic lithotripsy: effects on Caliceal Fluid temperature and thermal dose. J Endourol 35(8):1217–1222 Epub 2021/01/06. https://doi.org/10.1089/end.2020.1067
8. Aldoukhi AH, Ghani KR, Hall TL, Roberts WW (2017) Thermal response to high-power holmium laser lithotripsy. J Endourol 31(12):1308–1312. https://doi.org/10.1089/end.2017.0679PubMed PMID: 29048216 Epub 2017/10/20
9. Aldoukhi AH, Hall TL, Ghani KR, Maxwell AD, MacConaghy B, Roberts WW (2018) Caliceal Fluid Temperature during High-Power Holmium laser lithotripsy in an in vivo Porcine Model. J Endourol 32(8):724–729 Epub 2018/06/16. https://doi.org/10.1089/end.2018.0395
10. Buttice S, Sener TE, Proietti S, Dragos L, Tefik T, Doizi S et al (2016) Laser Usage? J Endourol 30(5):574–579 Epub 2016/02/04. https://doi.org/10.1089/end.2015.0747. Temperature Changes Inside the Kidney: What Happens During Holmium:Yttrium-Aluminium-Garnet
11. Dau JJ, Hall TL, Maxwell AD, Ghani KR, Roberts WW (2021) Effect of chilled irrigation on Caliceal Fluid temperature and Time to Thermal Injury threshold during laser lithotripsy: in Vitro Model. J Endourol 35(5):700–705 Epub 2020/11/13. https://doi.org/10.1089/end.2020.0896
12. Gallegos H, Bravo JC, Sepúlveda F, Astroza GM (2021) Intrarenal temperature measurement associated with holmium laser intracorporeal lithotripsy in an ex vivo model. Cent Eur J Urol 74(4):588–594 Epub 2022/01/28. https://doi.org/10.5173/ceju.2021.0092
13. Kallidonis P, Kamal W, Panagopoulos V, Vasilas M, Amanatides L, Kyriazis I et al (2016) Thulium Laser in the Upper urinary tract: does the Heat Generation in the Irrigation Fluid pose a risk? Evidence from an in vivo experimental study. J Endourol 30(5):555–559 Epub 2016/01/06. https://doi.org/10.1089/end.2015.0768
14. Maxwell AD, MacConaghy B, Harper JD, Aldoukhi AH, Hall TL, Roberts WW (2019) Simulation of laser lithotripsy-Induced Heating in the urinary tract. J Endourol 33(2):113–119 Epub 2018/12/27. https://doi.org/10.1089/end.2018.0485
15. Molina WR, Carrera RV, Chew BH, Knudsen BE (2021) Temperature rise during ureteral laser lithotripsy: comparison of super pulse thulium fiber laser (SPTF) vs high power 120 W holmium-YAG laser (Ho:YAG). World J Urol 39(10):3951–3956 Epub 2021/02/20. https://doi.org/10.1007/s00345-021-03619-3
16. Molina WR, Silva IN, Donalisio da Silva R, Gustafson D, Sehrt D, Kim FJ (2015) Influence of saline on temperature profile of laser lithotripsy activation. J Endourol 29(2):235–239 Epub 2014/08/27. https://doi.org/10.1089/end.2014.0305
17. Noureldin YA, Farsari E, Ntasiotis P, Adamou C, Vagionis A, Vrettos T et al (2021) Effects of irrigation parameters and access sheath size on the intra-renal temperature during flexible ureteroscopy with a high-power laser. World J Urol 39(4):1257–1262 Epub 2020/06/20. https://doi.org/10.1007/s00345-020-03287-9
18. Winship B, Terry R, Boydston K, Carlos E, Wollin D, Peters C et al (2019) Holmium:Yttrium-Aluminum-Garnet laser pulse type affects irrigation temperatures in a Benchtop Ureteral Model. J Endourol 33(11):896–901 Epub 2019/08/17. https://doi.org/10.1089/end.2019.0496
19. Winship B, Wollin D, Carlos E, Peters C, Li J, Terry R et al (2019) The rise and fall of high temperatures during Ureteroscopic Holmium laser lithotripsy. J Endourol 33(10):794–799 Epub 2019/04/25. https://doi.org/10.1089/end.2019.0084
20. Van Rhoon GC, Samaras T, Yarmolenko PS, Dewhirst MW, Neufeld E, Kuster N (2013) CEM43° C thermal dose thresholds: a potential guide for magnetic resonance radiofrequency exposure levels? Eur Radiol 23:2215–2227
21. Wu Z, Wei J, Sun C, Huangfu Q, Wang B, Huang G et al (2023) Temperature changes of renal calyx during high-power flexible ureteroscopic Moses Holmium laser lithotripsy: a case analysis study. Int Urol Nephrol 55(7):1685–1692 Epub 2023/05/05. https://doi.org/10.1007/s11255-023-03611-3
22. Æsøy MS, Juliebø-Jones P, Beisland C, Ulvik Ø (2024) Temperature Measurements During Flexible Ureteroscopic Laser Lithotripsy: A Prospective Clinical Trial. J Endourol. Epub 2024/01/08. https://doi.org/10.1089/end.2023.0660. PubMed PMID: 38185920
23. Teng J, Wang Y, Jia Z, Guan Y, Fei W, Ai X (2021) Temperature profiles of calyceal irrigation fluids during flexible ureteroscopic Ho:YAG laser lithotripsy. Int Urol Nephrol. ;53(3):415-9. Epub 2020/09/30. https://doi.org/10.1007/s11255-020-02665-x, PubMed PMID: 32989671
24. Hein S, Petzold R, Schoenthaler M, Wetterauer U, Miernik A (2018) Thermal effects of Ho: YAG laser lithotripsy: real-time evaluation in an in vitro model. World J Urol. ;36(9):1469-75. Epub 2018/04/25. https://doi.org/10.1007/s00345-018-2303-x. PubMed PMID: 29691640
25. Peteinaris A, Pagonis K, Vagionis A, Adamou C, Tsaturyan A, Ballesta Martínez B et al (2022) What is the impact of pulse modulation technology, laser settings and intraoperative irrigation conditions on the irrigation fluid temperature during

flexible ureteroscopy? An in vivo experiment using artificial stones. World J Urol 40(7):1853–1858. https://doi.org/10.1007/s00345-022-04002-6
26. Pietropaolo A, Bres-Niewada E, Skolarikos A, Liatsikos E, Kallidonis P, Aboumarzouk O et al (2019) Worldwide survey of flexible ureteroscopy practice: a survey from European Association of Urology sections of young academic urologists and uro-technology groups. Cent Eur J Urol 72(4):393–397 Epub 2020/02/06. https://doi.org/10.5173/ceju.2019.0041
27. Peteinaris A, Faitatziadis S, Tsaturyan A, Pagonis K, Liatsikos E, Kallidonis P (2022) MOSES™ pulse modulation technology versus conventional pulse delivery technology: the effect on irrigation fluid temperature during flexible ureteroscopy. Urolithiasis 50(5):613–618. https://doi.org/10.1007/s00240-022-01342-1
28. Wollin DA, Carlos EC, Tom WR, Simmons WN, Preminger GM, Lipkin ME (2018) Effect of laser settings and Irrigation Rates on Ureteral Temperature during Holmium laser lithotripsy, an in Vitro Model. J Endourol 32(1):59–63 Epub 2017/10/20. https://doi.org/10.1089/end.2017.0658
29. Louters MM, Dau JJ, Hall TL, Ghani KR, Roberts WW (2022) Laser operator duty cycle effect on temperature and thermal dose: in-vitro study. World J Urol 40(6):1575–1580 Epub 2022/02/28. https://doi.org/10.1007/s00345-022-03967-8
30. Rezakahn Khajeh N, Hall TL, Ghani KR, Roberts WW (2022) Pelvicaliceal volume and fluid temperature elevation during laser lithotripsy. J Endourol 36(1):22–28 Epub 2021/07/14. https://doi.org/10.1089/end.2021.0383
31. Pauchard F, Ventimiglia E, Corrales M, Traxer O (2022) A Practical Guide for Intra-Renal Temperature and Pressure Management during Rirs: What Is the Evidence Telling Us. J Clin Med. ;11(12). Epub 2022/06/25. https://doi.org/10.3390/jcm11123429. PubMed PMID: 35743499; PubMed Central PMCID: PMCPMC9224584
32. Aldoukhi A, Hall T, Ghani K, Roberts W (2020) Analysis of laser fiber to stone distance during different modes of laser lithotripsy. Eur Urol Open Sci 19:e340–e1
33. Liang H, Liang L, Yu Y, Huang B, Chen J, Wang C et al (2020) Thermal effect of holmium laser during ureteroscopic lithotripsy. BMC Urol 20:1–4
34. Gallegos H, Bravo JC, Sepúlveda F, Astroza GM (2021) Intrarenal temperature measurement associated with holmium laser intracorporeal lithotripsy in an ex vivo model. Cent Eur J Urol 74(4):588
35. Peteinaris A, Tsaturyan A, Bravou V, Tatanis V, Faria-Costa G, Pagonis K et al (2023) High-power laser lithotripsy - do we treat or harm? Histological evaluation of temperature effects in an in vivo study with thulium fiber laser. Cent Eur J Urol 76(1):44–48 Epub 2023/04/18. https://doi.org/10.5173/ceju.2023.24
36. Sapareto SA, Dewey WC (1984) Thermal dose determination in cancer therapy. Int J Radiat Oncol Biol Phys 10(6):787–800 Epub 1984/06/01. https://doi.org/10.1016/0360-3016(84)90379-1
37. Yarmolenko PS, Moon EJ, Landon C, Manzoor A, Hochman DW, Viglianti BL et al (2011) Thresholds for thermal damage to normal tissues: an update. Int J Hyperth 27(4):320–343 PubMed PMID: 21591897; PubMed Central PMCID: PMCPMC3609720
38. Bhojani N, Koo KC, Bensaadi K, Halawani A, Wong VK, Chew BH (2023) Retrospective first-in-human use of the LithoVue™ Elite ureteroscope to measure intrarenal pressure. BJU Int 132(6):678–685 Epub 2023/09/05. https://doi.org/10.1111/bju.16173

Publisher's Note Springer Nature remains neutral with regard to jurisdictional claims in published maps and institutional affiliations.

Springer Nature or its licensor (e.g. a society or other partner) holds exclusive rights to this article under a publishing agreement with the author(s) or other rightsholder(s); author self-archiving of the accepted manuscript version of this article is solely governed by the terms of such publishing agreement and applicable law.

尿路结石（2024）52：86
https://doi.org/10.1007/s00240-024-01592-1

研究

逆行肾内手术患者Ho：YAG激光碎石术中肾内温度变化的监测：一项新的试点研究

埃尔图格鲁·科塞[1] · Yakup Bostanci[2] · Murat Gulsen[2] · 费夫齐·萨欣[3] · Onur Kalayci[2] · Ender Ozden[2] · Yarkin Kamil Yakupoglu[2] · 萨比安·萨里卡亚[2]

接收日期：2024年4月1日/接受日期：2024年6月6日/网络发表日期：2024年6月13日
©作者（们）于2024年获得德国Springer-Verlag GmbH（Springer Nature旗下）的独家授权

摘要

Ho：YAG激光碎石术在治疗尿路结石中应用广泛，但其对肾组织的热效应仍存在争议。本研究旨在通过逆行肾内手术结合Ho：YAG激光技术，监测肾结石治疗过程中肾内温度变化。共纳入15例患者，采用不同激光功率（0.8J/10Hz、1.2J/12Hz）和冲洗模式（10cc/min、15cc/min、20cc/min、重力冲洗及手动泵冲洗）。将无菌热探头连接于柔性输尿管肾镜，经输尿管套管引入盏状系统。使用T型热探头记录温度变化，精度达±0.1°C。激光功率对平均温度有显著影响，14W与8W功率组间温差达4.981°C（p<0.001）。重力冲洗组平均温度升高2.075°C，手动泵冲洗组则降低2.828°C（p=0.038和p=0.005）。体重指数、激光功率、冲洗模式及操作者工作周期共同解释了平均温度变异性的49.5%（调整后R^2=0.495）。激光功率和操作人员工作周期对平均体温有积极影响，而体重指数和特定灌注模式则会产生负面影响。在Ho：YAG激光碎石术中，激光功率和灌注速率对肾内温度起着关键作用。采用最佳参数设置和灌注策略，是降低热损伤风险的关键。本研究强调，需要持续开展研究以深入理解并减轻激光碎石术中的热效应。

关键词肾内逆行手术·Ho：YAG激光·肾内温度·激光碎石术

介绍

逆行肾内手术（RIRS）是一种微创治疗手段，专门用于处理肾脏及上尿路结石，现已成为众多患者的首选治疗方案[1]。该手术凭借其高结石清除率等显著优势，正逐渐成为临床治疗的热门选择。

极低的发病率使其在临床应用中越来越受欢迎并得到广泛采用。自上世纪90年代问世以来，钬：钇铝石榴石（Ho：YAG）激光器已成为泌尿外科治疗尿路结石的标准工具，对各种成分的结石都具有碎石效果[2]。

随着技术进步，高功率激光系统已逐渐取代传统低功率激光系统，成为内镜泌尿外科领域的新型选择。其中，高功率钬掺杂钇铝石榴石（Ho：YAG）激光和铥光纤激光（TFL）系统尤为突出，其高频设置不仅能有效碎石，还能减少反冲现象，堪称理想替代方案[3，4]。但使用这类高功率激光系统时需注意，由于其能量传输能力远超传统低功率系统，可能导致组织热损伤风险显著增加。

✉ 埃尔图格鲁·科塞
ertugrul_kose@hotmail.com

1 土耳其萨姆松Ilkadim加齐州立医院泌尿科

2 土耳其萨姆松市Ondokuz Mayis大学医学院泌尿外科

3 土耳其萨姆松市Ondokuz Mayis大学工程学院机械工程系

激光参数设置[5]。相比其他类型的激光器，TFLs（准分子激光）凭借其独特的波长和工作模式具有显著优势。但需特别注意的是，若TFL（准分子激光）治疗过程中激光参数控制不当，或向组织输送的能量过量，仍可能引发热损伤。因此必须严格把控参数设置与操作技巧，才能确保治疗效果最大化并最大限度降低副作用风险。

当激光能量作用于结石时，会引发结石内部水分子的快速汽化，从而产生冲击波将结石击碎成更小碎片。此外，被肾盏液吸收的激光能量还会导致局部温度升高。关于钬：钇铝石榴石（Ho：YAG）激光的主要争议在于其可能对周围尿路上皮和肾脏组织产生的热效应[6]。温度升高的程度取决于多种因素，包括激光功率设置、照射时长、冲洗速率、结石特性，以及肾盏液的成分和体积。

动物模型和三维建模研究表明，在进行尿路结石激光碎石术时，肾内温度（IRT）会升高，相关研究已探讨了温度升高的有效参数和治疗效果[7–19]。然而，这种温度升高的临床意义仍存在争议。虽然适度的温度升高通常能被周围组织良好耐受，但过量热量可能导致肾实质或周围结构的热损伤。基于猪尿路系统在43 ℃发生蛋白质变性的研究[20]，现有研究将43℃设为温度阈值。目前针对肾结石激光碎石术中肾内温度监测的临床研究仍较为有限[21–23]。

本研究的主要目的是监测Ho：YAG激光治疗肾结石过程中红外热疗（IRT）的变化，次要目的是探究不同变量对平均温度的影响。

患者和方法

2023年3月至8月期间，本中心在伦理委员会批准（批准号：2023/13）后，对接受经尿道输尿管镜钬：钇铝石榴石激光碎石术的患者进行入组研究。纳入标准为：(1)年满18周岁，(2)确诊为肾结石，(3)结石最长直径小于2厘米。排除标准包括：(1)儿童患者，(2)先天性肾/输尿管畸形患者，(3)存在输尿管狭窄或合并输尿管结石患者，(4)妊娠期或哺乳期患者。所有符合条件的患者在入组前均签署了知情同意书。

为提高输尿管套管置入成功率并降低输尿管损伤风险，医生在置入6/26 DJ支架（美国波士顿科学公司）后7-10天实施手术。所有患者术前5天均接受无菌尿培养。所有手术均由经验丰富的外科医生Y.B.单独完成。

我们采用了一款88,598型4通道KSD记录仪作为测温系统，该设备可实现1秒间隔的数据采集。其测量范围覆盖-200°C至+350°C，测量精度达±0.1°C，配备直径0.3毫米的T型热电偶探头。在手术过程中进行内镜热成像（IRT）检测时，将热电偶探头固定于一次性柔性输尿管肾镜（德国WiScope®品牌）上，探头尖端距离远端10毫米处（见图1）。

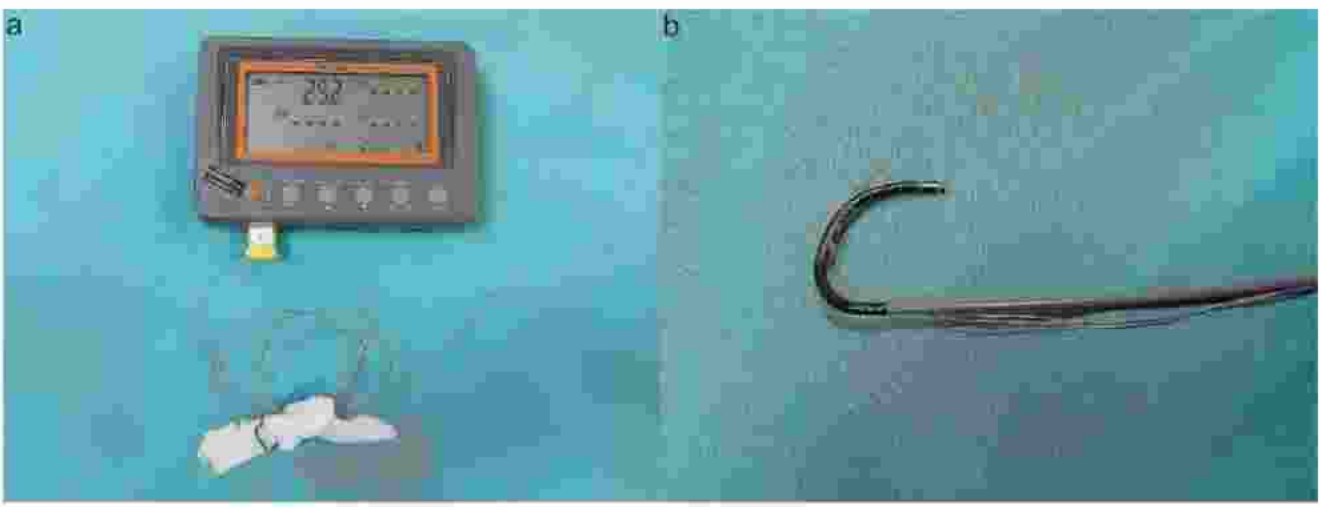


图1温度测量系统**a** T型导线温度传感器和温度计。**b**安装在输尿管肾镜上的温度传感器

通过13/15单腔输尿管导管鞘（Navigator™HD，美国波士顿科学公司），将输尿管肾镜插入收集系统。

我们使用了一套配备272μm激光光纤（FlexiFib，Lisa Laser Products，德国）的钬激光系统（Sphinx Jr.，Promed，德国）进行碎石术。每位患者均在室温（25.41±2.82°C）下使用生理盐水溶液进行碎石术。实验方案包括机械泵冲洗，具体采用血清输注泵，流速分别为10 ml/min、15 ml/min和20 ml/min。为此使用的激光功率为8 W（0.8 J/10 Hz）。除机械泵冲洗模式外，还采用了重力冲洗模式（手术台上方60厘米处）和手动泵冲洗模式（根据需要泵送以提高可视化质量），用于14 W（1.2 J/12 Hz）激光设置。

当软性输尿管肾镜抵达肾盏系统后，随即开始测量温度。若经内窥镜或X光检查确认无临床显著残留碎片（<3毫米），则停止测量。每个研究模型中，许多

表1患者围手术期及临床特征

特性	总体（*n*=15）
性别，n（%）	
男性	8 (53)
女性的	7 (47)
年龄（岁）	51.27±15.50
体重指数（kg/m²）	26.43±4.47
石方，n（%）	
右边的	7 (47)
左	8 (53)
石料数量，n（%）	
单曲	13 (86)
多选	2 (14)
石材位置，n（%）	
肾盂	9 (60)
上等片	2 (13)
中等片	2 (13)
多叶	2 (13)
石料尺寸（mm²）	139.49±15.07
CT值（HU）	1240 (520–1520)
不透明度，n（%）	
不透明	12 (80)
不透明	3 (20)
术前肌酐（mg/dL）	0.82±0.13
透视时间（秒）	18 (12–48)
激光时间（min）	15.26±7.04
碎石时间（min）	20.44±8.91
总能量(J)	17188±11430
术后肌酐（mg/dL）	0.80±0.12
并发症发生率（%）	没有一个
术后住院天数	1

*CT*计算机断层扫描，*HU*（亨氏单位）

记录了以下参数：激光持续时间（激光踏板有效工作时长）、碎石时间（从激光启动到最终停机的总时长，包含踏板开启与关闭的间隔）、操作员工作周期（ODC，即激光持续时间与碎石时间之比）、总能量以及IRT。

统计分析

本研究采用社会科学统计软件包25版（IBM SPSS®，纽约州阿蒙克）进行数据分析。通过夏皮罗-威尔克检验验证数据正态分布情况，正态分布数据以均值±标准差表示，非正态分布数据则采用中位数（最小值-最大值）呈现。对于正态分布数据，采用重复测量方差分析比较不同激光工作模式下各灌溉模式的效果，并通过Bonferroni校正进行多重比较。针对非正态分布数据，使用Friedman检验比较不同激光工作模式下的灌溉效果，多重比较采用Dunn检验。通过广义线性混合模型评估自变量对平均温度的影响，多重比较同样采用Bonferroni校正。线性回归分析用于确定平均温度的预测因子，$p<0.05$被视为具有统计学显著性。

结果

总体而言，本研究共纳入15名患者。表1显示了患者的临床和围手术期特征。平均年龄为51.27±15.50岁，平均体重指数（BMI）为26.43±4.47 kg/m²。结石平均大小为139.49±15.07毫米²，60%的患者结石位于肾盂。

为便于理解，图2中显示了“患者2”的肾内温度-时间曲线。在开始激光碎石术前，随着冲洗开始，IRT急剧下降，当8W时，随着冲洗速率的降低，IRT增加，当14W时，随着冲洗速率的增加，IRT下降。当从重力冲洗模式转换为手动泵冲洗模式时，IRT急剧下降。

我们分析了持续约四十秒激光激活病例的温度记录，研究了不同激光功率和灌注参数的影响。随着激光功率增加和灌注速率降低，盏状体液升温速度加快，最终达到恒温状态。同时发现，达到该温度所需时间会相应缩短。

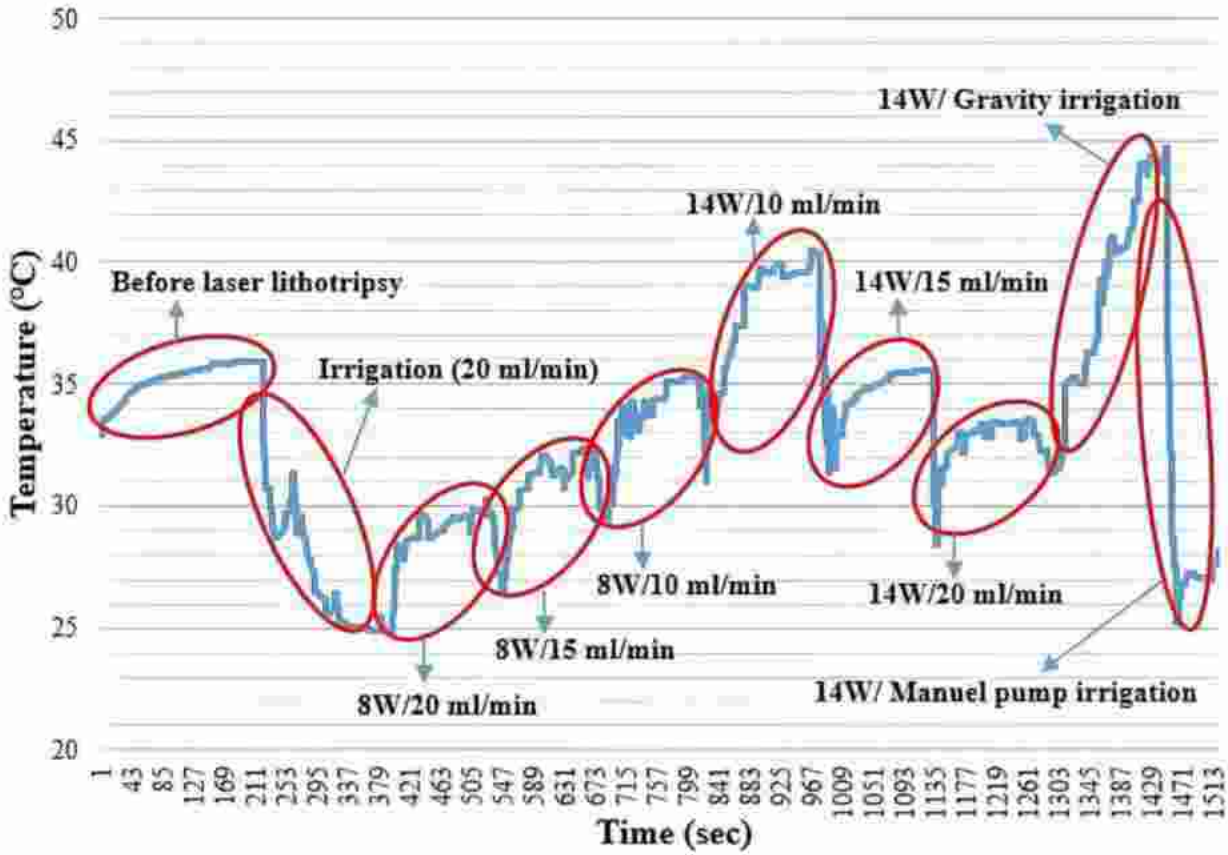


图2 “患者2”的温度-时间曲线

平台温度持续升高，激光功率与灌注模式呈现相似的关联性（图3）。

整体手术参数总结于表2中。在8 W工作模型中，最低、平均和最高IRT值分别在20 ml/min灌洗模型中获得（27.5±2.8°C、30.2±2.2°C 和 31.7±2.1°C；p=0.017、p=0.002和p=0.001）。在14 W工作模型中，虽然手动泵灌洗模型的IRT最低值和平均值最低（中位数分别为26.76 °C和31.80°C；p<0.001），但20 ml/min灌洗模型的IRT最高值最低（35.21±2.30°C；p=0.005）。8 W和14 W工作模型的总能量值相当。

表3展示了人口统计学变量和手术参数对平均内镜取石术（IRT）时间的影响。在单因素分析中，年龄、性别、结石大小、结石CT值、激光功率、冲洗模式和ODC值是显著影响平均IRT时间的参数。而在评估参数交互作用的多因素分析中，与单因素分析结果不同，性别参数未显示出显著影响。对平均温度的影响（p=0.616）。相比之下，总能量具有显著影响（p=0.012）。根据标准化β系数，激光功率对平均IRT的影响最为显著，14 W激光功率的平均IRT比8 W激光功率高4.981°C（p<0.001）。与20 ml/min灌溉模型相比，重力灌溉模型的平均IRT值高2.075°C，而手动泵灌溉模型则低2.828°C（分别为p=0.038和p=0.005）。

我们构建了一个多元线性回归模型，用于预测基于BMI、激光功率、灌洗模式和ODC的平均IRT（见表4）。计算得出的回归模型具有统计学显著性（p<0.001）。虽然激光功率和ODC对平均IRT有正向影响，但BMI和灌洗模式的增加预计会降低平均IRT。这些变量可解释约49.5%的平均IRT（调整后R^2=0.495）。

在8瓦激光功率治疗组中，所有灌洗治疗均未达到43°C的阈值。此外，在14瓦激光功率组中，有1名患者达到了

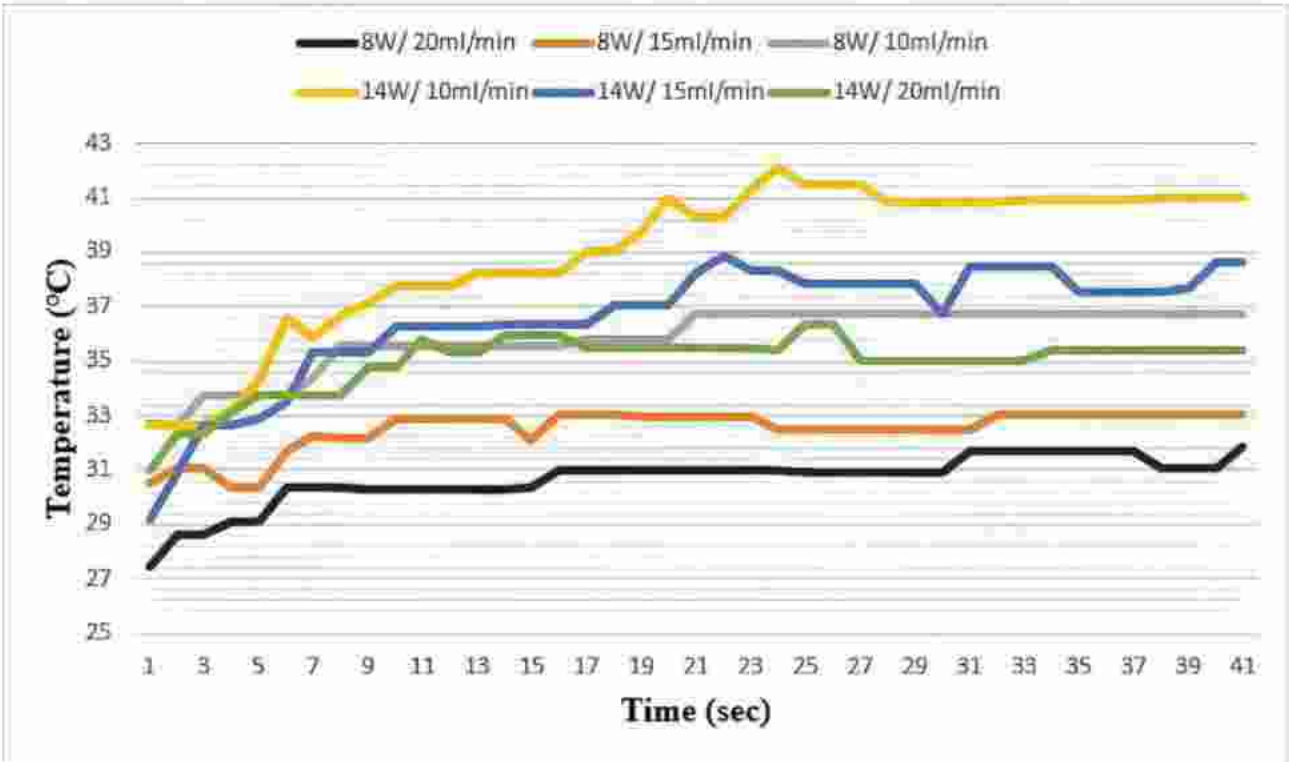


图3不同功率和灌溉设置下的温度-时间曲线

表2手术参数的基线特征和比较

	8 W						
	10 ml/min	15 ml/min	20 ml/min	手动泵	重力	检验统计量	p
总能量(J)	1069,7±628,2	999,4±377,1	883,8±325,4	否	否	0,833	0,659**
操作员值班周期	0,90（0,61-0,94）^{ab}	0,86（0,47-0,93）^{a}	0,91（0,52-1）^{b}	否	否	9,176	**0,01***
温度 (°C)				否	否		
最小平均	30,7±2^{a}	29±2,7^{ab}	27,5±2,8^{b}	否	否	8,174	**0,017****
最大值	33,7±2,3^{a}	31,4±2,3^{b}	30,2±2,2^{b}	否	否	12,516	**0,002****
	35,1±2,6^{a}	32,8±1,7^{b}	31,7±2,1^{b}	否	否	13,367	**0,001****
	14 W						
	10 ml/min	**15 ml/min**	**20 ml/min**	**手动泵**	**重力**	**检验统计量**	**p**
总能量(J)	2730,67±2590,70	2076,22±1702,33	1737,44±1205,76	3470,33±6801,19	2704,33±4703,37	5,689	0,224**
操作员值班周期	0,80±0,14^{a}	0,72±0,21^{ab}	0,69±0,23^{ab}	0,60±0,11^{b}	0,58±0,25^{ab}	10,96	**0,027****
温度（℃）最小值、平均值、最大值	32,65（30,98-35,73）^{a}	31,38（29,21-36,31）^{bc}	29,92（27,04–33,93）^{b}	26,76（25,28–29,21）^{c}	31,38（28,46-33,34）^{bc}	22,922	**<0,001***
	37,67（32,22–39,90）^{a}	36,27（30,80-40,42）^{c}	34,06（28,66-36,57）^{b}	31,80（28,25–33,24）^{c}	36,51（31,67-38,93）^{bc}	24,884	**<0,001***
	39,53±3,68^{b}	36,89±3,02^{ab}	35,21±2,30^{a}	38,62±3,92^{ab}	40,01±5,83^{ab}	15,039	**0,005****

*Friedman检验，**重复测量分析，a–c同一字母的灌注模型间无显著差异

表3自变量对平均温度的影响

	单变量					多变量				
	β1 (%95 CI)	S.E.M	β2	t	p**	β1 (%95 CI)	S.E.M	β2	t	p**
持续不断的						24,644 (20,843 – 28,444)	1,899	0,000	12,975	**< 0,001**
年龄	-0,074 (-0,127 - -0,022)	0,026	-0,275	-2,819	**0,006**	-0,105 (-0,137 - -0,072)	0,016	-0,390	-6,475	**< 0,001**
性别（参考：男性）	-2,087 (-3,345 - -0,829)	0,631	-0,318	-3,308	**0,001**	0,201 (-0,597–1)	0,399	0,031	0,504	0,616
BMI	-0,113 (-0,255–0,029)	0,071	-0,163	-1,593	0,116	0,064 (-0,018 – 0,145)	0,041	0,093	1,569	0,122
石料尺寸	0,024 (0,008 – 0,04)	0,008	0,292	2,997	**0,004**	0,019 (0,009 – 0,029)	0,005	0,231	3,769	**< 0,001**
CT石块值	0,003 (0,001 – 0,005)	0,001	0,272	3,095	**0,003**	0,003 (0,001 – 0,005)	0,001	0,272	3,363	**0,001**
激光功率（参考：8 W）	3,515 (2,208–4,822)	0,655	0,522	5,364	**< 0,001**	4,981 (4,072 – 5,89)	0,454	0,740	10,965	**< 0,001**
灌溉模型（参考：20 ml/min)										
15 ml/min	1,763 (-0,273–3,798)	1,020	0,234	1,728	0,089	1,169 (0,257–2,082)	0,456	0,155	2,565	**0,013**
10 ml/min	2,719 (0,952–4,486)	0,885	0,361	3,071	**0,003**	-1,128 (-2,326–0,07)	0,599	-0,150	-1,885	0,064
重力	5,181 (2,894–7,468)	1,146	0,526	4,522	**< 0,001**	2,075 (-0,027 – 4,176)	1,050	0,211	1,976	**0,038**
手动泵	0,177 (-1,64 – 1,993)	0,910	0,018	0,194	0,847	-2,828 (-4,745 - -0,911)	0,958	-0,287	-2,952	**0,005**
总能量	0 (-0,0002 – 0,0003)	0,000	0,030	0,280	0,780	-0,0002 (-0,0004 - -0,0001)	0,000	-0,232	-2,577	**0,012**
操作员值班周期	6,568 (3,045 – 10,092)	1,767	0,390	3,718	**< 0,001**	3,997 (0,545–7,449)	1,725	0,238	2,317	**0,024**

*BMI*体重指数，*CT*计算机断层扫描，*S.E.M*标准误差，*广义线性混合模型

表4平均气温预测因子分析结果

	β [1] (%95 CI)	β[2]	t	p*
持续不断的	29,227 (23,977–34,478)		11,111	**< 0,001**
BMI	-0,126 (-0,245 - -0,007)	-0,182	-2,118	**0,038**
激光功率	4,740 (3,462–6,018)	0,704	7,402	**< 0,001**
灌注模型	-1,173 (-1,627 - -0,719)	-0,474	-5,160	**< 0,001**
操作员值班周期	4,231 (1,091 – 7,371)	0,251	2,690	**0,009**

BMI*体重指数*，*线性回归模型（逐步法）$p<0,001$；$R^2=0.523$；$Adj.R^2=0,495$；Durbin-Watson=1,61]

在10 ml/min的灌溉模型中，IRT为43°C，而在重力灌溉模型中，有一名患者达到了这一IRT。

讨论

本研究发现，对于接受Ho：YAG激光进行RIRS治疗的患者，激光功率、冲洗模式以及ODC的影响和预测作用均与术中恢复时间（IRT）相关。据我们所知，这是首个针对Ho：YAG激光治疗RIRS患者时，除激光功率和冲洗模式外其他变量影响的临床研究。

根据热力学基本定律，在恒定环境中，单位时间内的热能应保持恒定，从而导致温度变化恒定（Q=mcΔT）。我们的研究表明，连续工作40秒的主动激光器可保持恒定热能输出。

当灌溉速率在某一单位范围内变化时，灌溉温度（IRT）会先上升后趋于稳定（图3）。在该动态模型中，环境条件并非恒定，这种稳定状态的形成可归因于未加热灌溉液流入杯状系统，同时加热后的灌溉液从杯状系统流出。这一现象与文献中已有研究结果[8，19，23，24]的结论一致。值得注意的是，当灌溉速率保持恒定时，IRT仍能维持稳定水平，这表明在临床研究中，平均灌溉温度比峰值温度更具参考价值。

激光参数经过个性化设置。随后可逐步提升脉冲能量，直至达到理想的粉尘化或碎裂效果。本研究发现，激光功率是决定平均红外温度（IRT）的最关键参数。通过回归分析预测模型显示，激光功率每增加1个单位，平均IRT将提升4.74°C（表4）。Aldoukhi等人的实验研究中，最高

在5W至40W激光功率范围内，当功率为40W且不采用灌注模式时，温度可达到70.3°C[8]。Peteinaris等人在猪模型研究中将54°C作为热损伤阈值，发现重力灌注模型中需使用超过40W的激光功率才能达到该阈值。相比之下，采用20W和40W激光功率时则能维持安全热范围[25]。Noureldin团队的猪模型研究显示，使用套管导管时，20W激光功率可确保间质性肾炎（IRT）处于安全范围；而在重力灌注模型中，当激光功率更高时，才可能引发泌尿系统热损伤的临界温度值会被达到[17]。

灌注模式已成为影响红外热成像（IRT）效果的关键参数。2019年针对泌尿科医生开展的调查显示，46%的医生更倾向于手动泵灌注法，27%的医生偏好重力灌注法[26]。研究数据显示，重力灌注法的平均IRT值显著高于其他灌注模式，而手动灌注法的平均IRT值最低（见表3）。Peteinaris团队的研究表明，在重力灌注模式下，当激光功率达到40瓦和60瓦、激活时间30秒时，即可达到热阈值；而采用类似激光参数的手动泵灌注模式仍能保持安全热范围[27]。另一项活体猪模型研究发现，无论是否使用输尿管套管，重力灌注模式在激光功率超过40瓦时都会产生危险的IRT值。相比之下，手动泵灌注模式仅在使用100瓦激光功率且未使用输尿管套管时才会达到热阈值[25]。

在临床操作中，暂停冲洗液流动可有效避免碎石术中结石的逆向运动。但需特别注意操作时的谨慎性。本研究中有一例患者在碎石术过程中因意外关闭冲洗系统，导致术中温度在短短5秒内骤升9°C，具体机制尚不明确。布蒂斯团队的体外研究表明，无论采用何种激光参数，持续冲洗都能有效抑制温度升高，而关闭冲洗则会引发快速升温[10]。沃林团队的实验性输尿管镜模型显示，所有激光功率（3.6-20W）在不持续冲洗时均达到热阈值[28]。海因团队报告称，无冲洗状态下激光应用会导致温度快速攀升，最大增幅达28K，100W功率时温度可飙升至68°C[24]。综合上述研究结果可知，持续冲洗对于维持安全热范围至关重要。

Louters等人的体外研究显示，ODC对温度的影响表明，随着ODC的增加，温度在更短时间内达到更高水平[29]。Aldoukhi等人的体外研究显示，热损伤阈值在40瓦激光功率下，仅需9秒即可实现50%的ODC[7]。体外实验表明，可将ODC作为限制输尿管或小盏等小腔体温度升高的方法[30]。Pauchard等人在关于肾内温度与压力的RIRS研究综述中指出，应暂停激光激活以降低高温风险[31]。本研究与文献一致地发现：当在各工作模型间切换时暂停激光激活，可显著降低IRT（图2）。此外，单因素和多因素分析均表明，ODC对平均IRT具有积极影响（表3）。

在我们的研究中，任何灌注模型在8 W激光功率下均未达到热阈值。相比之下，在14 W激光功率下，10 ml/min和重力灌注模型达到了43°C的IRT。Maxwell等人的一项体外研究使用5至40 W的激光功率和灌注模式（包括无灌注、15 ml/min和40 ml/min）对人类泌尿系统进行了建模。激光激活持续60秒。与我们的研究一致，他们发现当激光功率不超过20 W且灌注速率高于15 ml/min时，热阈值仍未达到[14]。类似地，Teng等人报告称，在其临床研究中，当激光功率低于20 W且灌注速率至少为15 ml/min时，IRT仍保持在安全热范围内[23]。Æsøy等人使用铥光纤激光器进行的临床研究也报告了类似结果，即在5 W和10 W激光功率及15 ml/min灌注速率下，温度未达到43°C[22]。目前，尚无针对RIRS的明确最佳激光设置或灌注模型。然而，低激光功率（<20 W）和中等灌注流量（15–30 ml/min）似乎是管理IRT的可行选择[31]。

我们深知激光频率是影响体外碎石术（IRT）的关键参数。Aldoukhi团队的体外研究显示，当频率为20赫兹时，仅有52%的发射脉冲能抵达结石；而频率提升至50赫兹和80赫兹时，这一比例分别降至23%和4%[32]。由此可见，随着频率升高，液体介质吸收的能量增加，导致体外碎石术温度升高。Liang等学者在输尿管镜碎石模型实验中发现，相同激光功率下高频模式产生的热量更多[33]。Hein团队通过对比低频高单脉冲能量与高频低单脉冲能量模型的体外研究发现，高频设置在低功率和高功率条件下分别使温度升高3.5%和8.8%[24]。Gallegos团队在猪模型研究中，分别于实验开始时和激光使用后1分钟测量IRT值，并将两次测量的温差定义为温度差（DT）。能量、频率、输尿管套管使用情况及液体高度等参数均需纳入考量。

研究发现，某些参数对DT有显著影响，与5Hz相比，15Hz频率下DT预测增加2.1°C[34]。Maxwell等人使用5-40W不同激光功率和不同冲洗模式进行研究，发现无论频率和脉冲设置如何，相同激光功率下的峰值温度值几乎相同[14]。

红外热（IRT）在临床实践中究竟有多重要？阿尔杜基团队在四只活体猪模型中采用Ho：YAG激光器进行肾内激光激活，功率40瓦持续60秒，未使用冲洗液，分别采用低流量和高流量冲洗，测得最高IRT值分别为84.8°C、63.9°C和43.6°C。组织病理学检查显示，未冲洗组出现肉眼可见的宏观改变，而低流量冲洗组仅有轻微变化，高流量冲洗组则未见热损伤迹象[9]。莫利纳团队在离体猪模型中通过手动冲洗、Ho：YAG激光器（6.4W和21W）及spTFL（6.4W和20W）构建输尿管结石模型，两种系统温度均低于临界值（43°C）。组织病理学检查证实碎石术后输尿管未出现热损伤[15]。皮泰纳里斯团队在两只活体猪模型中建立肾结石模型，使用8W铥光纤激光器进行60分钟激光碎石，两个模型的IRT值均在44°C至46°C之间。研究人员分别在第7天和第14天对肾脏进行了组织病理学检查。第7天的检查结果显示存在出血区域、尿路上皮分离、纤维蛋白沉积及固有层炎症等严重病理改变，而第14天的病理报告仅显示“轻微变化”35。因此，根据现有研究数据对这些病理变化进行定性评估存在较大难度。不过考虑到高温疗法长期影响的相关证据尚不充分，采用较低强度的红外线治疗似乎更为安全。

活体组织中产生的热细胞毒性效应，主要由温度和暴露时长决定。萨帕雷托与杜威提出的“43℃累积当量分钟（CEM43）”计算公式，专门用于评估热剂量——该数值基于43℃参考温度下的暴露时间计算得出[36]。动物实验表明，当尿路温度达到43℃时会发生蛋白质变性[20]，若CEM43持续时间超过70分钟，就会造成肾脏严重损伤[37]。鉴于目前文献尚未明确人体尿路系统的安全热剂量，本研究根据现有资料将43℃定为热损伤临界温度。

在RIRS手术中，为实现灌注热成像（IRT）监测，必须通过逆行或经皮途径将探头送入肾盏系统。尽管该系统具有精密的校准功能，但其校准可能影响灌注流量，导致IRT实际成像结果失真。在临床操作中，逆行入路相比经皮入路显得更为安全。该方法需配合输尿管套管使用，具有较高的可靠性。不过，目前仍需更多关于输尿管热成像监测（IRT）在输尿管镜肾镜联合手术（RIRS）中常规应用的临床研究。当前临床实践中，虽然已采用可监测肾内压力的柔性输尿管肾镜进行RIRS操作[38]，但专门用于IRT监测的仪器尚未问世。未来该领域的研究必然需要热探针技术的介入。

本研究存在若干局限性。首先，样本量较小可能导致人口均值估算存在偏差。其次，由于患者肾盏解剖结构和体积存在个体差异，即使变量相似也可能获得不同的红外热成像（IRT）结果。第三，由于无法始终保持激光光纤与结石及热探头的距离恒定，变量相似时可能产生不同IRT结果。第四，由于未使用多点热探头且无法测量各主要肾盏温度，记录温度可能无法准确反映平均IRT值。第五，监测设备无法实时显示温度信息，导致在达到临界温度时仍继续激光激活。第六，由于缺乏结石化学成分分析，无法探究温度曲线可能受到的影响。

结论

这项初步研究调查了Ho：YAG激光碎石术对肾盏内液体温度的影响，重点关注激光功率和冲洗速率的作用。结果显示，Ho：YAG激光功率和冲洗速率对平均温度具有相反的影响，其中激光功率是温度升高的最重要参数。以最低15 ml/min的速率持续冲洗有助于将温度维持在安全范围内，尤其是在中等激光功率下。此外，本研究揭示ODC是影响IRT的重要参数，表明定期停止激光激活的重要性。这些发现强调了需要进行更大规模人群的临床研究，以阐明激光碎石术过程中影响IRT动态的其他因素。

作者贡献E.K.：概念构思、数据整理、研究修订、方法论、撰写初稿。Y.B.：概念化，数据管理、方法论、撰写、审阅与编辑。M.G.：数据数据管理、正式分析。F.S.：资源、数据管理、正式分析S.S.、O.K.和E.O.：负责数据管理。撰写、审阅和编辑；Y.K.Y.：监督，撰写、审阅与编辑，S.S.：负责监督、撰写，审阅与编辑。所有作者均已阅读并批准最终版本。

手稿的版本。

资金作者未从任何组织获得提交工作的支持。

数据可用性：本研究期间未生成或分析任何数据集。

声明

利益冲突作者没有需要披露的相关财务或非财务利益。

参考文献

1. 曾G、赵Z、马宗G、皮尔尔M、钟S、斯科拉里科斯A等（2022）《欧洲泌尿外科学会尿路结石分会与国际尿路结石联盟关于肾结石逆行肾内手术治疗的联合共识》。《欧洲泌尿外科学焦点》8(5)：1461–1468.2021年11月28日电子版。doi.org/10.1016/j.euf.2021.10.011https://
2. Knudsen BE（2019）钬激光：YAG碎石术用激光光纤——重要性与创新点。《北美泌尿临床》46(2)：185–191。电子版2019年4月10日发布。https://doi.org/10.1016/j.ucl.2018.12.004
3. Traxer O，Keller EX（2020）铥光纤激光：治疗肾结石的新选择？与钬：YAG激光的比较。世界泌尿外科杂志38(8)：1883-1894。电子版2019年2月8日。<sp_
4. Traxer O，Rapoport L，Tsarichenko D，Dymov A，Enikeev D，Sorokin N等（2018）发表的V03-02号论文，是首项关于超脉冲铥光纤激光在碎石术中的临床研究，发表于《泌尿学杂志》199卷4S期，页码e321–e2。
5. White C，Aziz M（1985）材料激光与电子束辐照过程中的能量沉积、热流及快速凝固。橡树岭国家实验室
6. 洛佩斯ACN，达拉令V，卡雷拉RV，莫利纳WR，格利纳S（2021）输尿管镜检查期间肾内压力与温度的影响：是否重要？《巴西泌尿学杂志》2020年第47卷第2期，第436–442页，电子版发布于2020年12月8日。https://doi.org/10.1590/s1677-5538.ibju.2020.0428
7. 阿尔杜基AH，通JJ，马吉达兰尼SE，霍尔TL，加尼KR，霍林斯沃思JM等人（2021）在尿道镜碎石术中激光脉活模式：对盐状结构液体温度及热剂量的影响。《泌尿外科学杂志》35(8)：1217–1222，电子版发布于2021年1月6日。https://doi.org/10.1089/end.2020.1067
8. Aldoukhi AH，Ghani KR，Hall TL，Roberts WW（2017）高功率钬激光碎石术的热反应。J Endourol 31（12）：1308–1312。https://doi.org/10.1089/end.2017.0679 PubMed PMID：29048216 Epub 2017/10/20
9. Aldoukhi AH，Hall TL，Ghani KR，Maxwell AD，MacConaghy B，Roberts WW（2018）高功率钬激光碎石术中肾体内模型的肾盏液温度。J Endourol 32(8)：724–729 Epub 2018/06/16。https://doi.org/10.1089/end.2018.0395
10. Buttice S，Sener TE，Proietti S，Dragos L，Tefik T，Doizi S等（2016）激光应用？J Endourol 30(5)：574-579,2016年2月4日电子版。https://doi.org/10.1089/end.2015.0747。肾盏内的温度变化：钬：钇铝石榴石治疗期间发生了什么
11. Dau JJ，Hall TL，Maxwell AD，Ghani KR，Roberts WW（2021）冷却冲洗对激光碎石术中肾盏液温度和热损伤阈值时间的影响：体外模型。J Endourol 35(5)：700–705 Epub 2020/11/13。https://doi.org/10.1089/end.2020.0896
12. Gallegos H，Bravo JC，Sepulveda F，Astroza GM（2021）肾内温度测量与钬激光体腔碎石术在离体模型中的相关性。Cent Eur J Urol 74(4)：588–594 Epub 2022/01/28。https://doi.org/10.5173/ceju.2021.0092
13. Kallidonis P，Kamal W，Panagopoulos V，Vasilas M，Anastasiadis L，Kyriazis I et al（2016）Thulium Laser in the Upper urinary tract：does the Heat Generation in the Irrigation Fluid pose a risk? Evidence from an in vivo experimental study.J Endourol 30(5)：555–559 Epub 2016/01/06.https://doi.org/10.1089/end.2015.0768
14. Maxwell AD，MacConaghy B，Harper JD，Aldoukhi AH，Hall TL，Roberts WW（2019）激光碎石术所致尿路加热的模拟。J Endourol 33(2)：113–119 Epub 2018/12/27。https://doi.org/10.1089/end.2018.0485
15. Molina WR，Carrera RV，Chew BH，Knudsen BE（2021）输尿管激光碎石术期间的温度升高：超脉冲铥光纤激光器（SPTF）与高功率120 W钬YAG激光器（Ho：YAG）的比较。World J Urol 39（10）：3951–3956 Epub 2021/02/20。https://doi.org/10.1007/s00345-021-03619-3
16. Molina WR，Silva IN，Donalisio da Silva R，Gustafson D，Sehrt D，Kim FJ（2015）盐水对激光碎石术激活温度曲线的影响。J Endourol 29(2)：235–239 Epub 2014/08/27。https://doi.org/10.1089/end.2014.0305
17. Noureldin YA，Farsari E，Ntasiotis P，Adamou C，Vagionis A，Vrettos T et al（2021）灌注参数和套管尺寸对高功率激光柔性输尿管镜检查期间肾内温度的影响。World J Urol 39(4)：1257–1262 Epub 2020/06/20。https://doi.org/10.1007/s00345-020-03287-9
18. Winship B，Terry R，Boydston K，Carlos E，Wollin D，Peters C et al（2019）铥：钇铝石榴石激光脉冲类型对台式输尿管模型灌注温度的影响。J Endourol 33（11）：896–901 Epub 2019/08/17。https://doi.org/10.1089/end.2019.0496
19. Winship B，Wollin D，Carlos E，Peters C，Li J，Terry R et al（2019）输尿管镜钬激光碎石术期间高温的上升和下降。J Endourol 33（10）：794–799 Epub 2019/04/25。https://doi.org/10.1089/end.2019.0084
20. Van Rhoon GC，Samaras T，Yarmolenko PS，Dewhirst MW，Neufeld E，Kuster N（2013）CEM43°C热剂量阈值：避共振脏频暴露水平的潜在指南？Eur Radiol 23：2215–2227
21. 吴祥，魏杰，孙鹏，黄福，王兵，黄刚等（2023）在《国际泌尿肾病杂志》55卷7期发表《高倍率柔性输尿管镜下摩西钬激光碎石术中肾盏温度变化的病例分析研究》。电子版发表于2023年5月5日。https://doi.org/10.1007/s11255-023-03611-3
22. Æsøy MS，Juliebø-Jones P，Beisland C，UlvikØ（2024）柔性输尿管镜激光碎石术中的温度测量：一项前瞻性临床试验 。J Endourol.Epub 2024/01/08。https://doi.org/10.1089/end.2023.0660。PubMed PMID：38185920
23. 滕杰、王勇、贾志、吴勇、曹伟、艾旭（2021）柔性输尿管镜钬：钇铝石榴石激光碎石术中膀胱输尿管灌溉液温度分布研究。《国际泌尿与肾脏病学》，53(3)：415-9。电子版发布于2020年9月30日。https://doi.org/10.1007/s11255-020-02665-x。PubMed PMID：32989671
24. 海因S、佩措尔德R、舍恩塔勒M、韦特奥尔U、米尔尼克A（2018）钬：钇铝石榴石激光碎石术的热效应：体外模型中的实时评估。世界泌尿学杂志：36(9)：1469-75。电子版发布于2018年4月25日。https://doi.org/10.1007/s00345-018-2303-x。PubMed PMID：29691640
25. Peteinaris A，Pagonis K，Vagionis A，Adamou C，Tsaturyan A，Ballesta Martinez B等学者（2022年）研究了脉冲调制技术、激光参数设置及术中冲洗条件对冲洗液温度的影响。

输尿管镜检查是否灵活？一项使用人工结石的体内实验。《世界泌尿学杂志》40(7)：1853–1858。https://doi.org/10.1007/s00345-022-04002-6

26. 皮埃特罗保罗·A、布雷斯·涅瓦达·E、斯科拉里斯·A、柯亚齐科斯·E、卡利多尼斯·P、阿布马尔祖克·O等学者（2019）发表《全球非柔性输尿管镜检查实践调查：欧洲泌尿外科学会青年学术泌尿科医师及泌尿技术组调研报告》，该论文发表于《中欧泌尿学杂志》2020年第72卷第4期，页码393-397，电子版发布日期为2020年2月6日。https://doi.org/10.5173/ceju.2019.0041
27. Petenaris A，Faitatziadis S，Tsaturyan A，Pagonis K，Lintsikos E，Kallidonis P（2022）moses™脉冲调制技术与传统脉冲输送技术：对输尿管软镜检查期间灌注液温度的影响。Urolithiasis 50(5)：613–618。https://doi.org/10.1007/s00240-022-01342-1
28. Wollin DA，Carlos EC，Tom WR，Simmons WN，Preminger GM，Lipkin ME（2018）钬激光碎石术体外模型中激光设置和冲洗速率对输尿管温度的影响。J Endourol 32(1)：59-63。Epub 2017/10/20。https://doi.org/10.1089/end.2017.0658
29. Louters MM，Dau JJ，Hall TL，Ghani KR，Roberts WW（2022）激光操作员工作周期对温度和热剂量的影响：体外研究。《世界泌尿学杂志》40(6)：1575–1580，电子版发布于2022年2月28日。https://doi.org/10.1007/s00345-022-03967-8
30. Rezakahn Khajeh N，Hall TL，Ghani KR，Roberts WW（2022）激光碎石术期间肾盂肾盏体积和液体温度升高。J Endourol 36(1)：22–28 Epub 2021/07/14。https://doi.org/10.1089/end.2021.0383
31. Panchard F，Ventimiglia E，Corrales M，Traxer O（2022）《RIRS期间肾内温度和压力管理的实用指南：证据告诉我们什么》J Clin Med，11（12）.Epub 2022/06/25.https://doi.org/10.3390/jcm11123429.PubMed PMID：35743499；PubMed Central PMCID：PMCPMC9224584
32. Aldoukhi A，Hall T，Ghani K，Roberts W（2020）不同激光碎石术模式下激光光纤至结石距离的分析。《欧洲泌尿外科开放科学》19：e340–e1
33. 梁浩、梁立、余勇、黄兵、陈杰、王聪等（2020）钬激光在输尿管镜碎石术中的热效应研究。《BMC泌尿外科》20：1–4
34. 加列戈斯H，布拉沃JC，塞普尔维达F，阿斯特罗萨GM（2021）体外模型中钬激光碎石术的肾内温度测量研究。《中欧泌尿学杂志》74(4)：588
35. Peteinaris A，Tsaturyan A，Bravou V，Tatanis V，Faria-Costa G，Pagonis K等（2023）高功率激光碎石术——我们是治疗还是伤害？钬光纤激光在体内研究中温度效应的组织学评价。Cent Eur J Urol 76(1)：44–48 Epub 2023/04/18。https://doi.org/10.5173/ceju.2023.24
36. Sapareto SA，Dewey WC（1984）癌症治疗中的热剂量测定。Int J Radiat Oncol Biol Phys 10(6)：787-800，电子版1984/06/01。https://doi.org/10.1016/0360-3016（84）90379-1
37. 亚尔莫连科PS、根恩EJ、兰登C、爱祖尔A、霍克曼DW、斯科亚蒂BL等人（2011）正常组织热损伤阈值：最新进展。《国际高热杂志》27(4)：320–343 PubMed PMID：21591897；PubMed Central PMCID：PMCPMC3609720
38. Bhojani N，Koo KC，Bensaadi K，Halawani A，Wong VK，Chew BH（2023）人体首次应用Lith的回顾性研究oVue™Elite输尿管镜测量肾内压。BJU Int 132(6)：678–685 Epub 2023/09/05。https://doi.org/10.1111/bju.16173

出版商注Springer Nature对已发表地图和机构隶属关系的司法管辖权主张保持中立。

Springer Nature或其授权方（例如学会或其他合作伙伴）根据与作者或其他权利持有人签订的出版协议，对本文拥有独家权利；作者对本文已接受的稿件版本进行自我存档，完全受该出版协议条款和适用法律的约束。

输尿管结石患者行输尿管镜下钬激光碎石术治疗后输尿管狭窄发生情况及影响因素分析

张恒志[1]

【摘要】 **目的：**分析输尿管结石患者行输尿管镜下钬激光碎石术治疗后输尿管狭窄发生情况及影响因素。**方法：**选择 2022 年 2 月—2023 年 2 月贵阳贵航医院收治的 329 例行输尿管镜下钬激光碎石术治疗的输尿管结石患者作为研究对象。观察治疗后输尿管狭窄发生情况，分为狭窄组（n=21）、非狭窄组（n=308），比较两组一般资料，分析输尿管结石患者行输尿管镜下钬激光碎石术治疗后输尿管狭窄发生的影响因素。**结果：**329 例行输尿管镜下钬激光碎石术治疗的输尿管结石患者中，21 例治疗后发生输尿管狭窄，输尿管狭窄发生率为 6.38%。两组性别、年龄、体重指数、结石部位、患侧、合并尿路感染、结石残余、双 J 管留置时间比较，差异无统计学意义（P>0.05）；两组病程、结石直径、肾积水严重、结石嵌顿、炎性黏膜包裹比较，差异有统计学意义（P<0.05）。logistic 回归分析结果显示，病程长、结石直径大、肾积水严重、结石嵌顿、炎性黏膜包裹为输尿管镜下钬激光碎石术治疗后输尿管狭窄发生的影响因素（P<0.05）。**结论：**输尿管镜下钬激光碎石术治疗后仍存在一定的输尿管狭窄发生风险，病程长、结石直径大、肾积水严重、结石嵌顿、炎性黏膜包裹为其影响因素。

【关键词】 输尿管结石　钬激光碎石术　输尿管镜　输尿管狭窄

doi：10.14033/j.cnki.cfmr.2024.17.042　　文献标识码　B　　文章编号　1674-6805（2024）17-0166-04

Analysis of the Occurrence and Influencing Factors of Ureteral Stricture in Ureteral Calculi Patients after Ureteroscopic Holmium Laser Lithotripsy/ZHANG Hengzhi. //Chinese and Foreign Medical Research, 2024, 22(17): 166-169

[Abstract] **Objective:** To analyze the occurrence and influencing factors of ureteral stricture in ureteral calculi patients treated by ureteroscopic holmium laser lithotripsy. **Method:** A total of 329 patients with ureteral calculi who underwent ureteroscopic holmium laser lithotripsy treatment in Guiyang Guihang Hospital from February 2022 to February 2023 were selected as the study objects. The incidence of ureteral stricture after treatment was observed and divided into the stenosis group (n=21) and the non-stenosis group (n=308). The general data of the two groups were compared to analyze the influencing factors the occurrence of ureteral stricture in patients with ureteral calculi treated by ureteroscopic holmium laser lithotripsis. **Result:** Among 329 patients with ureteral calculi treated by ureteroscopic holmium laser lithotripsy, a total of 21 cases developed ureteral stricture after treatment, and the incidence of ureteral stricture was 6.38%. There were no significant differences in gender, age, body mass index, stone site, affected side, combined urinary tract infection, stone residue, and indindment time of double J-tube between the two groups (P>0.05). There were statistically significant differences in the course of disease, stone diameter, severe hydronephrosis, stone incarceration and inflammatory mucosal encapsulation between the two groups (P<0.05). logistic regression analysis showed that long course of disease, large stone diameter, severe hydronephrosis,

①贵航贵阳医院　贵州　贵阳　550009

stone incarceration, and inflammatory mucosal encapsulation were the influencing factors of ureteral stricture after ureteroscopic holmium laser lithotripsy (P<0.05). **Conclusion:** Ureteroscopic holmium laser lithotripsy has a certain risk of ureteral stricture, and the influencing factors are long course of disease, large stone diameter, severe hydronephrosis, stone incarceration, and inflammatory mucosal encapsulation.

[Key words] Ureteral calculi　Holmium laser lithotripsy　Ureteroscopic　Ureteral stricture

First-author's address: Guihang Guiyang Hospital, Guiyang 550009, China

输尿管结石是一个形成在输尿管中的固体结构，由于尿液中的某些物质沉积或结晶而形成，可以阻塞尿液的正常流动，并引起一系列的症状和并发症，导致尿液潴留，引起剧烈的腰背部疼痛、腹痛及尿频、尿急等不适症状[1]。输尿管镜下钬激光碎石术是一种治疗输尿管结石的微创手术，通过导入输尿管镜和钬激光设备可以精确地将激光能量聚焦在结石上，将结石分解成更小的颗粒，以便更容易排出体外[2]。然而，输尿管镜下钬激光碎石术治疗后仍然可能会出现术后输尿管狭窄，即输尿管内径变窄，会限制尿液的正常流动，引起尿液梗阻、尿痛、尿频等尿路症状，容易滞留尿液，增加尿路感染的风险，严重的输尿管狭窄还可能会导致肾脏受损，影响肾功能[3]。因此，需要采取预防措施来减少输尿管结石和术后输尿管狭窄的风险，现报告如下。

1　资料与方法

1.1　一般资料

选择 2022 年 2 月—2023 年 2 月贵阳贵航医院收治的 329 例行输尿管镜下钬激光碎石术治疗的输尿管结石患者作为研究对象。纳入标准：（1）符合《中国泌尿外科和男科疾病诊断治疗指南（2019 版）》[4]标准；（2）初次进行结石手术；（3）输尿管镜下钬激光碎石术适应证；（4）影像学确诊；（5）资料完整；（6）沟通、认知均正常；（7）单侧输尿管结石。排除标准：（1）精神障碍；（2）合并肾结石；（3）组织增生导致的输尿管狭窄；（4）输尿管狭窄病史；（5）多发输尿管结石；（6）既往有输尿管手术史；（7）严重躯体疾病。本研究经贵阳贵航医院医学伦理委员会批准，患者及家属知情同意。

1.2　方法

1.2.1　基线资料　设计一般资料调查表，仔细询问、调查并记录患者的相关资料，内容包括：（1）性别；（2）年龄；（3）体重指数；（4）病程；（5）结石直径；（6）结石部位（上段、中段、下段）；（7）患侧（左侧、右侧）；（8）肾积水程度（重度、轻中度）；（9）结石嵌顿（是、否）；（10）炎性黏膜包裹（是、否）；（11）合并尿路感染（是、否）；（12）结石残余（是、否）；（13）双 J 管留置时间（>4 周、≤4 周）。

1.2.2　输尿管狭窄评估及分组　输尿管狭窄判断：于输尿管镜下钬激光碎石术治疗后 3~6 周拔除双 J 管，并于拔除后的 1 周、2 周、1 个月、3 个月、6 个月进行复查，使用泌尿系彩超，如出现肾积水加重情况，需进一步进行 CT、造影等检查，若为输尿管狭窄造成肾积水加重，则判断为发生输尿管狭窄。观察治疗后输尿管狭窄发生情况，分为狭窄组（发生输尿管狭窄）、非狭窄组（未发生输尿管狭窄）。

1.3　统计学处理

本研究数据采用 SPSS 22.0 统计学软件进行分析和处理，计量资料以（$\bar{x}\pm s$）表示，采用 t 检验，计数资料以率（%）表示，采用 χ^2 检验，以 P<0.05 为差异有统计学意义。

2　结果

2.1　输尿管镜下钬激光碎石术治疗后输尿管狭窄的发生情况

329 例行输尿管镜下钬激光碎石术治疗的输尿管结石患者中，有 21 例治疗后发生输尿管狭窄，输尿管狭窄发生率为 6.38%。

2.2　狭窄组和非狭窄组一般资料比较

两组病程、结石直径、肾积水严重、结石嵌顿、炎性黏膜包裹比较，差异有统计学意义（P<0.05）；两组性别、年龄、体重指数、结石部位、患侧、合并尿路感染、结石残余、双 J 管留置时间比较，差异无统计学意义（P>0.05），见表 1。

2.3　输尿管镜下钬激光碎石术治疗后输尿管狭窄发生的影响因素分析

将输尿管狭窄发生情况作为应变量（发生输尿管狭窄=1，未发生输尿管狭窄=0），将病程（连续变量）、结石直径（连续变量）、肾积水程度（重度=1，轻中度=0）、结石嵌顿（是=1，否=0）、炎性黏膜包裹（是=1，否=0）作为自变量，经 logistic

回归分析结果显示，病程长、结石直径大、肾积水严重、结石嵌顿、炎性黏膜包裹为输尿管镜下钬激光碎石术治疗后输尿管狭窄发生的影响因素（$P<0.05$），见表 2。

表1 狭窄组和非狭窄组一般资料比较

组别	性别[例（%）]		年龄	体重指数	病程
	男	女	[岁，（$\bar{x}\pm s$）]	[kg/m^2，（$\bar{x}\pm s$）]	[个月，（$\bar{x}\pm s$）]
狭窄组（n=21）	11（52.38）	10（47.62）	50.13±5.52	22.12±0.86	5.05±0.50
非狭窄组（n=308）	175（56.82）	133（43.18）	50.87±5.74	22.06±0.79	4.13±0.52
χ^2/t 值	0.158		0.573	0.335	8.204
P 值	0.691		0.567	0.738	<0.001

组别	结石直径	结石部位[例（%）]			患侧[例（%）]	
	[cm，（$\bar{x}\pm s$）]	上段	中段	下段	左侧	右侧
狭窄组（n=21）	1.93±0.31	3（14.29）	10（47.62）	8（38.10）	11（52.38）	10（47.62）
非狭窄组（n=308）	1.38±0.25	37（12.01）	141（45.78）	130（42.21）	168（54.55）	140（45.45）
χ^2/t 值	9.598		0.177		0.037	
P 值	<0.001		0.915		0.847	

组别	肾积水[例（%）]		结石嵌顿[例（%）]		炎性黏膜包裹[例（%）]	
	重度	轻中度	是	否	是	否
狭窄组（n=21）	13（61.90）	8（38.10）	14（66.67）	7（33.33）	12（57.14）	9（42.86）
非狭窄组（n=308）	76（24.68）	232（75.32）	98（31.82）	210（68.18）	84（27.27）	224（72.73）
χ^2/t 值	13.808		10.633		8.488	
P 值	<0.001		0.001		0.003	

组别	合并尿路感染[例（%）]		结石残余[例（%）]		双J管留置时间[例（%）]	
	是	否	是	否	>4周	≤4周
狭窄组（n=21）	12（57.14）	9（42.86）	2（9.52）	19（90.48）	11（52.38）	10（47.62）
非狭窄组（n=308）	122（39.61）	186（60.39）	18（5.84）	290（94.16）	125（40.58）	183（59.42）
χ^2/t 值	2.503		0.045		1.128	
P 值	0.114		0.832		0.288	

表2 输尿管镜下钬激光碎石术治疗后输尿管狭窄发生的影响因素分析

因素	B	SE	Wald χ^2 值	P 值	OR 值	95%CI
病程	3.134	0.611	26.288	<0.001	22.963	6.930，76.084
结石直径	6.250	0.996	39.387	<0.001	518.191	73.579，3 649.443
肾积水程度	1.602	0.468	11.691	0.001	4.961	1.981，12.423
结石嵌顿	1.455	0.479	9.238	0.002	4.286	1.677，10.954
炎性黏膜包裹	1.269	0.459	7.633	0.006	3.556	1.446，8.744

3 讨论

输尿管结石阻塞尿液流动，造成尿液在尿路内滞留，易导致细菌感染，引发尿路感染的症状，如尿道灼热、尿频、尿急、尿痛等[5]。而且，结石经过输尿管时，可能会刮伤或刺激输尿管壁，引发输尿管炎症，甚至导致输尿管损伤，增加出血的风险。相比传统的手术方法，钬激光碎石术对周围组织损伤较小，可以最大限度地保护输尿管壁和其他组织，采用经尿道方式进行，无须开放手术，减少了术后的恢复时间和并发症的风险[6]。

本研究结果显示，329 例行输尿管镜下钬激光碎石术治疗的输尿管结石患者中，21 例治疗后发生输尿管狭窄，输尿管狭窄发生率为 6.38%。说明输尿管镜下钬激光碎石术治疗后仍存在一定的输尿管狭窄发生风险。经 logistic 回归分析结果显示，病程长、结石直径大、肾积水严重、结石嵌顿、炎性黏膜包裹为输尿管镜下钬激光碎石术治疗后输尿管狭窄发生的影响因素。分析原因为：（1）病程长说明结石已经存在较长时间并积聚成较大的固体物质，会导致输尿管黏膜的慢性刺激和炎症反应，进一步损伤输尿管组织，可能导致输尿管内组织的瘢痕形成和纤维化，增加输尿管狭窄的风险[7]。长期存在

的结石可能会引起其他并发症，例如肾功能异常或尿路感染，这些并发症本身就可能对输尿管组织造成进一步的损伤，增加术后发生输尿管狭窄的风险[8]。（2）钬激光碎石术是一种常用于治疗输尿管结石的手术方法，使用钬激光器产生的高能量光束将结石碎成小颗粒，以便更容易通过尿道排出体外。然而，当直径较大的结石被钬激光碎石术分解时，其中的碎片可能会比较粗糙，并可引发输尿管黏膜的炎症和损伤[9]。这些炎症反应可能导致组织增生和瘢痕形成，最终导致输尿管狭窄。此外，输尿管直径大的结石由于占据了更多的空间，可能会对周围组织施加更大的压力，增加了狭窄发生的风险[10]。（3）肾积水是指尿液在肾脏内无法正常排出，导致肾盂和输尿管扩张，重度肾积水意味着结石阻塞了输尿管的通路，导致尿液无法顺利流动，这种持续的阻塞会对输尿管壁施加压力，并引起炎症反应和组织损伤，当结石被钬激光碎石术分解时，由于长期的阻塞已经引起了严重的组织改变，再加上手术过程中的刺激，可能会增加输尿管狭窄的风险[11]。（4）结石嵌顿意味着结石阻塞了尿液的流动，会对输尿管壁施加压力，并引起炎症反应和组织损伤，当结石被钬激光碎石术分解时，由于结石嵌顿导致的组织损伤已经存在，再加上手术过程中的刺激，可能会增加输尿管狭窄的风险[12]。在进行钬激光碎石术时，为了辅助操作，可能会插入导丝或支架来保持输尿管通畅，然而，当结石嵌顿存在时，导丝或支架可能会更难插入，或者可能会引起更多的刺激和损伤，进一步增加了输尿管狭窄的风险[13]。（5）炎性黏膜包裹的输尿管结石通常会引起强烈的炎症反应，这是由于结石与输尿管黏膜之间的持续摩擦和刺激，当进行钬激光碎石术分解结石时，释放的结石碎片可能会进一步加剧炎症反应，持续的炎症反应会导致组织增生和纤维化，增加了输尿管狭窄的风险[14-15]。

综上所述，输尿管镜下钬激光碎石术治疗后仍存在一定的输尿管狭窄发生风险，病程长、结石直径大、肾积水严重、结石嵌顿、炎性黏膜包裹为其影响因素。

参 考 文 献

[1] 郭小强，夏强，顿文超. 输尿管软镜钬激光碎石术与输尿管硬镜碎石联合套石篮治疗输尿管上段结石的疗效比较[J]. 实用临床医药杂志，2023，27（2）：105-108.

[2] 秦刚，谢英金. 输尿管软镜下钬激光碎石术对复杂性上尿路结石患者疗效及术后复发的影响[J]. 实用医院临床杂志，2021，18（5）：166-169.

[3] LI X，QIAO J，XIONG S，et al. The surgical outcomes of reconstruction for the treatment of ureteral stricture after holmium laser lithotripsy: the comprehensive experiences[J]. Asian J Surg，2022，45（12）：2713-2718.

[4] 黄健. 中国泌尿外科和男科疾病诊断治疗指南（2019 版）[M]. 北京：科学出版社，2019：237-268.

[5] 唐朝，吴明霞. 输尿管镜下钬激光碎石术和气压弹道碎石术治疗老年输尿管结石的疗效及对患者肾功能的影响研究[J]. 贵州医药，2021，45（8）：1251-1252.

[6] 张江兵，曹护春，周岩，等. 改良输尿管镜钬激光碎石术治疗输尿管中、下段结石的有效性和安全性分析[J]. 蚌埠医学院学报，2021，46（3）：372-375.

[7] 万克松，王传圣，程华根，等. 输尿管镜碎石术后并发输尿管狭窄风险的列线图模型预测[J]. 国际泌尿系统杂志，2021，41（2）：323-327.

[8] 刘俊炜，杨嗣星（审校）. 输尿管结石术后发生输尿管狭窄的机制及相关危险因素分析[J]. 临床泌尿外科杂志，2022，37（6）：478-482.

[9] 孟凯，李东. 钬激光碎石术治疗输尿管结石后发生输尿管狭窄的危险因素分析[J]. 贵州医药，2020，44（9）：1440-1441.

[10] 乃比江·毛拉库尔班，姜孜麦麦提·艾合麦提江，夏韩，等. 基于贝叶斯网络模型分析输尿管结石患者碎石术后输尿管狭窄的发生因素[J]. 现代泌尿外科杂志，2022，27（11）：897-902.

[11] SHEN Y，XIANG A，SHAO S. Preoperative hydronephrosis is a predictive factor of ureteral stenosis after flexible ureteroscopy: a propensity scores matching analysis[J]. BMC Urol，2021，21（1）：153.

[12] 周乐，胡焕春，汪波. 单发输尿管结石患者行输尿管镜下钬激光碎石术后狭窄的危险因素分析[J]. 国际泌尿系统杂志，2020，40（2）：231-234.

[13] 王洪超，曹敬毅，孙卫兵，等. 输尿管软镜钬激光碎石术后继发输尿管狭窄的相关性因素分析[J]. 国际泌尿系统杂志，2022，42（3）：433-436.

[14] 张志成，廖继强. 输尿管镜下钬激光碎石术后输尿管狭窄的危险因素分析[J]. 中国药物与临床，2020，20（8）：1270-1272.

[15] 万优，许长宝，赵兴华，等. 输尿管上段嵌顿性结石术后发生输尿管狭窄的影响因素分析[J]. 微创泌尿外科杂志，2020，9（5）：324-329.

（收稿日期：2024-01-02）

·激光在泌尿外科领域的应用·

低功率钬激光瞬时切割对输尿管狭窄及组织纤维化的影响

彭永涵 李超 董浩 高小峰
海军军医大学第一附属医院泌尿外科，上海 200433
通信作者：高小峰，Email：gxfdoc@sina.com

【摘要】 **目的** 探索钬激光瞬时切割损伤对猪输尿管狭窄及组织纤维化的影响。**方法** 选取10头白雌猪，在双侧输尿管距肾盂输尿管连接部5、10、15、20 cm处分别标记为A、B、C、D组，各组激光参数设置如下：A组0.5 J×20 Hz（短脉冲），B组1.0 J×10 Hz（短脉冲），C组0.5 J×20 Hz（长脉冲）和D组1.0 J×10 Hz（长脉冲）。每组应用钬激光进行烧灼，能量设置统一为低功率（10 W），烧灼点取手术视野6点钟位置，烧灼时长约1 s。术后留置双J管1个月。术后4个月处死实验猪并剖取双肾、输尿管以及膀胱标本，沿长轴剖开输尿管，按术中标记距离及肉眼所见记录各组烧灼点狭窄情况，截取各组烧灼点输尿管组织，行组织病理学HE染色及Masson染色，分析组织损伤及纤维化情况。**结果** 本研究1头实验猪术中未能找到左侧输尿管开口，3头实验猪术后当天死亡，最终纳入6头猪，共12侧尿路标本进行分析，包含48个烧灼点。各烧灼点输尿管局部狭窄的发生率为64.6%（31/48），其中重度狭窄发生率为8.3%（4/48）。A、B、C、D组狭窄发生率分别为66.7%（8/12）、66.7%（8/12）、66.7%（8/12）、52.5%（8/12），各组在狭窄发生率（$P=1.000$）及狭窄程度（$P=0.075$）方面的差异均无统计学意义。组织病理学分析结果显示，A、B、C、D组的组织损伤深度[（1 645.46±277.01）、（1 976.59±222.62）、（1 841.37±189.59）、（2 055.66±206.40）μm，$P=0.560$]及胶原纤维面积百分比[（70.22±1.75）%、（69.48±1.34）%、（68.00±2.03）%、（74.39±1.20）%，$P=0.560$]差异均无统计学意义。**结论** 即使在低功率设置下，钬激光对输尿管组织的瞬时切割仍会导致较高的输尿管狭窄发生率。钬激光频率及脉冲长度选择对输尿管狭窄的发生率、组织病理损伤及纤维化程度无显著影响。

【关键词】 输尿管； 狭窄； 热损伤； 激光碎石术； 动物实验
基金项目：国家自然科学基金（82270805）
DOI：10.3760/cma.j.cn112330-20240614-00266

Effect of low-power Holmium laser instant cutting on ureteral stricture and tissue fibrosis

Peng Yonghan, Li Chao, Dong Hao, Gao Xiaofeng
Department of Urology, the First Affiliated Hospital of Naval Medical University, Shanghai 200433, China
Corresponding author: Gao Xiaofeng, Email: gxfdoc@sina.com

【**Abstract**】 **Objective** To investigate the effects of Holmium laser instant cutting damage on ureteral stricture and tissue fibrosis in pigs. **Methods** Ten female white pigs were selected, and the bilateral ureters were marked at 5 cm, 10 cm, 15 cm, and 20 cm from the ureteropelvic junction (UPJ), designated as groups A, B, C, and D, respectively. The laser parameters were set as follows: Group A 0.5 J×20 Hz (short pulse), Group B 1.0 J×10 Hz (short pulse), Group C 0.5 J×20 Hz (long pulse), and Group D 1.0 J×10 Hz (long pulse). Holmium laser ablation was performed at each group with a uniform low power setting (10 W) for approximately 1 second at the 6 o'clock position of the surgical field. A double J stent was placed for one month post-operation. The experimental pigs were euthanized three months after stent removal, and specimens of the kidneys, ureters, and bladder were collected. The ureters were longitudinally opened, and the stenosis at each marked ablation site was recorded and subjected to histopathological analysis. **Results** In this study, 1 pig failed to find the left ureteral opening during the operation, and 3 pigs died after operation. Six pigs with a total of 12 ureteral specimens were finally included. The incidence of local ureteral stricture at the ablation sites was 64.6% (31/48), with severe stricture occurring at 8.3% (4/48). The incidence of stricture in group A, B, C, and D were 66.7% (8/12), 66.7% (8/12), 66.7% (8/12), and 52.5% (8/12), respectively. There was no significant difference in the incidence

($P=1.000$) and degree ($P=0.075$) of stricture among the groups. Histopathological analysis showed no significant differences in tissue damage depth[(1 645.46±277.01) μm vs. (1 976.59±222.62) μm vs. (1 841.37±189.59) μm vs. (2 055.66±206.40) μm, $P=0.560$] and collagen fiber area percentage [(70.22±1.75)% vs. (69.48±1.34)% vs. (68.00±2.03)% vs. (74.39±1.20)%, $P=0.560$] among the groups. **Conclusions** Even under low power settings, instant cutting of ureteral tissue by Holmium laser results in a high incidence of ureteral stricture. The frequency and pulse length of the Holmium laser have no significant effect on the incidence of ureteral stricture, histopathological damage, or the degree of fibrosis.

[Key words] Ureter; Stricture; Thermal injury; Laser lithotripsy; Animal experiment
Fund program: National Natural Science Foundation of China (82270805)
DOI:10.3760/cma.j.cn112330-20240614-00266

目前,输尿管镜钬激光碎石术因其微创、精准的特点,已逐步成为治疗泌尿系结石的首选手术方法之一[1-2]。输尿管狭窄是输尿管镜钬激光碎石术后严重的长期并发症,发生率为0.3%~4.9%,且在过去几年呈上升趋势[3-5];若输尿管狭窄得不到及时有效的治疗,将可能对患者肾功能造成不可逆的损害,最终导致肾衰竭等严重后果[6],部分复杂性输尿管狭窄病例在后期修复性治疗方面往往面临巨大的挑战及风险[7-8],输尿管镜钬激光碎石术后输尿管狭窄的形成原因涉及多种因素,其中钬激光对输尿管直接或间接的损伤是其重要原因;既往研究结果显示,与气压弹道相比,钬激光碎石明显增加了输尿管狭窄的发生风险[9-10]。钬激光对输尿管组织的损伤主要来自于其直接切割效应及局部高温对周围组织的影响。近年来,关于钬激光引发的输尿管组织局部高温效应的研究逐渐增多;然而,关于钬激光瞬时切割作用对输尿管狭窄影响的研究尚未见报道。本研究于2019年11月至2020年3月通过建立钬激光瞬时切割输尿管损伤的动物模型,探讨钬激光瞬时切割性损伤对输尿管狭窄及组织纤维化的影响,并进一步探究不同能量参数设置在其中的作用。

材料与方法

一、研究对象及实验器材

以上海雌性白猪为实验对象,共10头,均为6个月龄,平均体重60 kg,饮食及排尿正常,由吴江市田宇生物科技有限公司提供;实验白猪自由饮食,适应性喂养2周后进行实验。实验采用F8.55一次性电子输尿管软镜(型号US31B-12,上海英诺伟医疗器械股份有限公司)及大功率钬激光治疗机(型号SRM-H3B,上海瑞柯恩激光技术有限公司)。

二、输尿管钬激光瞬时切割热损伤模型的建立

实验猪麻醉后使用输尿管软镜裸镜进入输尿管,行至肾盂输尿管连接部(ureteropelvic junction,UPJ)缓慢退镜,于双侧输尿管距离UPJ为5、10、15、20 cm处分别标记为A、B、C、D组。各组激光参数设置如下:A组0.5 J×20 Hz(短脉冲),B组1.0 J×10 Hz(短脉冲),C组0.5 J×20 Hz(长脉冲),D组1.0 J×10 Hz(长脉冲)。每组应用钬激光进行烧灼,能量设置统一为低功率(10 W),烧灼点取手术视野6点钟位置,烧灼时长约1 s。术后留置双J管1个月。术后4个月行输尿管镜检查,观察输尿管狭窄情况。处死实验猪后进行解剖,取双肾、输尿管以及膀胱标本。沿长轴剖开输尿管,按术中标记距离肉眼探查各组烧灼点狭窄情况,并截取各组烧灼点输尿管组织,分别进行组织病理学分析。

本研究中输尿管狭窄的判定标准:轻度狭窄为F6导管可通过,肉眼及镜下可见瘢痕形成及管腔变窄;重度狭窄为F6导管不能通过。

三、制片及病理学分析

送检标本经4%多聚甲醛固定,固定状态良好后,严格按照本单位病理实验检测SOP程序进行修剪、脱水、包埋、切片、染色、封片,最后镜检合格的样片。

病理学分析采用以下3种方法。①损伤深度分析:应用Image-Pro Plus 6.0软件,每张烧灼点病理切片选取8处,测量出组织的损伤深度并取平均值。②纤维化分析:病理切片行Masson染色,每组内每张切片随机挑选至少3个200倍视野进行拍照,应用Image-Pro Plus 6.0软件分别测量Masson染色阳性像素面积,结合视野像素面积,得出胶原纤维的面积百分比=胶原纤维像素面积/视野像素面积×100%。③组织学分析:病理切片HE染色,统计组织病变情况。

四、统计学方法

采用SPSS 26.0统计软件进行数据分析。计量资料均符合正态分布,以$\bar{x}\pm s$表示,组间比较采用ANOVA方差分析;分类变量以频率和百分比表示,

组间比较采用χ^2检验或 Fisher 精确检验；多组独立样本的等级资料，组间比较采用 Kruskal-Wallis 检验。以 $P<0.05$ 为差异有统计学意义。

结　果

一、输尿管镜检查及狭窄率分析

本研究 1 头实验猪术中未能找到左侧输尿管开口，3 头实验猪术后当天死亡；最终纳入 6 头猪，共 12 侧尿路标本进行分析，包含 48 个烧灼点。输尿管软镜下可见烧灼点狭窄以轻度为主，狭窄段输尿管可见黏膜缺血、苍白、瘢痕形成等改变，重度狭窄可观察到输尿管管腔闭锁（图 1）。狭窄总发生率为 64.6%（31/48），轻度狭窄发生率为 56.3%（27/48），重度狭窄为 8.3%（4/48）。其中，A 组未狭窄占比为 33.3%（4/12），轻度狭窄为 41.7%（5/12），重度狭窄为 25.0%（3/12）；B 组未狭窄占比为 33.3%（4/12），狭窄为 66.7%（5/12）且均为轻度狭窄；C 组未狭窄占比为 33.3%（4/12），轻度狭窄为 58.3%（7/12），重度狭窄为 25.0%（3/12）；D 组未狭窄占比为 47.5%（5/12），轻度狭窄为 58.3%（7/12），无重度狭窄发生。4 组标本在狭窄发生率（$\chi^2=0.42$，$P=1.000$）及狭窄程度（$K=1.360$，$P=0.075$）方面，差异均无统计学意义。

二、病理分析结果

获得烧灼病理切片 48 份，输尿管狭窄程度较轻时，输尿管组织病变主要以黏膜上皮肿胀、缺失为主，固有层及肌层水肿，肌纤维间隙增宽并有炎症细胞浸润；随着狭窄程度加重，输尿管局部肌层肌纤维消失，被大量增生的结缔组织取代（图 2）。A、B、C、D 组的组织损伤深度分别为（1 645.46 ± 277.01）、（1 976.59 ± 222.62）、（1 841.37 ± 189.59）、（2 055.66 ± 206.40）μm，各组间差异无统计学意义（$F=0.056$，$P=0.560$）；4 组病理标本胶原纤维面积的百分比分别为（70.22 ± 1.75）%、（69.48 ± 1.34）%、（68.00 ± 2.03）%、（74.39 ± 1.20）%，各组差异无统计学意义（$F=2.331$，$P=0.560$）。

讨　论

在钬激光碎石过程中，随着患者的呼吸活动，钬激光对输尿管黏膜的误击时有发生；在输尿管肿瘤的输尿管镜治疗中，更是需要使用激光直接烧灼肿瘤周围的黏膜组织，以实现肿瘤的完全剥离。尽管目前关于钬激光碎石过程中误击输尿管导致术后输尿管狭窄的数据仍然缺乏，但既往文献结果显示上尿路上皮肿瘤在接受激光治疗后，输尿管狭窄的并发症发生率最高可达 28.8%[1]，从而提示钬激光对输尿管黏膜直接烧灼可能会增加输尿管狭窄风险。本研究主要是建立钬激光对组织直接切割损伤的模型，为高度模拟临床钬激光碎石过程中误击输尿管的情况，本研究设置瞬时烧灼时间为 1 s，结果显示在钬激光烧灼处理部位输尿管狭窄的发生率高达 64.6%，重度狭窄发生率高达 8.3%。这一结果显示了钬激光对组织的直接损伤作用，而这方面在既往文献中较少被深入探讨。

钬激光的功率和能量设置是输尿管镜腔内碎石手术中的关键参数，术者根据结石的具体情况选择不同的参数以达到最佳的碎石效果。然而，钬激光不同能量参数对输尿管接触性损伤的影响尚未见相关文献报道。本研究结果表明，在相同钬激光功率设置下，钬激光的频率及脉冲长度对输尿管狭窄的

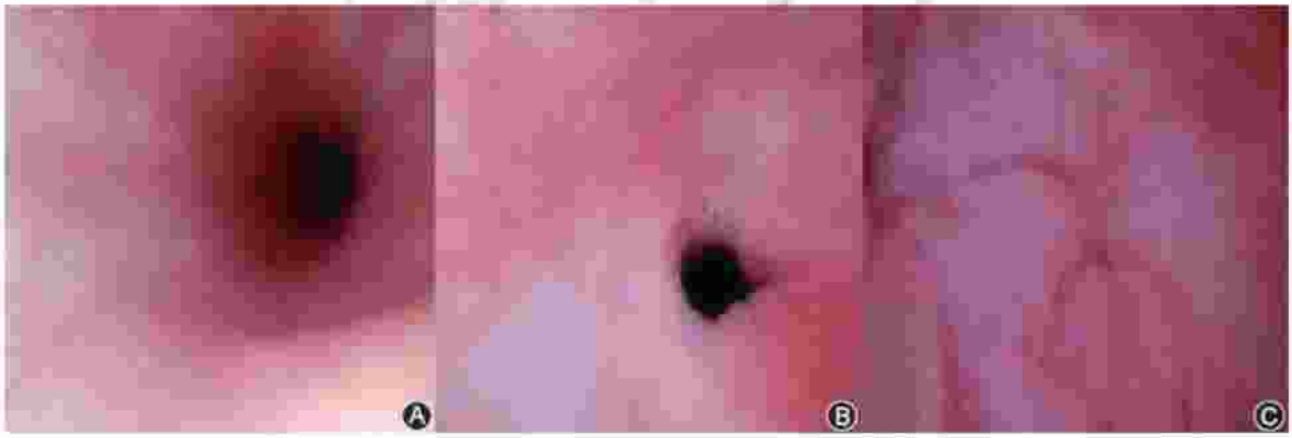


图 1　实验猪予钬激光瞬时切割输尿管损伤术后 4 个月输尿管软镜检查图像　A. 输尿管无狭窄，管腔通畅；B. 输尿管管腔轻度狭窄；C. 输尿管管腔完全闭锁

发生率、组织病理损伤及纤维化程度无显著影响。这一发现提示，在钬激光碎石术中，单纯通过调整频率和脉冲长度可能无法减少钬激光对输尿管组织的损伤。因此，术中采取各种策略避免钬激光误伤输尿管可能是降低输尿管狭窄的重要手段。目前关于钬激光功率及能量设置对输尿管损伤的研究主要集中在能量释放后局部温度升高的相关研究。已有研究结果表明，钬激光功率过高会增加肾脏热损伤的风险；当温度超过43℃时，高温导致的细胞毒性效应呈指数增加[12]。已有文献证实，高功率钬激光会导致局部温度迅速上升；但在低功率状态下，累积能量的发射也可能导致局部温度超过安全范围[13-14]。此外，脉冲模式对能量释放也有影响，长脉冲较短脉冲可能导致局部温度更高[15]。在本研究中，钬激光对输尿管进行瞬时切割，且在切割过程中保持输尿管软镜的正常灌注，因此，温度升高导致输尿管损伤的概率较小。

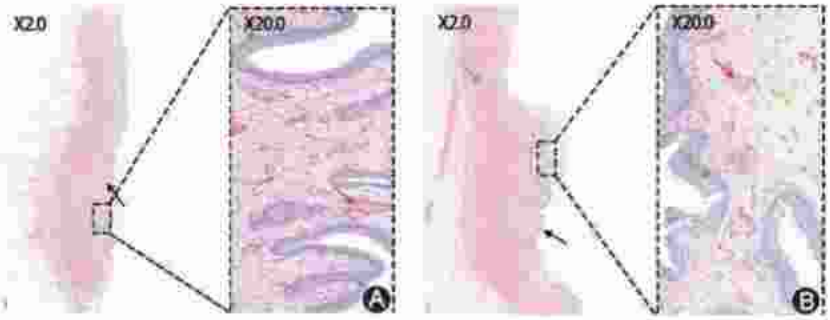


图 2　实验猪予钬激光瞬时切割输尿管后不同程度输尿管狭窄的组织学特征（HE 染色）A. 轻度狭窄段组织 HE 染色示，组织局部可见黏膜上皮细胞缺失（黑色箭头所示），较多上皮细胞肿胀，胞质疏松或呈空泡状（绿色箭头所示），固有层及肌层水肿，结缔组织排列疏松，肌纤维间隙增宽，较多血管淤血（红色箭头所示），并可见较多炎症细胞浸润（黄色箭头所示）；B. 重度狭窄段组织 HE 染色示，黏膜上皮细胞缺失（黑色箭头所示），较多上皮细胞肿胀，胞质疏松或呈空泡状（绿色箭头所示），固有层及肌层水肿，结缔组织排列疏松，肌纤维间隙增宽，较多血管淤血（红色箭头所示），并可见少量炎症细胞浸润（黄色箭头所示），肌层肌纤维消失，被大量增生的结缔组织取代（蓝色箭头所示）

钬激光的热效应对组织的损伤不仅包括温度升高的直接影响，还包括对光纤周围输尿管组织的广泛伤害。Ho 等[16]的研究结果显示，在热损伤的输尿管中，平滑肌消失，尿路上皮增生，周围软组织厚度增加，导致输尿管蠕动功能减弱，加重输尿管梗阻症状，进一步损害患肾功能。本研究得出类似的病理结果：当输尿管狭窄程度较轻时，主要表现为黏膜上皮坏死、脱落和缺失，受累输尿管的固有层常伴有炎症细胞浸润。随着狭窄的进展，固有层出现水肿，胶原纤维溶解，肌层平滑肌细胞开始出现坏死和溶解等病理改变。

尽管本研究提供了钬激光能量参数对输尿管损伤及纤维化影响的有价值数据，但仍存在局限性。首先，样本量较小，仅包括 10 头白雌猪，最终纳入分析的仅有 6 头，可能限制了结果的普遍性和统计学显著性。其次，本研究仅探讨了 10 W 功率下的不同频率和脉冲长度设置，未涉及其他能量水平。不同能量水平的钬激光可能对组织损伤和纤维化有不同影响，因此，未来研究应考虑更广泛的能量参数范围，以全面评估钬激光的效应。

综上所述，本研究建立了钬激光对输尿管瞬时切割的动物模型，结果显示即使在低功率设置下，钬激光的瞬时切割仍会导致较高的输尿管狭窄发生率，且部分病例出现重度狭窄。调整钬激光的频率及脉冲长度并未改善输尿管狭窄的发生率及组织纤维化的程度。因此，在进行输尿管镜钬激光碎石手术时，避免激光对输尿管组织的直接击打对于预防输尿管狭窄具有重要意义。

利益冲突　所有作者声明无利益冲突

作者贡献说明　彭冰涵：课题设计、论文撰写；李超、董浩：数据采集处理，图像采集；高小峰：研究指导、论文修改

参 考 文 献

[1] Oberlin DT, Flum AS, Bachrach L, et al. Contemporary surgical trends in the management of upper tract calculi[J]. J Urol, 2015, 193: 880-884. DOI: 10.1016/j.juro.2014.09.006.

[2] 高超，杨永安，马涛，等. 摩西钬激光与传统钬激光在输尿管软镜碎石术中的疗效比较[J]. 中华泌尿外科杂志, 2024, 45: 195-201. DOI: 10.3760/cma.j.cn112330-20231127-00153.

[3] Sumaya PL, May PC, Holt SK, et al. Ureteral strictures following ureteroscopy for kidney stone disease: a population-based assessment[J]. J Urol, 2022, 208: 1268-1275. DOI: 10.1097/JU.0000000000002929.

[4] Fam XI, Singam P, Ho CC, et al. Ureteral stricture formation after ureteroscope treatment of impacted calculi: a prospective study[J]. Korean J Urol, 2015, 56: 63-67. DOI: 10.4111/kju.2015.56.1.63.

[5] Moretto S, Saita A, Scoffone CM, et al. Ureteral stricture rate after endoscopic treatments for urolithiasis and related risk factors: systematic review and meta-analysis[J]. World J Urol, 2024, 42: 234. DOI: 10.1007/s00345-024-04933-2.

[6] Tyritzis SI, Wiklund NP. Ureteral strictures revisited…trying to see the light at the end of the tunnel: a comprehensive review[J]. J Endourol, 2015, 29: 124-136. DOI: 10.1089/end.2014.0522.

[7] 陈敏杰，高小峰. 自体补片技术治疗输尿管狭窄的研究进展[J]. 中华泌尿外科杂志, 2023, 44: 555-558. DOI: 10.3760/cma.j.cn112330-20230307-00071.

[8] 王振兴，杨昆林，赵扬，等. 腹腔镜输尿管末治疗输尿管长段狭窄的应用经验和临床疗效[J]. 中华泌尿外科杂志, 2024, 45: 91-

97. DOI:10.3760/cma.j.cn112330-20220418-00209.
[9] Li L, Pan Y, Weng Z, et al. A prospective randomized trial comparing pneumatic lithotripsy and Holmium laser for management of middle and distal ureteral calculi[J]. J Endourol, 2015,29:883-887. DOI: 10.1089/end.2014.0856.
[10] Dong H, Peng Y, Li L, et al. Prevention strategies for ureteral stricture following ureteroscopic lithotripsy[J]. Asian J Urol, 2018,5:94-100. DOI: 10.1016/j.ajur.2017.09.002.
[11] Giulioni C, Pirola GM, Maggi M, et al. Current evidence on utility, outcomes, and limitations of endoscopic laser ablation for localized upper urinary tract urothelial carcinoma: results from a scoping review[J]. Eur Urol Open Sci, 2023,59:7-17. DOI: 10.1016/j.euros.2023.11.005.
[12] Rice P, Somani BK, Nagele U, et al. Generated temperatures and thermal laser damage during upper tract endourological procedures using the Holmium: Yttrium-Aluminum-Garnet (Ho:YAG) laser: a systematic review of experimental studies[J]. World J Urol, 2022,40:1981-1992. DOI: 10.1007/s00345-022-03992-7.
[13] Alshukhi AH, Hall TL, Ghani KR, et al. Caliceal fluid temperature during high-power Holmium laser lithotripsy in an in vivo porcine model[J]. J Endourol, 2018,32:724-729. DOI: 10.1089/end.2018.0395.
[14] Hein S, Petzold R, Suarez-Ibarrola R, et al. Thermal effects of Ho:YAG laser lithotripsy during retrograde intrarenal surgery and percutaneous nephrolithotomy in an ex vivo porcine kidney model[J]. World J Urol, 2020,38:753-760. DOI: 10.1007/s00345-019-02808-5.
[15] Winship B, Terry R, Boydston K, et al. Holmium: Yttrium-Aluminum-Garnet laser pulse type affects irrigation temperatures in a benchtop ureteral model[J]. J Endourol, 2019,33:896-901. DOI: 10.1089/end.2019.0496.
[16] Ho DR, So SH, Chang PJ, et al. Biodegradable stent with mTOR inhibitor-eluting reduces progression of ureteral stricture[J]. Int J Mol Sci, 2021,22:5664. DOI: 10.3390/ijms22115664.

（收稿日期：2024-06-14）
（本文编辑：李晓燕）

《中华泌尿外科杂志》第十届编辑委员会组成名单

顾　　问	李　虹	李汉忠	叶章群				
总 编 辑	黄　健						
副总编辑	孔垂泽	王建业	谢立平	周利群			
编辑委员	白志明	毕建斌	陈　明	程　跃	程继文	崔心刚	戴　波
	傅　强	高　新	高　旭	高小峰	谷欣权	郭剑明	韩从辉
	何　翔	何志嵩	洪　锴	侯建全	胡小鹏	黄　健	黄教悌
	霍红梅	纪志刚	姜永光	江　军	孔垂泽	黎　玮	李　磊
	李传洪	李建兴	梁朝朝	廖利民	林天歆	刘　明	刘春晓
	罗光恒	马　鑫	马潞林	牛远杰	潘铁军	平　浩	齐　琳
	乔庐东	史本康	寿建忠	孙　发	孙　宁	唐　伟	田　野
	汪　朔	王　翼	王东文	王共先	王剑松	王建业	王坤杰
	王林辉	王少刚	王养民	王荫槐	王玉杰	王增军	魏　强
	吴　芃	吴　忠	夏术阶	肖克峰	谢克基	谢立平	邢金春
	邢念增	徐　涛	徐万海	许长宝	许传亮	许克新	薛　蔚
	严维刚	杨国胜	杨嗣星	杨文增	姚旭东	叶定伟	叶惟靖
	袁建林	曾国华	章小平	张　宁	张　骞	张　旭	张大宏
	张树栋	张耀光	甄立雄	郑军华	周芳坚	周辉震	周利群
	周占松	朱　刚	邹晓峰				

（以上名单全部按姓氏汉语拼音排序）

Turning up the HEAT

Surgical simulation of the Moses 2.0 laser in an anatomic model

Christopher Wanderling[1], Aaron Saxton[1], Dennis Phan[1], Karen Doersch[1], Lauren Shepard[1], Nathan Schuler[1], Thomas Osinski[1], Scott Quarrier[1], Ahmed Ghazi[2]

[1]University of Rochester Medical Center, Department of Urology, Rochester, NY, United States; [2]Brady Urological Institute, Johns Hopkins University, Baltimore, MD, United States

Cite as: Wanderling C, Saxton A, Phan D, et al. Turning up the HEAT: Surgical simulation of the Moses 2.0 laser in an anatomic model. Can Urol Assoc J 2024;18(7):E220-7. http://dx.doi.org/10.5489/cuaj.8273

Published online March 1, 2024

ABSTRACT

INTRODUCTION: With advancements in laser technology, urologists have been able to treat urinary calculi more efficiently by increasing the energy delivered to the stone. With increases in power used, there is an increase in temperatures generated during laser lithotripsy. The aim of this study was to evaluate the thermal dose and temperatures generated with four laser settings at a standardized power in a high-fidelity, anatomic model.

METHODS: Using high-fidelity, 3D-printed hydrogel models of a pelvicalyceal collecting system with a synthetic BegoStone implanted in the renal pelvis, surgical simulation of ureteroscopic laser lithotripsy was performed with the Moses 2.0 holmium laser. At a standard power (40 W) and irrigation pressure (100 cm H_2O), we evaluated operator duty cycle (ODC) variations with different time-on intervals at four different laser settings. Temperature was measured at two separate locations: at the stone and ureteropelvic junction.

RESULTS: Greater cumulative thermal doses and maximal temperatures were achieved with greater ODCs and longer laser activation periods. There were statistically significant differences between the thermal doses and temperature profiles of the laser settings evaluated. Temperatures were greater closer to the tip of the laser fiber.

CONCLUSIONS: Laser energy and frequency play an important role in the thermal loads delivered during laser lithotripsy. Urologists must perform laser lithotripsy cautiously when aggressively treating large renal pelvis stones, as dangerous temperatures can be reached. To reduce the risk of causing thermal tissue injury, urologists should consider reducing their ODC and laser-on time.

INTRODUCTION

Advancements in laser technology have allowed urologists to safely treat urolithiasis endoscopically for years. The holmium:yttrium-aluminum-garnet (Ho:YAG) laser has been accepted as a standard lithotripsy laser due to its ability to pulverize stones of many compositions.[1] With the increasing prevalence of high-powered lasers (≥100 W), more urologists have been utilizing this technology as they can deliver energy at higher frequencies (>120 Hz), leading to improved stone ablation efficiency and decreased operative time;[2] however, with increased power, there is increased heat generated. With this in mind, it is important to preserve patient safety while determining the most efficient method of stone ablation.

Lasers can be used for calculus ablation because the stone is able to absorb the emitted laser energy leading to stone fragmentation and melting; thus, temperature and thermal dose have been studied extensively. Thermal dose was first described by Sapareto and Dewey; it is the cumulative equivalent minutes held at 43°C (TD_{43}), and is a standard measure for tissue denaturation occurring when TD_{43} ≥120 equivalent minutes.[3-5] Previously this lab, along with others, have attempted to study thermal loads during ureteroscopic (URS) laser lithotripsy.

The majority of these studies have been performed in low-fidelity in-vitro models consisting of test tubes or syringes or with ex-vivo porcine kidney models. The weakness of the

KEY MESSAGES

- The time to TD_{43} was generally faster at the stone.
- Temperatures and cumulative thermal doses were greater closer to the laser fiber tip.
- Longer laser-on times yielded greater cumulative thermal doses, while shorter laser-off intervals reached the TD_{43} faster.
- ODCs of ≥75% reached the threshold of thermal injury.

in-vitro models is that they may not accurately simulate surgical conditions. Conversely, while ex-vivo models may be the closest simulation to surgery, animal models encompass financial and ethical dilemmas.

The goal of our study was to improve upon and confirm our prior studies, using a validated high-fidelity anatomic human kidney model.[1] Using image segmentation, 3D printing, and hydrogel casting, a model inclusive of a complete pelvicalyceal collecting system (PCS) with a ureteral access sheath (UAS) simulating the full-length ureter and incorporating a 2 cm BegoStone was fabricated. This model was then submerged in a water bath maintained at 37°C.

The aims of this study were to:

1. Evaluate the temperature profile of the Moses 2.0 Ho:YAG laser at the stone and ureteropelvic junction (UPJ) for four different 40 W laser settings (two fragmentation and two dusting) using three operator duty cycles (ODCs).
2. Evaluate and compare time to TD_{43} for each laser setting.

METHODS

Simulation model fabrication

Digital Imaging and Communications in Medicine (DICOM) data from a patient's CT scan was segmented into a 3D computer-aided design (CAD) model using Mimics software (Materialize, Leuven, Belgium). The 3D CAD model (including the PCS/ureter) was 3D-printed using hydrogel filament (Fusion3 Design, Greensboro, NC) with a synthetic BegoStone (prepared with 10:1 powder to water ratio by weight) positioned in the renal pelvis and coated with a second polyvinyl alcohol (PVA) mixture (Figures 1A & B). This was then implanted into a hydrogel kidney block. The model was submerged in a warm water bath at anatomic temperature (starting temperature 37.0°C +/- 2.0°C); the water was circulated using a sous vide precision cooker (Anova Applied Electronics, San Fransisco, CA). The final product underwent extensive mechanical and computational fluid dynamic (CFD) testing to replicate PCS properties, stone lithotripsy, and fluid flow (Figures 1C & D).

Laser lithotripsy

URS laser lithotripsy was performed at a standardized power (40 W, short pulse width, Moses Technology activated) with continuous normal saline irrigation (17.5 ml/min) via retrograde access with a flexible ureteroscope (LithoVue, Boston Scientific, Marlborough, MA, U.S.) and a 200 µm Ho:YAG laser fiber (Moses 2.0, Boston Scientific, Marlborough, MA, U.S.) (Figure 2).

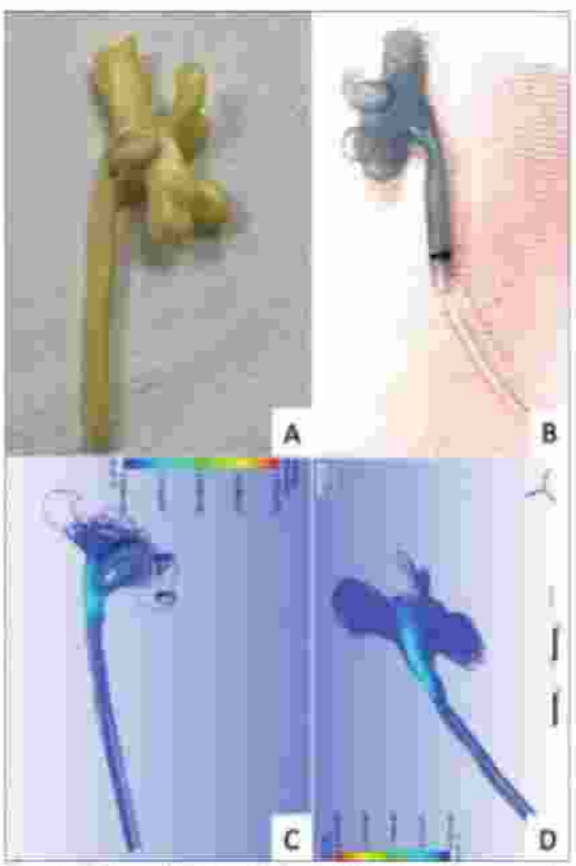


Figure 1. (A) 3D printed PVA PCS model with embedded BegoStone before coating with hydrogel. (B) Final hydrogel PCS model with drainage tubing secured acting as UPJ (stone inside model, unable to be visualized). (C&D) CFD testing of the model at 100 cm H$_2$O. CFD: computational fluid dynamic; PCS: pelvicalyceal collecting system; PVA: polyvinyl alcohol; UPJ: ureteropelvic junction.

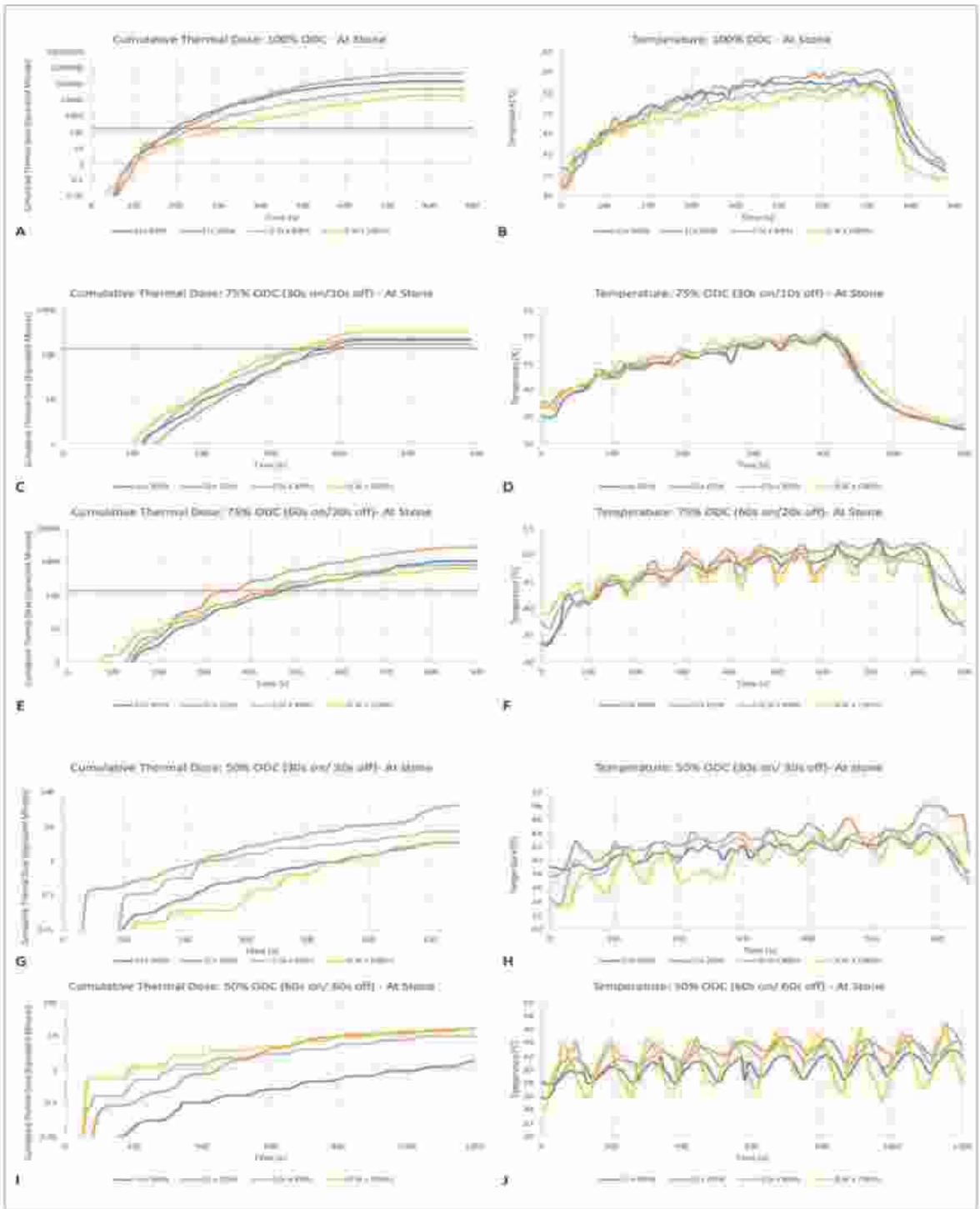


Figure 2. Temperature and thermal dose graphs of each laser setting at the stone. T043 (solid red line) is on the thermal dose graphs. 100% operator duty cycle (ODC). (A) thermal dose; (B) temperature. 75% ODC: 30 seconds on/10 seconds off; (C) thermal dose and (D) temperature 60 seconds on/20 seconds off; (E) thermal dose and (F) temperature 50% ODC: 30 seconds on/30 seconds off; (G) thermal dose and (H) temperature 60 seconds on/60 seconds off; (I) thermal dose; and (J) temperature.

Table 1. Comparison of cumulative thermal dose, time to TD43, and statistical comparison at the stone vs. UPJ

Laser setting	ODC	Time on (s)/ time off (s)	Cumulative thermal dose (CEM)		Time to thermal injury threshold (s)		p at vs. away from stone
			At stone	Away from stone	At stone	Away from stone	
1 J x 40 Hz	100%		**93909.8907**	**134501.2717**	**200**	**195**	<0.0001
	75%	30/10	**221.6387713**	**206.1101383**	**380**	**370**	<0.0001
		60/20	**1125.62778**	**1025.910058**	**440**	**465**	<0.0001
	50%	30/30	3.569467179	3.071237613	NR	NR	<0.0001
		60/60	3.233970832	1.882688132	NR	NR	<0.0001
2 J x 20 Hz	100%		**318276.667**	**449089.338**	**195**	**205**	<0.0001
	75%	30/10	**187.32621**	**169.9063665**	**395**	**395**	0.0004
		60/20	**3398.569694**	**2690.290273**	**325**	**330**	<0.0001
	50%	30/30	51.75861439	39.50125173	NR	NR	<0.0001
		60/60	24.86021107	18.09596256	NR	NR	<0.0001
0.5 J x 80 Hz	100%		**62134.7335**	**51936.32456**	**230**	**230**	<0.0001
	75%	30/10	**344.6057609**	**228.1060048**	**320**	**350**	<0.0001
		60/20	**1253.588927**	**788.0238063**	**395**	**435**	<0.0001
	50%	30/30	11.20336357	7.050187058	NR	NR	<0.0001
		60/60	23.62071365	9.677738417	NR	NR	<0.0001
0.4 J x 100 Hz	100%		**18045.01532**	**8502.241086**	**295**	**315**	<0.0001
	75%	30/10	**316.2694821**	**242.2321829**	**330**	**380**	<0.0001
		60/20	**739.8320632**	**627.1075826**	**410**	**450**	<0.0001
	50%	30/30	3.071237613	3.569467179	NR	NR	<0.0001
		60/60	18.93383935	17.0028632	NR	NR	<0.0001

Bolded cells indicate tests that exceeded threshold of thermal injury. NR indicates that the threshold of thermal injury was not reached. Statistics comparing cumulative thermal dose and calculated with Kruskal-Wallis. UPJ: ureteropelvic junction.

A 12/14 Fr, 40 cm UAS was inserted just distal to the UPJ to simulate a complete ureteral length. Four laser settings – two fragmentation (1 J x 40 Hz and 2 J x 20 Hz) and two dusting (0.5 J x 80 Hz, 0.4 J x 100 Hz) were tested. We evaluated 3 ODCs (50, 75, and 100%) with different laser-on (30, 60, and 120 s) times. Each experiment consisted of 10 cycles (1 cycle = 1 laser-on/laser-off sequence = 1 ODC); the 100% ODC consisted of pedal-on time of 12 minutes straight with no laser-off time. Five permutations of each laser setting were tested. A total of 20 experiments were performed. Temperature was measured continuously with data analysis performed in 10-second intervals.

Data collection and analysis

Temperature was recorded with K-type needle thermocouple probes and data logger (Omega, Norwalk, CT) at two standard positions (registered in the model) in the PCS – at the stone (renal pelvis) and UPJ. Additionally, a third temperature probe was inserted into the hydrogel block. Thermal dose was calculated with the Sapareto and Dewey formula. Statistical analysis for thermal dose was analyzed via area under the curve (AUC) and Kruskal-Wallis comparison and temperature data was analyzed via non-linear regression in a third-order polynomial (Prism 9). $P<0.05$ was considered statistically significant.

RESULTS

When evaluating the cumulative thermal dose, it was found to be higher *at the stone* than at the UPJ for each laser setting tested. There was a statistically significant difference between cumulative thermal dose at the stone and UPJ for each laser setting tested (Table 1).

Table 2. Comparison of maximal temperature, and statistical comparison at the stone vs. UPJ

Laser setting	ODC	Time on (s)/ time off (s)	Maximum temperature (°C)		p at vs. away from stone
			At stone	Away from stone	
1 J x 40 Hz	100%		**58.5**	**58.2**	<0.0001
	75%	30/10	**50.4**	**50.2**	<0.0001
		60/20	**52.9**	**51.6**	0.1618
	50%	30/30	44.1	43.1	0.0018
		60/60	42.8	43.3	0.1187
2 J x 20 Hz	100%		**60.5**	**59.9**	<0.0001
	75%	30/10	**50.1**	**50.1**	<0.0001
		60/20	**52.4**	**52.7**	0.0224
	50%	30/30	47.9	48.8	0.1638
		60/60	44.8	45.3	0.0301
0.5 J x 80 Hz	100%		**57.8**	**57.6**	<0.0001
	75%	30/10	**49.9**	**50.8**	<0.0001
		60/20	**51.2**	**52.1**	0.0014
	50%	30/30	45.2	44.4	<0.0001
		60/60	46.9	45.1	<0.0001
0.4 J x 100 Hz	100%		**56.7**	**55.3**	<0.0001
	75%	30/10	**50.8**	**49.9**	<0.0001
		60/20	**51.4**	**51.0**	<0.0001
	50%	30/30	44.4	43.8	<0.0001
		60/60	46.7	45.2	<0.0001

Bolded cells indicate tests that exceeded threshold of thermal injury. Statistics comparing temperature curves and calculated with non-linear regression in a third-order polynomial. UPJ: ureteropelvic junction

The threshold of thermal injury was reached for the 100 and 75% ODCs both at the stone and UPJ but was not reached in any 50% ODC. The threshold of thermal injury was reached faster for 100% ODC than either of the 75% ODC time intervals. For the 75% ODCs, the 30 seconds on/10 seconds off time interval reached the threshold faster for all laser settings tested, except for 2 J x 20 Hz, where the 60 seconds on/20 seconds off interval was faster. The time to reach the threshold of thermal injury was typically faster at the stone compared to the UPJ except for 1 J x 40 Hz (100% ODC, 30 seconds on/10 seconds off), where the UPJ reached the threshold faster; while for 2 J x 20 Hz (30 seconds on/10 seconds off) and 0.5 J x 80 Hz (100% ODC) the threshold was reached at approximately the same time (Table 1).

The cumulative thermal dose was greater for each laser setting with greater ODCs both at the stone and UPJ. 2 J x 20 Hz delivered the greatest cumulative thermal dose for each time interval tested except for 30 seconds on/10 seconds off, where it delivered the lowest cumulative thermal dose. There was no other generalizable pattern appreciated between the laser settings otherwise when compared against one another (Tables 1 and 2).

Considering maximal temperatures at the stone vs. UPJ, the temperatures were higher at the stone in 13/20 tests, higher at the UPJ in 6/20 tests, and in one test, the maximal temperature was the same (2 J x 20 Hz, 30 seconds on/10 seconds off). There was a statistically significant difference in the temperature curves for all but three tests (1 J x 40 Hz – 60 seconds on/20 seconds off and 60 seconds on/60 seconds off, 2 J x 20 Hz – 30 seconds on/30 seconds off). Temperatures were hotter with greater ODCs for each laser setting both at the stone and at the UPJ. Considering the 75% ODCs, hotter maximal temperatures were recorded with a longer laser-on time (60 seconds on/20 seconds off) for each laser setting both at the stone and at the UPJ. Considering the 50% ODCs, there were mixed results as to which laser time-on cycle generated hotter maximal temperatures; for the fragmentation settings, the 30 seconds on/30 seconds off cycle yielded hotter temperatures, while for the dusting settings, the 60 seconds on/60 seconds off cycle was hotter. This held true both at the stone and at the UPJ (Table 2).

While there was not an apparent trend as to which laser setting produced the hottest temperatures, we did appreciate statistically significant differences between laser settings which demonstrates that frequency and energy can strongly influence temperature and thermal dose, even at a standardized power. For 100% ODC, 2 J x 20 Hz was hottest at the stone and UPJ, while 0.4 J x 100 Hz was the lowest for both. For the other 4 ODC/time-on intervals evaluated, there was no overall trend (Tables 1 and 2).

Temperatures of the hydrogel block started at 37.0°C +/- 2.1°C and increased 1.0°C +/- 2.0°C. There were no statistically significant changes in temperature measured at this location. It was observed that the temperatures increased slightly more when the starting temperature was lower (<37°C) opposed to a minimal temperature fluctuation at higher starting temperatures (≥37°C).

DISCUSSION

In this study, we were able to establish that temperatures and cumulative thermal doses were greater closer to the tip of the last fiber, which has also been recognized in previous studies.[7] Additionally, we demonstrated that energy and frequency play a significant role in the thermal load delivered, and the previously accepted concept that power is the sole determinant of temperature may not be entirely accurate.[5,8-10] In general, greater thermal doses and maximal temperatures were achieved with greater ODCs and longer laser-on times for 100% and 75% ODCs, which is in agreement with previously published literature.[11,12] When comparing laser-on times for 75% ODC, 60 seconds on/20 seconds off delivered greater cumulative thermal doses and maximal temperatures for each laser setting both at the stone and UPJ.

Interestingly, when evaluating 50% ODCs, the fragmentation settings delivered greater cumulative thermal doses for shorter laser-on time (30 seconds on/30 seconds off) while the dusting settings delivered greater cumulative thermal doses for the longer laser-on time (60 seconds on/60 seconds off). When considering maximal temperatures, the same results held true, except for 1 J x 40 Hz at the UPJ (43.1°C for 30 seconds on/30 seconds off vs. 43.3°C for 60 seconds on/60 seconds off). This shows that the laser-off time may play a crucial role in fluid cool-down, as the longer the laser is off, the greater the opportunity that the fresh irrigation inflow can cool more of the PCS.

There have been numerous studies manipulating variables involved during URS laser lithotripsy. Dr. William Robert's laboratory at the University of Michigan has led many studies via in-vitro bench models and computational modelling. They have evaluated the Ho:YAG laser power (2.5–50 W), frequency (5–80 Hz), irrigation rate (0–40 ml/min), irrigation temperature (~0°C and 19°C), and ODC (≥50%).[13-17] Their work sought to adapt their previous findings to an in-vivo porcine model and found that temperatures capable of tissue damage were easily achieved but can be negated by increasing irrigation flow rate.[13] Other labs have also evaluated irrigation rates and have determined that increased irrigation rates can mitigate temperature increases during active lasing, as too can the use of a UAS.[18,19]

A recent study evaluated intraoperative irrigation fluid temperatures during URS treatment of urolithiasis. They compared laser settings of 1 J x 20 Hz and 0.5 J x 20 Hz with irrigation rates of 0 ml/min, 15 ml/min, and 30 ml/min. They found that with irrigation rates of 15 ml/min and 30 ml/min, a temperature of 43°C was not reached after 60 seconds straight of laser activation.[19] Our study used a UAS with a constant irrigation flow (100 cm H_2O=17.5 ml/min). We found that at a constant power, the threshold of thermal injury could be reached in as little as 195 seconds (2 J x 20 Hz at the stone and 1 J x 40 Hz at the UPJ). While there was a significant difference in power tested between Teng, et. al's study and ours, it is obvious that when treating larger stone burdens, urologists must be diligent when continuously lasing as temperatures can reach dangerous levels, even with UAS use.

It is important to consider that in this study, we were lasing a large calculus in the renal pelvis where there is more volume/area for fluid and irrigation flow. Previous studies have demonstrated that when lasing in smaller spaces, temperatures increased faster, and the threshold of thermal injury could be reached faster when compared to larger spaces.[20,21] In agreement with our prior evaluations and previous studies, the threshold of thermal injury was reached during ODCs greater than 70%.[11] This held true regardless of the laser settings tested and for laser-on time. Aldoukhi, et. al. performed a chart review of 63 URS cases and determined that during the 60 seconds of greatest power delivered, the ODC was 63%.[12]

Although studies have demonstrated that ODCs <70% are less likely to cross the threshold of thermal injury, it is important to consider that more powerful laser settings can deliver greater thermal loads in shorter amounts of time and with shorter ODCs. Additionally, when lasing in tighter spaces, such as a calyx opposed to the renal pelvis, it is reasonable to believe that the threshold of thermal injury could be reached even with lower ODCs or less powerful laser settings, particularly after a stone is broken; as the laser tip may be closer to the urothelium with no interruption from a stone, and it is not absorbing energy once pulverized. In an in-vitro model, it was found that the presence of a phantom BegoStone was related to lower rises in fluid temperatures when compared with no stone present at an array of powers tested (10, 20, 40, 60 W).[20]

It is recognized that BegoStones may possess distinctive photothermal properties compared with real urolithiasis during laser lithotripsy;[22] however, BegoStones are often accepted as a synthetic analogue for real urolithiasis during in-vitro urologic laser studies since they are able to be composed without significant difficulty in an efficacious manner and are able to be fabricated and reproduced with the same composition.

To date, this appears to be the first study evaluating thermal loads performed in a high-fidelity anatomic in-vitro model at anatomic temperature with a UAS used while actively lasing a phantom stone. Other studies have been performed using ex-vivo and in-vivo models with or without UAS that can simulate the complete ureteral length. It is well recognized that using a UAS can facilitate higher irrigation flow rates and modulate temperature increases more easily, in addition to reducing intrarenal pressures during irrigation.[12]

With regards to the power setting evaluated utilizing the Moses 2.0 Ho:YAG laser in this study, 40 W was chosen as the standard because this power allowed for the variation of both frequency and energy settings for four different laser settings — two dusting and two fragmentation — while maintaining constant power. It is recognized that urologists may commonly utilize lower power settings in clinical practice, however, the goal of this study was to evaluate variables besides power, since many previous studies have already compared different power settings.[4,5,13]

This study addressed some of the limitations of our previous studies which had been performed at room temperature. With this experimental model, we evaluated thermal dose and temperatures in the high-fidelity anatomic model performed at anatomic temperature with a UAS. This experimental design appears to be a quality, realistic in-vitro model for URS laser lithotripsy. The majority of previous studies have been performed with in-vitro test tube models or with ex-vivo porcine kidney models.

While we have addressed some limitations of our prior studies, we recognize that some limitations are present in this study. First, although this project was performed in a high-fidelity anatomic PCS model, some caution should be maintained when attempting to correlate this data to a surgical scenario. Second, only one PCS model was used in our evaluations in efforts to further reduce confounding variables influencing our results. Finally, although BegoStone models may simulate actual kidney stones, they may not act as an exact analogue. Our laboratory hopes to continue pursuing urologic laser research in the future, building on this study, and addressing some of these limitations.

This study had several strengths. First, this study evaluated four variables: laser frequency, laser energy, ODC, and laser time-on, in an anatomically correct, high-fidelity model that has been validated with mechanical and CFD testing; but this time, at anatomic temperature with the use of a UAS. Second, we were able to evaluate thermal load in two locations in the PCS. Finally, we were able to measure the temperatures while actively lasing a synthetic 2 cm calculus. The combination of these components into one model while analyzing four separate variables strengthens the results of this study. While prior studies have compared some of these factors affecting irrigation fluid temperature, the majority of these studies focus on fewer variables.

CONCLUSIONS

We were able to validate our previous studies and address several limitations with this experimental model. We confirmed that dangerous thermal loads can be delivered with greater ODCs and longer laser-on times. We demonstrated again that at a standardized power, energy and frequency manipulations can strongly influence thermal dose and temperatures. Based on the results of this study, it is important that urologists perform URS laser lithotripsy diligently, as irrigation fluid temperatures and cumulative thermal doses in the PCS can reach critical levels and potentially cause urothelial injury, regardless of laser setting.

COMPETING INTERESTS: The authors do not report any competing personal or financial interests related to this work.

ACKNOWLEDGEMENT: The authors would like to graciously thank Dr. William Roberts from the University of Michigan for providing his expertise, input, and guidance in our project. We largely based our protocol on the excellent work he lab has produced. He reviewed our data and provided insight for data evaluation to provide research results.

This paper has been peer-reviewed.

REFERENCES

1. Rassweiler JJ, Teber D, Kuntz R, Hofmann R. Complications of transurethral resection of ureteral stones. J Urol. 2006;175(1):299–303; discussion 303–304. https://doi.org/10.1016/S0022-5347(05)00081-4
2. Preminger GM, Tiselius HG, Assimos DG, et al. 2007 guideline for the management of ureteral calculi. J Urol. 2007;178(6):2418–34. https://doi.org/10.1016/j.juro.2007.09.014
3. Türk C, Petřík A, Sarica K, et al. EAU guidelines on interventional treatment for urolithiasis. Eur Urol. 2016;69(3):475–82. https://doi.org/10.1016/j.eururo.2015.07.041
4. Wollin DA, Carlos EC, Hollingsworth JM, et al. Real-time temperature measurement during ureteroscopic holmium laser lithotripsy and pneumatic lithotripsy. J Endourol. 2016;30(1):16–21. https://doi.org/10.1089/end.2015.0435
5. Wollin DA, Preminger GM. Thermal management during flexible ureteroscopy: calculating safe operative times while using holmium laser lithotripsy. J Endourol. 2018;32(2):160–5. https://doi.org/10.1089/end.2017.0722
6. Wollin DA, Preminger GM. Irrigation fluid temperature during ureteroscopic laser lithotripsy: in vitro and in vivo evaluation. J Endourol. 2015;29(12):1350–5. https://doi.org/10.1089/end.2015.0260
7. Sofer M, Watterson JD, Wollin TA, et al. Holmium:YAG lithotripsy for upper urinary tract calculi in 598 patients. J Urol. 2002;167(1):31–4. https://doi.org/10.1016/S0022-5347(05)65378-X
8. Wollin DA, Preminger GM. Thermal dose determination in stone therapy. Int J Radiat Oncol Biol Phys. 1988;15(3):707–800. https://doi.org/10.1016/0360-3016(88)90379-1
9. Maxwell AD, MacConaghy B, Harper JD, et al. Simulation of laser lithotripsy-induced heating in the urinary tract. J Endourol. 2019;33(2):113–9. https://doi.org/10.1089/end.2018.0485
10. Aldoukhi AH, Ghani KR, Hall TL, et al. Thermal response to high-power holmium laser lithotripsy. J Endourol. 2017;31(12):1208–12. https://doi.org/10.1089/end.2017.0679
11. Soliz P, Barbour E, Melnick R, et al. Development of a high-fidelity robot-assisted kidney transplant simulation platform using three-dimensional printing and hydrogel casting technologies. J Endourol. 2020;34(10):1088–94. https://doi.org/10.1089/end.2020.0441
12. Tzortzinis M, Loukidakos E, Sergis N, et al. Temperature changes during laser lithotripsy with the YAG laser and novel Tm:fiber laser: A comparative in-vitro study. World J Urol. 2020;38(12):3261–6. https://doi.org/10.1007/s00345-020-03122-1
13. De Coninck V, Dragonjac C, Traxer O. Wait! Determines the temperature during laser lithotripsy. World J Urol. 2022;40(5):1257–8.
14. Patwardhan R, Sontineni Ramanjaneyulu R, Melnick R. Temperature measurement of a novel pulsed thulium solid-state laser compared with a holmium:yttrium-aluminum-garnet laser. J Endourol. 2021;35(6):853–9. https://doi.org/10.1089/end.2020.0803

10. Abdunur WR, Cisneros RV, Chew BH, et al. Temperature rise during ureteral laser lithotripsy: Comparison of super pulse thulium fiber laser (SPTF) vs. high power 120 W holmium:YAG laser (Ho:YAG). World J Urol 2021;39:3951-6. https://doi.org/10.1007/s00345-021-03619-5
11. Cisneros AMR, Chew BJ, Hall TL, et al. Linear ejaculator duty cycle effect on temperature and thermal dose: In vitro study. World J Urol 2022;40:1575-80. https://doi.org/10.1007/s00345-022-03947-9
12. Abdunur AH, Chew BJ, Maghsoudi SE, et al. Patterns of laser activation during ureteroscopic lithotripsy: Effects on collected fluid temperature and thermal dose. J Endourol 2021;35:1217-22. https://doi.org/10.1089/end.2020.1067
13. Aldoukhi AH, Black KM, Hall TL, et al. Defining thermally safe laser lithotripsy power and irrigation parameters: In vitro model. J Endourol 2020;34:76-81. https://doi.org/10.1089/end.2019.0499
14. Chew BJ, Hall TL, Maxwell AD, et al. Effect of chilled irrigation on collected fluid temperature and time to thermal injury threshold during laser lithotripsy: In vitro model. J Endourol 2021;35:700-5. https://doi.org/10.1089/end.2020.0594
15. Aldoukhi AH, Hall TL, Ghani KR, et al. Collected fluid temperature during high-power holmium laser lithotripsy: In vivo porcine model. J Endourol 2018;32:774-9. https://doi.org/10.1089/end.2018.0395
16. Tsaturyan A, Proskurina A, Potminova L, et al. The effect of prolonged laser activation on irrigation fluid temperature: an in vitro experimental study. World J Urol 2022;40:1073-9. https://doi.org/10.1007/s00345-022-04000-8
17. Gallagher H, Moore RC, Sagalowsky E, et al. Intrarenal temperature measurement associated with holmium laser nephrostomy lithotripsy in an ex vivo model. Cent European J Urol 2021;74:588-94. https://doi.org/10.5173/ceju.2021.0092
18. Wroath W, Yilmaz M, Lattyer T, et al. Assessing critical temperature dose zones in the kidney by magnetic resonance imaging thermometry in an ex-vivo holmium:YAG laser lithotripsy model. World J Urol 2023;41:545-9. https://doi.org/10.1007/s00345-021-04255-1
19. Tang J, Wang Y, Jin Z, et al. Temperature profiles of saline irrigation fluids during flexible ureteroscopic Ho:YAG laser lithotripsy. Int Urol Nephrol 2021;53:415-9. https://doi.org/10.1007/s11255-020-02665-x
20. Tsaturyan A, Tsaturyan A, Martucci L, et al. Factors affecting the irrigation fluid temperature during laser lithotripsy: In vitro experimental study. Urology 2022;170:53-9. https://doi.org/10.1016/j.urology.2022.07.040
21. Aboukhir Alsayat N, Hall TL, et al. Pyelocaliceal volume and fluid temperature elevation during laser lithotripsy. J Endourol 2022;36:22-8. https://doi.org/10.1089/end.2021.0083
22. Wang HB, Bates N, Teichman JMH, et al. Mechanisms of pulse modulated holmium:YAG lithotripsy. J Endourol 2021;35:579-86. https://doi.org/10.1089/end.2021.0242
23. Tsaturyan A, Pogosov R, Vagapov A, et al. What is the impact of pulse modulation technology, laser settings and intracorporeal irrigation conditions on the irrigation fluid temperature during flexible ureteroscopy? An in vivo experiment using artificial stones. World J Urol 2022;40:1853-8. https://doi.org/10.1007/s00345-022-04002-6

CORRESPONDENCE: Dr. Christopher Wandling, University of Rochester Medical Center, Department of Urology, Rochester, NY, United States. Christopher_Wandling@URMC.Rochester.edu

加大加热

解剖模型中Moses2.0激光器的手术模拟

Christopher Wanderling [1]，Aaron saxton [1]，dennis Phan [1]，Karen doersch [1]，lauren shepard [1]，nathan schuler [1]，thomas osinski [1]，scott Quarrier [1]，ahmed ghazi [1]

[1]美国纽约州罗切斯特市罗切斯特大学医学中心泌尿外科；[2]美国马萨诸塞州伍斯特的伯利恒盖伦医院大学/布莱顿泌尿研究所

引用格式：Wanderling C，saxton A，Phan d，et al.turning up the heAt：surgical simulation of the moses 2.0 laser in an anatomic model.Can Urol Assoc J 2024；18(7)：E220-5.

2024年3月1日作稿发表

摘要

引言：随着激光技术的进步，泌尿科医生通过提高激光能量输送至结石的效率，能够更有效地治疗尿路结石。当激光功率增加时，激光碎石术过程中产生的温度也会随之升高。本研究旨在通过高保真解剖模型，评估在标准化功率条件下，四种不同激光设置所产生的热剂量和温度变化。

实验方法：采用高精度3D打印的肾盂输尿管集合系统水凝胶模型（模型中植入了合成贝戈斯通材料），使用摩西斯2.0钬激光系统进行输尿管镜激光碎石术的手术模拟。在标准功率（40瓦）和灌注压力（100厘米水柱）条件下，我们通过改变四个不同激光参数的开启时间间隔，评估了操作者工作循环（odC）的变化情况。温度测量在结石部位和输尿管肾盂连接处两个不同位置进行。

结果表明：随着臭氧浓度（odCs）的增加和激光激活时间的延长，累积热剂量和最高温度均显著升高。不同激光参数设置的热剂量和温度分布存在统计学显著差异，且激光光纤尖端附近的温度值更高。

结论：激光能量与频率在激光碎石术中对热负荷影响显著。泌尿科医生在对大型肾盂结石进行激进治疗时需格外谨慎，因可能产生危险温度。为降低热损伤风险，建议缩短激光脉冲宽度（odC）和激光持续时间。

介绍

激光技术的进步使泌尿科医生能够安全地通过内窥镜治疗尿路结石已有多年。钬钇铝石榴石（Ho：YAG）激光因其能粉碎多种成分的结石而被公认为标准碎石激光器。[1]随着高功率激光（>100W）的普及，越来越多的泌尿科医生开始采用这项技术，因为它们能以更高频率（>120 Hz）输送能量，从而提高结石消融效率并缩短手术时间；[2]但功率提升也带来了热量增加的问题。因此，在确定最有效的结石消融方法时，确保患者安全至关重要。

激光可应用于结石消融治疗，因其能有效吸收激光能量，促使结石碎裂并最终熔化。因此，温度与热剂量的研究已相当深入。热剂量最早由萨帕雷托和杜威提出，其定义为在43 ℃环境下保持的累积等效分钟数（td_{43}），该指标是衡量组织变性的标准参数，当td_{43}超过120等效分钟时即达到变性阈值。[3,4]此前本实验室联合多家机构，已着手研究输尿管镜（Urs）激光碎石术中的热负荷问题。

这些研究大多采用低保真度的体外模型，包括试管、注射器或离体猪肾模型。该模型的缺陷在于

重要消息

石头上的td时间$_{43}$通常更快。

■温度和累积热剂量在靠近激光光纤尖端处更大。

更长的激光开启时间产生更大的累积热剂量，而较短的激光关闭时间达到td$_{43}$更快。

■odCs ≥ 75%达到热损伤阈值。

体外模型的局限在于其无法准确模拟手术环境。而体外模型虽最接近真实手术，但动物模型却存在伦理与经济层面的双重困境。

本研究旨在通过采用经过验证的人体解剖肾脏高保真模型，改进并验证我们先前的研究成果。我们运用图像分割、3D打印和水凝胶铸造技术，成功构建了一个包含完整肾盂肾盏集合系统（PCs）的模型，该模型配备模拟全长输尿管的输尿管套管（UAs），并内置2厘米长的贝戈斯通假体。随后将该模型浸入37 ℃恒温水箱中进行实验。

本研究旨在：

1.评估摩西的温度分布

2.0号手术刀：采用银离子激光对结石及输尿管肾盂连接处（UPJ）进行治疗，设置四种40瓦激光功率（含两种碎石模式和两种碎粉模式），并配合三种不同工作模式（odCs）。

2.评估和比较$_{43}$每个激光设置的td时间。

方法

模拟器制造

通过mimics软件（比利时鲁汶Materialize公司）将患者CT扫描的数字医学影像与通信（dICom）数据分割为三维计算机辅助设计（CAD）模型。该三维CAD模型（包含肾盂/输尿管）采用水凝胶线材（Fusion3设计，美国北卡罗来纳州格林斯博罗）进行3D打印，其中合成Begostone材料（按10：1重量比配制的粉末与水混合物）被定位在肾盂区域，并在其表面涂覆第二层聚乙烯醇涂层。

将全氟乙烯（PVA）混合物（图1A和B）植入水凝胶肾脏模型中。随后将模型置于解剖温度（初始温度37.0 ℃± 2.0℃）的温水浴中，使用安诺瓦应用电子公司（美国旧金山）的精密真空低温锅进行水循环。最终产品经过广泛的机械性能和计算流体动力学（CFD）测试，以模拟肾小管特性、结石碎石效果及流体流动状态（图1C和d）。

激光碎石术

采用标准化功率（40 W，短脉冲宽度，激活moses技术）进行Urs激光碎石术，通过逆行通道使用柔性输尿管镜（lithoVue，Boston Scientific，马尔伯勒，马萨诸塞州，美国）和200μm ho：yAg激光光纤（moses 2.0，Boston Scientific，马尔伯勒，马萨诸塞州，美国）进行连续生理盐水冲洗（17.5 ml/min）（图2）。

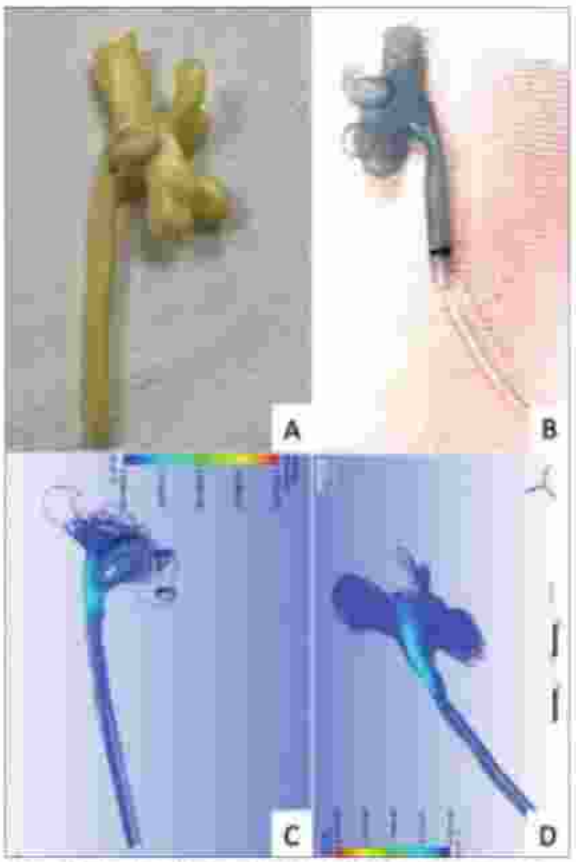


图1(A)采用3D打印技术制作的PVA肾盂输尿管连接系统模型。内置Begostone支架，并需未进行水凝胶包覆。(B)最终水凝胶铸型PCS模型，其内置导丝管用于连接。工作与输尿管肾盂连接处（UPJ）相对。模型内部结石碎粒大小显示于。（C&D）该模型在100厘米水柱[cm H2O]压力环境下的计算流体动力学（CFD）测试。CFD：计算流体动力学；PCS：肾盂肾盏连接系统；PVA：聚乙烯醇；UPJ：输尿管肾盂连接处。

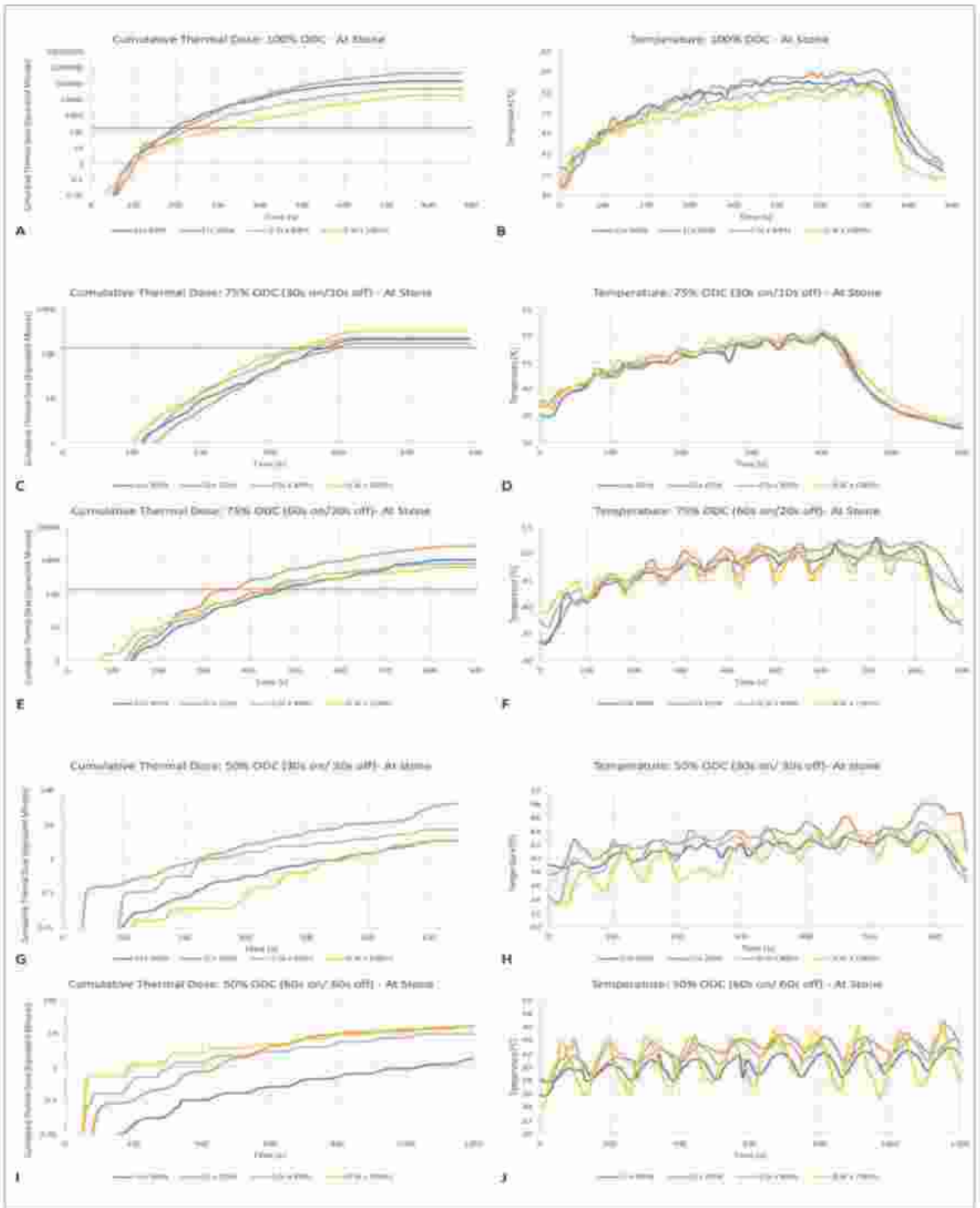


图2.各激光设置在结石处的温度与热剂量曲线。TD43（红色实线）对应热剂量曲线，显示100%操作员工作周期（ODC）。(A)热剂量；(B)温度。75%ODC：30秒开/10秒关；(C)热剂量与(D)温度；60秒开/20秒关；(E)热剂量与(F)温度；50%ODC：30秒开/30秒关；(G)热剂量与(H)温度；60秒开/60秒关；(I)热剂量；(J)温度。

表1.石块与UPJ在累积热剂量、TD43时间及统计学比较上的对比

激光设置	[illegible]	[illegible]（秒/秒）	累积热剂量（CEM）		热损伤阈值时间(s)		结石与UPJ
			[illegible]	远离石头	[illegible]	远离石头	
1 J x 40 Hz	100%		**93909.8907**	**134501.2717**	**200**	**195**	<0.0001
	75%	30/10	**221.6387713**	**206.1101383**	**380**	**370**	<0.0001
		60/20	**1125.62778**	**1025.910058**	**440**	**465**	<0.0001
	50%	30/30	3.569467179	3.071237613	NR	NR	<0.0001
		60/60	3.233970832	1.882688132	NR	NR	<0.0001
2 J x 20 Hz	100%		**318276.667**	**449089.338**	**195**	**205**	<0.0001
	75%	30/10	**187.32621**	**169.9063665**	**395**	**395**	0.0004
		60/20	**3398.569694**	**2690.290273**	**325**	**330**	<0.0001
	50%	30/30	51.75861439	39.50125173	NR	NR	<0.0001
		60/60	24.86021107	18.09596256	NR	NR	<0.0001
0.5 J x 80 Hz	100%		**62134.7335**	**51936.32456**	**230**	**230**	<0.0001
	75%	30/10	**344.6057609**	**228.1060048**	**320**	**350**	<0.0001
		60/20	**1253.588927**	**788.0238063**	**395**	**435**	<0.0001
	50%	30/30	11.20336357	7.050187058	NR	NR	<0.0001
		60/60	23.62071365	9.677738417	NR	NR	<0.0001
0.4 J x 100 Hz	100%		**18045.01532**	**8502.241086**	**295**	**315**	<0.0001
	75%	30/10	**316.2694821**	**242.2321829**	**330**	**380**	<0.0001
		60/20	**739.8320632**	**627.1075826**	**410**	**450**	<0.0001
	50%	30/30	3.071237613	3.569467179	NR	NR	<0.0001
		60/60	18.93383935	17.0028632	NR	NR	<0.0001

加粗单元格表示测试结果超过热损伤阈值，NR表示未达到该阈值。统计分析采用Kruskal-Wallis检验，比较累积热剂量。UPJ：输尿管肾盂连接处。

在膀胱颈（UPJ）远端插入12/14 Fr、40厘米的尿道扩张器（UAs）以模拟完整输尿管长度。测试了四种激光设置：两种碎石模式（1焦耳×40赫兹和2焦耳×20赫兹）以及两种碎石粉模式（0.5焦耳×80赫兹、0.4焦耳×100赫兹）。我们评估了三种碎石次数（50、75和100%），分别对应30秒、60秒和120秒的激光开启时间。每个实验包含10个周期（1个周期=1次激光开启/关闭序列=1次碎石次数）；100%碎石次数的实验采用连续12分钟的持续踩踏模式，不包含激光关闭时间。每种激光设置测试了五种组合方式，共进行20次实验。温度数据采用10秒间隔连续监测，并进行数据分析。

数据收集和分析

温度由K型针式热电偶探头与数据记录仪（Omega公司，诺沃克）进行记录。

Ct)在模型中注册的两个标准位置（位于肾盂和UPJ）的PCs区域进行测量。此外，第三个温度探头被插入水凝胶块中。热剂量通过萨帕雷托和杜威公式计算。热剂量的统计分析采用曲线下面积（AUC）和克鲁斯卡尔-沃利斯检验，温度数据则通过Prism 9软件中的三次多项式非线性回归进行分析。P<0.05被视为具有统计学意义。

结果

在评估累积热剂量时，发现*在每个测试激光设置下结石处*的累积热剂量高于UPJ处。在每个测试激光设置下，结石处与UPJ处的累积热剂量之间存在统计学显著性差异（表1）。

表2.石块与UPJ的最高温度及统计学对比

激光设置	[illegible]	[illegible]	最高温度（℃）		主场与客场对制
			[illegible]	邻居石头	
1 J x 40 Hz	100%		**58.5**	**58.2**	<0.0001
	75%	30/10	**50.4**	**50.2**	<0.0001
		60/20	**52.9**	**51.6**	0.1618
	50%	30/30	44.1	43.1	0.0018
		60/60	42.8	43.3	0.1187
2 J x 20 Hz	100%		**60.5**	**59.9**	<0.0001
	75%	30/10	**50.1**	**50.1**	<0.0001
		60/20	**52.4**	**52.7**	0.0224
	50%	30/30	47.9	48.8	0.1638
		60/60	44.8	45.3	0.0301
0.5 J x 80 Hz	100%		**57.8**	**57.6**	<0.0001
	75%	30/10	**49.9**	**50.8**	<0.0001
		60/20	**51.2**	**52.1**	0.0014
	50%	30/30	45.2	44.4	<0.0001
		60/60	46.9	45.1	<0.0001
0.4 J x 100 Hz	100%		**56.7**	**55.3**	<0.0001
	75%	30/10	**50.8**	**49.9**	<0.0001
		60/20	**51.4**	**51.0**	<0.0001
	50%	30/30	44.4	43.8	<0.0001
		60/60	46.7	45.2	<0.0001

加粗单元格表示温度超过热损伤阈值的测试结果。温度曲线的统计分析采用非线性回归方法，通过三次多项式进行计算。UPJ：肾盂输尿管移行部

在结石和UPJ条件下，100%和75%的odC均达到了热损伤阈值，而50%的odC则未达到该阈值。相较于75%的odC时间间隔，100%的odC达到热损伤阈值的速度更快。对于75%的odC，除2焦耳×20赫兹设置外，所有测试激光参数中30秒开/10秒关的时间间隔都更快达到阈值，但2焦耳×20赫兹设置中60秒开/20秒关的时间间隔更快。除1焦耳×40赫兹（100%odC，30秒开/10秒关）外，结石部位达到热损伤阈值的时间通常比UPJ更快；而2焦耳×20赫兹（30秒开/10秒关）和0.5焦耳×80赫兹（100%odC）的阈值达到时间基本相同（见表1）。

随着激光设置的增强，结石部位和UPJ区域的累积热剂量均呈现上升趋势。在所有测试时间间隔中，2 J x 20 Hz的激光设置累积热剂量最高，但30秒开/10秒关的设置却最低。除上述差异外，其他激光设置间未发现其他具有普遍性的规律（参见表1和表2）。

在石料与UPJ设备的最高温度对比中，13/20次测试显示石料温度更高，6/20次测试显示UPJ温度更高，仅有一项测试（2焦耳×20赫兹，30秒开/10秒关）的最高温度相同。除三项测试外（1焦耳×40赫兹——60秒开/20秒关和60秒开/60秒关，2焦耳×20赫兹——30秒开/30秒关），其余测试的温度曲线均存在统计学显著差异。在石料和UPJ设备中，各激光设置的光密度值（odCs）越大，温度越高。以75%光密度值为基准，各激光设置的激光开启时间越长（60秒开/20秒关），石料和UPJ设备的最高温度均更高。以50%光密度值为基准，不同激光开启周期对最高温度的影响结果存在差异：碎石模式下30秒开/30秒关周期温度更高，而除尘模式下60秒开/60秒关周期温度更高。这一规律在石料和UPJ设备中均成立（表2）。

虽然不同激光设置产生的最高温度没有明显趋势，但我们确实观察到统计学意义上的显著差异，这表明即使在标准化功率下，频率和能量仍能显著影响温度和热剂量。对于100%臭氧浓度（odC），2焦耳×20赫兹的设置在结石和UPJ部位温度最高，而0.4焦耳×100赫兹的设置在这两个部位温度最低。对于其他4种臭氧浓度/持续时间组合，整体上未发现明显趋势（见表1和表2）。

水凝胶块的温度起始值为$^{37.0℃\pm2.1℃}$，并以$^{1.0℃\pm2.0℃}$的速率持续升高。该位置测得的温度未出现统计学显著变化。观察发现，当起始温度较低（<37℃）时温度升高幅度略大，而当起始温度较高（>37 ℃）时温度波动幅度最小。

讨论

本研究证实，温度和累积热剂量在靠近最后一根光纤尖端的位置更高，这一发现与既往研究结果一致。[7]此外，我们证明能量和频率对热负荷具有显著影响，而传统观点认为功率是决定温度的唯一因素可能并不完全准确。[5,8-10]总体而言，当使用100%和75%的光密度时，光密度越高、激光开启时间越长，累积热剂量和最高温度就越高，这与已发表文献的结论一致。[11,12]在比较75%光密度的激光开启时间时，60秒开启/20秒关闭的模式在结石和UPJ部位的每个激光设置中，都能产生更高的累积热剂量和最高温度。

有趣的是，在评估50%臭氧浓度时，碎裂模式设置在较短激光开启时间（30秒开/30秒关）下能产生更高累积热剂量，而粉尘模式设置在较长激光开启时间（60秒开/60秒关）下则表现出更高累积热剂量。在考虑最高温度时，除UPJ模式下1焦耳×40赫兹的测试结果外（30秒开/30秒关43.3℃对比60秒开/60秒关43.3℃），其他条件均呈现相同规律。这表明激光关闭时间可能在流体冷却过程中起关键作用——激光关闭时间越长，新鲜灌注液流入冷却更多肺泡细胞的机会就越大。

在Urs激光碎石术中，已有大量研究对相关变量进行了操控。密歇根大学William Robert博士的实验室通过体外实验模型和计算建模开展了多项研究。他们评估了Ho：YAG激光功率（2.5-50 W）、频率（5-80 Hz）、冲洗速率（0-40 ml/min）、冲洗温度（约0 ℃和19 ℃）以及氧浓度（>50%）。[4,5,11-14]他们的研究试图将先前的发现应用于活体猪模型，发现能够造成组织损伤的温度很容易达到，但通过增加冲洗流速可以消除这种温度。[15]其他实验室也评估了冲洗速率，并确定增加冲洗速率可以减轻主动激光期间的温度升高，使用UAs同样可以达到这一效果。[16-18]

最近一项研究评估了在Urs治疗尿路结石期间术中冲洗液温度。他们比较了1 J x 20 Hz和0.5 J x 20 Hz的激光设置与0 ml/min、15 ml/min和30 ml/min的冲洗速率。他们发现，当冲洗速率为在15 ml/min和30 ml/min的条件下，连续60秒激光激活后仍未达到43 ℃的温度。[19]我们的研究使用了恒定灌注流量（100 cm^{-2} h=17.5 ml/min）的尿道成形器。我们发现，在恒定功率下，热损伤阈值最快可在195秒内达到（结石部位2焦耳×20赫兹，UPJ部位1焦耳×40赫兹）。尽管滕等人研究与我们的测试功率存在显著差异，但显然在治疗较大结石负荷时，泌尿科医生在连续激光治疗过程中必须格外谨慎，因为即使使用尿道成形器，温度也可能达到危险水平。

需要特别说明的是，本研究针对的是肾盂内较大的结石，该区域具有更大的容积和面积，有利于液体灌注与冲洗液流动。既往研究表明，相较于较小空间，激光治疗时温度上升更快，热损伤阈值可能更早达到。[20,21]与我们前期评估及既往研究结果一致，当结石占位率超过70%时即达到热损伤阈值。[1]这一结论不受测试的激光参数设置及激光作用时间的影响。Aldoukhi等学者通过对63例尿路结石病例的病历分析发现，在输送最大功率的60秒内，结石占位率可达63%。[1]

尽管研究表明光锥能量（odCs）低于70%时较难突破热损伤阈值，但需注意：高功率激光设备能在更短时间内产生更大热负荷，且光锥能量更低。此外，在膀胱颈与肾盂等狭窄空间进行激光治疗时，即使光锥能量较低或使用功率较小的激光设备，热损伤阈值仍可能被突破——特别是结石破碎后，此时激光尖端可能更接近尿路上皮，且碎石后不再吸收能量。体外实验显示，使用模拟贝戈斯结石时，与未放置结石的对照组相比，不同功率（10、20、40、60瓦）下液体温度升幅均有所降低。[20]

众所周知，与激光碎石术期间真正的尿路结石相比，Begostones可能具有独特的光热特性；[22]但是，在体外泌尿激光研究期间，Begostones通常被接受为真正的尿路结石的合成类似物，因为它们能够以有效的方式不费力地组成，并且能够以相同的组成进行制造和复制。

迄今为止，这似乎是首项在解剖温度条件下，于高保真解剖体外模型中进行热负荷评估的研究，该模型在使用超声导管（UAs）时同步对模拟结石进行激光治疗。其他研究已采用离体和体内模型进行实验，这些模型可模拟完整的输尿管长度，且部分研究使用了超声导管。学界普遍认为，使用超声导管不仅能提高冲洗流速、更精准地调控温度升高，还能有效降低冲洗过程中的肾内压。[17,23]

本研究采用moses2.0ho：yAg激光器评估功率参数时，将40瓦设定为标准功率。该功率值可在保持恒定功率的同时，实现频率与能量参数的四组不同激光模式调整——包含两种碎石模式和两种碎石粉碎模式。尽管泌尿科医生在临床实践中常采用较低功率，但本研究旨在突破单纯功率参数的局限，因为已有大量前期研究对比过不同功率设置的效果。[8,5,15]

本研究针对先前在室温环境下开展的研究存在局限性进行了改进。通过该实验模型，我们评估了在解剖温度条件下使用超声碎石仪（UAs）进行高精度解剖模型时的热剂量与温度参数。该实验设计为熊激光碎石术提供了一个高质量、高真实度的体外模型。值得注意的是，多数先前研究主要采用试管体外模型或离体猪肾模型进行实验。

尽管我们已对前期研究的局限性进行了改进，但本研究仍存在若干不足。首先，虽然本项目采用高精度解剖模型构建肾结石模型，但在将数据与实际手术场景对应时仍需保持审慎态度。其次，为最大限度减少干扰变量对结果的影响，本研究仅采用单一模型进行评估。最后，虽然Begostone模型能模拟真实肾结石，但其模拟效果可能无法完全复现真实病变。本实验室计划在后续研究中继续推进泌尿激光技术领域探索，基于本研究积累的经验，逐步解决上述局限性。

本研究具有多项优势。首先，我们通过解剖学精确的高保真模型（该模型已通过机械测试和CFd测试验证），评估了激光频率、激光能量、odC值及激光持续时间四个参数，且实验环境采用超声波阵列模拟解剖温度。其次，我们成功在人体解剖结构的两个特定部位评估了热负荷。

最终，我们成功实现了对合成2厘米结石进行激光治疗时的温度测量。通过整合这些组件构建单一模型并分析四个独立变量，本研究结果得到显著强化。尽管先前研究已探讨过影响灌注液温度的若干因素，但多数研究仅聚焦于较少变量。

结论

通过该实验模型，我们成功验证了前期研究结果并解决了若干局限性。我们证实，通过增加臭氧浓度和延长激光脉冲时间，可实现更高剂量的热负荷。研究再次表明，在功率、能量和频率标准化条件下，参数调整会显著影响热剂量和温度。本研究结果表明，泌尿科医生必须严格规范进行Urs激光碎石术操作——无论激光参数如何设置，输尿液温度和输尿管膀胱段的累积热剂量都可能达到临界值，进而引发尿路上皮损伤。

利益冲突声明：作者声明与本研究无任何个人或财务利益冲突。

致谢：作者感向Dr.爱以诚挚感谢。
我们衷心感谢密歇根大学的威廉·罗伯逊教授为本项目提供的专业指导与宝贵建议。本研究主要基于其实验室的卓越研究成果，经他审阅数据并提出数据评估的深入见解。最终取得了具有重要影响的研究成果。

这篇论文已经过同行评审。

参考文献

1. Kronenburg P, Somani B激光治疗结石的最新进展——系统综述。Curr Urol Rep 2018；19：45.https://doi.org/10.1007/s11934-018-0802-x
2. Deem CA, Simeon L, Alruwaily AF, et al.肾结石治疗中灵活输尿管镜检查技术发展模式：全球调查结果.J Endourol 2015;29:1221-30.https://doi.org/10.1089/end.2015.0160
3. Saguthio, SA., Denny WC.肾结石治疗中的热问题和解决方案。国际机械工业杂志 (Int J Mech Ind Eng 1984；10：795-806。https://doi.org/10.1016/0301-679X(84)90076-1
4. Maxwell AD, MacConaghy B, Harper JD, 等.温光碎石术的体模温度监测研究.J Endourol 2019;33:113-9.https://doi.org/10.1089/end.2018.0605
5. Abdelkhi AH, Ghani KR, Hill TL, 等.高功率钬激光碎石术的热安全问题.J Endourol 2017;31:1308-12.https://doi.org/10.1089/end.2017.0479
6. Saba P, Belfast L, Mehyk R, 等.采用三维打印解剖模型评估激光技术开发和医疗器械用钬激光模型平台.J Endourol 2020;34:1088-94.https://doi.org/10.1089/end.2020.0440
7. Tamkin M, Lashkhmi E, Singh N, et al.Ho:YAG激光与新型钬光纤激光在肾石术中的温度变化:一项体外对比研究.World J Urol 2020;38:3261-6.https://doi.org/10.1007/s00345-020-03251-1
8. De Coninck V, Defraigne C, Traxer O.激光碎石术中Watt温度测定法.World J Urol 2022；40：1257-8.
9. Petzold R, Suarez-Ibarrola R, Miernik A.新型脉冲钬固体激光器与铥光纤石英碎石激光器的最终评估。J Endourol 2021；35：851-9.https://doi.org/10.1089/end.2020.0803

10. Molina WR, Carrera RV, Chew BH, et al. 脉冲与连续光纤与术前间隙温度升高：超脉冲钬光钇铝石榴光谱（SPTP）与低功率120 W快速重复频率钕钇铝石榴石激光器（Ho：YAG）的比较。*Wrold J Urol*(2021)；39：3951-63.https://doi.org/10.1007/s00345-021-03694-1
11. Loures MM, Dan JI, Hall TL, 等.激光操作员工作周期对温度和热剂量的影响：体外研究。*世界泌尿学杂志* 2022;40:1575-80.https://doi.org/10.1007/s00345-022-03967-8
12. Aldoukhi AH, Dan JI, Majdalany SL, 等.脉冲管镜钬:钇:术中激光激活模式对器械体温及相关热剂量的影响.*J Endourol* 2021;35:1217-22.https://doi.org/10.1089/end.2020.0667
13. Aldoukhi AH, Black KM, Hall TL, 等.确定热安全激光钬:钇术动态调整新电源:体外模型.*J Endourol* 2020;34:79-84.http://doi.org/10.1089/end.2019.0499
14. Dan JI, Hall TL, Maxwell AD, 等.冷却冲洗对激光碎石术中肾盏前壁热损伤阈值时间的影响：体外模型.*J Endourol* 2021;35:700-5.https://doi.org/10.1089/end.2020.0806
15. Aldoukhi AH, Hall TL, Ghani KR, et al.脉冲前锥型单层与单纤激光钬:钇:铝石榴石碎石术期间的核体温监测.*J Endourol*.2018;32:724-9.https://doi.org/10.1089/end.2018.0305
16. Tsaturyan A, Petrosyan A, Pantazis L, et al.长脉冲钬:光激活对温度的影响：一项体外实验研究.*世界泌尿学杂志* 2022;40:1873-8.https://doi.org/10.1007/s00345-022-04000-8
17. Galligan H, Bravo JC, Sepulveda F, et al.在离体模型中与快脉光体型碎石术相关的管内温度测量。*Cent European J Urol* 2021；74：380-94.https://doi.org/10.5173/cej.2021.1092
18. Wroclawski R, Yilmaz M, Lorner T, 等.通过脉冲激光钬:钇:铝:石榴石(Ho:YAG)激光碎石术中的核心温度测量评估肾盂内温度升高.*World J Urol* 2023;41:543-9.https://doi.org/10.1007/s00345-023-04255-0
19. Tong J, Wang Y, Jin Z, 等.柔性输尿管镜钬:钇铝石榴石激光碎石术中肾积液灌注速度和灌注压对肾盂温度升高.*Int Urol Nephrol* 2021;53:415-9.https://doi.org/10.1007/s11255-020-02665-x
20. Petrosyan A, Tsaturyan A, Pantazis L, 等.激光碎石术中影响盏腔灌注温度的因素：体外实验研究.*Urology* 2022;170:53-9.https://doi.org/10.1016/j.urology.2022.08.028
21. Razzaghi Khajeh N, Hall TL, 等.激光碎石术中肾盂肾盏前壁热损伤阈值的预测.*J Endourol*.2022;36:22-8.https://doi.org/10.1089/end.2021.0082
22. King IB, Katta N, Teichman JMH, et al.基于周期的Ho:YAG碎石术的临床.*J Endourol* 2021;35:928-36.https://doi.org/10.1089/end.2021.0742
23. Petrosyan A, Paparel K, Vagenov A, 等.学者研究工场声调和技术.激光参数优化与术中治疗过程反馈调整相关的冲洗液温度问题.采用人工和自动计算体内实验.*世界泌尿学杂志*.2022;40:1953-8.https://doi.org/10.1007/s00345-022-04024-4

通讯作者：Christopher Wunderling博士，美国纽约州罗切斯特罗切斯特大学医学中心泌尿科，Christopher_Wunderling@UrmC.rochester.edu

World Journal of Urology (2024) 42:453
https://doi.org/10.1007/s00345-024-05162-3

RESEARCH

Temperature profile during endourological laser activation: introducing the thermal safety distance concept

Eugenio Ventimiglia[1,2,3,4] · Daniele Robesti[1,2] · Etienne Xavier Keller[3,4,5] · Christian Corsini[1,2] · Andrea Folcia[1,2] · Margherita Fantin[1,2] · Luigi Candela[6] · Edoardo Pozzi[1,2] · Alba Sierra[3,4,6] · Amelia Pietropaolo[3,7] · Bhaskar K. Somani[7] · Frederic Panthier[4,6] · Felipe Pauchard[4,8] · Ioannis Kartalas Goumas[9] · Luca Villa[1,2] · Francesco Montorsi[1,2] · Olivier Traxer[4,6] · Andrea Salonia[1,2] · Paola Saccomandi[10]

Received: 18 June 2024 / Accepted: 6 July 2024 / Published online: 29 July 2024
© The Author(s), under exclusive licence to Springer-Verlag GmbH Germany, part of Springer Nature 2024

Abstract

Purpose To examine temporal-spatial distribution of heat generated upon laser activation in a bench model of renal calyx. To establish reference values for a safety distance between the laser fiber and healthy tissue during laser lithotripsy.

Methods We developed an in-vitro experimental setup employing a glass pipette and laser activation under various intra-operative parameters, such as power and presence of irrigation. A thermal camera was used to monitor both temporal and spatial temperature changes during uninterrupted 60-second laser activation. We computed the thermal dose according to Sapareto and Dewey's formula at different distances from the laser fiber tip, in order to determine a safety distance.

Results A positive correlation was observed between average power and the highest recorded temperature (Spearman's coefficient 0.94, $p<0.001$). Irrigation was found to reduce the highest recorded temperature, with a maximum average reduction of 9.4 °C at 40 W ($p=0.002$). A positive correlation existed between average power and safety distance values (Spearman's coefficient 0.86, $p=0.001$). A thermal dose indicative of tissue damage was observed at 20 W without irrigation (safety distance 0.93±0.11 mm). While at 40 W, irrigation led to slight reduction in mean safety distance (4.47±0.85 vs. 5.22±0.09 mm, $p=0.08$).

Conclusions Laser settings with an average power greater than 10 W deliver a thermal dose indicative of tissue damage, which increases with higher average power values. According to safety distance values from this study, a maximum of 10 W should be used in the ureter, and a maximum of 20 W should be used in kidney in presence of irrigation.

Keywords Stone · Laser temperature · Thermal dose · Thermal safety · *In-vitro* model

✉ Eugenio Ventimiglia
eugenio.ventimiglia@gmail.com

1 Vita-Salute San Raffaele University, Milan, Italy

2 Division of Experimental Oncology, Unit of Urology, URI, IRCCS Ospedale San Raffaele, Via Olgettina, 60, Milan 20132, Italy

3 Young Academic Urologists (YAU), Urolithiasis and Endourology Working Party, Arnhem, The Netherlands

4 Progressive Endourological Association for Research and Leading Solutions (PEARLS), Paris, France

5 Department of Urology, University Hospital Zurich, University of Zurich, Zurich, Switzerland

6 Sorbonne Universite, GRC#20 Lithiase Urinaire, Hôpital Tenon, Paris, Île-de- France 27063, France

7 Department of Urology, University Hospital Southampton, Southampton, UK

8 Urology Department, Hospital Naval Almirante Nef, Viña del Mar 2520000, Av. Alessandri, Viña del Mar, Valparaíso, Chile

9 Dept. of Urology, Istituto Clinico Beato Matteo, Vigevano, Italy

10 Department of Mechanical Engineering, Politecnico di Milano, Milan 20156, Italy

Introduction

The physical principles of laser energy have revolutionized the endoluminal treatment of stone disease [1]. During laser lithotripsy, three major settings can be adjusted to adapt to different surgical conditions: pulse energy (J), pulse frequency (Hz), and pulse duration (µs). To regulate the total average power (W) given to the stone for ablation, the pulse energy and frequency are commonly titrated. High-power settings facilitate stone fragmentation or dusting regardless of stone size and composition [2]. Nevertheless, the potential benefit should be balanced with the increasing danger of thermal damage [3], a phenomenon that is temperature dependent.

The photothermal effect is the primary physical principle for the temperature to rise. The effects of this action on the surrounding tissues include coagulation, carbonization, and denaturation, ultimately leading to tissue scarring and fibrosis [4–6].

The extent of thermal damage is influenced by both the temperature of the tissue and the duration of heating. Traditionally, the formula developed by Sapareto and Dewey [7, 8] has been utilized to estimate tissue damage resulting from thermal exposure. This formula calculates the cumulative thermal dose necessary to achieve a specific biological effect, such as thermal necrosis or tissue ablation, typically observed at a temperature of 43 degrees Celsius lasting for at least 120 min. The cumulative equivalent minutes at 43 °C (CEM43) serve as a standardized measure of tissue heating, integrating both temperature and time factors of thermal energy delivery. In the context of lithotripsy, CEM43 is suggested as a relevant parameter for predicting tissue damage extent and optimizing safe laser parameters.

The aim of this study was to analyze the temporal-spatial distribution of generated heat following laser activation in a bench model of a renal calyx, in order to provide reference values for a safety distance between the laser fiber and healthy tissue during laser lithotripsy, based on CEM43 values.

Materials and methods

Experimental set-up

We developed an in-vitro experimental setup to study the variations in water temperature due to laser activation according to different intra-operative scenarios (Fig. 1). To simulate intra-operative conditions, we exploited a custom-built glass pipette with an open roof bulb simulating a renal calyx. The bulb diameter is 12 mm, while the opening is 10 mm. The stem of the bulb has a diameter of 5 mm, and it is 115 mm long. The glass pipette was filled with saline (NaCl 0.9%) and submerged in a container at 37 °C, replicating the temperature of the human body.

We tested our hypothesis in two different scenarios:

1. Laser activation without irrigation, with the laser fiber tip conducted at the center of the calix through a 4.8 Fr ureteral catheter (Coloplast, Humlebæk, Denmark, Fig. 1a).
2. Laser activation with irrigation, where a flexible ureteroscope (Lithovue, Boston Scientific, Marlborough, USA) was passed through a 12–14 Fr UAS (ReTrace, Coloplast, Humlebæk, Denmark) and conducted in the caliceal model. The laser fiber was then passed through the working channel of the scope and conducted at the

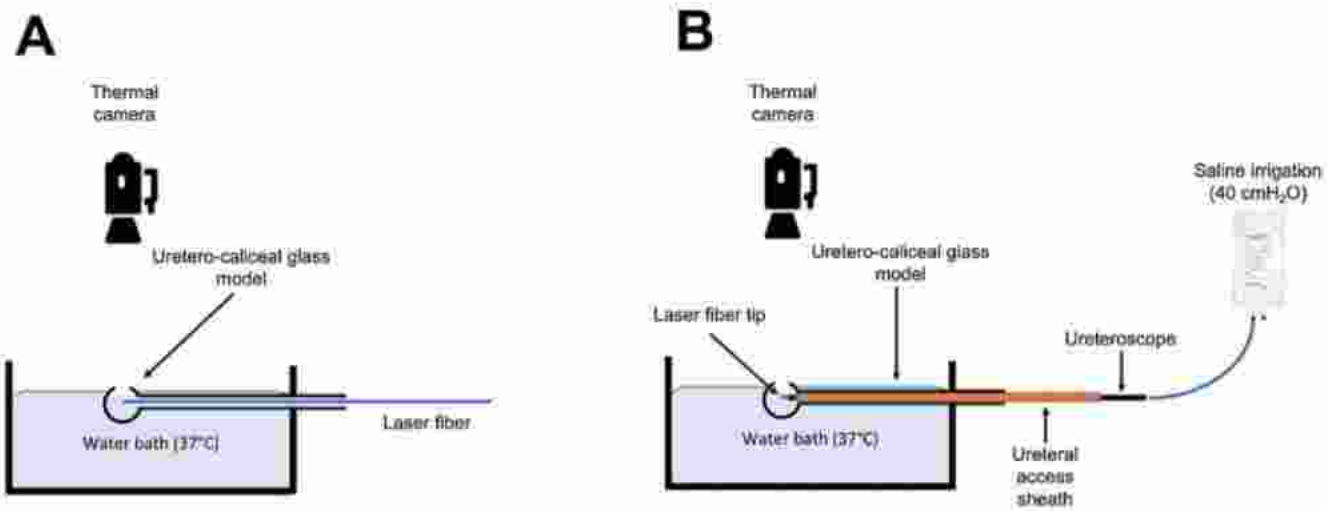


Fig. 1 Experimental setup for temperature recording during laser activation. **A**). Experimental setup in absence of irrigation **B**). Experimental setup in presence of irrigation

center of the laser. Saline at room temperature (21 °C) with a constant irrigating pressure of 40 cm H2O was used for irrigation (Fig. 1b). The irrigating pressure resulted in an average flow rate of 10 ml/min. The use of 12–14 Fr UAS enabled equilibrium between the inflow and outflow of fluid within the glass pipette, ensuring that the fluid level remained stable and prevented any overflow.

In both cases, a 200 µm laser fiber (Quanta System, Samarate, Italy) was used, with the laser fiber tip placed in a fixed position, 1 mm below the water surface. Laser fiber tip was cut before every test.

For live temperature monitoring during laser activation, a thermal camera set at 15 fps (FLIR E8 Pro, Teledyne FLIR LLC, Italy) was placed perpendicular to the open roof of the pipette. A thermal camera allows to keep track of both temporal and spatial changes in temperature.

All tests were performed using a high power Ho: YAG laser generator set with the lowest available peak power (Cyber Ho 150 W, Quanta System, Samarate, Italy). The spatial and temporal temperature fluctuations were documented and recorded during 60 s of uninterrupted laser activation, at different power and frequency settings with or without irrigation. Tested powers were 5 W, 10 W, 20 W, and 40 W. Each experimental configuration was repeated at least three times to ensure reliable results.

Image analysis

Image analysis was performed using FLIR Tools software version 6.x. The images were preprocessed to enhance image quality, remove noise, and normalize the temperature scale. Calibration was performed using reference objects with known temperatures to ensure accurate temperature measurements. To analyze the thermal images, a region of interest (ROI) was selected around the laser-irradiated area. The ROI consisted of a line perpendicular to the direction of the fiber laser, passing through the tip to capture the heat distribution accurately, over time. We exploited the customized image analysis algorithm to extract temperature information from the ROI.

Heat damage assessment

The effect of thermal damage on tissue depends on temperature and heating time. Dewey and Sapareto [7, 8] developed a metric known as thermal dose, which is calculated using the following experimental formula: $t_{43} = \sum_{t=0}^{t=\text{end}} R^{43-T} \Delta t$

where t represents the time in minutes, T denotes the temperature in degrees Celsius, and R is a constant that varies depending on T ($R = 0.5$ when $T > 43$, and $R = 0.25$ when $T < 43$). This formula enabled the computation of cumulative equivalent minutes at 43 °C (CEM43), which standardized cumulative temperature exposure across varying temperature profiles. Subsequently, a threshold of thermal injury of 120 equivalent minutes was established, consistent with existing literature [7, 8]. Accordingly, thermal damage is expected to occur when tissue is exposed to 43 °C for 120 min. Similarly, exposure to higher temperatures shortens the duration needed to obtain tissue damage.

Definition of safety distance

We utilized the collected data on temporal and spatial temperature variations during laser activation, captured by the thermal camera. Subsequently, we calculated CEM43 for every distance from the fiber tip to establish a safety margin for each power configuration, taking into account several surgical scenarios, i.e. presence or absence of irrigation.

Mean and standard deviation (SD) were calculated for each experimental replicate to analyze continuous variables. The comparison between different power settings was conducted using Student's t-test. The Spearman correlation was employed to examine the relationship between the average power and the highest recorded temperature, as well as between the average power and the safety distance values. The statistical analyses were performed using R software version 4.2.1 (www.r-project.org). All tests were two-sided, and a significance level of 0.05 was used.

Results

Recorded temperatures

Figure 2 shows an example of the spatial and temporal distribution of temperature obtained in a single replicate of our experimental setting. Highest temperature was recorded in proximity of the laser fiber, sharply declining when departing from it. Table 1 shows highest recorded temperatures 60 s after laser activations for all the analyzed scenarios. There was a statistically significant positive correlation between average power and highest recorded temperature (Spearman's correlation coefficient 0.94, $p < 0.001$). Highest temperature exceeded 43 °C with an average power ≥ 10 W in absence of irrigation. In presence of irrigation, highest temperature exceeded 43 °C with an average power ≥ 20 W. The use of irrigation was able to significantly lower highest recorded temperature with an average power ≥ 20 W, with a maximum average reduction of 9.4 °C at 40 W ($p = 0.002$).

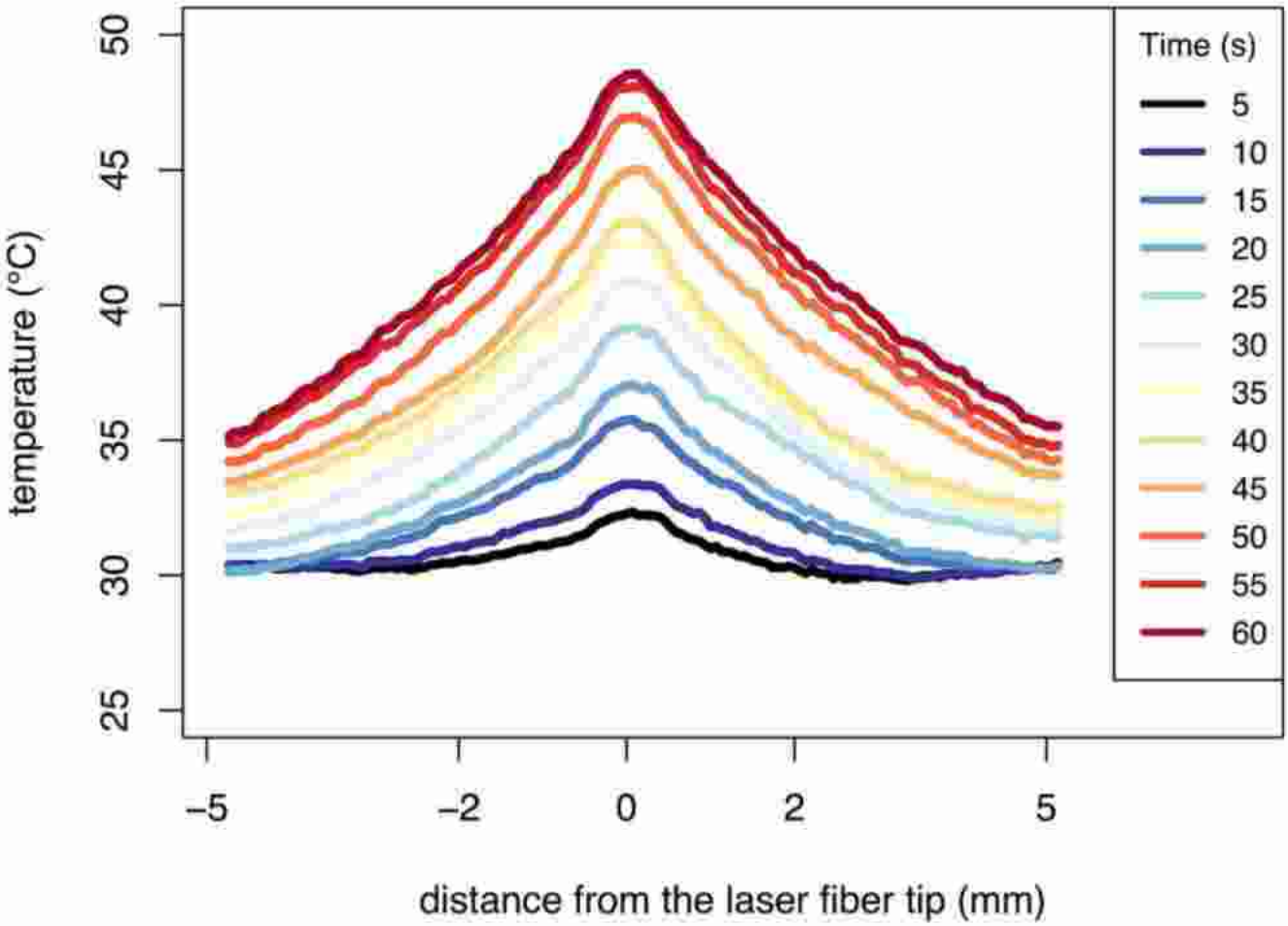


Fig. 2 Temporal and spatial distribution of recorded temperature during laser activation. The figure shows recorded temperatures for Ho: YAG laser according to the distance from the fiber tip and time of laser activation, when using 10 W of average power (5 J, 20 Hz, long pulse)

Table 1 Highest recorded temperature according to average power and use of irrigation

Average power	No irrigation, mean (SD)	Irrigation, mean (SD)	Temperature reduction	*p* value
5 W	40.1 (0.4) °C	39.1 (1.21) °C	1.0 °C	0.28
10 W	47.8 (0.3) °C	42.2 (2.2) °C	5.6 °C	0.04
20 W	56.4 (0.4) °C	50.7 (1.4) °C	5.7 °C	0.02
40 W	72.9 (0.9) °C	63.5 (0.9) °C	9.4 °C	0.002

Thermal dose and safety distance

A thermal dose indicative of tissue damage according to the CEM43 formula was observed with an average power of 20 W without irrigation, mean (SD) safety distance 0.93 (0.11) mm, and at 40 W irrespectively of the presence of irrigation (Fig. 3). For setting where CEM43 > 120 min, we estimated the thermal safety distance, defined as the distance from the laser fiber tip where thermal dose did not exceed the tissue damage threshold. There was a statistically significant positive correlation between average power and safety distance values (Spearman's correlation coefficient 0.86, $p = 0.001$). At maximum analyzed power, i.e. 40 W, irrigation provided a slight reduction in the mean (SD) safety distance, 4.47 (0.85) vs. 5.22 (0.09), although this difference was not statistically significant ($p = 0.08$).

Discussion

In this study, we report for the first time the temporal-spatial distribution of generated heat during laser lithotripsy. Using an in-vitro model, we described the rise in temperature as well as the thermal dose at different distances from the laser fiber tip. A rise in laser temperature > 43 °C was observed at 10 W without the use of irrigation and at 20 W in presence of irrigation. In order to better investigate the impact of generated heat, we estimated the thermal dose in terms

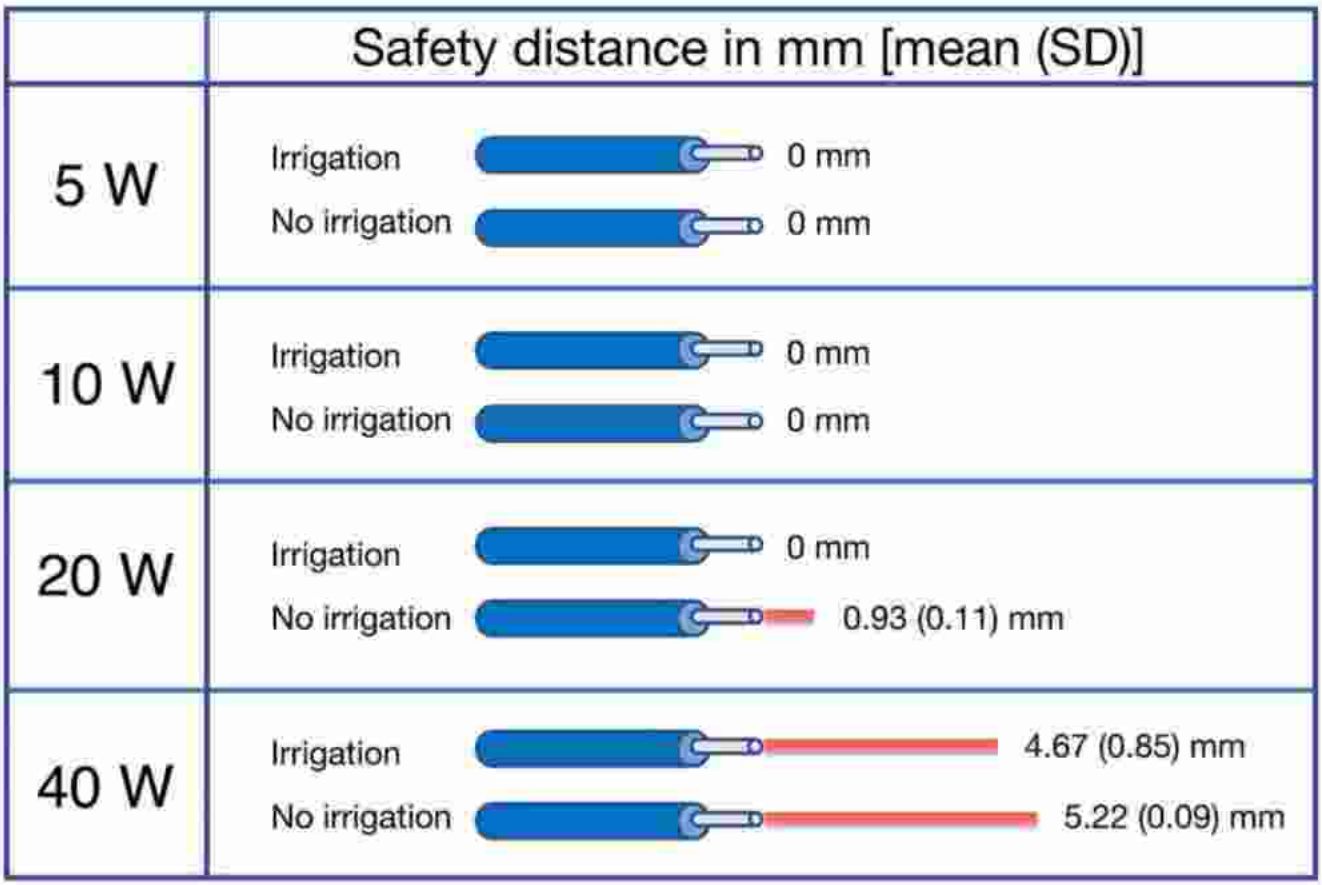


Fig. 3 Safety distance values according to the CEM43 formula for analyzed settings in presence and absence of irrigation (CEM43: cumulative equivalent minutes at 43 °C)

of CEM43 and defined the so-called thermal safety distance, i.e. the distance from the laser fiber tip where CEM43 remained below 120 min. We found that in the absence of irrigation, a thermal dose indicative of tissue damage was evident at 20 W, whereas in the presence of irrigation, it was instead evident at 40 W.

Several factors influence the thermal dose delivered during laser lithotripsy [9]. With regards to this, the choice of laser parameters is paramount: increasing average power of laser parameters [9, 10] invariably results in higher fluid temperature and thermal dose. It has been recommended that an average power > 25 W and > 15 W should not be used in the kidney and in the ureter, respectively [11]. Besides laser parameters, irrigation fluid is another important variable determining thermal dose values, influencing heat dissipation and cooling effects [12, 13]. Adequate irrigation helps mitigate thermal damage to surrounding tissues by dissipating heat and maintaining optimal operating conditions; however, increase in irrigation flow is likely paralleled by increase in intra-renal pressure, with possible drawbacks in terms of infectious complication risk. A recent bench [12] study showed that in order to mitigate the thermal effects of a 20 W laser regimen the irrigant flow should be set at 15 ml/s, i.e. elevating the water bag at 100 cm, far above the recommended 40 cmH20 threshold for irrigant pressure [14]. According to the same study, increasing power at 40 W required a 200 cmH_20 irrigant pressure in order to mitigate the thermal effect of such parameters [12].

It is therefore key not to focus only on temperature, but to stress the importance of the concept of thermal dose. Thermal tissue damage relies on both the degree of temperature increase and the duration it is sustained. Reporting outcomes solely based on peak temperature or time to reach a certain temperature may be misleading and provide an incomplete assessment of the risk of thermal injury. Sapareto and Dewey [7, 8] introduced the concept of thermal dose to standardize the relationship between temperature and time for tissues exposed to different temperatures. For instance, tissue maintained at 43 °C for 120 min accumulates the same thermal dose as tissue kept at 50 °C for 56 s or at 56 °C for 1 s [12]. Knowing the change in temperature and its temporal behavior, it is possible to estimate the cumulative equivalent minutes at 43 °C, and therefore to assess for any specific temperature record. This concept has

been confirmed in various tissue types, including the kidney [6]. Most soft tissues become nonviable with a CEM43 ranging surpassing 120 min [8, 15]. Our study stresses even more the importance of thermal dose over recorded temperature. An average power of 10 W without irrigation was shown to reach temperatures over 43 °C; however, thermal dose during the first 60 s of activation remained below the threshold of tissue damage. This happened also in the case of 20 W in presence of irrigation.

To date, proposed methodologies for investigating both temperature rise and thermal dose suffer from important limitations. The most evident is the lack of spatial definition, with point measurements which are unlikely to report a comprehensive scenario of heat diffusion and dissipation. Point estimates of temperature may be misleading, and considerably dependent on the distance from the selected point from the laser fiber tip. An important advantage of infrared thermometry is the temporal and spatial coverage of the changes in temperature [16], allowing us for the first time to define the concept of thermal safety distance.

There are clinically relevant implications in the results of our study. The safety distance values discourage the use of laser settings with an average power > 20 in the kidney, since thermal damage may arise even at 5 mm distance from the laser fiber tip. In the ureter, according to the safety distance values emerging from the current report, average power of laser settings should not overcome 10 W, since at 20 W tissue damage may arise up to 1 mm distance from the laser fiber tip. Preliminary clinical data seem to confirm this concept [17].

Our study is not devoid of limitation. First, being an in vitro study, our results will need to be substantiated in vivo. Second, the application of the thermal camera in an in vivo setting is not feasible at present, meaning that an alternative measurement modality will need to be implemented. Third, the implementation of stone into this model is experimentally not feasible, as the laser stone interaction would result in vertical movements, making signal to noise ratio of the thermal camera measurements too to be accurate. Fourth, the heat sink effect due to blood flaw was not recapitutalated in our model, as the glassy pipet was bathing in a still medium. Firth, the small gap between the water surface and the laser tip could potentially affect the measured temperature due to heat dispersion as it passes through the medium. However, since the fiber laser is maintained in a fixed position, this error would be constant across all measurements, still allowing for comparisons among different conditions.

Conclusions

Our experimental configuration highlights several crucial clinical implications: (1) the experimental data about safety distance advise against employing laser settings with an average power exceeding 20 W within the kidney or 10 W within the ureter; (2) Irrigation has the potential to lower the highest recorded temperature; however, we observed a marginal reduction of the safety distance values at high power-settings (3) High power settings do not appear to be safe even in presence of irrigation.

Acknowledgements none.

Author contributions E.V.: Manuscript writing/editing, Data analysis, Data collection or management D.R.: Manuscript writing/editing, Data analysisE.X.K.: project developmentC.C.: Manuscript writing, Data analysis, Protocol/project developmentA.F.: Manuscript editing, project developmentM.F.: Manuscript editing, Protocol/project developmentL.C.: project developmentE.P.: project developmentA.S.: project developmentA.P.: project developmentB.S.: project developmentF.P.: project developmentF.P.: project developmentI.K.G.: Critical Review, Protocol/project developmentL.V.: project developmentF.M.: Critical ReviewO.T.: Protocol/project development, Critical ReviewA.S.: Critical ReviewP.S.: Protocol/project development, Critical Review, Manuscript writing/editing, Data analysis.

Funding none.

Data availability No datasets were generated or analysed during the current study.

Declarations

Competing interests The authors declare no competing interests.

References

1. Panthier F, Ventimiglia E, Traxer O et al (2024) Lasers and stones: towards an Approach that depends on the Stone type? A point of View from PEARLS members. Eur Urol 85:e92–e93
2. Ventimiglia E, Pauchard F, Gorgen ARH et al (2021) How do we assess the efficacy of Ho:YAG low-power laser lithotripsy for the treatment of upper tract urinary stones? Introducing the Joules/mm(3) and laser activity concepts. World J Urol 39:891–896. https://doi.org/10.1007/s00345-020-03241-9
3. Sierra A, Corrales M, Kolvatzis M et al (2022) Thermal Injury and Laser Efficiency with Holmium YAG and Thulium Fiber Laser-An in Vitro Study. J Endourol 36:1599–1606. https://doi.org/10.1089/end.2022.0216
4. Buttice S, Sener TE, Proietti S et al (2016) Temperature changes inside the kidney: what happens during Holmium:Yttrium-Aluminum-Garnet laser usage? J Endourol 30:574–579. https://doi.org/10.1089/end.2015.0747
5. De Coninck V, Defraigne C, Traxer O (2022) Watt determines the temperature during laser lithotripsy. World J Urol 40:1257–1258
6. Yarmolenko PS, Moon EJ, Landon C et al (2011) Thresholds for thermal damage to normal tissues: an update. Int J Hyperth off J

Eur Soc Hyperthermic Oncol North Am Hyperth Gr 27:320–343. https://doi.org/10.3109/02656736.2010.534527
7. Sapareto SA, Dewey WC (1984) Thermal dose determination in cancer therapy. Int J Radiat Oncol Biol Phys 10:787–800. https://doi.org/10.1016/0360-3016(84)90379-1
8. van Rhoon GC, Samaras T, Yarmolenko PS et al (2013) CEM43°C thermal dose thresholds: a potential guide for magnetic resonance radiofrequency exposure levels? Eur Radiol 23:2215–2227. https://doi.org/10.1007/s00330-013-2825-y
9. Rice P, Somani BK, Nagele U et al (2022) Generated temperatures and thermal laser damage during upper tract endourological procedures using the holmium: yttrium-aluminum-garnet (Ho:YAG) laser: a systematic review of experimental studies. World J Urol 40:1981–1992. https://doi.org/10.1007/s00345-022-03992-7
10. Louters MM, Dau JJ, Hall TL et al (2022) Laser operator duty cycle effect on temperature and thermal dose: in-vitro study. World J Urol 40:1575–1580. https://doi.org/10.1007/s00345-022-03967-8
11. Panthier F, Abid N, Hoznek A et al (2023) 2022 recommendations of the AFU Lithiasis Committee: laser - utilization and settings. Prog en Urol J l'Association Fr D'urologie la Soc Fr D'urologie 33:825–842. https://doi.org/10.1016/j.purol.2023.08.008
12. Aldoukhi AH, Black KM, Hall TL et al (2020) Defining thermally safe laser lithotripsy power and irrigation parameters: in Vitro Model. J Endourol 34:76–81. https://doi.org/10.1089/end.2019.0499
13. Hein S, Petzold R, Schoenthaler M et al (2018) Thermal effects of Ho: YAG laser lithotripsy: real-time evaluation in an in vitro model. World J Urol 36:1469–1475. https://doi.org/10.1007/s00345-018-2303-x
14. Pauchard F, Bhojani N, Chew B, Ventimiglia E (2024) How to measure intra-renal pressure during flexible URS: historical background, technological innovations and future perspectives. Actas Urol Esp 48:42–51. https://doi.org/10.1016/j.acuroe.2023.10.007
15. Toupin S, Bour P, Lepetit-Coiffé M et al (2017) Feasibility of real-time MR thermal dose mapping for predicting radiofrequency ablation outcome in the myocardium in vivo. J Cardiovasc Magn Reson off J Soc Cardiovasc Magn Reson 19:14. https://doi.org/10.1186/s12968-017-0323-0
16. De Landro M, Felli E, Collins T et al (2021) Prediction of in vivo laser-Induced Thermal damage with Hyperspectral Imaging using deep learning. Sens (Basel) 21. https://doi.org/10.3390/s21206934
17. Æsøy MS, Juliebø-Jones P, Beisland C, Ulvik Ø (2024) Temperature measurements during flexible ureteroscopic laser lithotripsy: a prospective clinical trial. J Endourol 38:308–315. https://doi.org/10.1089/end.2023.0660

Publisher's Note Springer Nature remains neutral with regard to jurisdictional claims in published maps and institutional affiliations.

Springer Nature or its licensor (e.g. a society or other partner) holds exclusive rights to this article under a publishing agreement with the author(s) or other rightsholder(s); author self-archiving of the accepted manuscript version of this article is solely governed by the terms of such publishing agreement and applicable law.

《世界泌尿外科杂志》（2024）第42卷第453页
https://doi.org/10.1007/s00345-024-05162-3

研究

内窥镜激光激活过程中的温度分布：引入热安全距离概念

尤金尼奥·文蒂米利亚[1,2,3,4,5]、达尼埃莱·罗贝斯蒂[2,3,4,5]、埃蒂安·泽维尔·凯勒[1,2,5]、克里斯蒂安·科西尼[1,2]、路易吉·坎德拉[6,1,2]、阿尔巴·西埃拉[3,4,6,3,7]、阿梅莉亚·皮耶特罗保罗[7]、弗雷德里克·潘蒂耶[4,6,4,8,9,1,2]、巴沙卡尔·K·索马尼[1,2]、菲利佩·波沙尔[1,2,3,4,6,3,4,6,3,4,6

介绍

激光能量的物理原理彻底革新了腔内治疗结石疾病的方法[1]。在进行激光碎石术时，可通过调节脉冲能量(J)、脉冲频率（Hz）和脉冲持续时间（μs）这三个主要参数来适应不同手术需求。为了精确控制作用于结石的总平均功率(W)，通常需要对脉冲能量和频率进行微调。高功率设置能有效粉碎结石或使其碎裂成粉尘，无论结石大小和成分如何[2]。但需注意的是，这种潜在优势必须与热损伤风险的增加保持平衡[3]，而热损伤的发生具有温度依赖性特征。

光热效应是温度升高的主要物理原理，这种作用对周围组织的影响包括凝固、碳化和变性，最终导致组织瘢痕形成和纤维化[4—6]。

热损伤的程度受组织温度和加热时长的双重影响。传统上，萨帕雷托和杜威[7，8]提出的公式被用于评估热暴露导致的组织损伤。该公式通过计算达到特定生物效应（如热坏死或组织消融）所需的累积热剂量来实现，这种效应通常在43摄氏度持续至少120分钟的温度条件下出现。43℃累积等效分钟数（CEM43）作为组织加热的标准化指标，综合考量了热能传递的温度和时间因素。在碎石术中，CEM43被推荐为预测组织损伤程度和优化安全激光参数的重要参数。

本研究旨在通过激光碎石术实验模型，分析肾盏激光激活后产生的热量时空分布特征，基于CEM43值建立激光光纤与健康组织的安全距离参考标准。

材料和方法

实验设置

我们开发了一套体外实验装置，用于研究不同术中场景下激光激活引起的水温变化（图1）。为模拟术中条件，我们使用了一支定制的玻璃吸管，其顶部开有模拟肾盏的球形开口。该球形开口直径为12毫米，开口处直径为10毫米。球形开口的茎部直径为5毫米，长度为115毫米。玻璃吸管内填充了生理盐水（氯化钠0.9%），并浸入37°C的容器中，以模拟人体温度。

我们在两种不同场景下验证了假设：

1. 无需冲洗即可进行激光激活，具体操作是将激光光纤尖端经由4.8 Fr输尿管导管（丹麦Humlebæk公司Coloplast产品，见图1 a）导入杯状结构中心。
2. 采用激光联合灌洗技术进行激活，具体操作是将柔性输尿管镜（Lithovue，美国波士顿科学公司，马尔伯勒）经12-14 Fr UAS导管（ReTrace，丹麦科洛普拉斯公司，Humlebæk）插入膀胱杯模型。随后将激光光纤通过内镜工作通道引导至膀胱杯部位。

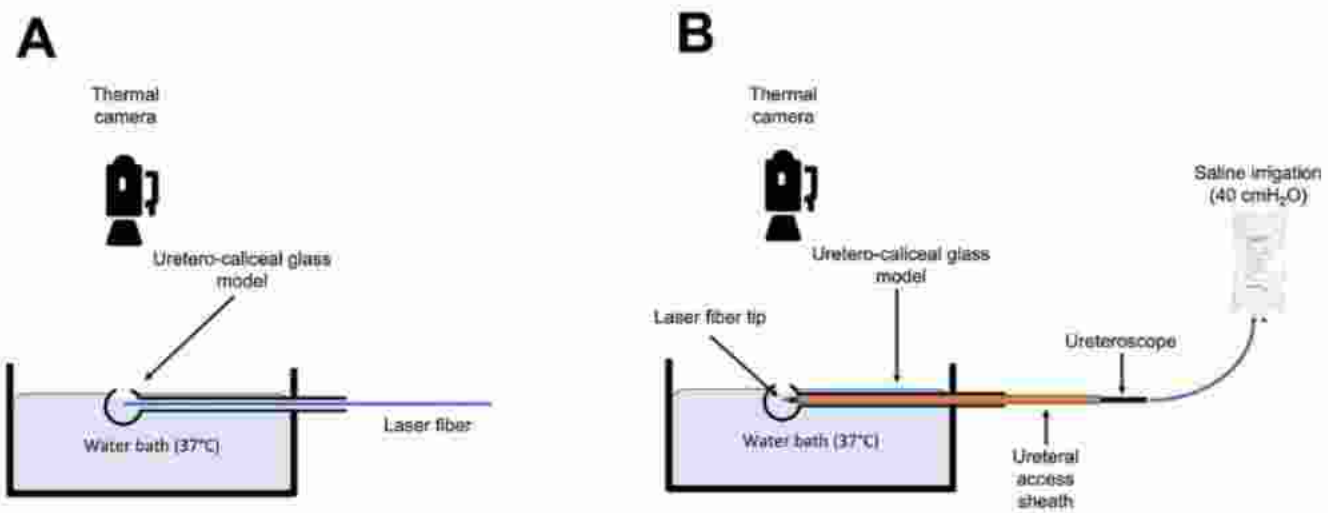


图1激光激活过程中温度记录的实验装置。**A**)无灌注的实验装置**B**)有灌注的实验装置

激光中心。使用室温（21°C）的生理盐水，以40厘米水柱的恒定灌注压力进行灌注（图1 b）。该灌注压力导致平均流速为10 ml/min。采用12–14 Fr UAS可使玻璃移液管内的液体流入与流出达到平衡，确保液位稳定并防止溢出。

两种情况下均采用200μm激光光纤（Quanta System，意大利萨马拉特），将光纤尖端固定于水下1毫米处。每次测试前均需对光纤尖端进行切割处理。

为实时监测激光激活过程中的温度，将热成像相机（FLIR E8 Pro，意大利Teledyne FLIR LLC公司）以15帧/秒的速率垂直安装在移液管的开口顶部。该设备可同步记录温度在时间和空间上的变化。

所有实验均采用高功率Ho：YAG激光发生器（Cyber Ho 150 W，Quanta System公司，意大利萨马拉特）进行，该设备具有最低可用峰值功率。在60秒连续激光激活期间，通过不同功率和频率设置（含/不含灌注）记录空间与时间温度波动。测试功率分别为5W、10W、20W和40W。每个实验配置至少重复三次以确保结果可靠性。

图像分析

图像分析采用FLIR Tools软件6.x版本完成。图像经过预处理以提升质量、消除噪声并标准化温度标度。通过已知温度的参考物体进行校准，确保温度测量的准确性。在热成像分析中，我们选取了激光照射区域周围的感兴趣区域（ROI）。该ROI由一条垂直于光纤激光器方向的线构成，该线穿过激光尖端以准确捕捉随时间变化的热分布。我们运用定制的图像分析算法，从ROI中提取温度信息。

热损伤评估

热损伤对组织的影响取决于温度
处理时间和加热时间。Dewey和Sapareto[7，8]开发了一个称为热剂量的指标，其计算使用以下实验公式：$t_{43}=\varepsilon_{i=0}^{n} R^{43-T} \Delta t_i$，其中t表示时间（分钟），T表示温度（摄氏度），R是一个随T变化的常数（当T>43时R=0.5，当T>43时R=0.25）

T<43）。该公式实现了43℃条件下累积等效分钟数（CEM43）的计算，将不同温度曲线下的累积热暴露时间标准化。随后，我们根据现有文献[7，8]确立了120分钟热损伤阈值。这意味着当组织在43℃环境下暴露120分钟时，就会发生热损伤。类似地，暴露在更高温度下时，组织损伤所需的暴露时间会相应缩短。

安全距离的定义

我们利用热成像仪采集的激光激活期间温度时空变化数据，计算出光纤尖端各距离处的CEM43值，从而为不同功率配置建立安全裕度，同时考虑了手术场景中的多种情况，包括是否进行灌洗。

为分析连续变量，我们计算了每个实验重复的平均值和标准差（SD）。采用学生t检验对不同功率设置进行比较。通过斯皮尔曼相关系数分析平均功率与最高记录温度之间的关系，以及平均功率与安全距离值之间的关联。统计分析使用R软件4.2.1版（www.r-project.org）完成。所有检验均为双侧检验，显著性水平设定为0.05。

结果

记录的温度

图2展示了本实验单次重复中测得的温度时空分布示例。激光光纤附近测得最高温度，远离该区域时温度急剧下降。表1列出了所有实验场景中激光激活60秒后的最高温度记录。平均功率与最高温度呈现统计学显著正相关（斯皮尔曼相关系数0.94，p<0.001）。在未使用灌溉的情况下，当平均功率≥10W时，最高温度超过43°C；使用灌溉时，当平均功率≥20W时，最高温度同样超过43°C。研究表明，使用灌溉可显著降低平均功率≥20W时的最高温度记录，其中在40W功率下平均温度降幅最大，达到9.4°C（p=0.002）。

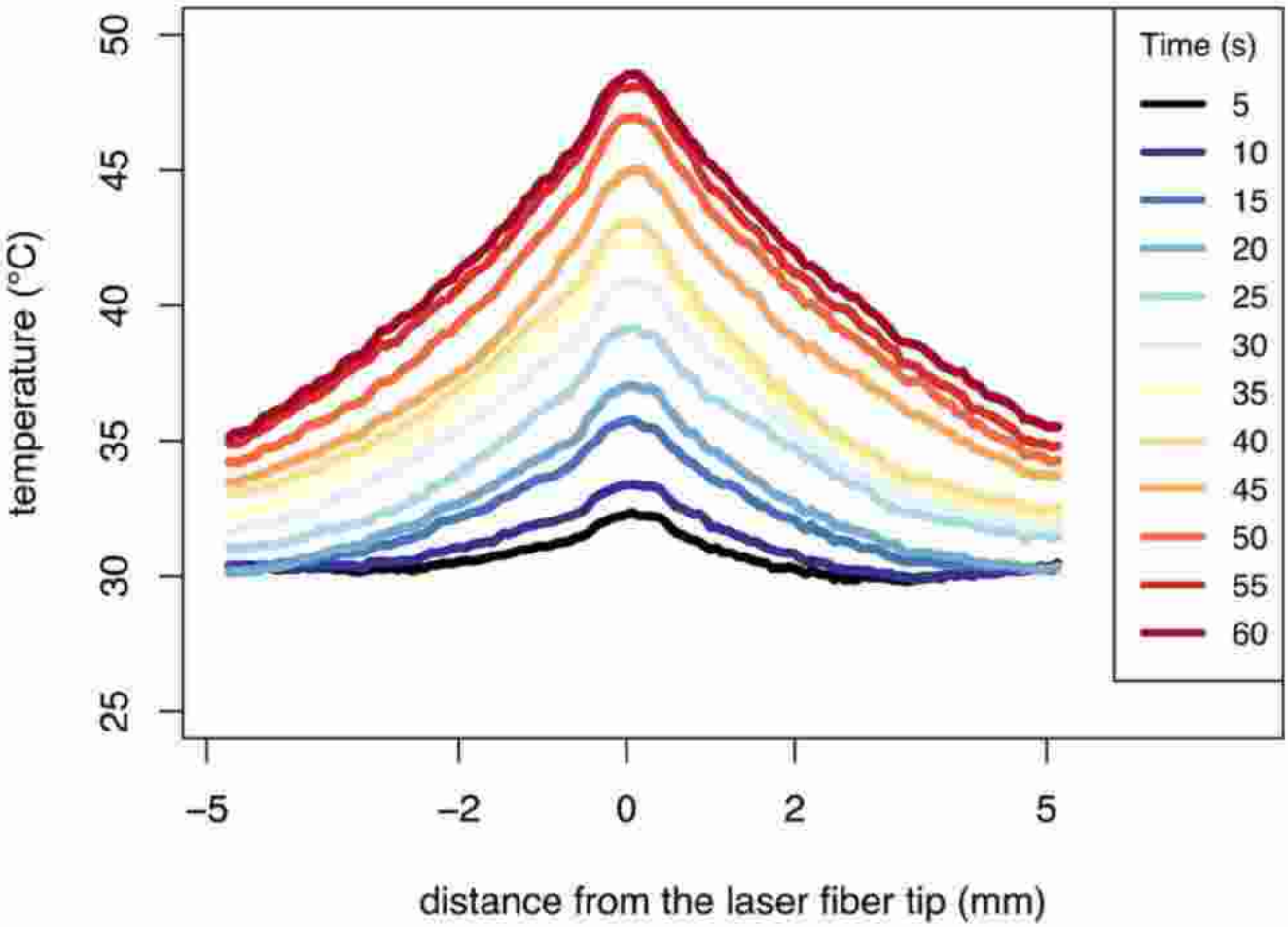


图2激光激活期间记录温度的时间和空间分布。该图显示了使用10W平均功率（5J，20Hz，长脉冲）时，Ho：YAG激光器根据光纤尖端距离和激光激活时间记录的温度。

表1根据平均功率和灌溉使用情况记录的最高温度

平均功率	无灌注，平均值（SD）	灌注，平均值（SD）	温度降低	p值
5 W	40.1 (0.4) °C	39.1 (1.21) °C	1.0 °C	0.28
10 W	47.8 (0.3) °C	42.2 (2.2) °C	5.6 °C	0.04
20 W	56.4 (0.4) °C	50.7 (1.4) °C	5.7 °C	0.02
40 W	72.9 (0.9) °C	63.5 (0.9) °C	9.4 °C	0.002

热剂量和安全距离

根据CEM43公式计算得出的热剂量指标显示，在未使用冲洗功能时，平均功率为20瓦时可观察到组织损伤迹象（平均安全距离0.93±0.11毫米，40瓦功率下该数值保持稳定）。对于CEM43值超过120分钟的治疗参数，我们通过热安全距离评估——即激光光纤尖端到热剂量未超过组织损伤阈值的最远距离。研究发现，平均功率与安全距离值之间存在统计学显著的正相关性（斯皮尔曼相关系数0.86，p=0.001）。在最大功率40瓦的测试条件下，使用冲洗功能可使平均热剂量值出现轻微下降。

（SD）安全距离，4.47（0.85）vs.5.22（0.09），尽管该差异无统计学意义（p=0.08）。

讨论

本研究首次揭示了激光碎石术过程中产生的热量在时空上的分布规律。通过体外模型，我们系统描述了激光光纤尖端不同距离处的温度升高情况及热剂量变化。实验数据显示：在10瓦功率下未使用冲洗时，激光温度升高超过43°C；而使用20瓦功率并配合冲洗时，温度增幅更为显著。为深入探究热量产生的影响，我们通过热剂量评估方法对相关参数进行了量化分析。

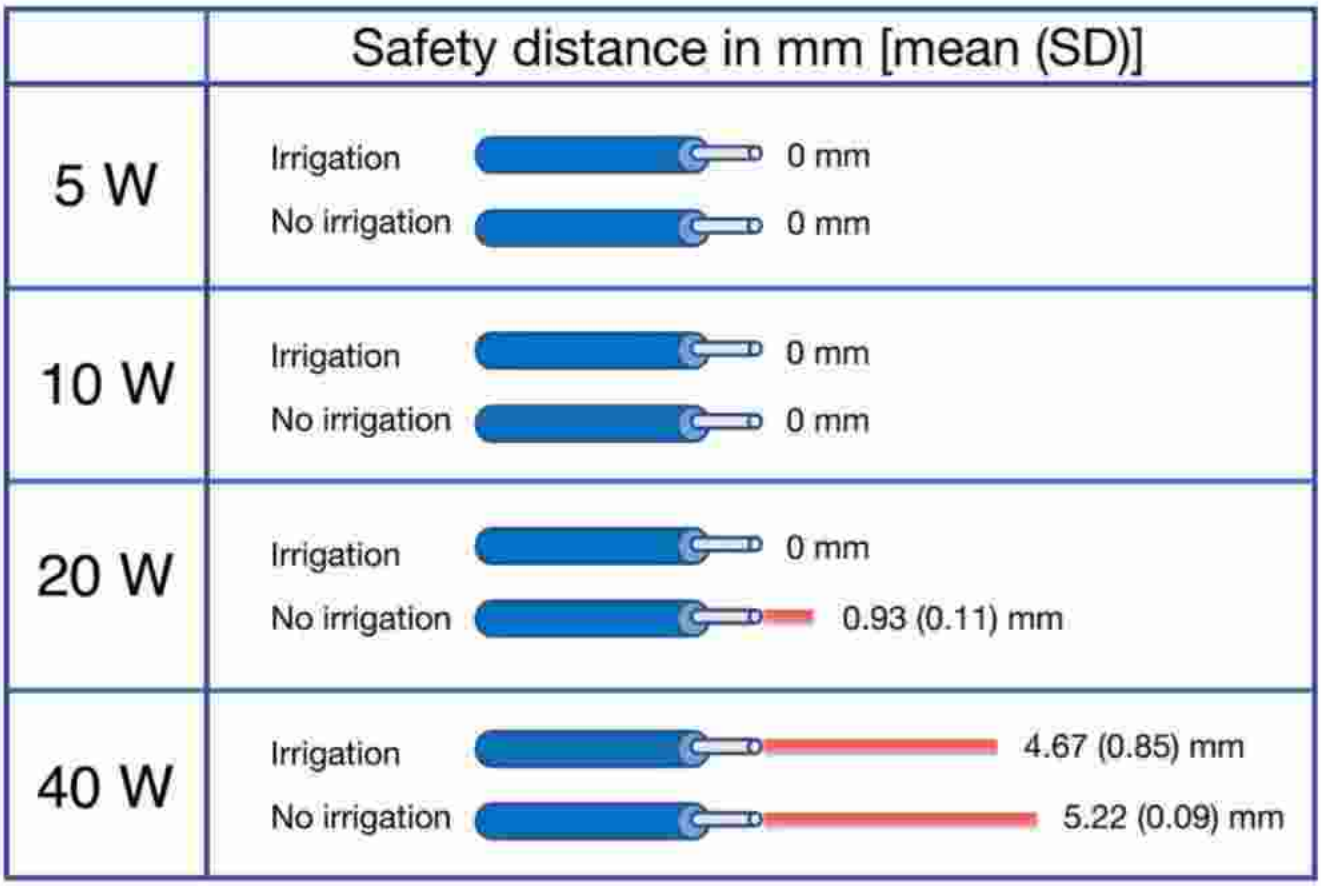


图3根据CEM43公式分析的设置在有无灌注情况下的安全距离值（CEM43：43°C下的累积等效分钟）

我们测定了CEM43的热效应，并定义了所谓的热安全距离——即激光光纤尖端持续保持CEM43值低于120分钟的区域。研究发现：在无灌注条件下，20瓦时即可检测到提示组织损伤的热剂量；而有灌注条件下，该阈值则需提升至40瓦才可检测到。

激光碎石术[9]过程中传递的热剂量受多重因素影响。其中激光参数的选择至关重要：平均功率越高[9，10]，液体温度和热剂量就越高。临床建议肾区平均功率不应超过25瓦，输尿管区域则不应超过15瓦[11]。除激光参数外，冲洗液也是决定热剂量的重要变量，它会影响热量散发和冷却效果[12，13]。适量冲洗液能通过散热维持最佳操作状态，有效减轻周围组织的热损伤；但冲洗流量增加可能伴随肾内压升高，从而增加感染并发症风险。最新实验室[12]研究表明，为减轻热效应

在20瓦激光治疗方案中，冲洗液流量应设置为15 ml/s，即将水袋抬高至100厘米，远高于推荐的40厘米水柱冲洗液压力阈值[14]。根据同一研究，当功率增加至40瓦时，需要200厘米水柱$_2$的冲洗液压力才能减轻此类参数的热效应[12]。

因此，我们不能只盯着温度数据，更要重视热剂量这个关键概念。组织热损伤的严重程度取决于温度上升幅度和持续时间。如果仅用峰值温度或达到特定温度所需时间来评估，可能会产生误导，无法全面评估热损伤风险。萨帕雷托和杜威[7，8]提出的热剂量概念，为不同温度环境下组织的温度-时间关系提供了标准化参照。例如，43℃持续120分钟的组织，其累积热剂量与50℃持续56秒或56℃持续1秒的组织相当[12]。通过掌握温度变化规律及其动态特征，我们就能估算出43℃条件下的累积等效时间，从而对任何特定温度记录进行风险评估。这一概念的提出，为热损伤评估提供了更科学的量化依据。

该现象已在多种组织类型中得到证实，包括肾脏[6]。当CEM43持续时间超过120分钟时，大多数软组织会失去活性[8，15]。我们的研究进一步强调了热剂量的重要性远超记录温度。数据显示，平均功率为10瓦且未进行冲洗时，温度可超过43°C；但激活启动后前60秒内的热剂量仍低于组织损伤阈值。即使在存在冲洗的情况下使用20瓦功率时，这一现象依然存在。

目前，针对温度升高和热剂量的研究方法仍存在明显局限。最突出的问题在于缺乏空间定义，仅凭点测量数据难以全面反映热量扩散与消散的完整过程。温度的点估计值可能具有误导性，且与激光光纤尖端到测量点的距离密切相关。红外测温技术的重要优势在于其能同时覆盖温度变化的时间维度和空间维度[16]，这使得我们首次能够明确界定热安全距离的概念。

本研究结果具有重要的临床意义。根据安全距离标准，肾脏部位的激光治疗应避免使用平均功率超过20瓦的激光设置，因为即使距离光纤尖端仅5毫米，也可能引发热损伤。对于输尿管部位，当前报告的安全距离数据表明，激光设置的平均功率不应超过10瓦——当功率达到20瓦时，距离光纤尖端仅1毫米处就可能造成组织损伤。初步临床数据似乎证实了这一观点[17]。

本研究存在若干局限性。首先，作为体外实验，我们的结果需要通过体内实验验证。其次，目前热成像相机在体内环境中的应用尚不可行，这意味着需要采用其他测量方式。第三，将结石植入该模型在实验层面不可行，因为激光与结石的相互作用会导致垂直位移，从而使热成像相机的信噪比无法准确测量。第四，由于玻璃移液管浸泡在静止介质中，我们的模型未能重现血液缺陷引发的散热效应。第五，水表面与激光尖端之间的微小间隙可能因介质中的热传导影响测量温度。不过，由于光纤激光器保持固定位置，这种误差在所有测量中保持恒定，仍可实现不同条件下的数据对比。

结论

我们的实验设计揭示了几个关键的临床意义：(1)安全距离的实验数据表明，肾脏内平均功率超过20瓦、输尿管内超过10瓦的激光设置不建议使用；(2)虽然冲洗可能降低最高记录温度，但我们发现高功率设置下的安全距离值仅有微小变化；(3)即使使用冲洗，高功率设置仍存在安全隐患。

无致谢。

作者贡献：E.V.：负责论文撰写/编辑、数据分析、数据收集或管理；D.R.：负责论文撰写/编辑、数据收集；analysisE.X.K.：负责项目开发；C.C.：负责论文撰写、数据分析、方案/项目开发；A.F.：负责论文编辑、项目开发；M.F.：负责论文编辑、方案/项目开发；L.C.：负责项目开发；E.P.：负责项目开发；A.S.：负责项目开发；A.P.：负责项目开发；B.S.：负责项目开发；F.P.：负责项目开发；F.P.：负责项目开发；developmentI.K.G.：负责方案/项目开发、批判性审阅；L.V.：负责项目开发；F.M.：负责批判性审阅；O.T.：负责方案/项目开发、批判性审阅；A.S.：负责批判性审阅；P.S.：负责方案/项目开发、批判性审阅、论文撰写/编辑、数据分析。

无资金。

数据可用性：本研究期间未生成或分析任何数据集。

声明

竞争利益作者声明无竞争利益。

参考文献

1. 潘蒂那尔F，文蒂米利亚E，特拉克塞尔O等（2024）激光与结石：是否应采用根结石类型而异的治疗策略？珍珠会员观点。《欧洲泌尿外科杂志》85：e92-e93
2. Ventimiglia E、Pauchard F、Gorgen ARH等学者（2021）在《世界泌尿学杂志》第39卷第891-896页发表论文《如何评估Ho：YAG低功率激光碎石术治疗上尿路结石的疗效？引入焦耳/毫米(3)和激光活性概念》。https://doi.org/10.1007/s00345-020-03241-9
3. Sierra A，Corrales M，Kolvatzis M et al（2022）稳定钬YAG和铒光纤激光治疗热损伤和激光效率的体外研究。J Endourol 36：1599–1606。https://doi.org/10.1089/end.2022.0216
4. Buttice S，Sener TE，Proietti S et al（2016）肾脏内部温度变化：钬：钇铝石榴石激光使用期间发生了什么？J Endourol 30：574–579。https://doi.org/10.1089/end.2015.0747
5. 德康尼克V，德弗兰C，特拉克塞O（2022）激光碎石术中瓦特值对温度的调控作用。《世界泌尿学杂志》40：1257–1258
6. 亚尔莫连科PS、穆恩EJ、兰登C等（2011）正常组织热损伤阈值：最新进展。《国际高热与肿瘤杂志》

欧洲超热肿瘤学会北美分会《超热肿瘤学》第27卷第320–343页。https://doi.org/10.3109/02656736.2010.534527

7. Sapareto SA，Dewey WC（1984）癌症治疗中的热剂量测定。Int J Radiat Oncol Biol Phys 10：787–800。https://doi.org/10.1016/0360-3016（84）90379-1
8. van Rhoon GC，SamarasT，YarmolenkoPS等（2013）CEM43°C热剂量阈值：磁共振射频暴露水平的潜在指南？《欧洲放射学》23：2215–2227。https://doi.org/10.1007/s00330-013-2825-y
9. 赖斯P，索马尼BK，纳格尔U等学者（2022）发表《钬钇石榴石（Ho：YAG）激光在上尿路内镜手术中的温度生成与热损伤：实验研究系统综述》一文，发表于《世界泌尿学杂志》，40：1981–1992年。https://doi.org/10.1007/s00345-022-03992-7
10. Louters MM，Dau JJ，Hall TL et al（2022）激光操作员工作周期对温度和热剂量的影响：体外研究。World J Urol 40：1575–1580。https://doi.org/10.1007/s00345-022-03967-8
11. Panthier F，Abid N，HoznekA等（2023）AFU膜酸盐结石委员会2022年建议：激光治疗的应用与参数设置。法国泌尿外科学会《泌尿外科进展杂志》33：825–842.https://doi.org/10.1016/j.purol.2023.08.008
12. Aldoukhi AH，Black KM，Hall TL et al（2020）确定热安全激光碎石术功率和冲洗参数：体外模型。J Endourol 34：76–81。https://doi.org/10.1089/end.2019.0499
13. Hein S，Petzold R，Schoenthaler M et al（2018）Ho：YAG激光碎石术的热效应：体外模型中的实时评估。World J Urol 36：1469–1475。https://doi.org/10.1007/s00345-018-2303-x
14. Pauchard F，Bhojani N，Chew B，Ventimiglia E（2024）如何在柔性URS期间测量肾内压力：历史背景、技术创新和未来展望。Actas Urol Esp 48：42–51。https://doi.org/10.1016/j.acuroe.2023.10.007
15. 图平S，布尔P，勒佩蒂-拜菲M等（2017）研究证实，实时磁共振热剂量成像技术可有效预测活体心肌射频消融术的治疗效果，相关成果发表于《心血管磁共振杂志》第19卷第14页。https://doi.org/10.1186/s12968-017-0323-0
16. De Landro M，Felli E，Collins T et al（2021）使用深度学习的高光谱成像对体内激光诱导热损伤的预测。Sens（Basel）21.https://doi.org/10.3390/s21206934
17. Æsøy MS，Juliebo-Jones P，Beisland C，UlvikØ（2024）柔性输尿管镜激光碎石术中的温度测量：一项前瞻性临床试验。J Endourol 38：308–315。https://doi.org/10.1089/end.2023.0660

出版者注：Springer Nature对已发表地图和机构隶属关系的司法管辖权主张保持中立。

Springer Nature或其授权方（例如学会或其他合作伙伴）根据与作者或其他权利持有人签订的出版协议，对本文拥有独家权利；作者对本文已接受的稿件版本进行自我存档，完全受该出版协议条款和适用法律的约束。

World Journal of Urology (2024) 42:588
https://doi.org/10.1007/s00345-024-05289-3

RESEARCH

An in vitro study of irrigation rate, operator duty cycle and intrarenal temperature in superpulse fiber thulium laser lithotripsy

Tianfu Ding[1] · Zheng Xu[1] · Zhongyue Huang[1] · Bo Xiao[1] · Weiguo Hu[1] · Jianxing Li[1]

Received: 11 July 2024 / Accepted: 23 September 2024 / Published online: 23 October 2024
© The Author(s) 2024

Abstract

Objective The present study aimed to examine the relationship between irrigation velocity, operator duty cycle (ODC), and intrarenal temperature during retrograde intrarenal surgery with a superpulse fiber thulium laser.

Methods Place the stones into the fresh isolated porcine kidneys, use puncture needle to place the temperature probe 2 mm around the stones, and place the pressure probes in the upper calyx, lower calyx, and renal pelvis. Place the entire setup in a 37 °C constant temperature water bath to simulate the human body environment. The laser power varies between 10 and 30 W, and the irrigation speed is 10-30 ml/min. Additionally, at a laser power of 20 W and an irrigation speed of 10 ml/min, different On-Duty Cycles (ODC) are set. Monitor the changes in temperature and pressure.

Results A direct proportionality of temperature in the kidney to the rate of irrigation has been reported between 10 W and 30 W laser powers. The percentage ratio of the rate of irrigation and power in the laser is 1:1, which can keep the temperature in the kidney at a safe level. At a laser power of 20 W and irrigation of 10 ml/min, the temperature inside the kidney increases sharply with the increase in ODC. By decreasing the ratio of ODC, the increase of temperature inside the kidney can be brought to a great reduction.

Conclusion Maintaining a 1:1 ratio between laser power and irrigation speed can effectively prevent thermal damage or injury to kidney tissue.Additionally, by adjusting the On-Duty Cycle (ODC) ratio, the intrarenal temperature can also be reduced.

Keywords Superpulse fiber thulium laser · Operator duty cycle (ODC) · Irrigation rate · Intrarenal temperature

Introduction

The continuous development of medical technology has resulted in the continued improvement of laser lithotripsy, which is now a mature treatment technique. Superpulsed fiber thulium laser with a 1940-nm wavelength has come to be one of the important candidates for lithotripsy. Due to the proximity of this wavelength to the absorption peak of water, the absorption coefficient of that wavelength in aqueous solutions is markedly higher than the conventional holmium laser at 2100 nm. This gives this wavelength a substantial edge over others in lithotripsy efficiency [1, 2]. Today, holmium laser lithotripsy is the preferred method for (flexible) URS, because of the wide range of applications and good outcomes in the procedure of lithotripsy [3]. What is more important is that besides showing stone-crushing efficiency superior to that with the holmium laser, the superpulsed fiber thulium laser also represents a new breakthrough in the treatment of the urinary tract stone, which features lower stone recoil force and thinner fiber diameter [4]. These features would thus indicate that the super-pulsed fiber thulium laser could be well applied and developed in the field of urinary stone treatment. The development of lithotripsy technology always attaches importance to the safety issue of laser lithotripsy as much as the stone comminution effect does. This work is aimed to optimize the temperature control and the irrigation flow rate during the process of laser lithotripsy to accomplish safe and effective therapy.

✉ Jianxing Li
lijianxing2015@163.com

[1] Department of Urology, Research Center for Urinary Disease, School of Clinical Medicine, Beijing Tsinghua Changgung Hospital, Tsinghua University, Beijing 102218, China

Materials and methods

In vitro modeling

This study utilized fresh ex vivo porcine kidneys, sourced under conditions that strictly adhered to ethical protocols, with all pigs being humanely euthanized. The research was conducted with the approval of the Ethics Review Committee and was granted the corresponding ethical approval number [IACUC-202306-P-001].The calculi specimens were obtained from our calculi specimen library, all of which underwent compositional analysis and were confirmed to be calcium oxalate monohydrate stones (CT value: 890 ± 123 HU). The study employed a range of equipment, including a single-use electronic ureteroscope with an outer diameter of F8.6 (ZebraScope Anhui Happiness Factory Medical Equipment Co., Ltd), a ureteral access sheath (F11/13 Laikai Medical Devices (Beijing) Co., Ltd), a super-pulsed thulium fiber laser with a 200 μm laser fiber (A-ONE Laikai Medical Devices (Beijing) Co., Ltd) , a multi-channel real-time thermometer (NF4000P-8 Guangzhou Ruimanting Instrument Factory) , a precision constant-flow experimental pump (BT-100 Hebei Rongbai Electric Appliance Factory) , High-precision digital pressure gauge (DT-1 Shanghai Ruxiang Instrument Factory) , a temperature-controlled water bath, physiological saline, and other essential surgical instruments.

The procedure involved the careful placement of the calculi into the renal pelvis, with temperature probes inserted using a puncture needle, positioned approximately 2 mm from the calculi within the renal pelvis. Ureteral access sheath was carefully inserted and secured to the ureter with ligatures. The pressure transducer is placed in the upper calyx, lower calyx, and renal pelvis using the same puncture needle. The entire setup was immersed in a temperature-controlled water bath, with the temperature maintained at 37 °C to simulate the human body's environmental temperature.

Experimental procedures

The laboratory temperature is set at 25 °C. The laser lithotripsy power is set at 10 W (1.0 J × 10 Hz, 0.1 J × 100 Hz), 15 W (1.5 J × 10 Hz, 0.15 J × 100 Hz), 20 W (2.0 J × 10 Hz, 0.1 J × 200 Hz), 25 W (2.5 J × 10 Hz, 0.1 J × 250 Hz), and 30 W (1.0 J × 10 Hz, 0.1 J × 300 Hz). The irrigation speed is set at 10, 15, 20, 25, and 30 ml/min (the irrigation fluid is physiological saline, and the temperature is 25 °C). The continuous laser excitation time is 120 s.

For the laser lithotripsy power of 20 W (2.0 J × 10 Hz) and the irrigation speed of 10 ml/min (the irrigation fluid is physiological saline, and the temperature is 25 °C), each 20 s constitute an operational cycle. The laser operates in the ODC mode, with 10 different ODC modes set to simulate various surgical strategies: ODC10%: The laser is activated for 2 s and then turned off for 18 s. ODC20%: Activated for 4 s, then off for 16 s. ODC30%: Activated for 6 s, then off for 14 s. ODC40%: Activated for 8 s, then off for 12 s. ODC50%: Activated for 10 s, then off for 10 s. ODC60%: Activated for 12 s, then off for 8 s. ODC70%: Activated for 14 s, then off for 6 s. ODC80%: Activated for 16 s, then off for 4 s. ODC90%: Activated for 18 s, then off for 2 s. ODC100%: The laser is continuously activated for 20 s without an off cycle. Each cycle is repeated 6 times to form a large group experiment.

Both of the temperature and pressure probes monitor the parameter in real-time at a frequency of once per second and records changes. The above experiments are repeated 5 times for each set of parameters, and a new kidney is used for each repetition.

Data collection and analysis

The experiments have been conducted at least in quintuplicate, and the data are given as averages. Data were graphed using ggplot2 in R version 4.3.3. Values are presented as mean ± standard deviation. Statistical analysis was conducted by paired t-test between two groups and nonparametric rank sum tests using multiple samples for multiple groups. The significant difference was set at $p < 0.05$.

Results

Changes in intrarenal temperature during continuous laser lithotripsy

At a lithotripsy power of 10 W, with irrigation speeds of 10 ml/min, 15 ml/min, 20 ml/min, 25 ml/min, and 30 ml/min, the intrarenal temperature reached a steady state with steady-state temperatures of 38.6 °C, 35 °C, 33.1 °C, 31.7 °C, and 30.7 °C, respectively, none of which exceeded the safety threshold (Fig. 1). At a lithotripsy power of 15 W, the intrarenal temperature continued to rise with an irrigation speed of 10 ml/min. However, at irrigation speeds of 15 ml/min, 20 ml/min, 25 ml/min, and 30 ml/min, the intrarenal temperature reached a steady state with steady-state temperatures of 38.4 °C, 35.9 °C, 34.7 °C, and 34.4 °C, respectively, none of which exceeded the safety threshold (Fig. 2). At a lithotripsy power of 20 W, the intrarenal temperature continued to rise with irrigation speeds of 10 ml/min and 15 ml/min. However, at irrigation speeds of 20 ml/min, 25 ml/min, and 30 ml/min, the intrarenal temperature

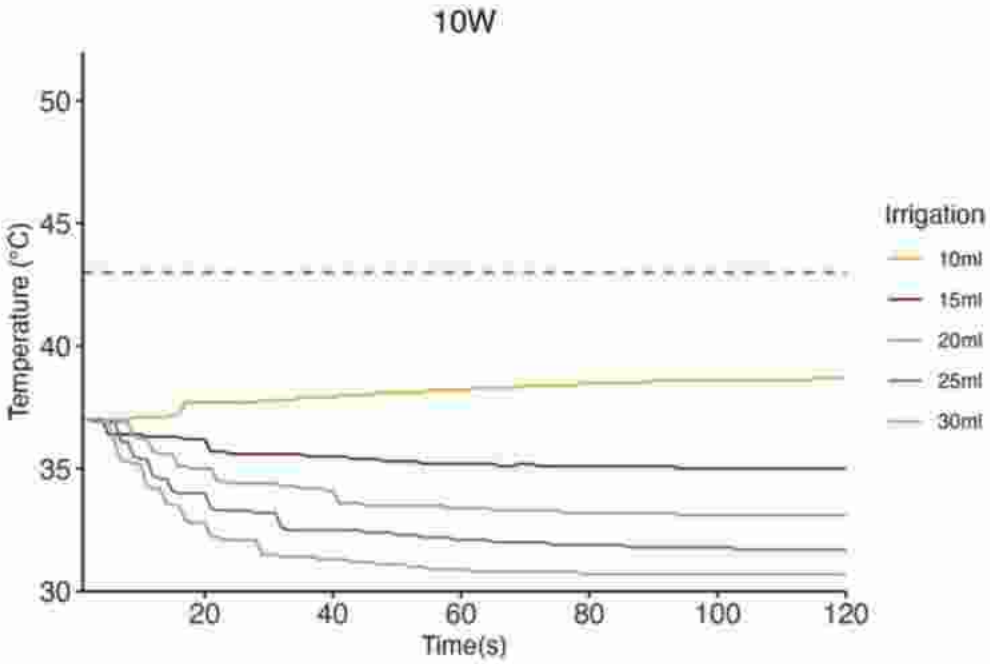


Fig. 1 Renal temperature at each irrigation speed at 10 W of gravel power

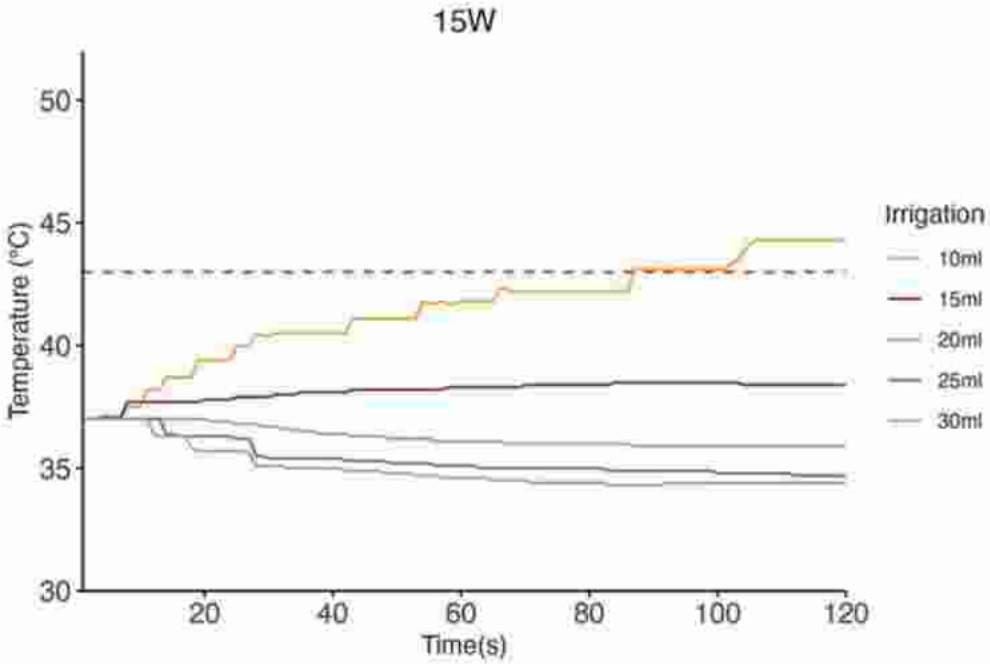


Fig. 2 Renal temperature at each irrigation speed at 15 W of gravel power

reached a steady state with steady-state temperatures of 38.7 °C, 36.3 °C, and 34.2 °C, respectively, none of which exceeded the safety threshold (Fig. 3). At a lithotripsy power of 25 W, the intrarenal temperature continued to rise with irrigation speeds of 10 ml/min, 15 ml/min, and 20 ml/min. However, at irrigation speeds of 25 ml/min and 30 ml/min, the intrarenal temperature reached a steady state with steady-state temperatures of 38.3 °C and 35.7 °C, respectively, neither of which exceeded the safety threshold (Fig. 4). At a lithotripsy power of 30 W, the intrarenal temperature continued to rise with irrigation speeds of 10 ml/min, 15 ml/min, 20 ml/min, and 25 ml/min. However, at an irrigation speed of 30 ml/min, the intrarenal temperature reached a steady state with a steady-state temperature of 37.5 °C, which did not exceed the safety threshold (Fig. 5). At different irrigation speeds, the intrarenal pelvic/calyceal pressure did not exceed 30mmH_2O (Table 1).

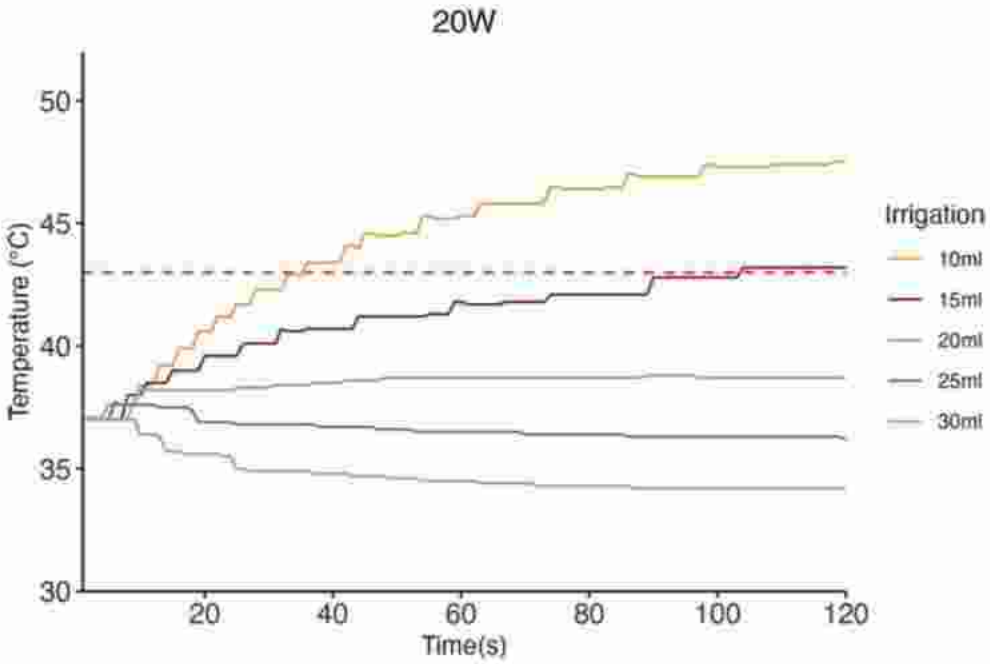


Fig. 3 Renal temperature at each irrigation speed at 20 W of gravel power

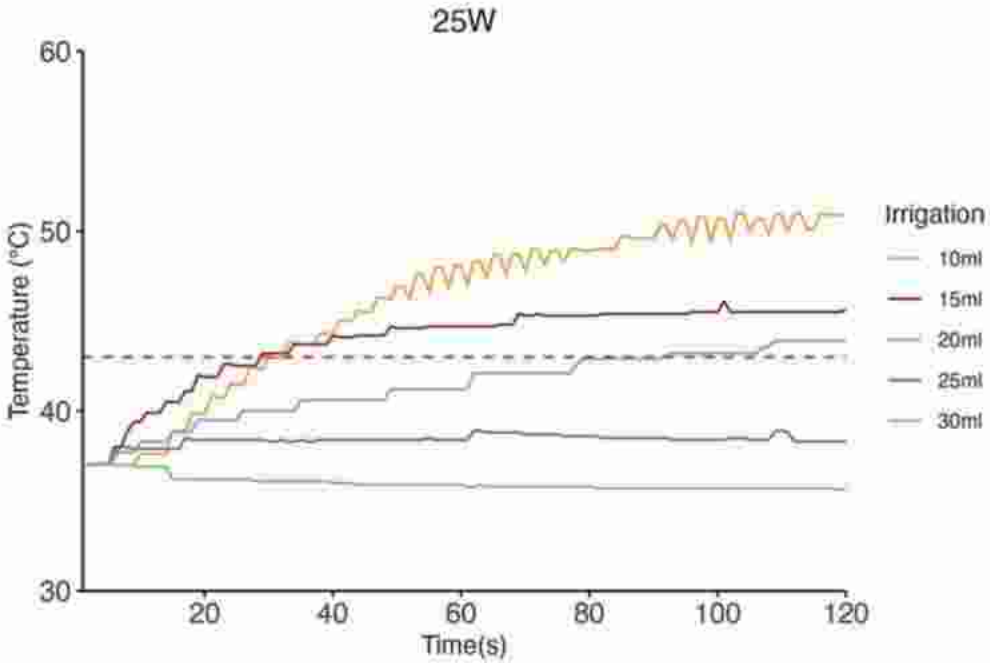


Fig. 4 Renal temperature at each irrigation speed at 25 W of gravel power

Changes in intrarenal temperature under different ODC ratios

When the On-Duty Cycle (ODC) is maintained below 60%, the steady-state intrarenal temperature tends to stabilize after reaching a certain value and does not further increase with the extension of time. In contrast, when the ODC exceeds 70%, the intrarenal temperature during the subsequent steady-state continues to rise over time (Fig. 6). With the increase of ODC, the highest intrarenal temperature shows a significant upward trend: ODC50%: 40.0 ± 0.52 °C; ODC 60%: 41.6 ± 0.38 °C; ODC 70%: 43.4 ± 0.48 °C; ODC 80%: 44.8 ± 0.73 °C; ODC 90%: 46.7 ± 0.54 °C (Table 2). When the ODC ratios are 70%, 80%, 90%, and 100%, respectively, the time for intrarenal temperature to reach the safety threshold temperature is 56.0 ± 1.0s, 51.8 ± 1.48s, 32.0 ± 1.58s, and 20.6 ± 1.14s, respectively (Table 3).

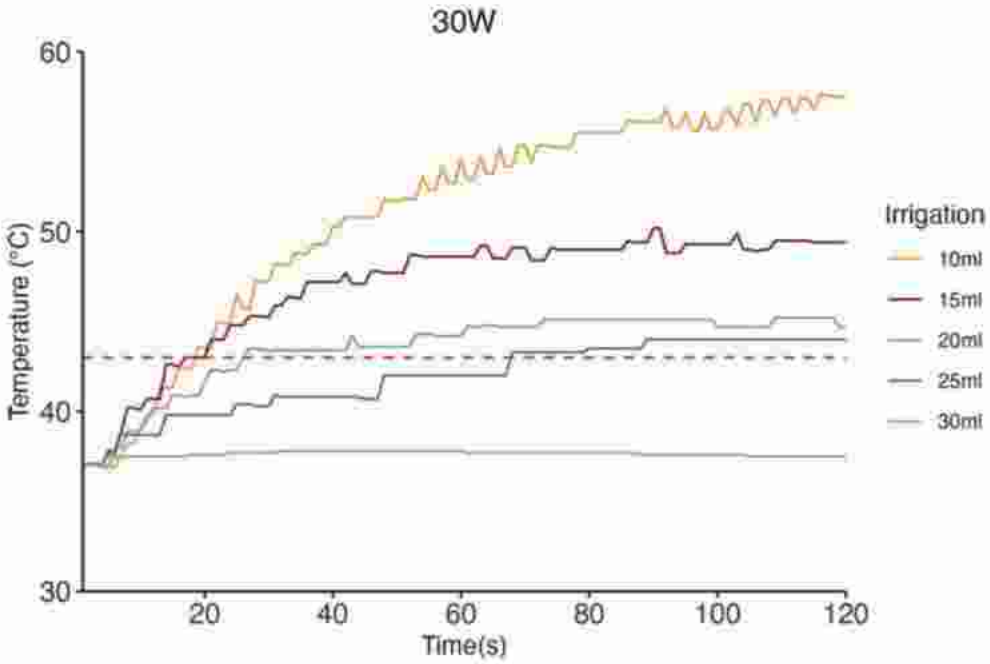


Fig. 5 Renal temperature at each irrigation speed at 30 W of gravel power

Table 1 The intrarenal pressure conditions under various irrigation speeds.（mmH_2O）

Irrigation speed	upper calyx	lower calyx	renal pelvis	F	*p*
10 ml/min	4.2 ± 0.07	3.85 ± 0.23	4.83 ± 0.09	33.46	<0.01
15 ml/min	4.6 ± 0.19	4.88 ± 0.08	5.48 ± 0.15	28.27	<0.01
20 ml/min	5.96 ± 0.04	6.08 ± 0.15	6.35 ± 0.12	10.05	<0.05
25 ml/min	6.18 ± 0.04	6.50 ± 0.28	9.08 ± 0.15	215.68	<0.01
30 mlmin	7.95 ± 0.54	8.65 ± 0.53	11.55 ± 0.15	54.82	<0.01

Table 3 The time required for different proportions of ODC to reach the safety threshold(s)

ODC Time	70%	80%	90%	100%
Time to reach the safety threshold	56.0 ± 1.0	51.8 ± 1.48	32.0 ± 1.58	20.6 ± 1.14

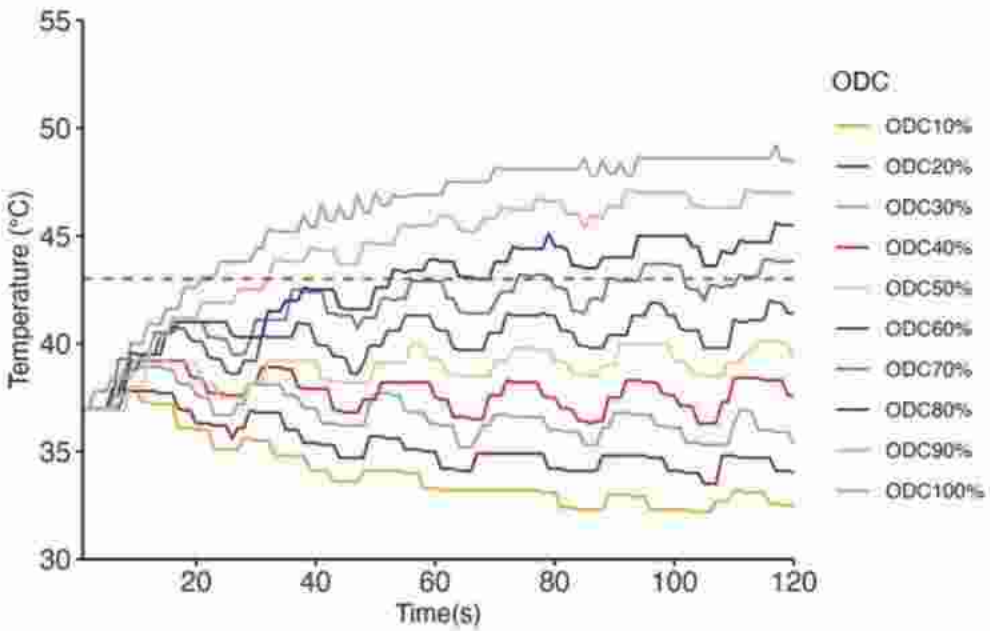


Fig. 6 Curve of renal temperature during the working cycle (ODC) of different proportions (laser power set to 20 W, irrigation speed is 10 ml/min)

Table 2 Different On-Duty Cycles (ODC) result in different intrarenal temperatures. (°C)

ODC	50%	60%	70%	80%	90%
Temperatures	40.0 ± 0.52	41.6 ± 0.38	43.4 ± 0.48	44.8 ± 0.73	46.7 ± 0.54

Discussion

Studies conducted earlier have shown that there is a considerable amount of cell necrosis in the human tissue above 43 °C temvperature and cell death further increases to 45 °C [5]. At a temperature of 60 °C, the proteins present in the tissue are irreversibly denatured; therefore, the structure of the tissue is permanently destroyed and its function is lost. This is why, to some extent, this is also considered as the temperature threshold for human tissue at 43 °C. During retrograde intrarenal surgery, the irrigation rate plays a very important factor in determining the temperature of the tissue [6]. The use of high irrigation rates will help avoid increased temperatures inside the kidney. A irrigation rate of 100 ml/min will maintain the temperature so that, even if the laser works continuously for one minute, the temperature does not exceed 38.5 °C [7]. But if the irrigation rate is too high, the intra-renal pressure will be increased, leading to postoperative pain and the patient being more prone to infection [8–10]. On the contrary, an inadequate irrigation rate might end up causing a high intraoperative temperature, leading to thermal injury in the tissues and affecting the visual field with an inability to wash away the stone powder in time, thus causing further damage to the tissues. And therefore, it is very important to measure the irrigation rate reasonably so that a surgical intervention in the patient can be safely made. In this experiment, we made a detailed observation and analysis of the temperature control used in laser lithotripsy. 10 W lithotripsy power and 10 ml/min irrigation rate kept the temperature of the kidney steady at a plateau in the early stage of the experiment, wherein this constant temperature was always below the safety threshold. The power of the laser had been increased to 15 W while proceeding with the experiment, although the irrigation rate remained the same. The temperature plateau reached 44 °C in the kidney, which was beyond the limit for safe human tissue. This damage was then effectively contained by increasing irrigation to a flow of 15 ml/min, such that the temperature was maintained at safe levels to prevent thermal injury. The results of the experiment show that with an increase in power, the temperature in the kidney grows appropriately to this change; conversely, an increase in the irrigation rate results in a decrease of the temperature in the kidney. Our observations correspond to the findings of Winship et al. [11], who conducted their experiments using 3.6 W, 6.4 W, 10 W, 16 W, and 20 W laser power with irrigation pressures of 0, 100, and 200 mmHg. These authors concluded that both the temperature in the kidney and the speed of irrigation determine the conducted temperature: the higher the laser power, the higher the temperature in the kidney; the faster the irrigation rate, the lower the temperature in the kidney [11]. The most striking result from this experiment is that when lithotripsy power and irrigation speed are varied together at a 1:1 ratio, the plateau temperature in the kidney stays below the safety threshold for all conditions. This approach is not only superior to the safety of the procedure but also provides physicians with a new way to adjust operational parameters in maximizing the benefit of lithotripsy while minimizing the possibility of thermal injury to the patient's kidney.

In our work, the 20 W lithotripter power and an irrigation flow rate of 10 mL/min were considered, paying particular attention to ODC values in a large range from 50 to 100%. This phenomenon is just the same as the classical sawtooth fluctuation wave which is corresponding to the laser periodical activation: the temperature in liquid increases rapidly when the laser is activated and decreases slowly to form a plateau when it is deactivated. The ODC ratio of the kidney showed a significantly raised level at the steady-state. This is similar to what was also observed in Louters et al. [12], so that a higher ODC increases temperature and energy release markedly. The steady-state renal temperature shows a trend of leveling off after attaining some value and does not increase further in case the ODC was kept below 60%. On the other hand, steady-state renal temperature increased to an increasing value after an ODC higher than 70%, and this may reflect increasing heat accumulation effect. It was also observed that a marked reduction in ODC, above an ODC of about 70%, considerably prolonged the time for which renal temperature to reach the safety threshold. This is likely due to the concordance with the results of Wanderling et al. [13]. The current theory is supported by the experimental results, which demonstrate that, over the very fine-tuning of the ODC required to minimize continuous activation time of the laser, the laser may be used for a greater length of time without crossing the safety temperature limit. One interesting point must be considered in this trial.

The experiment used a fixed superpulsed thulium fiber laser, one diameter of the fiber, and a ureteral guide sheath with a flexible ureteroscope. The effect of fiber diameter on temperature and size of the soft sheath is an area for future research. In addition, the fact that this was an in vitro experiment does not bring into play the physiological factors in the changes in temperature, like renal irrigation and urine production. More studies are essential to clarify whether experiments on animals present a solution to this problem. In a nut shell, the outcome of the study has indicated that the decrease in ODC ratio from applying retrograde intrarenal surgery can have the effect of substantially reducing the rise in renal temperature. This may provide a new safe and effective method for clinical application in surgery.

Conclusion

Therefore, reducing the ratio of ODC allows substantial relief in renal temperature elevation during super-pulse optical fiber thulium laser lithotripsy. When gravel power and irrigation speed have a 1:1 adjustment ratio, it can effectively keep renal temperature within safe limits, guarding against thermal injury of kidney tissue.

Author contributions Ding tianfu.Xu zheng.and Li jianxing. wrote the main manuscript text. Huang zhongyue. Xiao bo. and Huweiguo prepared all figures and table. All authors reviewed the manuscript.

Funding There was no source of funding for this project.

Data availability No datasets were generated or analysed during the current study.

Declarations

Competing interests The authors declare no competing interests.

Open Access This article is licensed under a Creative Commons Attribution-NonCommercial-NoDerivatives 4.0 International License, which permits any non-commercial use, sharing, distribution and reproduction in any medium or format, as long as you give appropriate credit to the original author(s) and the source, provide a link to the Creative Commons licence, and indicate if you modified the licensed material. You do not have permission under this licence to share adapted material derived from this article or parts of it. The images or other third party material in this article are included in the article's Creative Commons licence, unless indicated otherwise in a credit line to the material. If material is not included in the article's Creative Commons licence and your intended use is not permitted by statutory regulation or exceeds the permitted use, you will need to obtain permission directly from the copyright holder. To view a copy of this licence, visit http://creativecommons.org/licenses/by-nc-nd/4.0/.

References

1. Ventimiglia E, Robesti D, Bevilacqua L, Tondelli E, Oliva I, Orecchia L, Juliebø-Jones P, Pietropaolo A, De Coninck V, Esperto F, Tailly T, Ferretti S, Gauhar V, Somani B, Villa L, Keller EX, Salonia A, Traxer O, Kartalas Goumas I. What to expect from the novel pulsed thulium:YAG laser? A systematic review of endourological applications. World J Urol. 2023 Nov;41(11):3301-3308.
2. Kronenberg P, Traxer O. The laser of the future: reality and expectations about the new thulium fiber laser-a systematic review. Transl Androl Urol. 2019 Sep;8(Suppl 4):S398-S417.
3. Türk C, Petřík A, Sarica K, Seitz C, Skolarikos A, Straub M, Knoll T. EAU Guidelines on Interventional Treatment for Urolithiasis. Eur Urol. 2016 Mar;69(3):475-82.
4. Traxer O, Keller EX. Thulium fiber laser: the new player for kidney stone treatment? A comparison with Holmium:YAG laser. World J Urol. 2020 Aug;38(8):1883-1894.
5. Sapareto SA, Dewey WC. Thermal dose determination in cancer therapy. Int J Radiat Oncol Biol Phys. 1984 Jun;10(6):787-800.
6. Panthier F, Pauchard F, Traxer O. Retrograde intra renal surgery and safety: pressure and temperature. A systematic review. Curr Opin Urol. 2023 Jul 1;33(4):308-317.
7. Aldoukhi AH, Ghani KR, Hall TL, Roberts WW. Thermal Response to High-Power Holmium Laser Lithotripsy. J Endourol. 2017 Dec;31(12):1308-1312.
8. Rashid AO, Fakhulddin SS. Risk factors for fever and sepsis after percutaneous nephrolithotomy. Asian J Urol. 2016 Apr;3(2):82-87.
9. Alsyouf M, Abourbih S, West B, Hodgson H, Baldwin DD. Elevated Renal Pelvic Pressures during Percutaneous Nephrolithotomy Risk Higher Postoperative Pain and Longer Hospital Stay. J Urol. 2018 Jan;199(1):193-199.
10. Tokas T, Herrmann TRW, Skolarikos A, Nagele U; Training and Research in Urological Surgery and Technology (T.R.U.S.T.)-Group. Pressure matters: intrarenal pressures during normal and pathological conditions, and impact of increased values to renal physiology. World J Urol. 2019 Jan;37(1):125-131.
11. Winship B, Wollin D, Carlos E, Peters C, Li J, Terry R, et al. The Rise and Fall of High Temperatures During Ureteroscopic Holmium Laser Lithotripsy. J Endourol. 2019;33(10):794-799.
12. Louters MM, Dau JJ, Hall TL, Ghani KR, Roberts WW. Laser operator duty cycle effect on temperature and thermal dose: in-vitro study. World J Urol. 2022 Jun;40(6):1575-1580.
13. Wanderling C, Saxton A, Phan D, Doersch K, Shepard L, Schuler N, Osinski T, Quarrier S, Ghazi A. WATTS happening? Evaluation of thermal dose during holmium laser lithotripsy in a high-fidelity anatomic model. World J Urol. 2024 Mar 14;42(1):157.

Publisher's note Springer Nature remains neutral with regard to jurisdictional claims in published maps and institutional affiliations.

《世界泌尿外科杂志》（2024）第42卷第588页
https://doi.org/10.1007/s00345-024-05289-3

研究

超脉冲光纤铥激光碎石术中灌注率、操作者工作周期和肾内温度的体外研究

丁天福[1]·郑旭[1]·黄忠跃[1]·肖波[1]·胡伟国[1]·李建星[1]

接收日期：2024年7月11日/接受日期：2024年9月23日/网络发表日期：2024年10月23日
©作者2024

摘要

目的本研究旨在探讨使用超脉冲光纤铥激光进行逆行肾内手术时，灌注速度、操作者工作周期（ODC）与肾内温度之间的关系。

方法将结石置于新鲜分离的猪肾中，用穿刺针将温度探头置于结石周围2毫米处，并将压力探头放置于上盏、下盏及肾盂。将整个装置置于37°C恒温水浴中以模拟人体环境。激光功率在10至30瓦之间变化，灌注速度为10-30 ml/min。此外，在激光功率为20瓦且灌注速度为10 ml/min时，设置不同的工作周期（ODC）。监测温度和压力的变化。

结果在10 W至30 W激光功率范围内，肾脏温度与灌注速率呈正比关系。激光功率与灌注速率的百分比比率为1：1，可将肾脏温度维持在安全水平。当激光功率为20 W且灌注速率为10 ml/min时，肾脏内部温度会随着ODC值的增加而急剧上升。通过降低ODC值的比率，可显著减少肾脏内部温度的升高。

结论保持激光功率与冲洗速度1：1的比率可有效防止肾脏组织的热损伤或损伤。此外，通过调整工作循环（ODC）比率，也可降低肾内温度。

关键词超脉冲光纤铥激光器·操作员工作周期（ODC）·灌注率·肾内温度

介绍

医疗技术的持续发展推动了激光碎石术的不断进步，这项技术现已发展成熟。采用1940纳米波长的超脉冲光纤铥激光器，已成为碎石治疗的重要候选方案。由于该波长与水分子吸收峰高度重合，其在水溶液中的吸收系数显著高于传统2100纳米钬激光。这种特性使得该波长在临床应用中展现出独特优势。

钬激光碎石技术在碎石效率方面具有显著优势[1，2]。目前，由于其广泛的应用场景和良好的治疗效果，钬激光碎石已成为（柔性）上尿路系统结石的首选方案[3]。更重要的是，超脉冲光纤铥激光器不仅展现出优于钬激光的碎石效率，更在尿路结石治疗领域实现了重大突破——该技术具有更低的结石反弹力和更细的光纤直径[4]。这些特性表明，超脉冲光纤铥激光器在尿路结石治疗领域具有广阔的应用前景。在碎石技术的发展过程中，激光碎石的安全性始终与结石粉碎效果同等重要。本研究旨在优化激光碎石过程中的温度控制和冲洗液流速，以实现安全有效的治疗效果。

✉ 李建兴
lijianxing2015@163.com

1 中国北京清华大学医学院附属北京清华长庚医院泌尿外科，泌尿疾病研究中心，邮编：102218

材料和方法

体外建模

本研究采用新鲜离体猪肾样本，所有实验均在严格遵循伦理规范的条件下获取，所有实验猪均经过人道安乐死处理。研究获得伦理审查委员会批准，并取得伦理批件号[IACUC-202306-P-001]。结石样本取自本机构结石标本库，经成分分析确认为草酸钙单水合物结石（CT值：890±123 HU）。实验设备包括：外径F8.6的一次性电子输尿管镜（安徽幸福工厂医疗器械有限公司）、输尿管套管（F11/13莱凯医疗器械（北京）有限公司）、配备200μm光纤的钬光纤超脉冲激光器（A-ONE莱凯医疗器械（北京）有限公司）。（有限公司）配备多通道实时温度计（NF4000P-8广州瑞曼婷仪器厂）、精密恒流实验泵（BT-1河北荣柏电器厂）、高精度数字压力表（DT-1上海瑞祥仪器厂）、温控水浴、生理盐水等核心手术器械。

该手术流程包括将结石精准置入肾盂，通过穿刺针插入温度探头，使其距离肾盂内的结石约2毫米。随后小心插入输尿管套管，并用结扎线固定于输尿管。使用同一根穿刺针将压力传感器分别置入上盏、下盏及肾盂。整个装置被置于恒温水浴中，温度维持在37°C以模拟人体环境温度。

实验步骤

实验室温度设定为25℃。激光碎石功率设置为10W（1.0焦耳×10赫兹，0.1焦耳×100赫兹）、15W（1.5焦耳×10赫兹，0.15焦耳×100赫兹）、20W（2.0焦耳×10赫兹，0.1焦耳×200赫兹）和25W（2.5焦耳×10赫兹，0.1焦耳×250赫兹）。

30 W（1.0 J×10 Hz，0.1 J×300 Hz）。灌注速度设置为10、15、20、25和30 ml/min（灌注液为生理盐水，温度为25°C）。连续激光激发时间为120秒。

对于20瓦（2.0焦耳×10赫兹）的激光碎石功率和10毫升/分钟的灌注速度（灌注液为生理盐水，温度为25°C），每个20秒构成一个操作周期。激光器采用ODC模式运行，通过设置10种不同ODC模式来模拟多种手术策略：ODC10%：激光激活2秒后关闭18秒。ODC20%：激活4秒后关闭16秒。ODC30%：激活6秒后关闭14秒。ODC40%：激活8秒后关闭12秒。ODC50%：激活10秒后关闭10秒。ODC60%：激活12秒后关闭8秒。ODC70%：激活14秒后关闭6秒。ODC80%：激活16秒后关闭4秒。ODC90%：激活18秒后关闭2秒。ODC100%：激光持续激活20秒，不设关闭周期。每个周期重复6次，形成大规模实验组。

温度探头和压力探头均以每秒一次的频率实时监测参数并记录变化。每组参数的上述实验重复5次，且每次重复均使用新肾脏。

数据收集和分析

实验至少重复五次，数据以平均值给出。使用R版本4.3.3中的ggplot2绘制数据图。数值以均值±标准差表示。采用配对t检验进行两组间比较，采用非参数秩和检验进行多组间比较。显著性差异设定为$p<0.05$。

结果

连续激光碎石术中肾内温度的变化

在10 W的碎石功率下，当冲洗速度分别为10 ml/min、15 ml/min、20 ml/min、25 ml/min和30 ml/min时，肾内温度达到稳态，稳态温度分别为38.6°C、35°C、33.1°C、31.7°C和30.7°C，均未超过安全阈值（图1）。在15 W的碎石功率下，当冲洗速度为10 ml/min时，肾内温度继续上升。然而，当冲洗速度为15 ml/min、20 ml/min、25 ml/min和30 ml/min时，肾内温度达到稳态，稳态温度分别为38.4°C、35.9°C、34.7°C和34.4°C，均未超过安全阈值（图2）。在20 W的碎石功率下，当冲洗速度为10 ml/min和15 ml/min时，肾内温度继续上升。然而，当冲洗速度为20 ml/min、25 ml/min和30 ml/min时，肾内温度

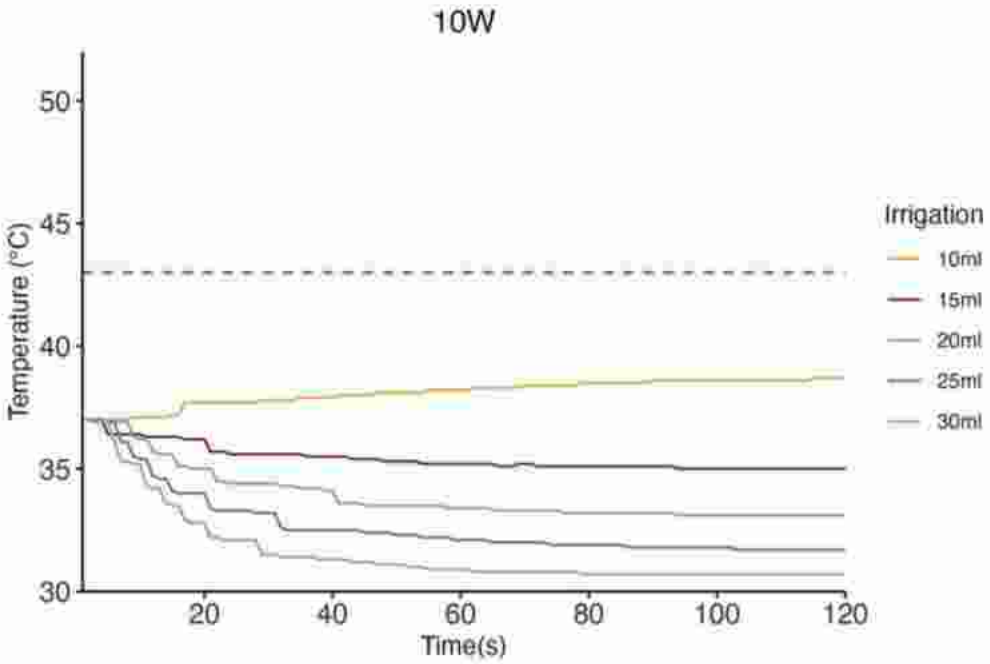


图1 10W碎石功率下各灌注速度的肾脏温度

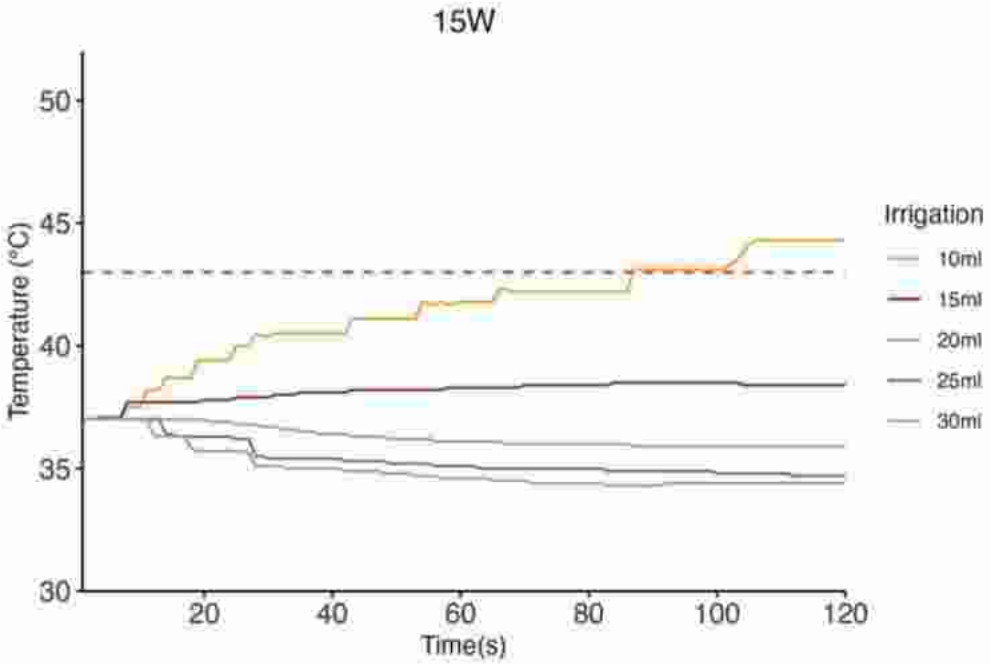


图2 15W碎石功率下各灌注速度的肾脏温度

达到稳态，稳态温度分别为38.7°C、36.3°C和34.2°C，均未超过安全阈值（图3）。在碎石功率为25W时，随着灌注速度为10ml/min、15ml/min和20ml/min，肾内温度持续上升。然而，在灌注速度为25ml/min和30ml/min时，肾内温度分别达到稳态，稳态温度为38.3°C和35.7°C，均未超过安全阈值（图4）。在碎石功率为30W时，随着灌注速度为10ml/min，肾内温度继续上升。min，15 ml/min，20 ml/min，和25 ml/min。然而，在30 ml/min的灌注速度下，肾内温度达到稳态，稳态温度为37.5°C，未超过安全阈值（图5）。在不同灌注速度下，肾内盆腔/盏压未超过30mmH $_2$O（表1）。

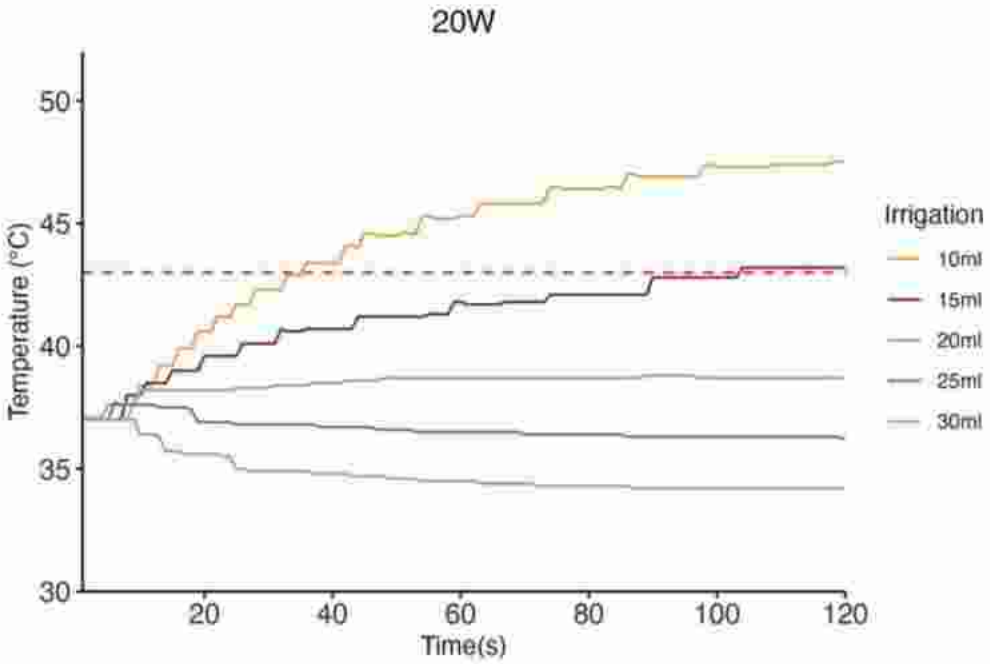


图3 20W碲石功率下各灌注速度的肾脏温度

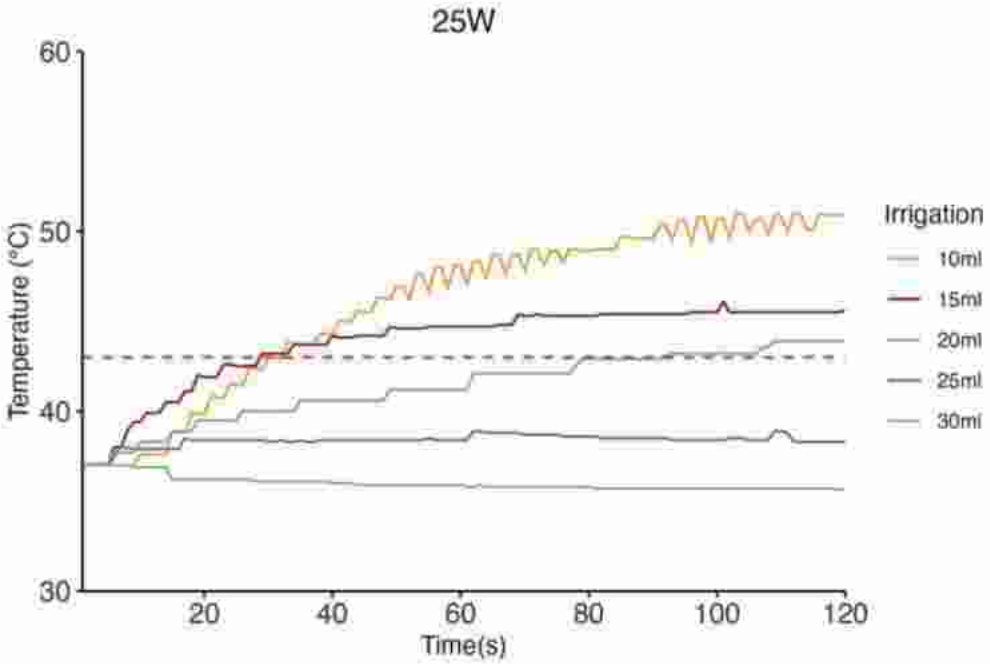


图4 25W碲石功率下各灌注速度的肾脏温度

不同ODC比值下的肾内温度变化

当工作循环率（ODC）维持在60%以下时，肾内稳态温度在达到某个临界值后趋于稳定，不会随时间推移继续升高。反之，当ODC超过70%时，后续稳态阶段的肾内温度会持续上升（图6）。随着ODC值的增加，最高肾内温度呈现显著上升趋势：ODC50%时为40.0±0.52°C；ODC 60%：41.6±0.38°C；ODC 70%：43.4±0.48°C；ODC 80%：44.8±0.73°C；ODC 90%：46.7±0.54°C（表2）。当ODC比率为70%、80%、90%和100%时，肾内温度达到安全阈值温度的时间分别为56.0±1.0s、51.8±1.48 s、32.0±1.58s和20.6±1.14s（表3）。

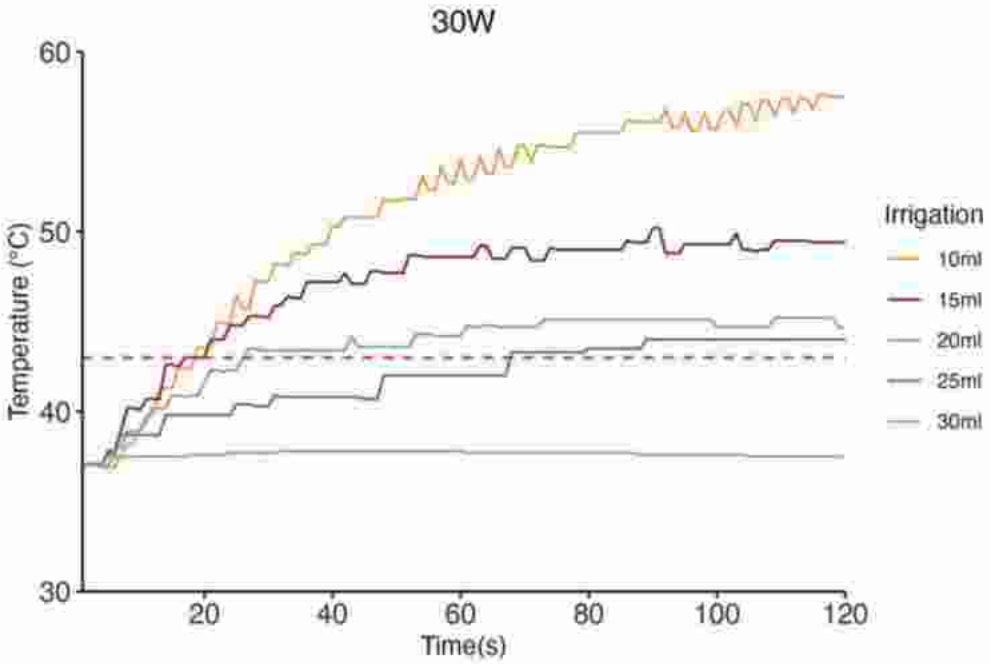


图5 30W碎石功率下各灌注速度的肾脏温度

表1不同冲洗速度下的肾内压力条件（mmH_2O）

灌注速度	较高的花萼	向下花萼	肾盂	F	*p*
10 ml/min	4.2±0.07	3.85±0.23	4.83±0.09	33.46	<0.01
15 ml/min	4.6±0.19	4.88±0.08	5.48±0.15	28.27	<0.01
20 ml/min	5.96±0.04	6.08±0.15	6.35±0.12	10.05	<0.05
25 ml/min	6.18±0.04	6.50±0.28	9.08±0.15	215.68	<0.01
30 mlmin	7.95±0.54	8.65±0.53	11.55±0.15	54.82	<0.01

表3不同比例ODC达到安全阈值所需时间（秒）

时间	70%	80%	90%	100%
到达安全区的时间	56.0±1.0	51.8±1.48	32.0±1.58	20.6±1.14

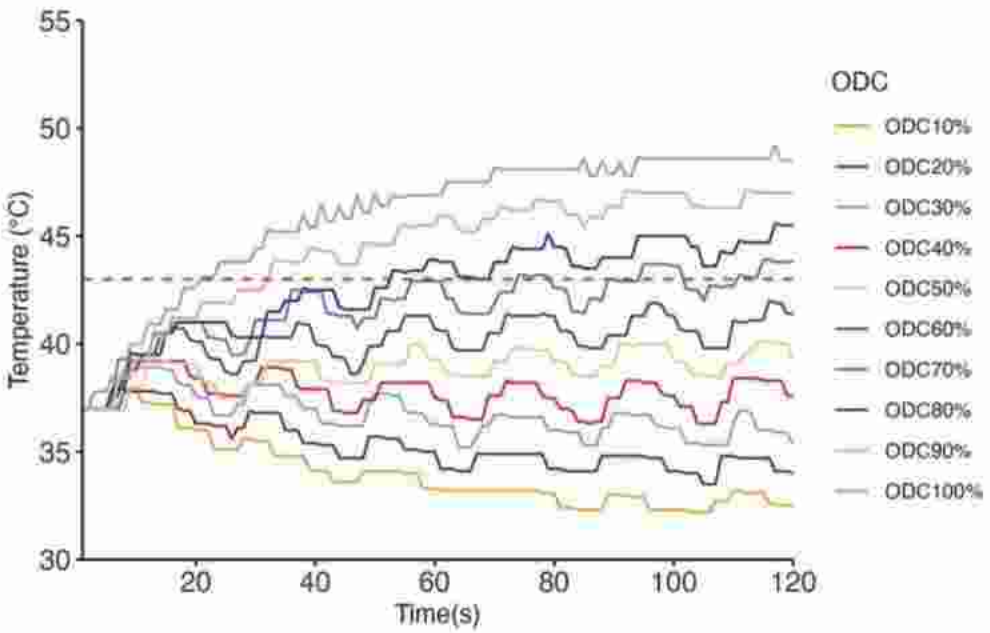


图6 不同比例工作周期（ODC）下肾脏温度曲线（激光功率设定为20 W，冲洗速度为10 ml/min）

表2不同工作循环（ODC）会导致肾内温度不同（℃）

	50%	60%	70%	80%	90%
温度	40.0±0.52	41.6±0.38	43.4±0.48	44.8±0.73	46.7±0.54

讨论

早期研究显示，人体组织中存在大量细胞坏死现象。43 温度降至0°C时，细胞死亡率进一步上升至45°C[5]当温度达到60°C时，组织中的蛋白质会发生不可逆的变性，导致组织结构永久破坏，功能丧失。因此，43°C也被视为人体组织的温度临界值。在逆行肾内手术中，灌注速率是决定组织温度的关键因素。[6]采用较高的冲洗速率有助于避免肾脏内部温度升高。当冲洗速率达到100毫升/分钟时，即使激光连续工作一分钟，温度也不会超过38.5°C[7]。但若冲洗速率过高，肾内压力会增加，可能导致术后疼痛并提高感染风险[8-10]。反之，冲洗速率不足则可能引发术中体温升高，导致组织热损伤，同时因无法及时冲洗出碎石粉而影响视野，进而造成组织进一步损伤。因此，合理控制冲洗速率对确保手术安全至关重要。在本实验中，我们对激光碎石术中的温度调控进行了详细观察与分析。10瓦碎石功率和10 ml/min的灌注速率使肾脏温度在实验初期保持稳定，该恒定温度始终低于安全阈值。实验进行时，激光功率已提升至15瓦，但灌注速率保持不变。肾脏温度平台达到44°C，这超出了人体组织的安全限度。随后通过将灌注速率增加至15 ml/min，有效控制了损伤，使温度维持在安全水平以防止热损伤。实验结果表明，随着功率增加，肾脏温度会相应升高；反之，灌注速率增加会导致肾脏温度下降。我们的观察结果与Winship等人的研究发现一致。[11]该研究团队采用3.6W、6.4W、10W、16W和20W三种不同功率的激光器，配合0mmHg、100mmHg和200mmHg三种灌注压力开展实验。研究发现，肾脏温度与灌注流速共同决定传导温度：激光功率越高，肾脏温度就越高；灌注流速越快，肾脏温度就越低[11]。这项实验最引人注目的发现是研究表明，当碎石术的功率与冲洗速度按1：1比例同步调节时，肾脏的平台温度始终低于安全阈值。这种操作方式不仅显著提升了手术安全性，更为临床医生提供了创新参数调控方案——在确保碎石术疗效最大化的同时，有效降低肾脏热损伤风险。

在我们的研究中，考虑了20瓦的碎石机功率和10毫升/分钟的灌注流速，特别关注了50%至100%范围内ODC值的变化。这一现象与经典的锯齿状波动波完全一致，对应于激光周期性激活：当激光激活时，液体温度迅速上升，停用时则缓慢下降形成平台期。肾脏的ODC比在稳态下显著升高，这与Louters等人[的观察结果相似。12]因此，当ODC值升高时，温度和能量释放会显著增加。稳态肾温在达到某个数值后趋于稳定，若将ODC值维持在60%以下则不会继续上升。另一方面，当ODC值超过70%后，稳态肾温会持续升高，这可能反映了热蓄积效应的增强。研究还发现，当ODC值超过约70%时，显著降低ODC值会大幅延长肾温达到安全阈值所需的时间。这可能与Wanderling等人的研究结果相吻合。[13]现有理论得到实验结果的支持，这些结果表明，在对激光器连续激活时间进行最小化所需的ODC微调过程中，激光器可在不突破安全温度阈值的情况下持续工作更长时间。值得注意的是，本研究中存在一个关键点需要特别关注。

本实验采用固定超脉冲钬光纤激光器、光纤直径为1毫米的导管，以及配备柔性输尿管镜的输尿管导引鞘。光纤直径对软鞘温度及尺寸的影响仍是未来研究方向。此外，由于该实验为体外操作，无法体现肾灌注、尿液生成等生理因素对温度变化的影响。需要更多研究来验证动物实验能否解决这一问题。简而言之，研究结果表明，通过逆行肾内手术降低ODC比值可显著抑制肾温升，这为临床手术提供了安全有效的解决方案。

结论

因此，降低ODC比值能显著缓解超脉冲光纤钬激光碎石术中的肾温升高。当碎石功率与冲洗速度保持1：1比例时，可有效将肾温控制在安全范围内，避免肾组织热损伤。

作者贡献丁天福、徐正、李建兴负责撰写论文主体内容；黄忠培、肖波、胡伟国负责制作全部图表；所有作者均参与论文审阅。

资金本项目无资金来源。

数据可用性：本研究期间未生成或分析任何数据集。

声明

竞争利益作者声明无竞争利益。

开放获取本文采用知识共享署名-非商业性使用-禁止演绎4.0国际许可协议授权，允许在任何媒介或格式下进行非商业性使用、分享、传播和复制，但需满足以下条件：正确标注原作者及来源信息、提供知识共享许可协议链接、注明是否修改过授权内容。根据该协议，您无权分享基于本文或其部分内容改编的衍生作品。文中图片或其他第三方素材均包含在知识共享许可协议中，除非在素材标注中另有说明。若素材未包含在知识共享许可协议中，且您的使用目的违反法律法规或超出许可范围，则需直接向版权方申请授权。如需查看本许可协议副本，请访问http://creativecommons.org/licenses/by-nc-nd/4.0/。

参考文献

1. 文蒂米利亚E，罗贝斯蒂D，贝维拉夸L，通德利E，奥利瓦I，奥雷基亚L，Juliebø-Jones P，皮埃勒罗保罗A，德科宁克V，埃斯佩尔托F，Tailly T，Ferretti S，Gauhar V，Somani B，Villa L，Keller EX，SaloniaA，Traxer O，Kartalas Goumas I.新型脉冲钬：YAG激光器有哪些应用前景？内镜泌尿外科应用的系统综述。《世界泌尿外科杂志》2023年11月；41（11）：3301-3308。
2. 克罗威伯格P，特拉克塞O.未来激光：新型钬光纤激光器的现实与展望——系统综述.Transl Androl Urol.2019年9月；8（Suppl 4）：S398-S417.
3. Turk C，Petrik A，Sarica K，Seitz C，Skolarikos A，Straub M，Knoll T.膀胱结石介入治疗指南.欧洲泌尿外科杂志.2016年3月；69(3)：475-82.
4. Traxer O，Keller EX.脉光纤激光：治疗肾结石的新选择？与钬：钇铝石榴石激光的对比。《世界泌尿学杂志》2020年8月；38(8)：1883-1894.
5. 萨帕雷托SA，杜威WC.癌症治疗中的热剂量测定.国际放射肿瘤学，生物学与物理学杂志.1984年6月；10(6)：787-800.
6. 潘蒂塔F，施沙尔F，特拉克塞尔O.肾内逆行手术与安全性：压力与温度。系统综述。Curr Opin Urol.2023年7月1日；33(4)：308-317.
7. 阿尔杜基AH，加尼KR，霍尔TL，罗伯茨WW.高功率钬激光碎石术的热反应。《泌尿外科学杂志》。2017年12月；31（12）：1308-1312。
8. 拉希德AO，汪赫鲁丁SS.经皮肾镜碎石术后发热与败血症的危险因素。《亚洲泌尿外科杂志》2016年4月第3卷第2期：82-87页。
9. Asyouf M，Abourbih S，West B，Hodgson H，Baldwin DD.经皮肾镜取石术期间肾盂压力升高会增加术后疼痛风险并延长住院时间。《泌尿学杂志》2018年1月；199(1)：193-199。
10. 托卡斯T，赫尔曼TRW，斯科拉里科斯A，纳格尔U：泌尿外科与技术培训与研究（T.R.U.S.T.）小组。压力至关重要：正常与病理状态下肾内压力及其数值升高对肾生理的影响。《世界泌尿学杂志》2019年1月；37(1)：125-131。
11. Winship B, Wollin D, Carlos E, Peters C, Li J, Terry R, 等学者在《泌尿外科学杂志》2019年第33卷第10期794-799页发表《输尿管镜钬激光碎石术中高温的兴起与消亡》一文。
12. Louters MM，Dau JJ，Hall TL，Ghani KR，Roberts WW.激光操作员工作周期对温度和热剂量的影响：体外研究。世界泌尿学杂志。2022年6月；40(6)：1575-1580。
13. Wanderling C，Saxton A，Pham D，Doerrich K，Shepard L，Schuler N，Osinski T，Quarrier S，Ghazi A.激光碎石术中热剂量评估：基于高精度解剖模型的热效应研究。《世界泌尿学杂志》2024年3月14日第42卷第1期第157页。

出版商注Springer Nature对已发表地图和机构隶属关系的管辖权主张保持中立。

Review Article

Investig Clin Urol 2025;66:1-10.
https://doi.org/10.4111/icu.20240369
pISSN 2466-0493 • eISSN 2466-054X

INVESTIGATIVE AND CLINICAL UROLOGY
ICUROLOGY

Rise in intraluminal temperature during ureteroscopy: Is this a concern?

Hyung Joon Kim[1], **Sung Kyu Hong**[1,2]

[1]Department of Urology, Seoul National University Bundang Hospital, Seongnam, [2]Department of Urology, Seoul National University College of Medicine, Seoul, Korea

The global increase in urolithiasis prevalence has led to a shift towards minimally invasive procedures, such as retrograde intrarenal surgery, supported by advancements in laser technologies for lithotripsy. Pulsed lasers, particularly the holmium YAG and the newer thulium fiber laser, have significantly transformed the management of upper urinary tract stones. However, the use of high-power lasers in these procedures introduces risks of heat-related injury. Laser lithotripsy works through photothermal and photomechanical effects to fragment stones, but up to 96% of the laser energy is converted into heat, increasing the risk of thermal damage to the surrounding urothelial mucosa. Studies show that even at low-power settings, intrarenal temperatures can exceed the threshold for cellular injury, particularly in confined spaces like the ureter. This narrative review explores strategies to mitigate thermal injury, including optimizing laser settings, improving irrigation flow rates, and incorporating novel methods such as cold irrigation, controlling outflow resistance, and using suction. Understanding these approaches is crucial to enhancing patient safety during high-power laser lithotripsy procedures.

Keywords: Lasers; Peroperative complications; Temperature; Ureteroscopy; Urolithiasis

This is an Open Access article distributed under the terms of the Creative Commons Attribution Non-Commercial License (http://creativecommons.org/licenses/by-nc/4.0) which permits unrestricted non-commercial use, distribution, and reproduction in any medium, provided the original work is properly cited.

INTRODUCTION

The prevalence of urolithiasis varies significantly across global populations and has seen a notable increase in recent decades [1]. Advances in technology have shifted surgical options toward minimally invasive endoscopic procedures, such as ureteroscopy and miniaturized percutaneous nephrolithotomy. The growing use of retrograde intrarenal surgery (RIRS), which utilizes flexible ureterorenoscopes, combined with innovations in laser technologies, has revolutionized the management of upper urinary tract stone disease [2,3].

Pulsed lasers are the primary and exclusive energy source used in flexible ureteroscopy across different energy sources for lithotripsy. The holmium YAG (HoYAG) laser has been the standard method for many years, evolving with high-power specs and modifiable pulse width. Thulium fiber laser (TFL) has recently emerged as a promising novel armamentarium for laser lithotripsy. TFL has a wide range of energy (0.025–6 J) and frequency (5–2,400 Hz), enabling less retropulsion and finer dusting [4,5]. A recent revisit of pulsed thulium YAG (Tm:YAG) gained attention for its specific characteristics as an alternative laser for lithotripsy, which awaits the accumulation of evidence [6].

Modern high-power lasers, with their higher frequency capabilities, have enabled faster surgeries. However, the use of high-power lasers in RIRS introduces heat-related challenges [7,8]. Lasers break down stones through two primary effects: photothermal and photomechanical. The photother-

Received: October 20, 2024 • **Revised:** December 12, 2024 • **Accepted:** December 16, 2024 • **Published online:** December 31, 2024
Corresponding Author: Sung Kyu Hong https://orcid.org/0000-0002-8344-6774
Department of Urology, Seoul National University Bundang Hospital, 82 Gumi-ro 173beon-gil, Bundang-gu, Seongnam 13620, Korea
TEL: +82-31-787-7343, E-mail: skhong@snubh.org

© The Korean Urological Association

mal effect, driven by electromagnetic radiation, heats the stone components, causing chemical decomposition through laser activation, boiling, or vaporizing surrounding water. The photomechanical effect occurs when water inside the stone's pores vaporizes, causing the stone to burst from within. When the pulse duration exceeds 10 μs, the photothermal effect dominates, while pulse durations beyond 200 μs render the photomechanical impact negligible [9]. During laser lithotripsy, the fluid surrounding the stones in the collecting system may experience a significant temperature rise, potentially leading to thermal injuries to the surrounding urothelial mucosa, as demonstrated in an *in vivo* porcine study [10].

METHODS

A literature search was conducted using the PubMed database from its inception to May 2024. The keywords used included "ureteroscopy," "heat," and "temperature." Boolean operators (AND, OR) were applied to refine the search results. The search included *in vitro*, human, and animal studies. Both original research and review articles were considered, along with additional articles identified through the references of selected works.

WHY DOES HEAT MATTER?

Concerns regarding potential indirect injuries to the urothelial mucosa during laser lithotripsy have grown as more stones are treated using high-power lasers (100–120 W), which may increase the risk of ureteral strictures or reduced renal function. While high-power laser systems enable higher frequencies, enhancing surgical efficiency, the energy levels have not changed significantly. However, not all pulses these systems generate are directed toward stone ablation. The primary advantage of high-power lasers lies in the dusting or pop-dusting techniques, which utilize higher frequencies. These strategies are increasingly favored over traditional stone fragmentation. Yet, as dusting becomes more prevalent, the predominant photothermal effect poses potential risks. Only 17% of laser pulses effectively strike the stone during high-power pop-dusting [11]. This not only reduces ablation efficiency but also raises the temperature inside the collecting system.

During laser lithotripsy, 91% to 96% of the laser energy is converted into heat, even during efficient stone ablation [10], which can potentially lead to tissue necrosis, as demonstrated in a pilot *in vivo* porcine study [12,13]. Both the peak temperature and the duration of exposure contribute to thermal cytotoxicity [14]. The potential for thermal cell injury can be estimated using the cumulative equivalent minutes at 43°C (CEM43°C) model, introduced by Sapareto and Dewey [15]. Thermal dose quantifies the biological risk of thermal injury from any time-temperature curve, with the threshold for injury and cell death set at 120 equivalent minutes. This corresponds to maintaining a temperature of 43°C for 120 minutes or shorter exposure times at higher temperatures: 44°C for 60 minutes, 45°C for 30 minutes, and 50°C for less than a minute. At 56°C, even one second of exposure can result in thermal injury. Animal studies have shown minor thermal damage at CEM43°C <20 minutes and significant damage at CEM43°C >70 minutes [16].

Studies have indicated that the threshold for cellular thermal damage is reached even at low-power settings (<30 W) [17]. A clinical study adjusting laser settings across different power levels (10–50 W) during ureteroscopy showed that intraluminal temperatures often exceeded 56°C, where thermal injury can occur within seconds at power levels above 15–20 W and, in all cases, above 25 W. Even at 10 W, temperatures of 43°C were reached at specific points [18]. Therefore, it is crucial to identify appropriate laser settings and develop strategies to minimize temperature-related complications.

WHAT FACTORS AFFECT TEMPERATURE DURING URETEROSCOPY

The thermal risk during laser lithotripsy is primarily influenced by two key factors: the amount of energy delivered and the heat capacity of the system. While laser power is the main determinant of energy delivery, the duration of laser activation and the operator duty cycle (ODC) also play critical roles. Heat capacity, on the other hand, is determined by the amount of heat the irrigation fluid can absorb. This is influenced by the volume of fluid present during laser activation—whether in the renal pelvis, calyx, or ureter—as well as the temperature and flow rate of the irrigation fluid. Additionally, the type of laser pulse used may contribute to temperature elevation.

1. Total power applied

Higher power settings result in more significant energy deposition, which increases the risk of thermal tissue injury. *In vitro* studies using different laser settings at a fixed flow rate show that the temperature rises proportionally to total power regardless of how pulse energy and frequency are combined [4,19-21]. Aldoukhi et al. [10] evaluated caliceal fluid temperature during high-power laser lithotripsy in an

https://doi.org/10.4111/icu.20240369

in vivo porcine model. At 40 W (0.5 J×80 Hz) for 60 seconds without irrigation, temperatures reached 60°C within 10 seconds of laser activation. The peak temperature was 84.8°C, and the mean time to reach the threshold for thermal injury (CEM43°C of 120 minutes) was 12.7 seconds [10]. In the same study, increasing irrigation rates to 15 mL/min and 40 mL/min reduced peak fluid temperatures to 58.5°C and 37.5°C, respectively. Teng et al. [22] investigated changes in calyceal irrigation fluid temperatures during HoYAG laser lithotripsy in a human trial. At 1 J×20 Hz without irrigation, the time required to reach 43°C was significantly shorter than at 0.5 J×20 Hz (8.84 seconds vs. 13.71 seconds) [22]. Both studies underscore the importance of adequate irrigation flow to mitigate temperature rises. Belle et al. [23], using a TFL in an *in vitro* silicone kidney-ureter model, demonstrated that high-power lasers are associated with an increased risk of thermal damage. They advocate for conservative laser settings during ureteroscopy laser lithotripsy to minimize this risk [23]. To avoid cellular thermal damage, temperature increases are proportional to power, with recommended limits of 20–30 W for the kidney and 10–15 W for the ureter [4,21,24].

2. Lasing time and pattern

The concept of "ODC" refers to the percentage of time the laser pedal is activated during a procedure. In an *in vitro* caliceal model, Aldoukhi et al. [25] measured thermal doses by applying 1,200 J of energy with different patterns of 50% ODC over 60 seconds. When 40 W was applied at 50% ODC with activation patterns of 30 seconds on/off and 15 seconds on/off, the thermal injury threshold was reached in 9 seconds. For a 10-second on/off pattern, the threshold was reached in 45 seconds, while shorter activation times did not reach the injury threshold. This suggests that, for equivalent energy delivery, more extended pedal activation patterns result in higher thermal doses [25]. Louters et al. [26] studied temperature changes related to escalating ODC by delivering 1,800 J of HoYAG laser energy at 30 W (0.5 J×60 Hz) to a fluid-filled glass bulb. Their findings showed higher ODCs increased maximum temperatures and thermal doses, with ODCs of 70% or more exceeding the thermal injury threshold. Comparatively, a 50% ODC required ten times longer to reach the thermal injury threshold and allowed for an eightfold increase in the maximal allowable energy compared to a 60% ODC [26]. However, caution is warranted when interpreting these results, as *in vivo* or *in vitro* studies may not fully reflect real clinical scenarios. For example, in actual practice, lasers are rarely activated continuously for 60 seconds. To better understand ODC in clinical settings, laser logs were analyzed from ureteroscopy cases, and it found that the mean ODC was 32%, meaning that during 1 minute of lasering, the laser was activated for approximately 20 seconds. During the minute of greatest energy delivery, the mean ODC reached 63% [25]. Awareness of these concepts is essential to reduce the risk of thermal injury during laser lithotripsy procedures. Effectively managing the ODC is one key strategy to control thermal dose and enhance patient safety.

3. Volume of fluid (renal pelvis/calyx/ureter)

Æsøy et al. [17] conducted a clinical trial involving ten patients to assess renal pelvis temperatures during sheathless RIRS. They observed that temperatures reached 43°C in three patients using 20 W and eight patients using 30 W. Their findings revealed an inverse correlation between intrarenal temperature and the anteroposterior diameter of the renal pelvis, underscoring the significance of fluid volume during laser activation [17]. Rezakahn Khajeh et al. [27] investigated fluid temperature elevation and thermal dose resulting from laser activation in fluid-filled glass bulbs simulating different calyx and renal pelvis volumes. At 40 W (0.5 J×80 Hz, short pulse [SP]), both temperature elevation and thermal dose were inversely related to the fluid volume and irrigation rate. In the smallest model (0.5 mL) without irrigation, the thermal injury threshold was reached in just 3 seconds, whereas in the largest model (60.8 mL), this threshold was not reached, regardless of irrigation. This suggests that the ureter, with its smaller fluid volume compared to the renal pelvis, is more prone to thermal injury.

Furthermore, the ureter is particularly vulnerable due to its lack of surrounding vasculature, which could otherwise provide a heat sink. Its narrow lumen also impedes irrigation flow, increasing the risk of circumferential injury and stricture formation [28]. Wang et al. [18] examined the thermal effects of laser lithotripsy within the ureter, increasing power from 10 to 50 W using a rigid ureteroscope with a 550 μm fiber. Across 30 datasets, the highest recorded temperatures exceeded 43°C in 100% of cases, with 63.3% of datasets showing peak temperatures above 56°C. As the power increased, the recorded temperatures generally rose in tandem [18]. For ureteral stones, a recommended approach involves (1) ensuring moderate irrigation, (2) limiting laser activation to 3- to 4-second bursts followed by 3- to 4-second pauses to allow temperature normalization, and (3) considering the use of lower power settings during prolonged procedures.

The risk of thermal injury is notably higher in cases of impacted ureteral stones, where irrigation flow is obstructed. In a 20 W dataset comparing seven cases of impacted stones

to four cases of non-impacted calculi, the mean intraoperative temperature of the irrigation fluid in the impacted stone group was significantly higher than in the non-impacted group (38.56℃±8.51℃ vs. 34.92℃±5.35℃, p<0.001). Given the ease of access to the renal pelvis with a flexible ureterorenoscope, a potential strategy is to reposition the stone from the proximal ureter into a broader, less thermally sensitive area, such as the calyx or renal pelvis [29,30].

4. Irrigation flow rate

Increasing the rate of continuous irrigation flow during laser lithotripsy is critical for reducing intrarenal temperature [1,31]. Thermography-based evaluations suggest that temperatures around the mucosa near stones can increase rapidly during laser lithotripsy, especially when irrigation is inadequate [32]. In an *in vitro* study, Villena et al. [33] demonstrated that each 20 mL/min increase in irrigation flow resulted in a significant reduction in intrarenal temperature by 4.7℃–9.2℃ (p<0.001) and a corresponding decrease in ureteral temperature by 2.6℃–8.8℃ (p=0.01). Experimental models further suggest that higher flow rates (50–100 mL/min) are necessary to maintain safe intrarenal temperature when using laser power settings of 20 W or higher. It is crucial to avoid laser activation without irrigation, as this can lead to temperatures exceeding 100℃, posing a serious risk of thermal injury [34]. Hein et al. [35] evaluated the thermal impact of laser power settings ranging from 5 to 100 W, in combination with various irrigation rates (0–100 mL/min at 37℃). Their findings indicate that even a low power setting of 5 W during RIRS can cause a harmful temperature increase if insufficient irrigation is applied. Based on their results, they developed a formula for estimating the temperature rise (ΔT) when using irrigation rates of ≥30 mL/min: ΔT=15 K×(power [W]/irrigation [mL/min]) [35].

In a human study, intrarenal temperature remained below 43℃ during 60 seconds of laser activation at both 1 J×20 Hz and 0.5 J×20 Hz, with irrigation flow rates of 15 mL/min or 30 mL/min. At an irrigation rate of 60 mL/min, the renal calyceal temperature was maintained within a safe range, even with continuous holmium laser activation up to 40 W. However, continuous activation of a HαYAG laser at 32 W or higher for more than 60 seconds with limited irrigation of 30 mL/min can lead to excessive local temperature elevation [36]. A thorough understanding of the relationship between laser power, irrigation rate, and intrarenal temperature is essential for safe and effective laser lithotripsy. In this context, Marom et al. [12] proposed thermal safety boundaries for ureteroscopy, offering a conceptual framework for selecting appropriate laser settings and irrigation rates to minimize the risk of thermal injury, based on findings from an *in vivo* porcine study.

5. Properties of laser

1) Laser type and mode

Although lasers share many similarities, they are not equivalent when it comes to laser-tissue interaction. They differ in key aspects such as temperature production, ablation depth, coagulation efficiency, and cutting speed [7].

The extent of high-temperature areas during laser activation was greater in long pulse (LP) mode and Moses mode (MM) compared to SP mode and virtual basket mode (VBM). In LP mode, high-temperature areas expanded primarily in an anterior direction during the early phase of laser irradiation, while in MM, they spread in a posterior direction during early laser activation [14].

TFL has different properties from solid-state lasers like HαYAG and Tm:YAG. Since water absorption of TFL is four times higher than HαYAG, concern on higher temperature was proposed. Peteinaris et al. [37] demonstrated histopathological alterations in porcine kidneys resulting from continuous temperature increases above 43℃ when using TFL at 8 W. *In vitro* study by Peng et al. [38] showed that during TFL lithotripsy at power settings of 15W without irrigation, temperatures exceeded 43℃ after 20 seconds of laser activation. At 15 mL/min irrigation and 30 W, temperatures exceeded 43℃ after 45 seconds of laser activation. Temperatures did not exceed 43℃ at 25 mL/min and 50 mL/min irrigation rates, even at 30 W [38].

In an *in vitro* study by Belle et al. [23], TFL produced significantly higher intraureteral temperatures at all power settings (3.6, 10, 20, and 30 W), with an 11% increase in temperature compared to HαYAG. However, both laser technologies may remain within safe thermal limits at high energy settings, provided there is sufficient irrigation at a rate of 35 cc/min [23].

Æsøy et al. [20] investigated the temperature profile during TFL and HαYAG laser activation using an *ex vivo* porcine model. The lasers were activated for 180 seconds, followed by an additional 60 seconds after deactivation, using TFL (150 μm and 200 μm) and HαYAG (270 μm) fibers at power settings of 2.4, 8, 20, and 30 W. The threshold for thermal cell injury (43℃) was not reached at 2.4 W or 8 W, regardless of fiber size. However, a more pronounced rise in temperature was observed at 20 W and higher.

In an *ex vivo* study, Molina et al. [4] compared the rise in ureteral fluid temperature during laser lithotripsy using the 120 W HαYAG (P120; Lumenis Ltd.) and the 60 W SuperPulsed TFL (SPTF; SOLTIVE™). Laser lithotripsy

https://doi.org/10.4111/icu.20240369

was performed with a 200 μm core fiber at dusting settings (SPTF—0.1 J×200 Hz, SP; HαYAG—0.3 J×70 Hz, LP) and fragmenting settings (0.8 J×8 Hz, SP for both) for 5 seconds. The study showed that at the fragmenting setting, the median temperature increase was higher for TFL than for HαYAG (33.3°C vs. 30.0°C). However, at dusting settings, the median temperature increase was not significantly different between the two lasers. At these settings, temperatures remained below 43°C during ureteral lithotripsy [4]. A recent systematic review of experimental studies comparing Tm:YAG, TFL, and HαYAG revealed similar temperature changes across lasers, with all maintaining a safe temperature profile at power settings below 40 W [7].

MOSES technology is a laser delivery mode based on the "Moses effect," where an initial laser pulse creates a vapor bubble that enhances the energy transmission of a closely following second pulse. This effect has been shown in *in vitro* studies to reduce retropulsion, allowing higher power to be applied without the need to chase the stone. Winship et al. [39] evaluated the impact of different laser pulse types on heat production using a benchtop ureteral model. They compared SP, LP, Moses contact (MC), and Moses distance (MD) modes. LP produced significantly higher temperatures at 0.8 J×8 Hz and 1 J×10 Hz compared to MM [39]. The observed differences in heat production between pulse types are likely multifactorial and not fully understood. One explanation could be that total laser power output varies with pulse type, even when user-controlled pulse energy and frequency settings are identical. Additionally, for a fixed number of pulses at a fixed pulse energy, a longer pulse duration results in more active laser time, reducing cooling intervals between pulses. At lower pulse energies, no significant difference in heat production was observed between pulse types, which aligns with findings by Hardy et al. [40] that pulse energy and duration are correlated. Thus, at very low energies, pulse length differences may not be substantial enough to impact temperature rise.

More recently, Yamashita et al. [32] observed dynamic thermal changes among various pulse modes during laser activation using thermography. After 15 seconds and 30 seconds of activation at 0.4 J×60 Hz, water surface temperatures reached 44.7°C±1.2°C and 46.5°C±0.5°C for LP, and 42.2°C±0.7°C and 44.3°C±0.6°C for SP, respectively, demonstrating greater heat production with LP compared to SP [32]. LP and MM reached thermal thresholds faster and generated larger high-temperature areas compared to SP and VBMs. In the early phase of laser activation, most heat is produced in the forward direction with SP and LP, while in MM, the heat spreads backward, likely due to the water flow generated by laser shots in each mode. In VBM, which also uses Moses technology, the high-temperature area behind the laser fiber tip was relatively smaller compared to MM [14]. The MD mode delivers energy more efficiently through a vapor channel, resulting in more energy being directed toward stone comminution and less toward fluid heating. This is supported by previous studies showing that the single-pulse crater volume for MD was greater than for SP at a 0.5 mm distance [41].

However, *in vivo* studies have shown that MOSES pulse delivery technology does not result in a significant difference in maximal intrarenal fluid temperature compared to conventional pulse technology during flexible ureteroscopy at the same power settings, highlighting the need for further clinical research [42].

2) Fiber size

Larger laser fibers have been shown to generate significantly higher temperatures compared to smaller fibers when used at equivalent power settings. In an *ex-vivo* porcine study, Æsøy et al. [20] demonstrated a significant difference in mean temperature at 20 W between 150 μm and 200 μm fibers (39.6°C vs. 44.9°C, p<0.001). Similarly, Buttice' et al. [43] reported faster temperature elevation during laser activation in a kidney model when using a 272 μm fiber compared to a 200 μm fiber. However, it is important to note that even with consistent irrigation pressure, the irrigation flow rate decreases when larger laser fibers are introduced into the working channel, due to increased inflow resistance. This reduction in flow may limit the cooling capacity of the irrigation fluid [44].

3) Laser fiber to tissue distance

A study by Yang et al. [45] demonstrated significantly higher temperatures at shorter distances from the laser tip, attributed to the high concentration of laser energy at the fiber's activation point. The authors suggest that maintaining more than 0.05 cm between the tissue and the fiber can enhance safety [45]. Ventimiglia et al. [21] found a statistically significant positive correlation between average laser power and safety distance in an *in vitro* model, applying the thermal dose concept. They recommend limiting laser settings to below 20 W in the kidney, as thermal damage can occur even at a 5 mm distance from the laser fiber tip. In the ureter, laser settings should remain under 10 W, as tissue damage has been observed at 20 W, even at distances up to 1 mm from the fiber tip [21].

WAYS TO OVERCOME INTRARENAL TEMPERATURE ISSUES

1. Adjust irrigation temperature

Dau et al. [46] investigated the effect of irrigation fluid temperature on reaching the threshold for thermal injury during HoYAG laser activation at 0.5 J×80 Hz (40 W) for 60 seconds using an *in vitro* model. Compared to room temperature (19°C) and warmed irrigation (37°C), cold irrigation (1°C) significantly slowed the rate of temperature rise, reduced the plateau temperature, and lowered the thermal dose during laser activation. Without irrigation, the threshold for thermal injury was reached after 13 seconds of laser activation. With 12 mL/min irrigation, the threshold was reached in 46 seconds with room temperature irrigation, but it was not reached with cold irrigation. The same group also evaluated the effect of cold saline on caliceal fluid temperature *in vivo* using a porcine model. Consistent with the *in vitro* findings, cold irrigation effectively mitigated intrarenal temperature without impacting core body temperature, even at the maximum flow rate of 15 mL/min for 60 minutes [47].

2. Adjusting outflow resistance

As discussed, high irrigation rates have been shown to effectively control thermal dose in experimental settings [1,8,19,28,31,48]. Achieving higher irrigation rates requires minimizing outflow resistance, which refers to the friction and other factors affecting fluid dynamics as the irrigation fluid exits alongside the ureteroscope. This resistance can be reduced by using pressure-mitigating devices such as ureteral access sheaths (UAS) or catheters [49]. Larger UAS sizes further decrease outflow resistance, thereby increasing flow rates and cooling the fluid, with minimal impact on intrarenal pressure.

In an *ex vivo* porcine kidney model, Gallegos et al. [50] evaluated intrarenal temperatures under various conditions, including different irrigation heights (30, 40, and 50 cmH_2O), laser frequency (Hz), laser energy (J), and the presence or absence of a UAS. Using a 9.5 Fr flexible ureterorenoscope and a 275 μm fiber in the working channel, the application of a 12/14 Fr UAS reduced temperatures by 8.8°C compared to the no-UAS condition, in a multivariate model adjusted for energy, frequency, and irrigation rate [50].

However, larger UAS may increase the risk of ureteral injury. Considering the average size of the human ureter is approximately 10 Fr (3–4 mm), the risk of ureteral injury can reach up to 46.5% when using a 12/14 Fr UAS [51]. To minimize injury, the ideal UAS should strike a balance between being small enough to reduce trauma and large enough to ensure adequate irrigation flow and low intrarenal pressure. When UAS is inserted, the outer diameter of the ureteroscope directly impacts the outflow resistance. In this context, the concept of the "ratio of endoscopy-sheath diameter (RESD)" is vital for optimizing outflow resistance. Fang et al. [52] investigated the relationship between intrarenal pressure and RESD, concluding that maintaining an RESD below 0.75 is essential for preserving safe intrarenal pressure which translated to efficient irrigation fluid turnover, helping to regulate intrarenal temperature.

With the availability of slimmer flexible ureterorenoscope, various combinations of UAS and ureteroscopes can be tailored to specific clinical scenarios, even for patients with narrow ureters, while staying within the safe RESD range.

One promising approach to minimizing thermal injury during laser lithotripsy is the use of suction. Initially applied in percutaneous nephrolithotomy for over 25 years, the concept of suction has recently gained attention in ureteroscopy. Suction is now used not only to remove stone dust in pursuit of stone-free outcomes but also to reduce intrarenal pressure and temperature, which have become significant concerns in the high-power laser era. Current methods of utilizing suction in ureteroscopy include suction ureteral access sheath (SUAS), flexible and navigable sheath (FANS), and direct in-scope suction (DISS). Suction actively lowers intrarenal pressure, and by replacing warmed irrigation fluid with cooler fluid, it may theoretically reduce the risk of exceeding thermal dose thresholds [53,54]. At the same RESD, SUAS has demonstrated greater effectiveness in reducing intrarenal pressure and enhancing irrigation flow rate compared to conventional UAS. An RESD of <0.85 is recommended for RIRS procedures utilizing SUAS [55]. Other than active suction, the siphoning effect, which is a simple hydrodynamic created by the height difference between the two points, can also be easily applied to control the flow, eventually affecting the change in temperature [56]. However, preclinical and clinical evidence on the effect of suction and siphoning effect on intrarenal temperature remains limited, highlighting the need for further research.

FUTURE PERSPECTIVE

Human studies investigating 'safe' thresholds for intrarenal temperatures remain limited (Table 1). While numerous *in vitro* and *in vivo* studies have proposed strategies to reduce intrarenal temperatures, caution must be exercised when interpreting these findings, as preclinical results do not always directly translate to clinical outcomes [29]. Emerg-

https://doi.org/10.4111/icu.20240369

Table 1. Clinical studies on IRT change during laser lithotripsy

Study	Working space (No. of subjects)	Laser activation protocol	Inflow condition	Temperature measurement tool	Key findings
Æsøy et al. [17] (2024)	Renal pelvis (n=10)	• Laser power: 5, 10, 20, and 30 W • 120 s with continuous laser activation and for another 60 s after deactivation • Laser was deactivated whenever the IRT reached 43°C.	• Sheathless FURSL • Gravitational irrigation (23°C) at 60 cm • TFL/150 μm fiber	K-type thermocouple inserted through the nephrostomy tube	• IRT correlated directly to power settings • Temperatures reached 43°C in three patients applying 20 W and in eight patients applying 30 W. • The shortest activation-time until threshold was 12 s and 28 s with 30 W and 20 W settings, respectively. • There was a significant correlation between IRT and renal APD. • Using a sheathless approach, power settings of 20 W should be avoided, especially in the context of a nondilated renal pelvis.
Teng et al. [22] (2021)	Renal pelvis (n=32)	• Laser power: 1 J/20 Hz and 0.5 J/20 Hz 1) Laser activation for 60 s in the calices with irrigation → Temperature changes were documented every 5 s. 2) Laser activated without irrigation → Time needed to reach 43°C was recorded. • Laser was deactivated whenever the IRT reached 43°C.	• Storz fiberoptic flexible ureteroscope • Ho:YAG/200 μm fiber • Irrigation flow rate: 0 mL/min, 15 mL/min and 30 mL/min • 12/14 Fr UAS	K-type thermocouple attached to the scope (tip 5 mm from the distal end)	• With 15 mL/min or 30 mL/min irrigation, 43°C was not reached after 60 s laser activation at both 1 J/20 Hz and 0.5 J/20 Hz. • At the power setting of 1 J/20 Hz and irrigation flow rate of 15 mL/min, the temperature rise was significantly higher than other groups. • Without irrigation, the time needed to reach 43°C at 1 J/20 Hz was significantly shorter than that at 0.5 J/20 Hz (8.84±1.41 s vs. 13.71±1.53 s).
Wu et al. [36] (2023)	Renal pelvis (n=22)	• Laser power: 24 W, 80 Hz/0.3 J and 32 W, 80 Hz/0.4 J • 60-s laser activation	• Olympus fiber-optic flexible ureteroscope • Ho:YAG MOSES/200 μm laser fiber • Room temperature irrigation (25°C) • 12/14 Fr UAS	Thermocouple attached to the scope (its tip 5 mm from the distal end)	1) Room temperature irrigation (25°C) • With 30 mL/min or 60 mL/min irrigation, IRT did not reach 43°C in any patient after 60 s laser activation. 2) Warm irrigation (37°C), • At the setting of 32 W, 30 mL/min and 40 W, 30 mL/min after continuing laser activation, IRT reached close to or over 43°C.
Wang et al. [18] (2019)	Ureter (n=27) (30 sets)	Laser power: 10–50 W (setting unknown)	• Semirigid ureteroscope (WOLF 8.0/9.8 Fr) • Ho:YAG/550 μm laser fiber	Thermocouple temperature measurement wire	• Highest temperatures in the 30 sets of data all exceeded 43°C (100%), with 19 sets (63.3%) having peak temperatures higher than 56°C.

IRT, intrarenal temperature; FURSL, flexible ureteroscopic lithotripsy; TFL, thulium fiber laser; APD, anterior-posterior diameter; Ho:YAG, holmium YAG; UAS, ureteral access sheaths.

ing technologies are now being incorporated into flexible ureterorenoscope systems, enabling real-time temperature monitoring to maintain temperatures within safer limits [45]. These advancements may improve our understanding of the impact of temperature on clinical outcomes during ureteroscopy.

CONCLUSIONS

Intrarenal temperatures can rise significantly during laser activation, with irrigation playing a critical role in temperature control. Understanding the concept of thermal dose is essential when performing high-power laser lithotripsy, particularly in confined anatomical spaces. Implementing strategies to regulate energy delivery and optimize the system's heat capacity is key to maintaining safe temperature levels and minimizing the risk of temperature-related complications during ureteroscopy.

CONFLICTS OF INTEREST

Sung Kyu Hong has been the Editor-in-Chief of Investigative and Clinical Urology since 2025. The other author has nothing to disclose.

FUNDING

None.

AUTHORS' CONTRIBUTIONS

Research conception and design: Hyung Joon Kim and Sung Kyu Hong. Data acquisition: Hyung Joon Kim. Statistical analysis: Hyung Joon Kim. Data analysis and interpretation: Hyung Joon Kim. Drafting of the manuscript: Hyung Joon Kim and Sung Kyu Hong. Critical revision of the manuscript: Hyung Joon Kim and Sung Kyu Hong. Administrative, technical, or material support: Hyung Joon Kim. Supervision: Sung Kyu Hong. Approval of the final manuscript: Hyung Joon Kim and Sung Kyu Hong.

REFERENCES

1. Wollin DA, Carlos EC, Tom WR, Simmons WN, Preminger GM, Lipkin ME. Effect of laser settings and irrigation rates on ureteral temperature during holmium laser lithotripsy, an in vitro model. J Endourol 2018;32:59-63.
2. Heers H, Turney BW. Trends in urological stone disease: a 5-year update of hospital episode statistics. BJU Int 2016;118:785-9.
3. Jung HD, Lee JY, Kang DH, Ko K, Koh DH, Kwon O, et al.; Korean Society of Endourology and Robotics (KSER) Publication and Research Committees. Korean Society of Endourology and Robotics (KSER) recommendation on the diagnosis, treatment, and prevention of urolithiasis. Investig Clin Urol 2023;64:325-37.
4. Molina WR, Carrera RV, Chew BH, Knudsen BE. Temperature rise during ureteral laser lithotripsy: comparison of super pulse thulium fiber laser (SPTF) vs high power 120 W holmium-YAG laser (Ho:YAG). World J Urol 2021;39:3951-6.
5. Chai CA, Inoue T, Somani BK, Yuen SKK, Ragoori D, Gadzhiev N, et al. Comparing thulium fiber versus high power holmium laser in bilateral same sitting retrograde intrarenal surgery for kidney stones: results from a multicenter study. Investig Clin Urol 2024;65:451-8.
6. Panthier F, Solano C, Chicaud M, Kutchukian S, Candela L, Doizi S, et al. Initial clinical experience with the pulsed solid-state thulium YAG laser from Dornier during RIRS: first 25 cases. World J Urol 2023;41:2119-25.
7. Ortner G, Rice P, Nagele U, Herrmann TRW, Somani BK, Tokas T. Tissue thermal effect during lithotripsy and tissue ablation in endourology: a systematic review of experimental studies comparing Holmium and Thulium lasers. World J Urol 2023;41:1-12.
8. Hein S, Petzold R, Schoenthaler M, Wetterauer U, Miernik A. Thermal effects of Ho: YAG laser lithotripsy: real-time evaluation in an in vitro model. World J Urol 2018;36:1469-75.
9. Jansen ED, Asshauer T, Frenz M, Motamedi M, Delacrétaz G, Welch AJ. Effect of pulse duration on bubble formation and laser-induced pressure waves during holmium laser ablation. Lasers Surg Med 1996;18:278-93.
10. Aldoukhi AH, Hall TL, Ghani KR, Maxwell AD, MacConaghy B, Roberts WW. Caliceal fluid temperature during high-power holmium laser lithotripsy in an in vivo porcine model. J Endourol 2018;32:724-9.
11. Aldoukhi AH, Roberts WW, Hall TL, Teichman JMH, Ghani KR. Understanding the popcorn effect during holmium laser lithotripsy for dusting. Urology 2018;122:52-7.
12. Marom R, Dau JJ, Hall TL, Ghani KR, Louters MM, Kim HJ, et al. Thermal safety boundaries for laser power and irrigation rate during ureteroscopy: in vivo porcine assessment with a Ho:YAG laser. Urology 2023;180:81-5.
13. Zhang X, Liu Z, Chen X, Li D, Yang Z, Gu J, et al. The effect of application of a Soton ureteroscope on infection after flexible ureteroscopy lithotripsy. Wideochir Inne Tech Maloinwazyjne 2022;17:232-9.
14. Yamashita S, Inoue T, Imai S, Maruyama Y, Iwahashi Y, Deguchi R, et al. Dynamic changes in fluid temperatures during

https://doi.org/10.4111/icu.20240369

laser irradiation using various laser modes: a thermography-based in vitro phantom study. J Clin Med 2023;12:1409.
15. Sapareto SA, Dewey WC. Thermal dose determination in cancer therapy. Int J Radiat Oncol Biol Phys 1984;10:787-800.
16. Yarmolenko PS, Moon EJ, Landon C, Manzoor A, Hochman DW, Viglianti BL, et al. Thresholds for thermal damage to normal tissues: an update. Int J Hyperthermia 2011;27:320-43.
17. Æsøy MS, Juliebø-Jones P, Beisland C, Ulvik Ø. Temperature measurements during flexible ureteroscopic laser lithotripsy: a prospective clinical trial. J Endourol 2024;38:308-15.
18. Wang XK, Jiang ZQ, Tan J, Yin GM, Huang K. Thermal effect of holmium laser lithotripsy under ureteroscopy. Chin Med J (Engl) 2019;132:2004-7.
19. Aldoukhi AH, Ghani KR, Hall TL, Roberts WW. Thermal response to high-power holmium laser lithotripsy. J Endourol 2017;31:1308-12.
20. Æsøy MS, Juliebø-Jones P, Beisland C, Ulvik Ø. Temperature profiles during ureteroscopy with thulium fiber laser and holmium:YAG laser: findings from a pre-clinical study. Scand J Urol 2022;56:313-9.
21. Ventimiglia E, Robesti D, Keller EX, Corsini C, Folcia A, Fantin M, et al. Temperature profile during endourological laser activation: introducing the thermal safety distance concept. World J Urol 2024;42:453.
22. Teng J, Wang Y, Jia Z, Guan Y, Fei W, Ai X. Temperature profiles of calyceal irrigation fluids during flexible ureteroscopic Ho:YAG laser lithotripsy. Int Urol Nephrol 2021;53:415-9.
23. Belle JD, Chen R, Srikureja N, Amasyali AS, Keheila M, Baldwin DD. Does the novel thulium fiber laser have a higher risk of urothelial thermal injury than the conventional holmium laser in an in vitro study? J Endourol 2022;36:1249-54.
24. Sierra A, Corrales M, Somani B, Traxer O. Laser efficiency and laser safety: holmium YAG vs. thulium fiber laser. J Clin Med 2022;12:149.
25. Aldoukhi AH, Dau JJ, Majdalany SE, Hall TL, Ghani KR, Hollingsworth JM, et al. Patterns of laser activation during ureteroscopic lithotripsy: effects on caliceal fluid temperature and thermal dose. J Endourol 2021;35:1217-22.
26. Louters MM, Dau JJ, Hall TL, Ghani KR, Roberts WW. Laser operator duty cycle effect on temperature and thermal dose: in-vitro study. World J Urol 2022;40:1575-80.
27. Rezakahn Khajeh N, Hall TL, Ghani KR, Roberts WW, Pelvicaliceal volume and fluid temperature elevation during laser lithotripsy. J Endourol 2022;36:22-8.
28. Winship B, Wollin D, Carlos E, Peters C, Li J, Terry R, et al. The rise and fall of high temperatures during ureteroscopic holmium laser lithotripsy. J Endourol 2019;33:794-9.
29. Dean NS, Krambeck AE. Endourologic procedures of the upper urinary tract and the effects on intrarenal pressure and temperature. J Endourol 2023;37:191-8.
30. Liang H, Liang L, Yu Y, Huang B, Chen J, Wang C, et al. Thermal effect of holmium laser during ureteroscopic lithotripsy. BMC Urol 2020;20:69.
31. Molina WR, Silva IN, Donalisio da Silva R, Gustafson D, Sehrt D, Kim EJ. Influence of saline on temperature profile of laser lithotripsy activation. J Endourol 2015;29:235-9.
32. Yamashita S, Inoue T, Imai S, Iwahashi Y, Deguchi R, Muraoka S, et al. Thermography-based comparison of irrigation temperatures between Moses mode and virtual basket mode: an in vitro phantom study. J Endourol 2023;37:179-84.
33. Villena JM, Elorrieta V, Salvadó JA. Temperature effect of Moses™ 2.0 during flexible ureteroscopy: an in vitro assessment. Cent European J Urol 2023;76:331-5.
34. Noureldin YA, Farsari E, Ntasiotis P, Adamou C, Vagionis A, Vrettos T, et al. Effects of irrigation parameters and access sheath size on the intra-renal temperature during flexible ureteroscopy with a high-power laser. World J Urol 2021;39:1257-62.
35. Hein S, Petzold R, Suarez-Ibarrola R, Müller PF, Schoenthaler M, Miernik A. Thermal effects of Ho:YAG laser lithotripsy during retrograde intrarenal surgery and percutaneous nephrolithotomy in an ex vivo porcine kidney model. World J Urol 2020;38:753-60.
36. Wu Z, Wei J, Sun C, Huangfu Q, Wang B, Huang G, et al. Temperature changes of renal calyx during high-power flexible ureteroscopic Moses holmium laser lithotripsy: a case analysis study. Int Urol Nephrol 2023;55:1685-92.
37. Peteinaris A, Tsaturyan A, Bravou V, Tatanis V, Faria-Costa G, Pagonis K, et al. High-power laser lithotripsy - do we treat or harm? Histological evaluation of temperature effects in an in vivo study with thulium fiber laser. Cent European J Urol 2023;76:44-8.
38. Peng Y, Liu M, Ming S, Yu W, Li L, Lu C, et al. Safety of a novel thulium fiber laser for lithotripsy: an in vitro study on the thermal effect and its impact factor. J Endourol 2020;34:88-92.
39. Winship B, Terry R, Boydston K, Carlos E, Wollin D, Peters C, et al. Holmium:yttrium-aluminum-garnet laser pulse type affects irrigation temperatures in a benchtop ureteral model. J Endourol 2019;33:896-901.
40. Hardy LA, Vinnichenko V, Fried NM. High power holmium: YAG versus thulium fiber laser treatment of kidney stones in dusting mode: ablation rate and fragment size studies. Lasers Surg Med 2019;51:522-30.
41. Aldoukhi AH, Roberts WW, Hall TL, Ghani KR. Watch your distance: the role of laser fiber working distance on fragmentation when altering pulse width or modulation. J Endourol 2019;33:120-6.
42. Peteinaris A, Faitatziadis S, Tsaturyan A, Pagonis K, Liatsikos

E, Kallidonis P. MOSES™ pulse modulation technology versus conventional pulse delivery technology: the effect on irrigation fluid temperature during flexible ureteroscopy. Urolithiasis 2022;50:613-8.

43. Butticè S, Sener TE, Proietti S, Dragos L, Tefik T, Doizi S, et al. Temperature changes inside the kidney: what happens during holmium:yttrium-aluminum-garnet laser usage? J Endourol 2016;30:574-9.
44. Rezakahn Khajeh N, Hall TL, Ghani KR, Roberts WW. Determination of irrigation flowrate during flexible ureteroscopy: methods for calculation using renal pelvis pressure. J Endourol 2022;36:1405-10.
45. Yang J, Li Z, Lai C, Xu K. An in vivo assessment of a novel temperature control flexible ureteroscope system for monitoring and controlling intrarenal temperature during flexible ureteroscopy. Urology 2024;191:38-44.
46. Dau JJ, Hall TL, Maxwell AD, Ghani KR, Roberts WW. Effect of chilled irrigation on caliceal fluid temperature and time to thermal injury threshold during laser lithotripsy: in vitro model. J Endourol 2021;35:700-5.
47. Dau JJ, Rezakahn Khajeh N, Hall TL, Roberts WW. Chilled irrigation for control of temperature elevation during ureteroscopic laser lithotripsy: in vivo porcine model. J Endourol 2022;36:403-9.
48. Aldoukhi AH, Black KM, Hall TL, Ghani KR, Maxwell AD, MacConaghy B, et al. Defining thermally safe laser lithotripsy power and irrigation parameters: in vitro model. J Endourol 2020;34:76-81.
49. Kim HJ, Louters MM, Dau JJ, Hall TL, Ghani KR, Roberts WW. Quantification of outflow resistance for ureteral drainage devices used during ureteroscopy. World J Urol 2023;41:873-8.
50. Gallegos H, Bravo JC, Sepúlveda F, Astroza GM. Intrarenal temperature measurement associated with holmium laser intracorporeal lithotripsy in an ex vivo model. Cent European J Urol 2021;74:588-94.
51. Traxer O, Thomas A. Prospective evaluation and classification of ureteral wall injuries resulting from insertion of a ureteral access sheath during retrograde intrarenal surgery. J Urol 2013;189:580-4.
52. Fang L, Xie G, Zheng Z, Liu W, Zhu J, Huang T, et al. The effect of ratio of endoscope-sheath diameter on intrapelvic pressure during flexible ureteroscopic lasertripsy. J Endourol 2019;33:132-9.
53. Solano C, Chicaud M, Kutchukian S, Candela L, Corrales M, Panthier F, et al. Optimizing outcomes in flexible ureteroscopy: a narrative review of suction techniques. J Clin Med 2023;12:2815.
54. Yuen SKK, Traxer O, Wroclawski ML, Gadzhiev N, Chai CA, Lim EJ, et al. Scoping review of experimental and clinical evidence and its influence on development of the suction ureteral access sheath. Diagnostics (Basel) 2024;14:1034.
55. Shi J, Huang T, Song B, Liu W, Cheng Y, Fang L. The optimal ratio of endoscope-sheath diameter with negative-pressure ureteral access sheath: an in vitro research. World J Urol 2024;42:122.
56. Kim HJ, Louters MM, Dau JJ, Hall TL, Ghani KR, Roberts WW. The impact of siphoning effect on renal pelvis pressure during ureteroscopy using an in vitro kidney and ureter model. World J Urol 2024;42:415.

https://doi.org/10.4111/icu.20240369

审阅文章

《临床泌尿学研究》2025；66：1-10。
https://doi.org/10.4111/icu.20240369 pISSN 2466-0493 • eISSN 2466-0540

ICUROLOGY

输尿管镜检查过程中腔内温度的升高：这是一个问题吗？

金炯俊[1]，Sung Kyu Hong[1, 2]

韩国首尔国立大学盆唐医院泌尿科，城南市；韩国首尔国立大学医学院泌尿科

全球尿路结石患病率的上升趋势推动了微创手术的发展，例如逆行肾镜碎石术，这得益于碎石激光技术的进步。脉冲激光技术，尤其是钬YAG激光和新型铥光纤激光，已显著改变了上尿路结石的治疗方式。然而，高功率激光在这些手术中的应用会带来热损伤风险。激光碎石术通过光热效应和光机械效应来粉碎结石，但高达96%的激光能量会转化为热量，增加了对周围尿路上皮黏膜的热损伤风险。研究表明，即使在低功率设置下，肾内温度也可能超过细胞损伤的临界值，尤其是在输尿管等狭窄空间。这篇综述探讨了减轻热损伤的策略，包括优化激光参数、改善冲洗液流速，以及引入冷冲洗、控制流出阻力和使用负压吸引等创新方法。掌握这些技术要点，对提高高功率激光碎石术中的患者安全性至关重要。

关键词：激光；围手术期并发症；温度；输尿管镜；尿路结石

本文为开放获取文章，根据知识共享署名非商业性使用许可协议（http://creativecommons.org/licenses/by-nc/4.0）发布，允许在任何媒介中不受限制地进行非商业性使用、传播和复制，前提是正确引用原始作品。

介绍

尿路结石的患病率在全球范围内存在显著差异，且近几十年来呈现明显上升趋势[1]。随着技术进步，外科治疗方案已转向微创内镜手术，例如输尿管镜检查和微型经皮肾镜碎石术。逆行肾镜手术（RIRS）的广泛应用——该技术通过柔性输尿管肾镜配合激光技术革新，已彻底改变了上尿路结石的诊疗模式[2,3]。

在碎石术中，脉冲激光是不同能量源中用于输尿管镜检查的主要且唯一能量源。钬掺杂钇铝石榴石（Ho：YAG）激光该技术作为标准方法已沿用多年，其功率规格不断提升且脉冲宽度可调。铥光纤激光器（TFL）近期崭露头角，成为激光碎石术领域极具潜力的新利器。TFL具备宽能量范围（0.025—6焦耳）和高频段（5—2,400赫兹），能有效减少后坐力并实现更精细的碎石效果[4,5]。近期对脉冲式钬掺杂钇铝石榴石（Tm：YAG）的重新评估，因其作为碎石术替代激光器的独特性能而备受关注，目前仍在等待更多实证数据的积累[6]。

现代高功率激光器凭借其更高的频率性能，使得手术速度显著提升。然而，在RIRS治疗中使用高功率激光器会引发热相关问题[7,8]。激光器通过光热效应和光机械效应两种主要作用机制来粉碎结石。光热效应

收稿日期：2024年10月20日•修订日期：2024年12月12日•录用日期：2024年12月16日•网络发表日期：2024年12月31日
通讯作者：Sung Kyu Hong https://orcid.org/0000-0002-8344-6774
首尔国立大学盆唐医院泌尿科。地址：韩国城南市盆唐区龟尾路82号173beon-gil，邮编13620，电话：+82-31-787-7343，电子邮箱：skhong@snubh.org

电磁辐射驱动的机械效应会使结石组件受热，通过激光激活、沸腾或周围水汽化引发化学分解。当结石内部孔隙中的水分汽化时，光机械效应就会发生，导致结石内部爆裂。当脉冲持续时间超过10μs时，光热效应会占据主导地位；而超过200μs的脉冲则会使光机械效应变得微不足道[9]。在激光碎石过程中，收集系统中结石周围的液体温度可能显著升高，正如一项*体内*猪实验所示[10]，这种高温可能对周围尿路上皮黏膜造成热损伤。

方法

我们使用PubMed数据库从建库至2024年5月期间进行了文献检索，检索关键词包括“输尿管镜检查”、“热”和“温度”，并采用布尔运算符（AND、OR）对检索结果进行细化，检索范围涵盖*体外*、人类和动物研究，既包含原始研究和综述文章，也包含通过选定文献的参考文献检索到的其他文献。

为什么热量很重要？

随着高功率激光（100-120瓦）在激光碎石术中的应用日益广泛，人们对输尿管黏膜可能遭受的间接损伤愈发担忧，这类技术可能增加输尿管狭窄或肾功能减退的风险。虽然高功率激光系统能实现更高频率、提升手术效率，但其能量水平并未显著改变。值得注意的是，并非所有脉冲都用于结石消融。高功率激光的主要优势在于其“粉尘消融”技术，该技术通过高频脉冲实现碎石效果，正逐渐取代传统碎石方式。然而随着粉尘消融技术的普及，其主导的光热效应也带来了潜在风险——在高功率粉尘消融中，仅有17%的激光脉冲能有效击中结石[11]。这不仅降低了消融效率，还会导致输尿管系统内部温度升高。

在激光碎石术中，91%至96%的激光能量转化为热能，即使在有效结石消融过程中[10]，这可能会导致组织坏死，*一项猪体内*预试验研究证实了这一点[12,13]。峰值温度和暴露时间都起着作用

热细胞毒性[14]。热损伤的潜在风险可通过萨帕雷托和杜威提出的累积等效分钟数（43°C，CEM43°C）模型进行评估[15]。热剂量指标用于量化任何温度-时间曲线引发的热损伤生物学风险，其损伤阈值设定为120等效分钟。具体而言，当温度维持在43°C时需暴露120分钟，或在更高温度下分别暴露60分钟（44°C）、30分钟（45°C）及不足一分钟（50°C）。在热效应阈值（56°C）下，即使仅暴露1秒也可能造成热损伤。动物实验表明，当暴露时间短于20分钟（CEM43°C<20分钟）时仅产生轻微热损伤，而超过70分钟（CEM43°C>70分钟）则会造成显著损伤[16]。

研究表明，即使在低功率设置（<30瓦）下，细胞热损伤的临界阈值也会被触发[17]。一项在输尿管镜检查过程中调整不同功率（10-50瓦）的临床研究显示，管腔温度常超过56°C阈值——当功率超过15-20瓦时，热损伤可能在数秒内发生，而所有案例中功率超过25瓦时都会出现这种情况。即便在10瓦功率下，某些特定部位的温度也达到了43°C[18]。因此，确定合适的激光参数并制定策略以减少温度相关并发症至关重要。

URETEROSCOPY过程中哪些因素会影响温度？

激光碎石术中的热风险主要受两大因素影响：能量输送量和系统热容量。虽然激光功率是能量输送的主要决定因素，但激光激活时长和操作者工作周期（ODC）也起着关键作用。热容量则取决于冲洗液的吸热能力，这受激光激活时冲洗液的体积（无论是在肾盂、肾盏还是输尿管中）、温度及流速的影响。此外，所使用的激光脉冲类型也可能导致温度升高。

1. 总功率已应用

功率设置越高，能量沉积越显著，从而增加热损伤风险。*体外*研究显示，在固定流量条件下使用不同激光参数时，温度升高与总功率成正比，且不受脉冲能量和频率组合方式的影响[4,19-21]。Aldoukhi等[10]曾评估过高功率激光碎石术中膀胱体液的温度变化。

https://doi.org/10.4111/icu.20240369

*体内*猪模型。在40瓦（0.5焦耳×80赫兹）功率下未进行冲洗时，激光激活后10秒内温度达到60°C。峰值温度为84.8°C，达到热损伤阈值（CEM43°C为120分钟）的平均时间为12.7秒[10]。在同一研究中，将冲洗速率提高至15 mL/min和40 mL/min时，峰值液体温度分别降至58.5°C和37.5°C。Teng等人[22]在人体试验中研究了Ho：YAG激光碎石术期间盏状结构冲洗液温度的变化。在1焦耳×20赫兹未冲洗条件下，达到43°C所需时间显著短于0.5焦耳×20赫兹条件（8.84秒对比13.71秒）[22]。两项研究均强调了适当冲洗流量对缓解温度升高的重要性。Belle等人[23]使用*体外*硅胶肾输尿管模型中的TFL激光器，证明高功率激光与热损伤风险增加相关。他们建议在输尿管镜激光碎石术中采用保守的激光设置以降低该风险[23]。为避免细胞热损伤，温度升高与功率成正比，建议肾脏功率限制为20—30 W，输尿管功率限制为10—15 W[4,21,24]。

2. 激光时间和模式

"ODC"（热损伤阈值百分比）的概念指的是激光踏板在治疗过程中被激活的时间占比。在*体外*骨膜模型中，Aldoukhi等人[25]通过采用50%ODC的不同能量模式，以1200焦耳总能量持续60秒进行热剂量测量。当以50%ODC强度施加40瓦功率，采用30秒开/关+15秒开/关的激活模式时，仅需9秒即可达到热损伤阈值。若改为10秒开/关模式，阈值则需45秒才能触发，而更短的激活时间则无法达到损伤阈值。这表明在能量输出相同的情况下，延长踏板激活时间会导致更高热剂量[25]。Louters团队[26]通过向充液玻璃灯管输送30瓦（0.5焦耳×60赫兹）的Ho：YAG激光能量（1800焦耳总能量），研究了ODC值递增引发的温度变化。研究发现，随着热损伤阈值（ODCs）的升高，最大温度和热剂量也随之增加，当ODCs达到70%及以上时，即可突破热损伤阈值。相比之下，50%的ODC需要多出十倍时间才能达到热损伤阈值，且与60%的ODC相比，其允许的最大能量增幅可达八倍[26]。但需注意，这些结果在解读时需谨慎，因为*体内*或*体外*研究可能无法完全反映真实临床场景。例如在实际操作中，激光设备很少会连续工作60秒。为了更好地理解临床环境中的ODC，la-研究人员对输尿管镜检查病例的激光治疗记录进行分析，发现平均ODC值为32%，这意味着在1分钟的激光治疗过程中，激光器实际工作时间约为20秒。当能量输送达到峰值时，平均ODC值可飙升至63%[25]。掌握这些关键概念对于降低激光碎石术中的热损伤风险至关重要。有效控制ODC值是调节热剂量、提升患者安全性的核心策略之一。

3. 液体积（肾盂/肾盏/输尿管）

Æsøy等人[17]开展了一项涉及10名患者的临床试验，旨在评估无鞘激光肾消融术（RIRS）期间肾盂温度的变化。研究发现，使用20瓦功率的患者中有3人出现肾盂温度高达43°C，而使用30瓦功率的患者中这一比例为8人。研究结果表明，肾盂温度与肾盂前后径呈负相关，这突显了激光激活过程中液体容量的重要性[17]。Rezakahn Khajeh等学者[27] 本研究通过模拟不同肾盏和肾盂体积的玻璃球体，探究了激光激活引发的流体温度升高及热剂量变化。在40瓦功率（0.5焦耳×80赫兹，短脉冲[SP]）条件下，温度升高和热剂量均与流体体积及冲洗速率呈负相关。最小模型（0.5毫升）未冲洗时，仅3秒即达到热损伤阈值；而最大模型（60.8毫升）无论是否冲洗均未达到该阈值。这表明与肾盂相比，输尿管因流体体积较小，更容易发生热损伤。

此外，输尿管因缺乏周围血管网络而特别脆弱，这些血管本可提供散热功能。其狭窄的管腔还会阻碍冲洗液流动，增加环形损伤和狭窄形成的风险[28]。王等学者[18]研究了输尿管内激光碎石术的热效应，使用550μm光纤的刚性输尿管镜将功率从10瓦提升至50瓦。在30组数据中，所有案例记录的最高温度均超过43°C，其中63.3%的数据组峰值温度超过56°C。随着功率增加，记录的温度普遍同步上升[18]。对于输尿管结石，推荐的治疗方案包括(1) 确保适度灌溉，(2)将激光激活限制为3-4秒的脉冲，随后暂停3-4秒以使温度恢复正常，(3)在长时间操作过程中考虑使用较低功率设置。

当输尿管结石发生嵌顿导致冲洗液流动受阻时，热损伤风险显著升高。一项20 W研究通过对比七例嵌顿结石病例发现

在四例非嵌顿结石病例中，嵌顿结石组的术中冲洗液平均温度显著高于非嵌顿组（38.56°C±8.51°C vs.34.92°C±5.35°C，p<0.001）。鉴于柔性输尿管肾镜可轻松进入肾盂，一种潜在策略是将结石从近端输尿管重新定位至更宽广、热敏感性更低的区域，例如肾盏或肾盂[29,30]。

4. 灌注流速

在激光碎石术中提高连续灌注流速对于降低肾内温度至关重要[1,31]。基于热成像的评估表明，在激光碎石术过程中，结石附近的黏膜周围温度可能迅速升高，尤其是在灌注不足时[32]。在一项*体外*研究中，Villena等人[33]证明，灌注流速每增加20 mL/min，肾内温度就会显著降低4.7°C—9.2°C（p<0.001），输尿管温度则相应下降2.6°C—8.8°C（p=0.01）。实验模型进一步表明，当使用20 W或更高功率的激光时，需要更高的流速（50—100 mL/min）来维持安全的肾内温度。必须避免在无灌注的情况下激活激光，因为这可能导致温度超过100°C，造成严重的热损伤风险[34]。Hein等人[35]评估了5至100 W不同功率激光与各种灌注速率（0—100 mL/min，37°C）组合的热影响，他们的研究结果表明，即使在RIRS期间使用5 W的低功率设置，如果灌溉量不足，也会导致有害的温度升高。基于他们的研究结果，他们开发了一个用于估算使用≥30 mL/min灌溉速率时温度升高（ΔT）的公式：ΔT=15 K×（功率[W]/灌溉[ML/min]）[35]。

在一项人体研究中，当使用1 J×20 Hz和0.5 J×20 Hz两种激光激活模式时，即使在15 mL/min或30 mL/min的灌注流速下，肾内温度在60秒内仍保持在43°C以下。当灌注流速为60 mL/min时，即使持续使用高达40 W的钬激光激活，肾盏温度仍能维持在安全范围内。然而，若以32 W或更高功率的Ho：YAG激光持续激活超过60秒，且灌注流速仅为30 mL/min，可能导致局部温度过度升高。

[36]要实现安全有效的激光碎石术，必须全面掌握激光功率、冲洗速率与肾内温度之间的关系。在此背景下，Marom等学者[12]为输尿管镜检查制定了热安全边界，为选择合适的激光参数和冲洗速率提供了理论框架。

根据一项*体内*猪研究的结果，将热损伤风险降至最低。

5. 激光器属性

1) 激光类型和模式

虽然激光器具有许多相似之处，但在激光与组织的相互作用方面并不等同。它们在温度产生、消融深度、凝固效率和切割速度等关键方面存在差异[7]。

激光激活过程中，长脉冲（LP）模式和Moses模式（MM）的高温区域范围，明显大于SP模式和虚拟篮模式（VBM）。具体来说，在LP模式下，高温区域在激光照射初期主要向前方扩展；而MM模式下，高温区域则在激光激活初期向后方扩散[14]。

TFL与Ho：YAG和Tm：YAG等固态激光器具有不同的特性。由于TFL的水吸收率是Ho：YAG的四倍，因此提出了对更高温度的担忧。Peteinaris等人[37]展示了在使用8 W TFL时，当温度持续升高至43°C以上时，猪肾脏出现组织病理学改变。Peng等人[38]的体外研究显示，在15 W功率设置下进行TFL碎石术且未冲洗时，激光激活20秒后温度超过43°C。在15 mL/min冲洗和30 W功率下，激光激活45秒后温度超过43°C。即使在30 W功率下，25 mL/min和50 mL/min的冲洗速率下温度也未超过43°C[38]。

Belle等人[23]的*体外*研究表明，TFL在所有功率设置（3.6、10、20和30 W）下产生的输尿管内温度显著高于Ho：YAG，温度比Ho：YAG高11%。然而，只要以35 cc/min的速率进行充分灌洗，两种激光技术在高能量设置下可能仍处于安全的热限内[23]。

Æsøy等人[20]采用*离体*猪模型研究了TFL和Ho：YAG激光激活过程中的温度变化。实验中，研究人员分别使用功率为2.4、8、20和30瓦的TFL光纤（150μm和200μm）及Ho：YAG光纤（270μm），每次激活持续180秒，停机后继续加热60秒。结果显示：在2.4瓦和8瓦功率下，无论光纤尺寸如何，温度均未达到热细胞损伤阈值（43°C）。但当功率提升至20瓦及以上时，温度升高现象显著加剧。

在一项*ex vivo*研究中，Molina等人[4]比较了使用120 W Ho：YAG（P120；Lumenis Ltd.）和60 W SuperPulsed TFL（SPTF：soltive™）进行激光碎石术时输尿管液温度的升高。

https://doi.org/10.4111/icu.20240369

实验采用200μm光纤进行碎石，分别设置为碎石模式（SP-TF—0.1焦耳×200赫兹，SP：Ho：YAG—0.3焦耳×70赫兹，LP）和碎石模式（两种模式均采用0.8焦耳×8赫兹，SP）持续5秒。研究显示，在碎石模式下，TFL激光器的温度中位数增幅高于Ho：YAG激光器（33.3°C对比30.0°C）。但在碎石模式下，两种激光器的温度中位数增幅无显著差异。在此模式下，输尿管碎石术期间温度始终低于43°C[4]。近期一项系统综述对比了Tm：YAG、TFL和Ho：YAG三种激光器的实验数据，发现各激光器的温度变化趋势相似，且在功率低于40瓦时均能保持安全的温度曲线[7]。

摩西技术是一种基于“摩西效应”的激光输送模式，其原理是通过初始激光脉冲产生气泡，从而增强紧随其后的第二脉冲能量传输效率。*体外研究*表明，这种效应能有效减少反冲现象，使得无需追踪结石即可施加更高功率。Winship等人[39]使用台式输尿管模型评估了不同激光脉冲类型对产热的影响，对比了SP、LP、摩西接触（MC）和摩西距离（MD）四种模式。实验数据显示，当脉冲能量为0.8焦耳×8赫兹和1焦耳×10赫兹时，LP模式产生的温度显著高于MM模式[39]。脉冲类型间的产热差异可能由多重因素共同作用，目前尚未完全阐明。一种可能的解释是：即使用户设定的脉冲能量和频率相同，不同脉冲类型会导致总激光功率输出差异。此外，在脉冲能量固定且脉冲次数不变的情况下，延长脉冲持续时间会增加激光作用时间，从而缩短脉冲间的冷却间隔。在较低脉冲能量下，不同脉冲类型产生的热量无显著差异，这与Hardy等人[40]关于脉冲能量与持续时间存在相关性的研究结果一致。因此，在极低能量条件下，脉冲长度的差异可能不足以影响温度上升。

近期，山下等人[32]通过热成像技术观察到，不同脉冲模式在激光激活过程中会产生动态热变化。当采用0.4焦耳×60赫兹的参数进行15秒和30秒激活时，水表面温度分别达到44.7°C±1.2°C（LP模式）和46.5°C±0.5°C（SP模式），而SP模式的温度分别为42.2°C±0.7°C和44.3°C±0.6°C，这表明LP模式的产热量显著高于SP模式[32]。与SP模式和VBMs模式相比，LP模式和MM模式能更快达到热阈值，并形成更大的高温区域。在激光激活初期，SP模式和LP模式主要产生前向热传导，而MM模式的热量会向后扩散，这可能是由于水分子的热传导特性所致。

不同模式下激光脉冲产生的流动特性存在差异。采用Moses技术的VBM系统中，激光光纤尖端后方的高温区域比MM系统更为紧凑[14]。MD模式通过蒸汽通道实现更高效的能量传输，使得更多能量用于石料粉碎而非流体加热。此前研究证实，在0.5毫米距离下，MD模式的单脉冲坑体积显著大于SP模式[41]。

然而，*体内*研究表明，在相同功率设置下，与传统脉冲技术相比，moses脉冲输送技术在输尿管镜软镜检查期间不会导致最大肾内液体温度产生显著差异，这强调了进一步临床研究的必要性[42]。

2) 纤维尺寸

研究表明，当功率设置相同时，大直径激光光纤产生的温度显著高于小直径光纤。在一项*离体猪*实验中，Æsøy团队[20]发现150μm和200μm光纤在20瓦功率下的平均温度存在显著差异（39.6°C对比44.9°C，$p<0.001$）。类似地，Buttice团队[43]在肾脏模型中发现，使用272μm光纤时，激光激活过程中的温度上升速度比200μm光纤更快。但需注意的是，即使保持恒定的灌注压力，当大直径光纤进入工作通道时，由于流入阻力增大，灌注液流量会随之减少。这种流量下降可能会影响灌注液的冷却效果[44]。

3) 激光光纤到组织距离

杨等人[45]的研究表明，随着与激光尖端距离的缩短，温度会显著升高，这归因于光纤激活点处激光能量的高浓度。研究者建议，保持组织与光纤之间超过0.05厘米的间距可提升安全性[45]。文蒂米利亚团队[21]通过*体外*模型应用热剂量概念，发现平均激光功率与安全距离存在统计学意义上的正相关关系。他们建议在肾脏治疗中将激光功率限制在20瓦以下，因为即使距离激光光纤尖端5毫米仍可能引发热损伤。对于输尿管治疗，激光功率应控制在10瓦以内，因为在距离光纤尖端仅1毫米处，20瓦功率仍会导致组织损伤[21]。

克服肾内温度问题的方法

1. 调节灌溉温度

Dau等人[46]使用*体外*模型研究了在0.5 J×80 Hz（40 W）条件下激活Ho：YAG激光器60秒时，灌注液温度对达到热损伤阈值的影响。与室温（19°C）和温热灌注（37°C）相比，冷灌注（1°C）显著减缓了温度上升速率，降低了平台温度，并在激光激活期间降低了热剂量。未进行灌注时，热损伤阈值在激光激活13秒后达到。使用12 mL/min的灌注液时，室温灌注下阈值在46秒内达到，而冷灌注则未达到。同一研究团队还使用猪模型评估了冷盐水*体内*对肾盏液温度的影响。与*体外*结果一致，即使在最大流速为15 mL/min持续60分钟的情况下，冷灌注也能有效降低肾内温度而不影响核心体温[47]。

2. 调节出液阻力

如前所述，高灌注速率已被证实能有效控制实验环境中的热剂量[1,8,19,28,31,48]。要实现更高的灌注速率，需要最大限度降低流出阻力——即当灌注液随输尿管镜排出时，流体动力学中涉及的摩擦力及其他影响因素。通过使用减压装置（如输尿管通路鞘UAS或导管）可有效降低此类阻力[49]。增大UAS尺寸能进一步降低流出阻力，从而提升流速并实现液体冷却，同时对肾内压力的影响微乎其微。

在一项*离体*猪肾模型研究中，Gallegos团队[50]通过多变量模型评估了不同条件下的肾内温度变化，实验参数包括冲洗高度（30、40和50厘米$_2$水柱）、激光频率（Hz）、激光能量(J)以及是否使用UAS。研究采用9.5 Fr柔性输尿管肾镜配合275μm光纤作为工作通道，结果显示：当使用12/14 Fr UAS时，经能量、频率和冲洗速率校正后的温度降幅达到8.8°C，较未使用UAS的对照组显著降低[50]。

然而，较大的导管尺寸（UAS）可能增加输尿管损伤风险。考虑到人类输尿管平均直径约为10 Fr（3-4毫米），使用12/14 Fr UAS时输尿管损伤风险可达46.5%[51]。为降低损伤风险，理想的导管尺寸需在创伤最小化与尺寸适配性之间取得平衡。

该数值足以确保充足的灌注流量和较低的肾内压力。当插入UAS时，输尿管镜的外径会直接影响流出阻力。在此背景下，“内镜-鞘管直径比（RESD）”这一概念对于优化流出阻力至关重要。方等人[52]研究了肾内压力与RESD的关系，得出结论：保持RESD低于0.75对于维持安全的肾内压力至关重要，这能实现灌注液的高效循环，进而帮助调节肾内温度。

得益于更纤细的柔性输尿管肾镜问世，医生可针对不同临床情况灵活组合UAS与输尿管镜，即便面对输尿管狭窄患者，仍能确保安全的RESD范围。

在激光碎石术中减少热损伤的一种有效方法是采用负压吸引技术。这项技术最初应用于经皮肾镜取石术已有25年以上历史，近年来在输尿管镜检查领域也逐渐受到重视。如今，负压吸引不仅用于清除结石碎屑以实现无结石效果，还能有效降低肾内压力和温度——这在高功率激光时代已成为重要考量因素。目前输尿管镜检查中常用的负压吸引技术包括负压输尿管套管（SUAS）、柔性导航套管（FANS）以及内镜直吸（DISS）。负压吸引能主动降低肾内压力，通过用低温冲洗液替代温热冲洗液，理论上可减少超过热剂量阈值的风险[53,54]。在相同RESD值下，SUAS在降低肾内压力和提升冲洗流量方面比传统肾盂输尿管连接术（UAS）更有效。对于采用SUAS的输尿管结石碎石术（RIRS），建议将RESD值控制在0.85以下[55]。除了主动抽吸外，虹吸效应——这种由两点高度差产生的简单流体动力学现象——同样能有效调控血流，进而影响体温变化[56]。不过，目前关于抽吸和虹吸效应对肾内温度影响的临床前及临床证据仍显不足，这凸显了开展深入研究的必要性。

未来视角

目前针对肾内温度安全阈值的人体研究仍较为有限（表1）。尽管已有大量*体外*和*体内*研究提出了降低肾内温度的策略，但需谨慎解读这些研究结果，因为临床前研究结果并不总能直接转化为临床疗效[29]。Emerg-

https://doi.org/10.4111/icu.20240369

表1.激光碎石术中IRT变化的临床研究

研究	工作的空间（编号主题	激光激活方案	流入条件	温度测量工具	主要发现
Æsøy等人[17] (2024)	肾盂 (n=10)	• 激光功率：5、10、20和30 W • 持续激光激活120秒，停用后监测60秒 • 当IRT达到43°C时，激光将被关闭。	• UreaMist FURS • 重力灌溉（23°C），60 cm • TFL/150μm光纤	K型热电偶插入肾造瘘管	• IRT与功率设置相关 • 使用20W的三名患者和使用30W的八名患者的体温均达到43°C。 • 在30瓦和20瓦两种功率设置下，达到阈值所需的最短激活时间分别为12秒和28秒。 • IRT与肾APD存在显著相关性。 • 采用无鞘管技术时，应避免使用20瓦的功率设置，尤其在肾盂未扩张的情况下。
滕等人[22] (2021)	肾盂 (n=32)	• 激光功率：1 J/20 Hz和0.5 J/20 Hz 1) 对花萼进行60秒激光激活并同步灌注——温度变化每5秒记录一次。 2) 激光激活无需冲洗——记录达到43°C所需时间。 • 当IRT达到43°C时，激光将被关闭。	• Storz纤维光导软性输尿管镜 • Ho：YAG/200μm光纤 • 灌注流速：0 mL/min、15 mL/min和30 mL/min • 12/14 Fr UAS	K型热电偶连接至内窥镜（尖端距离远端5 mm）	• 在15 mL/min或30 mL/min的灌溉条件下，无论是1 J/20 Hz还是0.5 J/20 Hz，60秒激光激活后均未达到43°C。 • 在功率设置为1 J/20 Hz和灌注流速为15 mL/min时，温度升高的幅度显著高于其他组。 • 在不进行灌溉的情况下，达到43°C所需的时间（1焦耳/20赫兹）显著短于0.5焦耳/20赫兹条件下的时间（8.84±1.41秒对比），13.71±1.53 s).
Wu等人[36] (2023)	肾盂 (n=22)	• 激光功率：24 W、80 Hz/0.3 J和32 W、80 Hz/0.4 J • 60s激光激活	• Olympus光纤输尿管镜 • Ho：YAG moses/200μm激光光纤 • 室温灌注（25°C） • 12/14 Fr UAS	将热电偶连接至内窥镜（其尖端距离远端5 mm）	1) 室温灌注（25°C） • 使用30 mL/min或60 mL/min的灌注液，任何患者在60秒激光激活后，IRT温度均未达到43°C。 2) 温水冲洗（37°C）， • 在32瓦、30毫升/分钟和40瓦、30毫升/分钟的设置下，继续激光激活后，IRT温度接近或超过43°C。
王等人[18] (2019)	输尿管（n=27）（30套）	激光功率：10-50 W（设置未知）	• 半刚性输尿管镜（WOLF 8.0/9.8 Fr） • Ho：YAG/550μm激光光纤	热电偶测温导线	• 30组数据中最高温度均超过43°C（100%），其中19组（63.3%）的峰值温度超过56°C。

IRT：肾内温度；FURSL：输尿管镜碎石术；TFL：钬光纤激光；APD：前后径；Ho：YAG：钬激光；UAS：输尿管套管。

如今，新技术已融入柔性输尿管肾镜系统，可实时监测温度，确保其保持在安全范围内[45]。这些技术进步有助于我们更深入地理解温度对输尿管镜检查临床效果的影响。

结论

在进行激光碎石术时，肾内温度可能显著升高，此时充分的冲洗液循环对控制温度至关重要。进行高功率激光碎石术时，特别是在解剖结构狭窄的部位，理解热剂量的概念尤为重要。通过优化能量输送策略并提升系统热容量，是维持安全温度水平、降低输尿管镜检查中温度相关并发症风险的关键所在。

利益冲突

洪承奎自2025年起担任《调查与临床泌尿学》主编，另一位作者无利益冲突。

资金

没有一个

作者贡献

研究构思与设计：金亨俊（Hyung Joon Kim）

成奎洪负责数据采集，金亨俊负责统计分析和数据分析解读，金亨俊同时参与论文初稿撰写与修订工作。行政、技术及物资支持由金亨俊提供，成奎洪负责项目监督，并对最终稿件进行审定。

剧本：金炯俊和洪成奎。

参考文献

1. 沃林DA、卡洛斯EC、海姆WR、盾蒙斯WN、普雷司格GM、利普金ME.激光参数与冲洗速率对钬激光碎石术中输尿管温度的影响（体外模型研究）。《泌尿内镜杂志》2018；32：59–63。
2. 赫尔斯H、特尼BW.泌尿系结石疾病趋势：医院就诊数据五年更新报告。BJU国际会议2016；118：785-9.
3. Jung HD、Lee JY、Kang DH、Ko K、Koh DH、Kwon O等：韩国内镜泌尿外科与机器人学会（KSER）出版与研究委员会。韩国内镜泌尿外科与机器人学会（KSER）关于尿路结石诊断、治疗及预防的建议。Investig Clin Urol 2023；64：325–37。
4. 莫利纳WR、卡雷拉RV、屈BH、克努森BE。输尿管激光碎石术中的温度升高：超脉冲铥光纤激光器（SPTF）与高功率120 W钬-钇铝石榴石激光器（Ho：YAG）的对比研究。《世界泌尿外科杂志》2021；39：3951–6。
5. Chai CA, Inoue T, Somani BK, Yuen SKK, Ragoori D, Gadzhiev N, et al.比较铥光纤与高功率钬激光在双侧同侧俯位进行肾镜取石术中的应用:一项多中心研究结果.Investig Clin Urol 2024;65:451–8.
6. Panthier F, Solano C, Chicaud M, Kutchukian S, Candela L, Doizi S, et al.Dornier脉冲式调态铥YAG激光在RIRS中的初步临床应用:前25例病例.《世界泌尿外科杂志》2023;41:2119–25.
7. 奥特纳G、赖斯P、纳格尔U、赫尔曼TRW、索马尼BK、托卡斯T.肾结石碎石术与组织消融术中的组织热效应：钬激光与铥激光实验研究的系统综述。《世界泌尿外科杂志》2023;41:1-12.
8. 海因S、佩格尔德R、奈恩塔勒M、韦特奥尔U、米尔尼克A.铒掺杂钇铝石榴石激光碎石术的热效应：体外模型实时评估。《世界泌尿学杂志》2018；36：1469–75。
9. 詹森ED、阿绍尔T、弗伦兹M、莫塔梅迪M、德拉克雷塔兹G、韦尔奇AJ。钬激光消融过程中脉冲持续时间对气泡形成及激光诱导压力波的影响。《激光外科与医学》1996；18：278–93。
10. 阿尔杜基AH、霍尔TL、加尼KR、麦克斯韦AD、麦克康纳吉B、罗伯茨WW.高功率钬激光碎石术中猪体内肾盂温度研究。《消化内镜杂志》2018；32：724–9。
11. Aldoukhi AH, Roberts WW, Hall TL, Teichman JMH, Ghani KR.理解钬激光碎石术中粉尘产生的爆米花效应。《泌尿外科》2018；122：52–7。
12. Marom R, Dau JJ, Hall TL, Ghani KR, Louters MM, Kim HJ, 等.输尿管镜检查中激光功率与冲洗速率的热安全边界:基于Ho:YAG激光的猪体内评估.《泌尿外科》2023;180:81–5.
13. Zhang X, Liu Z, Chen X, Li D, Yang Z, Gu J, et al.Soton输尿管镜在柔性输尿管镜碎石术后感染中的应用效果.Wideochir Inne Tech Maloinwazyjne 2022;17:232–9.
14. 山下S、井上T、今井S、丸山Y、岩桥Y、德口R等。流体温度在过程中的动态变化

https://doi.org/10.4111/icu.20240369

采用多种激光模式进行激光照射：一项基于热成像的体外模型研究。《临床医学杂志》2023；12：1409。

15. Sapareto SA，Dewey WC.乳腺癌治疗中的热剂量测定.国际放射肿瘤学、生物学与物理学杂志1984；10：787-800.

16. Yarmolenko PS, Moon EJ, Landon C, Manzoor A, Hochman DW, Viglianti BL, 等.正常组织热损伤阈值的最新进展.《国际热疗杂志》2011;27:320-43.

17. Æsøy MS，Julieba-Jones P，Beisland C，UlvikØ.柔性输尿管镜激光碎石术中的温度监测：一项前瞻性临床试验。《内镜泌尿外科杂志》2024；38：308-15。

18. 王XK、蒋ZQ、谭J、尹GM、黄K.输尿管镜下钬激光碎石的热效应.中国医学期刊（英文版）2019；132：2004-7.

19. 阿尔杜基AH，加尼KR，霍尔TL，罗伯茨WW.高功率钬激光碎石术的热反应。《泌尿外科学杂志》2017；31：1308-12。

20. Æsøy MS，Julieba-Jones P，Beisland C，UlvikØ.布鲁顿光纤激光与钬：钇铝石榴石激光输尿管镜检查中的温度曲线：一项临床前研究结果。Scand J Urol 2022；56：313-9.

21. Ventimiglia E, Robesti D, Keller EX, Corsini C, Folcia A, Fan tin M, 等.内窥镜激光激活过程中的温度分布提出热安全距离概念.《世界泌尿学杂志》2024;42:453.

22. 滕杰，王勇，贾志，关勇，曹伟，艾旭.柔性输尿管镜钬：钇铝石榴石激光碎石术中膀胱输尿管冲洗液的温度变化特征.国际泌尿肾病杂志2021；53：415-9.

23. Belle JD，Chen R，Srikureja N，Amasyali AS，Kehela M，Baldwin DD.体外研究显示新型钕光纤激光器是否比传统钬激光器更容易导致尿路上皮热损伤？《泌尿外科学杂志》2022；36：1249-54。

24. Sierra A，Corrales M，Somani B，Traxer O.激光效率与安全性：钬YAG激光器与钕光纤激光器的对比。《临床医学杂志》2022；12：149。

25. Aldoukhi AH, Dau JJ, Majdalany SE, Hall TL, Ghani KR, Hollingsworth JM, 等.尿道镜碎石术中激光激活模式对盐状体液体温度及热剂量的影响.《泌尿外科学杂志》2021;35:1217-22.

26. Louters MM，Dau JJ，Hall TL，Ghani KR，Roberts WW.激光操作员工作周期对温度和热剂量的影响：体外研究。World J Urol 2022；40：1575-80。

27. Rezakahn Khajeh N，Hall TL，Ghani KR，Roberts WW.激光碎石术中肾盂容量与尿液温度升高的研究。《泌尿外科学杂志》2022；36：22-8。

28. Winship B, Wollin D, Carlos E, Peters C, Li J, Terry R, et al.输尿管镜钬激光碎石术中高温波动的升降规律.《泌尿外科学杂志》2019;33:794-9.

29. 迪恩·NS，克拉姆贝克·AE。上尿路的内镜下手术及其对肾内压力的影响

温度。《J Endourol》2023；37：191-8。

30. Liang H, Liang L, Yu Y, Huang B, Chen J, Wang C, 等.霍尔姆激光在输尿管镜碎石术中的热效应.BMC Urol 2020;20:69.

31. 莫利纳WR、席尔瓦IN、多纳利西奥-达席尔瓦R、古斯塔夫森D、塞赫特D、金FJ。生理盐水对激光碎石术激活温度曲线的影响。《泌尿内镜杂志》2015；29：235-9。

32. Yamashita S, Inoue T, Imai S, Iwahashi Y, Deguchi R, Muraoka S, 等学者基于热成像技术对比了Moses模式与虚拟盲模式的灌注温度差异.该研究采用体外模型进行验证.相关成果发表于《泌尿外科学杂志》2023年第37卷第179-184页.

33. Villena JM，Elorrieta V，Salvado JA.Mo ⁴⁺/³⁺ 2.0在输尿管镜检查中的温度效应：体外评估.Cent European J Urol 2023；76：331-5.

34. Noureldin YA, Farsari E, Ntasiotis P, Adamou C, Vagionis A, Vrettos T, et al.高功率激光柔性输尿管镜检查中灌注参数与套管尺寸对肾内温度的影响.《世界泌尿外科杂志》2021;39:1257-1262.

35. 海因·S、佩措尔德·R、苏亚雷斯-伊巴罗拉·R、穆勒·PF、舍恩塔勒·M、米尔尼克·A.Ho：YAG激光碎石术在逆行肾内手术及经皮肾镜碎石术中的热效应研究——基于离体猪肾模型。《世界泌尿外科杂志》2020；38：753-60。

36. Wu Z, Wei J, Sun C, Huangfu Q, Wang B, Huang G, 等.高倍率柔性输尿管镜下钬激光碎石术中肾盏温度变化:病例分析研究.《国际泌尿与肾脏病学》2023;55:1685-92.

37. Peteinaris A, Tsaturyan A, Bravou V, Tatanis V, Faria-Costa G, Pagonis K, et al.高功率激光碎石术——是治疗还是伤害?钕光纤激光在体内研究中温度效应的组织学评估.Cent European J Urol 2023;76:44-8.

38. Peng Y, Liu M, Ming S, Yu W, Li L, Lu C, et al.新型钕光纤激光在碎石术中的安全性:体外热效应及其影响因子研究.《泌尿外科学杂志》2020;34:88-92.

39. Winship B, Terry R, Boydston K, Carlos E, Wollin D, Peters C, 等学者研究发现,钬激光(钇铝石榴石激光)脉冲类型会影响台式输尿管模型的灌注温度.相关成果发表于《泌尿外科学杂志》2019年第33卷第896-901页.

40. 哈迪LA，维尼琴科V，弗里德NM.高功率钬：YAG与钕光纤激光治疗肾结石的尘埃模式：消融率和碎片大小研究。Lasers Surg Med 2019；51：522-30。

41. Aldoukhi AH，Roberts WW，Hall TL，Ghani KR.注意工作距离：改变脉冲宽度或调制时激光光纤工作距离对碎石效果的影响。《泌尿外科学杂志》2019；33：120-6。

42. 德得亚里斯A、法伊塔齐亚迪斯S、茨图里扬A、巴戈尼斯K、利亚沃科斯

E，Kallidonis P.摩西™脉冲调制技术与传统脉冲输送技术：对输尿管软镜检查期间灌注液温度的影响。《泌尿系结石》2022；50：613-8。

43. 布蒂切S，塞纳尔TE，普罗耶蒂S，德拉戈斯L，特菲克T，多伊齐S等.肾脏温度变化：钬-钇-铝石榴石激光治疗期间的生理反应？《泌尿内镜杂志》2016；30：574-9.

44. Rezakahn Khajeh N，Hall TL，Ghani KR，Roberts WW.柔性输尿管镜检查时的灌注流量测定：基于肾盂压力的计算方法。《泌尿内镜杂志》2022；36：1405-10。

45. 杨杰，李志，赖聪，徐科.一种新型温控柔性输尿管镜系统的体内评估：用于输尿管镜检查期间监测和调控肾内温度。《泌尿外科》2024；191：38-44。

46. Dau JJ，Hall TL，Maxwell AD，Ghani KR，Roberts WW.冷却冲洗对激光碎石术中肾盂液温度及热损伤阈值时间的影响：体外模型。《泌尿内镜杂志》2021；35：700-5。

47. Dau JJ，Rezakahn Khajeh N，Hall TL，Roberts WW.冷却冲洗技术在尿道镜激光碎石术中控制温度升高的应用：猪体内模型研究。《泌尿内镜杂志》2022；36：403-9。

48. Aldoukhi AH, Black KM, Hall TL, Ghani KR, Maxwell AD, MacConaghy B. 等学者《热安全激光碎石术功率与灌洗参数的界定:体外模型研究》发表于《泌尿外科学杂志》2020年第34卷第76-81页.

49. Kim HJ，Louters MM，Dau JJ，Hall TL，Ghani KR，Roberts WW.输尿管引流管流出阻力的量化

输尿管镜检查中使用的器械。《世界泌尿外科杂志》2023；41：873-8。

50. 加列戈斯H，布拉沃JC，塞普尔维达F，阿斯托萨GM.体外模型中钬激光碎石术的肾内温度测量。《欧洲泌尿学中心期刊》2021；74：588-94。

51. Traxer O，Thomas A.逆行肾内手术中置入输尿管套管所致输尿管壁损伤的前瞻性评估与分类.J Urol 2013；189：580-4.

52. Fang L, Xie G, Zheng Z, Liu W, Zhu J, Huang T, 等学者研究了内窥镜鞘管直径比值对柔性输尿管镜激光碎石术中盆腔内压的影响.《内镜泌尿外科杂志》2019年第33卷第132-139页.

53. Solano C, Chicaud M, Kutchukian S, Candela L, Corrales M, Panthier F, 等.优化输尿管镜检查结果:吸引技术的叙述性综述.临床医学杂志2023;12:2815.

54. Yuen SKK, Traxer O, Wroclawski ML, Gadzhiev N, Chai CA, Lim EJ, 等.实验与临床证据的范围综述及其对吸引输尿管套管开发的影响.Diagnostics(巴塞尔)2024;14:1034.

55. 施杰，黄涛，宋冰，刘伟，程毅，方亮.负压输尿管套管内窥镜鞘管直径的最佳配比：体外实验研究.《世界泌尿外科杂志》
2024;42:122.

56. Kim HJ，Louters MM，Dau JJ，Hall TL，Ghani KR，Roberts WW.体外肾输尿管模型下输尿管镜检查对肾盂压力的虹吸效应影响.世界泌尿学杂志2024；42：415.

https://doi.org/10.4111/icu.20240369

DOI:10.16662/j.cnki.1674-0742.2024.02.086

输尿管狭窄在输尿管结石输尿管镜钬激光碎石术后患者中的发生情况及其危险因素研究

刘培，任海峰，代传真
印江县人民医院泌尿外科，贵州铜仁 555200

[摘要] **目的** 探讨输尿管结石输尿管镜钬激光碎石（Ureteroscopic Holmium Laser Lithotripsy，URHL）术后患者输尿管狭窄的发生情况及其影响因素。**方法** 方便选取2020年1月—2023年3月印江县人民医院泌尿外科收治的246例输尿管结石患者为研究对象，所有患者均接受URHL治疗。按照术后是否存在输尿管狭窄分为狭窄组（14例）、非狭窄组（232例）。统计两组患者的临床资料，对其进行单因素、多因素分析，以筛选输尿管结石URHL术后患者发生输尿管狭窄的危险因素。**结果** 单因素分析结果显示，狭窄组中病程≥3个月、结石直径>2 cm、存在息肉包裹、存在嵌顿结石、激光碎石时间>60 min的患者占比均显著高于非狭窄组，差异有统计学意义（P均<0.05）；多因素Logistic回归分析结果显示，病程≥3个月、结石直径>2 cm、存在息肉包裹、存在嵌顿结石、激光碎石时间>60 min均为输尿管结石URHL术后患者发生输尿管狭窄的危险因素，差异有统计学意义（OR=2.349、2.004、3.384、3.600、4.166，P均<0.05）。**结论** 病程≥3个月、结石直径>2 cm、存在息肉包裹、存在嵌顿结石、激光碎石时间>60 min均为输尿管结石URHL术后患者发生输尿管狭窄的危险因素，根据上述结果给予高危患者针对性干预措施，进而降低输尿管狭窄的发生风险。

[关键词] 输尿管狭窄；输尿管结石；输尿管镜；钬激光碎石术；危险因素
[中图分类号] R693.4 [文献标识码] A [文章编号] 1674-0742(2024)01(b)-0086-04

Occurrence and Risk Factors of Ureteral Stricture in Patients with Ureteral Calculi after Ureteroscopic Holmium Laser Lithotripsy

LIU Pei, REN Haifeng, DAI Chuanjino
Department of Urology, Yinjiang County People's Hospital, Tongren, Guizhou Province, 555200 China

[Abstract] Objective To investigate the occurrence and influencing factors of ureteral stricture after ureteroscopic holmium laser lithotripsy (URHL). **Methods** A total of 246 patients with ureteral calculi admitted to the Department of Urology of Yinjiang County People's Hospital from January 2020 to March 2023 were conveniently selected and treated with URHL. According to the presence or absence of ureteral stenosis, the patients were divided into stenosis group (14 cases) and non-stenosis group (232 cases). The clinical data of the two groups were analyzed, and univariate and multivariate analyses were performed to screen the risk factors of ureteral stricture in patients with ureteral calculi after URHL. **Results** Univariate analysis showed that the proportion of patients with disease course ≥3 months, stone diameter >2 cm, polyp encapsulation, incarcerated stones, laser lithotripsis time >60 min in the stenosis group were significantly higher than that in the non-stenosis group, and the differences were statistically significant (all P<0.05). Multivariate Logistic regression analysis showed that duration ≥3 months, stone diameter >2 cm, polyp encapsulation, incarcerated stones, and laser lithotripsy time >60 min were all risk factors for ureteral stricture after URHL, and the differences were statistically significant (OR=2.349, 2.004, 3.384, 3.600, 4.166, all P<0.05). **Conclusion** Duration ≥3 months, stone diameter >2cm, polyp encapsulation, incarcerated stones, and laser lithotripsy time >60 min are all risk factors for ureteral stricture in patients with URHL. Targeted interventions can be given to high-risk patients according to the above results, so as to reduce the risk of ureteral stricture.

[作者简介] 刘培（1980-），男，本科，主治医师，研究方向为泌尿系结石。

(C)1994-2024 China Academic Journal Electronic Publishing House. All rights reserved. http://www.cnki.net

[Key words] Ureteral stenosis; Ureteral calculi; Ureteroscope; Holmium laser lithotripsy; Risk factor

输尿管结石为泌尿外科常见疾病，大约有89%都来自于肾脏，主要临床表现为肾绞痛和血尿，给患者身体健康带来较大安全隐患[1]。随着医疗水平及设备的不断发展进步，结石输尿管镜钬激光碎石（Ureteroscopic Holmium Laser Lithotripsy，URHL）开始应用于输尿管结石患者的治疗中，但输尿管镜属于一种有创性检查，会导致患者的输尿管道出现不同程度的损伤，且输尿管的损伤会引发输尿管狭窄，而输尿管狭窄又会导致输尿管梗阻和肾功能进行性恶化[2-3]。目前对输尿管结石URHL术后患者发生输尿管狭窄的相关研究较少，但目前关于影响输尿管结石URHL术后患者发生输尿管狭窄的相关因素仍需要进一步进行探讨，评估术后发生输尿管狭窄的危险因素并进行术后及早预防，对改善患者预后具有重要意义[4]。因此，本研究方便选取2020年1月—2023年3月印江县人民医院泌尿外科收治的246例输尿管结石患者为研究对象，探讨输尿管结石URHL术后患者输尿管狭窄的发生情况及其影响因素，现报道如下。

1 资料与方法

1.1 一般资料

方便选取本院收治的246例输尿管结石患者为研究对象，所有患者均接受URHL治疗，按照术后是否发生输尿管狭窄分为狭窄组（14例）、非狭窄组（232例）。本研究经医院医学伦理委员会批准（231101）。

1.2 纳入与排除标准

纳入标准：与输尿管结石依据《中国泌尿外科疾病诊断治疗指南》[5]中的相关诊断标准高度符合者，均经泌尿系CT、腹部平片及CT尿路系统成像等确诊为输尿管结石者；入组前未接受其他治疗者等。排除标准：无法耐受输尿管手术者；合并肝癌、胃癌、肺癌等恶性肿瘤疾病者；先天性输尿管开口狭窄者。

1.3 方法

患者取截石位，采用腰硬麻或者全麻，常规消毒铺巾，采用输尿管镜及激光碎石机，直视下将硬性输尿管镜放置在尿道中，进入患者膀胱；确认患侧输尿管口后，将引导斑马导丝置入患侧输尿管，在导丝的引导下推入输尿管镜到达结石处；然后将220 μm钬激光光纤插入输尿管结石部，设置光纤功率为50 W，于直视下利用蚕食法将结石击碎成2~3 mm大小的碎片，依次检查上、中、下各盏，较大的结石用取石钳取出，然后残石碎片借助异物钳取出；完成碎石、取石后，留置F5-F7双J管于输尿管内引流1周，术后根据患者情况决定是否延长，保留导尿，所有操作均由同一医生完成。

1.4 观察指标

①输尿管狭窄发生情况：随访并记录患者术后3个月内输尿管狭窄发生情况，输尿管狭窄定义：术后复查CT尿路系统成像提示输尿管存在输尿管上段及肾盂扩张，且集合系统扩张>1 cm。②单因素分析：收集所有研究对象临床资料，包括性别、年龄、病程、体质指数、结石直径、结石部位、息肉包裹、嵌顿结石、激光碎石时间，并进行单因素分析。③多因素分析：自变量为单因素分析具有统计学意义的指标，因变量为术后随访是否发生输尿管狭窄，通过Logistic回归分析法分析输尿管结石URHL术后患者发生输尿管狭窄的影响因素。

1.5 统计方法

用SPSS 25.0统计学软件分析数据，性别、年龄、病程等为计数资料，用例数（n）和率（%）表示，行χ^2检验；体质指数为符合正态分布的计量资料，用（$\bar{x}\pm s$）表示，行t检验；Logistic回归分析筛选相关危险因素。P<0.05为差异有统计学意义。

2 结果

2.1 输尿管狭窄发生情况

246例输尿管结石患者术后3个月内共发生输尿管狭窄14例（5.69%）。

2.2 单因素分析

单因素分析结果显示，狭窄组中病程≥3个月、结石直径>2 cm、存在息肉包裹、存在嵌顿结石、激光碎石时间>60 min的患者占比均显著高于非狭窄组，差异有统计学意义（P均<0.05），见表1。

2.3 多因素分析

多因素分析结果显示，病程≥3个月、结石直径>2 cm、存在息肉包裹、存在嵌顿结石、激光碎石时间>60 min均为输尿管结石URHL术后患者发生输尿管狭窄的危险因素，差异有统计学意义（P均<0.05），见表2。

(C)1994-2024 China Academic Journal Electronic Publishing House. All rights reserved. http://www.cnki.net

表1 输尿管结石URHL术后患者发生输尿管狭窄的单因素分析

因素	非狭窄组（n=232）	狭窄组（n=14）	χ^2/t值	P值
性别[n(%)]			2.988	0.084
男	209(90.07)	10(71.43)		
女	23(9.91)	4(28.57)		
年龄[n(%)]			1.470	0.225
<65岁	87(37.50)	3(21.43)		
≥65岁	145(62.50)	11(78.57)		
病程[n(%)]			4.275	0.039
<3个月	147(63.36)	5(35.71)		
≥3个月	85(36.64)	9(64.29)		
体质指数[($\bar{x}\pm s$),kg/m^2]	26.07±0.17	25.99±0.14	1.729	0.085
结石直径[n(%)]			23.792	<0.001
<1 cm	159(68.53)	4(28.57)		
1~2 cm	53(22.84)	3(21.43)		
>2 cm	20(8.62)	7(50.00)		
结石部位[n(%)]			0.404	0.817
上段	29(12.50)	1(7.14)		
中段	103(44.40)	7(50.00)		
下段	100(43.10)	6(42.86)		
息肉包裹[n(%)]			3.895	0.048
是	66(28.45)	8(57.14)		
否	166(71.55)	6(42.86)		
嵌顿结石[n(%)]			8.214	0.004
是	78(33.62)	10(71.43)		
否	154(66.38)	4(28.57)		
激光碎石时间[n(%)]			7.348	0.025
<30 min	155(66.81)	6(42.86)		
30~60 min	71(30.60)	6(42.86)		
>60 min	6(2.59)	2(14.29)		

表2 输尿管结石输尿管镜钬激光碎石术后患者发生输尿管狭窄的多因素分析

变量	β值	S.E.值	Waldχ^2值	P值	OR值(95%CI)
病程≥3个月	0.854	0.217	15.488	<0.001	2.349(1.535~3.594)
结石直径>2 cm	0.695	0.201	11.956	0.001	2.004(1.351~2.971)
存在息肉包裹	1.219	0.346	12.412	<0.001	3.384(1.717~6.667)
存在嵌顿结石	1.281	0.418	9.392	0.002	3.600(1.587~8.168)
激光碎石时间>60 min	1.427	0.369	14.955	<0.001	4.166(2.021~8.587)

3 讨论

随着医疗技术的发展与进步，URHL逐渐成为治疗输尿管结石的主要术式，但术后可能会出现输尿管狭窄，其属于一种常见的术后并发症，会对患者的肾功能带来一定程度的影响。若能有效地评估URHL术后患者发生输尿管狭窄的可能性，并分析其发生的影响因素，可进一步提高手术治疗效果，为改善患者预后提供依据[9]。

本研究结果显示，病程≥3个月、结石直径>2 cm、存在息肉包裹、存在嵌顿结石、激光碎石时间>60 min均为输尿管结石URHL术后患者发生输尿管狭窄的危险因素，分析其原因可能为：输尿管结石病程长会加重肾积水程度，尿液引流不畅又易引发结石逐渐增大，同时病程长易导致梗阻处输尿管产生炎症刺激后引发增生，出现炎性肉芽组织形成息肉，增加手术的复杂性以及输尿管损伤的风险，最终导致输尿管狭窄发生率升高[7]。结石直径越大，引起的梗阻程度也就越大，在进行碎石、取石的过程中，手术时间越长，术中灌洗时间越长，越容易损伤输尿管黏膜，使其出现充血水肿的情况，易发生术后输尿管狭窄[10]。息肉包裹结石对输尿管黏膜有刺激作用，术中输尿管镜的应用会进一步对输尿管产生进一步刺激、同时也会对结石的移动产生限制作用，从而提高手术操作中损坏黏膜的风险，进而可促使输尿管狭窄的发生[8]。嵌顿结石为一种较为特殊的病理类型，出现输尿管嵌顿者的输尿管壁受到长时间压迫，会导致管壁间质逐渐纤维化、水肿，容易引发炎性息肉产生，增加手术过程中碎石的难度及术后输尿管狭窄发生的风险。部分患者碎石难度大，手术时间较长，由于钬激光能量较高，长时间使用进行碎石过程中，激光的能量可造成输尿管黏膜局部热灼伤，对输尿管损伤风险更高，增加输尿管狭窄发生风险。因此，临床医师术前根据患者病情综合评估，选择合适的碎石工具，尽量缩短碎石时间；术中处理较大坚硬甚至嵌顿的结石时，需在结石边缘多处采用"虫噬法"；对于息肉包裹结石，操作时从息肉基底部开始处理，仅建议处理突入输尿管管腔内的部分，避免广泛烧灼输尿管息肉；碎石过程中尽量保持光纤在视野范围内，在没有充分暴露视野时，切勿暴力操作，应注意观察输尿管情况，当结石与输尿管发生粘连时，应先将其用抓钳抓取粘连组织，露出结石后再碎石，在尽量避免激光直接接触输尿管黏膜的前提下粉碎结石；控制碎石手术时间，在保证引流通畅的情况下尽量保证流动水，进而减小激光的热蓄加效应[10]。

综上所述，病程≥3个月、结石直径>2 cm、存在息肉包裹、存在嵌顿结石、激光碎石时间≥60 min均为输尿管结石URHL术后患者发生输尿管狭窄的危险因素，因此，可根据上述结果给予高危患者针对性干预措施，进而降低输尿管狭窄的发生风险，值得临床上的进一步研究。

（下转第101页）

(C)1994-2024 China Academic Journal Electronic Publishing House. All rights reserved. http://www.cnki.net

（上接第88页）

[参考文献]

[1] 张志成,廖继强.输尿管镜下钬激光碎石术后输尿管狭窄的危险因素分析[J].中国药物与临床,2020,20(8):1270-1272.

[2] 阳建辉.输尿管软镜钬激光碎石术联合标准通道经皮肾镜取石术在上尿路结石中的应用效果分析[J/CD].现代医学与健康研究:电子版,2022,6(3):67-70.

[3] 王淇超,曹敬毅,孙卫兵,等.输尿管软镜钬激光碎石术后继发输尿管狭窄的相关性因素分析[J].国际泌尿系统杂志,2022,42(3):433-436.

[4] 周乐,胡换春,汪波.单发输尿管结石患者行输尿管镜下钬激光碎石术后狭窄的危险因素分析[J].国际泌尿系统杂志,2020,40(2):231-234.

[5] 那彦群,叶章群,孙光.中国泌尿外科疾病诊断治疗指南[M].北京:人民卫生出版社,2011:132-146.

[6] 覃柱艺.输尿管软镜钬激光碎石术治疗肾结石对患者结石清除率及CRP、IL-6、TNF-α的影响[J/CD].现代医学与健康研究:电子版,2019,3(19):37-39.

[7] 刘跃闻,李建中,周亚军,等.输尿管镜钬激光碎石术后继发输尿管狭窄的危险因素分析[J].临床泌尿外科杂志,2019,34(8):621-624.

[8] 吴佳成,姜力,陆雅君.经尿道输尿管镜治疗输尿管结石后发生输尿管狭窄的危险因素分析[J].国际泌尿系统杂志,2019,39(3):505-509.

[9] 孟凯,李东.钬激光碎石术治疗输尿管结石后发生输尿管狭窄的危险因素分析[J].贵州医药,2020,44(9):1440-1441.

[10] 黄爱平,蔡圆圆,钟昉昉.输尿管结石行钬激光碎石术后输尿管狭窄的危险因素分析[J].浙江临床医学,2019,21(5):606-607.

（收稿日期:2023-10-14）

(C)1994-2024 China Academic Journal Electronic Publishing House. All rights reserved. http://www.cnki.net

输尿管镜钬激光碎石术后输尿管狭窄的危险因素研究

夏天成[①] 高茂[①] 徐国政[①] 张帅[①]

【摘要】 **目的：**分析输尿管镜钬激光碎石术后输尿管狭窄的独立危险因素。**方法：**选择2021年1月—2023年6月在无锡第八人民医院接受输尿管镜钬激光碎石术治疗的320例输尿管结石患者，根据术后随访1年是否发生输尿管狭窄，将患者分为狭窄组（n=26）和未狭窄组（n=294）。采用单因素和多因素分析评价输尿管结石患者术后输尿管狭窄的独立危险因素。**结果：**单因素分析结果显示，狭窄组结石最大径≥2 cm、结石嵌顿、中重度肾积水和钬激光损伤黏膜的患者占比均高于未狭窄组，且手术时间长于未狭窄组，差异均有统计学意义（P<0.05）。logistic回归分析表明，结石直径≥2 cm、结石嵌顿、中重度肾积水、手术时间和发生钬激光损伤黏膜是输尿管镜钬激光碎石术后输尿管狭窄的独立危险因素（P<0.05）；通过ROC曲线下面积来验证logistic回归模型。ROC曲线结果显示，预测模型的敏感度为84.6%，特异度为85.7%，AUC为0.888。**结论：**结石直径、结石嵌顿、中重度肾积水、手术时间及钬激光损伤黏膜是输尿管镜钬激光碎石术后输尿管狭窄的独立危险因素，logistic回归模型具有较高的预测敏感度和特异度，可有效预测术后输尿管狭窄的发生，为临床决策提供了有力支持。

【关键词】 输尿管结石 钬激光碎石术 输尿管狭窄 危险因素

Study on the Risk Factors of Ureteral Stricture after Ureteroscopic Holmium Laser Lithotripsy/XIA Tiancheng, GAO Mao, XU Guozheng, ZHANG Shuai. //Medical Innovation of China, 2025, 22(06): 116-120

[Abstract] Objective: To analyze the independent risk factors of ureteral stricture after ureteroscopic holmium laser lithotripsy. **Method:** A total of 320 patients with ureteral calculi who received ureteroscopic holmium laser lithotripsy treatment in Wuxi No.8 People's Hospital from January 2021 to June 2023 were selected. According to whether ureteral stenosis occurred during 1 year postoperative follow-up, the patients were divided into a narrow group (n=26) and a non-narrow group (n=294). Independent risk factors for postoperative ureteral stricture in patients with ureteral calculi were evaluated by univariate and multivariate analysis. **Result:** The results of univariate analysis showed that the proportions of patients with maximum stone diameter ≥2 cm, stone incarceration, moderate and severe hydronephrosis and holmium laser injury of mucosa in the narrow group were higher than those in the non-narrow group, and the operation time was longer than that in the non-narrow group, the differences were statistically significant (P<0.05). logistic regression analysis showed that stone diameter ≥2 cm, stone entrapment, moderate and severe hydronephrosis, operation time and the occurrence of holmium laser damage were independent risk factors for ureteral stenosis after ureteroscopic holmium laser lithotripsy (P<0.05). The logistic regression model was verified by the area under ROC curve. ROC curve results showed that the sensitivity of the prediction model was 84.6%, the specificity was 85.7%, and the AUC was 0.888. **Conclusion:** Stone diameter, stone incarceration, moderate to severe hydronephrosis, operation time and holmium laser lesion of the mucosa are independent risk factors for ureteral stricture after ureteroscopic holmium laser lithotripsy. logistic regression model has high predictive sensitivity and specificity, which can effectively predict the occurrence of postoperative ureteral stenosis, and provide strong support for clinical decision-making.

[Key words] Ureteral calculi Holmium laser lithotripsy Ureteral stricture Risk factors

First-author's address: Department of Urology, Wuxi No.8 People's Hospital, Wuxi 214142, China

doi: 10.3969/j.issn.1674-4985.2025.06.027

①无锡市第八人民医院泌尿外科 江苏 无锡 214142
通信作者：夏天成

中国知网 https://www.cnki.net

输尿管结石由肾结石下降，排入输尿管所引起，其发病率呈上升趋势[1-2]。输尿管镜钬激光碎石术因其微创、高效和安全等优点而成为治疗输尿管结石的主要方法[3-5]。尽管该技术应用广泛，但术后输尿管狭窄的发生仍然是一个不容忽视的并发症[6-8]，给患者带来了较大的痛苦和经济负担。输尿管狭窄不仅影响患者的生活质量，还可能导致严重的泌尿系统并发症，如肾积水和肾功能衰竭等[9-10]。因此，研究输尿管镜钬激光碎石术后输尿管狭窄的危险因素具有重要的临床意义。本研究旨在通过回顾性分析输尿管结石患者的临床资料，利用单因素和多因素 logistic 回归分析方法，系统评估术后输尿管狭窄的独立危险因素，以期为临床预防和治疗提供科学依据。

1　资料与方法

1.1　一般资料

选取 2021 年 1 月—2023 年 6 月在无锡第八人民医院接受治疗的 320 例输尿管结石患者作为研究对象。纳入标准：（1）首次接受输尿管镜钬激光碎石术治疗。（2）具备完整的临床资料。（3）符合钬激光碎石术适应证的输尿管结石。排除标准：（1）恶性肿瘤、肝肾功能障碍及免疫系统疾病。（2）术前已放置输尿管支架。（3）有输尿管手术史、输尿管息肉、肾结石及既往输尿管狭窄病史。（4）术前检查提示有输尿管狭窄。（5）手术过程中发生意外损伤。本研究已获本院医学伦理委员会的审查和批准。

1.2　方法

收集并记录患者基本资料和疾病资料，所有患者均接受输尿管镜钬激光碎石术。术后通过门诊或电话随访 1 年，以记录输尿管狭窄的发生情况。单因素分析用于评估各因素与输尿管狭窄发生的关系，设定 P<0.05 为标准，将多变量纳入多元 logistic 回归分析，以筛选出影响输尿管镜下钬激光碎石术后并发输尿管狭窄的因素。

1.3　观察指标与评判标准

收集并比较患者的临床信息和基础数据。（1）病程：记录患者自诊断输尿管结石到手术的时间间隔；（2）体重、性别、年龄：记录患者的体重、性别和年龄；（3）钬激光对黏膜的损伤：在手术过程中记录钬激光对输尿管黏膜的损伤情况；（4）手术时间：记录从手术开始到结束的总时间；（5）肾积水程度：根据泌尿系 CT 扫描和超声检查结果进行判断，轻度肾积水为肾形态、肾实质厚度和回声正常、肾集合系统分离 2~3 cm，中度肾积水为肾柱显示不清，肾实质变薄，肾体积增大，肾集合系统分离 3~4 cm 并表现出明显的扩张，重度肾积水为肾柱出现放射状回声、肾实质明显变薄、区域位置为液性暗区、肾体积增大且形态异常；（6）结石大小：通过影像学检查（CT）测量并记录结石的最大直径。这些观察指标通过对比分析患者术后是否发生输尿管狭窄的组别差异，评估其对术后输尿管狭窄发生的影响，为临床预防和治疗提供依据。

1.4　统计学处理

本研究数据采用 SPSS 26.0 统计学软件进行分析和处理，计量资料以（$\bar{x}\pm s$）表示，组间比较采用独立样本 t 检验，组内比较采用配对 t 检验；计数资料以率（%）表示，采用 χ^2 检验。以 P<0.05 为差异有统计学意义。使用 R 软件建立一般 logistic 回归模型，并通过 ROC 曲线下面积进行验证。ROC 曲线下面积>0.7，表明模型具有良好的区分度。

2　结果

2.1　输尿管镜钬激光碎石术后输尿管狭窄的单因素分析

单因素分析结果显示，狭窄组结石最大径≥2 cm、结石嵌顿、中重度肾积水和钬激光损伤黏膜的患者占比均高于未狭窄组，且手术时间长于未狭窄组，差异均有统计学意义（P<0.05），见表 1。

2.2　输尿管镜钬激光碎石术后输尿管狭窄的多因素 logistic 回归分析

以是否发生输尿管狭窄为应变量（否 =0，是 =1），结石最大径（<2 cm 赋值为 0，≥2 cm 赋值为 1）、结石嵌顿（否赋值为 0，是赋值为 1）、肾积水程度（轻度赋值为 0，中度赋值为 1，重度赋值为 2）、钬激光损伤黏膜（否赋值为 0，是赋值为 1）和手术时间（赋值为实测值）为自变量，进行多因素 logistic 回归分析（引入水准为 0.05，剔除水准为 0.10）；结果显示，结石直径≥2 cm、结石嵌顿、中重度肾积水、手术时间和发生钬激光损伤黏膜是输尿管镜钬激光碎石术后输尿管狭窄的独立危险因素（P<0.05），见表 2。

2.3　输尿管镜钬激光碎石术后输尿管狭窄的 ROC 曲线

通过 ROC 曲线下面积来验证 logistic 回归模型。模型公式为 Logit（P）=-7.566+1.855 × 结石最大径 +1.949 × 结石嵌顿 +1.174 × 肾积水程度 +1.074 × 钬激光损伤黏膜 +0.034 × 手术时间。结果显示，该模型预测输尿管镜钬激光碎石术后输尿管狭窄的敏感度为 84.6%，特异度为 85.7%，约登指数为 0.703，AUC 为 0.888，95%CI 为（0.819，0.957），见图 1。

中国知网 https://www.cnki.net

表1 输尿管镜钬激光碎石术后输尿管狭窄的单因素分析

组别	病程[个月，（$\bar{x}\pm s$）]	年龄[岁，（$\bar{x}\pm s$）]	性别[例（%）]		受影响位置[例（%）]		BMI[kg/m^2，（$\bar{x}\pm s$）]
			男	女	左	右	
狭窄组（n=26）	5.36±1.26	47.97±4.34	16（61.54）	10（38.46）	14（53.85）	12（46.15）	23.69±2.41
未狭窄组（n=294）	5.12±0.97	47.64±5.13	180（61.22）	114（38.78）	167（56.80）	127（43.20）	23.96±2.28
t/χ^2值	1.178	0.318	0.001		0.085		0.576
P值	0.240	0.751	0.975		0.771		0.565

组别	血钙[mmol/L，（$\bar{x}\pm s$）]	手术时间[min，（$\bar{x}\pm s$）]	结石最大径[例（%）]		结石嵌顿[例（%）]	
			<2 cm	≥2 cm	是	否
狭窄组（n=26）	2.43±0.30	56.28±16.28	14（53.85）	12（46.15）	20（76.92）	6（23.08）
未狭窄组（n=294）	2.37±0.33	48.94±14.20	257（87.41）	37（12.59）	96（32.65）	198（67.35）
t/χ^2值	0.895	2.496	20.758		20.258	
P值	0.372	0.013	<0.001		<0.001	

组别	肾积水程度[例（%）]			尿路感染并发症[例（%）]		钬激光损伤黏膜[例（%）]	
	轻度	中度	重度	是	否	是	否
狭窄组（n=26）	3（11.54）	8（30.77）	15（57.69）	22（84.62）	4（15.38）	13（50.00）	13（50.00）
未狭窄组（n=294）	140（47.62）	88（29.93）	66（22.45）	210（71.43）	84（28.57）	82（27.89）	212（72.11）
t/χ^2值	18.686			2.083		5.594	
P值	<0.001			0.149		0.018	

表2 输尿管镜钬激光碎石术后输尿管狭窄的多因素logistic回归分析

影响因素	B	SE	Waldχ^2值	P值	OR值	95%CI
结石最大径	1.855	0.509	13.287	0.000	6.389	2.357，17.318
结石嵌顿	1.949	0.534	13.299	0.000	7.022	2.463，20.016
肾积水程度	1.174	0.325	13.040	0.000	3.236	1.711，6.120
钬激光损伤黏膜	1.074	0.492	4.768	0.029	2.927	1.116，7.674
手术时间	0.034	0.017	4.181	0.041	1.035	1.001，1.069
常量	−2.566	1.242	37.115	0.000	0.001	

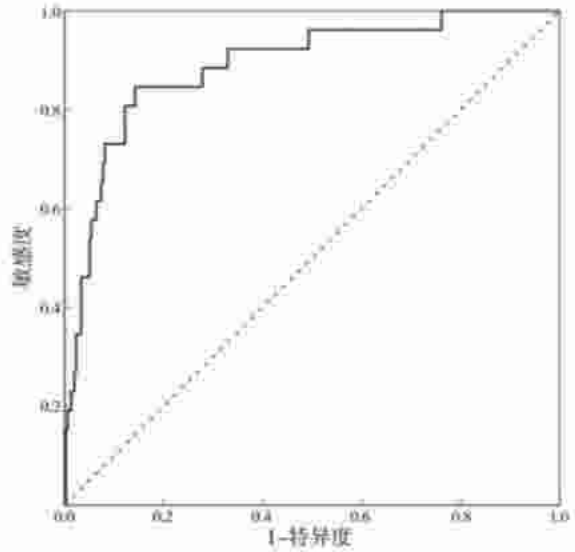


图1 输尿管镜钬激光碎石术后输尿管狭窄的ROC曲线

3 讨论

输尿管结石是泌尿系统中常见且高发的疾病，其主要表现为剧烈的腹痛、血尿和尿路梗阻，严重影响患者的生活质量[11-13]。随着微创手术技术的发展，输尿管镜钬激光碎石术因其创伤小、恢复快、疗效显著而成为治疗输尿管结石的首选方法[14-15]。然而，尽管该手术技术日益成熟，术后输尿管狭窄仍然是一个不可忽视的并发症，给患者带来了长期的健康风险和治疗挑战。术后输尿管狭窄的发生不仅影响患者的泌尿功能，还可能导致肾积水、感染等严重并发症，甚至危及肾功能[16-18]。研究表明，术后输尿管狭窄与术中操作、结石大小、结石嵌顿及肾积水程度等因素密切相关。Zheng等[19]的研究指出，结石嵌顿和肾积水是术后输尿管狭窄的重要风险因素，强调了术前和术中评估的必要性。此外，Wang等[20]的研究也发现，钬激光碎石术过程中产生的热效应可能导致黏膜损伤，进而增加狭窄的风险。基于此，明确术后输尿管狭窄的发生机制及其危险因素对提高手术疗效和预后具有重要意义。现有研究表明，结石大小、结石嵌顿时间、手术操作技术、术后护理等多种因素均可能影响术后输尿管狭窄的发生率。然而，这些研究多为单中心小样本

中国知网 https://www.cnki.net

研究，结果尚存在争议，且缺乏系统的回归分析。本研究通过回顾性分析大量输尿管结石患者的临床数据，利用单因素和多因素 logistic 回归分析评估了输尿管镜钬激光碎石术后输尿管狭窄的独立危险因素，旨在为临床实践提供科学依据，并探索有效的预防和干预措施。通过本研究，希望能够进一步揭示术后输尿管狭窄的发病机制，优化手术操作流程，制定个体化治疗方案，从而降低术后并发症的发生率，提高患者的生活质量。

本研究结果显示，结石最大径、结石嵌顿、肾积水程度、手术时间和钬激光损伤黏膜是输尿管狭窄的相关因素。进一步的 logistic 回归分析则揭示，结石直径大、结石嵌顿、中重度肾积水、手术时间长和钬激光损伤黏膜是独立的危险因素。首先，结石的最大径是影响术后输尿管狭窄发生的一个重要因素。较大的结石在碎石过程中需要更长的时间和更高的能量，这可能导致输尿管黏膜的广泛损伤和炎症反应，从而增加术后狭窄的风险。此外，较大的结石也更容易嵌顿在输尿管内，进一步加重局部的机械性损伤和炎症反应，影响输尿管的正常愈合过程。其次，结石嵌顿是另一个显著的独立危险因素。嵌顿的结石不仅增加了手术操作的难度，还会导致局部组织的缺血和坏死，这些病理变化都会促使输尿管黏膜的纤维化和瘢痕形成，最终导致狭窄的发生。因此，在术前影像学检查中发现结石嵌顿的患者，需特别注意术后狭窄的预防和管理。而肾积水程度也是影响术后狭窄的重要因素之一。本研究发现，中重度肾积水的患者更容易发生术后输尿管狭窄。这可能是由于肾积水导致的肾盂压力增高和输尿管扩张，使得输尿管壁的结构和功能发生改变，增加了手术后的恢复难度。此外，肾积水本身也可能反映了结石存在较长时间，导致更严重的局部炎症和纤维化。手术时间长和发生钬激光对黏膜的损伤也显著增加了术后输尿管狭窄的风险。较长的手术时间通常意味着更复杂的手术操作和更高的手术难度，增加了输尿管损伤的可能性。此外，长时间的手术操作会导致局部组织的持续性压力和缺血，进一步加剧术后纤维化和瘢痕形成。钬激光损伤黏膜是影响术后狭窄的另一重要因素。钬激光在碎石过程中产生的高能量可以有效粉碎结石，但同时也可能对输尿管黏膜造成热损伤和机械损伤。这些损伤会引起局部炎症反应，导致黏膜下层的纤维化，最终形成狭窄。因此，在手术过程中，需尽量减少激光对黏膜的直接照射，以降低术后狭窄的风险。基于这些发现，本研究还使用 R 软件建立了预测模型，并通过 ROC 曲线对模型进行了验证。结果显示，预测模型的敏感度为 84.6%，特异度为 85.7%，AUC 为 0.888。这表明该模型在预测输尿管镜钬激光碎石术后输尿管狭窄方面具有较高的准确性，能够有效区分高风险和低风险患者，从而帮助临床医生在术前制定更有效的治疗策略。

综上所述，本研究明确了结石最大径、结石嵌顿和肾积水程度等是独立危险因素。临床上，对于具有这些高危因素的患者，应在术前进行充分评估，术中采取精细操作，并在术后密切随访，以降低术后输尿管狭窄的发生风险，提高患者的预后和生活质量。这些发现为进一步优化输尿管结石的治疗策略提供了科学依据，也为今后的相关研究指明了方向。

参 考 文 献

[1] 王伟强，楼正达，郑军政，等 . 输尿管软镜钬激光碎石与硬镜气压弹道碎石治疗输尿管结石伴肾积水的疗效比较 [J]. 中国现代医学杂志，2020，30（24）：57-60.

[2] 汪涛，罗泽权，汪海燕 . 经皮肾镜碎石取石术与输尿管软镜钬激光碎石术在肾和输尿管结石中的应用效果对比 [J]. 中国医学创新，2024，21（9）：16-21.

[3] 李准民，龙跃，王维飞，等 .1 倍 ED95 罗库溴铵复合喉罩通气在输尿管镜钬激光碎石术中的应用效果 [J]. 中国现代手术学杂志，2023，27（2）：127-131.

[4] 欧元红，覃锐祥，沈霜，等 . 不同麻醉方式输尿管镜钬激光碎石术的疗效比较 [J]. 西部医学，2020，32（2）：225-228.

[5] 刘晨溪，曹雷，卢新喆，等 . 软性输尿管镜钬激光碎石术联合排石颗粒治疗老年上尿路结石病人的临床效果 [J]. 实用老年医学，2022，36（6）：584-587.

[6] 刘彦军，景治安，毛长青，等 . 软性与硬性输尿管镜钬激光碎石术治疗输尿管结石伴输尿管狭窄疗效比较 [J]. 新乡医学院学报，2020，37（10）：976-979.

[7] 张波，王朝晖，陈志，等 . 双镜种联合治疗输尿管镜钬激光碎石术引起的输尿管狭窄的疗效分析 [J]. 中华泌尿外科杂志，2017，38（10）：778-781.

[8] 张冠英，徐云，余泉峰，等 . 输尿管镜钬激光碎石术后输尿管狭窄的危险因素分析及再次手术的术式选择策略 [J]. 腹腔镜外科杂志，2023，28（11）：859-866.

[9] 廖文彪，杨厨星，宋超，等 . 输尿管镜钬激光碎石术后输尿管狭窄的处理方法：5 年单中心回顾性研究 [J]. 中华泌尿外科杂志，2021，42（12）：910-914.

[10] 吴晃，付宇强，何慕琪，等 . 舌黏膜在输尿管狭窄修复中的应用 [J]. 国际泌尿系统杂志，2023，43（4）：748-751.

[11] NAGENDRA V，DHANDE R，MISHRA G，et al.Hematuria

中国知网 https://www.cnki.net

小青龙汤合保元汤加减治疗慢性阻塞性肺疾病急性发作期外寒内饮证的效果

朱起储[①] 张新花[②] 张青妹[③]

【摘要】 **目的**：探究慢性阻塞性肺疾病（COPD）急性发作期外寒内饮证患者采用小青龙汤合保元汤加减治疗的临床效果。**方法**：择取大田县总医院收治62例确诊为COPD急性发作期外寒内饮证患者，入院接受治疗时间为2023年4月—2024年1月，通过病历号随机抽签分组法分为试验组（n=31）、对照组（n=31）。对照组采用西医基础治疗，试验组在对照组治疗方案基础上增加小青龙汤合保元汤加减治疗，两组均治疗14 d，对比两组临床总有效率、肺功能指标、炎症因子指标、免疫球蛋白指标、不良反应发生率。**结果**：治疗后试验组总有效率显著高于对照组，差异有统计学意义（P<0.05）；治疗后试验组肺功能指标[第1秒用力呼气容积（FEV_1）、用力肺活量（FVC）、FEV_1/FVC]水平均显著高于对照组，差异均有统计学意义（P<0.05）；治疗后试验组炎症因子指标[降钙素原（PCT）、C反应蛋白（CRP）、白介素-6（IL-6）]水平均显著低于对照组，差异均有统计学意义（P<0.05）；治疗后试验组免疫球蛋白指标[免疫球蛋白A（IgA）、免疫球蛋白G（IgG）、免疫球蛋白M（IgM）]水平均显著高于对照组，差异均有统计学意义（P<0.05）；两组不良反应发生率比较差异无统计学意义（P>0.05）。**结论**：COPD急性发作期外寒内饮证患者采用小青龙汤合保元汤加减治疗效果显著，可改善肺功能、缓解炎症反应、调节免疫功能，用药安全性较高。

【关键词】 小青龙汤 保元汤 慢性阻塞性肺疾病 外寒内饮证

①大田县总医院呼吸内科 福建 大田 366100
②大田县总医院心血管内科 福建 大田 366100
③大田县总医院（南院区）康复科 福建 大田 366100
通信作者：朱起储

as a sign of kidney stone disease evaluated using computed tomography: a review[J/OL].Cureus, 2023, 15(4): e38064[2024-06-21].https://www.ncbi.nlm.nih.gov/pmc/articles/PMC10212727/.DOI: 10.7759/cureus.38064. eCollection 2023 Apr.

[12] AYYAD M, AYAAD O.Measuring quality of life among patients with urinary stone disease: a qualitative study[J/OL].Journal of Renal Injury Prevention, 2022, 12(4): e32106[2024-06-21]. https://www.semanticscholar.org/paper/Measuring-quality-of-life-among-patients-with-stone-Ayyad-Ayaad/1f7ffe690090ff0c03f8da5f7a2ddd4e82522be53.DOI: 10.34172/jrip.2023.32106.

[13] DASGUPTA R, CAMERON S, AUCOTT L, et al.Shockwave lithotripsy versus ureteroscopic treatment as therapeutic interventions for stones of the ureter (TISU): a multicentre randomised controlled non-inferiority trial[J].European Urology, 2021, 80(1): 46-54.

[14] LI J, YU H, ZHOU P, et al.Application of flexible ureteroscopy combined with holmium laser lithotripsy and their therapeutic efficacy in the treatment of upper urinary stones in children and infants[J].Urology Journal, 2019, 16(4): 343-346.

[15] AKPAYAK I C, IKEH C D.Outcome of flexible ureteroscopy and holmium laser lithotripsy in the management of renal stones: a twoyear retrospective study[J].Nigerian Journal of Medicine, 2023, 32(3): 275-279.

[16] VASUDEVAN V P, JOHNSON E U, WONG K, et al. Contemporary management of ureteral strictures[J].Journal of Clinical Urology, 2019, 12(1): 20-31.

[17] XIONG S, WANG J, ZHU W, et al.Onlay repair technique for the management of ureteral strictures: a comprehensive review[J]. BioMed Research International, 2020: 6178286.

[18] ULVIK Ø, HARNESHAUG J R, GJENGSTØ P.Ureteral strictures following ureteroscopic stone treatment[J].Journal of Endourology, 2021, 35(7): 985-990.

[19] ZHENG J, WANG Y, CHEN B, et al.Risk factors for ureteroscopic lithotripsy: a case-control study and analysis of 385 cases of holmium laser ureterolithotripsy[J].Videosurgery and Other Miniinvasive Techniques, 2020, 15(1): 185-191.

[20] WANG X K, JIANG Z Q, TAN J, et al.Thermal effect of holmium laser lithotripsy under ureteroscopy[J].Chinese Medical Journal, 2019, 132(16): 2004-2007.

（收稿日期：2024-07-10）（本文编辑：马娇）

中国知网 https://www.cnki.net

World Journal of Urology (2025) 43:232
https://doi.org/10.1007/s00345-025-05553-0

RESEARCH

With great power comes great risk: High ureteral stricture rate after high-power, high-frequency Thulium fiber laser lithotripsy in ureteroscopy

Riccardo Villani[1] · Thibaut Dominique Liernur[2] · Olivier Laurent Windisch[2] · Massimo Valerio[2] · Fabian Thierry Schoofs[2] · Jia-Lun Kwok[3,4,5] · Alba Sierra[4,5,6,7] · Daniel Eberli[1] · Christophe Iselin[2,8] · Olivier Traxer[4,5,9,10] · Etienne Xavier Keller[1,4,5,7]

Received: 29 January 2025 / Accepted: 4 March 2025
© The Author(s) 2025

Abstract

Purpose To compare the safety and efficacy of Thulium Fiber Laser (TFL) using either manufacturer presets (MP) or individualized presets (IP) in ureteroscopy.

Methods Multi-institutional, retrospective analysis on the first patients treated with SOLTIVE® Premium (Olympus Medical Systems®) TFL in Switzerland in 2020. MP were used at the University Hospital of Geneva, while IP were used at the University Hospital of Zurich. Patient demographics, stone characteristics, and procedural details were collected. Primary outcome was postoperative ureteral stricture (US). Secondary outcome was stone-free rate (SFR).

Results A total of 158 patients were analyzed, 79 in each group. Demographics were similar between the two groups, except for a lower pre-stenting rate in the MP group (56% vs. 91%; $p<0.001$) and a higher rate of ureteral access sheath use in the MP group (65% vs. 44%; $p=0.011$). No significant differences in stone burden (median stone diameter 9 mm, median stone volume 267 mm^3), nor in the rate of impacted ureteral stones (29% vs. 34%; $p=0.49$). Mean power, maximal power, frequency settings, and energy consumption were significantly higher in the MP group. US rate was 11% in MP group compared to 1% in IP group ($p=0.009$). MP were a significant predictor of US on multivariable analysis (OR 12.4; $p=0.02$), independently from impacted ureteral stones. No difference in SFR between groups (85% and 84%; $p=0.67$).

Conclusion High-power, high-frequency laser settings from manufacturer laser presets increase the risk of US, without improving SFR. Future studies shall further evaluate optimal laser settings depending on patient characteristics and intraoperative situation.

Keywords Ureteroscopy · Lithotripsy · Thulium fiber laser · Ureteral stricture · Laser presets · Power

✉ Etienne Xavier Keller
etiennexavier.keller@usz.ch

1 Department of Urology, University Hospital Zurich, University of Zurich, Zurich, Switzerland

2 Department of Surgery, Service of Urology, University Hospital Geneva, University of Geneva, Geneva, Switzerland

3 Department of Urology, Tan Tock Seng Hospital, Singapore, Singapore

4 Progressive Endourological Association for Research and Leading Solutions (PEARLS), Paris, France

5 Section of Endourology, European Association of Urology, Arnhem, The Netherlands

6 Urology Department, Hospital Clinic de Barcelona, Villarroel 170, Barcelona 08036, Spain

7 Young Academic Urologists (YAU), Endourology & Urolithiasis Working Group, Arnhem, The Netherlands

8 Cabinet privé, 76b Av. de la Roseraie, Geneva, Switzerland

9 Service d'Urologie, Sorbonne Université, Hôpital Tenon, Paris, France

10 Sorbonne Université, GRC n°20, Groupe de Recherche Clinique sur la Lithiase Urinaire, Hôpital Tenon, Paris F-75020, France

Published online: 18 April 2025

Abbreviations

ASA	American Society of Anesthesiologists
BMI	Body Mass Index
CI	Confidence Interval
CT	Computer Tomography
DJ	Double-J
HU	Hounsfield Units
IP	Individual Presets
MP	Manufacturer Presets
HUG	Hôpitaux Universitaires de Genève
OR	Odds Ratio
SFR	Stone Free Rate
TFL	Thulium Fiber Laser
UAS	Ureteral Access Sheath
US	Ureteral Stricture
URS	Ureteroscopy
USZ	Universitätsspital Zürich

Introduction

Ureteroscopy (URS) is currently the most widely used operative technique for the treatment of urolithiasis [1]. For ureteroscopic laser lithotripsy, a series of pulsed lasers can be used: the Holmium: YAG laser, the pulsed Thulium: YAG laser and the superpulsed Thulium Fiber Laser (TFL) [2–4]. The TFL has shown superiority over the Holmium: YAG in several aspects (e.g. higher stone ablation, smaller stone fragments, lower retropulsion, smaller laser fibers, higher stone-free rate (SFR), shorter operative time), but safety warnings and reports from urologists surfaced the concern if TFL is associated with a higher risk of ureteral stricture (US) [2, 5–7]. The proposed mechanisms are wide and not sustained by robust evidence, with conflicting findings between in vitro studies [7–11]. The question, then, is how far we can push laser settings during URS to maximize efficacy while ensuring the patient's safety. An analysis of a Twitter pool of experts from October 2021 resulted in a high degree of variability in preferred laser settings, with no consensus [12]. De facto, many urologists worldwide rely on laser presets provided by manufacturers, which show a high degree of variability too [13].

In this context, the first two hospitals using TFL in clinical routine in Switzerland followed different approaches for laser presets: the University Hospital of Geneva (Hôpitaux Universitaires de Genève, HUG) used manufacturer presets (MP), while the University Hospital Zurich (Universitätsspital Zürich, USZ) used individual presets (IP) based on recommendations from a fellowship-trained urologist who had established internal hospital guidelines on laser settings (Fig. 1) [14–16].

This difference in practice was the basis for a comparison between patients treated at the HUG and USZ for analysis of safety and efficacy of TFL laser lithotripsy.

Materials and methods

We conducted a multi-institutional and retrospective analysis of the first patients who underwent URS-lithotripsy with the SOLTIVE® Premium TFL (Olympus Medical Systems®, Tokyo, Japan) in Switzerland, namely at the HUG and USZ. The HUG discontinued the use of the TFL after 79 patients. Accordingly, the first 79 patients treated at the USZ were included for analysis. Patients with history of prior reconstructive ureteral surgery or pre-existing strictures were excluded, as well as patient who underwent URS with stone extraction, but no laser lithotripsy. Data was extracted from the hospital's medical information system. The following patient characteristics were collected: age, sex, BMI, diabetes mellitus history, ASA score, and prior history of ipsilateral URS. Data regarding characteristics and location of the stones were also collected, including their location within the kidney or ureter (proximal, mid and distal ureter), number of stones, maximal diameter of the largest stone, stone volume, maximal stone density measured in Hounsfield Units (HU), as well as presence of hydronephrosis at the time of diagnosis. To accurately estimate the stone volume, we employed the ellipsoid volume formula ($4/3\ \pi\ a*b*c$, where a, b, and c represent the radius of the stone in three dimensions, calculated from pre-operative Computer-Tomography (CT) scans in both axial and coronal views). In case of multiple stones, we summed up each stone volume [17]. The presence of an impacted ureteral stone was retrieved from the medical files. The general practice in both institutions was to consider a ureteral stone as impacted if at least one of the following criteria was met: (a) presence of ureteral dilation proximal to the stone and moderate to severe hydronephrosis (grade$\geq$2) [18]; (b) difficulty passing a guidewire or ureteral catheter beyond the ureteral stone at first attempt; (c) stone remaining in the same location on two separate imaging studies taken at least two months apart [19]. Regarding the surgical procedure, we collected data on unilateral vs. bilateral URS, pre- and postoperative Double-J (DJ) ureteral stenting (pre-stenting in both institutions usually for 10–20 days; post-operative DJ-stenting usually 5–14 days), and ureteral access sheath (UAS) use. *Detailed surgical procedure steps and instruments are provided in Supplementary Material.* Since all surgeries were performed in a university hospital setting, each patient was treated by either a urologist with >100 URS experience or by a urology resident under the supervision of an experienced urologist.

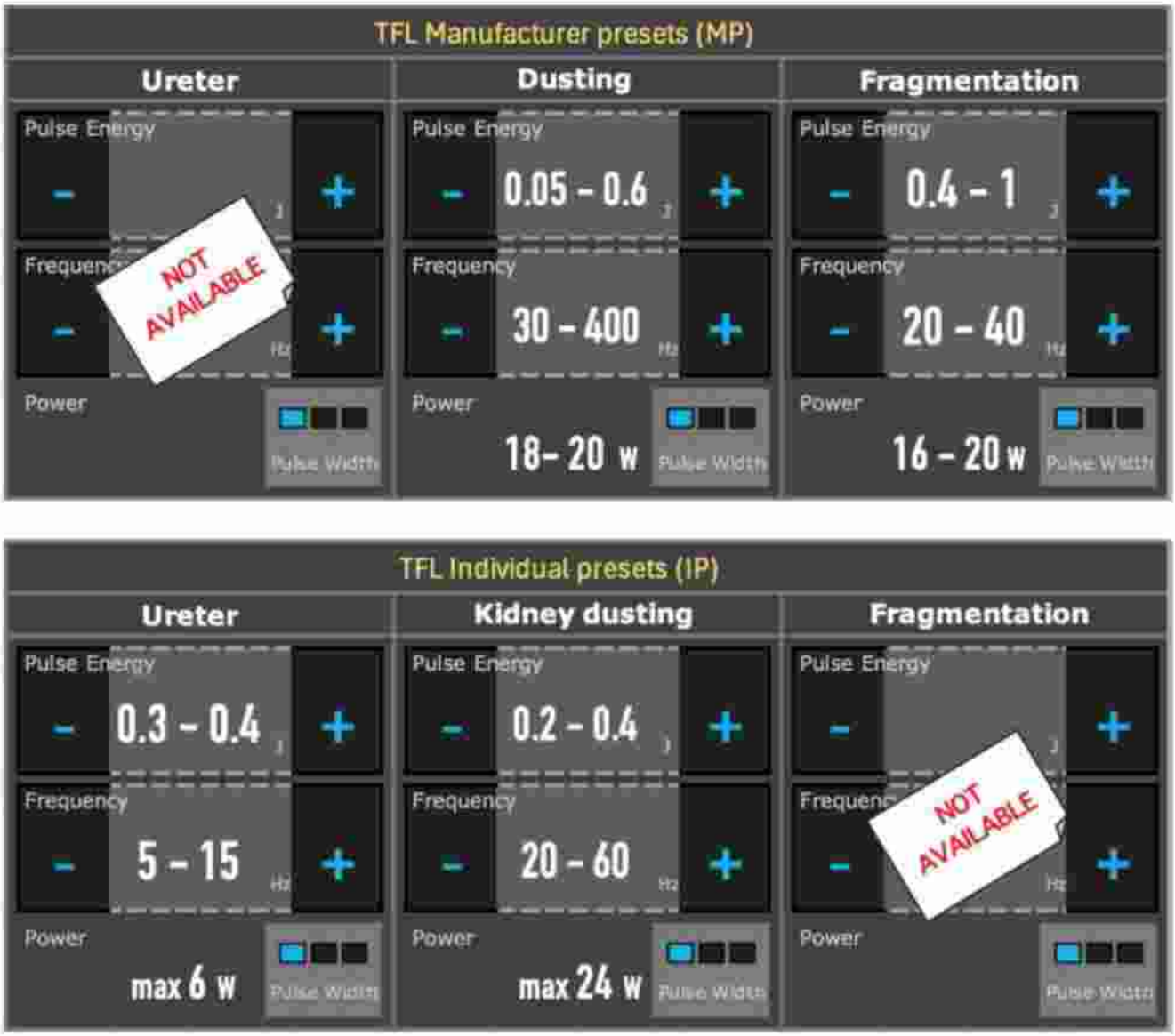


Fig. 1 Graphical user interface (GUI) comparison of manufacturer presets (MP) and individual presets (IP) for the Olympus SOLTIVE® Premium Thulium Fiber Laser (TFL) in 2020. Regarding manufacturer presets: Until July 2021, no manufacturer presets specifically intended for the ureter were available, nor was there any indication that the existing presets were designed for use in the kidney, but not the ureter. Regarding individual presets: Since the TFL was primarily introduced as a "dusting" laser, there were no individual presets dedicated to stone "fragmentation"

Laser settings were retrospectively extracted from the SOLTIVE® Premium laser generators, which have a record of the following parameters for each treated patient: type of laser fiber, active lasing time, total delivered energy, maximal power setting, as well as lowest and highest frequency settings. Mean power was calculated as total energy divided by lasing time. Mean laser energy consumption was calculated as total energy divided by stone volume (J/mm^3) [20].

Primary outcome was the presence of postoperative ureteral stricture (US). US was defined, according to Moretto et al., as signs of urinary flow impairment due to ureteral narrowing, associated with complications (such as pain, recurrent infections, or loss of renal function) and/or leading to re-intervention [21, 22]. In both institutions, patients underwent clinical evaluation and kidney-ultrasonography six weeks postoperatively. According to institutional guidelines, patients showing symptoms, impaired renal function, or hydronephrosis suggesting US were thoroughly evaluated. In such cases, the option of a retrograde ureteropyelography with diagnostic URS and/or dynamic scintigraphy was discussed. Other safety outcomes included intra-operative complications, as well as early (<1 month) and late (≥1 month) postoperative complications, classified according to the Clavien-Dindo grading system [23, 24].

Secondary outcome was the SFR, defined as the endoscopic absence of fragments greater than 2 mm and absence of fragments greater than 2 mm in follow-up imaging (ultrasonography in all patients, with additional imaging (e.g. CT) based on the surgeon's discretion) [25].

Statistical analysis

Associations between categorical variables were analyzed with Chi Square tests or Fischer's exact tests, as appropriate. Differences between continuous variables were analyzed with independent t-tests or Mann-Whitney U tests, as appropriate. Correlations between continuous variables was analyzed with Pearson correlations tests or Spearman's rho test, as appropriate. Logistic regression was used for the analysis of predictors of dichotomic outcomes. Patients with bilateral URS were included in a per-patient analysis. All statistical tests were two-sided and p-values < 0.05 were considered significant. Statistical analysis and graph plotting were performed with IBM SPSS Statistics 29.0 (IBM Corp., Armond, NY, USA).

Results

A total of 158 patients were available for analysis, 79 patients in each group, all treated between June 2020 and May 2021. Mean age was 53 years.

All patients underwent preoperative CT scan to assess stone burden. The majority of procedures were performed for kidney stones rather than ureteral stones. Specifically, 70% of patients had kidney stones (with/without concomitant ureteral stones), while 53% had ureteral stones (with/without concomitant kidney stones). There was a significant correlation between maximal stone size and stone volume (Spearman's rho 0.92; $p < 0.001$; Supplementary Fig. 1). Table 1 provides comprehensive patient characteristics.

Among baseline patient characteristics, diabetes mellitus was less prevalent in the MP group compared to the IP group (9% vs. 20%; $p = 0.04$). Additionally, the MP group had a significantly lower proportion of pre-stented cases (56% vs. 91%; $p < 0.001$). No other baseline variables showed significant differences between the two groups. Specifically, stone burden was comparable (median maximal stone size: 9 mm in both groups; $p = 0.39$; median stone volume 269 mm^3 in the MP group and 264 mm^3 in the IP group; $p = 0.67$). Similarly, the rate of impacted ureteral stones did not differ significantly between the MP and IP group (29% vs. 34%, respectively; $p = 0.49$).

Significant differences in procedural characteristics were observed between the two groups. The MP group demonstrated higher rate of UAS use, shorter active lasing times, higher energy consumption (J/mm^3), higher mean power, higher maximal power settings, and higher laser frequency settings (applicable to both lowest and highest frequency settings) compared to the IP group *(*Table 1*and* Fig. 2*)*.

No patient was lost to follow-up, and all patients underwent at least one first postoperative control within 3 months after surgery. Nine cases of US occurred in the MP group (11%) compared to one case (1%) in the IP group ($p = 0.009$). Impacted stone status, absence of pre-stenting, manufacturer laser presets, increasing total laser energy as well as increasing mean power were found as predictors of US on univariable analysis *(*Table 2*)*. On multivariable analysis, two independent variables emerged as predictors of US: impacted stone status (OR 7.10 (CI 1,67–30,1); $p = 0.008$) and manufacturer laser presets (OR 12,4 (CI 1,48–104); $p = 0.02$) *(*Table 2*)*.

Detailed patient characteristics and management of the 10 patients with US are presented in *Supplementary Table 1*. All patients had ureteral stones at initial diagnosis. All patients underwent retrograde ureteropyelography to locate and measure the US. The location of the US corresponded to the original stone location in 4 from 10 patients (40%), while further distally to the stone location in 4 patients (40%) and more proximally in the remaining 2 patients (20%). Most cases were managed with laparoscopic DaVinci-assisted ureteroplasty (using buccal mucosal graft or appendix flap) or ureteral reimplantation (50%) or balloon dilation and ureteral stenting (33%). Additionally, one case required nephrectomy, while another resolved spontaneously. Patients who underwent reconstruction were followed-up with clinical, ultrasound and renal function assessments for a minimum of 2 years with no loss of follow-up, showing excellent outcomes after reconstructive surgery, with no evidence of recurrence.

As for intraoperative, early postoperative, and late postoperative complications, no significant differences were observed between the MP and IP groups.

SFR did not significantly differ between groups (85% and 84% in the MP and IP group; $p = 0.67$).

Discussion

To the best of our knowledge, this is the first clinical study confirming the risks associated with the use of high-power, high-frequency settings from manufacturer laser presets in the context of ureteroscopic lithotripsy. Specifically, manufacturer laser presets led to a significantly higher risk of postoperative US (OR = 12.4; $p = 0.02$ on multivariable analysis), compared to more conservative, individualized laser presets, with no difference in SFR between both groups. Most cases of US required major surgical intervention. What

Table 1 Patient characteristics

Baseline characteristics					Procedural characteristics				
Variable	**Overall (*n* = 168)**	**Manufacturer laser presets (*n* = 79)**	**Individual laser presets (*n* = 79)**	p-value	**Variable**	**Overall (*n* = 168)**	**Manufacturer laser presets (*n* = 79)**	**Individual laser presets (*n* = 79)**	p-value
Age (mean, SD)	53 (17)	52 (19)	54 (15)	0.48*	**UAS use**	86 (54%)	51 (65%)	35 (44%)	**0.011****
Male : female ratio	2.1: 1	2.0: 1	2.2: 1	0.87**	**Postoperative DJ-stenting**	156 (99%)	79 (100%)	77 (98%)	0.16**
BMI (mean, SD) (kg/m²)	26 (5)	26 (5)	26 (5)	0.76*	**Laser fiber core diameter**				**<0.001****
					150 µm	84 (53%)	5 (6%)	79 (100%)	
					200 µm	68 (43%)	68 (86%)	0 (0%)	
					365 µm	6 (4%)	6 (8%)	0 (0%)	
Diabetes mellitus	23 (15%)	7 (9%)	16 (20%)	**0.04****	**Active lasing time (mm: ss) (median, IQR)**	06:28 (01:56–16:36)	04:38 (01:37–09:37)	13:05 (02:42–23:33)	**<0.001*****
ASA score				0.65**	**Total energy (KJ)**	6.26 (1.63–17.1)	6.50 (2.28–16.38)	5.98 (9.03–17.50)	0.41***
1	17 (11%)	9 (11%)	8 (10%)						
2	94 (59%)	50 (63%)	44 (56%)						
3	41 (26%)	17 (22%)	24 (30%)						
4	6 (4%)	3 (4%)	3 (4%)						
Prior history of URS	44 (28%)	22 (28%)	22 (28%)	1.00**	**Energy consumption (J/mm³) (median, IQR)**	18 (7–32)	20 (11–44)	17 (7–26)	**0.031*****
Stone location				0.94**	**Mean power (W) (median, IQR)**	19 (8–20)	20 (20–25)	8 (6–15)	**<0.001*****
Kidney	67 (43%)	33 (42%)	34 (43%)						
Ureter	48 (30%)	25 (32%)	23 (29%)						
Both	43 (27%)	21 (26%)	22 (28%)						
Ureteral stones' location				0.18**	**Maximal power setting (W) (mean, SD)**	21 (13)	27 (13)	15 (9)	**<0.001***
Proximal	54 (59%)	54 (59%)	31 (69%)						
Mid	25 (28%)	25 (28%)	8 (18%)						
Distal	9 (10%)	9 (10%)	4 (9%)						
Multiple	3 (3%)	3 (3%)	2 (4%)						
Number of stones (median, IQR)	1 (1–3)	1 (1–3)	2 (1–3)	0.28***	**Lowest frequency setting (Hz) (median, IQR)**	40 (10–200)	200 (100–200)	14 (5–30)	**<0.001*****
Maximal stone size (mm) (median, IQR)	9 (7–13)	9 (7–13)	9 (7–13)	0.39***	**Highest frequency setting (Hz) (median, IQR)**	100 (40–400)	400 (200–400)	40 (30–100)	**<0.001*****
Stone volume (mm³) (median, IQR)	267 (110–751)	269 (117–565)	264 (110–857)	0.67***	**Postoperative outcomes**				
Maximal stone density (HU) (mean, SD)	1142 (391)	1108 (382)	1177 (399)	0.27*	**Variable**	**Overall (*n* = 168)**	**Manufacturer laser presets (*n* = 79)**	**Individual laser presets (*n* = 79)**	p-value
Impacted stone	50 (32%)	23 (29%)	27 (34%)	0.49**	**Intraoperative complications**	Total: 8 (5%)	Total: 3 (4%)	Total: 2 (3%)	0.15**

Table 1 (continued)

Baseline characteristics					Procedural characteristics				
Variable	**Overall (*n* = 168)**	**Manufacturer laser presets (*n* = 79)**	**Individual laser presets (*n* = 79)**	p-value	**Variable**	**Overall (*n* = 168)**	**Manufacturer laser presets (*n* = 79)**	**Individual laser presets (*n* = 79)**	p-value
					Ureteral perforation	6 (4%)	2 (3%)	1 (1%)	
					Renal pelvis perforation	1 (1%)	1 (1%)	0 (0%)	
					Priapism	1 (1%)	0 (0%)	1 (1%)	
Preoperative hydronephrosis ≥ Grade 2	47 (30%)	21 (27%)	26 (33%)	0.38**	**Early postoperative complications**	Total: 8 (5%)			
	Total: 9 (11%)	Total: 5 (6%)	0.47**						
					CD I				
					Hematuria	2 (1%)		0 (0%)	
					CD II		2 (3%)		
					UTI	4 (3%)		3 (4%)	
					Delirium	1 (1%)	1 (1%)	1 (1%)	
					CD IV		0 (0%)		
					TIA	1 (1%)	0 (0%)	1 (1%)	
Bilateral URS	9 (6%)	4 (5%)	5 (6%)	0.73**	**Late postoperative complications**	Total: 10 (6%)	Total: 9 (11%)	Total: 1 (1%)	**0.009****
					CD IIIb				
					Ureteral stricture	10 (6%)	9 (11%)	1 (1%)	
					Others	0 (0%)	0 (0%)	0 (0%)	
Pre-stenting	116 (73%)	44 (56%)	72 (91%)	**<0.001****	**Stone free status**	132 (84%)	65 (82%)	67 (85%)	0.67**

*T-test, **Chi-square, ***Mann-Whitney U Test

SD = standard deviation; IQR = interquartile range; BMI = body mass index; ASA = American Society of Anesthesiologists; URS = ureteroscopy; HU = Hounsfield units; UAS = ureteral access sheath; TIA = transient ischemic attack; CD = Clavien-Dindo

had been previously hypothesized in several in vitro studies [7, 26] and highlighted by safety complaints [27–33], is now supported by compelling evidence provided by this study. It serves as a crucial caveat to all urologists performing ureteroscopic laser lithotripsy, underscoring the need for careful evaluation and adjustment of laser settings.

Recent systematic reviews have reported an overall 3% rate of US after URS [22, 23]. In the present study, the US rate in the MP group was 11%, arguably exceeding the safety threshold for this procedure. Understandably, the hospital involved (HUG) opted to discontinue the use of the TFL within less than a year after its acquisition. In contrast, use of IP resulted in a 1% US rate, indicating that ureteroscopic laser lithotripsy can be performed safely with the TFL when using IP.

Two critical factors likely explain the association between laser settings and US formation: high-power and high-frequency. High-power can result in excessive and rapid local energy delivery, potentially causing thermal tissue damage, which may ultimately lead to US formation [34–36]. Similarly, high-frequency is associated with suboptimal energy delivery to the stone surface, increasing the likelihood of inadvertent targeting of ureteral wall rather than the ureteral stone [26, 37].

Ultimately, high-power is mostly associated with high-frequency, and vice versa, because of the relatively narrow range of pulse energy used for laser lithotripsy (predominantly 0.4–1.5 J) [38]. In the present study, mean power, maximal power, lowest and highest frequency settings were all significantly higher in the MP group, compared to the IP group. Additionally, mean power was revealed as a significant predictor of US on univariable analysis (OR = 1.03 for each additional increase of 1 W; $p = 0.046$). Finally, laser energy consumption was significantly higher in the MP group compared to the IP group: 20 J/mm^3 vs. 17 J/mm^3 ($p = 0.031$) (the lower, the better, as highlighted by recent reports) [39, 40]. This difference in laser energy consumption is likely attributed to less precise targeting of the stone surface with high-frequency settings. This hypothesis is supported by the findings of two in vitro studies where higher frequency settings were associated with a less effective delivery of laser energy to the stone surface [41, 42].

Poor stone targeting due to impaired visibility during stone dust production and delayed human reaction time when off-target further exacerbates the hazards associated

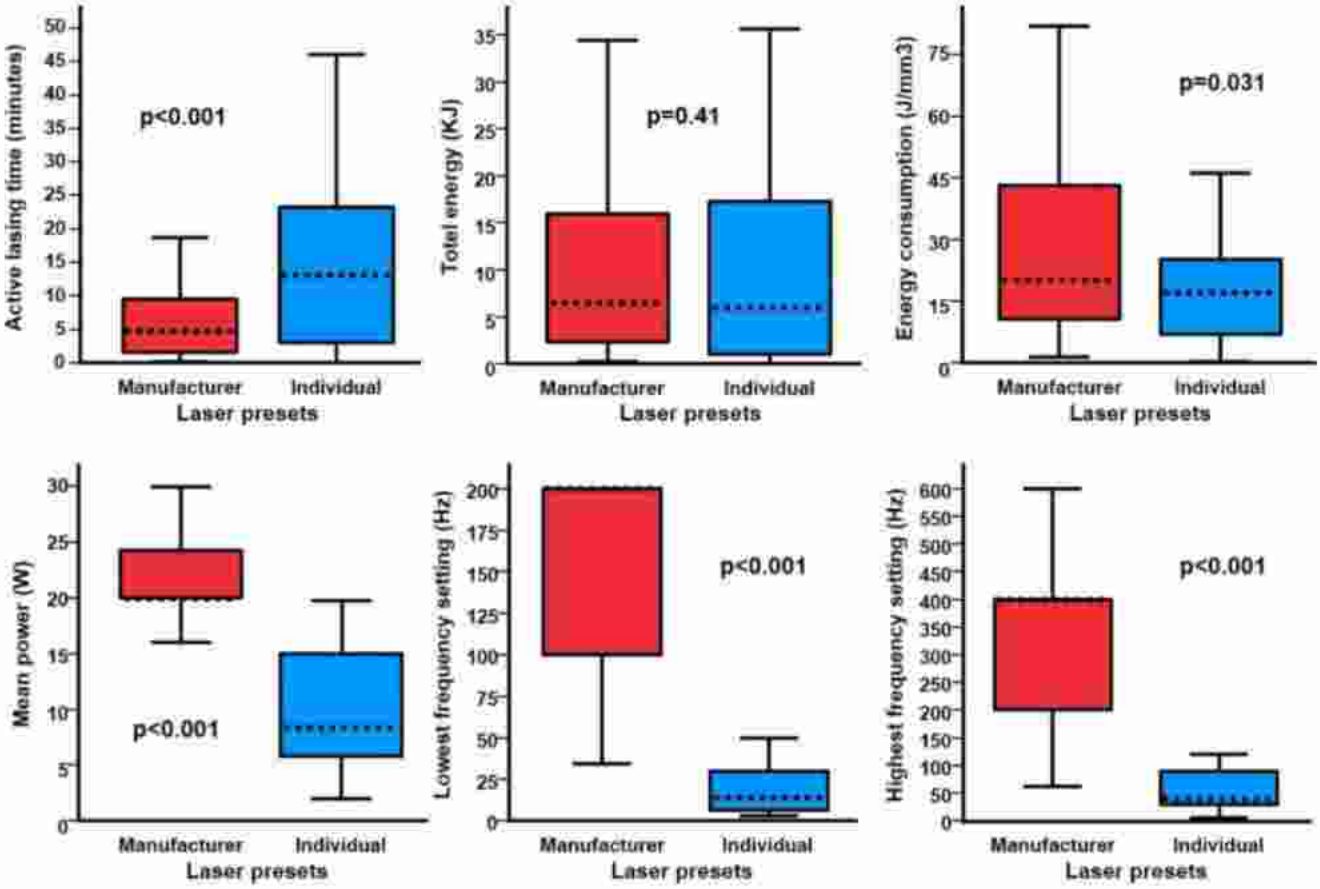


Fig. 2 Distribution of laser settings retrieved from the laser generators. Boxplots with median as dotted lines, boxes as 25th to 75th percentiles, and whiskers as 10th to 90th percentiles

with high-frequency lithotripsy [38]. In our study, most patients with US had laser frequency settings ranging from 100 to 400 Hz. Given a mean visual reaction time of at least 250 ms [43], most surgeons would likely release the laser pedal only after delivering 25 to 100 laser pulses in case of poor stone targeting or reduced visibility. These excessive, uncontrolled laser pulses not only possibly account for the observed differences in laser energy consumption, but might also have contributed to the formation of US in this study.

Presence of an impacted ureteral stone emerged as the second significant and independent predictor of US on multivariable analysis (OR = 7.10; $p = 0.008$). This finding aligns with a recent systematic review and meta-analysis, which confirmed impacted stone as an established predictor of US (OR = 7.47; $p = 0.01$, based on 5 studies including 13550 patients) [22]. In the present cohort, seven out of ten patients who developed US (70%) had impacted stones. However, 43 other patients with impacted stones did not develop US, underscoring the influence of competing risk factors such as high-power, high-frequency laser lithotripsy.

All cases of US occurred in patients with stones located in the ureter at initial diagnosis. Noteworthy, strictures occurred at the same location as the original stone in only 40% of all cases with US. This observation suggests that either stones were displaced between initial diagnosis and ureteroscopic laser lithotripsy, or that thermal tissue damages may have occurred distantly from the site of local laser energy delivery. Consequently, and until proven otherwise, high-power high-frequency laser lithotripsy should be considered hazardous for both ureteral and kidney stones. Future studies shall verify the hypothesis of distant heat-generated tissue damages by protocolling the site of laser emission in a prospective manner.

Interestingly, pre-stenting significantly reduced the risk for US on univariable analysis (OR = 0.2; $p = 0.022$). Although this finding may partly reflect practice differences between the two hospitals (56% pre-stenting in the MP group vs. 91% in the IP group; $p < 0.001$), it is plausible to hypothesize that pre-stenting contributes to US prevention by dilating the ureter and improving irrigation flow, therefore minimizing risks of ureteral trauma and optimizing conditions of laser lithotripsy [44]. Overall, pre-stenting is associated with higher SFR and fewer intra- and post-operative complications [45]. Further studies are needed to

Table 2 Logistic regression analysis for predictors of ureteral stricture

Variable	Univariable		Multivariable*	
	OR (95% CI)	***p***	**OR (95% CI)**	***p***
Age (continuous)	0.98 (0.94–1.02)	0.32		
Male vs. female	4.59 (0.57–37.3)	0.15		
BMI (kg/m2) (continuous)	1.03 (0.91–1.17)	0.64		
Diabetes mellitus	1.4 (0.3–7.6)	0.62		
Maximal stone size (mm) (continuous)	1.04 (0.94–1.15)	0.44		
Stone volume (mm^3) (continuous)	1.00 (1.00–1.00)	0.92		
Impacted ureteral stone	5.70 (1.41–23.1)	**0.015**	7.10 (1.67–30.1)	**0.008**
Preoperative hydronephrosis ≥ Grade 2	1.63 (0.44–6.06)	0.47		
Failed primary URS attempt	1.6 (0.3–8.1)	0.57		
Pre-stenting	0.2 (0.06–0.8)	**0.022**		
UAS use	0.8 (0.2–3.0)	0.77		
Manufacturer (MP) vs. individual laser presets (IP)	10.0 (1.24–81.2)	**0.031**	12.4 (1.48–104)	**0.02**
Laser fiber core diameter				
150 µm	1.00 (Ref.)			
200 µm	4.71 (0.94–23.5)	0.059		
365 µm	8.20 (0.63–106.6)	0.11		
Active lasing time (s) (continuous)	1.00 (1.00–1.00)	0.64		
Total energy (KJ) (continuous)	1.02 (1.00–1.04)	**0.026**		
Laser energy consumption (J/mm^3)	1.00 (0.99–1.02)	0.60		
Mean power (W)	1.03 (1.00–1.06)	**0.046**		
Maximal power setting (W)	1.02 (0.98–1.07)	0.28		
Lowest frequency setting (Hz)	1.00 (0.99–1.01)	0.12		
Highest frequency setting (Hz)	1.00 (0.99–1.01)	0.16		
Intraoperative ureteral or pelvic perforation	3.18 (0.34–30.2)	0.31		

*Only variables retained in a forward conditional multivariable analysis with an entry level at ≤ 0.05 and removal cut-off at ≥ 0.1 were retained in the model

OR = odds ratio; 95% CI = 95% confidence interval; BMI = body mass index

explore the impact of pre-stenting on reducing the risk of US.

Regarding the use of UAS, it was more frequently employed in the MP group (65% vs. 44% in the IP group; $p = 0.011$). Nevertheless, UAS use was not identified as a predictor of US. These findings are consistent with previous studies, which suggest that there is no established association between UAS placement during URS and the development of US [19, 46].

Neither stone size (maximal diameter) nor stone volume emerged as predictors of US in our study. Conversely, total delivered energy was identified as significant predictor of US on univariable analysis (OR = 1.02 for each additional 1 kJ; $p = 0.026$). This finding underscores that all laser parameters (power, frequency and cumulative delivered energy) should be cautiously selected and monitored during URS.

This study has several limitations. First, its retrospective design inherently introduces potential biases, limits retrieval of some information such as details on irrigation settings (pressure, manual pump, volume, rate, etc.) and does not warrant a follow-up longer than provided for by institutional guidelines. Second, the laser system does not provide detailed information regarding the mean frequency applied during the operation. This lack of granularity restricts our ability for analysis. Additionally, the study is based on data collected from two institutions, each employing different approaches to URS technique. A difference in surgeons' expertise between the two institutions cannot be formally excluded. Nevertheless, both are university hospitals from the same country with a urologist with > 100 URS experience present in each surgery, suggesting a minimal impact of possible differences in expertise. Another limitation is the relatively small sample size of 158 patients, which, while sufficient for preliminary observations and findings, may lack statistical power needed to detect subtle associations or rare complications. Despite these limitations, we consider the results of the present study to be robust, as all other significant variables that could influence the rate of US (such as age, ASA score, prior URS history, stone localization and burden, rate of impacted stones) were equally distributed between the two groups. The significant correlation between stone burden parameters (maximal stone size and stone volume) further underscores the quality of the data that was available for analysis. Of note, SFR was not based on systematic postoperative CT scan, potentially leading to an overestimation of success rates. The SFR shall be

interpreted accordingly. Larger prospective studies are warranted to confirm our findings and establish safety thresholds for laser settings in lithotripsy.

Conclusions

High-power, high-frequency settings from manufacturer laser presets significantly increase the risk of US formation, independently from impacted ureteral stones, and without improving SFR. Our findings underscore the importance of careful selection of laser settings during TFL lithotripsy, advocating for individualized laser presets with more conservative settings tailored to each patient and clinical scenario. Future research should prioritize prospective studies to evaluate the specific effects of individual laser parameters, such as power, frequency, cumulative delivered energy and laser energy consumption, in order to identify optimal settings, which can maximize efficacy while minimizing the risk of tissue damage. Additionally, the development of dynamic, real-time adjustable presets based on intraoperative feedback (irrigation flow and temperature, targeting of the stone, laser fiber working distance, stone particle size, stone type, stone ablation rate, etc.) represents a promising avenue for improving patient outcomes.

Supplementary Information The online version contains supplementary material available at https://doi.org/10.1007/s00345-025-05553-0.

Author contributions R.V. and E.X.K. wrote the main manuscript text, prepared Figs. 1 and 2; Table 1, and 2, as well as supplementary Fig. 1 and supplementary Table 1. O.T. and E.X.K. contributed to the research concept. R.V., E.X.K., M.V. and D.E. contributed to study protocol and development. R.V., E.X.K. and O.L.W. contributed to ethic committee registration for Geneva and Zurich. R.V. and T.D.L. contributed to data collection and management. R.V. and E.X.K. performed statistical analysis. All authors contributed to the data analysis, manuscript review and editing.

Funding Open access funding provided by University of Zurich
No funding was received for conducting this study.

Data availability No datasets were generated or analysed during the current study.

Declarations

Ethics approval and consent to participate All procedures performed in studies involving human participants were in accordance with the ethical standards of the institutional and/or national research committee and with the 1964 Helsinki declaration and its later amendments or comparable ethical standards. The local ethics committees approved the study protocol (Study ID: BASEC 2023 − 00660 and 2024 − 00272).

Competing interests The authors declare no competing interests.

Open Access This article is licensed under a Creative Commons Attribution 4.0 International License, which permits use, sharing, adaptation, distribution and reproduction in any medium or format, as long as you give appropriate credit to the original author(s) and the source, provide a link to the Creative Commons licence, and indicate if changes were made. The images or other third party material in this article are included in the article's Creative Commons licence, unless indicated otherwise in a credit line to the material. If material is not included in the article's Creative Commons licence and your intended use is not permitted by statutory regulation or exceeds the permitted use, you will need to obtain permission directly from the copyright holder. To view a copy of this licence, visit http://creativecommons.org/licenses/by/4.0/.

References

1. Geraghty RM, Jones P, Somani BK (2017) Worldwide trends of urinary stone disease treatment over the last two decades: A systematic review. J Endourol 31 https://doi.org/10.1089/end.2016.0895
2. Traxer O, Keller EX (2020) Thulium fiber laser: the new player for kidney stone treatment? A comparison with Holmium:YAG laser. World J Urol 38 https://doi.org/10.1007/s00345-019-02654-5
3. Ventimiglia E, Robesti D, Bevilacqua L et al (2023) What to expect from the novel pulsed Thulium:yag laser? A systematic review of endourological applications. World J Urol 41. https://doi.org/10.1007/s00345-023-04580-z
4. Traxer O, Sierra A, Corrales M (2022) Which is the best laser for lithotripsy? Thulium Fiber laser. Eur Urol Open Sci 44 https://doi.org/10.1016/j.euros.2022.05.020
5. Jiang P, Okhunov Z, Afyouni AS et al (2023) Comparison of superpulse Thulium Fiber laser *vs* Holmium laser for ablation of renal calculi in an *In vivo* Porcine model. J Endourol 37:335–340. https://doi.org/10.1089/end.2022.0445
6. Ulvik Ø, Æsøy MS, Juliebø-Jones P et al (2022) Thulium fibre laser versus Holmium:yag for ureteroscopic lithotripsy: outcomes from a prospective randomised clinical trial. Eur Urol 82:73–79. https://doi.org/10.1016/j.eururo.2022.02.027
7. Belle JD, Chen R, Srikureja N et al (2022) Does the novel Thulium Fiber laser have a higher risk of urothelial thermal injury than the conventional Holmium laser in an *In vitro* Study? J Endourol 36:1249–1254. https://doi.org/10.1089/end.2021.0842
8. Wanderling C, Saxton A, Phan D et al (2024) Getting hot in here! Comparison of Holmium vs. Thulium laser in an anatomic hydrogel kidney model. Urolithiasis 52:49. https://doi.org/10.1007/s00240-024-01541-y
9. Keller EX, De Coninck V, Talso M, Traxer O (2023) *Comment on*: Does the Novel Thulium Fiber Laser Have a Higher Risk of Urothelial Thermal Injury than the Conventional Holmium Laser in an *In Vitro* Study? by Belle. J Endourol 37:1164–1165. https://doi.org/10.1089/end.2022.0336
10. Æsøy MS, Juliebø-Jones P, Beisland C, Ulvik Ø (2022) Temperature profiles during ureteroscopy with Thulium fiber laser and Holmium:yag laser: findings from a pre-clinical study. Scand J Urol 56:313–319. https://doi.org/10.1080/21681805.2022.2104367
11. Molina WR, Carrera RV, Chew BH, Knudsen BE (2021) Temperature rise during ureteral laser lithotripsy: comparison of super pulse Thulium fiber laser (SPTF) vs high power 120 W Holmium-YAG laser (Ho:YAG). World J Urol 39:3951–3956. https://doi.org/10.1007/s00345-021-03619-3
12. Sierra A, Corrales M, Piñero A, Traxer O (2022) Thulium fiber laser pre-settings during ureterorenoscopy: Twitter's experts'

recommendations. World J Urol 40. https://doi.org/10.1007/s00345-022-03966-9
13. Sierra A, Corrales M, Piñero A et al (2022) Glossary of presettings given by laser companies: no consensus! World J Urol 40:2313–2321. https://doi.org/10.1007/s00345-022-04090-4
14. Keller Etienne Xavier https://x.com/exkeller/status/1315903100801216512. In: X
15. Keller Etienne Xavier https://x.com/exkeller/status/1316267242020106241/photo/2. In: X
16. Keller Etienne Xavier https://x.com/exkeller/status/1316644981004660737/photo/2. In: X
17. Panthier F, Kutchukian S, Ducousso H et al (2024) How to estimate stone volume and its use in stone surgery: a comprehensive review. Actas Urológicas Españolas (English Edition) 48. https://doi.org/10.1016/j.acuroe.2023.08.009
18. Fernbach SK, Maizels M, Conway JJ (1993) Ultrasound grading of hydronephrosis: introduction to the system used by the society for fetal urology. Pediatr Radiol 23:478–480. https://doi.org/10.1007/BF02012459
19. Tonyali S, Yilmaz M, Tzelves L et al (2023) Predictors of ureteral strictures after retrograde ureteroscopic treatment of impacted ureteral stones: A systematic literature review. J Clin Med 12 https://doi.org/10.3390/jcm12103603
20. Ventimiglia E, Pauchard F, Gorgen ARH et al (2021) How do we assess the efficacy of Ho:YAG low-power laser lithotripsy for the treatment of upper tract urinary stones? Introducing the Joules/mm3 and laser activity concepts. World J Urol 39:891–896. https://doi.org/10.1007/s00345-020-03241-9
21. Moretto S, Saita A, Scoffone CM et al (2024) An international Delphi survey and consensus meeting to define the risk factors for ureteral stricture after endoscopic treatment for urolithiasis. World J Urol 42:412. https://doi.org/10.1007/s00345-024-05103-0
22. Moretto S, Saita A, Scoffone CM et al (2024) Ureteral stricture rate after endoscopic treatments for urolithiasis and related risk factors: systematic review and meta-analysis. World J Urol 42:234. https://doi.org/10.1007/s00345-024-04933-2
23. De Coninck V, Keller EX, Somani B et al (2020) Complications of ureteroscopy: a complete overview. World J Urol 38:2147–2166. https://doi.org/10.1007/s00345-019-03012-1
24. Dindo D, Demartines N, Clavien PA (2004) Classification of surgical complications: A new proposal with evaluation in a cohort of 6336 patients and results of a survey. Ann Surg 240 https://doi.org/10.1097/01.sla.0000133083.54934.ae
25. Panthier F, Gauhar V, Ventimiglia E et al (2024) Rethinking Stone-free rates and surgical outcomes in endourology: A point of view from PEARLS members. Eur J Urol 86:198–199 https://doi.org/10.1016/j.eururo.2024.06.001
26. Sierra A, Corrales M, Kolvatzis M et al (2022) Thermal injury and laser efficiency with Holmium YAG and hulium Fiber laser—An *In vitro* study. J Endourol 36:1599–1606. https://doi.org/10.1089/end.2022.0216
27. (2020) https://www.accessdata.fda.gov/scripts/cdrh/cfdocs/cfMAUDE/detail.cfm?mdrfoi__id=12043126%26;pc=GEX. In: MAUDE Adverse Events
28. (2020) https://www.accessdata.fda.gov/scripts/cdrh/cfdocs/cfMAUDE/detail.cfm?mdrfoi__id=10782150%26;pc=GEX. In: MAUDE Adverse Events
29. (2022) https://www.accessdata.fda.gov/scripts/cdrh/cfdocs/cfMAUDE/detail.cfm?mdrfoi__id=15977674%26;pc=GEX&device_sequence_no=1. In: MAUDE Adverse Events
30. (2021) https://recalls-rappels.canada.ca/en/alert-recall/soltive-premium-superpulsed-laser-system-2021-06-22. In: CANADA Adverse Events
31. (2024) https://recalls-rappels.canada.ca/en/alert-recall/soltivet m-premium-superpulsed-tf-laser-system. In: CANADA Adverse Events
32. (2021) https://www.moph.gov.lb/userfiles/files/Medical%20Devices/Medical%20Devices%20Recalls%202021/19-07-2021/TFLPLSSOLTIVEPremiumSuperPulsedLaserSystem.pdf. In: Australian Government - Department of Health
33. (2021) https://ncmdr.sfda.gov.sa/Secure/CA/CaViewRecall.aspx?caId=10%26;rid=15757%26;AspxAutoDetectCookieSupport=1. In: Saudi Arabia
34. Pauchard F, Ventimiglia E, Corrales M, Traxer O (2022) A practical guide for Intra-Renal temperature and pressure management during Rirs: what is the evidence telling Us. J Clin Med 11:3429. https://doi.org/10.3390/jcm11123429
35. Ventimiglia E, Robesti D, Keller EX et al (2024) Temperature profile during endourological laser activation: introducing the thermal safety distance concept. World J Urol 42:453. https://doi.org/10.1007/s00345-024-05162-3
36. Corrales M, Panthier F, Solano C et al (2024) Laser safety, warnings, and limits in retrograde intrarenal surgery. Actas Urol Esp 48:19–24. https://doi.org/10.1016/j.acuro.2023.04.005
37. Sierra A, Solano C, Corrales M et al (2024) Steady-state versus burst lasing techniques for thulium fiber laser. World J Urol 42:487. https://doi.org/10.1007/s00345-024-05102-1
38. De Coninck V, Hente R, Claessens M et al (2021) High-power, High-frequency Ho:YAG lasers are not essential for retrograde intrarenal surgery. Eur Urol Focus 7:5–6. https://doi.org/10.1016/j.euf.2020.12.007
39. Keller EX, Kwok J-L, Panthier F et al (2024) Planning my ureteroscopic laser lithotripsy: how much energy and time should I reasonably expect? Integrating the concept of laser energy consumption (J/mm3). World J Urol 42:100. https://doi.org/10.1007/s00345-024-04790-z
40. Kwok J-L, De Coninck V, Ventimiglia E et al (2024) Laser ablation efficiency, laser ablation speed, and laser energy consumption during lithotripsy: what are they and how are they defined? A systematic review and proposal for a standardized terminology. Eur Urol Focus 10:599–611. https://doi.org/10.1016/j.euf.2023.10.004
41. Aldoukhi AH, Black KM, Hall TL et al (2020) Frequency threshold for ablation during Holmium laser lithotripsy: how high can you go?? J Endourol 34:1075–1081. https://doi.org/10.1089/end.2020.0149
42. Aldoukhi AH, Hall TL, Ghani KR, Roberts WW (2021) Strike rate: analysis of laser Fiber to stone distance during different modes of laser lithotripsy. J Endourol 35:355–359. https://doi.org/10.1089/end.2020.0298
43. Jain A, Bansal R, Kumar A, Singh K (2015) A comparative study of visual and auditory reaction times on the basis of gender and physical activity levels of medical first year students. Int J Appl Basic Med Res 5:124. https://doi.org/10.4103/2229-516X.157168
44. Jiang P, Afyouni A, Brevik A et al (2022) The impact of one week of Pre-Stenting on Porcine ureteral luminal circumference. J Endourol 36:885–890. https://doi.org/10.1089/end.2021.0771
45. Culvillo-Ramirez A, Angulo-Lozano JC, del Rio-Martinez CJ et al (2024) Safety and effectiveness of preoperative stenting compared to non-stenting in ureteroscopy for urinary stone disease: a meta-analysis of comparative studies. World J Urol 43:12. https://doi.org/10.1007/s00345-024-05365-8

46. de Amorim LGCR, Campos MEC, Dumont LS et al (2024) Retrograde intrarenal surgery with or without ureteral access sheath: a systematic review and meta-analysis of randomized controlled trials. Int Braz J Urol 50:670–682. https://doi.org/10.1590/s1677-5538.ibju.2024.0452

Publisher's note Springer Nature remains neutral with regard to jurisdictional claims in published maps and institutional affiliations.

《世界泌尿外科杂志》（2025）第43卷第232页
https://doi.org/10.1007/s00345-025-05553-0

研究

大功率带来大风险：输尿管镜下高频钬光纤激光碎石术后输尿管狭窄率高

Riccardo Villani [1]·Thibaut Dominique Liernur [2]·Olivier Laurent Windisch [2]·Massimo Valerio [2]·Fabian Thierry Schoofs [2]·Jia-Lun Kwok [3,4,5]·Alba Sierra [5,6,7]·Daniel Eberli [1]·Christophe Iselin [2,8]·Olivier Traxer [4,5,9,10]·Etienne Xavier Keller [1,4,5,7]

接收日期：2025年1月29日/接受日期：2025年3月4日
©作者2025

摘要

目的：比较输尿管镜检查中使用钬光纤激光（TFL）制造商预设（MP）或个性化预设（IP）的安全性和有效性。

方法本研究为多中心回顾性分析，针对2020年瑞士首例使用Sofivex® Premium（奥林巴斯医疗系统公司）TFL治疗的患者。其中MP组在日内瓦大学医院实施治疗，IP组在苏黎世大学医院实施治疗。研究收集了患者人口统计学特征、结石特性及手术细节等数据。主要结局指标为术后输尿管狭窄（超声检查），次要结局指标为结石清除率（SFR）。

研究结果显示，共纳入158例患者进行分析，每组79例。两组患者的人口学特征基本一致，但金属探头组（MP组）的术前置入率较低（56%对比91%；$p<0.001$）。输尿管套管使用率较高（65%对比44%；$p=0.011$）。结石负荷（中位结石直径9毫米，中位结石体积267 ^{3}毫米）和输尿管结石阻塞率（29%对比34%；$p=0.49$）均无显著差异。金属探头组的平均功率、最大功率、频率设置及能量消耗均显著高于普通探头组。金属探头组的超声检查率高达11%，而普通探头组仅为1%（$p=0.009$）。多变量分析表明，金属探头组是影响超声检查率的显著预测因素（比值比12.4；$p=0.02$），且该因素独立于输尿管结石阻塞存在。两组的超声检查率差异无统计学意义（85%对比84%；$p=0.67$）。

结论制造商激光预设的高功率、高频激光设置会增加超声检查风险，但未改善SFR。未来研究应根据患者特征和术中情况进一步评估最佳激光设置。

关键词输尿管镜检查·碎石术·钬光纤激光器·输尿管狭窄·激光预设值·功率

✉ 埃蒂安·泽维尔·凯勒
etiennexavier.keller@usz.ch

1 苏黎世大学医院泌尿外科，苏黎世大学，瑞士苏黎世

2 日内瓦大学医院外科泌尿科，日内瓦大学，瑞士

3 新加坡陈笃生医院泌尿外科，新加坡

4 研究与领先解决方案的渐进式内窥镜协会（pearls），法国巴黎

5 欧洲泌尿外科学会，荷兰阿纳姆，内镜泌尿外科

6 巴塞罗那医院诊所泌尿科，西班牙巴塞罗那08036，Villarroel 170

7 青年学术泌尿科医师（YAU），内镜泌尿外科与泌尿系结石工作组，荷兰阿纳姆

8 瑞士日内瓦玫瑰园大道76b号私人办公室

9 泌尿科，索邦大学，Tenon医院，巴黎，法国

10 索邦大学，GRC编号20，尿石症临床研究组，Tenon医院，巴黎F-75020，法国

Published online: 18 April 2025

缩写

ASA美国麻醉医师协会
BMI体重指数
CI 置信区间
CT计算机断层扫描
DJ 双J
HU Hounsfield单位
IP 个人预设
MP制造商预设
HUG日内瓦大学医院
OR比值比
SFR石头免费费率
TFL钬光纤激光器
UAS输尿管通路鞘
US输尿管狭窄
URS输尿管镜检查
USZ苏黎世大学医院

介绍

输尿管镜碎石术（URS）目前是治疗尿路结石最常用的技术[1]。在输尿管镜激光碎石术中，可采用多种脉冲激光器：钬：钇铝石榴石激光器、脉冲锕：钇铝石榴石激光器以及超脉冲锕光纤激光器（TFL）[2–4]。TFL在多个方面优于钬：钇铝石榴石激光器（如更高的结石消融率、更小的碎石颗粒、更低的后弹力、更细的光纤、更高的无结石率（SFR）、更短的手术时间），但泌尿科医生的安全警示和报告指出，TFL可能增加输尿管狭窄（US）的风险[2，5–7]。目前提出的致病机制范围广泛且缺乏有力证据支持，体外研究结果也存在矛盾[7–11]。因此，关键问题在于如何在确保患者安全的前提下，最大限度地提升输尿管镜碎石术的疗效，同时合理调整激光参数设置。对2021年10月Twitter专家库的分析显示，首选激光设置存在高度可变性，且无共识[12]。事实上，全球许多泌尿科医师依赖制造商提供的激光预设，这些预设也存在高度可变性[13]。

在此背景下，瑞士前两家在临床常规中使用TFL的医院在激光预设方面采用了不同的方法：日内瓦大学医院（HopitauxUniversitairesdeGeneve，HUG）使用制造商预设（MP），而苏黎世大学医院（UniversitatsspitalZurich，USZ）使用个体预设（IP），这是根据一位接受过专科培训的泌尿科医生的建议而制定的，该医生已建立了医院内部的激光设置指南(图1) [14-16]。

这种临床实践差异为比较HUG和USZ两家医院接受治疗的患者提供了基础，用于分析TFL激光碎石术的安全性和有效性。

材料和方法

我们对瑞士日内瓦大学医院（HUG）和洛桑大学医院（USZ）使用常规Premium TFL（奥林巴斯医疗系统公司，日本东京）进行上尿路碎石术（URS）的首批患者进行了多机构回顾性分析。HUG在完成79例患者治疗后停止使用TFL设备，因此本研究纳入了USZ医院前79例接受治疗的患者。排除标准包括：既往接受过输尿管重建手术或存在狭窄的患者，以及仅进行URS取石但未实施激光碎石术的患者。数据采集自医院医疗信息系统，收集的患者特征包括：年龄、性别、体重指数（BMI）、糖尿病病史、ASA分级评分及同侧输尿管URS既往治疗史。同时记录结石特征与位置信息，包括肾脏或输尿管近端、中段、远端的分布情况、结石数量、最大结石直径、结石体积、以亨氏单位（HU）表示的最大结石密度，以及诊断时是否存在肾积水。为准确估算结石体积，我们采用椭球体体积公式（4/3 π a*b*c，其中a、b、c分别代表结石在三维空间中的半径，数据来源于术前CT扫描的轴位和冠状位图像）。对于多发结石的情况，我们对每颗结石的体积进行累加[17]。通过查阅病历记录确认输尿管结石是否发生梗阻。两家医疗机构的常规诊疗标准是：若满足以下任一条件，则判定为输尿管结石梗阻：(a)结石近端存在输尿管扩张，且伴有中度至重度肾积水（分级≥2级）[18] (b)首次尝试时导丝或输尿管导管难以通过输尿管结石；(c)在至少间隔两个月的两次影像学检查中，结石仍位于原位[19]。关于手术操作，我们收集了单侧与双侧输尿管碎石术（URS）的数据，术前术后双J（DJ）输尿管支架置入情况（两家机构通常术前支架留置10-20天，术后支架留置5-14天），以及输尿管鞘管（UAS）使用情况。*详细手术步骤和器械信息详见补充材料*。由于所有手术均在大学附属医院完成，每位患者均由具有>100例URS经验的泌尿科医生或在资深泌尿科医生指导下进行的住院医师操作。

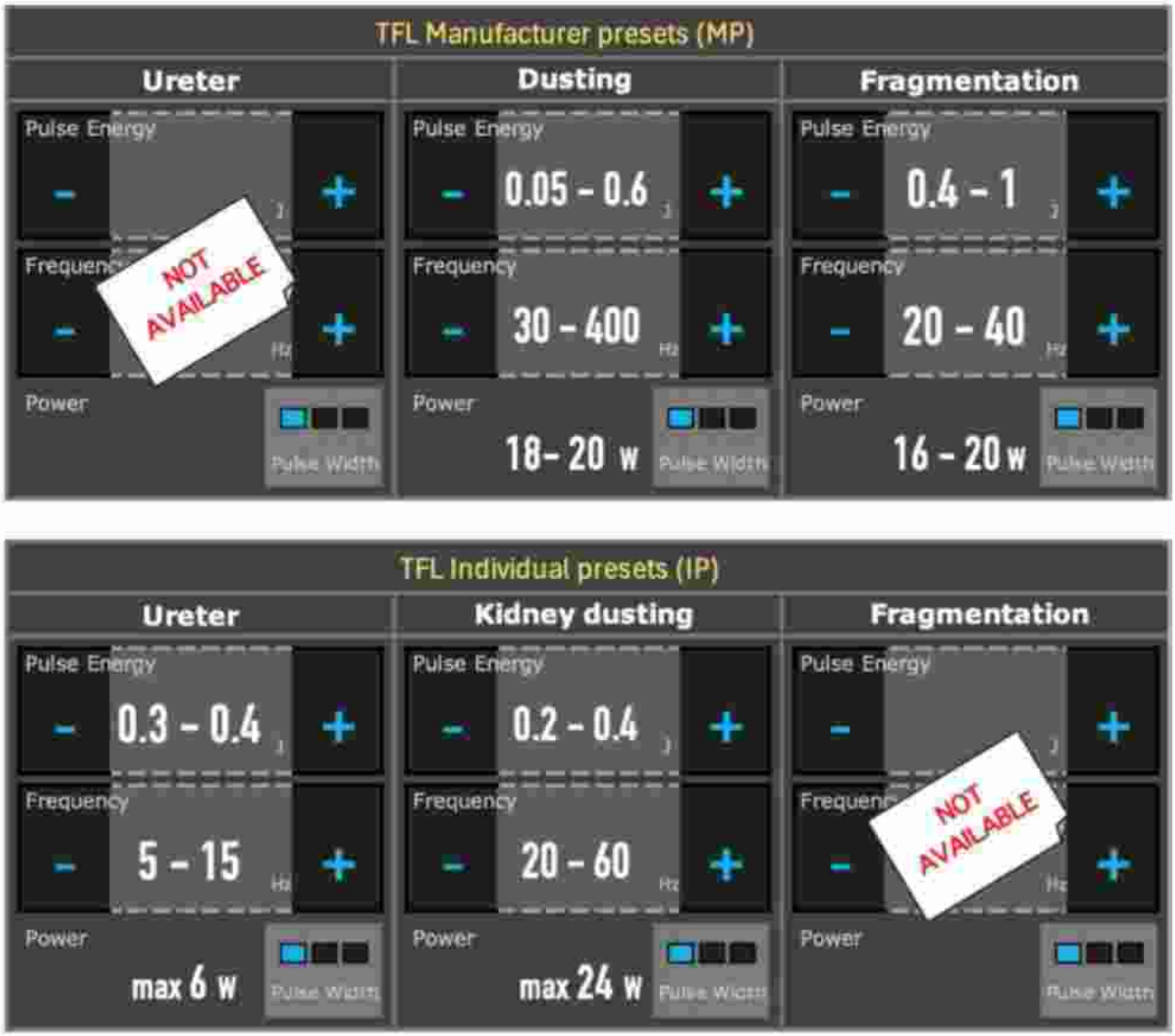


图1展示了2020年奥林巴斯Soltive® Premium钬光纤激光器（TFL）制造商预设（MP）与用户自定义预设（IP）的图形界面对比。关于制造商预设：截至2021年7月，市场上尚未出现专为输尿管设计的制造商预设方案，也未见相关技术指标的明确记载。

我们从soltive ® Premium激光治疗仪中回溯提取了治疗参数，该设备可记录每位患者的以下参数：激光光纤类型、有效激光时间、总能量输送量、最大功率设置以及最低和最高频率设置。平均功率计算方法为总能量除以激光时间。平均激光能量消耗则通过总能量除以结石体积（焦耳/立方毫米^3）得出[20]。

主要结局指标为术后输尿管狭窄（US）的存在。根据Moretto等人的定义，输尿管狭窄是指因输尿管变窄导致的尿流障碍，常伴随疼痛等症状。

现有预设模式专为肾脏设计，不适用于输尿管。关于单个预设模式：由于TFL最初主要作为碎石激光器推出，因此未提供专门用于结石碎石的预设模式。

（复发感染或肾功能丧失）和/或导致再次手术干预[21，22]。两家医疗机构均要求患者在术后六周接受临床评估和肾脏超声检查。根据机构诊疗指南，出现症状、肾功能受损或超声提示肾盂积水的患者需进行全面评估。对于此类病例，将讨论采用逆行输尿管肾盂造影结合诊断性尿路逆行扫描和/或动态显像检查方案。其他安全性指标包括术中并发症，以及根据Clavien-Dindo分级系统[23，24]分类的早期（<1个月）和晚期（≥1个月）术后并发症。

次要结局指标为SFR，定义为内镜检查未见大于2 mm的碎片，且随访影像（所有患者均进行超声检查，根据外科医生的判断可进行额外影像检查，如CT）中亦无大于2mm的碎片[25]。

统计分析

分类变量间的关联性分析采用卡方检验或费希尔精确检验，具体视情况而定。连续变量间的差异性分析采用独立样本t检验或曼-惠特尼U检验，视情况而定。连续变量间的相关性分析采用皮尔逊相关检验或斯皮尔曼rho检验，视情况而定。二分类结局预测因子的分析采用逻辑回归模型。双侧上尿路梗阻患者纳入个体患者分析。所有统计检验均为双侧检验，p值<0.05视为具有统计学意义。统计分析与图表绘制使用IBM SPSS Statistics 29.0软件（美国纽约州阿蒙德市IBM公司）完成。

结果

共有158名患者可供分析，每组79名，均在2020年6月至2021年5月期间接受治疗，平均年龄为53岁。

所有患者均接受术前CT扫描以评估结石负荷。多数病例为肾结石而非输尿管结石。具体而言，70%的患者患有肾结石（伴/不伴输尿管结石），而53%的患者为输尿管结石（伴/不伴肾结石）。结石最大尺寸与结石体积存在显著相关性（斯皮尔曼相关系数0.92；p <0.001；补充图1）。表1列出了患者的详细特征。

在基线患者特征方面，与IP组相比，MP组的糖尿病发病率较低（9%vs.20%；p=0.04）。此外，MP组的术前置入支架比例显著低于IP组（56%vs.91%；p <0.001）。两组在其他基线变量方面未见显著差异。具体而言，结石负荷相当（两组最大结石中位尺寸均为9毫米；p=0.39；MP组结石体积中位数269 mm^3，IP组264 mm^3；p=0.67）。同样，输尿管结石阻塞率在MP组和IP组间也无显著差异（分别为29%vs.34%；p=0.49）。

两组在操作特征上存在显著差异。MP组的UAS使用率更高，主动激光时间更短。与IP组相比，能量消耗更高（J/mm^3）、平均功率更高、最大功率设置更高、激光频率设置更高（适用于最低和最高频率设置）（表1和图2）。

所有患者均保持随访无失访，且术后3个月内均完成至少一次首次术后复查。MP组发生9例碎石（11%），而IP组仅1例（1%）（p=0.009）。单因素分析显示，结石阻塞程度、未置入支架、激光器预设参数、总激光能量递增及平均功率提升是碎石的预测因素（表2）。多因素分析中，结石阻塞程度（OR7.10（CI1.67–30.1）；p=0.008）和激光器预设参数（OR12.4（CI 1.48–104）；p=0.02）（表2）成为碎石的独立预测因素。

患者的详细特征及管理

10例US患者见*补充表*

1. 所有患者在初次诊断时均存在输尿管结石。所有患者均接受逆行输尿管尿路造影以定位并测量结石。超声显示的结石位置与10例患者中4例（40%）的原结石位置相符，另有4例（40%）显示结石位置更远端，其余2例（20%）显示结石位置更近端。多数病例采用腹腔镜达芬奇辅助输尿管成形术（使用颊黏膜移植片或阑尾瓣）或输尿管再植术（50%）或球囊扩张联合输尿管支架术（33%）进行治疗。此外，1例需行肾切除术，另1例结石自行消退。接受重建手术的患者至少随访2年，期间未出现失访情况，术后恢复良好，无复发迹象。

在术中、术后早期和术后晚期并发症方面，MP组和IP组之间未观察到显著差异。

SFR在两组间无显著差异（MP组和IP组分别为85%和84%；p=0.67）。

讨论

据我们所知，这是首项证实使用制造商预设的高功率、高频激光参数进行输尿管镜碎石术存在风险的临床研究。具体而言，与更为保守的个性化激光参数设置相比，制造商预设参数显著增加了术后超声检查风险（多变量分析显示比值比OR=12.4，p=0.02），但两组的碎石成功率（SFR）无显著差异。多数术后超声病例最终需要进行重大手术干预。

表1患者特征

基线特征					程序特征				
变量	全面的（*n*=168）	制造商 turer激光预设（*n*=79）	个人 激光预设值（*n*=79）	p值	变量	全面的（*n*=168）	制造商 turer激光预设（*n*=79）	个人 激光预设值（*n*=79）	p值
年龄（平均值，SD）	53 (17)	52 (19)	54 (15)	0.48*	UAS使用	86 (54%)	51 (65%)	35 (44%)	**0.011****
雄性：雌性比率	2.1: 1	2.0: 1	2.2: 1	0.87**	术后DJ支架植入术	156 (99%)	79 (100%)	77 (98%)	0.16**
BMI（均值，标准差）（kg/m^2）	26 (5)	26 (5)	26 (5)	0.76*	激光光纤芯径				**<0.001****
					150 µm	84 (53%)	5 (6%)	79 (100%)	
					200 µm	68 (43%)	68 (86%)	0 (0%)	
					365 µm	6 (4%)	6 (8%)	0 (0%)	
糖尿病	23 (15%)	7 (9%)	16 (20%)	**0.04****	有效激光时间（mm:ss）（中位数，IQR）	06:28 (01:56–16:36)	04:38 (01:37–09:37)	13:05 (02:42–23:33)	**<0.001*****
ASA评分				0.65**	总能量（KJ）	6.26 (1.63–17.1)	6.50 (2.28–16.38)	5.98 (9.03–17.50)	0.41***
1	17 (11%)	9 (11%)	8 (10%)						
2	94 (59%)	50 (63%)	44 (56%)						
3	41 (26%)	17 (22%)	24 (30%)						
4	6 (4%)	3 (4%)	3 (4%)						
既往尿路结石病史	44 (28%)	22 (28%)	22 (28%)	1.00**	能耗（J/mm^3）（中位数，IQR）	18 (7–32)	20 (11–44)	17 (7–26)	**0.031*****
石头位置				0.94**	平均功率(W)（中位数，IQR）	19 (8–20)	20 (20–25)	8 (6–15)	**<0.001*****
肾脏	67 (43%)	33 (42%)	34 (43%)						
输尿管	48 (30%)	25 (32%)	23 (29%)						
都	43 (27%)	21 (26%)	22 (28%)						
输尿管结石地点				0.18**	最大功率设置(W)（平均值，标准差）	21 (13)	27 (13)	15 (9)	**<0.001***
近端	54 (59%)	54 (59%)	31 (69%)						
中间	25 (28%)	25 (28%)	8 (18%)						
远端	9 (10%)	9 (10%)	4 (9%)						
多选	3 (3%)	3 (3%)	2 (4%)						
数量结石（中位数，IQR）	1 (1–3)	1 (1–3)	2 (1–3)	0.28***	最低频率设置-脉冲声（Hz）（中位数，IQR）	40 (10–200)	200 (100–200)	14 (5–30)	**<0.001*****
最大结石尺寸（mm）（中位数，IQR）	9 (7–13)	9 (7–13)	9 (7–13)	0.39***	最高频率组-脉冲声（Hz）（中位数，IQR）	100 (40–400)	400 (200–400)	40 (30–100)	**<0.001*****
石体积（mm^3）（中位数，Iqr）	267 (110–751)	269 (117–565)	264 (110–857)	0.67***	术后结局				
最大结石密度（HU）（平均值，SD）	1142 (391)	1108 (382)	1177 (399)	0.27*	变量	全面的（*n*=168）	**Manufac-** 激光扫描仪预先布置（*n*=79）	**Individ-** 紫外激光预先布置（*n*=79）	p值
受影响的石头	50 (32%)	23 (29%)	27 (34%)	0.49**	术中困难	总计：8（5%）	总计：3（4%）	总计：2（3%）	0.15**

表1（续）

基线特征					程序特征				
变量	全部的（*n*=168）	制造商turer激光预设（*n*=79）	个人激光预设值（*n*=79）	p值	变量	全部的（*n*=168）	制造商turer激光预设（*n*=79）	个人激光预设值（*n*=79）	p值
					输尿管穿孔肾盂穿孔阴	6 (4%) 1 (1%)	2 (3%) 1 (1%)	1 (1%) 0 (0%)	
					茎异常勃起	1 (1%)	0 (0%)	1 (1%)	
外科手术前的肾积水sis≥2级	47 (30%)	21 (27%)	26 (33%)	0.38**	术后早期并发症	总计：8（5%）			
	总计：9（11%）	总计：5（6%）	0.47**						
					CD I血尿	2 (1%)		0 (0%)	
					CD II	4 (3%)	2 (3%)	3 (4%)	
					UTI谵妄	1 (1%)	1 (1%)	1 (1%)	
					CD IV		0 (0%)		
					TIA	1 (1%)	0 (0%)	1 (1%)	
对侧尿路结石	9 (6%)	4 (5%)	5 (6%)	0.73**	术后晚期并发症	总计：10（6%）	总计：9（11%）	总计：1（1%）	**0.009****
					CD IIIb	10 (6%)	9 (11%)	1 (1%)	
					输尿管狭窄其他	0 (0%)	0 (0%)	0 (0%)	
支架植入前	116 (73%)	44 (56%)	72 (91%)	**<0.001****	石头完全获救	132 (84%)	65 (82%)	67 (85%)	0.67**

T检验，**卡方检验，***曼-惠特尼U检验

SD=标准差；IQR=四分位距；BMI=体重指数；ASA=美国麻醉医师协会；URS=输尿管镜检查；HU=豪斯菲尔德单位；UAS=输尿管导管鞘；TIA=一过性脑缺血发作；CD=克拉维恩-丁多分类

这一假设此前已在多项体外研究[7，26]中被提出，并因安全投诉[27-33]而备受关注，如今这项研究提供的有力证据为其提供了支持。对于所有实施输尿管镜激光碎石术的泌尿科医生而言，这都是一条至关重要的警示，强调了在评估和调整激光参数时必须谨慎操作。

近期系统综述显示，输尿管镜碎石术后发生输尿管狭窄（US）的总体发生率为3%[22，23]。本研究中，机械碎石组（MP组）的输尿管狭窄发生率达11%，这一比例显然已超过该手术的安全阈值。可以理解的是，相关医院（HUG）在引进TFL设备不到一年后便决定停用。相比之下，采用内镜碎石术（IP）的病例中输尿管狭窄发生率仅为1%，这表明使用内镜碎石术时，通过TFL进行输尿管镜激光碎石术是安全可行的。

激光参数与超声波形成之间的关联可能主要由两个关键因素决定：高功率和高频。高功率会导致局部能量传递过快过强，可能引发组织热损伤，从而最终形成超声波[34–36]。同样，高频参数会降低能量传递到结石表面的效率，增加了治疗风险。

非故意靶向输尿管壁而非输尿管结石[26，37]。

总体而言，高功率通常与高频相关联，反之亦然，这主要归因于激光碎石术中使用的脉冲能量范围相对狭窄（主要为0.4–1.5焦耳）[38]。本研究显示，MP组的平均功率、最大功率、最低频率和最高频率设置均显著高于IP组。此外，单变量分析表明平均功率是超声波能量的重要预测因子（每增加1瓦，比值比OR=1.03；p=0.046）。最后，MP组的激光能量消耗显著高于IP组：20焦耳/毫米^{3}对比17焦耳/毫米^3（p=0.031）（如近期研究所强调的，数值越低效果越好）[39，40]。这种能量消耗差异可能源于高频设置对结石表面的靶向精度较低。该假设得到两项体外研究的支持：高频设置会导致激光能量向结石表面的传递效率降低[41，42]。

结石定位不佳，因结石粉尘生成时能见度降低，且当偏离目标时人体反应时间延迟，这会进一步加剧相关危害。

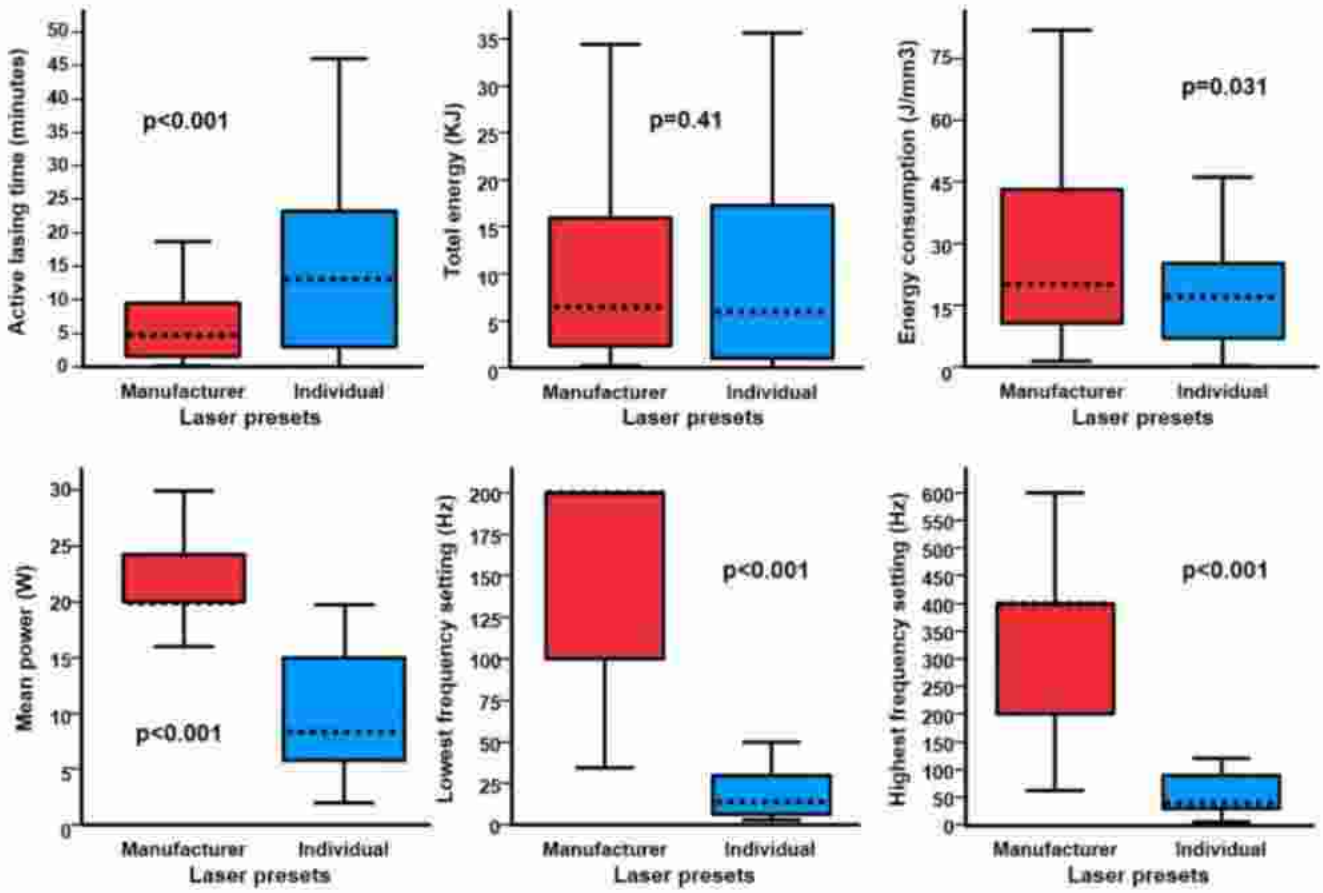


图2激光发生器获取的激光设置分布。箱线图中，中位数用虚线表示，箱体代表25%至75%百分位数，须线代表10%至90%百分位数。

采用高频碎石术[38]。本研究显示，多数接受超声碎石术的患者激光频率设置在100至400赫兹之间。根据平均视觉反应时间至少250毫秒[43]，多数外科医生在结石定位不佳或视野受限时，通常会在发射25到100个激光脉冲后才松开激光踏板。这些过度且不受控的激光脉冲，不仅可能导致观察到的激光能量消耗差异，还可能
本研究还对美国的形成作出了贡献。

多变量分析显示，输尿管结石嵌顿是超声检查的第二重要独立预测因素（比值比=7.10；p=0.008）。这一发现与近期系统综述和荟萃分析结果一致，该研究基于5项研究（共纳入13550名患者）证实嵌顿结石是超声检查的明确预测指标（比值比=7.47；p=0.01）[22]。在本研究队列中，出现超声检查的患者中有70%（7例/10例）存在结石嵌顿。然而，另有43例结石嵌顿患者未出现超声检查，这凸显了其他竞争性风险因素的影响，例如高功率高频激光碎石术等技术手段。

所有尿路结石病例均发生在初次诊断时输尿管已有结石的患者中。值得注意的是，这些病例均伴有输尿管狭窄。在采用超声检查的病例中，仅有40%的患者结石位置与最初发现时完全一致。这一发现表明，结石可能在初次诊断与输尿管镜激光碎石术之间发生位移，或者热损伤可能发生在激光能量作用区域之外。因此，在缺乏确凿证据证明之前，高功率高频激光碎石术对输尿管结石和肾结石都可能存在风险。未来研究应通过前瞻性方案，对激光发射部位进行标准化操作，以验证“远端热损伤”的假设。

值得注意的是，单变量分析显示术前置入支架可显著降低输尿管结石（US）风险（比值比=0.2；p=0.022）。尽管这一发现可能部分源于两家医院的诊疗差异（MP组术前置入支架56%vs.IP组91%；p<0.001），但可以合理推测：术前置入支架通过扩张输尿管并改善冲洗液流动，从而降低输尿管损伤风险，优化激光碎石术条件，进而预防结石形成[44]。总体而言，术前置入支架与更高的结石碎石率（SFR）及更少的术中术后并发症相关[45]。未来仍需进一步研究以验证这一结论。

表2输尿管狭窄预测因子的逻辑回归分析

变量	单变量		多变量*	
	或（95%置信区间）	*p*	或（95%置信区间）	*p*
年龄（连续）	0.98 (0.94–1.02)	0.32		
男性vs.女性	4.59 (0.57–37.3)	0.15		
BMI（kg/m2）（连续）	1.03 (0.91–1.17)	0.64		
糖尿病	1.4 (0.3–7.6)	0.62		
最大结石尺寸（mm）（连续）	1.04 (0.94–1.15)	0.44		
石方体积（mm^3）（连续）	1.00 (1.00–1.00)	0.92		
输尿管结石	5.70 (1.41–23.1)	**0.015**	7.10 (1.67–30.1)	**0.008**
术前肾积水≥2级	1.63 (0.44–6.06)	0.47		
主URS尝试失败	1.6 (0.3–8.1)	0.57		
支架植入前	0.2 (0.06–0.8)	**0.022**		
UAS使用	0.8 (0.2–3.0)	0.77		
制造商（MP）与激光光纤芯径的个体激光预设（IP）	10.0 (1.24–81.2)	**0.031**	12.4 (1.48–104)	**0.02**
150 µm	1.00 (参照)			
200 µm	4.71 (0.94–23.5)	0.059		
365 µm	8.20 (0.63–106.6)	0.11		
实际激光时间(s)（连续）	1.00 (1.00–1.00)	0.64		
总能量（KJ）（连续）	1.02 (1.00–1.04)	**0.026**		
激光能量消耗（J/mm^3）	1.00 (0.99–1.02)	0.60		
平均功率(W)	1.03 (1.00–1.06)	**0.046**		
最大功率设置(W)	1.02 (0.98–1.07)	0.28		
最低频率设置（Hz）	1.00 (0.99–1.01)	0.12		
最高频率设置（Hz）	1.00 (0.99–1.01)	0.16		
术中输尿管或肾盂穿孔	3.18 (0.34–30.2)	0.31		

在前向条件性多变量分析中，仅保留进入标准≤0.05且剔除阈值≥0.1的变量。最终纳入模型。

OR=比值比；95%CI=95%置信区间；BMI=体重指数

研究支架植入前的干预措施对降低清痛性结肠炎（US）风险的影响。

关于UAS的使用，MP组的使用频率更高（65%vs.IP组的44%；p=0.011）。然而，UAS的使用并未被确定为US的预测因素。这些发现与既往研究一致，既往研究表明URS期间放置UAS与US的发展之间没有明确的关联[19，46]。

在我们的研究中，无论是石块尺寸（最大直径）还是体积，均未被证实为超声波能量（US）的预测因子。相反，在单变量分析中，总能量传递量被确定为超声波能量的重要预测因子（每增加1 kJ，比值比OR=1.02；p=0.026）。这一发现强调，在尿路结石（URS）治疗过程中，所有激光参数（功率、频率和累积能量传递量）都应谨慎选择和监测。

本研究存在若干局限性。首先，其回顾性研究设计本身存在潜在偏倚，导致部分信息难以获取，例如灌注参数（压力、手动泵、体积、流速等）的详细数据，且未遵循机构指南要求的随访时长。其次，该激光系统未能提供所用平均频率的详细信息。

在手术过程中，这种缺乏细节的局限性制约了我们的分析能力。此外，本研究数据来自两家采用不同URS技术方案的医疗机构，两家机构外科医生的专业水平差异无法完全排除。不过，两家均为同国的大学附属医院，且每家手术室都配备有超过100次URS手术经验的泌尿科医生，这表明专业水平差异对结果的影响微乎其微。另一个局限是样本量相对较小（158例患者），虽然足以进行初步观察和得出结论，但可能缺乏检测细微关联或罕见并发症所需的统计效力。尽管存在这些局限，我们认为本研究结果具有可靠性，因为所有可能影响超声检查率的其他显著变量（如年龄、ASA评分、既往URS病史、结石位置及数量、结石阻塞率）在两组间分布均等。结石负荷参数（最大结石尺寸和结石体积）之间的显著相关性进一步凸显了可用于分析的数据质量。值得注意的是，SFR未基于系统性的术后CT扫描，这可能导致成功率被高估。SFR应

因此应相应地进行解释。有必要开展更大规模的前瞻性研究，以验证我们的发现，并为碎石术中激光参数的安全阈值提供依据。

结论

制造商预设的高功率、高频激光参数会显著增加超声碎石形成的风险，这种风险与输尿管结石本身无关，且无法提升碎石成功率。我们的研究结果强调了在TFL碎石术中谨慎选择激光参数的重要性，建议采用个体化激光预设方案，根据每位患者的具体情况和临床场景选择更为保守的参数设置。未来研究应优先开展前瞻性试验，评估功率、频率、累积能量输送量及激光能耗等具体参数对疗效的影响，从而确定既能最大化治疗效果又能最大限度降低组织损伤风险的最佳参数组合。此外，基于术中实时反馈（如冲洗液流量与温度、结石定位、光纤工作距离、结石粒径、结石类型、碎石速率等）开发动态实时可调预设方案，是提升患者治疗效果的极具潜力的研究方向。

补充信息在线版本包含补充材料，可在https://doi.org/10.1007/s00345-025-05553-0上找到。

作者贡献：R.V.和E.X.K.负责撰写论文主体内容，绘制1和2图表1及2表格，并补充绘制图1和表1。O.T.与E.X.K.共同参与研究方案设计。R.V.、E.X.K.、M.V.和D.E.负责研究方案制定与实施。R.V.、E.X.K.和O.L.W.共同完成日内瓦及苏黎世伦理委员会注册工作。R.V.与T.D.L.负责数据收集与管理。R.V.和E.X.K.完成统计分析。全体作者均参与数据分析、论文审阅与修改工作。

资金来源：苏黎世大学提供的开放获取资金。本研究未获得任何资金支持。

数据可用性：本研究期间未生成或分析任何数据集。

声明

伦理审批与参与同意所有涉及人类受试者的研究程序均遵循机构及/或国家研究委员会的伦理标准，同时符合1964年《赫尔辛基宣言》及其后续修订版本或同类伦理规范。本研究方案（研究编号：BASEC 2023-00660和2024-00272）已获得当地伦理委员会批准。

竞争利益作者声明无竞争利益。

开放获取本文采用知识共享署名4.0国际许可协议授权，允许在任何媒介或格式中自由使用、分享、改编、传播和复制，但需满足以下条件：正确标注原作者及来源信息、提供知识共享许可协议链接，并注明是否进行过修改。文中图片或其他第三方素材均包含在知识共享许可协议中。除非材料来源标注另有说明。若素材未包含在知识共享许可协议中，且您的使用方式未获法定授权或超出许可范围，则需直接向版权方申请授权。如需查看许可协议副本，请访问http://creativecommons.o rg/licenses/by/4.0/。

参考文献

1. Geraghty RM，Jones P，Somani BK（2017）过去二十年间全球尿路结石疾病治疗趋势：系统综述。J Endourol 31 https://doi.org/10.1089/end.2016.0 895
2. Traxer O，Keller EX（2020）钬光纤激光：治疗肾结石的新选择？与钬：YAG激光的比较。世界泌尿外科杂志38 https://doi.org/10.1007/s00345-019-0265 4-5
3. Ventimiglia E，Robesti D，Bevilacqua L等（2023）新型脉冲钬：YAG激光器有哪些应用前景？尿路内应用的系统综述。World J Urol 41，https://d oi.org/10.1007/s00345-023-04580-z
4. Traxer O，Sierra A，Corrales M（2022）哪种激光最适合碎石术？钬光纤激光。Eur Urol Open Sci 44 https://do i.org/10.1016/j.euros.2022.05.020
5. Jiang P，Okhunov Z，Afyouni AS et al（2023）*超脉冲钬光纤激光器与钬激光器在体内猪模型中引起肾结石的比较*。J Endourol 37：335–340，https://doi.org/10.1089/end.2022.0445
6. UlvikØ，Æsøy MS，Juliebø-Jones P等人（2022）在《欧洲泌尿外科杂志》第82卷第73-79页发表的前瞻性随机临床试验结果显示，钬光纤激光与钬激光在输尿管镜碎石术中的疗效对比。https://doi.org/10.1016/j.eururo.2022.02.027
7. Belle JD，Chen R，Srikureja N et al（2022）新型钬光纤激光器在体外比传统钬激光器在更高的尿路上皮热损伤风险吗？研究？J Endourol 36：1249–1254.https://doi.org/10.1089/end.2021.0842
8. Wanderling C，Saxton A，Phan D等（2024）这里很热！在解剖水凝胶肾脏模型中钬激光与铥激光的比较。Urolithiasis52：49，https://doi.org/10.1007/s00 240-024-01541-y
9. Keller EX，De Coninck V，Talso M，Traxer O（2023）对Belle所发表的《体外研究中新型钬光纤激光器是否比传统钬激光器更容易导致尿路上皮热损伤？》一文的评论。J Endourol 37：1164–1165，https://doi.org/10.1089/end.2022.0336
10. Æsøy MS，Juliebø-Jones P，Beisland C，UlvikØ（2022）采用钬光纤激光和钬：钇铝石榴石激光进行输尿管镜检查时的温度曲线：一项临床前研究的结果。Scand J Urol 56：313–319，https://doi.org/10.1080/21681805.2022.21043 67
11. Molina WR，Carrera RV，Chew BH，Knudsen BE（2021）输尿管激光碎石术中的温度升高：超脉冲钬光纤激光器（SPTF）与高功率120 W钬YAG激光器（Ho：YAG）的比较。World J Urol 39：3951–3956，https://doi.or g/10.1007/s00345-021-03619-3
12. 西耶拉·A、科拉莱斯·M、皮内罗·A、特拉克塞尔·O（2022）输尿管肾镜检查中钬光纤激光器的预设参数：Twitter专家的

建议。世界泌尿外科杂志40。https://doi.org/10.1007/s00345-022-03966-9

13. Sierra A，Corrales M，Pinero A等（2022）《激光公司预设参数术语表：尚未达成共识！》《世界泌尿学杂志》40：2313–2321.https://doi.org/10.1007/s00345-022-04090-4
14. 凯勒·艾蒂安·泽维尔https://x.com/exkeller/status/1515903100801216512.见：X
15. 凯勒·埃蒂安·泽维尔https://x.com/exkeller/status/1316267242020106241/照片/2。见：X
16. 凯勒·埃蒂安·泽维尔https://x.com/exkeller/status/1316644981004060737/photo/2。见：X
17. Panthier F，Kutchukian S，Ducousso H et al（2024）如何估计结石体积及其在结石手术中的应用：全面综述。Actas Urologicas Espanolas（英文版）48，<sp_2
18. Fernbach SK，Maizels M，Conway JJ（1993）肾积水的超声分级：胎儿泌尿学会使用的系统的介绍。Pediatr Radiol 23：478–480。https://doi.org/10.1007/BF02012459
19. 托纳利S、伊尔马兹M、茨韦尔夫L等（2023）逆行输尿管镜治疗输尿管结石术后输尿管狭窄的预测因素：系统性文献综述。J Clin Med 12.http s：//doi.org/10.3390/jcm12103603
20. Ventimiglia E，Pauchard F，GorgenARH et al（2021）我们如何评估Ho：YAG低功率激光碎石术治疗上尿路结石的疗效？介绍焦耳/mm3和激光活性概念。World J Urol 39：891–896。https：//doi.org/10.1007/s00345-020-03241-9
21. 莫雷托·S、普田·A、斯科丰·C·M等学者（2024年）通过国际德尔菲调查与共识会议，系统梳理了输尿管结石内镜治疗术后狭窄的危险因素。《J Urol》42：412。https://doi.org/10.1007/s00345-024-05103-0
22. 莫雷托·S、普田·A、斯科丰·C·M等（2024）《输尿管狭窄发生率与内镜治疗尿路结石相关风险因素的系统评价及荟萃分析》载于《世界泌尿学杂志》42：234.https://doi.org/10.1007/s00345-024-04933-2
23. 德·科宁克V、凯勒EX、索马尼B等人（2020）输尿管镜检查并发症：全面综述。《世界泌尿外科杂志》38：2147–2166. https://doi.org/10.1007/s00345-019-03012-1
24. Dindo D，Demartines N，Clavien PA（2004）外科并发症的分类：一项在6336例患者队列中进行评价的新建议和调查结果。Ann Surg 240.https://doi.org/10.1097/01.sla.0000133083.54934.ae
25. Panthier F，Gauhar V，Ventimiglia E等（2024）重新思考无结石率与泌尿外科手术结果：来自综述成员的观点。Eur J Urol 86：198–199 https://doi.org/10.1016/j.eururo.2024.06.001
26. Sierra A，Corrales M，Kolvatzis M et al（2022）热损伤和钬YAG与钬光纤激光器的效率——体外研究。J Endourol 36：1599–1606。https://doi.org/10.1089/end.2022.0216
27. （2020）https://www.accessdata.fda.gov/scripts/cdrh/cfdocs/cfMAUDE/detail.cfm?maudfoi_id=12043126%26；pc=GEX.见于：《不良事件报告系统》（MAUDE）
28. （2020）https://www.accessdata.fda.gov/scripts/cdrh/cfdocs/cfMAUDE/detail.cfm?maudfoi_id=10782150%26；pc=GEX.见于：《不良事件报告系统》（MAUDE）
29. （2022）https://www.accessdata.fda.gov/scripts/cdrh/cfdocs/cfMAUDE/detail.cfm?maudfoi_id=15977674%26；pc=GEX&device_sequence_no=1.见于：《不良事件报告系统》（MAUDE）
30. （2021）https://recalls-rappels.canada.ca/en/alert-recall/soltive-premium-superpulsed-laser-systems-2021-08-22.见：加拿大不良事件
31. （2024）https://recalls-rappels.canada.ca/en/alert-recall/soltivet m-premium-superpulsed-tf-laser-system.In：Canada Adverse Events
32. （2021）https://www.moph.gov.lb/userfiles/files/Medical%20Devices/Medical%20Devices%20Recalls%202021/19-07-2021/TFL PLSSOL-TIVEPremiumSuperPulsedLaserSystem.pdf.在：澳大利亚政府-卫生部
33. （2021）https://nemdr.sfda.gov.sa/Secure/CA/CaViewRecall.aspx?caid=10%26；rid=15757%26；AspxAutoDetectCookieSupport=1.在：沙特阿拉伯
34. Pauchard F，Ventimiglia E，Corrales M，Traxer O（2022）肾内温度与压力管理的实用指南：经肾镜手术期间的临床证据启示。《临床医学杂志》11：3429。https://doi.org/10.3390/jcm11123429
35. Ventimiglia E，Robesti D，Keller EX等（2024）尿道内激光激活过程中的温度分布：引入热安全距离概念。World J Urol 42：453。https://doi.org/10.1007/s00345-024-05162-3
36. Corrales M，Panthier F，Solano C等（2024）激光手术中的安全规范：警示与限制：逆行肾内手术中的应用。西班牙泌尿外科学会会刊48：19–24.https://doi.org/10.1016/j.acuro.2023.04.005
37. 西耶拉A、索拉诺C、科拉莱斯M等（2024）《稳态与脉冲激光技术在钬光纤激光器中的应用对比》载于《世界泌尿学杂志》42：487.https://doi.org/10.1007/s00345-024-05102-1
38. De Coninck V，Hente R，Claessens M et al（2021）高功率、高频Ho：YAG激光器不是逆行肾内手术的必需品。Eur Urol Focus 7：5–6。https://doi.org/10.1016/j.euf.2020.12.007
39. Keller EX，Kwok J-L，Panthier F et al（2024）规划我的尿道镜激光碎石术：我应该合理预期多少能量和时间？整合激光能量消耗的概念（J/mm3）。World J Urol 42：100。https://doi.org/10.1007/s00345-024-04790-z
40. Kwok J-L，De Coninck V，Ventimiglia E等（2024）碎石术中激光消融效率、激光消融速度和激光能量消耗：它们是什么以及如何定义？系统综述和标准化术语的建议。Eur Urol Focus 10：599–611。https://doi.org/10.1016/j.euf.2023.10.004
41. Aldoukhi AH，Black KM，Hall TL et al（2020）钬激光碎石术期间消融的频率阈值：你能达到多高？？J Endourol 34：1075–1081.https://doi.org/10.1089/end.2020.0149
42. Aldoukhi AH，Hall TL，Ghani KR，Roberts WW（2021）击中率：不同模式下激光碎石术中激光光纤至结石距离的分析。J Endourol 35：355–359。https://doi.org/10.1089/end.2020.0298
43. Jain A，Bansal R，Kumar A，Singh K（2015）医学一年级学生视觉和听觉反应时间的性别和身体活动水平比较研究。Int J Appl Basic Med Res 5：124。https://doi.org/10.4103/2229-516X.157168
44. Jiang P，AfyouniA，BrevikA et al（2022）J型支架置入术前对膀输尿管管腔周长的影响。J Endourol 36：885–890。https://doi.org/10.1089/end.2021.0771
45. Calvillo-Ramirez A，Angulo-Lozano JC，del Rio-Martinez CJ et al（2024）与非支架术相比，输尿管镜下支架术治疗尿路结石的安全性和有效性：比较研究的荟萃分析。World J Urol 43：12。https://doi.org/10.1007/s00345-024-05365-8

46.de Amorim LGCR，Campos MEC，Dumont LS等（2024）逆行性内手术：是否使用输尿管套管
一项随机对照试验的系统评价和荟萃分析。Int Braz J Urol 50：670–682。https://doi.org/10.1590/s1677-5538.ibju.2024.0452

出版商注Springer Nature对已发表地图和机构隶属关系的管辖权主张保持中立。

可控脉冲掺铥光纤激光器碎石特性实验研究

王子怡[1], 姚育成[1], 姚京云[2], 朱晓峰[3]
[1]湖北工业大学理学院, 武汉 430068;
[2]云南大学信息学院, 昆明 650091;
[3]武汉锴健科技有限责任公司, 武汉 430071

摘 要: 利用峰值功率 600 W 的掺铥光纤激光器, 用 Labview 程序外控激光脉冲参数进行体外碎石实验, 研究脉冲铥激光碎石规律, 为临床应用提供参考。结果表明, 脉冲铥激光具有较好的碎石能力, 设置能量 0.3 J 的脉冲铥激光冲击草酸钙结石时碎片颗粒大部分直径小于 0.5 mm, 具有较好的粉末化能力; 当脉冲能量较小时, 碎石效率随脉冲能量变大快速提高, 对于峰值功率 600 W 的铥激光, 双脉冲组合并不能产生明显的"摩西效应"使碎石效率提升; 另外掺铥光纤激光碎石时为提高碎石效率可能设置较大脉宽, 此条件下激光在水中的穿透距离较大, 实验中达到 5.4 mm, 因此, 手术中要充分考虑光纤端与周围组织的安全距离, 避免造成周围组织的损伤。

关键词: 激光碎石; 掺铥光纤激光器; 双脉冲组合; 组织损伤
中图分类号: TN249 **文献标识码**: A **doi**: 10.14016/j.cnki.jgzz.2025.03.045

Experimental study on the characteristics of pulse controlled thulium fiber laser lithotripsy

WANG Ziyi[1], YAO Yucheng[1], YAO Jingyun[2], ZHU Xiaofeng[3]
[1]*School of Science, Hubei University of Technology, Wuhan* 430068, *China*;
[2]*School of Information Science &Engineering, Yunnan University, Kunming* 650091, *China*;
[3]*Wuhan Radium Health Science and Technology Co., Ltd, Wuhan* 430071, *China*

Abstract: Using the peak power of 600 W thulium-doped fiber laser, the laser pulse parameters were controlled by Labview program to carry out the extracorporeal lithotripsy experiment, and the law of pulsed thulium laser lithotripsy was studied to provide reference for clinical application. The results show that the pulsed thulium laser has good lithotripsy ability. When the pulsed thulium laser with an energy of 0.3 J is set to impact calcium oxalate stones, most of the debris particles are less than 0.5 mm in diameter, which has good pulverization ability. When the pulse energy is small, the gravel efficiency increases rapidly with the increase of pulse energy. For the thulium laser with a peak power of 600 W, the double pulse combination does not produce obvious 'Moses effect' to improve the gravel efficiency. In addition, a large pulse width may be set to improve the efficiency of thulium-doped fiber laser lithotripsy. Under this condition, the penetration distance of laser in water is large, reaching 5.4mm in the experiment. Therefore, the safe distance between the fiber end and the surrounding tissue should be fully considered in the operation to avoid damage to the surrounding tissue.

Key words: laser lithotripsy; thulium-doped fiber laser; dual-pulse combination; tissue damage

1 引言

近年来, 软镜技术快速发展, 激光可通过光纤传导经输尿管进行肾盂内碎石从而避免了穿刺损伤, 激光碎石的优势得到充分发挥。激光碎石设备中, 1 940 nm 波长的脉冲铥光纤激光器(TFL)作为一种新兴技术备受关注, 与钬激光相比, 具有光纤芯径小、脉冲频率高、碎石粉末化好及反冲小等优点[1-5]。

收稿日期: 2024-09-13
基金项目: 武汉市科技计划项目(No. 2020BED021); 国家重点研发计划项目(No. 2023YFE0126400)
作者简介: 王子怡(1998-), 女, 硕士, 研究方向为光电子器件、激光技术及应用。E-mail: 717805320@qq.com
通讯作者: 姚育成(1975-), 男, 副教授, 研究方向为光电子器件、激光技术及应用。E-mail: yaoyucheng@libat.edu.cn

2021 年，Panthier 等人[6]体外研究比较了 TFL 和 Ho:YAG 在不同激光设置下用 150 μm 光纤和 272 μm 光纤的消融率，研究表明在相同的环境和光纤下，TFL 消融率至少是 Ho:YAG 消融率的两倍，比 Ho:YAG 产生更高的烧蚀体积。同年，Jones 等人[7]初步临床研究表明，超脉冲光纤铥激光碎石术因其能改善手术中的能见度，可以治疗结石类型范围大等优点，具备成为新一代碎石工具的潜力。2022 年，Ulvik 等人[8]对比了铥激光和钬激光碎石疗效差异，铥激光肾结石清除率要高于钬激光，术中出血发生率也低于钬激光。然而，在 2023 年许力为等人[9]的一项研究中，TFL 组与 HL 组比较患者术后并发症发生率略高，同年 Ahmad Para Sajad 等人[10]在临床研究指出，尽管 TFL 在输尿管镜激光碎石术中展现出显著优势，但其在术后输尿管狭窄的发生率与钬激光碎石相比却较高，这些发现给提出了新的挑战，需要进一步深入研究铥激光碎石特性，以降低并发症风险。通过实验研究不同脉冲形式下的铥激光碎石作用特性，研究不同参数铥激光碎石效率及效果，为临床应用提供参考。

2 铥激光碎石分析

铥激光碎石机制与钬激光相似，主要是光热效应以及光机械效应，即激光能量被结石中的水、有机物、矿物质吸收，结石孔隙间的水瞬间温度升高汽化，形成微爆使结石分解，另外被照射结石部分若温度高于物质阈值温度，可导致结石的热分解[11-13]，因此，铥激光碎石是一个复杂的物理化学过程，其特性直接决定了碎石效率及组织损伤。根据铥激光在水中的吸收系数分析，其穿透深度应该只有 0.1 mm，但通常碎石用的激光脉宽有几百微秒，其作用过程包含了空泡产生、膨胀、坍塌及冲击等多个过程，激光脉冲峰值功率、脉冲形式等参数决定了此过程特性。文献[14]研究了脉冲钬激光与水作用的微爆过程，其微爆空化气泡约 300 μs 时开始坍塌，脉冲宽度大于 300 μs 时，空化气泡进入混乱多泡状态。

激光作用过程特性直接决定了碎石效率和损伤范围[15-17]，提高单位能量碎石效率需要尽可能多的激光能量作用于结石或结石内空隙间的水，因此，理想的状态是合适的铥激光能量瞬时形成一个小空泡，让更多的激光能量穿过空泡作用到结石上。如双脉冲钬激光的“摩西效应”就是利用小能量脉冲产生气泡将水分开，然后使大能量脉冲激光作用于结石面提高碎石效率。

3 实验装置和方法

3.1 结石模型

不同的人体结石样本内外形貌、成分都有较大差异，不容易标定不同参数铥激光碎石效率及特性。肾结石成分主要为磷酸钙和草酸钙，其中草酸钙结石是较硬的一种，实验中制作草酸钙结石模型，分析铥激光碎石特性，同时用人体草酸钙结石样本（图 1b）验证铥激光碎石的有效性。

草酸钙结石的主要形成机制是钙、草酸盐结晶，而钙离子、草酸离子、尿酸离子和磷酸盐离子是晶体形成的主要促进剂，它们可以通过几种机制的激活来促进石材成分的结晶或聚集[18]。组织成分是影响激光与组织作用的最重要因素，根据草酸钙结石的主要成分，同时考虑结石硬度等特点，实验中结石模型是用一水草酸钙（$CaC_2O_4 \cdot H_2O$）和石膏粉（$CaSO_4 \cdot 2H_2O$）加清水凝结所形成的固体，结石中的羟基（-OH）是铥激光碎石的主要作用群体[12]。具体制作方法为：（1）将一水草酸钙、石膏粉和清水按 1∶2∶1 的比例混合加入到容器中；（2）搅拌至一水草酸钙和石膏粉混合均匀；（3）将混合物缓慢地倒入正方体模具中，静置待形成草酸钙结石样本模型（图 1 a）。



（a）结石模型



（b）人体草酸钙结石样本

图 1 结石模型及人体结石样本

3.2 实验装置及方法

如图 2 所示，实验装置由激光器、医疗光纤、脉冲驱动系统、信号检测示波器、双轴显微镜和方形石英烧杯等组成。其中激光器为峰值功率 600 W 的脉冲铥光纤激光器（上海科乃特激光科技有限公司产品），工作波长为 1 940 nm，光纤为芯径 370 μm 的低氢氧医疗光纤。脉冲驱动系统通过 Labview 软件自行编程

设置，并通过计算机串口连接驱动卡（型号：NI USB-6211，采样率：100 kHz）实现输出参数控制，改变方波的占空比以及相位大小实现任意脉冲波形驱动（图 3），同时信号由示波器实时检测，保证光脉冲的准确性。

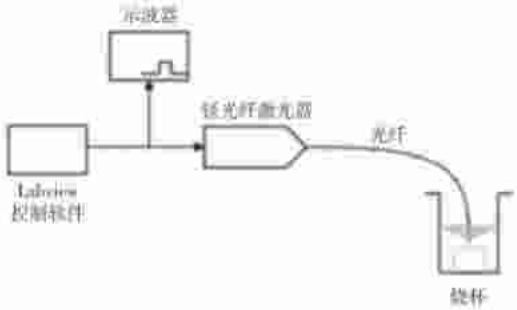


图 2 实验装置示意图



图 3 双脉冲波形

测量铥激光在水中的穿透深度时，将光纤浸入到方形烧杯的水中，调整光纤端部到水底部的距离，用黑色相纸观察到激光传出烧杯底部时，记录光纤端部到水底的距离标定激光脉冲穿透水的深度。激光穿透深度的数据通过多组实验，去掉误差较大的值，取 5 组一致性较好的平均值得出实验结果。另外设置不同的激光参数在水环境下进行碎石特性和碎石效率实验，通过多次重复减小随机误差，同时用内窥镜观察碎石过程（图 4）。



图 4 实验装置

激光碎石数据通过电子天平（型号：YJ-DTF-300，精度：0.001 g）称重获得，因为粉末化结石在水中不易收集，实验时先用电子天平称已经充分浸泡过水的结石质重，记录数据，碎石后再进行称重，实验前后的质量相减得到消融质量。经过多组实验后，去掉误差较大的值，取 5 组一致性较好的平均值得出结果。

4 实验结果及分析

4.1 不同参数的铥激光脉冲在水中的穿透深度

1 940 nm 的铥激光根据辐射波长水吸收系数计算在水中的穿透深度不足 0.1 mm，被视为一种安全的碎石激光，但实验中发现脉冲铥激光作用于水时，脉冲能量产生汽化空泡而使激光穿透更深的距离[20]。使用峰值功率为 600 W 的 TFL，设置脉宽从 100 μs~3 000 μs，测量激光脉冲穿透水的深度，结果如图 5 所示。

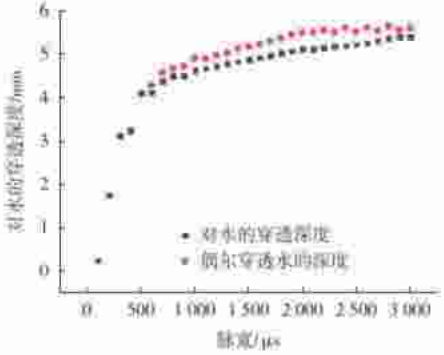


图 5 脉冲激光穿透水的深度

可以看出单脉冲铥激光在峰值功率 600 W 不变的情况下，激光在水中的穿透深度随脉宽增大（能量增大）而快速增大，但当脉宽达到 550 μs 后，穿透深度随脉宽变大趋势变缓。铥激光脉冲在 500 μs 时，其在水中的穿透深度为 4.1 mm，继续增大脉宽穿透深度达到 5.4 mm。另外一个明显特征是当激光脉宽小于 500 μs 时，固定脉宽的激光脉冲穿透水的深度基本保持一致，但当脉宽继续增大时，同样脉宽的激光脉冲在水中的穿透深度在一定范围内随机变化，推断此功率的铥激光作用时气泡的第一次坍缩和崩塌发生在大约 500 μs，对激光的吸收开始产生不确定性。

鉴于实验中铥激光脉冲小于 500 μs（能量 0.3 J）时，应该处于一次气泡形成过程，因此我们以 0.3 J 能量大小设置不同的双脉冲形式，分析峰值功率 600 W 的 TFL 产生的“摩西效应”特性，实验中分别以 100 μs+400 μs 和 200 μs+300 μs，300 μs+200 μs 和 400 μs+100 μs 四种组合测量不同脉冲间隔情况下双脉冲组合穿透水的特性，结果如图 6 所示。其中 100 μs+400 μs 的双脉冲组合在间隔 200 μs 时，穿透深度明显降低，在间隔 400 μs ~ 500 μs 时，穿透深度较大，略小于单脉冲情况的穿透深度，200 μs+300 μs 的双脉冲组合在水中的穿透深度一直较小。

以上实验可以看出脉冲参数对铥激光与水作用规律产生巨大影响，因为激光器峰值功率只有 600 W，作用过程中膨胀冲击和持续能量注入交织在

一起,无明显瞬态微爆特征,因此,高峰值能量的钬激光所能产生的明显"摩西效应"在低峰值功率的铥激光作用时并不明显,因为峰值功率低,不能在短时间内集中足够能量产生微爆形成明显分水孔洞,但长脉冲条件下产生的持续空泡使铥激光具有较大的水穿透深度,一定程度影响手术安全性。

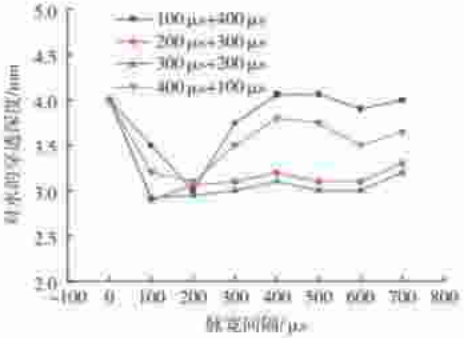


图6 双脉冲组合穿透水的深度

4.2 不同参数的铥激光脉冲碎石效率

将结石模型置于水中进行碎石实验,完成后使用电子天平进行称重,得到碎石质量,用以分析不同参数的激光碎石效率。实验过程中通过内窥镜观察,可以看到当激光照射到结石表面,瞬间会出现大量白色粉末扩散到周围的水中,同时会有一些粉末被吸引至消融凹坑附近,表明碎石时不断重复微爆冲击和气泡塌陷回吸等过程(图7)。



图7 激光碎结石模型

使用峰值功率为600 W占空比5%(平均功率30 W)的脉冲铥激光进行碎石,分析不同单脉冲能量的碎石效率,图8为碎石1分钟情况下不同脉宽参数的碎石质量。可以看出随着脉宽增大,碎石效率有明显提高。当单脉冲脉宽为1 ms(能量0.6 J)时,继续增大脉宽碎石效率增加变慢,当单脉冲脉宽为2 ms(能量1.2 J),继续增大脉宽碎石效率不再有明显变大。可以分析在小能量脉冲情况下,激光能量损失在水中的较多,作用到结石内部能量不足,形不成高效率的冲击作用,实验结果显示脉冲能量至少超过0.6 J。

根据理论分析,"摩西效应"可以产生更高的碎石效率,通过前面分析气泡塌陷的临界脉宽500 μs(能量0.3 J),继续延长脉宽微爆过程本身进入混乱状态,已经不能体现"摩西效应"的原理及结果,因此,选择总脉冲宽度500 μs进行碎石实验,为方便过程观察,设置较低频率(20 Hz,占空比1%),在100 μs+400 μs和200 μs+300 μs,300 μs+200 μs和400 μs+100 μs四组双脉冲组合形式和不同双脉冲间隔情况下进行碎石实验,碎石时间为3 min,碎石结果如图9所示。可以看出,激光与脉冲作用规律复杂,脉冲形式对碎石效率会产生较大影响,对于峰值功率600 W的铥激光脉冲组合,100 μs+400 μs双脉冲组合效率相对较高,碎石效率最高点为双脉冲间隔400 μs。

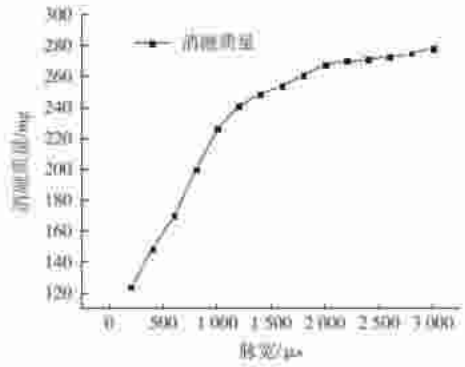


图8 不同脉宽情况下碎石效率

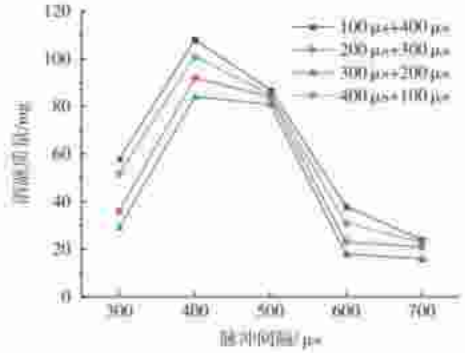


图9 双脉冲组合的激光消融质量

使用峰值功率为600 W占空比5%(平均功率30 W),设置100 μs+400 μs双脉冲组合形式(总能量0.3 J)、设置最佳效率状态即双脉冲组合间隔为400 μs进行碎石,1 min碎石质量为165.5±5 mg,与500 μs的单脉冲碎石质量158 mg比较(图8),碎石效率略有提高,因此双脉冲组合产生的"摩西效应"并不明显,同时根据图9可以判断,在此峰值功率情况下,大部分双脉冲组合形式低于单脉冲的碎石效率。可以分析"摩西效应"是高峰值功率双脉冲激光碎石时,前置小脉冲形成有效微爆,延迟一段时间使水有时间分开,避免更多的能量被吸收,从而提高碎石效率,因此,低峰值功率情况下进行双脉冲组合,不能起到相应作用。

随后,以同样激光参数对人体草酸钙结石样本进行碎石的操作,总能量仅0.3 J的铥激光脉冲具有一定碎石能力。如图10所示,实验中最小的碎片约为50 μm,碎片颗粒大部分小于0.5 mm,可以看出小能量脉冲铥激光碎石具有较好的粉末化能力。



图 10 人体草酸钙结石样本碎石

5 讨论

肾盂内激光碎石避免了穿刺损伤，但因输尿管细长而灌注液流量小，激光热量不易带走而容易引起肾盂烫伤，同时因输尿管及肾盂区域狭窄而容易损伤周围组织，因此，如何提高单位能量碎石效率，减小热冗余，如何避免或减小激光对周围组织的损伤变得尤为重要。通过实验可以得出，对于峰值功率 600 W 的 TFL 具有较强的碎石能力，在脉冲小于 1 ms（能量 0.6 J）时，随着脉宽变大，单位能量碎石效率快速提高，因此铥激光碎石脉冲能量不宜太小。但对于峰值功率不是很高的 TFL，提高脉冲能量要加大脉宽，此长脉宽激光脉冲与水作用会产生多次坍缩的微爆过程，使铥激光脉冲在水中具有大的穿透深度（实验中达到 5.4 mm），且穿透能力具有一定随机性，这在肾结石激光手术中容易损伤周围组织，因为部分损伤手术中并不容易直接观察到，最新研究 TFL 术后输尿管狭窄的较高发生率[10-11]应该与此相关。因峰值功率不高，通过双脉冲控制的 TFL 产生的“摩西效应”不明显。通过实验分析，TFL 具有较好的碎石潜力，但目前仍存在不足，随着峰值功率进一步提高，可实现良好的碎石应用。

参考文献

[1] Denstedt J, Gabrigna B F C. Thulium fiber laser lithotripsy: Is it living up to the hype? [J]. Asian Journal of Urology, 2023, 10(3): 289-297.

[2] Ventimiglia, Eugenio, Steeve Doizi, et al. Effect of temporal pulse shapeon urinary sto-nephantom retropulsion rate and ablation efficiency using Holmium:YAG and superpulse Thulium fibre lasers[J]. BJU International, 2020, 126(1):159-167.

[3] Andreeva Viktoria, Vinarov Andrey, Yaroslavsky Ilya, et al. Preclinical comparison of sup-erpulse thulium fiber laser and a holmium:YAG laser for lithotripsy[J]. World journal of urology, 2020, 38(2): 497-503.

[4] Hardy L A, Vinnichenko V, Fried N M. High power holmium: YAG versus thulium fiber laser treatment of kidney stones in dusting mode: ablation rate and fragment size studies[J]. Lasers in surgery and medicine, 2019, 51(6): 522-530.

[5] Traxer Olivier, Keller Etienne Xavier. Thulium fiber laser: the new player for kidney stone treatment? A comparison with Holmium: YAG laser[J]. World journal of urology, 2020, 38(8): 1883-1894.

[6] Panthier, Doizi, Lapouge, et al. Comparison of the ablation rates, fissures and fragments produced with 150 μm and 272 μm laser fibers with superpulsed thulium fiber laser: an in vitro study[J]. World journal of urology, 2021, 39(6): 1683-1691.

[7] Jones, Beisland, Ulvik, et al. Current status of thulium fibre laser lithotripsy: an uptodate review[J]. BJU International, 2021, 128(5): 531538.

[8] UlvikØyvind, Æsøy Mathias Sørstrand, Juliebø-Jones Patrick, et al. Thulium Fibre Laser versus Holmium:YAG for Ureteroscopic Lithotripsy: Outcomes from a Prospective Randomised Clinical Trial[J]. European urology, 2022, 82(1): 73-79.

[9] 许力为，虞晨昊，胡海义，等. 铥光纤激光碎石与钬激光碎石治疗上尿路结石的效果比较[J]. 中华医学杂志，2023，103(30)：2307-2313.

[10] Ahmad Para Sajad, Saleem Wani Mohammad, Hamid Arif, et al. Incidence of Ureteric-strictures Following Ureteroscopic Laser Lithotripsy: Holmium: YAG Versus Thulium Fiber Laser[J]. Urology research & practice, 2023, 49(3): 198-204.

[11] Fried N M, Irby P B. Advances in laser technology and fiberoptic delivery systems- in lithotripsy[J]. Nature Reviews Urology, 2018, 15(9): 563-573.

[12] Lekarev Vladimir, Dymov Alim, Vinarov Andrey, et al. Mechanism of Lithotripsy by Superpulse Thulium Fiber Laser and Its Clinical Efficiency[J]. Applied Sciencesb-asel, 2020, 10(21): 7480.

[13] 吕建林. 钬激光碎石术在复杂性肾结石治疗中的应用[J]. 激光杂志，2014，35(8)：97-98.

[14] Zhang J J, Xuan J R, Yu H G, et al. Study of cavitation bubble dynamics during H-o:YAG laser lithotripsy by high-speed camera[J]. S. N. , 2016, 9689: 96891-96891+7.

[15] Keller EX, de Coninck V, Audouin M, et al. Fragments and dust after Holmium laser lit-hotripsy with or without "Moses technology": How are they different? [J]. Biophotonics, 2019, 12(4): e201800227.

[16] 张安军，段嘉霖，邢新演，等. 掺铥激光在生物医疗领域的应用[J]. 激光与光电子学进展，2022，59(1)：50-63.

[17] Chiron P H, Berthe L L, Coninck V D. Comparison of vapor bubbles induced by an Ir-olmium:YAG Laser and a SuperPusled Thulium Fiber Laser. [J]. Journal of Endourology, 2018, 32: 40-45.

[18] Wang Z, Zhang Y, Zhang J, et al. Recent advances on the mechanisms of kidney stone formation (Review). [J]. International Journal of Molecular Medicine, 2021, 48(2): 149.

World Journal of Urology (2025) 43:221
https://doi.org/10.1007/s00345-025-05614-4

RESEARCH

Evaluating safe irrigation rates for Tm fiber laser lithotripsy to prevent thermal injury: an in vitro and numerical simulation

Rongwei Zha[1] · Du Wang[1] · Chenyang Wang[1] · Yunzhou Liao[1] · Xuehan Mei[1] · Zhilong Li[2] · Sheng Li[2] · Cheng Lei[1] · Xinghuan Wang[2]

Received: 8 November 2024 / Accepted: 1 April 2025
© The Author(s), under exclusive licence to Springer-Verlag GmbH Germany, part of Springer Nature 2025

Abstract

Purpose To evaluate temperature changes and thermal injury during thulium fiber laser (TFL) lithotripsy in the urinary tract and identify the safe irrigation rate, providing a reference for optimal parameter settings in clinical practice.

Methods An in vitro thermal injury experiment was conducted using a home-made TFL operating at 40 W. The experiment utilized a glass tube simulating the urinary tract. A peristaltic pump circulated 25 °C saline at irrigation rates ranging from 10 to 40 mL/min. Real-time temperature measurements were recorded using thermocouples, and thermal injury was assessed by calculating the thermal dose threshold. Additionally, a validated numerical simulation model was developed to analyze temperature distributions and predict safe irrigation rates at 20 and 30 W.

Results In the in vitro experiment, at 40 W, severe thermal injury occurred in the urinary tract when the irrigation rate was below 30 mL/min, particularly in the ureter and renal calyx. The numerical simulation model demonstrated a high degree of consistency with the experimental results. According to the simulation, at 30 W, thermal injury occurred in the renal calyx when the irrigation rate was below 20 mL/min. At 20 W, thermal injury was observed in the renal calyx when the irrigation rate was below 10 mL/min.

Conclusions The increase in temperature and the extent of thermal injury were strongly dependent on laser power and irrigation rate, with a lesser dependence on anatomical location. The accuracy of the numerical simulation was validated through experiments, demonstrating its capability to reliably predict temperature variations and thermal injury under different laser power settings and irrigation rates.

Keywords Thermal injury · Tm fiber laser lithotripsy · Numerical simulation · Irrigation rate · Urinary tract

Introduction

Laser lithotripsy (LL) has become one of the mainstream methods for treating urinary calculi [1]. Compared to traditional lithotripsy techniques, such as shockwave lithotripsy and pneumatic ballistic lithotripsy, LL combined with flexible ureteroscopy offers advantages in efficiency, precision, and versatility. However, the laser-induced photothermal effects [2] can potentially cause thermal injury to urinary tissues, leading to complications such as ureteral stricture [3] and thermal injury of the renal pelvis and calyx [4], which in turn may result in impaired renal function [5].

Ho: YAG LL has long been considered the gold standard for retrograde ureteroscopy procedures. In Ho: YAG LL, factors such as laser parameters, irrigation rate, and location within the urinary tract significantly affect fluid temperature and the extent of thermal injury [6, 7]. Recently, thulium fiber laser (TFL) lithotripsy has emerged as a strong alternative to Ho: YAG LL [8–10]. TFL has a water absorption coefficient four times higher than the Ho: YAG laser. It also features broader parameter ranges, including higher pulse repetition frequencies (up to 2400 Hz), wider pulse energies

✉ Du Wang
wdxz@foxmail.com

✉ Sheng Li
lisheng-znyy@whu.edu.cn

✉ Xinghuan Wang
wangxinghuan@whu.edu.cn

[1] The Institute of Technological Sciences, Wuhan University, Wuhan, China

[2] Department of Urology, Zhongnan Hospital of Wuhan University, Wuhan, China

Published online: 10 April 2025

(0.025–6 J), a flatter pulse waveform, and a peak power of 500 W [11]. These characteristics give TFL distinct advantages, such as faster stone ablation, finer stone dust, reduced retropulsion, and greater procedural flexibility, making it highly effective for lithotripsy [12]. Due to differences in the parameters of the two lasers, several studies have compared the thermal effects of TFL and Ho: YAG LL, with conflicting conclusions. Some studies have reported that TFL results in faster temperature rise and more pronounced thermal effects [13–15], while others have shown that the temperature profiles of TFL and Ho: YAG lasers are similar [16–18]. Consequently, it is essential to evaluate the safety parameters of TFL independently, as applying Ho: YAG laser parameters and irrigation rates directly may pose significant safety risks. Additionally, the use of high-power LL can result in higher stone ablation efficiency [19–21], but it also increases the risk of thermal injury [22]. Therefore, greater attention should be given to the thermal injury associated with high-power LL.

This study investigates temperature variations and thermal injury risks during thulium fiber laser (TFL) lithotripsy in the urinary tract, aiming to identify safe irrigation rates to mitigate these risks. A custom-designed glass tube model, which simulates the size and shape of the ureter, renal calyx, and renal pelvis, was used to provide a more accurate in vitro representation of the urinary tract. Advanced numerical simulation techniques were employed to model the temperature distribution and predict safe irrigation rates. Our findings provide a reliable method for assessing the thermal safety of TFL lithotripsy and propose an optimal irrigation rate to enhance the safety of LL procedures.

Materials and methods

Experimental setup

A testing apparatus was constructed to evaluate the extent of thermal injury during LL. This setup was designed to simulate the thermal effects induced by TFL lithotripsy at various locations within the urinary tract. A custom glass tube was used to replicate the anatomical structure of the urinary tract, with its upper, middle, and lower sections mimicking the shape and dimensions of the ureter, renal pelvis, and renal calyx, respectively (Fig. 1a). The tube, filled with physiological saline, was submerged in a water bath maintained at 37 °C. A homemade quasi-continuous-wave TFL (Table S1) was used in this study to deliver laser energy through an delivery fiber (diameter of 272 μm) positioned within the tube (Fig. 1b). Concurrently, a peristaltic pump delivered 25 °C saline from a reservoir through a syringe needle to the fiber tip for irrigation. The upper end of the glass tube was sealed with a rubber stopper, through which a long needle (irrigation inlet) extended into the test section of the glass tube. The delivery fiber was threaded through the needle to reach the test area. Additionally, a short needle (irrigation outlet) passed through the rubber stopper and was positioned at the upper end of the glass tube (Fig. S1). This setup simulates the irrigation system comprising a ureteral access sheath and a flexible ureteroscope. A K-type thermocouple, temperature sensing module, and data acquisition system were connected sequentially, with temperature recorded at a sampling rate of 1 Hz. The thermocouple was positioned flush with the fiber tip on the inner wall of the tube, allowing for accurate temperature measurements near the tube wall, which were then transmitted to a computer for storage.

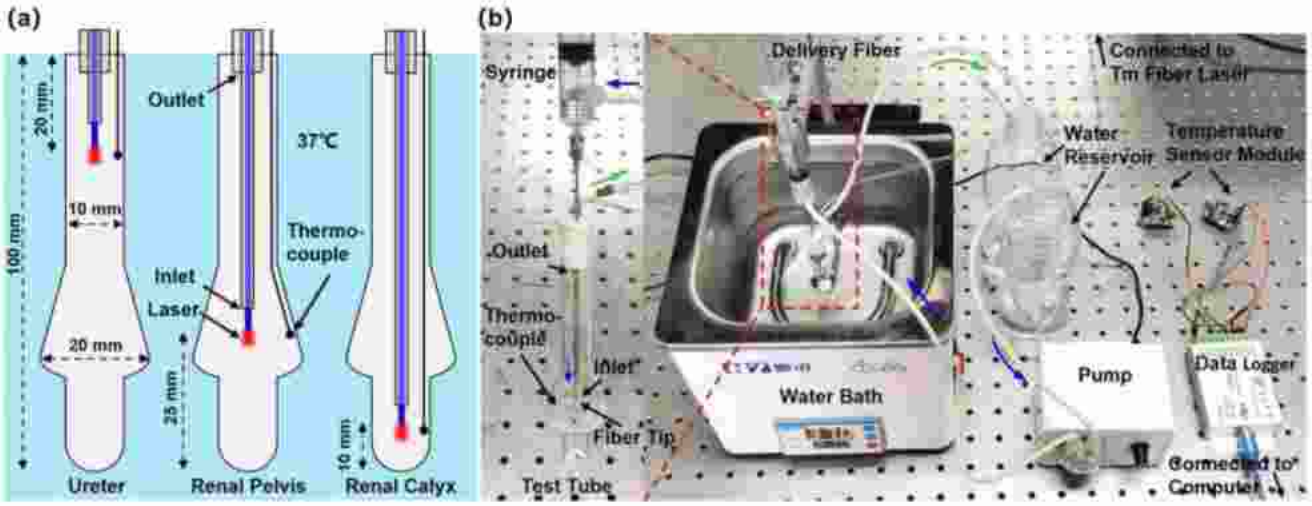


Fig. 1 Experimental setup: **a** Schematic of the glass tube simulating different regions of the urinary tract, **b** Laser thermal effect testing system, where the blue and green arrows represent the directions of inflow and outflow, respectively

Laser-induced thermal injury experiments were conducted at the upper (ureter), middle (renal pelvis), and lower (renal calyx) sections of the tube. The laser operated at an average power of 40 W (2 J × 20 Hz), with irrigation rates set at 10, 20, 30, and 40 mL/min. Once the temperature within the tube stabilized at 37 °C, the micro-pump was activated to initiate irrigation, and temperature data collection began. After 20 s, the laser was activated and operated continuously for 60 s. Following laser deactivation, irrigation and temperature recording continued for an additional 40 s.

Numerical simulation model

Numerical simulations were employed to calculate the temperature and flow fields during LL, enabling a better understanding of the mechanisms underlying laser-induced thermal injury and aiding in the prediction of optimal LL parameters. To ensure simulation accuracy and improve computational efficiency, an axisymmetric model was developed based on the experimental setup. The fiber tip was positioned at three specific locations within the simulated urinary tract regions: 20 mm from the top of the tube (ureter), 25 mm from the bottom (renal pelvis), and 10 mm from the bottom (renal calyx). Temperature probes were placed on the tube wall at each location to calculate inner wall temperatures. To provide a clearer description of the numerical simulation process, the supplementary materials include the thermal properties (Table S2) of the materials used in the simulation, the boundary conditions (Table S3 and Fig. S2), and the governing equations (Equations S1–S4). Additionally, simulations were conducted to analyze the temperature distribution and thermal injury in the renal calyx under 30 W and 20 W laser power settings.

Thermal dose

Thermal injury to biological tissue depends on both temperature elevation and exposure duration, and thermal dose is commonly used to quantify the extent of thermal injury in tissues. A standard method for calculating thermal dose involves converting the time-temperature profile into an equivalent exposure time at 43 °C, according to the following Eqs. [23],

$$TD_{43} = \int_0^{t_{end}} R^{43-T(t)} dt \tag{1}$$

where

$$R = \begin{cases} 0, & T \le 37°C \\ 0.25, & 37 < T < 43°C \\ 0.5, & T \ge 43°C \end{cases} \tag{2}$$

In Eqs. (1–2), T represents temperature, t is time, and R is a coefficient that varies with temperature. The thermal dose at 43 °C, denoted as TD_{43}, is expressed in minutes. Any temperature above 43 °C causes an exponential increase in the thermal dose. The time threshold for tissue injury is typically set at TD_{43} = 120 min. When TD_{43} exceeds 240 min, the tissue is considered to be denatured [24].

Results

In vitro experiments on thermal injury

At a laser power of 40 W, temperature variations were measured at three distinct urinary tract locations under different irrigation rates. Figure 2a-c presents the time-dependent inner wall temperature profiles for three distinct urinary tract regions. For each location, the maximum temperature (T-Max) decreased as the irrigation rate increased. The T-Max data for each urinary tract location are presented in Table 1. Under the low irrigation rate of 10 mL/min, the highest T-Max was observed in the renal calyx (60.2 °C), followed by the ureter (58.8 °C) and the renal pelvis (45.2 °C). At moderate irrigation rates of 20 and 30 mL/min, T-Max was highest in the ureter (51.2 and 45.2 °C), followed by the renal pelvis (49.4 and 43.8 °C) and renal calyx (48.6 and 44.5 °C). Under high irrigation rate of 40 mL/min, the T-Max values at the three sites were relatively similar, ranging from lowest to highest as follows: ureter (38.9 °C), renal pelvis (39.4 °C), and renal calyx (39.5 °C). As the irrigation rate increased, T-Max values for the three locations converged. Notably, at the high irrigation rate of 40 mL/min, T-Max for all locations remained below 43 °C, whereas at low and moderate irrigation rates, T-Max exceeded 43 °C in all locations.

The temperature curves were converted into thermal dose curves using Eq. 1 to evaluate the extent of thermal injury in urinary tract tissues. Figure 2d-f presents the time-dependent thermal dose curves. The laser is activated at 20 s, and the thermal dose increases rapidly over time. After the laser action ends at 80 s, the thermal dose reaches its maximum and remains constant. For a given location, higher irrigation rates delayed the time required to reach TD_{43} = 120 min. At low irrigation rates, the thermal doses at all three locations greatly exceeded the 120-minute and even 240-minute thresholds, indicating severe thermal injury in all regions. The risk of thermal injury was higher in the ureter and renal calyx compared to the renal pelvis. At an irrigation rate of 10 mL/min, the thermal doses for the renal pelvis, ureter, and renal calyx were 7.12×10^5, 3.60×10^4, and 2.03×10^6 min, respectively. At an irrigation rate of 20 mL/min, the thermal doses at the three locations were 7.20×10^3,

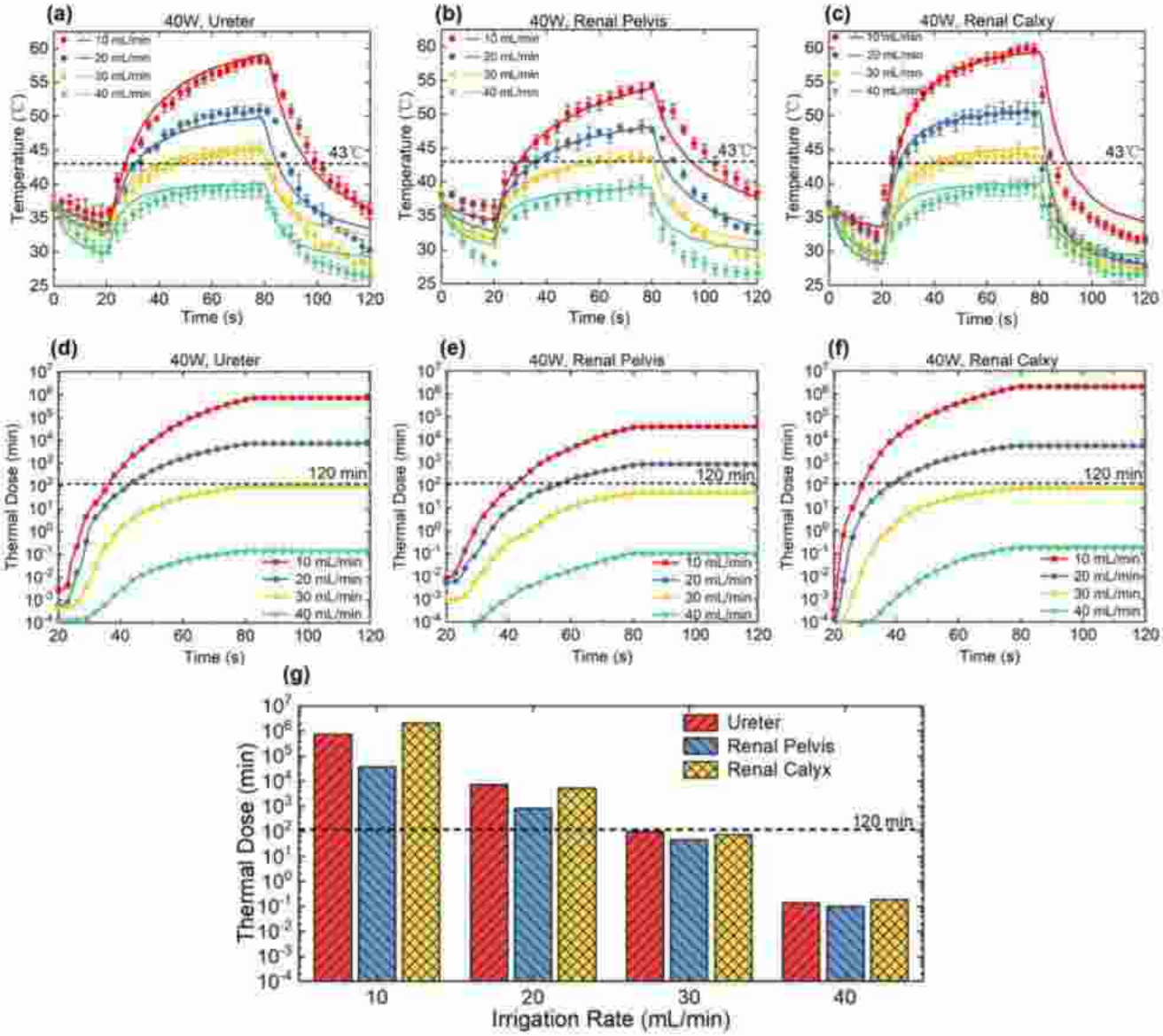


Fig. 2 Temperature and thermal dose at 40 W laser power, **a-c** measured temperatures (dots) and simulated temperatures (lines), **d-e** thermal dose calculated based on the temperatures, **g** total thermal dose after 120 s

Table 1 Maximum temperatures at different locations in the urinary tract

Urinary tract	T-Max (℃)			
	Irrigation rate (mL/min)			
	10	20	30	40
Ureter	58.8	51.2	45.2	38.9
Renal Pelvis	54.3	48.6	44.5	39.4
Renal Calyx	60.2	49.4	43.8	39.5

8.19×10^2, and 5.22×10^3 min, respectively. When the irrigation rate increased to 30 mL/min, the thermal doses at the ureter, renal calyx, and renal pelvis decreased significantly to 99.13, 46.07 and 73.59 min, respectively. These values were below the injury threshold, and no thermal injury was observed at any location. At the highest irrigation rate of 40 mL/min, the thermal dose at all locations was two orders of magnitude lower than the injury threshold, ensuring safe conditions across all regions.

Simulation of thermal injury

The numerical simulation model was employed to calculate temperature profiles and temperature field distributions at a laser power of 40 W. As shown in Fig. 2(a)-(c), the simulated data (lines) closely matched the experimental data (dots) across three urinary tract locations and four irrigation rates, demonstrating the model's high accuracy. Due to the smaller volume of the renal calyx, which makes it

more susceptible to thermal injury, the numerical simulation model was further used to analyze thermal injury in the renal pelvis at lower laser power settings (20 and 30 W) and to predict safe irrigation rates, as shown in Fig. 3. At a power of 30 W, the maximum temperatures at irrigation rates of 10, 20 and 30 mL/min were 47.4, 43.3 and 39.6 °C, respectively. Severe thermal injury occurred only at 10 mL/min, where the thermal dose reached 624.94 min, exceeding the injury threshold. At a power of 20 W, the maximum temperature at all irrigation rates remained below 43 °C, and no thermal injury was observed.

Figure 4 (a)-(c) show the temperature field distribution in different urinary tract regions at 79 s under high power 40 W. At a high irrigation rate of 40 mL/min, no significant heat accumulation was observed in any of the regions. In the ureter, the area affected by laser-induced heating displayed a spindle-like shape. At irrigation rates of 10 and 20 mL/min, substantial heat accumulation occurred, with a large high-temperature zone concentrated below the irrigation outlet in the ureter. At 30 mL/min, a slight degree of heat accumulation was observed. The laser-induced thermal effect zone in the renal pelvis forms an inverted triangle, with thermal accumulation mainly concentrated in the lower part of the renal pelvis and the upper part of the renal calyx. In contrast, the thermal effect in the renal calyx forms a triangle, with the highest temperature zone primarily located in the lower part of the renal calyx. Compared to the other sites, thermal accumulation in the renal pelvis was relatively lower. Furthermore, Fig. 4(d) and (e) present the temperature distributions in the renal calyx under 30 and 20 W laser power, respectively. Compared to 40 W, the thermal effect significantly weakened with reduced power. Notably, at 30 W power and an irrigation rate of 10 mL/min, distinct thermal accumulation was observed at the bottom of the renal calyx. However, at 20 W power, no significant thermal accumulation was observed within the renal calyx, consistent with the temperature trends shown in Fig. 3.

Discussion

As the use of high-power lasers increases, the risk of laser-induced thermal injury to the urinary system also rises [25, 26]. Understanding and controlling temperature elevations caused by laser application have become increasingly important for ensuring the safety of LL. An appropriate irrigation rate can effectively reduce the risk of thermal injury to tissues. However, laser-induced thermal injury varies across different regions of the urinary tract. Therefore, urologists must balance laser parameters, irrigation rate, and temperature control based on the specific region of the urinary tract being treated.

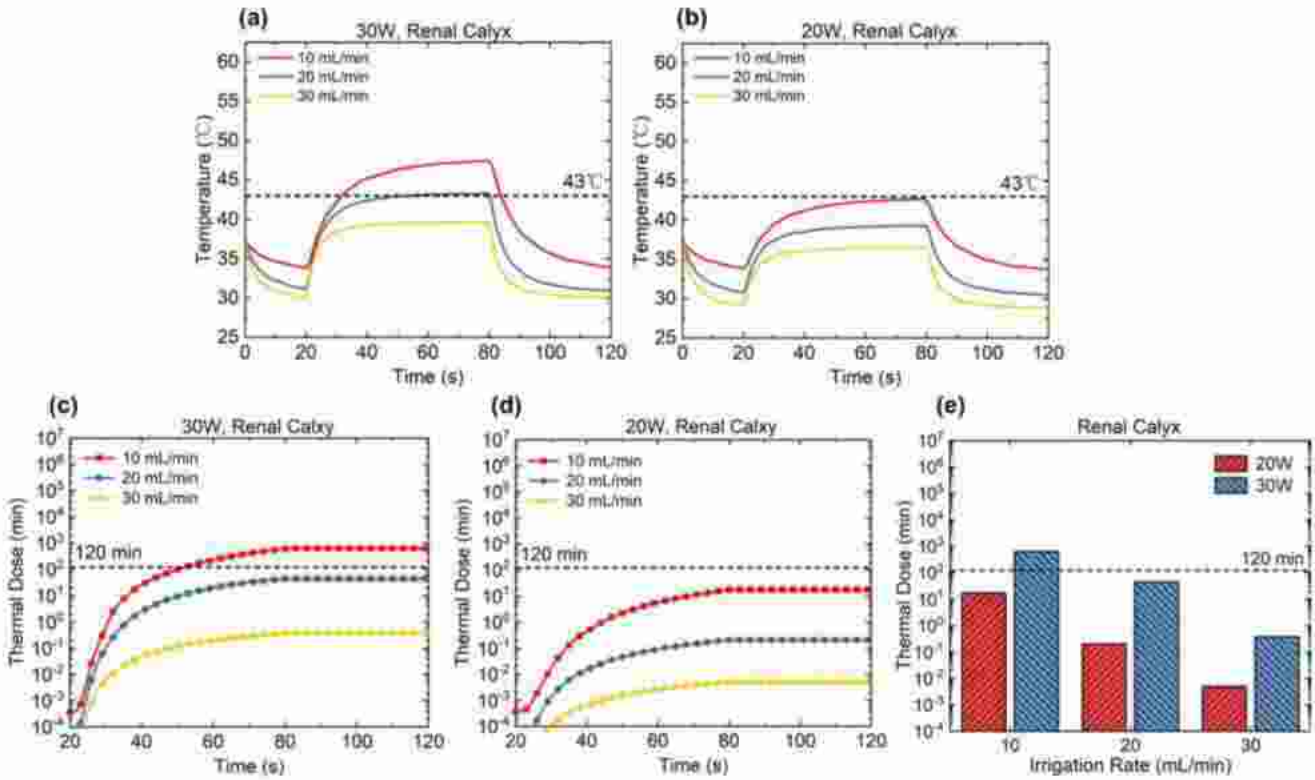


Fig. 3 Temperature profiles and thermal dose in the renal calyx obtained through simulation. **a-b** temperature profiles, **c-d** thermal dose, **e** total thermal dose after 120 s

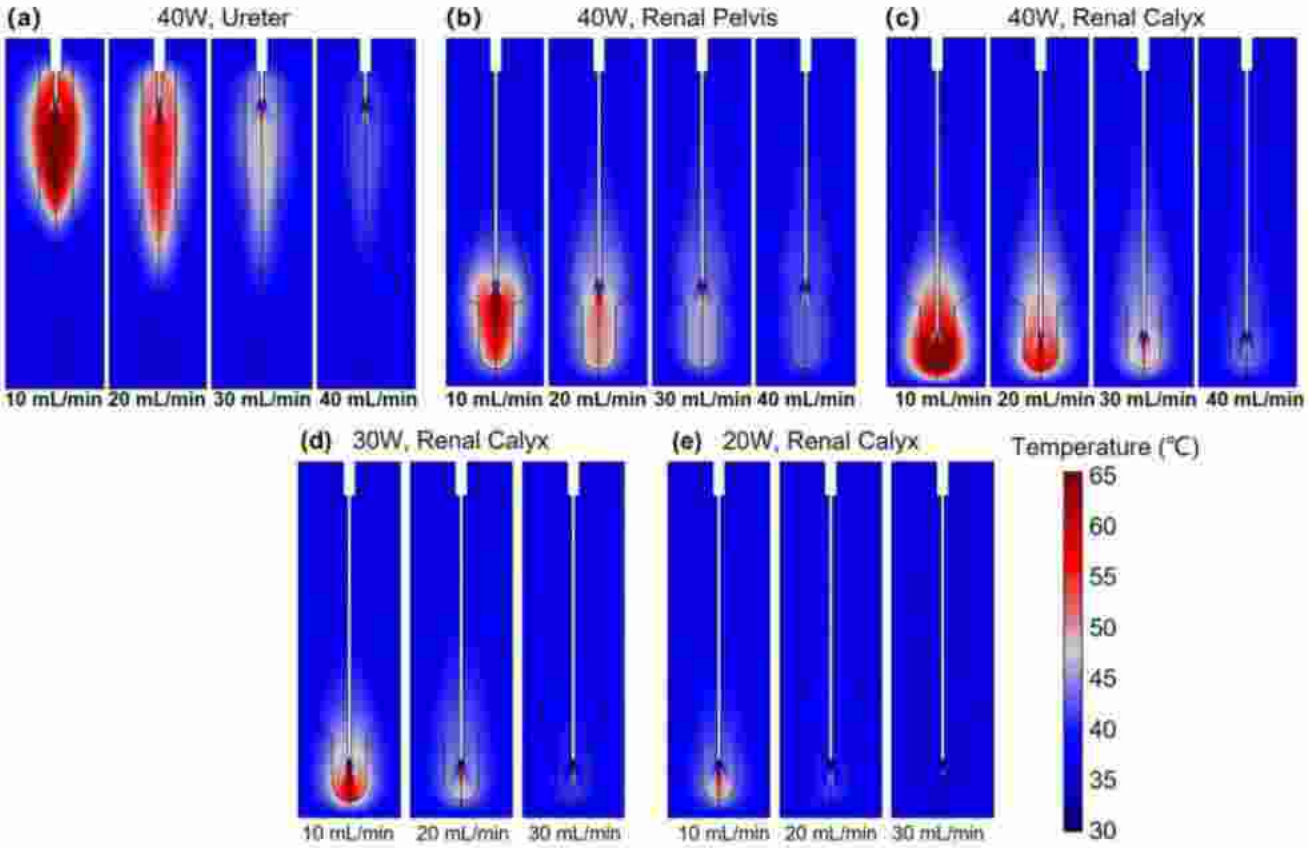


Fig. 4 Temperature field distribution from simulation, **a-c** 40 W in different urinary tract regions, **d** 30 W in the renal calyx, **e** 20 W in the renal calyx

Thermal injury in different regions of the urinary tract is closely related to their volume and shape. Under low irrigation rates, there is some space below the laser heating zone in the ureter and renal pelvis, which facilitates heat dissipation and results in relatively lower inner wall temperatures. The funnel-shaped structure of the renal pelvis further aids in the effective dispersion of heat within its cavity. In contrast, thermal injury is most pronounced in the renal calyx. Due to the narrow and enclosed structure of the calyx, heat generated in the laser heating area tends to accumulate, potentially causing thermal injury to the renal papilla. Therefore, increasing irrigation rates or adopting intermittent laser activation [14, 27], particularly in narrow spaces with limited heat diffusion, such as obstructed ureters or narrow renal calyces, is essential for safely reducing temperature thresholds during lithotripsy. Increasing the irrigation rate can effectively reduce the temperature and minimize the risk of thermal injury in the stone treatment area. This effect is attributed to the increased convective heat transfer coefficients at higher irrigation rates, which enhance cooling efficiency [28]. However, excessively high irrigation rates may lead to elevated intrarenal pressure, potentially causing pyelovenous backflow [29] or stone retropulsion. Therefore, to prevent thermal injury while minimizing the risk of elevated intrarenal pressure, a lower irrigation rate should be selected as the safe flow rate. Based on the in vitro experimental results, the safe irrigation rate for 40 W power was identified as 30 mL/min. According to the numerical simulation results, the safe irrigation rates for the renal calyx at 30 and 20 W were 20 and 10 mL/min, respectively. Since the renal calyx is the smallest of the three anatomical regions, its safe irrigation rate can also be considered a conservative reference for other urinary tract locations.

This study has several limitations. The experimental setup and simulation model represent a simplified version of the actual urinary tract structure, which cannot fully replicate its complex anatomical features. A three-dimensional simulation model based on CT data could provide greater precision and reliability in predicting thermal injury. Additionally, the rigidity of the glass material used in this study differs from the elasticity of the actual urinary system, so future research will focus on expanding TFL thermal injury experiments using silicone-based models or ex vivo porcine urinary tract models to better simulate real-life conditions. These advancements will provide a stronger scientific basis

for optimizing clinical LL techniques and enhancing safety assessments.

Conclusions

This study investigated the impact of irrigation rates on thermal injury in different regions during TFL lithotripsy. The results indicate that the increase in temperature and the extent of thermal injury were strongly dependent on laser power and irrigation rate, with a lesser dependence on anatomical location. The accuracy of the numerical simulation was validated through experiments, demonstrating its capability to reliably predict temperature variations and thermal injury under different laser power settings and irrigation rates. This study provides an effective method for assessing the risk of thermal injury during TFL lithotripsy and identifies a safe irrigation rate, offering valuable insights for enhancing the safety of LL procedures.

Supplementary Information The online version contains supplementary material available at https://doi.org/10.1007/s00345-025-05614-4.

Author contributions R.Z.: data analysis, data collection or management, and manuscript writing/editing; D.W.: supervision, project development and manuscript editing; C.W.: data collection, manuscript editing; Y.L.: data collection and analysis; X.M.: data collection and analysis; Z.L.: data analysis; S.L.: project development; C.L.: supervision, project development; X.W.: project development. All authors reviewed the manuscript.

Funding This work was supported by the Translational Medicine and Multidisciplinary Research Project of Zhongnan Hospital of Wuhan University (ZNJC202401).

Data availability No datasets were generated or analysed during the current study.

Declarations

Ethical approval No ethical approval as the study does not involve any human or animal participants.

Competing interests The authors declare no competing interests.

References

1. Zhu X, Li F, Hu X, Li H, Wu S, Jiang H (2023) A method for reducing thermal injury during the ureteroscopic holmium laser lithotripsy. Asian J Urol 10(1):89–95. https://doi.org/10.1016/j.ajur.2022.05.011
2. Kin Foong Chan PD, 1,4 T, Joshua Pfefer PD, 2 Joel MH, Teichman MD,3 and, Welch Ashleyj Ph.D.1,2 (2001) A perspective on laser lithotripsy: the fragmentation processes. J Endourol 15(3):https://doi.org/10.1089/089277901750161737
3. Chen S, Zhou L, Wei T et al (2017) Comparison of holmium: YAG laser and pneumatic lithotripsy in the treatment of ureteral stones: an update Meta-Analysis. Urol Int 98(2):125–133. https://doi.org/10.1159/000448692
4. Aldoukhi AH, Hall TL, Ghani KR, Maxwell AD, MacConaghy B, Roberts WW (2018) Caliceal fluid temperature during High-Power holmium laser lithotripsy in an in vivo Porcine model. J Endourol 32(8):724–729. https://doi.org/10.1089/end.2018.0395
5. El-Abd AS, Suliman MG, Abo Farha MO et al (2014) The development of ureteric strictures after ureteroscopic treatment for ureteric calculi: A long-term study at two academic centres. Arab J Urol 12(2):168–172. https://doi.org/10.1016/j.aju.2013.11.004
6. Aldoukhi AH, Black KM, Hall TL et al (2020) Defining thermally safe laser lithotripsy power and irrigation parameters: in vitro model. J Endourol 34(1):76–81. https://doi.org/10.1089/end.2019.0499
7. Tsaturyan A, Petcinaris A, Pantazis L et al (2022) The effect of prolonged laser activation on irrigation fluid temperature: an in vitro experimental study. World J Urol 40(7):1873–1878. https://doi.org/10.1007/s00345-022-04000-8
8. Traxer O, Pearle M (2024) Thulium fiber laser versus holmium:yttrium aluminum Garnet for lithotripsy: which is the winner?? Eur Urol 85(6):541–542. https://doi.org/10.1016/j.eururo.2024.02.023
9. Solano C, Corrales M, Panthier F, Candela L, Doizi S, Traxer O (2023) Navigating urolithiasis treatment: assessing the practicality and performance of thulium fiber laser, holmium YAG, and thulium YAG in real-world scenarios. World J Urol. https://doi.org/10.1007/s00345-023-04487-9
10. Emiliani E, Kanashiro A, Angerri O (2023) Lasers for stone lithotripsy: advantages/disadvantages of each laser source. Curr Opin Urol 33(4):302–307. https://doi.org/10.1097/MOU.0000000000001092
11. Mishra A, Medairos R, Chen J et al (2024) Exploring optimal settings for safe and effective thulium fibre laser lithotripsy in a kidney model. BJU Int 133(2):223–230. https://doi.org/10.1111/bju.16218
12. Ventimiglia E, Doizi S, Kovalenko A, Andreeva V, Traxer O (2020) Effect of Temporal pulse shape on urinary stone Phantom retropulsion rate and ablation efficiency using holmium:yag and super-pulse thulium fibre lasers. BJU Int 126(1):159–167. https://doi.org/10.1111/bju.15079
13. Belle JD, Chen R, Srikureja N, Amasyali AS, Kehcila M, Baldwin DD (2022) Does the novel thulium fiber laser have a higher risk of urothelial thermal injury than the conventional holmium laser in an in vitro study?? J Endourol 36(9):1249–1254. https://doi.org/10.1089/end.2021.0842
14. Wanderling C, Saxton A, Phan D et al (2024) Getting hot in here! Comparison of holmium vs. thulium laser in an anatomic hydrogel kidney model. Urolithiasis 52(1):49. https://doi.org/10.1007/s00240-024-01541-y
15. Taratkin M, Laukhtina E, Singla N et al (2020) Temperature changes during laser lithotripsy with Ho:YAG laser and novel Tm-fiber laser: a comparative in-vitro study. World J Urol 38(12):3261–3266. https://doi.org/10.1007/s00345-020-03122-1
16. Molina WR, Carrera RV, Chew BH, Knudsen BE (2021) Temperature rise during ureteral laser lithotripsy: comparison of super pulse thulium fiber laser (SPTF) vs high power 120 W holmium-YAG laser (Ho:YAG). World J Urol 39(10):3951–3956. https://doi.org/10.1007/s00345-021-03619-3
17. Ortner G, Rice P, Nagele U, Herrmann TRW, Somani BK, Tokas T (2022) Tissue thermal effect during lithotripsy and tissue ablation in endourology: a systematic review of experimental studies comparing holmium and thulium lasers. World J Urol 41(1):1–12. https://doi.org/10.1007/s00345-022-04242-6

18. Juliebo-Jones MSAE, Beisland P, Ulvik C O (2022) Temperature profiles during ureteroscopy with thulium fiber laser and holmium:yag laser: findings from a pre-clinical study. Scand J Urol 56(4):313–319. https://doi.org/10.1080/21681805.2022.2104367
19. Liu M, Peng Y, Wang Z et al (2021) Ablation efficiency of a novel thulium fiber laser: an in vitro study on laser setting and fiber usage. J Endourol 35(8):1211–1216. https://doi.org/10.1089/end.2020.1116
20. Shen Z, Liang J, Xie L, Liu C (2024) Ablation efficiency and laser safety of a novel superpulsed thulium fiber laser: a in vitro study. World J Urol 42(1):561. https://doi.org/10.1007/s00345-024-05266-w
21. Ventimiglia E, Pauchard F, Quadrini F et al (2021) High- and Low-Power laser lithotripsy achieves similar results: A systematic review and Meta-Analysis of available clinical series. J Endourol 35(8):1146–1152. https://doi.org/10.1089/end.2020.0090
22. Juliebo-Jones MSAE, Beisland P, Ulvik C O (2024) Temperature measurements during flexible ureteroscopic laser lithotripsy: A prospective clinical trial. J Endourol 38(4):308–315. https://doi.org/10.1089/end.2023.0660
23. Williams JG, Goldsmith L, Moulton DE, Waters SL, Turney BW (2021) A temperature model for laser lithotripsy. World J Urol 39(6):1707–1716. https://doi.org/10.1007/s00345-020-03357-y
24. Stephen A. Saparcto PD (1984) Thermal dose determination in cancer therapy
25. Winship B, Wollin D, Carlos E et al (2019) The rise and fall of high temperatures during ureteroscopic holmium laser lithotripsy. J Endourol 33(10):794–799. https://doi.org/10.1089/end.2019.0084
26. Aldoukhi AH, Ghani KR, Hall TL, Roberts WW (2017) Thermal response to High-Power holmium laser lithotripsy. J Endourol 31(12):1308–1312. https://doi.org/10.1089/end.2017.0679
27. Ding T, Xu Z, Huang Z, Xiao B, Hu W, Li J (2024) An in vitro study of irrigation rate, operator duty cycle and intrarenal temperature in superpulse fiber thulium laser lithotripsy. World J Urol 42(1):588. https://doi.org/10.1007/s00345-024-05289-3
28. Khabari A (2014) Natural and Forced Convective Heat Transfer Analysis of Nanostructured Surface. Proceedings of the World Congress on Engineering I:317–319
29. Tonyali S, von Bargen MF, Ozkan A, Gratzke C, Miernik A (2023) The heat is on: the impact of excessive temperature increments on complications of laser treatment for ureteral and renal stones. World J Urol 41(12):3853–3865. https://doi.org/10.1007/s00345-023-04652-0

Publisher's note Springer Nature remains neutral with regard to jurisdictional claims in published maps and institutional affiliations.

Springer Nature or its licensor (e.g. a society or other partner) holds exclusive rights to this article under a publishing agreement with the author(s) or other rightsholder(s); author self-archiving of the accepted manuscript version of this article is solely governed by the terms of such publishing agreement and applicable law.

《世界泌尿外科杂志》（2025）第43卷第221页
https://doi.org/10.1007/s00345-025-05614-4

研究

评估Tm光纤激光碎石术的安全灌注率以防止热损伤：体外和数值模拟

荣伟[1]·杜望[1]·王晨阳[1]·廖云洲[1]·梅雪涵[1]·李志龙[2]·李胜[2]·雷成[1]·王兴环[2]

接收日期：2024年11月8日/接受日期：2025年4月1日
©作者（们）于2025年获得德国Springer-Verlag GmbH（隶属Springer Nature集团）的独家授权

摘要

目的：评估钬光纤激光（TFL）碎石术中尿路温度变化及热损伤情况，确定安全冲洗速率，为临床实践中的最佳参数设置提供参考。

方法使用自制的40瓦TFL进行体外热损伤实验。实验采用模拟尿路的玻璃管，无蠕动泵以10至40 mL/min的冲洗速率循环25°C的生理盐水。通过热电偶记录实时温度测量值，并通过计算热剂量阈值评估热损伤。此外，还开发了一个经过验证的数值模拟模型，用于分析温度分布并预测20瓦和30瓦下的安全冲洗速率。

结果在体外实验中，当功率为40瓦时，若冲洗速率低于30毫升/分钟，尿路会发生严重热损伤，尤其在输尿管和肾盏中。数值模拟模型与实验结果高度一致。根据模拟结果，在30瓦功率下，当冲洗速率低于20毫升/分钟时，肾盏会发生热损伤。在20瓦功率下，当冲洗速率低于10毫升/分钟时，肾盏中可观察到热损伤。

结论温度升高和热损伤程度与激光功率和冲洗速率密切相关，与解剖位置的依赖性较弱。数值模拟的准确性通过实验得到验证，证明其能够可靠地预测不同激光功率设置和冲洗速率下的温度变化和热损伤。

关键词热损伤·Tm光纤激光碎石术·数值模拟·冲洗率·尿路

介绍

激光碎石术（LL）已成为治疗尿路结石的主流方法之一[1]。与传统的碎石术技术相比，如冲击波碎石术而气压弹道碎石术与LL联合应用的柔性输尿管镜技术，在效率、精准度和适用性方面具有显著优势。但激光诱导的光热效应[2]可能对尿路组织造成热损伤，引发输尿管狭窄[3]、肾盂及肾盏热损伤[4]等并发症，进而可能导致肾功能受损[5]。

Ho：YAGLL技术长期以来被视为逆行输尿管镜手术的金标准。在Ho：YAGLL过程中，激光参数、冲洗速率及尿路内定位等因素会显著影响液体温度和热损伤程度[6，7]。近年来，钬光纤激光（TFL）碎石术已崭露头角，成为Ho：YAGLL的有力替代方案[8–10]。TFL的水吸收系数是Ho：YAG激光的四倍，其参数范围也更为宽泛，包括最高可达2400赫兹的脉冲重复频率和更宽的脉冲能量范围。

✉ 杜王
wdxz@foxmail.com

✉ 盛丽
lisheng-znyy@whu.edu.cn

✉ 王星环
wangxinghuan@whu.edu.cn

1 中国武汉大学工学院

2 中国武汉大学中南医院泌尿外科

Published online: 10 April 2025

（0.025–6焦耳），更平缓的脉冲波形以及500瓦的峰值功率[11]。这些特性赋予TFL独特优势，例如更快的碎石速度、更细腻的碎石粉尘、更低的后向冲击力以及更高的操作灵活性，使其成为碎石术中的高效选择[12]。由于两种激光器参数存在差异，多项研究对比了TFL与Ho：YAG激光的热效应，但结论存在分歧。部分研究指出TFL会导致更快的温度升高和更显著的热效应[13–15]，而另一些研究则表明TFL和Ho：YAG激光的温度分布曲线相似[16–18]。因此，必须独立评估TFL的安全参数，因为直接套用Ho：YAG激光的参数和冲洗速率可能带来重大安全隐患。此外，使用高功率LL确实能提高碎石效率[19–21]，但同时也增加了热损伤风险[22]。因此，应更加重视高功率LL引发的热损伤问题。

本研究通过分析铥光纤激光（TFL）碎石术中温度波动与热损伤风险，旨在确定安全冲洗速率以降低相关风险。我们采用特制玻璃管模型模拟输尿管、肾盏及肾盂的尺寸与形态，从而在体外更精准地还原泌尿道结构。运用先进的数值模拟技术对温度分布进行建模，预测安全冲洗速率。研究结果为评估TFL碎石术的热安全性提供了可靠方法，并提出最佳冲洗速率方案以提升腔镜手术的安全性。

材料和方法

实验设置

为评估激光碎石术（LL）过程中热损伤的程度，我们研制了一套测试装置。该装置旨在模拟TFL碎石术在泌尿道不同部位引发的热效应。实验采用特制玻璃管模拟泌尿道解剖结构，其上、中、下三段分别对应输尿管、肾盂和肾盏的形态与尺寸（图1 a）。玻璃管内注入生理盐水后，置于37℃恒温水浴中。本研究使用自制的准连续波TFL系统（表S1），通过管内直径272μm的光纤传输激光能量（图1 b）。同时，蠕动泵将储液罐中的25℃生理盐水通过注射器针头输送至光纤尖端进行冲洗。玻璃管顶端用橡胶塞密封，一根长针（冲洗入口）穿过橡胶塞延伸至测试段。光纤通过针头穿线，直达测试区域。此外，一根短针（用于冲洗出口）穿过橡胶塞并定位在玻璃管的上端（图S1）。该装置模拟了包含输尿管套管和柔性输尿管镜的冲洗系统。K型热电偶、温度传感模块和数据采集系统依次连接，以1赫兹的采样率记录温度。热电偶与光纤尖端齐平地安装在管壁内侧，确保在管壁附近进行精确的温度测量，随后将数据传输至计算机进行存储。

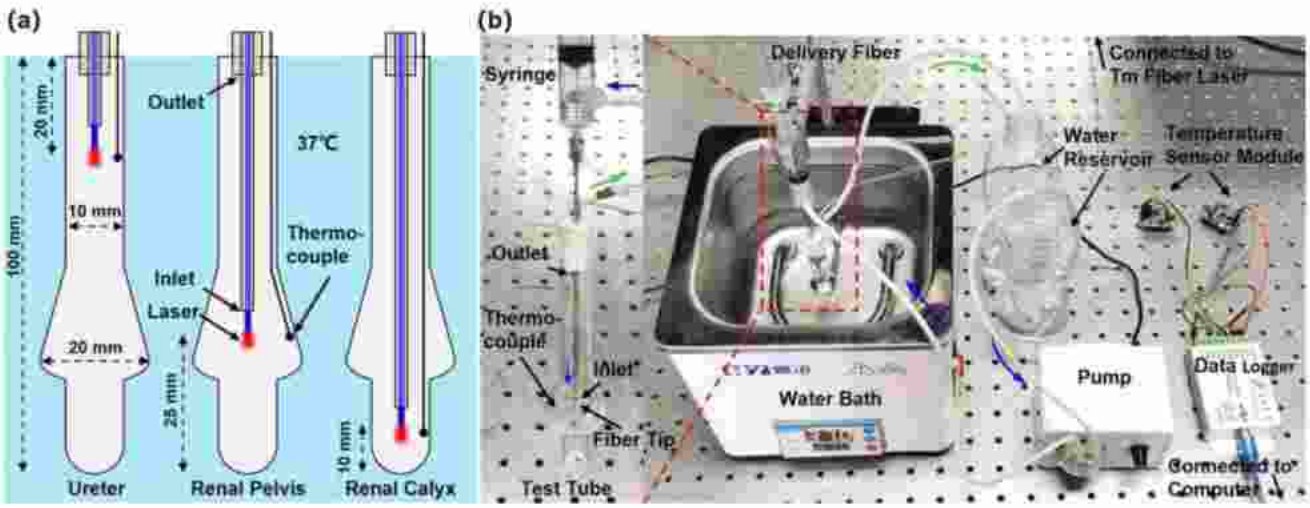


图1实验装置：a模拟不同尿路区域的玻璃管示意图，b激光热效应测试系统，其中蓝色和绿色箭头分别代表流入和流出方向

激光诱导热损伤实验在导管的上段（输尿管）、中段（肾盂）和下段（肾盏）进行。激光以平均功率40 W（2 J×20 Hz）运行，灌注速率设置为10、20、30和40 mL/min。当导管内的温度稳定在37°C时，激活微泵以启动灌注，并开始收集温度数据。20秒后，激光被激活并连续运行60秒。激光关闭后，灌注和温度记录继续进行40秒。

数值模拟模型

为精确计算激光乳化术（LL）过程中的温度场与流场分布，我们采用数值模拟技术，从而深入解析激光热损伤的形成机制，并为确定最佳LL参数提供理论依据。为确保模拟精度与计算效率，我们基于实验装置构建了轴对称模型。模拟尿路区域内的光纤尖端分别设置在三个关键位置：输尿管管口上方20毫米处、肾盂底部25毫米处及肾盏底部10毫米处。通过在管壁各点安装温度探头，实时监测管壁内部温度。为便于理解数值模拟流程，补充材料中详细列出了模拟材料的热学参数（表S2）、边界条件（表S3及图S2）以及控制方程（方程S1-S4）。此外，我们还针对肾盏区域开展了温度分布与热损伤分析，分别测试了30瓦与20瓦两种激光功率下的热效应。

热剂量

生物组织的热损伤程度取决于温度升高幅度和暴露时间，常用热剂量来量化组织损伤程度。标准计算方法是将时间-温度曲线转换为43°C等效暴露时间，具体计算公式如下：23],

$$TD_{43} = \int_0^{t_{end}} R^{43-T(t)} dt \tag{1}$$

在哪里

$$R = \begin{cases} 0, & T \le 37°C \\ 0.25, & 37 < T < 43°C \\ 0.5, & T \ge 43°C \end{cases} \tag{2}$$

在公式（1–2）中，T表示温度，t为时间，R是随温度变化的系数。43°C时的热剂量（记作TD_{43}）以分钟为单位。当温度超过43°C时，热剂量会呈指数级增长。组织损伤的时间阈值通常设定为TD_{43}=120分钟。当TD_{43}超过240分钟时，组织即被视为发生变性[24]。

结果

热损伤的体外实验

在40 W的激光功率下，测量了不同冲洗速率下三个不同尿路位置的温度变化。图2 a-c展示了三个不同尿路区域随时间变化的内壁温度分布。对于每个位置，最大温度（T-Max）随着冲洗速率的增加而降低。每个尿路位置的T-Max数据见表1。在10 mL/min的低冲洗速率下，肾盏的T-Max最高（60.2°C），其次是输尿管（58.8°C）和肾盂（45.2°C）。在20和30 mL/min的中等冲洗速率下，输尿管的T-Max最高（分别为51.2°C和45.2°C），其次是肾盂（分别为49.4°C和43.8°C）和肾盏（分别为48.6°C和44.5°C）。在40 mL/min的高冲洗速率下，三个部位的T-Max值相对接近，从低到高依次为：输尿管（38.9°C）、肾盂（39.4°C）和肾盏（39.5 °C）。随着冲洗速率的增加，三个位置的T-Max值趋于一致。值得注意的是，在40毫升/分钟的高灌溉速率下，所有位置的T-Max均保持在43°C以下；而当灌溉速率较低或中等时，所有位置的T-Max均超过43°C。

温度曲线通过公式1转换为热剂量曲线，以评估尿路组织的热损伤程度。图2 d-f展示了随时间变化的热剂量曲线。激光在20秒时激活，热剂量随时间迅速增加。激光作用在80秒结束时，热剂量达到最大值并保持恒定。对于给定位置，较高的冲洗速率会延迟达到TD_{43}=120分钟所需的时间。在低冲洗速率下，三个位置的热剂量均显著超过120分钟甚至240分钟阈值，表明所有区域均出现严重热损伤。与肾盂相比，输尿管和肾盏的热损伤风险更高。在10 mL/min的冲洗速率下，肾盂、输尿管和肾盏的热剂量分别为7.12×10^{5}、3.60×10^{4}和2.03×10^{6}分钟。在20 mL/min的冲洗速率下，三个位置的热剂量为7.20×10^{3}、

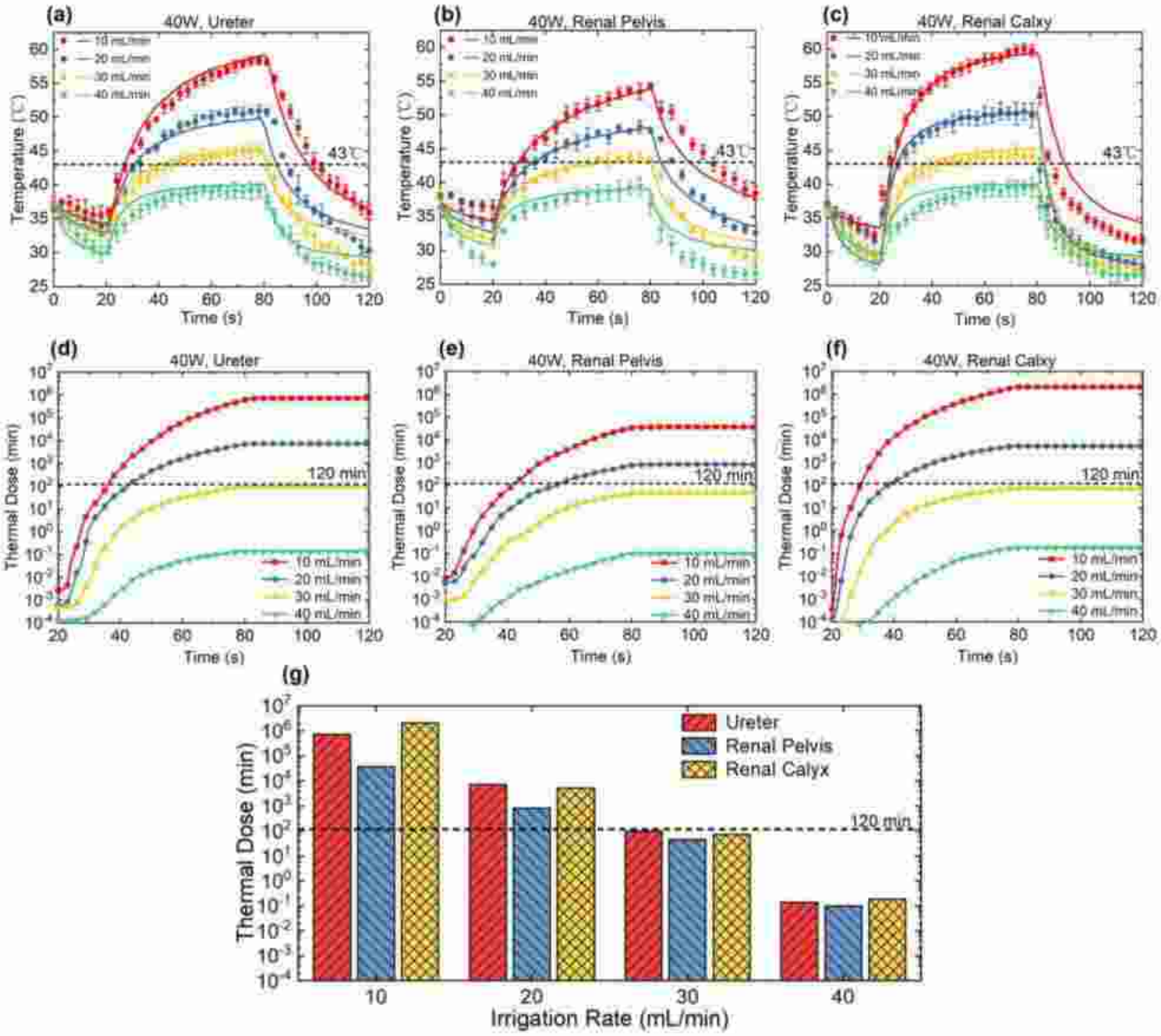


图2 40W激光功率下的温度和热剂量，**a-c**测量温度（点）和模拟温度（线），**d-e**根据温度计算的热剂量，**g** 120s后的总热剂量

表1尿液不同部位的最高温度

尿路	T-Max（℃）			
	灌注率（mL/min）			
	10	20	30	40
输尿管	58.8	51.2	45.2	38.9
肾盂	54.3	48.6	44.5	39.4
肾盏	60.2	49.4	43.8	39.5

8,19 当灌注速率增加到30 mL/min时，输尿管、肾盏和肾盂的热剂量分别显著降低至99.13、46.07和73.59分钟。这些数值均低于损伤阈值，且未出现热损伤。

在任何位置观测到的结果显示，在最高灌溉速率40 mL/min时，所有位置的热剂量比损伤阈值低两个数量级，确保了所有区域的安全条件。

热损伤模拟

本研究采用数值模拟模型，在40瓦激光功率条件下计算温度分布曲线及温度场分布。如图2(a)-(c)所示，模拟数据（曲线）与实验数据（散点）在三个尿路部位和四种冲洗速率下均高度吻合，充分验证了模型的高精度。由于肾盏体积较小，这使得

由于更易受到热损伤，数值模拟模型进一步用于分析较低激光功率设置（20和30 W）下肾盂的热损伤，并预测安全灌注速率，如图3所示。在30 W功率下，灌注速率分别为10、20和30 mL/min时的最大温度分别为47.4、43.3和39.6°C。仅在10 mL/min时发生严重热损伤，此时热剂量达到624.94 min，超过损伤阈值。在20 W功率下，所有灌注速率的最大温度均低于43°C，且未观察到热损伤。

图4(a)-(c)展示了在40 W高功率下79秒时不同尿路区域的温度场分布。在40 mL/min的高冲洗速率下，所有区域均未观察到显著的热量积聚。在输尿管中，激光诱导加热影响的区域呈现纺锤状。当冲洗速率降至10和20 mL/min时，出现明显的热量积聚，输尿管冲洗出口下方形成了一个大面积高温区。在30 mL/min时，观察到轻微的热量积聚。肾盂中的激光诱导热效应区呈倒三角形，热量积聚主要集中在肾盂下部和肾盏上部。相比之下，肾盏中的热效应呈三角形分布，最高温度区主要位于下部。

肾盏的一部分。与其他部位相比，肾盂中的热积累相对较低。此外，图4(d)和(e)分别展示了在30 W和20 W激光功率下肾盏内的温度分布。与40 W相比，功率降低时热效应显著减弱。值得注意的是，在30 W功率和10 mL/min的灌注速率下，肾盏底部观察到明显的热积累。然而，在20 W功率下，肾盏内未观察到显著的热积累，这与图3中所示的温度趋势一致。

讨论

随着高功率激光应用的日益普及，激光引发的泌尿系统热损伤风险也随之上升[25，26]。掌握并控制激光治疗导致的温度升高，已成为保障激光治疗安全的关键所在。适当控制冲洗速率能有效降低组织热损伤风险。但需注意，不同泌尿道区域对激光热损伤的敏感度存在差异。因此，泌尿科医生需根据具体治疗部位，灵活调整激光参数、冲洗速率及温度控制策略。

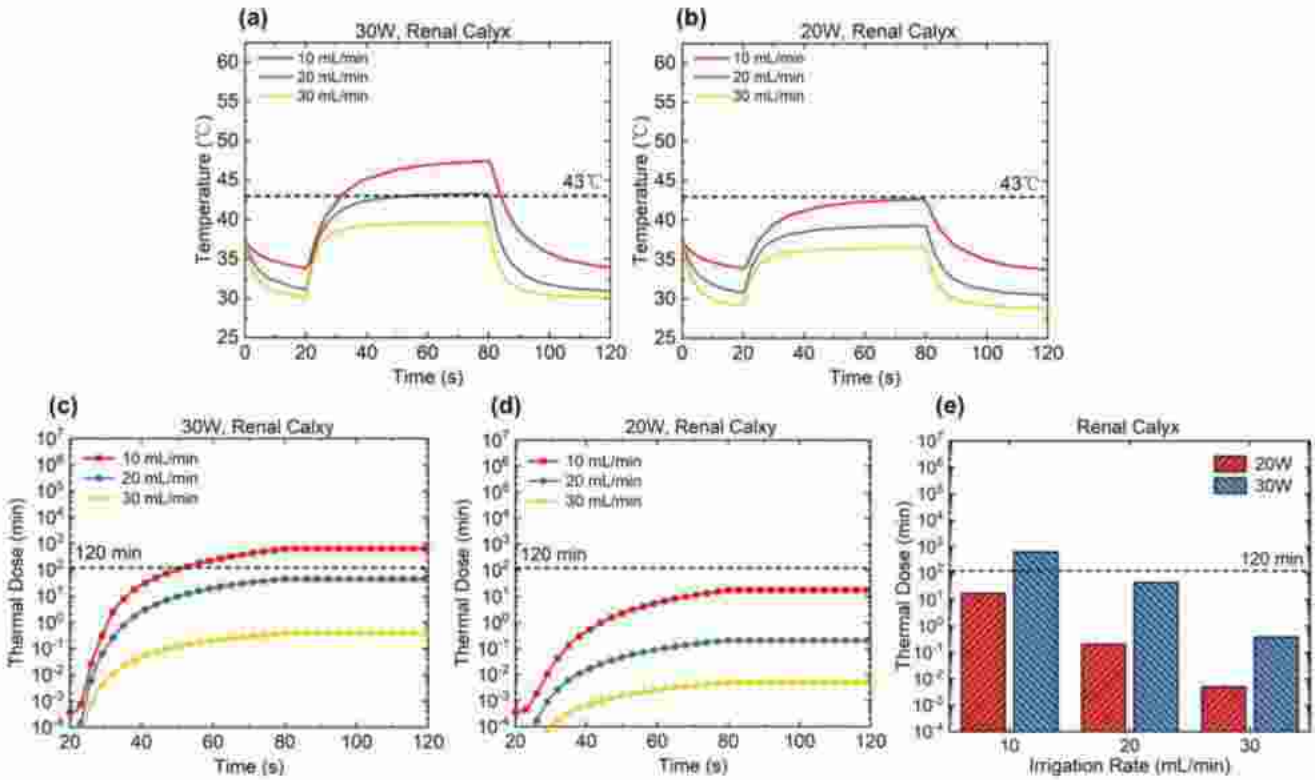


图3通过模拟获得的肾盏温度曲线和热剂量。**a-b**温度曲线，**c-d**热剂量，**e** 120秒后的总热剂量

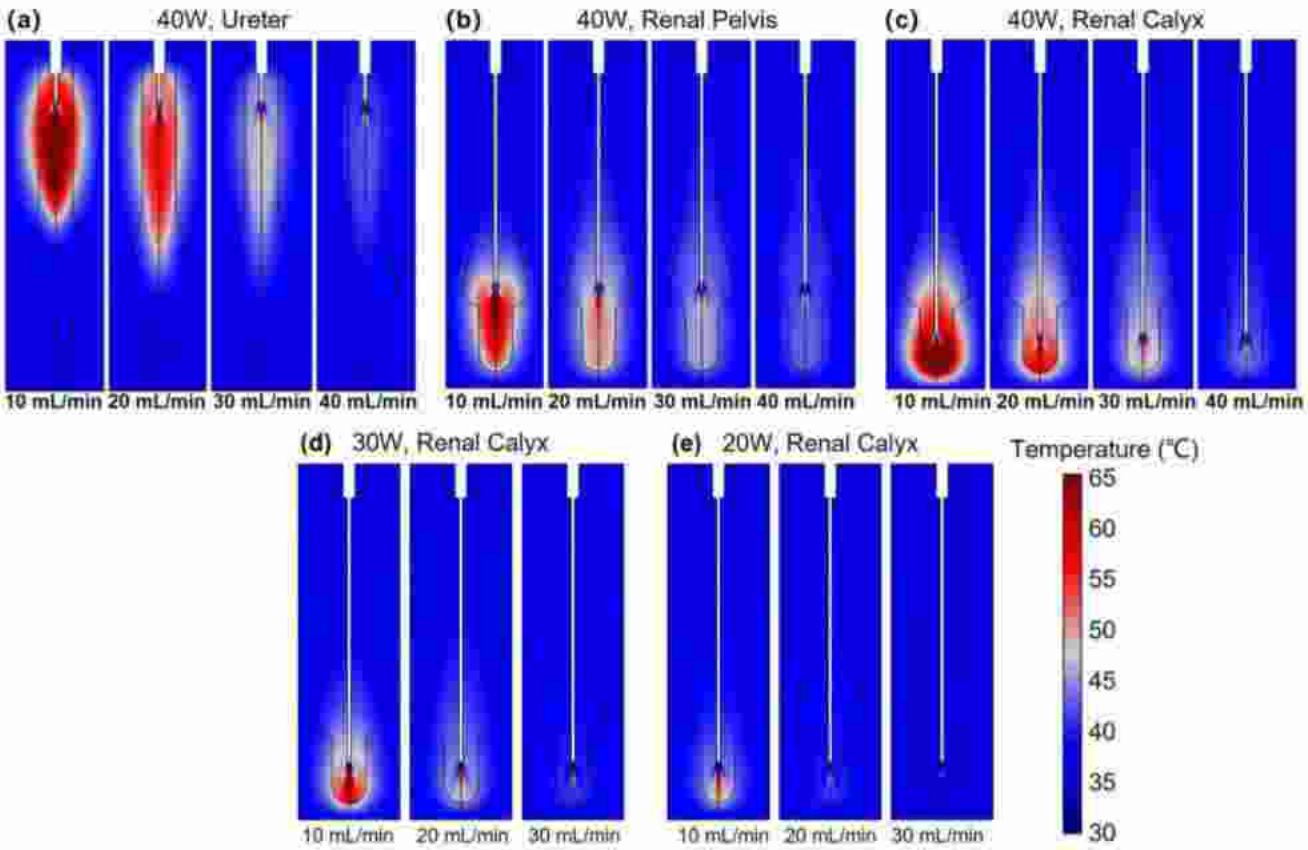


图4模拟温度场分布，**a-c**不同尿路区域40W，**d**肾盏30W，**e**肾盏20W

尿路不同部位的热损伤程度与其体积和形态密切相关。当冲洗速率较低时，输尿管和肾盂在激光加热区下方存在一定空间，这有利于热量散发，使内壁温度相对较低。肾盂漏斗状结构还能有效促进腔内热量扩散。相比之下，肾盏的热损伤最为显著。由于肾盏结构狭窄且封闭，激光加热区产生的热量容易积聚，可能对肾乳头造成热损伤。因此，在输尿管梗阻或肾盏狭窄等热扩散受限的狭窄空间进行碎石时，提高冲洗速率或采用间歇性激光激活[14，27]，对于安全降低温度阈值至关重要。增加冲洗速率能有效降低结石处理区域的温度，最大限度减少热损伤风险。这种效应归因于较高灌溉率时对流热传递系数的增加，从而提高了冷却效率[28]。然而，过高灌溉率可能导致肾内压力升高，从而可能引起肾盂静脉逆流[29]或结石后退。

因此，为了在最小化肾内压力升高的风险的同时防止热损伤，应选择较低的冲洗速率作为安全流速。根据体外实验结果，40瓦功率的安全冲洗速率被确定为30 mL/min。根据数值模拟结果，肾盏在30瓦和20瓦下的安全冲洗速率分别为20 mL/min和10 mL/min。由于肾盏是三个解剖区域中最小的，其安全冲洗速率也可作为其他尿路部位的保守参考。

本研究存在若干局限性。实验装置与模拟模型虽是对真实尿路结构的简化呈现，但无法完全复现其复杂的解剖特征。若采用基于CT数据的三维模拟模型，将能更精准可靠地预测热损伤。此外，本研究使用的玻璃材料刚性与真实尿路系统的弹性存在差异，因此未来研究将重点拓展TFL热损伤实验，通过硅胶基模型或离体猪尿路模型来更真实地模拟实际环境。这些改进将为相关研究奠定更坚实的科学基础。

用于优化临床LL技术并提升安全性评估。

结论

本研究探讨了TFL碎石术中不同灌注速率对热损伤的影响。研究结果表明，温度升高和热损伤程度主要取决于激光功率与灌注速率，而解剖位置的影响相对较小。通过实验验证了数值模拟的准确性，证明其能可靠预测不同激光功率设置和灌注速率下的温度变化及热损伤情况。本研究为评估TFL碎石术中的热损伤风险提供了有效方法，并确定了安全灌注速率，为提升LL手术安全性提供了重要参考依据。

补充信息在线版本包含补充材料，可在https://doi.org/10.1007/s00345-0 25-05614-4上找到。

作者贡献：R.Z.：数据分析、数据收集或管理、论文撰写/编辑；D.W.：项目开发、论文编辑；C.W.：数据收集、论文编辑；Y.L.：数据收集与分析；X.M.：数据收集与分析；Z.L.：数据分析；S.L.：项目开发；C.L.：项目开发；X.W.：项目开发。所有作者均参与论文审阅。

资金说明：本研究由武汉大学中南医院转化医学与多学科研究项目（项目编号：ZNJC202401）资助。

数据可用性：本研究期间未生成或分析任何数据集。

声明

伦理审批本研究不涉及人类或动物受试者，因此无需伦理审批。

竞争利益作者声明无竞争利益。

参考文献

1. 朱旭、李飞、胡晓、李浩、吴思、蒋浩（2023）输尿管镜钬激光碎石术中减少热损伤的方法。《亚洲泌尿外科杂志》10(1)：89–95。https://doi.org/10.1016/j.aj ur.2022.05.011
2. 金丰陈博士，1,4T，约书亚·佩奇博士，2乔尔 MH，泰奇曼医学博士，3和韦尔奇·阿什利博士12（2001年）激光碎石术的视角：碎石过程。J Endourol 15(3)ht tps：//doi.org/10.1089/089277901750161737
3. Chen S，Zhou L，Wei T et al（2017）钬：YAG激光与气压碎石术治疗输尿管结石的比较：最新Meta分析。Urol Int 98(2)：125–133。https://doi.org/10.1159/000448692
4. Aldoukhi AH，Hall TL，Ghani KR，Maxwell AD，MacConaghy B，Roberts WW（2018）高功率钬激光碎石术中猪体内模型的骨盆液温度。J Endourol 32(8)：724–729。https://doi.org/10.1089/end.2018.0395
5. El-Abd AS，Suliman MG，Abo Farha Mo等人（2014年）输尿管镜治疗输尿管结石后输尿管狭窄的发展：两个学术中心的长期研究。阿拉伯泌尿学杂志 12(2)：168-172。https://doi.org/10.1016/j.aju.2013.11.004
6. Aldoukhi AH，Black KM，Hall TL et al（2020）确定热安全激光碎石术功率和冲洗参数：体外模型。J Endourol 34(1)：76–81。https://doi.org/10.1089/end.201 9.0499
7. Tsaturyan A，Petcinaris A，Pantazis L et al（2022）长期激光激活对灌注液温度的影响：一项体外实验研究。World J Urol 40(7)：1873–1878。https://doi.org/10.1007/s00345-022-04000-8
8. Traxer O，Pearle M（2024）钕光纤激光器与钬-钇铝石榴石在碎石术中的比较：哪一种更胜一筹？？Eur Urol 85(6)：541–542。https://doi.org/10.1016/j.eururo.2024.02.023
9. 索拉诺C，科拉亚斯M，潘蒂耶尔F，坎德拉L，多伊兹S，特拉克塞尔O（2023）尿路结石治疗的导航：评估钕光纤激光、钬YAG和铥YAG在现实世界中的实用性和性能。世界泌尿学杂志。https://doi.or g/10.1007/s00345-023-04487-9
10. Emiliani E，KanashiroA，Angerri O（2023）激光碎石术：每种激光源的优缺点。Curr Opin Urol 33(4)：302–307。https://doi.org/10.1097/MOU.0000000000 01092
11. Mishra A，Medairos R，Chen J et al（2024）肾脏模型中安全有效钬光纤激光碎石术的最佳设置探索。BJU Int 133(2)：223–230。https://doi.org/10.1111/b ju.16218
12. 文蒂米利亚E，多伊齐S，科瓦连科A，安德烈娃V，特拉克塞O（2020）脉冲形状对尿路结石的影响：使用钬：钇铝石榴石和超脉冲钬光纤激光器的幻影后退率和消融效率。BJU Int126(1)：159–167。https://doi.org/10.1111/bju.15079
13. Belle JD，Chen R，Srikureja N，Amasyali AS，Keheila M，Baldwin DD（2022）一项体外研究中，新型钬光纤激光器是否比传统钬激光器具有更高的尿路上皮热损伤风险？？J Endourol 36(9)：1249–1254.https://d oi.org/10.1089/end.2021.0842
14. Wanderling C，Saxton A，Phan D et al（2024）Getting hot in here! Comparison of holmium vs.thulium laser in an anatomic hydrogel kidney model.Urolithiasis 52(1)：49.https://doi.org/10.1007/s00240-024-01541-y
15. Taratkin M，Laukhtina E，Singla N et al（2020）Ho：YAG激光和新型Tm光纤激光器进行激光碎石术期间的温度变化：一项比较体外研究。World J Urol 38（12）：3261–3266，https://doi.org/10.1007/s00345-020-03122-1
16. Molina WR，Carrera RV，Chew BH，Knudsen BE（2021）输尿管激光碎石术中的温度升高：超脉冲钬光纤激光器（SPTF）与高功率120 W钬YAG激光器（Ho：YAG）的比较。World J Urol 39（10）：3951–3956，https://d oi.org/10.1007/s00345-021-03619-3
17. 奥特纳G，赖斯P，纳格尔U，赫尔曼TRW，索马尼BK，托卡斯T（2022）《输尿管内泌尿外科碎石术与组织消融的热效应：钬激光与铥激光实验研究的系统综述》。《世界泌尿外科杂志》41(1)：1–12。https://doi.org/10.1007/s00345-022-04242-6

18. Juliebo-Jones MSAE，Beisland P，Ulvik C O（2022）采用钬光纤激光和钬：钇铝石榴石激光进行输尿管镜检查时的温度曲线：一项临床前研究的结果。Scand J Urol 56(4)：313–319。https://doi.org/10.1080/21681805.2022.2104367

19. 刘M，彭Y，王Z等（2021）新型钬光纤激光消融效率：激光设置和光纤使用体外研究。J Endourol 35(8)：1211–1216。https://doi.org/10.1089/end.2020.1116

20. 沈洋，梁杰，谢立，刘聪（2024）新型超脉冲钬光纤激光器的消融效率与激光安全性：一项体外研究。《世界泌尿外科杂志》42(1)：561。https://doi.org/10.1007/s00345-024-05266-w

21. Ventimiglia E，Pauchard F，Quadrini F et al（2021）高功率和低功率激光碎石术获得相似结果：现有临床系列的系统评价和荟萃分析。J Endourol 35(8)：1146–1152。https://doi.org/10.1089/end.2020.0090

22. Juliebo-Jones MSAE，Beisland P，Ulvik C O（2024）柔性输尿管镜激光碎石术期间的温度测量：一项前瞻性临床试验。J Endourol 38(4)：308–315。https://doi.org/10.1089/end.2023.0660

23. 威廉姆斯JG，戈德史密斯L，莫尔顿DE，沃特斯SL，特尼BW（2021）激光碎石术的温度模型。世界泌尿学杂志39(6)：1707-1716。https://doi.org/10.1007/s00345-020-03357-y

24. Stephen A.Sapareto PD（1984）癌症治疗中的热剂量测定

25. 温希普·B，沃林·D，卡洛斯·E等学者（2019）在《输尿管镜钬激光碎石术中高温的起落》一文中指出。

J Endourol 33（10）：794–799.https://doi.org/10.1089/end.2019.0084

26. Aldoukhi AH，Ghani KR，Hall TL，Roberts WW（2017）高功率钬激光碎石术的热反应。J Endourol 31（12）：1308–1312。https://doi.org/10.1089/end.2017.0679

27. 丁T，徐Z，黄Z，肖B，胡W，李J（2024）体外研究超脉冲光纤钬激光碎石术中冲洗率、操作室工作周期和肾内温度。世界泌尿外科杂志42(1)：588。https://doi.org/10.1007/s00345-024-05289-3

28. Khaburi A（2014）《纳米结构表面的自然与强制对流传热分析》，载于《世界工程大会论文集》第1卷，第317–319页

29. 托尼利S，贝根MF，奥兹坎A，格拉茨克C，米尔尼克A（2023）热效应：温度过度升高对输尿管和肾结石激光治疗并发症的影响。世界泌尿外科杂志41（12）：3853-3865。https://doi.org/10.1007/s00345-023-04652-0

出版商说明：Springer Nature对已发表地图和机构隶属关系的司法管辖权主张保持中立。

Springer Nature或其授权方（例如学会或其他合作伙伴）根据与作者或其他权利持有人签订的出版协议，对本文拥有独家权利；作者对本文已接受的稿件版本进行自我存档，完全受该出版协议条款和适用法律的约束。

Urolithiasis (2025) 53:169
https://doi.org/10.1007/s00240-025-01816-y

RESEARCH

High-power Ho:YAG lithotripsy increases subclinical renal stress: a prospective randomized KIM-1 study

Haider Nihad Izaddin Alalam[1] · Furkan Güldibi[1] · Mehmet Giray Sönmez[1] · Cemile Topçu[2] · Selçuk Güven[1] · Mehmet Balasar[1]

Received: 10 June 2025 / Accepted: 20 July 2025
© The Author(s), under exclusive licence to Springer-Verlag GmbH Germany, part of Springer Nature 2025

Abstract

This study aimed to compare the safety profile of high-power (HPL) and low-power (LPL) Holmium:YAG lasers in retrograde intrarenal surgery (RIRS), using urinary Kidney Injury Molecule-1 (KIM-1) as an early biomarker for acute kidney injury (AKI). Sixty patients with renal stones (1.5–2.5 cm) were prospectively randomized into HPL and LPL groups. Urinary KIM-1 and KIM-1/creatinine ratios were measured preoperatively and at 4 and 24 h postoperatively. Intraoperative parameters, stone-free rates (SFR), complications, and renal function (eGFR, serum creatinine) were also assessed. Intrarenal temperatures were recorded before and after lithotripsy. Operative time, SFR, complication rates, and renal function parameters were similar between groups ($p>0.05$). However, KIM-1 levels were significantly higher in the HPL group at 24 h postoperatively (278.8 ± 239.6 pg/mL vs. 170.3 ± 172.9 pg/mL, $p=0.003$), and the KIM-1/creatinine ratio was also elevated (5.5 ± 4.5 vs. 3.1 ± 2.0, $p=0.035$). No significant differences were observed in postoperative serum creatinine or eGFR. Intraoperative renal temperatures increased slightly in the HPL group, but the difference was not statistically significant. While high-power laser lithotripsy does not adversely affect global renal function, it is associated with elevated levels of renal injury biomarkers, suggesting greater subclinical renal stress.

Keywords Kidney stone · Retrograde intrarenal surgery · High-power laser · Low-power laser · KIM-1 · Urinary KIM-1

Introduction

Urolithiasis is a major global health issue, affecting 10 to 15% of the population and representing a prevalent urological condition that contributes significantly to morbidity [1]. Nephrolithiasis, a specific form of urolithiasis, refers to the presence of stones in the kidneys and is associated with a multifactorial etiology that includes genetic factors, obesity, and dehydration [2]. Retrograde intrarenal surgery (RIRS), shockwave lithotripsy (SWL), and percutaneous nephrolithotomy (PCNL) are the primary treatment modalities for managing kidney stones [3].

Retrograde intrarenal surgery (RIRS) is a minimally invasive procedure that employs a flexible ureteroscope (fURS) along with laser energy, commonly utilizing a holmium laser, for the treatment of renal stones [4]. Flexible ureteroscopy and laser lithotripsy (FURSL) particularly effective for stones that are small to medium-sized (typically < 2 cm) or located in anatomically challenging areas [5]. Due to advancements in technology and training, FURSL is now frequently used for stones up to 2 cm, achieving high stone-free rates and lower complication rates than PCNL [6]. The holmium:YAG (Ho:YAG) laser is regarded as the gold standard for laser lithotripsy in flexible ureteroscopy, offering efficient treatment for various kidney stone compositions [7].

Ho:YAG lithotripsy, utilizing a Holmium laser that emits light at a wavelength of 2100 nm, is highly absorbed by water, which results in minimal thermal injury to adjacent renal and ureteral tissues [8]. Ho:YAG lasers are commonly classified into two categories: low-power (LPL) and high-power lasers (HPL) [9]. Lasers with a single cavity that

✉ Haider Nihad Izaddin Alalam
hayderal-alim@hotmail.com

1 Urology Department, Faculty of Medicine, Necmettin Erbakan University, Konya, Turkey

2 Biochemistry Department, Faculty of Medicine, Necmettin Erbakan University, Konya, Turkey

Published online: 02 September 2025

produce up to 30 W of power are classified as LPL, while lasers with multiple cavities that produce over 30 W are categorized as HPL [10]. Previous similar studies have shown that the use of HPL significantly reduces operation time and hospitalization compared to LPL [11, 12]. Although, concerns have been raised regarding the short-term effects such as acute kidney injury (AKI) and long-term effects of high-power laser on the kidneys due to the high pressure and temperature generated [12].

Recently, new biomarkers for acute kidney injury (AKI) have been found. Key examples include NGAL, IL-18, KIM-1, and TIMP-2, which may help diagnose AKI early [13, 14]. Of the new biomarkers, urinary KIM-1 (KIM-1) stands out as a reliable indicator for detecting acute kidney injury (AKI). It has also been approved by the US Food and Drug Administration (FDA) for use in preclinical drug development [15]. KIM-1 is a specific marker of kidney tubule injury that is released into urine after acute kidney damage and is one of the first indicators of such injury. KIM-1 has been shown to be an effective biomarker for comparing the kidney damage caused by RIRS techniques [16].

In this study, we aimed to compare the safety of high-power and low-power laser lithotripsy using KIM-1, an early marker for acute kidney injury (AKI).

Materials and methods

This study was approved by the Ethics Committee of Necmettin Erbakan University Faculty of Medicine on July 7, 2023 (2023/4402). Written and verbally informed consent was obtained from all participants. The study was designed prospectively and funded by the Necmettin Erbakan University Scientific Research Projects Coordination Unit (Project No: 24TU18007).

Patient selection and study criteria

The study was conducted on patients aged 18–65 years who presented with kidney stones at the Urology Clinic of Necmettin Erbakan University Faculty of Medicine and underwent Retrograde Intrarenal Surgery (RIRS) between October 1, 2023, and May 1, 2024. A total of 60 patients were included, following strict inclusion and exclusion criteria to ensure a homogeneous patient group and enhance result reliability.

Eligible participants were healthy adults aged 18–75 years with CT-confirmed kidney stones (1.5–2.5 cm) and an eGFR of≥60. Exclusion criteria included pyuria, ureteral stones, positive urine culture, renal parenchymal thinning, recent surgery, kidney malformations, chronic kidney disease, solitary kidney, or nephrotoxic agent use. Patients who had undergone stone surgery in the past three months or were unable to undergo ureterorenoscopy due to ureteral strictures were also excluded.

Preoperative prophylaxis

All patients received antibiotic prophylaxis before surgery. A third-generation cephalosporin (ceftriaxone) was administered an hour preoperatively, while patients with allergies received an alternative antibiotic, such as ciprofloxacin or amikacin.

Urine sample collection and analysis

Urine samples were collected at three time points: preoperatively, 4 h postoperatively, and on the 24th hour postoperative. Samples were centrifuged at 3000 rpm for 10 min, separated into Eppendorf tubes, and stored at -80 °C until analysis. On the study day, the samples were thawed, and urinary KIM-1 levels (Elabscience Biotechnology Inc, USA) were measured. Urinary KIM-1/creatinine ratios were then calculated and compared across groups.

Devices and settings

A Redpine® RP-U-C12 Single-Use Video Flexible Ureteroscope (Guangzhou, China) was used for all procedures. For LPL used 272 µ fiber with Dornier® 30 W Laser (Germany) and for HPL used 272 µ fiber with Jenna Surgical® 150 W Laser (Germany). Laser technique chosen by block randomization.

Randomization method

Patients were randomized into High Power (HPL) or Low Power (LPL) groups using a block randomization method to ensure balanced group sizes. A total of 60 patients were assigned in blocks of four (15 blocks in total), with each block including 2 patients for HPL and 2 for LPL. The random sequence was computer-generated by an independent statistician and kept in sealed opaque envelopes, opened only at the time of enrollment. Both surgeons and patients were blinded to group assignment until allocation.

Intraoperative procedure and surgical technique

All procedures were performed by an experienced surgeon with a minimum of 60 RIRS cases. Surgeries were conducted under general anesthesia, with patients positioned in the dorsal lithotomy position. A sterile surgical field was

established, and all steps of the procedure followed strict aseptic protocols.

Intrarenal temperature measurement

Intrarenal temperature was measured at the beginning and end of lithotripsy using aspirated intrarenal fluid through the flexible ureterorenoscope channel.

Postoperative management

Patients were closely monitored for complications such as fever, hematuria, and urinary infections. Vital signs and hemodynamic stability were assessed regularly. On postoperative day 1, a plain abdominal X-ray was taken to evaluate residual stones and double-J stent positioning.

Outcome measures

The primary outcome measure was the stone-free rate, assessed by standard care imaging at three months post-procedure. Secondary outcome measures included intraoperative and postoperative complications, operative time, hospitalization time, postoperative fever, and DJ stent requirement. Operation time was defined as the total duration of the procedure in minutes. Postoperative fever incidence was recorded as a binary outcome (yes/no). Hospitalization time was inferred from perioperative management, although not explicitly stated in the data. The presence of residual stone and postoperative complications were evaluated and classified according to the Modified Clavien grading system.

In terms of biochemical markers, preoperative and postoperative serum creatinine, hemoglobin levels, and estimated glomerular filtration rate (eGFR) were measured and compared. Urinary Kidney Injury Molecule-1 (KIM-1) levels were recorded at baseline, 4th hour, and 24th hour postoperatively. Additionally, the ratio of KIM-1 to serum creatinine (KIM-1/Cr) was calculated at each of these time points to provide normalized values. Intraoperative thermal changes were evaluated by measuring intrarenal temperature before and after lithotripsy, with the difference noted in °C. Perioperative management parameters, including the presence or absence of pre- and postoperative DJ stents, were also documented as part of the outcome analysis.

Statistical analyses

Statistical analysis of the data obtained from the study was conducted using IBM SPSS Statistics software (Version 27, IBM Corp., Armonk, NY, USA) [17]. The normality distribution of continuous variables was evaluated using Kolmogorov–Smirnov and Shapiro–Wilk tests. Data with normal distribution were expressed as mean ± standard deviation (mean ± SD), while data without normal distribution were expressed as median (minimum–maximum) values. Independent Samples t-test was used to compare normally distributed continuous variables between groups, whereas Mann–Whitney U test was used for variables not showing normal distribution. Changes within a single group between preoperative and postoperative periods were assessed using Paired Samples t-test or Wilcoxon signed-rank test depending on the distribution. Categorical variables were summarized as frequencies and percentages, and comparisons between groups were conducted using Chi-square (χ^2) test or Fisher's exact test depending on expected cell counts. A multivariate logistic regression analysis was performed to determine the effect of independent variables on the dependent variable. For analyzing the changes in renal injury biomarkers (KIM-1 and KIM-1/creatinine ratios) over time, Repeated Measures ANOVA or Friedman test was used depending on distribution. In analyses where significant differences were identified, pairwise comparisons with Bonferroni correction were applied for post-hoc comparisons. In all statistical analyses, a p-value of <0.05 was considered statistically significant.

Results

The mean age of the 60 patients included in the study was 52.3 ± 12.4 years. Among the High Power laser group, the mean age was 51.5 ± 13.3 years, whereas it was 53.1 ± 11.6 years in the Low Power group. There was no significant difference between the groups (p = 0.636). Stone size averaged 16.5 ± 4.5 mm in the High Power group and 14.7 ± 4.0 mm in the Low Power group (p = 0.057). The stone density was 918 ± 266 HU in the High Power group and 961 ± 303 HU in the Low Power group, with no significant difference (p = 0.571). Preoperative double J (DJ) stent placement was performed in 43.3% (n = 26) of patients, with 36.7% (n = 11) in the High Power group and 50.0% (n = 15) in the Low Power group (p = 0.417) (Appendix Table 3).

The mean operative time for all patients was 70.7 ± 14.47 min, with 71.4 ± 13.6 min in the High Power group and 70.0 ± 15.5 min in the Low Power group, showing no significant difference (p = 0.202). Postoperative DJ stenting was performed in 88.3% (n = 53) of patients, with 83.3% (n = 25) in the High Power group and 93.3% (n = 28) in the Low Power group, showing no significant difference (p = 0.228). The residual stone rate in the study population was 20.0% (n = 12). These cases were equally divided between the groups, with 6 patients in the High Power group and 6 in the Low Power group (p = 1.00).

Table 1 Perioperative and Postoperative Outcomes

Parameters	Total (n = 60)	High Power (n = 30)	Low Power (n = 30)	P-value
Operation Time (min)	70.7 ± 14.47	71.4 ± 13.6	70.0 ± 15.5	0.202
Postoperative DJ stent	53 (88.3%)	25 (83.3%)	28 (93.3%)	0.228
Residual Stone	12 (20%)	6 (20%)	6 (20%)	1.000
Modified Clavien Grade 1	56 (93.3%)	29 (96.7%)	27 (90.0%)	0.301
Modified Clavien Grade 2	4 (6.7%)	1 (3.3%)	3 (10.0%)	
Modified Clavien Grade 3	0 (0%)	0 (0%)	0 (0%)	
Modified Clavien Grade 4	0 (0%)	0 (0%)	0 (0%)	
Modified Clavien Grade 5	0 (0%)	0 (0%)	0 (0%)	
Postoperative Fever	11 (18.3%)	6 (20%)	5 (16%)	0.556

Table 2 Comparison of Urinary KIM-1 and Creatinine Levels in Study Groups

Parameters	High Power (n = 30)	Low Power (n = 30)	P-value
KIM-1 Pre-op	66.0 ± 52.9	62.5 ± 42.1	0.807
KIM-1 Post-op 4th hour	186.2 ± 237.0	95.9 ± 63.9	0.114
KIM-1 Post-op 24th hour	278.8 ± 239.6	170.3 ± 172.9	0.003
Creatinine Pre-op (mg/dL)	41.09 ± 24.6	42.49 ± 35.7	0.450
Creatinine Post-op 4th hour (mg/dL)	50.86 ± 35.4	42.86 ± 25.4	0.549
Creatinine Post-op 24th hour (mg/dL)	62.82 ± 35.1	58.54 ± 31.5	0.626
KIM-1/Creatinine Pre-op	2.6 ± 3.0	2.7 ± 4.2	0.935
KIM-1/Creatinine Post-op 4th hour	4.9 ± 7.1	3.0 ± 3.1	0.287
KIM-1/Creatinine Post-op 24th hour	5.5 ± 4.5	3.1 ± 2.0	0.035

This equal distribution indicates that the laser power setting did not have a significant impact on stone-free outcomes in our study. Complications were classified using the Modified Clavien Classification, with Grade 1 complications observed in 93.3% (n = 56) of cases, including 96.7% (n = 29) in the High Power group and 90.0% (n = 27) in the Low Power group (p = 0.301). Grade 2 complications were found in 6.7% (n = 4) of cases, with 3.3% (n = 1) in the High Power group and 10.0% (n = 3) in the Low Power group. No Grade 3–4-5 complications were observed (Table 1).

Preoperatively, there was no significant difference in KIM-1 levels between the Low Power (62.5 ± 42.1 pg/mL) and High Power (66.0 ± 52.9 pg/mL) groups (p = 0.807). However, postoperative KIM-1 levels increased significantly in both groups, with a more pronounced elevation in the High Power group at both 4th (186.2 ± 237.0 pg/mL vs. 95.9 ± 63.9 pg/mL, p = 0.114) and 24th hours (278.8 ± 239.6 pg/mL vs. 170.3 ± 172.9 pg/mL, p = 0.003). Similarly, the KIM-1/Creatinine ratio was significantly higher at the 24th hour in the High Power group (5.5 ± 4.5 vs. 3.1 ± 2.0, p = 0.035), indicating increased renal stress (Table 2). These findings suggest that higher laser power is associated with greater postoperative renal injury biomarker elevation, although no acute renal dysfunction was observed based on serum creatinine and eGFR levels (Table 2) (Fig. 1).

There was no significant difference between preoperative and postoperative eGFR values in both groups. In the Low Power group, eGFR increased from 73.0 ± 20.7 to 75.5 ± 21.1 (p = 0.295), while in the High Power group, eGFR increased from 73.3 ± 19.2 to 76.5 ± 16.5 (p = 0.188). Similarly, serum creatinine levels showed a slight but non-significant postoperative decrease in both groups (p > 0.05), indicating that renal function remained stable postoperatively. Hemoglobin

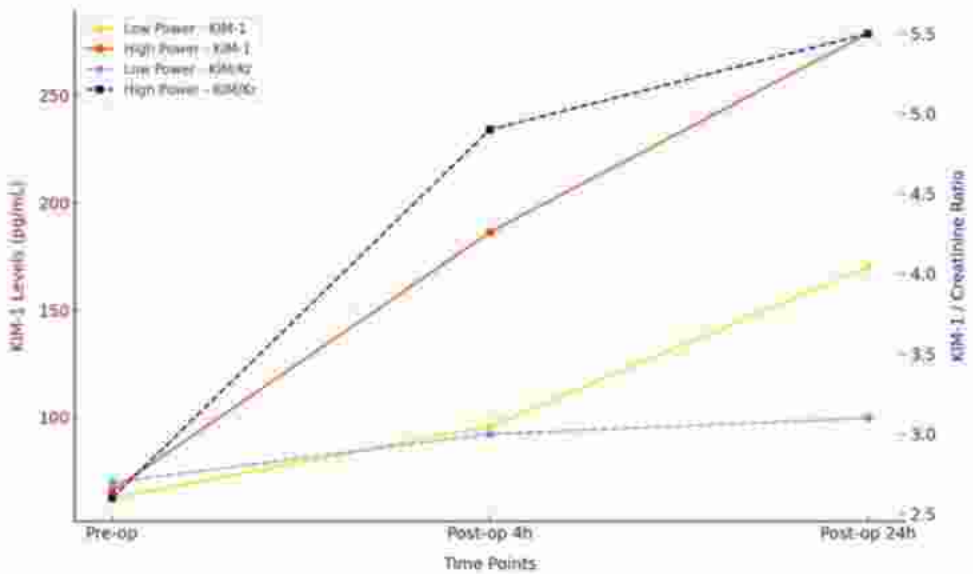


Fig. 1 KIM-1 And KIM-1/Creatinine Levels Over Time

levels also showed no significant changes, suggesting that blood loss was minimal. These results confirm that despite elevations in renal injury biomarkers, overall renal function was not significantly impaired, and no major postoperative complications related to renal dysfunction were observed (Appendix Table 5).

KIM-1 levels showed a steady increase in both groups postoperatively, but the High Power group exhibited significantly higher values at the 24th hour (278.8±239.6 pg/mL vs. 170.3±173 pg/mL, p=0.003). Similarly, the KIM-1/Creatinine ratio was higher in the High Power group at 24 h (5.5±4.5 vs. 3.1±2.0, p=0.035). These findings indicate that higher laser power correlates with greater renal stress and potential injury, despite stable renal function parameters. This suggests that subclinical renal stress may be more pronounced with high-power laser lithotripsy (Table 2) (Fig. 1).

Preoperatively, intra-renal temperatures were comparable in both groups (p=0.867). By the end of lithotripsy, temperatures increased slightly more in the High Power group (28.7±2.4 °C) compared to the Low Power group (28.2±2.4 °C), but the difference was not statistically significant (p=0.135). The mean temperature difference was also similar (2.56±1.4 °C vs. 2.49±1.5 °C, p=0.860) (Appendix Table 4) (Fig. 2).

Discussion

In our study, the effects of different laser power settings applied during retrograde intrarenal surgery (RIRS) on renal tissue were examined using biochemical markers. The demographic, clinical, and radiological parameters were similar in both groups, indicating that the findings were obtained from a homogeneous patient population. However, in the postoperative period, significant increases were observed in renal injury markers KIM-1 and KIM/spot urine creatinine ratios, particularly in patients treated with high-power laser. This suggests that high-power laser use may induce micro-level damage in renal parenchyma due to thermal and mechanical stress. The absence of significant differences between groups in operative time, stenting rates, complications, and residual stones further supports that these biomarker changes are directly related to laser power. Additionally, the lack of significant changes in glomerular filtration rate (eGFR), serum creatinine, and hemoglobin levels suggests that overall renal function was preserved, and that the increase in KIM-1 levels reflects the laser's tissue effects with high sensitivity. These findings highlight the potential of high-power lasers to cause renal tissue damage, emphasizing the importance of optimizing laser parameters in clinical practice.

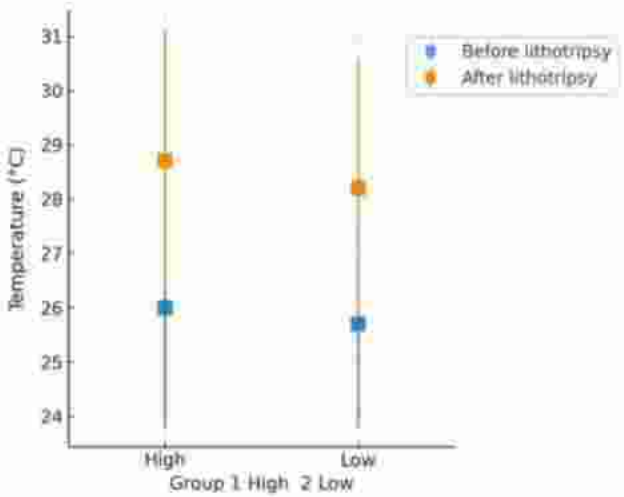


Fig. 2 Intrarenal temperatures were slightly higher in the high-power group, aligning with KIM-1 trends

Several studies in the literature have demonstrated that the use of high-power holmium lasers positively influences surgical efficiency. Rojo et al. [18] reported that in the pediatric population, high-power laser use resulted in shorter operative times and higher stone-free rates compared to low-power lasers. Similarly, Peretti et al. [19] found that low-energy but high-frequency laser settings significantly reduced operative time while achieving comparable stone-free rates to standard settings. Pietropaolo et al. [11] also reported that, in the treatment of lower pole stones, high-power laser use was associated with significantly higher stone-free rates and shorter operative times compared to low-power lasers. Additionally, Mekayten et al. [20] demonstrated that high-power laser significantly reduced stone dusting time regardless of stone density. Collectively, these studies suggest that high-power laser settings improve stone fragmentation efficiency, thereby leading to shorter operative durations and higher success rates in achieving stone-free status. Unlike previous studies, our findings revealed no significant differences in stone-free rates or operative times between the High Power and Low Power groups.

Shestha et al. [21] and Erol et al. [12] reported comparable success and complication rates between high-power and low-power laser groups. While Erol et al. found shorter operative time, hospital stay, and fluoroscopy duration with high-power lasers, our study confirmed similar success rates but observed no significant differences in hospital stay or fluoroscopy time between groups.

In light of our findings, low-power laser use may be particularly appropriate in patients with higher susceptibility to renal stress—such as those with solitary kidneys, early-stage renal dysfunction, or advanced age. Conversely, high-power laser settings may be more suitable for patients with adequate renal function, especially when maximizing

surgical efficiency and minimizing operative time are key considerations. Individualized laser parameter selection based on renal reserve and surgical goals is recommended to optimize both safety and efficacy.

While KIM-1 is a valuable and sensitive marker for detecting early subclinical kidney injury, its routine use in clinical practice is currently limited due to factors like high cost, limited availability, and lack of integration into standard care. At this stage, it may be more suitable for research purposes or in selected high-risk patients—such as those with impaired kidney function, a solitary kidney, or undergoing repeated endourological procedures—where closer renal monitoring could impact clinical decisions.

This study has several limitations, including its single-center design, small sample size (n = 60), and short follow-up period, which may limit the generalizability and long-term interpretation of the results. The exclusion of patients with renal stones < 1.5 cm restricts applicability to a broader population. Additionally, reliance on KIM-1 alone may be insufficient to fully assess renal injury, highlighting the need for more comprehensive biomarker panels and histopathological evaluation. The intrarenal temperature measurement method used was indirect and may not reflect real-time thermal dynamics. Finally, the lack of significant differences in some parameters may reflect limited statistical power. Despite these limitations, the study provides valuable insights into laser power, stone-free rates, and postoperative renal injury biomarkers in RIRS. Further validation of our findings requires multicenter, randomized controlled trials.

Conclusion

Our study demonstrates that although high-power laser lithotripsy provides comparable operative times and stone-free rates to low-power lasers, it is associated with significantly higher levels of renal injury biomarkers such as KIM-1 and KIM-1/creatinine ratio in the early postoperative period. These findings suggest a higher degree of subclinical renal stress in the high-power group. Despite stable serum creatinine and eGFR levels, the increased biomarker levels highlight the potential tissue-level effects of high-power laser usage. Further multicenter, randomized trials are needed to validate these results and guide safe laser parameter selection in RIRS.

Appendix

See Tables 3, 4, 5.

Table 3 Demographic and Baseline Clinical Characteristics

Parameters	Total (n = 60)	High Power (n = 30)	Low Power (n = 30)	P-value
Age (mean ± SD)	52.3 ± 12.4	51.5 ± 13.3	53.1 ± 11.6	0.636
Gender—Male	36 (60.0%)	19 (63.3%)	17 (56.7%)	0.598
Gender—Female	24 (40.0%)	11 (36.7%)	13 (43.3%)	
Comorbidity—DM	30 (42.0%)	12 (40%)	18 (60.0%)	0.121
Comorbidity—HT	9 (12.4%)	5 (16.7%)	4 (13.3%)	0.718
Comorbidity—CAD	17 (23.6%)	7 (23.3%)	10 (33.3%)	0.390
Comorbidity—COPD	2 (2.7%)	1 (3.3%)	1 (3.3%)	1.000
Comorbidity—Hyperlipidemia	2 (2.7%)	1 (3.3%)	1 (3.3%)	1.000
Opacity—Radiopaque	50 (83.3%)	26 (86.7%)	24 (80.0%)	0.488
Opacity—Radiolucent	10 (16.7%)	4 (13.3%)	6 (20.0%)	
Stone size (mm)	15.6 ± 4.3	16.5 ± 4.5	14.7 ± 4.0	0.057
Stone density (HU)	940 ± 284	918 ± 266	961 ± 303	0.571
Hydronephrosis—Yes	24 (41.4%)	15 (50%)	9 (32.1%)	0.168
Hydronephrosis—No	34 (58.6%)	15 (50%)	19 (67.9%)	
Stone side—Right	23 (38.3%)	8 (26.7%)	15 (50.0%)	0.063
Stone side—Left	37 (61.7%)	22 (73.3%)	15 (50.0%)	
Preoperative DJ stent—Yes	26 (43.3%)	11 (36.7%)	15 (50%)	0.417
Preoperative DJ stent—No	34 (56.7%)	19 (63.3%)	15 (50%)	

Table 4 Intrarenal Thermal Effect of Study Groups

Parameters	High Power (n = 30)	Low Power (n = 30)	P-value
Intrarenal temp before lithotripsy (°C)	26.0 ± 2.2	25.7 ± 1.9	0.867
Intrarenal temp after lithotripsy (°C)	28.7 ± 2.4	28.2 ± 2.4	0.135
Temperature difference (°C)	2.56 ± 1.4	2.49 ± 1.5	0.860

Table 5 Preoperative and Postoperative Biochemical Parameterse

Parameters	Low Power Pre-op	Low Power Post-op	P value	High Power Pre-op	High Power Post-op	P value
eGFR	73.0±20.7	75.5±21.1	0.295	73.3±19.2	76.5±16.5	0.188
Serum Creatinine	1.11±0.4	1.06±0.4	0.152	1.08±0.3	1.02±0.2	0.071
Hemoglobin	13.5±2.2	13.2±2.2	0.136	13.3±1.8	17.3±23.7	0.797

Author contributions HA: project development, manuscript writing, data managing, laboratory analysis, collection and storage of samples. FG: data analysis, manuscript Editing, editing of figures and tables. MGS: data analysis, manuscript editing, editing of tables. CT: laboratory analysis, sample collection and storage.SG: manuscript editing. MB: project development, manuscript editing, surgical application.

Funding The authors did not receive support from any organization for the submitted work. The authors state that they have no proprietary interest in the products named in this article. None of the authors involved in this study received financial support.

Data availability No datasets were generated or analysed during the current study.

Declarations

Competing interests The authors declare no competing interests.

Ethics approval Authors declared that the research was conducted according to the principles of the World Medical Association Declaration of Helsinki "Ethical Principles for Medical Research Involving Human Subjects". The study was performed in the Clinical Ethic Committee of Necmettin Erbakan University Faculty of Medicine (No: 2023/4402). Consent to participate All participants give their consent to participate in the study. Consent for publication All participants give permission to publication.

References

1. Desai M, Sun Y, Buchholz N, Fuller A, Matsuda T, Matlaga B et al (2017) Treatment selection for urolithiasis: percutaneous nephrolithomy, ureteroscopy, shock wave lithotripsy, and active monitoring. World J Urol 35(9):1395–1399. https://doi.org/10.1007/s00345-017-2030-8
2. Kaźmierczak J, Bartosiński R, Szustak J, Wijata A, Stępień Z, Dutkiewicz J et al (2025) Urolithiasis: Comprehensive Review of Etiology, Diagnosis and Treatment Quality in Sport 39:58490. https://doi.org/10.12775/QS.2025.39.58490
3. Zeng G, Zhao Z, Mazzon G, Pearle M, Choong S, Skolarikos A et al (2022) European association of urology section of urolithiasis and international alliance of urolithiasis joint consensus on retrograde intrarenal surgery for the management of renal stones. Eur Urol Focus 8(5):1461–1468. https://doi.org/10.1016/j.euf.2021.10.011
4. Inoue T, Okada S, Hamamoto S, Fujisawa M (2021) Retrograde intrarenal surgery: past, present, and future. Invest Clinic Urol 62(2):121–135. https://doi.org/10.4111/icu.20200526
5. Burr J, Ishii H, Simmonds N, Somani BK (2015) Is flexible ureterorenoscopy and laser lithotripsy the new gold standard for lower pole renal stones when compared to shock wave lithotripsy: comparative outcomes from a university hospital over similar time period. Cent Eur J Urol 68(2):183–186. https://doi.org/10.5173/ceju.2015.509
6. Barone B, Crocetto F, Vitale R, Di Domenico D, Caputo V, Romano F, et al. (2020) Retrograde intra renal surgery versus percutaneous nephrolithotomy for renal stones >2 cm. A systematic review and meta-analysis. Minerva urologica e nefrologica The Italian journal of urology and nephrology.;72(4):441–50. Epub 2020/02/23. https://doi.org/10.23736/s0393-2249.20.03721-2. PubMed PMID: 32083423.
7. Türk C, Petřík A, Sarica K, Seitz C, Skolarikos A, Straub M et al (2016) EAU guidelines on diagnosis and conservative management of urolithiasis. Eur Urol 69(3):468–474. https://doi.org/10.1016/j.eururo.2015.07.040
8. Sandhu AS, Srivastava A, Madhusoodanan P, Sinha T, Gupta SK, Kumar A et al (2007) Holmium: YAG laser for intra corporeal lithotripsy. Med J Armed Forces India 63(1):48–51. https://doi.org/10.1016/s0377-1237(07)80109-2
9. De Coninck V, Hente R, Claessens M, Duchateau A, Doizi S, Keller EX (2021) High-power, high-frequency Ho:YAG lasers are not essential for retrograde intrarenal surgery. Eur Urol Focus 7(1):5–6. https://doi.org/10.1016/j.euf.2020.12.007
10. Traxer O, Keller EX (2020) Thulium fiber laser: the new player for kidney stone treatment? A comparison with Holmium:YAG laser. World J Urol 38(8):1883–1894. https://doi.org/10.1007/s00345-019-02654-5
11. Pietropaolo A, Mani M, Hughes T, Somani BK. Role of low- versus high-power laser in the treatment of lower pole stones: prospective non-randomized outcomes from a university teaching hospital. Therapeutic advances in urology. 2022;. Epub 2022/06/03. https://doi.org/10.1177/17562872221097345. PubMed PMID: 35651485; PubMed Central PMCID: PMCPMC9149605.
12. Erol E, Eeer G, Kiremit MC, Gokce Mİ, Balasar M, Sarikaya AF et al (2024) Multicentric evaluation of high and low power lasers on RIRS success using propensity score analysis. Urolithiasis 52(1):32. https://doi.org/10.1007/s00240-024-01535-w
13. Kashani K, Cheungpasitporn W, Ronco C (2017) Biomarkers of acute kidney injury: the pathway from discovery to clinical adoption. Clin Chem Lab Med 55(8):1074–1089. https://doi.org/10.1515/cclm-2016-0973
14. Schrezenmeier EV, Barasch J, Budde K, Westhoff T, Schmidt-Ott KM. Biomarkers in acute kidney injury - pathophysiological basis and clinical performance. Acta physiologica (Oxford, England). 2017;219(3):554–72. Epub 2016/07/31. https://doi.org/10.1111/apha.12764. PubMed PMID: 27474473; PubMed Central PMCID: PMCPMC5575831.
15. Dieterle F, Sistare F, Goodsaid F, Papaluca M, Ozer JS, Webb CP et al (2010) Renal biomarker qualification submission: a dialog between the FDA-EMEA and predictive safety testing consortium. Nat Biotechnol 28(5):455–462. https://doi.org/10.1038/nbt.1625
16. Eeer G, Sönmez MG, Aydın A, Topçu C, Alalam HNI, Güven S et al (2022) Comparison of retrograde intrarenal stone surgery with and without a ureteral access sheath using kidney injury molecule-1 (KIM-1) levels: a prospective randomized study. Urolithiasis 50(5):625–633. https://doi.org/10.1007/s00240-022-01345-y
17. Corp. I. IBM SPSS Statistics for Windows, Version 27.0. Armonk, NY: IBM Corp. Released 2020; ( ):. Epub doi:, PubMed PMID:; PubMed Central PMCID: PMC
18. García Rojo E, Traxer O, Vallejo Arzuyús DM, Castellani D, Ferreti S, Gatti C, et al. Comparison of Low-Power vs High-Power

Holmium Lasers in Pediatric Retrograde Intrarenal Surgery Outcomes. Journal of endourology. 2023;37(5):509–15. Epub 2023/03/03. https://doi.org/10.1089/end.2022.0778. PubMed PMID: 36860192.

19. Peretti D, Dalmasso E, Pecoraro A, Ambruosi C, Venzano F, Fiori C et al (2022) Low-energy high-frequency Ho-YAG lithotripsy: is RIRS going forward? A case-control study. Urolithiasis 50(1):79–85. https://doi.org/10.1007/s00240-021-01282-2
20. Mekayten M, Lorber A, Katafigiotis I, Sfoungaristos S, Leotsakos I, Heifetz EM et al (2019) Will stone density stop being a key factor in endourology? The impact of stone density on laser time using Lumenis Laser p120w and standard 20 W laser: a comparative study. J Endourol 33(7):585–589. https://doi.org/10.1089/end.2019.0181
21. Shrestha A, Corrales M, Adhikari B, Chapagain A, Traxer O (2022) Comparison of low power and high power holmium YAG laser settings in flexible ureteroscopy. World J Urol 40(7):1839–1844. https://doi.org/10.1007/s00345-022-04040-0

Publisher's Note Springer Nature remains neutral with regard to jurisdictional claims in published maps and institutional affiliations.

Springer Nature or its licensor (e.g. a society or other partner) holds exclusive rights to this article under a publishing agreement with the author(s) or other rightsholder(s); author self-archiving of the accepted manuscript version of this article is solely governed by the terms of such publishing agreement and applicable law.

尿路结石（2025）53：169
https://doi.org/10.1007/s00240-025-01816-y

研究

高功率Ho：YAG碎石术增加亚临床肾应激：一项前瞻性随机KIM-1研究

海德尔·尼哈德·伊扎丁·阿拉拉姆[1] · Furkan Guldibi [1] · Mehmet Giray Sonmez [1] · Cemile Topcu [2] · Selcuk Guven [1] · Mehmet Balasar [1]

接收日期：2025年6月10日/接受日期：2025年7月20日
©作者（们）于2025年获得德国Springer-Verlag GmbH（隶属Springer Nature集团）的独家授权

摘要

本研究旨在比较高功率（HPL）和低功率（LPL）钬：钇铝石榴石激光在逆行肾内手术（RIRS）中的安全性，使用尿液肾损伤分子-1（KIM-1）作为急性肾损伤（AKI）的早期生物标志物。60名肾结石患者（1.5–2.5厘米）被前瞻性随机分为HPL组和LPL组。术前及术后4小时和24小时分别测量尿液KIM-1水平和KIM-1/肌酐比值。同时评估术中参数、无结石率（SFR）、并发症及肾功能（eGFR、血清肌酐）。记录碎石术前后肾内温度。两组的手术时间、SFR、并发症发生率及肾功能参数无显著差异（p>0.05）。然而，术后24小时HPL组的KIM-1水平显著升高（278.8±239.6 pg/mL vs.170.3±172.9 pg/mL，p=0.003），KIM-1/肌酐比值也升高（5.5±4.5 vs.3.1±2.0，p=0.035）。术后血清肌酐或eGFR未见显著差异。HPL组患者术中肾温度略有升高，但差异无统计学意义。虽然高功率激光碎石术不会对整体肾功能造成不良影响，但其伴随的肾损伤生物标志物水平升高提示存在更严重的亚临床肾功能压力。

关键词肾结石·逆行肾内手术·高功率激光·低功率激光·KIM-1·尿KIM-1

介绍

尿路结石症是全球范围内的重大公共卫生问题，影响着全球10%-15%的人口，作为常见的泌尿系统疾病，对发病率具有显著贡献[1]。肾结石症作为尿路结石症的一种特殊类型，特指肾脏内结石的存在，其病因复杂多样，涉及遗传因素、肥胖和脱水等多重因素[2]。目前治疗肾结石的主要方式包括逆行肾镜取石术（RIRS）、体外冲击波碎石术（SWL）和经皮肾镜取石术（PCNL）[3]。

逆行肾镜手术（RIRS）是一种微创治疗方案，通过柔性输尿管镜（fURS）配合激光能量（通常采用钬激光）来清除肾结石[4]。在处理中小型结石（通常<2 cm）或位于解剖结构复杂区域的结石时，柔性输尿管镜联合激光碎石术（FURSL）效果尤为显著[5]。随着技术进步和专业培训的提升，如今FURSL已广泛应用于直径达2厘米的结石治疗，其结石清除率高且并发症发生率低于传统碎石术（PCNL）[6]。在柔性输尿管镜碎石术中，钬：钇铝石榴石（Ho：YAG）激光被公认为激光碎石的金标准，能高效处理各类肾结石成分[7]。

Ho指出：采用波长2100纳米钬激光的YAG碎石术，由于水分子对其光波具有高吸收特性，可将热损伤控制在肾脏及输尿管邻近组织的最小范围[8]。Ho进一步说明：YAG激光器主要分为低功率（LPL）和高功率（HPL）两类[9]。单腔结构的激光器

✉ 海德尔·尼哈德·伊扎丁·阿拉拉姆
hayderal-alim@hotmail.com

1 土耳其科尼亚市内杰梅廷-埃尔巴坎大学医学院泌尿外科

2 土耳其科尼亚市内杰梅廷-埃尔巴坎大学医学院生物化学系

Published online: 02 September 2025

功率不超过30瓦的激光设备被归类为LPL级，而具有多个腔体且功率超过30瓦的激光器则被归类为HPL级[10]。先前类似研究表明，与LPL级相比，使用HPL级设备能显著缩短治疗时间并减少住院需求[11，12]。不过，由于高强度激光会产生高压高温，学界对急性肾损伤（AKI）等短期影响以及高功率激光对肾脏的长期危害提出了担忧[12]。

近期，医学界发现了急性肾损伤（AKI）的新型生物标志物。其中，白细胞介素-18（NGAL）、白细胞介素-18（IL-18）、肾小管上皮细胞生长因子1型（KIM-1）和血管紧张素II受体抗抗剂2（TIMP-2）等指标，为早期诊断AKI提供了重要依据[13，14]。在这些新发现的生物标志物中，尿液中的KIM-1（肾小管上皮细胞生长因子1型）尤为突出，已成为检测急性肾损伤（AKI）的可靠指标。该标志物已获得美国食品药品监督管理局（FDA）批准，可用于临床前药物研发[15]。KIM-1作为肾小管损伤的特异性标志物，会在急性肾损伤发生后随尿液排出，是此类损伤最早出现的预警信号之一。研究还表明，KIM-1可作为有效生物标志物，用于评估不同透析技术（如血液透析、腹膜透析、血液滤过、血液透析滤过等）对肾脏造成的损伤程度[16]。

本研究旨在通过急性肾损伤（AKI）早期标志物KIM-1，对比高功率与低功率激光碎石术的安全性差异。

材料和方法

本研究于2023年7月7日获得内杰梅廷·埃尔巴坎大学医学院伦理委员会批准（编号：2023/4402）。所有参与者均签署了书面知情同意书并接受了口头说明。研究采用前瞻性设计，由该校科学研究项目协调单位资助（项目编号：24TU18007）。

患者选择和研究标准

本研究在2023年10月1日至2024年5月1日期间，于内杰梅廷·埃尔巴坎大学医学院泌尿科诊所开展，对象为18-65岁肾结石患者。通过严格筛选纳入标准和排除标准，最终筛选出60例患者，确保研究对象同质性，从而提升结果可靠性。所有患者均接受了逆行肾镜手术（RIRS）。

符合入选标准的受试者为18-75岁健康成年人，需经CT确诊的肾结石（1.5-2.5厘米）且估算肾小球滤过率（eGFR）≥60。排除标准包括：尿脓症、输尿管结石、尿培养阳性、肾实质变薄、近期接受过手术、肾脏畸形或慢性排除标准包括肾病、单侧肾或使用肾毒性药物。此外，过去三个月内接受过结石手术或因输尿管狭窄无法进行输尿管肾镜检查的患者亦被排除。

术前预防

所有患者术前均接受抗生素预防治疗。术前1小时给予第三代头孢菌素（头孢曲松），对有过敏史的患者则改用环丙沙星或阿米卡星等替代抗生素。

尿液样本采集和分析

尿液样本在三个时间点采集：术前、术后4小时及术后24小时。样本经3000转/分钟离心10分钟后，分装至Eppendorf离心管中，于-80℃冷冻保存待测。实验当天解冻样本后，使用美国Elabscience生物技术公司试剂盒测定尿液KIM-1水平，随后计算尿液KIM-1/肌酐比值，并进行组间比较分析。

设备和设置

所有手术均采用Redpine®RP-U-C12一次性视频输尿管镜（中国广州）完成。LPL手术使用272μ光纤搭配Dornier®30 W激光（德国），而HPL手术则采用272μ光纤配合Jenna Surgical®150 W激光（德国）。具体激光技术选择通过区组随机化确定。

随机化方法

为确保两组样本量均衡，采用区组随机化方法将患者随机分配至高功率组（HPL）或低功率组（LPL）。研究共纳入60名患者，按四人一组进行分组（共15个区组），每个区组包含2名HPL组患者和2名LPL组患者。随机序列由独立统计学家通过计算机生成，并密封在不透明信封中，仅在入组时开封。在分组完成前，外科医生和患者均不知晓具体分组情况。

术中操作和手术技术

所有手术均由一位拥有至少60例RIRS病例经验的资深外科医生完成。手术在全身麻醉下进行，患者采取背部截石位。手术区域保持无菌状态。

该程序已建立，且所有步骤均严格遵循无菌操作规范。

肾内温度测量

在碎石术开始和结束时，通过输尿管肾镜的柔性通道抽取肾内液体，以此测量肾内温度。

术后管理

密切监测患者发热、血尿、尿路感染等并发症，定期评估生命体征和血流动力学稳定性。术后第1天行腹部平片检查，评估残留结石及双J支架置入位置。

结果测量

主要结局指标为术后3个月通过标准影像学检查评估的无结石率。次要结局指标包括术中及术后并发症、手术时间、住院时间、术后发热情况以及是否需要植入DJ支架。手术时间定义为整个手术过程的总耗时（以分钟为单位）。术后发热发生率记录为二元结局指标（是/否）。住院时间根据围手术期管理情况推算得出，尽管数据中未明确说明。残留结石的存在及术后并发症均依据改良Clavien分级系统进行评估和分类。

在生化指标方面，研究团队对术前术后血清肌酐、血红蛋白水平及估算肾小球滤过率（eGFR）进行了检测与对比。尿肾损伤分子-1（KIM-1）水平分别在术前基线、术后4小时及24小时进行记录。此外，通过计算各时间点KIM-1与血清肌酐的比值（KIM-1/Cr）获得标准化数值。术中热变化通过测量碎石术前后肾内温度差值（以°C为单位）进行评估。围手术期管理参数（包括术前术后双侧肾动脉支架置入情况）也被纳入结果分析范围。

统计分析

采用IBM SPSS Statistics软件（版本27，IBM公司，美国纽约州阿蒙克）[17]对研究数据进行统计学分析。通过该软件评估连续变量的正态分布情况。采用柯尔莫哥洛夫-斯米尔诺夫检验和夏皮罗-威尔克检验。正态分布数据以均值±标准差（均值±SD）表示，非正态分布数据则以中位数（最小值-最大值）呈现。对于组间正态分布连续变量的比较，采用独立样本t检验；对于非正态分布变量则使用曼-惠特尼U检验。同一组患者术前与术后的变化情况，根据数据分布采用配对样本t检验或威尔科克森符号秩检验进行评估。分类变量以频数和百分比形式汇总，组间比较根据预期单元格数采用卡方（χ^2）检验或费舍尔精确检验。通过多变量逻辑回归分析评估自变量对因变量的影响。针对肾损伤生物标志物（KIM-1及KIM-1/肌酐比值）的动态变化分析，根据数据分布采用重复测量方差分析或弗里德曼检验。在发现显著差异的分析中，采用Bonferroni校正进行两两比较以进行事后检验。所有统计分析中，p值<0.05均视为具有统计学意义。

结果

本研究纳入的60例患者平均年龄为52.3±12.4岁。高功率激光组的平均年龄为51.5±13.3岁，低功率组为53.1±11.6岁，两组间无显著差异（p=0.636）。结石平均大小方面，高功率组为16.5±4.5毫米，低功率组为14.7±4.0毫米（p=0.057）。结石密度方面，两组分别为918±266 HU和961±303 HU，差异无统计学意义（p=0.571）。术前双J型支架置入率方面，高功率组为36.7%（n=11），低功率组为50.0%（n=15），两组差异无统计学意义（p=0.417）（详见附表3）。

所有患者的平均手术时间为70.7±14.47分钟，其中高功率组为71.4±13.6分钟，低功率组为70.0±15.5分钟，两组间无显著差异（p=0.202）。术后进行DJ支架置入术的患者比例为88.3%（n=53），高功率组为83.3%（n=25），低功率组为93.3%（n=28），两组间无显著差异（p=0.228）。研究人群的残留结石率为20.0%（n=12），两组间病例数均等分布，各6例（p=1.00）。

表1术中和术后结局

参数	总计（n=60）	高功率（n=30）	低功率（n=30）	概率值
操作时间（分钟）	70.7±14.47	71.4±13.6	70.0±15.5	0.202
术后DJ支架	53 (88.3%)	25 (83.3%)	28 (93.3%)	0.228
残留石	12 (20%)	6 (20%)	6 (20%)	1.000
改良型克拉一年级	56 (93.3%)	29 (96.7%)	27 (90.0%)	0.301
改良型克拉二年级	4 (6.7%)	1 (3.3%)	3 (10.0%)	
改良型克拉三年级	0 (0%)	0 (0%)	0 (0%)	
改良型克拉五年级	0 (0%)	0 (0%)	0 (0%)	
改良型克拉五年级	0 (0%)	0 (0%)	0 (0%)	
术后发热	11 (18.3%)	6 (20%)	5 (16%)	0.556

表2研究中尿KIM-1和肌酐水平的比较组

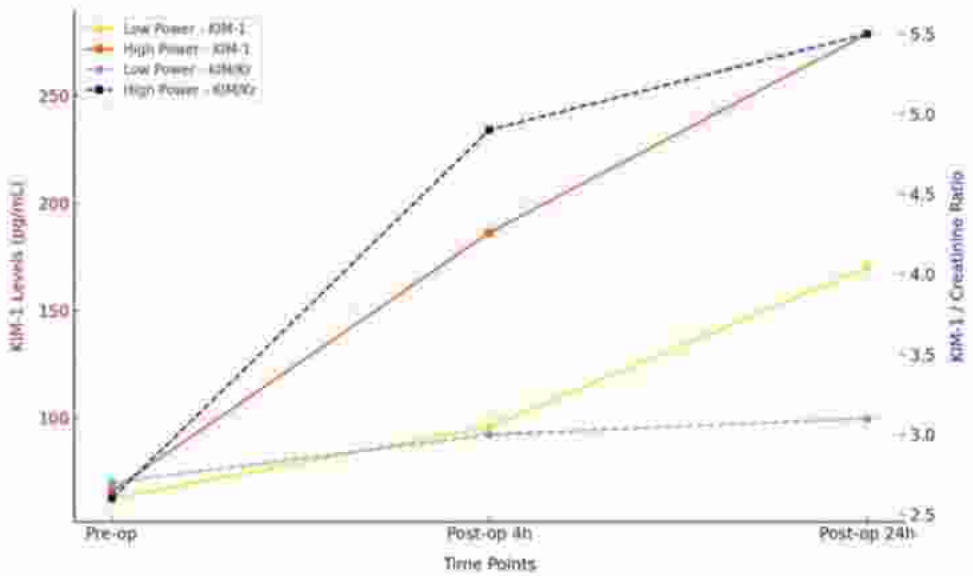
参数	高功率（n=30）	低功率（n=30）	概率值
KIM-1 Pre-op	66.0±52.9	62.5±42.1	0.807
术后第4小时KIM-1	186.2±237.0	95.9±63.9	0.114
术后24小时的KIM-1	278.8±239.6	170.3±172.9	0.003
肌酐术前（mg/dL）	41.09±24.6	42.49±35.7	0.450
肌酐术后4小时（mg/dL）	50.86±35.4	42.86±25.4	0.549
肌酐术后24小时（mg/dL）	62.82±35.1	58.54±31.5	0.626
KIM-1/Creatinine Pre-op	2.6±3.0	2.7±4.2	0.935
术后第4小时的KIM-1/肌酐	4.9±7.1	3.0±3.1	0.287
术后24小时的KIM-1/肌酐	5.5±4.5	3.1±2.0	0.035

这种均衡分布表明，在本研究中，激光功率设置对结石清除率没有显著影响。我们采用改良克雷文分类法对并发症进行分级，其中1级并发症发生率为93.3%（n=56），高功率组为96.7%（n=29），低功率组为90.0%（n=27）（p=0.301）。2级并发症发生率为6.7%（n=4），高功率组为3.3%（n=1），低功率组为10.0%（n=3）。未观察到3-4-5级并发症（见表1）。

术前，低功率组（62.5±42.1 pg/mL）与高功率组（66.0±52.9 pg/mL）的KIM-1水平无显著差异（p=0.807）。然而，术后两组的KIM-1水平均显著升高，其中高功率组在第4小时（186.2±237.0 pg/mL vs.95.9±63.9 pg/mL，p=0.114）和第24小时（278.8±239.6 pg/mL vs.170.3±172.9 pg/mL，p=0.003）的升高更为明显。同样，高功率组在第24小时的KIM-1/肌酐比值显著更高（5.5±4.5 vs.3.1±2.0，p=0.035），表明肾应激增加（表2）。这些结果表明，更高的激光功率与术后肾损伤生物标志物的升高相关，尽管根据血清肌酐和eGFR水平未观察到急性肾功能障碍（表2）（图1）。

两组患者术前与术后估算肾小球滤过率（eGFR）均无显著差异。低功率组eGFR从73.0±20.7提升至75.5±21.1（p=0.295），而高功率组则从73.3±19.2增至76.5±16.5（p=0.188）。血清肌酐水平在术后两组均出现轻微下降（p>0.05），但未达统计学显著性，表明术后肾功能保持稳定。血红蛋白

图1 KIM-1和KIM-1/肌酐水平随时间的变化



水平也未显示任何显著变化，这表明失血量极小。这些结果证实，尽管肾损伤生物标志物升高，但整体肾功能未出现显著损害，且未观察到与肾功能障碍相关的重大术后并发症（附表5）。

两组术后KIM-1水平均呈现稳定上升趋势，但高功率组在24小时时的数值显著更高（278.8±239.6 pg/mL vs.170.3±173 pg/mL，p=0.003）。同样，高功率组在24小时时的KIM-1/肌酐比值也更高（5.5±4.5 vs.3.1±2.0，p=0.035）。这些发现表明，尽管肾功能参数稳定，但更高的激光功率与更大的肾应激和潜在损伤相关。这提示亚临床肾应激在高功率激光碎石术中可能更为显著（表2）（图1）。

术前，两组的肾内温度相当（p=0.867）。碎石术结束时，高功率组的温度（28.7±2.4°C）比低功率组（28.2±2.4°C）略高，但差异无统计学意义（p=0.135）。平均温度差也相似（2.56±1.4°C vs.2.49±1.5°C，p=0.860）（附表4）（图2）。

讨论

本研究通过生化标志物检测，系统评估了逆行肾内手术（RIRS）中不同激光功率设置对肾组织的影响。两组患者的人口学特征、临床表现及影像学参数均无显著差异，表明研究结果具有普适性。

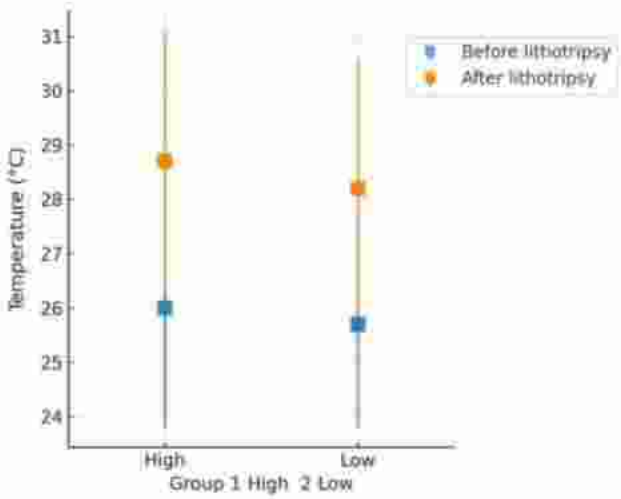


图2高功率组的肾内温度略高与KIM-1趋势一致的组

研究数据来源于同质化患者群体。然而在术后阶段，高功率激光治疗组的肾损伤标志物KIM-1及尿液中KIM-1与肌酐比值出现显著升高，这表明高功率激光可能因热机械应力导致肾实质微损伤。各组在手术时间、支架置入率、并发症及残留结石方面未见显著差异，进一步证实这些生物标志物变化与激光功率直接相关。此外，肾小球滤过率（eGFR）、血清肌酐和血红蛋白水平未见明显变化，说明整体肾功能保持稳定，KIM-1水平升高反映了激光对组织的高敏感性损伤效应。这些发现凸显了高功率激光可能引发肾组织损伤的潜在风险，强调了临床实践中优化激光参数的重要性。

多项研究表明，使用高功率钬激光器可显著提升手术效率。Rojo等人[18]研究显示，在儿童患者群体中，高功率激光治疗相较于低功率激光，能缩短手术时间并提高无结石率。Peretti等学者[19]研究发现，采用低能量但高频的激光设置，不仅显著缩短了手术时间，其结石清除率也与标准设置相当。Pietropaolo等[11]研究还指出，在治疗下极结石时，与低功率激光相比，高功率激光能显著提高无结石率并缩短手术时间。此外，Mekayten等人[20]研究证实，无论结石密度如何，高功率激光都能显著缩短碎石时间。综合来看，这些研究结果表明，高功率激光参数能有效提升碎石效率，从而缩短手术时间并提高结石清除成功率。与以往研究不同，我们的数据显示高功率组与低功率组在结石清除率和手术时间上均无显著差异。

谢斯塔等人[21]以及Erol等人[12]研究显示高功率激光组与低功率激光组的手术成功率及并发症发生率具有可比性。尽管Erol等学者发现高功率激光组的手术时间、住院时长及透视检查时间较短，但本研究证实两组成功率相当，且未发现住院时间或透视检查时间存在显著差异。

根据我们的研究结果，低功率激光治疗可能特别适合肾功能易受损伤的患者，例如单侧肾脏患者、早期肾功能不全或高龄人群。相反，高功率激光治疗可能更适合肾功能正常患者，特别是在需要最大化治疗效果时。

手术效率和缩短手术时间是关键考量因素。建议根据肾功能储备和手术目标进行个体化激光参数选择，以优化安全性和有效性。

尽管KIM-1作为检测早期亚临床肾损伤的敏感指标具有重要价值，但由于成本高昂、供应有限且尚未纳入标准诊疗流程等因素，其临床常规应用目前仍受限。现阶段该指标更适合用于科研研究或特定高危人群——例如肾功能不全患者、单侧肾脏患者或需反复接受泌尿系统手术的患者——这些情况下更密切的肾脏监测可能对临床决策产生重要影响。

本研究存在若干局限性，包括单中心设计、样本量较小（n=60）以及随访周期较短，这些因素可能限制研究结果的普适性和长期解读价值。排除肾结石直径小于1.5厘米的患者，限制了研究适用人群的广泛性。此外，仅依赖KIM-1指标可能不足以全面评估肾损伤，这凸显了构建更全面的生物标志物组合及组织病理学评估的必要性。研究采用的肾内温度测量方法为间接法，可能无法真实反映实时热力学动态。最后，部分参数未呈现显著差异，可能与统计效力不足有关。尽管存在这些局限，本研究仍为激光功率、无结石率及RIRS术后肾损伤生物标志物提供了重要参考。未来需通过多中心随机对照试验进一步验证研究结果。

结论

我们的研究表明，虽然高功率激光碎石术在手术时间和无结石率方面与低功率激光相当，但术后早期阶段的肾损伤生物标志物（如KIM-1和KIM-1/肌酐比值）水平显著升高。这些发现表明高功率组存在更高程度的亚临床肾功能压力。尽管血清肌酐和估算肾小球滤过率（eGFR）水平稳定，但生物标志物水平的升高凸显了高功率激光可能对组织产生的影响。未来需要开展更多多中心随机对照试验来验证这些结果，并指导RIRS治疗中安全的激光参数选择。

附录

见表3、4、5。

表3人口统计学和基线临床特征

参数	总计（n=60）	高功率 (n=30)	低功耗 (n=30)	概率值
年龄（平均值±SD）	52.3±12.4	51.5±13.3	53.1±11.6	0.636
性别—男性	36 (60.0%)	19 (63.3%)	17 (56.7%)	0.598
性别—女性	24 (40.0%)	11 (36.7%)	13 (43.3%)	
合并症—糖尿病	30 (42.0%)	12 (40%)	18 (60.0%)	0.121
合并症—HT	9 (12.4%)	5 (16.7%)	4 (13.3%)	0.718
合并症—CAD	17 (23.6%)	7 (23.3%)	10 (33.3%)	0.390
合并症—COPD	2 (2.7%)	1 (3.3%)	1 (3.3%)	1.000
合并症—高脂血症	2 (2.7%)	1 (3.3%)	1 (3.3%)	1.000
不透明-显影	50 (83.3%)	26 (86.7%)	24 (80.0%)	0.488
混浊-透光	10 (16.7%)	4 (13.3%)	6 (20.0%)	
石料尺寸（mm）	15.6±4.3	16.5±4.5	14.7±4.0	0.057
结石密度（HU）	940±284	918±266	961±303	0.571
肾积水-是	24 (41.4%)	15 (50%)	9 (32.1%)	0.168
肾积水-无	34 (58.6%)	15 (50%)	19 (67.9%)	
石侧—右	23 (38.3%)	8 (26.7%)	15 (50.0%)	0.063
石侧—左	37 (61.7%)	22 (73.3%)	15 (50.0%)	
术前DJ支架—是	26 (43.3%)	11 (36.7%)	15 (50%)	0.417
术前DJ支架—否	34 (56.7%)	19 (63.3%)	15 (50%)	

表4研究组的肾内热效应

参数	高权力 (n=30)	低权力 (n=30)	概率值
碎石术前肾内温度（℃）	26.0±2.2	25.7±1.9	0.867
碎石术后肾内温度（℃）	28.7±2.4	28.2±2.4	0.135
温差（℃）	2.56±1.4	2.49±1.5	0.860

表5术前和术后生化参数c

参数	低功率预操作	术后低功率	P值	高功率预操作	术后高功率	P值
eGFR	73.0±20.7	75.5±21.1	0.295	73.3±19.2	76.5±16.5	0.188
血清肌酐	1.11±0.4	1.06±0.4	0.152	1.08±0.3	1.02±0.2	0.071
血红蛋白	13.5±2.2	13.2±2.2	0.136	13.3±1.8	17.3±23.7	0.797

作者贡献HA：项目开发、论文撰写、数据管理、实验室分析、样本采集与保存。FG：数据分析、论文编辑、图表编辑。MGS：数据分析、论文编辑、表格编辑。CT：实验室分析、样本采集与保存。SG：论文编辑。MB：项目开发、论文编辑、手术应用。

资金作者未从任何机构获得资助。作者声明对文中提及的产品不享有任何所有权。参与本研究的作者均未获得任何经济资助。

数据可用性：本研究期间未生成或分析任何数据集。

声明

竞争利益作者声明无竞争利益。

伦理审批作者声明本研究遵循世界医学协会《赫尔辛基宣言》“涉及人类受试者的医学研究伦理原则”。本研究已通过内杰梅廷-埃尔巴坎大学医学院临床伦理委员会审核（编号：2023/4402）。参与同意所有受试者均签署知情同意书，明确表示自愿参与研究、发表同意所有受试者均授权允许论文公开发表。

参考文献

1. Desai M，Sun Y，Buchholz N，Fuller A，Matsuda T，Matlaga B等（2017）尿路结石的治疗选择：经皮肾镜碎石术、输尿管镜检查、冲击波碎石术和主动监测。World J Urol 35(9)：1395-1399。https://doi.org/10.1007/s00345-017-2030-8
2. Kazmierczak J，Bartosinski R，Szustak J，Wijata A，Stepien Z，Dutkiewicz J等（2025）尿石症：病因、诊断和治疗质量的综合评价.运动医学39：58490。https://doi.org/10.12775/QS.2025.39.58490
3. 曾G，赵Z，马宗G，皮尔尔M，钟S，斯科拉里蒂斯A等（2022）欧洲泌尿外科学会结石病学分会与国际结石病学联盟关于肾结石治疗逆行性肾内手术的联合共识。Eur Urol Focus 8(5)：1461–1468。https://doi.org/10.1016/j.euf.2021.10.011
4. 井上T，川田S，宫本S，藤泽M（2021）逆行肾内手术：历史、现状与未来。Invest Clinic Urol 62(2)：121–135。https://doi.org/10.4111/icu.20200526
5. 伯尔J，石井H，西蒙兹N，索马尼BK（2015）：与冲击波碎石术相比，灵活输尿管肾镜术和激光碎石术是否是治疗肾下极结石的新金标准？——来自某大学医院同期比较研究结果。《中欧泌尿学杂志》68(2)：183–186。https://doi.org/10.5173/ceju.2015.509
6. Barone B，Crocetto F，Vitale R，Di Domenico D，Caputo V，Romano P等学者（2020）发表的《逆行肾内手术与经皮肾镜碎石术治疗2纸米以上肾结石的系统评价与荟萃分析》一文，刊载于《Minerva urologica e nefrologica》（意大利泌尿与肾脏病学杂志）第72卷第4期，页码441-50。该文献于2020年2月23日通过https://doi.org/10.23736/s0393-2249.20.03721-2平台发布，PubMed PMID编号为32083423。
7. 图尔克C，佩特里克A，萨里察K，塞泰C，斯科拉里科斯A，施特贾布M等（2016）《关于尿路结石诊断和保守治疗的指南》，《欧洲泌尿学》69(3)：468–474。https://doi.org/10.1016/j.eururo.2015.07.040
8. Sandhu AS，Srivastava A，Madhusoodanan P，Sinha T，Gupta SK，Kumar A等（2007）钬：用于体内碎石术的YAG激光。印度武装部队医学杂志63(1)：48-51。https://doi.org/10.1016/s0377-1237（07）80109-2
9. De Coninck V，Hente R，Claessens M，Duchateau A，Doizi S，Keller EX（2021）高功率、高频Ho：YAG激光器不是逆行肾内手术的必需品。Eur Urol Focus 7(1)：5–6.https://doi.org/10.1016/j.euf.2020.12.007
10. Traxer O，Keller EX（2020）铒光纤激光：治疗肾结石的新选择？与钬：YAG激光的比较。世界泌尿外科杂志38(8)：1883–1894。https://doi.org/10.1007/s00345-019-02654-5
11. PietropaoloA，ManiM，Hughes T，SomaniBK.低功率与高功率激光治疗下极结石的疗效对比：某大学附属医院前瞻性非随机研究结果.《泌尿外科治疗进展》.2022；.Epub 2022/06/03.https://doi.org/10.1177/17562872221097345.PubMed PMID：35651485；PubMed Central PMCID：PMCPMC9149605.
12. Erol E，Ecer G，Kiremit MC，Gokce MI，Balasar M，Sarikaya AF等（2024）倾向评分分析法对高功率和低功率激光治疗RIRS成功率的多中心评价。《尿石症》52(1)：32。https://doi.org/10.1007/s00240-024-01535-w
13. Kashani K，Cheungpasitporn W，Ronco C（2017）急性肾损伤的生物标志物：从发现到临床应用的途径。Clin Chem Lab Med 55(8)：1074–1089。https://doi.org/10.1515/cclm-2016-0973
14. Schrezenmeier EV，Barasch J，Budde K，Westhoff T，SchmidtOtt KM.急性肾损伤中的生物标志物——病理生理学基础和临床表现。Acta physiologica（牛津，英国）。2017；219(3)：554–72。Epub 2016/07/31。https://doi.org/10.1111/apha.12764.PubMed PMID：27474473；PubMed Central PMCID：PMCPMC5575831。
15. Dieterle F，Sistare F，Goodsaid F，Papaluca M，Ozer JS，Webb CP et al（2010）肾脏生物标记物资格提交：FDA-EMEA和预测安全性测试联盟之间的对话。Nat Biotechnol 28(5)：455–462。https://doi.org/10.1038/nbt.1625
16. Ecer G，Sonmez MG，AydinA，Topcu C，Alalam HNI，Guven S等（2022）肾损伤分子-1（KIM-1）水平对比逆行肾内碎石术与输尿管套管术：一项前瞻性随机研究。《泌尿外科疾病》50(5)：625–633。https://doi.org/10.1007/s00240-022-01345-y
17. IBM SPSS Windows统计软件，版本27.0。纽约州阿蒙克：IBM公司，2020年发布；（）：Epub doi：；PubMed PMID：；PubMed Central PMCID：PMC
18. 加西亚-罗霍卡、特拉克莱尔O、瓦利霍-阿尔萨克斯-DM、卡斯特拉尼D、费雷蒂S、加蒂C等学者，低功率与高功率技术对比研究

钬激光在小儿逆行性肾内手术中的疗效。《内镜泌尿外科杂志》。2023；37(5)：509–15。电子版发布于2023年3月3日。https://doi.org/10.1089/end.2022.0778。PubMed PMID：36860192。

19. Peretti D，Dalmasso E，Pecoraro A，Ambruosi C，Venzano F，Fiori C et al（2022）低能量高频Ho-YAG碎石术：RIRS会继续发展吗？病例对照研究。Urolithiasis 50(1)：79–85。https://doi.org/10.1007/s00240-021-01282-2

20. Mekayten M，LorberA，Katafigiotis I，Sfoungaristos S，Leotsakos I，Heifetz EM等（2019）结石密度会不再是输尿管内镜手术的关键因素吗？使用Lumenis Laser p120w和标准20 W激光器的结石密度对激光时间的影响：一项比较研究。J Endourol 33(7)：585-589。https://doi.org/10.1089/end.2019.0181

21. 施雷斯塔A、科拉莱斯M、阿迪卡里B、查帕甘A、特拉克瑟O (2022) 低功率与高功率钬YAG的比较输尿管镜检查中的激光参数设置。《世界泌尿外科杂志》40(7)：1839–1844. https://doi.org/10.1007/s00345-022-04040-0

出版商声明：Springer Nature对已发表地图和机构隶属关系中的司法管辖权主张保持中立。

Springer Nature或其授权方（例如学会或其他合作伙伴）根据与作者或其他权利持有人签订的出版协议，对本文拥有独家权利：作者对本文已接受的稿件版本进行自我存档，完全受该出版协议条款和适用法律的约束。

Check for updates

JOURNAL OF ENDOUROLOGY
Volume 39, Number 8, August 2025
© Mary Ann Liebert, Inc.
Pp. 794–803
DOI: 10.1089/end.2025.0036

High-Power Lasers Induce Dose-Dependent Acute Kidney Injury

Mantu Gupta,[1] Kavita Gupta,[1] Roman Shimonov,[1] Raymond Khargi,[1] Anna Ricapito,[1] Blair Gallante,[1] Christopher Connors,[1] Dara Lundon,[1] Manishkumar Patel,[2] Seunghee Kim-Schulze,[2] William Atallah,[1] Natasha Kyprianou,[1,3] and Alan J. Yaghoubian[1]

Abstract

Introduction and Objective: High-powered lasers have been hypothesized to cause kidney injury; however, no human studies have confirmed or quantified this damage. Our objective was to identify and quantify damage and explore factors affecting degree of injury in patients undergoing retrograde intrarenal surgery (RIRS) with thulium fiber laser (TFL) and Holmium:YAG (Ho:YAG) lasers.

Methods: Patients undergoing RIRS for unilateral nonobstructing renal stones were randomized to receive lithotripsy with either a 60 W SuperPulse TFL or 120 W pulse-modulated Ho:YAG laser. A control group of patients undergoing RIRS without laser use were used for comparison. Urine samples were collected at 3 time points as follows: preoperative, 1 hour postoperative, and 10 days postoperative. Samples were analyzed using ELISA for key biomarkers—kidney injury molecule-1, neutrophil gelatinase-associated lipocalin (NGAL), and β2-microglobulin—normalized to urine creatinine. Primary outcome was the extent of renal injury based on biomarker elevation.

Results: Ninety-one patients with similar baseline patient and stone characteristics were randomized (46 TFL, 45 Ho:YAG). Both lasers led to significant biomarker elevation, which trended toward but did not reach baseline by postoperative day 10. The Ho:YAG laser resulted in a sustained increase in NGAL at 10 days. Multivariate analysis demonstrated that injury is dose dependent on total laser energy used ($p < 0.001$, $p = 0.006$) and worse in older patients ($p = 0.009$) and in those with metabolic syndrome ($p = 0.002$), with slower recovery in both these groups, but not with the type of laser used. Multiple levels of the nephron are involved.

Conclusions: There is notable kidney injury induced by both SuperPulse TFL and pulse-modulated Ho:YAG lasers in a dose-dependent manner, but the 2 lasers do not differ in the degree of injury. Injury occurs at multiple levels. Age and metabolic syndrome affect the amount of injury and recovery from injury. Further studies evaluating factors that can mitigate damage from high-energy lasers are needed.

Keywords: urinary biomarkers, kidney injury, thulium fiber laser, pulse-modulated Ho:YAG

Introduction

Lifetime incidence of kidney stones in the United States approaches 10%.[1] Ideally, treatment would be efficient, efficacious, and minimize renal damage. Shockwave lithotripsy (SWL) procedures, considered less invasive, have decreased as better endoscopes and high-powered lasers (HPLs) have made retrograde intrarenal surgery (RIRS) more efficient. Holmium:YAG (Ho:YAG) lasers have been enhanced with pulse modulation and high-frequency capabilities. The recently introduced SuperPulse thulium fiber laser (TFL) is capable of frequencies as high as 2400 Hz.[2] HPLs increase

[1]Department of Urology, Icahn School of Medicine at Mount Sinai, New York, New York, USA.
[2]Human Immune Monitoring Center, Icahn School of Medicine at Mount Sinai, New York, New York, USA.
[3]Department of Oncological Sciences, Tisch Cancer Institute, Icahn School of Medicine at Mount Sinai, New York, New York, USA.
Portions of the abstract were previously published in The Journal of Urology, Volume 211, Issue 5S, May 2024, Page: e983.

the efficiency of stone ablation, but *in vitro* and human studies show that they increase surrounding fluid temperature, and *in vitro* studies show histologic evidence of kidney injury. No human studies have measured or compared degree of kidney injury from HPLs.[3–6] Urine biomarkers noninvasively quantify renal injury *in vivo*.[7,8] We used urinary biomarkers to quantify renal injury caused by HPLs during RIRS.

Methods

Study design

We conducted an IRB-approved single center, randomized control trial (IRB 21-00084) on patients over 18 years old with renal stones 6 mm to 20 mm undergoing laser RIRS. Eligible patients were consented in the preoperative area by a member of the surgical team. Exclusion criteria included ureteral stones, hydronephrosis, chronic kidney disease (CKD) (eGFR <60), solitary kidney, prestented patients, prior ureteroscopy within 9 weeks, urinary retention, neurogenic bladder, or urinary tract infection within 2 weeks. Intraoperative exclusion criteria included findings of bladder stone(s), urothelial tumor(s), new onset obstruction absent on preoperative imaging, or failure to reach the stone. There were no deviations from the protocol. The study was registered with clinicaltrials.gov (NCT05350423).

Randomization and procedure

The purpose was to evaluate noninferiority of two laser modalities with regard to occult kidney damage defined as producing a change in eGFR of 1 mg/mL based on two prior studies by Fahmy and colleagues and van Timmeren and associates.[9,10] Fahmy prospectively compared urinary kidney injury molecule-1 (KIM-1) levels after SWL and laser RIRS. SWL in 50 patients resulted in KIM-1 increasing from 5.78 to 10.14 ng/mL after 2 hours ($p < 0.001$), but RIRS in 10 patients effected no change (5.78 to 5.49 ng/mL). van Timmeren and coworkers evaluated 11 healthy controls and 53 patients with varying kidney diseases and found a −27.5 correlation ($p = 0.016$) between KIM-1 and eGFR. That is, a 1 ng/mL rise in KIM-1 correlated to a 27.5 mL/min decline in eGFR. To power our study using an eGFR change of 10 mg/mL with an allocation ratio of 1:1, 99% power, noninferiority limit of 20%, and alpha of 5% using the noninferiority power calculation, we required 49 patients in each study arm. Factoring a 10% dropout rate, we sought to enroll 108 patients. Patients were randomized to Ho:YAG (Lumenis P120 with Moses 2.0) or SuperPulse TFL (Olympus Soltive Premium). Block randomization was performed via sealedenvelope.com with the scheme stored on a password-protected computer. Patients and surgeons were blinded to group allocation by not revealing the treatment until a stone was visualized.

The first sample (preoperative [V1]) was collected after induction of anesthesia and prior to surgical intervention using a Foley catheter. Procedures were conducted by experienced endourologists (M.G. and W.A.) with standardized methodology, including use of a Storz Flex-X2 7.5F flexible ureteroscope, no ureteral access sheaths (UASs), and use of only gravity irrigation at 80 cm H_2O (~ 60 mm Hg) with no pressurized, mechanical, or hand irrigation systems. Upon entering the renal pelvis, full pyeloscopy ensured that the stone burden was consistent with preoperative imaging. Treatment allocation was revealed by a research assistant, and the allocated laser was brought into the room. Patients consenting for the study who had ureteroscopy, but did not require laser treatment (stones basket extracted or stone in question submucosal/parenchymal and not amenable to treatment), served as the control group to assure that laser energy itself, not ureteroscopy, was responsible for biomarker elevation.

In standard practice, although not using a UAS or using pressurized irrigation, we do frequently pause and aspirate renal pelvic fluid during treatment to prevent generating high temperatures with high-power settings and to improve observation. Starting settings were 0.5 J and 5 Hz for Ho:YAG and 1 J and 2 Hz for TFL and increased to 0.5 J and 50 Hz (25 watts) in every patient to achieve high-powered dusting with the goal to generate particles smaller than the laser fiber (200 μm). Power is increased to 25 watts only for brief intervals, not exceeding 5 seconds. For duty cycle management, laser activation is limited to 10-second bursts, followed by a mandatory 20-second pause to reduce cumulative heat deposition. In addition, frequent aspiration of the collecting system fluid is performed between laser activations to further mitigate thermal buildup.

Laser settings, total laser energy, laser on/off time, lasing time, and operative time were documented. Visible laser-induced tissue damage was documented and graded as follows:

- Level 0: No visible damage to mucosa; minor erythema because of scope-related trauma.
- Level 1: Blanching or fluffing of mucosa after contact with laser; no evidence of mucosal disruption (bleeding should not be present).
- Level 2: Penetration to submucosal tissues; obvious defect in mucosal layer after contact with laser, +/- bleeding, no extravasation of contrast.
- Level 3: Full-thickness perforation of renal pelvis (contrast extravasation) or observation of renal parenchyma or fat.

All procedures (including control patients) concluded with placement of a 6F silicone stent (Black Silicone Filiform Double Pigtail Ureteral Stent, Cook Medical, Indiana, USA) and a 16F Foley catheter as per study protocol.

The second urine sample (1 hour postoperative [V2]) was obtained 1 hour postoperatively in the recovery room via the aspiration side port of the indwelling Foley catheter at catheter removal, and the third sample (10 days postoperative [V3]) 10 days postoperatively via a voided urine sample just prior to stent removal.

Urinary biomarker analysis

Urine samples were analyzed for spot urine creatinine and by ELISA for 3 biomarkers as follows: KIM-1, neutrophil gelatinase-associated lipocalin (NGAL), and β2-microglobulin (β2M)—all normalized to the simultaneously collected urine creatinine levels. Levels of KIM-1, NGAL, and β2M were determined by the commercially available MILLIPLEX® Kidney Injury Magnetic Bead Luminex Assay Panels (EMD Millipore/Millipore Sigma, Billerica, Massachusetts). Urine samples were centrifuged at 13,500 RPM for 10 minutes at

4°C to clear precipitates prior to assay. Samples were diluted 1:2 for KIM-1, 1:100 for NGAL, and 1:500 for β2M with assay buffer and measured in duplicate on 96-well plates. Incubation was done overnight (16–18 hours) with primary capture antibody at 4°C followed by detection antibody at room temperature for 1 hour and then for 30 minutes with streptavidin–phycoerythrin. Plates were read on the Luminex Flexmap 3D System. Data were analyzed using MILLIPLEX Analyst 5.1 software (EMD Millipore/Millipore Sigma, Billerica, Massachusetts).

Outcomes

Primary outcome was extent of renal injury measured by changes in urinary biomarkers from baseline. Secondary outcomes were total laser energy used, lasing time, lithotripsy time, laser ablation efficiency, laser energy consumption, laser ablation speed, laser activity (operator duty cycle), postoperative complications, readmissions, and emergency room visits for 3 months after operation.

Statistics

Baseline characteristics and stone information are shown in Table 1 and operative data in Table 2. Statistical significance was assessed using Mann–Whitney *U* tests for continuous variables and either Chi-squared or Fisher's Exact tests for categorical variables. Trends in KIM-1, NGAL, and β2M levels from V1 to V3 were calculated for Ho:YAG, TFL, and control groups (Fig. 2). Paired sample *t*-tests assessed whether changes in biomarker concentration from V1 to V2, V2 to V3, and V1 to V3 were significant for each group, including controls (Fig. 3). Multivariate linear regression analysis was performed to evaluate laser type as a predictor of percent change of biomarkers from V1 to V2, V2 to V3, and V1 to V3 (Table 3). *Variables in the multivariate model were selected a priori or if they demonstrated a p-value less than 0.1 on univariate analysis.* Collectively, these included operative group, age, presence of metabolic syndrome, preoperative eGFR, operative time, and total laser energy. All statistical analyses were performed using SPSS Statistics Version 28 (IBM Corp., Armonk, N.Y., USA) with a two-tailed alpha of 0.05 indicating significance.

Results

Between October 2021 and July 2023, 108 patients meeting inclusion criteria were enrolled (Fig. 1). Patients were randomized to the HPL groups equally, 54 in each arm. Ultimately, there were 46 TFL patients, 45 Ho:YAG, and 5 controls.

Demographics and baseline characteristics were comparable (Table 1). Total energy used was similar between HPL groups (1.7 kJ interquartile range [IQR]:1.0–4.8 *vs* 1.98 kJ IQR:1.31–4.43, p = 0.727). Calculated laser efficiency metrics (laser ablation efficiency, energy consumption, operator duty cycle/activity, and ablation speed) did not differ. Evidence of visible kidney damage did not differ ($p = 0.164$). Grade 3 injury did not occur. Grade 2 injury (penetration into submucosa) was higher for Ho:YAG than TFL (21.7% *vs* 8.9%). Stone composition was most commonly calcium oxalate (77.8% *vs* 78.3%, $p = 0.299$). Complications were similar (6.7% *vs* 10.9%, $p = 0.677$).

Both lasers caused drastic and statistically significant increases in biomarkers (median values in ng/mL TFL: 0.011 to 00.025 KIM-1, 0.526 to 2.518 NGAL, 2.126 to 25.623 β2M; HoYAG: 0.012 to 0.024 KIM-1, 0.572 to 2.448 NGAL, 2.775 to 17.147 β2M), which trended toward, but did not always reach, baseline at day 10 (Figs. 2 and 3).

TABLE 1. DEMOGRAPHICS AND PREOPERATIVE INFORMATION

	Holmium group (n = 45)	*Thulium group (n = 46)*
Age [IQR]	56.0 [39.0–67.5]	59.0 [46.5–63.5]
BMI [IQR]	27.4 [23.8–30.4]	25.8 [23.8–29.4]
Gender, *n* (%)		
Male	18 (40.0)	23 (50.0)
Female	27 (60.0)	23 (50.0)
ASA Score, *n* (%)		
1	4 (8.9)	1 (2.2)
2	33 (73.3)	35 (76.1)
3	8 (17.8)	9 (19.6)
4	0 (0.0)	1 (2.2)
Diabetes, *n* (%)	7 (15.6)	10 (21.7)
Diuretics, *n* (%)	3 (6.7)	5 (10.9)
ACE Inhibitors, *n* (%)	6 (13.6)	6 (13.0)
Anticoagulants, *n* (%)	2 (4.4)	1 (2.2)
Previous Stone Surgery, *n* (%)	17 (37.8)	24 (52.2)
Laterality, *n* (%)		
Left	24 (53.3)	25 (54.3)
Right	21 (46.7)	21 (45.7)
Total Stone Burden, mm [IQR]	12.0 [9.0–19.0]	13.0 [9.0–19.0]
Stone Volume, mm3 [IQR]	214.0 [82.8–310.6]	176.9 [91.9–292.3]
HU [IQR]	837.5 [473.5–1144.0]	992 [824.8–1194.0]
Preoperative Creatinine [IQR]	0.80 [0.67–0.99]	0.80 [0.71–0.98]
Preoperative eGFR [IQR]	92.0 [76.5–106.0]	92.5 [84.8–103.0]

IQR = interquartile range.

TABLE 2. OPERATIVE INFORMATION AND OUTCOMES FOR HOLMIUM VERSUS THULIUM STUDY GROUPS

	Holmium group (n = *45*)	*Thulium group* (n = *46*)	p-*value*
Operative Time, mins [IQR]	56.0 [42.0–68.0]	52.5 [42.8–72.3]	0.846
Total Laser Energy, kJ [IQR]	1.7 [1.0–4.8]	1.98 [1.3–4.4]	0.727
Total Laser Time, sec [IQR]	432.5 [197.0–910.5]	469.0 [282.0–1077.0]	0.495
Total Lithotripsy Time, sec [IQR]	2160.0 [1320.0–2880.0]	1950.0 [1365.0–3135.0]	0.846
Laser Efficiency [IQR]			
Laser Energy Consumption(J/mm3)	13.4 [4.9–25.4]	12.9 [6.8–35.5]	0.435
Laser Activity (Operator Duty Cycle) (%)	25.2 [10.6–44.0]	33.8 [17.7–49.2]	0.212
Laser Ablation Speed (mm3/s)	0.38 [0.21–1.21]	0.27 [0.17–0.55]	0.264
Visible Damage			0.164
No visible damage	10 (21.7)	8 (17.8)	
Mucosa only-blanching	26 (56.5)	33 (73.3)	
Penetration into submucosa	10 (21.7)	4 (8.9)	
Stone Composition, *n* (%)			0.299
>50% CaOx	35 (77.8)	36 (78.3)	
>50% UA	3 (6.7)	0 (0.0)	
>50% HA	3 (6.7)	6 (13.0)	
Other / Unknown	4 (8.9)	4 (8.7)	
Clavien–Dindo Complications, *n* (%)			0.677
None	42 (93.3)	41 (89.1)	
I	1 (2.2)	4 (8.7)	
II	1 (2.2)	1 (2.2)	
III	0 (0.0)	0 (0.0)	

Continuous variables reported as medians. *p*-Values derived from Chi-squared tests, Fisher's exact tests, or Mann–Whitney *U* tests, with significance set to $p < 0.05$.
IQR = interquartile range.

In clear contradistinction, controls had relatively little increase and normalization by day 10. Persistent elevation of biomarkers was both laser and biomarker dependent. Baseline levels of all 3 biomarkers were low and equal between groups (Fig. 2). Elevation of NGAL and KIM-1 was marked, but virtually identical regardless of laser type. Elevation of β2M was also marked; although greater for TFL than holmium, this did not reach statistical significance. By day 10, decreasing values indicated tissue recovery, but in most cases were still statistically significantly higher than baseline (Fig. 3). The decrease in KIM-1 from V2 to V3 was significant for TFL but not holmium. The values of NGAL, in particular, did not substantially decrease by day 10 especially for Ho:YAG patients.

Multivariate analysis to define factors affecting kidney injury focused on clinical conditions, as well as treatment parameters (Table 3). Age and metabolic syndrome influenced kidney injury. Older patients had a greater elevation in KIM-1 ($p = 0.005$), slower recovery in NGAL ($p = 0.031$), and were more likely to have persistent elevation in NGAL from baseline ($p = 0.009$). Age did not independently influence levels of β2M. Patients with metabolic syndrome had a significantly slower recovery in β2M from V2 to V3 and were more likely to have persistent elevation in β2M ($p = 0.008$, $p = 0.002$). Metabolic syndrome did not similarly influence NGAL or KIM-1 levels. The more total laser energy used, the slower the recovery of elevated KIM-1 and β2M levels from V2 to V3 and the more likely there would be persistent elevation at V3 ($p = 0.006$, $p = 0.019$, $p < 0.001$, $p = 0.001$). This effect was not seen with NGAL, but laser-treated patients in general had slower recovery in NGAL and persistent elevation in NGAL, regardless of total energy used. Operating room time did not independently correlate with biomarker elevation. In addition, type of laser used was not independently associated with biomarker level changes.

Discussion

HPLs have been engineered to make RIRS more efficient and improve stone-free rates. The Ho:YAG laser, introduced in 1993, has evolved with pulse modulation and high-frequency capabilities, enhancing energy delivery and reducing operative times via improved dusting capability.[11–13] SuperPulse TFL has come into common use with advantages of less retropulsion and better dusting capabilities than older Ho:YAG systems.[2] There is no consensus on which technology is superior or induces less damage. *In vitro* studies have raised concern that HPLs can cause temperature-induced renal injury. However, there is a paucity of clinical data evaluating injury. We quantified urinary biomarkers specific for kidney and urothelial injury before and after RIRS and correlated these markers to different intraoperative variables.

Kidney injury can be evaluated by serum creatinine and eGFR derived from serum creatinine, but these levels do not demonstrate a linear relationship with kidney injury. A patient with two normal kidneys can have one removed without affecting serum creatinine or eGFR. In a study of 120 patients undergoing RIRS, there was no significant decrease in eGFR; however, older age, longer ureteroscopy, thinner renal parenchyma, and ureteral stones were risk factors for renal function deterioration.[14] Another study found that only 4.9% of 163 patients had a significant decrease in GFR after RIRS.[15] Our data also showed no significant change in eGFR 10 days postoperatively. Serum creatinine is affected by factors unrelated to kidney function (e.g., diet, hydration status, and muscle mass). More importantly, serum

TABLE 3. MULTIVARIATE LINEAR REGRESSION ANALYSIS FOR CHANGES IN BIOMARKERS ACROSS COLLECTION TIMES

	V1 → V2 Delta (%)		*V2 → V3 Delta (%)*		*V1 → V3 Delta (%)*	
Factor	*Standardized β coefficient*	p-*value*	*Standardized β coefficient*	p-*value*	*Standardized β coefficient*	p-*value*
KIM-1						
Operative Group						
Control	Ref	—	Ref	—	Ref	—
Holmium	0.228	0.440	−0.205	0.564	0.086	0.810
Thulium	0.446	0.132	−0.294	0.406	0.061	0.865
Age, years	−0.362	**0.005***	0.152	0.280	−0.108	0.416
Metabolic Syndrome	−0.121	0.286	0.087	0.475	−0.059	0.608
eGFR	−0.023	0.856	0.145	0.296	0.115	0.371
Operative Time, mins	0.098	0.420	0.024	0.854	0.084	0.512
Total Laser Energy, kJ	−0.140	0.262	0.387	**0.006***	0.319	**0.019***
NGAL						
Operative Group						
Control	Ref	—	Ref	—	Ref	—
Holmium	0.055	0.916	−0.064	0.903	−0.059	0.909
Thulium	0.067	0.897	−0.134	0.798	−0.153	0.768
Age, years	−0.128	0.336	−0.298	**0.031***	−0.341	**0.009***
Metabolic Syndrome	−0.102	0.377	0.029	0.803	0.026	0.815
eGFR	−0.023	0.860	−0.020	0.880	−0.047	0.709
Operative Time, mins	0.198	0.120	−0.035	0.789	0.014	0.913
Total Laser Energy, kJ	0.137	0.289	0.060	0.645	0.050	0.695
Beta-2						
Operative Group						
Control	Ref	—	Ref	—	Ref	—
Holmium	0.128	0.728	−0.086	0.794	0.034	0.918
Thulium	0.325	0.379	0.010	0.975	0.110	0.736
Age, years	0.040	0.779	0.068	0.597	0.004	0.976
Metabolic Syndrome	−0.107	0.394	0.300	**0.008***	0.328	**0.002***
eGFR	−0.217	0.126	0.088	0.492	−0.083	0.473
Operative Time, mins	0.237	0.072	−0.228	0.054	−0.116	0.315
Total Laser Energy, kJ	−0.074	0.583	0.441	**<0.001***	0.400	**0.001***

Significance set to $p < 0.05$ (bolded and * for reference).
KIM-1 = kidney injury molecule-1; NGAL = neutrophil gelatinase-associated lipocalin; V1 = preoperative; V2 = 1 hour postoperative; V3 = 10 days postoperative.

creatinine and eGFR have poor sensitivity for detecting early or small insults to renal tubular cells and are better for long term and sustained kidney damage. Several urinary protein biomarkers are markers of renal cellular injury. Compared with eGFR, these markers detect renal insult earlier and have significantly higher sensitivity. However, their specificity can be limited; elevations may occur because of nonrenal factors such as systemic inflammation, dehydration, or other organ injuries, which do not necessarily indicate renal damage. Biomarkers can provide insight into the nature of the damage, as some studies suggest that specific patterns of elevation may correlate with reparable *vs* nonreparable damage. The kinetics of these biomarkers can differ; we chose two markers of acute kidney injury, NGAL and KIM-1, that peak rapidly after injury and return to baseline quickly, and one (β2M) that is a better measure of chronic injury. β2M has been validated as a measure of glomerular and proximal tubular damage.[16] We noted that β2M did not return to baseline after 10 days. In addition, β2M elevation was influenced by metabolic syndrome ($p = 0.008$), whereas NGAL and KIM-1 were not. The effect of metabolic syndrome on both the persistent elevation of β2M and slow recovery of elevated β2M is consistent with decreased renal reserve. Previous studies have supported that β2M is associated with metabolic disease, early diabetic nephropathy, and early CKD.[17] Patients with metabolic syndrome have a higher likelihood of having poor renal reserve. Even subtle kidney injury could be more difficult to recover from in this subset of patients.

Total laser energy correlated with both slower recovery and persistent elevation of KIM-1 and β2M levels at 10 days. This is direct evidence that laser energy not only causes renal injury but also is dose dependent, with more energy causing more damage and slower recovery. The effect on KIM-1 and β2M raises concern for tubular and glomerular injury. Our findings suggest that providers should be mindful of total energy used by HPLs during RIRS, especially in patients with preexisting kidney disease.

Although β2M reflects glomerular and proximal tubular damage, NGAL is produced in the distal nephron and is synthesized in response to kidney injury.[18] Albert and colleagues found that urinary and plasma NGAL indicate early tubular injury before declining filtration function.[19] Memmos and associates, comparing low-power Ho:YAG RIRS with mini-PCNL and standard PCNL, found that KIM-1 and NGAL levels rose continuously from 2 to 24 to 48 hours, but no difference between treatment arms.[17] Our study similarly

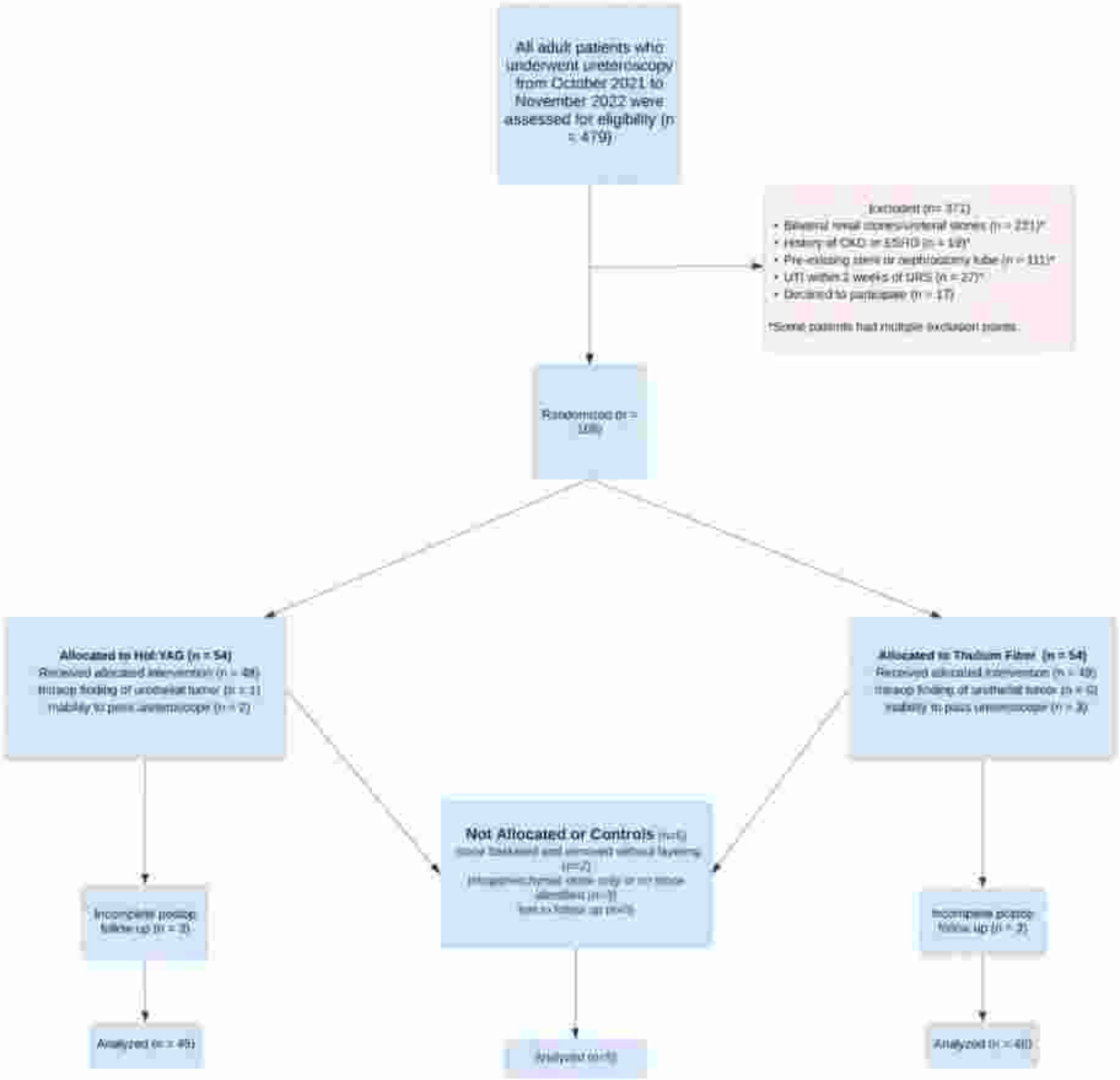


FIG. 1. Flow Diagram.

found that NGAL rises for both HPLs as early as 1 hour postoperatively. Levels stay elevated on day 10. Persistent elevation of NGAL is concerning, indicating that injury is profound and long-lasting. How long-lasting is yet to be determined, as we did not go beyond 10 days. The slow recovery of injury and persistent elevation of NGAL above baseline were independently influenced by age ($p = 0.031$ and $p = 0.009$, respectively), the implication being that older patients recover more slowly from kidney damage and NGAL can detect this. Our data suggest that providers should be particularly careful when treating older patients with HPLs.

Age was also the only parameter independently associated with degree of injury at 1 hour postoperatively, and the best marker for this was KIM-1. KIM-1, expressed during acute tubular necrosis and produced by the proximal convoluted tubule, is higher in ischemic ATN than chronic renal failure.[18] In addition, UASs have been found to reduce KIM-1 elevation after RIRS.[19] In our study, KIM-1 trended downward, but did not reach baseline by day 10. KIM-1, similar to B2M, was influenced by total laser energy ($p < 0.006$), with more laser energy used associated with a steeper rise from V1 to V2 and slower recovery from V2 to V3. These findings suggest that HPLs induce ATN, that degree of injury is higher in older patients, and that recovery is slower in patients who receive more laser energy in a dose-dependent manner.

The study by Memmos and colleagues did not check levels beyond 48 hours.[17] We did not check levels between 1 hour and 10 days postprocedure, but noted that by 10 days levels had decreased for most biomarkers. Combining our findings with theirs, it is likely that values peak a few days postoperation and by 10 days are already on the decline. These assumptions are in line with a prospective study evaluating KIM-1 after PCNL and RIRS, in which KIM-1 levels were found to decrease to baseline between 4 hours and 14 days postoperatively.[20] Further studies are needed to evaluate long-term values of biomarkers and to correlate biomarkers with other measures of kidney injury such as nuclear renal scans.

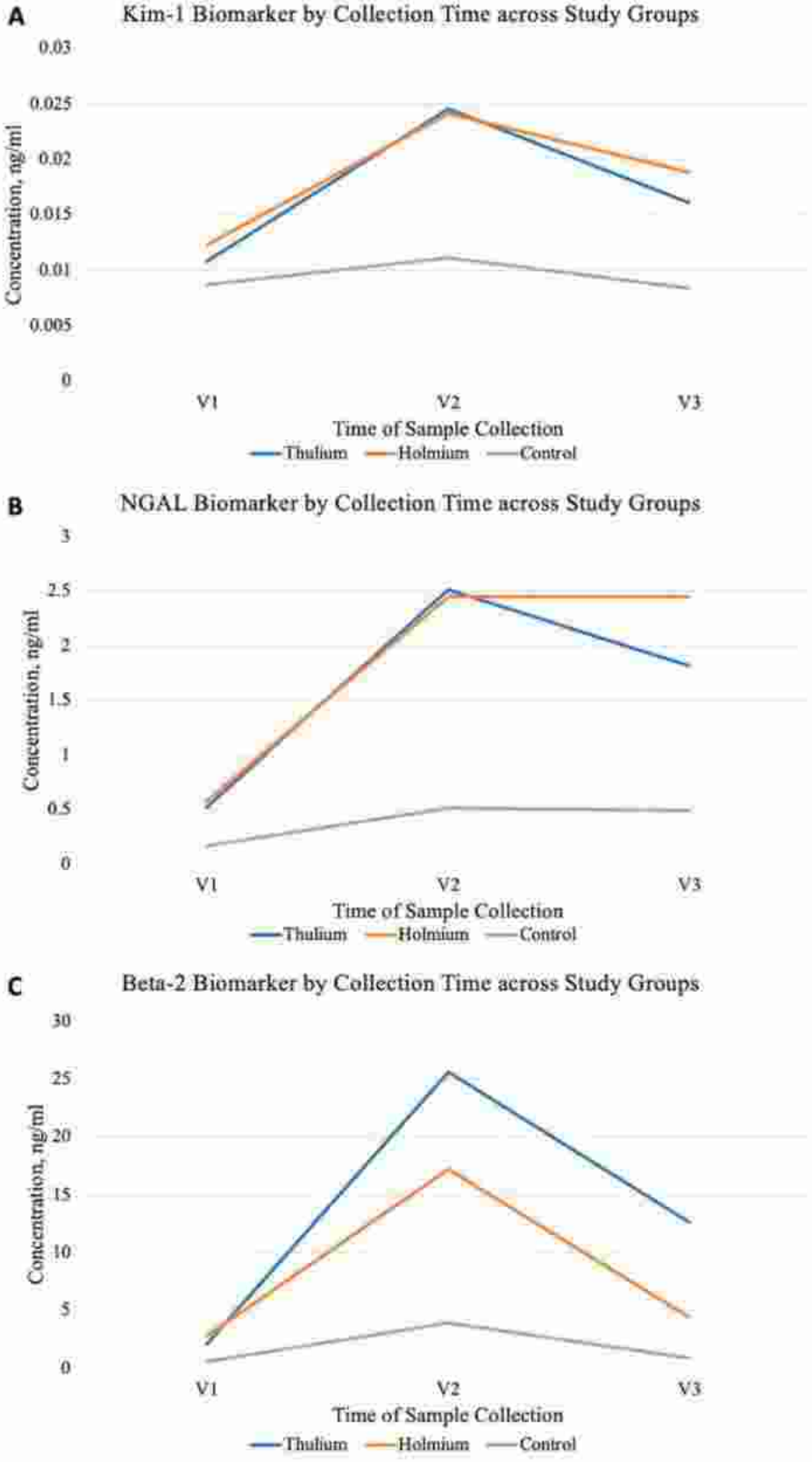


FIG. 2. Linear representation of Biomarker Collection by Time across all Study Groups.

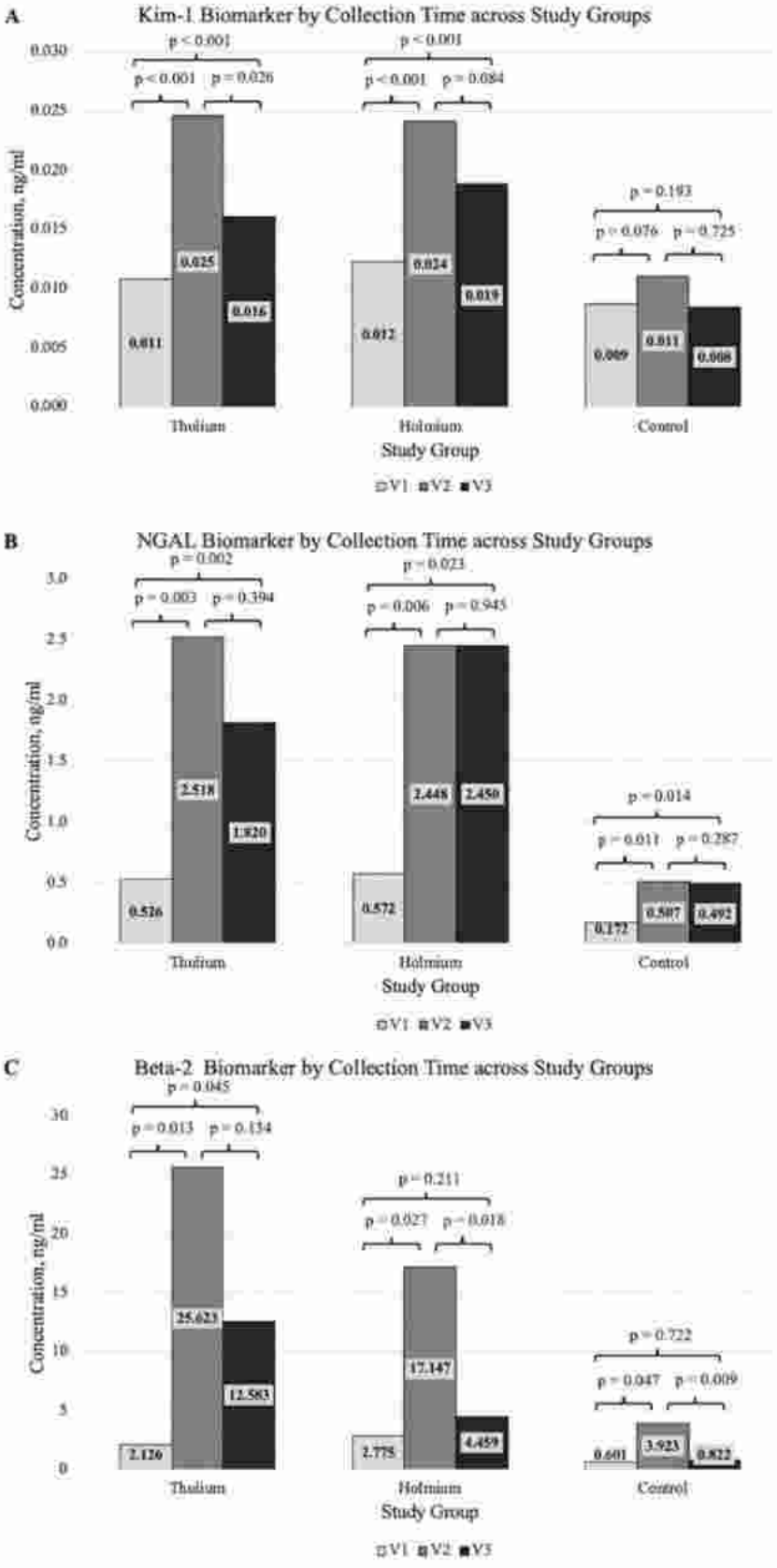


FIG. 3. Bar graph representation of Biomarker Collection by Time across all Study Groups.

Our findings indicate that renal cellular damage occurs, but not how. Laser energy produces thermal damage to surrounding tissues directly and by heating irrigation fluid, resulting in damage by coagulation, carbonization, and denaturation in a dose-dependent manner. *In vivo* porcine studies show that 40 W can increase temperatures to concerning levels if irrigation is low.[3] In our study, total laser energies of 3.14 kJ (TFL) and 3.36 kJ (Ho:YAG) resulted in evidence of cellular damage by biomarker elevation. The direct relationship between temperature increases secondary to HPLs and thermal injury is currently being studied at our institution.

This study had several limitations. We only analyzed urinary biomarkers from a single kidney, and the exact cause of injury, potentially temperature or intrarenal pressure (IRP), remained unclear. Although we attempted to minimize IRP using gravity irrigation (<60 mm Hg) and frequent aspiration of the renal pelvis, we could not definitively confirm consistently low IRP or intrarenal temperature. Furthermore, despite using similar settings for both lasers, subtle differences in their parameters existed. We also did not investigate the impact of lower or higher energy settings (above 25 W) on kidney damage. Future research could explore alternative laser settings and assess whether UASs and increased irrigation flow can mitigate the observed damage.

Conclusions

There is notable dose-dependent laser-induced renal parenchymal damage for both TFL and Ho:YAG lasers. Older age and metabolic syndrome predispose to greater injury and slower recovery. Damage occurs at multiple levels of the nephron. Although the safety profiles of both lasers are similar, there are notable differences in recovery from injury. Further studies evaluating factors that can ameliorate kidney injury caused by HPLs are needed.

Authors' Contributions

Conception and design: A.J.Y., K.G., M.G., N.K., and D.L. Data analysis and interpretation: B.G., C.C., K.G., M.G., R.K., W.A., D.L., and A.R. Data acquisition: R.S., C.C., B.G., K.G., W.A., A.R. M.P., and S.K.-S. and Drafting the article: K.G., M.G., and A.J.Y. Critical revision of the article for scientific and factual content: K.G., M.G., R.K., W.A., and A.J.Y. Statistical analysis: D.L., C.C., and K.G. Supervision: K.G., M.G., W.A., M.P., and S.K.-S.

Author Disclosure Statement

There are no competing financial interests for all authors.

Funding Information

Valentine Fellow Scholarship Grant from the New York Academy of Medicine and Lumenis.

References

1. Scales CD, Jr, Smith AC, Hanley JM, et al.: Urologic Diseases in America Project. Prevalence of kidney stones in the United States. Eur Urol 2012;62(1):160–165; doi: 10.1016/j.eururo.2012.03.052
2. Kronenberg P, Traxer O. The laser of the future: Reality and expectations about the new thulium fiber laser-a systematic review. Transl Androl Urol 2019;8(Suppl 4): S398–S417; doi: 10.21037/tau.2019.08.01
3. Aldoukhi AH, Ghani KR, Hall TL, et al. Thermal response to high-power holmium laser lithotripsy. J Endourol 2017; 31(12):1308–1312; doi: 10.1089/end.2017.0679
4. Hardy LA, Wilson CR, Irby PB, et al. Thulium fiber laser lithotripsy in an in vitro ureter model. J Biomed Opt 2014;19(12):128001; doi: 10.1117/1.Jbo.19.12.128001
5. Maxwell AD, MacConaghy B, Harper J, et al. Simulation of laser lithotripsy-induced heating in the urinary tract. J Endourol 2019;33(2):113–119; doi: 10.1089/end.2018.0485
6. Peng Y, Liu M, Ming S, et al. Safety of a novel thulium fiber laser for lithotripsy: An In vitro study on the thermal effect and its impact factor. J Endourol 2020:34(1):88–92: doi: 10.1089/end.2019.0426
7. Beker BM, Corleto MG, Fieiras C, et al. Novel acute kidney injury biomarkers: Their characteristics, utility and concerns. Int Urol Nephrol 2018;50(4):705–713; doi: 10.1007/s11255-017-1781-x
8. Griffin BR, Faubel S, Edelstein CL. Biomarkers of drug-induced kidney toxicity. Ther Drug Monit 2019;41(2): 213–226; doi: 10.1097/ftd.0000000000000589
9. Fahmy N, Sener A, Sabbisetti V, et al. Urinary expression of novel tissue markers of kidney injury after ureteroscopy, shockwave lithotripsy, and in normal healthy controls. J Endourol 2013;27(12):1455–1462; doi: 10.1089/end.2013.0188
10. van Timmeren MM, Van Den Heuval MC, Bailly V, et al. Tubular kidney injury molecule-1 (KIM-1) in human renal disease. J Pathol 2007;212(2):209–217; doi: 10.1002/path.2175
11. Sanchez-Puy A, Bravo-Balado A, Diana P, et al. New generation pulse modulation in holmium:YAG Lasers: A systematic review of the literature and meta-analysis. J Clin Med 2022;11(11):3208; doi: 10.3390/jcm11113208
12. Wright AE, Rukin NJ, Somani BK. Ureteroscopy and stones: Current status and future expectations. World J Nephrol 2014;3(4):243–248; doi: 10.5527/wjn.v3.i4.243
13. Knoedler MA, Li S, Best SL, et al. Clinical impact of the institution of moses technology on efficiency during retrograde ureteroscopy for stone disease: Single-Center experience. J Endourol 2022;36(1):65–70; doi: 10.1089/end.2021.0251
14. Liu Y, Jian Z, Ma Y, et al. Changes of renal function after retrograde intrarenal surgery using flexible ureteroscope in renal stone patients. Transl Androl Urol 2021;10(6):2320–2331; doi: 10.21037/tau-20-1521
15. Hoarau N, Martin F, Lebdai S, et al. Impact of retrograde flexible ureteroscopy and intracorporeal lithotripsy on kidney functional outcomes. Int Braz J Urol 2015;41(5): 920–926; doi: 10.1590/s1677-5538.Ibju.2014.0402
16. Ogiste JS, Nejat RJ, Rashid HH, et al. The role of mannitol in alleviating renal injury during extracorporeal shock wave lithotripsy. J Urol 2003;169(3):875–877; doi: 10.1097/01.ju.0000050320.56369.01
17. Memmos D, Sarafidis P, Alexandrou ME, et al. The effect of standard percutaneous nephrolithotomy, miniaturized percutaneous nephrolithotomy and retrograde intrarenal surgery on biomarkers of renal injury: A randomized clinical trial. Clin Kidney J 2023;16(11):2216–2225; doi: 10.1093/ckj/sfad120
18. Han WK, Bailly V, Abichandani R, et al. Kidney injury molecule-1 (KIM-1): A novel biomarker for human renal

proximal tubule injury. Kidney Int 2002;62(1):237–244; doi: 10.1046/j.1523-1755.2002.00433.x

19. Ecer G, Sonmez MG, Aydin A, et al. Comparison of retrograde intrarenal stone surgery with and without a ureteral access sheath using kidney injury molecule-1 (KIM-1) levels: a prospective randomized study. Urolithiasis 2022;50(5): 625–633; doi: 10.1007/s00240-022-01345-y
20. Balasar M, Pişkin MM, Topcu C, Demir LS, Gürbilek M, Kandemir A, Öztürk A. Urinary kidney injury molecule-1 levels in renal stone patients. World J Urol 2016;34(9): 1311–1316; doi: 10.1007/s00345-016-1765-y 26795762

Address correspondence to:
Mantu Gupta, MD, FRCS
Department of Urology
Icahn School of Medicine at Mount Sinai
425 W. 59th St.
New York, NY 10019
USA

E-mail: drmantugupta@gmail.com

Abbreviations Used

β2M = β2-microglobulin
CKD = Chronic kidney disease
HPL = High-powered Laser
Ho:YAG = Holmium:YAG
HU = Hounsfield units
IRP = Intrarenal pressure
IQR = Interquartile range
KIM-1 = Kidney injury molecule-1
NGAL = Neutrophil gelatinase-associated lipocalin
RIRS = Retrograde intrarenal surgery
SWL = Shockwave lithotripsy
TFL = Thulium fiber laser
UAS = Ureteral access sheath
V1 = Preoperative
V2 = 1 hour postoperative
V3 = 10 days postoperative
vs = Versus

Check for updates

《血管内泌尿外科杂志》第39卷第8期，
2025年8月 * Mary Ann Liebert出版社
Pp. 794–803
DOI：10.1089/end.2025.0036

高功率激光可诱发剂量依赖性急性肾损伤

曼图·古普塔[1]、卡维塔·古普塔[1]、罗曼·希莫诺夫[1]、雷蒙德·卡尔吉[1]、安娜·里卡皮托[1]、布莱尔·加兰特[1]、克里斯托弗·康纳斯[1]、达拉·伦登[1]、马尼什库马尔·帕特尔[2]、成熙·金-舒尔泽[2]、威廉·阿塔拉[1]、娜塔莎·基普里亚努[1,3]以及艾伦·J·亚古比安[1]

摘要

引言与目的：已有假说认为高功率激光可能引起肾损伤；然而尚无人体研究证实或量化这种损伤。本研究旨在识别并量化使用钬光纤激光（TFL）和钬:YAG激光（Ho:YAG）进行逆行肾内手术（RIRS）患者所遭受的损伤程度，并探讨影响损伤严重程度的因素。

方法：接受单侧非梗阻性肾结石 RIRS 治疗的患者被随机分配使用60W SuperPulse TFL 激光或120W脉冲调制Ho:YAG激光进行碎石治疗。另设未使用激光的 RIRS 对照组作为比较组。分别在以下三个时间点采集尿液样本：术前、术后1小时及术后10天。采用 ELISA 法检测关键生物标志物——肾损伤分子-1、中性粒细胞明胶酶相关脂质运载蛋白（NGAL）和 β2 -微球蛋白，并以尿肌酐为基准进行标准化处理。主要结局指标基于生物标志物升高程度评估肾脏损伤程度。

结果：91例具有相似基线患者特征和结石特征的患者被随机分组（男性46 TFL，女性45）。Ho：YAG激光）。两种激光均导致生物标志物水平显著升高，其升高趋势接近但未达到基线值。术后第10天。Ho:YAG激光治疗使 NGAL 在10天时持续升高。多变量分析表明，损伤程度与所用激光总能量呈剂量依赖性关系（$p < 0.001$，$p = 0.006$）；老年患者（$p = 0.009$）及代谢综合征患者（$p = 0.002$）的损伤更严重，且这两组患者的恢复速度均较慢，但与所使用的激光类型无关。肾单位的多个层面均受累。

结论：SuperPulse TFL 激光与脉冲调制Ho:YAG激光均能以剂量依赖方式引起显著的肾脏损伤，但两种激光造成的损伤程度并无差异。损伤发生在多个解剖层面。年龄和代谢综合征会影响损伤程度及损伤恢复情况。需进一步研究评估可减轻高能激光所致损伤的因素。

关键词：尿液生物标志物、肾损伤、钬光纤激光、脉冲调制Ho:YAG激光

引言

美国的肾结石终身发病率接近10%。[1]理想情况下，治疗方案应兼具高效性、显著疗效，并最大限度减少肾脏损伤。冲击波碎石术（SWL）因其侵入性较低而被广泛应用；随着内窥镜技术的进步和高功率激光（HPL）的应用，逆行肾内手术（RIRS）的效率也显著提升。钬：YAG（Ho:YAG）激光器已通过脉冲调制技术及高频输出能力得到显著提升。最新推出的SuperPulse钬光纤激光器（TFL）可实现高达2400Hz的频率输出。[2]

[1]美国纽约州西奈山伊坎医学院泌尿外科。
[2]人类免疫监测中心，美国纽约州西奈山伊坎医学院。
[3]美国纽约州西奈山伊坎医学院普施癌症研究所肿瘤科学系。
该摘要的部分内容此前已发表于《泌尿学杂志》第211卷第5S期（2024年5月），页码：e983。

HPLs提高了结石消融的效率，但体外实验和人体研究表明其会升高周围液体温度；体外研究还提供了肾脏损伤的组织学证据。目前尚无人体研究对高能量激光（HPL）所致肾脏损伤程度进行量化或比较。[3-6]尿液生物标志物可无创地定量评估体内肾损伤情况。[7,8]我们采用尿液生物标志物来量化RIRS过程中高能量激光引起的肾损伤。

方法

研究设计

我们开展了一项经机构审查委员会（IRB）批准的单中心随机对照试验（IRB 21-00084），研究对象为年龄超过18岁、患有6毫米至20毫米肾结石并接受激光RIRS治疗的患者。符合入选条件的患者均在术前由手术团队成员签署知情同意书。排除标准包括输尿管结石、肾积水、慢性肾脏病（CKD）（估算肾小球滤过率<60）、单侧肾脏、已置入支架的患者、近9周内接受过输尿管镜检查、尿潴留、神经源性膀胱或近2周内发生尿路感染；术中排除标准包括发现膀胱结石、尿路上皮肿瘤、术前影像未显示的新发梗阻或未能抵达结石部位。本研究未偏离既定方案，已在calin trials.gov网站注册（注册号：NCT05350423）。

随机化与操作流程

本研究旨在根据Fahmy及其同事与van Timmeren及其团队先前的两项研究中定义的隐匿性肾损伤（即估算肾小球滤过率[eGFR]变化达1 mg/mL）标准，评估两种激光治疗方案的非劣效性。[9,10]Fahmy前瞻性比较了SWL与激光RIRS术后尿液中肾脏损伤分子-1（KIM-1）水平的变化：50例患者接受SWL治疗后2小时KIM-1水平从5.78 ng/mL升至10.14 ng/mL（$p < 0.001$），而10例患者接受RIRS治疗后未见变化（5.78 ng/mL至5.49 ng/mL）。van Timmeren及其团队对11名健康对照者及53例不同肾脏疾病患者进行评估，发现KIM-1与eGFR之间存在-27.5的相关性（$p = 0.016$）；即KIM-1升高1 ng/mL对应eGFR下降27.5 mL/min。为基于eGFR变化10 mg/mL、分配比例1:1、检验效能99%、非劣效界值20%及α=5%的非劣效性功效计算设计本研究，每组需纳入49例患者；考虑到10%的脱落率，最终计划招募108例患者。受试者被随机分配至YAG激光组（Lumenis P120设备搭配Moses 2.0系统）或SuperPulse TFL激光组（Olympus Soltive Premium设备）。采用sealedenvelope.com平台进行区组随机化，方案存储于密码保护计算机中。患者与外科医生均对分组情况设盲，在结石显影前不透露具体治疗方案。

首份样本（术前[V1]）于麻醉诱导后、手术干预前通过福莱导管采集。所有操作均由经验丰富的腔内泌尿外科医师（M.G.与W.A.）采用标准化方法完成，包括使用Storz Flex-X2 7.5F柔性输尿管镜、不使用输尿管通路鞘（UAS），仅采用80 cm H_2（约60 mmHg）的重力灌洗方式，未使用加压式、机械式或手动灌洗系统。进入肾盂后，通过完整肾盂镜检查确认结石负荷与术前影像结果一致。治疗方案由研究助理确定，并将指定激光设备带入手术室。同意参与研究且接受输尿管镜检查但无需激光治疗的患者（已取出结石篮或结石位于黏膜下/实质层且无法治疗），作为对照组以确保生物标志物升高是由激光能量本身而非输尿管镜检查所致。

在标准操作中，即使未使用UAS或加压冲洗系统，我们仍会在治疗过程中频繁暂停并抽吸肾盂液体，以避免使用高功率设置导致温度过高，并改善观察效果。初始参数设置为：Ho:YAG激光器采用0.5 J、5 Hz；TFL激光器采用1 J、2 Hz；随后针对每位患者均调增至0.5 J、50 Hz（25瓦），以实现高功率喷砂，使产生的颗粒尺寸小于激光光纤直径（200微米）。功率仅短暂提升至25瓦，且每次不超过5秒。为控制工作周期，激光激活时间限制为10秒脉冲，之后必须进行20秒的强制暂停，以减少累积热量沉积。此外，在两次激光激活之间需频繁抽吸收集系统的液体，进一步降低热积聚风险。

记录了激光参数、总激光能量、激光开关时间、激光照射时间和手术时间。可见的激光诱导组织损伤情况按以下标准进行记录和分级：

0级：黏膜无可见损伤；因器械操作相关创伤导致轻微红斑。

1级：接触激光后黏膜出现苍白或绒毛状变；无黏膜损伤证据（不应存在出血）。

第2级：穿透至黏膜下组织；接触激光后黏膜层出现明显缺损，伴或不伴出血，未见造影剂外渗。

3级：肾盂全层穿孔（需注射造影剂）

血管化）或肾实质及脂肪组织的观察。

所有操作步骤（包括对照组患者）均按照研究方案完成，最终置入了6F硅胶支架（Black Silicone Filiform Double Pigtail输尿管支架，美国印第安纳州Cook Medical公司生产）及16F福莱导管。

第二份尿液样本（术后1小时[V2]）于术后1小时在恢复室通过留置福莱导尿管的抽吸侧端口在导管拔除时采集；第三份样本（术后10天[V3]）则于术后第10天、支架取出前即刻通过排尿方式采集。

尿液生物标志物分析

对尿液样本进行了随机尿肌酐检测，并采用ELISA法测定以下三种生物标志物：KIM-1、中性粒细胞明胶酶相关脂质运载蛋白（NGAL）以及β2-微球蛋白（β2M）。所有指标均以同期采集的尿肌酐水平进行标准化校正。KIM-1、NGAL和β2M的浓度均通过市售的®肾脏损伤磁珠Luminex多重检测组合试剂盒（EMD Millipore/Millipore Sigma，美国马萨诸塞州比勒里卡）测定。尿样在4℃下以13500 RPM离心

10分钟以清除沉淀。样品分别用测定缓冲液按1:2比例稀释KIM-1、1:100比例稀释 NGAL 、1:500比例稀释 β2M ，并在96孔板中进行双重复检测。先于4°C与一抗孵育过夜（16–18小时），随后在室温下与检测抗体孵育1小时，再与链霉亲和素-藻红蛋白孵育30分钟。使用 Luminex Flexmap 3D系统读取结果数据，并采用 Milliplex Analyst 5.1 软件（EMD Millipore/Millipore Sigma公司，美国马萨诸塞州比勒里卡）进行分析。

结果

主要结局指标为通过尿液生物标志物较基线水平的变化评估的肾损伤程度。次要结局指标包括：使用的总激光能量、激光照射时间、碎石手术时间、激光消融效率、激光能耗、激光消融速度、激光活性（操作者工作周期）、术后并发症、再入院率以及术后3个月内的急诊就诊次数。

统计量

基线特征及结石信息详见表1，手术数据见表2。连续变量采用Mann-Whitney U检验评估统计学显著性，分类变量则采用卡方检验或Fisher精确检验。针对Ho：YAG组、TFL 组及对照组，计算了V1 至V3 期间KIM-1、NGAL 和 β2M 水平的变化趋势（<sp_3图2）；采用配对样本t检验分析各组（包括对照组）从V1到V2、V2到V3以及V1到V3的生物标志物浓度变化是否具有显著性（<sp_4图3）；通过多元线性回归分析评估激光类型对V1至V2、V2至V3及V1至V3期间生物标志物百分比变化的影响（<sp_5表3）。多元模型中的变量均经过预先筛选或在单变量分析中显示ap值小于0.1；这些变量包括手术组别、年龄、代谢综合征存在情况、术前估算肾小球滤过率（eGFR）、手术时间及总激光能量。所有统计分析均使用 SPSS Statistics 28版软件（IBM公司，纽约州阿蒙克）完成。（美国），双尾α值为0.05，表明具有统计学显著性。

结果

2021年10月至2023年7月期间，共纳入108例符合入选标准的患者（图1）。所有患者均被均等地随机分配至 HPL 组。每组各54例。最终研究共包含46例 TFL 患者、45例Ho:YAG治疗组患者及5例对照组患者。

两组患者的人口统计学特征及基线参数具有可比性（表1）。 HPL 组与 TFL 组的总能耗相近（1.7 kJ四分位数范围[IQR]：1.0–4.8 vs 1.98 kJ IQR ：1.31–4.43，p=0.727）；计算得出的激光效率指标（激光消融效率、能量消耗、操作者工作负荷/活动量及消融速度）均无显著差异；可见肾脏损伤的发生率亦无统计学差异（p=0.164）；未出现3级损伤；Ho:YAG激光组的2级损伤（穿透至黏膜下层）发生率高于 TFL 激光组（21.7% vs 8.9%）；结石成分以草酸钙最为常见（77.8% vs 78.3%，p=0.299）；并发症发生情况无显著差异。相似（6.7% 对比 10.9%，p = 0.677）。

两种激光均导致生物标志物出现显著且具有统计学意义的升高（ng/mL TFL 中的中位值：KIM-1从0.011升至0.025、 NGAL 从0.526升至2.518、 β2M 从2.126升至25.623；HoYAG从0.012升至0.024 KIM-1、 NGAL 从0.572 升至2.448、 β2M 从2.775 升至17.147），其变化趋势在第10天接近但未完全恢复至基线水平（图2和图3）。

表1. 人口统计学资料与术前信息

	钬组（n = 45）	铥组（n = 46）
年龄 [IQR]	56.0 [39.0–67.5]	59.0 [46.5–63.5]
BMI [IQR]	27.4 [23.8–30.4]	25.8 [23.8–29.4]
性别，n（%）		
男性	18(40.0)	23(50.0)
女性	27(60.0)	23(50.0)
ASA评分，n（%）		
1	4(8.9)	1(2.2)
2	33(73.3)	35(76.1)
3	8(17.8)	9(19.6)
4	0(0.0)	1(2.2)
糖尿病，n（%）	7(15.6)	10(21.7)
利尿剂，n（%）	3(6.7)	5(10.9)
血管紧张素转换酶抑制剂，n（%）	6(13.6)	6(13.0)
抗凝剂，n（%）	2(4.4)	1(2.2)
既往骨外科手术史，n（%）：	17(37.8)	24(52.2)
手术侧别，n（%）		
左侧	24(53.3)	25(54.3)
右侧	21(46.7)	21(45.7)
总石料负荷，mm [IQR]	12.0[9.0–19.0]	13.0[9.0–19.0]
石料体积，mm^3 [IQR]	214.0[82.8–310.6]	176.9[91.9–292.3]
HU [IQR]	837.5[473.5–1144.0]	992[824.8–1194.0]
术前肌酐[IQR]	0.80[0.67–0.99]	0.80[0.71–0.98]
术前估算肾小球滤过率[IQR]	92.0[76.5–106.0]	92.5[84.8–103.0]

IQR = 四分位距。

表2. 钬与钍研究组的运营信息及结果

	钬组（n = 45）	钍组（n = 46）	p 值
手术时间，分钟 [IQR]	56.0 [42.0–68.0]	52.5 [42.8–72.3]	0.846
总激光能量，kJ [IQR]	1.7 [1.0–4.8]	1.98 [1.3–4.4]	0.727
总激光时间，秒 [IQR]	432.5 [197.0–910.5]	469.0 [282.0–1077.0]	0.495
总碎石时间，秒[IQR]	2160.0 [1320.0–2880.0]	1950.0 [1365.0–3135.0]	0.846
激光效率[IQR]			
激光能耗（J/mm³）	13.4 [4.9–25.4]	12.9 [6.8–35.5]	0.435
激光工作时间（操作员使用周期）（%）	25.2 [10.6–44.0]	33.8 [17.7–49.2]	0.212
激光消融速度（mm³/s）	0.38 [0.21–1.21]	0.27 [0.17–0.55]	0.264
可见损伤			0.164
无可见损坏	10 (21.7)	8 (17.8)	
仅黏膜苍白	26 (56.5)	33 (73.3)	
穿透至黏膜下层	10 (21.7)	4 (8.9)	
石料成分（百分比）：			0.299
>50% CaO_x	35 (77.8)	36 (78.3)	
>50% UA	3 (6.7)	0 (0.0)	
>50% HA	3 (6.7)	6 (13.0)	
其他／未知	4 (8.9)	4 (8.7)	
克拉维恩-丁多并发症，n（%）			0.677
无	42 (93.3)	41 (89.1)	
I	1 (2.2)	4 (8.7)	
II	1 (2.2)	1 (2.2)	
III	0 (0.0)	0 (0.0)	

连续变量以中位数表示。p值通过卡方检验、Fisher精确检验或Mann-Whitney U检验得出。显著性水平设定为$p < 0.05$。

IQR = 四分位距。

与之形成鲜明对比的是，对照组在第10天时生物标志物的升高幅度和恢复正常水平均相对较小。生物标志物的持续升高既取决于激光类型，也取决于具体生物标志物本身。所有三种生物标志物的基线水平均较低且各组间无显著差异（图2）。NGAL 和KIM-1的升高幅度显著，但与激光类型无关；β2M 的升高同样明显——尽管 TFL 激光组的升高幅度大于钬激光组，但未达到统计学显著性。至第10天，数值下降表明组织已恢复，但在大多数病例中仍显著高于基线水平（图3）。从V2到V3阶段，KIM-1在 TFL 激光组中的下降具有显著性，而在钬激光组则无此现象。尤其是 NGAL 值，在第10天时并未出现明显下降，这在Ho:YAG激光治疗组患者中尤为明显。

为明确影响肾损伤的因素，我们进行了多变量分析，重点关注临床状况及治疗参数（表3）。年龄和代谢综合征均对肾损伤具有显著影响：老年患者KIM-1水平升高更明显（$p = 0.005$），NGAL 恢复速度更慢（$p = 0.031$），且 NGAL 较基线水平持续升高的可能性更高（$p = 0.009$）；年龄则未独立影响 β2M 水平。代谢综合征患者从V2期到V3期的 β2M 恢复速度显著延迟，且 β2M 持续升高的概率更高（$p = 0.008$，$p = 0.002$）；而代谢综合征对 NGAL 或KIM-1水平无类似影响。激光总能量使用量越大，KIM-1和 β2M 水平从V2期到V3期的恢复速度越慢，且在V3期出现持续升高的可能性越高（$p = 0.006$，$p = 0.019$，$p < 0.001$）；这一效应在 NGAL 中未观察到，但无论激光总能量如何，接受激光治疗患者的 NGAL 恢复速度普遍较慢且 NGAL 水平持续升高。手术时间与生物标志物升高无独立相关性。此外，所使用的激光类型与生物标志物水平变化无独立关联。

讨论

高脉冲激光（HPL）经过改良设计，可提升 RIRS 手术效率并提高无结石率。1993年问世的Ho:YAG激光器已发展出脉冲调制和高频功能，通过增强碎石能力改善能量输送效果并缩短手术时间[11–13]；SuperPulse TFL 系统相较于传统Ho:YAG系统具有反冲力更小、碎石性能更优的优势，已得到广泛应用[2]。目前学界尚未就哪种技术更具优势或损伤更小达成共识。体外研究提示HPL可能引发温度诱导性肾损伤，但评估此类损伤的临床数据仍十分匮乏。我们量化了 RIRS 术前术后特异性反映肾脏及尿路上皮损伤的尿液生物标志物，并将其与不同术中参数进行关联分析。

肾损伤可通过血清肌酐及基于血清肌酐计算的估算肾小球滤过率（eGFR）进行评估，但这些指标与肾损伤程度并无线性关系。即使患者双肾功能正常，切除一侧肾脏也不会影响血清肌酐或eGFR水平。一项针对120例接受输尿管肾镜取石术（RIRS）患者的研究表明，eGFR并未出现显著下降；然而，高龄、较长的输尿管镜操作时间、较薄的肾实质以及输尿管结石均是肾功能恶化的危险因素[14]。另一项研究显示，在163例接受 RIRS 的患者中，仅4.9%的患者术后GFR出现显著下降[15]。我们的数据同样表明术后10天eGFR未见显著变化。血清肌酐受多种与肾功能无关的因素影响（如饮食、水合状态及肌肉质量），更重要的是，血清

表3. 不同采集时间点生物标志物变化的多变量线性回归分析

	V1 → V2 的变化值（百分比）		V2 → V3 的变化幅度（%）		V1 → V3 的变化值（百分比）	
因子	标准化 β 系数	p 值	标准化 β 系数	p 值	标准化 β 系数	p 值
KIM-1						
手术组对照	Ref	—	Ref	—	Ref	—
钬	0.228	0.440	−0.205	0.564	0.086	0.810
铥	0.446	0.132	−0.294	0.406	0.061	0.865
年龄（岁）	−0.362	**0.005***	0.152	0.280	−0.108	0.416
代谢综合征	−0.121	0.286	0.087	0.475	−0.059	0.608
eGFR	−0.023	0.856	0.145	0.296	0.115	0.371
手术时间（分钟）	0.098	0.420	0.024	0.854	0.084	0.512
总激光能量，kJ	−0.140	0.262	0.387	**0.006***	0.319	**0.019***
NGAL						
手术组对照	Ref	—	Ref	—	Ref	—
钬	0.055	0.916	−0.064	0.903	−0.059	0.909
铥	0.067	0.897	−0.134	0.798	−0.153	0.768
年龄（岁）	−0.128	0.336	−0.298	**0.031***	−0.341	**0.009***
代谢综合征	−0.102	0.377	0.029	0.803	0.026	0.815
eGFR	−0.023	0.860	−0.020	0.880	−0.047	0.709
手术时间（分钟）	0.198	0.120	−0.035	0.789	0.014	0.913
总激光能量，kJ	0.137	0.289	0.060	0.645	0.050	0.695
β-2						
手术组对照	Ref	—	Ref	—	Ref	—
钬	0.128	0.728	−0.086	0.794	0.034	0.918
铥	0.325	0.379	0.010	0.975	0.110	0.736
年龄（岁）	0.040	0.779	0.068	0.597	0.004	0.976
代谢综合征	−0.107	0.394	0.300	**0.008***	0.328	**0.002***
eGFR	−0.217	0.126	0.088	0.492	−0.083	0.473
手术时间（分钟）	0.237	0.072	−0.228	0.054	−0.116	0.315
总激光能量，kJ	−0.074	0.583	0.441	**<0.001***	0.400	**0.001***

显著性阈值设为＜0.05（加粗及*号表示参考）。

KIM-1=肾损伤分子-1；NGAL =中性粒细胞明胶酶相关脂质运载蛋白；V1=术前；V2=术后1小时；V3=术后10天。

肌酐和估算肾小球滤过率（eGFR）在检测肾小管细胞早期或轻微损伤方面敏感性较低，但更适用于评估长期持续性肾损伤。多种尿液蛋白生物标志物可作为肾细胞损伤的指标；与eGFR相比，这些标志物能更早发现肾损伤且灵敏度显著更高，但其特异性可能有限——其升高可能由全身性炎症、脱水或其他器官损伤等非肾脏因素引起，并不必然反映肾损伤。生物标志物可帮助判断损伤性质，部分研究表明特定升高水平模式可能提示损伤是否可修复。这些标志物的动态变化特征各异：我们选取了两种急性肾损伤标志物 NGAL 和KIM-1（二者在损伤后迅速达峰并快速恢复至基线水平），以及一种更能反映慢性损伤的标志物 β2M（该指标已被证实可有效评估肾小球及近端肾小管损伤[16]）。值得注意的是，β2M 在10天后仍未恢复至基线水平；此外，β2M 升高程度受代谢综合征影响（p=0.）。008），而 NGAL 和 KIM-1则未受影响。代谢综合征对 β2M 持续升高及升高水平缓慢恢复的影响，与肾储备功能下降相一致。既往研究已证实这一结论。

研究支持 β2M 与代谢性疾病、早期糖尿病肾病及早期慢性肾脏病（CKD）存在关联。[17]代谢综合征患者出现肾功能储备受损的可能性更高。即使轻微的肾损伤，在此类患者中也更难恢复。

总激光能量与恢复速度减慢以及第10天时KIM-1和 β2M 水平持续升高均存在关联。这直接证明激光能量不仅会导致肾损伤，且具有剂量依赖性——能量越高，损伤越严重，恢复也越缓慢。其对KIM-1和 β2M 的影响令人担忧肾小管及肾小球损伤的发生风险。我们的研究结果表明，临床医生在进行 RIRS 治疗时应特别关注高功率激光器（HPL）所消耗的总能量，尤其是对于已有肾脏疾病的患者。

虽然 β2M 可反映肾小球及近端肾小管损伤，但 NGAL 是在远端肾单位产生，并作为肾脏损伤的应答产物而合成。[18]Albert及其团队发现，在滤过功能下降之前，尿液和血浆中的 NGAL 水平即可提示早期肾小管损伤。[19]Memmos研究团队通过比较低功率Ho:YAG RIRS 、微型 PCNL 与标准 PCNL 的结果发现，KIM-1和 NGAL 水平在2至24小时乃至48小时内持续升高，但各治疗组间无显著差异。[17]我们的研究结果发现

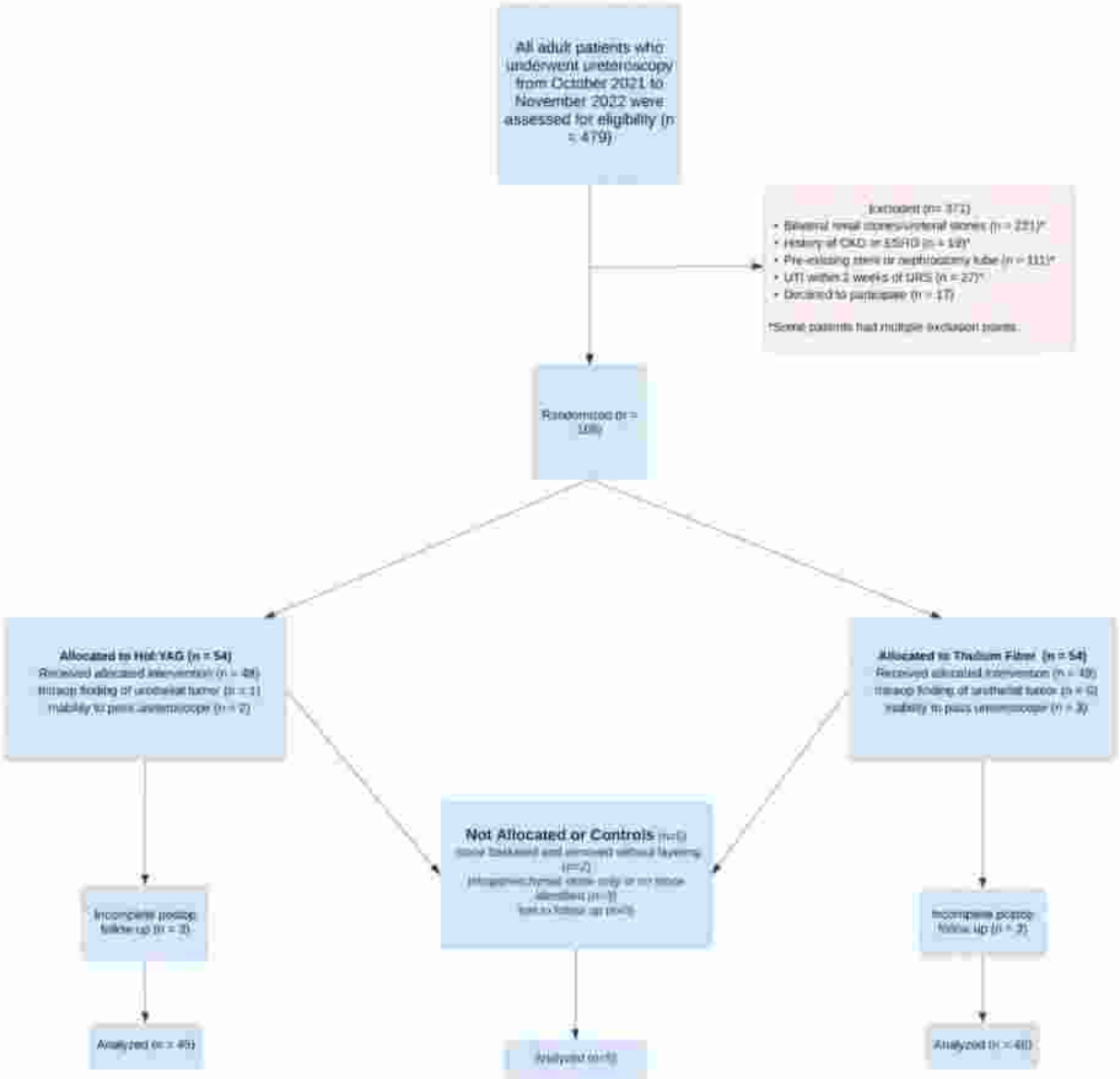


图 1. 流程图。

两种肾盂输尿管连接部（HPL）的 NGAL 值在术后仅1小时即开始升高，并持续至第10天仍保持高位。NGAL 值的持续升高令人担忧，表明损伤程度严重且持久。其持续时间尚待确定（因为我们未超过10天进行随访）。损伤恢复缓慢以及 NGAL 值持续高于基线水平均与年龄独立相关（分别为p=0.031和p=0.009），这意味着老年患者从肾脏损伤中恢复的速度较慢，而 NGAL 检测可反映这一特征。我们的数据表明，临床医生在治疗老年HPL患者时应格外谨慎。

年龄也是唯一与术后1小时损伤程度独立相关的参数，其中KIM-1是最佳标志物。KIM-1在急性肾小管坏死期间表达，并由近端曲小管[18]产生。在缺血性 ATN 中，肾小管的KIM-1水平高于慢性肾功能衰竭患者。此外，研究发现UAS能降低 RIRS 后的KIM-1升高[19]。本研究中，KIM-1呈下降趋势，但至第10天仍未恢复至基线水平。与B2M类似，KIM-1受总激光能量影响（$p < 0.006$）：使用的激光能量越大，从V1到V2阶段的升高幅度越显著，而从V2到V3阶段的恢复速度则越慢。这些结果表明：高强度激光可诱发 ATN；老年患者的损伤程度更为严重；接受较高激光能量治疗的患者其恢复速度呈剂量依赖性减缓。

Memmos及其同事的研究并未检测术后48小时后的指标水平。[17]我们虽未检测术后1小时至10天期间的指标水平，但注意到大多数生物标志物在10天时其水平均已下降。结合我们的研究结果与他们的数据，可以推测相关指标值在术后数天达到峰值，并于10天时开始下降。这些推论与一项评估 PCNL 和 RIRS 术后KIM-1水平的前瞻性研究结果一致——该研究发现术后4至14天内KIM-1水平会降至基线水平。[20]未来仍需开展进一步研究以评估生物标志物的长期变化趋势，并将其与其他肾损伤评估指标（如核素肾脏扫描）进行关联分析。

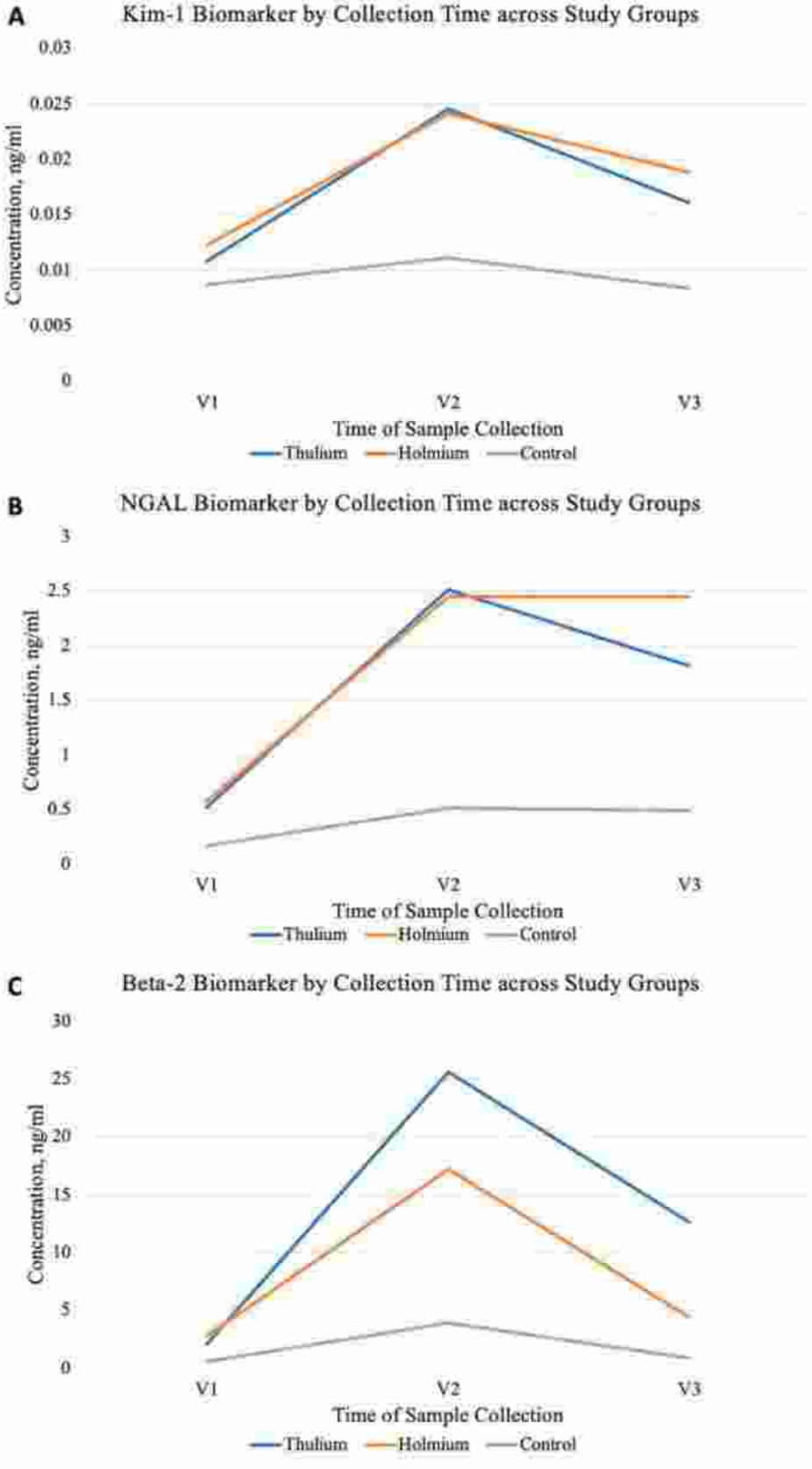


图2. 所有研究组中生物标志物采集量随时间变化的线性关系图。

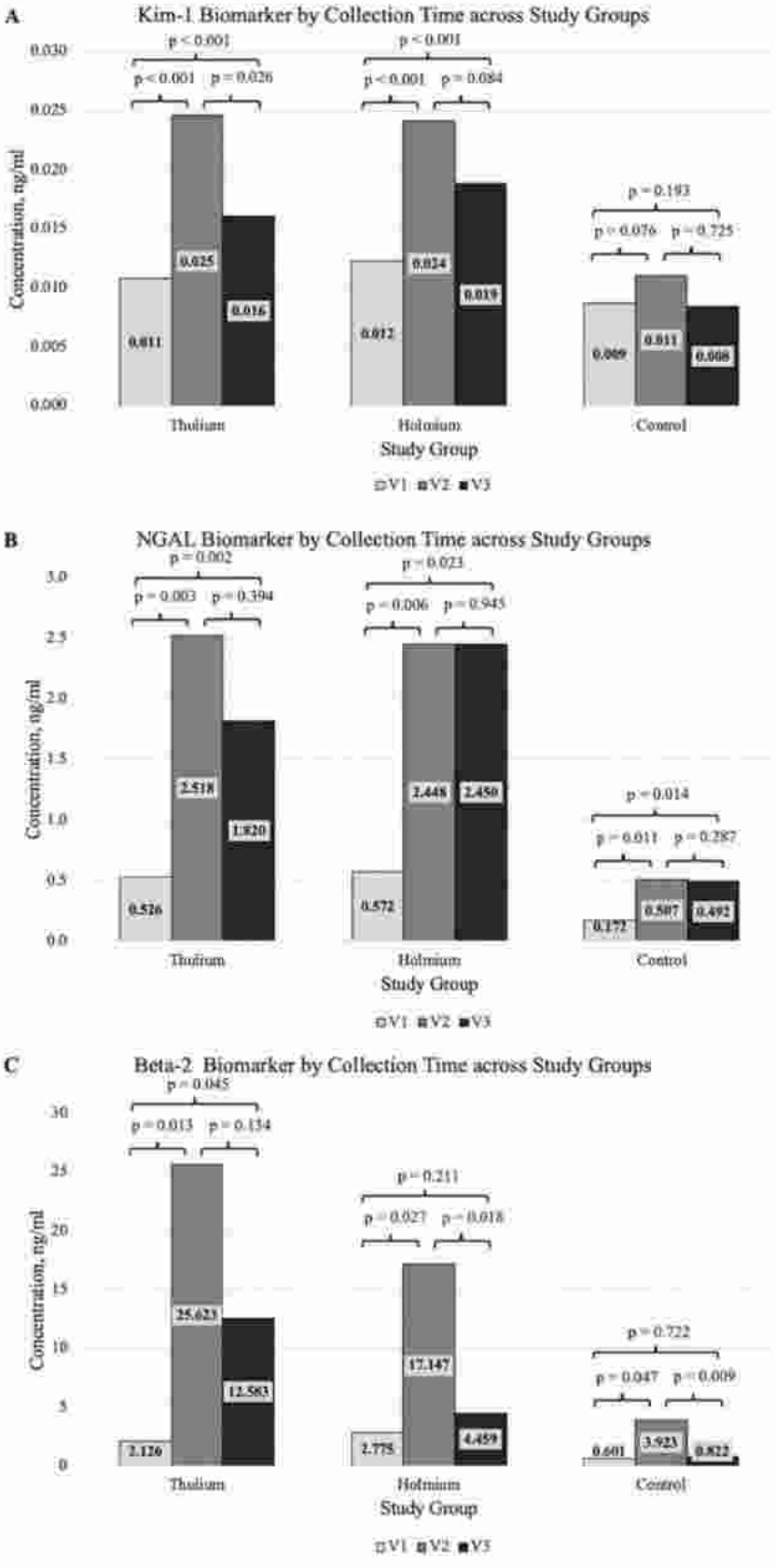


图3. 所有研究组中生物标志物采集量随时间变化的条形图表示。

我们的研究结果表明肾脏细胞确实会受到损伤，但具体机制尚不明确。激光能量既直接对周围组织产生热损伤，也会通过加热冲洗液导致损伤，从而以剂量依赖的方式引发凝固、碳化及蛋白质变性等损伤反应。体内猪模型研究表明，当冲洗液流量较低时，40瓦的激光功率可使温度升至危险水平[3]。本研究中，总激光能量分别为3.14 kJ（TFL）和3.36 kJ（Ho:YAG）时均通过生物标志物水平升高证实了细胞损伤的存在。目前我们机构正在进一步研究高脉冲激光引起的温度升高与热损伤之间的直接关联。

本研究存在若干局限性：我们仅分析了单侧肾脏的尿液生物标志物，而损伤的确切原因（可能是温度或肾内压力 IRP）仍不明确；尽管我们尝试通过重力灌注（<60 mmHg）和频繁冲洗肾盂来降低 IRP，但未能确证 IRP 或肾内温度始终处于较低水平；此外，虽然两台激光设备采用相似参数设置，其具体参数仍存在细微差异；我们亦未探讨较低或较高能量设置（高于25 W）对肾脏损伤的影响。未来研究可探索其他激光参数配置，并评估超声辅助手术（UAS）及增加灌注流量是否能减轻观察到的损伤。

结论

无论是 TFL 激光还是Ho:YAG激光，均会引发显著的剂量依赖性激光诱导肾实质损伤。年龄较大和代谢综合征患者更易遭受严重损伤且恢复速度较慢。损伤可发生于肾单位的多个层面。尽管两种激光的安全性特征相似，但其损伤后的恢复情况存在显著差异。须需开展进一步研究以明确能够减轻高功率激光所致肾损伤的相关因素。

作者的贡献

概念与设计：A.J.Y.、K.G.、M.G.、N.K. 和 D.L.；数据分析与解读：B.G.、C.C.、K.G.、M.G.、R.K.、W.A.、D.L. 和 A.R.；数据采集：R.S.、C.C.、B.G.、K.G.、W.A.、A.R.、M.P. 和 S.K.-S.；文章起草：K.G.、M.G. 和 A.J.Y.；针对文章的科学性和事实准确性进行批判性修订：K.G.、M.G.、R.K.、W.A. 和 A.J.Y.；统计分析：D.L.、C.C. 和 K.G.；监督工作：K.G.、M.G.、W.A.、M.P. 和 S.K.-S.

作者披露声明

所有作者均不存在相互冲突的经济利益。

资金信息

纽约医学科学院与Lumenis公司联合颁发的瓦伦丁研究员奖学金。

参考文献

1. Scales CD, Jr, Smith AC, Hanley JM, et al.; Urologic Diseases in America Project. Prevalence of kidney stones in the United States. Eur Urol 2012;62(1):160 - 165; doi: 10.1016/j.eururo.2012.03.052
2. Kronenberg P, Traxer O. The laser of the future: Reality and expectations about the new thulium fiber laser-a systematic review. Transl Androl Urol 2019;8(Suppl 4): S398 - S417; doi: 10.21037/tau.2019.08.01
3. Aldoukhi AH, Ghani KR, Hall TL, et al. Thermal response to high-power holmium laser lithotripsy. J Endourol 2017; 31(12):1308 - 1312; doi: 10.1089/end.2017.0679
4. Hardy LA, Wilson CR, Irby PB, et al. Thulium fiber laser lithotripsy in an in vitro ureter model. J Biomed Opt 2014;19(12):128001; doi: 10.1117/1.Jbo.19.12.128001
5. Maxwell AD, MacConaghy B, Harper J, et al. Simulation of laser lithotripsy-induced heating in the urinary tract. J Endourol 2019;33(2):113 - 119; doi: 10.1089/end.2018.0485
6. Peng Y, Liu M, Ming S, et al. Safety of a novel thulium fiber laser for lithotripsy: An in vitro study on the thermal effect and its impact factor. J Endourol 2020;34(1):88 - 92; doi: 10.1089/end.2019.0426
7. Beker BM, Corleto MG, Fieiras C, et al. Novel acute kidney injury biomarkers: Their characteristics, utility and concerns. Int Urol Nephrol 2018;50(4):705 - 713; doi: 10.1007/s11255-017-1781-x
8. Griffin BR, Faubel S, Edelstein CL. Biomarkers of drug-induced kidney toxicity. Ther Drug Monit 2019;41(2): 213 - 226; doi: 10.1097/ftd.0000000000000589
9. Fahmy N, Sener A, Sabbisetti V, et al. Urinary expression of novel tissue markers of kidney injury after ureteroscopy, shock-wave lithotripsy, and in normal healthy controls. J Endourol 2013;27(12):1455 - 1462; doi: 10.1089/end.2013.0188
10. van Timmeren MM, Van Den Heuval MC, Bailly V, et al. Tubular kidney injury molecule-1 (KIM-1) in human renal disease. J Pathol 2007;212(2):209 - 217; doi: 10.1002/path.2175
11. Sanchez-Puy A, Bravo-Balado A, Diana P, et al. New generation pulse modulation in holmium:YAG Lasers: A systematic review of the literature and meta-analysis. J Clin Med 2022;11(11):3208; doi: 10.3390/jcm11113208
12. Wright AE, Rukin NJ, Somani BK. Ureteroscopy and stones: Current status and future expectations. World J Nephrol 2014;3(4):243 - 248; doi: 10.5527/wjn.v3.i4.243
13. Knoedler MA, Li S, Best SL, et al. Clinical impact of the institution of moses technology on efficiency during retrograde ureteroscopy for stone disease: Single-Center experience. J Endourol 2022;36(1):65 - 70; doi: 10.1089/end.2021.0251
14. Liu Y, Jian Z, Ma Y, et al. Changes of renal function after retrograde intrarenal surgery using flexible ureteroscope in renal stone patients. Transl Androl Urol 2021;10(6):2320 - 2331;doi: 10.21037/tau-20-1521
15. Hoarau N, Martin F, Lebdai S, et al. Impact of retrograde flexible ureteroscopy and intracorporeal lithotripsy on kidney functional outcomes. Int Braz J Urol 2015;41(5): 920 - 926; doi: 10.1590/s1677-5538.Ibju.2014.0402
16. Ogiste JS, Nejat RJ, Rashid HH, et al. The role of mannitol in alleviating renal injury during extracorporeal shock wave lithotripsy. J Urol 2003;169(3):875 - 877; doi: 10.1097/01.ju.0000050320.56369.01
17. Memmos D, Sarafidis P, Alexandrou ME, et al. The effect of standard percutaneous nephrolithotomy, miniaturized percutaneous nephrolithotomy and retrograde intrarenal surgery on biomarkers of renal injury: A randomized clinical trial. Clin Kidney J 2023;16(11):2216 - 2225; doi: 10.1093/ckj/sfad120
18. Han WK, Bailly V, Abichandani R, et al. Kidney injury molecule-1 (KIM-1): A novel biomarker for human renal

proximal tubule injury. Kidney Int 2002;62(1):237 - 244; doi: 10.1046/j.1523-1755.2002.00433.x
19. Ecer G, Sonmez MG, Aydin A, et al. Comparison of retrograde intrarenal stone surgery with and without a ureteral access sheath using kidney injury molecule-1 (KIM-1) levels: a prospective randomized study. Urolithiasis 2022;50(5): 625 - 633; doi: 10.1007/s00240-022-01345-y
20. Balasar M, Pis¸kin MM, Topcu C, Demir LS, Gürbilek M, Kandemir A, Öztürk A. Urinary kidney injury molecule-1 levels in renal stone patients. World J Urol 2016;34(9): 1311 - 1316; doi: 10.1007/s00345-016-1765-y 26795762

通讯地址：Mantu Gupta，医学博士，加拿大皇家外科医学院院士，泌尿外科系
西奈山伊坎医学院
美国纽约州纽约市西59街425号，邮编10019

电子邮件：drmantugupta@gmail.com

使用的缩写词

β2M = β2 -微球蛋白
CKD = 慢性肾脏病
HPL = 高功率激光器；
Ho:YAG=钬：钇铝石榴石
HU = 亨氏单位
IRP = 肾内压
IQR = 四分位距；
KIM-1 = 肾损伤分子-1
NGAL = 中性粒细胞明胶酶相关脂质运载蛋白；
RIRS = 肾内逆行手术
SWL = 冲击波碎石术
TFL = 长锥姆光纤激光器
UAS = 输尿管军刺鞘；
V1 = 术前
V2 = 术后1小时
V3 = 术后第10天
vs = 对比；与.....相比

World Journal of Urology (2025) 43:354
https://doi.org/10.1007/s00345-025-05713-2

RESEARCH

Characterisation of iatrogenic human ureteral laser injury - results from ex vivo testing with a Ho: YAG laser at commonly used lithotripsy settings

S. O'Meara[1,2] · K. Sheehan[3,4] · J. Fay[5] · T. O'Grady[3,5] · S. M. Croghan[1,2] · E. M. Cunnane[7,8] · D. Hogan[6] · G. G. Calpin[6] · B. Somani[10] · M. T. Walsh[7,8] · F. J. O'Brien[9] · N. F. Davis[1,2,6]

Received: 11 October 2024 / Accepted: 18 May 2025
© The Author(s) 2025

Abstract

Introduction Modern endourology relies on Ho: YAG lasers for definitive management of urolithiasis. Current safety data is drawn predominantly from Ho: YAG laser testing in animal tissue. We aim to evaluate and characterise the grades of iatrogenic human ureteral injury due to contact with a Ho: YAG laser at commonly used lithotripsy settings.

Methodology Human ureters were collected from consenting adults at the time of radical nephrectomy. A custom rig was developed to secure a 273micron (μm) laser fibre in contact with the urothelium for periods of 5, 10 and 20 s. Testing settings used included 8 Hz (Hz) and 800millijoules (mJ), 10 Hz/1000 mJ, and 5 Hz/1500 mJ. Grades of ureteric injury were then characterised with histopathology.

Results A total of 31 specimens were tested and the mean specimen thickness was 2.2 mm (range 0.9–3.1 mm). The depth of laser-related injury ranged from urothelium alone to full thickness perforation at all settings depending on the duration of laser contact with tissue and specimen thickness. No full thickness perforation was seen in specimens ≥ 3 mm, even at 20 s of contact duration at 10 Hz/1000 mJ. However, in specimens < 1 mm the level of injury depth ranged from urothelium to full thickness perforation at 5 s of testing.

Discussion Ho: YAG laser causes variable levels of injury, with both superficial and extensive injury noted. The thickness of the ureter may determine the extent of trauma following laser contact. Concerningly, full thickness ureter perforation may occur with commonly used laser settings at short laser contact durations.

Keywords Urolithiasis · Laser · Endourology · Iatrogenic injury · Stricture

✉ S. O'Meara
sorchaomeara@rcsi.ie

1 Strategic Academic Recruitment (StAR) Programme, Royal College of Surgeons in Ireland, Dublin, Ireland

2 Dept. of Urology, Blackrock Health, Blackrock, Dublin, Ireland

3 Dept. of Pathology, Royal College of Surgeons in Ireland, Dublin, Ireland

4 Dept. of Pathology, Blackrock Health, Dublin, Ireland

5 RCSI biobank, Dept. of Pathology, Royal College of Surgeons in Ireland, Dublin, Ireland

6 Dept. of Urology, Beaumont Hospital, Dublin, Ireland

7 Biomaterials Cluster, Bernal Institute, University of Limerick, Limerick, Ireland

8 School of Engineering, University of Limerick, Limerick, Ireland

9 Tissue Engineering Research Group, Royal College of Surgeons in Ireland, Dublin, Ireland

10 Department of Urology, University Hospital Southampton NHS Foundation Trust, Southampton SO16 6YD, UK

Published online: 04 June 2025

Abbreviations

Fr	French
H&E	Hematoxylin and eosin
Hz	Hertz
Ho:YAG	Holmium: yttrium–aluminium–garnet
IRP	Intra–renal pressures
IRT	Intra–renal temperature
mj	Millijoules
TFL	Thulium fibre laser
Tm:YAG	Thulium–yttrium–aluminum–garnet
nm	Nanometers
NS0.9%	Normal Saline 0.9%
µm	Micron

Introduction

The holmium: yttrium-aluminium-garnet (Ho: YAG) surgical laser has a defined role in lithotripsy and tissue ablation in endourology. Its depth of tissue penetration is approximately 0.4 millimetres (mm) which contributes to the laser's favourable safety profile, with clinical studies reporting low rates of tissue trauma [1–7]. Despite its common use, there is ongoing debate regarding the optimal Ho: YAG settings for efficient stone or tissue destruction while ensuring patient safety [8–12]. Recent ex-vivo animal studies have suggested that the actual depth of tissue trauma is deeper than the penetration depth previously described [6, 13].

Studies evaluating the detrimental impact of Ho: YAG laser contact with human ureteric tissue are lacking, with available safety data relying on experiments in animal tissue [6, 9, 13–16]. One previous study in ex-vivo human ureter tissue evaluated the time to visual perforation when the laser fibre was in tangential contact with the specimen [17]. The objective of the present study is to evaluate and characterise the histological grades of iatrogenic human ureteral injury due to contact from the Ho: YAG laser at commonly used lithotripsy settings.

Methodology

Overview of experimental design

Ex-vivo testing of Ho: YAG laser was performed in direct contact with human ureteric tissue to evaluate the impact of commonly used laser settings, duration of contact and specimen characteristics on the level of laser injury. Following development and testing of an experimental protocol, a custom rig was developed to simulate clinical settings. The ureter was tested within one hour of collection, and testing was performed in a water bath at physiological temperature, with the laser in direct contact with the ureter. Histological review of specimens was used to determine the extent of laser injury and to evaluate for perforation of the ureter. Perforation was defined as trauma extending through all ureteric anatomical layers including the adventitia.

Specimen preparation

Following approval from our institutional research and ethics committee (Ref: 22/20), human ureteric specimens were extracted from consenting adults at the time of radical nephrectomy for renal malignancy. Intra-operatively, the ureter was divided at the bifurcation of the common iliac vessels and extracted with the kidney. Immediately after nephrectomy, the ureter was trimmed of peri-ureteric fat and transected at the renal pelvis. (Fig. 1a) The specimen was stored in normal saline 0.9% (NS0.9%) at 37.5 °C for a maximum of one hour prior to testing. The ureter was incised along its longitudinal axis to expose the urothelium for testing. (Fig. 1b) Specimen thickness was measured at three points using a digital calliper, and the mean of the three measurements used for specimen thickness.

Experimental set-up

A custom rig was developed for ex-vivo testing as in Fig. 2. Specimens were secured on sponge (Fig. 1b) and submerged in a water bath of NS0.9% at 37.5 °C. A 273 µm (micron) Ho: YAG laser fibre (Dornier MedTech Flexifiber©) was passed through a 6Fr (french) ureteric catheter and secured in place. The laser fibre was placed in direct contact with the urothelium in a parallel position to simulate the laser fibre position in the ureter when the patient is in the lithotomy position during ureteroscopy surgery.

Laser testing

A Dornier MedTech Medilas H20 Ho: YAG laser was used for all experiments. Applied settings were 8 Hz (Hertz) and 800 mJ (millijoules), 10 Hz and 1000 mJ, and 5 Hz and 1500 mJ for durations of 5, 10 and 20 s. Following testing, specimens were analysed for macroscopic trauma. Blue dye (Cancer diagnostics Inc. Tissue Marking Dye©) was used to mark the area adjacent to testing and then immediately placed in formalin.

Tissue processing

Samples were fixed, sectioned, and stained using hematoxylin and eosin (H&E) prior to microscopic and histological evaluation (Fig. 3A-L)). All specimens were reviewed by a blinded histopathologist who graded the depth and extent



Fig. 1 Caption: Preparation of human ureter
Legend: Steps of specimen preparation, with fresh ureter transected at the renal pelvis immediately following nephrectomy (**A**). The specimen is then trimmed and divided longitudinally to expose the urothelium, and is secured on a custom sponge using silk sutures (**B**). Following treatment, the specimens are trimmed and the area of treatment marked with blue dye prior to placement in formalin (**C**)

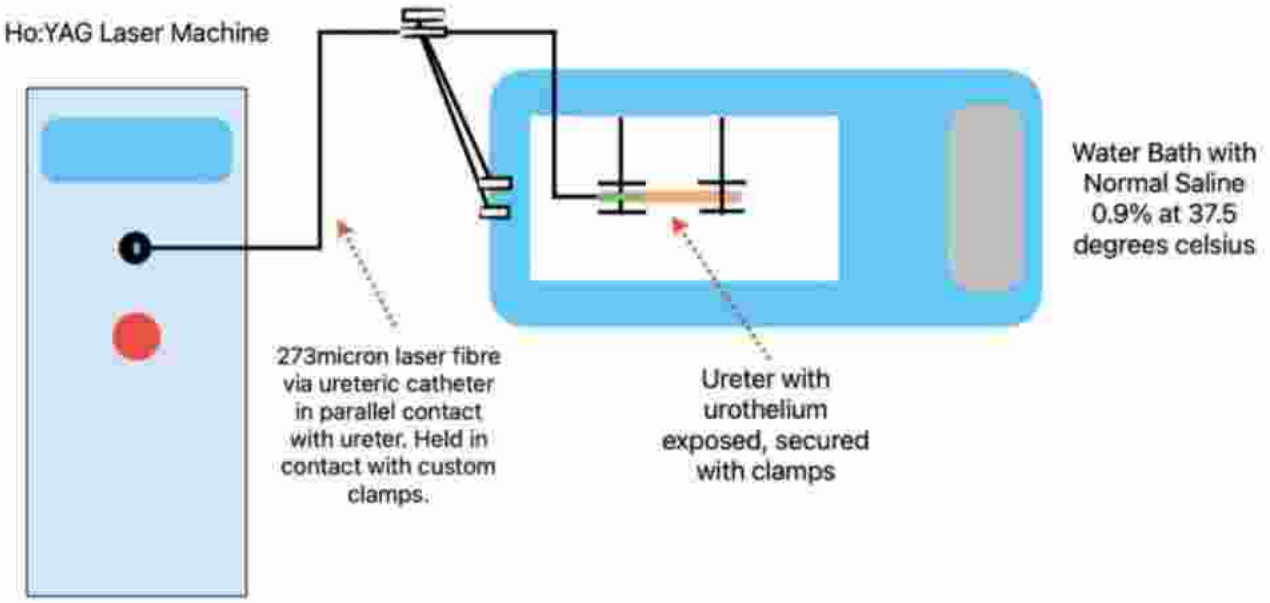


Fig. 2 Caption: Simplified diagram of experimental rig set-up
Legend: The specimen was secured as in Fig. 1B and placed in 37.5 C water bath with normal saline 0.9% A custom rig was used to hold the 273 μm Dornier Ho: YAG laser fibre which was passed through a 5Fr ureteric catheter and placed in direct contact parallel to the urothelium

of ureteral injury in each specimen. The level of iatrogenic trauma was defined by the deepest layer of tissue affected; urothelium, lamina propria, superficial muscularis, full thickness muscularis and adventitial perforation. Perforation was defined as trauma extending from the urothelium through all ureteric layers to include the adventitia.

Data analysis

Tissue characteristics and treatment variables (contact duration, laser settings) were inputted into Microsoft Excel to allow generation of descriptive statistics. Chi-Squared Test and Students Paired T-Tests were used to evaluate for statistically significant relationships between tissue and treatment

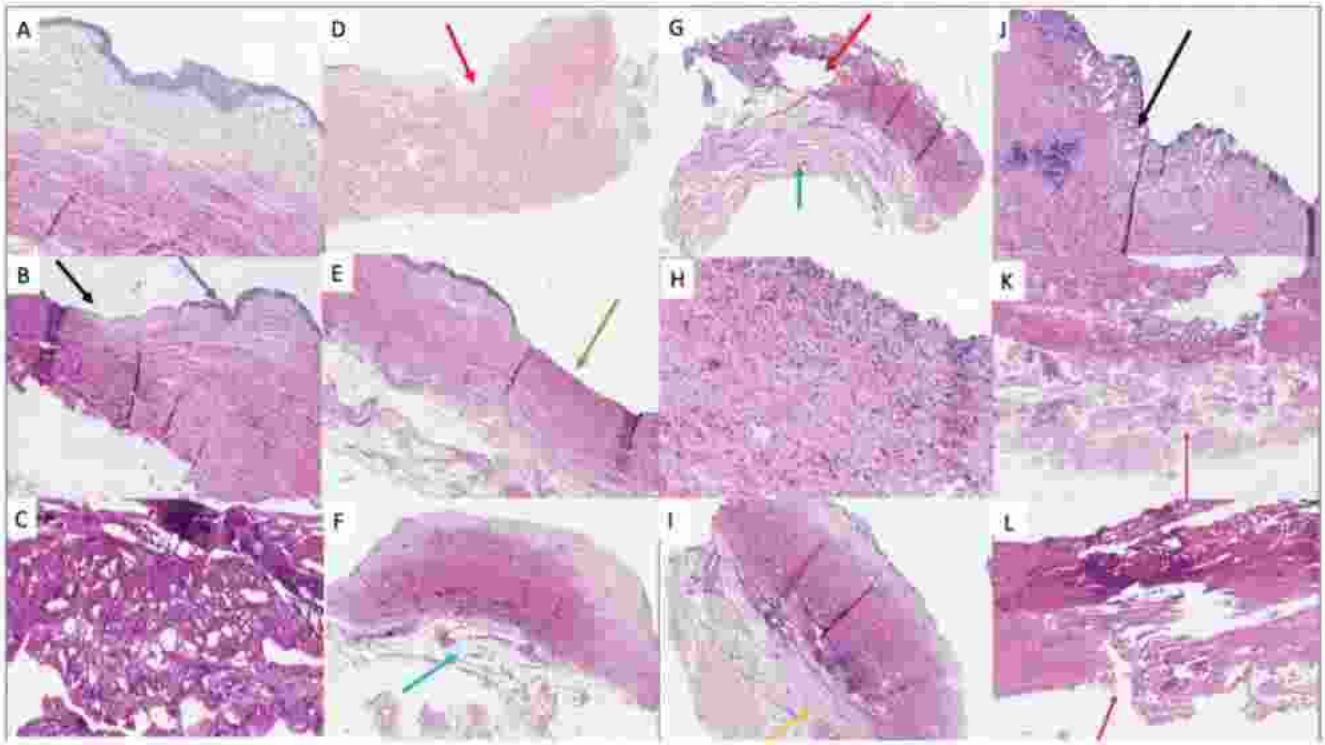


Fig. 3 Caption: Representative images of human ureter following fixation, H&E staining and sectioning with image. **A**: Normal ureter anatomy at 400x of magnification. **B**: Illustrates the transition from normal (blue arrow) to abnormal interface (black arrow) following treatment with Ho: YAG laser. **C**: High power view showing changes (60x magnification) that are suggestive of more severe trauma to the ureter with blurring of cell nuclei with significant distortion and homogenisation of the tissue with prominent vacuolar change. **D-F**: Laser trauma in specimens treated at 8 Hz and 800 mJ at 400x magnification. **D** shows trauma extending to the urothelium only in a 0.9 mm thick specimen treated for 5 s. There is focal loss of transitional epithelium (red arrow), but normal epithelium either side of this. The underlying layers of the ureter appear normal, with no obvious cautery damage. **E** is representative of a 0.9 mm specimen treated for 10 s with laser trauma extending to the superficial muscularis with mild homogenisation and blurring of nuclei (green arrow). The remainder of the muscularis layers appear normal, with no significant cautery damage or vacuolar change. **F** demonstrates adventitial perforation (blue arrow) after 20 s of treatment in a 2 mm thick specimen. **G-I**: Treatment at 10 Hz and 1000 mJ is displayed in figures **G-I** at 400x magnification. Figure **G** is a representative image from a 2 mm specimen treated for 7 s with trauma extending from the urothelium to the muscle (red arrow) but preservation of the outer adventitia (green arrow). A representative high-power image(300x) from a 3 mm specimen treated for 10 s is seen in figure **H**, with abnormal nuclei in the lamina propria. However, the remaining three specimens treated for 10 s all had injury extending to the superficial half of the muscularis. Treatment of a 2 mm thick specimen for 20 s shows changes extending from urothelium through to full thickness of muscularis but with preservation of the adventitia (yellow arrow). Figures **J-L** show representative images following treatment at 5 Hz and 1500 mJ. Full thickness perforation or full thickness muscularis trauma was seen in all specimens tested at this setting excluding one. Figure **J** is a representative image at 200x magnification from a 1.7 mm specimen treated for 5 s showing full thickness muscularis changes but no perforation (black arrow). Adventitial perforation (red arrows) is seen in Figure **K** after 10 s of laser contact in a 2.1 mm specimen and Figure **L** after 20 s of laser contact in a 2.75 mm laser specimen (400x magnification)

variables and full thickness ureter perforation. A p value of >0.05 was deemed statistically significant.

Results

Specimen characteristics

In total, 31 human ureter samples were tested from 8 consenting adults at the time of radical nephrectomy for suspected renal malignancy. The characteristics of each specimen are summarised in Table 1. The mean specimen thickness was 2.2 mm (range 0.9–3.1 mm). A histological sample of tissue showing normal ureter unaffected by laser trauma and the transition from normal ureter to laser trauma is illustrated in Fig. 3A and B.

Laser settings and duration of contact

The depth of laser related injury ranged from urothelium only to full thickness perforation at all settings tested (Fig. 3; Table 1). The abnormalities noted on histological analysis include blurring of nuclei, homogenisation of tissue and vacuolar change (Fig. 3C). Overall, the abnormalities were focal and appeared milder at lower power and frequency settings (8 Hz/800 mJ) but more extensive at higher power

Table 1 Specimen characteristics, testing protocols and anatomical level of laser related trauma

Settings Used	*N*	Nephrectomy Side	Anatomical Location	Previous Urology Intervention	Patient Sex	Specimen Thickness (mm)	Laser Contact Duration (s)	Level of Injury	
8 Hz	1	Left	Proximal	-	M	0.9	5	Urothelium	
800 mJ	2	Right	Proximal	Ureteroscopy	F	1.47	5	Muscularis	Inner half
	3	Right	Proximal	Ureteroscopy	F	1.47	5	Muscularis	Inner half
	4	Left	Proximal	-	M	0.9	10	Muscularis	Inner half
	5	Left	Proximal	-	M	0.9	10	Perforation	
	6	Left	Proximal	-	M	0.9	10	Urothelium	
	7	Left	Proximal	-	F	2	20	Muscularis	Full thickness
	8	Left	Proximal	-	F	2	20	Perforation	
	9	Left	Proximal	-	F	2	20	Muscularis	Inner Half
10 Hz	10	Right	Proximal	-	M	2	7	Muscularis	Full thickness
1000 mJ	11	Right	Proximal	-	M	1	6	Perforation	
	12	Right	Proximal	-	F	3	5	Muscularis	Full thickness
	13	Right	Proximal	-	F	3	5	Urothelium	
	14	Right	Proximal	-	F	3	10	Muscularis	Inner half
	15	Right	Proximal	-	F	3	10	Lamina Propria	
	16	Right	Proximal	-	F	3.1	10	Muscularis	Inner half
	17	Right	Proximal	-	F	3.1	10	Muscularis	Inner half
	18	Right	Proximal	-	M	3	20	Muscularis	Full thickness
	19	Right	Proximal	-	M	3	20	Muscularis	Inner half
	20	Right	Proximal	-	M	2	20	Muscularis	Full thickness
5 Hz	21	Right	Proximal	-	M	2.1	5	Perforation	
1500 mJ	22	Left	Proximal	-	F	1.7	5	Muscularis	Full Thickness
	23	Left	Proximal	-	F	1.7	5	Muscularis	Full Thickness
	24	Left	Proximal	-	M	2.75	10	Muscularis	Full thickness
	25	Right	Proximal	-	M	2.1	10	Muscularis	Full thickness
	26	Right	Proximal	-	M	2.1	10	Lamina Propria	
	27	Right	Proximal	-	M	2.1	10	Perforation	
	28	Left	Proximal	-	M	2.75	20	Muscularis	Full thickness
	29	Left	Proximal	-	M	2.75	20	Muscularis	Full thickness
	30	Left	Proximal	-	M	2.75	20	Perforation	
	31	Left	Proximal	-	M	2.75	20	Muscularis	Full thickness

(10 Hz/1000 mJ and 5 Hz/1500 mJ). This relationship was not statistically significant ($p=0.5$).

Testing settings of 8 Hz/800 mJ resulted in a range of injury from confined to the urothelium to full thickness perforation (Table 1; Figs. 3D-F). At short contact durations of 5 s, injury extended to the superficial level of muscle or urothelium only (Fig. 3D). At 20 s of contact, injury involved superficial muscle in one specimen, full thickness muscle trauma and full thickness ureter perforation (Fig. 3F). The specimens tested for 5 s all had thickness of 1.5 mm or less, compared to 2 mm at 20 s of treatment.

Laser settings of 10 Hz/1000 mJ were associated with injury, extending and ranging from urothelium only to full thickness perforation (Table 1; Fig. 3G-I). At the shortest duration of 5 s, injury varied from urothelium only to full thickness perforation (Fig. 3G). The specimen with full thickness perforation had a thickness of 1 mm. At 10 s injury extended to superficial muscle or lamina propria only, and at 20 s of contact duration injury involved muscularis in all cases (Figs. 3H-I).

The final settings of 5 Hz/1500 mJ had full thickness muscle injury or full thickness perforation in all specimens tested, excluding one which was confined to the lamina propria. (Table 1; Fig. 3J-L) Cautery changes extending to full thickness adventitia perforation and full thickness muscularis injury were seen at 5 s of contact at these settings (Fig. 3J). At 10 s of contact, injury extended to the lamina propria in one specimen, full thickness muscle trauma in one specimen and full thickness ureter perforation in the final specimen (Fig. 3K). At 20 s of contact, trauma extended from full thickness of the ureter in three specimens to perforation in one specimen (Fig. 3L). All specimens treated for 20 s at this setting were 2.75 mm thick (Table 1).

Overall, the level of injury seen with 5–10 s of treatment at any setting ranged from urothelium only to full thickness perforation depending on specimen thickness and laser power settings (Table 1). At 20 s of contact the minimal level of injury seen is superficial muscularis injury ($n=2$, 20%), however the majority of specimens had full thickness muscle changes or perforation ($n=8$, 80%).

Specimen thickness

There was variation in the thickness of specimens with a range from 0.9 to 3.1 mm. No full thickness perforation was seen in specimens≥3 mm ($n=8$), even at 20 s of contact duration at 10 Hz/1000 mJ (Table 1). Specimens of ≤1 mm ($n=5$) had levels of injury ranging from urothelium only to full thickness perforation. The remainder of specimens ranged from 1.1 to 2.9 mm ($n=18$) with level of injury involving lamina propria, muscularis and full thickness perforation. There is a trend towards perforation with reduced specimen thickness, this was not statistically significant ($p=0.18$).

Discussion

We present histological results of laser injury in human ureter using clinically relevant laser settings. Full thickness ureter perforation can occur at short contact durations and at low laser settings. The level of trauma produced by the laser is variable, with both superficial and extensive injury noted in different specimens at the same settings and duration of contact. Importantly, the thickness of ureteral specimens appears to be relevant in determining the extent of ureteral trauma following laser contact.

Our results show the impact of laser trauma to the ureter on a histological level with both thermal and mechanical injury. Thermal injury is noted as charring of tissue, blurring of nuclei, homogenisation of tissue and vacuolar change. Mechanical injury is noted as the destruction of tissue, with loss of tissue layers. The level of trauma varied from urothelium only to full thickness perforation through the adventitia. Similar injury types have been described in porcine studies with thermal laser injury noted as a discolouration rim of the entrance crater, the extent of which varied according to pulse rate [18]. Early studies in human ureter describe photothermal coagulation necrosis and fissures extending through ureteral layers [17]. Piergovanni et al. performed in-vivo porcine testing with delayed histological evaluation up to six days [16]. They described extensive lesions of partial or total necrosis of the porcine ureteral wall and urothelium with partial necrosis of muscle and lamina propria, and complete necrosis of urothelium [16]. This suggests that our results may underestimate the true extent of injury to the ureter with direct laser contact. In the real-life setting, the impact of inflammatory mediators and other clinical parameters may worsen the extent of injury seen.

The Ho: YAG laser has a good safety profile with a low risk of complications, however contemporary series have reported a stricture rate of up to 3% post ureteroscopy [19, 20]. This is higher than the rate of strictures seen with stones only, suggesting that the underlying pathology is related to treatment [20]. These strictures can be significant, with patients requiring further intervention including reconstructive surgery in 4.8% and nephrectomy in 1.7% [20]. Although the mechanisms for stricture formation are not fully understood and there are multiple potential contributing factors and ureteral perforation was identified as an independent significant risk factor for stricture formation [19]. It is theorised that the combination of periureteral fibrosis caused by urine extravasation and the inflammatory reaction caused by thermal injury leads to stricture formation [20]. Full thickness perforation was identified in $n=6$ (19.4%) of our specimens, including at short contact durations and commonly used laser settings. We suggest that endourologists should exercise caution even at settings that are considered conventionally safe, as inadvertent contact between the laser and urothelium may have considerable clinical consequences for the patient.

As seen in Table 1, there was variation in the thickness of ureteric specimens tested ranging from 0.9 to 3.1 mm. Previous anatomical and imaging based studies have also reported wide ranges of ureteral thickness [21–23]. Ureter wall thickness can be measured on axial non-contrast computed tomography, the clinical relevance of this measurement is yet to be fully determined [23]. A recent meta-analysis showed a statistically significant correlation between wall thickness and spontaneous stone passage in the setting of urolithiasis, with higher rates of stone passage seen in thinner wall thickness measurements [22]. Ureter wall thickness has also been shown to impact the likelihood of successful external shockwave lithotripsy, with increasing thickness associated with lower success rates [22, 24]. In our results the extent of laser related injury varied according to specimen thickness, although not statistically significant there was a trend towards less severe injury in thicker specimens. No full thickness perforation was seen in specimens≥3 mm, while in thinner specimens full thickness perforation was seen at 5 and 10 s contact. In the setting of stone impaction, the ureter may become inflamed, friable and prone to injury, so thicker tissue may also see significant trauma. Further studies comparing imaging based measurement of ureter wall thickness with pathological specimens and standardised imaging-based wall thickness measurement protocols are required. In the interim, surgeons should

be aware that ureter thickness varies widely from patient-to-patient, and that this may carry with it a higher risk of ureteral perforation at commonly used laser settings with inadvertent laser contact.

Selection of the appropriate laser settings depends on many factors including stone type, size and location, surgeon preference and experience, and anatomical features. The ''optimal' settings have yet to be defined and we chose to test commonly used laser settings that would represent the minimum and maximum expected power and frequency used in the ureter [9]. A previous review described "typical" fragmentation settings of 6–10 Hz and 1.0–1.2 J, with dusting settings of 0.2–0.4 J and 12–15 Hz [8]. A recent survey showed a preference for Ho: YAG for ureteral lithotripsy, with 80.8% of international experts surveyed choosing it over thulium fibre (TFL) or thulium-yttrium-aluminum-garnet (Tm: YAG) lasers [25]. The median maximum power used was 1000 mJ with a range of 500-1500 mJ, and a median maximum frequency of 15 Hz with a range of 6–50 Hz [25]. The settings we have chosen reflect commonly used settings in clinical practice and it is concerning to note that even at short contact durations (5 s) there can be injury extending to the muscularis, or indeed full thickness perforation.

Our testing was performed with a 273 µm fibre, the use of larger fibres may cause more significant injury at shorter durations or lower energy settings. Santa Cruz et al. evaluated Ho: YAG laser injuries in porcine ureter with a 365 µm fibre [15]. They describe ureter perforation at a minimum time frame regardless of frequency and power when in direct contact with the ureteric wall. At the minimum power setting of 1.0 W (200 mJ/5Hz) Ho: YAG produced a perforation within 1 s with a total energy of <0.01 kJ when placed in direct contact with the ureteral wall at a ninety degree angle [15]. There are some limitations to these results; the laser was placed perpendicular to the outer aspect of the ureter (adventitia), which does not represent the typical clinical scenario. Other experiments with a 400 µm fibre on porcine ureter saw perforation with 0.02 kJ of energy applied, but the authors did not describe the duration of laser to urothelium contact [16]. Early testing in human ureter with a 400 µm fibre saw rapid perforation in <1 s at 1500 mJ and 5 Hz, while in our specimens injury ranged from muscle to full thickness perforation at 5 s of contact at the same settings, and even at 20 s of contact there was only perforation in one of four specimens [17].

Ho: YAG has been the laser of choice for endourologists for over two decades with TFL representing the most common alternative due to its good dusting efficiency, low retropulsion and small fibre [25, 26]. In-vivo stone ablation in porcine ureters showed minimal urothelial damage with TFL or Ho: YAG on repeat inspection at 3 weeks and histological review of specimens [26]. Specific ex-vivo testing of TFL in direct perpendicular contact with porcine ureter showed a time to perforation of 7.9 s at 150 Hz and 1.8 s at 500 Hz [18]. Our results show full thickness perforation at 5 s of contact with 5 Hz and 10 Hz. Furthermore, we performed testing with the laser fibre parallel rather than perpendicular to the ureter in order to represent the position of the laser fibre in the ureter in conventional lithotomy position. This suggests the Ho: YAG laser may be safer than TFL, however comparative studies in human tissue are needed as well as further in-vivo testing to evaluate for other parameters that may contribute to tissue injury.

The limitations to our study include *ex*-vivo experiments and the contact durations sampled. Ex-vivo testing has its limits, as the impact of inflammatory mediators and tissue repair is absent. Intraoperative variations such as ureter oedema, inflammation, intra ureteric pressure, intra ureteric temperature and the manual pressure applied to the laser fibre could also affect the time to ureter perforation. We are limited with the in-vivo testing we can perform in human tissue, as it would not be appropriate to intentionally laser human ureter and remove it for pathological analysis. Nonetheless our ex-vivo findings contribute knowledge of Ho: YAG laser interaction with human tissue as current data relies mainly on animal studies [15, 16, 18]. Although providing useful information about the extent and type of injury associated with laser usage, the clinical application of these studies is limited as the laser was either applied to the ureter at a perpendicular angle or to the adventitia rather than the urothelium. The one previous study that evaluated laser injury in ex-vivo human tissue used a 400 µm fibre which is not commonly used in the ureter [17]. It is also unclear at what angle the laser was placed in contact with the ureter, and only a small number of specimens were tested ($n=7$) [17]. Our experiments were performed with a 273 µm fibre which was in parallel contact to the ureter to simulate the position the laser fibre is in during ureteroscopy with the patient in the lithotomy position. A limitation to our study may include the contact durations chosen of 5, 10 and 20 s. We chose these as we considered them to show the extremes of laser contact that the ureter may be exposed to. Previous studies have focused on time to perforation using video or visual contact to confirm it, however it is not possible to determine microscopic perforation based on this basis alone and we wanted to evaluate the extent/depth of injury as opposed to purely full-thickness perforation [16, 17].

Conclusion

This is the first study to evaluate laser injury in human ureter at commonly used laser settings with the Ho: YAG laser. Our results show that full thickness perforation and muscle injury occurs at commonly used laser settings. Further in-vivo testing is required to evaluate for other contributing parameters such as ureteric thickness and the impact of the inflammatory response in the ureter to laser contact and temperature. We suggest that the impact of laser contact may be more important than previously documented. In addition to stone parameters, measurement of ureteric thickness, with non-contrast CT, should be considered during pre-operative surgical evaluation of symptomatic urolithiasis patients. With the advent of new laser types, more powerful equipment and a move towards minimally invasive techniques we must advocate that the clinical implications of iatrogenic laser contact with human urothelium should not be forgotten.

Acknowledgements The authors wish to acknowledge the assistance of Grace Hogan, Derek Borwick and Martin Dunphy for their assistance in specimen storage and sourcing of appropriate equipment.

Author contributions SOM, EC and ND wrote the main manuscript. ND, FJOB, MTW, BS were involved in supervision and experiment design. KS, JF and TOG processed and reviewed all specimens, and were involved in development of protocol for tissue processing and handling. DH, GC and SOM performed experiments. SOM, EC, SC, KS processed data and generated results. All authors reviewed manuscript.

Funding Open Access funding provided by the IReL Consortium

Data availability No datasets were generated or analysed during the current study.

Declarations

Ethical approval Ethical approval was received from Beaumont Hospital research and ethics committee (ref 22/20). Financial support was provided via the StAR Programme through the Royal College of Surgeons of Ireland and Blackrock Health. The authors have no other financial or ethical disclosures.

Competing interests The authors declare no competing interests.

Open Access This article is licensed under a Creative Commons Attribution 4.0 International License, which permits use, sharing, adaptation, distribution and reproduction in any medium or format, as long as you give appropriate credit to the original author(s) and the source, provide a link to the Creative Commons licence, and indicate if changes were made. The images or other third party material in this article are included in the article's Creative Commons licence, unless indicated otherwise in a credit line to the material. If material is not included in the article's Creative Commons licence and your intended use is not permitted by statutory regulation or exceeds the permitted use, you will need to obtain permission directly from the copyright holder. To view a copy of this licence, visit http://creativecommons.org/licenses/by/4.0/.

References

1. Scarpa RM et al (1999) Holmium:YAG laser ureterolithotripsy. Eur Urol 35(3):233–238
2. Shroff S et al (1996) The holmium: YAG laser for ureteric stones. Br J Urol 78(6):836–839
3. Bagley D, Erhard M (1995) Use of the holmium laser in the upper urinary tract. Tech Urol 1(1):25–30
4. Devarajan R et al (1998) Holmium: YAG Lasertripsy for ureteric calculi: an experience of 300 procedures. Br J Urol 82(3):342–347
5. Jiang H et al (2007) Ureteroscopic treatment of ureteral calculi with holmium: YAG laser lithotripsy. J Endourol 21(2):151–154
6. Emiliani E et al (2018) The true ablation effect of holmium YAG laser on soft tissue. J Endourol 32(3):230–235
7. Wollin DA et al (2018) Effect of laser settings and irrigation rates on ureteral temperature during holmium laser lithotripsy, an in vitro model. J Endourol 32(1):59–63
8. Matlaga BR et al (2018) Ureteroscopic laser lithotripsy: A review of dusting vs fragmentation with extraction. J Endourol 32(1):1–6
9. Sierra A et al (2022) Glossary of pre-settings given by laser companies: no consensus! World J Urol 40(9):2313–2321
10. Ventimiglia E (2019) T.O. *Laser Lithotripsy Principles*. Available from: https://caunet.org/en/news/laser-lithotripsy-principles-2/
11. Skolarikos A, Petřík ANA, Somani B, Thomas K, Gambaro G, Davis NF, Geraghty R, Lombardo R, Tzelves L, Shepherd R (2022) *EAU Guidelines on Urolithiasis*.
12. Tzelves L et al (2021) Basic and advanced technological evolution of laser lithotripsy over the past decade: an educational review by the European society of urotechnology section of the European association of urology. Turk J Urol 47(3):183–192
13. Johnson DE, Cromeens DM, Price RE (1992) Use of the holmium:yag laser in urology. Lasers Surg Med 12(4):353–363
14. Hardy LA et al (2014) Thulium fiber laser lithotripsy in an in vitro ureter model. J Biomed Opt 19(12):128001
15. Santa-Cruz RW, Leveillee RJ, Krongrad A (1998) Ex vivo comparison of four lithotripters commonly used in the ureter: what does it take to perforate? J Endourol 12(5):417–422
16. Piergiovanni M et al (1994) Ureteral and bladder lesions after ballistic, ultrasonic, electrohydraulic, or laser lithotripsy. J Endourol 8(4):293–299
17. Sayer J et al (1993) Ureteral lithotripsy with the holmium:yag laser. J Clin Laser Med Surg 11(2):61–65
18. Wilson CR et al (2015) Collateral damage to the ureter and nitinol stone baskets during thulium fiber laser lithotripsy. Lasers Surg Med 47(5):403–410
19. Ulvik Ø, Harneshaug JR, Gjengstø P (2021) Ureteral Strictures Following Ureteroscopic Stone Treat J Endourol 35(7):985–990
20. Sunaryo PL et al (2022) Ureteral strictures following ureteroscopy for kidney stone disease: A Population-based assessment. J Urol 208(6):1268–1275
21. De Nunzio C et al (2022) Ureteral wall thickness and distal ureteral density in patients with residual fragments after Ho:YAG laser semi-rigid ureterolithotripsy. Lasers Med Sci 38(1):19
22. Dean NS et al (2023) Ureteral wall thickness is an effective predictor of ureteral stone impaction and management outcomes: A systematic review and Meta-analysis. J Urol 210(3):430–437
23. Yoshida T et al (2017) Ureteral wall thickness as a preoperative Indicator of impacted stones in patients with ureteral stones undergoing ureteroscopic lithotripsy. Urology 106:45–49

24. Güler Y (2023) Non-contrast computed tomography-based factors in predicting ESWL success: A systematic review and meta-analysis. Prog Urol 33(1):27–47
25. Ortner G et al (2024) Experts' recommendations in laser use for the treatment of urolithiasis: a comprehensive guide by the European section of Uro-Technology (ESUT) and Training-Research in urological surgery and technology (T.R.U.S.T.)-Group. World J Urol 42(1):33
26. Sierra A et al (2022) Laser efficiency and laser safety: holmium YAG vs. Thulium Fiber laser. J Clin Med, 12(1)

Publisher's note Springer Nature remains neutral with regard to jurisdictional claims in published maps and institutional affiliations.

《世界泌尿学杂志》（2025年）第43卷第354页
https://doi.org/10.1007/s00345-025-05713-2

研究

医源性人类输尿管激光损伤的表征——基于常用碎石设置下Ho：YAG激光离体测试的结果

S.O' Meara[1,2] · K. Sheehan[3,4] · J. Fay[5] · T. O' Grady[3,5] · S. M. Croghan[1,2] · E. M. Cunnane[7,8] · D. Hogan[6] · G. G. Calpin[6] · B. Somani[10] · M. T. Walsh[7,8] · F. J. O' Brien[9] · N. F. Davis[1,2,8]

收到日期：2024年10月11日/接受日期：2025年5月18日
© 作者 2025

摘要

引言 现代经尿道泌尿外科手术依赖Ho：YAG激光器对尿石症进行根治性治疗。目前的安全性数据主要来源于Ho：YAG激光器在动物组织中的测试。我们的目标是评估和表征该激光器的分级。在常用碎石治疗参数下，接触Ho：YAG激光导致的人类输尿管损伤模型

方法学 在根治性肾切除术时，从同意参与研究的成年人体内采集输尿管。我们开发了一种定制装置，用于将273微米（μm）激光光纤与尿路上皮接触5、10和20秒。测试设置包括8赫兹（Hz）和800毫焦（mJ）、10赫兹/1000毫焦以及5赫兹/1500毫焦。随后通过组织病理学对输尿管损伤程度进行表征。

实验结果 显示，共检测31个样本，平均厚度为2.2毫米（范围0.9-3.1毫米）。激光损伤深度根据激光与组织接触时间和样本厚度的不同，在不同参数设置下呈现从仅损伤尿路上皮到全层穿孔的多种情况。值得注意的是，即使在10赫兹/1000毫焦耳的参数下持续接触20秒，厚度≥3毫米的样本也未出现全层穿孔。但在厚度<1毫米的样本中，经过5秒测试后，损伤深度范围从仅损伤尿路上皮到完全穿透组织层不等。

讨论 Ho：YAG激光可造成不同程度的损伤，包括浅表损伤和广泛性损伤。输尿管的厚度可能决定激光接触后的创伤程度。令人担忧的是，使用常用的激光设置和短时间的激光接触可能造成输尿管全层穿孔。

关键词 膀胱结石病·激光·腔内泌尿外科·医源性损伤·狭窄

✉ S.O' Meara
sorchaomeara@rcsi.ie

1 战略学术招聘（StAR）计划，爱尔兰皇家外科学院，爱尔兰都柏林

2 泌尿外科，Blackrock Health，Blackrock，都柏林，爱尔兰

3 爱尔兰都柏林皇家外科医师学院病理学系

4 爱尔兰都柏林Blackrock Health病理学系

5 RCSI生物样本库，病理学系，爱尔兰皇家外科医师学会，爱尔兰都柏林

6 爱尔兰都柏林博蒙特医院泌尿外科

7 生物材料集群，伯纳尔研究所，利默里克大学，爱尔兰利默里克

8 利默里克大学工程学院，爱尔兰利默里克

9 爱尔兰皇家外科学院组织工程研究组，爱尔兰都柏林

10 英国南安普敦SO16 6YD，南安普敦大学医院NHS基金会信托机构泌尿外科

Published online: 04 June 2025

缩略语

Fr French 法国
H&E Hematoxylin and eosin 苏木精-伊红
Hz Hertz 赫兹
Ho:YAG Holmium: yttrium – aluminium – garnet 钬：钇铝石榴石
IRP Intra – renal pressures 肾内压力
IRT Intra – renal temperature 肾内温度
mj Millijoules 毫焦耳
TFL Thulium fibre laser 铥光纤激光器
Tm:YAG Thulium – yttrium – aluminum – garnet 铥：钇铝石榴石
nm Nanometers 纳米
NS0.9% Normal Saline 0.9% 生理盐水 0.9%
µm Micron 微米

介绍

钬：钇铝石榴石（Ho：YAG）手术激光在泌尿内镜领域的碎石术和组织消融术中具有明确应用价值。其组织穿透深度约为0.4毫米（mm），这一特性使得该激光具有良好的安全性，临床研究显示其组织损伤发生率较低[1–7]。尽管应用广泛，但关于如何在确保患者安全的前提下，选择最优化的Ho：YAG参数以实现高效结石或组织破坏，目前仍存在学术争议[8–12]。最新离体动物研究表明，实际组织损伤深度可能比既往描述的穿透深度更深[6，13]。

目前针对Ho：YAG激光与人类输尿管组织接触危害性的研究尚不充分，现有安全性数据主要基于动物实验[6，9，13–16]。此前一项离体人类输尿管组织研究评估了激光光纤与样本接触时出现可见穿孔所需时间[17]。本研究旨在通过分析常用碎石治疗参数下Ho：YAG激光接触导致的人类输尿管医源性损伤，评估并表征其组织学分级特征。

方法学

实验设计概述

为评估常用激光参数、接触时长及样本特性对激光损伤程度的影响，研究人员将Ho：YAG激光与人输尿管组织直接接触进行离体测试。在制定实验方案并完成测试后，开发了定制化装置以模拟临床环境。输尿管样本采集后1小时内即进行测试，实验在生理温度的水浴中完成。

将激光直接接触输尿管。通过组织学标本复查评估激光损伤程度及输尿管穿孔情况。穿孔定义为创伤穿透所有输尿管解剖层（包括外膜）。

标本制备

经本机构研究与伦理委员会批准（批准号：22/20），我们从同意参与研究的成年患者肾癌根治术中获取输尿管标本。术中于髂总动脉分叉处切断输尿管并连带肾脏一并取出。肾切除术后立即清除输尿管周围脂肪组织，并在肾盂处进行横断。（图1 a）标本置于0.9%生理盐水（NS0.9%）中，37.5°C保存不超过1小时后进行检测。沿输尿管纵轴切开以暴露尿路上皮组织用于检测。（图1 b）使用数字卡尺在三个位置测量标本厚度，取三次测量的平均值作为最终厚度数据。

实验装置

如图2所示，我们开发了一种用于离体测试的定制化装置。将标本固定在海绵上（图1 b），并浸入37.5°C的0.9%生理盐水水浴中。将一根273 µm（微米）Ho：YAG激光光纤（Dornier MedTech Flexifiber©）通过6Fr（法国）输尿管导管穿入并固定到位。该激光光纤与尿路上皮直接接触，其平行位置模拟了患者在输尿管镜手术中采取碎石位时激光光纤在输尿管内的位置。

激光检测

所有实验均采用Dornier MedTech Medilas H20 Ho：YAG激光器。实验参数设置为：8 Hz（赫兹）与800 mJ（毫焦耳）、10 Hz与1000 mJ、5 Hz与1500 mJ，持续时间分别为5秒、10秒和20秒。测试完成后，对样本进行宏观创伤分析。使用蓝色染料（Cancer diagnostics Inc. Tissue Marking Dye©）标记测试区域邻近部位，随后立即置于福尔马林中。

组织处理

样本经固定、切片后，采用苏木精-伊红（H&E）染色法进行显微镜及组织学评估（图3 A-L）。所有标本均由盲法组织病理学家审核，并对每个标本的输尿管损



图1 题注：人输尿管的制备
图例：标本制备步骤。肾切除术后立即在肾盂处切断新鲜输尿管（**A**）。然后将标本修剪并纵向分离，以暴露尿路上皮，并使用用丝线固定在定制薄膜上（**B**）。处理后，标本被修剪，处理区域用蓝色染料标记，然后放入福尔马林中（**C**）

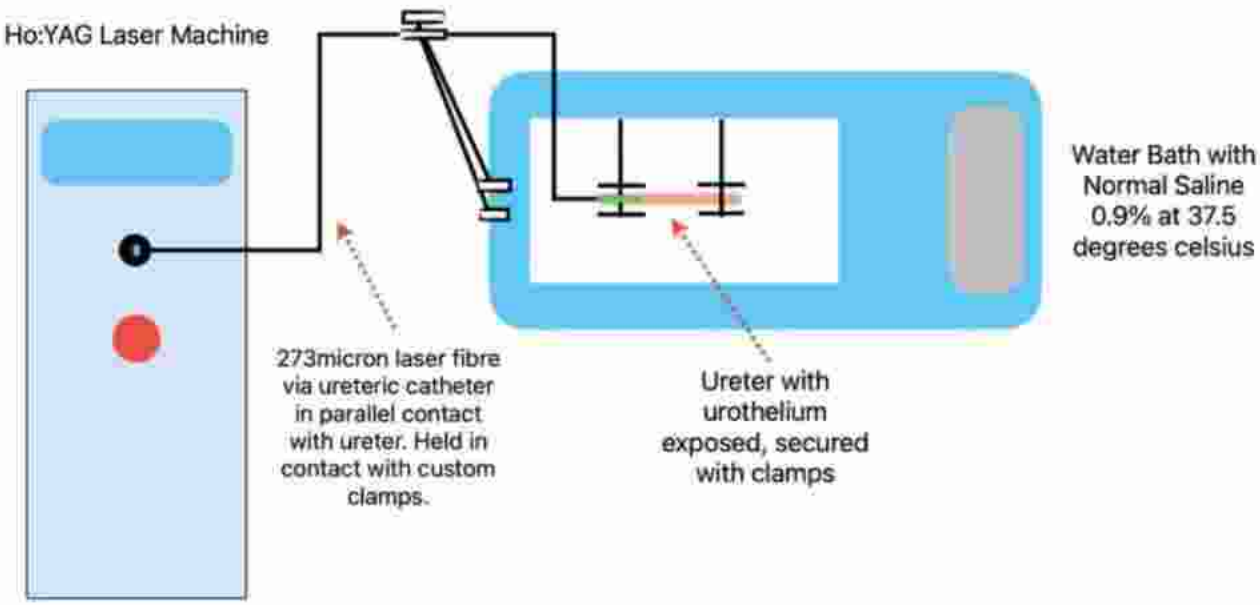


图2 题注：实验装置简化示意图
图例：如图1B所示，将标本固定在含有0.9%生理盐水的37.5℃水浴中。使用定制的装置固定273 μm Dornier Ho: YAG激光纤维，该纤维通过5Fr输尿管导管并与尿路上皮平行直接接触

伤深度和范围进行分级。医源性创伤的严重程度根据受累最深的组织层来定义：尿路上皮、固有层、浅肌层、全层肌层及外膜穿孔。穿孔的定义为创伤从尿路上皮贯穿所有输尿管层，包括外膜。

数据分析

将组织特征和治疗变量（接触时间、激光参数）输入Microsoft Excel以生成描述性统计。卡方检验和学生配对t检验用于评估组织和治疗变量与全层输尿管穿

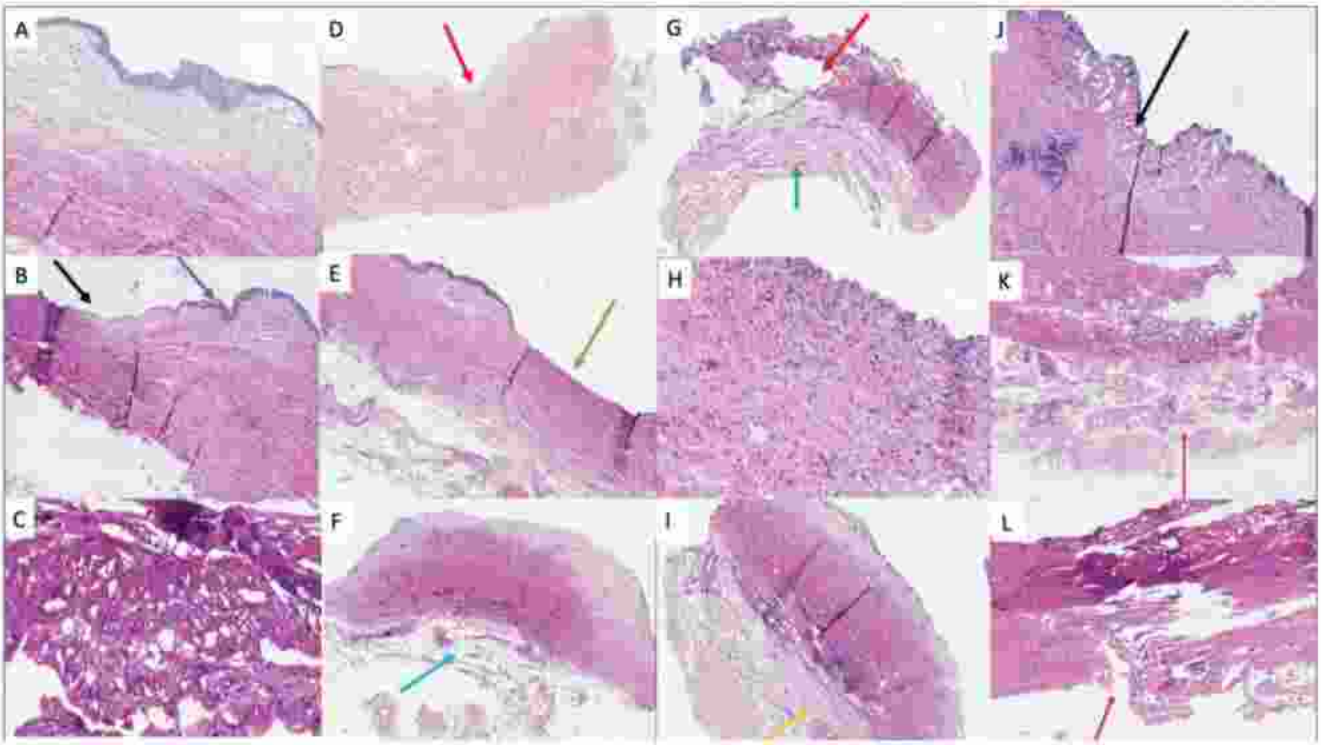


图3 题注：人类输尿管固定、H&E染色及切片后的代表性图像。**A**：400倍放大下的正常输尿管解剖结构。**B**：展示经Ho：YAG激光处理后从正常界面（蓝色箭头）向异常界面（黑色箭头）的转变。**C**：60倍放大下的高倍视野显示输尿管遭受更严重损伤的迹象：细胞核模糊、组织显著变形与均质化，可见明显空泡改变。**D-F**：8Hz，800mJ激光处理样本在400倍放大下的损伤情况。**D**展示仅在0.9毫米厚样本中延伸至尿路上皮的损伤（处理时间5秒）。局部移行上皮缺失（红色箭头），但两侧上皮结构正常。输尿管底层未见明显烧灼损伤。**E**展示0.9毫米样本经10秒激光处理后损伤延伸至浅肌层，可见轻度组织均质化及细胞核模糊（绿色箭头）。肌层的其余部分看起来正常，没有明显的电灼损伤或空泡改变。在2mm厚的标本中，**F**显示了20秒治疗后的外膜穿孔（蓝色箭头）。**G-I**：在400倍放大的的G-I图中显示了10 Hz和1000 mJ的治疗。图**G**展示了2毫米样本经7秒处理后的典型图像，可见损伤范围从尿路上皮延伸至肌层（红色箭头），但外膜层（绿色箭头）得以保留。图**H**展示了3毫米样本经10秒处理后的典型300倍高倍图像，固有层出现异常细胞核。然而其余三个经10秒处理的样本均显示损伤延伸至肌层浅层。2毫米厚样本经20秒处理后，损伤范围从尿路上皮贯穿至肌层全层，但外膜层（黄色箭头）仍保持完整。图**J-L**展示了5赫兹频率和1500毫焦耳量处理后的典型图像。在此参数设置下，所有测试样本（除一个外）均出现肌层全层穿孔或损伤。图**J**展示了1.7毫米样本经5秒处理后的200倍放大图像，可见肌层全层改变但未出现穿孔（黑色箭头）。在2.1 mm标本中，激光接触10秒后可见外膜穿孔（红色箭头）；在2.75 mm激光标本中，激光接触20秒后可见外膜穿孔（400倍放大）（图**K**和图**L**）。

孔之间的统计学显著性关系。。Ap值>0.05被认为具有统计学意义。

结果

标本特征

本研究共检测了8名同意参与的成年患者在根治性肾切除术（疑似肾恶性肿瘤）时提供的31份人类输尿管样本。各标本特征汇总于表1中。标本平均厚度为2.2毫米（范围0.9–3.1毫米）。图3A和B显示了未受激光损伤影响的正常输尿管的组织学样本，以及从正常输尿管到激光损伤的转变。

激光设置与接触持续时间

在所有测试参数下，激光损伤深度从仅累及尿路上皮到全层组织穿孔不等（图3；表1）。组织学分析显示的异常包括细胞核模糊、组织均质化及空泡样改变（图3C）。在低功率和频率（8 Hz/800 mJ）下，异常程度较轻，但在高功率（10 Hz/1000 mJ和5 Hz/1500 mJ）下，

表1标本特征、检测方案和激光相关创伤的解剖学水平

已用设置	N	肾切除术侧切	解剖学位置	既往泌尿外科介入治疗	患者性别	标本厚度（毫米）	激光接触持续时间（秒）	损伤程度	
8 Hz	1	左	近端的	-	M	0.9	5	尿路上皮	
800 mJ	2	右	近端的	输尿管镜检查	F	1.47	5	肌性	内半部
	3	右	近端的	输尿管镜检查	F	1.47	5	肌性	内半部
	4	左	近端的	-	M	0.9	10	肌性	内半部
	5	左	近端的	-	M	0.9	10	穿孔	
	6	左	近端的	-	M	0.9	10	尿路上皮	
	7	左	近端的	-	F	2	20	肌性	全层厚度
	8	左	近端的	-	F	2	20	穿孔	
	9	左	近端的	-	F	2	20	肌性	内半部
10 Hz	10	右	近端的	-	M	2	7	肌性	全层厚度
1000 mJ	11	右	近端的	-	M	1	6	穿孔	
	12	右	近端的	-	F	3	5	肌性	全层厚度
	13	右	近端的	-	F	3	5	尿路上皮	
	14	右	近端的	-	F	3	10	肌性	内半部
	15	右	近端的	-	F	3	10	固有层	
	16	右	近端的	-	F	3.1	10	肌性	内半部
	17	右	近端的	-	F	3.1	10	肌性	内半部
	18	右	近端的	-	M	3	20	肌性	全层厚度
	19	右	近端的	-	M	3	20	肌性	内半部
	20	右	近端的	-	M	2	20	肌性	全层厚度
5 Hz	21	右	近端的	-	M	2.1	5	穿孔	
1500 mJ	22	左	近端的	-	F	1.7	5	肌性	满的厚度
	23	左	近端的	-	F	1.7	5	肌性	满的厚度
	24	左	近端的	-	M	2.75	10	肌性	全层厚度
	25	右	近端的	-	M	2.1	10	肌性	全层厚度
	26	右	近端的	-	M	2.1	10	固有层	
	27	右	近端的	-	M	2.1	10	穿孔	
	28	左	近端的	-	M	2.75	20	肌性	全层厚度
	29	左	近端的	-	M	2.75	20	肌性	全层厚度
	30	左	近端的	-	M	2.75	20	穿孔	
	31	左	近端的	-	M	2.75	20	肌性	全层厚度

异常范围较广泛。该关系无统计学意义（$p=0.5$）。

在8赫兹/800毫焦耳的测试参数下，损伤程度从仅限于尿路上皮到完全穿透全层不等（表1；图3 D-F）。当接触时间缩短至5秒时，损伤仅限于肌肉或尿路上皮的浅表层（图3 D）。而接触20秒后，一个样本出现浅层肌肉损伤、肌肉全层创伤及输尿管全层穿孔（图3 F）。经测试发现，5秒处理的样本厚度均不超过1.5毫米，而20秒处理的样本厚度达到2毫米。

当激光参数设置为10赫兹/1000毫焦耳时，可引发损伤，损伤范围从仅累及尿路上皮到全层组织穿孔不等（表1；图3 G-I）。在最短5秒的照射时间下，损伤程度同样呈现从尿路上皮到全层穿孔的渐进变化（图3 G）。其中全层穿孔样本的厚度达到1毫米。接触10 s时损伤范围仅为浅表肌层或固有层，接触20 s时损伤均累及肌层（图3H-I）。

在5赫兹/1500毫焦耳的最终参数设置下，所有测试样本均出现全层肌肉损伤或全层穿孔，仅有一例损伤局限于固有层（表1；图3 J-L）。接触5秒时，这些参数设置下可见烧灼伤扩展至全层外膜穿孔和全层肌层损伤（图3 J）。接触10秒时，一个样本的损伤扩展至固有层，一个样本出现全层肌肉创伤，最后一个样本则发生全层输尿管穿孔（图3 K）。接触20秒时，三个样本的创伤从输尿管全层延伸至穿孔，一个样本出现穿孔（图3 L）。所有在此参数设置下处理20秒的样本厚度均为2.75毫米（表1）。

总体而言，在任何设置下，5-10秒治疗所见损伤程度范围从仅尿路上皮损伤到全层穿孔，具体取决于标本厚度和激光功率设置（表1）。在20秒接触时间下，所见最小损伤程度为浅层肌层损伤（n=2,20%），但大多数标本出现全层肌肉改变或穿孔（n=8,80%）。

标本厚度

样本厚度存在差异，范围在0.9至3.1毫米之间。在接触持续时间为20秒、频率为10赫兹/1000毫焦耳的条件下，厚度≥3毫米的样本（样本量n=8）均未出现全层穿孔（表1）。厚度≤1毫米的样本（样本量n=5）损伤程度从仅累及尿路上皮到全层穿孔不等。其余样本厚度介于1.1至2.9毫米之间（样本量n=18），损伤范围涉及固有层、肌层直至全层穿孔。样本厚度越薄，出现穿孔的趋势越明显，但该趋势无统计学意义（p=*0.18*）。

讨论

我们展示了采用临床相关激光参数对人输尿管进行激光损伤后的组织学结果。在短接触时间和低激光参数下，输尿管可能发生全层穿孔。激光产生的创伤程度具有变异性，即使在相同参数和接触时间下，不同标本中均可见浅表性与广泛性损伤。值得注意的是，输尿管标本的厚度似乎与激光接触后输尿管创伤程度的判定相关。

我们的研究结果从组织学层面揭示了激光对输尿管造成的热损伤与机械损伤双重作用。热损伤表现为组织焦化、细胞核模糊、组织均质化及空泡改变；机械损伤则表现为组织破坏及多层组织缺失。损伤程度从仅累及尿路上皮到穿透外膜形成全层穿孔不等。类似损伤模式在猪模型研究中也有记载，其中热激光损伤表现为入口凹陷边缘变色，其范围随脉冲频率变化[18]。早期人类输尿管研究描述了光热凝固性坏死及贯穿输尿管各层的裂隙[17]。Piergovanni等学者通过活体猪模型实验进行延迟组织学评估（最长达六天）[16]，发现猪输尿管壁及尿路上皮出现广泛部分或完全坏死，肌层与固有层部分坏死，尿路上皮完全坏死[16]。这表明我们的结果可能低估直接激光接触对输尿管造成的实际损伤程度。在真实临床环境中，炎症介质及其他临床参数的影响可能导致观察到的损伤程度加重。

Ho：YAG激光具有良好的安全性，并发症风险较低。但最新研究数据显示，输尿管镜术后狭窄发生率最高可达3%[19，20]。这一比例高于单纯结石引发的狭窄发生率，表明潜在病理机制与治疗方式存在关联[20]。这些狭窄可能较为严重，其中4.8%的患者需接受重建手术，1.7%的患者则需行肾切除术。

[20]尽管狭窄形成的机制尚未完全阐明，且存在多种潜在致病因素，但输尿管穿孔已被确认为狭窄形成的独立显著危险因素[19]。理论推测认为，尿液外渗导致的输尿管周围纤维化与热损伤引发的炎症反应共同作用，最终导致狭窄形成[20]。在本研究样本中，共发现6例（19.4%）出现全层穿孔，其中包含接触时间较短及常规激光参数设置的情况。我们建议，即使在传统认为安全的参数设置下，泌尿外科医生仍需保持谨慎，因为激光与尿路上皮的意外接触可能对患者造成重大临床后果。

如表1所示，受检输尿管标本的厚度存在0.9至3.1毫米的差异。既往基于解剖学和影像学的研究也报道了输尿管厚度的广泛范围[21–23]。输尿管壁厚度可通过轴位非增强计算机断层扫描进行测量，但该测量指标的临床意义尚未完全明确[23]。近期一项荟萃分析显示，在尿石症患者中，壁厚与结石自发排出率存在统计学显著相关性，壁厚较薄的标本结石排出率更高[22]。研究还表明，输尿管壁厚会影响体外冲击波碎石术的成功率，壁厚增加与成功率降低相关[22，24]。本研究结果显示，激光损伤程度与标本厚度相关，尽管无统计学显著性，但较厚标本的损伤程度呈现轻度趋势。在≥3毫米的标本中未观察到全层穿孔，而较薄标本在接触5秒和10秒时可见全层穿孔。在结石嵌顿情况下，输尿管可能发生炎症、变脆并易受损伤，因此较厚组织也可能出现显著创伤。需要进一步开展基于影像学测量的输尿管壁厚度与病理标本及标准化影像学壁厚测量方案的对比研究。在此期间，外科医师应

意识到，不同患者的输尿管厚度有很大差异，这可能会导致在常用激光设置下无意中接触到输尿管穿孔的较高风险。

激光参数的选择需综合考虑结石类型、大小、位置、术者偏好与经验以及解剖结构等多重因素。目前尚未明确“最佳”参数设置，我们选择测试代表输尿管碎石术常规使用的最小和最大预期功率及频率的激光参数[9]。既往综述指出，“典型”碎石参数为6-10 Hz和1.0-1.2 J，碎石参数为0.2-0.4 J和12-15 Hz[8]。最新调查显示，80.8%的国际专家更倾向于使用Ho：YAG激光进行输尿管碎石术，而非钬光纤（TFL）或铥-钇-铝石榴石（Tm：YAG）激光[25]。所用参数的中位最大功率为1000 mJ（范围500-1500 mJ），中位最大频率为15 Hz（范围6-50 Hz）[25]。我们选择的参数反映了临床实践中的常规设置，值得注意的是，即使接触时间较短（5秒），仍可能导致肌层损伤甚至全层穿孔。

我们的实验使用273 μm 光纤进行测试，若改用更大规格的光纤，在较短照射时间或较低能量设置下可能导致更严重的损伤。Santa Cruz等学者曾采用365 μm 光纤评估Ho：YAG激光对猪输尿管的损伤效果[15]。他们指出，当激光以直角接触输尿管壁时，无论照射频率和功率如何，输尿管穿孔的最短时间阈值始终存在。在最低功率1.0 W（200 mJ/5Hz）条件下，Ho：YAG激光以直角接触输尿管壁时，仅需1秒即可产生穿孔，总能量 < 0.01 kJ[15]。但该研究存在局限性：激光器垂直置于输尿管外层（外膜）的实验设置，与临床典型场景不符。另有研究使用400 μm 光纤对猪输尿管进行实验，发现0.02 kJ能量即可引发穿孔，但作者未说明激光与尿路上皮接触的持续时间[16]。在人类输尿管中使用400 μm 光纤进行早期测试时，在1500 mJ和5 Hz条件下，1秒内即发生快速穿孔；而在我们的样本中，相同设置下接触5秒时，损伤范围从肌肉到全层穿孔不等，即使接触20秒，四个样本中也仅有一个出现穿孔[17]。

Ho：YAG激光是泌尿外科医生二十多年来首选的激光，TFL因其良好的粉尘效率、低反冲力和细光纤而成为最常用的替代选择[25，26]。在猪输尿管的体内结石消融实验中，TFL或Ho：YAG在3周复查时均显示出最小的尿路上皮损伤和组织学样本测试结果[26]。针对TFL在与猪输尿管直接垂直接触时的离体测试显示：150赫兹频率下穿孔时间为7.9秒，500赫兹频率下为1.8秒[18]。我们的实验结果显示，在5赫兹和10赫兹频率下，接触5秒即可引发全层穿孔。此外，我们采用激光光纤平行于输尿管而非垂直接触的方式进行测试，以模拟传统输尿管切开术中激光光纤的实际位置。这表明Ho：YAG激光可能比TFL更安全，但仍需通过人体组织对比研究及更多体内测试来评估其他可能导致组织损伤的参数。

本研究的局限性主要体现在*离体实验*和采样接触时长两个方面。离体测试存在固有缺陷，无法评估炎症介质作用及组织修复过程的影响。术中变量如输尿管水肿、炎症反应、管内压力、温度以及激光光纤的手动按压力度，都可能影响输尿管穿孔时间。虽然我们无法在人体组织中进行离体测试（因故意激光切割人类输尿管进行病理分析并不合适），但离体实验结果仍为钬：YAG激光与人体组织的相互作用提供了新认知——当前相关数据主要依赖动物实验[15，16，18]。尽管这些研究揭示了激光损伤的范围和类型，但由于激光仅以垂直角度作用于输尿管或仅作用于外膜而非尿路上皮，其临床应用价值仍存在局限。既往评价离体人体组织中激光损伤的研究使用了400 μm 光纤，该光纤在输尿管中并不常用[17]。目前还不清楚激光与输尿管接触的角度，且仅对少量标本进行了测试（n=7）。

[17]本研究采用273 μm 光纤与输尿管平行接触的方式进行实验，以此模拟患者处于截石位时输尿管镜检查中激光光纤的实际接触位置。本研究的一个局限性可能在于所选择的接触时长为5秒、10秒和20秒，我们选择这些时长是因为认为它们能展示输尿管可能暴露的激光接触极端情况。既往研究主要通过视频或视觉接触来确认穿孔时间，但仅凭此无法判断显微穿孔程度，而我们旨在评估损伤范围/深度，而非单纯判断是否为全层穿孔[16，17]。

结论

本研究首次评估了Ho：YAG激光在常用参数设置下对人类输尿管的损伤效应。结果显示，在常规激光参数下会发生全层穿孔及肌层损伤。需进一步开展体内实验以评估其他影响因素，如输尿管壁厚度及炎症反应对激光接触与温度的响应。我们认为激光接触的影响可能比既往文献记载更为显著。除结石参数外，对有症状的泌尿系结石患者进行术前评估时，应考虑采用非增强CT测量输尿管壁厚度。随着新型激光设备的问世、功率增强及微创技术的普及，我们必须强调：医源性激光接触对人类尿路上皮的临床影响不容忽视。

致谢作者感谢Grace Hogan、Derek Borwick和Martin Dunphy在标本储存和适当设备采购方面的协助。

作者贡献SOM、EC 和 ND 撰写了主要手稿。ND、FJOB、MTW 和 BS 参与了监督和实验设计。KS、JF 和 TOG 处理并审查了所有样本，并参与了组织处理和操作流程的开发。DH、GC 和 SOM 进行了实验。SOM、EC、SC 和 KS 处理了数据并生成了结果。所有作者均审阅了手稿。

资金IReL联盟提供的开放存取资金

数据可用性本研究期间没有生成或分析数据集。

声明

伦理审批本研究已获得博蒙特医院研究与伦理委员会的伦理批准（批准号：22/20）。资金支持由爱尔兰皇家外科医师学会（Royal College of Surgeons of Ireland）和贝莱德健康（Blackrock Health）通过StAR计划提供。作者声明无其他财务或伦理利益冲突。

竞争利益作者声明无竞争利益。

开放获取本文采用知识共享署名4.0国际许可协议授权，允许您在任何媒介或格式中自由使用、分享、改编、分发和复制，但需满足以下条件：标明原作者及来源、提供知识共享许可协议链接，并注明是否进行过修改。文中涉及的图片或第三方素材均包含在知识共享许可范围内，除非特别注明版权归属。若素材未包含在知识共享许可中，或您的使用方式超出法定授权范围，需直接向版权持有者申请许可。

如需查看本许可证副本，请访问http://creativecommons.org/licenses/by/4.0/。

参考文献

1. Scarpa RM et al (1999) Holmium:YAG laser ureterolithotripsy. Eur Urol 35(3):233 – 238
2. Shroff S et al (1996) The holmium: YAG laser for ureteric stones. Br J Urol 78(6):836 – 839
3. Bagley D, Erhard M (1995) Use of the holmium laser in the upper urinary tract. Tech Urol 1(1):25 – 30
4. Devarajan R et al (1998) Holmium: YAG Lasertripsy for ureteric calculi: an experience of 300 procedures. Br J Urol 82(3):342 – 347
5. Jiang H et al (2007) Ureteroscopic treatment of ureteral calculi with holmium: YAG laser lithotripsy. J Endourol 21(2):151 – 154
6. Emiliani E et al (2018) The true ablation effect of holmium YAG laser on soft tissue. J Endourol 32(3):230 – 235
7. Wollin DA et al (2018) Effect of laser settings and irrigation rates on ureteral temperature during holmium laser lithotripsy, an in vitro model. J Endourol 32(1):59 – 63
8. Matlaga BR et al (2018) Ureteroscopic laser lithotripsy: A review of dusting vs fragmentation with extraction. J Endourol 32(1):1 – 6
9. Sierra A et al (2022) Glossary of pre-settings given by laser companies: no consensus! World J Urol 40(9):2313 – 2321
10. Ventimiglia E (2019) T.O. *Laser Lithotripsy Principles*. Available from: https://eaunet.org/en/news/laser-lithotripsy-principles-2/
11. Skolarikos A, Petřík ANA, Somani B, Thomas K, Gambaro G, Davis NF, Geraghty R, Lombardo R, Tzelves L, Shepherd R (2022) *EAU Guidelines on Urolithiasis*.
12. Tzelves L et al (2021) Basic and advanced technological evolution of laser lithotripsy over the past decade: an educational review by the European society of urotechnology section of the European association of urology. Turk J Urol 47(3):183 – 192
13. Johnson DE, Cromeens DM, Price RE (1992) Use of the holmium:yag laser in urology. Lasers Surg Med 12(4):353 – 363
14. Hardy LA et al (2014) Thulium fiber laser lithotripsy in an in vitro ureter model. J Biomed Opt 19(12):128001
15. Santa-Cruz RW, Leveillee RJ, Krongrad A (1998) Ex vivo comparison of four lithotripters commonly used in the ureter: what does it take to perforate? J Endourol 12(5):417 – 422
16. Piergiovanni M et al (1994) Ureteral and bladder lesions after bal ?listic, ultrasonic, electrohydraulic, or laser lithotripsy. J Endourol 8(4):293 – 299
17. Sayer J et al (1993) Ureteral lithotripsy with the holmium:yag laser. J Clin Laser Med Surg 11(2):61 – 65
18. Wilson CR et al (2015) Collateral damage to the ureter and nitinol stone baskets during thulium fiber laser lithotripsy. Lasers Surg Med 47(5):403 – 410
19. Ulvik Ø, Harneshaug JR, Gjengstø P (2021) Ureteral Strictures Following Ureteroscopic Stone Treat J Endourol 35(7):985 – 990
20. Sunaryo PL et al (2022) Ureteral strictures following ureteroscopy for kidney stone disease: A Population-based assessment. J Urol 208(6):1268 – 1275
21. De Nunzio C et al (2022) Ureteral wall thickness and distal ureteral density in patients with residual fragments after Ho:YAG laser semi-rigid ureterolithotripsy. Lasers Med Sci 38(1):19
22. Dean NS et al (2023) Ureteral wall thickness is an effective predictor of ureteral stone impaction and management outcomes: A systematic review and Meta-analysis. J Urol 210(3):430 – 437
23. Yoshida T et al (2017) Ureteral wall thickness as a preoperative Indicator of impacted stones in patients with ureteral stones undergoing ureteroscopic lithotripsy. Urology 106:45 – 49

24. Güler Y (2023) Non-contrast computed tomography-based factors in predicting ESWL success: A systematic review and meta-analysis. Prog Urol 33(1):27 – 47
25. Ortner G et al (2024) Experts' recommendations in laser use for the treatment of urolithiasis: a comprehensive guide by the European section of Uro-Technology (ESUT) and Training-Research in urological surgery and technology (T.R.U.S.T.)-Group. World J Urol 42(1):33
26. Sierra A et al (2022) Laser efficiency and laser safety: holmium YAG vs. Thulium Fiber laser. J Clin Med, 12(1)

Publisher's note Springer Nature remains neutral with regard to jurisdictional claims in published maps and institutional affiliations.

World Journal of Urology (2026) 44:81
https://doi.org/10.1007/s00345-025-06165-4

RESEARCH

Thermal injury and treatment efficiency during thulium fiber laser lithotripsy: insights from an in vivo porcine model

Ezra J. Margolin[1] · Arpit Mishra[2] · David L. Barquin[1] · Aaron W. Stewart[1] · Nicklas A. Sarantos[1] · Jeremy A. Kurnot[1] · Logan W. Grimaud[1] · Thomas E. Schroeder[1] · Megan E. Bock[1] · Jiaoti Huang[3] · Jodi Antonelli[1] · Glenn M. Preminger[1] · Charles D. Scales[1] · Robert A. Medairos[1] · Pei Zhong[2] · Michael E. Lipkin[1]

Received: 14 November 2025 / Accepted: 15 December 2025
© The Author(s), under exclusive licence to Springer-Verlag GmbH Germany, part of Springer Nature 2026

Abstract

Purpose To evaluate the risk of thermal injury and the treatment efficiency during thulium fiber laser (TFL) lithotripsy of renal and ureteral stone phantoms in an in vivo porcine model.

Methods BegoStone phantoms were sequentially implanted and treated in the kidneys and ureters of five live anesthetized pigs using ureteroscopy and a 200-µm TFL fiber. Room-temperature saline irrigation (20 mL/min) was used. Intraluminal temperatures were monitored using thermocouples. Nine kidney stone treatments were performed at 0.8 J/12 Hz, 0.2 J/100 Hz, and 1 J/20 Hz. Twelve ureteral stone treatments were performed at 0.8 J/12 Hz, 2 J/5 Hz, 0.2 J/100 Hz, and 1 J/20 Hz. Treatment efficiency was assessed by measuring residual stone mass. Histopathological examinations assessed for thermal injury.

Results In kidney treatments, maximum temperatures were lower at 10 W settings (median 33.2˚C) than at 20 W (45.7˚C, $p=0.020$). Histology revealed major thermal injury in 1/3 treatments at 10 W and 4/6 at 20 W ($p=0.524$). In ureter treatments, temperatures did not differ significantly between 10 W (median 36.3˚C) and 20 W (44.6˚C, $p=0.109$) settings. However, major histologic thermal injury occurred in 1/6 treatments at 10 W and 6/6 at 20 W ($p=0.015$). Median treatment efficiency was 0.57 mg/sec (kidney) and 0.35 mg/sec (ureter), with no significant differences among settings.

Conclusion TFL lithotripsy at 20 W can exceed thermal safety thresholds, especially in the ureter. Treatment at 10 W appears safer without significantly compromising efficiency, supporting its use for minimizing thermal injury risk.

Keywords Nephrolithiasis · Ureteroscopy · Laser lithotripsy · Translational research · Thermal injury

Introduction

The thulium fiber laser (TFL) is gaining widespread adoption among urologists for ureteroscopic kidney stone treatment. TFL has several potential advantages compared to the holmium: yttrium-aluminum-garnet (Ho: YAG) laser, including reduced stone retropulsion and improved ablation efficiency. These benefits are attributed to TFL's lower peak power, longer pulse duration, and approximately fourfold greater absorption in water, compared to Ho: YAG [1, 2]. Given these distinctions, TFL is expected to generate distinct thermal profiles during laser lithotripsy (LL).

TFL's high absorption in water has raised concerns for elevated intraluminal temperatures with potential to cause thermal injury to the urothelium during treatment. Prior benchtop studies have demonstrated that high-power TFL lithotripsy may pose a greater risk of thermal injury to the kidney and ureter than Ho: YAG [3–8]. These concerns contributed to post-market safety communications from TFL manufacturers have warned against exceeding 20 W in the ureter due to the risk of thermal injury [9]. Despite these warnings, real-time studies evaluating both temperature elevations and tissue-level effects during TFL lithotripsy remain sparse.

✉ Michael E. Lipkin
michael.lipkin@duke.edu

1 Department of Urology, Duke University Medical Center, 40 Duke Medicine Cir, Clinic 1G, Durham, NC 27710, USA

2 Thomas Lord Department of Mechanical Engineering and Materials Science, Duke University, Durham, NC, USA

3 Department of Pathology, Duke University Medical Center, Durham, NC, USA

Published online: 11 January 2026

Prior in vivo porcine research has demonstrated elevated intraluminal temperatures associated with high-power TFL during ureteroscopy, though these experiments were performed without the presence of stones [10]. Despite these findings, few studies have directly evaluated the histopathological consequences of TFL on renal and ureteral tissues [6, 11, 12]. In this study, we aimed to assess the potential for thermal injury risk during TFL lithotripsy of renal and ureteral stones in an in vivo porcine model, with a specific emphasis on intraluminal temperature monitoring, thermal dose estimation, and histological outcomes. This work addresses a critical knowledge gap regarding the tissue-level consequences of thermal exposure during TFL lithotripsy.

Materials and methods

Procedure

Institutional Animal Care and Use Committee approval was obtained for this study (protocol number: A071-24-03). We performed stone implantation followed by ureteroscopy and LL on five live anesthetized female pigs (75–100 lbs). Each pig underwent sequential implantation and treatment of 4–6 × 10 mm pre-weighed cylindrical soft BegoStone phantoms (BEGO™, Lincoln, RI) in both kidneys and ureters. Stone phantoms were prepared with a 5:2 powder-to-water ratio and soaked in water for 24 h before implantation to achieve mechanical properties comparable to human kidney stones [13], similar to our recent publications [4, 14, 15]. Stone implantation was performed by urology residents, while ureteroscopy with LL was performed by an endourology fellow.

General anesthesia was administered. Each procedure began with cystoscopy and bilateral ureteral catheterization, followed by a laparotomy and proximal ureterotomy for stone implantation. After placing two stones in the kidney, the ureterotomy was closed using 4 − 0 absorbable suture, and the absence of leakage was confirmed. An 11/13 Fr ureteral access sheath was placed over a wire into the distal ureter, and a single-use flexible ureteroscope (AXIS II, Dornier MedTech, Germany; outer diameter 8.7 Fr) was advanced through the sheath to manipulate stones into separate non-adjacent calyces, resulting in a sheath-to-scope ratio of 1.26. Using endoscopic guidance, K-type thermocouples (5SRTC-TT-K-36-36, OMEGA, Norwalk, CT, USA) with 0.13 mm sensor diameter were inserted through the renal parenchyma into the calyceal lumen, adjacent to the stone-tissue boundary for temperature monitoring. The distance between the thermocouple tip and the fiber/stone interface was standardized as much as possible across experiments. Endoscopic video footage was recorded.

Treatment and sham protocols

LL and sham procedures were alternated in a predetermined order (Supplementary Table 1). LL was performed using a TFL system (IPG Photonics, Marlborough, MA, USA) using a 200-µm fiber (NA = 0.22). In the kidney, LL employed a dusting technique aiming to reduce kidney stone to particles smaller than 0.25 mm. LL proceeded until the stone was completely treated or had moved from the initial location and was no longer adjacent to the thermocouple. After kidney procedures, a stone was implanted into the proximal ureter via a new ureterotomy, and a thermocouple was placed through the wall of the ureter adjacent to the stone. Ureteral stones were placed distal to the ureterotomy and treated ureteroscopically using fragmentation technique targeting fragments < 3 mm. The process was repeated in the distal ureter using a new ureterotomy and new stones. The entire procedure was repeated on the contralateral side, such that each pig underwent two treatments and two sham procedures per kidney and ureter. Upon completion of the bilateral procedures, the pigs were euthanized, and their kidneys and ureters were explanted for histopathological examination.

Three laser settings were tested in the kidney (0.8 J/12 Hz, 0.2 J/100 Hz, 1 J/20 Hz), and four settings were tested in the ureter (0.8 J/12 Hz, 2 J/5 Hz, 0.2 J/100 Hz, 1 J/20 Hz), selected based on prior benchtop evidence suggesting both efficacy and safety [4]. Each setting was tested in three experiments. All procedures used room temperature 0.9% saline irrigation at a rate of 20 mL/min, controlled and delivered using a peristaltic pump (Masterflex®). All TFL treatments involved alternating 30-second cycles of laser activation and rest until the stone was completely treated or had moved from the initial location. Sham procedures replicated the full intervention without laser activation and consisted of ureteroscopy with temperature monitoring adjacent to the stone for a duration of 5 min. There were three protocol deviations: one kidney treatment (Pig 1) used a different laser cycle and was excluded from analysis, and two sham procedures in the ureter (Pigs 4 and 5) were replaced by additional treatments.

Temperature analysis

Temperature changes were monitored every 0.2 s. For each experiment, the maximum sustained temperature (T_{max}) was defined as the highest temperature maintained for at least 3 s. While the T_{max} values were compared to a safety threshold of 43 °C, which is widely used as a reference point for evaluating thermal exposure and is considered the point above which cell death may begin [16, 17], tissue injury depends on both magnitude and duration of heating. To quantify this,

we calculated the thermal dose using cumulative equivalent minutes at 43 °C (CEM43) based on the recorded temperatures, using the formula:

$$\mathrm{CEM43} = \int_0^{t_{final}} R^{43-T} dt$$

where R is 0.25 for T < 43 °C and 0.5 for T ≥ 43 °C [18]. Thermal doses were compared against a safety threshold of 120 min, beyond which thermal injury is expected to occur in most tissues [19].

Histopathological analysis

The kidneys and ureters were grossly inspected for evidence of thermal injury and necrosis. Tissue sections from kidney and ureters were taken to include cross sections of the lumens of renal pelvis/calyces and ureter. The tissue sections were formalin-fixed and embedded in paraffin. Slides were cut from the paraffin tissue blocks, stained with hematoxylin and eosin and examined microscopically by an experienced genitourinary pathologist (JH) for the presence or absence of thermal injury.

Mechanical injury was characterized by denuded urothelium, focal hemorrhage, and vascular congestion. Minor thermal injury was defined as focal or superficial collagen homogenization (<1 mm), while major thermal injury was defined as by global and deep collagen homogenization (>1 mm), fibrin deposition, edema, and loss of cellular details.

Efficiency and fragment distribution

During gross pathology analysis, residual stone fragments were collected, air-dried, and weighed. Fragments were sequentially sieved through mesh sizes of 3, 1, and 0.25 mm. In the kidney, fragments larger than 0.25 mm were considered untreated. In the ureter, fragments larger than 3 mm were considered untreated. The mass of treated stones was determined by subtracting the mass of untreated fragments from the initial mass. Treatment efficiency was calculated as treated stone mass per laser activation time (mg/sec).

Statistical analysis

Continuous variables were compared across laser settings using Wilcoxon rank-sum tests for pairwise comparisons and Kruskal-Wallis tests for multi-group comparisons. Binary variables were compared using Fisher's exact tests. Statistical testing was performed using Stata 12.1 (StataCorp, College Station, TX, USA).

Results

We performed 21 treatment procedures (9 in the kidney and 12 in the ureter), along with 18 sham procedures (10 in the kidney and 8 in the ureter).

Kidney stone treatments: thermal injury

Temperature curves for kidney stone treatments are shown in Fig. 1A-C, with corresponding T_{max} and thermal doses summarized in Table 1. At 0.8 J/12 Hz, temperatures remained below body temperature with minimal thermal dose. At 0.2 J/100 Hz, one treatment exceeded the temperature threshold of 43°C. All treatments at 1 J/20 Hz reached T_{max} > 43°C, and two exceeded thermal doses of 120 min. Compared to 10 W settings, treatments at 20 W showed significantly higher T_{max} (median 45.7 vs. 33.2°C, p=0.020) and greater thermal dose (median 55.8 vs. 1.89×10^{-4} min, p=0.039).

Gross pathology revealed extensive urothelium damage in two treatments at 1 J/20 Hz (Supplementary Fig. 1A, Table 1), with no visible injury in other treatments or sham procedures (Supplementary Fig. 1B). Gross injury was present in 0/3 treatments at 10 W and 2/6 treatments at 20 W (p=0.500).

Histological evaluation showed major thermal injury in 1/3 experiments at 0.8 J/12 Hz and 0.2 J/100 Hz (Supplementary Fig. 2A, Table 1). All 3 experiments at 1 J/20 Hz resulted in major thermal injury. No histologic injury was observed in other treatment groups or any sham procedure (Supplementary Fig. 2B). Major thermal injury was noted in 1/3 treatments at 10 W and 4/6 treatments at 20 W (p=0.524).

Ureteral stone treatments: thermal injury

Temperature curves for the ureter treatments are shown in Fig. 1D-G. At 0.8 J/12 Hz and 2 J/5 Hz, temperatures stayed below body temperature, with thermal doses under 1 min in 5/6 experiments (Table 1). At 0.2 J/100 Hz and 1 J/20 Hz, 3/6 experiments had T_{max} > 43°C, and 3/6 had thermal doses > 120 min. No statistically significant difference was found between 20 W and 10 W settings in T_{max} (median 44.6 vs. 36.3°C, p=0.109) or thermal dose (153 vs. 0.0736 min, p=0.200).

Gross pathology showed extensive urothelial damage in two treatments at 0.2 J/100 Hz and two treatments at 1 J/20 Hz (Supplementary Fig. 1C, Table 1), with no visible injuries at any 10 W settings (Supplementary Fig. 1D). Gross injury was seen in 0/6 treatments at 10 W and 4/6 at 20 W (p=0.061).

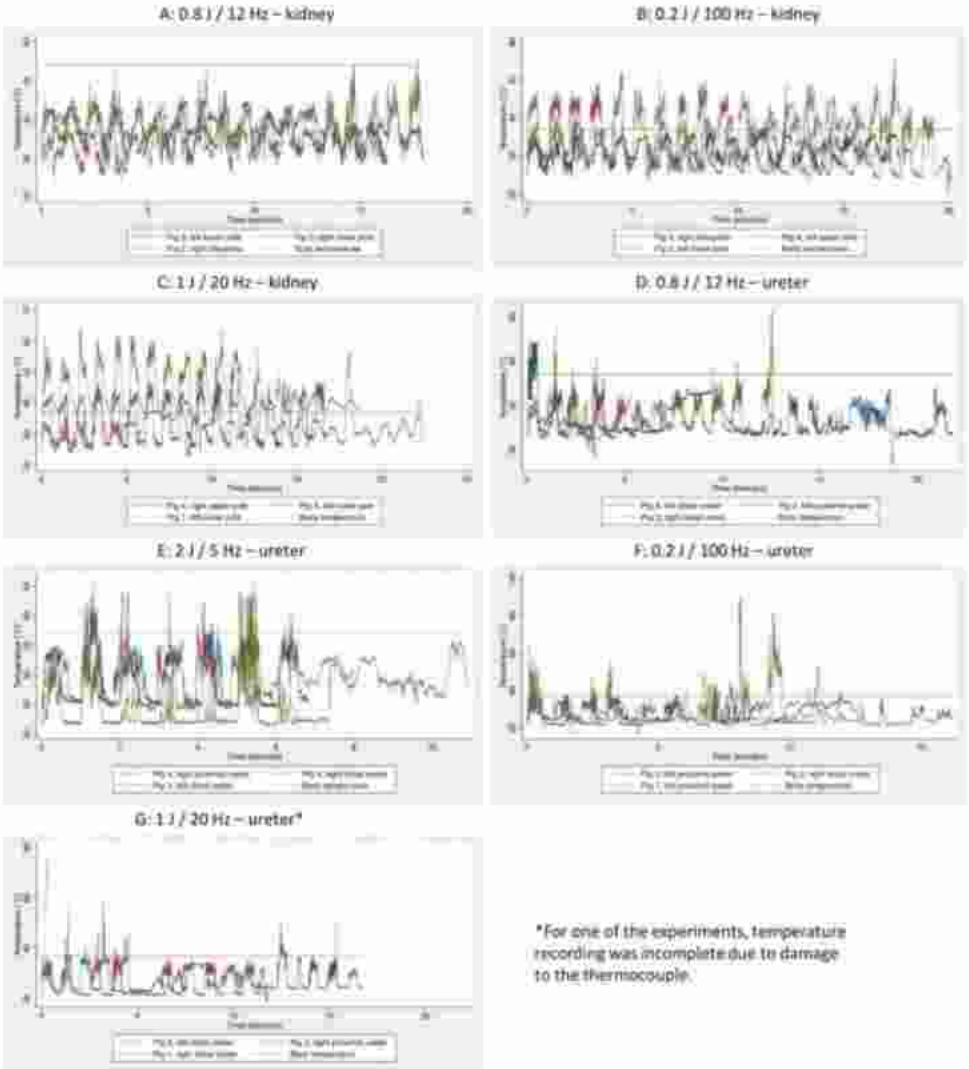


Fig. 1 Temperature curves during laser treatments at different settings in the (**a**–**c**) kidney and (**d**–**g**) ureter. Horizontal orange line represents body temperature

Table 1 Maximum temperature, thermal dose, gross pathology, and histopathological findings following treatment at different laser settings in the kidney and ureter ($n = 3$ for each setting); temperature and thermal dose data displayed as median (range); tissue injury data displayed as number of experiments demonstrating the specified injury

Organ	Power (W)	Pulse Energy (J)	Frequency (Hz)	Maximum temperature T_{max} (°C)	Thermal Dose, CEM43 (min)	Gross tissue injury	Histological thermal tissue injury		
							None	**Mild**	**Severe**
Kidney	10	0.8	12	33.2 (31.5–33.7)	1.89×10^{-4} (1.25×10^{-6} – 0.280)	0	2	0	1
	20	0.2	100	40.7 (36.4–47.6)	2.25 (4.10×10^{-3} – 103)	0	2	0	1
	20	1	20	54.3 (43.8–57.8)	394 (8.22–1.32×10^{5})	2	0	0	3
Ureter	10	0.8	12	37.3 (31.7–38.0)	0.326 (6.45×10^{-5} – 5.72)	0	0	2	1
	10	2	5	35.9 (31.8–36.7)	0.0453 (0.0449–0.102)	0	0	3	0
	20	0.2	100	49.3 (34.8–55.9)	33.9 (1.63×10^{-4} – 6.64×10^{9})	2	0	0	3
	20	1	20	39.9 (32.9–69.4)	272 (0.0349–7.82×10^{7})	2	0	0	3

Histologically, major thermal injury was observed in 1/3 experiments at 0.8 J/12 Hz (Supplementary Fig. 2C) and minor thermal injury in 2/3 experiments (Supplementary Fig. 2D, Table 1). All 2 J/5 Hz treatments exhibited minor injury. Both 0.2 J/100 Hz and 1 J/20 Hz resulted in major thermal injury in 3/3 experiments. Mechanical injury (but no thermal injury) was found in 7/8 sham procedures (Supplementary Fig. 2E). Major thermal injury occurred in 1/6 treatments at 10 W and 6/6 at 20 W ($p=0.015$).

Treatment efficiency

During kidney stone treatments, a median of 84% (range 54–90%) of the stone mass was treated across all laser settings. Median procedure and median laser activation times were 20.2 min (17.9–24.3) and 9.8 min (8.2–12.1), respectively. Overall treatment efficiency was 0.57 mg/Sect. (0.29–0.64), and efficiency at each laser setting is shown in Supplementary Fig. 3A. There was no significant variation in treatment efficiency among settings ($p=0.670$).

During ureteral stone treatments, 77% (range 49–100) of the stone mass was treated across all settings, with median procedure time of 12.3 min (8.5–24.2), and median laser activation time of 6.1 min (4.3–12.2). Overall treatment efficiency was 0.35 mg/Sect. (0.15–0.55), and efficiency at each laser setting is shown in Supplementary Fig. 3B. No significant variation in treatment efficiency among settings was observed ($p=0.161$).

Fragment size distribution

Across all ureteral stone treatments, a median of 86% (range 59–100%) of treated stone mass consisted of particles<0.25 mm. Fragments 0.25-1 mm accounted for <1% (0–3%), and fragments 1–3 mm accounted for 13% (0–40%). The largest proportion of 1–3 mm fragments was seen with 2 J/5 Hz (35%), but no statistically significant differences in fragment size distribution were observed across settings ($p=0.122$, Supplementary Fig. 4).

Discussion

This is the first study to evaluate both thermal injury and treatment efficiency following TFL lithotripsy in a porcine model. Under controlled conditions with 20 mL/min room-temperature irrigation and alternating 30-second cycles of laser activation and rest, we found that 20 W settings can lead to elevated intraluminal temperatures and thermal tissue injury in both the kidney and ureter, whereas 10 W settings proved to be generally safe, maintaining temperatures below physiological thresholds and causing only minor histological changes on the tissue.

During kidney stone treatments, 20 W laser settings consistently produced temperatures exceeding 43 °C, a threshold previously associated with thermal injury [16, 17]. Correspondingly, our histopathological analysis confirmed evidence of global injury throughout the treatment area both grossly and microscopically at these elevated temperatures. A similar trend was observed in the ureter, where 10 W treatments maintained safe temperature ranges, while 20 W settings frequently resulted in dangerously high temperatures and tissue damage. Tissue injury was uncommon at 10 W but frequent at 20 W.

Our analysis of treatment efficiency showed no significant difference between 10 W and 20 W settings in either the kidney or ureter, though this is limited by small sample size. While higher powers likely improve treatment efficiency, we believe that the difference is modest and is outweighed by the increased risk of thermal injury.

Given its favorable safety and efficiency profile, we recommend 0.8 J/12 Hz as an effective setting for stone dusting using TFL. We have previously shown that this setting results in more efficient stone dusting compared to low-energy/high-frequency settings like 0.2 J/50 Hz [4, 14]. Due to its high water absorption, low peak power, and long pulse width, TFL achieves effective stone dusting at settings traditionally used for fragmentation. This was further supported by a randomized controlled trial where patients treated with TFL at 1 J/10 Hz had more efficient stone treatment than those treated at 0.1 J/100 Hz [20].

In situations when fragmentation is more desirable, we believe that settings with higher pulse energy may be most effective. In this study, 2 J/5 Hz produced more extractable fragments suitable for basketing compared to other settings. This aligns with findings from our benchtop ureteral model, where 2 J/5 Hz provided superior fragmentation without exceeding safe thermal thresholds [21]. While care must be taken to avoid inadvertently firing the laser in contact with the urothelium, the low frequency and effective fragmentation should help urologists keep the laser farther from the tissue surface while maintaining good control.

This study has several limitations: a relatively small sample size, inability to precisely control calyceal volume, use of BegoStone phantoms rather than human stones, a limited number of settings tested, and unclear clinical significance of the histologically observed injuries. Additionally, our findings are specific to TFL and should not be extrapolated to Ho: YAG or other laser technologies. These findings also may not apply to other irrigation parameters or laser activation cycles. Despite these limitations, this study offers valuable in vivo evidence to guide urologists in selecting laser settings for kidney and ureteral stone treatment using TFL.

Conclusions

This in vivo porcine study demonstrates that TFL lithotripsy at 20 W power, under standard irrigation and laser activation parameters, can result in elevated intraluminal temperatures and thermal tissue injury to both the kidney and ureter. In contrast, treatment at 10 W appears to be thermally safe without significantly compromising treatment efficiency.

Supplementary Information The online version contains supplementary material available at https://doi.org/10.1007/s00345-025-06165-4.

Acknowledgements The authors would like to express their gratitude to the following individuals and departments for their invaluable contributions to this study: Duke Vivarium, Division of Laboratory Animal Services, Duke University: Heather Lewis, Marisa Tonner, Aura Cortes de Gomez, Fernando Orozco, Kelly Shaw, Angela Garner, Lindsey Morgan, Ianthia Parker, Andres Schreiner, Lauren Dunlap, Danielle Cecil, and many others from the DLAR Vivarium, Pharmacy, and Animal Ordering Team.Research Histology Lab, Department of Pathology, Duke University Medical Center: Emily Knutson and Thomas RibarThe authors also acknowledge Sonia Doss, who expertly administered our experiments as the QA & Regulatory Compliance Associate on behalf of IACUC (Registry Number: A071-24-03).

Author contributions Conceptualization: Ezra Margolin, Arpit Mishra, Jodi Antonelli, Glenn Preminger, Charles Scales, Robert Medairos, Pei Zhong, Michael Lipkin; Methodology: Ezra Margolin, Arpit Mishra, Jodi Antonelli, Glenn Preminger, Charles Scales, Robert Medairos, Pei Zhong, Michael Lipkin; Formal analysis and investigation: Ezra Margolin, Arpit Mishra, David Barquin, Aaron Stewart, Nicklas Sarantos, Jeremy Kurnot, Logan Grimaud, Thomas Schroeder, Megan Bock, Jiaoti Huang; Writing – original draft preparation: Ezra Margolin; Writing – review and editing: Ezra Margolin, Arpit Mishra, Jiaoti Huang, Jodi Antonelli, Glenn Preminger, Charles Scales, Robert Medairos, Pei Zhong; Funding acquisition: Pei Zhong; Resources: Pei Zhong; Supervision: Pei Zhong, Michael Lipkin.

Funding This project is supported by the National Institutes of Health (NIH) through grants 1P20DK135107-03, 1R01DK138972-01A1 and 2R01DK052985-28.

Data availability No datasets were generated or analysed during the current study.

Declarations

Conflict of interst GMP and MEL are consultants for Boston Scientific. All other authors have no conflicts of interest to declare.

References

1. Lekarev V, Dymov A, Vinarov A, Sorokin N, Minaev V, Minaev N, Tsypina S, Yusupov V (2020) Mechanism of lithotripsy by superpulse thulium fiber laser and its clinical efficiency. Appl Sci 10(21):7480
2. Jiang P, Okhunov Z, Afyouni AS, Ali S, Hosseini Sharifi SH, Bhatt R, Brevik A, Ayad M, Larson K, Osann K, Patel RM, Landman J, Clayman RV (2023) Comparison of superpulse thulium fiber laser vs holmium laser for ablation of renal calculi in an in vivo Porcine model. J Endourol 37(3):335–340. https://doi.org/10.1089/end.2022.0445
3. Sierra A, Corrales M, Kolvatzis M, Panthier F, Piñero A, Traxer O (2022) Thermal injury and laser efficiency with holmium YAG and thulium fiber laser-An in vitro study. J Endourol 36(12):1599–1606. https://doi.org/10.1089/end.2022.0216
4. Mishra A, Medairos R, Chen J, Soto-Palou F, Wu Y, Antonelli J, Preminger GM, Lipkin ME, Zhong P (2024) Exploring optimal settings for safe and effective thulium fibre laser lithotripsy in a kidney model. BJU Int 133(2):223–230. https://doi.org/10.1111/bju.16218
5. Belle JD, Chen R, Srikureja N, Amasyali AS, Kehcila M, Baldwin DD (2022) Does the novel thulium fiber laser have a higher risk of urothelial thermal injury than the conventional holmium laser in an in vitro study? J Endourol 36(9):1249–1254. https://doi.org/10.1089/end.2021.0842
6. Molina WR, Carrera RV, Chew BH, Knudsen BE (2021) Temperature rise during ureteral laser lithotripsy: comparison of super pulse thulium fiber laser (SPTF) vs high power 120 W holmium-YAG laser (Ho:YAG). World J Urol 39(10):3951–3956. https://doi.org/10.1007/s00345-021-03619-3
7. Hardy LA, Wilson CR, Irby PB, Fried NM (2014) Thulium fiber laser lithotripsy in an in vitro ureter model. J Biomed Opt 19(12):128001. https://doi.org/10.1117/1.Jbo.19.12.128001
8. Wanderling C, Saxton A, Phan D, Doersch KM, Shepard L, Schuler N, Hassig S, Quarrier S, Osinski T, Ghazi A (2024) Getting hot in here! Comparison of holmium vs. thulium laser in an anatomic hydrogel kidney model. Urolithiasis 52(1):49. https://doi.org/10.1007/s00240-024-01541-y
9. Class 2 Device Recall Olympus (2021) U.S. Food and Drug Administration. https://www.accessdata.fda.gov/scripts/cdrh/cfdocs/cfres/res.cfm?id=188172. Accessed 25 April 2025
10. Okhunov Z, Jiang P, Afyouni AS, Ayad M, Arada R, Brevik A, Akopian G, Patel RM, Landman J, Clayman RV (2021) Caveat emptor: the heat is ON-An in vivo evaluation of the thulium fiber laser and temperature changes in the Porcine kidney during dusting and fragmentation modes. J Endourol 35(11):1716–1722. https://doi.org/10.1089/end.2021.0206
11. Peteinaris A, Tsaturyan A, Bravou V, Tatanis V, Faria-Costa G, Pagonis K, Faitatziadis S, Vagionis A, Liatsikos E, Kallidonis P (2023) High-power laser lithotripsy - do we treat or harm? Histological evaluation of temperature effects in an in vivo study with thulium fiber laser. Cent Eur J Urol 76(1):44–48. https://doi.org/10.5173/ceju.2023.24
12. Sierra A, Corrales M, Somani B, Traxer O (2022) Laser efficiency and laser safety: holmium YAG vs. Thulium fiber laser. J Clin Med 12(1). https://doi.org/10.3390/jcm12010149
13. Esch E, Simmons WN, Sankin G, Cocks HF, Preminger GM, Zhong P (2010) A simple method for fabricating artificial kidney stones of different physical properties. Urol Res 38(4):315–319. https://doi.org/10.1007/s00240-010-0298-x
14. Chen J, Mishra A, Medairos R, Antonelli J, Preminger GM, Lipkin ME, Zhong P (2023) In vitro investigation of stone ablation efficiency, Char formation, spark generation, and damage mechanism produced by thulium fiber laser. Urolithiasis 51(1):124. https://doi.org/10.1007/s00240-023-01501-y
15. Chen J, Li D, Yu W, Ma Z, Li C, Xiang G, Wu Y, Yao J, Zhong P (2022) The effects of scanning speed and standoff distance of the fiber on dusting efficiency during short pulse holmium: YAG laser lithotripsy. J Clin Med 11(17). https://doi.org/10.3390/jcm11175048
16. Kim M, Kim G, Kim D, Yoo J, Kim D-K, Kim H (2019) Numerical study on effective conditions for the induction of apoptotic temperatures for various tumor aspect ratios using a

single Continuous-Wave laser in photothermal therapy using gold nanorods. Cancers 11(6):764
17. Dewhirst MW, Viglianti BL, Lora-Michiels M, Hoopes PJ, Hanson M (2003) Thermal dose requirement for tissue effect: experimental and clinical findings. Proc SPIE Int Soc Opt Eng 4954:37. https://doi.org/10.1117/12.476637
18. Sapareto SA, Dewey WC (1984) Thermal dose determination in cancer therapy. Int J Radiat Oncol Biol Phys 10(6):787–800. https://doi.org/10.1016/0360-3016(84)90379-1
19. Yarmolenko PS, Moon EJ, Landon C, Manzoor A, Hochman DW, Viglianti BL, Dewhirst MW (2011) Thresholds for thermal damage to normal tissues: an update. Int J Hyperth 27(4):320–343. https://doi.org/10.3109/02656736.2010.534527
20. Pathak N, Gowda N, Coelho V, Shete N, Singh A, Ganpule A, Sabnis R, Desai M (2024) Prospective randomized controlled trial to compare dusting vs fragmentation using thulium fiber laser in retrograde intrarenal surgery. J Endourol 38(2):102–107. https://doi.org/10.1089/end.2023.0167
21. Mishra A, Margolin EJ, Medairos RA, Antonelli J, Preminger GM, Lipkin ME, Zhong P (2025) Optimizing fragmentation with the thulium fiber laser in ureteral stone lithotripsy: an In-Vitro study. J Endourol

Publisher's note Springer Nature remains neutral with regard to jurisdictional claims in published maps and institutional affiliations.

Springer Nature or its licensor (e.g. a society or other partner) holds exclusive rights to this article under a publishing agreement with the author(s) or other rightsholder(s); author self-archiving of the accepted manuscript version of this article is solely governed by the terms of such publishing agreement and applicable law.

《世界泌尿学杂志》（2026年）第44卷第81页
https://doi.org/10.1007/s00345-025-06165-4

研究

铥光纤激光碎石术中的热损伤与治疗效率：基于活体猪模型的观察

Ezra J. Margolin[1] · Arpit Mishra[2] · David L. Barquin[1] · Aaron W. Stewart[1] · Nicklas A. Sarantos[1] · Jeremy A. Kurnot[1] · Logan W. Grimaud[1] · Thomas E. Schroeder[1] · Megan E. Bock[1] · Jiaoti Huang[3] · Jodi Antonelli[1] · Glenn M. Preminger[1] · Charles D. Scales[1] · Robert A. Medairos[1] · Pei Zhong[2] · Michael E. Lipkin[1]

接收日期：2025年11月14日/接受日期：2025年12月15日
© 作者（们），经德国施普林格出版社（Springer-Verlag GmbH）独家授权，施普林格自然出版社旗下 2026

摘要

目的评估铥光纤激光（TFL）碎石术在活体猪模型中对肾及输尿管结石模型的热损伤风险与治疗效果。

方法使用输尿管镜和200- µm TFL 纤维，依次将BegoStone体模植入并处理五只麻醉活体猪的肾脏和输尿管。采用室温生理盐水冲洗（20 mL/min）。通过热电偶监测管腔温度。在0.8 J/12 Hz、0.2 J/100 Hz和1 J/20 Hz条件下进行了九次肾结石处理。在0.8 J/12 Hz、2 J/5 Hz、0.2 J/100 Hz和1 J/20 Hz条件下进行了十二次输尿管结石处理。通过测量残留结石质量评估治疗效率。组织病理学检查评估热损伤情况。

结果在肾脏治疗中，10 W设置下的最高温度（中位数33.2°C）低于20 W（45.7°C，p= 0.020）。组织学显示1/3的10 W治疗和4/6的20 W治疗存在严重热损伤（p= 0.524）。在输尿管治疗中，10 W（中位数36.3°C）与20 W（44.6°C，p= 0.109）设置下的温度无显著差异。然而，1/6的10 W治疗和6/6的20 W治疗出现严重组织学热损伤（p= 0.015）。治疗效率中位数为0.57 mg/秒（肾脏）和0.35 mg/秒（输尿管），各设置间无显著差异。

结论TFL 20W的碎石治疗可能超过热安全阈值，尤其在输尿管部位。10W治疗在不显著降低效率的前提下安全性更高，这支持了其用于最小化热损伤风险的应用。

关键词肾结石 · 输尿管镜检查 · 激光碎石术 · 转化研究 · 热损伤

介绍

铥光纤激光器（TFL）在泌尿外科医师中正被广泛应用于输尿管镜下肾结石治疗。与钬激光（Ho:YAG）相比，TFL 具有多项潜在优势，包括降低结石反冲力和改善消融效果。效率。这些优势归因于 TFL 较低的峰值功率、更长的脉冲持续时间，以及与Ho:YAG相比在水中吸收能力约高出四倍[1，2]。鉴于这些差异，TFL 在激光碎石术（LL）过程中预计将产生不同的热分布特征。

TFL 在水中的高吸收性引发了对治疗过程中腔内温度升高的担忧，这种高温可能对尿路上皮造成热损伤。此前的台架研究表明，与Ho:YAG激光相比，高功率 TFL 碎石术可能对肾脏和输尿管造成更大的热损伤风险[3–8]。这些担忧促使 TFL 制造商在上市后安全公告中警告，由于存在热损伤风险，输尿管的功率不得超过20瓦[9]。尽管有这些警告，但评估 TFL 碎石术中温度升高和组织水平效应的实时研究仍然较为匮乏。

✉ 迈克尔·E·利普金
迈克尔·利普金@杜克大学邮箱

1 杜克大学医学中心泌尿外科，地址：美国北卡罗来纳州达勒姆市杜克医学环路40号1G诊室，邮编27710

2 托马斯·洛德，美国北卡罗来纳州达勒姆市杜克大学机械工程与材料科学系

3 美国北卡罗来纳州达勒姆市杜克大学医学中心病理学系

Published online: 11 January 2026

先前的猪体内研究已证实，输尿管镜检查中使用高功率 TFL 会导致管腔内温度升高，但这些实验均未涉及结石存在[10]。尽管有这些发现，直接评估 TFL 对肾脏和输尿管组织组织病理学影响的研究仍较少[6、11、12]。本研究旨在通过猪体内模型评估肾结石和输尿管结石 TFL 碎石术中的热损伤风险，重点监测管腔内温度、热剂量估算及组织学结果。这项工作填补了关于 TFL 碎石术中热暴露对组织水平影响的关键知识空白。

材料与方法

程序

本研究已获得机构动物护理与使用委员会批准（方案编号：A071-24-03）。我们对五头活体麻醉雌性猪（体重75-100磅）实施了结石植入术，随后进行输尿管镜检查及输尿管镜下取石术（LL）。每头猪双侧肾脏及输尿管依次植入并处理4-6个10毫米预称重的圆柱形BegoStone软质模型（BEGO ™，美国罗德岛州林肯市）。模型采用5:2粉末与水配比制备，植入前浸泡24小时以获得与人类肾结石相当的力学特性。[13]与我们近期发表的文献[4，14，15]类似。结石植入术由泌尿外科住院医师完成，而采用LL技术的输尿管镜检查则由血管内泌尿外科专科医师实施。

实施全身麻醉后，所有操作均以膀胱镜检查及双侧输尿管插管开始，随后进行剖腹手术及近端输尿管切开术以置入结石。在肾脏内放置两颗结石后，使用4-0可吸收缝线缝合输尿管切口，并确认无渗漏。通过导丝将11/13 Fr输尿管通路鞘置入远端输尿管，随后将一次性使用柔性输尿管镜（AXIS II，德国Dornier MedTech公司；外径8.7 Fr）经鞘推进，将结石分入不相邻的肾盏，实现鞘管与内镜的1.26倍比。在内镜引导下，将传感器直径0.13 mm的K型热电偶（型号5SRTC-TT-K-36-36，美国康涅狄格州诺沃克市omega公司）经肾实质插入肾盏腔，邻近结石组织边界进行温度监测。实验中尽可能标准化热电偶尖端与光纤/结石界面的距离。全程记录内镜视频影像。

治疗与假手术方案

LL（激光碎石）与假手术按预定顺序交替进行（补充表1）。LL采用 TFL 系统（IPG Photonics，美国马萨诸塞州马尔伯勒）配合200 μm 光纤（数值孔径=0.22）实施。肾脏治疗中，LL采用喷砂技术将结石粉碎至小于0.25毫米的颗粒。治疗持续至结石完全清除或移出初始位置且不再邻近热电偶。肾脏治疗后，通过新尿道切开术将结石植入近端输尿管，并在结石邻近处的输尿管壁置入热电偶。输尿管结石则置于远端输尿管处，采用碎石技术（目标碎屑<3毫米）进行输尿管镜下碎石治疗。该流程在远端输尿管重复实施新尿道切开术及新结石。整个操作在对侧重复进行，确保每头猪每侧肾脏及输尿管各接受两次治疗及两次假手术。双侧手术完成后，处死实验动物并摘取肾脏与输尿管进行组织病理学检查。

在肾脏中测试了三种激光设置（0.8 J/12 Hz、0.2 J/100 Hz、1 J/20 Hz），在输尿管中测试了四种设置（0.8 J/12 Hz、2 J/5 Hz、0.2 J/100 Hz、1 J/20 Hz），这些设置是基于先前的台面证据（表明其既有效又安全）[4]而选定的。每种设置均进行了三次实验测试。所有操作均使用室温0.9%生理盐水冲洗，流速为20 mL/min，通过蠕动泵（Masterflex ®）进行控制和输送。所有 TFL 治疗均采用30秒的激光激活与休息交替循环，直至结石完全处理或从初始位置移出。假手术复制了完整的干预过程但不激活激光，包括在结石附近进行5分钟的输尿管镜检查并监测温度。存在三种方案偏离：一只肾脏治疗（猪1）使用了不同的激光循环，因此被排除在分析之外；输尿管中的两例假手术（猪4和5）被额外治疗所替代。

温度分析

温度变化每0.2秒监测一次。每次实验中，最大持续温度（Tmax）定义为至少维持3秒的最高温度。虽然T_{max}值与43°C的安全阈值进行对比——该阈值被广泛用作评估热暴露的参考点，并被认为是可能引发细胞死亡的临界点[16，17]，但组织损伤取决于加热的强度和持续时间。为量化这一点，

我们根据记录的温度，采用43°C下的累积当量分钟数（CEM43）计算热剂量，计算公式如下：

$$CEM43 = \int_0^{t_{final}} R^{43-T} dt$$

其中R在T < 43°C时为0.25，在T ≥ 43°C时为0.5[18]。热剂量与120分钟的安全阈值进行对比，超过该阈值后，大多数组织预计会发生热损伤[19]。

组织病理学分析

对肾脏和输尿管进行大体检查以观察热损伤和坏死的证据。取肾脏和输尿管的组织切片，包括肾盂/盏腔和输尿管腔的横截面。组织切片经福尔马林固定后石蜡包埋。从石蜡组织块中切取切片，经苏木精和伊红染色后，由经验丰富的泌尿生殖系统病理学家（JH）在显微镜下检查是否存在热损伤。

机械性损伤的特征表现为尿路上皮剥脱、局灶性出血及血管充血。轻度热损伤定义为局灶性或浅表性胶原均质化（<1毫米），而重度热损伤则定义为胶原均质化范围广泛且深度超过1毫米、纤维蛋白沉积、水肿及细胞细节丧失。

效率与片段分布

在大体病理学分析过程中，收集残留结石碎片，经空气干燥后称重。碎片依次通过3、1和0.25毫米筛网进行筛分。在肾脏中，大于0.25毫米的碎片被视为未处理。在输尿管中，大于3毫米的碎片被视为未处理。处理后结石的质量通过初始质量减去未处理碎片的质量来确定。处理效率以每秒激光激活时间处理的结石质量（mg/sec）计算。

统计分析

连续变量采用Wilcoxon秩和检验进行配对比较，采用Kruskal-Wallis检验进行多组比较。二分类变量采用Fisher精确检验进行比较。统计分析使用Stata 12.1软件（StataCorp，美国德克萨斯州大学城）完成。

结果

我们共实施了21例治疗手术（肾脏9例，输尿管12例），以及18例假手术（肾脏10例，输尿管8例）。

肾结石治疗：热损伤

肾结石治疗的温度曲线如图1A-C所示，相应的T_{max}和热剂量总结于表1。在0.8 J/12 Hz时，温度保持在体温以下且热剂量极低。在0.2 J/100 Hz时，一次治疗超过43°C的温度阈值。所有1 J/20 Hz的治疗均达到T_{max} > 43 °C，其中两次超过120分钟的热剂量。与10 W设置相比，20 W的治疗显示出显著更高的T_{max}（中位数45.7 vs. 33.2°C，p= 0.020）和更大的热剂量（中位数55.8 vs. 1.89×10^{-4}分钟，p= 0.039）。

大体病理学检查显示，在1 J/20 Hz的两种处理中存在广泛的尿路上皮损伤（补充图1A，表1），而在其他处理或假手术中未观察到明显损伤（补充图1B）。在10 W的处理中，0/3组存在大体损伤；在20 W的处理中，2/6组存在大体损伤（p=0.500）。

组织学评估显示，在0.8 J/12 Hz和0.2 J/100 Hz条件下，1/3实验组出现严重热损伤（补充图2A，表1）。所有3个1 J/20 Hz实验组均导致严重热损伤。其他处理组及假手术组均未观察到组织学损伤（补充图2B）。在10 W条件下，1/3处理组出现严重热损伤；在20 W条件下，4/6处理组出现严重热损伤（p=0.524）。

输尿管结石治疗：热损伤

输尿管治疗的温度曲线如图1D-G所示。在0.8 J/12 Hz和2 J/5 Hz条件下，温度始终低于体温，5/6次实验的热剂量低于1分钟（表1）。在0.2 J/100 Hz和1 J/20 Hz条件下，3/6次实验的T_{max}>43°C，3/6次实验的热剂量 >120分钟。20 W与10 W设置在T_{max}（中位数44.6 vs. 36.3°C，p=0.109）或热剂量（153 vs. 0.0736分钟，p=0.200）方面均未发现统计学显著差异。

大体病理学显示，在0.2 J/100 Hz和1 J/20 Hz的两种处理条件下存在广泛的尿路上皮损伤（补充图1C，表1），而在任何10 W设置下均未观察到可见损伤（补充图1D）。在10 W条件下，0/6次处理和20 W条件下4/6次处理出现大体损伤（p=0.061）。

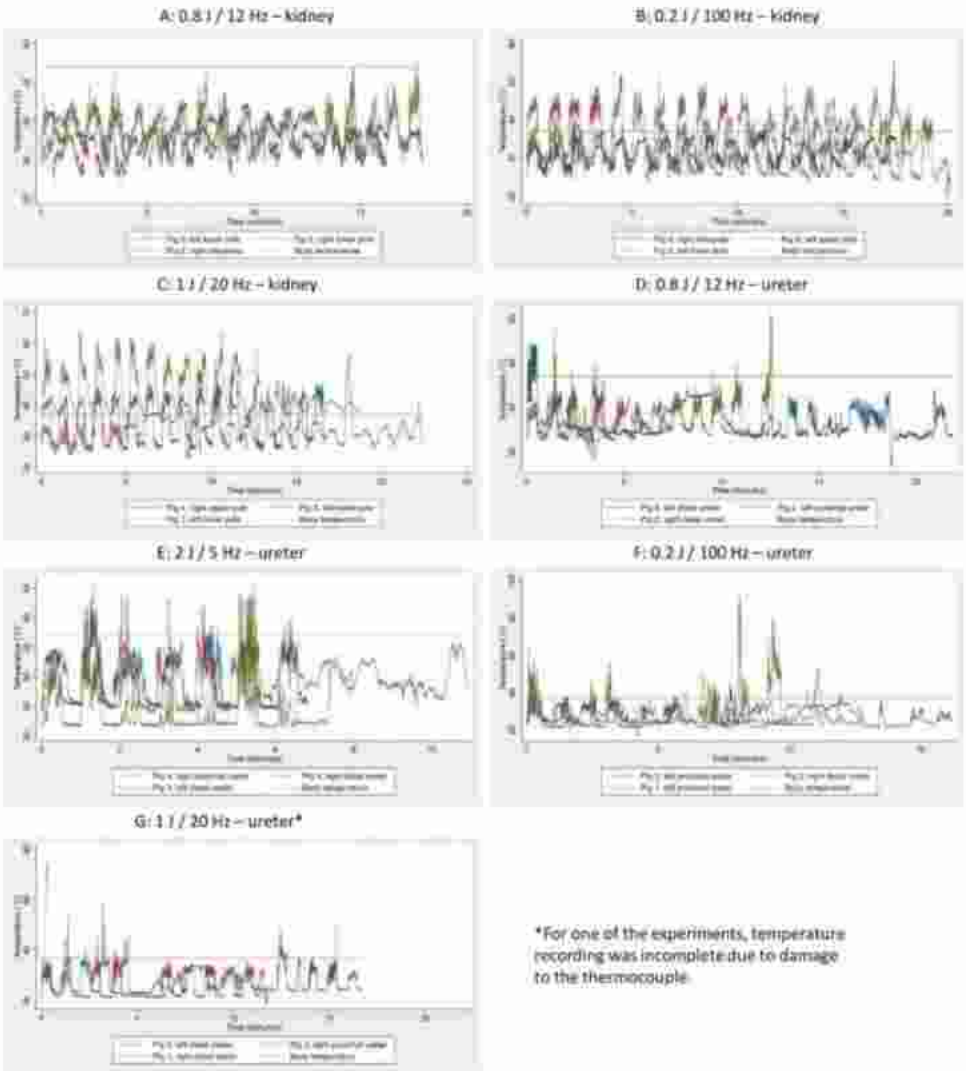


图1不同设置下激光治疗期间肾脏（**a–c**）与输尿管（**d–g**）的温度曲线。水平橙色线代表体温

表1不同激光参数下肾脏和输尿管治疗后的最高温度、热剂量、大体病理学及组织病理学结果（n=3，每种参数）；温度和热剂量数据以中位数（范围）表示；组织损伤数据以显示特定损伤的实验次数表示

机构	权力 (W)	脉搏	频繁性 蹲客	最大 温 度 T $_{max}$ （℃）	热剂量，CEM43 分	总	热组织组织学检查 伤害		
							没有一个	轻度	重度
肾脏	10	0.8	12	33.2 (31.5–33.7)	1.89×10^{-4} (1.25×10^{-6}–0.280)	0	2	0	1
	20	0.2	100	40.7 (36.4–47.6)	2.25 (4.10×10^{-3}–103)	0	2	0	1
	20	1	20	54.3 (43.8–57.8)	394 ($8.22–1.32\times10^{5}$)	2	0	0	3
输尿管	10	0.8	12	37.3 (31.7–38.0)	0.326 (6.45×10^{-5}–5.72)	0	0	2	1
	10	2	5	35.9 (31.8–36.7)	0.0453 (0.0449–0.102)	0	0	3	0
	20	0.2	100	49.3 (34.8–55.9)	33.9 (1.63×10^{-4}–6.64×10^{9})	2	0	0	3
	20	1	20	39.9 (32.9–69.4)	272 (0.0349–7.82×10^{7})	2	0	0	3

组织学观察显示，在0.8焦耳/12赫兹的实验中，三分之一的样本出现严重热损伤（补充图2C），三分之二的样本出现轻微热损伤（补充图2D，表1）。所有2焦耳/5赫兹的处理组均仅出现轻微损伤。0.2焦耳/100赫兹和1焦耳/20赫兹的处理组在全部三个实验中均引发严重热损伤。机械损伤（但无热损伤）在八分之七的假手术组中被发现（补充图2E）。在10瓦功率下，六分之一的处理组出现严重热损伤；20瓦功率下，六分之六的处理组出现严重热损伤（p=0.015）。

治疗效率

在肾结石治疗过程中，所有激光设置下结石质量的中位处理率为84%（范围54-90%）。中位手术时间与中位激光激活时间分别为20.2分钟（17.9-24.3）和9.8分钟（8.2-12.1）。总体治疗效率为0.57毫克/秒（0.29-0.64），各激光设置下的效率如补充图3A所示。不同设置间的治疗效率无显著差异（p=0.670）。

在输尿管结石治疗过程中，77%（范围49-100）的结石体积在所有激光设置下均被处理，中位手术时间为12.3分钟（8.5-24.2），中位激光激活时间为6.1分钟（4.3-12.2）。总体治疗效率为0.35毫克/节（0.15-0.55），各激光设置下的效率如补充图3B所示。未观察到不同设置间治疗效率存在显著差异（p=0.161）。

碎片大小分布

在所有输尿管结石治疗中，中位数86%（范围59-100%）的治疗结石质量由<0.25 mm的颗粒组成。0.25-1 mm碎片占比<1%（0-3%），1-3 mm碎片占比13%（0-40%）。1-3 mm碎片的最大比例见于2 J/5 Hz（35%），但不同治疗方案间碎片大小分布未观察到统计学显著差异（p=0.122，补充图4）。

讨论

这是首个在猪模型中评估TFL碎石术后热损伤及治疗效率的研究。在室温下以20 mL/min冲洗并交替进行30秒激光激活与休息的受控条件下，我们发现20 W设置会导致肾脏和输尿管的管腔内温度升高及热组织损伤，而10 W设置总体上是安全的，可维持温度低于生理阈值，仅引起组织轻微的组织学改变。

在肾结石治疗过程中，20瓦激光设置始终产生超过43°C的温度，该阈值此前已被证实与热损伤相关[16，17]。相应地，我们的组织病理学分析证实，在这些高温条件下，治疗区域的宏观和微观层面均存在整体性损伤证据。输尿管也呈现类似趋势：10瓦治疗可维持安全温度范围，而20瓦设置则常导致危险高温和组织损伤。10瓦组的组织损伤较为罕见，但20瓦组则频繁出现。

我们对治疗效率的分析显示，10 W与20 W设置在肾脏或输尿管中均未显示出显著差异，尽管这一结论受限于样本量较小。虽然更高功率可能提高治疗效率，但我们认为该差异较为有限，且被热损伤风险增加所抵消。

鉴于其良好的安全性和效率特性，我们推荐将0.8 J/12 Hz作为使用TFL进行碎石治疗的有效参数。我们先前的研究表明，与0.2 J/50 Hz等低能量/高频参数相比，该参数能实现更高效的碎石效果[4，14]。由于TFL具有高吸水性、低峰值功率和长脉冲宽度的特点，它在传统碎石治疗参数下仍能实现有效碎石。这一结论在随机对照试验中得到进一步验证：接受1 J/10 Hz TFL治疗的患者，其碎石治疗效果优于0.1 J/100 Hz组[20]。

在需要更精细碎裂的情况下，我们认为脉冲能量较高的设置可能效果更佳。本研究中，2焦耳/5赫兹的参数设置比其他参数能产生更多适合碎石的可提取碎片。这与我们在台式输尿管模型中的实验结果一致——该参数在不超出安全热阈值的前提下实现了更优的碎裂效果[21]。虽然需注意避免激光意外接触尿路上皮组织，但低频段与高效碎裂特性有助于泌尿科医生在保持良好控制的同时，将激光源与组织表面的距离控制得更远。

本研究存在若干局限性：样本量相对较小、无法精确控制肾盏体积、使用BegoStone模拟体而非人体结石、测试的激光参数设置有限，且组织学观察到的损伤临床意义尚不明确。此外，本研究结果仅适用于TFL，不应外推至Ho:YAG或其他激光技术。这些发现可能也不适用于其他冲洗参数或激光激活周期。尽管存在这些局限性，本研究仍为泌尿科医师选择TFL治疗肾及输尿管结石的激光参数提供了有价值的体内证据。

结论

这项猪体内研究证实，采用20W功率的 TFL 碎石术，在标准冲洗和激光激活参数下，可能导致肾盂和输尿管管腔内温度升高并造成热损伤。相比之下，10W功率的治疗在不显著降低治疗效率的前提下，具有热安全性。

补充信息在线版本包含补充材料，可在https://doi.org/10.1007/s00345-0 25-06165-4获取。

致谢作者谨向以下个人及部门致以诚挚谢意，感谢他们为本研究作出的宝贵贡献：杜克大学实验动物服务中心杜克动物饲养中心：Heather Lewis、Marisa Tonner、Aura Cortes de Gomez、Fernando Orozco、Kelly Shaw、Angela Garner、Lindsey Morgan、Ianthia Parker、Andres Schreiner、Lauren Dunlap、Danielle Cecil，以及 DLAR 动物饲养中心、药房和动物订购团队的众多同仁。杜克大学医学中心病理学系研究组织学实验室：Emily Knutson和Thomas Ribar。作者还特别感谢Sonia Doss，她作为 IACUC（注册号：A071-24-03）的质控与合规助理，专业指导了我们的实验工作。

作者贡献概念化：Ezra Margolin、Arpit Mishra、Jodi Antonelli、Glenn Preminger、Charles Scales、Robert Medairos、Pei Zhong、Michael Lipkin；方法论：Ezra Margolin、Arpit Mishra、Jodi Antonelli、Glenn Preminger、Charles Scales、Robert Medairos、Pei Zhong、Michael Lipkin；形式分析与调查：Ezra Margolin、Arpit Mishra、David Barquin、Aaron Stewart、Nicklas Sarantos、Jeremy Kurnot、Logan Grimaud、Thomas Schroeder、Megan Bock、Jiaoti Huang；撰写——初稿准备：Ezra Margolin；撰写——审阅与编辑：Ezra Margolin、Arpit Mishra、Jiaoti Huang、Jodi Antonelli、Glenn Preminger、Charles Scales、Robert Medairos、Pei Zhong；资金获取：Pei Zhong；资源：Pei Zhong；监督：Pei Zhong、Michael Lipkin。

资助本项目由美国国立卫生研究院（NIH）通过以下资助项目支持：1P20DK135107-03、1R01DK138972-01A1及2R01DK052985-28。

数据可用性本研究期间未生成或分析任何数据集。

声明

利益冲突GMP 与MEL为波士顿科学公司顾问。其他所有作者均无利益冲突需要声明。

参考文献

1. 列卡列夫 V、迪莫夫 A、维纳罗夫 A、索罗金 N、米纳耶夫 V、米纳耶夫 N、齐皮娜 S、尤苏波夫 V（2020）超脉冲钬光纤激光碎石术的机制及其临床疗效。应用科学 10（21）:7480
2. Jiang P，Oklunov Z，Afyouni AS，Ali S，Hosseini Sharifi SH，Bhatt R，Brevik A，Ayad M，Larson K，Osann K，Patel RM，Landman J，Clayman RV（2023）超脉冲钬激光的比较研究光纤激光与钬激光在猪体内模型中用于肾结石消融的比较研究。《内镜泌尿外科杂志》37(3):335-340。https://doi.org/10.1089/lue.2022.0445
3. Sierra A，Corrales M，Kolvatzis M，Panthier F，Pinero A，Traxer O（2022）钬YAG激光与钬光纤激光的热损伤及激光效率——一项体外研究。《关节外科学杂志》36（12）:1599–1606。https://doi.org/10.1089/end.2022.0216
4. Mishra A，Medairos R，Chen J，Soto-Palou F，Wu Y，Antonelli J，Preminger GM，Lipkin ME，Zhong P（2024）探索肾盂模型中安全有效钬光纤激光碎石术的最佳参数设置。BJU Int 133(2):223–230.https://doi.org/10.1111/b ju. 16218
5. Belle JD，Chen R，Srikureja N，Amasyali AS，Kehcila M，Baldwin DD（2022）体外研究显示新型钬光纤激光器是否比传统钬激光器具有更高的尿路上皮热损伤风险？《内镜泌尿外科杂志》36(9):1249–1254.https://doi.org/10.1089/end.2021.0842
6. Molina WR，Carrera RV，Chew BH，Knudsen BE（2021）输尿管激光碎石术中的温度升高：超脉冲钬光纤激光（SPTF）与高功率120 W钬YAG激光（Ho:YAG）的比较。世界泌尿外科杂志 39（10）:3951–3956.https://d oi.org/10.1007/s00345-021-03619-3
7. Hardy LA，Wilson CR，Irby PB，Fried NM（2014）钨光纤激光在体外输尿管模型中的碎石术。《生物医学光学杂志》19（12）:128001。https://doi.org/10.1117/1.Jbo.19.12.128001
8. Walterding C，Saxton A，Phan D，Doersch KM，Shepard L，Schuler N，Hassig S，Quarrier S，Osinski T，Ghazi A（2024）在这里变得火热！钬激光与钬激光在解剖学水凝胶肾盂模型中的比较。Urolithiasis 52(1):49.https://doi.org/10.1007/s00240-024-01541-y
9. 2类器械召回Olympus（2021年）美国食品药品监督管理局。https://www.accessdata.fda.gov/scripts/cdrh/cfd ocs/cfres/res.cfm?id=188172。访问日期：2025年4月25日
10. Okhunov Z，Jiang P，Afyouni AS，Ayad M，Arada R，Brevik A，Akopian G，Patel RM，Landman J，Clayman RV（2021）Caveat emptor: the heat is ON——钬光纤激光在粉尘和碎裂模式下对猪肾脏温度变化的体内评估。J Endourol 35（11）:1716–1722.https://doi.org/10.1089/end.2021.0206
11. Peteinaris A，Tsaturyan A，Bravou V，Tatanis V，Faria-Costa G，Pagonis K，Faitatziadis S，Vagionis A，Liatsikos E，Kallidonis P（2023）高功率激光碎石术——我们是在治疗还是在伤害？钬光纤激光体内研究中温度效应的组织学评估。《欧洲泌尿外科杂志》76(1):44–48。https://doi.org/10.5173/ceju.2023.24
12. Sierra A，Corrales M，Somani B，Traxer O（2022）激光效率与激光安全性：钬YAG激光器与钬光纤激光器。《临床医学杂志》12(1).https://doi.org/10.3390/jcm12010149
13. Esch E，Simmons WN，Sankin G，Cocks HF，Preminger GM，Zhong P（2010）制备不同物理特性的人工肾结石的简易方法。Urol Res 38(4):315–319.https://doi.org/10.1007/s00240-010-0298-x
14. Chen J，Mishra A，Medairos R，Antonelli J，Preminger GM，Lipkin ME，Zhong P（2023）钬光纤激光体外研究结石消融效率、Char形成、火花产生及损伤机制。Urolithiasis 51(1):124.https://doi.org/10.1007/s00240-023-01501-y
15. 陈杰、李迪、余伟、马子、李晨、向刚、吴勇、姚杰、钟鹏（2022）短脉冲钬:YAG激光碎石术中扫描速度与光纤支架距离对除尘效率的影响。临床医学杂志 11（17）。https://doi.org/10.3390/jcm111750 48
16. Kim M，Kim G，Kim D，Yoo J，Kim D-K，Kim H（2019）关于不同肿瘤长宽比诱导凋亡温度的有效条件数值研究

金纳米棒光热治疗中单个连续波激光的应用。《癌症》11(6):764

17. DewhirstMW，VigliantiBL，Lora-MichielsM，HoopesPJ，HansonM（2003）组织效应的热剂量需求：实验与临床研究结果。SPIE 国际光学工程学会会刊4954:37。https://doi.org/10.1117/12.476637
18. Sapareto SA，Dewey WC（1984）癌症治疗中的热剂量测定。国际放射肿瘤学与生物物理学杂志 10(6):787–800.http s://doi.org/10.1016/0360-3016（84）90379-1
19. Yarmolenko PS，Moon EJ，Landon C，ManzoorA，Hochman DW，Viglianti BL，Dewhirst MW（2011）正常组织热损伤阈值：最新进展。国际高热杂志 27(4):320–343.ht tps://doi.org/10.3109/02656736.2010.534527
20. Pathak N，Gowda N，Coelho V，Shete N，Singh A，Gaupale A，Subnis R，Desai M（2024）前瞻性随机对照试验：比较钬纤维喷雾与碎裂疗法

器光在进行经内手术中的应用。《内镜泌尿外科杂志》38(2):102–107。https://doi.org/10.1089/end.2022.0167
21. Mishra A，Margolin EJ，Medairos RA，Antonelli J，Preminger GM，Lipkin ME，Zhong P（2025）钨光纤激光在输尿管结石碎石术中优化碎石效果的体外研究。《内镜泌尿外科杂志》

出版者注斯普林格·自然出版社对于已出版地图中的管辖权主张及机构隶属关系保持中立立场。

施普林格·自然出版社或其授权方（如学术团体或其他合作伙伴）根据与作者或其他权利持有人签订的出版协议，对该文章享有独家权利；作者对已接受稿件版本的自存档行为，仅受该出版协议条款及适用法律约束。

Check for updates

JOURNAL OF ENDOUROLOGY
Volume 40, Number 1, January 2026
© Mary Ann Liebert (NY), LLC
Pp. 17–25
DOI: 10.1177/08927790251392232

Laser Lithotripsy Induces Dose-Dependent Temperature Elevation During Retrograde Intrarenal Surgery

Kavita Gupta, MD,[1] Christopher Connors, BS,[1] Ziv Savin, MD,[1] Dara Lundon, MD,[1] Raymond Khargi, MD,[1] Vinay Durbhakula, BS,[1] Kasmira Gupta, BS,[2] Blair Gallante, MPH,[1] William M. Atallah, MD,[1] and Mantu Gupta, MD[1]

Abstract

Objective: Real-time assessment of calyceal and tissue temperatures during laser lithotripsy.
Methods: Patients eligible for endoscopic combined intrarenal surgery were assigned to Soltive 60 W SuperPulsed thulium fiber laser (TFL; Olympus, Inc.) or holmium:YAG (Ho:YAG; Lumenis Pulse™ 120H) based on availability. After translocation of stones, a 1.5-mm multipoint thermal sensor needle measuring temperatures 5, 15, 25, and 35 mm from the tip was placed percutaneously with ultrasound guidance. The 5-mm mark recorded calyceal fluid temperature and the others parenchymal temperatures for 2 minutes during fragmentation (1 J/2 Hz TFL and 0.5 J/5 Hz Ho:YAG, 2–2.5 W), dusting (0.3 J/50 Hz, 15 W), and pop-dusting (0.5 J/80 Hz, 40 W). If tissue temperature exceeded 43°C, lasering was paused. After measurements, tract dilation and percutaneous nephrolithotomy were performed. Categorical data were compared using chi-square or Fisher's exact tests and continuous variables via *t*-tests.
Results: The 20 patients (10 TFL and 10 Ho:YAG) had similar baseline characteristics. During fragmentation, calyceal (T_{calyx}) and parenchymal (T_{tissue}) temperatures never exceeded 41°C. During dusting, T_{calyx} exceeded 43°C in four patients for each laser and T_{tissue} exceeded 43°C in one Ho:YAG patient (49°C after 60 seconds). Maximum calyceal temperature (T_{max}) in TFL and Ho:YAG patients was 51°C and 56°C ($p = 0.18$), respectively. During pop-dusting, T_{calyx} exceeded 43°C in 10 TFL and 8 Ho:YAG patients, and average maximum temperature ($avgT_{max}$) was significantly higher for TFL (52.9°C *vs* 45.1°C, $p = 0.027$). The tissue T_{max} was 47°C and 49°C ($p = 0.96$), respectively, with 43°C exceeded in three TFL and three Ho:YAG patients.
Conclusion: During high-powered lasering, temperatures can exceed 43°C in as little as 15 seconds. This is concerning since temperatures >43°C may be associated with permanent tissue injury.

Keywords: lasers, renal temperature, ureteroscopy

Introduction

Retrograde intrarenal surgery (RIRS) using holmium:YAG (Ho:YAG) and thulium fiber laser (TFL) systems for lithotripsy has become the most common surgical treatment for kidney stones.[1] Although advancements in laser technology, particularly the development of high-power modalities, have enhanced stone ablation efficiency, concerns have been raised regarding the potential for thermal injury to surrounding urothelial tissues.[2]

Energy emitted by a laser used in ureteroscopy (URS) may dissipate, in the form of heat, into surrounding tissues, potentially causing thermal damage such as coagulation, carbonization, and protein denaturation.

Existing literature highlights the importance of modifiable surgical parameters, including irrigation temperature and flow rate, utilization of ureteral access sheaths (UASs), laser settings (power, pulse duration, and frequency), and operator duty cycle, in lowering intrarenal temperatures and thus mitigating potential thermal damage during URS.[3–5]

However, no human studies, to date, have been done to measure both renal parenchymal and calyceal temperatures during RIRS with lithotripsy with both pulse-modulated Ho:YAG (Lumenis Pulse™ 120H) and SuperPulsed TFL (Olympus, Inc.) systems. The primary objective of this study was to measure human intracalyceal and renal parenchymal temperature changes in real time during endoscopic stone surgery with two high-power laser systems. Secondary objectives

[1]Department of Urology, Icahn School of Medicine at Mount Sinai, New York, New York, USA.
[2]Albert Einstein College of Medicine, New York, New York, USA.
The abstract was previously published in *The Journal of Urology*, Volume 213, Issue 5S, May 2025.

included correlating irrigation fluid temperatures with parenchymal temperatures in real time during endoscopic stone and determining which modifiable surgical factors influence renal temperature changes during endoscopic stone surgery with high-power laser systems. Another secondary objective included comparing calyceal and renal parenchymal temperature changes between the pulse-modulated Ho:YAG and SuperPulsed TFL systems.

Methods

Study design

An Institutional Review Board approved (IRB STUDY-23-00046) from December 2023 to July 2024 recruited patients with unilateral stone burden requiring a combined approach (endoscopic combined intrarenal surgery [ECIRS]) at Mount Sinai Medical Center. Although surgeon preference plays a role, the primary indications for ECIRS included a large stone burden (≥2 cm) and multiple stones in different calyces, in an effort to prevent the need for a multiaccess percutaneous nephrolithotomy (PCNL). Patients were then screened for the following inclusion criteria: minimum age of 18 years; nonpregnant and able to provide informed consent; preoperative creatinine ≤1.3 mg/dL; negative preoperative urine culture; and preoperative CT scan within 60 days of surgery. Exclusion criteria included nephrolithiasis procedure (i.e., shockwave lithotripsy, URS/laser lithotripsy [LLT], or PCNL) within the previous 90 days; preoperative indwelling urinary drain (ureteral stent and percutaneous nephrostomy tube); history of urinary diversion; congenital kidney anomalies, solitary or atrophic kidney; and preexisting urinary tract obstruction or ureteral stricture disease.

Procedure

Stone burden was defined as the sum of the single longest diameters of all stones, as measured in the coronal dimension. For a more precise measurement, total stone volume was calculated by summing the volumes of individual stones. Maximal width and length were measured on axial views and height on coronal views, all under ≥8× magnification. Using these dimensions, individual volumes were determined via manual calculation with the European Association of Urology ellipsoid formula: $V = 0.167 \times \pi \times L \times W \times H$.

Patients were assigned to receive LLT with either a TFL (60 W Soltive™ SuperPulsed) or Ho:YAG (Lumenis Pulse™ 120H) laser system based on the availability of the laser system.

All patients were positioned in the modified Barts flank-free position followed by standard sterile preparation and draping. Cystoscopy was performed followed by flexible URS (Flex X2, Karl Storz) under direct vision into the renal collecting system. The procedure was performed without the use of a UAS. A comprehensive pyeloscopy was performed to identify and characterize the stone burden. As is our standard procedure with ECIRS, all stones were translocated using a basket to a favorable calyx for LLT followed by percutaneous evacuation of all stones, stone particles, and dust. All patients received gravity irrigation at room temperature with saline irrigant bags placed 80 cm above the patient's abdomen (distance from top of the abdomen to the bottom of the irrigant bag). Although the precise volume of infused fluid was not measured, our standard protocol for URS involves using no more than a single 1-L saline bag.

After translocation of stones, a 1.5-mm multipoint thermal sensor (MTS) needle (Boston Scientific) was utilized to get percutaneous access to the favorable renal calyx in place of using a 18 g access needle (Fig. 1). The MTS needle was inserted into the collecting system under ultrasound and fluoroscopic guidance. Moreover, with the flexible ureteroscope in position, the needle penetration was observed in real time. After the needle was positioned properly with the distal most sensor in the calyx, it was calibrated according to protocol to ensure accurate functionality.

The Soltive 60 W SuperPulsed TFL (Olympus, Inc.) or Lumenis P120 Ho:YAG laser with MOSES™ technology (Boston Scientific) systems was used for LLT with a 200-μm laser fiber. Temperature data were collected from each patient during LLT using three commonly used laser settings. Fragmentation was performed with the following settings: 1 J/2 Hz (TFL) and 0.5 J/5 Hz (Ho:YAG), 2–2.5 W with the aim to break stones into large pieces. Dusting was performed with the following settings: 0.3 J/50 Hz, 15 W with the aim to pulverize stone into fine powder in a continuous "painting" motion over the stone's surface. Pop-dusting was performed with the following settings: 0.5 J/80 Hz, 40 W with the aim to rapidly fragment kidney stones into extremely fine, powder-like pieces. Each laser mode was used for 2 minutes, with intracalyceal and parenchymal tissue temperatures measured in real time. If tissue temperature exceeded 43°C, lasering was paused. Before commencing a new laser setting, the temperature of the caliceal fluid and renal parenchyma was allowed to return to baseline body temperature prior to initiating a new laser setting.

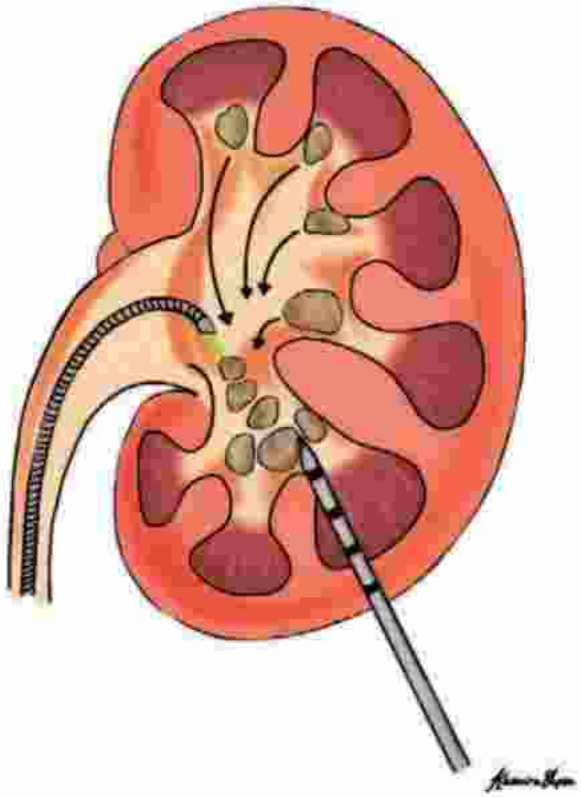


FIG. 1. Diagram of translocation of stones to a favorable calyx and percutaneous placement of multipoint thermal sensor with calyceal (5 mm) and parenchymal (15 mm [1 cm], 25 mm [2 cm], and 35 mm [3 cm]) marks.

During LLT, temperature measurements were recorded using the MTS needle at 5 mm (calyceal), 15 mm (1 cm), 25 mm (2 cm), and 35 mm (3 cm) from the probe's tip. The 5-mm sensor was located just within the collecting system, whereas the other sensors measured temperatures along the parenchyma (medulla and cortex) in real time. At each site along the MTS needle, we monitored for temperatures over 43°C and recorded the duration for which this threshold was surpassed. The operating surgeon assessed and graded any laser-induced damage intraoperatively, immediately following the completion of lithotripsy. The laser damage was graded with the following criteria: Grade 0: none, Grade 1: mucosal, Grade 2: submucosal, and Grade 3: full thickness.[6]

Following temperature measurements, a fascial dilator was placed over the MTS needle under direct vision, to facilitate the placement of a guidewire and to perform balloon dilation of the tract to 24F followed by PCNL of all stones and fragments and dust in standard fashion. At the conclusion of the case, the surgeon decided as usual if a ureteral stent or nephrostomy tube was necessary. Categorical data were compared using chi-square or Fisher's exact tests, whereas continuous variables were analyzed via *t*-tests. Normality of distributions for all comparisons was assessed via Kolmogorov–Smirnov and Shapiro–Wilk tests of normality. Given that the majority of comparisons/distributions in our study did not violate the assumption of normality, we opted to compare data between our groups using means/*t*-tests and standard deviations.

Results

Between December 2023 and July 2024, a total of 26 patients met the inclusion criteria for ECIRS. Six patients were preoperatively excluded according to exclusion criteria, resulting in a final analysis of 20 patients, with 10 in each treatment arm (Fig. 2).

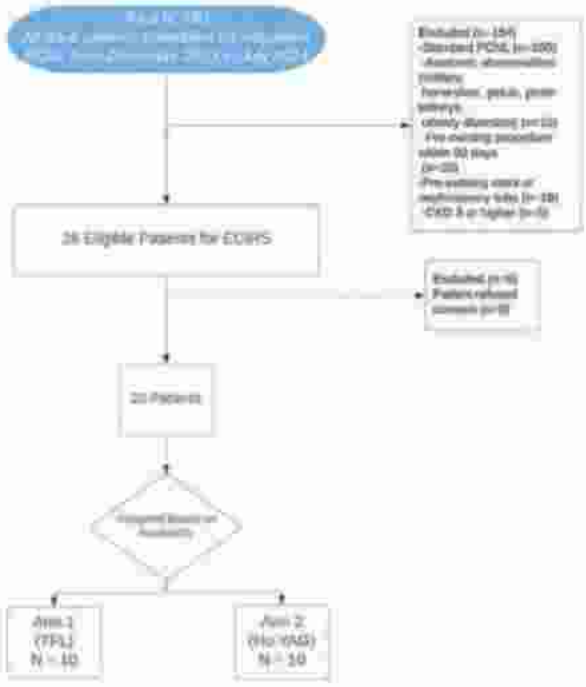


FIG. 2. Flow diagram.

There were no differences in demographics, stone characteristics, and clinical characteristics between both groups (Table 1). Total operative time, operator duty cycle, and frequency of visible laser damage were similar between both groups. Nine out of 20 (45%) were done totally tubeless, without stents or nephrostomy tubes. The remaining 11 had stents but no nephrostomy tubes.

Mean baseline calyceal temperatures (T_{calyx}) for Ho:YAG and TFL were below 33°C across all time points for both groups (Table 2). During fragmentation, 1 J and 2 Hz, 2 W, mean calyceal temperatures for Ho:YAG and TFL were 31.8°C *vs* 32.5°C at 0 seconds, 33.4°C *vs* 33.3°C at 60 seconds, and 34.0°C *vs* 33.4°C at 120 seconds ($p = 0.404$, $p = 0.941$, $p = 0.699$; Fig. 3). During dusting, 0.3 J and 50 Hz, 15 W, mean T_{calyx} for Ho:YAG and TFL was 32.5°C *vs* 31.9°C at 0 seconds, 39.1°C *vs* 42.1°C at 60 seconds, and 37.6°C *vs* 42.6°C at 120 seconds ($p = 0.526$, $p = 0.289$, $p = 0.082$). During dusting, T_{calyx} exceeded 43°C in four TFL patients and four Ho:YAG patients (mean T_{max}: 44.3°C *vs* 40.4°C, $p = 0.175$). Maximum calyceal temperature (T_{max}) in TFL and Ho:YAG patients was 51°C and 56°C ($p = 0.18$), respectively. During pop-dusting, 0.5 J and 80 Hz, mean T_{calyx} for Ho:YAG and TFL was 33.0°C *vs* 32.7°C at 0 seconds, 43.0°C *vs* 47.3°C at 60 seconds, and 40.0°C *vs* 51.2°C at 90 seconds ($p = 0.754$, $p = 0.264$, $p = 0.071$). The T_{calyx} exceeded 43°C in 10 TFL and 8 Ho:YAG patients with a significantly higher mean T_{max} in the TFL arm (TFL: 52.9°C, Ho:YAG: 45.1°C, $p = 0.027$).

Mean baseline parenchymal temperatures (T_{tissue}) for both groups were also comparable and remained below 36°C across all time points. During fragmentation, mean T_{tissue} at the 15-mm probe tip for Ho:YAG and TFL was 34.2°C *vs* 35.2°C at 0 seconds, 34.7°C *vs* 35.3°C at 60 seconds, and 34.8°C *vs* 32.3°C at 120 seconds ($p = 0.087$, $p = 0.468$, $p = 0.430$). Maximum calyceal and parenchymal temperatures averaged below 36°C and never exceeded 43°C during fragmentation (Table 3).

During dusting, mean T_{tissue} at the 15-mm probe tip for Ho:YAG and TFL was 35.0°C *vs* 35.0°C at 0 seconds, 36.9°C *vs* 36.5°C at 60 seconds, and 36.3°C *vs* 36.6°C at 120 seconds ($p = 1.000$, $p = 0.805$, $p = 0.554$). The mean parenchymal T_{max} at 15 mm was 37.6°C and 37.2°C during dusting in the Ho:YAG and TFL groups, respectively ($p = 0.788$; Fig. 4). T_{tissue} during dusting only exceeded 43°C in one patient in the Ho:YAG cohort (49°C after 60 seconds at the 15 mm probe; Fig.5). At the 25 mm and 35 mm markers, the mean T_{max} was <37°C for both Ho:YAG and TFL with no significant statistical differences between groups. During pop-dusting, mean T_{tissue} at the 15-mm probe tip for Ho:YAG and TFL was 34.6°C *vs* 35.1°C at 0 seconds, 38.4°C *vs* 38.3°C at 60 seconds, and 39.0°C *vs* 39.5°C at 90 seconds ($p = 0.607$, $p = 0.954$, $p = 0.899$). The mean parenchymal T_{max} at 15 mm was 39.8°C and 39.9°C during pop-dusting in the Ho:YAG and TFL groups, respectively ($p = 0.958$). T_{tissue} during pop-dusting exceeded 43°C two times in the Ho:YAG cohort and three in the TFL cohort, which all occurred at the 15 mm probe (Fig. 6). At the 25-mm and 35-mm probes, mean T_{max} was comparable between groups and averaged below 37°C during pop-dusting.

Table 1. Baseline Characteristics and Operative Information Between Ho:YAG and TFL Groups

	Ho:YAG	*TFL*	p *Value*
Age [STD]	54.8 [16.3]	58.6 [11.6]	0.556
BMI [STD]	28.4 [3.5]	26.6 [7.4]	0.512
Gender, *n* (%)			0.170
Male	2 (80.0)	4 (40.0)	
Female	2 (20.0)	6 (60.0)	
ASA score, *n* (%)			0.211
2	10 (100.0)	7 (70.0)	
3	0 (0.0)	3 (30.0)	
Diabetes, *n* (%)	1 (10.0)	0 (0.0)	1.000
Diuretics, *n* (%)	0 (0.0)	0 (0.0)	—
ARB or ACE inhibitor, *n* (%)	1 (10.0)	3 (30.0)	0.582
Anticoagulants, *n* (%)	0 (0.0)	1 (10.0)	1.000
Antiplatelets, *n* (%)	1 (10.0)	0 (0.0)	1.000
History of recurrent UTI, *n* (%)	0 (0.0)	2 (20.0)	0.474
Positive preop urine culture, *n* (%)	1 (10.0)	0 (0.0)	1.000
Preoperative creatinine [STD]	1.0 [0.2]	1.0 [0.3]	0.979
Preoperative EGFR [STD]	88.2 [23.7]	79.2 [20.4]	0.376
Previous stone surgery, *n* (%)	7 (70.0)	8 (80.0)	1.000
ESWL	0 (0.0)	1 (10.0)	1.000
URS	4 (40.0)	3 (30.0)	1.000
PCNL	2 (20.0)	4 (40.0)	0.628
Laterality, *n* (%)			1.000
Left	6 (60.0)	6 (60.0)	
Right	4 (40.0)	4 (40.0)	
Renal pelvis AP diameter, cm [STD]	2.2 [0.8]	2.0 [0.7]	0.503
Total stone burden, mm [STD]	21.7 [10.0]	22.2 [10.6]	0.906
Stone volume, mm^3 [STD]	3292.0 [3140.1]	2157.6 [2607.6]	0.391
HU [STD]	876.9 [370.5]	801.9 [173.6]	0.572
Size of laser fiber, nm, *n* (%)			0.057
150	1 (10.0)	6 (60.0)	
200	9 (90.0)	4 (40.0)	
Visible laser damage, *n* (%)			0.141
Grade 0: none	5 (50.0)	9 (90.0)	
Grade 1: mucosal	5 (50.0)	1 (10.0)	
Grade 2: submucosal	0 (0.0)	0 (0.0)	
Grade 3: full thickness	0 (0.0)	0 (0.0)	
Total laser energy used, kJ [STD]	3.8 [1.5]	5.2 [1.3]	**0.038***
Operator duty cycle, minutes [STD]	16.02 [2.02]	16.33 [3.09]	0.790
Pedal time, minutes [STD]	4.81 [0.61]	4.90 [0.93]	0.801
Total operative time, minutes [STD]	76.7 [15.9]	70.7 [13.9]	0.390

Continuous variables reported as medians. *p* Values derived from chi-square tests, Fisher's exact tests, or *t*-tests, with significance set to $p < 0.05$ (bolded and * for reference).

AP = anterior posterior; ESWL = extracorporeal shock wave lithotripsy; Ho:YAG = holmium:YAG; PCNL = percutaneous nephrolithotomy; STD = standard deviation; TFL = thulium fiber laser; URS = ureteroscopy.

Discussion

High-powered lasers have demonstrated increased efficiency in LLT; however, they also pose a risk of elevating intrarenal temperatures, potentially leading to thermal injury to the kidney. This study evaluates calyceal and parenchymal temperature elevations up to 120 seconds following the activation of high-powered lasers. Additionally, we analyzed the minimum, maximum, and mean calyceal and parenchymal temperatures during laser activation using both pulse-modulated Ho:YAG and SuperPulsed TFL systems.

With the advent of high-powered lasers, several modifiable risk factors have been investigated to mitigate the risk of thermal injury, one of which is laser settings. In this study, we observed that with low-powered settings (2–2.5 W), renal temperatures—including both calyceal and parenchymal measurements—remained below 43°C for both TFL and Ho:YAG systems. In contrast, high-powered settings (>15 W) led to temperatures exceeding 43°C within as little as 15 seconds. Similarly, a study that measured calyceal fluid temperature utilizing a Type K thermocouple during retrograde LLT with a TFL laser at incremental settings reported that a temperature of 43°C was reached in 3 out of 10 patients at 20 W and in 8 out of 10 patients at 30 W, whereas it remained below this threshold at 5 W and 10 W.[7] In an *in vivo* porcine model, all dusting and most fragmentation settings (dusting: 0.5 J, 80 Hz, 40 W; low-power fragmentation: 1 J, 10 Hz, 10 W; high-power fragmentation: 1.5 J, 20 Hz, 30 W) resulted in calyceal temperatures reaching or exceeding 44°C.[8] All the settings >5 W in our study and in

Table 2. Temperature Outcomes Between Ho:YAG and TFL Groups

	Mean calyceal temperature, °C			*Mean 15 mm temperature, °C*			*Mean 25 mm temperature, °C*			*Mean 35 mm temperature, °C*		
	Ho:YAG	*TFL*	p *Value*	*Ho:YAG*	*TFL*	p *Value*	*Ho:YAG*	*TFL*	p *Value*	*Ho:YAG*	*TFL*	p *Value*
Baseline [STD]												
0 seconds	32.2 [1.8]	31.6 [3.4]	0.628	34.7 [1.6]	34.9 [1.4]	0.776	35.0 [1.6]	35.8 [0.8]	0.172	34.8 [1.7]	35.5 [1.0]	0.274
30 seconds	32.4 [1.8]	31.9 [2.6]	0.626	34.9 [1.5]	35.1 [1.1]	0.741	35.1 [1.5]	35.8 [0.8]	0.219	35.0 [1.6]	35.4 [1.0]	0.515
60 seconds	32.6 [1.8]	32.2 [2.4]	0.684	34.9 [1.5]	35.1 [1.1]	0.741	35.0 [1.6]	35.8 [0.8]	0.172	34.8 [1.8]	35.4 [1.0]	0.359
90 seconds	0.0 [0.0]	0.0 [0.0]	—	0.0 [0.0]	0.0 [0.0]	—	0.0 [0.0]	0.0 [0.0]	—	0.0 [0.0]	0.0 [0.0]	—
120 seconds	0.0 [0.0]	0.0 [0.0]	—	0.0 [0.0]	0.0 [0.0]	—	0.0 [0.0]	0.0 [0.0]	—	0.0 [0.0]	0.0 [0.0]	—
Fragmentation [STD]												
0 seconds	31.8 [1.5]	32.5 [2.1]	0.404	34.2 [1.4]	35.2 [1.0]	0.087	34.4 [1.5]	35.3 [1.1]	0.141	35.0 [1.5]	35.3 [1.3]	0.632
30 seconds	32.6 [2.5]	33.6 [3.0]	0.425	34.5 [1.9]	35.3 [1.2]	0.274	34.6 [1.6]	35.1 [1.0]	0.424	34.8 [1.8]	35.1 [1.3]	0.675
60 seconds	33.4 [3.1]	33.3 [2.8]	0.941	34.7 [2.3]	35.3 [1.2]	0.468	34.7 [1.8]	35.1 [1.0]	0.543	34.8 [1.9]	35.0 [1.2]	0.782
90 seconds	33.5 [3.1]	33.1 [3.0]	0.771	34.8 [2.3]	35.4 [1.3]	0.482	35.0 [1.8]	35.2 [0.9]	0.755	35.0 [1.9]	34.9 [1.4]	0.896
120 seconds	34.0 [3.4]	33.4 [3.4]	0.699	34.8 [2.3]	32.3 [9.3]	0.430	34.8 [1.9]	35.2 [1.0]	0.564	35.0 [1.9]	34.9 [1.4]	0.896
Dusting [STD]												
0 seconds	32.5 [1.8]	31.9 [2.3]	0.526	35.0 [1.6]	35.0 [1.1]	1.000	35.1 [1.4]	35.2 [1.0]	0.861	35.3 [1.4]	35.3 [1.3]	1.000
30 seconds	36.4 [4.2]	39.0 [4.2]	0.182	35.3 [2.0]	35.7 [1.4]	0.613	35.4 [1.5]	35.4 [1.4]	1.000	35.5 [1.7]	35.4 [1.6]	0.894
60 seconds	39.1 [6.4]	42.1 [5.9]	0.289	36.9 [4.5]	36.5 [2.3]	0.805	36.1 [2.4]	36.1 [2.3]	1.000	35.4 [1.6]	35.9 [2.6]	0.635
90 seconds	37.5 [3.4]	42.1 [5.6]	0.069	35.5 [1.5]	36.1 [1.6]	0.428	35.6 [1.2]	35.3 [1.0]	0.512	35.4 [1.7]	35.0 [1.4]	0.647
120 seconds	37.6 [3.2]	42.6 [6.6]	0.082	36.3 [1.2]	36.6 [1.3]	0.554	35.9 [1.1]	35.6 [0.9]	0.634	35.6 [1.5]	35.1 [1.2]	0.505
Pop-dusting [STD]												
0 seconds	33.0 [2.1]	32.7 [2.2]	0.754	34.6 [2.7]	35.1 [1.4]	0.607	34.7 [2.6]	35.4 [0.7]	0.434	34.7 [2.5]	35.3 [0.8]	0.492
30 seconds	41.2 [6.8]	43.4 [6.8]	0.479	37.9 [4.1]	37.6 [3.2]	0.858	36.7 [1.9]	36.0 [1.5]	0.370	36.0 [1.8]	35.8 [1.2]	0.772
60 seconds	43.0 [5.3]	47.3 [10.1]	0.264	38.4 [2.8]	38.3 [2.5]	0.954	36.8 [2.1]	36.1 [1.4]	0.463	36.1 [2.1]	35.9 [1.3]	0.795
90 seconds	40.0 [4.2]	51.2 [6.9]	0.071	39.0 [4.2]	39.5 [4.0]	0.899	36.0 [0.0]	36.8 [1.6]	0.259	34.5 [0.7]	36.3 [1.5]	0.077
120 seconds	38.0 [.]	53.5 [9.2]	—	37.0 [.]	40.0 [0.0]	—	36.0 [.]	36.5 [0.7]	—	35.0 [.]	35.0 [1.4]	—

p Values derived from *t*-tests, with significance set to $p < 0.05$ (bolded and * for reference).

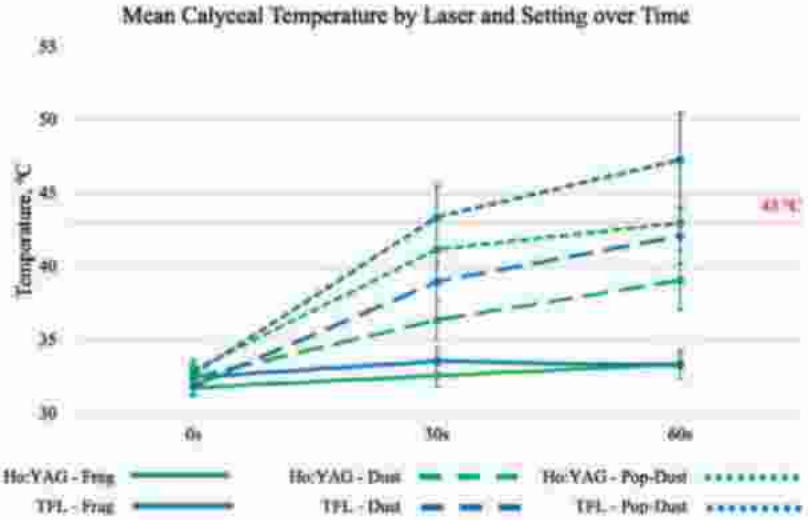


FIG. 3. Mean calyceal temperature by laser and setting over time. Error bars represent standard error of the mean.

prior *in vivo* studies have resulted in calyceal temperatures reaching or exceeding 43°C. These findings underscore the direct relationship between laser power settings and peak calyceal fluid temperatures. During pop-dusting, the average maximum temperature ($avgT_{max}$) was significantly higher for TFL than for pulse-modulated Ho:YAG. This finding is consistent with a previous *in vitro* URS study using an impacted ureteral stone model with no outflow where they found that TFL produced significantly higher temperatures than Dornier and Empower HL lasers across most power settings ($p < 0.001$).[9] The sole exception occurred at 20 W, where no significant difference was observed between TFL

TABLE 3. TEMPERATURE OUTCOMES BETWEEN HO:YAG AND TFL GROUPS

	Ho:YAG	*TFL*	p *Value*
Maximum calyceal temperature, °C [STD]			
Baseline	32.7 [1.9]	32.5 [2.6]	0.846
Fragmentation	34.1 [3.4]	34.4 [3.0]	0.837
Dusting	40.4 [5.8]	44.3 [6.5]	0.175
Pop-dusting	45.1 [5.2]	52.9 [8.6]	0.027*
Maximum 15 mm temperature, °C [STD]			
Baseline	34.9 [1.5]	35.1 [1.1]	0.741
Fragmentation	34.9 [2.2]	35.6 [1.2]	0.387
Dusting	37.6 [4.1]	37.2 [2.0]	0.788
Pop-dusting	39.8 [4.2]	39.9 [4.1]	0.958
Maximum 25 mm temperature, °C [STD]			
Baseline	35.1 [1.5]	35.8 [0.8]	0.219
Fragmentation	35.0 [1.8]	35.5 [1.0]	0.445
Dusting	36.6 [2.2]	36.3 [2.2]	0.760
Pop-dusting	37.0 [1.9]	36.7 [1.3]	0.687
Maximum 35 mm temperature, °C [STD]			
Baseline	35.0 [1.6]	35.5 [1.0]	0.419
Fragmentation	35.3 [1.6]	35.3 [1.3]	1.000
Dusting	35.8 [1.4]	36.1 [2.4]	0.736
Pop-dusting	36.4 [1.5]	36.2 [1.2]	0.749
Time to maximum temperature, seconds [STD]			
Baseline	—	—	—
Fragmentation	60.0 [.]	67.5 [45.0]	—
Dusting	76.7 [37.1]	82.5 [21.2]	0.693
Pop-dusting	49.5 [31.5]	75.0 [35.9]	0.136
Time to 43 °C (if reached), seconds [STD]			
Baseline ($n = 0$)	—	—	—
Fragmentation ($n = 0$)	—	—	—
Dusting (H: $n = 3$; T: $n = 6$)	60.0 [30.0]	50.0 [24.5]	0.648
Pop-dusting (H: $n = 7$; T: $n = 9$)	45.0 [22.5]	43.3 [15.8]	0.871

p Values derived from *t*-tests, with significance set to $p < 0.05$ (bolded and * for reference).

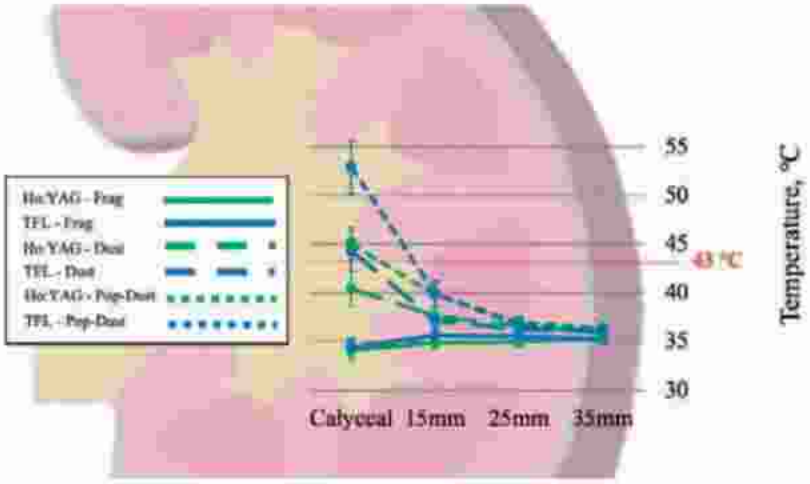


FIG. 4. Mean T_{max} at each renal landmark by laser and setting. Error bars represent standard error of the mean.

and Empower HL. However, the study's methodology presents a key limitation. Temperature was measured with a thermocouple placed in the ureteral fluid, just 2 mm from the laser fiber. When treating an impacted stone, this method is known to yield falsely elevated readings, which may not accurately reflect the true temperature of the ureteral tissue. Calyceal fluid temperatures do not necessarily indicate that renal tissue temperatures increase, and parenchymal temperature elevations may be more indicative of renal injury because of high-powered lasers.

Given the importance of parenchymal temperatures in evaluating potential tissue injury, our study measured medullary and cortical temperatures at approximately 1, 2, and 3 cm from the tip of the renal papilla. According to the thermal dose model described by Sapareto and Dewey, tissue maintained at 43°C for 120 minutes experiences an equivalent thermal dose to tissue maintained at 50°C for 56 seconds or 56°C for 1 second. This concept has been validated across multiple tissue types, including renal tissue.[10,11] Thermal cell injury is known to occur progressively at sustained temperatures above 43°C.[12] Our study demonstrated that under high-powered laser settings, calyceal and parenchymal temperatures exceeded 43°C in as little as 15 seconds. Specifically, during dusting (0.3 J, 50 Hz, 15 W), parenchymal temperatures exceeded 43°C in 1/20 patients (Ho:YAG patient), reaching 49°C after 60 seconds at the 15-mm marker. At the 25-mm and 35-mm markers, the mean peak temperature remained below 37°C for both Ho:YAG and TFL, with no significant differences between the two groups. However, during pop-dusting (0.5 J, 80 Hz), parenchymal temperatures exceeded 43°C in 5/20 patients (2 Ho:YAG patients and 3 TFL patients), all occurring at the 15-mm marker. At the 25-mm and 35-mm markers, mean peak temperatures remained below 37°C across both groups. Notably, with pop-dusting, parenchymal temperatures exceeded 43°C in as little as 20 seconds.

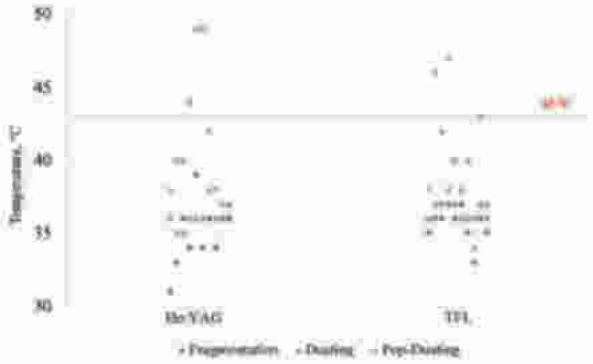


FIG. 5. Individual maximum temperature readings at 15-mm probe for Ho:YAG and TFL across laser settings. Ho:YAG = holmium:YAG; TFL = thulium fiber laser.

Conversely, findings from an *in vivo* porcine study indicated that temperatures surpassing 43°C did not penetrate deeper within the kidney.[4] Even under the most unfavorable conditions—including prewarmed irrigation, absence of a UAS, and the use of a single-lumen ureteroscope—renal temperatures remained below 43°C. This phenomenon is likely attributable to increased ureteral peristalsis and the heat-sinking properties of porcine renal tissue. Our findings from the first *in vivo* assessment of human renal parenchymal temperature during RIRS with LLT highlight the importance of optimizing laser settings to minimize the risk of thermal injury while maintaining procedural efficacy. In addition, our findings of elevated parenchymal temperatures during lithotripsy, coupled with the advent of new high-powered lasers, underscore the urgent need to study the associated risk of thermal damage.

Calyceal and parenchymal temperatures are influenced not only by transmitted energy but also by the surrounding medium and flow dynamics, including renal pelvis anteroposterior diameter (APD) and irrigation/outflow characteristics. *In vitro* studies have demonstrated that decreasing irrigation flow rate leads to elevated calyceal temperatures.[13] Specifically, Wollin et al. reported that with no flow, all maximum temperatures exceeded 43°C, surpassing those observed with lower-energy settings of the Lumenis Pulse 100 W Ho:YAG at 0.8 J/8 Hz, 1 J/10 Hz, and 1 J/20 Hz ($p < 0.05$). The mechanism by which irrigation lowers calyceal temperature is attributed to heat transfer to the irrigant as it passes over the lasered stone.[14] In a similar *in vitro* study, the highest temperature recorded was 70.3°C, occurring with no irrigation after 60 seconds of continuous laser firing (pulse 120 W Ho:YAG, 1.0 J ×

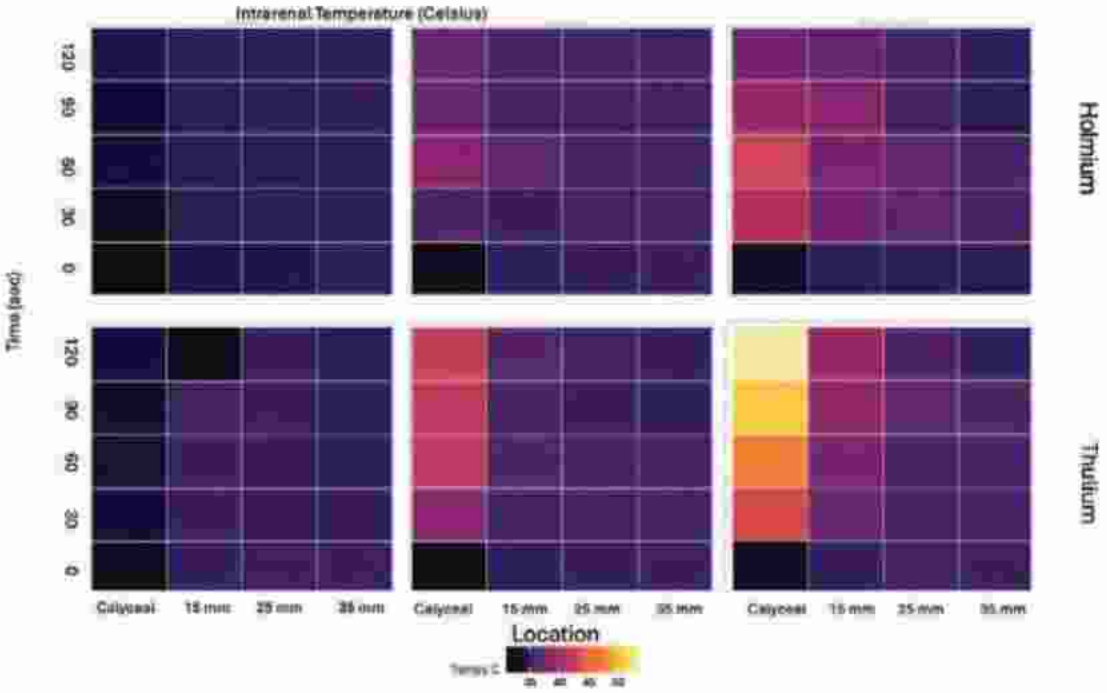


FIG. 6. Heat map representation of calyceal and parenchymal temperatures for both pulse-modulated Ho:YAG and SuperPulsed TFL for all settings.

40 Hz). Notably, fluid temperature in the test tube was measured via a thermocouple positioned 5 mm from the tube's bottom.[15] These *in vitro* studies employed a thermocouple within a static fluid environment (tube or water bath), lacking outflow. When extrapolating *in vitro* findings to *in vivo* conditions, the interplay between irrigation and outflow becomes critical.[8] An *in vivo* porcine study investigating various irrigation and outflow scenarios, including single- *vs* dual-lumen ureteroscopes, warmed *vs* room-temperature irrigation, and with/without a 14 F UAS with the SuperPulsed TFL, identified the use of a UAS as the most significant factor affecting intrarenal temperature. Temperatures reached or exceeded 44°C across all laser and irrigation settings when a UAS was not employed.[4] The present study, conducted without UAS, using room-temperature irrigation and single-lumen ureteroscopes, represents a "worst-case scenario." Although previous research suggests an inverse correlation between intrarenal temperature and APD, this association was not observed in the current study. Although APD can reflect renal pelvic volume, it does not consistently predict renal outflow. This discrepancy may stem from variations in temperature measurement methodologies.

We acknowledge several limitations in our study. To ensure a standardized methodology across laser types, we performed RIRS without a sheath and with gravity irrigation via a single-lumen ureteroscope—which is our standard method. We acknowledge that this is a "worse-case scenario," but RIRS is commonly done in this manner, including at our own center. Although this approach enhances comparability, it may reduce the generalizability of our findings. Despite the limited sample size, the qualitative data provide compelling evidence of clinical relevance. Despite these limitations, we believe our study is well designed and provides valuable insights into an underexplored topic such as temperature dynamics during URS, particularly within the renal parenchyma.

Conclusions

High-powered settings in both Ho:YAG and TFL raise greater concerns regarding calyceal and parenchymal heating (>43°C) and the risk of renal injury compared with low-powered settings. The duration of high-powered energy activation should be carefully considered. Our study highlights the need for further research to explore parenchymal temperatures and their possible association with renal injury.

Authors' Contributions

K.G.: Conceptualization and study design. C.C., V.D., and K.G.: Data collection. C.C., K.G., and D.L.: Data analysis. K.G., K.G., D.L., and Z.S.: Writing. R.K., W.M.A., B.G., K.G., and M.G.: Review and editing.

Authors' Disclosure Statement

There are no competing financial interests.

Funding Information

This study was supported by the Ferdinand C. Valentine Fellowship Award for Research in Urology, Boston Scientific Corporation (equipment only).

References

1. Monga M, Murphy M, Paranjpe R, et al. Prevalence of stone disease and procedure trends in the United States. Urology 2023;176:63–68.
2. Aldoukhi AH, Hall TL, Ghani KR, et al. Caliceal fluid temperature during high-power holmium laser lithotripsy in an in vivo porcine model. J Endourol 2018;32(8):724–729.
3. Molina WR, Silva IN, Donalisio da Silva R, et al. Influence of saline on temperature profile of laser lithotripsy activation. J Endourol 2015;29(2):235–239.
4. Okhunov Z, Jiang P, Afyouni AS, et al. Caveat emptor: The heat is "ON"-An in vivo evaluation of the thulium fiber laser and temperature changes in the porcine kidney during dusting and fragmentation modes. J Endourol 2021;35(11):1716–1722.
5. Aldoukhi AH, Dau JJ, Majdalany SE, et al. Patterns of laser activation during ureteroscopic lithotripsy: Effects on caliceal fluid temperature and thermal dose. J Endourol 2021;35(8):1217–1222.
6. Gupta M, Gupta K, Shimonov R, et al. High-Power lasers induce dose-dependent acute kidney injury. J Endourol 2025;39(8):794–803.
7. MSAE, Juliebo-Jones P, Beisland C, Ulvik, O. Temperature measurements during flexible ureteroscopic laser lithotripsy: A prospective clinical trial. J Endourol 2024;38(4):308–315.
8. Okhunov Z, Duty B, Smith AD, Okeke Z. Management of urolithiasis in patients after urinary diversions. BJU Int 2011;108(3):330–336.
9. Belle JD, Chen R, Srikureja N, et al. Does the novel thulium fiber laser have a higher risk of urothelial thermal injury than the conventional holmium laser in an in vitro study? J Endourol 2022;36(9):1249–1254.
10. Sapareto SA, Dewey WC. Thermal dose determination in cancer therapy. Int J Radiat Oncol Biol Phys 1984;10(6):787–800.
11. van Rhoon GC, Samaras T, Yarmolenko PS, et al. CEM43 degrees C thermal dose thresholds: A potential guide for magnetic resonance radiofrequency exposure levels? Eur Radiol 2013;23(8):2215–2227.
12. Krishnaprasad K, Pathi RT, Nazar M. Factors affecting the thermal effects of lasers in lithotripsy: A literature review. Asian J Urol 2025;12(1):23–32.
13. Williams JG, Goldsmith L, Moulton DE, et al. A temperature model for laser lithotripsy. World J Urol 2021;39(6):1707–1716.
14. Wollin DA, Carlos EC, Tom WR, et al. Effect of laser settings and irrigation rates on ureteral temperature during holmium laser lithotripsy, an in vitro model. J Endourol 2018;32(1):59–63.
15. Aldoukhi AH, Ghani KR, Hall TL, et al. Thermal response to high-power holmium laser lithotripsy. J Endourol 2017;31(12):1308–1312.

Address correspondence to:
Kavita Gupta, MD
Icahn School of Medicine at Mount Sinai
425 W. 59th Street, Suite 4F
New York, NY 10019
USA

E-mail: kgoopt@gmail.com

Abbreviations Used

$avgT_{max}$	= average maximum temperature
ECIRS	= endoscopic combined intrarenal surgery
Ho:YAG	= holmium:YAG
MTS	= multipoint thermal sensor
PCNL	= percutaneous nephrolithotomy
RIRS	= retrograde intrarenal surgery
T_{calyx}	= calyceal temperature
T_{tissue}	= parenchymal temperature
T_{max}	= maximum temperature
TFL	= thulium fiber laser
UAS	= ureteral access sheath
URS	= ureteroscopy

Check for updates

《血管内泌尿外科杂志》第40卷第1期，
2026年1月
* 玛丽·安·利伯特（纽约），有限
责任公司，第17–25页
DOI: 10.1177/08927790251392232

激光碎石术在逆行肾内手术期间可引起剂量依赖性的温度升高

卡维塔·古普塔医学博士[1]、克里斯托弗·康纳斯理学士[1]、齐夫·萨文医学博士[1]、达拉·伦登医学博士[1]、雷蒙德·卡尔吉医学博士[1]、维奈·杜尔巴库拉理学士[1]、卡斯米拉·古普塔理学士[2]、布莱尔·加兰特公共卫生硕士[1]、威廉·M·阿塔拉医学博士[1]以及曼图·古普塔医学博士[1]

摘要

目的：实时监测激光碎石术过程中肾盏及组织温度的变化。
方法：符合内镜下联合肾内手术指征的患者根据设备可用情况，分别接受Soltive 60 W超脉冲铥光纤激光（TFL；Olympus公司）或钬:YAG激光（Ho:YAG；Lumenis Pulse伽 120H）治疗。结石移位后，在超声引导下经皮置入一根1.5毫米多点温度传感器针，其尖端距结石表面分别为5、15、25和35毫米处。在碎石阶段（TFL 激光：1 J/2 Hz；Ho:YAG激光：0.5 J/5 Hz，功率2–2.5 W）、粉尘粉碎阶段（0.3 J/50 Hz，功率15 W）及爆破粉碎阶段（0.5 J/80 Hz，功率40 W），该针头在5毫米标记点持续记录肾盏液温及其他各点的肾实质温度，记录时长为2分钟。若组织温度超过43°C，则暂停激光治疗。完成温度测量后，实施输尿管扩张术及经皮肾镜取石术。分类数据采用卡方检验或Fisher精确检验进行比较，连续变量则采用t检验分析。
结果：20例患者（10例 TFL 激光组和10例Ho:YAG激光组）具有相似的基线特征。在碎石过程中，肾盏（T_{calyx}）与实质组织（T_{tissue}）温度均未超过41°C；在喷砂处理期间，每种激光组各有4例患者的T_{calyx}温度超过43°C，其中1例Ho:YAG激光组患者T_{tissue}温度超过43°C（60秒后达49°C）。TFL 激光组与Ho:YAG激光组患者的最高肾盏温度（T_{max}）分别为51°C和56°C（p=0.18）；喷砂处理时，10例 TFL 激光组与8例Ho:YAG激光组患者的T_{calyx}温度均超过43°C，且 TFL 组的平均最高温度（avgT_{max}）显著更高（52.9°C vs 45.1°C，p=0.027）；组织T_{max}分别为47°C和49°C（p=0.96），其中3例 TFL 激光组与3例Ho:YAG激光组患者的温度超过43°C。结论：高功率激光治疗时，温度可在短短15秒内超过43°C，这一现象值得关注，因>43°C的温度可能导致永久性组织损伤。

关键词：激光、肾温度、输尿管镜检查

引言

使用钬激光（Ho:YAG）和铥光纤激光（TFL）系统的逆行肾内手术（RIRS）治疗肾结石已成为最常用的手术治疗方法。[1]

尽管激光技术的进步（尤其是高功率模式的发展）显著提高了结石消融效率，但关于其可能对周围尿路上皮组织造成热损伤的问题仍存在担忧。[2]

输尿管镜检查（URS）中使用的激光所发射的能量可能以热的形式散逸至周围组织，从而可能导致热损伤，如凝固、碳化及蛋白质变性。

现有文献强调了可调节手术参数的重要性，包括灌注温度与流量、输尿管通路鞘（UAS）的使用、激光参数设置（功率、脉冲持续时间及频率）以及操作者的工作负荷，这些因素均有助于降低肾内温度，从而减轻经肾上尿路取石术（URS）过程中可能发生的热损伤。[3–5]

然而，迄今为止尚未有研究同时测量使用脉冲调制Ho:YAG激光（Lumenis Pulse伽 120H）和超脉冲 TFL 激光（奥林巴斯公司）系统进行碎石 RIRS 时肾脏实质与肾盏的温度变化。本研究的主要目的是实时监测两种高功率激光系统在内镜下取石手术过程中人体肾盏及肾脏实质温度的变化；次要目标包括：

[1]美国纽约州西奈山伊坎医学院泌尿外科。
[2]阿尔伯特·爱因斯坦医学院，美国纽约州纽约市。
该摘要此前已发表于《泌尿外科杂志》第213卷第5S期（2025年5月）。

实时关联内镜下取石过程中灌注液温度与肾实质温度的关系，并确定在使用高功率激光系统的内镜取石术中，哪些可调控的手术因素会影响肾脏温度变化；另一项次要目标则是比较脉冲调制Ho:YAG系统与超脉冲TFL系统在肾盏及肾实质温度变化方面的差异。

方法

研究设计

一项经机构审查委员会批准（IRB研究编号23-00046）的研究于2023年12月至2024年7月期间在西奈山医疗中心招募了需要采用联合治疗方案（内镜下联合肾内手术[ECIRS]）的单侧结石负荷患者。尽管外科医生的选择具有一定影响，但 ECIRS 的主要适应症包括较大的结石负荷（≥2厘米）以及不同肾盏内的多发结石，旨在避免需要进行多入路经皮肾镜取石术（PCNL）。患者需满足以下纳入标准：年龄不低于18岁；非妊娠状态且能够签署知情同意书；术前肌酐水平≤1.3 mg/dL；术前尿培养阴性；且术前CT扫描时间距手术不超过60天。排除标准包括：过去90天内接受过肾结石治疗（如冲击波碎石术、尿路镜/激光碎石术[LLT]或 PCNL）；术前留置导尿管（输尿管支架或经皮肾造瘘管）；有尿流改道史；先天性肾脏异常（孤立肾或萎缩肾）；以及既往存在尿路梗阻或输尿管狭窄疾病。

程序；流程

结石负荷定义为所有结石在冠状面测量的各最长直径之和。为获得更精确的测量值，通过累加单个结石体积得出总结石体积。最大宽度与长度均在轴位片上测量，高度则在冠状面测量，所有测量均在 ≥8· 放大镜下进行。基于这些尺寸参数，采用欧洲泌尿外科学会椭球公式$V=0.167 \cdot \pi \cdot L \cdot W \cdot H$手动计算各结石体积。

根据激光系统的可用性，患者被分配使用 TFL（60W Soltive伽 超脉冲激光器）或Ho:YAG（Lumenis Pulse伽 120H）激光系统进行 LLT 治疗。

所有患者均采用改良Barts无侧腹位体位。随后进行标准无菌准备及铺巾。完成膀胱镜检查后，在直视下使用可弯曲尿路镜（Flex X2，Karl Storz）探查肾集合系统。整个操作未使用 UAS 。同时实施全面肾盂镜检查以明确结石数量及分布特征。遵循我们对 ECIRS 的标准操作流程，所有结石均通过收集篮转移至适宜的肾盏进行 LLT，随后经皮清除所有结石、碎石及碎屑。所有患者均接受室温下的重力灌洗，灌洗液袋置于患者腹部上方80厘米处（从腹部顶部至灌洗液袋底部的距离）。虽未精确测量灌注液体量，但我们的尿路镜标准方案规定使用的生理盐水袋不超过1升。

结石移位后，采用1.5毫米多点热传感器（MTS）针头（波士顿科学公司产品）替代18G穿刺针（图1）实现经皮入路进入适宜的肾盏。在超声及荧光透视引导下将MTS针头置入集合系统；同时借助可弯曲输尿管镜定位，实时观察针头穿刺过程。当针头正确就位且最远端传感器位于肾盏内时，按操作规程进行校准以确保其功能准确。

采用Soltive 60W SuperPulsed TFL 激光器（奥林巴斯公司）或配备 MOSES伽 技术的Lumenis P120 Ho:YAG 激光器（波士顿科学公司）系统，配合200微米激光光纤进行 LLT 治疗。在 LLT 过程中，使用三种常用激光参数对每位患者采集温度数据：碎石参数为1J/2Hz（TFL 激光）和0.5J/5Hz（Ho:YAG 激光），功率为2-2.5W，旨在将结石破碎成较大碎片；粉尘化参数为0.3J/50Hz、15W，通过持续“喷涂”方式将结石表面粉碎为细粉；爆破粉碎参数为0.5J/80Hz、40W，旨在快速将肾结石破碎成极细的粉末状颗粒。每种激光模式均持续作用2分钟，并实时监测肾盏内及肾实质组织温度——若温度超过43℃则暂停激光治疗；更换新参数前，需待肾盏液与肾实质温度恢复至基础体温后方可继续操作。

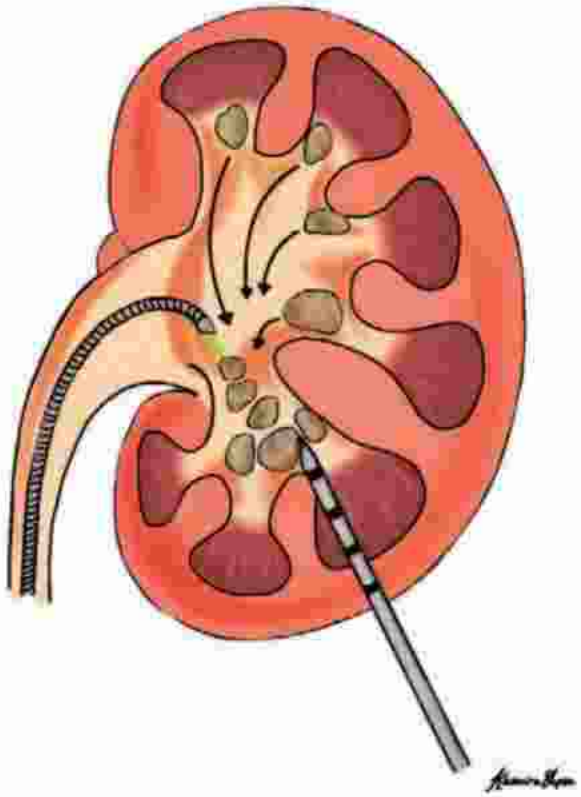


图1. 结石向适宜杯状腔转移的示意图，以及带有杯状标记（5 mm）和实质标记（15 mm [1 cm]、25 mm [2 cm] 及35 mm [3 cm]）的多点热传感器经皮置入示意图。

在LLT过程中，使用MTS针头分别在距探头尖端5毫米（肾盏）、15毫米（1厘米）、25毫米（2厘米）和35毫米（3厘米）处记录温度值。5毫米传感器位于收集系统内部，其余传感器则实时监测肾实质（髓质与皮质）的温度分布。我们在MTS针头各位置均监测超过43°C的温度，并记录该阈值被突破的持续时间。术中完成碎石术后，主刀医生立即对激光引起的损伤进行评估和分级。激光损伤分级标准如下：0级：无损伤；1级：6级。

黏膜层，2级：黏膜下层；3级：全层。

完成温度测量后，在直视下将筋膜扩张器置于MTS针上方，以便置入导丝并实施管腔球囊扩张至24F尺寸，随后按标准流程PCNL所有结石、碎片及碎屑。手术结束时，外科医生照常评估是否需要置入输尿管支架或肾造瘘管。分类数据采用卡方检验进行比较。

分类变量采用卡方检验或Fisher精确检验，连续变量则采用t检验进行分析。所有比较的分布正态性均通过Kolmogorov-Smirnov检验和Shapiro-Wilk检验进行评估。鉴于本研究中大多数比较/数据分布均符合正态性假设，我们选择使用均值/t检验及标准差来比较组间数据。

结果

2023年12月至2024年7月期间，共有26例患者符合ECIRS研究的纳入标准。根据排除标准，术前有6例患者被排除，最终分析样本量为20例，各治疗组各10例（图2）。

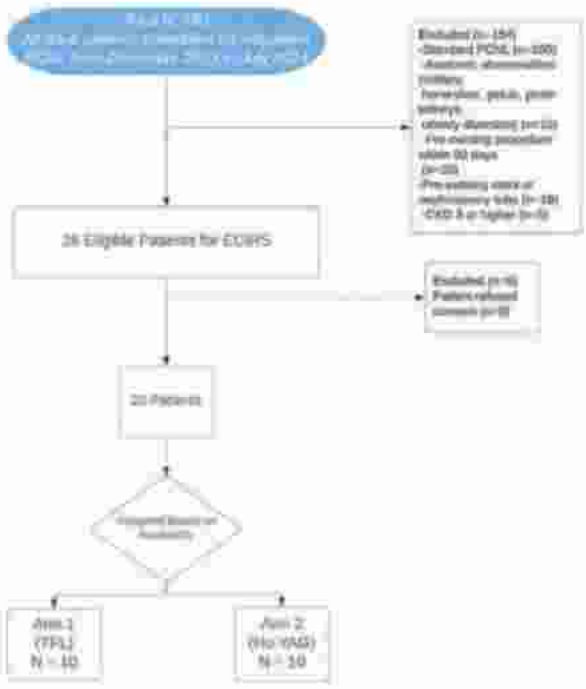


图2. 流程图。

两组患者在人口统计学特征、结石特性及临床特征方面均无显著差异（表1）。两组的总手术时间、操作者工作负荷以及可见激光损伤的发生频率均相似。20例手术中，9例（45%）完全采用无导管术式，未使用支架或肾造瘘管；其余11例虽置入支架但未使用肾造瘘管。

Ho:YAG与TFL两组患者的平均基线杯状体温度（T_{calyx}）在所有时间点均低于33°C（表2）。在碎裂过程中（0.3 J、50 Hz、15 W），Ho:YAG与TFL的平均T_{calyx}分别为：0秒时31.8°C vs 32.5°C，60秒时33.4°C vs 33.3°C，120秒时34.0°C vs 33.4°C（p = 0.404、p = 0.941、p = 0.699；图3）；在喷粉过程中（0.5 J、80 Hz、15 W），两组的平均T_{calyx}分别为：0秒时32.5°C vs 31.9°C，60秒时39.1°C vs 42.1°C，120秒时37.6°C vs 42.6°C（p = 0.526、p = 0.289、p = 0.082）；其中TFL组与Ho:YAG组各有4例患者出现T_{calyx}超过43°C（平均T_{max}：44.3°C vs 40.4°C，p = 0.175）。最高杯状体温度（T_{max}）分别为51°C和56°C（p = 0.18）；在弹丸喷粉过程中（0.5 J、80 Hz），两组的平均T_{calyx}分别为：0秒时33.0°C vs 32.7°C，60秒时43.0°C vs 47.3°C，90秒时40.0°C vs 51.2°C（p = 0.754、p = 0.264、p = 0.071）。在10例TFL患者和8例Ho:YAG患者中，T_{calyx}温度超过43°C，且TFL组的平均T_{max}显著更高（TFL组：52.9°C；Ho:YAG组：45.1°C，p=0.027）。

两组的平均基线实质温度（T_{tissue}）也具有可比性，并在所有时间点均保持低于36°C。在碎裂过程中，Ho:YAG激光与TFL激光在15毫米探头尖端处的平均T_{tissue}值分别为：0秒时34.2°C对比35.2°C、60秒时34.7°C对比35.3°C、120秒时34.8°C对比32.3°C（p值分别为0.087、0.468和0.430）。碎裂期间，肾盏及实质的最大平均温度始终低于36°C且从未超过43°C（表3）。

在喷粉过程中，Ho:YAG组与TFL组在15毫米探头尖端的平均T_{tissue}分别为：0秒时35.0°C vs 35.0°C；60秒时36.9°C vs 36.5°C；120秒时36.3°C vs 36.6°C（p = 1.000、p = 0.805、p = 0.554）。两组在15毫米处的平均实质T_{max}分别为：Ho:YAG组37.6°C，TFL组37.2°C（p = 0.788；图4）。仅在Ho:YAG组中有一例患者在喷粉期间T_{tissue}超过43°C（15毫米探头处60秒后为49°C；图5）。在25毫米和35毫米标记点处，Ho:YAG组与TFL组的平均T_{max}均低于37°C，组间无显著统计学差异。在弹射喷粉过程中，Ho:YAG组与TFL组在15毫米探头尖端的平均T_{tissue}分别为：0秒时34.6°C vs 35.1°C；60秒时38.4°C vs 38.3°C；90秒时39.0°C vs 39.5°C（p = 0.607、p = 0.954、p = 0.899）。两组在弹射喷粉时15毫米处的平均实质T_{max}分别为39.8°C和39.9°C（p=0.958）。在Ho:YAG组中，弹丸抛射过程中T_{tissue}超过43°C的情况出现两次；在TFL组中则出现三次，所有情况均发生在15毫米探头处（图6）。而在25毫米和35毫米探头处，两组的平均T_{max}值相当，且弹丸抛射期间的平均温度均低于37°C。

表1. YAG组与 TFL 组之间的基线特征及操作信息

	Ho:YAG	*TFL*	p 价值
年龄 [STD]	54.8 [16.3]	58.6 [11.6]	0.556
BMI [STD]	28.4 [3.5]	26.6 [7.4]	0.512
性别，n（%）			0.170
男性	2 (80.0)	4 (40.0)	
女性	2 (20.0)	6 (60.0)	
ASA评分，n（%）			0.211
2	10 (100.0)	7 (70.0)	
3	0 (0.0)	3 (30.0)	
糖尿病，n（%）	1 (10.0)	0 (0.0)	1.000
利尿剂，n（%）	0 (0.0)	0 (0.0)	—
ARB或ACE抑制剂，n（%）	1 (10.0)	3 (30.0)	0.582
抗凝剂，n（%）	0 (0.0)	1 (10.0)	1.000
抗血小板药物，n（%）	1 (10.0)	0 (0.0)	1.000
复发性尿路感染病史，n（%）	0 (0.0)	2 (20.0)	0.474
术前尿培养阳性，n（%）	1 (10.0)	0 (0.0)	1.000
术前肌酐[STD]	1.0 [0.2]	1.0 [0.3]	0.979
术前 EGFR [STD]	88.2 [23.7]	79.2 [20.4]	0.376
既往结石手术史，n（%）	7 (70.0)	8 (80.0)	1.000
ESWL	0 (0.0)	1 (10.0)	1.000
URS	4 (40.0)	3 (30.0)	1.000
PCNL	2 (20.0)	4 (40.0)	0.628
偏侧性，n（%）：			1.000
左侧	6 (60.0)	6 (60.0)	
右侧	4 (40.0)	4 (40.0)	
肾盂前后径，cm[STD]	2.2 [0.8]	2.0 [0.7]	0.503
总结石负荷，mm (STD]	21.7 [10.0]	22.2 [10.6]	0.906
石体体积，mm^3 [STD]	3292.0 [3140.1]	2157.6 [2607.6]	0.391
HU [STD]	876.9 [370.5]	801.9 [173.6]	0.572
激光光纤的直径（单位：纳米），n（%）			0.057
150	1 (10.0)	6 (60.0)	
200	9 (90.0)	4 (40.0)	
可见激光损伤，n（%）			0.141
0级：无	5 (50.0)	9 (90.0)	
1级：黏膜	5 (50.0)	1 (10.0)	
2级：黏膜下层	0 (0.0)	0 (0.0)	
3级：全层	0 (0.0)	0 (0.0)	
所用总激光能量，kJ [STD]	3.8 [1.5]	5.2 [1.3]	0.038*
操作员工作周期，分钟 [STD]	16.02 [2.02]	16.33 [3.09]	0.790
踏板时间，分钟 [STD]	4.81 [0.61]	4.90 [0.93]	0.801
总手术时间（分钟）[STD]	76.7 [15.9]	70.7 [13.9]	0.390

连续变量以中位数表示。p值通过卡方检验、Fisher精确检验或t检验得出，显著性水平设定为$p < 0.05$（加粗及*号表示参考）。

AP=前后位；ESWL =体外冲击波碎石术；Ho:YAG=钬:YAG激光；PCNL =经皮肾镜取石术；STD=标准差；TFL =钬光纤激光；URS=输尿管镜检查。

讨论

高功率激光器在 LLT 治疗中已展现出更高的效率；然而，它们也可能导致肾内温度升高，从而可能引发肾脏热损伤。本研究评估了高功率激光激活后长达120秒内的肾盏及肾实质温度变化，并分别采用脉冲调制Ho:YAG激光系统和超脉冲 TFL 激光系统，分析了激光激活期间肾盏与肾实质的最低、最高及平均温度值。

随着高功率激光器的问世，学界已对多种可调控的风险因素进行了研究以降低热损伤风险，其中激光参数设置便是关键因素之一。本研究发现，在低功率设置（2–2.5 W）下，无论是 TFL 还是Ho:YAG系统，肾脏温度（包括肾盏和肾实质测量值）均始终低于43°C；而高功率设置（>15 W）则可在短短15秒内使温度超过43°C。另一项采用K型热电偶在 TFL 激光递行 LLT 过程中测量肾盏液温的研究表明：在20 W功率下，10例患者中有3例达到43°C；30 W时该比例升至8例；而5 W和10 W功率下温度始终低于此阈值[7]。在猪体内模型中，所有碎屑化模式及大部分碎裂模式（碎屑化：0.5 J，80 Hz，40 W；低功率碎裂：1 J，10 Hz，10 W；高功率碎裂：1.5 J，20 Hz，30 W）均导致肾盏温度达到或超过44°C[8]。在我们的研究和先前的体内研究中，

表2. Ho组与YAG组及 TFL 组之间的温度结果

	肾盏平均温度，℃			平均温度：15 摄氏度			平均温度为 25 摄氏度			平均温度为 35 摄氏度		
	Ho:YAG	*TFL*	p 价值	*Ho:YAG*	*TFL*	p 价值	*Ho:YAG*	*TFL*	p 价值	*Ho:YAG*	*TFL*	p 价值
基线[STD]												
0 秒	32.2 [1.8]	31.6 [3.4]	0.628	34.7 [1.6]	34.9 [1.4]	0.776	35.0 [1.6]	35.8 [0.8]	0.172	34.8 [1.7]	35.5 [1.0]	0.274
30秒	32.4 [1.8]	31.9 [2.6]	0.626	34.9 [1.5]	35.1 [1.1]	0.741	35.1 [1.5]	35.8 [0.8]	0.219	35.0 [1.6]	35.4 [1.0]	0.515
60秒	32.6 [1.8]	32.2 [2.4]	0.684	34.9 [1.5]	35.1 [1.1]	0.741	35.0 [1.6]	35.8 [0.8]	0.172	34.8 [1.8]	35.4 [1.0]	0.359
90秒	0.0 [0.0]	0.0 [0.0]	—	0.0 [0.0]	0.0 [0.0]	—	0.0 [0.0]	0.0 [0.0]	—	0.0 [0.0]	0.0 [0.0]	—
120秒	0.0 [0.0]	0.0 [0.0]	—	0.0 [0.0]	0.0 [0.0]	—	0.0 [0.0]	0.0 [0.0]	—	0.0 [0.0]	0.0 [0.0]	—
碎片化 [STD] 0 秒	31.8 [1.5]	32.5 [2.1]	0.404	34.2 [1.4]	35.2 [1.0]	0.087	34.4 [1.5]	35.3 [1.1]	0.141	35.0 [1.5]	35.3 [1.3]	0.632
30秒	32.6 [2.5]	33.6 [3.0]	0.425	34.5 [1.9]	35.3 [1.2]	0.274	34.6 [1.6]	35.1 [1.0]	0.424	34.8 [1.8]	35.1 [1.3]	0.675
60秒	33.4 [3.1]	33.3 [2.8]	0.941	34.7 [2.3]	35.3 [1.2]	0.468	34.7 [1.8]	35.1 [1.0]	0.543	34.8 [1.9]	35.0 [1.2]	0.782
90秒	33.5 [3.1]	33.1 [3.0]	0.771	34.8 [2.3]	35.4 [1.3]	0.482	35.0 [1.8]	35.2 [0.9]	0.755	35.0 [1.9]	34.9 [1.4]	0.896
120秒	34.0 [3.4]	33.4 [3.4]	0.699	34.8 [2.3]	32.3 [9.3]	0.430	34.8 [1.9]	35.2 [1.0]	0.564	35.0 [1.9]	34.9 [1.4]	0.896
粉末化[STD]												
0 秒	32.5 [1.8]	31.9 [2.3]	0.526	35.0 [1.6]	35.0 [1.1]	1.000	35.1 [1.4]	35.2 [1.0]	0.861	35.3 [1.4]	35.3 [1.3]	1.000
30秒	36.4 [4.2]	39.0 [4.2]	0.182	35.3 [2.0]	35.7 [1.4]	0.613	35.4 [1.5]	35.4 [1.4]	1.000	35.5 [1.7]	35.4 [1.6]	0.894
60秒	39.1 [6.4]	42.1 [5.9]	0.289	36.9 [4.5]	36.5 [2.3]	0.805	36.1 [2.4]	36.1 [2.3]	1.000	35.4 [1.6]	35.9 [2.6]	0.635
90秒	37.5 [3.4]	42.1 [5.6]	0.069	35.5 [1.5]	36.1 [1.6]	0.428	35.6 [1.2]	35.3 [1.0]	0.512	35.4 [1.7]	35.0 [1.4]	0.647
120秒	37.6 [3.2]	42.6 [6.6]	0.082	36.3 [1.2]	36.6 [1.3]	0.554	35.9 [1.1]	35.6 [0.9]	0.634	35.6 [1.5]	35.1 [1.2]	0.505
爆破粉末化[STD] 0 秒	33.0 [2.1]	32.7 [2.2]	0.754	34.6 [2.7]	35.1 [1.4]	0.607	34.7 [2.6]	35.4 [0.7]	0.434	34.7 [2.5]	35.3 [0.8]	0.492
30秒	41.2 [6.8]	43.4 [6.8]	0.479	37.9 [4.1]	37.6 [3.2]	0.858	36.7 [1.9]	36.0 [1.5]	0.370	36.0 [1.8]	35.8 [1.2]	0.772
60秒	43.0 [5.3]	47.3 [10.1]	0.264	38.4 [2.8]	38.3 [2.5]	0.954	36.8 [2.1]	36.1 [1.4]	0.463	36.1 [2.1]	35.9 [1.3]	0.795
90秒	40.0 [4.2]	51.2 [6.9]	0.071	39.0 [4.2]	39.5 [4.0]	0.899	36.0 [0.0]	36.8 [1.6]	0.259	34.5 [0.7]	36.3 [1.5]	0.077
120秒	38.0 [.]	53.5 [9.2]	—	37.0 [.]	40.0 [0.0]	—	36.0 [.]	36.5 [0.7]	—	35.0 [.]	35.0 [1.4]	—

p值源自t检验，显著性阈值设定为<0.05（加粗及*号表示参考）。

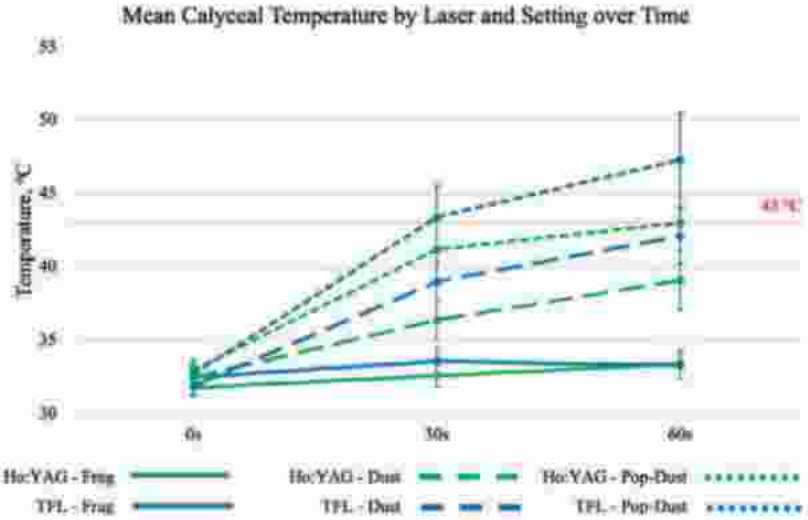


图3. 不同激光参数及设置条件下随时间变化的肾盏平均温度。误差线表示均值的标准误。

所有> 5w的设置都导致肾盏温度达到或超过43° C。这些结果凸显了激光功率设置与肾盏液峰值温度之间的直接关联。在弹丸式碎石过程中，TFL 激光器的平均最高温度（avgT_{max}）显著高于脉冲调制型Ho:YAG激光器。这一发现与先前一项采用无流出道冲击性输尿管结石模型的体外URS研究结果一致——该研究指出，在大多数功率设置下，TFL 激光器产生的温度均显著高于Dornier和Empower HL激光器（$p < 0.001$）。[9]唯一例外出现在20 W功率下；此时 TFL 激光器与Empower HL激光器之间未观察到显著差异。

表3. Ho组、YAG组与 TFL 组之间的温度结果

	Ho:YAG	*TFL*	p 价值
最大杯状结构温度，℃ [标准值]	32.7 [1.9]	32.5 [2.6]	0.846
基线	34.1 [3.4]	34.4 [3.0]	0.837
碎片化	40.4 [5.8]	44.3 [6.5]	0.175
粉末化	45.1 [5.2]	52.9 [8.6]	0.027*
爆破粉末化			
最高温度为 15 摄氏度 [STD]	34.9 [1.5]	35.1 [1.1]	0.741
基线值	34.9 [2.2]	35.6 [1.2]	0.387
碎片化	37.6 [4.1]	37.2 [2.0]	0.788
粉末化	39.8 [4.2]	39.9 [4.1]	0.958
爆破粉末化			
最高温度：25 摄氏度 [STD]	35.1 [1.5]	35.8 [0.8]	0.219
基线值	35.0 [1.8]	35.5 [1.0]	0.445
碎片化	36.6 [2.2]	36.3 [2.2]	0.760
粉末化	37.0 [1.9]	36.7 [1.3]	0.687
爆破粉末化			
最高温度为 35 摄氏度 [STD]	35.0 [1.6]	35.5 [1.0]	0.419
基线值	35.3 [1.6]	35.3 [1.3]	1.000
碎片化	35.8 [1.4]	36.1 [2.4]	0.736
粉末化	36.4 [1.5]	36.2 [1.2]	0.749
爆破粉末化			
达到最高温度所需时间（秒）[STD]	—	—	—
基线值	60.0 [.]	67.5 [45.0]	—
碎片化	76.7 [37.1]	82.5 [21.2]	0.693
粉末化	49.5 [31.5]	75.0 [35.9]	0.136
爆破粉末化			
达到43°C所需时间（如已达到），秒 [STD]			
基线值（n = 0）	—	—	—
碎片化（n = 0）	—	—	—
粉末化（H组：n=3；T组：n=6）	60.0 [30.0]	50.0 [24.5]	0.648
爆破粉末化（女性：n=7；男性：n=9）	45.0 [22.5]	43.3 [15.8]	0.871

p值源自t检验，显著性水平设定为<0.05（加粗及*号表示参考）。

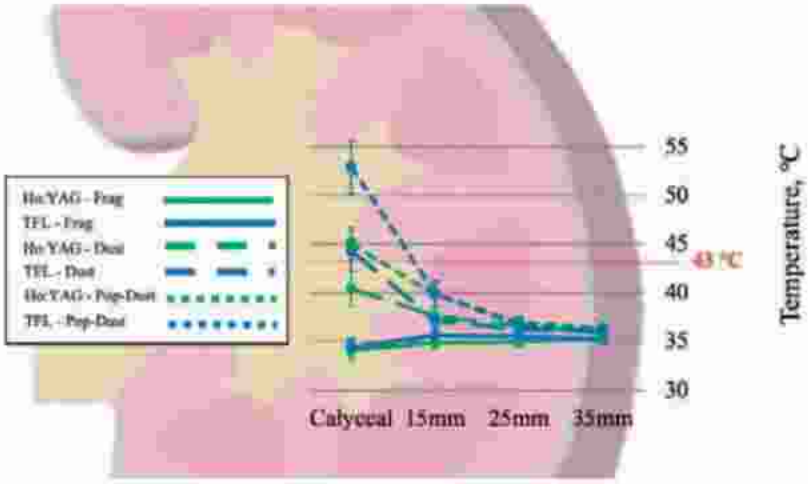


图4. 不同激光参数及设置下各肾脏标志点处的平均T_{max}值。误差线表示均值的标准误。

然而，该研究的方法存在一个关键局限性：温度测量采用置于输尿管液中、距激光光纤仅2毫米处的热电偶进行。在治疗嵌顿结石时，已知此方法会得出错误升高的读数，无法准确反映输尿管组织的真实温度；肾盏液温度并不必然表明肾组织温度升高；而由于高功率激光的影响，肾实质温度升高可能更提示存在肾损伤。

鉴于实质温度在评估潜在组织损伤中的重要性，本研究测量了距肾乳头顶端约1、2和3厘米处的髓质与皮质温度。根据Sapareto和Dewey提出的热剂量模型，组织在43°C下维持120分钟所承受的热剂量，等同于在50°C下维持56秒或在56°C下维持1秒所产生的热剂量。这一概念已在包括肾组织在内的多种组织类型中得到验证[10,11]。已知在持续高于43°C的温度下，热细胞损伤会逐渐发生[12]。我们的研究表明，在高功率激光条件下，肾盏及肾实质温度可在短短15秒内超过43°C；具体而言，在点状照射模式（0.3 J，50 Hz，15 W）下，1/20的患者（Ho: YAG激光组）肾实质温度超过43°C；至60秒时，15 mm标记处温度已达49°C；而在25 mm和35 mm标记处，Ho: YAG与 TFL 激光组的平均峰值温度均低于37°C，两组间无显著差异；然而在点阵照射模式下（0.在5 J、80Hz条件下，20例患者中有5例（2例YAG激光患者和3例 TFL 激光患者）的实质温度超过43°C，均出现在15毫米标记处。在25毫米和35毫米标记处，两组患者的平均峰值温度均保持在37°C以下。值得注意的是，采用弹射式碎石时，实质温度可在短短20秒内超过43°C。

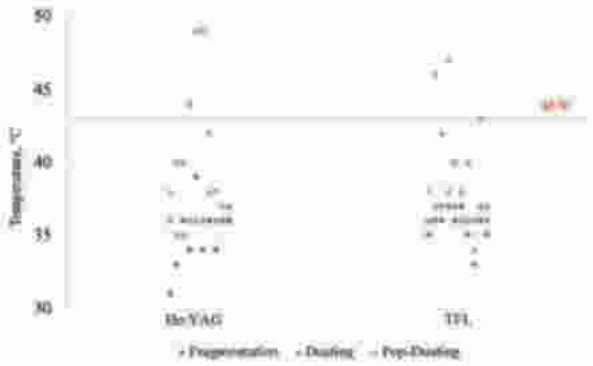


图5展示了不同激光参数下15毫米探头测得的Ho:YAG和TFL 激光器各自的最高温度读数。Ho:YAG指钬:YAG激光器；TFL 指铥光纤激光器。

相反，一项猪体内研究结果表明，超过43°C的温度无法深入肾脏内部。[4]即使在最不利条件下（包括预热灌注、未使用 UAS 以及使用单腔输尿管镜），肾组织温度仍保持在43°C以下。这一现象很可能归因于输尿管蠕动增强以及猪肾组织具有散热特性。我们首次对人类接受 LLT 碎石术（RIRS）过程中肾实质温度进行的体内评估结果表明，优化激光参数对于在保证治疗效果的同时降低热损伤风险至关重要。此外，我们在碎石术期间观察到肾实质温度升高的现象，加之新型高功率激光器的出现，更凸显了研究相关热损伤风险的紧迫性。

肾盏及肾实质温度不仅受透射能量的影响，还受到周围介质及流体动力学因素的影响，包括肾盂前后径（APD）以及灌注/流出特性。体外研究表明，降低灌注流量会导致肾盏温度升高[13]；具体而言，Wollin等人报道在无灌注条件下，所有最高温度均超过43°C，显著高于使用Lumenis Pulse 100 W Ho:YAG激光器在0.8 J/8 Hz、1 J/10 Hz和1 J/20 Hz低能量设置下观测到的数值（$p < 0.05$）。灌注降低肾盏温度的作用机制归因于液体在流经激光照射结石时发生的热传递[14]。另一项类似的体外研究中，连续激光照射60秒后（使用120 W Ho: YAG激光器，脉冲能量1.0 Jx40Hz）未进行灌注时记录到的最高温度为70.3°C。

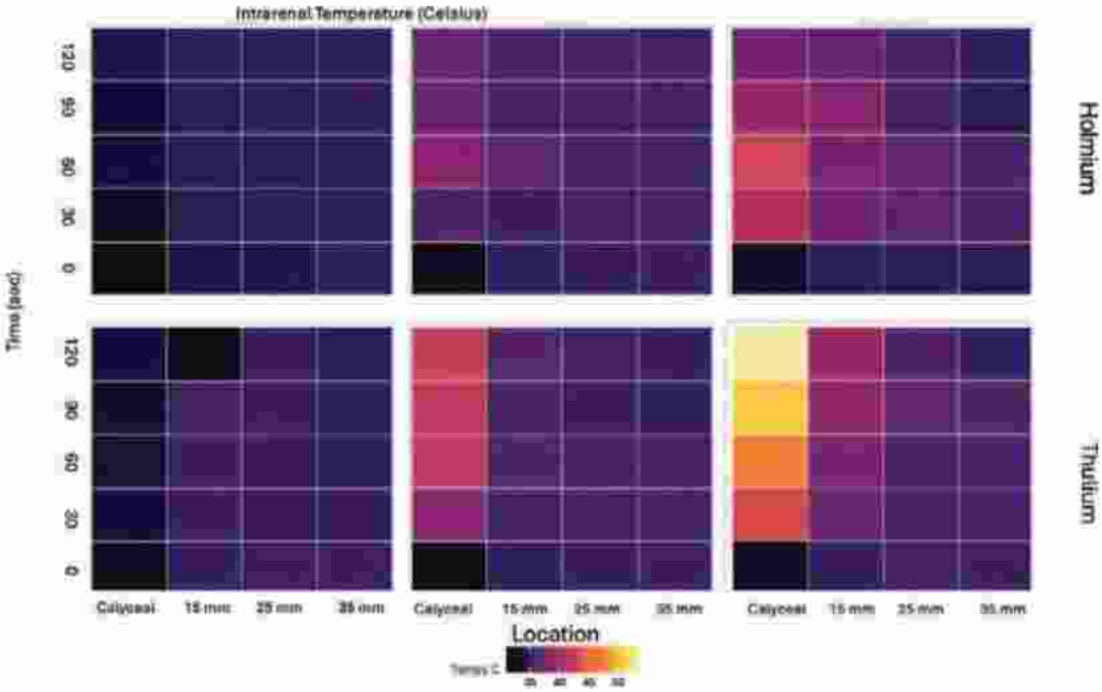


图6.展示了所有参数设置下脉冲调制Ho:YAG激光与超脉冲 TFL 激光在花萼组织及薄壁组织中的温度热力分布图。

值得注意的是，试管中的液体温度为
通过距离管壁5毫米处设置的热电偶进行测量。
底部。[15]这些体外研究在静态流体环境（管腔或水浴）中使用了热电偶，且缺乏流出液。当将体外实验结果外推至体内条件时，灌注液与流出液之间的相互作用变得至关重要。[8]一项针对猪模型的体内研究探讨了多种灌注与流出液方案（包括单腔与双腔输尿管镜、温水与室温灌注液、使用/不使用配备SuperPulsed TFL 系统的14F UAS 导管），结果表明 UAS 导管的使用是影响肾内温度的最关键因素：未使用 UAS 导管时，所有激光与灌注设置下的温度均达到或超过44°C。[4]本研究在不使用 UAS 导管、采用室温灌注液及单腔输尿管镜的情况下进行，代表了“最坏情况”。尽管既往研究表明肾内温度与 APD 值呈负相关，但本研究并未观察到这种关联。虽然 APD 值可反映肾盂容积，但并不能稳定预测肾脏流出液量：这种差异可能源于不同温度测量方法的差异。

我们承认本研究存在若干局限性。为确保不同激光类型间方法学的一致性，我们采用单腔输尿管镜在无鞘管且借助重力冲洗条件下实施了 RIRS 术——这正是我们的标准操作流程。我们承认这属于“最极端情况”，但此类 RIRS 手术的常规操作方式包括本中心亦如此。尽管该方法提升了结果的可比性，但可能降低研究结论的普适性。尽管样本量有限，定性数据仍提供了有力的临床相关性证据。尽管存在这些局限，我们认为本研究设计严谨，并为输尿管镜检查过程中（尤其是肾实质内）温度动态这一尚未充分研究的领域提供了重要见解。

结论

与低功率设置相比，Ho:YAG和 TFL 的高功率设置会引发更严重的担忧，包括肾盏及肾实质温度升高（>43° C）以及肾损伤风险。高功率能量激活的持续时间需谨慎考量。本研究强调需开展进一步研究以探讨肾实质温度及其与肾损伤之间的潜在关联。

作者的贡献

K.G.：概念构建与研究设计；C.C.、V.D.及K.G.：数据收集；C.C.、K.G.及D.L.：数据分析。
K.G.、K.G.、D.L.和 Z.S.：撰写；R.K.、W.M.A.、B.G.、K.G.和 M.G.：审阅与编辑。

作者披露声明

不存在相互冲突的财务利益。

资金信息

本研究由波士顿科学公司颁发的费迪南德·C·瓦伦丁泌尿外科研究奖学金（仅限设备费用）资助。

参考文献

1. Monga M, Murphy M, Paranjpe R, et al. Prevalence of stone disease and procedure trends in the United States. Urology 2023;176:63 - 68.
2. Aldoukhi AH, Hall TL, Ghani KR, et al. Caliceal fluid temperature during high-power holmium laser lithotripsy in an in vivo porcine model. J Endourol 2018;32(8): 724 - 729.
3. Molina WR, Silva IN, Donalisio da Silva R, et al. Influence of saline on temperature profile of laser lithotripsy activation. J Endourol 2015;29(2):235 - 239.
4. Okhunov Z, Jiang P, Afyouni AS, et al. Caveat emptor: The heat is "ON" -An in vivo evaluation of the thulium fiber laser and temperature changes in the porcine kidney during dusting and fragmentation modes. J Endourol 2021;35(11):1716 - 1722.
5. Aldoukhi AH, Dau JJ, Majdalany SE, et al. Patterns of laser activation during ureteroscopic lithotripsy: Effects on caliceal fluid temperature and thermal dose. J Endourol 2021; 35(8):1217 - 1222.
6. Gupta M, Gupta K, Shimonov R, et al. High-Power lasers induce dose-dependent acute kidney injury. J Endourol 2025;39(8):794 - 803.
7. MSAE, Juliebo-Jones P, Beisland C, Ulvik, O. Temperature measurements during flexible ureteroscopic laser lithotripsy: A prospective clinical trial. J Endourol 2024; 38(4):308 - 315.
8. Okhunov Z, Duty B, Smith AD, Okeke Z. Management of urolithiasis in patients after urinary diversions. BJU Int 2011;108(3):330 - 336.
9. Belle JD, Chen R, Srikureja N, et al. Does the novel thulium fiber laser have a higher risk of urothelial thermal injury than the conventional holmium laser in an in vitro study? J Endourol 2022;36(9):1249 - 1254.
10. Sapareto SA, Dewey WC. Thermal dose determination in cancer therapy. Int J Radiat Oncol Biol Phys 1984;10(6): 787 - 800.
11. van Rhoon GC, Samaras T, Yarmolenko PS, et al. CEM43 degrees C thermal dose thresholds: A potential guide for magnetic resonance radiofrequency exposure levels? Eur Radiol 2013;23(8):2215 - 2227.
12. Krishnaprasad K, Pathi RT, Nazar M. Factors affecting the thermal effects of lasers in lithotripsy: A literature review. Asian J Urol 2025;12(1):23 - 32.
13. Williams JG, Goldsmith L, Moulton DE, et al. A temperature model for laser lithotripsy. World J Urol 2021;39(6): 1707 - 1716.
14. Wollin DA, Carlos EC, Tom WR, et al. Effect of laser settings and irrigation rates on ureteral temperature during holmium laser lithotripsy, an in vitro model. J Endourol 2018;32(1):59 - 63.
15. Aldoukhi AH, Ghani KR, Hall TL, et al. Thermal response to high-power holmium laser lithotripsy. J Endourol 2017;31(12):1308 - 1312.

通讯地址：Kavita Gupta，医学博士
西奈山伊坎医学院，地址：纽约州纽约市西 59 街 425 号 4F 室，邮编 10019
美国

电子邮件：kgoopt@gmail.com

使用的缩写词

$avgT_{max}$= 平均最高温度
ECIRS：内镜下联合腔内手术；
Ho：YAG=钬：YAG
MTS= 多点热传感器
PCNL = 经皮肾镜取石术
RIRS：逆行肾内手术
T_{calyx}= 花萼温度
T_{tissue}= 实质温度T_{max}= 最高温度
TFL = 钬 光纤激光器
UAS = 输尿管穿刺鞘
URS = 输尿管镜检查

Check for updates

JOURNAL OF ENDOUROLOGY
Volume 00, Number 00, Month 2026
Mary Ann Liebert, A Part of Sage
© The Author(s)
Pp. 000–000
DOI: 10.1177/08927790261457175

Bubble Trouble: The Thermal Risk of Ureteral Laser Lithotripsy in an Air Bubble

Gabriel E. Martin, MD, Kallan Richards, Daniel Jhang, MD, Adel Battikha, Ninous Betdashtoo, Jongwan Park, Faith Ajayi, Zhamshid Okhunov, MD, and D. Duane Baldwin, MD

Abstract

Introduction: During ureteroscopic laser lithotripsy (URSL), unsafe elevations in ureteral temperature are thought to contribute to ureteral stricture formation. Cellular damage begins at 43°C, and proteins denature instantly at 60°C. Air bubbles may inadvertently migrate into the collecting system during URSL. The purpose of this study was to evaluate ureteral temperatures during simulated URSL in an air bubble with a holmium (Ho:YAG) and thulium fiber laser (TFL).

Methods: BegoStone phantoms were positioned distal to the ureteropelvic junction in a model kidney and ureter submerged in a 35°C saline bath. A 7.5 Fr flexible ureteroscope was advanced to the stone, and continuous saline irrigation at 22°C was maintained at 15 mL/min. A needle thermocouple positioned 2 mm from the laser fiber tip monitored ureteral wall temperature. A 200 μm laser fiber was then advanced until it contacted the stone. The Ho:YAG and TFL were used in 5 trials each to ablate stones at 3, 10, and 20 W in saline and in a 3 mL air bubble.

Results: In the control condition, neither laser exceeded 43°C at 3, 10, or 20 W. In an air bubble, ureteral temperatures exceeded 43°C after 1 second at 3 W for both TFL and Ho:YAG. At 10 W, the Ho:YAG exceeded 43°C after 1 second, while the TFL exceeded 60°C. The average temperature exceeded 60°C at 20 W for both lasers after 1 second. Both lasers generated much higher temperatures in an air bubble than in saline at all time points ($p = 0.008$), with maximum temperature exceeding 250°C for both lasers.

Conclusion: In this benchtop model, laser activation in an air bubble for 1 second exceeded the thermal safety threshold at ≥ 3 W and risks protein denaturation at ≥ 20 W. This study highlights the importance of avoiding air bubbles during URSL to maintain safe ureteral temperatures. Further studies are needed to validate these findings *in vivo*.

Keywords: thermal injury, air bubble, laser lithotripsy, ureteroscopy, holmium laser, thulium fiber laser

Introduction

The prevalence of nephrolithiasis has been increasing in recent years, with a concomitant increase in ureteroscopic laser lithotripsy (URSL).[1,2] During URSL, thermal effect from lasers likely secondary to unsafe elevations in ureteral temperature are related to ureteral stricture formation.[3] Previous research has shown that temperature rises with higher power settings, larger laser fiber sizes, and smaller volumes of fluid in which laser activation occurs.[4,5] During ureteroscopy, the volume of fluid in the ureter is small, which portends greater risk of thermal injury compared to the kidney or bladder.[6] Thus, this has been an area of active research to help improve patient outcomes. Previous studies have shown that adequate irrigation, chilled irrigation, shorter laser activation cycles, and lower power settings can reduce thermal injury.[7,8] Additionally, the thulium fiber laser (TFL) is now known to produce higher temperatures than the holmium:yttrium aluminum garnet laser (Ho:YAG), prompting extra caution when using the TFL.[9] There is no clear threshold for thermal injury in the current literature. Several studies have shown that proteins denature at 60°C using proteins *in vitro*, this has been used as a thermal damage limit previously in urologic research, although this is not specific to the urinary tract.[10] In cell culture, a breakpoint in the rate of cell death was detected around 43°C, so this too has been used as a thermal damage limit in urologic studies.[11,12] Likely the most specific measurement for this area of research uses the cumulative equivalent minutes at 43°C (CEM_{43}), which converts temperature over time into a single number (the CEM_{43} or thermal isoeffect dose), which

Department of Urology, Loma Linda University Health, Loma Linda, California, USA.

can quantify thermal dose exposure.[11,13] Prior research has shown that CEM_{43} >70 minutes has caused significant injury (including coagulative necrosis) specifically to the kidney; they also showed acute and minor damage was observed even at CEM_{43} <20 minutes.[11,14] Despite this, there is still no defined safe thermal dose for the human urinary tract, but these thresholds are used in research evaluating the thermal impact of laser lithotripsy. Based on the aforementioned research, we can presume that temperatures reaching or exceeding 43°C are unsafe and temperatures reaching or exceeding 60°C and a CEM_{43} > 70 cause irreversible thermal injury.

Air bubbles may be inadvertently introduced into the collecting system during URSL. There has been no investigation of the safety of laser lithotripsy in an air bubble. This benchtop study evaluates ureteral temperatures and thermal dose during simulated URSL in an air bubble with a Ho:YAG and TFL.

Materials and Methods

A computed tomography scan of a kidney was converted into a three-dimensional (3D) model of a kidney using 3D slicer 5.2.2 (Kitware, NY), and a ureter was created using Autodesk Fusion 360 (Autodesk, San Francisco, CA). These models were used to print molds using an Ultimaker 3 Extended (Ultimaker, Geldermalsen, Netherlands) 3D printer. Liquid Dragon Skin™ 20 silicone (Smooth-On, Inc., Macungie, PA) was used in conjunction with the molds to create the model kidney and ureter. Identical, spherical, 10 mm calcium oxalate monohydrate consistency BegoStone phantoms (Bego GmbH, Germany) were created and positioned 1 cm distal to the ureteropelvic junction to simulate a ureteral stone. The model with a ureteral stone was submerged in a 35°C saline bath using an electric immersion heater (Pong-Dang, Gyeonggi-do, South Korea) to simulate ureteral temperature during an endoscopic surgical procedure (Fig. 1). A 7.5 Fr single-use digital flexible ureteroscope (Pusen Medical Technology, Zhuhai, China) was introduced into the model ureter and advanced up to the stone. A 3 mL air bubble was introduced through the ureteroscope for the air bubble arm of the study; the bubble remained in a stable position during irrigation and laser lithotripsy. Continuous saline irrigation at room temperature (22°C) was maintained at 15 mL/min using the Thermedx FluidSmart System (Thermedx LLC, Solon, OH). A 200 µm laser fiber was advanced through the scope until the laser fiber contacted the stone. A T-29X Micro Needle Insect Type T Thermocouple Probe (ThermoWorks, American Fork, UT) was inserted through the ureter wall perpendicular to the laser fiber at the level where the fiber contacted the stone and positioned 2 mm lateral to the laser fiber tip (Fig. 1C). The laser fiber was positioned in saline during the saline trials and air during the air bubble trials. The thermocouple response time is 1 second in liquid, with an accuracy of ± 0.1°C. A digital data acquisition system, including a MAX31855 T-Type Thermocouple Sensor breakout board (ThermoWorks, American Fork, UT), recorded temperature data with readings every 6.0 seconds. The Empower H100 Ho:YAG laser

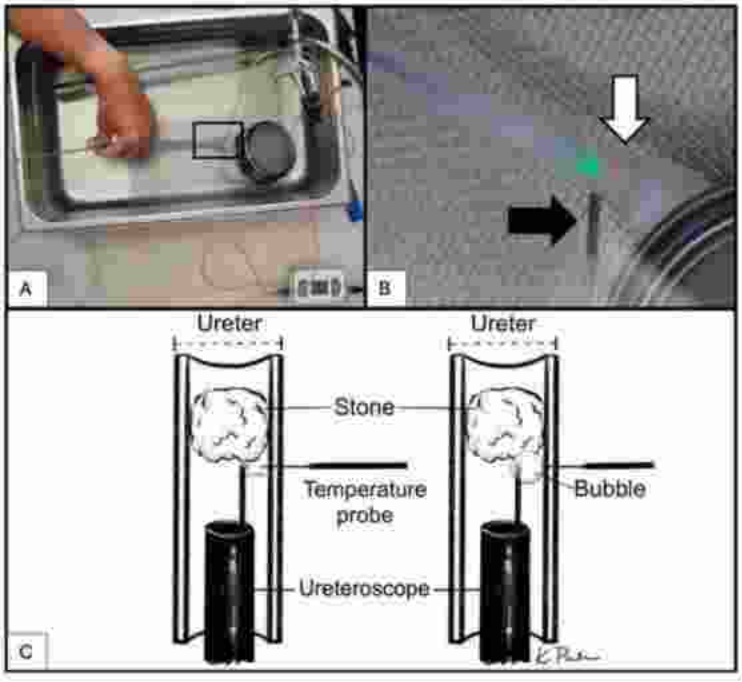


FIG. 1. Model kidney and ureter experimental setup. **(A)** shows the silicone model kidney and ureter submerged in a 35°C saline bath with ureteroscope entering from distal ureter. A sieve sits atop the model kidney to keep it submerged. The black rectangle is the area shown in panel B. **(B)** shows a close-up of the ureteropelvic junction with 10 mm BegoStone (*white arrow*) in place and a thermocouple (*black arrow*) positioned 2 mm from the tip of the laser fiber (*green* aiming beam can be seen in the picture). **(C)** shows a cross-sectional illustration of the model ureter depicting the saline control condition (*left*) and air bubble condition (*right*). The laser fiber was placed in contact with the stone, the thermocouple was inserted through the ureter wall perpendicular to the laser fiber at the level where the fiber contacted the stone, and positioned 2 mm lateral to the laser fiber tip.

(Olympus, Center Valley, PA) and SOLTIVE™ Premium SuperPulsed TFL laser (Olympus, Center Valley, PA) were each used with their respective 200 μm laser fibers to ablate stones for 7 seconds at three different power settings: 3 W (0.3 J/10 Hz), 10 W (1 J/10 Hz), and 20 W (1 J/20 Hz) in saline (as a control) and within a 3 mL air bubble. Both lasers used the manufacturer's preset short pulse width/duration setting for all powers tested. The model was allowed to return to baseline temperature, and the saline in the model was replaced between each trial. For the saline arm, temperature was recorded at baseline (0 seconds, pre-laser activation), after 6 seconds of laser activation, and after 12 seconds of laser activation. For the air bubble arm, temperature was recorded at baseline (0 seconds, pre-laser activation), after 1 second of laser activation, and after 7 seconds of laser activation. Five measurements were taken for each unique combination of laser type (TFL, Ho:YAG), power setting (3, 10, and 20 W), and medium (saline, air bubble) at the above time points for a total of 180 measurements.

Thermal dose exposure was calculated using the CEM_{43} equations established by Sapareto and Dewey.[13] Unsafe temperature was defined as >43°C, and the threshold for thermal injury was defined as CEM_{43} >70 minutes or temperature >60°C. Data analysis was conducted using SPSS Statistics (IBM, Chicago, IL). Statistical significance was assessed using the Mann–Whitney U tests with Bonferroni correction for multiple comparisons. The Mann–Whitney U tests were performed to compare temperature and CEM_{43} values between saline control and 1 second air bubble activation for each laser at each power setting. With six comparisons performed, the corrected significance level was set at $p < 0.0083$ ($\alpha = 0.05/6$).

Results

Temperature profiles were substantially different between the saline control and air bubble groups across all tested power settings (Table 1). Average temperatures in the saline control never exceeded the 43°C safety threshold for either laser at any power setting. At the highest power setting (20 W) after 12 seconds of laser activation, temperatures only reached 38.6°C for TFL and 37.9°C for Ho:YAG. In contrast, laser activation within air bubbles resulted in unsafe temperatures across all tested conditions. At one second of laser activation in an air bubble, the average temperature exceeded the 43°C safety threshold for both lasers at all power settings. Even at the lowest power setting (3 W), mean temperatures were 44.1°C for TFL and 45.0°C for Ho:YAG. At one second of laser activation in an air bubble, average temperature exceeded the 60°C thermal injury threshold at 10 W and 20 W for TFL and at 20 W for Ho:YAG. At 20 W, the maximum temperatures recorded were 98.4°C for TFL and 92.8°C for Ho:YAG at 1 second and 257.2°C for TFL and 278.2°C for Ho:YAG at 7 seconds. Temperature increase in air bubbles demonstrated both power-dependent and time-dependent patterns (Fig. 2), with 1 second of laser activation producing an average of 68% increase in temperature at 3 W across both lasers, 82% at 10 W, and 113% at 20 W. Continued laser activation for 7 seconds resulted in even more dramatic increases of 139% at 3 W, 165% at 10 W, and 394% at 20 W.

In addition to temperature measurements, CEM_{43} values were calculated to account for both the magnitude of temperature and the length of exposure. CEM_{43} of saline controls remained well below the thermal damage threshold (CEM_{43} < 70 minutes) for both lasers across all power settings. At 1 second, air bubble CEM_{43} exceeded the thermal damage threshold at 10 W for the TFL alone and 20 W for both lasers. At 7 seconds, air bubble CEM_{43} values exceeded the thermal damage threshold at all power settings for both lasers (Table 2).

Comparisons demonstrated statistically significant temperature and CEM_{43} increases for 1-second air bubble activation compared to saline controls for both lasers across all power settings ($p = 0.008$ for all comparisons) with complete statistical separation between conditions (U = 25.0 for all comparisons) (Table 3).

Discussion

The findings of this study demonstrate that laser activation within air bubbles poses immediate thermal risk during URSL, with unsafe temperatures occurring at all tested power settings, regardless of laser type or activation duration. This study represents the first investigation of thermal

Table 1. Average Temperature by Laser Type, Power, and Activation Time

Laser power and setting	*Laser active time (s)*	*TFL saline control average temperature (°C)*	*Ho:YAG saline control average temperature (°C)*	*Laser active time (s)*	*TFL air bubble average temperature (°C)*	*Ho:YAG air bubble average temperature (°C)*
3 W (0.3 J/10 Hz)	0	25.98	25.97	0	35.52	35.02
	6	26.78	25.98	1	44.09[a]	44.97[a]
	12	26.69	26.52	7	64.74[b]	61.52[b]
10 W (1 J/10 Hz)	0	26.89	26.03	0	37.08	34.23
	6	35.24	29.56	1	63.78[b]	54.24[a]
	12	34.01	29.29	7	88.01[b]	82.66[b]
20 W (1 J/20 Hz)	0	27.73	24.52	0	37.64	35.72
	6	38.08	35.40	1	80.71[b]	76.20[b]
	12	38.56	37.88	7	193.30[b]	170.21[b]

Saline control temperatures were recorded at baseline (0 seconds), 6 seconds, and 12 seconds of laser activation.
Air bubble temperatures were recorded at baseline (0 seconds), 1 second, and 7 seconds of laser activation.
[a]Thermal safety threshold (43°C) exceeded.
[b]Thermal injury threshold (60°C) exceeded.

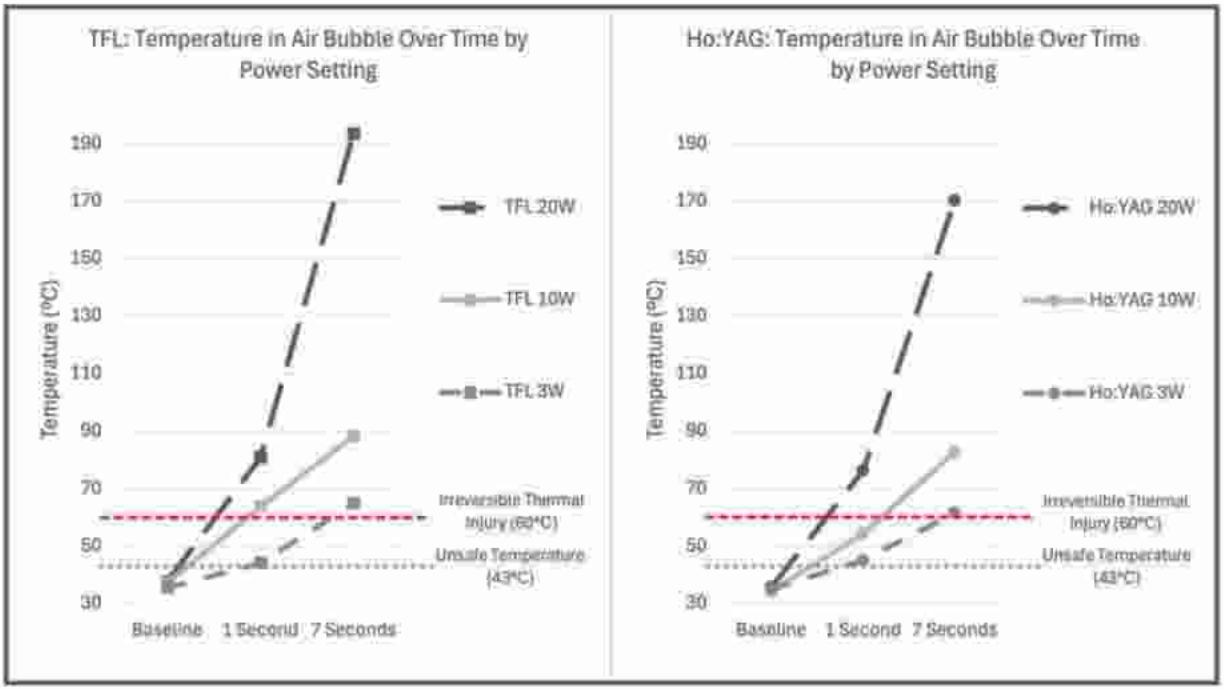


FIG. 2. Laser temperature profiles by power setting and time. Temperature measurements for TFL and Ho:YAG laser activation in an air bubble at three power settings (3, 10, and 20 W) over time (baseline without laser activation, after 1 second of laser activation, and after 7 seconds of laser activation). Unsafe temperature threshold (43°C) and irreversible thermal injury threshold (60°C) are shown. Both laser types demonstrate power-dependent and time-dependent increases in temperature.

safety during laser lithotripsy in an air bubble, revealing a previously unrecognized and potentially serious intraoperative hazard.

Looking at the data from the saline controls alone, the average temperature never exceeded the 43°C safety threshold with up to 12 seconds of laser activation for either laser at any power setting. This demonstrates what is known, that laser lithotripsy in saline with irrigation is generally safe, with faster irrigation and lower power settings providing safer thermal profiles.[7,8]

In stark contrast, laser activation for even 1 second in an air bubble exceeded the thermal safety threshold for both lasers at all power settings. At the lowest power setting (3 W), both TFL and Ho:YAG exceeded the 43°C safety threshold at 1 second and the 60°C thermal injury threshold at 7 seconds in an air bubble. At 20 W, both lasers exceeded the 60°C thermal injury threshold at 1 second in an air bubble. At all power settings, temperature readings were significantly higher at 1 second in air compared to saline with complete separation between groups. Even at a minimal clinical power of 3 W, the findings are concerning, suggesting that no safe operating parameters exist for laser activation within air bubbles. In addition, the maximum recorded temperatures are alarming. The maximum temperature recorded after 1 second of laser activation at 20 W was near the boiling point of normal saline at 98°C, and the maximum temperature after 7 seconds at 20 W was comparable to temperatures reached by electrocautery devices at 278°C.[15] This suggests that even brief, inadvertent laser activation in an air bubble could have devastating consequences for the ureter.

The CEM_{43} thermal dose analysis provides a separate, meaningful assessment of thermal damage risk, accounting

TABLE 2. AVERAGE CEM_{43} BY LASER TYPE, POWER, AND ACTIVATION TIME

Laser power and setting	*Laser active time (s)*	*TFL saline control average CEM_{43} (min)*	*Ho:YAG saline control average CEM_{43} (min)*	*Laser active time (s)*	*TFL air bubble average CEM_{43} (min)*	*Ho:YAG air bubble average CEM_{43} (min)*
3 W (0.3 J/10 Hz)	6	9.93E-07	7.50E-07	1	1.09E-02	1.25E-02
	12	2.26E-06	1.66E-06	7	7.46E + 05[a]	1.47E + 05[a]
10 W (1 J/10 Hz)	6	2.55E-05	2.65E-06	1	2.97E + 03[a]	5.54E-01
	12	3.27E-04	1.08E-05	7	6.38E + 18[a]	2.10E + 14[a]
20 W (1 J/20 Hz)	6	9.14E-05	1.19E-05	1	5.47E + 08[a]	6.35E + 06[a]
	12	3.99E-03	1.23E-03	7	3.95E + 55[a]	1.94E + 48[a]

Saline control CEM_{43} values were calculated for 6 seconds and 12 seconds of laser activation. Air bubble CEM_{43} values were calculated for 1 second, and 7 seconds of laser activation.

[a]Thermal injury threshold (CEM_{43} > 70 minutes) exceeded.

TABLE 3. STATISTICAL ANALYSIS OF SALINE AND AIR BUBBLE TEMPERATURE AND CEM_{43}

Setting and laser compared (saline vs *1 second in air bubble)*	*Variable compared*	*U*	p-*Value*
3W TFL	Temperature	25	0.008
3W Ho:YAG	Temperature	25	0.008
10W TFL	Temperature	25	0.008
10W Ho:YAG	Temperature	25	0.008
20W TFL	Temperature	25	0.008
20W Ho:YAG	Temperature	25	0.008
3W TFL	CEM_{43}	25	0.008
3W Ho:YAG	CEM_{43}	25	0.008
10W TFL	CEM_{43}	25	0.008
10W Ho:YAG	CEM_{43}	25	0.008
20W TFL	CEM_{43}	25	0.008
20W Ho:YAG	CEM_{43}	25	0.008

Mann–Whitney U tests were performed with Bonferroni correction for multiple comparisons. Corrected significance level $p < 0.0083$. For each laser and power setting, the temperature of laser activation in saline was compared to laser activation in an air bubble for 1 second. All air bubble temperature and CEM_{43} values were significantly higher ($p = 0.008$ for all), with complete separation between groups ($U = 25$).

for temperature and duration. At all power settings, the CEM_{43} values were significantly higher at 1 second in air compared to saline with complete separation between groups. The minimum average increase in CEM_{43} in an air bubble was 1,099,819% at 3 W 1-second compared to saline control. The maximum average increase was 9.9×10^{59}% at 20 W at 7 seconds. Importantly, previous research demonstrated $CEM_{43} < 20$ minutes still caused acute minor thermal damage, but acute and severe thermal damage occurred at $CEM_{43} > 70$ minutes.[14] Despite the drastic increase in CEM_{43}, the 1 second air bubble group did not exceed the thermal damage threshold ($CEM_{43} > 70$) for either laser at 3 W, or for Ho:YAG at 10 W. This adds value to the temperature data, suggesting that 1 second activation damage may be less severe at 3 W for both lasers or 10 W with Ho:YAG, while the remainder of the conditions are much more severe, drastically surpassing the thermal damage threshold. This confirms that moderate and high-power settings operating in an air bubble have no margin for error.

The dramatic temperature differences between operating a laser in saline compared to an air bubble can be attributed to several converging physical mechanisms. The specific heat of a substance is the amount of heat energy required to raise the temperature of one gram of a substance by one degree Celsius. Water has a high specific heat, of 4.184 Joules per gram per degree Celsius (J/g °C), while air at sea level has a much lower specific heat of 1.007 J/g °C.[16] With a specific heat four times that of air, water can absorb significantly more thermal energy before experiencing a rise in temperature. In addition, the speed at which heat leaves the region of light absorption, termed thermal diffusion time, is a function of optical penetration depth and thermal diffusivity of the medium (the rate of heat transfer within a material).[17]

$$\textit{Thermal diffusion time} = \frac{(\textit{optical penetration depth})^2}{4 \times (\textit{thermal diffusivity})}$$

Optical penetration depth is much greater and thermal diffusivity is much smaller in air/vapor compared to liquid water. Thus, thermal diffusion time is significantly decreased in air/vapor compared to liquid water.[18,19] Taking this a step further, we consider the "Moses effect." Upon laser activation, saline is evaporated rapidly, creating an expanding vapor bubble. As the density of water vapor is ~1672 times less than that of liquid water, the vapor bubble allows laser energy transmission directly to the exposed calculus surface.[20] This is concerning when considering that in a macroscopic air bubble, the heat generated by the laser is transmitted not only to the stone but the ureteral wall. In the context of our study, air behaves more closely to water vapor than liquid water, with greater photon transmission and conversion of photons to heat. These principles illustrate that laser activation within air (rather than saline) allows for greater heat generation, accumulation, and transfer to surrounding tissue.

Recent data examining thermal properties of TFL demonstrated that pulse width/duration increased as pulse energy increased, with pulse duration being 3–4 times longer on the long preset (compared to short). The authors concluded that TFL has the potential for long pulse durations, potentially exceeding thermal relaxation time, which poses an independent risk for excessive heat generation and nonspecific thermal injury.[21] This may help explain why TFL breached the 60°C thermal injury threshold at a lower power setting (10 W) compared to Ho:YAG, as TFL pulse durations lengthen with increasing pulse energy even on the short preset.

Moreover, the flow of irrigation fluid provides heat removal through the process of convective cooling. Water runs over the surface of the stone and nearby tissue, removing heat and cooling them.[22] In contrast to flowing water, the air bubble is stagnant, with the temperature rising commensurate with the energy it is absorbing. The air bubble hinders the effectiveness of this convective cooling by creating a microenvironment where water is absent and unable to absorb excess heat. The heat continually accumulates in the air bubble, on the surface of the stone, and the surrounding tissue, and convective cooling is limited only to the surface of the air bubble.

Given the thermal injury risk posed by laser activation in an air bubble, urologists should take precautionary measures to avoid lasering within them. In particular, care should be taken by the person irrigating to prevent inadvertent air bubble introduction into the collecting system.

This benchtop study clearly demonstrates the potential thermal danger of laser lithotripsy in an air bubble but has several limitations. The *in vitro* silicone model and stone do not perfectly replicate every aspect of clinical ureteroscopy, including true impact on ureteral tissue, but use of a benchtop model allowed us to better understand the thermal effect of lasering in an air bubble and standardize conditions for all trials. Future clinical studies in an animal model with histopathologic assessment would help better assess thermal injury. The thermocouple sensor was only capable of recording temperatures at 6 second intervals. Because the temperature was so great in an air bubble at 12 seconds that the endoscope and temperature probe risked damage, temperature measurements were taken at 1 second of laser activation and 7 seconds of laser activation for the air bubble trials; further study could evaluate second-by-second temperature

changes that are directly compared between saline and air. The 3 mL volume was selected as a worst-case scenario to maximize sensitivity for detecting thermal differences. Further study should evaluate different sized air bubbles.

In our experience, several simple actions can help avoid bubble introduction into the collecting system, including priming/flushing the irrigation tubing, expelling bubbles from irrigation syringes prior to connecting, irrigating with the syringe oriented vertically and pointed toward the floor (to keep bubbles trapped at the top of the syringe), and not instilling the entire volume of the syringe (in case any bubbles are trapped at the top of the syringe). Future research should explore other methods of preventing air bubble migration into the collecting system and techniques for removal when present.

These findings highlight a previously unrecognized yet significant safety hazard that may be silently contributing to ureteral injury and stricture formation. The universal breach of the thermal safety threshold at all power settings at 1 second of laser activation and progression to thermal injury with moderate-to-high power settings at 1 second is alarming. This study provides clear guidance for clinical practice: surgeons should avoid laser activation within an air bubble, regardless of power setting or intended activation duration.

Conclusion

In this benchtop model, laser activation within an air bubble for even 1 second exceeded the thermal safety threshold at power settings ≥3 W; further clinical studies are needed to validate these findings *in vivo*. Introduction of air bubbles during ureteroscopic laser lithotripsy should be avoided, and further techniques to remove air bubbles once present should be developed.

Acknowledgments

The authors would like to thank and acknowledge Dr. Kimberly Park for her contribution through the illustration of the experimental setup (Fig. 1C).

Authors' Contributions

G.E.M.: Conceptualization (lead), methodology (supporting), formal analysis (lead), investigation (lead), data curation (lead), writing—original draft (lead), writing—review and editing (lead), and visualization (lead). K.R.: Methodology (lead), investigation (supporting), data curation (supporting), writing—original draft (supporting), and project administration (lead). D.J.: Investigation (supporting) A.B.: Investigation (supporting), and methodology (supporting). N.B.: Investigation (supporting) J.P.: Investigation (supporting). F.A.: Investigation (supporting). Z.O.: Supervision (supporting). D.D.B.: Conceptualization (supporting), supervision (lead).

Author Disclosure Statements

No competing financial interests exist.

Funding Information

This project received no funding.

References

1. Stamatelou K, Goldfarb D. Epidemiology of kidney stones. Healthcare (Basel) 2023;11(3):424; doi: 10.3390/healthcare11030424
2. Monga M, Murphy M, Paranjpe R, et al. Prevalence of stone disease and procedure trends in the United States. Urology 2023;176:63–68; doi: 10.1016/j.urology.2023.03.040
3. Dong H, Peng Y, Li L, et al. Prevention strategies for ureteral stricture following ureteroscopic lithotripsy. Asian J Urol 2018;5(2):94–100; doi: 10.1016/j.ajur.2017.09.002
4. Æsøy M, Juliebø-Jones P, Beisland C, et al. Temperature profiles during ureteroscopy with thulium fiber laser and holmium: YAG laser: Findings from a pre-clinical study. Scand J Urol 2022;56(4):313–319; doi: 10.1080/21681805.2022.2104367
5. Rezakahn Khajeh N, Hall T, Ghani K, et al. Pelvicaliceal volume and fluid temperature elevation during laser lithotripsy. J Endourol 2022;36(1):22–28; doi: 10.1089/end.2021.0383
6. Louters M, Kim H, Dau J, et al. Characterization of fluid dynamics and temperature profiles during ureteroscopy with laser activation in a model ureter. J Endourol 2022;36(12):1593–1598; doi: 10.1089/end.2022.0275
7. Wollin D, Carlos E, Tom W, et al. Effect of laser settings and irrigation rates on ureteral temperature during holmium laser lithotripsy, an in vitro model. J Endourol 2018;32(1):59–63; doi: 10.1089/end.2017.0658
8. Rice P, Somani B, Nagele U, et al. Generated temperatures and thermal laser damage during upper tract endourological procedures using the holmium: Yttrium-Aluminum-Garnet (Ho:YAG) laser: A systematic review of experimental studies. World J Urol 2022;40(8):1981–1992; doi: 10.1007/s00345-022-03992-7
9. Belle J, Chen R, Srikureja N, et al. Does the novel thulium fiber laser have a higher risk of urothelial thermal injury than the conventional holmium laser in an in vitro study? J Endourol 2022;36(9):1249–1254; doi: 10.1089/end.2021.0842
10. Sourial M, Ebel J, Francois N, et al. Holmium-YAG laser: Impact of pulse energy and frequency on local fluid temperature in an in-vitro obstructed kidney calyx model. J Biomed Opt 2018;23(10):1–4; doi: 10.1117/1.JBO.23.10.105002
11. Van Rhoon G, Samaras T, Yarmolenko P, et al. CEM43°C thermal dose thresholds: A potential guide for magnetic resonance radiofrequency exposure levels? Eur Radiol 2013;23(8):2215–2227; doi: 10.1007/s00330-013-2825-y
12. Kose E, Bostanci Y, Gulsen M, et al. Monitoring intrarenal temperature changes during Ho: YAG laser lithotripsy in patients undergoing retrograde intrarenal surgery: A novel pilot study. Urolithiasis 2024;52(1):86; doi: 10.1007/s00240-024-01592-1
13. Sapareto S, Dewey W. Thermal dose determination in cancer therapy. Int J Radiat Oncol Biol Phys 1984;10(6):787–800; doi: 10.1016/0360-3016(84)90379-1
14. Yarmolenko P, Moon E, Landon C, et al. Thresholds for thermal damage to normal tissues: An update. Int J

Hyperthermia 2011;27(4):320–343; doi: 10.3109/02656736.2010.534527
15. Loh S, Carlson G, Chang E, et al. Comparative healing of surgical incisions created by the PEAK PlasmaBlade, conventional electrosurgery, and a scalpel. Plast Reconstr Surg 2009; 124(6):1849–1859; doi: 10.1097/PRS.0b013e3181bcee87
16. Flowers P, Theopold K, Langley R, et al. Chemistry 2e. OpenStax: Houston, Texas; 2019.
17. Chan K, Pfefer T, Teichman J, et al. A perspective on laser lithotripsy: The fragmentation processes. J Endourol 2001; 15(3):257–273; doi: 10.1089/089277901750161737
18. Shen J, Zhou J, Gu C, et al. A simplified model for thermal-wave cavity self-consistent measurement of thermal diffusivity. Rev Sci Instrum 2013;84(12):124902; doi: 10.1063/1.4846255
19. Teichman JMH, Vassar GJ, Glickman RD. Holmium: Yttrium-aluminum-garnet lithotripsy efficiency varies with stone composition. Urology 1998;52(3):392–397; doi: 10.1016/S0090-4295(98)00239-8
20. Chan K, Vassar G, Pfefer T, et al. Holmium:YAG laser lithotripsy: A dominant photothermal ablative mechanism with chemical decomposition of urinary calculi. Lasers Surg Med 1999;25(1):22–37; doi: 10.1002/(SICI)1096-9101(1999)25:1<22::AID-LSM4>3.0.CO;2-6
21. Riedinger E, Mohaghegh M, Leshchenko V, et al. Thulium fiber laser: Long pulse width as an independent risk factor for excessive heat generation. J Endourol 2025;39(11): 1158–1164; doi: 10.1177/08927790251377787
22. Lienhard VJ, Lienhard J. , IV.. A Heat Transfer Textbook. Phlogiston Press: Cambridge MA; 2024.

Address correspondence to:
D. Duane Baldwin, MD
Department of Urology
Loma Linda University Health
Room A560
11234 Anderson Street
Loma Linda, CA 92354
USA

E-mail: dbaldwin@llu.edu

Abbreviations Used

CEM_{43}	= cumulative equivalent minutes at 43°C
°C	= degrees Celsius
F	= French
Hz	= hertz
Ho:YAG	= holmium:yttrium aluminum garnet laser
J	= Joules
µm	= micrometer
mL	= milliliter
mm	= millimeter
Min	= minutes
3D	= three-dimensional
TFL	= thulium fiber laser
URSL	= ureteroscopic laser lithotripsy
W	= watts

Check for updates

《血管内泌尿外科杂志》第00卷第00期，
2026年1月：玛丽·安·利伯特，《智慧的一
部分》
© 作者（们）
Pp. 000–000
DOI: 10.1177/08927790261457175

气泡问题：输尿管激光碎石术中气泡带来的热风险

加布里埃尔·E·马丁医学博士、卡兰·理查兹、丹尼尔·张医学博士、阿德尔·巴蒂卡、尼努斯·贝特达什图、琼万·朴、费思·阿贾
伊、扎姆希德·奥赫诺夫医学博士以及D·杜安·鲍德温医学博士

摘要

引言：在输尿管镜激光碎石术（URSL）过程中，输尿管温度的异常升高被认为会促进输尿管狭窄的发生。细胞损伤始于43°C，蛋白质在60°C时即发生变性。在 URSL 操作期间，气泡可能意外进入集合系统。本研究旨在评估使用钬（Ho:YAG）光纤激光器和铥光纤激光器（TFL）进行模拟 URSL 时输尿管内的温度变化。

方法：将BegoStone仿体置于模型肾脏的输尿管肾盂连接部远端，并使输尿管浸没于35°C的生理盐水中。使用7.5 Fr可弯曲输尿管镜推进至结石处，同时以15 mL/min的流速持续灌注22°C的生理盐水。位于激光光纤尖端2 mm处的针式热电偶用于监测输尿管壁温度。随后推进直径为200 μm的激光光纤直至接触结石。分别采用Ho:YAG和 TFL 激光器各进行5次试验，在生理盐水及含3 mL气泡的环境中以3 W、10 W和20 W功率对结石进行消融。

结果：在对照条件下，两种激光在3、10或20瓦功率下均未超过43°C。在气泡环境中，TFL 和Ho:YAG激光在3瓦功率下作用1秒后输尿管温度均超过43°C；10瓦功率时，Ho:YAG激光1秒后温度超过43°C，而 TFL 激光则超过60°C；20瓦功率时两种激光1秒后的平均温度均超过60°C。在所有时间点，两种激光在气泡环境中的温度均显著高于生理盐水环境（p=0.008），且两种激光的最大温度均超过250°C。

结论：在该台式实验模型中，激光在气泡内持续激活1秒时，其功率 ≥ 3 W and risks protein denaturation at ≥ 20W即已超过热安全阈值。本研究强调了 URSL 过程中避免气泡存在对维持输尿管安全温度的重要性。需进一步开展体内研究以验证这些发现。

关键词：热损伤、气泡、激光碎石术、输尿管镜检查、钬激光、铥光纤激光

引言

近年来，肾结石的患病率不断上升，与之相伴的是输尿管镜激光碎石术（URSL）的增多。[1,2]在URSL过程中，可能继发于不安全的输尿管温度升高的激光热效应与输尿管狭窄的形成相关。[3]之前的研究表明，随着功率设置的提高，激光光纤尺寸的增大，以及激光激活的流体体积的减小，温度会升高。[4,5]在输尿管镜检查过程中，输尿管内的液体量较小，这预示着比肾脏或膀胱更大的热损伤风险。[6]因此，这是一个积极研究以帮助改善患者结局的领域。已有研究表明，充分的灌洗、冷冻灌洗、更短的激光激活周期和更低的功率设置可以减少热损伤。[7,8]此外，目前已知铥光纤激光器（TFL）比钬：钇铝石榴石激光器（Ho:YAG）产生更高的温度，提示在使用TFL时要格外小心。[9]目前文献中没有明确的热损伤阈值。一些研究表明体外蛋白质在60℃时发生变性，这在之前的泌尿学研究中被用作热损伤极限，尽管这不是泌尿道特有的。[10]在细胞培养中，细胞死亡率的断点在43℃左右被检测到，因此这也被用作泌尿学研究中的热损伤极限。[11,12]这一研究领域最具体的测量方法可能是使用43℃下的累积等效分钟（CEM_{43}），它将温度随时间的变化转化为单个数字（CEM_{43}或热效应剂量），

泌尿外科，洛马林达大学健康中心，美国加利福尼亚州洛马林达市。

可以量化热剂量暴露。[11,13]先前研究表明，CEM_{43}>70分钟可导致肾脏出现显著损伤（包括凝固性坏死）；研究还表明即使在CEM_{43}<20分钟时也会观察到急性及轻微损伤。[11,14]尽管如此，目前仍未明确界定人类泌尿系统的安全热剂量阈值，但这些阈值被用于评估激光碎石术热效应的研究中。基于上述研究，我们可以推断：温度达到或超过43°C即不安全；温度达到或超过60°C且CEM_{43} 70分钟则会导致不可逆的热损伤。

在URSL过程中，气泡可能无意间进入收集系统。目前尚未有针对激光碎石术在气泡环境中安全性的研究。本台式实验评估了使用Ho:YAG激光器和TFL设备在气泡环境中进行模拟URSL时输尿管温度及热剂量的变化情况。

材料与方法

采用3D slicer 5.2.2软件（Kitware公司，纽约）将肾脏的计算机断层扫描图像转换为三维（3D）肾脏模型，并使用Autodesk Fusion 360软件（Autodesk公司，旧金山）构建输尿管模型。利用这些模型通过Ultimaker 3 Extended 3D打印机（Ultimaker公司，荷兰格尔德马尔森）打印模具，并配合Liquid Dragon Skin伽20硅胶材料（Smooth-On公司，宾夕法尼亚州麦克恩吉）制作出肾脏及输尿管模型。同时制备了相同的球形、直径10毫米、呈一水草酸钙形态的BegoStone仿体模型（Bego GmbH公司，德国），并将其置于输尿管肾盂连接处远端1厘米处以模拟输尿管结石。为模拟内镜手术过程中的输尿管温度环境（图1），将含输尿管结石的模型置于35°C生理盐水中，并使用电浸式加热器（Pong-Dang公司，韩国京畿道）进行恒温维持。随后将7.5 Fr一次性数字柔性输尿管镜（普森医疗科技公司，中国珠海）置入模型输尿管中，并推进至结石位置。通过输尿管镜向研究使用的气泡肾内注入了3 mL空气泡；该气泡在冲洗及激光碎石过程中始终保持稳定位置。使用Thermedx FluidSmart系统（Thermedx LLC，美国俄亥俄州索伦市）以15 mL/min的流速持续进行室温（22°C）生理盐水冲洗。将一根200 μm激光光纤经内镜推进至与结石接触处。在激光光纤与结石接触处垂直于光纤方向穿入一根T-29X微针昆虫型T型热电偶探头（ThermoWorks，美国犹他州阿美利科），并将其定位在激光光纤尖端外侧2 mm处（图1C）。在生理盐水试验中激光光纤置于生理盐水中，在气泡试验中则置于空气中。该热电偶在液体中的响应时间为1秒，测量精度为±0.1°C。采用包含MAX31855 T型热电偶传感器扩展板（ThermoWorks，美国犹他州阿美利科）的数字数据采集系统，每6.0秒记录一次温度数据。Empower H100 Ho:YAG激光

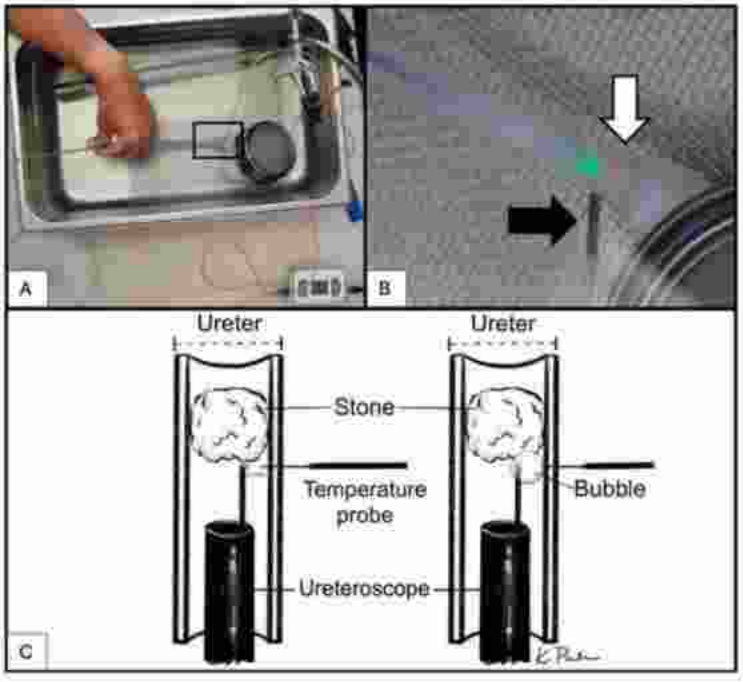


图1. 肾脏与输尿管模型实验装置示意图。(A)展示浸没于35°C生理盐水浴中的硅胶制肾脏及输尿管模型，输尿管镜从远端输尿管插入；模型肾脏上方设有筛网以确保其持续浸没。黑色矩形区域即为图B所示部分。(B)显示输尿管肾盂连接处的特写图像；其中置有10毫米BegoStone结石（白色箭头指示），热电偶（黑色箭头指示）位于激光光纤尖端外侧2毫米处（图中可见绿色瞄准光束）。(C)为模型输尿管的横截面示意图，分别展示生理盐水对照组（左）与气泡存在状态（右）；激光光纤与结石接触；热电偶垂直于激光光纤穿过输尿管壁，在光纤与结石接触处水平位置安装，并距激光光纤尖端外侧2毫米处布置。

(Olympus, Center Valley, PA)和SOLTIVE™Premium SuperPulsed TFL 激光器(Olympus, Center Valley, PA)，配合各自的200微米激光光纤，在生理盐水（作为对照组）及3毫升气泡环境中，以三种不同功率设置（3 W（0.3 J/10 Hz）、10 W（1 J/10 Hz）和20 W（1 J/20Hz））对结石进行7秒消融。所有测试功率下均采用制造商预设的短脉冲宽度/持续时间参数。实验结束后使模型恢复至基线温度，并在每次试验后更换模型内的生理盐水。对于生理盐水组：分别记录基线状态（0秒，激光激活前）、激光激活6秒后及激活12秒后的温度；对于气泡组：分别记录基线状态（0秒，激光激活前）、激活1秒后及激活7秒后的温度。针对每种激光类型（TFL、Ho:YAG）、功率设置（3 W、10 W、20 W）及介质（生理盐水、气泡）的组合，在上述时间点各进行5次测量，共计完成180次测量。

热剂量暴露量采用Sapareto和Dewey建立的CEM_{43}公式进行计算[13]。不安全温度定义为>43°C，热损伤阈值则设定为CEM_{43}>70分钟或温度>60°C。数据分析使用SPSS Statistics（IBM公司，芝加哥，伊利诺伊州）软件完成：统计学显著性采用曼-惠特尼U检验并结合Bonferroni多重比较校正法进行评估。针对每种激光器及各功率设置，均通过曼-惠特尼U检验比较生理盐水对照组与1秒气泡激活组之间的温度值及CEM_{43}值。共进行六次比较，校正后的显著性水平设定为$p<0.0083$（$\alpha=0.05/6$）。

结果

在所有测试功率设置下，生理盐水对照组与气泡组的温度曲线均存在显著差异（表1）。生理盐水对照组在任何功率设置下，激光器的平均温度均未超过43°C的安全阈值。在最高功率设置（20 W）下，激光激活12秒后，TFL 激光器的平均温度仅为38.6°C，Ho:YAG激光器为37.9°C；相比之下，在所有测试条件下，气泡内的激光激活均导致不安全的温度升高。

在气泡内仅激活1秒时，两种激光器在所有功率设置下的平均温度均超过43°C的安全阈值；即使在最低功率设置（3 W）下，TFL 激光器的平均温度仍达44.1°C，Ho:YAG激光器达45.0°C；激活1秒时，TFL 激光器在10 W和20 W功率下的平均温度均超过60°C的热损伤阈值，Ho:YAG激光器在20 W时亦如此；在20 W功率下，TFL 激光器1秒时记录到的最高温度为98.4°C，Ho:YAG激光器为92.8°C；而7秒时，TFL 激光器最高温度达257.2°C，Ho:YAG激光器则高达278.2°C。气泡温度的升高呈现出功率依赖性和时间依赖性两种模式（图2）：激光激活1秒时，在3 W功率下两种激光器的平均温度均升高68%，10 W时升高82%，20 W时升高113%；持续激活7秒后，温度增幅更为显著：3 W时升高139%，10 W时升高165%，20 W时升高394%。

除温度测量外，还计算了CEM_{43}值以同时反映温度幅度和暴露时长。CEM_{43}值在所有功率设置下均显示生理盐水对照组远低于热损伤阈值（CEM_{43}< 70分钟）。在1秒时，气泡CEM_{43}值仅在 TFL 激光器的10W功率下、以及两种激光器的20W功率下超过热损伤阈值；至7秒时，两种激光器在所有功率设置下的气泡CEM_{43}值均超过该阈值（表2）。

比较结果显示，在所有功率设置下，与生理盐水对照组相比，两种激光在1秒气泡激活条件下均出现具有统计学显著性的温度及CEM_{43}值升高（所有比较的p值均为0.008），且各实验条件间存在完全统计学差异（所有比较的U值均为25.0）（表3）。

讨论

本研究结果表明，在 URSL 过程中，气泡内的激光激活会立即带来热风险；在所有测试功率设置下均会出现不安全的温度值，且与激光类型或激活时长无关。本研究是首次针对

表1. 按激光类型、功率及激活时间划分的平均温度

激光功率及参数设置	激光激活时间（秒）	TFL 生理盐水对照组平均 CEM_{43}（分）	Ho：YAG生理盐水对照组平均CEM_{43}（分）	激光激活时间（秒）	TFL 气泡平均 CEM_{43}（分）	Ho：YAG气泡平均CEM_{43}（分）
3 W (0.3 J/10 Hz)	0	25.98	25.97	0	35.52	35.02
	6	26.78	25.98	1	44.09[a]	44.97[a]
	12	26.69	26.52	7	64.74[b]	61.52[b]
10 W (1 J/10 Hz)	0	26.89	26.03	0	37.08	34.23
	6	35.24	29.56	1	63.78[b]	54.24[a]
	12	34.01	29.29	7	88.01[b]	82.66[b]
20 W (1 J/20 Hz)	0	27.73	24.52	0	37.64	35.72
	6	38.08	35.40	1	80.71[b]	76.20[b]
	12	38.56	37.88	7	193.30[b]	170.21[b]

生理盐水对照温度分别在激光激活开始时（0秒）、6秒和12秒记录；气泡温度则在激光激活开始时（0秒）、1秒和7秒记录。

[a]热安全阈值（43°C）已被超过。

[b]热损伤阈值（60°C）已被超过。

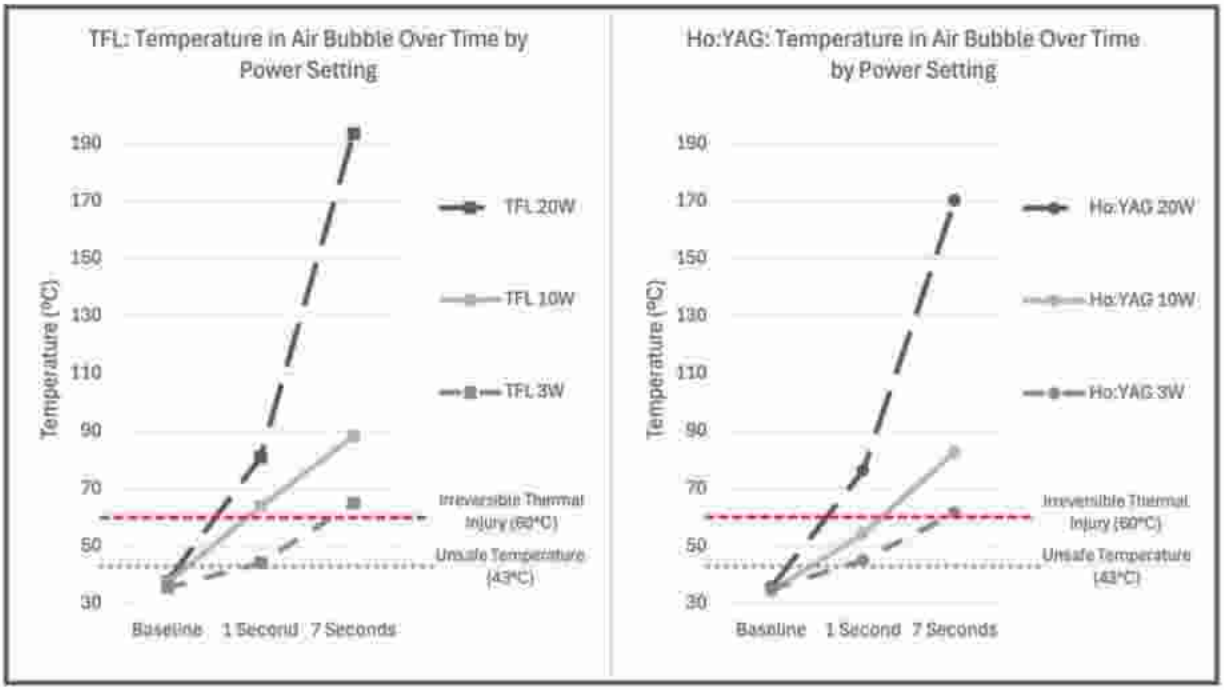


图2展示了不同功率设置和时间条件下激光器的温度分布曲线。图中呈现了TFL型与Ho:YAG型激光器在气泡内三种功率（3W、10W和20W）下随时间变化的温度测量结果（包括未激活时、激活1秒后及激活7秒后的基线值），并标注了不安全温度阈值（43°C）和不可逆热损伤阈值（60°C）。两种激光器均表现出随功率和时间增加而升高的温度趋势。

激光碎石术中气泡内的热安全性问题进行了调查，揭示了一种此前未被认识且可能构成严重术中风险的因素。

仅观察生理盐水对照组的数据即可发现：在任何功率设置下，无论使用哪种激光器，平均温度均未超过43°C的安全阈值（激光激活时间最长为12秒）。这证实了已知结论：采用生理盐水并配合灌注液的激光碎石术通常具有安全性，且更快的灌注速度和更低的功率设置可提供更安全的热分布。[7,8]

与之形成鲜明对比的是，在气泡环境中即使仅持续1秒的激光激活，两种激光器在所有功率设置下均超过了热安全阈值。在最低功率（3 W）条件下，TFL激光和Ho:YAG激光在气泡环境中均于1秒时超过43°C的安全阈值，并在7秒时超过60°C的热损伤阈值；而在20 W功率下，两种激光在1秒时均超过60°C的热损伤阈值。在所有功率设置下，气泡环境中的温度读数在1秒时均显著高于生理盐水环境，且各组数据差异显著。即便在临床最低功率3 W条件下，研究结果仍令人担忧，表明在气泡环境中进行激光激活并不存在安全的操作参数。此外，记录到的最大温度值也极为惊人：20 W功率下激光激活1秒后的最高温度接近生理盐水的沸点（98°C），而7秒后的最高温度则与电灼设备产生的温度（278°C）相当。[15]这表明即使是在气泡环境中短暂、非故意的激光激活，也可能对输尿管造成严重损害。

CEM_{43}热剂量分析提供了一个单独的、有意义的热损伤风险评估，

表2. 按激光类型、功率及激活时间划分的CEM_{43}平均值

激光功率及参数设置	激光激活时间（秒）	TFL生理盐水对照组平均CEM_{43}（分）	Ho：YAG生理盐水对照组平均CEM_{43}（分）	激光激活时间（秒）	TFL 气泡平均值CEM_{43} (min)	Ho：YAG气泡平均值CEM_{43} (min)
3 W (0.3 J/10 Hz)	6	9.93E-07	7.50E-07	1	1.09E-02	1.25E-02
	12	2.26E-06	1.66E-06	7	7.46E + 05[a]	1.47E + 05[a]
10 W (1 J/10 Hz)	6	2.55E-05	2.65E-06	1	2.97E + 03[a]	5.54E-01
	12	3.27E-04	1.08E-05	7	6.38E + 18[a]	2.10E + 14[a]
20 W (1 J/20 Hz)	6	9.14E-05	1.19E-05	1	5.47E + 08[a]	6.35E + 06[a]
	12	3.99E-03	1.23E-03	7	3.95E + 55[a]	1.94E + 48[a]

生理盐水对照组的CEM_{43}值分别在激光激活6秒和12秒时计算；气泡组的CEM_{43}值则分别在激光激活1秒和7秒时计算。

[a]热损伤阈值（CEM_{43}> 70分钟）已超过。

表3. 生理盐水与空气的统计分析
气泡温度与CEM_{43}

环境与激光对比（生理盐水 vs 空气泡中1秒）	比较的变量	U	p 值
3W TFL	温度	25	0.008
3W Ho:YAG	温度	25	0.008
10W TFL	温度	25	0.008
10W Ho:YAG	温度	25	0.008
20W TFL	温度	25	0.008
20W Ho:YAG	温度	25	0.008
3W TFL	CEM_{43}	25	0.008
3W Ho:YAG	CEM_{43}	25	0.008
10W TFL	CEM_{43}	25	0.008
10W Ho:YAG	CEM_{43}	25	0.008
20W TFL	CEM_{43}	25	0.008
20W Ho:YAG	CEM_{43}	25	0.008

采用曼-惠特尼U检验并结合Bonferroni校正进行多重比较，校正后的显著性水平为$p < 0.0083$。针对每种激光类型及功率设置，将盐水环境中的激光激活温度与空气泡环境中持续1秒的激光激活温度进行对比。所有空气泡温度及CEM_{43}值均显著更高（各项p值均为0.008），且组间差异显著（U = 25）。

考虑了温度和持续时间。在所有功率设置下，空气泡中1秒时的CEM_{43}值均显著高于生理盐水组，且各组间差异显著。在3 W、1秒条件下，气泡中CEM_{43}的最小平均增幅为1,099,819%，而生理盐水对照组则无显著变化；最大平均增幅出现在20 W、7秒时，达9.9×10^{59}%。值得注意的是，既往研究已证实$CEM_{43} \geq 20$分钟仍可导致急性轻度热损伤，而急性及严重热损伤则出现于$CEM_{43} > 70$分钟时[14]。尽管CEM_{43}急剧升高，但1秒气泡组在3 W激光或10 W Ho:YAG激光条件下均未超过热损伤阈值（$CEM_{43} > 70$）。这进一步验证了温度数据：对于两种激光在3 W功率下、或Ho:YAG激光在10 W功率下，1秒激活损伤可能较轻微；其余条件下的损伤则更为严重，远超热损伤阈值。这表明在气泡环境中运行的中高功率设置不存在容错空间。

激光器在生理盐水环境与气泡环境中工作时存在的显著温差，可归因于多种相互作用的物理机制。物质的比热容是指使一克物质温度升高一度摄氏度所需的热能。水的比热容高达每克每摄氏度4.184焦耳（J/g·°C），而海平面空气的比热容则低得多，仅为1.007 J/g·°C。[16]由于水的比热容是空气的四倍，因此在温度上升之前能够吸收更多的热能。此外，热量从光吸收区域逸出的速度（即热扩散时间）取决于介质的光学穿透深度和热扩散率（即热量在材料内部的传递速率）。[17]

$$\text{热扩散时间} = \frac{(\text{光学穿透深度})^2}{4\times(\text{热扩散率})}$$

与液态水相比，空气/蒸汽中的光穿透深度要大得多，而热扩散系数则小得多。因此，空气/蒸汽中的热扩散时间显著短于液态水。[18,19]进一步而言，我们考虑"摩西效应"：激光激活时，生理盐水会迅速蒸发形成膨胀的气泡。由于水蒸气密度比液态水低约1672倍，该气泡可使激光能量直接传递至暴露的结石表面。[20]这尤其值得关注——因为在宏观气泡中，激光产生的热量不仅传递给结石，还会传导至输尿管壁。在本研究背景下，空气的行为更接近水蒸气而非液态水，具有更高的光子传输率及光子向热能转化效率。这些原理表明，在空气中（而非生理盐水中）进行激光激活能够实现更强的热量产生、积聚以及向周围组织的传递。

近期针对 TFL 热学特性的研究数据显示，脉冲宽度/持续时间随脉冲能量增加而延长；在长预设模式下，脉冲持续时间较短预设模式延长3至4倍。作者得出结论：TFL 具有实现长脉冲持续时间的潜力，其持续时间可能超过热弛豫时间，从而独立引发过热现象及非特异性热损伤[21]。这或许能解释为何与Ho:YAG激光器相比，TFL 在较低功率设置（10 W）下即可突破60°C的热损伤阈值——即使采用短预设模式，TFL 的脉冲持续时间仍会随脉冲能量增加而延长。

此外，灌溉液的流动通过对流冷却过程实现散热功能。水流经结石表面及周围组织时，可带走热量并使其降温。[22]与流动的水相比，气泡中的空气处于静止状态，其温度随吸收的能量而升高。气泡会形成缺乏水分、无法吸收多余热量的微环境，从而削弱对流冷却的效果。热量持续在气泡内部、结石表面及周围组织中积聚，导致对流冷却仅限于气泡表面区域。

鉴于激光在气泡中作用可能造成的热损伤风险，泌尿科医师应采取预防措施避免在气泡内进行激光治疗。尤其需要由冲洗操作人员格外注意，防止意外将气泡引入收集系统。

这项台式研究明确揭示了激光碎石术在气泡环境中可能带来的热危害，但存在若干局限性。体外硅胶模型和结石模型虽无法完全复现临床输尿管镜检查的每个细节（包括对输尿管组织的真实影响），但采用台式模型使我们能够更深入地了解激光在气泡环境中的热效应，并统一所有试验条件。未来在动物模型中开展结合组织病理学评估的临床研究将有助于更准确地评估热损伤风险。热电偶传感器仅能以6秒为间隔记录温度数据；由于气泡环境中第12秒时温度极高，可能导致内窥镜及温度探头受损，因此在气泡实验中分别于激光激活后第1秒和第7秒进行测温；进一步的研究可以评估直接比较

生理盐水和空气之间每秒的温度变化。选择3mL体积作为最坏情况，以最大化检测温度差异的灵敏度。后续研究应评估不同尺寸的气泡。

根据我们的经验，采取几项简单措施即可有效避免气泡进入收集系统：包括对灌注管进行预充/冲洗；连接前将灌注注射器内的气泡排出；使用垂直放置且朝向地面的注射器进行灌注（使气泡滞留在注射器顶部）；以及避免注入注射器的全部液体体积（以防气泡滞留于注射器顶部）。未来研究应探索其他防止气泡进入收集系统的方法以及现有气泡的清除技术。

这些研究结果揭示了一个此前未被认识但具有显著危害性的安全风险，该风险可能在不知不觉中导致输尿管损伤及狭窄形成。在所有功率设置下，激光激活仅1秒即普遍超过热安全阈值；而在中高功率设置下，仅1秒即可进展为热损伤。这一现象令人担忧。本研究为临床实践提供了明确指导：外科医生应避免在气泡内进行激光激活，无论其功率设置或预期激活时长如何。

结论

在此台式模型中，即使仅在气泡内进行1秒的激光激活，在功率设置≥3 W时即超过热安全阈值；需进一步临床研究以在体内验证这些发现。输尿管镜激光碎石术过程中应避免引入气泡，并需开发进一步消除已存在气泡的技术。

致谢

作者谨此感谢并致谢Kimberly Park博士通过绘制实验装置示意图（图1C）所作出的贡献。

作者的贡献

G.E.M.：概念化（主导）、方法论（支持）、形式分析（主导）、调查研究（主导）、数据管理（主导）、初稿撰写（主导）、修订与编辑（主导）及可视化设计（主导）。K.R.：方法论（主导）、调查研究（支持）、数据管理（支持）、初稿撰写（支持）及项目管理（主导）。D.J.：调查研究（支持）。A.B.：调查研究（支持）及方法论（支持）。N.B.：调查研究（支持）。J.P.：调查研究（支持）。
F.A.：研究（支持性工作）。Z.O.：监督（支持性工作）。D.D.B.：概念化（支持性工作）及监督（主导工作）。

作者披露声明

不存在任何竞争性的财务利益。

资金信息

该项目未获得任何资金支持。

参考文献

1. Stamatelou K, Goldfarb D. Epidemiology of kidney stones. Healthcare (Basel) 2023;11(3):424; doi: 10.3390/healthcare11030424
2. Monga M, Murphy M, Paranjpe R, et al. Prevalence of stone disease and procedure trends in the United States. Urology 2023;176:63–68; doi: 10.1016/j.urology.2023.03.040
3. Dong H, Peng Y, Li L, et al. Prevention strategies for ure teral stricture following ureteroscopic lithotripsy. Asian J Urol 2018;5(2):94–100; doi: 10.1016/j.ajur.2017.09.002
4. Esøy M, Juliebø-Jones P, Beisland C, et al. Temperature profiles during ureteroscopy with thulium fiber laser and holmium: YAG laser: findings from a preclinical study. Scand J Urol 2022;56(4):313–319; doi: 10.1080/21681805.2022.2104367
5. Rezakahn Khajeh N, Hall T, Ghani K, et al. Pelvicaliceal volume and fluid temperature elevation during laser litho tripsy. J Endourol 2022;36(1):22–28; doi: 10.1089/end.2021.0383
6. Louters M, Kim H, Duu J, et al. Characterization of fluid dynamics and temperature profiles during ureteroscopy with laser activation in a model ureter. J Endourol 2022;36(12):1593–1598; doi: 10.1089/end.2022.0275
7. Wollin D, Carlos E, Tom W, et al. Effect of laser settings and irrigation rates on ureteral temperature during holmium laser lithotripsy, an in vitro model. J Endourol 2018;32(1):59–63; doi: 10.1089/end.2017.0658
8. Rice P, Somani B, Nagele U, et al. Generated temperatures and thermal laser damage during upper tract endourological procedures using the holmium: Yttrium-Aluminum-Garnet(Ho:YAG) laser: A systematic review of experimental stud ies. World J Urol 2022;40(8):1981–1992; doi: 10.1007/s00345-022-03992-7
9. Belle J, Chen R, Srikureja N, et al. Does the novel thulium fiber laser have a higher risk of urothelial thermal injury than the conventional holmium laser in an in vitro study? J Endourol 2022;36(9):1249–1254; doi: 10.1089/end.2021.0842
10. Sourial M, Ebel J, Francois N, et al. Holmium-YAG laser:Impact of pulso energy and frequency on local fluid temper ature in an in-vitro obstructed kidney calyx model. J Biomed Opt 2018;23(10):1–4; doi: 10.1117/1.JBO.23.10.105002
11. Van Rhoon G, Samaras T, Yarmolenko P, et al. CEM43℃ thermal dose thresholds: A potential guide for magnetic res onance radiofrequency exposure levels? Eur Radiol 2013;23(8):2215–2227; doi: 10.1007/s00330-013-2825-y
12. Kose E, Bostanci Y, Gulsen M, et al. Monitoring intrarenal temperature changes during Ho: YAG laser lithotripsy in patients undergoing retrograde intrarenal surgery: A novel pilot study. Urolithiasis 2024;52(1):86; doi: 10.1007/s00240-024-01592-1
13. Sapareto S, Dewey W. Thermal dose determination in can cer therapy. Int J Radiat Oncol Biol Phys 1984;10(6):787–800; doi: 10.1016/0360-3016(84)90379-1
14. Yarmolenko P, Moon E, Landon C, et al. Thresholds for thermal damage to normal tissues: An update. Int J

Hyperthermia 2011;27(4):320 – 343; doi: 10.3109/02656736.2010.534527
15. Loh S, Carlson G, Chang E, et al. Comparative healing of surgical incisions created by the PEAK PlasmaBlade, conventional electrosurgery, and a scalpel. Plast Reconstr Surg 2009;124(6):1849 – 1859; doi: 10.1097/PRS.0b013e3181bcee87
16. Flowers P, Theopold K, Langley R, et al. Chemistry 2e. OpenStax: Houston, Texas; 2019.
17. Chan K, Pfefer T, Teichman J, et al. A perspective on laser lithotripsy: The fragmentation processes. J Endourol 2001;15(3):257 – 273; doi: 10.0890/89277901750161737
18. Shen J, Zhou J, Gu C, et al. A simplified model for thermalwave cavity self-consistent measurement of thermal diffusivity. Rev Sci Instrum 2013;84(12): 124902; doi: 10.1063/1.4846255
19. Teichman JMH, Vassar GJ, Glickman RD. Holmium: Yttrium-aluminum-garnet lithotripsy efficiency varies with stone composition. Urology 1998;52(3):392 – 397; doi: 10 .1016/S0090-4295(98)00239-8
20. Chan K, Vassar G, Pfefer T, et al. Holmium:YAG laser lithotripsy: A dominant photothermal ablative mechanism with chemical decomposition of urinary calculi. Lasers Surg Med 1999;25(1):22 – 37; doi: 10.1002/(SICI)1096-9101(1999)25: 1<22::AID-LSM4>3.0.CO;2-6
21. Riedinger E, Mohaghegh M, Leshchenko V, et al. Thulium fiber laser: Long pulse width as an independent risk factor for excessive heat generation. J Endourol 2025;39(11): 1158 – 1164; doi: 10.1177/08927790251377787
22. Lienhard VJ, Lienhard J. , IV., A Heat Transfer Textbook. Phlogiston Press: Cambridge MA; 2024.

地址通信请寄至：
D. 杜安·鲍德温医学博士，泌尿外科
洛马琳达大学医务室 A560
美国加利福尼亚州洛马林达市安德森街11234号，邮编92354
电子邮件：dbaldwin@llu.edu

使用的缩写

CEM43=43° C下的累积等效分钟数
℃=摄氏度
F=法国的
Hz=赫兹
Ho：YAG=钬：钇铝石榴石激光器
J=焦耳
μm=微米
mL=毫升
mm=毫米
Min=分钟
3D=三维的
TFL=铥光纤激光器
URSL=输尿管镜激光碎石术
W=瓦特

·综述·

激光碎石对泌尿系统组织热损伤的研究进展

关汉添[1] 郑晓鹏[2] 曾国华[1]

[1]广州医科大学附属第一医院泌尿外科 广东省泌尿疾病重点实验室，广州 510230；[2]郑州大学附属第一医院泌尿外科，郑州 450000

通信作者：曾国华，Email：2008690094@gzhmu.edu.cn

【摘要】 泌尿系结石的治疗已由传统开放手术过渡到微创手术，激光技术的发展有力地推动了这一过程。而激光通过光热效应产生的热能除能击碎结石外，也能导致组织热损伤，造成局部组织坏死或瘢痕形成。激光碎石过程中热损伤的发生是多种因素共同影响的结果。本文阐述了激光碎石过程中可能导致热损伤发生的因素，如激光、术者、灌注和光纤等因素，并总结如何通过控制各因素来降低热损伤发生的风险，为保证激光碎石安全性提供理论依据。

【关键词】 尿路结石； 碎石术； 激光； 热效应； 损伤

基金项目：广州医科大学科研能力提升计划（GMUCR2024-01006）；第六批“广东特支计划”科技创新领军人才项目

DOI：10.3760/cma.j.cn112330-20250211-00051

Research progress on laser-induced thermal injury to the urinary system during lithotripsy

Guan Hantian[1], Zheng Xiaopeng[2], Zeng Guohua[1]

[1]Department of Urology, The First Affiliated Hospital of Guangzhou Medical University, Guangdong Provincial Key Laboratory of Urological Diseases, Guangzhou 510230, China; [2]Department of Urology, The First Affiliated Hospital of Zhengzhou University, Zhengzhou 450000, China

Corresponding author: Zeng Guohua, Email: 2008690094@gzhmu.edu.cn

【Abstract】 The treatment of urolithiasis has evolved from traditional open surgery to minimally invasive procedures, which significantly facilitated by the development of laser technology. While laser energy effectively fragments calculi through photothermal effects, it can also induce thermal injury to surrounding tissues, leading to localized necrosis or scar formation. The occurrence of thermal injury during laser lithotripsy is influenced by multiple interacting factors. This article reviews the key contributors to the injury, including laser-related parameters, operator techniques, irrigation conditions, and fiber characteristics. Furthermore, it summarizes strategies for mitigating thermal damage by optimizing these variables, providing a theoretical foundation for enhancing the safety of laser lithotripsy.

【Key words】 Urolithiasis; Lithotripsy; Laser; Thermal effect; Injury

Fund program: Plan on Enhancing Scientific Research in Guangzhou Medical University (GMUCR2024-01006); The 6th Batch of "Guangdong Special Support Program" for Science and Technology Innovation Leaders Project

DOI：10.3760/cma.j.cn112330-20250211-00051

激光技术自90年代在泌尿外科逐步开始使用，腔内碎石是其应用的主要方向。泌尿外科常用激光器主要有掺钕激光器（Nd：YAG）、掺铥（Tm：YAG）或钬（Ho：YAG）激光器和铥光纤激光器（thulium fiber laser，TFL），其中Ho：YAG运用最广泛。激光碎石的主要原理是激光的光热效应，激光能量被结石表面和水吸收后迅速转化为热能，产生高温蒸汽泡和冲击波使结石碎裂[1]。目前在临床上常用的操作模式主要有两种：“粉尘化”碎石（低能高频）可以将结石粉碎成细粉状，有助于减少网篮的使用；“爆米花”式碎石（高能低频）更适合处理较硬结石，使之破碎为较大碎片。

热能在激光碎石过程中发挥着重要作用，但其在腔内并非是定向传导的，若大量热量持续作用于组织容易发生热损伤，进而导致组织局部坏死和瘢痕形成[2-3]。热损伤的发生和严重程度受多种因素的共同影响，如激光的功率和脉冲、激光持续发射时间、灌注流速、镜鞘比和光纤类型等。本文归纳激光碎石相关的热损伤因素，并结合文献和本中心经验，探讨其预防策略。

在激光碎石过程中，当温度持续达到43 ℃会导致周围组织热损伤，当温度超过56 ℃时，仅1 s就能导致组织热损伤[1-4]。因此，术者应熟悉激光碎石相关参数和影响因素，以

降低热损伤发生的风险。

一、激光因素

1. 激光器选择：目前在泌尿外科常用的激光器中，Tm:YAG 的能量转换效率低，热量管理困难，多用于软组织切割。Ho:YAG 和 TFL 是泌尿外科激光碎石常用的激光器。Ho:YAG 使用固体激光晶体技术，通过脉冲形式输出能量；TFL 采用光纤激光技术，输出更稳定的连续波或超高频脉冲波。TFL 因发射激光的波长与水的吸收峰更接近，在同样的参数设置下，与 Ho:YAG 相比 TFL 的碎石效率更高[4]。TFL 在提高碎石效率的同时，也带来更明显的热效应，同样的参数设置下，TFL 造成的腔内温度升高程度和速度远大于 Ho:YAG[4-7]。Bedle 等[5]研究发现，当功率超过 30 W 时，TFL 能使温度显著升高至热损伤阈值，而同样功率下 Ho:YAG 的腔内温度仅为 38 ℃。尽管 TFL 的碎石效率高于 Ho:YAG，但同时也存在更高的热损伤风险，因此应针对结石类型和硬度等因素进行选择。Ho:YAG 的能量以脉冲形式释放，适合采用“高能低频”设置使用“爆米花”式碎石，快速破碎较硬或聚集的结石，后续使用网篮清除较大的碎石以避免“石街”形成；TFL 的能量输出特点则适宜采用“低能高频”设置使用“粉尘化”模式处理较大或复杂结石。

2. 激光功率：尽管目前并没有研究结果显示使用高功率激光碎石的效率高于使用低功率，但美国大部分泌尿外科医师仍习惯使用高功率碎石[8]。一项临床前瞻性研究结果显示[9]，对于直径 < 2 cm 肾结石，使用低或高功率激光碎石，手术时间和结石清除率并没有明显差异。在常规激光碎石操作中，使用高功率碎石更容易导致腔内温度快速升高，若温度持续超过阈值则会导致热损伤发生。一项体外研究结果证明[10]，在不进行灌注的情况下，激光功率设置为 40 W，仅需 10 s 肾内温度即升至 50 ℃；即使使用 14 – 15 ml/min 流速灌注，10 s 后温度仍为 44.9 ℃。因此，腔内温度与激光功率直接相关，功率越高腔内温度升高越迅速、持续时间越长，组织损伤越严重[4,11]。当碎石操作需要使用高功率设置时，需要保证有充分的灌注以避免腔内温度过高导致的组织热损伤[4,11]。总的来说，不应盲目追求高功率，如需高功率碎石，应保证充分灌注以降低热损伤风险。

3. 脉冲：脉冲参数包括脉冲能量、脉冲频率和脉冲宽度。碎石过程中仅脉冲相关参数变化也会使腔内温度产生变化，并可能造成组织热损伤。高脉冲能量更容易产生高热量使腔内温度迅速升高。Sourial 等[6]同样认为高脉冲能量会带来更高的加热速率。脉冲频率与腔内温度呈正相关，脉冲频率升高会增加组织热损伤事件发生的风险。Aldoukhi 等[6]和冯媛媛等[7]的研究结果同样证明了上述结论。另外 Aldoukhi 等[6]还探讨了脉冲频率与碎石效果的关系，发现脉冲频率存在一个阈值，当频率升高超过该值，碎石效果提升并不明显。因此，在实际操作中盲目提高脉冲频率并不可取。脉冲宽度指单个激光脉冲的持续时间，增加脉冲宽度能使光热效应更明显，产生更多热量[12]。激光碎石时应综合脉冲设置及其他参数，控制热损伤风险。

二、术者因素

在讨论激光碎石导致的热损伤时，操作占空比（operator duty cycle，ODC）是一个不可回避的重要因素。ODC 是指踏板激活时间的占比，以 10 s 为计，若激光激活 7 s 后关闭 3 s，则 ODC 为 70%。ODC 越高产生热量越多，腔内温度升高越快，更容易发生热损伤。既往研究结果表明[10]，ODC 为 50% 时到达热损伤阈值所需的时间为 60% 的 10 倍（948 s 与 94 s），提示 ODC 的高低与腔内温度呈正相关[7]。值得注意的是，尽管激光关闭后温度可以缓慢恢复到基线水平，但热剂量仍会维持在一定水平，即热剂量具有累积效应，因此单次激光激活的时间也是影响腔内温度的重要因素。Aldoukhi 等[13]发现温度峰值高低与踏板激活时间呈正相关，激光激活模式设置为开/关 15 s 进行 2 个循环，仅 9 s 就能达到热损伤阈值。总而言之，在激光碎石时应尽量避免持续长时间激活激光，并将 ODC 控制在 50% 以下，以减少热剂量积累，从而降低热损伤的风险。

三、灌注因素

1. 结石部位：结石形成的不同部位决定了激光激活时周围液体的体积，进而影响热剂量的积累。结石形成部位狭小，激光激活时更容易导致温度升高。既往研究结果表明[11,13-14]，肾盂对激光碎石产生热量的耐受能力最强，输尿管次之，肾盏最弱，这是由于流体体积小的部位单位时间内受到的热剂量大导致。因此，在进行激光碎石时，应明确不同部位对热量的耐受能力，降低组织热损伤风险。此外，若结石在热量耐受能力较弱的部位，应尽量避免原位碎石，可尝试将结石转移至较能耐受热量的肾盂再进行碎石；若结石无法转移，则应从结石的中央开始碎石，并远离组织。

2. 灌注压力：灌注充分是维持腔内温度稳定的前提，当使用高功率激光设置时充分灌注更为重要，激光碎石过程中灌注越充分，导致热损伤的风险越低[14]。但充分灌注并不意味着盲目加大灌注，盲目加大灌注容易导致腔内灌注压力过大，造成尿路黏膜损伤、撕裂和细菌侵入，增加术后感染的风险[15-16]。因此，激光碎石时应合理控制灌注压力，既保证视野清晰便于操作，又能稳定腔内温度。灌注压力受灌注体积、流速、液体流出方式、光纤直径和鞘通道直径等多因素影响。

灌注流速指单位时间内进入腔内的灌注液体积。既往多项研究[11,13,15,17-18]结果显示，增加灌注流速可显著降低激光碎石导致的温度升高，且降温效果与灌注流速呈正相关。增加灌注流速的同时还需要保证灌注液流出顺畅才能维持灌注压力稳定，否则容易增加肾盂静脉回流、感染、菌血症和器官损伤等相关并发症的风险。在使用低功率（< 30 W）碎石时，将平均流速控制在 25 – 30 ml/min 可以提供较好的操作环境和保证腔内温度稳定。在使用高功率碎石时，增加灌注流速可以保证充分灌注，同时搭配使用负压吸引鞘将灌注压力控制在 130 – 150 mmHg（1 mmHg = 0.133 kPa）内能有效降低术后感染风险。近期文献报道的智能控压控温软镜系统和末端可弯曲负压吸引鞘的应用[19-21]，则能更有效地管理腔内温度，他们分别通过智能调控进出水平衡和柔性解剖适

配，压力闭环控制，在提高结石清除率的同时降低了热损伤风险。

尽管光纤直径并不会对腔内升温模式有直接的影响[34]，但光纤直径与鞘通道直径的比例却能直接影响灌注液回流，进而影响灌注压力和腔内温度。Noureldin 等[35]比较不同直径输尿管鞘对腔内温度的影响，发现使用大直径输尿管鞘更能缓解激光碎石导致的温度升高。尽管鞘直径越大缓解腔内温度升高效果越显著[36]，但在实际操作中不可能无限制地增加鞘直径，鞘直径过大可能会造成周围组织压迫，使局部组织缺血坏死等损伤。因此，控制镜鞘比 < 0.75 能有效将灌注压力维持在安全水平，并能保证灌注液回流的效果，有效降低热损伤风险[34-35]。

3. 灌注温度：Dan 等[37]提出，在激光碎石过程中使用冷灌注（4 ℃）替代室温灌注（20 ℃）或温灌注（37 ℃）能有效降低激光激活产生的热剂量，冷灌注与室温灌注相比能使腔内温度保持在较低水平和降低温度峰值。Dan 等[37]在动物模型实验中发现使用冷灌注时峰值温度、热剂量和到达热损伤阈值时间等均明显降低。4 ℃灌注液虽然能高效带走热量，但冷灌注液持续与尿路黏膜接触也可能导致体温降低甚至失温[38]，因此在实际操作中应使用室温灌注。

四、光纤因素

激光通过在二氧化硅芯内反射被输送到光纤尖端，影响光纤性能的因素主要包括：光纤直径、柔韧性和耐久性等。光纤直径对灌注参数产生间接影响，根据 Poiseuille 定律，流动阻力与半径的四次方成反比，而流动阻力又能影响灌注液流出速率，从而影响灌注压力和热量带出效率。因此减小光纤直径可降低流动阻力，增加灌注液回流，减小灌注压力，降低组织热损伤风险。此外，减小光纤直径可以增加结石单位面积的辐射暴露，利于击碎结石[39]。值得注意的是，小直径光纤更容易发生尖端回烧的问题，光纤尖端回烧会降低碎石效率。因此在使用小直径光纤时，可使用低能、短脉冲设置来延缓尖端回烧。

五、总结和展望

激光技术推动了泌尿系结石治疗由开放手术向微创治疗转变，减少了患者的创伤和负担。激光碎石具有高效、精准和普适等特点，但也存在术中组织热损伤风险。针对不同情况需要对激光设置、灌注参数等进行相应调整，以最大程度保证碎石效果和安全性。Ho:YAG 作为现阶段普及度最高的激光器，是激光碎石的主流选择，为降低使用钬激光碎石的热损伤风险，更推荐使用低功率（< 10 W）、高能低频、短脉宽的设置进行碎石[40]，同时使用室温灌注液进行灌注，并将流速控制在 30 ml/min。TFL 虽尚未大规模普及，但碎石效率更高，适合需"粉尘化"处理的较大或复杂结石，并且能降低网篮使用率。有条件的地区还能使用负压吸引鞘促进灌注液回流，维持腔内压力为 130 – 150 mmHg。此外镜鞘比也应控制在 < 0.75，尽量避免在输尿管、肾盏等对热量耐受能力低的部位进行碎石，碎石时应尽量远离组织黏膜，避免长时间持续激活激光[41]，控制 ODC < 50%。

增强碎石效果、提高精准性和保证安全性将是未来激光碎石技术的发展方向。得益于近期出现的智能控压控温软镜系统和末端可弯曲负压吸引鞘等新技术，激光碎石的效率和安全性得到了提升，患者的术后恢复快、并发症减少。人工智能和纳米技术有望与激光碎石技术融合，实现对热损伤的精准控制和智能预防。首先，人工智能可以通过整合和分析大量手术影像、激光参数、灌注参数和术中温度等数据，建立预测模型，为医师决策提供参考和辅助作用，甚至实时自动调整各项激光参数。其次，电子集成技术和柔性材料的发展，使未来在内窥镜上集成多个温度监测仪器成为可能，多个温度检测点有助于实时获取腔内热量分布情况，结合人工智能技术进行三维热量分布建模，有助于直观了解腔内热量分布，避免在高热区域持续操作。未来可开发导热性能良好的纳米材料，在管鞘或光纤周围制成镀膜，甚至直接使用高导热材料制成管鞘或光纤保护套，促进腔内热量传导至体外。另外，研制热效应更小的激光器或磁力引导的纳米碎石机器人同样是未来激光碎石的发展方向。将人工智能技术和纳米技术应用于激光碎石虽然颇具前景，但距离其临床转化仍面临多方面挑战，仍需多学科协同推进，方可实现从实验研究向标准化临床应用的跨越。

利益冲突 所有作者声明无利益冲突

参 考 文 献

[1] 刘凡，邵小斌，张敏，等. 泌尿系结石钬激光碎石热效应研究进展[J]. 国际泌尿系统杂志，2019，39(2)：351-353. DOI：10.3760/cma.j.issn.1673-4416.2019.02.049.

[2] 吴桐，赵胜云，施旭东，等. 热损伤致输尿管狭窄机制的研究进展[J]. 国际泌尿系统杂志，2023，43(5)：938-941. DOI：10.3760/cma.j.cn431460-20220129-00240.

[3] 张旭辉，刘凡，秦琪琪，等. 泌尿系结石钬激光碎石热效应的体外研究[J]. 中华实验外科杂志，2019，36(12)：2160-2162. DOI：10.3760/cma.j.issn.1001-9030.2019.12.010.

[4] Tonyali S, van Buren MF, Ozkan A, et al. The heat is on: the impact of excessive temperature increments on complications of laser treatment for ureteral and renal stones [J]. World J Urol, 2023, 41(12): 3853-3865. DOI: 10.1007/s00345-023-04652-0.

[5] He M, Dong Y, Cai W, et al. Recent advances in the treatment of renal stones using flexible ureteroscopy [J]. Int J Surg, 2024, 110(7): 4320-4328. DOI: 10.1097/js9.0000000000001345.

[6] 梁磊，肖博，丁天福，等. 钬激光与钬激光碎石时升温曲线和稳态温度的差异[J]. 中华泌尿外科杂志，2023，44(2)：134-139. DOI：10.3760/cma.j.cn112330-20220219-00056.

[7] Kim HJ, Ghani KR. Which is the best laser for lithotripsy? Holmium laser [J]. Eur Urol Open Sci, 2022, 44(10): 27-29. DOI: 10.1016/j.euros.2022.05.017.

[8] Belle JD, Chen R, Srikureja N, et al. Does the novel thulium fiber laser have a higher risk of urothelial thermal injury than the conventional holmium laser in an in vitro study? [J]. J Endourol, 2022, 36(9): 1249-1254. DOI: 10.1089/end.2021.0842.

[9] Shrestha A, Corrales M, Adhikari B, et al. Comparison of low power and high power holmium YAG laser settings in flexible ureteroscopy [J]. World J Urol, 2022, 40(7): 1839-1844. DOI: 10.1007/s00345-022-04040-0.

[10] Aldoukhi AH, Ghani KR, Hall TL, et al. Thermal response to high-power holmium laser lithotripsy [J]. J Endourol, 2017, 31(12): 1308-1312. DOI: 10.1089/end.2017.0679.

[11] Æsøy MS, Julieba-Jones P, Bessland C, et al. Temperature

measurements during flexible ureteroscopic laser lithotripsy: a prospective clinical trial [J]. J Endourol, 2024, 38(4): 308-315. DOI:10.1089/end.2023.0660.

[12] Wei W, Chen M, Xie L, et al. Comparison of temperature and renal tissue thermal damage by holmium laser with different energy parameters during lithotripsy: in vitro porcine kidney model [J]. Int Urol Nephrol, 2024, 56(8): 2539-2545. DOI: 10.1007/s11255-024-03943-8.

[13] Aldoukhi AH, Hall TL, Ghani KR, et al. Caliceal fluid temperature during high-power holmium laser lithotripsy in an in vivo porcine model [J]. J Endourol, 2018, 32(8): 724-729. DOI:10.1089/end.2018.0395.

[14] Wollin DA, Carlos EC, Tom WR, et al. Effect of laser settings and irrigation rates on ureteral temperature during holmium laser lithotripsy, an in vitro model [J]. J Endourol, 2018, 32(1): 59-63.DOI:10.1089/end.2017.0658.

[15] Nouri hin YA, Farsari E, Ntasiotis P, et al. Effects of irrigation parameters and access sheath size on the intra-renal temperature during flexible ureteroscopy with a high-power laser [J]. World J Urol, 2021, 39(4): 1257-1262.DOI:10.1007/s00345-020-03287-9.

[16] Sourial MW, Elbel J, Francois N, et al. Holmium-YAG laser: impact of pulse energy and frequency on local fluid temperature in an in-vitro obstructed kidney calyx model [J]. J Biomed Opt, 2018, 23(10): 1-4.DOI:10.1117/1.JBO.23.10.105002.

[17] 冯媛媛, 陈明惠, 谈维杰, 等. 脉冲钬激光碎石热效应的实验研究[J]. 光学技术, 2020, 46(4): 507-512.DOI:10.13741/j.cnki.11-1879/o4.2020.04.022.

[18] Aldoukhi AH, Black KM, Hall TL, et al. Frequency threshold for ablation during holmium laser lithotripsy: how high can you go? [J]. J Endourol, 2020, 34(10): 1075-1081.DOI:10.1089/end.2020.0149.

[19] Yamashita S, Inoue T, Imai S, et al. Dynamic changes in fluid temperatures during laser irradiation using various laser modes: a thermography-based in vitro phantom study [J]. J Clin Med, 2023, 12(4): 1409.DOI:10.3390/jcm12041409.

[20] Louters MM, Dau JJ, Hall TL, et al. Laser operator duty cycle effect on temperature and thermal dose: in-vitro study [J]. World J Urol, 2022, 40(6): 1575-1580. DOI: 10.1007/s00345-022-03967-8.

[21] Ding T, Xu Z, Huang Z, et al. An in vitro study of irrigation rate, operator duty cycle and intrarenal temperature in superpulse fiber thulium laser lithotripsy [J]. World J Urol, 2024, 42(1): 588.DOI:10.1007/s00345-024-05289-3.

[22] Aldoukhi AH, Dau JJ, Majdalany SE, et al. Patterns of laser activation during ureteroscopic lithotripsy: effects on caliceal fluid temperature and thermal dose [J]. J Endourol, 2021, 35(8): 1217-1222.DOI:10.1089/end.2020.1067.

[23] Rezakahn Khajeh N, Hall TL, Ghani KR, et al. Pelvicaliceal volume and fluid temperature elevation during laser lithotripsy [J]. J Endourol, 2022, 36(1): 22-28. DOI: 10.1089/end.2021.0383.

[24] 朱澄村, 程飙, 饶帅, 等. 输尿管软镜碎石术治疗上尿路结石的疗效和安全性[J]. 中华泌尿外科杂志, 2020, 41(1): 41-45. DOI:10.3760/cma.j.issn.1000-6702.2020.01.008.

[25] Dean NS, Krambeck AE. Endourologic procedures of the upper urinary tract and the effects on intrarenal pressure and temperature [J]. J Endourol, 2023, 37(2): 191-198. DOI: 10.1089/end.2022.0630.

[26] Panthier F, Pauchard F, Traxer O. Retrograde intra renal surgery and safety: pressure and temperature. A systematic review [J]. Curr Opin Urol, 2023, 33(4): 308-317. DOI: 10.1097/mou.0000000000001102.

[27] Tsaturyan A, Petrimaris A, Pantazis L, et al. The effect of prolonged laser activation on irrigation fluid temperature: an in vitro experimental study [J]. World J Urol, 2022, 40(7): 1873-1878.DOI:10.1007/s00345-022-04000-8.

[28] Kose E, Bostanci Y, Gulsen M, et al. Monitoring Intrarenal temperature changes during Ho: YAG laser lithotripsy in patients undergoing retrograde intrarenal surgery: a novel pilot study [J]. Urolithiasis, 2024, 52(1): 86. DOI: 10.1007/s00240-024-01592-1.

[29] 吴至楷, 刘成, 杨江华, 等. 智能控压控温软镜系统联合超脉冲光纤钬激光在上尿路结石治疗中的应用[J]. 中华泌尿外科杂志, 2024, 45(7): 527-531. DOI:10.3760/cma.j.cn112330-20240621-00279.

[30] 王冬冬, 郭振坤, 朱要辉, 等. 头端可弯曲负压吸引鞘在肾结石治疗中的效果[J]. 新疆医学, 2025, 55(5): 589-592. DOI: 10.3760/cma.j.issn.1001-5183.2025.05.114.

[31] Zeng G, Jiang K, Liu S, et al. Flexible ureteroscopy with a flexible and navigable suction ureteral access sheath versus mini-percutaneous nephrolithotomy for treatment of 2-3 cm renal stones: an international, multicenter, randomized, non-inferiority trial [J]. Eur Urol, 2026, 89(1): 45-54.DOI: 10.1016/j.eururo.2025.06.001.

[32] Petrimaris A, Tsaturyan A, Pantazis L, et al. Factors affecting the irrigation fluid temperature during laser lithotripsy: in vitro experimental study [J]. Urology, 2022, 170(12): 53-59.DOI: 10.1016/j.urology.2022.07.060.

[33] Rukawender K, Dybowski B. The effect of laser settings and ureteral access sheath size on intrapelvic temperature during holmium laser lithotripsy [J]. Appli Sci, 2024, 14(8): 3501. DOI: 10.3390/app14083501.

[34] Ding T, Xu Z, Huang Z, et al. Optimizing aspiration efficiency in RIRS: the impact of ratio of endoscope-sheath diameter, irrigation flow, and negative pressure in an in vitro study [J]. Urolithiasis, 2025, 53(1): 102.DOI: 10.1007/s00240-025-01773-6.

[35] Shi J, Huang T, Song B, et al. The optimal ratio of endoscope-sheath diameter with negative-pressure ureteral access sheath: an in vitro research [J]. World J Urol, 2024, 42(1): 122.DOI: 10.1007/s00345-024-04815-7.

[36] Dau JJ, Hall TL, Maxwell AD, et al. Effect of chilled irrigation on caliceal fluid temperature and time to thermal injury threshold during laser lithotripsy: in vitro model [J]. J Endourol, 2021, 35(5): 700-705.DOI: 10.1089/end.2020.0896.

[37] Dau JJ, Rezakahn Khajeh N, Hall TL, et al. Chilled irrigation for control of temperature elevation during ureteroscopic laser lithotripsy: in vivo porcine model [J]. J Endourol, 2022, 36(3): 403-409.DOI: 10.1089/end.2021.0537.

[38] 辛锋, 刘久华, 范利. 不同温度灌洗液对输尿管软镜下钬激光碎石术后寒战及发性反应的影响分析[J]. 国际外科学杂志, 2024, 51(1): 43-48. DOI: 10.3760/cma.j.cn115396-20231007-00081.

[39] Fried NM, Irby PB. Advances in laser technology and fibre-optic delivery systems in lithotripsy [J]. Nate Rev Urol, 2018, 15(9): 563-573.DOI: 10.1038/s41585-018-0035-8.

[40] 靳松, 肖博, 敏超后, 等. 针状肾镜钬激光碎石术中结石周围温度变化的研究[J]. 中华泌尿外科杂志, 2020, 41(11): 861-864. DOI: 10.3760/cma.j.cn112330-20200520-00411.

[41] 中华医学会泌尿外科学分会结石学组, 中华医学会泌尿外科学分会激光学组, 中国泌尿系结石联盟. 钬激光在尿路结石治疗中的规范应用中国专家共识[J]. 中华泌尿外科杂志, 2022, 43(10): 721-724. DOI: 10.3760/cma.j.cn112330-20220909-00498.

（收稿日期：2025-03-11）

（本文编辑：黄鹿）

scientific reports

Check for updates

OPEN

Defining the safe operational window for holmium laser lithotripsy in impacted ureteral stones: an analysis of power, operator duty cycle, and irrigation flow

Jinquan Luo, Xinyi Li, Rui Ren, Yueming Li, Hao Wu, Lijie Zhang, Runqiang Yuan & Mancheng Gong✉

Iatrogenic thermal injury is a proposed mechanism for ureteral strictures that may occur following holmium laser lithotripsy for impacted stones. The safe operational parameters, including laser power, operator duty cycle (ODC), and irrigation flow rate, remain poorly defined. We utilized a high-fidelity, ex vivo 3D-printed silicone model to simulate the scenario of an impacted ureteral calculus. A full-factorial experimental design was employed to evaluate all combinations of laser power (10, 20, 30, and 40 W), irrigation flow rates (10 and 20 mL/min), and 50% ODC patterns (1 s/1 s, 3 s/3 s, and 5 s/5 s). The primary outcome was the cumulative thermal dose (CEM43) accumulated over a 90-s operational period. At power levels of 10 W and 20 W, nearly all combinations resulted in negligible CEM43 accumulation, measured at less than 0.06 min. A critical transition occurred at 30 W, where the combination of low flow (10 mL/min) and a prolonged laser-on time (5 s) resulted in CEM43 levels exceeding 120 min within the 90-s experiment, specifically reaching 336.18 min. At 40 W, the thermal risk was substantially elevated. Increasing the irrigation flow from 10 to 20 mL/min at 40 W, while maintaining a 3-s laser-on time, reduced CEM43 levels from a hazardous 309.80 min to 11.11 min. However, a 5-s laser-on time at 40 W consistently resulted in hazardous CEM43 levels, regardless of the flow rate. Thermal risk during laser lithotripsy is governed by the interplay of power, ODC, and flow. In this ex vivo model, 10 W was safe across all tested conditions. While 20 W is generally safe, prolonged activation at low flow should be avoided. Risk increases markedly above 30 W, where safety requires high flow and short activation bursts, conditions with a safety margin in theory, but not reproducibly so in practice. Moreover, because CEM43 is cumulative, the 90-s experimental window does not reflect total clinical activation time; longer activation may exceed injury thresholds even for settings that appeared safe in this model. Clinicians should therefore interpret these data with caution and use lower power setting.

Keywords Holmium laser lithotripsy, Ureteral stones, Thermal injury, Laser safety, Impacted stones

Urolithiasis is a prevalent global health issue, among which ureteral stones, accounting for 30–55% of all cases, can lead to complications such as flank pain, urinary tract infections, and ureteral strictures[1,2]. For impacted ureteral stones, which are characterized by prolonged entrapment leading to mucosal edema, inflammation, and fibrosis, ureteroscopic laser lithotripsy presents a particular challenge[3]. The precise definition of stone impaction is not easy to establish, with literature often defining it by clinical criteria. These include: (1) failure of guidewire to advance beyond the stone at the first attempt, (2) mild to severe hydronephrosis due to the stone and (3) stone remaining in the same position for two months or longer[4,5]. These stones are associated with significantly

Department of Urology, The People's Hospital of Zhongshan, No. 2 Sunwen East Road, Zhongshan, Guangdong, China. ✉email: gongmancheng@126.com

higher rates of postoperative complications, most notably ureteral strictures, with incidence reported as high as 4.9–34% compared to 1.9% for non-impacted stones[6–8].

A primary mechanism underlying iatrogenic injury is thermal damage resulting from holmium laser activation. The conversion of laser energy into heat within the irrigation fluid can raise temperatures to levels that induce coagulative necrosis of the urothelium. The degree of this damage depends on both the temperature and the duration of exposure, which is formally quantified as the thermal dose (Cumulative Equivalent Minutes at 43 °C, or CEM43). A CEM43 threshold of 120 min is acknowledged as the critical limit for tissue necrosis[9,10].

The risk of accumulating a damaging thermal dose is governed by key operative parameters. While laser power is a fundamental driver of heat generation[11], the operator duty cycle (ODC)—defining the pattern of intermittent laser activation—has been identified as an independent critical factor. High ODCs can lead to dangerous thermal doses even at moderate power settings[12]. Irrigation flow rate serves as the principal cooling mechanism, yet its efficacy in the confined space of an impacted ureter, where fluid circulation is inherently restricted, remains a critical concern[13].

Although previous in-vitro studies have explored these parameters individually, a systematic quantification of their combined effects under conditions that replicate the clinical challenge of an impacted stone is lacking. The specific operational boundaries for safely performing lithotripsy in this high-risk scenario are poorly defined. Therefore, this study aimed to systematically evaluate the effects of ODC, laser power, and irrigation flow rate on the risk of urothelial thermal injury using a high-fidelity, ex vivo 3D-printed model of an impacted ureteral stone. By calculating the cumulative thermal dose (CEM43), we sought to identify the safe operational windows that maintain the thermal dose below the critical threshold of 120 min, thereby providing an experimental basis for the safe and efficient management of impacted ureteral stones.

Methods

Experimental setup and materials

3D-printed ureteral model

A unilateral kidney and ureter model (including the renal pelvis and calyces) was reconstructed using Mimics Research 21.0 software (Materialise, Belgium). The model was fabricated using a silicone liquid 3D printer with 10A softness addition-cure liquid silicone. The inner diameter of the ureteral lumen was 4.8 mm, simulating the average caliber of a normal human ureter. A hydrogel support bath was employed to prevent structural deformation during printing. After printing, the model was washed to remove residual hydrogel, resulting in a hollow, anatomically accurate kidney-ureter model.

Stone samples

Standardized Begostone artificial stones with a diameter of 12 ± 2 mm were used. Additionally, human calcium oxalate stones of similar size, obtained from a patient with multiple bladder stones (with informed consent), were also utilized.

Surgical and laser equipment

A rigid ureteroscope (Fr9.8/8.0, Richard Wolf, Germany) was used and secured in a fixed clamp during experiments. A holmium laser system was used to perform lithotripsy (SRM-H1C, Raykeen, Shanghai, China) along with a laser fiber (550 μm). With the aid of the endoscope, the laser fiber was placed to the center of ureteral lumen and its tip was adjusted to remain approximately 1 mm from the stone surface before the stout fixation. Laser output power was selected in 4 levels 10 W (0.5 J/20 Hz), 20 W (1.0 J/20 Hz), 30 W (1.5 J/20 Hz) and, 40 W (2.0 J/20 Hz). All power settings were checked and verified by an independent power meter before the experiments (Figure S1).

Irrigation system

An irrigation pump (LC690, Shenzhou, Shenzhen, China) delivered normal saline at the temperature of 22–23 °C at the two rates of 10 mL/min and 20 mL/min. Before each series of experiments, a test for a particular flow rate was conducted with effluent collected for 1 min in a pre-weighed container, permitting volume calculation from the mass and density ($\rho = 1.03$ g/cm^3) of the effluent. Three measurements were made independently and only permits flow rates within ± 0.5 mL/min of target for later experiments.

Temperature monitoring

The temperature was monitored with a high-accuracy thermometer (KPS-YET, Kaipusen, Jiangsu, China) with a resolution of 0.01 °C with two built-in thermocouples. Before their utilization, the thermocouples went through a calibration phase, after which they were installed at two strategic locations: below the stone (T1) and above the stone (closer to the obstruction, T2). The tip of the thermocouple was placed roughly 1 mm away from the stone surface, with only the sensing portion inserted into the ureteral lumen to assess mucosal temperature. The built-in data acquisition system of the equipment recorded temperature data every second.

Experimental environment

The experiments were conducted with the model being submerged in a thermostatic water bath at 37 ± 0.5 °C (Fig. 1A). All the assemblies including the ureteroscope and the printed model were immobilized with fixture clamps to maintain spatial and angular stability of the assemblies throughout the experiments.

Operator duty cycle (ODC) settings

To simulate intermittent laser activation, three ODC patterns were implemented: 1 s on / 1 s off, 3 s on / 3 s off, and 5 s on / 5 s off, all corresponding to a 50% duty cycle.

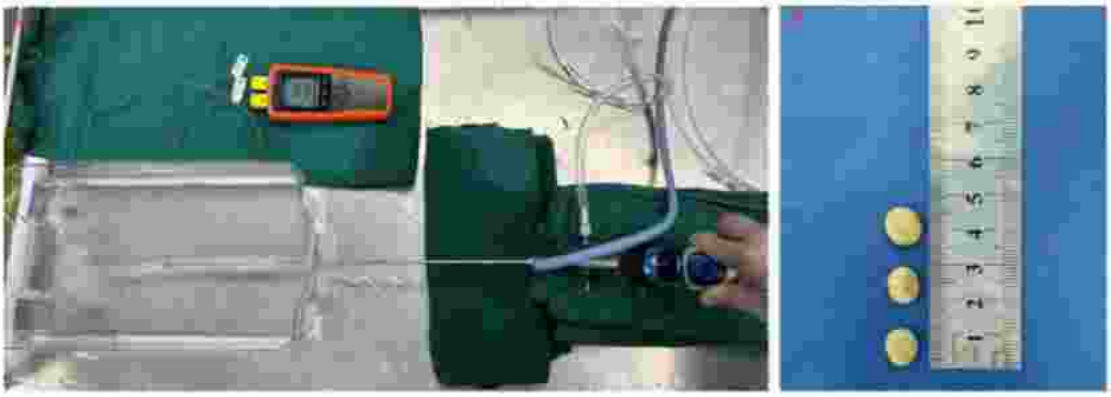


Fig. 1. Experimental materials and setup. (**A**) The configuration of the experimental setup. (**B**) Three representative human ureteral stone samples used in the experiments.

Experimental procedure

The experimental procedures can be seen in Text S1, Supplementary materials.

Thermal injury assessment and data analysis

The primary outcome was the CEM43 value, calculated from the 1-s interval temperature data at the T1 (highest risk location) and T2 site using the Sapareto & Dewey formula[9,14]:

$$\mathrm{CEM43} = \sum t_i \times R^{(43-T_i)}$$

where t_i is the time interval, T_i is the average temperature during that interval, $R = 0.5$ for $T_i \geq 43$ °C, and $R = 0.25$ for $T_i < 43$ °C.

Statistical analysis

Data were processed using SPSS version 26.0. CEM43 at 90 s were expressed as mean ± standard deviation (SD).

Results

Real-time temperature profiles

The dynamic changes in temperature during the laser activation period were recorded for all parameter combinations (Fig. 2).

At a laser power of 10 W, all temperature profiles, irrespective of the flow rate or ODC laser-on time, remained below the 43 °C threshold throughout the 90 s duration. An increase in laser power to 20 W resulted in temperature profiles that, in most cases, also remained below 43 °C. A single exception was observed with the combination of low flow rate (10 mL/min) and the longest ODC laser-on time (5 s), where the recorded temperature surpassed 43 °C. A notable change in thermal activity occurred at the 30 W mark. At low flow rates (10 mL/min), all three settings (1 s, 3 s, 5 s) of ODC laser-on time produced temperatures higher than 43 °C. At the maximum flow rate of 20 mL/min, for both the 1 s and 3 s heating times, the temperature did not exceed 43 °C. However, the longer 5 s laser-on time resulted in the temperature exceeding 43 °C. At a maximum laser power of 40 W, the temperature profiles showed that all parameter combinations gave rise to temperatures in excess of 43 °C. The magnitude of temperature elevation above 43 °C and the duration of exposure were significantly affected by the irrigation flow rate and ODC laser-on time.

The CEM43 assessment

The thermal safety of various holmium laser settings was systematically evaluated in an in vitro model by measuring the CEM43. The comprehensive results are presented in Table 1.

The data identified laser power as the primary determinant of thermal risk. At power settings of 10 W and 20 W, the accumulated CEM43 after 90 s was negligible (< 0.06 min) under most tested conditions, indicating a wide thermal safety margin. The sole exception was the combination of 20 W, 10 mL/min, and a 5-s laser-on time, which yielded a low but measurable CEM43 of 1.27 ± 0.19 min. A critical transition was observed at 30 W. While most combinations remained safe, the use of low flow rate (10 mL/min) with an extended laser-on time (5 s) led to rapid accumulation of thermal dose, exceeding the 120-min threshold within the experiment (336.18 ± 50.43 min). At 40 W, thermal risk was substantially elevated. High irrigation flow (20 mL/min) effectively mitigated risk at shorter laser-on times (1 s, 3 s), maintaining CEM43 at 11.11 ± 1.67 min or lower. However, prolonging activation to 5 s at 40 W consistently resulted in hazardous CEM43 levels, regardless of flow rate (1069.35 ± 85.55 min at 10 mL/min; 159.77 ± 23.97 min at 20 mL/min).

The resultant thermal doses (CEM43) for human stones demonstrated a preliminary consistency with the data obtained from Begostones under identical settings (Table S1). Furthermore, the real-time temperature profiles of human stones (Figure S2) closely mirrored those of Begostones.

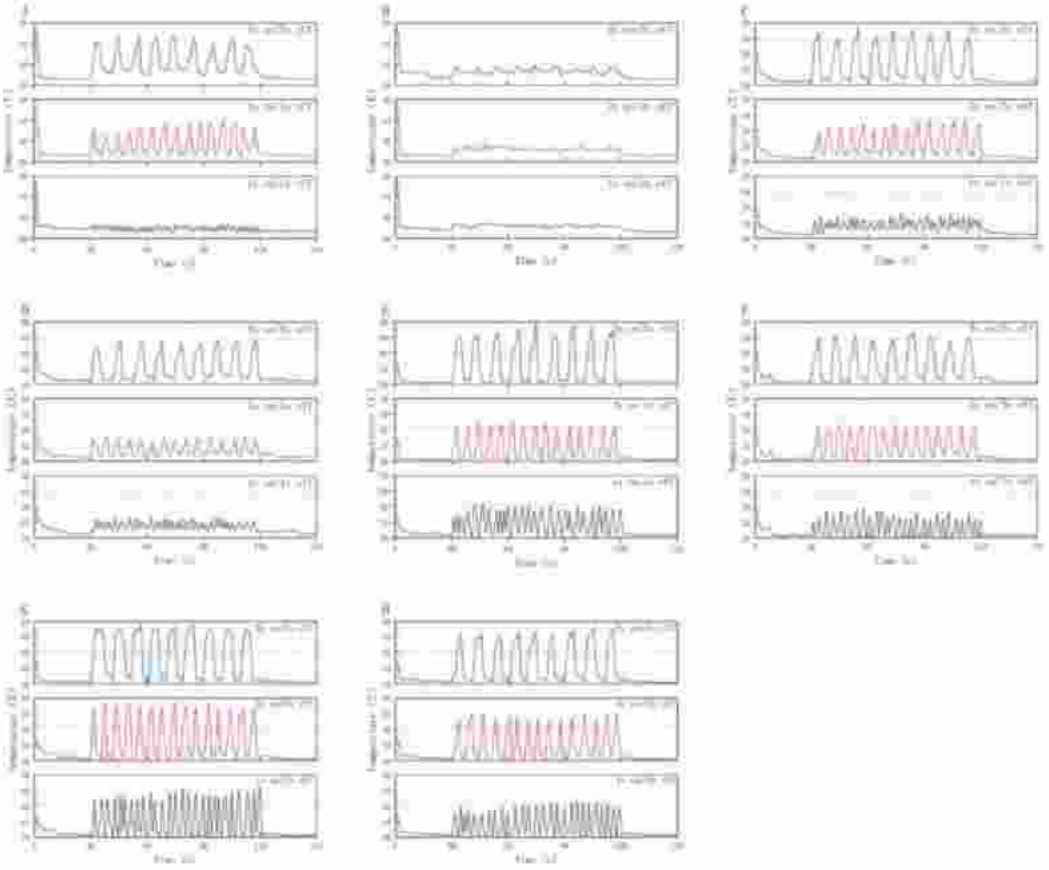


Fig. 2. Temperature variations under different laser energies, flow rates, and duty cycles. (**A**, **B**) represent the results for 10 ml/min and 20 ml/min flow rates, respectively, under 10 W laser energy. (**C**, **D**) represent the results for 10 ml/min and 20 ml/min flow rates, respectively, under 20 W laser energy. (**E**, **F**) represent the results for 10 ml/min and 20 ml/min flow rates, respectively, under 30 W laser energy. (**G**, **H**) represent the results for 10 ml/min and 20 ml/min flow rates, respectively, under 40 W laser energy. In each panel, the temperature variation curves represent duty cycles of 1 s on/1 s off, 3 s on/3 s off, and 5 s on/5 s off, respectively. The red dashed line indicates the 43 °C threshold.

The temperature and CEM43 data presented above were measured at the T1 position. Temperatures at the T2 measurement point remained below 43 °C under all tested conditions (data not shown).

Discussion

This study systematically quantified the effects of ODC, laser power, and irrigation flow rate on the accumulation of thermal dose during holmium laser lithotripsy in a high-fidelity model of an impacted upper ureteral stone. Our primary finding is that while laser power is the dominant determinant of thermal risk, the ODC and irrigation flow rate are critical modifiers that can either mitigate or exacerbate this risk, defining the narrow safety margins in high-power settings.

The data identify a clear risk stratification based on laser power. For all tested conditions at 10 W, and for the majority at 20 W, the accumulated CEM43 after 90 s was negligible (≤ 0.06 min), effectively posing no thermal injury risk for clinically relevant activation periods. This finding provides robust experimental support for the safety of low-to-moderate power settings, as suggested by prior expert recommendations[11,15–17]. A critical transition to risk occurred at 30 W, where the combination of parameters determined whether the 120-min injury threshold was breached within the 90-s observation window. Specifically, the 30 W, 10 mL/min, 5 s combination produced a CEM43 of 336.18 ± 50.43 min, far exceeding the threshold. This highlights that even at 30 W, unsafe practices can swiftly lead to potentially damaging thermal doses. At the highest power of 40 W, the thermal risk was substantially elevated. However, our data clearly demonstrate the profound mitigating effect of irrigation: at 40 W with a 3-s laser-on time, increasing flow from 10 to 20 mL/min reduced the accumulated CEM43 from a hazardous 309.80 ± 24.78 min to a substantially lower 11.11 ± 1.67 min. Consistent with the findings of Rice et al., high-flow irrigation (36–40 mL/min) has been demonstrated to significantly reduce intraluminal temperature[18].

Our findings underscore that the operator duty cycle (ODC) is a critical modulator of thermal risk, whose impact is contingent on laser power and irrigation flow. At power settings ≥ 30 W, extending the laser-on time from 1 s or 3 s to 5 s was frequently the difference between accumulating a minimal versus a damaging thermal dose. For instance, at 40 W with 20 mL/min flow, extending the laser-on time from 3 to 5 s caused the CEM43 to

Flow rate (ml/min)	Laser power (W)	ODC laser-on time (s)	CEM43 at 90 s (min), Mean ± SD
10	10	1	$(3.17 \pm 0.95) \times 10^{-6}$
10	10	3	$(4.15 \pm 1.25) \times 10^{-6}$
10	10	5	$(7.32 \pm 2.20) \times 10^{-6}$
20	10	1	$(6.71 \pm 2.01) \times 10^{-6}$
20	10	3	$(5.45 \pm 1.64) \times 10^{-6}$
20	10	5	$(6.06 \pm 1.82) \times 10^{-6}$
10	20	1	$(1.08 \pm 0.32) \times 10^{-5}$
10	20	3	$(14.7 \pm 2.94) \times 10^{-5}$
10	20	5	1.27 ± 0.19
20	20	1	$(3.69 \pm 1.11) \times 10^{-6}$
20	20	3	$(9.56 \pm 2.87) \times 10^{-6}$
20	20	5	$(5.90 \pm 1.18) \times 10^{-5}$
10	30	1	$(34.4 \pm 6.88) \times 10^{-5}$
10	30	3	0.418 ± 0.083
10	**30**	**5**	**336.18 ± 50.43**
20	30	1	$(2.16 \pm 0.65) \times 10^{-5}$
20	30	3	$(11.3 \pm 2.26) \times 10^{-5}$
20	30	5	0.472 ± 0.071
10	40	1	20.54 ± 3.08
10	**40**	**3**	**309.80 ± 24.78**
10	**40**	**5**	**1069.35 ± 85.55**
20	40	1	0.323 ± 0.065
20	40	3	11.11 ± 1.67
20	**40**	**5**	**159.77 ± 23.97**

Table 1. Accumulated CEM43 during 90-Second Laser Activation. ‘CEM43, Cumulative Equivalent Minutes at 43 °C. Bold entries indicate parameter combinations where the mean CEM43 value at 90 s exceeded the 120-min safety threshold, identifying them as high-risk settings.

increase from 11.11 ± 1.67 min to 159.77 ± 23.97 min, crossing the injury threshold. This aligns with prior studies where ODC was identified as a important variable controlling temperature rise[12,19]. The dramatic effect of ODC patterns is quantified in the work of Louters et al., showing that a change from 50 to 60% ODC can shorten the time to injury by an order of magnitude[19]. Our data, consistent with clinical observations of transient high-ODC activation[20], demonstrate that managing ODC is essential for safe lithotripsy, especially when utilizing higher power settings.

Another interesting observation was the rapid temperature change. Before any irrigation procedure, the temperature at the T1 measuring point took only 2 s to go below 30 °C and stabilize at 27 °C or so. Likewise, when the laser stopped working, the temperature at T1 measuring point was less than 30 °C within 2 s. According to studies involving non-impacted stones, the cooling rate is even faster than that observed in those studies. Song et al. note that typical pre-irrigation requires approximately 10 s to cool the field to a temperature range of 29–31 °C, despite utilizing a higher irrigation flow rate of 78–91 mL/min with a semi-rigid ureteroscope[21]. We hypothesize that the presence of an impacted stone obstructs the normal retrograde flow of irrigation fluid within the ureter, thereby promoting rapid local fluid turnover and facilitating heat dissipation. This mechanism may explain why in our experiments (30 W or 40 W), if there was adequate irrigation, and the laser-on time was short enough to allow safe delivery of laser energy without thermal damage.

The most important clinical benchmark to detect ureteral thermal injury remains the CEM43 threshold of 120 min, which is based on prior hyperthermia research[9,10,22]. Nonetheless, data from Pauchard et al. show that renal thermal injury may occur with a CEM43 value ranging from 20 to 70 min indicating that clinically significant injury may occur with a lower thermal dose than believe[22]. As a result, future studies are required to further characterize the thermal injury threshold for the renal pelvis and ureter. Meanwhile, a more conservative choice of parameters should be considered to create a major margin of safety.

The results of our study have direct and important clinical implications. The increasing occurrence of ureteral strictures post-ureteroscopy (especially impacted stones[6]) may be due to the uneducated use of the high-power laser settings without adequate attention to activation patterns and irrigation. Our findings provide practical, evidence-based recommendations for safely performing treatments based on thermal dose accumulated during a typical activation of 90 s. For a high margin of safety, the power setting of 10 W was safe for all flow rate and ODC combinations tested. Although 20 W power settings are usually safe, 20 W settings should not be used for prolonged activation at low flow rates. The safety at 30 W is highly dependent on the adjuvant parameters. It is recommended to use a high rate of irrigation flow (20 mL/min). At low irrigation flow (10 mL/min), surgeons must avoid prolonged continuous activation (e.g., 5-s laser-on time) at this power level, as this combination leads to a rapid accumulation of a damaging thermal dose (CEM43 > 336 min). Using 40 W power comes

with high risks and therefore, should be used wisely. Its use is justified only with high flow rates (20 mL/min) and short ODC laser-on times (≤ 3 s). Thus, the surgeon must be acutely aware of the cumulative (and total) duration of laser activation to remain below the injury threshold. Notably, upward modification of the flow rate of irrigation could be helpful in clinical practice to decrease the thermal effect of laser activation at high power. However, this must also feature a patent outflow tract to prevent a rise in intrarenal pressure and, hence, the risk of postoperative infection and related complications. We suggest that in situations where outflow is compromised—such as in the presence of ureteral strictures or tortuosity—the use of high-power laser settings should be avoided. Furthermore, the operational window of 40 W is very narrow, so the surgeon needs to strictly control both the time of individual activation pulses and the number of activations.

Despite its strengths, our study has several limitations. As an ex vivo model, it lacks the heat-sink effect of blood perfusion and the dynamic physiological responses of living tissue. Furthermore, the thermal properties of the silicone model and artificial stones differ from human tissue, our validation with a limited number of human stones (n = 3) necessitates further investigation. For all experiments a 550 µm laser fiber was used. The larger fiber provides a lower energy density at the stone surface as compared to smaller fibers like the 200 µm fiber limiting its ablation capacity. In clinical settings, this may lead surgeons to compensate by selecting higher power settings or prolonging activations, resulting in excessive thermal exposure. More importantly, the model idealized several clinical conditions, by assuming a patent irrigation pathway and a central non-contacting laser fiber. Impacted stones, in fact, frequently result in impaired irrigation. Furthermore, surgical technique, particularly among inexperienced surgeons, may lead to fiber interacting with the mucosa, resulting in direct ureteral injury[23]. These factors could generate heating on a more rapid time scale than observed here, which means our experimental estimates could represent a best-case thermal scenario. The model was also not able to factor in the fragmentation of the stone. The stone may fragment into smaller pieces, consuming laser energy and altering heat generation. As a result, while experienced surgeons operating in controlled situations may get the safety profiles described, less experienced operators or cases with poorer irrigation ought to use more conservative parameters. Future experiments should try to reproduce these thermal dose thresholds under more difficult clinically relevant conditions.

Conclusion

The risk of thermal injury during laser lithotripsy depends on power, ODC, and flow rate. In this ex vivo model, the power setting of 10 W was safe for all flow rate and ODC combinations tested. Although 20 W power settings are usually safe, 20 W settings should not be used for prolonged activation at low flow rates. As soon as the power level rises above 30 W, safety increasingly depends on high flow rates and limiting activation bursts, suitable levels that can only be achieved with a safety margin, but not reproducibly so in practice. In addition, since CEM43 is a cumulative parameter, the 90-s experimental window which was used in this study does not represent the total clinical activation time, and prolonged activation could exceed the injury threshold, even at settings which seem safe in this model. For this reason, clinicians should interpret these data with caution and use lower power setting.

Data availability

The datasets generated during and/or analyzed during the current study are available from the corresponding author on reasonable request.

Received: 28 December 2025; Accepted: 18 March 2026
Published online: 28 March 2026

References

1. Sorokin, I. et al. Epidemiology of stone disease across the world. *World J. Urol.* **35**, 1301–1320. https://doi.org/10.1007/s00345-017-2008-6 (2017).
2. Jahrreiss, V., Seitz, C. & Quhal, F. Medical management of urolithiasis: Great efforts and limited progress. *Asian J. Urol.* **11**, 149–155. https://doi.org/10.1016/j.ajur.2023.05.001 (2024).
3. Hu, H. et al. Ureteral stricture formation after removal of proximal ureteral stone: Retroperitoneal laparoscopic ureterolithotomy versus ureteroscopy with Holmium: YAG laser lithotripsy. *PeerJ* **5**, e3483. https://doi.org/10.7717/peerj.3483 (2017).
4. Fam, X. I. et al. Ureteral stricture formation after ureteroscope treatment of impacted calculi: A prospective study. *Korean J. Urol.* **56**, 63. https://doi.org/10.4111/kju.2015.56.1.63 (2015).
5. Tonyali, S. et al. Predictors of ureteral strictures after retrograde ureteroscopic treatment of impacted ureteral stones: A systematic literature review. *JCM* **12**, 3603. https://doi.org/10.3390/jcm12103603 (2023).
6. Moretto, S. et al. Ureteral stricture rate after endoscopic treatments for urolithiasis and related risk factors: Systematic review and meta-analysis. *World J. Urol.* **42**, 234. https://doi.org/10.1007/s00345-024-04933-2 (2024).
7. Yamashita, S., Inoue, T., Kohjimoto, Y. & Hara, I. Comprehensive endoscopic management of impacted ureteral stones: Literature review and expert opinions. *Int. J. Urol.* **29**, 799–806. https://doi.org/10.1111/iju.14908 (2022).
8. Tonyali, S. et al. Factors associated with ureteral strictures following ureteroscopy for impacted ureteral stones? A multicenter study by EAU-YAU endourology and urolithiasis working party. *Actas Urológicas Españolas (English Edition)* **47**, 631–637. https://doi.org/10.1016/j.acuroe.2023.04.005 (2023).
9. Sapareto, S. A. & Dewey, W. C. Thermal dose determination in cancer therapy. *Int. J. Radiat. Oncol. Biol. Phys.* **10**, 787–800. https://doi.org/10.1016/0360-3016(84)90379-1 (1984).
10. Aldoukhi, A. H. et al. Caliceal fluid temperature during high-power Holmium laser lithotripsy in an *in vivo* porcine model. *J. Endourol.* **32**, 724–729. https://doi.org/10.1089/end.2018.0395 (2018).
11. De Coninck, V., Defraigne, C. & Traxer, O. Watt determines the temperature during laser lithotripsy. *World J. Urol.* **40**, 1257–1258. https://doi.org/10.1007/s00345-021-03848-6 (2022).
12. Wanderling, C. et al. WATTS happening? Evaluation of thermal dose during holmium laser lithotripsy in a high-fidelity anatomic model. *World J. Urol.* **42**, 157. https://doi.org/10.1007/s00345-024-04821-9 (2024).

13. Ventimiglia, E. et al. Temperature profile during endourological laser activation: Introducing the thermal safety distance concept. *World J. Urol.* **42**, 453. https://doi.org/10.1007/s00345-024-05162-3 (2024).
14. Van Rhoon, G. C. et al. CEM43°C thermal dose thresholds: A potential guide for magnetic resonance radiofrequency exposure levels?. *Eur. Radiol.* **23**, 2215–2227. https://doi.org/10.1007/s00330-013-2825-y (2013).
15. Panthier, F. et al. 2022 Recommendations of the AFU Lithiasis Committee: Laser – Utilization and settings. *Prog. Urol.* **33**, 825–842. https://doi.org/10.1016/j.purol.2023.08.008 (2023).
16. Aldoukhi, A. H. et al. Defining thermally safe laser lithotripsy power and irrigation parameters: In vitro model. *J. Endourol.* **34**, 76–81. https://doi.org/10.1089/end.2019.0499 (2020).
17. Pauchard P, Corrales M, Perri D, et al (2025) Intrarenal Fluid Temperature During Laser Lithotripsy: A Mini Review by the European Association of Urology Endourology Section. European Urology Focus S2405456925001221. https://doi.org/10.1016/j.euf.2025.05.009
18. Rice, P. et al. Generated temperatures and thermal laser damage during upper tract endourological procedures using the Holmium: Yttrium–Aluminum-Garnet (Ho:YAG) laser: A systematic review of experimental studies. *World J. Urol.* **40**, 1981–1992. https://doi.org/10.1007/s00345-022-03992-7 (2022).
19. Louters, M. M. et al. Laser operator duty cycle effect on temperature and thermal dose: In-vitro study. *World J. Urol.* **40**, 1575–1580. https://doi.org/10.1007/s00345-022-03967-8 (2022).
20. Aldoukhi, A. H. et al. Patterns of laser activation during ureteroscopic lithotripsy: Effects on caliceal fluid temperature and thermal dose. *J. Endourol.* **35**, 1217–1222. https://doi.org/10.1089/end.2020.1067 (2021).
21. Song, B. et al. Impact of negative-pressure ureteral access sheath on preventing "boiled ureter" during holmium laser lithotripsy. *World J. Urol.* **43**, 371. https://doi.org/10.1007/s00345-025-05743-w (2025).
22. Pauchard, F. et al. Rethinking thermal safety in laser lithotripsy: A systematic review of thermal dose thresholds. *Curr. Opin. Urol.* **36**, 96. https://doi.org/10.1097/MOU.0000000000001346 (2026).
23. Sierra, A. et al. Thermal injury and laser efficiency with Holmium YAG and Thulium fiber laser—An in vitro study. *J. Endourol.* **36**, 1599–1606. https://doi.org/10.1089/end.2022.0216 (2022).

Author contributions

JQL, XYL, RR contributed equally to this work. Study conception and design: JQL, RR Data collection: JQL, XYL, YML Analysis and interpretation of results: JQL, RR, WH Draft manuscript preparation: JQL, LIZ Critical revision and editing of the manuscript: MCG Supervision: RQY, MCG.

Declarations

Competing interests

The authors declare no competing interests.

Ethical approval

This study was approved by the Medical Ethics Committee of The People's Hospital of Zhongshan, and informed consent was obtained from the patient for their use in research. All procedures performed in studies involving human participants were in accordance with the ethical standards of the institutional and/or national research committee and with the 1964 Helsinki declaration and its later amendments or comparable ethical standards.

Additional information

Supplementary Information The online version contains supplementary material available at https://doi.org/10.1038/s41598-026-45412-5.

Correspondence and requests for materials should be addressed to M.G.

Reprints and permissions information is available at www.nature.com/reprints.

Publisher's note Springer Nature remains neutral with regard to jurisdictional claims in published maps and institutional affiliations.

Open Access This article is licensed under a Creative Commons Attribution-NonCommercial-NoDerivatives 4.0 International License, which permits any non-commercial use, sharing, distribution and reproduction in any medium or format, as long as you give appropriate credit to the original author(s) and the source, provide a link to the Creative Commons licence, and indicate if you modified the licensed material. You do not have permission under this licence to share adapted material derived from this article or parts of it. The images or other third party material in this article are included in the article's Creative Commons licence, unless indicated otherwise in a credit line to the material. If material is not included in the article's Creative Commons licence and your intended use is not permitted by statutory regulation or exceeds the permitted use, you will need to obtain permission directly from the copyright holder. To view a copy of this licence, visit http://creativecommons.org/licenses/by-nc-nd/4.0/.

© The Author(s) 2026

科学报告

Check for updates

打开

确定钬激光碎石术治疗嵌顿性输尿管结石的安全操作窗口：对功率、操作者工作周期及冲洗流量的分析

罗金泉、李新义、任瑞、李宇明、吴浩、张丽杰、袁润强与龚曼成✉

医源性热损伤是针对钬激光碎石术治疗嵌顿结石后可能发生的输尿管狭窄的一种潜在机制。包括激光功率、操作者工作周期（ODC）以及冲洗流速在内的安全操作参数仍缺乏明确界定。我们采用高精度的离体3D打印硅胶模型模拟输尿管嵌顿结石的情景，并采用全因子实验设计评估了激光功率（10、20、30和40 W）、冲洗流速（10和20 mL/min）以及50% ODC 模式（1 s/1 s、3 s/3 s和5 s/5 s）的所有组合效应。主要观察指标为90秒操作期间累积的热剂量（CEM43）。在10 W和20 W功率水平下，几乎所有组合产生的CEM43累积值均可忽略不计（测量时间小于0.06分钟）。当功率达到30 W时出现关键转变：低流量（10 mL/min）与延长激光开启时间（5 s）相结合，在90秒实验中导致CEM43值超过120分钟，具体达到336.18分钟；而40 W功率下的热损伤风险显著升高。在保持激光开启时间为3秒、功率为40 W的条件下，将灌注流量从10 mL/min增加至20 mL/min后，CEM43水平从危险值309.80分钟降至11.11分钟。然而，在40 W功率下将激光开启时间延长至5秒时，无论流量如何变化，均持续导致CEM43水平达到危险水平。激光碎石术中的热风险由功率、ODC 值和流量三者的相互作用共同决定。在此离体模型中，10 W在所有测试条件下均属安全范围；虽然20 W通常也是安全的，但应避免在低流量下长时间激活。当功率超过30 W时，风险显著增加——此时安全性要求采用高流量和短时间脉冲激活模式，理论上存在安全裕度，但在实践中难以复现。此外，由于CEM43具有累积性，90秒的实验时间窗并不能反映实际临床激活总时长；即使在本模型中看似安全的参数设置下，更长的激活时间也可能超过损伤阈值。因此临床医生应谨慎解读这些数据并使用较低功率设置。

关键词钬激光碎石术、输尿管结石、热损伤、激光安全性、嵌顿结石

尿路结石症是全球范围内普遍存在的健康问题，其中输尿管结石占所有病例的30%-55%，可导致侧腹痛、尿路感染及输尿管狭窄等并发症[1,2]。对于嵌顿性输尿管结石（其特征为长期滞留导致黏膜水肿、炎症及纤维化），输尿管镜激光碎石术面临特殊挑战[3]。结石嵌顿的确切定义难以明确，文献多依据临床标准进行界定，包括：(1)首次尝试时导丝未能通过结石；(2)因结石导致轻度至重度肾积水；(3)结石在原位停留两个月或更长时间[4,5]。这些结石与

中山市人民医院泌尿外科，地址：广东省中山市孙文东路2号
中国。✉邮箱：gongmancheng@126.com

术后并发症发生率显著升高相关，尤其是输尿管狭窄；据报道其发生率高达4.9%至34%，而非嵌顿性结石的发生率为1.9%[6–8]。

医源性损伤的主要机制是钬激光激活引起的热损伤。激光能量在灌注液中转化为热量，可使温度升高至诱发尿路上皮凝固性坏死的程度。这种损伤的程度取决于温度和暴露时间，后者被正式量化为热剂量（43°C下的累积等效分钟数，即CEM43）。公认CEM43阈值为120分钟是组织坏死的关键临界值[9,10]。

累积有害热剂量的风险受关键操作参数的调控。虽然激光功率是热量产生的主要驱动因素[11]，但操作者的工作周期（ODC）——即激光间歇激活的模式——已被确认为独立的关键影响因素。即使在中等功率设置下，较高的工作周期也会导致危险的热剂量[12]。灌注流速是主要的冷却机制，但在输尿管梗阻这种液体循环天然受限的狭小空间内，其冷却效果仍是一个关键问题[13]。

尽管先前的体外研究已分别探讨了这些参数，但针对模拟嵌顿结石临床挑战条件下的其综合效应进行系统性量化分析仍存在空白。在此高风险情境下安全实施碎石术的具体操作规范尚未明确界定。因此，本研究旨在利用高精度离体三维打印的输尿管嵌顿结石模型，系统评估 ODC 、激光功率及冲洗流速对尿路上皮热损伤风险的影响。通过计算累积热剂量（CEM43），我们旨在确定能将热剂量维持在120分钟临界阈值以下的安全操作范围，从而为输尿管嵌顿结石的安全高效治疗提供实验依据。

方法

实验装置与材料

3D打印输尿管模型

采用Mimics Research 21.0软件（比利时Materialise公司）重建了单侧肾脏及输尿管模型（包含肾盂和肾盏）。该模型使用含10A软度的加固化液态硅胶的硅胶液体3D打印机制备而成。输尿管腔内径为4.8毫米，模拟了正常人类输尿管的平均口径。打印过程中采用水凝胶支撑浴防止结构变形；打印完成后对模型进行清洗以去除残留水凝胶，最终获得一个空心且解剖结构精确的肾-输尿管模型。

石料样本

采用直径为12±2毫米的标准化贝戈石人工结石。此外，还使用了从一名患有多发性膀胱结石患者（经知情同意）体内获取的、尺寸相似的人体草酸钙结石。

外科及激光设备

实验中使用了刚性输尿管镜（Fr9.8/8.0，德国Richard Wolf公司生产），并在操作过程中用固定夹固定。采用钬激光系统（SRM -H1C型，中国上海Raykeen公司）配合激光光纤（550 μm）进行碎石治疗。借助内窥镜将激光光纤置于输尿管腔中心，并调整其尖端距结石表面保持约1毫米距离后进行半固固定。激光输出功率设置为四个档位：10 W（0.5 J/20 Hz）、20 W（1.0 J/20 Hz）、30 W（1.5 J/20 Hz）和40 W（2.0 J/20 Hz）。所有功率参数均在实验前由独立功率计进行校验确认（图S1）。

灌流系统

一台灌注泵（LC690，神州公司，深圳，中国）以10 mL/min和20 mL/min两种流速输送温度为22–23°C的生理盐水。每次实验系列开始前，均针对特定流速进行测试：将流出液收集于预先称重的容器中1分钟，根据流出液体积与质量及密度（$\rho = 1.03\ g/cm^3$）计算体积。实验独立进行三次测量，仅允许最终实验中的流速值与目标值偏差在±0.5 mL/min范围内。

温度监测

温度使用高精度温度计（KPS -YET，中国江苏省开普森）进行监测，该仪器配备两个内置热电偶，分辨率为0.01°C。使用前，热电偶均经过校准，随后被安装在两个关键位置：结石下方（T1）及结石上方（靠近阻塞处，T2）。热电偶尖端距结石表面约1毫米，仅其感应部分插入输尿管腔内以测量黏膜温度；设备内置的数据采集系统每秒记录一次温度数据。

实验环境

实验中将模型浸入温度恒定为37±0.5°C的水浴中进行（图1A）。包括输尿管镜及打印模型在内的所有组件均使用固定夹固定，以确保实验过程中各组件的空间位置和角度稳定性。

操作员工作周期（ODC）设置

为模拟间歇性激光激活，采用了三种 ODC 模式：1秒开启/1秒关闭、3秒开启/3秒关闭以及5秒开启/5秒关闭，均对应50%的占空比。

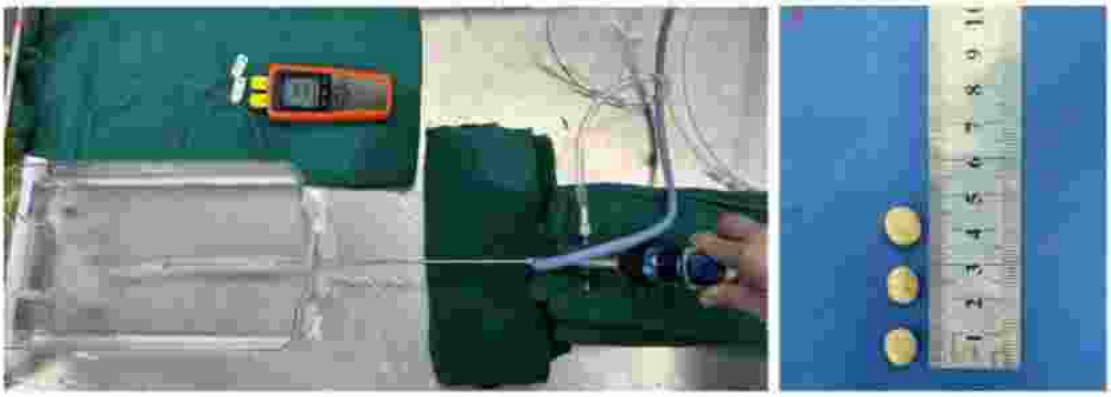


图 1 。实验材料与装置配置。（**A**）实验装置的结构示意图；（**B**）实验中使用的三种代表性人类输尿管结石样本。

实验步骤

实验步骤详见文本S1及补充材料。

热损伤评估与数据分析

主要结局指标为CEM43值，该值根据Sapareto与Dewey公式[9,14]，利用T1（最高风险部位）和T2位点的1秒时间间隔温度数据计算得出：

$$\mathrm{CEM43} = \sum t_i \times R^{(43 - T_i)}$$

其中t_i为时间间隔，T_i为该区间内的平均温度；当$T_i \geq 43°C$时$R=0.5$，当$T<43°C$时$R=0.25$。

统计分析

数据使用 SPSS 26.0版进行处理。CEM43在90秒时的数据以均值±标准差（SD）表示。

结果

实时温度分布曲线

在激光激活期间，所有参数组合下的温度动态变化均被记录（图2）。

在激光功率为10 W时，无论流速或 ODC 激光开启时间如何，所有温度曲线在整个90秒实验期间均保持在43°C阈值以下。将激光功率增加至20 W后，大多数情况下的温度曲线仍低于43°C。仅在低流速（10 mL/min）与最长 ODC 激光开启时间（5秒）组合的情况下观察到一个例外：该条件下记录的温度超过了43°C。在30 W功率点处出现了显著的热活动变化：在低流速（10 mL/min）条件下，三种 ODC 激光开启时间设置（1秒、3秒、5秒）均导致温度高于43°C；而在最大流速20 mL/min下，无论是1秒还是3秒的加热时间，温度均未超过43°C；但较长的5秒激光开启时间则使温度超过43°C。当激光功率达到最大值40 W时，所有参数组合均导致温度超过43°C。温度升高幅度及暴露持续时间均受灌注流速和 ODC 激光开启时间的显著影响。

CEM43评估

通过测量CEM43值，在体外模型中系统评估了不同钬激光参数设置下的热安全性。完整结果见表1。

数据表明激光功率是热风险的主要决定因素。在10 W和20 W的功率设置下，大多数测试条件下90秒后的累积CEM43值可忽略不计（<0.06分钟），表明存在较大的热安全裕度。唯一的例外是20 W、10 mL/min流速以及5秒激光照射时间的组合，该组合产生了较低但可测量的CEM43值（1.27 ± 0.19分钟）。在30 W时观察到关键转变点：虽然大多数组合仍属安全范围，但低流速（10 mL/min）配合延长激光照射时间（5秒）会导致热剂量迅速累积，在实验中超过了120分钟的安全阈值（336.18 ± 50.43分钟）。当功率达到40 W时，热风险显著升高。高灌注流量（20 mL/min）能有效降低短激光照射时间（1秒、3秒）下的风险，使CEM43值维持在11.11 ± 1.67分钟或更低水平；然而，在40 W功率下将激活时间延长至5秒则始终导致危险的CEM43值（在20 mL/min流速下为1069.35 ± 85.55 min at 10 <| term_0|>； 159.77 ± 23.97分钟）。

人体结石的最终热剂量（CEM43）与在相同条件下从Begostones实验中获得的数据初步一致（表S1）。此外，人体结石的实时温度曲线（图S2）与Begostones实验中的曲线高度吻合。

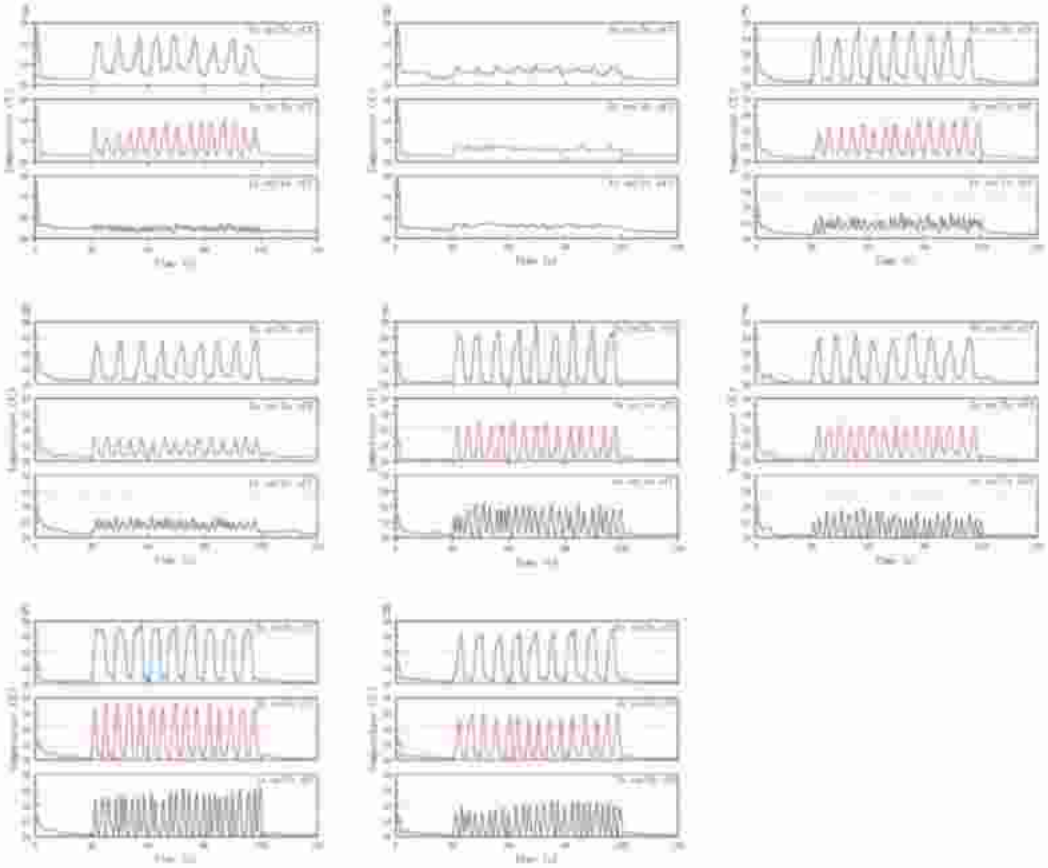


图 2。不同激光能量、流速和占空比下的温度变化。（**A**、**B**）分别表示在10 W激光能量下，流速为10 ml/min和20 ml/min时的结果；（**C**、**D**）分别表示在20 W激光能量下，流速为10 ml/min和20 ml/min时的结果；（**E**、**F**）分别表示在30 W激光能量下，流速为10 ml/min和20 ml/min时的结果；（**G**、**H**）分别表示在40 W激光能量下，流速为10 ml/min和20 ml/min时的结果。各图中的温度变化曲线分别对应1秒开启/1秒关闭、3秒开启/3秒关闭以及5秒开启/5秒关闭的占空比。红色虚线表示43°C的阈值。

上述温度及CEM43数据均在T1位置测量获得。在所有测试条件下，T2测量点的温度均保持低于43°C（数据未显示）。

讨论

本研究在高仿真度的嵌顿性上段输尿管结石模型中，系统量化了ODC 值、激光功率及冲洗流速对钬激光碎石术过程中热剂量累积的影响。我们的主要发现是：虽然激光功率是决定热损伤风险的主要因素，但 ODC 值与冲洗流速则是关键调节变量——它们既能降低也能加剧该风险，从而明确了高功率操作下的安全阈值范围。

数据明确揭示了基于激光功率的明显风险分级。在所有10 W测试条件下，以及大多数20 W条件下，90秒后的累积CEM43值可忽略不计（≤0.06分钟），在临床相关的激活期间实际上不存在热损伤风险。这一发现为低至中等功率设置的安全性提供了坚实的实验支持，这与先前专家建议[11,15–17]一致。风险的关键转折点出现在30 W时；参数组合决定了是否会在90秒观察窗口内突破120分钟损伤阈值。具体而言，30 W、10 mL/min、5秒的参数组合产生的CEM43值为336.18 ± 50.43分钟，远超该阈值。这表明即使在30 W功率下，不当操作也可能迅速导致潜在有害的热剂量。在最高40 W功率下，热风险显著升高；但我们的数据清楚地证明了冲洗液的显著缓解作用：在40 W、激光开启时间为3秒的情况下，将流量从10 mL/min增加至20 mL/min可使累积CEM43值从危险值309大幅降低。从80 ± 24.78分钟显著缩短至11.11 ± 1.67分钟。与Rice等人的研究结果一致，高流量灌注（36–40 mL/min）已被证实能显著降低管腔内温度[18]。我们的研究结果表明，操作者工作周期（ODC）是热风险的关键调节因素，其影响取决于激光功率和灌注流量。在功率设置≥30 W时，将激光开启时间从1秒或3秒延长至5秒，往往决定了是否仅积累最低热剂量还是导致损伤性热剂量。例如，在40 W功率、20 mL/min流量条件下，将激光开启时间从3秒延长至5秒，导致CEM43

流速（ml/min）	激光功率（瓦）	ODC 激光作用时间（秒）	CEM43累积值（分钟）：均值平均值±标准差
10	10	1	$(3.17 \pm 0.95) \times 10^{-6}$
10	10	3	$(4.15 \pm 1.25) \times 10^{-6}$
10	10	5	$(7.32 \pm 2.20) \times 10^{-6}$
20	10	1	$(6.71 \pm 2.01) \times 10^{-6}$
20	10	3	$(5.45 \pm 1.64) \times 10^{-6}$
20	10	5	$(6.06 \pm 1.82) \times 10^{-6}$
10	20	1	$(1.08 \pm 0.32) \times 10^{-3}$
10	20	3	$(14.7 \pm 2.94) \times 10^{-3}$
10	20	5	1.27 ± 0.19
20	20	1	$(3.69 \pm 1.11) \times 10^{-6}$
20	20	3	$(9.56 \pm 2.87) \times 10^{-6}$
20	20	5	$(5.90 \pm 1.18) \times 10^{-3}$
10	30	1	$(34.4 \pm 6.88) \times 10^{-3}$
10	30	3	0.418 ± 0.083
10	**30**	**5**	**336.18 ± 50.43**
20	30	1	$(2.16 \pm 0.65) \times 10^{-3}$
20	30	3	$(11.3 \pm 2.26) \times 10^{-3}$
20	30	5	0.472 ± 0.071
10	40	1	20.54 ± 3.08
10	**40**	**3**	**309.80 ± 24.78**
10	**40**	**5**	**1069.35 ± 85.55**
20	40	1	0.525 ± 0.065
20	40	3	11.11 ± 1.67
20	**40**	**5**	**159.77 ± 23.97**

表1。激光激活90秒期间CEM43的累积值。*CEM43：43°C下的累积等效分钟数。粗体条目表示在90秒时平均CEM43值超过120分钟安全阈值的参数组合，表明这些设置属于高风险状态。

CEM43±1.67分钟增加到159.77±23.97分钟，超过了损伤阈值。这与先前研究结果一致，即 ODC 被确定为控制体温升高的重要变量[12,19]。Louters等人的研究量化了 ODC 模式的显著影响，表明将 ODC 从50%调整至60%可使受伤时间缩短一个数量级[19]。我们的数据与关于短暂高 ODC 激活的临床观察结果一致[20]，证明调控 ODC 对于安全进行碎石术至关重要，尤其是在使用较高功率设置时。

另一个有趣的观察结果是温度变化极为迅速。在任何冲洗操作开始前，T1测量点的温度仅需2秒即可降至30°C以下并稳定在约27°C。同样，当激光停止工作时，T1测量点的温度也在2秒内降至30°C以下。根据针对非嵌顿结石的研究表明，其冷却速率甚至快于这些研究中观察到的结果。Song等人指出，尽管使用了流速为78–91 mL/min的半刚性输尿管镜[21]，典型的冲洗前过程仍需要约10秒才能将输尿管腔温降至29–31°C范围。我们推测，嵌顿结石的存在会阻碍冲洗液在输尿管内的正常逆行流动，从而促进局部液体快速更新并加速散热。这一机制或许可以解释为何在我们的实验（30 W或40 W功率下）中，只要冲洗充分且激光照射时间足够短以确保安全传递激光能量而不造成热损伤，就能实现有效降温。

检测输尿管热损伤最重要的临床标准仍是CEM43阈值（120分钟），该阈值基于先前的高温研究[9,10,22]。然而，Pauchard等的研究数据表明，当CEM43值在20至70分钟范围内时仍可能发生肾热损伤，这说明临床显著损伤所需的热剂量可能低于既往认知[22]。因此，未来需要进一步明确肾盂和输尿管的热损伤阈值。同时，应采用更为保守的参数选择以确保足够的安全裕度。

我们的研究结果具有直接且重要的临床意义。输尿管镜检查后输尿管狭窄（尤其是嵌顿性结石[6]）的发生率日益增加，可能与未充分了解高功率激光参数设置、忽视激活模式及冲洗方式有关。我们的研究结果基于典型90秒激活过程中累积的热剂量，提出了安全实施治疗的实用、循证建议。为确保较高的安全裕度，在所有测试的流速和 ODC 组合下，10 W的功率设置均是安全的。尽管20 W功率设置通常也是安全的，但在低流速条件下不应长时间使用该功率设置。30 W下的安全性高度依赖于辅助参数；建议采用较高的冲洗流速（20 mL/min）。在低冲洗流速（10 mL/min）下，外科医生必须避免在此功率水平下进行长时间连续激活（例如激光开启时间达5秒），因为这种组合会导致有害热剂量迅速累积（CEM43>336分钟）。使用40瓦的

功率存在较高风险，因此需谨慎使用。仅在高流速（20 mL/min）且激光开启时间短（≤3秒）的情况下才具有合理性。因此，外科医生必须严格注意激光激活的累计（及总）持续时间，以确保低于损伤阈值。值得注意的是，在临床实践中，适当提高灌注流速有助于减轻高功率激光激活产生的热效应。但前提是输尿管流出道必须通畅，以防止肾内压力升高，从而降低术后感染及相关并发症的风险。我们建议在流出道受阻的情况下（如存在输尿管狭窄或迂曲时），应避免使用高功率激光参数。此外，40 W的操作窗口范围非常狭窄，因此外科医生需严格控制单次激活脉冲的时间及激活次数。

尽管本研究具有诸多优势，但仍存在若干局限性。作为离体模型，其缺乏血液灌注带来的散热效应以及活体组织的动态生理反应；此外，硅胶模型与人工结石的热学特性均不同于人体组织，我们在有限数量的人体结石样本（n=3）中进行的验证结果仍需进一步研究。所有实验均使用550μm激光光纤——相较于200μm等较细光纤，较大光纤在结石表面产生的能量密度较低，从而限制了其消融效果。在临床实践中，这可能导致外科医生通过选择更高功率或延长激光作用时间来弥补，进而导致过度热暴露。更重要的是，该模型假设了通畅的冲洗通道及居中的非接触式激光光纤，从而理想化了多种临床情况；而实际上，嵌顿结石常会导致冲洗功能受损。此外，手术操作技术（尤其是对经验不足的外科医生而言）可能使激光光纤与黏膜发生接触，直接造成输尿管损伤[23]。这些因素可能在比本研究观察到的更短的时间尺度内产生热量，这意味着我们的实验估算结果可能代表了最理想的情况下的热效应模型。该模型还未能考虑结石的碎裂现象——结石可能会断裂成更小的碎片，从而消耗激光能量并改变热量生成情况。因此，虽然经验丰富的外科医生在受控环境下手术时可能达到所述的安全参数水平，但经验不足的操作者或灌注条件较差的病例则应采用更为保守的参数设置。未来实验应尝试在更具临床挑战性的条件下复现这些热剂量阈值。

结论

激光碎石术中热损伤的风险取决于功率、ODC 值及流速。在本离体模型中，10 W的功率设置在所有测试的流速与 ODC 值组合下均安全可靠。虽然20 W功率通常也是安全的，但在低流速条件下不应长时间使用该功率。一旦功率超过30 W，安全性就日益依赖于高流速以及限制激活脉冲次数——这些适宜参数仅能通过安全裕度实现，但在实际操作中难以稳定复现。此外，由于CEM43是累积参数，本研究采用的90秒实验时间窗并不能代表完整的临床激活时长；即使在该模型中看似安全的参数设置下，长时间激活仍可能超过损伤阈值。因此，临床医生应谨慎解读这些数据并选择较低功率设置。

数据可用性

本研究期间生成和/或分析所得的数据集可根据合理要求向通讯作者索取。

接收日期：2025年12月28日；接受日期：2026年3月18日
Published online: 28 March 2026

参考文献

1. Sorokin, I. et al. Epidemiology of stone disease across the world. *World J. Urol.* **35**, 1301 – 1320. https://doi.org/10.1007/s00345-01 7-2008-6 (2017).
2. Jahrreiss, V., Seitz, C. & Quhal, F. Medical management of urolithiasis: Great efforts and limited progress. *Asian J. Urol.* **11**, 149 – 155. https://doi.org/10.1016/j.ajur.2023.05.001 (2024).
3. Hu, H. et al. Ureteral stricture formation after removal of proximal ureteral stone: Retroperitoneal laparoscopic ureterolithotomy versus ureteroscopy with Holmium: YAG laser lithotripsy. *PeerJ* **5**, e3483. https://doi.org/10.7717/peerj.3483 (2017).
4. Fam, X. I. et al. Ureteral stricture formation after ureteroscope treatment of impacted calculi: A prospective study. *Korean J. Urol.* **56**, 63. https://doi.org/10.4111/kju.2015.56.1.63 (2015).
5. Tonyali, S. et al. Predictors of ureteral strictures after retrograde ureteroscopic treatment of impacted ureteral stones: A systematic literature review. *JCM* **12**, 3603. https://doi.org/10.3390/jcm12103603 (2023).
6. Moretto, S. et al. Ureteral stricture rate after endoscopic treatments for urolithiasis and related risk factors: Systematic review and meta-analysis. *World J. Urol.* **42**, 234. https://doi.org/10.1007/s00345-024-04933-2 (2024).
7. Yamashita, S., Inoue, T., Kohjimoto, Y. & Hara, I. Comprehensive endoscopic management of impacted ureteral stones: Literature review and expert opinions. *Int. J. Urol.* **29**, 799 – 806. https://doi.org/10.1111/iju.14908 (2022).
8. Tonyali, S. et al. Factors associated with ureteral strictures following ureteroscopy for impacted ureteral stones? A multicenter study by EAU-YAU endourology and urolithiasis working party. *Actas Urológicas Españolas (English Edition)* **47**, 631 – 637. https://doi.org/10.1016/j.acuroe.2023.04.005 (2023).
9. Sapareto, S. A. & Dewey, W. C. Thermal dose determination in cancer therapy. *Int. J. Radiat. Oncol. Biol. Phys.* **10**, 787 – 800. https://doi.org/10.1016/0360-3016(84)90379-1 (1984).
10. Aldoukhi, A. H. et al. Caliceal fluid temperature during high-power Holmium laser lithotripsy in an *in vivo* porcine model. *J. Endourol.* **32**, 724 – 729. https://doi.org/10.1089/end.2018.0395 (2018).
11. De Coninck, V., Defraigne, C. & Traxer, O. Watt determines the temperature during laser lithotripsy. *World J. Urol.* **40**, 1257 – 1258. https://doi.org/10.1007/s00345-021-03848-6 (2022).
12. Wanderling, C. et al. WATTS happening? Evaluation of thermal dose during holmium laser lithotripsy in a high-fidelity anatomic model. *World J. Urol.* **42**, 157. https://doi.org/10.1007/s00345-024-04821-9 (2024).

13. Ventimiglia, E. et al. Temperature profile during endourological laser activation: Introducing the thermal safety distance concept. *World J. Urol.* **42**, 453. https://doi.org/10.1007/s00345-024-05162-3 (2024).
14. Van Rhoon, G. C. et al. CEM43°C thermal dose thresholds: A potential guide for magnetic resonance radiofrequency exposure levels?. *Eur. Radiol.* **23**, 2215 – 2227. https://doi.org/10.1007/s00330-013-2825-y (2013).
15. Panthier, F. et al. 2022 Recommendations of the AFU Lithiasis Committee: Laser – Utilization and settings. *Prog. Urol.* **33**, 825 – 842. https://doi.org/10.1016/j.purol.2023.08.008 (2023).
16. Aldoukhi, A. H. et al. Defining thermally safe laser lithotripsy power and irrigation parameters: In vitro model. *J. Endourol.* **34**, 76 – 81. https://doi.org/10.1089/end.2019.0499 (2020).
17. Pauchard F, Corrales M, Perri D, et al (2025) Intrarenal Fluid Temperature During Laser Lithotripsy: A Mini Review by the European Association of Urology Endourology Section. European Urology Focus S2405456925001221. https://doi.org/10.1016/j.euf.2025.05.009
18. Rice, P. et al. Generated temperatures and thermal laser damage during upper tract endourological procedures using the Holmium: Yttrium – Aluminum-Garnet (Ho:YAG) laser: A systematic review of experimental studies. *World J. Urol.* **40**, 1981 – 1992. https://doi.org/10.1007/s00345-022-03992-7 (2022).
19. Louters, M. M. et al. Laser operator duty cycle effect on temperature and thermal dose: In-vitro study. *World J. Urol.* **40**, 1575 – 1580. https://doi.org/10.1007/s00345-022-03967-8 (2022).
20. Aldoukhi, A. H. et al. Patterns of laser activation during ureteroscopic lithotripsy: Effects on caliceal fluid temperature and thermal dose. *J. Endourol.* **35**, 1217 – 1222. https://doi.org/10.1089/end.2020.1067 (2021).
21. Song, B. et al. Impact of negative-pressure ureteral access sheath on preventing "boiled ureter" during holmium laser lithotripsy. *World J. Urol.* **43**, 371. https://doi.org/10.1007/s00345-025-05743-w (2025).
22. Pauchard, F. et al. Rethinking thermal safety in laser lithotripsy: A systematic review of thermal dose thresholds. *Curr. Opin. Urol.* **36**, 96. https://doi.org/10.1097/MOU.0000000000001346 (2026).
23. Sierra, A. et al. Thermal injury and laser efficiency with Holmium YAG and Thulium fiber laser—An in vitro study. *J. Endourol.* **36**, 1599 – 1606. https://doi.org/10.1089/end.2022.0216 (2022).

作者贡献

JQL、XYL和RR对本研究贡献均等。研究构思与设计：JQL、RR；数据收集：JQL、XYL、YML；结果分析与解读：JQL、RR、WH；初稿撰写：JQL、LJZ；关键性审阅、稿件修订与编辑：MCG监督：RQY、MCG。

声明；宣言

竞争性利益

作者声明无利益冲突。

伦理审批

本研究已获得中山人民医院医学伦理委员会批准，并已获得患者对其参与研究的知情同意。所有涉及人类受试者的研究程序均符合机构及/或国家研究委员会的伦理标准、1964年《赫尔辛基宣言》及其后续修正案或同等伦理规范。

附加信息

补充信息：在线版本包含补充材料，可访问https://doi.org/10.1038/s41598-026-45412-5获取。

来函及材料索取请求应发送至 M.G. 邮箱。

重印及授权信息可访问www.nature.com/reprints**获取。**

出版方说明：Springer Nature 对已出版地图中的管辖权主张及机构隶属关系均保持中立立场。

开放获取本文依据知识共享署名-非商业性使用-禁止演绎 4.0 国际许可协议授权，允许以任何媒介或格式进行非商业性使用、分享、分发及复制，但须满足以下条件：正确标注原作者及来源信息、提供知识共享许可协议链接、并注明是否对授权内容进行了修改。根据该许可协议，您无权分享基于本文或其部分内容改编的材料。文中所含图像或其他第三方素材均纳入文章的知识共享许可范围（除非在引用说明中另有特别注明）。若素材未包含在文章知识共享许可范围内、且您的使用目的超出法定许可范围或违反相关法规，则需直接向版权方申请授权。如需查看该许可协议副本，请访问http://creativecommons.org/licenses/by-nc-nd/4.0/。

© 作者 2026

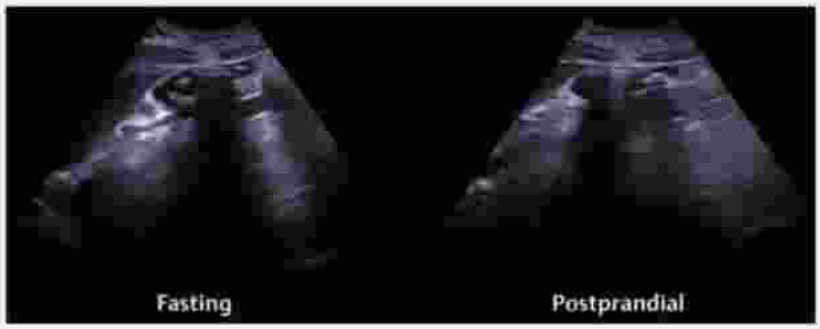
Article published online: 2026-05-21

Gallbladder perforation during peroral holmium laser lithotripsy

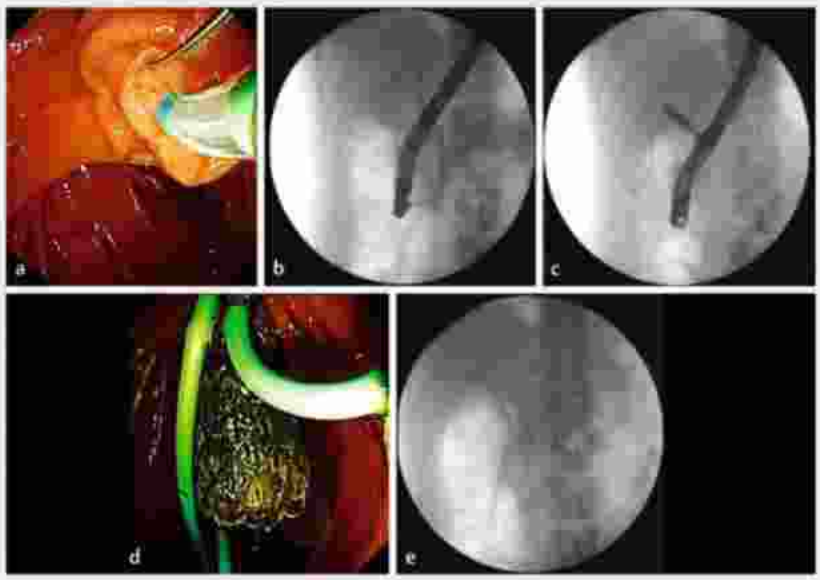
OPEN ACCESS

A 26-year-old woman presented with intermittent right upper quadrant abdominal pain for 6 months. Abdominal ultrasonography revealed multiple stones in the gallbladder (largest size: 22×9 mm; wall thickness: 2 mm) and an ejection fraction of 80% on a fatty meal test (▶ **Fig. 1**). Given the patient's strong preference for gallbladder preservation, peroral gallbladder-preserving cholelithotomy using a choledochoscope (eyeMAX, 9-Fr, Micro-Tech, China) was planned [1]. During the procedure, a guidewire was inserted into the gallbladder using endoscopic retrograde cholangiopancreatography techniques, and a fully covered metal stent (120×10 mm, Micro-Tech, China) was implanted across the papilla, bridging the duodenum and gallbladder (▶ **Fig. 2**). One week later, the choledochoscope was easily advanced through the stent into the gallbladder, where multiple large stones were identified (▶ **Fig. 3**). Subsequently, holmium laser lithotripsy was performed (▶ **Video 1**). However, the laser inadvertently penetrated the gallbladder wall, resulting in acute gallbladder perforation. A nasobiliary tube was immediately placed for bile drainage, and subsequent continuous negative-pressure drainage was applied. After 1 week, choledochoscopy confirmed the complete healing of the perforation. A second lithotripsy session was performed for the residual stones, followed by complete stone extraction (▶ **Fig. 4**). The patient was discharged shortly thereafter and remained asymptomatic during the 7-month follow-up. To the best of our knowledge, this is the first reported endoscopic detection and management of gallbladder perforation occurring during peroral holmium laser lithotripsy.

Endoscopy_UCTN_Code_CPL_1AK_2AF



▶ **Fig. 1** Abdominal ultrasonography indicated multiple large stones in the gallbladder and an ejection fraction of 80% on a fatty meal test.



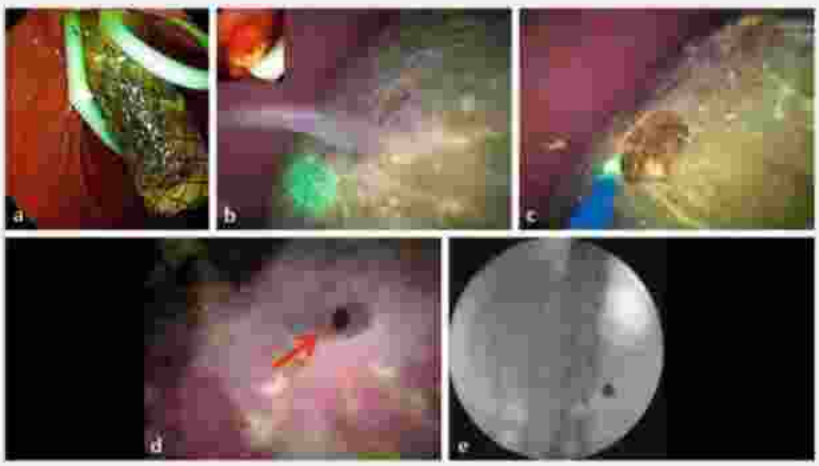
▶ **Fig. 2** **a–c** Guidewire insertion into the gallbladder using ERCP techniques and **d, e** stent placement across the papilla bridging the duodenum and gallbladder. ERCP, endoscopic retrograde cholangiopancreatography.

Contributors' Statement

Rui Zhu: Data curation, Formal analysis, Writing – original draft. Hui Long: Writing – review & editing. Yue Zhu: Resources, Software. Qiu Zhao: Resources. Hongling Wang: Supervision. Fan Wang: Project administration.

Funding Information

Key Laboratory Project of Hubei Province of Hubei Province of Tianyou Hospital Affiliated to Wuhan University of Science & Technology
OHIC2023K01



▶ **Fig. 3** **a, b** Peroral choledochoscope detection of multiple large stones in the gallbladder. **c** Holmium laser lithotripsy. **d** Gallbladder perforation occurring during the lithotripsy (arrow). **e** Nasobiliary tube placement for continuous negative-pressure bile drainage.



▶ **Fig. 4** **a** The second lithotripsy session, **b–d** stone extraction, and **e** complete healing of the perforation in the gallbladder after 1 week.

Conflict of Interest

The authors declare that they have no conflict of interest.

The authors

Rui Zhu[1], Hui Long[1], Yue Zhu[2], Qiu Zhao[2], Hongling Wang[2], Fan Wang[2]

1. Department of Gastroenterology, Tianyou Hospital Affiliated to Wuhan University of Science and Technology, Wuhan, China
2. Department of Gastroenterology, Wuhan University Zhongnan Hospital, Wuhan, China



Video 1 Gallbladder perforation during peroral holmium laser lithotripsy.

Corresponding author

Fan Wang
Department of Gastroenterology, Wuhan University Zhongnan Hospital, Wuhan 430071, China
fanndywang@126.com

Reference

[1] Zou Q, Du J, Lin Y et al. Application of holmium laser in endoscopic retrograde cholangiopancreatographygall gallbladder-preserving cholecystolithotomy. Endoscopy 2025; 57 (Suppl. 01): E118–E119. doi:10.1055/a-2499-7536

Bibliography

Endoscopy 2026; 58: E622–E623
DOI 10.1055/a-2868-7854
ISSN 0013-726X

© 2026. The Author(s).
This is an open access article published by Thieme under the terms of the Creative Commons Attribution License, permitting unrestricted use, distribution, and reproduction so long as the original work is properly cited. (https://creativecommons.org/licenses/by/4.0/)

Georg Thieme Verlag KG, Oswald-Hesse-Str. 50, 70469 Stuttgart, Germany

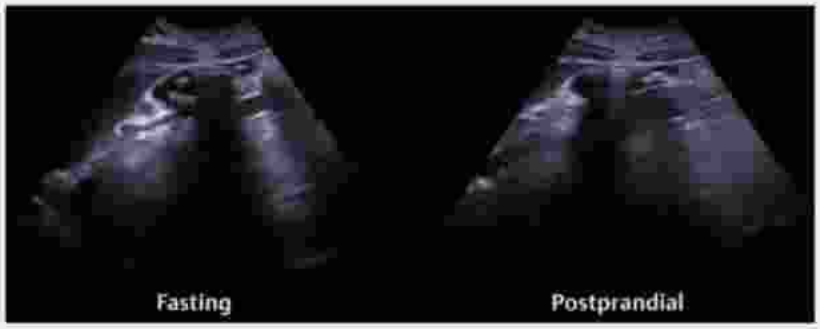
文章在线发表日期：2026-05-21

经口钬激光碎石术期间发生的胆囊穿孔

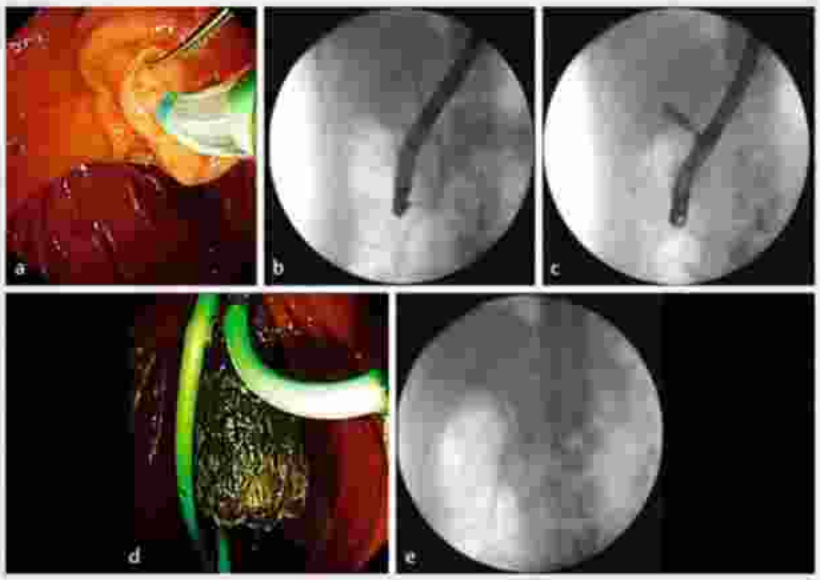
OPEN ACCESS

一名26岁女性因持续6个月的右上腹间歇性疼痛就诊。腹部超声检查显示胆囊内存在多枚结石（最大尺寸：22×9毫米，壁厚：2毫米）。脂肪餐试验中的排空分数为80%（▶图1）。鉴于患者强烈要求保留胆囊，医生计划采用胆道镜（Eye MAX，9-Fr，Micro-Tech，中国）行经口保胆性胆总管切开术[1]。术中通过内镜逆行胆胰管造影技术将导丝置入胆囊，并植入完全覆膜的金属支架（120×10毫米，Micro-Tech，中国）跨越乳头，连接十二指肠与胆囊（▶图2）。一周后，胆道镜顺利经支架进入胆囊，发现多个大结石（▶图3）。随后实施钬激光碎石术（▶视频1）。但激光意外穿透胆囊壁，导致急性胆囊穿孔。立即置入鼻胆管进行胆汁引流，并随后实施持续负压引流。一周后，胆总管造影证实穿孔已完全愈合。针对残留结石进行了第二次碎石治疗。随后成功完全取出结石（▶图4）。患者随后即出院，在为期7个月的随访期间均无症状。据我们所知，这是首例报道在经口钬激光碎石术过程中通过内镜检测并处理胆囊穿孔的病例。

Endoscopy_UCTN_Code_CPL_1AK_2AF



▶图1 腹部超声检查显示胆囊内存在多枚大结石，且脂肪餐试验中的排空分数为80%。



▶图2a–c：采用 ERCP 技术将导丝置入胆囊；图d、e：支架跨乳头植入，连接十二指肠与胆囊。ERCP：内镜逆行胰胆管造影。

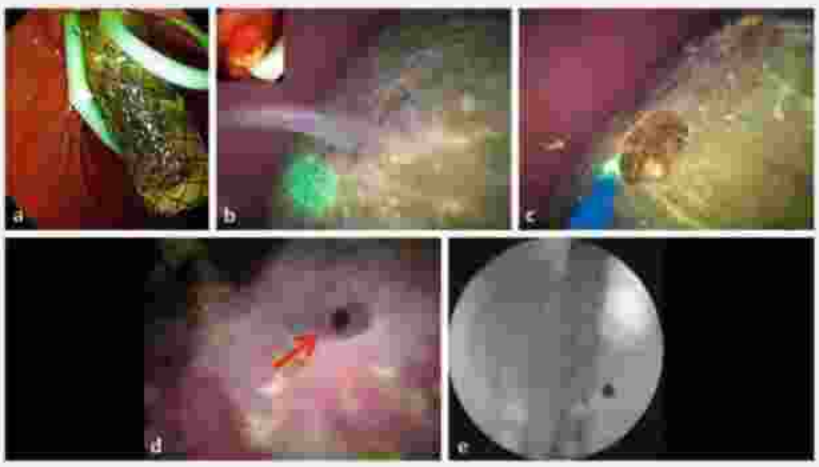
贡献者声明

朱瑞：数据管理、形式分析、初稿撰写；龙辉：审阅与编辑；朱悦：资源与软件支持；赵秋：资源支持；王洪玲：超级计算支持。唐雷，岳王：项目管理。

资金信息

武汉理工大学附属天佑医院湖北省重点实验室项目

OHIC2023K01



▶图3 a、b 经口胆总管镜检发现胆囊内存在多枚大结石。c 钬激光碎石术。d 碎石术过程中发生的胆囊穿孔（箭头所示）。e 安置鼻胆管以实现持续负压胆汁引流。



▶图4a为第二次碎石治疗，b–d为结石取出过程，e为术后1周胆囊穿孔完全愈合。

违背公众利益的行为

作者声明不存在利益冲突。

作者们

[redacted]

1 武汉理工大学天佑医院消化内科，中国武汉

2 武汉大学中南医院消化内科，中国武汉



▶视频1 经口钬激光碎石术期间发生的胆囊穿孔。

通讯作者

汪王

武汉大学中南医院消化内科，中国武汉

430071

fanndywang@126.com

参考：依据

[1] Zou Q, Du J, Lin Y 等.全金属激光在内镜逆行胰胆管造影术中用于胆囊保全性胆囊结石切开术的应用.《内镜学》2025;57(增刊01):E118–E119. doi:10.1055/a-2499-7536

参考文献

《内镜学》2026年；第58卷：E622–E623

DOI 10.1055/a-2868-7854

ISSN 0013-726X

© 2026。作者（们）。

本文为Thieme出版社根据知识共享署名许可协议发布的开放获取文章，允许在正确引用原始作品的前提下自由使用、传播和复制。

(https://creativecommons.org/licenses/by/4.0/)

乔治·蒂梅出版社（Georg Thieme Verlag KG），奥斯瓦尔德-黑塞街50号，70469斯图加特，德国